VOLUME 28 / NUMBER 15
AUGUST 8, 1990
ACC. NOS. N90-21722 TO N90-22529

STAR
AN ABSTRACT JOURNAL

Scientific and Technical Aerospace Reports

PRODUCED BY THE
SCIENTIFIC AND TECHNICAL
INFORMATION
DIVISION

NASA

NATIONAL AERONAUTICS AND SPACE ADMINISTRATION

WHAT YOU CAN DO FOR *STAR*

All users of this abstract service are urged to forward reports to be considered for announcement in *STAR*. This will aid NASA in its efforts to provide the fullest possible coverage of all scientific and technical publications that might support aeronautics and space research and development. If you have prepared relevant reports (other than those that you will transmit to NASA, DOD, or DOE through the usual contract- or grant-reporting channels), please send them for consideration to the NASA Scientific and Technical Information Facility, P.O. Box 8757, BWI Airport, MD 21240.

Reprints of journal articles, book chapters, and conference papers are also welcome. These will be considered for announcement in *STAR's* companion journal, *International Aerospace Abstracts*.

You may specify a particular source to be included in a report announcement if you wish; otherwise the report will be placed on public sale at the National Technical Information Service. Copyrighted publications will be announced but not distributed or sold.

PURCHASE OF *STAR*

The semimonthly issues are available to registered users on annual subscription from the NASA Scientific and Technical Information Facility, ATTN: Registration Services, P.O. Box 8757, BWI Airport, MD 21240. *STAR* is publicly available on annual subscription from the Superintendent of Documents, U.S. Government Printing Office, Washington, DC 20402.

PUBLISHED BY:

UNITED STATES GOVERNMENT
NATIONAL AERONAUTICS AND SPACE ADMINISTRATION
SCIENTIFIC AND TECHNICAL INFORMATION DIVISION
Scientific and Technical Aerospace Reports, Volume 28, is prepared by the NASA Scientific and Technical Information Facility operated for the National Aeronautics and Space Administration by RMS Associates.

The Administrator of the National Aeronautics and Space Administration has determined that the publication of this periodical is necessary in the transaction of the public business required by law of this agency. Use of funds for printing this periodical has been approved by the Director of the Office of Management and Budget through March 22, 1991.

US ISSN 0036-8741

Scientific and Technical Aerospace Reports (STAR) is issued twice a month and contains abstracts and indexes of meeting papers, conference proceedings, and unlimited distribution reports that have been added to the NASA Scientific and Technical Information Database during the preceding period. These citations may also be accessed online via NASA/RECON or via AIAA's Aerospace Database (File 108) through Dialog Information Services, Inc.

STAR subject coverage includes all aerospace-related areas that will help NASA achieve its mission. Material is gathered from all over the world and includes significant input from many countries under exchange and access agreements.

Consult the indexes at the back of this volume to help zero in on what you are looking for. These include:

Subject Index
Personal Author Index
Corporate Source Index
Contract Number Index
Report/Accession Number Index

STAR's companion abstract journal *International Aerospace Abstracts* should be used if you are looking for references to periodicals, books, and published meeting papers or conference proceedings.

Questions and comments should be addressed to:

NASA Scientific and Technical Information Facility
User Services
P.O. Box 8757
BWI Airport, MD 21240
301-621-0150

VOLUME 28 NUMBER 15 / AUGUST 8, 1990

TABLE OF CONTENTS

AERONAUTICS

Includes aeronautics (general); aerodynamics; air transportation and safety; aircraft communications and navigation; aircraft design, testing and performance; aircraft instrumentation; aircraft propulsion and power; aircraft stability and control; and research and support facilities (air).

For related information see also *Astronautics.*

01 AERONAUTICS (GENERAL) 2045

02 AERODYNAMICS 2045

Includes aerodynamics of bodies, combinations, wings, rotors, and control surfaces; and internal flow in ducts and turbomachinery.

For related information see also *34 Fluid Mechanics and Heat Transfer.*

03 AIR TRANSPORTATION AND SAFETY 2049

Includes passenger and cargo air transport operations; and aircraft accidents.

For related information see also *16 Space Transportation* and *85 Urban Technology and Transportation.*

04 AIRCRAFT COMMUNICATIONS AND NAVIGATION 2050

Includes digital and voice communication with aircraft; air navigation systems (satellite and ground based); and air traffic control.

For related information see also *17 Space Communications, Spacecraft Communications, Command and Tracking* and *32 Communications and Radar.*

05 AIRCRAFT DESIGN, TESTING AND PERFORMANCE 2050

Includes aircraft simulation technology.

For related information see also *18 Spacecraft Design, Testing and Performance* and *39 Structural Mechanics.* For land transportation vehicles see *85 Urban Technology and Transportation.*

06 AIRCRAFT INSTRUMENTATION 2052

Includes cockpit and cabin display devices; and flight instruments.

For related information see also *19 Spacecraft Instrumentation* and *35 Instrumentation and Photography.*

07 AIRCRAFT PROPULSION AND POWER 2052

Includes prime propulsion systems and systems components, e.g., gas turbine engines and compressors; and onboard auxiliary power plants for aircraft.

For related information see also *20 Spacecraft Propulsion and Power, 28 Propellants and Fuels,* and *44 Energy Production and Conversion.*

08 AIRCRAFT STABILITY AND CONTROL 2053

Includes aircraft handling qualities; piloting; flight controls; and autopilots.

For related information see also *05 Aircraft Design, Testing and Performance.*

09 RESEARCH AND SUPPORT FACILITIES (AIR) 2055

Includes airports, hangars and runways; aircraft repair and overhaul facilities; wind tunnels; shock tubes; and aircraft engine test stands.

For related information see also *14 Ground Support Systems and Facilities (Space).*

ASTRONAUTICS

Includes astronautics (general); astrodynamics; ground support systems and facilities (space); launch vehicles and space vehicles; space transportation; space communications, spacecraft communications, command and tracking; spacecraft design, testing and performance; spacecraft instrumentation; and spacecraft propulsion and power.

For related information see also *Aeronautics.*

12 ASTRONAUTICS (GENERAL) 2056

For extraterrestrial exploration see *91 Lunar and Planetary Exploration.*

13 ASTRODYNAMICS 2056

Includes powered and free-flight trajectories; and orbital and launching dynamics.

14 GROUND SUPPORT SYSTEMS AND FACILITIES (SPACE) 2057

Includes launch complexes, research and production facilities; ground support equipment, e.g., mobile transporters; and simulators.

For related information see also *09 Research and Support Facilities (Air).*

15 LAUNCH VEHICLES AND SPACE VEHICLES 2057

Includes boosters; operating problems of launch/space vehicle systems; and reusable vehicles.

For related information see also *20 Spacecraft Propulsion and Power.*

16 SPACE TRANSPORTATION N.A.

Includes passenger and cargo space transportation, e.g., shuttle operations; and space rescue techniques.

For related information see also *03 Air Transportation and Safety* and *18 Spacecraft Design, Testing and Performance.* For space suits see *54 Man/System Technology and Life Support.*

17 SPACE COMMUNICATIONS, SPACECRAFT COMMUNICATIONS, COMMAND AND TRACKING N.A.

Includes telemetry; space communications networks; astronavigation and guidance; and radio blackout.

For related information see also *04 Aircraft Communications and Navigation* and *32 Communications and Radar.*

18 SPACECRAFT DESIGN, TESTING AND PERFORMANCE 2058

Includes satellites; space platforms; space stations; spacecraft systems and components such as thermal and environmental controls; and attitude controls.

For life support systems see *54 Man/System Technology and Life Support*. For related information see also *05 Aircraft Design, Testing and Performance, 39 Structural Mechanics,* and *16 Space Transportation.*

19 SPACECRAFT INSTRUMENTATION N.A.

For related information see also *06 Aircraft Instrumentation* and *35 Instrumentation and Photography.*

20 SPACECRAFT PROPULSION AND POWER 2060

Includes main propulsion systems and components, e.g. rocket engines; and spacecraft auxiliary power sources.

For related information see also *07 Aircraft Propulsion and Power, 28 Propellants and Fuels, 44 Energy Production and Conversion,* and *15 Launch Vehicles and Space Vehicles.*

CHEMISTRY AND MATERIALS

Includes chemistry and materials (general); composite materials; inorganic and physical chemistry; metallic materials; nonmetallic materials; propellants and fuels; and materials processing.

23 CHEMISTRY AND MATERIALS (GENERAL) N.A.

24 COMPOSITE MATERIALS 2062

Includes physical, chemical, and mechanical properties of laminates and other composite materials.

For ceramic materials see *27 Nonmetallic Materials.*

25 INORGANIC AND PHYSICAL CHEMISTRY 2066

Includes chemical analysis, e.g., chromatography; combustion theory; electrochemistry; and photochemistry.

For related information see also *77 Thermodynamics and Statistical Physics.*

26 METALLIC MATERIALS 2068

Includes physical, chemical, and mechanical properties of metals, e.g., corrosion; and metallurgy.

27 NONMETALLIC MATERIALS 2070

Includes physical, chemical, and mechanical properties of plastics, elastomers, lubricants, polymers, textiles, adhesives, and ceramic materials.

For composite materials see *24 Composite Materials.*

28 PROPELLANTS AND FUELS 2072

Includes rocket propellants, igniters and oxidizers; their storage and handling procedures; and aircraft fuels.

For related information see also *07 Aircraft Propulsion and Power, 20 Spacecraft Propulsion and Power,* and *44 Energy Production and Conversion.*

29 MATERIALS PROCESSING 2072

Includes space-based development of products and processes for commercial application.

For biological materials see *55 Space Biology.*

ENGINEERING

Includes engineering (general); communications and radar; electronics and electrical engineering; fluid mechanics and heat transfer; instrumentation and photography; lasers and masers; mechanical engineering; quality assurance and reliability; and structural mechanics.

For related information see also *Physics.*

31 ENGINEERING (GENERAL) 2073

Includes vacuum technology; control engineering; display engineering; cryogenics; and fire prevention.

32 COMMUNICATIONS AND RADAR 2074

Includes radar; land and global communications; communications theory; and optical communications.

For related information see also *04 Aircraft Communications and Navigation* and *17 Space Communications, Spacecraft Communications, Command and Tracking.* For search and rescue see *03 Air Transportation and Safety,* and *16 Space Transportation.*

33 ELECTRONICS AND ELECTRICAL ENGINEERING 2088

Includes test equipment and maintainability; components, e.g., tunnel diodes and transistors; microminiaturization; and integrated circuitry.

For related information see also *60 Computer Operations and Hardware* and *76 Solid-State Physics.*

34 FLUID MECHANICS AND HEAT TRANSFER 2089

Includes boundary layers; hydrodynamics; fluidics; mass transfer and ablation cooling.

For related information see also *02 Aerodynamics* and *77 Thermodynamics and Statistical Physics.*

35 INSTRUMENTATION AND PHOTOGRAPHY 2101

Includes remote sensors; measuring instruments and gauges; detectors; cameras and photographic supplies; and holography.

For aerial photography see *43 Earth Resources and Remote Sensing.* For related information see also *06 Aircraft Instrumentation* and *19 Spacecraft Instrumentation.*

36 LASERS AND MASERS 2102

Includes parametric amplifiers.

For related information see also *76 Solid-State Physics.*

37 MECHANICAL ENGINEERING 2104

Includes auxiliary systems (nonpower); machine elements and processes; and mechanical equipment.

38 QUALITY ASSURANCE AND RELIABILITY 2108

Includes product sampling procedures and techniques; and quality control.

39 STRUCTURAL MECHANICS 2109

Includes structural element design and weight analysis; fatigue; and thermal stress.

For applications see *05 Aircraft Design, Testing and Performance* and *18 Spacecraft Design, Testing and Performance.*

GEOSCIENCES

Includes geosciences (general); earth resources and remote sensing; energy production and conversion; environment pollution; geophysics; meteorology and climatology; and oceanography.

For related information see also *Space Sciences*.

42 GEOSCIENCES (GENERAL) **N.A.**

43 EARTH RESOURCES AND REMOTE SENSING **2121**

Includes remote sensing of earth resources by aircraft and spacecraft; photogrammetry; and aerial photography.

For instrumentation see *35 Instrumentation and Photography.*

44 ENERGY PRODUCTION AND CONVERSION **2123**

Includes specific energy conversion systems, e.g., fuel cells; global sources of energy; geophysical conversion; and windpower.

For related information see also *07 Aircraft Propulsion and Power, 20 Spacecraft Propulsion and Power,* and *28 Propellants and Fuels.*

45 ENVIRONMENT POLLUTION **2124**

Includes atmospheric, noise, thermal, and water pollution.

46 GEOPHYSICS **2127**

Includes aeronomy; upper and lower atmosphere studies; ionospheric and magnetospheric physics; and geomagnetism.

For space radiation see *93 Space Radiation.*

47 METEOROLOGY AND CLIMATOLOGY **2130**

Includes weather forecasting and modification.

48 OCEANOGRAPHY **2134**

Includes biological, dynamic, and physical oceanography; and marine resources.

For related information see also *43 Earth Resources and Remote Sensing.*

LIFE SCIENCES

Includes life sciences (general); aerospace medicine; behavioral sciences; man/system technology and life support; and space biology.

51 LIFE SCIENCES (GENERAL) **2135**

52 AEROSPACE MEDICINE **2136**

Includes physiological factors; biological effects of radiation; and effects of weightlessness on man and animals.

53 BEHAVIORAL SCIENCES **2137**

Includes psychological factors; individual and group behavior; crew training and evaluation; and psychiatric research.

54 MAN/SYSTEM TECHNOLOGY AND LIFE SUPPORT **2138**

Includes human engineering; biotechnology; and space suits and protective clothing.

For related information see also *16 Space Transportation.*

55 SPACE BIOLOGY **N.A.**

Includes exobiology; planetary biology; and extraterrestrial life.

MATHEMATICAL AND COMPUTER SCIENCES

Includes mathematical and computer sciences (general); computer operations and hardware; computer programming and software; computer systems; cybernetics; numerical analysis; statistics and probability; systems analysis; and theoretical mathematics.

59 MATHEMATICAL AND COMPUTER SCIENCES (GENERAL) **N.A.**

60 COMPUTER OPERATIONS AND HARDWARE **2144**

Includes hardware for computer graphics, firmware, and data processing.

For components see *33 Electronics and Electrical Engineering.*

61 COMPUTER PROGRAMMING AND SOFTWARE **2145**

Includes computer programs, routines, algorithms, and specific applications, e.g., CAD/CAM.

62 COMPUTER SYSTEMS **2149**

Includes computer networks and special application computer systems.

63 CYBERNETICS **2152**

Includes feedback and control theory, artificial intelligence, robotics and expert systems.

For related information see also *54 Man/System Technology and Life Support.*

64 NUMERICAL ANALYSIS **2159**

Includes iteration, difference equations, and numerical approximation.

65 STATISTICS AND PROBABILITY **2163**

Includes data sampling and smoothing; Monte Carlo method; and stochastic processes.

66 SYSTEMS ANALYSIS **2163**

Includes mathematical modeling; network analysis; and operations research.

67 THEORETICAL MATHEMATICS **2163**

Includes topology and number theory.

PHYSICS

Includes physics (general); acoustics; atomic and molecular physics; nuclear and high-energy physics; optics; plasma physics; solid-state physics; and thermodynamics and statistical physics.

For related information see also *Engineering.*

70 PHYSICS (GENERAL) **2163**

For precision time and time interval (PTTI) see *35 Instrumentation and Photography;* for geophysics, astrophysics or solar physics see *46 Geophysics, 90 Astrophysics,* or *92 Solar Physics.*

71 ACOUSTICS 2163

Includes sound generation, transmission, and attenuation.

For noise pollution see *45 Environment Pollution.*

72 ATOMIC AND MOLECULAR PHYSICS 2165

Includes atomic structure, electron properties, and molecular spectra.

73 NUCLEAR AND HIGH-ENERGY PHYSICS 2166

Includes elementary and nuclear particles; and reactor theory.

For space radiation see *93 Space Radiation.*

74 OPTICS 2167

Includes light phenomena and optical devices.

For lasers see *36 Lasers and Masers.*

75 PLASMA PHYSICS 2167

Includes magnetohydrodynamics and plasma fusion.

For ionospheric plasmas see *46 Geophysics.* For space plasmas see *90 Astrophysics.*

76 SOLID-STATE PHYSICS 2170

Includes superconductivity.

For related information see also *33 Electronics and Electrical Engineering* and *36 Lasers and Masers.*

77 THERMODYNAMICS AND STATISTICAL PHYSICS 2174

Includes quantum mechanics; theoretical physics; and Bose and Fermi statistics.

For related information see also *25 Inorganic and Physical Chemistry* and *34 Fluid Mechanics and Heat Transfer.*

SOCIAL SCIENCES

Includes social sciences (general); administration and management; documentation and information science; economics and cost analysis; law, political science, and space policy; and urban technology and transportation.

80 SOCIAL SCIENCES (GENERAL) N.A.

Includes educational matters.

81 ADMINISTRATION AND MANAGEMENT 2175

Includes management planning and research.

82 DOCUMENTATION AND INFORMATION SCIENCE 2175

Includes information management; information storage and retrieval technology; technical writing; graphic arts; and micrography.

For computer documentation see *61 Computer Programming and Software.*

83 ECONOMICS AND COST ANALYSIS N.A.

Includes cost effectiveness studies.

84 LAW, POLITICAL SCIENCE AND SPACE POLICY 2181

Includes NASA appropriation hearings; aviation law; space law and policy; international law; international cooperation; and patent policy.

85 URBAN TECHNOLOGY AND TRANSPORTATION N.A.

Includes applications of space technology to urban problems; technology transfer; technology assessment; and surface and mass transportation.

For related information see *03 Air Transportation and Safety, 16 Space Transportation,* and *44 Energy Production and Conversion.*

SPACE SCIENCES

Includes space sciences (general); astronomy; astrophysics; lunar and planetary exploration; solar physics; and space radiation.

For related information see also *Geosciences.*

88 SPACE SCIENCES (GENERAL) 2181

89 ASTRONOMY 2181

Includes radio, gamma-ray, and infrared astronomy; and astrometry.

90 ASTROPHYSICS 2185

Includes cosmology; celestial mechanics; space plasmas; and interstellar and interplanetary gases and dust.

For related information see also *75 Plasma Physics.*

91 LUNAR AND PLANETARY EXPLORATION 2191

Includes planetology; and manned and unmanned flights.

For spacecraft design or space stations see *18 Spacecraft Design, Testing and Performance.*

92 SOLAR PHYSICS 2193

Includes solar activity, solar flares, solar radiation and sunspots.

For related information see *93 Space Radiation.*

93 SPACE RADIATION 2193

Includes cosmic radiation; and inner and outer earth's radiation belts.

For biological effects of radiation see *52 Aerospace Medicine.* For theory see *73 Nuclear and High-Energy Physics.*

GENERAL

Includes aeronautical, astronautical, and space science related histories, biographies, and pertinent reports too broad for categorization; histories or broad overviews of NASA programs.

99 GENERAL 2194

Note: N.A. means that no abstracts were assigned to this category for this issue.

SUBJECT INDEX **I-1**
PERSONAL AUTHOR INDEX **I-55**
CORPORATE SOURCE INDEX **I-61**
CONTRACT NUMBER INDEX **I-71**
REPORT/ACCESSION NUMBER INDEX .. **I-73**
APPENDIX—ABOUT STAR **A-1**

TYPICAL CITATION AND ABSTRACT

NASA SPONSORED
ON MICROFICHE

ACCESSION NUMBER → **N90-10004*#** Sverdrup Technology, Inc., Cleveland, OH. ← **CORPORATE SOURCE**
TITLE → **A SUPERSONIC THROUGH-FLOW FAN ENGINE AIRFRAME INTEGRATION STUDY Final Report**
AUTHOR → Paul J. Barnhart Sep. 1989 11 p Presented at the Aircraft Design, Systems and Operations Conference, Seattle, WA, 31 Jul. - 2 Aug. ← **PUBLICATION DATE**
1989; cosponsored by AIAA, AHS, and ASEE
CONTRACT OR GRANT → (Contract NAS3-25266)
REPORT NUMBERS → (NASA-CR-185140; E-5068; NAS 1.26:185140; AIAA-89-2140)
AVAILABILITY SOURCE → Avail: NTIS HC A03/MF A01 CSCL 01A ← **COSATI CODE**
PRICE CODE

Engine airframe integration effects are investigated for superonsic through-flow fan engines installed on a Mach 3.20 supersonic cruise vehicle. Six different supersonic through-flow fan engine installations covering the effects of engine size, nacelle contour, nacelle placement, and approximate bypass plume effects are presented. The different supersonic through-flow fan installations are compared with a conventional turbine bypass engine configuration on the same basic airframe. The supersonic through-flow fan engine integrations are shown to be comparable to the turbine bypass engine configuration on the basis of installed nacelle wave drag. The supersonic through-flow fan engine airframe integrated vehicles have superior aerodynamic performance on the basis of maximum lift-to-drag ratio than the turbine bypass engine installation over the entire operating Mach number range from 1.10 to 3.20. When approximate bypass plume modeling is included, the supersonic through-flow fan engine configuration shows even larger improvements over the turbine bypass engine configuration. Author

VOLUME 28 NUMBER 15 / AUGUST 8, 1990

Scientific and Technical Aerospace Reports

A Semimonthly Publication of the National Aeronautics and Space Administration

01 AERONAUTICS (GENERAL)

N90-21722* National Aeronautics and Space Administration, Washington, DC.
AERONAUTICAL ENGINEERING: A CONTINUING BIBLIOGRAPHY WITH INDEXES (SUPPLEMENT 250)
Dec. 1988 123 p
(NASA-SP-7037(250); NAS 1.21:7037(250)) Avail: NTIS HC A06; NTIS standing order as PB89-914100, $11.50 domestic, $23.00 foreign CSCL 01B

This bibliography lists 420 reports, articles, and other documents introduced into the NASA scientific and technical information system in February, 1990. Subject coverage includes: design, construction and testing of aircraft and aircraft engines; aircraft components, equipment and systems; ground support systems; and theoretical and applied aspects of aerodynamics and general fluid dynamics. Author

N90-21723*# National Aeronautics and Space Administration. Lewis Research Center, Cleveland, OH.
THE VIBRO-ACOUSTIC MAPPING OF LOW GRAVITY TRAJECTORIES ON A LEARJET AIRCRAFT
C. M. Grodsinsky and T. J. Sutliff May 1990 16 p Presented at the 2nd Workshop on Microgravity Experimentation, Ottawa, Ontario, 8-9 May 1990; sponsored by National Research Council of Canada
(NASA-TM-103103; E-5427; NAS 1.15:103103) Avail: NTIS HC A03/MF A01 CSCL 01B

Terrestrial low gravity research techniques have been employed to gain a more thorough understanding of basic science and technology concepts. One technique frequently used involves flying parabolic trajectories aboard the NASA Lewis Research Center Learjet aircraft. A measurement program was developed to support an isolation system conceptual design. This program primarily was intended to measure time correlated high frequency accelerations (up to 100 Hz) present at various locations throughout the Learjet during a series of trajectories and flights. As suspected, the measurements obtained revealed that the environment aboard such an aircraft can not simply be described in terms of the static level low gravity g vector obtained, but that it also must account for both rigid body and high frequency vibro-acoustic dynamics. Author

N90-21724*# Purdue Univ., West Lafayette, IN.
WINCOF-I CODE FOR PREDICTION OF FAN COMPRESSOR UNIT WITH WATER INGESTION Interim Report
S. N. B. Murthy and A. Mullican Mar. 1990 88 p
(Contract NAG3-481; DTFA03-83-A-00328)
(NASA-CR-185157; NAS 1.26:185157; DOT/FAA/CT-TN89/63; M/NAFA/89-1) Avail: NTIS HC A05/MF A01 CSCL 01B

The PURDUE-WINCOF code, which provides a numerical method of obtaining the performance of a fan-compressor unit of a jet engine with water ingestion into the inlet, was modified to take into account: (1) the scoop factor, (2) the time required for the setting-in of a quasi-steady distribution of water, and (3) the heat and mass transfer processes over the time calculated under 2. The modified code, named WINCOF-I was utilized to obtain the performance of a fan-compressor unit of a generic jet engine. The results illustrate the manner in which quasi-equilibrium conditions become established in the machine and the redistribution of ingested water in various stages in the form of a film out of the casing wall, droplets across the span, and vapor due to mass transfer. Author

N90-21725*# National Aeronautics and Space Administration. Lewis Research Center, Cleveland, OH.
PERFORMANCE CHARACTERISTICS OF A ONE-THIRD-SCALE, VECTORABLE VENTRAL NOZZLE FOR SSTOVL AIRCRAFT
Barbara S. Esker and Jack G. McArdle 1990 12 p Proposed for presentation at the 26th Joint Propulsion Conference, Orlando, FL, 16-18 Jul. 1990; cosponsored by AIAA, ASME, SAE, and ASEE
(NASA-TM-103120; E-5448; NAS 1.15:103120; AIAA-90-2271) Avail: NTIS HC A03/MF A01 CSCL 01B

Several proposed configurations for supersonic short takeoff, vertical landing aircraft will require one or more ventral nozzles for lift and pitch control. The swivel nozzle is one possible ventral nozzle configuration. A swivel nozzle (approximately one-third scale) was built and tested on a generic model tailpipe. This nozzle was capable of vectoring the flow up to + or - 23 deg from the vertical position. Steady-state performance data were obtained at pressure ratios to 4.5, and pitot-pressure surveys of the nozzle exit plane were made. Two configurations were tested: the swivel nozzle with a square contour of the leading edge of the ventral duct inlet, and the same nozzle with a round leading edge contour. The swivel nozzle showed good performance overall, and the round-leading edge configuration showed an improvement in performance over the square-leading edge configuration. Author

02 AERODYNAMICS

Includes aerodynamics of bodies, combinations, wings, rotors, and control surfaces; and internal flow in ducts and turbomachinery.

For related information see also *34 Fluid Mechanics and Heat Transfer.*

N90-21726# National Aerospace Lab., Tokyo (Japan).
NUMERICAL SIMULATION OF HYPERSONIC FLOW AROUND A SPACE PLANE. PART 2: APPLICATION TO HIGH ANGLES OF ATTACK FLOW
Yukimitsu Yamamoto Feb. 1989 22 p
(NAL-TR-1011T; ISSN-0389-4010) Avail: NTIS HC A03/MF A01

A flux-split upwind TVD (Total Variation Diminishing) scheme was applied to the hypersonic flow around a space plane proposed by the National Aerospace Laboratory (NAL). Thin-layer Navier-Stokes equations in a finite volume formulation are solved by using an implicit approximately factored ADI (alternating direction implicit) algorithm. Numerical computations are performed for a Mach number of 7.0 and Reynolds number of 4.4 x 10(exp 6) at angles of attack up to 50 degrees. Numerical results are compared with experimental data obtained from the hypersonic wind tunnel tests at NAL. Through these comparisons, it is demonstrated that the present TVD Navier-Stokes code has excellent capabilities for evaluating total aerodynamic performance and investigating aerodynamic heating, and which are of great significance in the design of a space plane configuration. Author

N90-21727*# National Aeronautics and Space Administration. Lewis Research Center, Cleveland, OH.
SWEPT WING ICE ACCRETION MODELING
Mark G. Potapczuk and Colin S. Bidwell 1990 26 p Presented at the 28th Aerospace Sciences Meeting, Reno, NV, 8-11 Jan. 1990; sponsored by AIAA
(NASA-TM-103114; E-5238; NAS 1.15:103114; AIAA-90-0756)
Avail: NTIS HC A03/MF A01 CSCL 01A

An effort to develop a three-dimensional modeling method was initiated. This first step towards creation of a complete aircraft icing simulation code builds on previously developed methods for calculating three-dimensional flow fields and particle trajectories combined with a two-dimensional ice accretion calculation along coordinate locations corresponding to streamlines. This work is a demonstration of the types of calculations necessary to predict a three-dimensional ice accretion. Results of calculations using the 3-D method for a MS-317 swept wing geometry are projected onto a 2-D plane normal to the wing leading edge and compared to 2-D results for the same geometry. It is anticipated that many modifications will be made to this approach, however, this effort will lay the groundwork for future modeling efforts. Results indicate that the flow field over the surface and the particle trajectories differed for the two calculations. This led to lower collection efficiencies, convective heat transfer coefficients, freezing fractions, and ultimately ice accumulation for the 3-D calculation. Author

N90-21728 Council for National Academic Awards (England).
THE INTERACTION BETWEEN A PLANE SHOCK WAVE AND A CYLINDRICAL AFTERBODY Ph.D. Thesis
Guo-Chun Shen 1988 227 p
Avail: Univ. Microfilms Order No. BRDX86625

Shock wave cylinder interaction flows were studied at M = 2.5 for a range of shock strengths, lateral distances between shock generator and cylinder, and model nose length. Oil flow patterns, schlieren photographs, and model surface pressure distributions were obtained, and some tests were also made at M = 1.5. Topological laws and physical consistency criteria were applied to analyze the flow structure inferred from observation and a number of published flow structures analyzed and improved. Extension of relevant topological laws to deal with special features are proposed for the interpretation of the shock/cylinder interaction flowfield. In the light of this, a published interpretation of the surface flow patterns for a shock/cylinder interaction at M = 3.0 was critically examined and structures for both the surfaces and the external flow proposed. Also topologically and physically consistent surface flow patterns and external flow structures in cross flow planes were constructed at M = 2.5 and M = 1.5 together with a 3-D sketch of the entire flowfield. Dissert. Abstr.

N90-21729# National Oceanic and Atmospheric Administration, Silver Spring, MD. Air Resources Lab.
WIND TUNNEL INVESTIGATION OF THREE SONIC ANEMOMETERS
C. Bruce Baker, Robert E. Eskridge, Paul S. Conklin, and Kenneth R. Knoerr (Duke Univ., Durham, NC.) Oct. 1989 38 p
(PB90-149808; NOAA-TM-ERL-ARL-178) Avail: NTIS HC A03/MF A01 CSCL 01A

The flow distortion induced by three different sonic anemometer arrays was systematically studied in a wind tunnel. Blockage effects due to the probe arrays in the tunnel were negligible. The sonics were rotated through + or - 90 deg in the horizontal and + or - 15 deg in the vertical at three different speeds. It was found that the flow distortion parameterization must be done for the entire probe assembly and that a wind tunnel is necessary to provide the controlled condition necessary to obtain the shape of the response curve for each geometric configuration. The error in the horizontal components of the wind speed was found to be as much as 15 percent. The estimation of wind direction calculated from the horizontal components has an accuracy of 3 deg. Momentum flux measurements under convective conditions would be better measured with sonic arrays that have all three components in front of the support arm. Author

N90-21730 Georgia Inst. of Tech., Atlanta.
TOWARDS A UNIFIED ANALYSIS METHODOLOGY FOR COMPOSITE ROTOR BLADES Ph.D. Thesis
Ali Rana Atilgan 1989 342 p
Avail: Univ. Microfilms Order No. DA9005467

Two distinct analysis methodologies are presented for composite rotor blades. The first approach formulates a simple, analytical composite beam model in order to predict static and dynamic behavior. In this model, both cross-section and elastic analyses are developed analytically. Results can be obtained either in closed form or in only a few minutes on a personal computer. This approach is needed as a cause-effect relationship between configuration and response must be clearly understood and numerous preliminary design iterations may be required. The second theory is formulated for nonhomogeneous, anisotropic elastic beams with initial curvature and shear. The cross-sectional deformations are derived from three-dimensional elasticity by a perturbation procedure which generates a hierarchy of equations. In this methodology, a linear two-dimensional cross-section analysis whose results determine the constitutive law for a nonlinear one-dimensional elastic analysis is presented. A general mixed hybrid finite element variational principle to solve the one-dimensional elastica equations is formulated. This is an amenable approach and practical tool for detailed design analysis/optimization. This work aims to construct a unified structural technology for both preliminary design and detailed analysis of composite rotor blades. Validation of these approaches through tests on model configurations and comparison with the existing literature are given. Dissert. Abstr.

N90-21731 Georgia Inst. of Tech., Atlanta.
DEVELOPMENT AND APPLICATION OF A GENERALIZED DYNAMIC WAKE THEORY FOR LIFTING ROTORS Ph.D. Thesis
Chengjian He 1989 214 p
Avail: Univ. Microfilms Order No. DA9005480

Rotorcraft aeroelasticity and aeromechanics analysis requires a consistent mathematical model that has an appropriate combination of structural dynamics and unsteady aerodynamics. To provide rotorcraft dynamists with an efficient unsteady wake model, an intermediate level unsteady induced-flow theory suitable for rotorcraft aeroelastic stability, vibration control, and aeroelastic tailoring studies is being developed. The unsteady wake theory is developed for lifting rotors based on an acceleration potential for an actuator disk. The induced inflow at the rotor disk is expressed in terms of a Fourier series azimuthally and a polynomial distribution radially. A system of first-order, ordinary differential equations in the time domain, formulated from first principles, describes the flow. The pressure at the rotor disk is discretized at each motor blade to allow for the effect of finite number of blades. This formulation is well fitted to rotor aeroelastic analysis. The research has resulted in closed-form, analytical expressions for the induced-flow influence coefficients, one of the most critical parts in the development of the theory in forward flight. Encouragingly, the results show an overall good correlation with recent measurement data, both time-averaged and time-dependent, with the Army's Langley facility. The theory correctly predicts such essential characteristics as fore-to-aft induced-flow gradient, dissymmetric side-to-side induced-flow distribution in forward flight, and saw-tooth, triangular wave form of unsteady inflow associated with the passage of rotor blades. The theory also reveals the significant distance between the time-averaged induced flow at points fixed in space and instantaneous induced flow in the blade-fixed rotating system. Dissert. Abstr.

N90-21732 Virginia Polytechnic Inst. and State Univ., Blacksburg.

EFFECTIVE METHODS OF CONTROLLING A JUNCTION VORTEX SYSTEM IN AN INCOMPRESSIBLE, THREE-DIMENSIONAL, TURBULENT FLOW Ph.D. Thesis

Jaiwon Shin 1989 685 p

Avail: Univ. Microfilms Order No. DA9003609

An experimental investigation was conducted to find effective methods of controlling a junction vortex system around and in the wake of a NACA 0020 body with a 1.5:1 elliptical nose mounted normal to the flat surface. Control of the junction vortex system was investigated using more slender noses and leading edge fillets. The study includes surface flow visualizations, and extensive mean flow measurements. The mean flow measurements consist of velocity, total pressure, and static pressure distributions. The results of the mean flow measurements around and in the wake of a NACA 0020 body with a 1.5:1 elliptical nose show the presence of a large, dominant vortex, or a primary horseshoe vortex, in the junction between the body and the flat surface. A smaller, co-rotating vortex relative to the primary horseshoe vortex was observed at the 100 percent chord position, which is believed to be identified with the corner separation at the junction near the trailing edge. Mean flow measurements of the flow field around and in the wake of a NACA 0020 body with more slender noses were acquired. The results indicate that the more slender nose generated a weaker primary horseshoe vortex. The results also suggest that the weak primary horseshoe vortex developed by the more slender nose was dissipated alongside the body to the point where it had a very small effect on the flow field at the 100 percent chord position. The results of the mean flow measurements around and in the wake of a NACA 0020 body with a 1.5:1 elliptical nose with leading edge fillets indicate that the leading edge fillets were very effective in reducing the strength and size of the primary horseshoe vortex. The vorticity identified with the corner separation vortex was observed in the wake for both leading edge shape changes and fillets. The results show that the corner separation vortex dominates the flow in the wake due to the weak effects of the primary horseshoe vortex. Dissert. Abstr.

N90-21733*# National Aeronautics and Space Administration. Lewis Research Center, Cleveland, OH.

CONTROL OF FLOW SEPARATION AND MIXING BY AERODYNAMIC EXCITATION

Edward J. Rice and John M. Abbott 1990 13 p Proposed for presentation at the 17th Congress of the International Council of the Aeronautical Sciences, Stockholm, Sweden, 9-14 Sep. 1990; sponsored by AIAA

(NASA-TM-103131; E-5462; NAS 1.15:103131) Avail: NTIS HC A03/MF A01 CSCL 01A

The recent research in the control of shear flows using unsteady aerodynamic excitation conducted at the NASA Lewis Research Center is reviewed. The program is of a fundamental nature, concentrating on the physics of the unsteady aerodynamic processes. This field of research is a fairly new development with great promise in the areas of enhanced mixing and flow separation control. Enhanced mixing research includes influence of core turbulence, forced pairing of coherent structures, and saturation of mixing enhancement. Separation flow control studies included are for a two-dimensional diffuser, conical diffusers, and single airfoils. Ultimate applications include aircraft engine inlet flow control at high angle of attack, wide angle diffusers, highly loaded airfoils as in turbomachinery, and ejector/suppressor nozzles for the supersonic transport. An argument involving the Coanda Effect is made that all of the above mentioned application areas really only involve forms of shear layer mixing enhancement. The program also includes the development of practical excitation devices which might be used in aircraft applications. Author

N90-21734*# Pennsylvania State Univ., University Park. Dept. of Aerospace Engineering.

PREDICTION OF FORCES AND MOMENTS FOR FLIGHT VEHICLE CONTROL EFFECTORS. PART 1: VALIDATION OF METHODS FOR PREDICTING HYPERSONIC VEHICLE CONTROLS FORCES AND MOMENTS Final Report

Mark D. Maughmer, L. Ozoroski, T. Ozoroski, and D. Straussfogel May 1990 140 p

(Grant NAG1-849)

(NASA-CR-186571; NAS 1.26:186571) Avail: NTIS HC A07/MF A01 CSCL 01A

Many types of hypersonic aircraft configurations are currently being studied for feasibility of future development. Since the control of the hypersonic configurations throughout the speed range has a major impact on acceptable designs, it must be considered in the conceptual design stage. The ability of the aerodynamic analysis methods contained in an industry standard conceptual design system, APAS II, to estimate the forces and moments generated through control surface deflections from low subsonic to high hypersonic speeds is considered. Predicted control forces and moments generated by various control effectors are compared with previously published wind tunnel and flight test data for three configurations: the North American X-15, the Space Shuttle Orbiter, and a hypersonic research airplane concept. Qualitative summaries of the results are given for each longitudinal force and moment and each control derivative in the various speed ranges. Results show that all predictions of longitudinal stability and control derivatives are acceptable for use at the conceptual design stage. Results for most lateral/directional control derivatives are acceptable for conceptual design purposes; however, predictions at supersonic Mach numbers for the change in yawing moment due to aileron deflection and the change in rolling moment due to rudder deflection are found to be unacceptable. Including shielding effects in the analysis is shown to have little effect on lift and pitching moment predictions while improving drag predictions. Author

N90-21735*# Pennsylvania State Univ., University Park. Dept. of Aerospace Engineering.

PREDICTION OF FORCES AND MOMENTS FOR FLIGHT VEHICLE CONTROL EFFECTORS. PART 2: AN ANALYSIS OF DELTA WING AERODYNAMIC CONTROL EFFECTIVENESS IN GROUND EFFECT Final Report

Mark D. Maughmer, L. Ozoroski, T. Ozoroski, and D. Straussfogel May 1990 116 p

(Grant NAG1-849)

(NASA-CR-186572; NAS 1.26:186572) Avail: NTIS HC A06/MF A01 CSCL 01A

Many types of hypersonic aircraft configurations are currently being studied for feasibility of future development. Since the control of the hypersonic configurations throughout the speed range has a major impact on acceptable designs, it must be considered in the conceptual design stage. Here, an investigation of the aerodynamic control effectiveness of highly swept delta planforms operating in ground effect is presented. A vortex-lattice computer program incorporating a free wake is developed as a tool to calculate aerodynamic stability and control derivatives. Data generated using this program are compared to experimental data and to data from other vortex-lattice programs. Results show that an elevon deflection produces greater increments in C sub L and C sub M in ground effect than the same deflection produces out of ground effect and that the free wake is indeed necessary for good predictions near the ground. Author

N90-21736*# Eloret Corp., Sunnyvale, CA.

MODELING OF VORTEX-INDUCED OSCILLATIONS BASED ON INDICIAL RESPONSE APPROACH Final Technical Report, 1 May 1989 - 30 Apr. 1990

Khiem Van Truong 15 May 1990 32 p

(Contract NCC2-634)

(NASA-CR-186560; NAS 1.26:186560) Avail: NTIS HC A03/MF A01 CSCL 01A

The indicial response approach, a modeling approach originally used for studying nonlinear problems in flight dynamics is applied to the study of vortex-induced oscillations phenomena. The indicial response of the velocity field is derived for the problem studied with emphasis on physical postulates involved. A full account of fluid dynamics effects is taken by considering the incompressible Navier-Stokes equations. The theory is applied to the particular case of flow past a cylinder in periodically forced motion to derive some salient features. The indicial response approach is shown to be equivalent to a currently popular approach based on the use of the amplitude equation. Jump and hysteresis phenomena that experiments indicate occur within the lock-in regime (where the velocity field oscillates at the forcing frequency) are captured by the approach. Author

N90-21737# Sandia National Labs., Albuquerque, NM.
SLOTTED-WALL RESEARCH WITH DISK AND PARACHUTE MODELS IN A LOW-SPEED WIND TUNNEL
J. M. Macha, R. J. Buffington, J. F. Henfling, D. VanEvery, and J. L. Harris (DSMA International, Inc., Mississauga, Ontario) 1990 20 p Presented at the 16th AIAA Aerodynamic Ground Testng Conference, Seattle, WA, 18-20 Jun. 1990
(Contract DE-AC04-76DP-00789)
(DE90-002989; SAND-89-2666C; CONF-900672-1) Avail: NTIS HC A03/MF A01

An experimental investigation of slotted-wall blockage interference was conducted using disk and parachute models in a low speed wind tunnel. Test section open area ratio, model geometric blockage ratio, and model location along the length of the test section were systematically varied. Resulting drag coefficients were compared to each other and to interference-free measurements obtained in a much larger wind tunnel where the geometric blockage ratio was less than 0.0025. DOE

N90-21738*# Johnson Aeronautics, Palo Alto, CA.
AIRLOADS, WAKES, AND AEROELASTICITY
Wayne Johnson Apr. 1990 54 p Presented at AGARD Special Course on Aerodynamics of Rotorcraft, Brussels, Belgium, 2-5 Apr. 1990; Ankara, Turkey, 9-11 Apr. 1990; and Moffett Field, CA, 14-17 May 1990 Sponsored by Army Aviation Systems Command, Saint Louis, MO
(Contract NAS2-11555)
(NASA-CR-177551; A-90165; NAS 1.26:177551; USAAVSCOM-TM-90-A-005) Avail: NTIS HC A04/MF A01 CSCL 01A

Fundamental considerations regarding the theory of modeling of rotary wing airloads, wakes, and aeroelasticity are presented. The topics covered are: airloads and wakes, including lifting-line theory, wake models and nonuniform inflow, free wake geometry, and blade-vortex interaction; aerodynamic and wake models for aeroelasticity, including two-dimensional unsteady aerodynamics and dynamic inflow; and airloads and structural dynamics, including comprehensive airload prediction programs. Results of calculations and correlations are presented. Author

N90-21739*# National Aeronautics and Space Administration. Ames Research Center, Moffett Field, CA.
EXTENSION OF A STREAMWISE UPWIND ALGORITHM TO A MOVING GRID SYSTEM
Shigeru Obayashi (MCAT Inst., San Jose, CA.), Peter M. Goorjian, and Guru P. Guruswamy Apr. 1990 22 p
(NASA-TM-102800; A-90101; NAS 1.15:102800) Avail: NTIS HC A03/MF A01 CSCL 01A

A new streamwise upwind algorithm was derived to compute unsteady flow fields with the use of a moving-grid system. The temporally nonconservative LU-ADI (lower-upper-factored, alternating-direction-implicit) method was applied for time marching computations. A comparison of the temporally nonconservative method with a time-conservative implicit upwind method indicates that the solutions are insensitive to the conservative properties of the implicit solvers when practical time steps are used. Using this new method, computations were made for an oscillating wing at a transonic Mach number. The computed results confirm that the present upwind scheme captures the shock motion better than the central-difference scheme based on the beam-warming algorithm. The new upwind option of the code allows larger time-steps and thus is more efficient, even though it requires slightly more computational time per time step than the central-difference option. Author

N90-21740# Technische Univ., Delft (Netherlands). Faculty of Aerospace Engineering.
A COMPUTER PROGRAM FOR THE PREDICTION OF NOZZLE-PROPELLER PERFORMANCE
Ivan S. Gibson Feb. 1989 60 p
(LR-578; ETN-90-96342) Avail: NTIS HC A04/MF A01

A programmers guide and users manual for a FORTRAN program called IDUK are presented. The program allows for the calculation of the hydrodynamic performance of single and multi-element nozzles with either fixed or controllable pitch marine propellers of known geometry. Each program input option is fully described. The corresponding computer output is presented and examined. A listing of the program and all subroutines is presented. ESA

N90-21741# Technische Univ., Delft (Netherlands). Faculty of Aerospace Engineering.
THEORY AND NUMERICAL ANALYSIS OF SINGLE AND MULTI-ELEMENT NOZZLE PROPELLERS
Ivan S. Gibson Feb. 1989 67 p
(LR-579; ETN-90-96343) Avail: NTIS HC A04/MF A01

Theoretical and numerical analysis methods developed to predict the operating performance of nozzle or ducted propellers in axisymmetric flow are described. Surface vorticity techniques are used to model the nozzle and hub. A lifting line theory for both three dimensional and finite blade effects is described. Radial variation of axial inflow velocity are accommodated for in the theory, to allow for systematic calculations of device performance in the wakefield behind a ship's after body. Recommendations for further study are presented. ESA

N90-21742# Technische Univ., Delft (Netherlands). Faculty of Aerospace Engineering.
RECENT IMPROVEMENTS IN THE SCOPE AND ACCURACY OF THE PERFORMANCE PREDICTION OF NOZZLE PROPELLERS
Ivan S. Gibson Jul. 1989 38 p
(LR-598; ETN-90-96353) Avail: NTIS HC A03/MF A01

Updated theoretical analysis developed to predict the operating performance of a nozzle or ducted propeller in axisymmetric flow is presented. Improvements in the calculation of the cavitation number at the propeller blade sections are described. Research results on which future development of the theoretical model might be built are discussed. The sequence that must be followed in order to achieve successful nozzle-propeller configuration design is outlined. A one-shot method which helps to avoid adverse boundary layer separation effects on the nozzle thrust is described. ESA

N90-21743# Technische Univ., Delft (Netherlands). Faculty of Aerospace Engineering.
ON THE DIRECT SIMULATION OF VORTEX SHEDDING
C. W. M. vanderGeld Feb. 1989 136 p Prepared in cooperation with Prins Maurits Lab. TNO, Rijswijk, Netherlands
(LR-513; PML-1987-C17; SFCC-Publ-40; ETN-90-96375) Avail: NTIS HC A07/MF A01

The simulation of vortex shedding in Solid Fuel Combustion Chambers (SFCCs) is described. For the simulation of time dependent two-dimensional flow across solid boundaries, a simple model with discrete vortices is found to be efficient and realistic. Away from solid boundaries, flow field computations are shown to be accurate. Close to the boundaries, vortices are initiated at so-called creation points. The set-up of these creation points is closely examined. The incorportion of diffusion of individual vortex blobs due to viscosity is used to make the flow simulation more realistic. ESA

N90-21744*# National Aeronautics and Space Administration. Langley Research Center, Hampton, VA.
THREE-DIMENSIONAL SIMULATION OF VORTEX BREAKDOWN
G. Kuruvila and M. D. Salas Jun. 1990 75 p
(NASA-TM-102664; NAS 1.15:102664) Avail: NTIS HC A04/MF A01 CSCL 01A

The integral form of the complete, unsteady, compressible, three-dimensional Navier-Stokes equations in the conservation form, cast in generalized coordinate system, are solved, numerically, to simulate the vortex breakdown phenomenon. The inviscid fluxes are discretized using Roe's upwind-biased flux-difference splitting scheme and the viscous fluxes are discretized using central differencing. Time integration is performed using a backward Euler ADI (alternating direction implicit) scheme. A full approximation multigrid is used to accelerate the convergence to steady state. Author

N90-21745*# Analytical Services and Materials, Inc., Hampton, VA.
A MULTIBLOCK/MULTIZONE CODE (PAB 3D-v2) FOR THE THREE-DIMENSIONAL NAVIER-STOKES EQUATIONS: PRELIMINARY APPLICATIONS Final Report
Khaled S. Abdol-Hamid May 1990 48 p
(Contract NAS1-18599)
(NASA-CR-182032; NAS 1.26:182032) Avail: NTIS HC A03/MF A01 CSCL 01A

The development and applications of multiblock/multizone and adaptive grid methodologies for solving the three-dimensional simplified Navier-Stokes equations are described. Adaptive grid and multiblock/multizone approaches are introduced and applied to external and internal flow problems. These new implementations increase the capabilities and flexibility of the PAB3D code in solving flow problems associated with complex geometry. Author

N90-21746*# National Aeronautics and Space Administration. Ames Research Center, Moffett Field, CA.
ANALYTICAL STUDY OF THE ORIGIN AND BEHAVIOR OF ASYMMETRIC VORTICES
Murray Tobak, David Degani (Technion - Israel Inst. of Tech., Haifa.), and Gregory G. Zilliac Apr. 1990 19 p
(NASA-TM-102796; A-90089; NAS 1.15:102796) Avail: NTIS HC A03/MF A01 CSCL 01A

An hypothesis advanced originally to explain computational observations is supported by theoretical considerations: The asymmetric mean flow observed on bodies of revolution at moderate to high angles of attack is the result of a convective instability of an originally symmetric flow to a time-invariant space-fixed disturbance. Additionally, the time-dependent fluctuations characteristic of the flow at higher angles of attack (up to 90 deg) are the result of an absolute instability of an originally steady flow to a small temporal disturbance of finite duration. Within a common domain, the instability mechanisms may coexist. The experimentally confirmed existence of bistable states, wherein the side-force variation with nose roll angle approaches a square-wave distribution, is attributed to the dominant influence of a pair of trailing vortices from the ogival forebody. Their existence is made possible by the appearance of foci of separation in the skin-friction line pattern beyond a critical angle of attack. The extreme sensitivity of the asymmetric flow orientation to nose geometry, demonstrated experimentally, is attributed to the presence of an indeterminate phase in the family of possible solutions for the three-dimensional wave system. Author

N90-21980# Aerospatiale, Chatillon (France). Tactical Missiles Div.
GEOMETRY AND GRIDS OF COMPLEX CONFIGURATIONS FOR AERODYNAMIC CALCULATION [GEOMETRIE ET MAILLAGE DE CONFIGURATIONS COMPLEXES POUR LES CALCULS AERODYNAMIQUES]
Gilbert Ranoux, Jerome Lordon, and Jean Diet *In* AGARD, Applications of Mesh Generation to Complex 3-D Configurations Mar. 1990 16 p In FRENCH; ENGLISH summary (For primary document see N90-21975 15-34)
Copyright Avail: NTIS HC A14/MF A02; Non-NATO Nationals requests available only from AGARD/Scientific Publications Executive

N90-21982# Mississippi State Univ., Mississippi State. Dept. of Aerospace Engineering.
UNSTEADY EULER SOLUTIONS ON DYNAMIC BLOCKED GRIDS FOR COMPLEX CONFIGURATIONS
David L. Whitfield, J. Mark Janus, and Abdollah Arabshahi *In* AGARD, Applications of Mesh Generation to Complex 3-D Configurations Mar. 1990 13 p (For primary document see N90-21975 15-34)
Copyright Avail: NTIS HC A14/MF A02; Non-NATO Nationals requests available only from AGARD/Scientific Publications Executive

N90-21985# Messerschmitt-Boelkow-Blohm G.m.b.H., Munich (Germany, F.R.). Military Aircraft Div.
GRID PATCHING APPROACHES FOR COMPLEX THREE-DIMENSIONAL CONFIGURATIONS
W. Schwarz, G. Hartmann, and M. A. Schmatz *In* AGARD, Applications of Mesh Generation to Complex 3-D Configurations Mar. 1990 14 p (For primary document see N90-21975 15-34)
Copyright Avail: NTIS HC A14/MF A02; Non-NATO Nationals requests available only from AGARD/Scientific Publications Executive

N90-21996*# National Aeronautics and Space Administration. Ames Research Center, Moffett Field, CA.
APPLICATION OF THE TRANAIR RECTANGULAR GRID APPROACH TO THE AERODYNAMIC ANALYSIS OF COMPLEX CONFIGURATIONS
Forrester T. Johnson, Satish S. Samant, Michael B. Bieterman, Robin G. Melvin, David P. Young, John E. Bussoletti (Boeing Advanced Systems Co., Seattle, WA.), and Mike D. Madson *In* AGARD, Applications of Mesh Generation to Complex 3-D Configurations Mar. 1990 12 p Sponsored in part by Boeing Co. (For primary document see N90-21975 15-34)
(Contract NAS2-12513)
Copyright Avail: NTIS HC A14/MF A02; Non-NATO Nationals requests available only from AGARD/Scientific Publications Executive CSCL 20D

03 AIR TRANSPORTATION AND SAFETY

Includes passenger and cargo air transport operations; and aircraft accidents.

For related information see also *16 Space Transportation* and *85 Urban Technology and Transportation.*

N90-21747*# Rice Univ., Houston, TX. Aero-Astronautics Group.
OPTIMIZATION AND GUIDANCE OF FLIGHT TRAJECTORIES IN THE PRESENCE OF WINDSHEAR Final Report, 1984 - 1989
A. Miele 1989 73 p Sponsored by Boeing Commercial Airplane Co. and Air Line Pilots Association
(Grant NAG1-516)
(NASA-CR-186163; NAS 1.26:186163; AAR-244) Avail: NTIS HC A04/MF A01 CSCL 01C

Research on the optimization and guidance of flight trajectories in the presence of windshear performed in the period 1984 to 1989 is discussed. The research concerns windshear recovery systems and covers two major areas of investigation: optimal trajectories for takeoff, abort landing, and penetration landing; and guidance schemes for takeoff, abort landing, and penetration landing. Author

N90-21748# National Transportation Safety Board, Washington, DC.

AIRCRAFT ACCIDENT REPORT, UNITED AIRLINES FLIGHT 811, BOEING 747-122, N4713U, HONOLULU, HAWAII, FEBRUARY 24, 1989

16 Apr. 1990 75 p
(PB90-910401; NTSB/AAR-90/01) Avail: NTIS HC A04/MF A01 CSCL 01C

Factual information related to the sudden opening of an improperly latched cargo door in flight on United Airlines flight 811 near Honolulu, Hawaii, on 24 Feb. 1989 are presented. The safety issues discussed include the design and certification of the Boeing 747 cargo doors; the operation and maintenance of the cargo doors; portable emergency oxygen bottles; storage compartments over emergency exit doors; flight attendant communications during an emergency; life preservers; and aircraft rescue and firefighting. Recommendations addressing these issues were made to the Federal Aviation Administration, the State of Hawaii, and the U.S. Department of Defense. Author

04 AIRCRAFT COMMUNICATIONS AND NAVIGATION

Includes digital and voice communication with aircraft; air navigation systems (satellite and ground based); and air traffic control.

For related information see also *17 Space Communications, Spacecraft Communications, Command and Tracking* and *Communications and Radar*.

N90-21749# Minority Services, Inc., Washington, DC.

MICROWAVE LANDING SYSTEM (MLS) REMOTE MONITORING SUBSYSTEM/REMOTE MAINTENANCE MONITORING SYSTEM Interface Control Report

Alex E. Smith and Susan H. Houston (Lisan Corp., Washington, DC.) Jun. 1989 82 p Sponsored by FAA, Washington, DC
(DOT/FAA/PS-89/2) Avail: NTIS HC A05/MF A01

This interface control report standardizes the communications protocol between the Remote Maintenance Monitoring System of the National Airspace System and microwave landing systems of different design. The interface requirements include the electrical, mechanical, data link control, and application level interface requirements between the microwave landing system and the Remote Maintenance Monitoring System. Communications functions specified include the establishment and termination of transmissions, and the structure, format, and encoding of messages and commands for transmission. Additionally the logical unit and datapoint addresses are defined for all microwave landing system monitored parameters and status parameters. Author

N90-21750# Minority Services, Inc., Washington, DC.

MICROWAVE LANDING SYSTEM (MLS) MULTIPLE SYSTEM DESIGN INTEROPERABILITY INTERFACE CONTROL REPORT Final Report

John E. Kacur Jun. 1989 28 p Sponsored by Federal Aviation Administration, Washington, DC
(DOT/FAA/SA-89/2) Avail: NTIS HC A03/MF A01

The communications interface between two Microwave Landing Systems one each installed at opposite runway ends and which are each of a different design/manufacture is standardized. The interface requirements include the physical, data link control and application level requirements and are established to promote the interoperability of the systems. Functions specified include the establishment and termination of transmissions, and the structure, format, and encoding of messages and commands for transmission. The logical units and datapoints for all Microwave Landing System monitored parameters and status parameters are addressed. Additionally, a synchronization function is established to provide a timing reference to assure interference free transmission of the signals-in-space from each of the two MLSs. The operation, encoding and format of the synchronization function is provided. Author

N90-21751# Technische Univ., Delft (Netherlands). Dept. of Aerospace Engineering.

FIRST-ORDER WEIGHT CORRECTIONS FOR REAL-TIME FLIGHT PATH MANAGEMENT

H. G. Visser Feb. 1989 35 p
(LR-580; ETN-90-96344) Avail: NTIS HC A03/MF A01

The usefulness of singular perturbation methods in developing real time automatic flight trajectory synthesis algorithms is investigated. Using the minimum principle of optimal control theory, approximate feedback type solutions are developed. It is concluded that the approximations are not practical for onboard applications in commercial jet transports. Singular perturbation analysis does provide valuable insight into the solution behavior, which may eventually help in the development of simplified algorithms. Numerical experiments are suggested to validate the concept and serve as a basis for quantitative comparison. ESA

N90-21752# Technische Univ., Delft (Netherlands). Faculty of Aerospace Engineering.

AN APPROACH TO ON-BOARD OPTIMIZATION OF CRUISE AT CONSTANT ALTITUDE

H. G. Visser Dec. 1989 52 p
(LR-581; ETN-90-96345) Avail: NTIS HC A04/MF A01

The derivation and evaluation of an automatic flight trajectory synthesis algorithm is described. The algorithm can generate both time-free and time-fixed fuel-optimal cruise trajectories. The algorithm is based on a regularly perturbed optimal control formulation of cruise at constant altitude. Complicating effects such as winds aloft, off nominal ambient temperatures and engine losses are embedded in the dynamic model using a regular perturbation approach. It is shown that by including the weight dynamics in the system formulation, the performance of the algorithm is improved. ESA

N90-22232*# Georgia Inst. of Tech., Atlanta.

PASSIVE NAVIGATION USING IMAGE IRRADIANCE TRACKING

P. K. A. Menon (National Aeronautics and Space Administration. Ames Research Center, Moffett Field, CA.) *In* NASA, Ames Research Center, Vision Science and Technology at NASA: Results of a Workshop Feb. 1990 p 38 (For primary document see N90-22216 15-54)
(Grant NAG2-463)
Avail: NTIS HC A04/MF A01 CSCL 17G

N90-22238*# National Aeronautics and Space Administration. Ames Research Center, Moffett Field, CA.

KALMAN FILTER BASED RANGE ESTIMATION FOR AUTONOMOUS NAVIGATION USING IMAGING SENSORS

Banavar Sridhar *In its* Vision Science and Technology at NASA: Results of a Workshop Feb. 1990 p 47-48 (For primary document see N90-22216 15-54)
Avail: NTIS HC A04/MF A01 CSCL 17G

05 AIRCRAFT DESIGN, TESTING AND PERFORMANCE

Includes aircraft simulation technology.

For related information see also *18 Spacecraft Design, Testing and Performance* and *39 Structural Mechanics.*For land transportation vehicles see *85 Urban Technology and Transportation.*

N90-21753*# Georgia Inst. of Tech., Atlanta. School of Aerospace Engineering.

A COMPARISON OF TIME-OPTIMAL INTERCEPTION TRAJECTORIES FOR THE F-8 AND F-15 Final Technical Report

Anthony J. Calise and James B. Pettengill Jan. 1990 30 p
(Contract NCC2-506)
(NASA-CR-186300; NAS 1.26:186300) Avail: NTIS HC A03/MF A01 CSCL 01C

The simulation results of a real time control algorithm for onboard computation of time-optimal intercept trajectories for the F-8 and F-15 aircraft are given. Due to the inherent aerodynamic and propulsion differences in the aircraft, there are major differences in their optimal trajectories. The significant difference in the two aircrafts are their flight envelopes. The F-8's optimal cruise velocity is thrust limited, while the F-15's optimal cruise velocity is at the intersection of the Mach and dynamic pressure constraint boundaries. This inherent difference necessitated the development of a proportional thrust controller for use as the F-15 approaches it's optimal cruise energy. Documented here is the application of singular perturbation theory to the trajectory optimization problem, along with a summary of the control algorithms. Numerical results for the two aircraft are compared to illustrate the performance of the minimum time algorithm, and to compute the resulting flight paths. Author

N90-21754*# George Washington Univ., Washington, DC. Science Communication Studies.
PUBLICATIONS OF THE NASA CONTROLLED ECOLOGICAL LIFE SUPPORT SYSTEM (CELSS) PROGRAM, 1979-1989
Janice S. Wallace and Janet V. Powers Washington NASA May 1990 68 p
(Contract NASw-4324)
(NASA-CR-4297; NAS 1.26:4297) Avail: NTIS HC A04/MF A01 CSCL 01C

Publications of research sponsored by the NASA Controlled Ecological Life Support System (CELSS) Program from 1979 to 1989 are listed. The CELSS Program encompasses research and technology with the goal of developing an autonomous bioregenerative life support system that continually recycles the solid, liquid, and gaseous materials essential for human life. The bibliography is divided into four major subject areas: food production, nutritional requirements, waste management, and systems management and control. Author

N90-21755*# North American Aircraft Operations, Los Angeles, CA.
CONCEPTUAL DESIGN OPTIMIZATION STUDY Final Report, Aug. 1987 - Nov. 1988
S. J. Hollowell, E. R. Beeman, II, and R. M. Hiyama Washington NASA May 1990 118 p
(Contract NAS1-18015)
(NASA-CR-4298; NAS 1.26:4298; NA-88-1877) Avail: NTIS HC A06/MF A01 CSCL 01C

The feasibility of applying multilevel functional decomposition and optimization techniques to conceptual design of advanced fighter aircraft was investigated. Applying the functional decomposition techniques to the conceptual design phase appears to be feasible. The initial implementation of the modified design process will optimize wing design variables. A hybrid approach, combining functional decomposition techniques for generation of aerodynamic and mass properties linear sensitivity derivatives with existing techniques for sizing mission performance and optimization, is proposed. Author

N90-21756*# National Aeronautics and Space Administration. Ames Research Center, Moffett Field, CA.
IDENTIFICATION OF XV-15 AEROELASTIC MODES USING FREQUENCY-DOMAIN METHODS
Cecil W. Acree, Jr. and Mark B. Tischler Feb. 1989 28 p Previously announced in IAA as A89-41092 Prepared in cooperation with Army Aviation Research and Development Command, Moffett Field, CA
(NASA-TM-101021; A-88268; NAS 1.15:101021; USAAVSCOM-CP-89-A-001) Avail: NTIS HC A03/MF A01 CSCL 01C

The XV-15 Tilt-Rotor wing has six major aeroelastic modes that are close in frequency. To precisely excite individual modes during flight test, dual flaperon exciters with automatic frequency-sweep controls were installed. The resulting structural data were analyzed in the frequency domain (Fourier transformed) with cross spectral and transfer function methods. Modal frequencies and damping were determined by performing curve fits to transfer function magnitude and phase data and to cross spectral magnitude data. Results are given for the XV-15 with its original metal rotor blades. Frequency and damping values are also compared with earlier predictions. Author

N90-21757*# National Aeronautics and Space Administration. Ames Research Center, Moffett Field, CA.
AN UPWIND-DIFFERENCING SCHEME FOR THE INCOMPRESSIBLE NAVIER-STOKES EQUATIONS
Stuart E. Rogers (Sterling Software, Palo Alto, CA.) and Dochan Kwak Nov. 1988 31 p
(NASA-TM-101051; A-89002; NAS 1.15:101051) Avail: NTIS HC A03/MF A01 CSCL 01C

The steady state incompressible Navier-Stokes equations in 2-D are solved numerically using the artificial compressibility formulation. The convective terms are upwind-differenced using a flux difference split approach that has uniformly high accuracy throughout the interior grid points. The viscous fluxes are differenced using second order accurate central differences. The numerical system of equations is solved using an implicit line relaxation scheme. Although the current study is limited to steady state problems, it is shown that this entire formulation can be used for solving unsteady problems. Characteristic boundary conditions are formulated and used in the solution procedure. The overall scheme is capable of being run at extremely large pseudotime steps, leading to fast convergence. Three test cases are presented to demonstrate the accuracy and robustness of the code. These are the flow in a square-driven cavity, flow over a backward facing step, and flow around a 2-D circular cylinder. Author

N90-21758*# National Aeronautics and Space Administration. Ames Research Center, Moffett Field, CA.
QUIET MODE FOR NONLINEAR ROTOR MODELS
R. E. McFarland Apr. 1990 38 p
(NASA-TM-102236; A-89247; NAS 1.15:102236) Avail: NTIS HC A03/MF A01 CSCL 01C

High frequency harmonics are generated by helicopter rotor systems, and nonlinear blade-element models of these systems create the same harmonics. In discrete real-time rotorcraft simulation, however, especially for handling qualities research, they are more of a nuisance than a benefit. The cycle times required to adequately represent them are rarely obtainable. The result is that distinct frequencies alias into the pilot and simulator bandwidths, thereby decreasing simulation fidelity. However, use of an interpolation procedure permits the observation of harmonics at their proper frequency locations, and an accompanying notch filter may then be used to attenuate the harmonics prior to decimation. Rotorcraft simulations using these techniques are not contaminated with the spurious frequencies that create variable trim points, produce erroneous stability and control derivative data, and obscure time histories. Author

N90-21984# National Aerospace Lab., Amsterdam (Netherlands).
DESIGN AND TESTING OF A MULTIBLOCK GRID-GENERATION PROCEDURE FOR AIRCRAFT DESIGN AND RESEARCH
J. W. Boerstoel, J. M. J. W. Jacobs, A. Kassies, A. Amendola, R. Tognaccini, and P. L. Vitagliano (Aeritalia S.p.A., Pomigliano D'Arco, Italy) *In* AGARD, Applications of Mesh Generation to Complex 3-D Configurations Mar. 1990 16 p (For primary document see N90-21975 15-34)
Copyright Avail: NTIS HC A14/MF A02; Non-NATO Nationals requests available only from AGARD/Scientific Publications Executive

N90-21986# British Aerospace Public Ltd. Co., Hatfield (England). Airlines Div.
MULTIBLOCK TOPOLOGY SPECIFICATION AND GRID GENERATION FOR COMPLETE AIRCRAFT CONFIGURATIONS
Steve Allwright *In* AGARD, Applications of Mesh Generation to

Complex 3-D Configurations Mar. 1990 11 p (For primary document see N90-21975 15-34)
Copyright Avail: NTIS HC A14/MF A02; Non-NATO Nationals requests available only from AGARD/Scientific Publications Executive

06 AIRCRAFT INSTRUMENTATION

Includes cockpit and cabin display devices; and flight instruments.

For related information see also *19 Spacecraft Instrumentation* and *35 Instrumentation and Photography.*

N90-21759# Federal Aviation Administration, Atlantic City, NJ.
ENHANCED LOW LEVEL WIND SHEAR (LLWAS) 6-SENSOR IMPROVEMENT USER'S MANUAL FOR DATA PROCESSING OF FIELD DATA
Eric J. Hoover May 1990 30 p
(DOT/FAA/CT-TN90/8) Avail: NTIS HC A03/MF A01

The Low Level Wind Shear Alert System (LLWAS) data collection includes only those Fairchild/Weston 6 and N Sensor sites qualified to copy data to TK50 magnetic tape cartridges. The data is prescribed to be collected on a 90-day schedule for 6-Sensor airports, and a 60-day schedule for N-Sensor airports. The data is copied onto the TK50 cartridge and then mailed to FAATC, ANC-230, Atlantic City International Airport, Atlantic City, New Jersey. Information is provided for the processing of the LLWAS-recorded wind data at the Federal Aviation Administration Technical Center Data Analysis Facility. Author

07 AIRCRAFT PROPULSION AND POWER

Includes prime propulsion systems and systems components, e.g., gas turbine engines and compressors; and onboard auxilliary power plants for aircraft.

For related information see also *20 Spacecraft Propulsion and Power, 28 Propellants and Fuels,* and *44 Energy Production and Conversion.*

N90-21760*# McDonnell Aircraft Co., Saint Louis, MO.
EXHAUST ENVIRONMENT MEASUREMENTS OF A TURBOFAN ENGINE EQUIPPED WITH AN AFTERBURNER AND 2D NOZZLE Final Report
L. O. Brase Washington May 1990 59 p Sponsored in part by Air Force Wright Research and Development Center and Pratt and Whitney
(NASA-CR-4289; E-5302; NAS 1.26:4289) Avail: NTIS HC A04/MF A01 CSCL 21E

A test to measure the acoustic noise and static pressure environment on a structure exposed to engine exhaust flow was conducted at the NASA Lewis Research Center Propulsion Systems Laboratory by using an F100 derivative engine with a two-dimensional convergent-divergent (2D/CD) non-flight-weight demonstrator nozzle. A highly instrumented, water cooled flat panel was placed behind the 2D/CD nozzle, and tests were conducted at simulated Mach/altitude flight conditions with the engine at military or maximum-afterburner power setting. The panel instrumentation consisted of acoustic pressure microphones, thermocouples, and static-pressure pickups. Measurements indicated that the exhaust environment may excite structural resonances up to 10,000 HZ and that overall sound pressure levels decrease with increasing altitude. Author

N90-21761*# Pratt and Whitney Aircraft, West Palm Beach, FL.
ASSESSMENT OF HIGH TEMPERATURE SUPERCONDUCTING (HTS) ELECTRIC MOTORS FOR ROTORCRAFT PROPULSION Final Report
Jay Doernbach Apr. 1990 49 p
(Contract NAS3-25117)
(NASA-CR-185222; NAS 1.26:185222; PW-FR-20668) Avail: NTIS HC A03/MF A01 CSCL 21E

The successful development of high temperature superconductors (HTS) could have a major impact on future aeronautical propulsion and aeronautical flight vehicle systems. Applications of high temperature superconductors have been envisioned for several classes of aeronautical systems, including subsonic and supersonic transports, hypersonic aircraft, V/STOL aircraft, rotorcraft and solar powered aircraft. The potential of HTS electric motors and generators for providing primary shaft power for rotorcraft propulsion is examined. Three different sized production helicopters were investigated; namely, the Bell Jet Ranger, the Sikorsky Black Hawk and the Sikorsky Super Stallion. These rotorcraft have nominal horsepower ratings of 500, 3600, and 13400 respectively. Preliminary results indicated that an all-electric HTS drive system produces an improvement in rotorcraft Takeoff Gross Weight (TOGW) for those rotorcraft with power ratings above 2000 horsepower. The predicted TOGW improvements are up to 9 percent for the medium-sized Sikorsky Black Hawk and up to 20 percent for the large-sized Sikorsky Super Stallion. The small-sized Bell Jet Ranger, however, experienced a penalty in TOGW with the all-electric HTS drive system. Author

N90-21762*# National Aeronautics and Space Administration. Lewis Research Center, Cleveland, OH.
ON THE USE OF EXTERNAL BURNING TO REDUCE AEROSPACE VEHICLE TRANSONIC DRAG
Charles J. Trefny 1990 12 p Proposed for presentation at the 26th Joint Propulsion Conference, Orlando, FL, 16-18 Jul. 1990; cosponsored by AIAA, ASME, SAE, and ASEE
(NASA-TM-103107; E-5431; NAS 1.15:103107; AIAA-90-1935) Avail: NTIS HC A03/MF A01 CSCL 21E

The external combustion of hydrogen to reduce the transonic drag of aerospace vehicles is currently being investigated. A preliminary analysis based on a constant pressure control volume is discussed. Results indicate that the specific impulse of the external burning process rivals that of a turbojet and depends on the severity of the initial base drag as well as on the Mach flight number and the equivalence ratio. A test program was conducted to investigate hydrogen-air flame stability at the conditions of interest and to demonstrate drag reduction on a simple expansion ramp. Initial test results are presented and compared with the control-volume analysis. The expansion ramp surface pressure coefficient showed little variation with fuel pressure and altitude, in disagreement with the analysis. Flame stability results were encouraging and indicate that stable combustion is possible over an adequate range of conditions. Facility interference and chemical kinetics phenomena that make interpretation of subscale ground test data difficult are discussed. Author

N90-21763*# Sverdrup Technology, Inc., Brookpark, OH.
PRELIMINARY DESIGN OF A LONG-ENDURANCE MARS AIRCRAFT Final Report
Anthony J. Colozza Apr. 1990 14 p Proposed for presentation at the 26th Joint Propulsion Conference, Orlanda, FL, 16-18 Jul. 1990; sponsored by AIAA, SAE, ASME and ASEE
(Contract NAS3-25266)
(NASA-CR-185243; E-5475; NAS 1.26:185243; AIAA-90-2000) Avail: NTIS HC A03/MF A01 CSCL 21E

The preliminary design requirements of a long endurance aircraft capable of flight within the Martian environment was determined. Both radioisotope/heat engine and PV solar array power production systems were considered. Various cases for each power system were analyzed in order to determine the necessary size, weight and power requirements of the aircraft. The analysis method used was an adaptation of the method developed by Youngblood and Talay of NASA-Langley used to design a high altitude earth based aircraft. The analysis is set up to design an aircraft which, for the given conditions, has a minimum wingspan and maximum endurance parameter. The results showed that, for a first approximation, a long endurance aircraft is feasible within the

Martian environment. The size and weight of the most efficient solar aircraft were comparable to the radioisotope powered one. Author

N90-21981# Societe Nationale d'Etude et de Construction de Moteurs d'Aviation, Moissy-Cramayel (France).
MESH GENERATION FOR FLOW COMPUTATION IN TURBOMACHINE
M. Goutines, G. Karadimas, and C. Hah (General Electric Co., Schenectady, NY.) *In* AGARD, Applications of Mesh Generation to Complex 3-D Configurations Mar. 1990 13 p (For primary document see N90-21975 15-34)
Copyright Avail: NTIS HC A14/MF A02; Non-NATO Nationals requests available only from AGARD/Scientific Publications Executive

08 AIRCRAFT STABILITY AND CONTROL

Includes aircraft handling qualities; piloting; flight controls; and autopilots.

For related information see also *05 Aircraft Design, Testing and Performance.*

N90-21764 Rutgers Univ., New Brunswick, NJ.
NUMERICAL INVESTIGATION OF SOME CONTROL METHODS FOR 3-D TURBULENT INTERACTIONS DUE TO SHARP FINS Ph.D. Thesis
Datta V. Gaitonde 1989 203 p
Avail: Univ. Microfilms Order No. DA8923594

Numerical efforts are described for the modification and control of 3-D shock wave-turbulent boundary layer interactions due to supersonic flow past sharp fin/fins mounted on a flat plate. The first set of computations investigates the effect of bleed on single figure configurations (SFCs). For a strong interaction, suction is applied on two regions-Region 1 covering the area on the flat plate between the line of upstream influence and the theoretical inviscid shock line (TISL) and Region 2 covering the remaining portion of the plate between the TISL and the base of the fin. The largest suction case corresponds to bleeding of roughly 25 percent of the incoming boundary layer. Numerical pilot pressure and yaw angles are compared with experimental data obtained in the absence of bleed. Comparison with experimental data and analysis of the computed results indicates that the effect of bleed is primarily due to reduce the surface angularity and upstream influence. The motivation for the second set of computations derives from the conclusion of Mee and Stalker that shock-shock intersections may be capable of producing a given pressure rise with less likelihood of separation. Three computations on symmetric double fin configurations are described. The first (5 x 5 deg) corresponds to the strongest interaction. The overall comparison with experiment is good with modest discrepancies in extent of upstream influence. No flow separation is observed. Two other configurations (4 x 4 deg and 8 x 8 deg) are also simulated. Analysis of the computed flowfield indicates that the first is a weak interaction. In contrast, the 8 x 8 configuration displays an interesting surface pattern with turning angles larger than the shock angle. The consequent separated flowfield is examined with particle traces. Dissert. Abstr.

N90-21765 Stanford Univ., CA.
OPTIMAL CONTROL OF AN AIRCRAFT FLYING THROUGH A DOWNBURST Ph.D. Thesis
Yi Yuan Zhao 1989 280 p
Avail: Univ. Microfilms Order No. DA8925985

A downburst is a mass of cold air that descends to the ground in a column with a diameter of .1 to 1 kilometer. It lasts only five to ten minutes, but during that time, it creates vertical winds up to 50 ft per second and, as it spreads out near the ground, horizontal winds up to 100 ft/sec. The exsistence of downbursts was only recently discovered. Downbursts are the suspected cause of several aircraft accidents. The best way to handle a downburst is not to fly through it. However, a downburst is difficult to detect until the aircraft starts into it. Thus the problem of how to fly an aircraft through a downburst is of interest. The problem is considered mainly at take-off but also the landing problem is discussed. Downbursts are modeled by three dimensional vortex rings. The concept of pseudo-energy is introduced, which is the kinetic energy of an aircraft relative to the airmass plus the potential energy of the aircraft relative to the inertial ground. The control of an aircraft flying through a downburst is formulated as a dynamic optimization problem with a minimum altitude constraint and two different performance measures. A generalized gradient algorithm is developed to solve this problem numerically. Paths are determined through a downburst that maximize the pseudo-energy just after penetration (survival), and minimize deviation from the intended flight path (performance maintaining). Since the intensity of a downburst is difficult to assess use is recommended of the survival flight path strategy when the pilot believes he has entered a downburst. This strategy involves immediate application of maximum thrust, along with rapid descent to the minimum safe altitude; this increases airspeed and places the aircraft in a region of lower downdraft velocity. Simulation results suggest that the Delta Flight 191 would not have crashed if the proposed strategy had been followed. Dissert. Abstr.

N90-21766 Virginia Polytechnic Inst. and State Univ., Blacksburg.
OPTIMAL AND NEAR-OPTIMAL MEDIUM RANGE AIR-TO-AIR MISSILE GUIDANCE AGAINST MANEUVERING TARGETS Ph.D. Thesis
Renjith R. Kumar 1989 226 p
Avail: Univ. Microfilms Order No. DA9000633

Optimal intercept trajectories for a boost-sustain-coast medium-range air-to-air missile are synthesized using optimal control theory. Optimality in time/range/energy at intercept of a target is the main objective. Attainable sets and their boundaries are obtained and used to generate optimal intercept points in a three-dimensional scenario. A three-phase closed-loop guidance scheme is used to generate an efficient guidance law against a maneuvering target. In the present study, target maneuvers are restricted to the horizontal plane. An initial boost-phase with near-optimal guidance in the prescence of active control constraints and thrust switches is simulated. Target maneuvers are neglected during this phase. A new method of gain evaluation is detailed. A midcourse guidance scheme with neighboring guidance, transversal comparisons, and chasing center-of-attainability of target to augment performance is studied. Modifications in terminal guidance using proportional navigation, such as chasing the center-of-attainability of target, altitude shaping, and drag-resolution schemes are used to attempt better performance at intercept. A composite guidance strategy using a combination of neighboring guidance and proportional navigation for the midcourse guidance is introduced. The excellent performance of this guidance strategy and the improvement in storage requirements for on-board use make it a very special scheme. Dissert. Abstr.

N90-21767 North Carolina State Univ., Raleigh.
AN EXPERIMENTAL INVESTIGATION OF THE PHYSICAL MECHANISMS CONTROLLING THE ASYMMETRIC FLOW PAST SLENDER BODIES AT LARGE ANGLES OF ATTACK Ph.D. Thesis
Cary A. Moskovitz 1989 99 p
Avail: Univ. Microfilms Order No. DA9001176

An experimental investigation of the effects of geometric perturbations on the asymmetric flow past slender bodies was conducted. The perturbations included variations in model tip sharpness, roughness and shape as well as discrete surface perturbations represented by beads of varying height and diameter attached to the model surface. Two cone/cylinder models having 9 and 10 deg semi-apex angles and a 3.0 caliber tangent ogive model, all having base diameters of 3.5 in were tested at laminar flow conditions at angles of attack from 30 to 60 deg. Data were taken with each model from 3 circumferential rows of pressure taps at a flow speed of 45 ft/s corresponding to a Reynolds number of 8.4 x 10(exp 4) based on model base diameter. Also, a helium bubble flow visualization technique was used at a speed of 15 ft/s corresponding to a Reynolds number of 2.5 x 10(exp 4). Beads were tested by placing the model at a roll position having either a symmetric or a highly asymmetric flowfield, and then attaching a bead to the model surface at varying axial and circumferential positions. Bead effectiveness was judged by the extent to which the flowfield was affected. Data showed the beads to be very effective when placed approximately 140 deg from the windward ray, and to decrease in effectiveness with decreasing bead size and distance from the tip. The data showed no significant change in this behavior with variations in angle of attack and tip bluntness. Tests without beads, conducted with sets of tips manufactured to identical specifications, showed the behavior of sectional side-force with roll position to be a function of machining imperfections and surface roughness. Dissert. Abstr.

N90-21768 California Univ., Los Angeles.

AEROELASTIC SIMULATION OF HIGHER HARMONIC CONTROL Ph.D. Thesis

Lawson Hayes Robinson 1989 305 p

Avail: Univ. Microfilms Order No. DA9001751

The development of an aeroelastic analysis of a helicopter and its application to the simulation of helicopter vibration through Higher Harmonic Control (HHC) are described. This analysis is based on an existing aeroelastic code which was modified to allow the modeling of high frequency blade root pitch changes which are used by HHC to modify blade inertia and aerodynamic loads to alleviate vibrations. An improved implementation of a finite-state, time-domain model of unsteady aerodynamics is developed to capture high frequency aerodynamic effects. Helicopter trim parameters are determined using an improved trim procedure accounting for flap, lag, and torsional deformations of the blade. A procedure for calculating 4/rev. rotor hub loads is developed and control algorithms are incorporated in the analysis to determine the optimal HHC inputs necessary to minimize these rotor hub loads. Using this analysis, a study is carried out of the effects on a hingeless rotor of unsteady, as opposed to quasisteady, aerodynamics. Several different HHC algorithms are implemented on a hingeless rotor using both quasisteady and unsteady aerodynamic models, and their effectiveness in reducing rotor hub vibratory shears is compared. Simulations of roughly equivalent articulated and hingeless rotors are carried out, and it is found that hingeless rotors can require considerably larger HHC inputs to reduce rotor vibratory hub shears. This analysis is used to simulate the application of HHC to the rotor of an OH6A light helicopter. This helicopter was used in flight tests of HHC and results from those tests are compared to the results of this simulation. Dissert. Abstr.

N90-21769 California Univ., Los Angeles.

ADVANCES IN OPTIMAL ACTIVE CONTROL TECHNIQUES FOR AEROSPACE SYSTEMS; APPLICATION TO AIRCRAFT ACTIVE LANDING GEAR Ph.D. Thesis

Khai Tran Vu 1989 163 p

Avail: Univ. Microfilms Order No. DA8926454

The problem of runaway denial is a real threat to the Air Force. The effectiveness of a counterattack after a hostile airraid depends on the capabilities of the airbase to make rapid runway repair. Aircrafts with conventional landing gears can operate on rough repaired surfaces under certain limited conditions. When the surface roughness is severe, and the taxing speed of the aircraft over the runway is high, landing gear forces start exceeding design structural limits causing catastrophic failures and damages to the aircraft. Active control landing gears present a solution to this problem. An active control landing gear can reduce landing impact loads, provide better ground handling capabilities to the aircraft, and negotiate runway damages more effectively than a conventional landing gear. Optimal control techniques can be applied on active landing gears to provide the best control laws for different conditions. A performance index can be chosen to minimize the load transmitted to the aircraft and the aircraft vertical and angular motion thus improving aircraft stability and ground handling characteristics. Active control concept is discussed and then the problem of optimal control of active landing gears (semi-active concept) is described. The problem formulation is done for an aircraft that has three landing gears (one nose gear and two main gears) and flexible dynamics. The technique of steepest descent that is used to solve the resulting nonlinear two point boundary problem is given together with numerical results of an exemplary optimal solution. Dissert. Abstr.

N90-21770 Texas Univ., Austin.

A DECENTRALIZED LINEAR QUADRATIC CONTROL DESIGN METHOD FOR FLEXIBLE STRUCTURES Ph.D. Thesis

Tzu-Jeng Su 1989 204 p

Avail: Univ. Microfilms Order No. DA9005673

A decentralized suboptimal linear quadratic control design procedure which combines substructural synthesis, model reduction, decentralized control design, subcontroller synthesis, and controller reduction is proposed for the design of reduced-order controllers for flexible structures. The procedure starts with a definition of the continuum structure to be controlled. An evaluation model of finite dimension is obtained by the finite element method. Then, the finite element model is decomposed into several substructures by using a natural decomposition called substructuring decomposition. Each substructure, at this point, still has too large a dimension and must be reduced to a size that is Riccati-solvable. A Krylov model reduction algorithm is proposed to reduce the spillover of control energy. The Krylov reduced model has the property of matching low-frequency moments of the full-order system. Then, based on the reduced substructure model, a subcontroller is designed by an Linear Quadratic (LQ) optimal control method for each substructure independently. After all subcontrollers are designed, a controller synthesis method called Substructural Controller Synthesis is employed to synthesize all subcontrollers into a global controller. The assembling scheme used is the same as that employed for the structure matrices. Finally, a controller reduction scheme, called the Equivalent Impulse Response Energy Controller (EIREC) reduction algorithm, is used to reduce the global controller to a reasonable size for implementation. The EIREC reduced controller preserves the impulse response energy of the full-order controller and has the property of matching low-frequency moments and low-frequency power moments. Dissert. Abstr.

N90-21771 Texas A&M Univ., College Station.

A VIDEO-BASED EXPERIMENTAL INVESTIGATION OF WING ROCK Ph.D. Thesis

Steven Lynn Morris 1989 260 p

Avail: Univ. Microfilms Order No. DA9007508

The primary objective of this research was to develop a definitive theory on the cause of wing rock. The study was based on dynamic measurements in both a water tunnel and a wind tunnel on a sharp-edged delta wing with an 80 deg leading-edge sweep angle. Experimental data were compared with analytical results from a mathematical model and a fourth order Runge-Kutta integration. In the water tunnel tests, conducted at alpha = 35 deg and Reynolds numbers from 3 x 10(exp 4)/ft to 7.5 x 10(exp 4)/ft, the movement of the leading edge vortices and the model motion were simultaneously tracked and analyzed using a video-based motion analysis system, Expert Vision. Quantified vortex movement data were not obtained in the wind tunnel study; however, an extensive investigation of wing rock dynamics was performed at angles of attack from 24 to 50 deg and Reynolds numbers from 1.09 x 10(exp 5)/ft to 3.44 x 10(exp 5)/ft. The initial phase of the study validated Expert Vision accuracy using stationary and forced oscillation tests on 70 and 80 deg delta wings. Vortex trajectory, core velocity, and burst point results from stationary tests were in good agreement with published data. Wing rock is caused by the dynamic behavior of the leading-edge vortices. Specifically, the alternate lift-off and reattachment of the vortices generate an asymmetry in vortex lift and cause changes in rolling moment that initiate and sustain roll oscillations. Since wind tunnel and water tunnel tests showed opposite direction hysteresis loops, it was concluded that roll damping could not be the primary aerodynamic mechanism that sets the limit on roll amplitude. Wing rock dynamics were significantly different between water tunnel and wind tunnel experiments. Apparent mass terms must be included in the equations of motion when converting water tunnel acceleration data to rolling moment coefficients; with no apparent mass correction, C(sub l) calculated from accelerations in the water tunnel were about 15 times greater than those from the wind tunnel. Dissert. Abstr.

N90-21772*# Boeing Commercial Airplane Co., Seattle, WA.
A CONFLICT ANALYSIS OF 4D DESCENT STRATEGIES IN A METERED, MULTIPLE-ARRIVAL ROUTE ENVIRONMENT Final Report
K. H. Izumi and C. S. Harris 10 May 1990 48 p
(Contract NAS1-18027)
(NASA-CR-182019; NAS 1.26:182019) Avail: NTIS HC A03/MF A01 CSCL 17G

A conflict analysis was performed on multiple arrival traffic at a typical metered airport. The Flow Management Evaluation Model (FMEM) was used to simulate arrival operations using Denver Stapleton's arrival route structure. Sensitivities of conflict performance to three different 4-D descent strategies (clear-idle Mach/Constant AirSpeed (CAS), constant descent angle Mach/CAS and energy optimal) were examined for three traffic mixes represented by those found at Denver Stapleton, John F. Kennedy and typical en route metering (ERM) airports. The Monte Carlo technique was used to generate simulation entry point times. Analysis results indicate that the clean-idle descent strategy offers the best compromise in overall performance. Performance measures primarily include susceptibility to conflict and conflict severity. Fuel usage performance is extrapolated from previous descent strategy studies. Author

N90-21773*# National Aeronautics and Space Administration. Ames Research Center, Moffett Field, CA.
DIRECT INVERSION OF RIGID-BODY ROTATIONAL DYNAMICS
Ralph Bach and Russell Paielli May 1990 16 p Presented at the 1990 American Control Conference, San Diego, CA, 23-25 May 1990
(NASA-TM-102798; A-90098; NAS 1.15:102798) Avail: NTIS HC A03/MF A01 CSCL 01C

The global linearization (inversion) of rigid-body rotational dynamics is reviewed and representations in terms of quaternions and direction cosines are compared. Certain properties common to quaternions and direction cosines that make their use preferable to Euler angles and that simplify the inversion procedure are described. Applications of the inversion procedure for state estimation and attitude control are discussed. To avoid complexities caused by aerodynamics, an example of direct inversion for linear feedback control of spacecraft attitude is given. Author

09 RESEARCH AND SUPPORT FACILITIES (AIR)

Includes airports, hangars and runways; aircraft repair and overhaul facilities; wind tunnels; shock tubes; and aircraft engine test stands.

For related information see also *14 Ground Support Systems and Facilities (Space).*

N90-21774# Federal Aviation Administration, Atlantic City, NJ. Technical Center.
EVALUATION OF A PROTOTYPE LIGHTED BALL MARKER FOR POWERLINE OBSTRUCTIONS
Eric S. Katz Mar. 1990 12 p
(DOT/FAA/CT-TN90/12) Avail: NTIS HC A03/MF A01

A prototype lighted ball marker was evaluated. The lighted ball marker is a powerline obstruction marker that is designed to illuminate when it is placed directly on a high voltage powerline. Three of these ball markers were installed on a powerline near the FAA Technical Center and were tested for conspicuity during nighttime, Visual Flight Rules (VFR) conditions. Results of the evaluation indicate that the lighted ball markers provide a pilot with adequate advance warning that a powerline obstruction is being approached. Complete and partial failures of the prototype markers under evaluation indicated that reliability problems may be anticipated unless design corrections are made to production units. Author

N90-21775*# North Carolina State Univ., Raleigh. Dept. of Mechanical and Aerospace Engineering.
ANALYSIS OF A SIX-COMPONENT, FLOW-THROUGH, STRAIN-GAGE, FORCE BALANCE USED FOR HYPERSONIC WIND TUNNEL MODELS WITH SCRAMJET EXHAUST FLOW SIMULATION M.S. Thesis Final Report
Marc W. Kniskern 1990 57 p
(Contract NCC1-129)
(NASA-CR-186585; NAS 1.26:186585) Avail: NTIS HC A04/MF A01 CSCL 14B

The thermal effects of simulant gas injection and aerodynamic heating at the model's surface on the measurements of a non-watercooled, flow through balance were investigated. A stainless steel model of a hypersonic air breathing propulsion cruise missile concept (HAPCM-50) was used to evaluate this balance. The tests were conducted in the 20-inch Mach 6 wind tunnel at NASA-Langley. The balance thermal effects were evaluated at freestream Reynolds numbers ranging from .5 to 7 x 10(exp 6) ft and angles of attack between -3.5 to 5 deg at Mach 6. The injection gases considered included cold air, hot air, and a mixture of 50 percent Argon and 50 percent Freon-12. The stagnation temperatures of the cold air, hot air, and Ar-Fr(12) reached 111, 214, and 283 F, respectively within the balance. A bakelite sleeve was inserted into the inner tube of the balance to minimize the thermal effects of these injection gases. Throughout the tests, the normal force, side force, yaw moment, roll moment, and pitching moment balance measurements were unaffected by the balance thermal effects of the injection gases and the wind tunnel flow. However, the axial force (AF) measurement was significantly affected by balance heating. The average zero shifts in the AF measurements were 1.9, 3.8, and 5.9 percent for cold air, hot air, and Ar-Fr(12) injection, respectively. The AF measurements decreased throughout these tests which lasted from 70 to 110 seconds. During the cold air injection tests, the AF measurements were accurate up to at least ten seconds after the model was injected into the wind tunnel test section. For the hot air and Ar-Fr(12) tests, the AF measurements were accurate up to at least five seconds after model injection. Author

N90-21776*# Pittsburgh Univ., PA. Dept. of Electrical Engineering.
THE INSERTION OF HUMAN DYNAMICS MODELS IN THE FLIGHT CONTROL LOOPS OF V/STOL RESEARCH AIRCRAFT. APPENDIX 2: THE OPTIMAL CONTROL MODEL OF A PILOT IN V/STOL AIRCRAFT CONTROL LOOPS Final Report
Mark E. Zipf 1989 210 p
(Grant NAG3-729)
(NASA-CR-186598; NAS 1.26:186598) Avail: NTIS HC A10/MF A02 CSCL 05H

An overview is presented of research work focussed on the design and insertion of classical models of human pilot dynamics within the flight control loops of V/STOL aircraft. The pilots were designed and configured for use in integrated control system research and design. The models of human behavior that were considered are: McRuer-Krendel (a single variable transfer function model); and Optimal Control Model (a multi-variable approach based on optimal control and stochastic estimation theory). These models attempt to predict human control response characteristics when confronted with compensatory tracking and state regulation tasks. An overview, mathematical description, and discussion of predictive limitations of the pilot models is presented. Design strategies and closed loop insertion configurations are introduced and considered for various flight control scenarios. Models of aircraft dynamics (both transfer function and state space based) are developed and discussed for their use in pilot design and application. Pilot design and insertion are illustrated for various flight control objectives. Results of pilot insertion within the control loops of two V/STOL research aricraft (Sikorski Black Hawk UH-60A, McDonnell Douglas Harrier II AV-8B) are presented and compared against actual pilot flight data. Conclusions are reached on the ability of the pilot models to adequately predict human behavior when confronted with similar control objectives. Author

N90-21777*# Pittsburgh Univ., PA. Dept. of Electrical Engineering.

AN ADAPTIVE HUMAN RESPONSE MECHANISM CONTROLLING THE V/STOL AIRCRAFT. APPENDIX 3: THE ADAPTIVE CONTROL MODEL OF A PILOT IN V/STOL AIRCRAFT CONTROL LOOPS M.S. Thesis. Final Report

Senol Kucuk 1988 183 p
(Grant NAG3-729)
(NASA-CR-186599; NAS 1.26:186599) Avail: NTIS HC A09/MF A01 CSCL 05H

Importance of the role of human operator in control systems has led to the particular area of manual control theory. Human describing functions were developed to model human behavior for manual control studies to take advantage of the successful and safe human operations. A single variable approach is presented that can be extended for multi-variable tasks where a low order human response model is used together with its rules, to adapt the model on-line, being capable of responding to the changes in the controlled element dynamics. Basic control theory concepts are used to combine the model, constrained with the physical observations, particularly, for the case of aircraft control. Pilot experience is represented as the initial model parameters. An adaptive root-locus method is presented as the adaptation law of the model where the closed loop bandwidth of the system is to be preserved in a stable manner with the adjustments of the pilot handling qualities which relate the latter to the closed loop bandwidth and damping of the closed loop pilot aircraft combination. A Kalman filter parameter estimator is presented as the controlled element identifier of the adaptive model where any discrepancies of the open loop dynamics from the presented one, are sensed to be compensated. Author

N90-21778*# National Aeronautics and Space Administration. Ames Research Center, Moffett Field, CA.

THEORETICAL AND EXPERIMENTAL STUDY OF FLOW-CONTROL DEVICES FOR INLETS OF INDRAFT WIND TUNNELS

James C. Ross Sep. 1989 74 p
(NASA-TM-100050; A-88040; NAS 1.15:100050) Avail: NTIS HC A04/MF A01 CSCL 14B

The design of closed circuit wind tunnels has historically been performed using rule of thumb which have evolved over the years into a body of useful guidelines. The development of indraft wind tunnels, however, has not been as well documented. The design of indraft wind tunnels is therefore generally performed using a more intuitive approach, often resulting in a facility with disappointing flow quality. The primary problem is a lack of understanding of the flow in the inlet as it passes through the required antiturbulence treatment. For wind tunnels which employ large contraction ratio inlets, this lack of understanding is not serious since the relatively low velocity of the flow through the inlet treatment reduces the sensitivity to improper inlet design. When designing a small contraction ratio inlet, much more careful design is needed in order to reduce the flow distortions generated by the inlet treatment. As part of the National Full Scale Aerodynamics Complex Modification Project, 2-D computational methods were developed which account for the effect of both inlet screens and guide vanes on the test section velocity distribution. Comparisons with experimental data are presented which indicate that the methods accurately compute the flow distortions generated by a screen in a nonuniform velocity field. The use of inlet guide vanes to eliminate the screen induced distortion is also demonstrated both computationally and experimentally. Extensions of the results to 3-D is demonstrated and a successful wind tunnel design is presented. Author

12 ASTRONAUTICS (GENERAL)

For extraterrestrial exploration see *91 Lunar and Planetary Exploration.*

N90-21779*# National Aeronautics and Space Administration, Washington, DC.

FINAL (TIER 1) ENVIRONMENTAL IMPACT STATEMENT FOR THE GALILEO AND ULYSSES MISSIONS

Nov. 1988 106 p
(NASA-TM-102917; NAS 1.15:102917) Avail: NTIS HC A06/MF A01 CSCL 22A

Presented here is a Final (Tier 1) Environmental Impact Statement (EIS) addressing the potential environmental consequences associated with continuing the modifications of the Galileo and Ulysses spacecraft for launch using a booster/upper stage combination that is different from the one planned for use prior to the Challenger accident, while conducting the detailed safety and environmental analysis in order to preserve the October 1989 launch opportunity for Galileo and an October 1990 launch opportunity for Ulysses. While detailed safety and environmental analyses associated with the missions are underway, they currently are not complete. Nevertheless, sufficient information is available to enable a choice among the reconfiguration alternatives presented. Relevant assessments of the potential for environmental impacts are presented. Author

13 ASTRODYNAMICS

Includes powered and free-flight trajectories; and orbital and launching dynamics.

N90-21780*# Rice Univ., Houston, TX. Astro-Astronautics Group.

OPTIMAL TRAJECTORIES FOR THE AEROASSISTED FLIGHT EXPERIMENT. PART 4: DATA, TABLES, AND GRAPHS

A. Miele, T. Wang, W. Y. Lee, H. Wang, and G. D. Wu 1989 132 p Sponsored in part by Boeing Military Airplane Co., Seattle, WA
(Contract JPL-956415; NAG8-755)
(NASA-CR-186164; NAS 1.26:186164; AERO-ASTRONAUTICS-243-Pt-4) Avail: NTIS HC A07/MF A01 CSCL 22A

The determination of optimal trajectories for the aeroassisted flight experiment (AFE) is discussed. Data, tables, and graphs relative to the following transfers are presented: (IA) indirect ascent to a 178 NM perigee via a 197 NM apogee; and (DA) direct ascent to a 178 NM apogee. For both transfers, two cases are investigated: (1) the bank angle is continuously variable; and (2) the trajectory is divided into segments along which the bank angle is constant. For case (2), the following subcases are studied: two segments, three segments, four segments, and five segments; because the time duration of each segment is optimized, the above subcases involve four, six, eight, and ten parameters, respectively. Presented here are systematic data on a total of ten optimal trajectories (OT), five for Transfer IA and five for Transfer DA. For comparison purposes and only for Transfer IA, a five-segment reference trajectory RT is also considered. Author

14 GROUND SUPPORT SYSTEMS AND FACILITIES (SPACE)

Includes launch complexes, research and production facilities; ground support equipment, e.g., mobile transporters; and simulators.

For related information see also *09 Research and Support Facilities (Air).*

N90-21781 Texas Univ., Austin.
CURRENT MANAGEMENT FOR IMPROVED RAILGUN PERFORMANCE Ph.D. Thesis
Joseph Henry Beno, Jr. 1989 238 p
Avail: Univ. Microfilms Order No. DA9005530

Continued railgun development toward high energy devices that launch useful projectiles and have a lifetime of hundreds to thousands of shots, requires progress in two related aspects of accelerator design: rail containment structures must be made capable of withstanding greater rail repulsion forces without causing accelerators to become too bulky for their intended use; and rails must sustain minimal heat-related damage during projectile launch. These issues are related because they primarily represent direct effects of railgun current and its distribution. The potential for managing rail current and its distribution to alleviate the two aforementioned problems is investigated. Techniques for calculating pulsed, rail current distribution, in the infinite conductivity approximation, and resultant projectile force are developed. Then, passive, current management methods - involving multiple rail pairs to distribute currents and rail-repulsive forces in a few, evenly-spaced, radial directions, for easier rail containment - are explored. Optimized multi-rail, railgun cross-sectional shapes that produce more projectile force than conventional two-rail railguns operating under the same local peak current density constraints are determined. These railguns have nontraditional bore shapes, i.e., not square or round. The use of neighboring, current-carrying conductors to actively influence rail current distribution is then studied. Optimized, square- and round-bore, railgun geometries, employing separately powered auxiliary conductors, are developed. Compared with conventional, two-rail railguns, or normal, augmented, two-rail railguns, these designs produce three to seven fold increases in projectile force, for the same local peak current density limits. Additionally, the possibility of restricting current to inner rail surfaces to ease armature design and interfacing is explored. Dissert. Abstr.

N90-22085*# Centre National d'Etudes Spatiales, Toulouse (France).
A DYNAMIC MOTION SIMULATOR FOR FUTURE EUROPEAN DOCKING SYSTEMS
G. Brondino, Ph. Marchal, D. Grimbert, and P. Noirault (MATRA Espace, Paris-Velizy, France) *In* NASA, John F. Kennedy Space Center, The 24th Aerospace Mechanisms Symposium Apr. 1990 p 75-87 (For primary document see N90-22079 15-39)
Avail: NTIS HC A16/MF A03 CSCL 14B

N90-22103*# Lockheed Space Operations Co., Cocoa Beach, FL.
CLEAN ACCESS PLATFORM FOR ORBITER
H. Morrison and J. Harris *In* NASA, John F. Kennedy Space Center, The 24th Aerospace Mechanisms Symposium Apr. 1990 p 329-340 (For primary document see N90-22079 15-39)
Avail: NTIS HC A16/MF A03 CSCL 14B

15 LAUNCH VEHICLES AND SPACE VEHICLES

Includes boosters; operating problems of launch/space vehicle systems; and reusable vehicles.

For related information see also *20 Spacecraft Propulsion and Power.*

N90-21782 Columbia Univ., New York, NY.
EQUILIBRIUM AND STABILITY ANALYSIS OF MAGNETOSPHERIC PLASMAS Ph.D. Thesis
Christopher Peter J. Paranicas 1989 123 p
Avail: Univ. Microfilms Order No. DA9005918

The equilibrium and stability properties of plasmas in the Earth's magnetotail and Jupiter's magnetosphere are considered. A sufficient condition for the stability to ballooning modes of axisymmetric plasmas with equilibrium field-aligned flows is derived. These modes are found to be unstable, independent of the pressure gradient, if the flow speed approaches a critical speed of the plasma. This analysis is applied to the Jovian magnetosphere and the flow speeds are found to be too small to drive this resonant destabilization. However, in the inner magnetosphere, which is a region of essentially corotational flow, the sufficient condition for stability is violated because of the large destabilizing flow terms. Similar results in the middle magnetosphere are obtained, where field-aligned flows large enough to violate the condition for stability are consistent with the present data. Finally, equilibrium and stability in the Earth's magnetotail are discussed. A relaxation process to describe equilibrium states is considered. These solutions have the structure of flux ropes containing field-aligned currents. These results agree with data from the two observations ISEE-1 and ISEE-2. A sufficient condition for the stability of these states is formulated. Dissert. Abstr.

N90-21783# Technische Univ., Delft (Netherlands). Faculty of Aerospace Engineering.
THE INITIAL IMPERFECTION DATABANK AT THE DELFT UNIVERSITY OF TECHNOLOGY, PART 3
A. W. H. Klompe and P. C. denReyer Mar. 1989 65 p
(LR-568; ETN-90-96336) Avail: NTIS HC A04/MF A01

The results of an initial imperfection survey of 8 conical shells of nominally identical dimensions produced by the same fabrication process are presented. These shells are the interstage shells between stages 1 and 2 of the Ariane launch vehicle. The modal components of the measured imperfection surfaces, as a function of the circumferential and axial wave numbers, are calculated. A summary of information for each shell is provided. The results of the initial imperfection survey of 5 cylindrical shells, and of the interstage shells between stages 2 and 3 are presented in a companion report. ESA

N90-22086*# Lockheed Missiles and Space Co., Sunnyvale, CA.
THE DEVELOPMENT OF A COMPLEMENTARY EXPENDABLE LAUNCH VEHICLE INTERFACE FOR AN STS DEPLOYABLE PAYLOAD
Ed Eubanks and John Gibb *In* NASA, John F. Kennedy Space Center, The 24th Aerospace Mechanisms Symposium Apr. 1990 p 89-104 (For primary document see N90-22079 15-39)
Avail: NTIS HC A16/MF A03 CSCL 22B

16 SPACE TRANSPORTATION

Includes passenger and cargo space transportation, e.g., shuttle operations; and space rescue techniques.

For related information see also *03 Air Transportation and Safety* and *18 Spacecraft Design, Testing and Performance.* For space suits see *54 Man/System Technology and Life Support.*

No abstracts in this category.

17 SPACE COMM., SPACECRAFT COMM., COMMAND & TRACKING

Includes telemetry; space communications networks; astronavigation and guidance; and radio blackout.

For related information see also *04 Aircraft Communications and Navigation* and *32 Communications and Radar.*

N90-21884*# Jet Propulsion Lab., California Inst. of Tech., Pasadena.
GALILEO EARTH APPROACH NAVIGATION USING CONNECTED-ELEMENT INTERFEROMETER PHASE-DELAY TRACKING
S. W. Thurman *In its* The Telecommunications and Data Acquisition Report 15 Feb. 1990 p 34-47 (For primary document see N90-21880 15-32)
Avail: NTIS HC A15/MF A02 CSCL 09F

N90-21885*# Jet Propulsion Lab., California Inst. of Tech., Pasadena.
USING CONNECTED-ELEMENT INTERFEROMETER PHASE-DELAY DATA FOR MAGELLAN NAVIGATION IN VENUS ORBIT
S. W. Thurman and G. Badilla *In its* The Telecommunications and Data Acquisition Report 15 Feb. 1990 p 48-54 (For primary document see N90-21880 15-32)
Avail: NTIS HC A15/MF A02 CSCL 17G

N90-21903*# Jet Propulsion Lab., California Inst. of Tech., Pasadena.
MARK 4-A DSCC (MAGELLAN-ERA) TELEMETRY SYSTEM DESCRIPTION
D. L. Ross *In its* The Telecommunications and Data Acquisition Report 15 Feb. 1990 p 263-273 (For primary document see N90-21880 15-32)
Avail: NTIS HC A15/MF A02 CSCL 09F

18 SPACECRAFT DESIGN, TESTING AND PERFORMANCE

Includes satellites; space platforms; space stations; spacecraft systems and components such as thermal and environmental controls; and attitude controls.

For life support systems see *54 Man/System Technology and Life Support.* For related information see also *05 Aircraft Design, Testing and Performance, 39 Structural Mechanics,* and *16 Space Transportation.*

N90-21784 Colorado Univ., Boulder.
ROBUST CONTROL OF FLEXIBLE STRUCTURES Ph.D. Thesis
Nassim Mohammed Arbouz 1989 101 p
Avail: Univ. Microfilms Order No. DA8923474

The control of flexible mechanical systems has application to control of space systems, aircraft, robotics and active optics, to name a few. These systems have distributed-parameter dynamics; their natural damping is very small; they have many densely packed low-frequency modes; and their model parameters are uncertain. Moreover, performance requirements such as pointing accuracy, shape control, and bandwidth are very stringent and make the problem of structural vibration more acute. Another important application of flexible structural control is in robotics. The goal is to develop lighter and faster robots capable of moving larger payloads with low energy requirements. The single-input, single-output control of flexible structures is first examined. Important time and frequency-domain properties that characterize elastic systems were established. Particularly, an interesting pattern of movement of the plant zeros was demonstrated as a function of the sensor location. This zero motion has a considerable implication on control design. A compensation method was then presented based on a frequency minimax technique, and a search procedure which always converges to the optimal controller. The concept of generalized lead-lag compensation was proposed. This method is intended for the noncollocated control of flexible structures. A theorem giving necessary and sufficient conditions for the existence of such a stabilizing controller is proved, and a systematic design procedure is given. The multi-output control of flexible structures was also investigated. An optimal sensor placement procedure, based on eigenstructure assignment, is developed for the robust control of elastic systems.
Dissert. Abstr.

N90-21785*# Boeing Aerospace Co., Kent, WA.
BI-DIRECTIONAL THRUSTER DEVELOPMENT AND TEST REPORT Final Report, Jul. - Oct. 1989
A. D. Jacot, G. S. Bushnell, and T. M. Anderson Feb. 1990 94 p
(Contract NAS1-18762)
(NASA-CR-182013; NAS 1.26:182013) Avail: NTIS HC A05/MF A01 CSCL 22B

The design, calibration and testing of a cold gas, bi-directional throttlable thruster are discussed. The thruster consists of an electro-pneumatic servovalve exhausting through opposite nozzles with a high gain pressure feedback loop to optimize performance. The thruster force was measured to determine hysteresis and linearity. Integral gain was used to maximize performance for linearity, hysteresis, and minimum thrust requirements. Proportional gain provided high dynamic response (bandwidth and phase lag). Thruster performance is very important since the thrusters are intended to be used for active control. Author

N90-21786# Instituto de Pesquisas Espaciais, Sao Jose dos Campos (Brazil).
ANALYSIS, SELECTION, AND IMPLEMENTATION OF PROCEDURES WHICH APPROVE OPTIMAL ARTIFICIAL SATELLITE MANEUVERS M.S. Thesis [ANALISE, SELECAO E IMPLEMENTACAO DE PROCEDIMENTOS QUE VISEM MANOBRAS OTIMAS DE SATELITES ARTIFICIAIS]
Antonio Fernando BertachinideAlmeidaPrado Oct. 1989 235 p
In PORTUGUESE; ENGLISH summary
(INPE-5003-TDL/397) Avail: NTIS HC A11/MF A02

The problem of spacecraft orbit transfer with minimum fuel consumption is considered, in terms of selecting, implementing, and testing numerical optimal solutions. After a search in the literature and analysis of results available, two schemes of solution to the problem were selected which are considered to be satisfactory. In one of these schemes the associated optimal control problem is numerically treated by using a direct search approach together with suboptimal parameterized control. In the other, a hybrid approach is used where the determination of the initial value of Lagrange multipliers, to solve the equations given by the Maximum Principle, is transformed in a direct search problem. In both cases, the numerical solution of the problem in each iteration is reduced to one of nonlinear programming, which is then solved with a projection of the gradient method. With the results obtained, it was possible to suggest a new version which considers errors in constraints satisfaction. Author

N90-21787# Instituto de Pesquisas Espaciais, Sao Jose dos Campos (Brazil). Departamento de Controle e Guiagem.

ACCURATE NONLINEAR CONTROL FOR SATELLITES USING REACTION WHEELS [CONTROLE NAO-LINEAR EXATO PARA SATELITES USANDO RODAS DE REACAO]

Antonio Felix Martin Neto Oct. 1989 6 p In PORTUGUESE; ENGLISH summary Presented at the 3rd Latin American Conference on Automation, Vina del Mar, Chile, 7-11 Nov. 1988
(INPE-4983-PRE/1546) Avail: NTIS HC A02/MF A01

The problem of maneuvering a satellite relative to a desired noninertial reference by using interval reaction wheels is examined by the use of linearizing transformations and the concept of relative quaternion. The satellite dynamic equations are transformed into an equivalent linear from which considers the fact that the control purpose is to align the satellite with a moving reference frame (e.g., an earth resource satellite). The equations so obtained are used to design control strategies for stabilizing the satellite attitude by linear techniques. This approach is more useful in algorithm design for on-board autonomous processors than the technique using inertial quaternion since the laws obtained are function of the noninertial sensor (sun sensor, or earth sensors) outputs and of the inertial sensor (gyroscopes) outputs. Author

N90-21788# Instituto de Pesquisas Espaciais, Sao Jose dos Campos (Brazil).

EXPERIMENTAL DETERMINATION OF THERMAL CONDUCTANCE IN BOLTED JOINT IMPACT IN SATELLITES [DETERMINACAO EXPERIMENTAL DA CONDUTANCIA TERMICA DE JUNTAS PARAFUSADAS ENCONTRADAS EM SATELITES]

Marcia Barbosa Henri Mantelli and Jose Edson Basto Aug. 1989 6 p In PORTUGUESE; ENGLISH summary Presented at the 10th Brazilian Conference on Mechanical Engineering, Rio de Janeiro, Brazil, 4-8 Dec. 1989
(INPE-4989-PRE/1551) Avail: NTIS HC A02/MF A01

The goal is to determine the thermal conductance of bolted joints between panels for the first Brazilian satellite. This is achieved by a comparison among experimental values, numerical values based on the finite difference method, and theoretical results. These joints were submitted to tests in a vacuum-thermal chamber of the laboratory of satellite thermal control subsystem development, at INPE. Author

N90-21789*# Colorado Univ., Boulder. Center for Space and Geosciences Policy.

THE ADVANCED COMMUNICATIONS TECHNOLOGY SATELLITE (ACTS) CAPABILITIES FOR SERVING SCIENCE

Thomas R. Meyer 15 May 1990 143 p
(Grant NAGw-1105)
(NASA-CR-186584; NAS 1.26:186584) Avail: NTIS HC A07/MF A01 CSCL 22B

Results of research on potential science applications of the NASA Advanced Communications Technology Satellite (ACTS) are presented. Discussed here are: (1) general research on communications related issues; (2) a survey of science-related activities and programs in the local area; (3) interviews of selected scientists and associated telecommunications support personnel whose projects have communications requirements; (4) analysis of linkages between ACTS functionality and science user communications activities and modes of operation; and (5) an analysis of survey results and the projection of conclusions to a national scale. Author

N90-21790*# National Aeronautics and Space Administration. Goddard Space Flight Center, Greenbelt, MD.

DEVELOPMENT AND INTEGRATION OF THE CAPILLARY PUMPED LOOP GAS AND HITCHHIKER FLIGHT EXPERIMENTS

D. Butler and R. McIntosh Apr. 1990 17 p
(NASA-TM-100756; Rept-90B00081; NAS 1.15:100756) Avail: NTIS HC A03/MF A01 CSCL 22B

The Capillary Pumped Loop (CPL) is a thermal control system with high density heat acquisition and transport capability. A small spaceflight version of the CPL was built and flown as a GAS experiment on STS 51-D in April 1985 and STS 51-G in June 1985, and as a Hitchhiker-G experiment on STS 61-C in January 1986. The purpose of the experiments was to demonstrate the capability of a capillary pumped system under microgravity conditions for use in the thermal control of large scientific instruments, advanced orbiting spacecraft, and space station components. The development, integration, and test activities of the CPL are described. Author

N90-21791# Los Alamos National Lab., NM.

SCALING OF NONNUCLEAR KINETIC-ENERGY ANTISATELLITES

Gregory H. Canavan May 1990 22 p
(Contract W-7405-eng-36)
(DE90-009758; LA-11716-MS) Avail: NTIS HC A03/MF A01

Nonnuclear antisatellites could release particles in the paths of satellites. The antisatellite would have about a twofold mass advantage in attrition and about a tenfold advantage in suppression over the defensive satellite. Antisatellites would weigh 5 to 10 tons; satellite shields could weigh a factor of 2 to 4 less. Exchange ratios scale strongly on antisatellite mass, maneuver, and range. Such antisatellites would be less effective against directed energy satellites, which could clear their paths or destroy the antisatellites before deployment. DOE

N90-21792*# Southwest Research Inst., San Antonio, TX. Dept. of Space Sciences.

PIC CODE MODELING OF SPACECRAFT CHARGING POTENTIAL DURING ELECTRON BEAM INJECTION INTO A BACKGROUND OF NEUTRAL GAS AND PLASMA, PART 1

J. K. Koga, C. S. Lin, and R. M. Winglee (Colorado Univ., Boulder.) [1989] 48 p
(Grant NAGw-1231)
(NASA-CR-186602; NAS 1.26:186602) Avail: NTIS HC A03/MF A01 CSCL 22B

Injections of nonrelativistic electron beams from an isolated equipotential conductor into a uniform background of plasma and neutral gas were simulated using a 2-D electrostatic particle code. The ionization effects on spacecraft charging are examined by including interactions of electrons with neutral gas. The simulations show that the conductor charging potential decreases with increasing neutral background density due to the production of secondary electrons near the conductor surface. In the spacecraft wake, the background electrons accelerated towards the charged spacecraft produce an enhancement of secondary electrons and ions. Simulations run for longer times indicate that the spacecraft potential is further reduced and short wavelength beam-plasma oscillations appear. The results are applied to explain the spacecraft charging potential measured during the SEPAC experiments from Spacelab 1. Author

19 SPACECRAFT INSTRUMENTATION

For related information see also *06 Aircraft Instrumentation* and *35 Instrumentation and Photography.*

No abstracts in this category.

20 SPACECRAFT PROPULSION AND POWER

Includes main propulsion systems and components, e.g., rocket engines; and spacecraft auxilliary power sources.

For related information see also *07 Aircraft Propulsion and Power, 28 Propellants and Fuels, 44 Energy Production and Conversion,* and *15 Launch Vehicles and Space Vehicles.*

N90-21793*# United Technologies Corp., San Jose, CA. Chemical Systems Div.
HYBRID PROPULSION TECHNOLOGY PROGRAM. VOLUME 1: CONCEPTIONAL DESIGN PACKAGE Final Technical Report, 6 Mar. 1989 - 28 Sep. 1989
Gordon E. Jensen, Allen L. Holzman, Steven O. Leisch, Joseph Keilbach, Randy Parsley, and John Humphrey 15 Oct. 1989 247 p
(Contract NAS8-37778)
(NASA-CR-183953; NAS 1.26:183953; Proj-2027-FR-Vol-1)
Avail: NTIS HC A11/MF A02 CSCL 21H

A concept design study was performed to configure two sizes of hybrid boosters; one which duplicates the advanced shuttle rocket motor vacuum thrust time curve and a smaller, quarter thrust level booster. Two sizes of hybrid boosters were configured for either pump-fed or pressure-fed oxygen feed systems. Performance analyses show improved payload capability relative to a solid propellant booster. Size optimization and fuel safety considerations resulted in a 4.57 m (180 inch) diameter large booster with an inert hydrocarbon fuel. The preferred diameter for the quarter thrust level booster is 2.53 m (96 inches). As part of the design study critical technology issues were identified and a technology acquisition and demonstration plan was formulated. Author

N90-21794*# United Technologies Corp., San Jose, CA. Chemical Systems Div.
HYBRID PROPULSION TECHNOLOGY PROGRAM. VOLUME 2: TECHNOLOGY DEFINITION PACKAGE Final Technical Report, 6 Mar. 1989 - 28 Sep. 1989
Gordon E. Jensen, Allen L. Holzman, Steven O. Leisch, Joseph Keilbach, Randy Parsley, and John Humphrey 15 Oct. 1989 110 p
(Contract NAS8-37778)
(NASA-CR-183954; NAS 1.26:183954; Proj-2027-FR-Vol-2)
Avail: NTIS HC A06/MF A01 CSCL 21H

A concept design study was performed to configure two sizes of hybrid boosters; one which duplicates the advanced shuttle rocket motor vacuum thrust time curve and a smaller, quarter thrust level booster. Two sizes of hybrid boosters were configured for either pump-fed or pressure-fed oxygen feed systems. Performance analyses show improved payload capability relative to a solid propellant booster. Size optimization and fuel safety considerations resulted in a 4.57 m (180 inch) diameter large booster with an inert hydrocarbon fuel. The preferred diameter for the quarter thrust level booster is 2.53 m (96 inches). The demonstration plan would culminate with test firings of a 3.05 m (120 inch) diameter hybrid booster. Author

N90-21795*# National Aeronautics and Space Administration. Lewis Research Center, Cleveland, OH.
FREE-SPACE POWER TRANSMISSION
Washington Nov. 1989 189 p Workshop held in Cleveland, OH, 29-30 Mar. 1988
(NASA-CP-10016; E-4161; NAS 1.55:10016) Avail: NTIS HC A09/MF A02 CSCL 10B

NASA Lewis Research Center organized a workshop on technology availability for free-space power transmission (beam power). This document contains a collection of viewgraph presentations that describes the effort by academia, industry, and the national laboratories in the area of high-frequency, high-power technology applicable to free-space power transmission systems. The areas covered were rectenna technology, high-frequency, high-power generation (gyrotrons, solar pumped lasers, and free electron lasers), and antenna technology. For individual titles, see N90-21796 through N90-21805.

N90-21796*# Raytheon Co., Waltham, MA.
AN ALL ELECTRONIC TRANSPORTATION SYSTEM FROM LEO TO GEO AND BEYOND
William C. Brown *In* NASA, Lewis Research Center, Free-Space Power Transmission Nov. 1989 p 7-17 Presented at the Lunar Bases and Space Activities of the 21st Century, Houston, TX, 5-7 Apr. 1988 (For primary document see N90-21795 15-20)
Avail: NTIS HC A09/MF A02 CSCL 10B

System description and moon mission interface; LEO to GEO flight times; technology readiness and modular construction; system capacity and costs; and reduction of propellant mass are outlined. This presentation is represented by viewgraph only. B.G.

N90-21797*# Georgia Inst. of Tech., Atlanta.
MILLIMETER WAVELENGTH RECTENNA DEVELOPMENT
James Gallagher and Mark Gouker *In* NASA, Lewis Research Center, Free-Space Power Transmission Nov. 1989 p 19-35 (For primary document see N90-21795 15-20)
Avail: NTIS HC A09/MF A02 CSCL 10B

Rectennas were studied with the intent of converting the Earth's (black body) radiation into dc power for satellites in earth orbit. Power densities; metal-oxide-metal diodes; antenna design configurations; fluid patterns; substrate mounted antennas; and directions for future work are outlined. This presentation is represented by viewgraphs only. B.G.

N90-21798*# National Aeronautics and Space Administration. Langley Research Center, Hampton, VA.
LARGE SPACE SYSTEMS ANTENNA TECHNOLOGY
Thomas G. Campbell *In* NASA, Lewis Research Center, Free-Space Power Transmission Nov. 1989 p 37-49 (For primary document see N90-21795 15-20)
Avail: NTIS HC A09/MF A02 CSCL 10B

Program objectives; approach; surface characterization of large scale antennas; adaptive feed-multimode horn and array configuration; and technology benefits of CSEI program are outlined. This presentation is represented by viewgraphs only. B.G.

N90-21799*# L'Garde, Inc., Tustin, CA.
INFLATABLE ANTENNAS FOR MICROWAVE PWOER TRANSMISSION
Geoff Williams *In* NASA, Lewis Research Center, Free-Space Power Transmission Nov. 1989 p 51-65 (For primary document see N90-21795 15-20)
Avail: NTIS HC A09/MF A02 CSCL 10B

Operational phase of the inflatable radiator; inflatable space structures; advantages; inflated thin-film satellites; antenna configuration; 3 meter diameter test paraboloid (HAIR program); and weight breakdown for the 100 meter diameter reflector are outlined. This presentation is represented by viewgraphs only. B.G.

N90-21800*# Lawrence Livermore National Lab., CA.
FREE ELECTRON LASERS DRIVEN BY LINEAR INDUCTION ACCELERATORS: HIGH POWER RADIATION SOURCES
T. J. Orzechowski *In* NASA, Lewis Research Center, Free-Space Power Transmission Nov. 1989 p 67-96 (For primary document see N90-21795 15-20)
Avail: NTIS HC A09/MF A02 CSCL 10B

The technology of Free Electron Lasers (FELs) and linear induction accelerators (LIAs) is addressed by outlining the following topics: fundamentals of FELs; basic concepts of linear induction accelerators; the Electron Laser Facility (a microwave FEL); PALADIN (an infrared FEL); magnetic switching; IMP; and future directions (relativistic klystrons). This presentation is represented by viewgraphs only. B.G.

N90-21801*# Case Western Reserve Univ., Cleveland, OH.
ANALYSIS OF A HIGH HARMONIC RECTANGULAR GYROTRON USING RIBBON BEAMS c35
Altan M. Ferendeci *In* NASA, Lewis Research Center, Free-Space Power Transmission Nov. 1989 p 97-114 (For primary document see N90-21795 15-20)
Avail: NTIS HC A09/MF A02 CSCL 14B

Cylindrical cavity structures and electron orbits; a grooved gyrotron using a ribbon beam; construction details; radiation patterns; radiation distribution; phase distribution; energy curves; and advantages are outlined. This presentation is represented by viewgraphs and charts only. B.G.

N90-21802*# Massachusetts Inst. of Tech., Cambridge.
OPERATION OF A STEP TUNABLE MEGAWATT GYROTRON
K. E. Kreischer and R. J. Temkin *In* NASA, Lewis Research Center, Free-Space Power Transmission Nov. 1989 p 115-125 Sponsored in part by DOE (For primary document see N90-21795 15-20)
Avail: NTIS HC A09/MF A02 CSCL 10B

An electron cyclotron resonance maser; gyrotron fundamental oscillator; advantages of gyrotrons; a schematic of the experiment; gyrotron design theory; 1 MW design parameters; compact ignition tokamak; and a gyrotron with quasi-optical output coupler are briefly presented. This presentation is represented by viewgraphs only. B.G.

N90-21803*# Massachusetts Inst. of Tech., Cambridge.
THE 10-100 kW SUBMILLIMETER GYROTRON
S. Spira, K. E. Kreischer, and R. J. Temkin *In* NASA, Lewis Research Center, Free-Space Power Transmission Nov. 1989 p 127-136 (For primary document see N90-21795 15-20)
Avail: NTIS HC A09/MF A02 CSCL 10B

High frequency high harmonic gyrotrons; cyclotron autoresonance maser (CARM); CARM amplifier schematics; MIT electron gun; and baseline design for the 140 GHz CARM amplifier are briefly reviewed. This presentation is represented by viewgraphs only. Author

N90-21804*# National Aeronautics and Space Administration. Langley Research Center, Hampton, VA.
SOLAR-PUMPED LASER FOR FREE SPACE POWER TRANSMISSION
Ja H. Lee *In* NASA, Lewis Research Center, Free-Space Power Transmission Nov. 1989 p 137-152 (For primary document see N90-21795 15-20)
Avail: NTIS HC A09/MF A02 CSCL 10B

Laser power transmission; laser systems; space-borne and available lasers; 2-D and 1 MW laser diode array systems; technical issues; iodine solar pumped laser system; and laser power transmission applications are presented. This presentation is represented by viewgraphs only. Author

N90-21805*# Department of Energy, Washington, DC.
HIGH POWER MILLIMETER WAVE SOURCE DEVELOPMENT PROGRAM
T. V. George *In* NASA, Lewis Research Center, Free-Space Power Transmission Nov. 1989 p 153-157 (For primary document see N90-21795 15-20)
Avail: NTIS HC A09/MF A02 CSCL 10B

High power millimeter wave sources for fusion program; ECH source development program strategy; and 1 MW, 140 GHz gyrotron experiment design philosophy are briefly outlined. This presentation is represented by viewgraphs only. B.G.

N90-21806*# Large Scale Programs Inst., Austin, TX.
A SUPERCONDUCTING QUENCHGUN FOR DELIVERING LUNAR DERIVED OXYGEN TO LUNAR ORBIT Final Report
Nathan Nottke and Curt R. Bilby Apr. 1990 51 p
(Grant NAG3-928)
(NASA-CR-185161; NAS 1.26:185161; LSPI-901) Avail: NTIS HC A04/MF A01 CSCL 22D

The development of a parametric model for a superconducting quenchgun for launching lunar derived liquid oxygen to lunar orbit is detailed. An overview is presented of the quenchgun geometry and operating principles, a definition of the required support systems, and the methods used to size the quenchgun launcher and support systems. An analysis assessing the impact of a lunar quenchgun on the OEXP Lunar Evolution Case Study is included. Author

N90-21807*# Large Scale Programs Inst., Austin, TX.
A TRAJECTORY GENERATION AND SYSTEM CHARACTERIZATION MODEL FOR CISLUNAR LOW-THRUST SPACECRAFT. VOLUME 2: TECHNICAL MANUAL
David J. Korsmeyer, Elfego Pinon, III, Brendan M. OConnor, and Curt R. Bilby May 1990 61 p
(Grant NAG3-928)
(NASA-CR-185172; NAS 1.26:185172; LSPI-903) Avail: NTIS HC A04/MF A01 CSCL 21H

The documentation of the Trajectory Generation and System Characterization Model for the Cislunar Low-Thrust Spacecraft is presented in Technical and User's Manuals. The system characteristics and trajectories of low thrust nuclear electric propulsion spacecraft can be generated through the use of multiple system technology models coupled with a high fidelity trajectory generation routine. The Earth to Moon trajectories utilize near Earth orbital plane alignment, midcourse control dependent upon the spacecraft's Jacobian constant, and capture to target orbit utilizing velocity matching algorithms. The trajectory generation is performed in a perturbed two-body equinoctial formulation and the restricted three-body formulation. A single control is determined by the user for the interactive midcourse portion of the trajectory. The full spacecraft system characteristics and trajectory are provided as output. Author

N90-21808*# National Aeronautics and Space Administration. Lewis Research Center, Cleveland, OH.
EFFECT OF LEO CYCLING ON 125 Ah ADVANCED DESIGN IPV NICKEL-HYDROGEN BATTERY CELLS
John J. Smithrick and Stephen W. Hall (Naval Weapons Support Center, Crane, IN.) 1990 8 p Proposed for presentation at the 25th Intersociety Energy Conversion Engineering Conference, Reno, NV, 12-17 Aug. 1990; cosponsored by AIChE, SAE, ACS, AIAA, ASME, and IEEE
(NASA-TM-103128; E-5458; NAS 1.15:103128) Avail: NTIS HC A02/MF A01 CSCL 10A

An advanced 125 Ah individual pressure vessel (IPV) nickel-hydrogen cell was designed. The primary function of the advanced cell, is to store and deliver energy for long term, low earth-orbit (LEO) spacecraft missions. The new features of this design are: (1) use of 26 percent rather than 31 percent potassium hydroxide (KOH) electrolyte, (2) use of a patented catalyzed wall wick, (3) use of serrated edge separators to facilitate gaseous oxygen and hydrogen flow within the cell, while still maintaining physical contact with the wall wick for electrolyte management, and (4) use of a floating rather than a fixed stack (state-of-the-art) to accommodate nickel electrode expansion. Six 125 Ah flight cells based on this design were fabricated by Eagle-Picher. Three of the cells contain all of the advanced features (test cells) and three are the same as the test cells except they don't have catalyst on the wall wick (control cells). All six cells are in the process of being evaluated in a LEO cycle life test. The cells have accumulated about 4700 LEO cycles (60 percent DOD 10 C). There have been no cell failures, the catalyzed wall wick cells however, are performing better. Author

N90-21809*# United Technologies Research Center, East Hartford, CT.
FRAMEWORK FOR A SPACE SHUTTLE MAIN ENGINE HEALTH MONITORING SYSTEM Final Report
Michael W. Hawman, William S. Galinaitis, Sharayu Tulpule, Anita K. Mattedi, and Jeffrey Kamenetz (United Technologies Corp., Windsor Locks, CT.) May 1990 189 p
(Contract NAS3-25626)

(NASA-CR-185224; NAS 1.26:185224; UTRC-R90-997978)
Avail: NTIS HC A09/MF A01 CSCL 21H

A framework developed for a health management system (HMS) which is directed at improving the safety of operation of the Space Shuttle Main Engine (SSME) is summarized. An emphasis was placed on near term technology through requirements to use existing SSME instrumentation and to demonstrate the HMS during SSME ground tests within five years. The HMS framework was developed through an analysis of SSME failure modes, fault detection algorithms, sensor technologies, and hardware architectures. A key feature of the HMS framework design is that a clear path from the ground test system to a flight HMS was maintained. Fault detection techniques based on time series, nonlinear regression, and clustering algorithms were developed and demonstrated on data from SSME ground test failures. The fault detection algorithms exhibited 100 percent detection of faults, had an extremely low false alarm rate, and were robust to sensor loss. These algorithms were incorporated into a hierarchical decision making strategy for overall assessment of SSME health. A preliminary design for a hardware architecture capable of supporting real time operation of the HMS functions was developed. Utilizing modular, commercial off-the-shelf components produced a reliable low cost design with the flexibility to incorporate advances in algorithm and sensor technology as they become available. Author

N90-21810*# Colorado State Univ., Fort Collins. Dept. of Mechanical Engineering.
ADVANCED ELECTRIC PROPULSION RESEARCH, 1989 Annual Report, 1 Jan. 1989 - 1 Jan. 1990
Paul J. Wilbur Apr. 1990 21 p
(Grant NGR-06-002-112)
(NASA-CR-185237; NAS 1.26:185237) Avail: NTIS HC A03/MF A01 CSCL 21C

Results of an experimental study of the characteristics of ion thruster hollow cathodes operating at high discharge currents (up to 60 A) are presented in a companion report. This work shows that ions produced near the cathode orifice can acquire sufficient energy to induce the high sputter erosion rates on cathode potential surfaces that have been observed in ion thrusters. A mechanism by which these ions could be produced is also described. A second, brief study showing how a discharge chamber model developed previously can be applied to determine optimal values for one or more discharge chamber design parameters is presented. The experimental approach being used to study the plasma potential field and charge-exchange ion production rate downstream of the accelerator grid of an ion thruster is discussed and preliminary results are presented. Author

N90-21811*# Thiokol Corp., Brigham City, UT. Nozzle/TVC Design.
FLIGHT MOTOR SET 360L002 (STS-27R). VOLUME 5: NOZZLE COMPONENT Final Report
S. A. Meyer Mar. 1990 342 p
(Contract NAS8-30490)
(NASA-CR-183945; NAS 1.26:183945; TWR-17541-5) Avail: NTIS HC A15/MF A02 CSCL 21H

A review of the performance and post-flight condition of the STS-27 Redesigned Solid Rocket Motor (RSRM) nozzles is presented. Thermal/Structural instrumentation data is reviewed, and applicable Discrepancy Reports (DRs) and Process Departures (PDs) are presented. The Nozzle Component Program Team (NCPT) performance evaluation and the Redesign Program Review Board (RPRB) assessment is included. The STS-27 nozzle assemblies were flown on the RSRM Second Flight (Space Shuttle Atlantis) on 2 December 1988. The nozzles were a partially submerged convergent and/or divergent movable design with an aft pivot point flexible bearing. The nozzle assemblies incorporated the following features: RSRM forward exit cone with snubber assembly, RSRM fixed housing, Structural backup Outer Boot Ring (OBR), RSRM cowl ring, RSRM nose inlet assembly, RSRM throat assembly, RSRM aft exit cone assembly with Linear-Shaped Charge (LSC), RTV backfill in Joints 1, 3, and 4, Use of EA913 NA adhesive in place of EA913 adhesive, Redesigned nozzle plug, and Carbon Cloth Phenolic (CCP) with 750 ppm sodium content. The CCP material usage for the STS-27 forward nozzle and aft exit cone assemblies is shown. Author

N90-21812*# National Aeronautics and Space Administration. Lewis Research Center, Cleveland, OH.
PHOTOVOLTAIC POWER FOR SPACE STATION FREEDOM
Cosmo R. Baraona 1990 8 p Presented at the 21st Photovoltaic Specialists Conference, Orlando, FL, 21-25 May 1990; sponsored by IEEE
(NASA-TM-102569; E-5391; NAS 1.15:102569) Avail: NTIS HC A02/MF A01 CSCL 10B

Space Station Freedom is described with special attention given to its electric power system. The photovoltaic arrays, the battery energy storage system, and the power management, and distribution system are also discussed. The current design of Freedom's power system and the system requirements, trade studies, and competing factors which lead to system selections are referenced. This will be the largest power system ever flown in space. This system represents the culmination of many developments that have improved system performance, reduced cost, and improved reliability. Key developments and their evolution into the current space station solar array design are briefly described. The features of the solar cell and the array including the development, design, test, and flight hardware production status are given. Author

N90-21813*# Thiokol Corp., Brigham City, UT. Space Operations.
SHELF LIFE EXTENSION FOR THE LOT AAE NOZZLE SEVERANCE LSCS Final Test Report
M. Cook Apr. 1990 43 p
(Contract NAS8-30490)
(NASA-CR-183878; NAS 1.26:183878; TWR-50010) Avail: NTIS HC A03/MF A01 CSCL 21H

Shelf life extension tests for the remaining lot AAE linear shaped charges for redesigned solid rocket motor nozzle aft exit cone severance were completed in the small motor conditioning and firing bay, T-11. Five linear shaped charge test articles were thermally conditioned and detonated, demonstrating proper end-to-end charge propagation. Penetration depth requirements were exceeded. Results indicate that there was no degradation in performance due to aging or the linear shaped charge curving process. It is recommended that the shelf life of the lot AAE nozzle severance linear shaped charges be extended through January 1992. Author

23 CHEMISTRY AND MATERIALS (GENERAL)

No abstracts in this category.

24 COMPOSITE MATERIALS

Includes physical, chemical, and mechanical properties of laminates and other composite materials.
For ceramic materials see *27 Nonmetallic Materials.*

N90-21814 Massachusetts Univ., Amherst.
INTERFACIAL STUDIES IN FIBER-REINFORCED THERMOPLASTIC-MATRIX COMPOSITES Ph.D. Thesis
Richard L. Brady 1989 121 p
Avail: Univ. Microfilms Order No. DA9001485

Structure/property relationships in fiber-reinforced thermoplastic-matirix composites are stressed. Effort was focused on the interface: interfacial crystallization and fiber/matrix adhesion. Included are investigations on interfacial nucleation and morphology, measurement of fiber/matrix adhesion, effects of interfacial adsorption and crystallization of fiber/matrix adhesion, and composites reinforced with thermotropic liquid crystal copolyester fibers. Crystallization of a copolyester and poly (butylene terephthalate) with glass, carbon, or aramid fibers was studied with regard to interfacial morphology. Techniques employed included hot-stage optical microscopy and differential scanning calorimetry. In order to better monitor fiber/matrix adhesion, a buckled plate test was developed. The test measures transverse toughness as the parameter characterizing interfacial adhesion in unidirectional, continuous-fiber composites. The test is simple to perform yet has advantages over other interfacial evaluation techniques. The buckled plate test was found to be a sensitive measure of fiber/matrix adhesion. The buckled plate test was used along with the transverse tensile test to examine how interfacial adsorption and crystallization affect fiber/matrix adhesion in polycarbonate/carbon fiber composites. Studies of the fiber/matrix interface were extended to composites reinforced with thermotropic liquid crystal copolyester fibers. Poor fiber transverse properties rather than fiber/matrix adhesion appear to limit composite transverse properties. Author

N90-21815 Reading Univ. (England).

RESIDUAL STRESSES IN LAMINATED THERMOPLASTIC MATRIX COMPOSITES Ph.D. Thesis

Adrian Timothy Parkyn 1988 207 p
Avail: Univ. Microfilms Order No. BRDX86647

Residual stresses appear in composite laminates as a consequence of the differences in the thermoelastic properties of the fiber and the matrix and the temperature excursion involved during fabrication. These stresses may cause out-of-plane deformation and reduction in laminate strength. The stress distribution in the laminate is a function of stacking sequence and orientation of the plies. Laminates were fabricated from the APC-2 carbon fiber/PEEK composite system with a variety of stacking sequences. In the majority of the work cross-ply laminates were used in order to maximize the residual stresses; a number of angle ply laminates were also constructed with the laminae oriented at 45 deg to the principal laminate direction. Predictions based on classical lamination theory were compared to the levels of residual stress measured by a variety of techniques involving laminate curvature and residual strength. The results obtained indicate that the predictions are accurate provided the changes in thermoelastic properties with temperature are taken into account. The time dependences of the residual stress was studied; it was found that residual stress relaxation in a laminate can be predicted from the relaxation rate of a unidirectional laminate by making use of lamination theory. Effective means were found to accelerate the rate at which stress relaxation occurs in either laminates or single components. Residual stresses on a micro-laminar scale lead to fiber buckling with consequent reduction in both tensile and comprehensive strength. By the use of models the factors which affect buckling in single fibers were studied and related to the phenomena observed in APC-2 mouldings. Also, estimates were made of the stresses causing buckling in APC-2. Dissert. Abstr.

N90-21816 Northwestern Univ., Evanston, IL.

DEVELOPMENT OF ULTRASONIC NONDESTRUCTIVE METHODS FOR DEFECT AND DAMAGE CHARACTERIZATION IN COMPOSITE MATERIALS Ph.D. Thesis

Shi-Chang Wooh 1989 216 p
Avail: Univ. Microfilms Order No. DA9001889

Quantitative ultrasonic methods were studied and developed for detection and characterization of defects in graphite/epoxy after fabrication and inservice. Several types of defects were investigated: embedded film patch in a quasi-isotropic laminate, impact damage in a quasi-isotropic laminate, matrix cracking due to static loading of a crossply laminate, fatigue damage in a crossply laminate, thermally induced cracks in a thick crossply laminate, fabrication defects in thick unidirectional laminates including inclusions, interlaminar grease spots, fiber fractures, and porosity. Computer-aided digital data acquisition and processing was developed and used for acoustic imaging. Image enhancement techniques, such as mapping and contrast stretching, median filtering, histogram equalization, thresholding, sharpening, one-dimensional segmentation, and log operation, were developed and used as needed. Comprehensive characterization of the damage state was possible by constructing a perspective three-dimensional image of defects. Echos were detected to determine the location of flaws and the storage requirement of the huge database was reduced by the use of a data compression and pattern recognition scheme. There is no method which can be adequately used with certainty for all configurations. Therefore, test procedures and standards must be developed and tailored to meet specific needs by considering the material, geometry, type of damage, or failure mechanism. Dissert. Abstr.

N90-21817*# Mississippi State Univ., Mississippi State. Dept. of Chemical Engineering.

PROCEEDINGS OF THE ADVISORY COMMITTEE ON STANDARDIZATION OF CARBON-PHENOLIC TEST METHODS AND SPECIFICATIONS

William B. Hall 1 Apr. 1990 200 p Meeting held in Tempe, AZ, 16 Nov. 1989
(Grant NAG8-545)
(NASA-CR-186478; NAS 1.26:186478) Avail: NTIS HC A09/MF A02 CSCL 11D

Topics addressed include: Polyacrylonitrile (PAN) activity; low fired PAN fiber program review; carbon fabric oxidation mass loss; gel permeation chromatography (GPC) test methodology; carbon assay testing; and NAR rayon yarn specifications. For individual titles, see N90-21818 through N90-21819.

N90-21818*# National Aeronautics and Space Administration. Marshall Space Flight Center, Huntsville, AL.

DEVELOPMENT OF LOW THERMAL CONDUCTIVITY PAN-BASED CARBON FIBERS FOR SOLID ROCKET MOTOR NOZZLE APPLICATIONS

R. Clinton and Pat C. Pinoli (Lockheed Missiles and Space Co., Palo Alto, CA.) *In* Mississippi State Univ., Proceedings of the Advisory Committee on Standardization of Carbon-Phenolic Test Methods and Specifications 1 Apr. 1990 24 p (For primary document see N90-21817 15-24)
Avail: NTIS HC A09/MF A02 CSCL 11D

The program plan for the development of low thermal conductivity PAN-based carbon fibers is presented and is separated into two phases. During the first phase, fiber trials are to be conducted by the participating carbonizers and two candidate fiber types are to be supplied by each. Fibers will be characterized and composite test articles constructed and tested in forty pound charge motor firings. From these results, the number of candidates will be reduced to five for further characterization in the second phase. In Phase 2, screening level mechanical and thermal properties will be generated. Carbon phenolic test articles will be fabricated using each of the selected fibers for performances testing in the MSFC Testbed's 2 inch throat solid rocket motor. Candidates will be ranked according to the results from those tests. The results will be compared to those generated on the PAN-based ablatives currently being evaluated under SPIP Subtask 3.2.1.3 to determine whether any candidates merit further evaluation. The influence of process temperature on critical properties of PAN-based carbon fibers is discussed and historical data is presented. The derived technical requirements for the development of low thermal conductivity PAN-based carbon fibers and the fiber characterization test methodologies are described. Author

N90-21819*# National Aeronautics and Space Administration. Marshall Space Flight Center, Huntsville, AL.

TESTING CARBON FABRIC FOR OXIDATION MASS LOSS

William B. Hall, Lou Ann Fikes, and Pat C. Pinoli (Lockheed Missiles and Space Co., Palo Alto, CA.) *In* Mississippi State Univ., Proceedings of the Advisory Committee on Standardization of

Carbon-Phenolic Test Methods and Specifications 1 Apr. 1990
7 p (For primary document see N90-21817 15-24)
Avail: NTIS HC A09/MF A02 CSCL 11D

Rayon based carbon fabric was studied to assess reactivity to air oxidation/gasification. Excessive laboratory variability of mass loss data by conventional thermal gravimetric analysis mandated a more fundamental approach to determine the sensitivity factors which influence the gasification process. Reaction activation energy and pre-exponential factor derived from the Arrhenius equation were used to assess the role of fabric firing temperature and Na catalytic action. Low temperature oxidation (400 to 500 C) was found to be most strongly influenced by Na catalytic action. At 400 C the oxidation rate was increased by 681 percent by 2,240 ppm Na. The presence of water soluble Na anion significantly reduced the reaction activation energy from 34 to 21 Kcal/mole. The effect of firing temperature shifted the pre-exponential factors progressively from 2.49 x 10(exp 6) to 2.63 x 10(exp 3) g/g-sec after 2,500 C heat treatment. The Arrhenius temperature dependency was also used to assess laboratory to laboratory variances. Reaction rate data generated at ICI Fiberite, Tempe, Arizona, and Lockheed Research was found to deviate by 13 C, when compared at 525 C isothermal temperature. Author

N90-21820 Virginia Polytechnic Inst. and State Univ., Blacksburg.
STRENGTH IN NOTCHED AND IMPACT-DAMAGED LAMINATES Ph.D. Thesis
Mohamad Samih El-Zein 1989 84 p
Avail: Univ. Microfilms Order No. DA9003589

The strength of notched and impact damaged laminates was studied. The solution for a place containing an elliptic opening and inclusion was used as given by Lekhnitskii. The solution for the infinite plate, combined with laminate analysis to determine the ply stresses, and the average stress criterion proposed by Whitney and Nuismer were used to predict the notched strength. However, unlike Whitney and Nuismer, the average stress criterion was used at the ply level. The strength of off-axis unidirectional laminates was predicted by using a matrix oriented failure criterion applied at a critical point on the boundary of the hole. A good agreement between the experimental and predicted data was obtained. On the other hand, an attempt made to predict the notched strength of angle-ply laminates was not as successful. This is believed to be due to the different failure modes existing among different (+/- theta) sub s laminates. The controversy on whether the characteristic dimension is a material or geometric property, together with the belief that the physics of fracture of composites is better represented at the ply level, was the motivation to seek an invariant equation which describes the dependence of the characteristic dimension, D(sub o). A quantitative approach to determine the characteristic dimension in the average stress criterion was proposed. A good agreement between experimental and predicted data was found. It was also found that contrary to prior claims, the value of D(sub o) does not depend on the diameter of the hole, when used at the ply level. The tensile strength after impact (TSAI) was investigated. An approach based on modeling the delaminated area as an elliptic inclusion was used. Dissert. Abstr.

N90-21821*# National Aeronautics and Space Administration. Lewis Research Center, Cleveland, OH.
COMPUTATIONAL SIMULATION OF STRUCTURAL FRACTURE IN FIBER COMPOSITES
Christos C. Chamis and P. L. N. Murthy 7 Feb. 1990 20 p
Presented at the 8th Conference on Fibrous Composites in Structural Design, Norfolk, VA, 28 Nov. - 1 Dec. 1989; sponsored in part by DOD and FAA
(NASA-TM-102505; E-5307; NAS 1.15:102505) Avail: NTIS HC A03/MF A01 CSCL 11D

A methodology was developed for the computational simulation of structural fracture in fiber composites. This methodology consists of step-by-step procedures for mixed-mode fracture in generic components and an integrated computer code, Composite Durability Structural Analysis (CODSTRAN). The generic types of composite structural fracture include: (1) single and combined mode fracture in beams; 2) laminate free-edge delamination fracture; and (3) laminate center flaw progressive fracture. Structural fracture is identified by rapid changes in one or all of the following: (1) displacements, (2) frequencies, (3) the buckling loads, or (4) the strain energy release rate. These rapid changes are herein assumed to denote imminent structural fracture. Based on these rapid changes, parameters are identified which can be used as guidelines for structural fracture, inspection intervals and retirement for cause. Author

N90-21822* National Aeronautics and Space Administration. Langley Research Center, Hampton, VA.
IMPACT TOLERANT MATERIAL Patent
Joseph S. Heyman, inventor (to NASA) 27 Mar. 1990 7 p
Filed 15 Mar. 1989
(NASA-Case-LAR-12887-3; US-Patent-4,911,062; US-Patent-Appl-SN-323236; US-Patent-Class-89-36.02; US-Patent-Class-181-286; US-Patent-Class-181-290) Avail: US Patent and Trademark Office CSCL 11D

A material is protected from acoustic shock waves generated by impacting projectiles by means of a backing. The backing has an acoustic impedance that efficiently couples the acoustic energy out of the material.
Official Gazette of the U.S. Patent and Trademark Office

N90-21823# Oak Ridge National Lab., TN.
MECHANICAL PROPERTIES OF CARBON-IMPLANTED NIOBIUM
S. J. Zinkle and J. S. Huang (Lawrence Livermore National Lab., CA.) 1990 6 p Presented at the Spring Meeting of the Materials Research Society, San Francisco, CA, 16-21 Apr. 1990
(Contract DE-AC05-84OR-21400)
(DE90-009864; CONF-900466-8) Avail: NTIS HC A02/MF A01

Polycrystalline niobium specimens were implanted with either 200 keV carbon ions or a combination of 50, 100, and 200 keV carbon ions to peak concentrations of 0.6 to 50 at. (percent). Microindentation techniques were used to measure the hardness and elastic modulus of the implanted layer. Both the hardness (H) and modulus (E) showed dramatic increases due to the carbon implantation. The measured peak hardness and modulus following uniform implantation with 16 at. percent C were 15 times and 3 times that of niobium, respectively, which is comparable to the literature values for NbC. The peak hardness and modulus for the implanted specimens were observed at an indent depth of approximately 40 nm, which is about one-eighth of the depth of the implanted carbon layer. The decrease in the indentation mechanical properties at deeper indent depths is due to the interaction of long-ranging strain fields underneath the indenter with the niobium substrate. DOE

N90-21824*# National Aeronautics and Space Administration. Lewis Research Center, Cleveland, OH.
METCAN VERIFICATION STATUS
Christos C. Chamis, J. J. Caruso, H.-J. Lee, and P. L. N. Murthy May 1990 16 p
(NASA-TM-103119; E-5443; NAS 1.15:103119) Avail: NTIS HC A03/MF A01 CSCL 11D

The status of the verification (comparisons of predictions with experimental data) of the METCAN (METal-matrix Composite ANalyzer) code at high temperature is summarized. Verification includes select available room temperature of W/Cu composites for different fiber volume ratios. It also includes high temperature properties for thermal expansion, moduli, strength and stress/strain behavior for SiC/Ti composites. Furthermore it includes limited cases for thermal fatigue strength degradation. The verification results summarized herein indicate that METCAN simulates complex high temperature metal matrix composite bahavior with reasonable accuracy and that it can be used with confidence to identify in-situ nonlinear behavior that influences composite properties. Author

N90-21825*# National Aeronautics and Space Administration. Lewis Research Center, Cleveland, OH.

PROGRESSION OF DAMAGE AND FRACTURE IN COMPOSITES UNDER DYNAMIC LOADING

Levon Minnetyan (Clarkson Univ., Potsdam, NY.), Pappu L. N. Murthy, and Christos C. Chamis 1990 17 p Presented at the 31st Structures, Structural Dynamics, and Materials Conference, Long Beach, CA, 2-4 Apr. 1990; cosponsored by AIAA, ASME, ASCE, AHS, and ASCE Previously announced in IAA as A90-29318
(NASA-TM-103118; E-5442; NAS 1.15:103118) Avail: NTIS HC A03/MF A01 CSCL 11D

A new computational simulation method is presented to evaluate the dynamic aspects of composite structural response and durability that have not been simulated previously. Composite structural behavior under any loading condition, geometry, composite system, laminate configuration, and boundary conditions can now be simulated. Structural degradation, delamination, fracture, and damage propagation are included in the simulation. An angle-plied composite plate structure under normal impact loading is used as an example to demonstrate the versatility of the simulation method. Author

N90-21826*# National Aeronautics and Space Administration. Lewis Research Center, Cleveland, OH.

MATRIX DENSITY EFFECTS ON THE MECHANICAL PROPERTIES OF SiC/RBSN COMPOSITES

Ramakrishna T. Bhatt (Army Aviation Systems Command, Cleveland, OH.) and James D. Kiser 1990 17 p Presented at the 14th Annual Conference on Composites and Advanced Ceramics, Cocoa Beach, FL, 14-17 Jan. 1990; sponsored by American Ceramic Society
(NASA-TM-103098; E-5306; NAS 1.15:103098; AVSCOM-TR-90-C-008) Avail: NTIS HC A03/MF A01 CSCL 11D

The room temperature mechanical properties were measured for SiC fiber reinforced reaction-bonded silicon nitride composites (SiC/RBSN) of different densities. The composites consisted of approx. 30 vol percent uniaxially aligned 142 micron diameter SiC fibers (Textron SCS-6) in a reaction-bonded Si3N4 matrix. The composite density was varied by changing the consolidation pressure during RBSN processing and by hot isostatically pressing the SiC/RBSN composites. Results indicate that as the consolidation pressure was increased from 27 to 138 MPa, the average pore size of the nitrided composites decreased from 0.04 to 0.02 microns and the composite density increased from 2.07 to 2.45 gm/cc. Nonetheless, these improvements resulted in only small increases in the first matrix cracking stress, primary elastic modulus, and ultimate tensile strength values of the composites. In contrast, HIP consolidation of SiC/RBSN resulted in a fully dense material whose first matrix cracking stress and elastic modulus were approx. 15 and 50 percent higher, respectively, and ultimate tensile strength values were approx. 40 percent lower than those for unHIPed SiC/RBSN composites. The modulus behavior for all specimens can be explained by simple rule-of-mixture theory. Also, the loss in ultimate strength for the HIPed composites appears to be related to a degradation in fiber strength at the HIP temperature. However, the density effect on matrix fracture strength was much less than would be expected based on typical monolithic Si3N4 behavior, suggesting that composite theory is indeed operating. Possible practical implications of these observations are discussed. Author

N90-21827# Oxford Univ. (England). Dept. of Engineering Science.

MODELLING OF THE IMPACT RESPONSE OF FIBRE-REINFORCED COMPOSITES Progress Report No. 6

Y. L. Li (Northwestern Polytechnical Univ., Xian, China), C. Ruiz, and J. Harding 1989 131 p
(Grant AF-AFOSR-0129-87)
(OUEL-1784/89; ETN-90-96412) Avail: NTIS HC A07/MF A01

Progress during the 2nd year of a 3 year program is reported. Results on an extended series of tensile impacts on hybrid carbon/glass and carbon/Kevlar laminates are given. A testing technique for determining the effect of strain rate on interlaminar shear strength in composite materials was developed and results are observed. Theoretically, the stress distribution in a hybrid carbon/glass tensile specimen was determined using the ABAQUS finite element package. Observations are detailed. A finite element analysis of the stress distribution around the specimen/loading-bar interface shows the present rectangular ended design of loading-bar to be as good as any of the more refined geometries studied. ESA

N90-21828# Oxford Univ. (England). Dept. of Engineering Science.

FAILURE ANALYSIS OF WOVEN HYBRID COMPOSITE USING A FINITE ELEMENT METHOD

Y. L. Li (Northwestern Polytechnical Univ., Xian, China), C. Ruiz, and J. Harding 1989 40 p
(Grant AF-AFOSR-0129-87)
(OUEL-1791/89; ETN-90-96416) Avail: NTIS HC A03/MF A01

A finite element method is used to determine the stress and strain distribution around a failure link in a carbon reinforced ply in a woven carbon/glass laminate under tensile loading. On the assumption that delamination follows this initial tensile failure in a carbon link, the new stress and strain distribution is determined. The effect of stacking sequence on the failure of a woven hybrid laminate is discussed. ESA

N90-21829 Purdue Univ., West Lafayette, IN.

ENERGY RELEASE RATE ANALYSIS OF INTERFACIAL CRACKS IN COMPOSITES Ph.D. Thesis

Muthuswamy Ganapathy Manoharan 1989 107 p
Avail: Univ. Microfilms Order No. DA9008661

Analytical methods were developed to study the basic nature of the coupled opening, in-plane shearing, and antiplane shearing fracture behavior of an interfacial crack between two anisotropic media. Mode 1, Mode 2, and Mode 3 strain energy release rates for a crack lying along the interface of two anisotropic solids subjected to uniform axial strain are investigated using integral transform method and also by the finite element method. It is shown that due to violent oscillatory crack tip behavior, the strain energy release rates for Modes 1, 2, and 3 do not converge to definite values. However the total energy release rate is well defined. A method for separating the effective strain energy release rates for three fracture modes is suggested. A particular case of an interfacial crack between two orthotropic solids subjected to uniform tensile and shear stresses is also studied. Tests were performed to study the growth of delamination cracks due to bending in a graphite/epoxy (90(5)/0(5)/90(5)). A closed form expression for energy release rate is obtained using laminate plate theory and is compared with the finite element analysis result. These results combined with the experimentally determined critical load are used to calculate the critical energy release range G(sub c). Critical energy release rate is also determined experimentally using compliance method. Dissert. Abstr.

N90-21830 Purdue Univ., West Lafayette, IN.

THE CONTROLLED-DAMAGE CONCEPT IN DESIGN OF LAMINATED COMPOSITES Ph.D. Thesis

Timothy Lee Norman 1989 186 p
Avail: Univ. Microfilms Order No. DA9008672

Laminated composites are highly susceptible to foreign object impact damage. One common form of impact damage is delamination. An attempt to control delamination, referred to as the controlled damage concept (CDC), uses adhesive strips at the 0/90 graphite/epoxy composite interface. The concept is demonstrated through high velocity impact tests, which show that delamination is substantially reduced when adhesive is used. The effect of the CDC on stiffness and notched and unnotched strength is investigated. A micromechanical model developed for stiffness predictions of CDC composites is found in good agreement with experimentally obtained mechanical properties. Interlaminar fracture toughness of composites with adhesive is investigated through the use of a nonlinear quasi static analytical beam model developed. The critical strain energy release rate G(sub)c determined from the beam model using static crack growth data, indicates substantial increases in G(sub)c for CDC composites. Critical load and crack growth data obtained from instrumented drop impact tests verify the use of the model for low velocity impact problems where contact times are large. Dissert. Abstr.

25 INORGANIC AND PHYSICAL CHEMISTRY

Includes chemical analysis, e.g., chromatography; combustion theory; electrochemistry; and photochemistry.

For related information see also *77 Thermodynamics and Statistical Physics.*.

N90-21831 Northwestern Univ., Evanston, IL.
STUDIES ON REACTIVE FLOWS Ph.D. Thesis
Wen-Jenn Sheu 1989 114 p
Avail: Univ. Microfilms Order No. DA9001868

Theoretical, numerical and experimental studies are presented on the upstream interactions between premixed flamelets in turbulent combustions, the effect of centrifugal acceleration due to the rotation on Bunsen flames, extinction of counterflow diffusion flames in a counter-rotating finite jet, and nonplanar flame configurations in stagnation point flow. The processes during the upstream flame interactions are numerically investigated using two ozone decomposition planar flames propagating towards each other. The flame temperature and speed during the whole interaction process are also analyzed. One basic kind of rotational effects on the shape and stability of the premixed flames stabilized in Bunsen burner is theoretically and experimentally studied. The relation between the flame stabilization by the burner rim and rotation across the flame is examined. In addition the stable and unstable flame configuration are identified. In the study of the extinction characteristics of diffusion flames in opposed-jet flows with angular velocities which are equal in magnitude but opposite in directions, the extinction characteristics with vorticity in the flow were explored. The general configurations of premixed flame fronts in a stagnation point flow is pursued. Some flame shapes other than planar flames were verified. A simple mathematical model is given to provide the explicit expressions of flame fronts. The implications of these studies to the modeling of turbulent combustion are discussed. Dissert. Abstr.

N90-21832# Massachusetts Univ., Amherst. Dept. of Chemical Engineering.
MOLECULAR THEORY OF FLUID PHASE EQUILIBRIA Final Report, 1 Jan. 1986 - 30 Jun. 1989
Peter A. Monson 21 Aug. 1989 48 p
(Contract GRI-5086-260-1223)
(PB90-131277; GRI-89/0183) Avail: NTIS HC A03/MF A01 CSCL 07D

A statistical mechanical theory that predicts the contributions to the structure and thermodynamics of fluids arising from multipolar interactions or other long ranged forces in the presence of nonspherical molecular shape was developed. Fluid phase diagrams were determined for single component diagrams for fluids modeled with site-site Lennard-Jones 12-6 potentials. The results were used to show how molecular shape effects determine departures from corresponding states. The phase diagrams of diatomic molecules with dipole-dipole interactions were also studied. Increasing the dipole moment in common with increased nonspherical molecular shape increased departures from corresponding states. However, polarity and nonspherical molecular shape are coupled in a nontrivial manner and the effects on the phase diagram are not additive. The theory was extended to mixtures. A preliminary study of the role played by molecular shape differences in determining excess properties was made along with a study of the vapor-liquid critical lines for binary mixtures of spherical and nonspherical molecules using the Ornstein-Zernike and Site-site Ornstein-Zernike equations in the Percus-Yevick approximation. A study was begun of the properties of dilute solutions using distribution function theories. Calculations of the infinite dilution partial molar volume and distribution functions for binary Lennard-Jones 12-6 mixtures with one component at infinite dilution were made. Author

N90-21833# Oak Ridge National Lab., TN. Chemical Technology Div.
PHOTOSYNTHETIC WATER SPLITTING, PHASE 2 Final Report, Feb. 1984 - Jun. 1989
E. Greenbaum Sep. 1989 28 p
(Contracts GRI-5083-260-0880; DE-AC05-84OR-21400)
(PB90-132671; ORNL/TM-11302; GRI-89/0255) Avail: NTIS HC A03/MF A01 CSCL 07D

The key conclusion is that the concept of producing hydrogen fuel via microalgal water splitting is scientifically sound. From an economic and engineering point of view, however, key problems associated with the method of fuel production are costs of the photobiological reactors and separation of the hydrogen fuel from other product gases such as oxygen. Additional basic research in the area is also needed to address the problem of the photo-response of the system at high solar irradiances. High solar energy conversion efficiencies of production of molecular hydrogen are observed in the linear low-intensity region of the light-saturation curve of photosynthesis but decrease significantly at high irradiances. A logical course of action based on results derived from the exploratory basic research project would focus in two areas of applied research and one area of basic research. The applied research should be in the areas of photobiological reactor design and development and separations technology for the separation of stoichiometric ratios of hydrogen and oxygen. Basic research should focus on the nature of the light-saturation processes of photosynthesis. Author

N90-21834# California Univ., Berkeley. Dept. of Mechanical Engineering.
FIRE PROPAGATION IN CONCURRENT FLOWS Final Progress Report, 1 Aug. 1988 - 31 Jul. 1989
A. C. Fernandez-Pello Dec. 1989 26 p
(Grant NIST 60NANB-7-D0737)
(PB90-151754; NIST/GCR-89/569) Avail: NTIS HC A03/MF A01 CSCL 21B

A research program is being carried out to study the mechanisms controlling the spread of fire in a forced gas flow. Particular emphasis is given to the case when the gas flow is concurrent with the direction of fire spread. The research tasks completed include an experimental study of the effect of the flame spread rate of the turbulence intensity of a concurrent air flow, and a theoretical analysis of the effect of a prescribed gas velocity profile on the flame spread rate predictions. The results of the experiments show that for flames spreading over thick PMMA sheets, the flame spread process is significantly affected by the show turbulence intensity. For a fixed flow velocity, the flame spread rate decreases as the turbulent intensity is increased. This appears to be mainly due to the shortening of the flame length. Schlieren images of the process indicate that the decrease of the flame length may be the result of the intense entrainment of cold air in the flame at the higher turbulent intensities. The results of the theoretical analysis indicate that the gas velocity profile influences strongly the flame spread rate predictions. GRA

N90-21835 New South Wales Univ., Kensington (Australia). School of Chemistry.
PRODUCTION AND ANALYSIS BY MASS SPECTROMETRY OF BEAMS OF POLYGLYCOL IONS Abstract Only Ph.D. Thesis
Muljadji Agma Mar. 1989 2 p
Avail: Issuing Activity

Successful field desorption mass spectrometry necessarily requires a reliable means of production of activated field desorption emitters. That is to say, the ability to reliably grow carbonaceous microneedles on the thin filament wire surface of the emitter. For some time the standard activated emitters, which were constructed from 10 micron diameter tungsten wire, have demonstrated their usefulness over other types of emitters. The need however for more robust emitters in high acceleration potential experiments designed to study the collision dynamics of multiatomic ions has stimulated the development and application of larger diameter filament wires in the emitters. The method of production and application of new 25 micron wire emitters, as well as the standard 10 micron wire emitter are presented. Additional features of the larger wire emitters is that they generate more intense ion beams as well as show increased periods of ion field desorption. These last two features have facilitated repetitive scans in the mass-analyzed ion kinetic energy experiments which has led to more reliable and reproducible results. A final observation is that the larger wire emitters generally reduce the amount of fragmentation of the polymer ions in the field desorption experiments. The production and analysis of several field desorbed polyglycol ions including polyethylene glycols up to a nominal mass-average molecular mass of 3400 u and polypropylene glycols up to a nominal mass-average molecular mass-average of 4000 u were studied using a large double focussing mass spectrometer. The emitter potential spectra, mass spectra, and unimolecular as well as collision-induced decomposition spectra are presented. The results show that the field desorption of the polyglycol polymers depends upon several parameters such as the morphology of the emitter, the chemical and physical, as well as, the electrical properties of the sample. Analysis of the polyglycol mass spectra and the mass-analyzed ion kinetic energy spectra, obtained with and without the presence of a collision gas, has allowed the information of numerous fragmentation pathways as well as the prediction of the relative stability of the polyglycol ions. Author

N90-21836*# National Aeronautics and Space Administration. Marshall Space Flight Center, Huntsville, AL.

THE TEMPERATURE VARIATION OF HYDROGEN DIFFUSION COEFFICIENTS IN METAL ALLOYS

M. D. Danford Apr. 1990 18 p
(NASA-TM-100397; NAS 1.15:100397) Avail: NTIS HC A03/MF A01 CSCL 07D

Hydrogen diffusion coefficients were measured as a function of temperature for a few metal alloys using an electrochemical evolution technique. Results from these measurements are compared to those obtained by the time-lag method. In all cases, diffusion coefficients obtained by the electrochemical method are larger than those by the time-lag method by an order of magnitude or more. These differences are attributed mainly to hydrogen trapping. Author

N90-21837# Rice Univ., Houston, TX.

INFRARED ABSORPTION SPECTROSCOPY AND CHEMICAL KINETICS OF FREE RADICALS Progress Report

Robert F. Curl and Graham P. Glass Mar. 1990 6 p
(Contract DE-FG05-85ER-13439)
(DE90-009469; DOE/ER-13439/5) Avail: NTIS HC A02/MF A01

Research on reactions of free radicals continued. Progress is briefly described in the following areas: (1) pressure effects in reactions of C2H with CO and C2H6: rate constants; (2) NO HNO produced in the thermal DeNOx process; and (3) product branching ratios for NH2 and NO between 300 and 1200 K. DOE

N90-21838# Lawrence Livermore National Lab., CA.

A COMPARISON OF THE AUTOIGNITION CHEMISTRY OF n-BUTANE AND ISOBUTANE IN AN INTERNAL COMBUSTION ENGINE

R. D. Wilk, R. M. Green, W. J. Pitz, C. K. Westbrook, S. Addagarla, D. L. Miller, and N. P. Cernansky 1990 19 p Presented at the Annual Society of Acoustical Engineers Congress, Detroit, MI, 26 Feb. - 2 Mar. 1990
(Contracts W-7405-eng-48; DE-FG04-87AL-44658)
(DE90-009474; UCRL-102784; CONF-900282-3) Avail: NTIS HC A03

Butane is the simplest alkane fuel for which more than a single structural isomer is possible. N-butane and isobutane are used in a test engine to examine the importance of molecular structure in determining knock tendency, and the experimental results are interpreted using a detailed chemical kinetic model. A sampling valve was used to extract reacting gases from the combustion chamber of the engine. Samples were withdrawn at different times during the engine cycle, providing concentration histories of a wide variety of reactant, olefin, carbonyl, and other intermediate and product species. The chemical kinetic model predicted the formation of all the intermediate species measured in the experiments. The agreement between the measured and predicted values is mixed and is discussed. Calculations show that RO2 isomerization reactions are more important contributors to chain branching in the oxidation of n-butane than in isobutane. Chain branching in isobutane oxidation is dependent on H-atom abstraction reactions involving HO2 and CH3O2 radicals that occur at higher temperatures than RO2 isomerization reactions. Therefore, an isobutane mixture must be raised to a higher temperature than a n-butane mixture to achieve the same overall rate of reaction. DOE

N90-21839# Lawrence Livermore National Lab., CA.

TRANSIENT EFFECTS IN BRILLOUIN GAIN SPECTROSCOPY IN SOLIDS

Gregory W. Faris, Leonard E. Jusinski, Mark J. Dyer, William K. Bischel, and A. Peet Hickman (SRI International Corp., Menlo Park, CA.) 7 Dec. 1989 7 p
(Contract W-7405-eng-48)
(DE90-009476; UCRL-CR-103294; MP-89-227) Avail: NTIS HC A02/MF A01

Transient effects on Brillouin gain spectroscopy in solids are examined. A method for accurate measurements of Brillouin peak gain coefficients and linewidths valid in the transient regime is described. Detailed measurements in crystals are presented. DOE

N90-21840# Lawrence Livermore National Lab., CA.

HIGH RESOLUTION STIMULATED RAMAN-BRILLOUIN SPECTROSCOPY IN GASES AND SOLIDS

William K. Bischel, Mark J. Dyer, Gregory W. Faris, A. Peet Hickman, and Leonard E. Jusinski (SRI International Corp., Menlo Park, CA.) Dec. 1989 4 p Sponsored by ONR
(Contract W-7405-eng-48)
(DE90-009535; UCRL-CR-103296) Avail: NTIS HC A02/MF A01

High resolution, quasi-cw, stimulated Raman-gain spectroscopy has become a standard technique for the study of molecular energy levels. In this paper we apply this technique to the study of two diverse problems: a determination of the ac Stark effect for the vibrational levels of H(sub 2), and a demonstration of the first high resolution stimulated Brillouin gain spectra in glasses and crystals. DOE

N90-21841# Lawrence Livermore National Lab., CA.

BRILLOUIN GAIN SPECTROSCOPY IN GLASSES AND CRYSTALS

Gregory W. Faris (SRI International Corp., Menlo Park, CA.) Dec. 1989 7 p
(Contract W-7405-eng-48)
(DE90-009536; UCRL-CR-103297) Avail: NTIS HC A02/MF A01

Gain spectroscopy is a well established technique for the study of nonlinear scattering phenomena. Several capabilities of gain spectroscopy make the technique very powerful for frequency domain measurements of scattering processes. The use of gain spectroscopy is illustrated by the application of the technique to Brillouin measurements in solids. DOE

N90-21842*# National Aeronautics and Space Administration. Lewis Research Center, Cleveland, OH.

DETAILED MECHANISM FOR OXIDATION OF BENZENE

David A. Bittker May 1990 32 p
(NASA-TM-102443; E-5224; NAS 1.15:102443) Avail: NTIS HC A03/MF A01 CSCL 07D

A detailed mechanism for the oxidation of benzene is presented and used to compute experimentally obtained concentration profiles and ignition delay times over a wide range of equivalence ratio and temperature. The computed results agree qualitatively with all the experimental trends. Quantitative agreement is obtained with several of the composition profiles and for the temperature dependence of the ignition delay times. There are indications, however, that some important reactions are as yet undiscovered in this mechanism. Recent literature expressions have been used for the rate coefficients of most important reactions, except for some involving phenol. The discrepancy between the phenol pyrolysis rate coefficient used in this work and a recent literature expression remains to be explained. Author

N90-21843*# National Aeronautics and Space Administration. Lewis Research Center, Cleveland, OH.
STUDIES ON THE USE OF SUPERCRITICAL AMMONIA FOR CERAMIC NITRIDE SYNTHESIS AND FABRICATION
Linda Cornell, Y. C. Lin (Case Western Reserve Univ., Cleveland, OH.), and Warren H. Philipp Apr. 1990 17 p
(NASA-TM-102570; E-4441; NAS 1.15:102570) Avail: NTIS HC A03/MF A01 CSCL 07D

The extractability of ammonia halides (including ammonium thiocyanate) formed as byproducts from the synthesis of Si(NH)2 via ammonolysis of the corresponding silicon tetrahalides using supercritical NH3 as the extraction medium was investigated. It was found that the NH4SCN byproduct of ammonolysis of Si(SCN)4 can be almost completely extracted from the insoluble Si(NH)2 forming a promising system for the synthesis of pure Si(NH)2, one of the best precursors for Si3N4. In addition it was found that Si3N4, AlN, BN, and Si(NH)2 are insoluble in SC ammonia. Also discussed are design considerations for a supercritical ammonia extraction unit. Author

N90-21844*# National Aeronautics and Space Administration. Lewis Research Center, Cleveland, OH.
ELECTROCHEMICAL IMPREGNATION AND CYCLE LIFE OF LIGHTWEIGHT NICKEL ELECTRODES FOR NICKEL-HYDROGEN CELLS
Doris L. Britton 1990 6 p Presented at the 34th International Power Sources Conference, Cherry Hill, NJ, 25-28 Jun. 1990; cosponsored by Army and IEEE
(NASA-TM-103140; E-5492; NAS 1.15:103140) Avail: NTIS HC A02/MF A01 CSCL 07D

Development of a high specific energy nickel electrode is the main goal of the lightweight nickel electrode program at NASA-Lewis. The approach was to improve the nickel electrode by continuing combined in-house and contract efforts to develop a more efficient and lighter weight electrode for the nickel-hydrogen cell. Lightweight plaques are used as conductive supports for the nickel hydroxide active material. These plaques are commercial products that are fabricated into nickel electrodes by electrochemically impregnating them with active material. The electrodes are life cycle tested in a low Earth orbit regime at 40 and 80 percent depths-of-discharge. Author

N90-21845# Technische Univ., Delft (Netherlands). Faculty of Aerospace Engineering.
THE PYROLYSIS OF POLYMETHYLMETHACRYLATE DURING COMBUSTION IN A SOLID FUEL COMBUSTION CHAMBER
J. P. deWilde Dec. 1987 80 p Revised Prepared in cooperation with Prins Maurits Lab. TNO, Rijkswijk, Netherlands
(LR-531; PML-1987-C142; SFCC-Publ-49; ETN-90-96376) Avail: NTIS HC A05/MF A01

Both experimental results and literature concerning polymethylmethacrylate pyrolysis are presented. The use of existing bulk pyrolysis equipment for the study of pyrolysis under combustion conditions is shown to be inadequate. Comparison of bulk pyrolysis results with pyrolysis results obtained under combustion conditions does not allow any definite conclusions to be drawn. The composition of pyrolysis products is shown to be pressure dependent. Measurement of surface temperature is carried out using crystals. The temperature appears to be higher than 850 K. Ways of quickly stopping the combustion are described. ESA

N90-21846# Technische Univ., Delft (Netherlands). Faculty of Aerospace Engineering.
SOLID FUEL COMBUSTION CHAMBER Progress Report No. 13, Jan. - Jun. 1988
H. Wittenberg, P. A. O. G. Korting, B. T. C. Zandbergen, ed., T. Wijchers, P. J. M. Elands, J. P. deWilde, and F. Dijkstra Oct. 1988 36 p Prepared in cooperation with Prins Maurits Lab. TNO, Rijswijk, Netherlands
(LR-562; PML-1988-C137; SFCC-Publ-55; ETN-90-96377) Avail: NTIS HC A03/MF A01

An update on the Solid Fuel Combustion Chamber (SFCC) project resources and project constraints is presented. Project management and organization are described. An overview of the activities carried out by the theoretical and experimental working groups is presented. Student involvement in the project is outlined. An overview of publications, reports, presentations and contacts is given. A general assessment of project status and an outline of the project's next half year period is presented. ESA

N90-21847# Technische Univ., Delft (Netherlands). Faculty of Aerospace Engineering.
SOLID FUEL COMBUSTION CHAMBER Progress Report No. 14, Jul. - Dec. 1988
H. Wittenberg, P. A. O. G. Korting, B. T. C. Zandbergen, ed., T. Wijchers, P. J. M. Elands, J. P. deWilde, and F. Dijkstra Apr. 1989 31 p Sponsored by Netherlands Technology Foundation; Organization for Applied Scientific Research; and Working Group for the Use of Supercomputers Prepared in cooperation with Prins Maurits Lab. TNO, Rijswijk, Netherlands
(LR-591; PML-1989-C67; SFCC-Publ-56; ETN-90-96379) Avail: NTIS HC A03/MF A01

An overview of the research carried out from July to December 1988 on the Solid Fuel Combustion Chamber (SFCC) project is presented. Management, finance and personnel of the project are discussed. The activities carried out by the theoretical and experimental working groups are described. Student involvement in the project is outlined. Utilization aspects of the project such as the granting of a European patent for the sonic control and measuring choke are presented. An overview of publications, reports, presentations and contacts is presented. The updated phase 2 of the project is described. ESA

N90-21848# Instituto de Pesquisas Espaciais, Sao Jose dos Campos (Brazil).
NUMERICAL SIMULATION MODEL OF HYDRAZINE ATTITUDE CONTROL THRUSTERS
Philippe R. B. Devloo and Sonia M. GomesdeG. Villalobos Nov. 1989 6 p Presented at the 10th Brazilian Congress of Mechanical Engineering, Rio de Janeiro, Brazil, 5-8 Dec. 1989
(INPE-4965-PRE/1534) Avail: NTIS HC A02/MF A01

The purpose is to simulate the physical and chemical phenomena associated with the decomposition of hydrazine over a catalytic bed. The mathematical model consists of the basic conservation laws, (mass, momentum, and energy) augmented with nonlinear terms corresponding to heat exchange, mass exchange, heat release, and friction. This model results in a set of one dimensional nonlinear partial differential equation (PDE) similar in nature to Euler equations for compressible fluid flow. The numerical algorithm used is finite element algorithm derived from the Streamline Upwind Petrov Galerkin (SUPG) method. Author

26 METALLIC MATERIALS

Includes physical, chemical, and mechanical properties of metals, e.g., corrosion; and metallurgy.

N90-21849*# Carnegie-Mellon Univ., Pittsburgh, PA.
THE EFFECT OF HYDROGEN AND MICROSTRUCTURE ON THE DEFORMATION AND FRACTURE BEHAVIOR OF A SINGLE CRYSTAL NICKEL-BASE SUPERALLOY Final Report Ph.D. Thesis
William S. Walston Apr. 1990 254 p

(Grant NAG3-463)
(NASA-CR-185219; NAS 1.26:185219) Avail: NTIS HC A12/MF A02 CSCL 11F

A study was conducted on the effects of internal hydrogen and microstructure on the deformation and fracture of a single crystal nickel-base superalloy. In particular, room temperature plane strain fracture toughness and tensile tests were performed on hydrogen-free and hydrogen charged samples of PWA 1480. The role of microstructure was incorporated by varying the levels of porosity and eutectic gamma/gamma prime through hot isostatic pressing and heat treatment. The room temperature behavior of PWA 1480 was unusual because precipitate shearing was not the primary deformation mechanism at all strains. At strains over 1 percent, dislocations were trapped in the gamma matrix and an attempt was made to relate this behavior to compositional differences between PWA 1480 and other superalloys. Another unique feature of the tensile behavior was cleavage of the eutectic gamma/gamma prime, which is believed to initiate the failure process. Fracture occurred on (111) planes and is likely a result of shear localization along these planes. Elimination of the eutectic gamma/gamma prime greatly improved the tensile ductility, but pososity had no effect on tensile properties. Large quantities of hydrogen (1.74 at. percent) were gas-phase charged into the material, but surprisingly this was not a function of the amount of porosity or eutectic gamma/gamma prime present. Desorption experiments suggest that the vast majority of hydrogen is at reversible lattice trapping sites. This large, uniform concentration of hydrogen dramatically reduced the tensile strain to failure, but only slightly affected the reduction in area. Available hydrogen embrittlement models were examined in light of these results and it was found that the hydrogen enhanced localized plasticity model can explain much of the tensile behavior. K(IC) fracture toughness tests were conducted, but it was necessary to also perform J(IC) tests to provide valid data. Author

N90-21850# Army Communications-Electronics Command, Fort Monmouth, NJ.

METHOD OF MAKING A CATHODE FROM TUNGSTEN POWDER Patent Application

Louis E. Branovich, inventor (to Army), Bernard Smith, inventor (to Army), Gerard L. Freeman, inventor (to Army), and Donald W. Eckart, inventor (to Army) 22 Jan. 1990 8 p
(AD-D014434; US-Patent-Appl-SN-468335) Avail: NTIS HC A02/MF A01 CSCL 09/1

This invention relates in general to a method of making a cathode for operation in microwave devices and in particular to a method of making a cathode for operation in microwave devices from tungsten powder using as an impregnant the product formed from adding about 1 mole of a member selected from the group consisting of zirconium, zirconium dioxide, hafnium, hafnium dioxide, uranium, uranium dioxide, titanium, and titanium dioxide to about 50 to about 100 moles of a compound selected from the group consisting of Ba3Al2O6, Ba3WO6, and Ba4Al2O7. GRA

N90-21851# Westinghouse Hanford Co., Richland, WA.

FRACTURE TOUGHNESS AND TENSILE PROPERTIES OF ALLOY HT9 IN THIN SECTIONS UNDER HIGH NEUTRON FLUENCES

F. H. Huang Mar. 1990 40 p Presented at the 15th Symposium on Effects of Radiation on Materials, Nashville, TN, 17-21 Jun. 1990
(Contract DE-AC06-87RL-10930)
(DE90-008386; WHC-SA-0475; CONF-900623-2) Avail: NTIS HC A03/MF A01

The effect of neutron radiation on the mechanical properties of alloy HT9 was evaluated by conducting postirradiation tensile and fracture toughness tests. Samples of HT9 were irradiated in the Experimental Breeder Reactor 2 (EBR-2) and Fast Flux Test Facility (FFTF) as part of material experiments. In addition, selected samples were obtained from a duct used in fuel pin tests in FFTF. The peak neutron fluence for these samples was 15.9 x 10(exp 22) n/sq cm (E is greater than 0.1 MeV), or about 80 dpa. Results of tests conducted at 205 C and at ambient temperature showed that the irradiation temperature had a larger influence on the mechanical behavior than neutron fluence. Irradiation at temperatures below 400 C produces a significant increase in the yield strength of HT9. At 360 C, an increase of more than 80 percent was found for tests conducted at ambient temperature. Tests on notched tensile specimens that had been irradiated at low temperature exhibited a linear elastic behavior with failure occurring with no yielding or elongation. DOE

N90-21852# Oak Ridge National Lab., TN. Metals and Ceramics Div.

WELDING BEHAVIOR AND WELDING METALLURGY OF DUCTILE INTERMETALLIC ALLOYS

S. A. David and M. L. Santella 1990 14 p Presented at the 1st United States-Japan Symposium on Advances in Welding Metallurgy, San Francisco, CA, 7-8 Jun. 1990
(Contract DE-AC05-84OR-21400)
(DE90-008908; CONF-9006149-1) Avail: NTIS HC A03/MF A01

Welding behavior and welding metallurgy of several ordered intermetallic alloys are reviewed comprehensively. Weldability of these alloys was found to be a strong function of composition, welding process and process parameters. Phase transformations associated with the weld thermal cycle play a critical role in determining the weldability of these alloys. Defect-free welds were produced in several of these alloys. DOE

N90-21853# Oak Ridge National Lab., TN. Metals and Ceramics.

THE EFFECT OF AGING AT 343 C ON TYPE 308 STAINLESS STEEL WELDMENTS

D. J. Alexander, K. B. Alexander, M. K. Miller, and R. K. Nanstad 1990 7 p Presented at the Pressure Vessels and Piping Conference: Be in Tune for the 90's, Nashville, TN, 17-21 Jun. 1990
(Contract DE-AC05-84OR-21400)
(DE90-009232; CONF-900617-7) Avail: NTIS HC A02/MF A01

The effect of long term aging at intermediate temperatures on the mechanical properties of stainless steel welds was studied. Three type 308 multipass shielded metal-arc welds with ferrite levels of 4, 8, and 12 percent were aged up to 343 C. Tensile tests showed little effect of aging on either the yield or ultimate tensile strengths, but the impact toughness was significantly degraded. The extent of the degradation increased with increasing ferrite content and increasing aging time. Examination of the microstructure with transmission electron microscopy and atom probe field-ion microscopy revealed that the ferrite phase had undergone spinodal decomposition as a result of aging. In addition, G-phase particles were observed at dislocations, and finer G-phase particles were homogeneously distributed throughout the ferrite phase. The changes in the mechanical properties and the fractography are discussed in light of the observed changes in the microstructure. DOE

N90-21854# California Univ., San Diego, La Jolla. Dept. of Applied Mechanics and Engineering Science.

MARTENSITIC TRANSFORMATION INDUCED BY STRESS PULSES Final Report

M. A. Meyers and G. Ravishandran Mar. 1990 5 p Prepared for Lawrence Livermore National Lab., CA
(Contract W-7405-eng-48)
(DE90-009534; UCRL-CR-103260) Avail: NTIS HC A02/MF A01

The objectives of this research program were to establish the preferential sites for martensite nucleation in ferrous alloys. A Fe-30 wt percent Ni alloy was used in this investigation. The tensile pulse technique was used to produce a short-duration tensile pulse that triggers the formation of martensite above M(sub s). The tensile pulse is produced by impact in a gas gun. DOE

N90-21855# Idaho National Engineering Lab., Idaho Falls.
MICROSTRUCTURE AND MECHANICAL PROPERTIES OF NICKEL ALUMINIDE POWDERS CONSOLIDATED BY EXTRUSION AND HOT ISOSTATIC PRESSING
R. N. Wright, J. R. Knibloe, and R. L. Williamson Jan. 1990 44 p
(Contract DE-AC07-76ID-01570)
(DE90-009777; EGG-MS-8865) Avail: NTIS HC A03/MF A01

The influence of alloying additions of iron and chromium, alone and in combination with molybdenum and zirconium, on the heat treatment response and mechanical properties of powder metallurgy Ni3 Al based materials consolidated by hot extrusion has been characterized in detail. Consolidation of the nickel aluminide powders by hot isostatic pressing (HIP) has been examined as an alternative to extrusion. Densification has been simulated using a model that describes consolidation by the additive effects of plastic flow, power-law creep, boundary diffusion, and Nabarro-Herring and Coble creep. The model has been used to develop maps that describe densification for any combination of time, temperature, and pressure. The best available material property data and parameters from experiments have been used to develop maps that describe HIP consolidation experiments with reasonable accuracy. Finite element models were developed as an extension of the HIP map approach to provide detailed simulations of particle deformation during densification. Preliminary results for both monosized and bimodal particle distributions indicate that this particle level approach is useful for simulating microstructural development resulting from different combinations of consolidation parameters. DOE

N90-21856# National Physical Lab., Teddington (England). Div. of Materials Applications.
VAMAS PROJECT ON VARIABLE WELD PENETRATION: SURFACE TENSION OF THE STEELS
R. F. Brooks and K. C. Mills Aug. 1989 17 p
(NPL-DMA(A)-188; ISSN-0143-7313; ETN-90-96435) Copyright Avail: NTIS HC A03/MF A01

Surface tension values were derived for casts of 304 and 316 stainless steels with both high and low sulfur contents for temperatures between 1570 to 1800 C. The results indicated that the high sulfur casts had low surface tension values and positive temperature coefficients whereas low sulfur casts had high surface tensions and negative coefficients. The plot of the coefficient as a function of the sulfur content of the steel indicated that the crossover from a negative to a positive coefficient occurred at a sulfur content of about 50 ppm. ESA

N90-21857 Purdue Univ., West Lafayette, IN.
THREE-DIMENSIONAL FATIGUE CRACK CLOSURE BEHAVIOR OF METALS Ph.D. Thesis
David Stanley Dawicke 1989 173 p
Avail: Univ. Microfilms Order No. DA9008596

The three-dimensional variation in plasticity induced fatigue crack closure behavior of metals is described. Experimental determination of the plasticity induced fatigue crack closure behavior of 2024-T351 aluminum was made using fatigue striations, strain gages, and displacement gages. A three-dimensional elastic finite element analysis was conducted to calculate the three-dimensional fatigue crack closure behavior. The experimental measurements and the finite element calculations indicate that, for metals, a significant three-dimensional variation in plasticity induced fatigue crack closure behavior exists. Near the surface, where the stress state was plane stress, high crack opening loads were measured and calculated. In the interior, where the stress state was plane strain, lower crack opening loads were measured and calculated. Dissert. Abstr.

27 NONMETALLIC MATERIALS

Includes physical, chemical, and mechanical properties of plastics, elastomers, lubricants, polymers, textiles, adhesives, and ceramic materials.

For composite materials see *24 Composite Materials.*

N90-21858*# National Aeronautics and Space Administration. Lewis Research Center, Cleveland, OH.
POLYSILOXANES DERIVED FROM THE CONTROLLED HYDROLYSIS OF TETRAETHOXYSILANE AS PRECURSORS TO SILICA FOR USE IN CERAMIC PROCESSING
Warren H. Philipp Jan. 1990 21 p
(NASA-TM-102489; E-4527; NAS 1.15:102489) Avail: NTIS HC A03/MF A01 CSCL 11C

Synthesis, properties, and potential applications in ceramic processing for two polysiloxane silica precursors derived from the controlled hydrolysis of tetraethoxysilane (TEOS) are presented. The higher molecular weight TEOS-A is a thick adhesive liquid of viscosity 8000 to 12,000 c.p. having a SiO2 char yield of about 55 percent. The lower molecular weight TEOS-B is a more fluid liquid of viscosity 150 to 200 c.p. having a SiO2 char yield of about 52 percent. The acid catalyzed hydrolysis of TEOS to hydrated silica gel goes through a series of polysiloxane intermediates. The rate of this transition increases with the quantity of water added to the TEOS; thus, for ease of polymer isolation, the amount of water added must be carefully determined so as to produce the desired polymer in a reasonable time. The water to TEOS mole ratio falls in the narrow range of 1.05 for TEOS-A and 0.99 for TEOS-B. Further polymerization or gelation is prevented by storing at -5 C in a freezer. Both polysiloxanes thermoset to a glassy solid at 115 C. The liquid polymers are organic in nature in that they are miscible with toluene and ethanol, slightly souble in heptane, but immiscible with water. For both polymers, results on viscosity versus time are given at several temperatures and water additions. Based on these results, some examples of practical utilization of the precursors for ceramic fabrication are given. B.H.A.

N90-21859 Northwestern Univ., Evanston, IL.
A STRESS-STRENGTH INTERFERENCE APPROACH TO FAST AND DELAYED FRACTURE RELIABILITY ANALYSIS FOR CERAMIC COMPONENTS Ph.D. Thesis
Franz Boehm 1989 117 p
Avail: Univ. Microfilms Order No. DA9001775

A probabilistic approach to fast and delayed fracture reliability analysis of ceramic components is formulated. By employing the Poisson postulate to determine the distribution of the number of cracks in a solid, the component reliability is first expressed in terms of the component volume, the reference crack density, and the fracture probability for a single crack. The fracture probability is then evaluated using the stress-strength interference theory by requiring that the stress on the crack and the strength of the crack each be given as a probability distribution function. The probability function for stress is evaluated by using Batdorf's definition of equivalent stress to transform the spatial stress field obtained from a finite element stress analysis into a cumulative distribution function using the assumption of uniformly distributed and oriented cracks. For fast fracture the stress-strength formulation yields results to the finite element method proposed by Gyekenyesi. The stress-strength formalism, however, differs in the following aspect; it explicitly evaluates the cumulative density function of the equivalent stress on a crack. The explicit stress-strength interference representation provides a framework for the analysis of delayed fracture. The formalism is generalized to treat the effect of proof testing on the delayed fracture reliability components. Dissert. Abstr.

N90-21860 Brown Univ., Providence, RI.
FRACTURE MECHANICS OF MONOLITHIC CERAMIC MATERIALS UNDER SMALL SCALE MICROCRACKING CONDITIONS Ph.D. Thesis
Antonios E. Giannakopoulos 1989 166 p
Avail: Univ. Microfilms Order No. DA9002230

It is shown that the shielding effect of a distribution of microcracks is maximized when the microcracks develop normal to the direction of maximum tension. In passing, mode 1 asymptotic solutions for a class of anisotropic damage models are derived. Asymptotic and full field finite element solutions are given for a semi-infinite planar crack in a monolithic ceramic subjected to remote mixed mode loading. The material is assumed to undergo damage in the form of elastic degradation as a result of stable microcracking. Microcracks are assumed to be preferentially oriented normal to the direction of maximum tension. An outcome of the analysis is that microcracks shield the crack tip less effectively under mode 2 than under mode 1 conditions. Other issues addressed concern the relation between the mixities of the applied loads and the near-tip fields, the path independence of the J integral, the validity of deformation theories of damage under proportional loading, and the conditions for dominance of the singular near-tip fields. Finite element calculations are presented for a semi-infinite crack in a brittle solid undergoing microcracking normal to the maximum tensile direction. Microcracks are presumed stable and a saturation stage is postulated wherein the effective elastic moduli attain steady state values. Mode 1, mode 2, and mixed mode loading conditions are investigated. In these two latter cases, the method of analysis employed allows for cracks to grow out of their initial planes. The mixed mode loading case investigated corresponds to taking equal values of the remote mode 1 and 2 stress intensity factors. Contrary to what is observed in the mode 1 case, no appreciable R-curve behavior is found under mode 2 or mixed mode conditions. Dissert. Abstr.

N90-21861# Clemson Univ., SC. School of Textiles.

TERNARY REACTIONS AMONG POLYMER SUBSTRATE-ORGANOHALOGEN-ANTIMONY OXIDES UNDER PYROLYTIC, OXIDATIVE AND FLAMING CONDITIONS

M. J. Drews, C. W. Jarvis, and G. C. Lickfield Jan. 1989 64 p
(Grant NIST 60NANB-4-D0033)
(PB90-154766; NIST/GCR-89/558) Avail: NTIS HC A04/MF A01 CSCL 11C

The objectives of the flame retardant chemistry study into the ternary reactions which occur among polymer substrates, organohalogen compounds and antimony oxides in the condensed phase under pyrolytic and combustion conditions were to elucidate in detail the principle solid state reactions which result in the formation of volatile antimony containing species and the role of the polymer substrate in the reactions. A mechanistic basis was established for the role of the metal species in the degradation reactions which were observed in the solid state. The results from small scale degradation studies were related to the combustion behavior measured in the cone calorimeter and useful parameters were established between the observed solid state chemistry and the combustion behavior. GRA

N90-21862*# National Aeronautics and Space Administration. Lewis Research Center, Cleveland, OH.

SELF-LUBRICATING POLYMER COMPOSITES AND POLYMER TRANSFER FILM LUBRICATION FOR SPACE APPLICATIONS

Robert L. Fusaro Feb. 1990 49 p
(NASA-TM-102492; E-5284; NAS 1.15:102492) Avail: NTIS HC A03/MF A01 CSCL 11C

The use of self-lubricating polymers and polymer composites in space is somewhat limited today. In general, they are only used when other methods are inadequate. There is potential, however, for these materials to make a significant impact on future space missions if properly utilized. Some of the different polymers and fillers used to make self-lubricating composites are surveyed. The mechanisms of composite lubrication and wear, the theory behind transfer film lubricating mechanisms, and some factors which affect polymer composite wear and transfer are examined. In addition, some of the current space tribology application areas for self-lubricating polymer composites and polymer transfer are mentioned. Author

N90-21863 National Physical Lab., Teddington (England). Div. of Materials Applications.

NEW CORROSION RESISTANT CERAMIC COATINGS BY LASER PROCESSING

S. R. J. Saunders, A. A. Ansari, M. J. Bennett, A. T. Tuson, F. Fellowes, and W. M. Steen (Liverpool Univ., England) Aug. 1988 12 p Presented at an International Conference on Laser Technologies in Industry, Porto, Portugal, 6-8 Jun. 1988
(AERE-R-13166) Copyright Avail: Issuing Activity

Fabrication of thick oxide ceramic coatings upon a metal substrate by laser processing was investigated. Crucial parameters studied included beam power, diameter, overlap and transverse speed, feed powder size and coating environment. Coatings were characterized by a range of surface analytical techniques. The corrosion protection afforded by a coating was assessed in both oxidizing and sulphidizing environments. Author

N90-21864*# National Aeronautics and Space Administration. Goddard Space Flight Center, Greenbelt, MD.

THERMOMECHANICAL PROPERTIES OF POLYMERIC MATERIALS AND RELATED STRESSES

Sheng Yen Lee Apr. 1990 26 p
(NASA-TM-100758; Rept-90B00071; NAS 1.15:100758) Avail: NTIS HC A03/MF A01 CSCL 11C

The thermomechanical properties of a number of widely used polymeric materials were determined by thermomechanical analysis and dynamic mechanical analysis. A combined profile of the coefficient of thermal expansion and the modulus change over a wide temperature range obtained by the analyses shows clearly the drastic effect of the glass transition on both the CTE and the modulus of a polymer, and the damaging potential due to such effect. Author

N90-21865# Sandia National Labs., Albuquerque, NM.

SURFACE STRUCTURE AND CHEMISTRY OF HIGH SURFACE AREA SILICA GELS

C. J. Brinker, R. K. Brow, D. R. Tallant, and R. J. Kirkpatrick (Illinois Univ., Urbana.) 1989 22 p Presented at the 10th University Conference on Glass Science, State College, Jun. 1989
(Contract DE-AC04-76DP-00789)
(DE90-007684; SAND-89-0183C; CONF-8906295-1) Avail: NTIS HC A03/MF A01

Combined Raman and Si-29 NMR investigations of high surface area silica gels indicate that dehydroxylation of the a-SiO2 surface results preferentially in the formation of cyclic trisiloxanes (3-membered rings). Estimates of the maximum experimentally observed concentration of 3-membered rings correspond to a surface coverage of about 28 to 58 percent. Two consequences of 3-membered rings on the a-SiO2 surface are enhanced hydrolysis rates and increased skeletal densities. DOE

N90-21866# Allied-Signal Corp., Kansas City, MO.

NEW FLEXIBLE CIRCUIT MATERIAL EVALUATION

David J. Fossey Mar. 1990 11 p Presented at the 4th International SAMPE Electronic Materials and Processes Conference, Albuquerque, NM, 12-14 Jun. 1990
(Contract DE-AC04-76DP-00613)
(DE90-008313; KCP-613-4303; CONF-9006121-3) Avail: NTIS HC A03/MF A01

A project has been undertaken to evaluate new sources of flexible circuit materials for use by Allied-Signal, Inc., Kansas City Division. The vast majority of current flexible circuits are fabricated from polyimide film and acrylic adhesive circuit materials. One new polyimide film was evaluated as an alternate dielectric film. Thirteen (13) suppliers of flexible circuit materials have been identified. The results of the mechanical and electrical properties evaluation study of some of the new sources of flexible circuit materials are discussed. DOE

N90-21867# Lawrence Livermore National Lab., CA. Environmental Sciences Div.
STABILITY STUDIES OF A pH-SENSITIVE POLYMER MATRIX: APPLICATIONS TO FIBER OPTIC pH SENSORS
M. Allen Northrup, Kevin Langry, and S. Michael Angel Mar. 1990 10 p Presented at the SPIE Optics, Electro-Optics, and Laser Applications in Science and Engineering Conference and Exhibition, Los Angeles, CA, 15-19 Jan. 1990
(Contract W-7405-eng-48)
(DE90-009579; UCRL-JC-103167; CONF-900140-19) Avail: NTIS HC A02/MF A01

A ratiometric pH-sensitive fluorescent dye (hydroxypyrenetrisulfonic acid) was covalently attached to an acrylamide polymer. These pH-sensitive copolymers were either covalently bonded to the end of an optical fiber or polymerized into separate gels. Long-term, accelerated aging studies were performed on the fibers and gels in 43 C distilled H_2O. The fiber-immobilized optrodes gave good pH responses for up to 2 months. The pH-sensitive gels were physically attached to optical fibers and gave very good pH responses for over one year. These physically immobilized, one-year-old, pH-sensitive copolymers provided optrodes with linear pH responses between pH 6 and 8 and resolution greater than 0.25 pH unit. A simple photostability experiment on these optrodes showed that they were very photostable. The results indicate that pH-sensitive copolymers in a simple optrode design can be employed as pH sensors with useful lifetimes exceeding one year. DOE

28 PROPELLANTS AND FUELS

Includes rocket propellants, igniters, and oxidizers; their storage and handling procedures; and aircraft fuels.

For related information see also *07 Aircraft Propulsion and Power, 20 Spacecraft Propulsion and Power,* and *44 Energy Production and Conversion.*

N90-21868# Army Missile Command, Redstone Arsenal, AL.
EXTRACTION OF RECOVERY OF PLASTICIZERS FROM SOLID PROPELLANTS AND MUNITIONS Patent Application
William S. Melvin, inventor (to Army) 16 Oct. 1989 22 p
(AD-D014433; US-Patent-Appl-SN-422161) Avail: NTIS HC A03/MF A01 CSCL 19/1

A method to extract and recover plasticizers and their stabilizers from solid propellants, explosives, and pyrotechnics (PEP source compositions) employs near critical liquid (NCL) or supercritical fluid (SCF) CO_2 as the solvent. The extraction and ingredient recovery method provides an environmentally acceptable alternative to traditional open burning and destruction of PEP source compositions. CO_2 solvent is nontoxic, nonflammable, noncorrosive, inexpensive, and does not generate any additional toxic or hazardous wastes. The solvent is totally inert when it is confined, pressurized, and possibly heated in direct contact with an energetic propellant heated in direct contract motor or similar pressure vessel. CO(2) readily undergoes a gas-to-liquid phase change to NCL readily undergoes a gas-to-liquid phase change to NCL conditions when confined and compressed to a pressure of 831 psig or greater at ambient temperature. By further increasing the pressure and temperature of NCL CO_2 to 1058 psig and 31.3 C or greater, respectively, SCF conditions of CO_2 are obtained. GRA

N90-21869*# National Aeronautics and Space Administration. Lewis Research Center, Cleveland, OH.
HIGH SPEED COMMERCIAL TRANSPORT FUELS CONSIDERATIONS AND RESEARCH NEEDS
C. M. Lee and R. W. Niedzwiecki 1989 10 p Presented at the Symposium on the Structure of Future Jet Fuels 2, Miami Beach, FL, 10-15 Sep. 1989; sponsored by American Chemical Society
(NASA-TM-102535; E-5345; NAS 1.15:102535) Avail: NTIS HC A02/MF A01 CSCL 21D

NASA is currently evaluating the potential of incorporating High Speed Civil Transport (HSCT) aircraft in the commercial fleet in the beginning of the 21st century. NASA sponsored HSCT enabling studies currently underway with airframers and engine manufacturers, are addressing a broad range of technical, environmental, economic, and related issues. Supersonic cruise speeds for these aircraft were originally focused in the Mach 2 to 5 range. At these flight speeds, both jet fuels and liquid methane were considered potential fuel candidates. For the year 2000 to 2010, cruise Mach numbers of 2 to 3+ are projected for aircraft fuel with thermally stable liquid jet fuels. For 2015 and beyond, liquid methane fueled aircraft cruising at Mach numbers of 4+ may be viable candidates. Operation at supersonic speeds will be much more severe than those encountered at subsonic flight. One of the most critical problems is the potential deterioration of the fuel due to the high temperature environment. HSCT fuels will not only be required to provide the energy necessary for flight, but will also be subject to aerodynamic heating and, will be required to serve as the primary heat sink for cooling the engine and airframe. To define fuel problems for high speed flight, a fuels workshop was conducted at NASA Lewis Research Center. The purpose of the workshop was to gather experts on aviation fuels, airframe fuel systems, airport infrastructure, and combustion systems to discuss high speed fuel alternatives, fuel supply scenarios, increased thermal stability approaches and measurements, safety considerations, and to provide directional guidance for future R and D efforts. Subsequent follow-up studies defined airport infrastructure impacts of high speed fuel candidates. The results of these activities are summarized. In addition, an initial case study using modified in-house refinery simulation model Gordian code (1) is briefly discussed. This code can be used to simulate different types of refineries, emphasizing jet fuel production and relative cost factors. Author

29 MATERIALS PROCESSING

Includes space-based development of products and processes for commercial applications.

For biological materials see *55 Space Biology.*

N90-21870*# Life Systems, Inc., Cleveland, OH.
IMPACT OF LOW GRAVITY ON WATER ELECTROLYSIS OPERATION Final Report
F. T. Powell, F. H. Schubert, and M. G. Lee Mar. 1989 53 p
(Contract NAS9-17966)
(NASA-CR-185521; NAS 1.26:185521; TR-1028-5) Avail: NTIS HC A04/MF A01 CSCL 22A

Advanced space missions will require oxygen and hydrogen utilities for several important operations including the following: (1) propulsion; (2) electrical power generation and storage; (3) environmental control and life support; (4) extravehicular activity; (5) in-space manufacturing and (6) in-space science activities. An experiment suited to a Space Shuttle standard middeck payload has been designed for the Static Feed Water Electrolysis technology which has been viewed as being capable of efficient, reliable oxygen and hydrogen generation with few subsystem components. The program included: end use design requirements, phenomena to be studied, Space Shuttle Orbiter experiment constraints, experiment design and data requirements, and test hardware requirements. The objectives are to obtain scientific and engineering data for future research and development and to focus on demonstrating and monitoring for safety of a standard middeck payload. B.H.A.

N90-21871*# National Aeronautics and Space Administration. Lewis Research Center, Cleveland, OH.
PROBABILISTIC ANALYSIS OF BLADED TURBINE DISKS AND THE EFFECT OF MISTUNING
A. R. Shah, V. K. Nagpal (Sverdrup Technology, Inc., Cleveland, OH.), and Christos C. Chamis 1990 11 p Presented at the 31st Structures, Structural Dynamics and Materials Conference, Long Beach, CA, 2-4 Apr. 1990; sponsored by AIAA, ASME, ASCE,

AHS and ASC Previously announced in IAA as A90-29327
(NASA-TM-102564; E-5388; NAS 1.15:102564) Avail: NTIS HC A03/MF A01 CSCL 22A

Probabilistic assessment of the maximum blade response on a mistuned rotor disk is performed using the computer code NESSUS. The uncertainties in natural frequency, excitation frequency, amplitude of excitation and damping are included to obtain the cumulative distribution function (CDF) of blade responses. Advanced mean value first order analysis is used to compute CDF. The sensitivities of different random variables are identified. Effect of the number of blades on a rotor on mistuning is evaluated. It is shown that the uncertainties associated with the forcing function parameters have significant effect on the response distribution of the bladed rotor. Author

31 ENGINEERING (GENERAL)

Includes vacuum technology; control engineering; display engineering; cryogenics; and fire prevention.

N90-21872*# Phobos Industrial Applications Corp., Austin, TX.

A ROBOTICALLY CONSTRUCTED PRODUCTION AND SUPPLY BASE ON PHOBOS

4 May 1989 142 p
(Contract NASw-4435)
(NASA-CR-186234; NAS 1.26:186234) Avail: NTIS HC A07/MF A01 CSCL 13B

PHOBIA Corporation is involved with the design of a man-tenable robotically constructed, bootstrap base on Mars' moon, Phobos. This base will be a pit-stop for future manned missions to Mars and beyond and will be a control facility during the robotic construction of a Martian base. An introduction is given to the concepts and the ground rules followed during the design process. Details of a base design and its location are given along with information about some of the subsystems. Since a major purpose of the base is to supply fuel to spacecraft so they can limit their fuel mass, mining and production systems are discussed. Surface support activities such as docks, anchors, and surface transportation systems are detailed. Several power supplies for the base are investigated and include fuel cells and a nuclear reactor. Tasks for the robots are defined along with descriptions of the robots capable of completing the tasks. Finally, failure modes for the entire PHOBIA Corporation design are presented along with an effects analysis and preventative recommendations. Author

N90-21873 Auburn Univ., AL.

UTILIZATION OF WATER HYACINTHS TO UPGRADE HEAVILY LOADED WASTEWATER TREATMENT PLANT EFFLUENTS Ph.D. Thesis

Anthony Stephen McAnally 1989 349 p
Avail: Univ. Microfilms Order No. DA8925641

Many municipal wastewater treatment plants are presently failing to meet their discharge permit requirements. Recently, considerable attention has been focused on the use of aquatic plants of various types to treat municipal wastewaters. While several species of plants have been found to be useful in this regard, water hyacinths appear to offer the most promise in areas where the climate is mild enough for them to flourish during most of the year. Accordingly, the primary purpose was to test the acceptability of such systems for use in southern states such as Alabama. A wastewater treatment plant located at Union Springs, Alabama was selected as the study site. The experimental water hyacinth system was configured as a set of two treatment trains with two growth channels in series for each train. One train was harvested and the other was not. Each growth channel was constructed of 3/4-inch marine plywood and was 8 feet wide, 2 feet deep and 32 feet long. Observations indicate that a water hyacinth treatment system can be a reliable method for upgrading secondary effluents to advanced secondary levels in central Alabama. The reliable treatment period will extend from about May through December with no plant protection (possibly longer in Southern Alabama). Dissert. Abstr.

N90-21874# Swedish Inst. for Materials Testing, Boras. Div. of Fire Technology.

TEST METHOD FOR FIRE EXTINGUISHING POWDER, NORDTEST PROJECT 675-87

Henry Persson 1989 66 p
(PB90-166984; SP-RAPP-1989:15; ISBN-91-7848-165-1; ISSN-0284-5172) Avail: NTIS HC A04/MF A01 CSCL 13B

A proposal for a test method for fire extinguishing powders, including the results of reference tests which form the basis of the method, is presented. The proposal for the test method is based on ISO 7202 Fire Protection-Fire Extinguishing Media-Powder; certain items have, however, been supplemented and changed. The test method aims at providing both qualitative and quantitative information about the composition and extinguishing efficiency of various powders on A-, B-, and C-fires, respectively. The specific extinguishing media requirement REMP (Required Extinguishing Media Portion) is provided as a quantitative measure of the efficiency of the powder. The REMP-value is the ratio between the weight of powder supplied and the weight of propane gas supplied, which implies that the lower the REMP-value, the more effective the powder. Author

N90-21875# Sandia National Labs., Albuquerque, NM.

THE INFLUENCE OF LARGE, COLD OBJECTS ON ENGULFING FIRE ENVIRONMENTS

V. F. Nicolette and D. W. Larson 1989 28 p Presented at the 5th AIPA/ASME Thermophysics and Heat Transfer Conference, Seattle, WA, 18-20 Jun. 1990
(Contract DE-AC04-76DP-00789)
(DE90-003342; SAND-89-2175C; CONF-900619-2) Avail: NTIS HC A03/MF A01

Appropriate thermal boundary conditions for analytical predictions of the thermal response of large, cold objects (such as nuclear spent-fuel shipping casks) engulfed in flames are not well understood. These objects have been shown experimentally to respond differently to engulfing flames than small calorimeters, and traditional scaling parameters are not successful in explaining these observed differences. One possible explanation is that a large, cold object interacts with and cools the surrounding flames, resulting in lower incident heat fluxes to the large object. A simple model is constructed to investigate this hypothesis. Results of calculations with the model indicate that such an interaction does occur and can significantly reduce incident heat fluxes to large objects. This implies that appropriate thermal boundary conditions for large, cold objects engulfed in flames are dependent on the size, shape, and thermal response of the object. DOE

N90-21876# Oak Ridge National Lab., TN. Energy Div.

EXPERIMENTAL PERFORMANCE OF OZONE-SAFE ALTERNATIVE REFRIGERANTS: EXPERIMENTAL PERFORMANCE COMPARISONS OF R32, R125, R143a, R218, R134a, R152a, R124, R142b, RC318 AND R143 IN A REFRIGERATION CIRCUIT

James R. Sand, Edward A. Vineyard, and Richard J. Nowak (Purdue Univ., West Lafayette, IN.) 1990 23 p Presented at the Annual Meeting of The American Society of Heating, Refrigerating and Air-Conditioning Engineers, St. Louis, MO, 9-13 Jun. 1990
(Contract DE-AC05-84OR-21400)
(DE90-009227; CONF-9006117-4) Avail: NTIS HC A03/MF A01

Several compounds proposed as near term or longer range substitutes for the regulated chlorofluorocarbon (CFC) refrigerants were tested in a breadboard vapor-compression circuit, and their performance was evaluated relative to more commonly used refrigerants. The limited physical property information available in the literature for these alternative compounds was used to fit an equation of state so coefficients of performance (COPs) and capacities calculated from refrigerant property subroutines could be compared to those obtained experimentally. Comparisons of measured and modeled performance are given for 11 alternatives

and for R22, R12, and R114. Estimates of compressor efficiency with each refrigerant are provided. Several of the alternatives exhibited better performance than the more widely used refrigerants at some or all of the conditions tested. Ozone-safe, alternative refrigerants that performed better than CFC counterparts at selected conditions are R152a, R143a, R134a, R134, and R142b.
DOE

N90-21877# Technische Univ., Delft (Netherlands). Faculty of Aerospace Engineering.
DEVELOPMENT, IMPLEMENTATION AND TEST OF A COMPUTER PROGRAM FOR THE PRODUCTION OF AXISYMMETRIC PATTERN MOULDS ON A NUMERICALLY CONTROLLED MILLING MACHINE
Ivan S. Gibson May 1989 63 p
(LR-593; ETN-90-96351) Avail: NTIS HC A04/MF A01

The development of a computer program, written to drive a numerically controlled milling machine, is described. The ideas, defining parameters, and numerical methods adopted during the writing process are described. The milling machine is used for the production of axisymmetric pattern molds used in the manufacture of an annular (nozzle) from a number of annular segments. Each segment is constructed from plastic laminates incorporating male/female couplings which are bonded together to form the complete product. The practical utility of a number of surface spline fitting methods is investigated. The smoothness requirements appropriate to the mold production method adopted are discussed. Photographs of the molds and a listing of the computer program are included.
ESA

N90-21878 Illinois Univ., Urbana-Champaign.
NONLINEAR SPLINE OPERATOR INTERPOLATION AND SLIDING CONTROL OF DEFORMABLE MANEUVERING BODIES Ph.D. Thesis
Fakhreddine Karray 1989 132 p
Avail: Univ. Microfilms Order No. DA9010910

For purposes of achieving high performances of tracking, and precision pointing of a flexible structure subject to large angular maneuvers (such as the slewing maneuver of a large space structure), a newly developed off-line modeling procedure combined with a robust control technique is investigated and then implemented to the moving structure. The modeling issue is first discussed, and two different procedures for dealing with the nonlinear dynamics of a given deformable structure are described. The coupled dynamic of vibration, translation, and rotation are derived for a completely decretized model and then for a hybrid model. Deformation estimates are then computed through two types of observers: the well-known extended Kalman filter and the feedback linearized based observer. Knowing that hardware costs, as well as on-time computational problems arise whenever dealing with such observers, especially for high dimensional systems, another alternative is then to be sought. An off-line modeling technique is developed using the nonlinear optimal interpolator theory. This interpolator is used basically to reduce the dimension of the original system to the one determined by the number of applied test inputs. Estimates of the deformations, as well as error bounds on their measurements are then computed. Finally, and in order to insure a robust performance of the moving structure subject to induced deformations, and structural parameters variations, a procedure based on the sliding manifolds technique is used. Combination of such a technique, with the outputs of the optimal interpolator constitutes an excellent alternative for the system to achieve robust tracking performances in presence of disturbances and parameter uncertainties.
Dissert. Abstr.

32 COMMUNICATIONS AND RADAR

Includes radar; land and global communications; communications theory; and optical communications.

For related information see also *04 Aircraft Communications and Navigation* and *17 Space Communications, Spacecraft Communications, Command and Tracking.* For search and rescue see *03 Air Transportation and Safety,* and *16 Space Transportation.*

N90-21879 Ohio State Univ., Columbus.
RECOGNITION AND ANALYSIS OF AIRCRAFT TARGETS BY RADAR, USING STRUCTURAL PATTERN REPRESENTATIONS DERIVED FROM POLARIMETRIC SIGNATURES Ph.D. Thesis
Neil Frederick Chamberlain 1989 276 p
Avail: Univ. Microfilms Order No. DA9001927

Automatic recognition of aircraft by means of radar signals is examined. In particular, the problem of utilizing polarimetric information from the monostatic, wideband, scattering matrix to target classification and analysis is considered. The approach taken is to effect a decomposition of the target in terms of its predominant scattering centers and their polarimetric properties. This polarimetric target model is based on a new formalism for the description of the vector behavior of wideband electromagnetic planewaves, called transient polarization. The transient polarization response of a radar object is a 3-dimensional, time-dependent electric field locus. Conceptually, this signature can be envisioned as the result of transmitting a short circularly polarized pulse toward the object. Transient polarization states are expressed as a 3-tuple of time-dependent polarimetric parameters: amplitude, ellipticity, and tilt. Scattering centers are identified by the peaks in the amplitude. The polarimetric parameters of canonical targets, simplified aircraft target combinations, and scaled model commercial airliners are analyzed. The performance of radar target identification systems employing polarimetric features is evaluated by means of Monte-Carlo simulation studies. Both decision-theoretic and language-theoretic techniques are used for this purpose. A target is represented as a string of polarimetrically-related symbols, and is classified using syntactic methods. Target classification simulations show that polarimetric pattern representations extracted from transient polarization responses may be used for reliable and flexible target classification. In addition, the polarimetric techniques developed may be used as a tool for concise characterization and analysis of time-domain electromagnetic scattering.
Author

N90-21880*# Jet Propulsion Lab., California Inst. of Tech., Pasadena.
THE TELECOMMUNICATIONS AND DATA ACQUISITION REPORT Progress Report, Oct. - Dec. 1989
E. C. Posner, ed. 15 Feb. 1990 335 p
(NASA-CR-186479; JPL-TDA-PR-42-100; NAS 1.26:186479)
Avail: NTIS HC A15/MF A02 CSCL 17B

Archival reports are given on developments in programs managed by JPL's Office of Telecommunications and Data Acquisition (TDA), including space communications, radio navigation, radio science, ground-based radio and radar astronomy, and the Deep Space Network (DSN) and its associated Ground Communications Facility (GCF) in planning, supporting research and technology, implementation, and operations. Also included is TDA-funded activity at JPL on data and information systems and reimbursable DSN work performed for other space agencies through NASA. In the search for extraterrestrial intelligence (SETI), implementation and operations for searching the microwave spectrum are reported. Use of the Goldstone Solar System Radar for scientific exploration of the planets, their rings and satellites, asteroids, and comets are discussed. For individual titles, see N90-21881 through N90-21905.

N90-21881*# Jet Propulsion Lab., California Inst. of Tech., Pasadena.
PRECISE ESTIMATION OF TROPOSPHERIC PATH DELAYS WITH GPS TECHNIQUES
S. M. Lichten *In its* The Telecommunications and Data Acquisition

Report 15 Feb. 1990 p 1-12 (For primary document see N90-21880 15-32)
Avail: NTIS HC A15/MF A02 CSCL 17B

Tropospheric path delays are a major source of error in deep space tracking. However, the tropospheric-induced delay at tracking sites can be calibrated using measurements of Global Positioning System (GPS) satellites. A series of experiments has demonstrated the high sensitivity of GPS to tropospheric delays. A variety of tests and comparisons indicates that current accuracy of the GPS zenith tropospheric delay estimates is better than 1-cm root-mean-square over many hours, sampled continuously at intervals of six minutes. These results are consistent with expectations from covariance analyses. The covariance analyses also indicate that by the mid-1990s, when the GPS constellation is complete and the Deep Space Network is equipped with advanced GPS receivers, zenith tropospheric delay accuracy with GPS will improve further to 0.5 cm or better. Author

N90-21882*# Jet Propulsion Lab., California Inst. of Tech., Pasadena.
THE DETERMINATION OF MAXIMUM DEEP SPACE STATION SLEW RATES FOR A HIGH EARTH ORBITER
J. A. Estefan n its The Telecommunications and Data Acquisition Report 15 Feb. 1990 p 13-20 (For primary document see N90-21880 15-32)
Avail: NTIS HC A15/MF A02 CSCL 17B

As developing national and international space ventures, which seek to employ NASA's Deep Space Network (DSN) for tracking and data acquisition, evolve, it is essential for navigation and tracking system analysts to evaluate the operational capability of Deep Space Station antennas. To commission the DSN for use in tracking a highly eccentric Earth orbiter could quite possibly yield the greatest challenges in terms of slewing capability; certainly more so than with a deep-space probe. The focus here is on the determination of the maximum slew rates needed to track a specific high Earth orbiter, namely the Japanese MUSES-B spacecraft of the Very Long Baseline Interferometry Space Observatory Program. The results suggest that DSN 34-m antennas are capable of meeting the slew rate requirements for the nominal MUSES-B orbital geometries currently being considered. Author

N90-21883*# Jet Propulsion Lab., California Inst. of Tech., Pasadena.
MICROWAVE ANALOG FIBER-OPTIC LINK FOR USE IN THE DEEP SPACE NETWORK c74
R. T. Logan, Jr., G. F. Lutes, and L. Maleki *In its* The Telecommunications and Data Acquisition Report 15 Feb. 1990 p 21-33 (For primary document see N90-21880 15-32)
Avail: NTIS HC A15/MF A02 CSCL 20F

A novel fiber-optic system with dynamic range of up to 150 dB-Hz for transmission of microwave analog signals is described. The design, analysis, and laboratory evaluations of this system are reported, and potential applications in the NASA/JPL Deep Space Network are discussed. Author

N90-21884*# Jet Propulsion Lab., California Inst. of Tech., Pasadena.
GALILEO EARTH APPROACH NAVIGATION USING CONNECTED-ELEMENT INTERFEROMETER PHASE-DELAY TRACKING c17
S. W. Thurman *In its* The Telecommunications and Data Acquisition Report 15 Feb. 1990 p 34-47 (For primary document see N90-21880 15-32)
Avail: NTIS HC A15/MF A02 CSCL 09F

The application of a Connected-Element Interferometer (CEI) to the navigation of the Galileo spacecraft during its encounter with Earth in December 1990 is investigated. A CEI tracking demonstration is planned for the week of November 11 through 18, 1990, from 27 days to 20 days prior to Earth encounter on December 8. During this period, the spacecraft will be tracked daily with Deep Space Network Stations 13 and 15 at Goldstone. The purpose of this work is twofold: first, to establish and define the navigation performance expected during the tracking demonstration and, second, to study, in a more general sense, the sensitivity of orbit demonstration results obtained with CEI to the data density within CEI tracking passes and to important system parameters, such as baseline orientation errors and the phase-delay measurement accuracy. Computer simulation results indicate that the use of CEI data, coupled with conventional range and Doppler data, may reduce the uncertainty in the declination of the spacecraft's incoming trajectory by 15 to 66 percent compared with the operational solution using range and Doppler data only. The level of improvement depends upon the quantity and quality of the CEI data. Author

N90-21885*# Jet Propulsion Lab., California Inst. of Tech., Pasadena.
USING CONNECTED-ELEMENT INTERFEROMETER PHASE-DELAY DATA FOR MAGELLAN NAVIGATION IN VENUS ORBIT c17
S. W. Thurman and G. Badilla *In its* The Telecommunications and Data Acquisition Report 15 Feb. 1990 p 48-54 (For primary document see N90-21880 15-32)
Avail: NTIS HC A15/MF A02 CSCL 17G

The pointing accuracy needed to support Magellan's Synthetic Aperture Radar mapping of Venus places stringent requirements on navigation accuracy. This need is met with a combination of two-way Doppler and narrowband delta Very Long Baseline Interferometer (delta VLBI) data, which are capable of determining the spacecraft's orbit to the required level, typically about one-kilometer position uncertainty. Differenced Doppler (two-way Doppler minus three-way Doppler) is also capable of meeting mission navigation requirements, and serves as a backup to narrowband delta VLBI. The Magellan Project specifies that the turn-around time for processing narrowband delta VLBI data must be 12 hours or less, a very difficult requirement to meet operationally. The use of phase-delay data, taken from a Connected-Element Interferometer (CEI) with a 21-km baseline, for Magellan orbit determination was investigated to determine if navigation performance comparable with narrowband delta VLBI and differenced Doppler could be achieved. CEI possesses an operational advantage over delta VLBI data in that the observables are constructed in near-real time, thus greatly reducing the turn-around time needed to process the data, relative to the off-line system used to generate delta VLBI observables. Unfortunately, the results indicate that CEI data are much less powerful than narrowband delta VLBI and differenced Doppler for orbiter navigation, although there was some marginal improvement over the navigation performance obtained when only two-way Doppler data were used. Author

N90-21886*# Jet Propulsion Lab., California Inst. of Tech., Pasadena.
VOLTAGE SOURCE ac-TO-dc CONVERTERS FOR HIGH-POWER TRANSMITTERS c33
R. Cormier *In its* The Telecommunications and Data Acquisition Report 15 Feb. 1990 p 55-68 (For primary document see N90-21880 15-32)
Avail: NTIS HC A15/MF A02 CSCL 09C

This work was done to optimize the design of the components used for the beam power supply, which is a component of the transmitters in the Deep Space Network (DSN). The major findings are: (1) the difference in regulation between a six-pulse and a twelve-pulse converter is at most 7 percent worse for the twelve-pulse converter; (2) the commutation overlap angle of a current source converter equals that of a voltage source converter with continuous line currents; (3) the sources of uncharacteristic harmonics are identified with SPICE simulation; (4) the use of an imperfect phase-shifting transformer for the twelve-pulse converter generates a harmonic at six times the line frequency; and (5) the assumptions usually made in analyzing converters can be relaxed with SPICE simulation. The results demonstrate the suitability of using SPICE simulation to obtain detailed performance predictions of ac-to-dc converters. Author

N90-21887*# Jet Propulsion Lab., California Inst. of Tech., Pasadena.

DUAL-SHAPED OFFSET REFLECTOR ANTENNA DESIGNS FROM SOLUTIONS OF THE GEOMETRICAL OPTICS FIRST-ORDER PARTIAL DIFFERENTIAL EQUATIONS

V. Galindo-Israel, W. Imbriale, K. Shogen, and R. Mittra (Illinois Univ., Urbana.) *In its* The Telecommunications and Data Acquisition Report 15 Feb. 1990 p 69-80 (For primary document see N90-21880 15-32)

Avail: NTIS HC A15/MF A02 CSCL 17B

In obtaining solutions to the first-order nonlinear partial differential equations (PDEs) for synthesizing offset dual-shaped reflectors, it is found that previously observed computational problems can be avoided if the integration of the PDEs is started from an inner projected perimeter and integrated outward rather than starting from an outer projected perimeter and integrating inward. This procedure, however, introduces a new parameter, the main reflector inner perimeter radius p(o), when given a subreflector inner angle 0(o). Furthermore, a desired outer projected perimeter (e.g., a circle) is no longer guaranteed. Stability of the integration is maintained if some of the initial parameters are determined first from an approximate solution to the PDEs. A one-, two-, or three-parameter optimization algorithm can then be used to obtain a best set of parameters yielding a close fit to the desired projected outer rim. Good low cross-polarization mapping functions are also obtained. These methods are illustrated by synthesis of a high-gain offset-shaped Cassegrainian antenna and a low-noise offset-shaped Gregorian antenna. Author

N90-21888*# Jet Propulsion Lab., California Inst. of Tech., Pasadena.

A REAL-TIME SIGNAL COMBINING SYSTEM FOR Ka-BAND FEED ARRAYS USING MAXIMUM-LIKELIHOOD WEIGHT ESTIMATES

V. A. Vilnrotter and E. R. Rodemich *In its* The Telecommunications and Data Acquisition Report 15 Feb. 1990 p 81-99 (For primary document see N90-21880 15-32)

Avail: NTIS HC A15/MF A02 CSCL 17B

A real-time digital signal combining system for use with Ka-band feed arrays is proposed. The combining system attempts to compensate for signal-to-noise ratio (SNR) loss resulting from antenna deformations induced by gravitational and atmospheric effects. The combining weights are obtained directly from the observed samples by using a sliding-window implementation of a vector maximum-likelihood parameter estimator. It is shown that with averaging times of about 0.1 second, combining loss for a seven-element array can be limited to about 0.1 dB in a realistic operational environment. This result suggests that the real-time combining system proposed here is capable of recovering virtually all of the signal power captured by the feed array, even in the presence of severe wind gusts and similar disturbances. Author

N90-21889*# Jet Propulsion Lab., California Inst. of Tech., Pasadena.

ULTRALOW NOISE PERFORMANCE OF AN 8.4-GHz MASER-FEEDHORN SYSTEM

D. L. Johnson, S. M. Petty, J. J. Kovatch, and G. W. Glass *In its* The Telecommunications and Data Acquisition Report 15 Feb. 1990 p 100-110 (For primary document see N90-21880 15-32)

Avail: NTIS HC A15/MF A02 CSCL 17B

A total system noise temperature of 6.6 K was demonstrated with an 8.4-GHz traveling wave maser and feedhorn operating in a cryogenic environment. Both the maser and feedhorn were inserted in the helium cryostat, with the maser operating in the 1.6-K liquid bath and the feedhorn cooled in the helium gas, with a temperature gradient along the horn ranging from the liquid bath temperature at its lower end to room temperature at its top. The ruby maser exhibited 43 dB of gain with a bandwidth of 76 MHz(-3 dB) centered at 8400 MHz. Discussions of the maser, cooled feedhorn, and cryostat designs are presented along with a discussion of the noise temperature measurements. Author

N90-21890*# Jet Propulsion Lab., California Inst. of Tech., Pasadena.

RADIOMETRIC TESTS ON WET AND DRY ANTENNA REFLECTOR SURFACE PANELS

T. Y. Otoshi and M. M. Franco *In its* The Telecommunications and Data Acquisition Report 15 Feb. 1990 p 111-130 (For primary document see N90-21880 15-32)

Avail: NTIS HC A15/MF A02 CSCL 17B

The results of X-band noise temperature tests on two types of antenna surface panels are presented. The first type tested was a solid antenna panel, while the second type was a perforated panel with 3/16-in.-diameter holes. Measurements were made at 8.45 GHz using an X-band radiometric system. Included in this article are measured noise temperature contributions from: (1) thermal diffusive white paint on solid and perforated panels, and (2) water sprayed on both painted and unpainted perforated panels. Experiments on perforated panels were restricted to the 3/16-in.-diameter hole panels formerly used on Deep Space Network 64-m antennas. Rigorous calibration equations, applicable to a variety of antenna panel and dichroic plate test configurations, are presented. It was demonstrated that an accurate, stable radiometric measurement system of the type used for the results of this research makes it possible to obtain information that would be much more difficult to obtain using other techniques. Author

N90-21891*# Jet Propulsion Lab., California Inst. of Tech., Pasadena.

A FUNCTIONAL DESCRIPTION OF THE ADVANCED RECEIVER

S. Hinedi *In its* The Telecommunications and Data Acquisition Report 15 Feb. 1990 p 131-149 (For primary document see N90-21880 15-32)

Avail: NTIS HC A15/MF A02 CSCL 17B

The breadboard Advanced Receiver 2 (ARX 2) that is currently being built for future use in NASA's Deep Space Network (DSN) is described. The hybrid analog/digital receiver performs multiple functions including carrier, subcarrier, and symbol synchronization. Tracking can be achieved for residual, suppressed, or hybrid carriers and for both sinusoidal and square-wave subcarriers. Other functions such as time-tagged Doppler extraction and monitor/control are also discussed, including acquisition algorithms and lock-detection schemes. System requirements are specified and a functional description of the ARX 2 is presented. The various digital signal-processing algorithms used are also discussed and illustrated with block diagrams. Author

N90-21892*# Jet Propulsion Lab., California Inst. of Tech., Pasadena.

QPSK CARRIER-ACQUISITION PERFORMANCE IN THE ADVANCED RECEIVER 2

S. Hinedi and B. Shah *In its* The Telecommunications and Data Acquisition Report 15 Feb. 1990 p 150-159 (For primary document see N90-21880 15-32)

Avail: NTIS HC A15/MF A02 CSCL 17B

The frequency-acquisition performance of the Costas cross-over loop which is used in the Advanced Receiver 2 (ARX 2) to perform Quadrature Phase Shift Keying (QPSK) carrier tracking is described. The performance of the Costas cross-over loop is compared to two other QPSK carrier tracking loops: the MAP estimation loop and the generalized Costas loop. Acquisition times and probabilities of acquisition as functions of both loop signal-to-noise ratio and frequency-offset to loop-bandwidth ratio are obtained using computer simulations for both type-2 and type-3 loops. It is shown that even though the MAP loop results in the smallest squaring loss for all signal-to-noise ratios, the MAP loop is sometimes outperformed by the other two loops in terms of acquisition time and probability. Author

N90-21893*# Jet Propulsion Lab., California Inst. of Tech., Pasadena.

DIGITAL DOPPLER EXTRACTION DEMONSTRATION WITH THE ADVANCED RECEIVER

S. Hinedi, R. Bevan, H. DelCastillo, P. Kinman, D. Chong, and R.

Labelle *In its* The Telecommunications and Data Acquisition Report 15 Feb. 1990 p 160-173 (For primary document see N90-21880 15-32)
Avail: NTIS HC A15/MF A02 CSCL 17B

A digital Doppler extraction demonstration with the Advanced Receiver 2 (ARX 2) tracking Pioneer 10 and Voyager 2 is described. The measured results are compared with those of the Block 4 receiver that was operating in parallel with the ARX 2. It is shown that the ARX 2 outperforms the Block 4 receiver in terms of Allan variance of the Doppler residuals, the amount of which depends on the scenario of interest. Author

N90-21894*# Jet Propulsion Lab., California Inst. of Tech., Pasadena.

EXACT CLOSED-FORM EXPRESSIONS FOR THE PERFORMANCE OF THE SPLIT-SYMBOL MOMENTS ESTIMATOR OF SIGNAL-TO-NOISE RATIO

S. Dolinar *In its* The Telecommunications and Data Acquisition Report 15 Feb. 1990 p 174-179 (For primary document see N90-21880 15-32)
Avail: NTIS HC A15/MF A02 CSCL 17B

Previously, the performance of the split-symbol moments estimator (SSME) of signal-to-noise ratio (SNR) has been evaluated by means of approximate expressions for the estimator mean and variance. These are asymptotic formulas in the sense that they become accurate as the number of estimator samples gets large. Here, exact closed-form expressions are obtained for the same quantities. These expressions confirm the accuracy of the previously derived asymptotic results, and, unlike the asymptotic formulas, they are useful even when the number of samples is small. It is also shown that the conventional split-symbol estimator can be trivially scaled to form a signal-to-noise ratio estimator which is precisely unbiased (as long as the estimate is based on more than two split-symbols). Author

N90-21895*# Jet Propulsion Lab., California Inst. of Tech., Pasadena.

A VLSI DECOMPOSITION OF THE DEBRUIJN GRAPH

O. Collins (Johns Hopkins Univ., Baltimore, MD.), S. Dolinar, R. McEliece, and F. Pollara *In its* The Telecommunications and Data Acquisition Report 15 Feb. 1990 p 180-190 (For primary document see N90-21880 15-32)
Avail: NTIS HC A15/MF A02 CSCL 17B

A new Viterbi decoder for convolutional codes with constraint lengths up to 15, called the Big Viterbi Decoder, is under development for the Deep Space Network. It will be demonstrated by decoding data from the Galileo spacecraft, which has a rate 1/4, constraint-length 15 convolutional encoder on board. Here, the mathematical theory underlying the design of the very-large-scale-integrated (VLSI) chips that are being used to build this decoder is explained. The deBruijn graph B sub n describes the topology of a fully parallel, rate 1/v, constraint length n+2 Viterbi decoder, and it is shown that B sub n can be built by appropriately wiring together (i.e., connecting together with extra edges) many isomorphic copies of a fixed graph called a B sub n building block. The efficiency of such a building block is defined as the fraction of the edges in B sub n that are present in the copies of the building block. It is shown, among other things, that for any alpha less than 1, there exists a graph G which is a B sub n building block of efficiency greater than alpha for all sufficiently large n. These results are illustrated by describing a special hierarchical family of deBruijn building blocks, which has led to the design of the gate-array chips being used in the Big Viterbi Decoder. Author

N90-21896*# Jet Propulsion Lab., California Inst. of Tech., Pasadena.

VALIDITY OF THE TWO-LEVEL MODEL FOR VITERBI DECODER GAP-CYCLE PERFORMANCE

S. Dolinar and S. Arnold *In its* The Telecommunications and Data Acquisition Report 15 Feb. 1990 p 191-202 (For primary document see N90-21880 15-32)
Avail: NTIS HC A15/MF A02 CSCL 17B

A two-level model has previously been proposed for approximating the performance of a Viterbi decoder which encounters data received with periodically varying signal-to-noise ratio. Such cyclically gapped data is obtained from the Very Large Array (VLA), either operating as a stand-alone system or arrayed with Goldstone. This approximate model predicts that the decoder error rate will vary periodically between two discrete levels with the same period as the gap cycle. It further predicts that the length of the gapped portion of the decoder error cycle for a constraint length K decoder will be about K-1 bits shorter than the actual duration of the gap. The two-level model for Viterbi decoder performance with gapped data is subjected to detailed validation tests. Curves showing the cyclical behavior of the decoder error burst statistics are compared with the simple square-wave cycles predicted by the model. The validity of the model depends on a parameter often considered irrelevant in the analysis of Viterbi decoder performance, the overall scaling of the received signal or the decoder's branch-metrics. Three scaling alternatives are examined: optimum branch-metric scaling and constant branch-metric scaling combined with either constant noise-level scaling or constant signal-level scaling. The simulated decoder error cycle curves roughly verify the accuracy of the two-level model for both the case of optimum branch-metric scaling and the case of constant branch-metric scaling combined with constant noise-level scaling. However, the model is not accurate for the case of constant branch-metric scaling combined with constant signal-level scaling. Author

N90-21897*# Jet Propulsion Lab., California Inst. of Tech., Pasadena.

FINDING THE COMPLETE PATH AND WEIGHT ENUMERATORS OF CONVOLUTIONAL CODES

I. Onyszchuk *In its* The Telecommunications and Data Acquisition Report 15 Feb. 1990 p 203-213 (For primary document see N90-21880 15-32)
Avail: NTIS HC A15/MF A02 CSCL 17B

A method for obtaining the complete path enumerator T(D, L, I) of a convolutional code is described. A system of algebraic equations is solved, using a new algorithm for computing determinants, to obtain T(D, L, I) for the (7,1/2) NASA standard code. Generating functions, derived from T(D, L, I) are used to upper bound Viterbi decoder error rates. This technique is currently feasible for constraint length K less than 10 codes. A practical, fast algorithm is presented for computing the leading nonzero coefficients of the generating functions used to bound the performance of constraint length K less than 20 codes. Code profiles with about 50 nonzero coefficients are obtained with this algorithm for the experimental K = 15, rate 1/4, code in the Galileo mission and for the proposed K = 15, rate 1/6, 2-dB code. Author

N90-21898*# Jet Propulsion Lab., California Inst. of Tech., Pasadena.

AN ADAPTIVE VECTOR QUANTIZATION SCHEME

K.-M. Cheung *In its* The Telecommunications and Data Acquisition Report 15 Feb. 1990 p 214-220 (For primary document see N90-21880 15-32)
Avail: NTIS HC A15/MF A02 CSCL 17B

Vector quantization is known to be an effective compression scheme to achieve a low bit rate so as to minimize communication channel bandwidth and also to reduce digital memory storage while maintaining the necessary fidelity of the data. However, the large number of computations required in vector quantizers has been a handicap in using vector quantization for low-rate source coding. An adaptive vector quantization algorithm is introduced that is inherently suitable for simple hardware implementation because it has a simple architecture. It allows fast encoding and decoding because it requires only addition and subtraction operations. Author

N90-21899*# Jet Propulsion Lab., California Inst. of Tech., Pasadena.

A VLSI DESIGN FOR A SYSTOLIC VITERBI DECODER

T. K. Truong, E. Satorius, M. T. Shih, and I. S. Reed (University of Southern California, Los Angeles.) *In its* The Telecommunications and Data Acquisition Report 15 Feb. 1990 p 221-233 (For primary document see N90-21880 15-32)
Avail: NTIS HC A15/MF A02 CSCL 17B

A systolic Viterbi decoder for convolutional codes is developed. This decoder uses the trace-back method to reduce the amount of data needed to be stored in registers. It is shown that this new algorithm requires a smaller chip size and achieves a faster decoding time than other existing methods. Author

N90-21900*# Jet Propulsion Lab., California Inst. of Tech., Pasadena.
RADAR RFI AT GOLDSTONE DSS 12 AND DSS 16
S. D. Slobin and T. K. Peng *In its* The Telecommunications and Data Acquisition Report 15 Feb. 1990 p 234-247 (For primary document see N90-21880 15-32)
Avail: NTIS HC A15/MF A02 CSCL 17B

Radio frequency interference (RFI) from the DSS 14 Goldstone Solar System Radar (GSSR) was investigated at DSS 12 and DSS 16 with the goal of assisting in the choice of the location of future DSN antennas. Total power measurements at both locations were made at the S-band carrier frequency of 2320 MHz. X-band measurements at the carrier frequency of 8495 MHz could not be made. Exciter-chain output spectrum and klystron output spectrum measurements were made at S- and X-bands using a probable worst-case modulation of the radar signal (short pseudorandom number (PN) code length and short pulse length). Based on these measurements, it is estimated that RFI levels in the DSN receiving bands at both sites (above 10-deg elevation) would be below -192 dBm for a 1-Hz bandwidth Author

N90-21901*# Jet Propulsion Lab., California Inst. of Tech., Pasadena.
IMPROVING A DATA-ACQUISITION SOFTWARE SYSTEM WITH ABSTRACT DATA TYPE COMPONENTS c61
S. D. Howard *In its* The Telecommunications and Data Acquisition Report 15 Feb. 1990 p 248-251 (For primary document see N90-21880 15-32)
Avail: NTIS HC A15/MF A02 CSCL 09B

Abstract data types and object-oriented design are active research areas in computer science and software engineering. Much of the interest is aimed at new software development. Abstract data type packages developed for a discontinued software project were used to improve a real-time data-acquisition system under maintenance. The result saved effort and contributed to a significant improvement in the performance, maintainability, and reliability of the Goldstone Solar System Radar Data Acquisition System. Author

N90-21902*# Jet Propulsion Lab., California Inst. of Tech., Pasadena.
STRUCTURAL FATIGUE IN THE 34-METER HA-DEC ANTENNAS c39
R. A. VanHek and B. P. Saldua *In its* The Telecommunications and Data Acquisition Report 15 Feb. 1990 p 252-262 (For primary document see N90-21880 15-32)
Avail: NTIS HC A15/MF A02 CSCL 20K

Structural modifications to the 34-m hour-angle-declination antennas, coupled with the use of the antennas beyond their intended lifespans, have led to structural fatigue, as evidenced by damage to the declination drive gear and cracks on the structural members and gussets. An analysis and simulation were made of the main antenna structural members. The analysis showed that the total stress to the antenna structure substantially exceeds the maximum levels recommended by the American Institute of Steel Construction (AISC). Although each of the separate static conditions of stress is only 50 percent of the total stress and does not reach the AISC reduced yield limit, fatigue can and did occur, causing the material to crack in the weakest places. Author

N90-21903*# Jet Propulsion Lab., California Inst. of Tech., Pasadena.
MARK 4-A DSCC (MAGELLAN-ERA) TELEMETRY SYSTEM DESCRIPTION c17
D. L. Ross *In its* The Telecommunications and Data Acquisition Report 15 Feb. 1990 p 263-273 (For primary document see N90-21880 15-32)
Avail: NTIS HC A15/MF A02 CSCL 09F

An update to the description of the Deep Space Communications Complex portion of the Mark 4-A Telemetry system is given. This system is currently implemented at all signal processing centers. The upgrade of the telemetry system was undertaken primarily in support of the Voyager-Neptune Encounter and the Magellan mission. The Mark 3 Telemetry System is the predecessor of the Mark 4-A system. Author

N90-21904*# Jet Propulsion Lab., California Inst. of Tech., Pasadena.
A HIGHER DENSITY VLBI CATALOG FOR NAVIGATING MAGELLAN AND GALILEO
J. S. Ulvestad, O. J. Sovers, and C. S. Jacobs *In its* The Telecommunications and Data Acquisition Report 15 Feb. 1990 p 274-300 (For primary document see N90-21880 15-32)
Avail: NTIS HC A15/MF A02 CSCL 17B

The density of radio sources near the ecliptic in the astrometric JPL Very Long Baseline Interferometry (VLBI) catalog has been increased by over 50 percent since 1985. This density increase has been driven by the need for more sources for the VLBI navigation of the Magellan and Galileo spacecraft, but the sources also will be usable for Mars Observer and other future missions. Since the last catalog, including observations made through 1985, was published in 1988, a total of 21 radio sources has been added that fulfill the following criteria: (1) they lie within 10 deg of the ecliptic plane; (2) their correlated flux densities are above 0.2 Jy on at least one of the Deep Space Network intercontinental baselines at both 2.3 and 8.4 GHz; and (3) the source positions are known to better than 5 milliarcseconds (25 nanoradians). The density of such sources in the catalog has been increased from 15.6 per steradian to 25.2 per steradian. Ten more sources have been added that fulfill the last two criteria given above and lie between 10 deg and 20 deg from the ecliptic plane. Analysis shows that there may be approx. 70 more sources with correlated flux densities above 0.2Jy that are within approx. 20 deg of the ecliptic. However, VLBI navigation observations of the new and prospective sources with the 250-kHz bandwidth of the current operational system will require the use of two 70-m antennas in most cases. Including both old and new sources, if two 34-m antennas are used, there will be usable navigation sources within 10 deg of a spacecraft in only 30 percent of the ecliptic, and sources within 20 deg of a spacecraft over 70 percent of the ecliptic. Author

N90-21905*# Jet Propulsion Lab., California Inst. of Tech., Pasadena.
AN 8.4-GHz DUAL-MASER FRONT-END SYSTEM FOR PARKES REIMPLEMENTATION c36
D. L. Trowbridge, J. R. Loreman, T. J. Brunzie, and R. Quinn *In its* The Telecommunications and Data Acquisition Report 15 Feb. 1990 p 301-319 (For primary document see N90-21880 15-32)
Avail: NTIS HC A15/MF A02 CSCL 20E

An 8.4-GHz front-end system consisting of a feedhorn, a waveguide feed assembly, dual masers, and downconverters was reimplemented at Parkes as part of the Parkes Canberra Telemetry Array for the Voyager Neptune encounter. The front-end system was originally assembled by the European Space Agency and installed on the Parkes antenna for the Giotto project. It was also used on a time-sharing basis by the Deep Space Network as part of the Parkes Canberra Telemetry Array to enhance the data return from the Voyager Uranus encounter. At the conclusion of these projects in 1986, part of the system was then shipped to JPL on loan for reimplementation at Parkes for the Voyager Neptune encounter. New design and implementation required to make the system operable at Parkes included new microwave front-end control cabinets, closed-cycle refrigeration monitor system, noise-adding radiometer system, front-end controller assembly, X81 local oscillator multiplier, and refurbishment of the original dual 8.4-GHz traveling-wave masers and waveguide feed system. The front-end system met all requirements during the encounter and was disassembled in October 1989 and returned to JPL. Author

N90-21906 Essex Univ., Colchester (England).
BROADCAST FILE DISTRIBUTION ON PACKET SATELLITE NETWORKS Ph.D. Thesis
J. S. J. Daka 1989 216 p
Avail: Univ. Microfilms Order No. BRD-87426

A packet satellite network provides a completely connected network with a fixed delay (about 250 milliseconds). These are provided on a global scale (up to one third of the Earth) within the antenna pattern coverage area or footprint. File distribution is an application which can benefit from such a network. In file distribution a single file is distributed to multiple sites. Total connectivity offered by a packet satellite network to achieve highly efficient file distributions can be taken advantage of. Some of the methods used to distribute files are examined, with the intention of improving the techniques. Three bulk distribution protocols are suggested and analyzed. These are the Modified Full Memory go-back-n Protocol, an Improved Broadcast File Transfer Protocol, and a Recipient Driven Broadcast File Transfer Protocol. For the Recipient Driven Broadcast File Transfer Protocol, an algorithm is proposed which attempts to coordinate the actions of the recipients, giving the protocol better performance especially when there is a large number of receivers. For the connection phase, a protocol called Continuous Attempts Until Connection is suggested, which offers a shorter connection time especially in environments of higher error rates. Dissert. Abstr.

N90-21907# Advisory Group for Aerospace Research and Development, Neuilly-Sur-Seine (France). Electromagnetic Wave Propagation Panel.
ATMOSPHERIC PROPAGATION IN THE UV, VISIBLE, IR, AND mm-WAVE REGION AND RELATED SYSTEMS ASPECTS
Mar. 1990 363 p In ENGLISH and FRENCH Meeting held in Copenhagen, Denmark, 9-13 Oct. 1989
(AGARD-CP-454; ISBN-92-835-0548-4) Copyright Avail: NTIS HC A16/MF A03; Non-NATO Nationals requests available only from AGARD/Scientific Publications Executive

Atmospheric propagation of electromagnetic waves at frequencies above 30 GHz is of importance to many current and future military applications. Propagation phenomena affect and often limit navigation, communications, surveillance, search, target acquisition, fire control, autonomous weapons guidance, kill assessment, countermeasures and medium to high power laser applications. Recent advances in components and technology have prompted extensive studies and applications in the above wavelength region. An exchange of information between scientists and engineers involved in research and development in this wavelength region is expected to benefit further development of systems and explore new areas of research as well as military and civilian applications. Topics discussed are: propagation measurements; propagation modes; sensing of the propagation environment; system aspects and performance modeling; and countermeasures. For individual titles, see N90-21908 through N90-21942.

N90-21908# Admiralty Research Establishment, Portsdown (England).
A SURVEY OF THE MARITIME-AEROSOL DATA COLLECTED AT SOUTH UIST AND THE IMPLICATIONS FOR THE LOWTRAN MARITIME AEROSOL MODEL c45
N. P. Tolliday, M. H. Smith, P. M. Park, and I. E. Consterdine (Manchester Univ., England) *In* AGARD, Atmospheric Propagation in the UV, Visible, IR, and MM-Wave Region and Related Systems Aspects Mar. 1990 11 p (For primary document see N90-21907 15-32)
Copyright Avail: NTIS HC A16/MF A03; Non-NATO Nationals requests available only from AGARD/Scientific Publications Executive

Over the period 1979 until 1988, a Maritime Aerosol Study was performed. A survey of the results obtained and some comments on how well the data conforms to the LOWTRAN maritime aerosol model are presented. Aerosol loadings and spectral distributions were measured, over numerous 2 to 4 week periods since 1979, at a coastal site on the island of South Uist, situated off north-west Scotland. Aerosol size distributions, covering the radius range 0.08 to 23.5 microns, were measured by Particle Measuring Systems optical particle counters, together with basic meteorological observations. Two further field projects were conducted at this site during the spring and summer of 1986. The spring project was characterized by an intense cyclone which gave rise to local wind speeds exceeding 40 m/s while, during the summer, much calmer conditions prevailed with an extended period of very low wind speeds. These observations demonstrated that volumetric loadings of marine aerosol continue increasing for all measured wind speeds, contrary to earlier speculation suggesting a limit beyond 12 to 15 m/s. The low wind speed period permitted the relaxation response of the atmosphere to be investigated, and the decay of the aerosol loadings, for various size catagories, over this period was found to be consistent with a simple turbulent deposition model. Variations in aerosol spectral shape with wind speed will be presented, and demonstrate that particulate volume and surface area are dominated by the larger particles for moderate and high wind speeds. The consequences of these findings for the LOWTRAN Maritime Aerosol Model and for atmospheric propagation at visible and infrared wavelengths are discussed. Author

N90-21909# Centre National de la Recherche Scientifique, Paris (France).
THE MEDITERRANEAN MARINE ENVIRONMENT AND ITS EFFECTS ON AEROSOLS AND INFRARED TRANSMISSION Thesis c45
Mireille Tanguy *In* AGARD, Atmospheric Propagation in the UV, Visible, IR, and MM-Wave Region and Related Systems Aspects Mar. 1990 13 p In FRENCH (For primary document see N90-21907 15-32)
Copyright Avail: NTIS HC A16/MF A03; Non-NATO Nationals requests available only from AGARD/Scientific Publications Executive

A series of experiments conducted depend on the validation of the LOWTRAN 6 code by the computation of the atmospheric transmission of infrared rays through the marine boundary layer in the Mediterranean region. The opto-electronic device implanted in the coast is made up of a transmissometer, which aids in the measurement of transmission in the 3 to 5 and 8 to 12 micron frequencies, along a horizontal path at 8 km and an altitude 40 m above sea level. In order to compare data from different readings, an automatic weather station and an optical sonde (CSASP-100-HV) work in parallel. Also, a study was made of the behavior of aerosol density as a localization function of the measurement along with weather conditions during the summer on board national French navy ships. Transl. by E.R.

N90-21910*# National Aeronautics and Space Administration. Langley Research Center, Hampton, VA.
NEW SPECTRAL FEATURES OF STRATOSPHERIC TRACE GASES c45
A. Goldman, F. J. Murcray, R. D. Blatherwick, J. J. Kosters, F. H. Murcray, D. G. Murcray (Denver Univ., CO.), and C. P. Rinsland *In* AGARD, Atmospheric Propagation in the UV, Visible, IR, and MM-Wave Region and Related Systems Aspects Mar. 1990 13 p (For primary document see N90-21907 15-32)
Copyright Avail: NTIS HC A16/MF A03; Non-NATO Nationals requests available only from AGARD/Scientific Publications Executive CSCL 04A

A new Michelson-type interferometer system operating in the infrared at very high resolution (0.002 to 0.003 wavenumber FWHM) was used to record numerous balloon-borne solar absorption spectra of the stratosphere, ground-based solar absorption spectra, and laboratory spectra of molecules of atmospheric interest. Results obtained are reported for several important stratospheric trace gases, HNO3, ClONO2, HO2NO2, NO2, and COF2, in the 8 to 12 micron spectral region. Many features of these gases were identified in the stratospheric spectra. Comparison of the spectra with line-by-line simulations shows previous spectral parameters are often inadequate. New analysis of high resolution laboratory and atmospheric spectra and improved theoretical calculations will be required for all bands. Preliminary versions of several sets of improved line parameters are presented. Author

N90-21911# Science Applications International Corp., Billerica, MA.

MINIMIZING THE EFFECTS OF THE ATMOSPHERE IN THE OBSERVATION OF ULTRAVIOLET RADIATION c45

A. V. Dentamaro, C. G. Stergis, and V. C. Baisley (Air Force Geophysics Lab., Hanscom AFB, MA.) *In* AGARD, Atmospheric Propagation in the UV, Visible, IR, and MM-Wave Region and Related Systems Aspects Mar. 1990 11 p (For primary document see N90-21907 15-32)

Copyright Avail: NTIS HC A16/MF A03; Non-NATO Nationals requests available only from AGARD/Scientific Publications Executive

Ground measurements were performed which provide an accurate method of measuring ultra-violet radiation sources propagating through the atmosphere. This method of measurement effectively minimizes the influence of the atmosphere in the detection of UV sources at equal or greater altitude at the specific time the measurements are being made, allowing evaluation of propagation losses. Radiation of wavelength 3000 to 3700 A was collected and recorded by a UV imager mounted onto an 18 inch Cassegrain telescope situated on Santa Ynez Mountain, California at an altitude of 1.26 km above sea level. Various meteorological and topographical conditions determine the transmittance of the incident starlight through the atmosphere. Measurements were taken under optimum conditions (little or no cloud cover, visibility greater than 20 km). The atmospheric transmittance code LOWTRAN 6 was used to generate transmittance as a function of observation angle and meteorological range (quantitative measurement of visibility). Comparing the measured intensity of one star to its known absolute intensity above the atmosphere determines the transmittance for any point in the sky. In addition, extinction coefficients were measured at the observation point and at ground level using a photometer and a standard UV source. Both the stellar and photometer data indicate that the meteorological range during the ten day period of observation varied from 20 to 30 km. Therefore, the method was useful in accounting for changes in the atmosphere. Under these optimum viewing conditions, ground-based measurements of various high altitude sources of radiation such as rocket plumes or vehicle glow with a maximum error due to transmission losses of 10 percent should be possible. Author

N90-21912# National Oceanic and Atmospheric Administration, Boulder, CO. Wave Propagation Lab.

SCINTILLATION OF MILLIMETER-WAVE INTENSITY AND PHASE CAUSED BY TURBULENCE AND PRECIPITATION c45

R. J. Hill, S. F. Clifford, R. J. Lataitis, and A. D. Sarma *In* AGARD, Atmospheric Propagation in the UV, Visible, IR, and MM-Wave Region and Related Systems Aspects Mar. 1990 6 p Sponsored in part by National Research Council (For primary document see N90-21907 15-32)
(Contract MIPR-125-88)

Copyright Avail: NTIS HC A16/MF A03; Non-NATO Nationals requests available only from AGARD/Scientific Publications Executive

A propagation experiment over exceptionally flat farm land was performed near Flatville, Illinois. Extensive micrometeorological (abbreviated as micromet) measurements were made simultaneously. Because of the excellent horizontal homogeneity of the site, these micromet data determine the turbulence statistics along the entire propagation path. Instrumentation for measurements of rain as well as fog and snow were deployed. There were five experiment sessions, each about one month long Several millimeter-wave frequencies between 116 and 230 GHz were used. Results for data during inclement weather were reported. Some results of these studies are reviewed and new results are presented for temporal spectra of intensity and phase difference obtained during precipitation. Author

N90-21913# Science Research Council, Didcot (England).

MILLIMETRIC, INFRARED, AND OPTICAL PROPAGATION STUDIES OVER A 500 m PATH

C. J. Gibbins *In* AGARD, Atmospheric Propagation in the UV, Visible, IR, and MM-Wave Region and Related Systems Aspects Mar. 1990 13 p (For primary document see N90-21907 15-32)

Copyright Avail: NTIS HC A16/MF A03; Non-NATO Nationals requests available only from AGARD/Scientific Publications Executive

A 500 m propagation range was developed with transmission links operating at frequencies of 37, 57, 97, 137, and 210 GHz and at wavelengths of 10.6 and 0.63 microns. A comprehensive set of meteorological observations includes rainfall and snowfall rates, raindrop size distributions, temperature and humidity, microwave refractive index, surface pressure, and wind velocity. Measurements from the range are being used to compile an extensive propagation and meteorological database with which a variety of studies are being carried out; these include detailed investigations into individual events, aimed towards obtaining a deeper understanding of the interaction between electromagnetic radiation and the prevailing meteorological phenomena such as rain, snow, fog, and atmospheric turbulence. Statistical analysis of the database, on the other hand, is directed towards obtaining information on the reliability of future communications systems, so that average and extreme values of systems performance can be assessed. Such studies facilitate the development of prediction procedures based on existing meteorological data for future systems planning, and an assessment of the relative merits of different wavebands, important to the increasing development and deployment of multi-spectral sensors. Author

N90-21914# Naval Ocean Systems Center, San Diego, CA. Ocean and Atmospheric Sciences Div.

EVAPORATION DUCT EFFECTS AT MILLIMETER WAVELENGTHS

K. D. Anderson *In* AGARD, Atmospheric Propagation in the UV, Visible, IR, and MM-Wave Region and Related Systems Aspects Mar. 1990 13 p (For primary document see N90-21907 15-32)

Copyright Avail: NTIS HC A16/MF A03; Non-NATO Nationals requests available only from AGARD/Scientific Publications Executive

The evaporation duct strongly influences low-altitude over-the horizon propagation at millimeter wavelengths. Results from more than 2000 hours of propagation and meteorological measurements were made at 94 GHz on a 40.6 km over-horizon, over-water path along the southern California coast show that the average received power was 63 dB greater than expected for propagation in a nonconducting, or normal, atmosphere; 90 percent of the measurements were at least 55 dB greater than the normal atmosphere. A numerical model of transmission loss based on observed surface meteorology is discussed and results are compared to measured transmission loss. On average, modeling results underestimate the transmission loss by 10 dB. In addition, results from modeling based on an independent climatology of evaporation duct heights for the area are shown to be adequate for most propagation assessment purposes. The reliability and reasonable accuracy of the model provide a strong justification for utilizing the technique to assess millimeter wave communication and radar systems operating in many, if not all, ocean regions. Author

N90-21915# Shape Technical Center, The Hague (Netherlands).

REPORT ON STC/TECHNISCHE UNIVERSITEIT (TU) DELFT EXTREMELY HIGH FREQUENCY (EHF) RADIO RELAY STUDY

N. P. Mansfield, L. P. Ligthart, R. J. Niemeijer, and J. S. vanSinttruyen (Technische Hogeschool, Delft, Netherlands) *In* AGARD, Atmospheric Propagation in the UV, Visible, IR, and MM-Wave Region and Related Systems Aspects Mar. 1990 6 p (For primary document see N90-21907 15-32)
Copyright Avail: NTIS HC A16/MF A03; Non-NATO Nationals requests available only from AGARD/Scientific Publications Executive

Preliminary results of a joint extremely high frequency (EHF) radio relay trial between SHAPE Technical Center (STC) and the Delft University of Technology (DUT) are presented. The trial was established to study the effects of meteorological disturbances, of which rain is the principal cause, on a digital radio relay path 12.7 km long operating at 37.5 GHz. Practical use for these radio relay links is found in local grade connections in an Integrated Services Digital Network (ISDN). Author

N90-21916# Selenia S.p.A., Rome (Italy).

THE mm-WAVE REGION PROPAGATION EXPERIMENTS BY SATELLITE

Paolo Ricci and Antonio Florio *In* AGARD, Atmospheric Propagation in the UV, Visible, IR, and MM-Wave Region and Related Systems Aspects Mar. 1990 10 p (For primary document see N90-21907 15-32)
Copyright Avail: NTIS HC A16/MF A03; Non-NATO Nationals requests available only from AGARD/Scientific Publications Executive

The RF propagation experiments, related to the earth space communications by means of geostationary satellites, at frequencies exceeding the 30 GHz value, as lower limit of the mm-wave region, are examined. The Selenia Spazio activity is outlined. Olympus system in-orbit tests will have experiments at 20/30 GHz, just below the mm-wave band, and includes a 12.5 GHz beacon which will be used as reference to crosscorrelate the behavior at different frequencies, to extend the measurement dynamics of the coherent receivers, and as possible reference for antenna autotracking. The next step will be with Italsat, the Italian satellite scheduled for launch at the end of '90, allowing the first mm-wave propagation experiment for space communications at 40/50 GHz, across the outmost of the European zone. A third beacon at lower frequency (20 GHz) is foreseen as multipurpose reference. The functional configuration of the earth stations is presented and the related propagation experiments are described in terms of performances and from an operational point of view. Copolar/crosspolar characteristics and scintillation phenomena are included. The triple frequency configuration (20/40/50 GHz) and the use of radiometric and meteorological sensors, associated with the earth station, will give the opportunity to crosscorrelate the experiments results and to extend their dynamics capabilities. The propagation experiments results at 40/50 GHz will have interest for secure communications and countermeasures. The use of higher frequency values, until and beyond 100 GHz, is envisaged in other study activities for atmospheric propagation experiments. The mm-wave propagation experiment results can provide suitable guidelines for link design optimization and to identify the opportunity of using frequency/polarization/site diversity configurations in the different communication scenarios. Author

N90-21917# Air Force Geophysics Lab., Hanscom AFB, MA.

LOWTRAN 7: STATUS, REVIEW, AND IMPACT FOR SHORT-TO-LONG-WAVELENGTH INFRARED APPLICATIONS

F. X. Kneizys, G. P. Anderson, Eric P. Shettle, L. W. Abreu, J. H. Chetwynd, Jr., J. E. A. Selby, W. O. Gallery, and S. A. Clough (Atmospheric and Environmental Research, Inc., Cambridge, MA.) *In* AGARD, Atmospheric Propagation in the UV, Visible, IR, and MM-Wave Region and Related Systems Aspects Mar. 1990 11 p (For primary document see N90-21907 15-32)
Copyright Avail: NTIS HC A16/MF A03; Non-NATO Nationals requests available only from AGARD/Scientific Publications Executive

A summary of the recent improvements, modifications, and updates to the LOWTRAN 7 atmospheric transmittance and radiance computer program will be given. There were some significant changes to the LOWTRAN model in the latest version, LOWTRAN 7, that affect the manner in which the basic atmospheric transmittance and radiance calculations are performed as well as providing the user with greater flexibility and more capabilities. The LOWTRAN 7 code now calculates atmospheric transmittance, atmospheric background radiance, single-scattered and earth-reflected solar and lunar radiance, direct solar irradiance, and multiple-scattered solar and thermal radiance. The spectral range of the code was extended from 0 to 50,000 cm at a spectral resolution of 20 cm. The program can cope with an observer/target geometry and can include the effects of molecular, aerosol, fog, rain, and cloud absorption and scattering. Some of the basic changes to LOWTRAN 7, in particular the introduction of new molecular absorption transmission functions and separating the transmittances due to CO2, N2O, CO, CH4 and O2, will give rise to differences in the transmittance and radiance calculations (compared to those obtained with LOWTRAN 6) depending on the observer/target viewing geometry and spectral region. The dual purpose is to indicate how the new changes to LOWTRAN 7 affect atmospheric transmittance and background radiance calculations for specific applications. Both high-altitude, long-range and low-altitude, moderate-range scenarios are stressed and will show the impact that the recent changes to LOWTRAN 7 have made on the short, medium and long wavelength infrared atmospheric attenuation and background radiance, compared to calculations with LOWTRAN 6. Author

N90-21918# Atmospheric Sciences Lab., White Sands Missile Range, NM.

PROPAGATION ENVIRONMENTS, EFFECTS, AND DECISION AIDS

F. E. Niles, M. G. Heaps, R. C. Shirkey, L. D. Duncan, and M. A. Seagraves *In* AGARD, Atmospheric Propagation in the UV, Visible, IR, and MM-Wave Region and Related Systems Aspects Mar. 1990 8 p (For primary document see N90-21907 15-32)
Copyright Avail: NTIS HC A16/MF A03; Non-NATO Nationals requests available only from AGARD/Scientific Publications Executive

Reconnaissance, surveillance, target acquisition, communications, and weapon systems are becoming more sophisticated and are becoming more dependent on the propagation of electromagnetic of acoustic energy through the atmosphere. Weather and battle activity will constantly change the atmospheric conditions and hence the propagation environments when the systems are employed. The effects of these changing propagation environments must be understood for optimum system design, assessment of system performance, development of countermeasures, development of tactics and doctrine, and development of decision aids. In 1978 the U.S. Army Atmospheric Effects Laboratory (ASL) began the development of the Electro-Optical Systems Atmospheric Effects Library (EOSAEL) in order to quantify some of the battlefield atmospheric effects. EOSAEL has had several releases; and the latest, EOSAEL 87, contains 26 modules that can be separated into 6 generic classes: gases, natural aerosols, battlefield aerosols, radiative transfer, laser propagation, and target acquisition and system performance. Combining information on weather and battle activity with an understanding of atmospheric effects has allowed ASL to produce tactical decision aids (TDAs) for many friendly and threat electro-optical systems. This developmental software is scheduled to be fielded on the Integrated Meteorological System (IMETS). Author

N90-21919# Air Force Geophysics Lab., Hanscom AFB, MA.

MODELS OF AEROSOLS, CLOUDS, AND PRECIPITATION FOR ATMOSPHERIC PROPAGATION STUDIES c46

Eric P. Shettle *In* AGARD, Atmospheric Propagation in the UV, Visible, IR, and MM-Wave Region and Related Systems Aspects

Mar. 1990 14 p (For primary document see N90-21907 15-32)
Copyright Avail: NTIS HC A16/MF A03; Non-NATO Nationals requests available only from AGARD/Scientific Publications Executive

A number of models are reviewed for the atmospheric aerosols, clouds, and precipitation and their effects on the propagation of electromagnetic radiation at wavelengths from the ultraviolet through the microwave spectral regions. The focus is on the models developed at AFGL and elsewhere primarily for use in the atmospheric propagation models LOWTRAN (Kneizys et al., 1983 and 1988) and FASCODE (Clough et al., 1986), but also examines other particulate models. The scattering and absorption properties of the different particulate models are presented. Applications of the various models are discussed with recommendations on when it is most appropriate to use which aerosol or cloud model. Sensitivities of calculated transmittances and background radiances to the different types of particulate models are examined for a range of wavelengths. Author

N90-21920# Defence Research Establishment Valcartier (Quebec).

INTERPRETING METEOROLOGICAL DATA REPORTS FOR LOWTRAN NAVY AEROSOL MODEL EXTINCTION CALCULATIONS c47

A. J. Beaulieu *In* AGARD, Atmospheric Propagation in the UV, Visible, IR, and MM-Wave Region and Related Systems Aspects Mar. 1990 9 p (For primary document see N90-21907 15-32)
Copyright Avail: NTIS HC A16/MF A03; Non-NATO Nationals requests available only from AGARD/Scientific Publications Executive

To evaluate the aerosol extinction, one of the most advanced models is the LOWTRAN 6 Navy Aerosol model. However, evaluating the extinction corresponding to weather conditions derived from meteorological reports is often difficult because these reports lack one critical parameter required by the model: the Air Mass parameter value. Using default values for this parameter can lead to substantial errors in the extinction at the longer wavelengths. Furthermore, the LOWTRAN model does not accept values of relative humidities greater than 98 percent. These deficiencies become serious when it is desired to derive statistics of the IR extinction from meteorological records. A meteorological data interpreter model has been developed to overcome these problems. This model uses the visibility to determine the effective Air Mass parameter as well as adjusting the RH, the wind velocities and the precipitation rates through a series of logical selections to arrive at a physically consistent solution with respect to the available data. This model was tested on a large number of weather scenarios which shows its validity and its effects on IR system performance assessment. Author

N90-21921# Naval Research Lab., Washington, DC.

THE NAVAL OCEANIC VERTICAL AEROSOL MODEL Progress Report c46

Stuart G. Gathman, Gerrit deLeeuw, Kenneth L. Davidson, and Douglas R. Jensen (Naval Ocean Systems Center, San Diego, CA.) *In* AGARD, Atmospheric Propagation in the UV, Visible, IR, and MM-Wave Region and Related Systems Aspects Mar. 1990 11 p Sponsored in part by National Research Council (For primary document see N90-21907 15-32)
Copyright Avail: NTIS HC A16/MF A03; Non-NATO Nationals requests available only from AGARD/Scientific Publications Executive

The Naval Oceanic Vertical Aerosol Model (NOVAM) was formulated to estimate the vertical structure of the optical and infrared extinction coefficients in the marine atmospheric boundary layer (MABL). NOVAM was designed to predict the non-uniform and non-logarithmic extinction profiles which are often observed. It is based on a combination of empirical and physical models which describe the aerosol dynamical behavior. The extinction properties are calculated from the aerosol profiles using the Mie theory. For the initial evaluation of NOVAM, data from the July 1987 FIRE experiment (conducted off the coast of southern California) was used. Aerosol particle size distributions, aerosol scattering, and required meteorological parameters throughout the MABL were obtained from both airborne and surface-based platforms (aircraft, ship and balloon instrumentation packages). The aerosol-derived extinction properties throughout the MABL are compared with the NOVAM estimates. Author

N90-21922# Institute for Telecommunication Sciences, Boulder, CO.

MODELING MILLIMETER-WAVE PROPAGATION EFFECTS IN THE ATMOSPHERE

H. J. Liebe and G. A. Hufford *In* AGARD, Atmospheric Propagation in the UV, Visible, IR, and MM-Wave Region and Related Systems Aspects Mar. 1990 13 p Sponsored in part by Naval Ocean Systems Center (For primary document see N90-21907 15-32)
Copyright Avail: NTIS HC A16/MF A03; Non-NATO Nationals requests available only from AGARD/Scientific Publications Executive

Two millimeter-wave propagation models, called MPM and MZM, are discussed. The first one predicts, at frequencies up to 1000 GHz, loss and delay effects for a nonprecipitating atmosphere. Contributions from dry air and water vapor are addressed, as well as suspended water droplets that simulate fog or cloud conditions. For clear air, a local spectral line base is employed (44 O2 + 30 H2O lines) complemented by an empirical water-vapor continuum. Droplet effects are treated with the approximate Rayleigh scattering theory. Input variables are barometric pressure, temperature, relative humidity, and droplet concentration. At heights between 30 and 100 km, the spectral lines of oxygen result in an anisotropic medium due to the geomagnetic Zeeman effect. The computer program MZM was developed to analyze propagation of plane, polarized radio waves in the vicinity (+ or - MHz) of O2 line centers positioned in the 60-GHz band and at 119 GHz. Results are displayed that demonstrate many aspects of the unusual wave propagation through the mesosphere. Author

N90-21923# Forschungsinstitut fuer Optik, Tuebingen (Germany, F.R.).

MODELLING OF OPTICALLY AND IR EFFECTIVE ATMOSPHERIC TURBULENCE c47

V. Thiermann and A. Kohnle *In* AGARD, Atmospheric Propagation in the UV, Visible, IR, and MM-Wave Region and Related Systems Aspects Mar. 1990 12 p (For primary document see N90-21907 15-32)
Copyright Avail: NTIS HC A16/MF A03; Non-NATO Nationals requests available only from AGARD/Scientific Publications Executive

The problem area of modeling atmospheric turbulence, which is limiting electro-optical, especially laser systems performance is examined. The practical use of Monin-Oboukhov (MO) similarity for predicting the structure constant c(sup 2)(sub n) and the inner length scale l(sub n) of refractive index fluctuations are discussed. Even though MO similarity originally was stated for an ideal surface layer which is nearly nowhere found, it can be expected to be helpful also in natural terrain under real meteorological conditions. A set of parameterizations of the surface fluxes, which are required in the MO similarity expressions, is proposed. These parameterizations need only very basic environmental input data. Results of an experiment are presented showing reasonable agreement between model predictions and direct measurements at different heights. Model input parameters were measured explicitly here. In many cases, input parameters have to be estimated or there are only simple, not fully representative measurements available. A sensitivity analysis with respect to all input parameters is performed. The overall model error in high refractivity turbulence level situations is found to be about half an order of magnitude for c(sup 2)(sub n) if summed up over all contributions. For the inner scale l(sub n) this is less than 40 percent. Author

N90-21924# Yale Univ., New Haven, CT. Dept. of Applied Physics.

HIGH INTENSITY LASER BEAM INTERACTIONS WITH SINGLE DROPLETS **c36**

Richard K. Chang and Alfred S. Kwok *In* AGARD, Atmospheric Propagation in the UV, Visible, IR, and MM-Wave Region and Related Systems Aspects Mar. 1990 12 p (For primary document see N90-21907 15-32)
(Contract DAAL03-88-K-0040; AF-AFOSR-0100-88)
Copyright Avail: NTIS HC A16/MF A03; Non-NATO Nationals requests available only from AGARD/Scientific Publications Executive

High density laser beam propagation in the atmosphere requires knowledge of the linear and nonlinear optical interactions of the UV, visible, and IR radiation with individual water droplets. The spherical water-air interface of droplets (with radii larger than the wavelength) can enhance the incident laser intensity inside the droplet and in the air, provide optical feedback which can lower the threshold for stimulated nonlinear emission when the wavelength is in the transparent range of water, and modify the internal intensity distribution and, thereby, distort the droplet shape when the incident radiation is in the transparent or absorbing range of water. Nonlinear optical research with single micrometer-size water droplets irradiated by high intensity laser radiation in the transparent and absorbing regions of water is reviewed. Author

N90-21925# York Univ. (Ontario). Centre for Research in Earth and Space Science.

INCLUSION OF CLOUDS AND RAIN IN ATMOSPHERIC SLANT PATH CALCULATIONS

C. W. Lui, M. W. P. Cann, and R. W. Nicholls *In* AGARD, Atmospheric Propagation in the UV, Visible, IR, and MM-Wave Region and Related Systems Aspects Mar. 1990 9 p Prepared in cooperation with Institute for Space and Terrestrial Science, York, Ontario (For primary document see N90-21907 15-32)
Copyright Avail: NTIS HC A16/MF A03; Non-NATO Nationals requests available only from AGARD/Scientific Publications Executive

The computation of aerosol absorption and scattering coefficients is normally a lengthy process, so that atmospheric slant path calculations rely on selections from pre-calculated data. An investigation in which the calculated coefficients are stored in a parameterized form is described. The object was to encompass a wide variety of cloud and rain types in a data set of manageable proportions. Atmospheric aerosols and rain are characterized by the mass density, size distribution n(r), and shapes of the constituent water drops or ice crystals. Particle shapes may be irregular - in ice clouds, snow and rain for example - but for the calculations reported here are assumed to be spheres of equivalent volume. The modified gamma function, first proposed by D. Deirmendjian, as n(r) is adopted. The original form of the function contains four parameters. To facilitate the parameterization, we regroup them into two physically meaningful parameters r(sub c) (critical radius) and delta = alpha gamma, proportional to the slope of n(r) around r(sub c). Then the absorption and scattering coefficients calculated from Mie theory are expressed as a polynomial in temperature and frequency. These coefficients in the polynomials are stored for retrieval and interpolation during a slant path calculation. The parameterization is quite general and includes the Marshall-Palmer relation for rain, the Laws and Parsons and inverse power distributions. Author

N90-21926# GEC-Marconi Electronics Ltd., Chelmsford (England).

INFRARED PROPAGATION IN THE AIR-SEA BOUNDARY LAYER

R. Larsen, K. A. Preedy, and G. Drake (GEC Sensors Ltd., Basildon, England) *In* AGARD, Atmospheric Propagation in the UV, Visible, IR, and MM-Wave Region and Related Systems Aspects Mar. 1990 6 p Sponsored by Ministry of Defence, England (For primary document see N90-21907 15-32)
Copyright Avail: NTIS HC A16/MF A03; Non-NATO Nationals requests available only from AGARD/Scientific Publications Executive

Over the oceans and other large bodies of water the structure of the lowest layers of the atmosphere is often strongly modified by evaporation of water vapor from the water surface. At radio wavelengths this layer will usually be strongly refracting or ducting, and the layer is commonly known as the evaporation duct. However, the refractive index of air at infrared wavelengths differs from that at radio wavelengths, and the effects of the marine boundary layer on the propagation of infrared radiation are examined. Meteorological models of the air-sea boundary layer are used to compute vertical profiles of temperature and water-vapor pressure. From these are derived profiles of atmospheric refractive index at radio wavelengths and at infrared wavelengths in the window regions of low absorption. For duct propagation to occur it is necessary that the refractivity of air decreases rapidly with increasing height above the surface. At radio wavelengths this usually occurs when there is a strong lapse of water vapor pressure with increasing height. By contrast, at infrared wavelengths the refractive index is almost independent of water vapor pressure, and it is found that an infrared duct is formed only when there is a temperature inversion. Author

N90-21927# Defence Research Establishment Valcartier (Quebec).

A TEMPERATURE-DEPENDENT REGULAR INFRARED BAND MODEL FOR ABSORPTION AND DISPERSION

P. L. Roney *In* AGARD, Atmospheric Propagation in the UV, Visible, IR, and MM-Wave Region and Related Systems Aspects Mar. 1990 10 p (For primary document see N90-21907 15-32)
Copyright Avail: NTIS HC A16/MF A03; Non-NATO Nationals requests available only from AGARD/Scientific Publications Executive

A temperature-dependent infrared band model for the absorption and refraction of spectral lines, simultaneously broadened by Doppler and collisional effects, is developed. The model also takes into account the effects of line-coupling. The case of a simple diatomatic molecule, in the rotating oscillator approximation is treated. The result is given in the form of an infinite series which converges rapidly and is appropriate for efficient computation. Author

N90-21928# Air Force Geophysics Lab., Hanscom AFB, MA.

UV SPECTRAL SIMULATIONS USING LOWTRAN 7

G. P. Anderson, F. X. Kneizys, Eric P. Shettle, L. W. Abreu, J. H. Chetwynd, Jr., R. E. Huffman, and L. A. Hall *In* AGARD, Atmospheric Propagation in the UV, Visible, IR, and MM-Wave Region and Related Systems Aspects Mar. 1990 9 p (For primary document see N90-21907 15-32)
Copyright Avail: NTIS HC A16/MF A03; Non-NATO Nationals requests available only from AGARD/Scientific Publications Executive

LOWTRAN 7 is a low-resolution propagation model and computer code for predicting atmospheric transmittance and background radiance from 0 to 50,000/cm (wavelengths greater than 0.2 micron). The current model, released in February 1989, is a major extension of the LOWTRAN 6 model. In addition to incorporating new and improved molecular band models (primarily influencing IR calculations), LOWTRAN 7 was particularly adapted for basic ultraviolet transmittance and radiance calculations. It now contains a 0.2 nm resolution extra-terrestrial solar source function along with temperature-dependent O3 (Hartley-Huggins) and pressure-dependent O2 (Herzberg continuum) absorption cross sections. The O2 Schumann-Runge band absorption was patterned after the IR band model. As with past versions of LOWTRAN, the line-of-sight viewing and solar incidence geometry can be arbitrarily configured for either direct or backscattered calculations. Both solar and thermal multiple scattering are accommodated. Initial validations of the UV portions of LOWTRAN 7 were made against two separate AFGL spectrometers. Excellent agreement was found with UV data from a balloon-borne spectrometer designed to measure in situ solar irradiance within the stratosphere. These direct solar observations, all at high sun angles, were made at stratospheric altitudes. Ultraviolet background measurements in the 0.2 to 0.29 micron wavelength region were made from the S3-4 satellite in a polar, sun-synchronous, nadir-viewing orbit. For moderate to high solar incidence angles, the backscatter comparisons with LOWTRAN 7 are again reasonable (generally within 10 percent). With the sun on the horizon, however, the twilight airglow becomes a dominant feature; such emission sources are not incorporated into LOWTRAN. Author

N90-21929# Science Research Council, Didcot (England). Radio Communications Research Unit.

MILLIMETRE-WAVE PROPAGATION IN THE EVAPORATION DUCT

M. F. Levy and K. H. Craig *In* AGARD, Atmospheric Propagation in the UV, Visible, IR, and MM-Wave Region and Related Systems Aspects Mar. 1990 10 p (For primary document see N90-21907 15-32)

Copyright Avail: NTIS HC A16/MF A03; Non-NATO Nationals requests available only from AGARD/Scientific Publications Executive

Recent developments in propagation modeling based on the Parabolic Equation Method allow the forecasting of two-dimensional antenna coverage diagrams at millimeter wavelengths, in a dispersive atmosphere with arbitrary two-dimensional variation of the refractive index. The model was applied successfully to mm-wave propagation in the evaporation duct. The evaporation duct height is not sufficient to characterize mm-wave propagation, and information on the water vapor content is essential for the correct modeling of atmospheric absorption. Turbulence simulations were carried out, showing marked scintillation, effects in the evaporation duct. The method can be applied to arbitrary refractivity spectra, and gives a complete numerical description of the field statistics. Author

N90-21930# Maryland Univ., College Park. Inst. for Physical Science and Technology.

LIDAR MEASUREMENTS OF THE OPTICAL PROPAGATION ENVIRONMENT

Thomas D. Wilkerson, Upendra N. Singh, Anthony Notari, and W. Charles Braun *In* AGARD, Atmospheric Propagation in the UV, Visible, IR, and MM-Wave Region and Related Systems Aspects Mar. 1990 12 p (For primary document see N90-21907 15-32)

(Contract N00014-85-K-0582)

Copyright Avail: NTIS HC A16/MF A03; Non-NATO Nationals requests available only from AGARD/Scientific Publications Executive

Results of lidar measurements are reported, particularly the layering of tropospheric haze and extinction/backscatter by cirrus clouds at visible wavelengths. This work includes the operation of a fixed lidar at College Park, and a transportable lidar for geographic locations of interest to DoD. A sensitivity baseline for these lidars was established using Rayleigh backscatter from the altitude molecular atmosphere. Profiles of temperature and density cover the altitude range 30 to 80 km. For cirrus clouds, measured relationships between extinction and backscatter make it possible to estimate the long-range horizontal visibility through cirrus layers via calibrated backscatter observations. Inversion of tropospheric haze measurements to vertical profiles of extinction is reported. Applicability of lidar probe methods to energy and information transfer through the atmosphere is summarized. Upper atmosphere observations are discussed, relevant to the prediction of atmospheric effects on reentry vehicles. Author

N90-21931# Defence Research Establishment Valcartier (Quebec).

LIDAR MEASUREMENT OF CONCENTRATION AND TURBULENCE IN BATTLEFIELD OBSCURANTS

B. T. N. Evans and G. Roy *In* AGARD, Atmospheric Propagation in the UV, Visible, IR, and MM-Wave Region and Related Systems Aspects Mar. 1990 12 p (For primary document see N90-21907 15-32)

Copyright Avail: NTIS HC A16/MF A03; Non-NATO Nationals requests available only from AGARD/Scientific Publications Executive

Concentration inhomogeneities, caused by turbulence, in obscurant clouds are studied by using a rapidly scanning lidar. Spatial correlograms in the three spatial directions are derived and are related to atmospheric stability. Implications of these inhomogeneities for obscurant effectiveness and interdevice comparison are discussed. Author

N90-21932# Wisconsin Univ., Madison.

CIRRUS CLOUD OPTICAL PROPERTIES MEASURED WITH THE UNIVERSITY OF WISCONSIN HIGH SPECTRAL RESOLUTION AND VOLUME IMAGING LIDARS

E. W. Eloranta and C. J. Grund *In* AGARD, Atmospheric Propagation in the UV, Visible, IR, and MM-Wave Region and Related Systems Aspects Mar. 1990 5 p (For primary document see N90-21907 15-32)

Copyright Avail: NTIS HC A16/MF A03; Non-NATO Nationals requests available only from AGARD/Scientific Publications Executive

The High Spectral Resolution Lidar (HSRL) provides calibrated range-resolved measurements of atmospheric optical parameters. These measurements include: the optical backscatter cross section, extinction cross section, optical depth and, when the absorption cross section is negligible, the backscatter phase function. Calibrated measurements are achieved by partitioning the lidar signal into separate aerosol and molecular scattering components. The separation is possible because the molecular signal is spectrally broadened by Doppler shifts from the thermal velocities of the molecules while the aerosol return spectrum is nearly unaffected by the slow Brownian motions of the aerosols. Visible and subvisible cirrus cloud optical properties measured at a wavelength of 510 nm with the HSRL are presented. Backscatter cross sections between 10(exp -5)/(km sr) to 0.18/(km sr) were measured along with backscatter phase functions in the range between .02/sr and .065/sr. Clouds with optical depths ranging from .003 to 2.9 were observed. An example of the tenuous enhanced backscattering often observed with the HSRL at cirrus altitudes is presented. Examples are provided of the mid-cloud altitudes, the optical thickness, and the backscatter phase function observed in cirrus clouds with the HSRL. The mid-cloud temperatures reported were derived from radiosonde data. Optical thickness of cirrus clouds are plotted as a function of their mid-cloud temperature. Results are presented along with measurements obtained from the HSRL. A comparison is shown of cirrus cloud optical depths measured with the HSRL and thermal emissivities measured by satellite with the CO(sup -2) slicing method. These preliminary observations lend support to the model results of Hansen (1971). A Volume Imaging Lidar (VIL) optimized for three-dimensional mapping of atmospheric structure was also operated. This lidar couples a 0.6J, 30 Hz Nd-YAG laser, with a 0.5 m diameter receiver, a 20 degree/sec beam scanning unit and data system capable of acquiring, displaying and storing data at sustained high rates. Author

N90-21933# Fraunhofer-Inst. fuer Atmosphaerische Umweltforschung, Garmisch-Partenkirchen (Germany, F.R.).

VERIFICATION OF KLETT'S METHOD BY COMPARISON OF LIDAR AND TRANSMISSOMETER MEASUREMENTS

Walter Carnuth *In* AGARD, Atmospheric Propagation in the UV, Visible, IR, and MM-Wave Region and Related Systems Aspects Mar. 1990 12 p (For primary document see N90-21907 15-32)

(Contract T/RF-35/G0056/G1237)

Copyright Avail: NTIS HC A16/MF A03; Non-NATO Nationals requests available only from AGARD/Scientific Publications Executive

Lidar measurements are performed in 532 nm wavelength along a slant path from ground level at 730 m MSL to a 1780 m mountain peak at 7 km horizontal distance, and extinction profiles derived from them by Klett's inversion method. This method, proceeding in the backward direction, avoids the instabilities occurring with the classical forward inversion, but requires a reference extinction value at the end of the lidar path. In this case, it is derived from visual range data obtained by an integrating nephelometer which is operated by a broadband optical transmissometer (350 to 900 nm). The data are compared with those calculated by integration of the lidar extinction profiles. Author

N90-21934# Naval Ocean Systems Center, San Diego, CA. Ocean and Atmospheric Sciences Div.

TECHNIQUE FOR SELECTING AN AEROSOL MODEL USEFUL FOR INFRARED ATMOSPHERIC TRANSMITTANCE CALCULATIONS

Herbert G. Hughes *In* AGARD, Atmospheric Propagation in the UV, Visible, IR, and MM-Wave Region and Related Systems Aspects Mar. 1990 8 p (For primary document see N90-21907 15-32)
(NR Proj. RM-35G80)
Copyright Avail: NTIS HC A16/MF A03; Non-NATO Nationals requests available only from AGARD/Scientific Publications Executive

Vertical profiles of meteorological parameters are used with the LOWTRAN 6 atmospheric transmittance/radiance computer code to model measurements of near horizon infrared radiances. It is shown that calculations with the Navy Maritime Aerosol Model can exactly reproduce the measured horizon pixel radiance using non-unique combinations of air mass factors and surface visibilities. This feature is the result of the visibility scaling factor of the size distribution remaining nearly constant for any appropriate combination of the two factors, and the relative insensitivity of the calculated extinction coefficients for the far infrared wavelengths to the air mass factor term. Using measurements taken on two consecutive days during low wind speed conditions, it is shown that any appropriate combination of the two factors will allow the calculated and measured radiances at other angles above the horizon to differ less than 2 percent. These agreements place confidence in using the selected aerosol model in transmittance calculations for the far infrared wavelength bands over other propagation paths. Author

N90-21935# Massachusetts Univ., Amherst. Microwave Remote Sensing Lab.

RADAR SCATTEROMETRY AND POLARIMETRY AT 220 GHz

Robert E. McIntosh and James B. Mead *In* AGARD, Atmospheric Propagation in the UV, Visible, IR, and MM-Wave Region and Related Systems Aspects Mar. 1990 8 p (For primary document see N90-21907 15-32)
Copyright Avail: NTIS HC A16/MF A03; Non-NATO Nationals requests available only from AGARD/Scientific Publications Executive

Two high-power portable radars operating in the 220 GHz absorption window were developed. The first, an incoherent 215 GHz scatterometer was used for reflectivity measurements of foliage, fallen snow, clouds and fog between ranges of .1 and 2 km. An incoherent 225 GHz polarimetric radar was also developed which is capable of fully characterizing the Stokes scattering matrix of distributed targets. Both radars employ an Extended Interaction (Klystron) Oscillator (EIO) as the transmitting source. These tubes produce a 60 W pulse of 50 to 600 ns duration and operate at a maximum duty cycle of .005. High efficiency Schottky barrier diode mixers are attached directly to the feed horns of the receiver antennas to minimize loss. Work at 215 GHz, including a review of the hardware and measurements of clouds and fog is summarized. The 225 GHz polarimeter will be discussed in greater depth, including a review of the theory of polarimetry, a description of the hardware and a calibration technique requiring only a single in-scene reflector. Preliminary polarimetric measurements of a dihedral reflector and foliage are presented and discussed. Author

N90-21936# Michigan Univ., Ann Arbor. Dept. of Electrical Engineering and Computer Science.

MILLIMETER-WAVE BISTATIC SCATTERING BY TERRAIN

Fawwaz T. Ulaby *In* AGARD, Atmospheric Propagation in the UV, Visible, IR, and MM-Wave Region and Related Systems Aspects Mar. 1990 12 p (For primary document see N90-21907 15-32)
Copyright Avail: NTIS HC A16/MF A03; Non-NATO Nationals requests available only from AGARD/Scientific Publications Executive

Interference caused by bistatic and forward scattering by terrain can often lead to degradation in performance for electromagnetic sensors and communications systems. The results of a study conducted to evaluate the directional distribution of bistatic scattering from terrain surfaces at 35 GHz are described. A calibrated radar system was used in a bistatic mode to measure the scattering from a variety of smooth and rough surfaces and from standing trees for all four linear polarization combinations HH, HV, VH, and VV. The measurements were made as a function of the azimuth and elevation angles of the receive antenna direction for fixed directions of the transmit antenna. The scattering data for trees were used to develop a new model for the phase matrix of foliage which can then be used in conjunction with transport theory to compute bistatic scattering by forest canopies for any incident and scattered directions. This approach was found to give excellent agreement with backscatter measurements conducted at 35 GHz, 94 GHz, and 140 GHz. Author

N90-21937# Naval Research Lab., Washington, DC.

MODELLING UV-VISIBLE RADIATION OBSERVED FROM SPACE

D. E. Anderson, Jr. and D. J. Strickland (Computational Physics, Inc., Annandale, VA.) *In* AGARD, Atmospheric Propagation in the UV, Visible, IR, and MM-Wave Region and Related Systems Aspects Mar. 1990 11 p (For primary document see N90-21907 15-32)
Copyright Avail: NTIS HC A16/MF A03; Non-NATO Nationals requests available only from AGARD/Scientific Publications Executive

Development of space-based passive remote systems for observing and tracking artificial radiation sources in the earth's atmosphere requires the characterization of the natural radiation background. Recent advances in detector technology and theoretical modeling have led to improved understanding of the UV-visible (1000 to 5000A) atmospheric background radiation. There are two principal sources of naturally occurring UV-visible atmospheric radiation: Rayleigh and Mie scattering of sunlight; and auroral and airglow emission. The first source is generated primarily in the troposphere, but is affected by the presence of aerosols and ozone in the stratosphere up to 40 km. In addition, clouds, surface reflection and multiple scattering can have a significant affect on the radiation field. The relative importance of these sources to nadir emission is shown. In particular, it is found that for wavelengths greater than 3000 A as much as 60 percent of the nadir emission can be due to multiple scattering. The second source, auroral and airglow emission, emanates from the mesosphere above 50 km and the thermosphere below 1000 km altitude and exhibits remarkable geographic and geomagnetic variability. A description of these radiation fields and models developed to analyze satellite remote sensing data in the UV-visible region of the spectrum are presented. Emission levels from both sources are compared and expected geographic and solar cycle variability identified. Author

N90-21938# Admiralty Research Establishment, Portsmouth (England).

CALCULATION OF IR PROPAGATION STATISTICS IN THE EASTERN ATLANTIC FOR SURVEILLANCE SYSTEM PERFORMANCE ASSESSMENT

J. M. Ridout *In* AGARD, Atmospheric Propagation in the UV, Visible, IR, and MM-Wave Region and Related Systems Aspects Mar. 1990 5 p (For primary document see N90-21907 15-32)
Copyright Avail: NTIS HC A16/MF A03; Non-NATO Nationals requests available only from AGARD/Scientific Publications Executive

The assessment of Infrared Search and Track systems requires a knowledge of the atmospheric propagation conditions in the geographic region of interest and how often these conditions arise. One area of interest to the UK Royal Navy is the Eastern Atlantic from the Iberian Basin in the South to the Greenland Sea in the North. A description of the meteorological conditions in this area in terms of air mass type has become available under NATO. The data were used with the LOWTRAN 6 computer program to determine the atmospheric transmissions in the 3 to 5 and 8 to 12 micron bands and the associated occurrence values used to produce cumulative probabilities of occurrence of a given transmission. This data base gives the conditions in terms of air mass type which may distort the probability curves. A further meteorological data base is available which gives the atmospheric conditions over a period of several years for Weather Ship J in the West European Basin and a subset of this was used to provide a check on the above calculations for this restricted region. It is shown that the degree of correlation between the two methods is reasonably good and that using the air mass type of approach is satisfactory. The effect of the calculated probability curves in sub regions of the Eastern Atlantic region on the selection of IR surveillance systems is indicated. Author

N90-21939# Science and Technology Corp., Las Cruces, NM.

COMPUTATION OF BROAD SPECTRAL BAND ELECTRO-OPTICAL SYSTEM TRANSMITTANCE RESPONSE CHARACTERISTICS TO MILITARY SMOKES AND OBSCURANTS USING FIELD TEST DATA FROM TRANSMISSOMETER SYSTEM MEASUREMENTS

W. Michael Farmer, Roger Davis, Robert Laughman, and Wendall Watkins (Atmospheric Sciences Lab., White Sands Missile Range, NM.) *In* AGARD, Atmospheric Propagation in the UV, Visible, IR, and MM-Wave Region and Related Systems Aspects Mar. 1990 12 p (For primary document see N90-21907 15-32)
Copyright Avail: NTIS HC A16/MF A03; Non-NATO Nationals requests available only from AGARD/Scientific Publications Executive

Electro-optical weapon system developers and users must know the smoke/obscurant countermeasure transmittance levels required to defeat their systems. This information is required in order to establish both operational smoke screen requirements and system scenario applicability. Transmittance data acquired in field tests such as the Smoke Week tests, Smoke/Obscurants were developed for this purpose. Narrow-band transmittance data can be analyzed using the Beer-Bouguer transmittance law to evaluate the performance of narrow-band electro-optical weapon systems such as laser rangefinders. However, broadband transmittance data for smokes such as phosphorus, fog oil, and dust in the visible, 3 to 5, or 8 to 12 micron bands cannot be evaluated directly using the Beer-Bouguer transmission law for broadband electro-optical systems such as FLIRs. A method for transforming field-measured transmittance data into equivalent electro-optical system transmittance is required. The transmissometer system analysis developed in the Project Manager, Smoke/Obscurants TRANSmissometer VALidation (TRANSVAL) program has provided the basis for developing such a method. The method developed in the TRANSVAL program for computing equivalent broadband electro-optical sensor transmittance from field test data is described. It is shown that band averages of the mass extinction coefficient used with the Beer-Bouguer transmission law do not yield correct estimates of equivalent electro-optical system transmittance. Examples are provided to illustrate the kinds of errors that can arise if sensor performance is incorrectly interpreted using field test data. Author

N90-21940# Atmospheric Sciences Lab., White Sands Missile Range, NM.

EFFECT OF ATMOSPHERIC TURBULENCE ON ELECTRO-OPTICAL SYSTEMS

Walter B. Miller, Jennifer C. Ricklin, and David H. Marlin *In* AGARD, Atmospheric Propagation in the UV, Visible, IR, and MM-Wave Region and Related Systems Aspects Mar. 1990 10 p (For primary document see N90-21907 15-32)
Copyright Avail: NTIS HC A16/MF A03; Non-NATO Nationals requests available only from AGARD/Scientific Publications Executive

The IMTURB model characterizes the effects of clear air optical turbulence on electro-optical (EO) imaging devices and laser transmitters operating in the atmospheric surface boundary layer and is valid for wavelengths from the visible through the far infrared. Similarity theory and the Kolmogorov principle of universal equilibrium are employed to characterize optical turbulence structure over regions typical of applications, based on simple environmental observables. A profile for the refractive index structure parameter is estimated, then used as input to a weak perturbation propagation model. Receiver coherence diameter, log-amplitude variance, scintillation averaging length, isoplanatism effective path length, and related subsidiary propagation statistics are then estimated for a selected propagation path. Outer and inner scale profiles are also estimated for advanced applications. Model results for two sample cases are discussed. Author

N90-21941# British Aerospace Public Ltd. Co., Bristol (England). Dept. of Advanced Information Processing.

ATMOSPHERIC MODELLING STUDIES: A MODELLING COMPARISON BETWEEN IR AND MILLIMETRIC ATMOSPHERIC PROPAGATION

A. R. Tooth *In* AGARD, Atmospheric Propagation in the UV, Visible, IR, and MM-Wave Region and Related Systems Aspects Mar. 1990 5 p (For primary document see N90-21907 15-32)
Copyright Avail: NTIS HC A16/MF A03; Non-NATO Nationals requests available only from AGARD/Scientific Publications Executive

When viewing through the atmosphere, whether by naked eye or with some electro-optic sensor, viewing performance is largely dictated by the composition of the intervening atmosphere. The composition of this atmosphere is continually changing with the fluctuations of the prevailing meteorology and will also differ in different geographical locations. Despite the fact that it is known that prevailing meteorology affects sensor and consequently overall system performance the phenomena is seldom explored and is often made excessively complicated. A technique developed at the Sowerby Research Centre, at British Aerospace, allows the meteorological effect to be rigorously, but simply, evaluated. Using the technique that was developed, in conjunction with atmospheric propagation models, for example LOWTRAN, realistic comparisons can be performed between different waveband IR systems and different millimetric frequency systems. Author

N90-21942# Office National d'Etudes et de Recherches Aerospatiales, Paris (France).

FAST METHOD FOR COMPUTING INFRARED TRANSMISSION, COMPUTATION EXAMPLES

A. M. Bouchardy and A. P. Junchat (Centre d'Electronique de l'Armement, Rennes Armees, France) *In* AGARD, Atmospheric Propagation in the UV, Visible, IR, and MM-Wave Region and Related Systems Aspects Mar. 1990 8 p In FRENCH (For primary document see N90-21907 15-32)
Copyright Avail: NTIS HC A16/MF A03; Non-NATO Nationals requests available only from AGARD/Scientific Publications Executive

A fast method for computing infrared transmission is described, it allows an effective transmission computation of a horizontal path with good precision. Two examples of applications of this method are presented. The first is a description of a weather station which allows the determination of infrared transmission from the ground. The second is from an atlas of infrared transmissions in France. Transl. by E.R.

N90-21943# Helsinki Univ. of Technology, Espoo (Finland). Lab. of Computer and Information Science.

ADAPTIVE FREQUENCY ESTIMATION BY MUSIC (MULTIPLE SIGNAL CLASSIFICATION) METHOD

Juha Karhunen, Esko Nieminen, and Jyrki Joutsensalo 1989 25 p
(PB90-166794; A-11; ISBN-951-754-989-X; ISSN-0783-7445)
Avail: NTIS HC A03/MF A01 CSCL 20N

During the last years, the eigenvector-based method called MUSIC has become very popular in estimating the frequencies of sinusoids in additive white noise. Adaptive realizations of the MUSIC method are studied using simulated data. Several of the adaptive realizations seem to give in practice equally good results as the nonadaptive standard realization. The only exceptions are instantaneous gradient type algorithms that need considerably more samples to achieve a comparable performance. A new method is proposed for constructing initial estimates to the signal subspace. The method improves often dramatically the performance of instantaneous gradient type algorithms. The new signal subspace estimate can also be used to define a frequency estimator directly or to simplify eigenvector computation. Author

N90-21944# Lawrence Livermore National Lab., CA.
COMPUTER SIMULATION OF IONOSPHERIC RADIO FREQUENCY HEATING
R. A. Close, B. S. Bauer, A. Y. Wong, A. B. Langdon, W. L. Kruer, and E. Mjolhus (Tromsoe Univ., Norway) 1 Dec. 1989 34 p
(Contracts W-7405-eng-48; N00014-78-C-0754)
(DE90-009478; UCRL-CR-103232) Avail: NTIS HC A03/MF A01

Linear and nonlinear absorption of electromagnetic waves in a warm, magnetized, nonuniform plasma is studied using an electromagnetic particle simulation code (ZOHAR) with either 1 or 2 spatial and 3 velocity dimensions. With fixed ions, finite temperature, and finite wave amplitude, transmission of the ordinary mode to the slow extraordinary wave (Z mode) is found to agree with cold plasma theory for linear conversion, and interference of mode converted waves is observed. With mobile ions and a parabolic density profile which peaks at the critical layer (omega (sub p) = omega), the wave electric field is enhanced (factor of ten or more) near the critical layer where the wave becomes electrostatic, and small scale density fluctuations (cavitons) are observed delta (l) approx. 10 lambda (sub D); delta n/n approx. = 0.1, typical of strong Langmuir turbulence. Wave damping and particle acceleration are also observed. Application to ionospheric heating is discussed. DOE

N90-21945# Academy of Sciences of the Ukrainian SSR, Kharkov. Inst. of Radio Astronomy.
THEORY OF A PERIODIC CYLINDRICAL WAVEGUIDE WITH A NONUNIFORM METAL-DIELECTRIC FILLING
V. B. Kazanski and I. V. Kocarowska 1988 56 p In RUSSIAN, ENGLISH summary
(DE90-620099; INIS-SU-154) Avail: NTIS (US Sales Only) HC A04/MF A01

A theory of wave propagation through a screened annular waveguide with a piecewise-continuous fielding is developed. The coupled fields in the dielectric layers are described with the aide of a characteristic matrix. The conditions at the discrete boundary yield a set of functional equations characteristic of the Riemann-Hilbert problem. The propagation constant follows from the condition that the determinantal of the equivalent algebraic set should be equal to zero. Analysis of the field phase and reduced amplitude in a wide range of variation of the waveguide parameters suggests promising performance characteristics of the structure as a prototype mode and spatial spectrum selector. DOE

N90-21946# Technische Univ., Delft (Netherlands). Faculty of Technical Mathematics and Informatics.
MULTIRESOLUTION AND TIME-FREQUENCY REPRESENTATIONS OF SIGNALS
J. A. H. Alkemade and P. L. Vermeer 1989 65 p
(Rept-89-47; ISSN-0922-5461; ETN-90-96363) Copyright Avail: NTIS HC A04/MF A01

Two approaches to the intimately related time-frequency and multiresolution representations are reviewed. Time-frequency representations formed using shifted and frequency modulated versions of a window function are described. Gabor functions result if a Gaussian window function is used. Application of the approaches to image analysis problems such as edge detection is discussed. The analysis and filtering of time-varying signals are identified as other applications of the approaches. The use of the wavelet transform on multigrid methods is outlined. ESA

N90-21947# Technische Univ., Delft (Netherlands).
ELECTROMAGNETIC INVERSE PROFILING OF STRATIFIED MEDIA Ph.D. Thesis
Michael Cosmas Silve Zeijlmans 1989 190 p
(ETN-90-96402) Avail: NTIS HC A09/MF A01

A method of solution of inverse profiling problems is presented. It is based on the application of an otimization algorithm. The characteristic of such a method is that a model object is introduced with a known profile that depends on a number of profile parameters. In the process an error function is minimized, using a Levenberg-Marquardt algorithm. Field derivatives with respect to the profile parameters of the model object are applied. The existence of errors in the measured data, which are input data of the Levenberg-Marquardt algorithm, is assumed. Numerical results with the inversion algorithm are obtained for two problems in civil engineering and geophysics. ESA

N90-21948# Royal Signals and Radar Establishment, Malvern (England).
MULTIWAVE DIFFRACTION ANALYSIS OF TRANSMISSION PHASE GRATINGS
C. W. Slinger Sep. 1989 19 p
(RSRE-Memo-4325; BR112014; ETN-90-96427) Copyright Avail: NTIS HC A03/MF A01

A multiwave coupled wave analysis of phase modulated, transmission gratings is made. The aim is to calculate the first order diffraction efficiency as a function of the modulation and a volume parameter, for arbitrary phase profiles. Sinusoidal, square, triangular and sawtooth gratings are investigated in detail through the thin, multiwave and volume diffraction regimes, using analytic and numerical techniques. The relative merits of these profiles are discussed in terms of efficiency and ease of fabrication. High efficiencies (greater than 90 percent) are found to be possible in the multiwave regime. ESA

N90-21949 Duke Univ., Durham, NC.
PASSIVE SHAPE CONTROL OF SPACE ANTENNAS WITH DETERMINATE TRUSS SUPPORT STRUCTURES Ph.D. Thesis
Ahmet Bulent Trak 1989 130 p
Avail: Univ. Microfilms Order No. DA9010373

The shape control of space antennas by a passive method is investigated. The application of the passive approach to the shape control of determinate trusses is emphasized. The passive control is achieved by modifying the nodal coordinates of the structure such that the modified structure deforms to the original (unmodified) geometry under the given loading. The modified geometry is obtained by changing the coordinates iteratively. Mathematically, the technique can be represented as the simple iteration method for solving nonlinear equations. The technique was illustrated in four cases. Two loading conditions and a tetrahedral truss were considered. In Case 1, a modified geometry, which would deform to the original geometry, was sought. In Case 2, a modified surface geometry, which would deform to the original surface geometry, was sought. In Case 3, a single modified geometry, which would satisfy both loading conditions, was sought. In Case 4, an indeterminate truss was investigated under a single loading condition. Dissert. Abstr.

N90-21997# Deutsche Forschungsanstalt fuer Luft- und Raumfahrt, Oberpfaffenhofen (Germany, F.R.). Institut fuer Hochfrequenztechnik.
THE SOLUTION OF SCATTERING AND RADIATION PROBLEMS FOR COMPLEX CONFIGURATIONS BASED ON 3-D GRID AND PATCH MODELS
V. Stein *In* AGARD, Applications of Mesh Generation to Complex 3-D Configurations Mar. 1990 22 p Sponsored in part by Bundesamt fuer Wehrtechnik und Beschaffung, Koblenz, Fed. Republic of Germany (For primary document see N90-21975 15-34)

Copyright Avail: NTIS HC A14/MF A02; Non-NATO Nationals requests available only from AGARD/Scientific Publications Executive

33 ELECTRONICS AND ELECTRICAL ENGINEERING

Includes test equipment and maintainability; components, e.g., tunnel diodes and transistors; microminiaturization; and integrated circuitry.

For related information see also *60 Computer Operations and Hardware* and *76 Solid-State Physics.*

N90-21950 Carnegie-Mellon Univ., Pittsburgh, PA.
PRINCIPLES OF VERY LARGE SCALE INTEGRATED (VLSI) SYSTEM PLANNING Ph.D. Thesis
Allen Mark Dewey 1989 236 p
Avail: Univ. Microfilms Order No. DA9006202

One of the first steps in the VLSI (very large scale integration) design process is to determine the particular design approach that will result in the most efficient implementation of the initial specifications or to conclude that the specifications are not realizable. As the complexity of design grows, the traditional trial-and-error design methodology becomes increasingly cost prohibitive because the number of possible design alternatives, as well as the cost of a complete synthesis and fabrication cycle, grows dramatically. VLSI System Planning addresses this problem by modeling the practices of an expert designer in providing guidance at the initial stage of the design process as to the most promising design alternatives and giving a preliminary indication of the estimated performance. A benefit of VLSI System Planning is that a more credible system-level specification can be developed. Another benefit is that the expensive resources of a full development cycle can be more judiciously targeted to only the select set of plans that are the most likely to meet the design goals. Finally, the designer can avoid costly redesigns when, halfway into an expensive design cycle, it is discovered that the final implementation will fall short of the performance goals.
Dissert. Abstr.

N90-21951* National Aeronautics and Space Administration. Pasadena Office, CA.
BALANCED BRIDGE FEEDBACK CONTROL SYSTEM Patent
Boris J. Lurie, inventor (to NASA) (California Inst. of Tech., Pasadena.) 27 Mar. 1990 14 p Filed 21 Mar. 1989
(NASA-Case-NPO-17430-1-CU; US-Patent-4,912,386; US-Patent-Appl-SN-332677; US-Patent-Class-318-615; US-Patent-Class-318-434; US-Patent-Class-318-561; US-Patent-Class-318-618; US-Patent-Class-388-821) Avail: US Patent and Trademark Office CSCL 09A

In a system having a driver, a motor, and a mechanical plant, a multiloop feedback control apparatus for controlling the movement and/or positioning of a mechanical plant, the control apparatus has a first local bridge feedback loop for feeding back a signal representative of a selected ratio of voltage and current at the output driver, and a second bridge feedback loop for feeding back a signal representative of a selected ratio of force and velocity at the output of the motor. The control apparatus may further include an outer loop for feeding back a signal representing the angular velocity and/or position of the mechanical plant.
Official Gazette of the U.S. Patent and Trademark Office

N90-21952*# Cleveland State Univ., OH. Dept. of Electrical Engineering.
ANALYTICAL AND EXPERIMENTAL STUDY OF HIGH PHASE ORDER INDUCTION MOTORS Final Technical Report
Eugene A. Klingshirn Aug. 1989 120 p
(Grant NAG3-108)
(NASA-CR-186580; NAS 1.26:186580) Avail: NTIS HC A06/MF A01 CSCL 09A

Induction motors having more than three phases were investigated to determine their suitability for electric vehicle applications. The objective was to have a motor with a current rating lower than that of a three-phase motor. The name chosen for these is high phase order (HPO) motors. Motors having six phases and nine phases were given the most attention. It was found that HPO motors are quite suitable for electric vehicles, and for many other applications as well. They have characteristics which are as good as or better than three-phase motors for practically all applications where polyphase induction motors are appropriate. Some of the analysis methods are presented, and several of the equivalent circuits which facilitate the determination of harmonic currents and losses, or currents with unbalanced sources, are included. The sometimes large stator currents due to harmonics in the source voltages are pointed out. Filters which can limit these currents were developed. An analysis and description of these filters is included. Experimental results which confirm and illustrate much of the theory are also included. These include locked rotor test results and full-load performance with an open phase. Also shown are oscillograms which display the reduction in harmonic currents when a filter is used with the experimental motor supplied by a non-sinusoidal source. Author

N90-21953*# Colorado State Univ., Fort Collins. Dept. of Mechanical Engineering.
HOLLOW CATHODE OPERATION AT HIGH DISCHARGE CURRENTS M.S. Thesis
Verlin Joe Friedly Apr. 1990 92 p
(Grant NGR-06-002-112)
(NASA-CR-185238; NAS 1.26:185238) Avail: NTIS HC A05/MF A01 CSCL 09A

It was shown that ion thruster hollow cathode operation at high discharge current levels can induce reduced thruster lifetimes by causing cathode insert overheating and/or erosion of surfaces located downstream of the cathode. The erosion problem has been particularly baffling because the mechanism by which it occurs has not been understood. The experimental investigation described reveals the energies of the ions produced close to the cathode orifice can be several times the anode-to-cathode potential difference generally considered available to accelerate them. These energies (of order 50 eV) are sufficient to cause the observed erosion rates. The effects of discharge current (to 60 A), magnetic field configuration and the cathode flowrate, orifice diameter and insert design on the energies and current densities of these jet ions are examined. A model describing the mechanism by which the high energy ions could be produced when the anode-cathode potential difference is insufficient is proposed. The effects of discharge current on cathode temperature and internal pressure are also examined experimentally and described phenomenologically. Author

N90-21954*# Sandia National Labs., Albuquerque, NM. Exploratory Batteries Div.
AGING CHARACTERISTICS OF LI/SO(SUB 2) CELLS
Samuel C. Levy and Darryl A. Bouchard 1990 6 p Presented at the 34th International Power Sources Symposium, Cherry Hill, NJ, 25-28 Jun. 1990
(Contract NASA Order A-41521; DE-AC04-76DP-00789)
(NASA-CR-180432; NAS 1.26:180432; DE90-009333; SAND-89-2313C; CONF-9006146-2) Avail: NTIS HC A02/MF A01 CSCL 10C

Delays in the launch of the Galileo probe to Jupiter have resulted in a new trajectory that will increase the fly-out time such that batteries will be greater than seven years old at the time of descent into the Jovian atmosphere. The longest real time data for flight design cells was five years at the time of launch. A program was initiated to establish a methodology and data base so that the performance of these cells may be predicted at the time they are expected to complete the mission. Cells from five lots and five storage temperatures, ranging from one year to seven years in age, were studied. Chemical analysis was performed on one cell from each lot/storage group. The remaining cells in each group were discharged at the mission load and temperature. Additional cells were placed on high temperature accelerated storage, and then discharged. DOE

N90-21955# Sandia National Labs., Albuquerque, NM.
ACTIVE PRIMARY LITHIUM THIONYL CHLORIDE BATTERY FOR ARTILLERY APPLICATIONS
Arlen R. Baldwin, Frank M. Delnick, and David L. Miller (Eagle-Picher Industries, Inc., Joplin, MO.) 1990 11 p Presented at the 34th International Power Sources Symposium, Cherry Hill, NJ, 25-28 Jun. 1990
(Contract DE-AC04-76DP-00789)
(DE90-009511; SAND-89-2382C; CONF-9006146-3) Avail: NTIS HC A03/MF A01

Sandia National Laboratories and Eagle Picher Industries have successfully developed an Active Lithium Thionyl Chloride (ALTC) power battery for unique artillery applications. Details of the design and the results of safety and performance will be presented. DOE

N90-21956# Lawrence Livermore National Lab., CA.
AN ASSESSMENT OF THE HARDNESS OF MINIATURE VACUUM TUBES TO HIGH-VOLTAGE TRANSIENTS
William J. Orvis Mar. 1990 6 p Presented at the High Powered Microwave and Broadband Radio Frequency Propagation/Phenomenology/Methodology Workshop, Livermore, CA, 23-26 Oct. 1989
(Contract W-7405-eng-48)
(DE90-009541; UCRL-101792; CONF-891097-5) Avail: NTIS HC A02/MF A01

Miniature vacuum tubes are vacuum switching and control devices fabricated on a silicon wafer, using the same technology as is used to make integrated circuits. They operate in much the same manner as conventional vacuum tubes, but with two important differences: they are micron sized devices, and they employ field emission instead of thermionic emission as the electron source. As these devices have a vacuum as their active region, they will be extremely hard to nuclear radiation and relatively insensitive to temperature effects, they are also expected to be extremely fast devices. We have estimated here that their hardness to high-voltage transients will be at least as good as existing semiconductor devices and possibly better. DOE

N90-21957# Edgerton, Germeshausen and Grier, Inc., Idaho Falls, ID.
LABORATORY TESTING OF ENERGY RESEARCH CORPORATION ERC 160 NiCd 6 VOLT TRACTION BATTERY
Jasper E. Hardin and H. E. Knauts Dec. 1989 31 p
(Contract DE-AC07-76ID-01570)
(DE90-009629; EGG-EP-8918) Avail: NTIS HC A03/MF A01

The purpose of this report is to describe the testing performed on the Energy Research Corp. NiCd 160 nickel-cadmium 6 volt traction battery by the INEL Electric Vehicle Battery Laboratory, to present the results and conclusions of this testing, and to make appropriate recommendations. DOE

N90-21958# Edgerton, Germeshausen and Grier, Inc., Idaho Falls, ID.
LABORATORY TESTING OF SAFT SEH-5-200 6 VOLT TRACTION BATTERY
Jasper E. Hardin Dec. 1989 23 p
(Contract DE-AC07-76ID-01570)
(DE90-009787; EGG-EP-8917) Avail: NTIS HC A03/MF A01

The purpose of this report is to describe the testing performed on the Saft SEH-5-200 flooded nickel cadmium traction battery by the INEL Electric Vehicle Battery Laboratory, to present the results and conclusions of this testing, and to make appropriate recommendations. DOE

N90-21886*# Jet Propulsion Lab., California Inst. of Tech., Pasadena.
VOLTAGE SOURCE ac-TO-dc CONVERTERS FOR HIGH-POWER TRANSMITTERS
R. Cormier *In its* The Telecommunications and Data Acquisition Report 15 Feb. 1990 p 55-68 (For primary document see N90-21880 15-32)
Avail: NTIS HC A15/MF A02 CSCL 09C

34 FLUID MECHANICS AND HEAT TRANSFER

Includes boundary layers; hydrodynamics; fluidics; mass transfer; and ablation cooling.

For related information see also *02 Aerodynamics* and *77 Thermodynamics and Statistical Physics.*

N90-21959 State Univ. of New York at Buffalo, Amherst.
PREDICTION OF LENGTH SCALES IN A MACH REFLECTION FLOWFIELD Ph.D. Thesis
David Jason Azevedo 1989 206 p
Avail: Univ. Microfilms Order No. DA8921522

A planar symmetric wedge configuration representative of a simple high-speed intake in steady flow was investigated. Of interest are the complex reflection patterns that develop when the leading-edge shocks intersect at angles above a certain critical value that is less than the wedge detachment angle. Of particular interest is the analytical prediction of the size and location of the almost-normal shock that is produced in these Mach reflection situations. The size of both the Mach shock and the attendant subsonic region behind it is important in that the highest noise levels in supersonic flows appears to be associated with these embedded subsonic regions. A control-volume analysis was carried out for this two-dimensional geometry in order to determine the various length scales associated with Mach reflection. The usual inviscid conservation equations were applied, and were supplemented by constitutive relations based on the flowfield geometry. The results of these predictions were compared with the steady-flow experiments of Hornung and Robinson (1982), for freestream Mach numbers from 2.8 to 5. Modification of these assumptions to better represent the test environment improved the predictions. Dissert. Abstr.

N90-21960 Colorado Univ., Boulder.
THERMOMECHANICALLY-INDUCED CONVECTIVE MOTION AND NATURAL CONVECTION IN CONFINED GASEOUS HELIUM SUBJECTED TO BOUNDARY HEATING Ph.D. Thesis
Sutrisno 1989 186 p
Avail: Univ. Microfilms Order No. DA8923534

A theoretical analysis of the effects of a gravity field on gaseous helium confined in a slender two dimensional box when boundary heating suddenly takes place at the wall is described. The gravity field is applied vertically. A heat flux, capable of producing an appreciable wall temperature increase, is applied uniformly along the longer vertical walls. A systematic analysis using various perturbation techniques is carried out in the central region away from the upper and lower insulated boundaries. A complete system of conservation equations governing viscous, heat conducting and compressible flow is employed. Analysis on the acoustic timescale shows that conduction heating takes place only in a thin, continuously growing boundary layer near the heated wall. On the conduction timescale, both acoustic and conduction phenomena occur simultaneously in the container. Multiple timescale methods are employed to separate the high frequency acoustic equations from the lower frequency conduction equations. In this fully conductive system, energy is transferred by conduction among the fluid particles which at the same time experience thermal expansion and compression. Dissert. Abstr.

N90-21961*# Prairie View Agricultural and Mechanical Coll., TX. Dept. of Mechanical Engineering.
FLOW BOILING WITH ENHANCEMENT DEVICES FOR COLD PLATE COOLANT CHANNEL DESIGN Semiannual Report
Ronald D. Boyd, Sr. and Alvin Smith 27 Feb. 1990 157 p
(Grant NAG9-310)
(NASA-CR-186358; NAS 1.26:186358) Avail: NTIS HC A08/MF A01 CSCL 20D

The use of flow boiling for thermal energy transport is intended to provide an alternative for accommodating higher heat fluxes in commercial space systems. The objectives are to: (1) examine the variations in both the mean and local (axial and circumferential) heat transfer coefficients for a circular coolant channel with either smooth walls, spiral fins, or both spiral fins and a twisted tape; (2) examine the effects of channel diameter and subcooling; and (3) develop an improved reduction analysis and/or suggest possible heat transfer correlation of the present data. Freon-11 is the working fluid. Two-dimensional (circumferential and axial) wall temperature distributions were measured for coolant channels with the above noted internal geometries. The flow regimes which are being studied are: (1) single phase; (2) subcooled flow boiling; and (3) stratified flow boiling. The inside diameter of all test sections is near 1.0 cm. Cicumferentially averaged heat transfer coefficients at several axial locations were obtained for selected coolant channels for a mass velocity of 210 kg/sq m s, an exit pressure of 0.19 MPa (absolute), and an inlet subcooling of 20.8 C. Overall (averaged over the entire channel) heat transfer coefficients were compared for the above channel geometries. This comparison showed that the channel with large pitch spiral fins had higher heat transfer coefficients at all power levels. B.H.A.

N90-21962*# National Aeronautics and Space Administration. Lewis Research Center, Cleveland, OH. Inst. for Computational Mechanics in Propulsion.

NUMERICAL INVESTIGATION OF SEPARATED TRANSONIC TURBULENT FLOWS WITH A MULTIPLE-TIME-SCALE TURBULENCE MODEL

S.-W. Kim Jan. 1990 40 p
(NASA Order C-99066-G)
(NASA-TM-102499; ICOMP-90-04; E-5295; NAS 1.15:102499)
Avail: NTIS HC A03/MF A01 CSCL 20D

A numerical investigation of transonic turbulent flows separated by curvature and shock wave - boundary layer interaction is presented. The free stream Mach numbers considered are 0.4, 0.5, 0.6, 0.7, 0.8, 0.825, 0.85, 0.875, 0.90, and 0.925. In the numerical method, the conservation of mass equation is replaced by a pressure correction equation for compressible flows and thus incremental pressure is solved for instead of density. The turbulence is described by a multiple-time-scale turbulence model supplemented with a near-wall turbulence model. The present numerical results show that there exists a reversed flow region at all free stream Mach numbers considered whereas various k-epsilon turbulence models fail to predict such a reversed flow region at low free stream Mach numbers. The numerical results also show that the size of the reversed flow region grows extensively due to the shock wave - turbulent boundary layer interaction as the free stream Mach number is increased. These numerical results show that the turbulence model can resolve the turbulence field subjected to extra strains caused by the curvature and the shock wave - turbulent boundary layer interaction and that the numerical method yields a significantly accurate solution for the complex compressible turbulent flow. Author

N90-21963 Washington Univ., Seattle.

AN EXPERIMENTAL INVESTIGATION OF MIXING IN BUOYANT FLOWS Ph.D. Thesis

Hamid Johari 1989 127 p
Avail: Univ. Microfilms Order No. DA9000255

Entrainment and molecular scale mixing in turbulent, axisymmetric thermals and plumes released into an unconfined, nonstratified, quiescent environment in the large Schmidt number fluid were investigated. Visualization experiments in a water tank using both chemically reactive and passive laser-induced fluorescence techniques revealed that the plume far-field is organized by large scale arrowhead-shaped structures having a fairly uniform concentration of the mixed fluid. A simple model is proposed which addresses the far-field mixing features of the plume. Experiments revealed that the turbulent thermal has an oblate spheroidal shape with an approximately uniform concentration of the mixed fluid in the far-field. Ambient fluid is entrained primarily through incursions in the rear of the thermal due to the velocity induced by the vorticity field. The first parcels of mixed fluid appear in the center, around the thermal's axis of symmetry, and are then distributed throughout the thermal. The molecular scale mixing rate was found to be proportional to the entrainment rate in both thermals and plumes. Furthermore, these buoyant flows are very efficient in processing the entrained fluid as compared to other free turbulent shear flows. When atmospheric evaporative cooling effects are simulated in the water tank using chemicals, the trajectory of the thermal depends strongly on the buoyancy reversal parameter D*. Most surprising, the molecular mixing rate of the evaporating thermal is independent of D* while the thermal ascends. Engulfment of pure, unmixed ambient fluid deep into the flow was observed in both of the flow types investigated. This is one of the main indications that large scale motions control the mixing and entrainment processes of buoyant flows. This investigation suggests a model for the instantaneous concentration field of the mixed fluid within these flows which differs considerably from models based on gradient diffusion. Dissert. Abstr.

N90-21964 Michigan Univ., Ann Arbor.

INTERACTION OF A TURBULENT ROUND JET WITH THE FREE SURFACE Ph.D. Thesis

Koorosh Madnia 1989 176 p
Avail: Univ. Microfilms Order No. DA9001677

An experimental study of the interaction of an underwater turbulent round jet with the free surface was conducted. Flow visualization, surface curvature measurements, and hot film velocity measurement were used to study this flow. It is shown that surface waves are generated by the large scale vortical structures in the jet flow as they approach the free surface. These waves propagate at angle with respect to the flow direction. The propagation angle increases as the strength of the interaction is increased by increasing the momentum flux of the jet or reducing the distance of the jet to the free surface or both. Propagation of these waves in the flow direction is suppressed by the surface current produced by the jet. The fundamental scaling parameters of the free-surface jet is determined. The velocity scale is the velocity obtained from the combination of jet momentum, density and depth of the jet and the scale is the distance of the jet to the free surface. It is shown that the centerline velocity decay when scaled with these parameters collapses to a universe curve for different depths of the jet. The asymptotic decay in the far field is reduced by a factor of 2(sup 1/2) compared to the free jet due to the confinement by the free surface. The growth rate of the free-surface jet is found in good agreement with the free jet. However the eccentricity of the jet cross section caused by the displacement of the jet centerline persists for large distances downstream, beyond 40 times the initial depth of the jet centerline. Measurements are also reported on the flow field of a jet moving parallel to a solid surface. These results are compared with the results for the free surface jet. Dissert. Abstr.

N90-21965 Michigan Univ., Ann Arbor.

HOMOGENEOUS DILUTE TURBULENT PARTICLE-LADEN WATER FLOWS Ph.D. Thesis

Ramkumar N. Parthasarathy 1989 171 p
Avail: Univ. Microfilms Order No. DA9001695

An experimental and theoretical study of a homogeneous particle-laden turbulent flow was conducted, involving glass particles falling in a stagnant water bath. The experiments included various loadings of nearly monodisperse particles having mean diameters of 0.5, 1.0, and 2.0 mm. Measurements included liquid and particle velocities, and the temporal spectra and spatial correlations of liquid-phase velocity fluctuations. The motion of isolated particles falling in stagnant water was also calibrated using shadowgraph movies. An approximate analysis for liquid-phase properties was developed, based on linear superposition of randomly-arriving particle velocity fields. In addition, stochastic simulation, solving the Lagrangian equations of motion of the particles, were used to predict particle properties. For present test conditions, liquid velocity fluctuations correlated solely as a function of the rate of dissipation of kinetic energy in the liquid. The analysis predicted many of the features of the flows reasonably well but must be improved to obtain satisfactory predictions of the temporal and spatial scales of the flow. After accounting for

effects of particle size variations and self-induced motion, the stochastic simulation predicted particle properties reasonably well.
Author

N90-21966 California Univ., Davis.
AN INVESTIGATION OF TURBULENCE STRUCTURE IN A LOW REYNOLDS NUMBER INCOMPRESSIBLE TURBULENT BOUNDARY LAYER Ph.D. Thesis
Constantine John Strataridakis 1989 183 p
Avail: Univ. Microfilms Order No. DA9002779

Hot-wire anemometry measurements in an incompressible turbulent boundary-layer flow over a flat plate at zero pressure gradient were made using two X-probes simultaneously. The experiment was performed in the large Atmospheric Boundary-Layer Wind tunnel at the University of California, Davis. The 7.32 meter long flat plate installed within the wind tunnel generated approximately 20 cm thick boundary layer, R (sub theta) approximately 4,000. Mean velocity and turbulence intensity data very close to the wall (y(+) is greater than or = to 1) were measured with a single hot wire to improve the measurement resolution. Space-time correlations of mu' and upsilon' velocities and of their instantaneous product were obtained with a pair of X-wires. The mean convection velocities, the extent in space, the mean inclination angles, and coherence characteristics of the mu', upsilon' and (mu')(upsilon') large-scale structures are presented. (The (mu')(upsilon') results are presented for the first time.) The mu' structure is inclined at a small angle (19 deg) to the wall, while the upsilon' and (mu')(upsilon') structures propagate almost at wall-normal directions. Each of the mu' and upsilon' structures appears elongated in the direction of the corresponding velocity fluctuation and is limited to delta-extent in the other two directions. The similarity between the upsilon' and (mu')(upsilon') suggests that the (mu')(upsilon') might mainly be a consequence of the motion of the upsilon' structure. Finally, a possible explanation for the differences between the (mu')(upsilon'), upsilon' and the mu' structures is the existence of different coherent scales, one dominating mu' and the other dominating upsilon' and (mu')(upsilon'). Dissert. Abstr.

N90-21967 California Inst. of Tech., Pasadena.
TOPICS IN VORTEX METHODS FOR THE COMPUTATION OF THREE- AND TWO-DIMENSIONAL INCOMPRESSIBLE UNSTEADY FLOWS Ph.D. Thesis
Gregoire Stephane Winckelmans 1989 290 p
Avail: Univ. Microfilms Order No. DA9000611

Contributions to vortex methods for the computation of incompressible unsteady flows are presented. Three methods are investigated. The first method is the inviscid method of vortex filaments in three dimensions, and the following topics are presented: review of the method of regularized vortex filaments and of convergence results for multiple-filament computations; modeling of a vortex tube by a single filament convected with the regularized Biot-Savart velocity applied on the centerline; and development of a new regularization of the Biot-Savart law that reproduces the lowest mode dispersion relation to the rectilinear vortex tube in the range of large to medium wavelengths. Next the method of vortex particles in three dimensions is investigated, and the following contributions are discussed: review of the method of singular vortex particles; review of the method of regularized vortex particles and of convergence results, and introduction of a new algebraic smoothing with convergence properties; development of a new viscous method in which viscous diffusion is taken into account by a scheme that redistributes the particle strength vectors, and application of the method to the computation of the fusion of two vortex rings; investigation of the particle method with respect to the conservation laws and derivation of expressions for the evaluation of the quadratic diagnostics. The third method considered is the method of contour dynamics in two dimensions. The particular efforts presented are: review of the classical inviscid method and development of a new vector particle version of the method, both singular and regularized; development of a viscous version of the method of regularized particles and application of the method to computation of the reconnection of two vortex patches of same sign vorticity; and investigation of the particle method with respect to the conservation laws and derivation of new expressions for the evaluation of linear and quadratic diagnostics. Dissert. Abstr.

N90-21968 California Inst. of Tech., Pasadena.
EXPERIMENTAL AND ANALYTICAL INVESTIGATIONS OF GRANULAR MATERIALS: SHEAR FLOW AND CONVECTIVE HEAT TRANSFER Ph.D. Thesis
Hojin Ahn 1989 164 p
Avail: Univ. Microfilms Order No. DA9000549

Granular materials flowing down an inclined chute were studied experimentally and analytically. Characteristics of convective heat transfer to granular flows were also investigated experimentally and numerically. Experiments on continuous, steady flows of granular materials in an inclined chute were conducted with the objectives of understanding the characteristics of chute flows and of acquiring information on the rheological behavior of granular material flow. Existing constitutive equations and governing equations were used to solve for fully developed chute flows of granular materials, and thus the boundary value problem was formulated with two parameters (the coefficient of restitution between particles, and the chute inclination) and three boundary values at the chute base wall (the values of solid fraction, granular temperature, and mean velocity at the wall). The boundary value problem was numerically solved by the shooting method. These analytical results were also compared with the present experimental values and with the computer simulations by other investigators in their literature. Experiments on heat transfer to granular flows over a flat heating plate were conducted with three sizes of glass beads, polystyrene beads, and mustard seeds. A modification on the existing model for the convective heat transfer was made using the effective Nusselt number and the effective Peclet number, which include the effects of solid fraction variations. The slightly modified model could describe the heat transfer characteristics of both fast and slow flows (supercritical and subcritical). A numerical analysis of the transfer to granular flows was also performed. The results were compared with the present experimental data, and reasonable agreement was found in the comparison.
Dissert. Abstr.

N90-21969# North Carolina State Univ., Raleigh.
INVERSE PROBLEMS OF HEAT CONDUCTION Ph.D. Thesis
Gregory Paul Flach 1988 184 p
Avail: Univ. Microfilms Order No. DA8909216

Inverse heat conduction problems in four categories are solved. Periodic surface conditions, periodic contact conductance, spatially varying thermal properties, and transient surface conditions are determined based on measurements of the interior temperature distribution of a solid. The effectiveness of the proposed methods is illustrated through simulated, and occasionally actual, experimental applications. Confidence bounds are derived to estimate the statistical level of uncertainty in the computed results. A method based on the use of periodic B-splines and the integral transform technique is proposed for the solution of quasi-steady periodic linear inverse heat conduction problems. The approach is applied to an inverse heat conduction problem of determining the periodically time-varying contact conductance between two periodically contacting surfaces. The technique is based on solving two single-region inverse problems for the periodic contact surface temperature and heat flux of each solid. A method for simultaneously estimating spatially varying thermal conductivity and heat capacity per unit volume under the conditions of a flash method type of experiment is developed. A variable-order variable-step sequential method is presented for solving the nonlinear one-dimensional inverse heat conduction problem. Results from a statistical analysis are shown to predict the stability or instability for a given selection of the parameters controlling the inverse method. Dissert. Abstr.

N90-21970# Mississippi Univ., University. Computational Hydroscience and Engineering.
AUTOMATED ANALYSIS OF MEASURED TURBULENT BOUNDARY FLOW
Sergio E. Adeff, Shu-Yi Wang, and Neil L. Coleman Dec. 1989 289 p Sponsored by Agricultural Research Service, Beltsville, MD
(PB90-147844) Avail: NTIS HC A13/MF A02 CSCL 20D

Velocity profiles in bounded shear flows in laboratory flume with various flow intensities and depths and two very different roughness magnitudes and types were measured and analyzed. A new computational procedure was developed to define a virtual origin and successfully applied as part of a larger program named VELMEAS; this computational program was developed as an accurate and expendable tool for analyzing boundary layer flows; it is also suitable for collecting and analyzing any set of data samples produced in voltage form. Basic statistical and regression analysis are performed efficiently, and the boundary layer analysis is documented in graphic and table form. Many graphs illustrating boundary layer phenomena are included. The source FORTRAN code is also included. GRA

N90-21971 Virginia Polytechnic Inst. and State Univ., Blacksburg.
LASER DOPPLER ANEMOMETRY MEASUREMENTS OF A CONFINED TURBULENT WATER JET WITH A UNIFORM BACKGROUND FLOW Ph.D. Thesis
Cheng-Hsing Hsu 1989 135 p
Avail: Univ. Microfilms Order No. DA9003594

An axisymmetric, turbulent water jet with several very slow, coflowing external streams was measured with a frequency-shifted laser Doppler anemometer. The objective was to approximate a jet submerged in an ambient fluid of infinite domain by using a confined jet in a uniform coflow. The coflow prevents flow reversal outside the jet, but if the coflow velocity is not small compared to the jet velocity, the jet will no longer be self-preserving. Thus, the objective is reached in the limit as the coflow approaches zero, but in the absence of reverse flow. In the present study, a jet with several slow coflows was examined to investigate this behavior, the data was extrapolated to the limit (U(sub s)/U(sub j) = 0) to obtain the free jet results and reduce uncertainty in earlier data. The Reynolds number based on the jet diameter and exit velocity was 32100. Conservation of momentum of the jet was demonstrated up to the measurement limit of x/d = 100. Its distribution suggests that the near field axial pressure variation has significant effects on the momentum flux. This study indicates that a slow coflowing stream is an ideal way to eliminate the recirculating zone present outside jets without coflows. By reducing the coflow to a negligible velocity with constant Craya-Curtet number, researchers can greatly reduce the wide experimental variation in jet entrainment and spreading rates found in different facilities. The results also indicated that a confined jet with a very slow coflow without recirculation can asymptotically approach the conditions of a free jet. An estimate of the variation of the duct size versus the velocity ratio is obtained. It suggests that it is not possible to reduce the velocity ratio to an arbitrarily small value without backflow because the duct would become impractically large. Dissert. Abstr.

N90-21972 Iowa State Univ. of Science and Technology, Ames.
A DUAL POTENTIAL FORMULATION OF THE NAVIER-STOKES EQUATIONS Ph.D. Thesis
Steven Gerard Gegg 1989 220 p
Avail: Univ. Microfilms Order No. DA9003519

A dual potential formulation for numerically solving the Navier-Stokes equations is developed and presented. The velocity field is decomposed using a scalar and vector potential. Vorticity and dilatation are used as the dependent variables in the momentum equations. Test cases in two dimensions verify the capability to solve flows using approximations from potential flow to full Navier-Stokes simulations. A three-dimensional incompressible flow formulation is also described. An interesting feature of this approach to solving the Navier-Stokes equations is the decomposition of the velocity field into a rotational part (vector potential) and an irrotational part (scalar potential). The Helmholtz decomposition theorem allows this splitting of the velocity field. A time-accurate, iterative algorithm is used for the uncoupled solution of the governing equations. Several levels of flow approximation are available within the framework of this method. Potential flow, Euler and full Navier-Stokes solutions are possible using the dual potential formulation. Solution efficiency can be enhanced in a straightforward way. The relative merits of non-primitive variables versus primitive variables for solution of the Navier-Stokes equations are also discussed. Dissert. Abstr.

N90-21973 Virginia Polytechnic Inst. and State Univ., Blacksburg.
CONVERGENCE ACCELERATION OF UPWIND RELAXATION METHODS FOR THE NAVIER-STOKES EQUATIONS Ph.D. Thesis
Arthur Canning Taylor, III 1989 173 p
Avail: Univ. Microfilms Order No. DA9003612

Two methods for improving the computational efficiency of upwind relaxation algorithms for the Navier-Stokes equations are proposed and tested. More efficient procedures were developed for obtaining steady-state solutions to these equations. In the first method investigated, the use of multiple relaxation sweeps (i.e., inner iterations) at each time step replaces the more conventional use of a single relaxation pass. This results in an accelerated (even quadratic) rate of error reduction per time step. An upwind line Gauss-Seidel algorithm which uses inner iterations is applied to a supersonic and a subsonic test case. In the supersonic test case, this method only requires about 65 percent of the CPU time which is used by the most efficient line relaxation method without inner iterations. The second method investigated is a new upwind relaxation algorithm for high speed viscous flows. This new method is a modified version of the standard line Gauss-Seidel algorithm, where as a convergence acceleration strategy, the thin wall-bounded subsonic regions of the flow are given a special treatment. Once the initial transient in the solution is overcome, the new algorithm is more efficient by a factor of over five in the first test case, and in the second test case, is more efficient by a factor of about two. Dissert. Abstr.

N90-21974*# National Aeronautics and Space Administration. Lewis Research Center, Cleveland, OH.
ANALYSIS OF THERMAL ENERGY STORAGE MATERIAL WITH CHANGE-OF-PHASE VOLUMETRIC EFFECTS
Thomas W. Kerslake and Mounir B. Ibrahim (Cleveland State Univ., OH.) Feb. 1990 34 p Presented at the 1990 International Solar Energy Conference, Miami, FL, 1-4 Apr. 1990; sponsored by ASME
(NASA-TM-102457; E-5244; NAS 1.15:102457) Avail: NTIS HC A03/MF A01 CSCL 20D

NASA's Space Station Freedom proposed hybrid power system includes photovoltaic arrays with nickel hydrogen batteries for energy storage and solar dynamic collectors driving Brayton heat engines with change-of-phase Thermal Energy Storage (TES) devices. A TES device is comprised of multiple metallic, annular canisters which contain a eutectic composition LiF-CaF2 Phase Change Material (PCM) that melts at 1040 K. A moderately sophisticated LiF-CaF2 PCM computer model is being developed in three stages considering 1-D, 2-D, and 3-D canister geometries, respectively. The 1-D model results indicate that the void has a marked effect on the phase change process due to PCM displacement and dynamic void heat transfer resistance. Equally influential are the effects of different boundary conditions and liquid PCM natural convection. For the second stage, successful numerical techniques used in the 1-D phase change model are extended to a 2-D (r,z) PCM containment canister model. A prototypical PCM containment canister is analyzed and the results are discussed. Author

N90-21975# Advisory Group for Aerospace Research and Development, Neuilly-Sur-Seine (France). Fluid Dynamics Panel.

APPLICATIONS OF MESH GENERATION TO COMPLEX 3-D CONFIGURATIONS

Mar. 1990 302 p In ENGLISH and FRENCH Meeting held in Loen, Norway, 24-25 May 1989
(AGARD-CP-464; ISBN-92-835-0551-4) Copyright Avail: NTIS HC A14/MF A02; Non-NATO Nationals requests available only from AGARD/Scientific Publications Executive

This Symposium was sponsored to provide a survey of the capabilities of the CFD community for griding complex 3-D configurations. The intent was to provide some insight to the present state of grid generation for complex configurations to help assess whether this task presents a long-term stumbling block to the routine use of CFD in aerodynamic applications. To this end, the meeting was structured in five sessions: General Surveys, Algebraic Grid Generation, Block Structured Meshes, Multi-block-Adaptive Meshes, and Unstructured Meshes. It was amply demonstrated that the viability of a numerical solution depends directly on the quality of the mesh and surface representation as measured by its spacing and resolution. Results indicate that geometry discretization and generation of meshes for complex 3-D configurations in aerospace will continue to be time- and cost-consuming operations for some time to come. For individual titles, see N90-21976 through N90-21997.

N90-21976# European Space Agency. European Space Research and Technology Center, ESTEC, Noordwijk (Netherlands). Aerothermodynamics Section.

RECENT DEVELOPMENTS IN GRID GENERATION

J. Haeuser and A. Vinckier *In* AGARD, Applications of Mesh Generation to Complex 3-D Configurations Mar. 1990 15 p (For primary document see N90-21975 15-34)
Copyright Avail: NTIS HC A14/MF A02; Non-NATO Nationals requests available only from AGARD/Scientific Publications Executive

An overview is given on recent developments in grid generation with emphasis on the results presented in the proceedings of the Second International Conference in Numerical Grid Generation in Computational Fluid Mechanics '88. Grid generation is essential for the solution of all kinds of fluid physics problems. It also reports briefly about the grid generation activities mainly to be used for Hermes. It is particularly important in cases where very different length scales are present, as, for example, in the case of turbulence, which can be considered as the pacing item in present day fluid physics. The main issue deals with multi-block grids in 3-D, but unstructured grids are also briefly mentioned. The important topics in multi-block grid generation are outlined and various approaches to their solution are discussed. The following main building blocks were identified: topology of the grid, that is how neighboring blocks are identified and what their relative orientation is to each other; patched (nonoverlapping grid that has grid line continuity only) or matched grids (grids with slope continuity, i.e., continuous tangent vector); block decomposition, which has to be automated if hundreds or thousands of blocks are being used; surface grid generation and analytical description of smooth surfaces to avoid the generation of shocks or expansion fans; grid point clustering (static grids); grid adaptation (dynamic grids) according to specified gradients or function values performed either by redistribution or by local enrichment; and postprocessing of grids to visualize and to achieve a specified grid quality at certain points or along certain lines or planes (interactive process). Author

N90-21977# Mississippi State Univ., Mississippi State. Dept. of Aerospace Engineering.

GENERAL STRUCTURED GRID GENERATION SYSTEMS

Joe F. Thompson *In* AGARD, Applications of Mesh Generation to Complex 3-D Configurations Mar. 1990 8 p (For primary document see N90-21975 15-34)
Copyright Avail: NTIS HC A14/MF A02; Non-NATO Nationals requests available only from AGARD/Scientific Publications Executive

Current techniques for the generation of composite-block structured grids for general 3D configurations are discussed. The various aspects of grid generation involved are noted, and their incorporation in general codes is cited. Current techniques for adaptive grids for general configurations are also discussed. Author

N90-21978# Volvo Flygmotor A.B., Trollhaettan (Sweden).

ALGEBRAIC BLOCK-STRUCTURED GRID GENERATION BASED ON A MACRO-BLOCK CONCEPT

Lars-Erik Eriksson and Erland Orbekk (Norges Tekniske Hoegskole, Trondheim.) *In* AGARD, Applications of Mesh Generation to Complex 3-D Configurations Mar. 1990 11 p (For primary document see N90-21975 15-34)
Copyright Avail: NTIS HC A14/MF A02; Non-NATO Nationals requests available only from AGARD/Scientific Publications Executive

An algebraic technique for generating block-structured grids of arbitrary topology is described. The method is based on a macro-block concept which allows the usage of large blocks with partial block boundary interfacing. Various spline procedures are used for curve generation and for constrained surface grids whereas all unconstrained surfaces and volumes are gridded by transfinite interpolation. Instead of using derivative information to control the grid in each block the present method is based on the idea of generating as many interior guiding surfaces as required for grid control and gridding each resulting sub-block independently of other sub-blocks. The resulting metric discontinuities, both inside blocks and between blocks, are smoothed either by a local algebraic smoothing procedure or by a global elliptic type smoothing procedure or combinations of both. The complete method was coded in a highly modular way and includes all graphics routines. Several 3-D multi-block grid examples are presented and discussed. Author

N90-21979*# National Aeronautics and Space Administration. Langley Research Center, Hampton, VA.

APPLICATIONS OF ALGEBRAIC GRID GENERATION

Peter R. Eiseman (Columbia Univ., New York, NY.) and Robert E. Smith *In* AGARD, Applications of Mesh Generation to Complex 3-D Configurations Mar. 1990 12 p (For primary document see N90-21975 15-34)
Copyright Avail: NTIS HC A14/MF A02; Non-NATO Nationals requests available only from AGARD/Scientific Publications Executive CSCL 20D

Techniques and applications of algebraic grid generation are described. The techniques are univariate interpolations and transfinite assemblies of univariate interpolations. Because algebraic grid generation is computationally efficient, the use of interactive graphics in conjunction with the techniques is advocated. A flexible approach, which works extremely well in an interactive environment, called the control point form of algebraic grid generation is described. The applications discussed are three-dimensional grids constructed about airplane and submarine configurations. Author

N90-21980# Aerospatiale, Chatillon (France). Tactical Missiles Div.

GEOMETRY AND GRIDS OF COMPLEX CONFIGURATIONS FOR AERODYNAMIC CALCULATION [GEOMETRIE ET MAILLAGE DE CONFIGURATIONS COMPLEXES POUR LES CALCULS AERODYNAMIQUES] c02

Gilbert Ranoux, Jerome Lordon, and Jean Diet *In* AGARD, Applications of Mesh Generation to Complex 3-D Configurations Mar. 1990 16 p In FRENCH; ENGLISH summary (For primary document see N90-21975 15-34)
Copyright Avail: NTIS HC A14/MF A02; Non-NATO Nationals requests available only from AGARD/Scientific Publications Executive

The methods which are used at Aerospatiale Tactical Missiles Division in order to calculate missile aerodynamics numerically in an industrial way are described. The problems in linking geometry and mesh are stressed. After a few comments about computer aided design (CAD) and its use in a mesh generation scheme, two procedures are presented: the first one, based on the space marching principle, is designed for supersonic flows and the second one proposes a multizonal approach for transonic and subsonic flows. Mesh examples and flow results are given for different types of configurations in order to illustrate the two procedures. Author

N90-21981# Societe Nationale d'Etude et de Construction de Moteurs d'Aviation, Moissy-Cramayel (France).
MESH GENERATION FOR FLOW COMPUTATION IN TURBOMACHINE **c07**
M. Goutines, G. Karadimas, and C. Hah (General Electric Co., Schenectady, NY.) *In* AGARD, Applications of Mesh Generation to Complex 3-D Configurations Mar. 1990 13 p (For primary document see N90-21975 15-34)
Copyright Avail: NTIS HC A14/MF A02; Non-NATO Nationals requests available only from AGARD/Scientific Publications Executive

Building grids for flow computation in turbomachine applications is examined. H,I,C, and O types are discussed for 2D or 3D, inviscid or viscous flow cases. The given examples concern 3D Euler application on a fan with part-span damper and splitter, 2D Navier-Stokes on turbine and compressor transonic cascades, and 3D Navier-Stokes on a transonic fan. Author

N90-21982# Mississippi State Univ., Mississippi State. Dept. of Aerospace Engineering.
UNSTEADY EULER SOLUTIONS ON DYNAMIC BLOCKED GRIDS FOR COMPLEX CONFIGURATIONS **c02**
David L. Whitfield, J. Mark Janus, and Abdollah Arabshahi *In* AGARD, Applications of Mesh Generation to Complex 3-D Configurations Mar. 1990 13 p (For primary document see N90-21975 15-34)
Copyright Avail: NTIS HC A14/MF A02; Non-NATO Nationals requests available only from AGARD/Scientific Publications Executive

A numerical method for solving the three-dimensional unsteady Euler equation on dynamic multiblocked grids about complex configurations in transonic flow is presented. Two configurations are considered. The first is a wing-pylon-store configuration with the store in the captive position, and then vertically launched from the wing-pylon. The second is a counter-rotating unducted propfan. The numerical results are validated by comparisons with available experimental data. Author

N90-21983# General Dynamics/Fort Worth, TX. Computational Fluid Dynamics Group.
A STRUCTURED APPROACH TO INTERACTIVE MULTIPLE BLOCK GRID GENERATION
J. P. Steinbrenner, J. R. Chawner, and C. L. Fouts *In* AGARD, Applications of Mesh Generation to Complex 3-D Configurations Mar. 1990 12 p (For primary document see N90-21975 15-34)
Copyright Avail: NTIS HC A14/MF A02; Non-NATO Nationals requests available only from AGARD/Scientific Publications Executive

The sheer variety of problems found in Computational Fluid Dynamics (CFD) has dictated a need for grid generation methods of the utmost generality. Experience has shown that user interaction and graphical feedback are two necessary features of a successful method as well. Employing these ideas, a structured method of grid generation was developed, allowing a grid system to be constructed through the use of four specialized codes, accessed on two machines. These codes are based on the multiple block concept, whereby the flowfield domain is decomposed into a number of contiguous subdomains, allowing for efficient grid generation and flowfield solution. The first of these codes aids the user in inspecting the flow domain and in developing a suitable blocking strategy for the block system. A second code is then used to establish the exact connections between abutting blocks and to set flow boundary conditions on all surfaces of the block system. This connectivity and boundary condition data is accessed in the final two codes to construct the grid itself. The third code generates the surfaces of each block in the system, and the final code distributes grid points on the block interiors. The intricacies of these codes are explained along with an example, conclusions and projections for further work. Author

N90-21984# National Aerospace Lab., Amsterdam (Netherlands).
DESIGN AND TESTING OF A MULTIBLOCK GRID-GENERATION PROCEDURE FOR AIRCRAFT DESIGN AND RESEARCH **c05**
J. W. Boerstoel, J. M. J. W. Jacobs, A. Kassies, A. Amendola, R. Tognaccini, and P. L. Vitagliano (Aeritalia S.p.A., Pomigliano D'Arco, Italy) *In* AGARD, Applications of Mesh Generation to Complex 3-D Configurations Mar. 1990 16 p (For primary document see N90-21975 15-34)
Copyright Avail: NTIS HC A14/MF A02; Non-NATO Nationals requests available only from AGARD/Scientific Publications Executive

A multiblock grid-generation procedure embedded in a numerical flow simulation system is described. Major features of the grids are: suitable for complex aerodynamic configurations; grid lines continuous, in particular, over block faces; grid lines not slope-continuous over block faces, topology and geometry of block decomposition first specified, and then grid-point distributions; application of transfinite interpolation and elliptic techniques. It is possible to construct multiblock grids around complex configurations with 250 to 1000 blocks, and to compute (Euler) flows on such grids. New technical concepts are proposed, to improve the accuracy of the flow simulation results, and to reduce manhour investments in the construction of multiblock grids. These concepts concern the use of compound faces and edges; the application of grid refinement per block and per coordinate direction, to remove the constraining effect of grid-line continuity on grid-point-density control; the use of new techniques for analytic aerodynamic geometry modeling, to reduce the dependence on non-CFD geometry software packages; the control of grid quality and acceptability with weight functions in the independent variables of the 3D vector functions defining the geometrical shape of edges, faces and blocks; and use of hyperblocks to speed up the block decomposition. Author

N90-21985# Messerschmitt-Boelkow-Blohm G.m.b.H., Munich (Germany, F.R.). Military Aircraft Div.
GRID PATCHING APPROACHES FOR COMPLEX THREE-DIMENSIONAL CONFIGURATIONS **c02**
W. Schwarz, G. Hartmann, and M. A. Schmatz *In* AGARD, Applications of Mesh Generation to Complex 3-D Configurations Mar. 1990 14 p (For primary document see N90-21975 15-34)
Copyright Avail: NTIS HC A14/MF A02; Non-NATO Nationals requests available only from AGARD/Scientific Publications Executive

Three examples of different grid generation procedures are reported. The first one is based on a single-block approach but nevertheless it is able to handle very complex aircraft configurations and requires only a minimum of user input. This system was the base for the development of the following patched grid method. The next example shows the application of the patched grid technique for the zonal solution of Euler, boundary-layer and Navier-Stokes equations and demonstrates the ability of this method to achieve the necessary local grid refinement for viscous calculations. Finally an application of a patched grid method for an Euler code with a shock fitting approach for supersonic calculations is presented. The grid near the body surface is fixed while the grid in the outer region is moved so that it can be adapted to the location of the bow shock. Author

N90-21986# British Aerospace Public Ltd. Co., Hatfield (England). Airlines Div.
MULTIBLOCK TOPOLOGY SPECIFICATION AND GRID GENERATION FOR COMPLETE AIRCRAFT CONFIGURATIONS **c05**

Steve Allwright *In* AGARD, Applications of Mesh Generation to Complex 3-D Configurations Mar. 1990 11 p (For primary document see N90-21975 15-34)
Copyright Avail: NTIS HC A14/MF A02; Non-NATO Nationals requests available only from AGARD/Scientific Publications Executive

The ability to calculate the flow around complex geometries is fundamentally controlled by the ability to generate grids of suitable structure and quality around the configurations of interest. The approach to Multiblock topology specification and grid generation pursued within British Aerospace, targeted to make Multiblock flow prediction methods available for use at all stages of the aerodynamic design process is discussed. The grids and computed flow solutions for a number of complex geometries are shown, and the capability for rapid systematic analysis of similar configuration geometries is illustrated. Author

N90-21987# Politecnico di Torino (Italy). Dept. of Aerospace Engineering.

THREE-DIMENSIONAL ADAPTIVE GRIDS WITH LIMITED SKEWNESS **c61**

Renzo Arina *In* AGARD, Applications of Mesh Generation to Complex 3-D Configurations Mar. 1990 8 p (For primary document see N90-21975 15-34)
Copyright Avail: NTIS HC A14/MF A02; Non-NATO Nationals requests available only from AGARD/Scientific Publications Executive

A grid generation technique for curved surfaces and three-dimensional regions is presented. In the two-dimensional case the set of solutions of the proposed grid generator belongs to the class of quasiconformal mappings, and it is shown that under appropriate conditions, it represents unfolded orthogonal coordinates. The isothermic coordinates are a particular case of this wider family of mappings. In three dimensions the solution of the mapping system is harmonic. Different kinds of stretching including an adaptive control of the mesh clustering are presented. Author

N90-21988# Royal Aerospace Establishment, Farnborough (England).

FEATURE-ASSOCIATED MESH EMBEDDING FOR COMPLEX CONFIGURATIONS

C. M. Albone and Gaynor Joyce (City Univ., London, England) *In* AGARD, Applications of Mesh Generation to Complex 3-D Configurations Mar. 1990 12 p (For primary document see N90-21975 15-34)
Copyright Avail: NTIS HC A14/MF A02; Non-NATO Nationals requests available only from AGARD/Scientific Publications Executive

The mesh-generation scheme described was designed to cope with complex geometric and flow features by employing many regular three-dimensional overlying meshes. Features are classified according to the number of geometric constraints to which they are subject, and each feature has its own purpose-built mesh. Four different mesh topologies are required to deal with all possible geometric and flow features. Progress to date is described and meshes for simple three-dimensional configurations are shown together with results of some Euler flow calculations. Author

N90-21989# Dornier-Werke G.m.b.H., Friedrichshafen (Germany, F.R.). Computational Fluid Dynamics Group.

ON THE WAY TO AN INTEGRATED MESH GENERATION SYSTEM FOR INDUSTRIAL APPLICATIONS

W. Seibert, W. Fritz, and S. Leicher *In* AGARD, Applications of Mesh Generation to Complex 3-D Configurations Mar. 1990 12 p (For primary document see N90-21975 15-34)
Copyright Avail: NTIS HC A14/MF A02; Non-NATO Nationals requests available only from AGARD/Scientific Publications Executive

The main features of some specialized batch modules, which were developed recently to meet the requirements of a grid generation for complex configurations, are described. One module is a combination of an algebraic grid generator for the determination of a surface grid and the far field boundary, and an hyperbolic grid generator for the sectionwise calculation of the corresponding orthogonal internal grid lines. Two other modules are concentrated on solution adaptive grids - either using algebraic redistribution proportional to the curvature of a typical flow filed describing function, or by solving elliptical partial differential equations resulting from the transformation of the Poisson equation from the physical space into the computational space. Adaption of the grid to pressure gradients and to the total pressure loss is done by replacing the source terms. The first part, however, is the description of the graphic-interactive program-system INGRID, which already comprises several standard techniques to generate composite volume grids around arbitrary complex configurations, and which has the potential to become an integrated system to match the demands for a general productive mesh generation method. As application examples several grids are shown, illustrating actual problems of external aircraft aerodynamics, ground-vehicle aerodynamics and of internal pipe flow. Author

N90-21990# Office National d'Etudes et de Recherches Aerospatiales, Paris (France). Direction de l'Aerodynamique.

GENERATION, OPTIMIZATION, AND ADAPTATION OF MULTIDOMAIN MESHES AROUND COMPLEX CONFIGURATIONS [GENERATION, OPTIMISATION, ET ADAPTATION DE MAILLAGES MULTIDOMAINES AUTOUR DE CONFIGURATIONS COMPLEXES]

Olivier-Pierre Jacquotte *In* AGARD, Applications of Mesh Generation to Complex 3-D Configurations Mar. 1990 11 p In FRENCH Original language document was announced in IAA as A89-48756 (For primary document see N90-21975 15-34)
Copyright Avail: NTIS HC A14/MF A02; Non-NATO Nationals requests available only from AGARD/Scientific Publications Executive

A method for the construction, optimization, and adaptation of three-dimensional structured meshes around complex configurations is presented. The first step consists of the algebraic generation of a multidomain mesh by dividing the calculation domain into structured hexahedral subdomains. A variational method is then developed to improve the qualities of the mesh (in particular its metrical properties) and to adapt it to the physical solution to be calculated on the mesh. The method has been used to obtain results for such configurations as a turbine blade, a hollow nacelle, and the Aster missile. Author

N90-21991# Aircraft Research Association Ltd., Bedford (England).

A DISCUSSION ON ISSUES RELATING TO MULTIBLOCK GRID GENERATION

J. M. Georgala and J. A. Shaw *In* AGARD, Applications of Mesh Generation to Complex 3-D Configurations Mar. 1990 13 p Sponsored in part by Ministry of Defence, England (For primary document see N90-21975 15-34)
Copyright Avail: NTIS HC A14/MF A02; Non-NATO Nationals requests available only from AGARD/Scientific Publications Executive

Efforts aimed at bringing a multiblock grid generation system to the state of maturity necessary for practical use are discussed. Attention is focused upon the interrelated areas of topology generation and grid control. An algorithm for automatically decomposing a flow domain about an aircraft configuration into a component-adaptive topology is given. Two techniques for controlling the resulting grid topology are described. The first automatically produces default grids, which will generally be of an acceptable quality. The second is a user-friendly interactive grid editor which allows any deficiencies in the default grids to be rapidly identified and modified. Examples of the multiblock approach are applied to a range of aircraft geometries. Author

N90-21992# Avions Marcel Dassault-Breguet Aviation, Saint-Cloud (France). Departement des Etudes Theoriques Aerodynamiques.
AUTOMATIC GRID GENERATION IN COMPLEX THREE-DIMENSIONAL CONFIGURATIONS USING A FRONTAL SYSTEM [GENERATION DE MAILLAGE AUTOMATIQUE DANS DES CONFIGURATIONS TRIDIMENSIONNELLES COMPLEXES UTILISATION D'UNE METHODE DE FRONT]
F. Huet *In* AGARD, Applications of Mesh Generation to Complex 3-D Configurations Mar. 1990 12 p In FRENCH (For primary document see N90-21975 15-34)
Copyright Avail: NTIS HC A14/MF A02; Non-NATO Nationals requests available only from AGARD/Scientific Publications Executive

Among the types of grid generation, the frontal construction method, starting from the limiting preset parameters, seems to be the most promising with respect to complex configurations within the framework of the finite element method. Its flexibility and its great adaptability makes it a tool with a very large area of application. The algorithm presented functions for the grids of complex configurations encounterd in aeronautics: engine nozzles with multiflow, Hermes shuttle, and Falcon. Transl. by E.R.

N90-21993*# University Coll. of Swansea (Wales). Dept. of Civil Engineering.
UNSTRUCTURED FINITE ELEMENT MESH GENERATION AND ADAPTIVE PROCEDURES FOR CFD
J. Peraire, K. Morgan, and J. Peiro *In* AGARD, Applications of Mesh Generation to Complex 3-D Configurations Mar. 1990 12 p Sponsored by NASA; Avions Marcel Dassault; and Civil and Military Aircraft Div., British Aerospace Public Ltd. Co. (For primary document see N90-21975 15-34)
Copyright Avail: NTIS HC A14/MF A02; Non-NATO Nationals requests available only from AGARD/Scientific Publications Executive CSCL 20D

A method is described for generating unstructured meshes of triangles or tetrahedra for computational domains of complex geometrical shape. To illustrate the power of the approach, it is applied to the solution of flows past several complete aircraft configurations. The advocated approach allows for the natural incorporation of mesh adaptivity and this is demonstrated for both inviscid and viscous computations in two and three dimensions. Author

N90-21994*# George Washington Univ., Washington, DC. School of Engineering and Applied Science.
GENERATION AND ADAPTATION OF 3-D UNSTRUCTURED GRIDS FOR TRANSIENT PROBLEMS
Rainald Loehner *In* AGARD, Applications of Mesh Generation to Complex 3-D Configurations Mar. 1990 17 p Sponsored in part by DNA; Air Force Ballistic Missile Office; and NRL (For primary document see N90-21975 15-34)
(Contracts NAS1-18419; NAS1-18670)
Copyright Avail: NTIS HC A14/MF A02; Non-NATO Nationals requests available only from AGARD/Scientific Publications Executive CSCL 20D

Grid generation and adaptive refinement techniques suitable for the simulation of strongly unsteady flows past geometrically complex bodies in 3-D are described. The grids are generated using the advancing front technique. Emphasis is placed not to generate elements that are too small, as this would severely increase the cost of simulations with explicit flow solvers. The grids are adapted to an evolving flowfield using simple h-refinement. A grid change is performed every 5 to 10 timesteps, and only one level of refinement/coarsening is allowed per mesh change. Author

N90-21995# Princeton Univ., NJ. Dept. of Mechanical and Aerospace Engineering.
UNSTRUCTURED MESH GENERATION BY A GENERALIZED DELAUNAY ALGORITHM c61
Timothy J. Baker *In* AGARD, Applications of Mesh Generation to Complex 3-D Configurations Mar. 1990 10 p Sponsored in part by IBM (For primary document see N90-21975 15-34)
Copyright Avail: NTIS HC A14/MF A02; Non-NATO Nationals requests available only from AGARD/Scientific Publications Executive

A method for generating tetrahedral meshes will be described. The algorithm is based on the Delaunay triangulation and can treat objects of essentially arbitrary complexity. In order to preserve the surface triangulation of solid objects, it is necessary to override the Delaunay property and redefine the triangulation when points are introduced close to solid boundaries. Details of the generalized algorithm are presented and an efficient implementation of the triangulation method is described. Author

N90-21996*# National Aeronautics and Space Administration. Ames Research Center, Moffett Field, CA.
APPLICATION OF THE TRANAIR RECTANGULAR GRID APPROACH TO THE AERODYNAMIC ANALYSIS OF COMPLEX CONFIGURATIONS c02
Forrester T. Johnson, Satish S. Samant, Michael B. Bieterman, Robin G. Melvin, David P. Young, John E. Bussoletti (Boeing Advanced Systems Co., Seattle, WA.), and Mike D. Madson *In* AGARD, Applications of Mesh Generation to Complex 3-D Configurations Mar. 1990 12 p Sponsored in part by Boeing Co. (For primary document see N90-21975 15-34)
(Contract NAS2-12513)
Copyright Avail: NTIS HC A14/MF A02; Non-NATO Nationals requests available only from AGARD/Scientific Publications Executive CSCL 20D

A numerical method is described which uses a rectangular grid to solve the nonlinear full potential equation about complex configurations. The grid is locally refined to resolve high velocity gradients arising from leading edge expansions or shock waves. The grid penetrates the boundary (described by networks of quadrilateral panels) and is generated automatically. Discrete operators are constructed using the finite element method. The system of nonlinear discrete equations is solved iteratively using a Krylov subspace method preconditioned by an exterior Poisson solver and a direct sparse solver. The primary emphasis is to provide design engineers with an aerodynamic analysis tool (the TRANAIR code) which is accurate, reliable, economical, and flexible to use. Computational results for many interesting configurations are presented. Author

N90-21997# Deutsche Forschungsanstalt fuer Luft- und Raumfahrt, Oberpfaffenhofen (Germany, F.R.). Institut fuer Hochfrequenztechnik.
THE SOLUTION OF SCATTERING AND RADIATION PROBLEMS FOR COMPLEX CONFIGURATIONS BASED ON 3-D GRID AND PATCH MODELS c32
V. Stein *In* AGARD, Applications of Mesh Generation to Complex 3-D Configurations Mar. 1990 22 p Sponsored in part by Bundesamt fuer Wehrtechnik und Beschaffung, Koblenz, Fed. Republic of Germany (For primary document see N90-21975 15-34)
Copyright Avail: NTIS HC A14/MF A02; Non-NATO Nationals requests available only from AGARD/Scientific Publications Executive

The increasing interest in predicting the scattering and radiation characteristics of objects with a complicated structure has stimulated the development of several theories. A rigorous treatment of the electrodynamic problem requires the solution of a boundary value problem based on Maxwell's differential equations or on the equivalent integral equations. The application of rigorous methods for objects whose dimensions are large compared to the wavelength is limited by the required computer memory and execution time. Therefore, methods which solve the boundary value problem approximately come into consideration. Each type of solution method involves a typical model either of the surface or the volume of the structure and its surroundings. So, geometric models consisting of canonical shapes, wire-grids, surface patches, and volume cells are described and the requirements of the specific solution methods are discussed. In some cases estimations for the necessary modeling accuracy are given. Methods which are based on geometrical-optics principles require models where the surface parts which are illuminated by the incident wave and the surface parts which are hidden can be separated for each aspect angle. Such a procedure is discussed as well as the procedure to treat double reflections. Some computational examples for radiation and scattering processes are given and comparisons with measurements are made. Author

N90-21998# Laboratorio de Computacao Cientifica, Rio de Janeiro (Brazil).

HIGH ORDER P-G FINITE ELEMENTS FOR CONVECTION-DOMINATED PROBLEMS

Eduardo DubrodoCarmo and Augusto Cesar Galeio Jun. 1989 13 p
(DE90-614743; LNCC-020/89) Avail: NTIS (US Sales Only) HC A03/MF A01

From the error analysis presented in this paper it is shown that the C Consistent Approximation Upwind method derived by Dutra do Carmo and Galeao (3) preserves the same order of approximation obtained with Streamline Upwind Petrov-Galerkin (cf. Books and Hughes (2)) when advection and/or diffusion regular solutions are considered, and improves the accuracy of the approximate boundary layer solution when high order interpolating polynomials are used near sharp layers. DOE

N90-21999* National Aeronautics and Space Administration. Lyndon B. Johnson Space Center, Houston, TX.

PRESSURIZED BELLOWS FLAT CONTACT HEAT EXCHANGER INTERFACE Patent

Fred E. Voss, inventor (to NASA), Harold R. Howell, inventor (to NASA), and Roger V. Winkler, inventor (to NASA) (LTV Aerospace and Defense Co., Dallas, TX.) 20 Mar. 1990 7 p Filed 30 Sep. 1988
(NASA-Case-MSC-21271-1; US-Patent-4,909,313; US-Patent-Appl-SN-252077; US-Patent-Class-165-78; US-Patent-Class-165-96; US-Patent-Class-165-46; US-Patent-Class-165-32) Avail: US Patent and Trademark Office CSCL 20D

Disclosed is an interdigitated plate-type heat exchanger interface. The interface includes a modular interconnect to thermally connect a pair or pairs of plate-type heat exchangers to a second single or multiple plate-type heat exchanger. The modular interconnect comprises a series of parallel, plate-type heat exchangers arranged in pairs to form a slot therebetween. The plate-type heat exchangers of the second heat exchanger insert into the slots of the modular interconnect. Bellows are provided between the pairs of fins of the modular interconnect so that when the bellows are pressurized, they drive the plate-type heat exchangers of the modular interconnect toward one another, thus closing upon the second heat exchanger plates. Each end of the bellows has a part thereof a thin, membrane diaphragm which readily conforms to the contours of the heat exchanger plates of the modular interconnect when the bellows is pressurized. This ensures an even distribution of pressure on the heat exchangers of the modular interconnect thus creating substantially planar contact between the two heat exchangers. The effect of the interface of the present invention is to provide a dry connection between two heat exchangers whereby the rate of heat transfer can be varied by varying the pressure within the bellows.
Official Gazette of the U.S. Patent and Trademark Office

N90-22000*# Kansas Univ. Center for Research, Inc., Lawrence. Flight Research Lab.

MODERN DEVELOPMENTS IN SHEAR FLOW CONTROL WITH SWIRL Final Report

Saeed Farokhi and R. Taghavi May 1990 48 p
(Contract NCC3-56)
(NASA-CR-186586; NAS 1.26:186586; KU-FRL-724-4) Avail: NTIS HC A03/MF A01 CSCL 20D

Passive and active control of swirling turbulent jets is experimentally investigated. Initial swirl distribution is shown to dominate the free jet evolution in the passive mode. Vortex breakdown, a manifestation of high intensity swirl, was achieved at below critical swirl number ($S = 0.48$) by reducing the vortex core diameter. The response of a swirling turbulent jet to single frequency, plane wave acoustic excitation was shown to depend strongly on the swirl number, excitation Strouhal number, amplitude of the excitation wave, and core turbulence in a low speed cold jet. A 10 percent reduction of the mean centerline velocity at $x/D = 9.0$ (and a corresponding increase in the shear layer momentum thickness) was achieved by large amplitude internal plane wave acoustic excitation. Helical instability waves of negative azimuthal wave numbers exhibit larger amplification rates than the plane waves in swirling free jets, according to hydrodynamic stability theory. Consequently, an active swirling shear layer control is proposed to include the generation of helical instability waves of arbitrary helicity and the promotion of modal interaction, through multifrequency forcing. Author

N90-22001# Sandia National Labs., Albuquerque, NM. Fluid and Thermal Sciences Dept.

PARTIAL ACOUSTIC FILTERING APPLIED TO THE EQUATIONS OF COMPRESSIBLE FLOW

J. R. Torczynski 1990 18 p Presented at the International Symposium on Nonsteady Fluid Dynamics, Toronto, Ontario, 4-7 Jun. 1990
(Contract DE-AC04-76DP-00789)
(DE90-000673; SAND-89-1927C; CONF-900651-1) Avail: NTIS HC A03/MF A01

Gas contained in a rectangular enclosure of large length and small width is subjected to large, transient, spatially nonuniform, volumetric heating. The heating timescale is much longer than the time required for an acoustic wave to traverse the width but can be comparable to the time required for an acoustic wave to traverse the length. Approximate equations are derived from the 2-D equations of mass, momentum, and energy conservation for a perfect gas without viscosity or thermal conductivity. This is accomplished by applying partial acoustic filtering to the equations of motion: pressure waves traversing the width are removed while pressure waves traversing the length are retained. The pressure is partitioned into the average pressure across the width, which is O(1), and the small remaining perturbation that is the difference between the pressure and its average. The resulting equations are hyperbolic for the average pressure term but are elliptic for the perturbation pressure term. If an explicit numerical method is used to solve the approximate system, the maximum allowable time step is potentially much larger than the time step for the original system, which is dominated by resolution of pressure waves propagating across the width. Application of partial acoustic filtering to 3-D geometries is discussed. DOE

N90-22002# West Virginia Univ., Morgantown. Dept. of Mechanical and Aerospace Engineering.

NUMERICAL SIMULATION OF LIQUID CIRCULATION IN A BUBBLY COLUMN

Ismail Celik and Yi-Zun Wang 1990 24 p Presented at the Symposium on Numerical Methods for Multi-Phase Flows, Toronto, Canada, 3-9 Jun. 1990
(Contract DE-FG22-87PC-79935)
(DE90-005226; DOE/PC-79935/13; CONF-9006107-1) Avail: NTIS HC A03/MF A01

The gas-liquid flow inside a vertically situated circular, isothermal column reactor was simulated numerically. The gas-liquid flow is assumed to be in the bubbly flow regime which is characterized by a suspension of discrete air bubbles in a continuous liquid phase such as glycerol water. The mathematical formulation is based on the conservation of mass and momentum principle for the liquid phase. The gas velocity distribution is calculated via an empirically prescribed slip velocity as a function of void fraction. The interface viscous drag forces are prescribed empirically. A profile shape is assumed for the void ratio distribution and the magnitude of it is calculated as part of the solution. The influence of various profile shapes is investigated. Results with the void ratio distribution calculated from the conservation of mass equation for the gas phase are also presented. The mathematical model was implemented by modifying a readily available computer code for single phase newtonian fluid flows. The numerical discretization is based on a finite volume approach. DOE

N90-22003# Argonne National Lab., IL.
DEVELOPMENT OF A COMPUTATIONAL FLUID DYNAMICS AND CHEMISTRY MODEL FOR THE FOULING OF JET FUELS
J. L. Krazinski, S. P. Vanka, J. A. Pearce, and W. M. Roquemore (Air Force Aero Propulsion Lab., Wright-Patterson AFB, OH.) 1990 41 p Presented at the 35th International Gas Turbine and Aeroengine Congress and Exposition, Brussels, Belgium, 11-14 Jun. 1990 Sponsored by Air Force Aero Propulsion Lab., Wright-Patterson AFB, OH and Pittsburgh Energy Technology Center, PA
(Contract W-31-109-eng-38)
(DE90-005664; CONF-900615-1) Avail: NTIS HC A03/MF A01

A new approach has been devised in which Computational Fluid Dynamic and Chemistry (CFDC) models are employed to predict the fluid mechanics, heat transfer, and deposition in fuel system components. The structure of this model is such that it has the potential of being used as a tool for research or to assist in the design of heat exchangers or other fuel system components. The model contains several unknown parameters that must be calibrated using experimental data for a particular fuel. This paper describes the development of the model, a method of calibrating the model, and a sensitivity analysis of the effects of different model parameters on predicted deposition rates in a heated tube. DOE

N90-22004# Edgerton, Germeshausen and Grier, Inc., Idaho Falls, ID.
ON DUAL LAGRANGIAN HYPERBOLIC MODELS FOR ONE DIMENSIONAL TWO PHASE FLOW PROBLEMS
Arthur S.-L. Shieh 1990 16 p Presented at the Symposium on Numerical Methods for Multi-phase Flows, Toronto, Ontario, 3-9 Jun. 1990 Submitted for publication
(Contract DE-AC07-76ID-01570)
(DE90-007012; EGG-M-89359; CONF-9006107-2) Avail: NTIS HC A03/MF A01

A dual Lagrangian computational hyperbolic model for two-phase flow is presented. The implicit Richtmeyer-von Neumann method is used to solve the resulting difference equations. The method is unconditionally stable and solves the shock tube with no mass diffusion. DOE

N90-22005# Los Alamos National Lab., NM.
EXPERIMENTAL OBSERVATIONS ON TRANSITION TO TURBULENCE IN CONFINED COAXIAL JETS AND OTHER BOUNDARY LAYER FLOWS
Robert A. Gore, Clayton T. Crowe, and Adrian Bejan (Duke Univ., Durham, NC.) 1990 7 p Presented at the International Symposium on Nonsteady Fluid Dynamics, Toronto, Ontario, 4-7 Jun. 1990
(Contract W-7405-eng-36)
(DE90-008939; LA-UR-90-857; CONF-900651-2) Avail: NTIS HC A02/MF A01

Experiments performed demonstrate the transition to turbulent flow of water jets discharging coaxially into a stream confined in a round duct. The critical Reynolds number is shown to be a strong function of velocity ratio. From the flow visualization it is shown that a proportionality between the laminar length of the jet (L) and the wavelength (lambda) can be seen in the region of transition to turbulence. The proportionality coincides with similar observations concerning the transition to turbulence in various other flows. A brief argument based on scale analysis is presented for the confined coaxial jet and round plume. The apparent universality of the L/(lambda) (approximately) O(10) scaling law supports the conclusion that the laminar sections of all naturally progressing boundary layer-type flows are geometrically similar. DOE

N90-22006# Los Alamos National Lab., NM.
TURBULENCE IN SLURRY PIPE FLOW
Robert A. Gore and Clayton T. Crowe (Washington State Univ., Pullman.) 1990 6 p Presented at the International Symposium on Nonsteady Fluid Dynamics, Toronto, Ontario, 4-7 Jun. 1990
(Contract W-7405-eng-36)
(DE90-008940; LA-UR-90-856; CONF-900651-3) Avail: NTIS HC A02/MF A01

The present state of knowledge of liquid-solid flows (slurries) is far behind than that for single phase flows. Very few geometries have been examined with a slurry and only with a limited variation of system parameters i.e., fluid viscosity, particle diameter, etc. This paper presents the first part of a study which examines the effects of the addition of a solid to the flow through a confined coaxial jet. Presented here will be the initial conditions for the jet which correspond to fully developed pipe flow. DOE

N90-22007# Pittsburgh Energy Technology Center, PA.
MATHEMATICAL MODELING OF FLUID-SOLID MIXTURES
K. R. Rajagopal (Pittsburgh Univ., PA.), M. Massoudi, and J. M. Ekmann Mar. 1990 10 p
(DE90-009152; DOE/PETC/TR-90/5) Avail: NTIS HC A03/MF A01

The flows of a mixture of solid particles and a fluid have relevance to several important technological applications. There are primarily two approaches that have been used for modeling such solid-fluid systems. In the first approach, the model is obtained by some kind of averaging of the equations of motion. In the second approach, the basic conservation laws are postulated and the ideas in continuum mechanics are used to arrive at appropriate constitutive relations. In this report we use this approach called mixture theory to derive the governing equations of motion for a steady one-dimensional fully developed pipe flow of a mixture of particles and a fluid. We present a brief historical account of the modeling of stress tensors for particles and the fluid. Finally, we discuss the importance of the boundary conditions. DOE

N90-22008# Lawrence Livermore National Lab., CA. Dept. of Chemistry and Materials Science.
PLANE STOKES FLOW DRIVEN BY CAPILLARITY ON A FREE SURFACE: OVERVIEW AND STATUS
Robert W. Hopper 11 Mar. 1990 6 p Presented at the 5th International Colloquium on Free Boundary Problems: Theory and Applications, Montreal, Quebec, 13-22 Jun. 1990
(Contract W-7405-eng-48)
(DE90-009186; UCRL-JC-103243; CONF-900684-1) Avail: NTIS HC A02/MF A01

The creeping viscous incompressible plane flow in a region, bounded by a simple smooth closed curve and driven solely by surface tension was studied. Such problems are self-contained in that the applied tractions are intrinsic in the geometry. The objective is to determine exactly the time evolution of the shape of the region. The problems are fundamentally nonlinear due to the large changes in shape, and it is emphasized that no mathematical approximations are made. For finite regions, the shape in the complex z-plane is described in terms of a time dependent conformal mapping function (Omega zeta ,t) on the fixed region the absolute value of zeta is less than or = 1 of the complex. In practice, it has been necessary to conjecture an explicit parametric form omega ((zeta);a(sub 1)(t), a(sub 2)(t), ...)) whose validity must be verified using the shape evolution equation. Suitable parameterizations are not always obvious. When the conjectured form hold and the equations can be solved, the equation of the shape with time is obtained in simple, exact and closed form except for the value of the time, which requires a mere quadrature. Internal velocity and stress fields can be obtained. DOE

N90-22009# Lawrence Livermore National Lab., CA. Dept. of Chemistry and Materials Science.
PLANE STOKES FLOW DRIVEN BY CAPILLARITY ON A FREE SURFACE: OVERVIEW AND STATUS
Robert W. Hopper 26 Mar. 1990 8 p Presented at the 5th International Colloquium on Free Boundary Problems: Theory and Applications, Montreal, Quebec, 13-22 Jun. 1990 Revised
(Contract W-7405-eng-48)

(DE90-009290; UCRL-JC-103243-Rev-1; CONF-900684-1-Rev-1) Avail: NTIS HC A02/MF A01

The creeping viscous incompressible plane flow in a region, bounded by a simple smooth closed curve and driven solely by surface tension was studied. Such problems are self-contained in that the applied tractions are intrinsic in the geometry. The objective is to determine exactly the time evolution of the shape of the region. The problems are fundamentally nonlinear due to the large changes in shape, and it is emphasized that no mathematical approximations are made. Mathematical details, discussions of general concepts, and references to related work are included which deals primarily with finite regions. Further articles are in preparation, including extensions to unbounded and doubly-connected regions. DOE

N90-22010# Edgerton, Germeshausen and Grier, Inc., Idaho Falls, ID.

TOODEE: A TWO-DIMENSIONAL, TIME-DEPENDENT HEAT CONDUCTION PROGRAM

Brent J. Sackett, Richard G. Ambrosek, and John A. McClure, comp. Jan. 1990 131 p
(Contract DE-AC07-76ID-01570)
(DE90-009631; EGG-NE-8863) Avail: NTIS HC A07/MF A01

TOODEE is a two-dimensional, time-dependent heat conduction computer program written in FORTRAN. This program is suitable for investigating general transient and/or steady-state problems. Typical of (but not limited to) the type of problems for which the program has been used are the calculation of temperature distributions in reactor fuel elements during power excursions. The mesh for the program is formed by variably spaced orthogonal curves in either slab or cylindrical geometry. The cylindrical geometry may be either axisymmetric, with space variables R-Z, or polar, with space variables R-(theta). Conditions to be specified independently at each boundary are either surface temperatures or heat transfer coefficients and either exterior temperatures of flow rates. Materials and coolant properties required in the program are evaluated from FORTRAN arithmetic functions supplied by the user. These properties may be time and/or temperature dependent. In addition, nonisotropic thermal conductivities and expansion coefficients may be defined. Phase changes are permitted in all materials except coolants. DOE

N90-22011*# National Aeronautics and Space Administration. Lewis Research Center, Cleveland, OH.

COMPUTATIONAL MODELING AND VALIDATION FOR HYPERSONIC INLETS

Louis A. Povinelli 1990 11 p Presented at the 75th Symposium on Hypersonic Combined Cycle Propulsion, Madrid, Spain, 28 May - 1 Jun. 1990; sponsored by Propulsion and Energetics Panel of AGARD
(NASA-TM-103111; E-5435; NAS 1.15:103111) Avail: NTIS HC A03/MF A01 CSCL 20D

Hypersonic inlet research activity at NASA is reviewed. The basis is the experimental tests performed with three inlets: the NASA Lewis Research Center Mach 5, the McDonnell Douglas Mach 12, and the NASA Langley Mach 18. Both three-dimensional parabolized Navier-Stokes and Navier-Stokes codes were used to compute the flow within the three inlets. Modeling assumptions in the codes involve the turbulence model, the nature of the boundary layer, shock wave boundary layer interaction, and the flow spilled to the outside of the inlet. Use of the codes in conjunction with the experimental data are helping to develop a clearer understanding of the inlet flow physics and to focus on the modeling improvements required in order to arrive at validated codes. Author

N90-22012# Technische Univ., Delft (Netherlands). Faculty of Aerospace Engineering.

BIFURCATIONS IN VISCOUS FLOW FIELDS. ON THE GENESIS AND DEVELOPMENT OF TOPOLOGICALLY COMPLICATED SEPARATED FLOW STRUCTURES

Pieter Gerrit Bakker Feb. 1989 87 p
(PB90-167156; LR-576; ETN-90-96341) Avail: NTIS HC A05/MF A01

A qualitative theory of dynamical systems with topological considerations is applied to steady viscous flows. Local solutions of the Navier-Stokes equations are constructed in the phase space and a classification of possible flow topologies near fixed and moving walls is presented. A detailed study of the unfoldings and bifurcation behavior of higher order singular points is described. It is concluded that despite their rare appearance in practice, higher order singularities are the cornerstones of a method providing local solution to Navier-Stokes equations. ESA

N90-22013# Technische Univ., Delft (Netherlands). Faculty of Aerospace Engineering.

THE CALIBRATION AND MEASURING PROCEDURE OF A FIVE-HOLE HEMISPHERICAL HEAD PROBE IN COMPRESSIBLE FLOW

E. M. Houtman and W. J. Bannink Apr. 1989 32 p
(LR-585; ETN-90-96348; PB90-166554) Avail: NTIS HC A03/MF A01

Probe pressures are used to determine relative flow angles, Mach number and total pressure around the probe. Calibration functions developed with the aid of the theory of flow around a sphere are described. The probe is calibrated at angles up to 60 degrees relative to its axis and at Mach numbers between 0.55 and 1.76. Flow angles are determined within an accuracy of 0.5 degrees, and Mach numbers within an accuracy of 0.03 if a fine interval of probe angles is applied. Determination of flow parameters in an unknown flow is achieved by using calculations of low order polynomials determined from calibration data in a limited region around a measuring point. ESA

N90-22014# National Aerospace Lab., Amsterdam (Netherlands).

EUROPEAN RESEARCH ON VISCOUS FLOW (EUROVISC) Annual Report No. 17, 1988

J. P. F. Lindhout, ed., J. Cousteix, ed., D. A. Humphreys, ed., W. Kordulla, ed., and P. D. Smith, ed. (Royal Aeronautical Society, London, England) Jan. 1989 163 p
(NLR-TP-89077-U; ETN-90-96399) Avail: NTIS HC A09/MF A01

A survey of research work going on today in Europe on viscous flow problems, is given. The reports of associations include: the experimental investigation of the turbulent shear layers of a swept wing, experimental turbulent boundary layers in ducts, the missions of CERFACS and studies on numerical methods in fluid mechanics. Specific activities within the high speed aerodynamics, study of transition models, both active and passive laminar flow control, experimental techniques and computational methods, are discussed. ESA

N90-22015# Technische Univ., Delft (Netherlands).

PROPAGATION OF TRANSIENT ACOUSTIC WAVES IN POROUS MEDIA Ph.D. Thesis

Sytze Marten deVries 1989 182 p
(ETN-90-96401) Avail: NTIS HC A09/MF A01

The scope of a macroscopic linear acoustic theory for impulsive wave propagation in a porous medium is investigated. A closed form expression for the acoustic traction in the space-time domain of the wave was derived. With Laplace and Fourier transformations applied to wave equations, the transform-domain field equations arise as a system of differential equations in the coordinate normal to the boundary. The corresponding system's matrix, eigenvalues and eigenvectors are presented. ESA

N90-22016*# National Aeronautics and Space Administration. Lewis Research Center, Cleveland, OH.

AN UNSTEADY TIME ASYMPTOTIC FLOW IN THE SQUARE DRIVEN CAVITY

John W. Goodrich 1990 12 p Presented at the IMACS 1st International Conference on Computational Physics, Boulder, CO, 11-15 Jun. 1990; cosponsored by International Association of

Mathematics and Computers in Simulation and Colorado Univ.
(NASA-TM-103141; E-5493; NAS 1.15:103141) Avail: NTIS HC A03/MF A01 CSCL 20D

Summary details of an aperiodic time asymptotic numerical solution for the square drive cavity at Re = 10000 are presented. The data presented is for 6100 less than t less than or equal to 7100, and is representative of the data that characterizes the aperiodic asymptotic state. Author

N90-22017*# Arizona Univ., Tucson. Dept. of Aerospace and Mechanical Engineering.

INSTABILITIES AND SUBHARMONIC RESONANCES OF SUBSONIC HEATED ROUND JETS, VOLUME 2 Ph.D. Thesis Final Report

Lian Lai Ng 1990 186 p
(Contract NAS1-18599; NAG3-485)
(NASA-CR-186058; NAS 1.26:186058) Avail: NTIS HC A09/MF A01 CSCL 20D

When a jet is perturbed by a periodic excitation of suitable frequency, a large-scale coherent structure develops and grows in amplitude as it propagates downstream. The structure eventually rolls up into vortices at some downstream location. The wavy flow associated with the roll-up of a coherent structure is approximated by a parallel mean flow and a small, spatially periodic, axisymmetric wave whose phase velocity and mode shape are given by classical (primary) stability theory. The periodic wave acts as a parametric excitation in the differential equations governing the secondary instability of a subharmonic disturbance. The (resonant) conditions for which the periodic flow can strongly destabilize a subharmonic disturbance are derived. When the resonant conditions are met, the periodic wave plays a catalytic role to enhance the growth rate of the subharmonic. The stability characteristics of the subharmonic disturbance, as a function of jet Mach number, jet heating, mode number and the amplitude of the periodic wave, are studied via a secondary instability analysis using two independent but complementary methods: (1) method of multiple scales, and (2) normal mode analysis. It is found that the growth rates of the subharmonic waves with azimuthal numbers beta = 0 and beta = 1 are enhanced strongly, but comparably, when the amplitude of the periodic wave is increased. Furthermore, compressibility at subsonic Mach numbers has a moderate stabilizing influence on the subharmonic instability modes. Heating suppresses moderately the subharmonic growth rate of an axisymmetric mode, and it reduces more significantly the corresponding growth rate for the first spinning mode. Calculations also indicate that while the presence of a finite-amplitude periodic wave enhances the growth rates of subharmonic instability modes, it minimally distorts the mode shapes of the subharmonic waves. Author

N90-22018 Colorado Univ., Boulder.

UNSTEADY SEPARATED FLOWS PRODUCED BY COMPLEX HARMONIC MOTIONS: INVESTIGATION OF WING-FLOW INTERACTIONS ELICITED BY A MECHANICAL MODEL SIMULATING DRAGONFLY WING KINEMATICS Ph.D. Thesis

Daniel Chasman 1989 196 p
Avail: Univ. Microfilms Order No. DA9009142

Attention was drawn to the flying skill of dragonflies by many aerodynamicists. While some have tried to explain this exceptional flight capability using known steady aerodynamics, there was growing realization by others that the dragonfly uses principles of unsteady separated flow to sustain flight. The moving wings generate shear flows that accumulate vorticity and form vortices. In an effort to describe the phenomenon and possibly derive some of the underlying unsteady principles, a mechanical model of the dragonfly was built simulating all aspects of wing kinematics of the dragonfly. Flow visualization tests revealed complex yet highly organized flow during changes in parameters of the model wing kinematics. Each wing kinematic element produces a distinct vortex structure. Parameters such as reduced frequency, pitching/plunging frequency ratio, wing phase relations and non-pitched angle of attack control the wing-flow interactions. Changes in the parameters result in changes in the interactons that were cataloged into wing-vortex and vortex-vortex interactons. In the narrow range of parameter combinations that is used by the dragonfly, vortices fuse with each other to form much larger and more cohesive vortex structures. A complex starting vortex mechanism was identified. Since each of the kinematic elements possesses a starting motion, a vortex is initiated when each motion starts. Upon motion termination, the vortex sheds. In harmonic motion this vortex production and shedding occurs with every new cycle. Eight kinematic elements per cycle produce eight vortex structures that interact harmonically to generate instantaneous aerodynamic force. Thus, complex harmonic wing motion produces complex harmonic circulation using mechanisms very similar to the interference phenomena of waves. Tuning of parameter values controls this interference. Dissert. Abstr.

N90-22019 North Carolina State Univ., Raleigh.

DEVELOPMENT OF A DEFECT STREAM FUNCTION, LAW OF THE WALL/WAKE METHOD FOR COMPRESSIBLE TURBULENT BOUNDARY LAYERS Ph.D. Thesis

Richard Alan Wahls 1989 123 p
Avail: Univ. Microfilms Order No. DA9008765

The method presented is designed to improve the accuracy and computational efficiency of existing numerical methods for the solution of flows with compressible turbulent boundary layers. A compressible defect stream function formulation of the governing equations assuming an arbitrary turbulence model is derived. This formulation is advantageous because it has a constrained zero-order approximation with respect to the wall shear stress and the tangential momentum equation has a first integral. Previous problems with this type of formulation near the wall are eliminated by using empirically based analytic expressions to define the flow near the wall. The van Driest law of the wall for velocity and the modified Crocco temperature-velocity relationship are used. The associated compressible law of the wake is determined and it extends the valid range of the analytic expressions beyond the logarithmic region of the boundary layer. The need for an inner-region eddy viscosity model is completely avoided. The near-wall analytic expressions are patched to numerically computed outer region solutions at a point determined during the computation. A new boundary condition on the normal derivative of the tangential velocity at the surface is presented; this condition replaces the no-slip condition and enables numerical integration to the surface with a relatively coarse grid using only an outer region turbulence model. The method was evaluated for incompressible and compressible equilibrium flows and was implemented into an existing Navier-Stokes code using the assumption of local equilibrium flow with respect to the patching. The method has proven to be accurate and efficient. Dissert. Abstr.

N90-22020 Iowa Univ., Iowa City.

NUMERICAL STUDY OF LAMINAR AND TURBULENT FLOWS PAST TWO-DIMENSIONAL AND AXISYMMETRIC BODIES Ph.D. Thesis

Seok Ki Choi 1989 266 p
Avail: Univ. Microfilms Order No. DA9009294

A numerical study of laminar and turbulent flows past two-dimensional bodies and axisymmetric bodies is presented. Numerical methods are developed to solve Navier-Stokes equations for two-dimensional and axisymmetric flows in the arbitrary geometries. The complex physical geometry is resolved by use of numerically generated, body-fitted coordinates. The governing equations are written in the transformed domain using the orthogonal velocity components as dependent variables for momentum equation. The governing equations are discretized using both the finite analytic method and the finite volume method. Both one velocity staggered grid method and two velocities staggered method are employed for grid arrangements. The velocity and pressure coupling techniques in these grid arrangements are presented. The solution procedure of the SIMPLER numerical algorithm is used with a parabolic marching technique and a global pressure calculation method. For turbulent flow calculations, both the k-epsilon turbulence model and the two-layer model are used. Calculations are performed for laminar and turbulent flows past a finite flat plate and turbulent flow past axisymmetric bodies with different solution domains, numerical methods and turbulence models. Calculations include the development of a wake function method for the prediction of turbulent wake of a flat plate, predictions of laminar and turbulent flows past a finite flat plate, predictions of turbulent flow past axisymmetric bodies by the wall function method and by the two-layer turbulence model and predictions of turbulent flow past finite axisymmetric bodies. Comparisons of predictions by finite analytic method with those by finite volume method are made for some calculations.

Dissert. Abstr.

35 INSTRUMENTATION AND PHOTOGRAPHY

Includes remote sensors; measuring instruments and gages; detectors; cameras and photographic supplies; and holography.

For aerial photography see *43 Earth Resources and Remote Sensing.* For related information see also *06 Aircraft Instrumentation,* and *19 Spacecraft Instrumentation.*

N90-22021*# National Aeronautics and Space Administration. Lewis Research Center, Cleveland, OH.

SCATTERED-LIGHT SCANNER MEASUREMENTS OF CRYOGENIC LIQUID-JET BREAKUP

Robert D. Ingebo and Donald R. Buchele 1990 14 p Presented at the 2nd International Congress Optical Particle Sizing, Tempe, AZ, 5-9 Mar. 1990; sponsored by Arizona State Univ.
(NASA-TM-102432; E-5200; NAS 1.15:102432) Avail: NTIS HC A03/MF A01 CSCL 14B

The effect of highly turbulent Mach 1 gas flow and high thermal gradients on drop size measurements was investigated with a scattered light scanner. The instrument, developed at NASA-Lewis, was used to measure characteristic drop diameters or cyrogenic liquid sprays. By correcting for gas turbulence and thermal gradient affects, it was possible to obtain good reproducible data with the scattered light scanner. Tests were conducted primarily in the aerodynamic-stripping regime of liquid atomization and it was found that the loss of small droplets due to vaporization and dispersion had a marketed effect on drop size measurements. The nitrogen gas flow rate exponent of 1.33 is the same as that predicted by atomization theory for liquid jet breakup in high velocity gas flow. However, when the sprays were sampled farther downstream of the atomizer, at axial distances of 2.5 and 4.5 cm, the exponent for W sub n decreased 1.2 and 0.9, respectively. This was attributed to the loss of small droplets due to vaporization when values of downstream axial distances exceeded 1.3 cm. Author

N90-22022*# Purdue Univ., West Lafayette, IN. School of Mechanical Engineering.

SATURATED FLUORESCENCE MEASUREMENTS OF THE HYDROXYL RADICAL IN LAMINAR HIGH-PRESSURE FLAMES Final Report

Campbell D. Carter, Galen B. King, and Normand M. Laurendeau Feb. 1990 222 p
(Grant NAG3-351)
(NASA-CR-185218; NAS 1.26:185218) Avail: NTIS HC A10/MF A02 CSCL 14B

The efficacy of laser saturated fluorescence (LSF) for OH concentration measurements in high pressure flames was studied theoretically and experimentally. Using a numerical model describing the interaction of hydroxyl with nonuniform laser excitation, the effect of pressure on the validity of the balanced cross-rate model was studied along with the sensitivity of the depopulation of the laser-coupled levels to the ratio of rate coefficients describing: (1) electronic quenching to (sup 2) Sigma (+) (v double prime greater than 0), and (2) vibrational relaxation from v double prime greater than 0 to v double prime = 0. At sufficiently high pressures and near-saturated conditions, the total population of the laser-coupled levels reaches an asymptotic value, which is insensitive to the degree of saturation. When the ratio of electronic quenching to vibrational relaxation is small and the rate of coefficients for rotational transfer in the ground and excited electronic states are nearly the same, the balanced cross-rate model remains a good approximation for all pressures. When the above ratio is large, depopulation of the laser-coupled levels becomes significant at high pressures, and thus the balanced cross-rate model no longer holds. Under these conditions, however, knowledge of the depletion of the laser-coupled levels can be used to correct the model. A combustion facility for operation up to 20 atm was developed to allow LSF measurements of OH in high pressure flames. Using this facility, partial saturation in laminar high pressure (less than or equal to 12.3 atm) C2H6/O2/N2 flames was achieved. To evaluate the limits of the balanced cross-rate model, absorption and calibrated LSF measurements at 3.1 and 6.1 atm were compared. The fluorescence voltages were calibrated with absorption measurements in an atmospheric flame and corrected for their finite sensitivity to quenching with: (1) estimated quenching rate coefficients, and (2) an in situ measurement from a technique employing two fluorescence detection geometries.

Author

N90-22023* National Aeronautics and Space Administration. John F. Kennedy Space Center, Cocoa Beach, FL.

INDUCTION-TYPE METAL DETECTOR WITH INCREASED SCANNING AREA CAPABILITY Patent

Edward S. Lesky, inventor (to NASA), Alan J. Reid, inventor (to NASA), Wilton E. Bushong, inventor (to NASA), and Duane P. Dickey, inventor (to NASA) 27 Mar. 1990 11 p Filed 28 Oct. 1988
(NASA-Case-KSC-11386-1; US-Patent-4,912,414; US-Patent-Appl-SN-264107; US-Patent-Class-324-329) Avail: US Patent and Trademark Office CSCL 14B

A metal detector includes a detector head having a primary or transmit coil for the transmission of electromagnetic radiation and having a plurality of secondary or receiving coils associated for having voltages induced by transmissions from the primary coil. The presence of metallic objects within the detector head affects the voltage level induced in the secondary coils, a condition which may be detected as indicative of such presence of metallic objects. Each detector head preferably includes a primary coil about the periphery, with a plurality of secondary coils, all in the same plane with the primary coil, situated axially in from the periphery of the detector head in a mutually non-overlapping configuration, preferably about the center of such detector head. A plurality of such detector heads may be supported in coplanar alignment by a common non-metallic support structure for scanning relatively larger areas at a time. The primary coil of each respective detector head may be sequentially pulsed and selectively spaced to avoid interference with adjacent detector heads, thereby avoiding certain inherent disadvantages in applying conventional single detector head frequency-dependent tuned coil technology to multiple head use in an integral metal detector system.

Official Gazette of the U.S. Patent and Trademark Office

N90-22024* National Aeronautics and Space Administration. Lewis Research Center, Cleveland, OH.

ZERO-G PHASE DETECTOR AND SEPARATOR Patent

Steven J. Schneider, inventor (to NASA) 27 Mar. 1990 7 p Filed 21 Mar. 1989
(NASA-Case-LEW-14844-1; US-Patent-4,911,738; US-Patent-Appl-SN-326766; US-Patent-Class-55-160; US-Patent-Class-55-203; US-Patent-Class-55-204; US-Patent-Class-210-512.1; US-Patent-Class-210-97) Avail: US Patent and Trademark Office CSCL 14B

The gaseous phase is detected and then separated from a liquid phase in a fluid. This is accomplished by centrifuging the liquid phase while the gaseous phase migrates to the axis. When the expected phase is detected at a predetermined port, a signal is generated to open the liquid or gas valve at the respective outlet ports and to modulate these valves in such a manner as to withdraw fluid at the same volume rate at which it is admitted.

Official Gazette of the U.S. Patent and Trademark Office

N90-22025* National Aeronautics and Space Administration. Langley Research Center, Hampton, VA.
DEVICE FOR QUICKLY SENSING THE AMOUNT OF O2 IN A COMBUSTION PRODUCT GAS Patent
Jag J. Singh, inventor (to NASA), William T. Davis, inventor (to NASA), and Richard L. Puster, inventor (to NASA) 27 Mar. 1990 7 p Filed 9 Mar. 1988
(NASA-Case-LAR-13816-1; US-Patent-4,911,890; US-Patent-Appl-SN-165945; US-Patent-Class-422-62; US-Patent-Class-422-98; US-Patent-Class-422-111; US-Patent-Class-422-126; US-Patent-Class-436-55; US-Patent-Class-436-137; US-Patent-Class-436-143) Avail: US Patent and Trademark Office CSCL 14B

A sensing device comprising an O2 sensor, a pump, a compressor, and a heater is provided to quickly sense the amount of O2 in a combustion product gas. A sample of the combustion product gas is compressed to a pressure slightly above one atmosphere by the compressor. Next, the heater heats the sample between 800 C and 900 C. Next, the pump causes the sample to be flushed against the electrode located in O2 sensor 6000 to 10,000 times per second. Reference air at approximately one atmosphere is provided to the electrode of O2 sensor. Accordingly, the O2 sensor produces a voltage which is proportional to the amount of oxygen in the combustion product gas. This voltage may be used to control the amount of O2 entering into the combustion chamber which produces the combustion product gas. Official Gazette of the U.S. Patent and Trademark Office

N90-22026# Allied-Signal Corp., Kansas City, MO. Dept. of Analytical Sciences.
SMALL STRAIN GAGE APPLICATIONS 2
Edward G. Wenski Mar. 1990 15 p Presented at the Society for Experimental Mechanics Conference, Albuquerque, NM, 4-6 Jun. 1990
(Contract DE-AC04-76DP-00613)
(DE90-008312; KCP-613-4302; CONF-9006124-1) Avail: NTIS HC A03/MF A01

This paper describes a number of small strain gage applications conducted recently at Allied-Signal Inc., Kansas City Division. These stress analyses used some of the smallest strain gages commercially available on the market today. Although data reduction techniques remain the same for these small-scale analyses, gaging techniques differ from application to application. This paper discusses three different strain gage applications using 0.015 grid area strain gages. DOE

N90-22027# National Physical Lab., Teddington (England). Div. of Materials Metrology.
LONG TERM INTENSITY STABILITY OF AUGER ELECTRON SPECTROMETERS: INSTRUCTIONS FOR THE INTERLABORATORY COMPARISON
M. P. Seah and G. C. Smith Dec. 1989 6 p
(NPL-DMM(A)-1; ISSN-0143-7313; ETN-90-96434) Copyright Avail: NTIS HC A02/MF A01

The previous interlaboratory comparison of the intensity-energy transmission function of Auger electron spectrometers showed that the response of cylindrical mirror analyzer systems was dominated by the Channel Electron Multiplier (CEM) or first dynode detector efficiency. A study is presented which repeats the calibration work for appropriate respondees, in the direct mode only, to define the extent to which this calibration has altered over the intervening 18 months as the CEM ages. ESA

N90-21801*# Case Western Reserve Univ., Cleveland, OH.
ANALYSIS OF A HIGH HARMONIC RECTANGULAR GYROTRON USING RIBBON BEAMS
Altan M. Ferendeci *In* NASA, Lewis Research Center, Free-Space Power Transmission Nov. 1989 p 97-114 (For primary document see N90-21795 15-20)
Avail: NTIS HC A09/MF A02 CSCL 14B

N90-22082*# Centre National d'Etudes Spatiales, Toulouse (France).
SPOT 4 SPACE MAGNETIC RECORDER MECHANISMS
A. Borrien, E. Vialatoux, J. L. Lhermet, and A. Didier (Schlumberger Industries, Velizy, France) *In* NASA, John F. Kennedy Space Center, The 24th Aerospace Mechanisms Symposium Apr. 1990 p 25-39 (For primary document see N90-22079 15-39)
Avail: NTIS HC A16/MF A03 CSCL 14B

N90-22083*# Lockheed Aircraft Corp., Palo Alto, CA. Research Lab.
DEVELOPMENT OF THE CLAES INSTRUMENT APERTURE DOOR SYSTEM
D. M. Stubbs *In* NASA, John F. Kennedy Space Center, The 24th Aerospace Mechanisms Symposium Apr. 1990 p 41-56 (For primary document see N90-22079 15-39)
Avail: NTIS HC A16/MF A03 CSCL 14B

N90-22098*# TRW Space Technology Labs., Redondo Beach, CA.
ACTIVE CONTROL OF BEARING PRELOAD USING PIEZOELECTRIC TRANSLATORS
Ted W. Nye *In* NASA, John F. Kennedy Space Center, The 24th Aerospace Mechanisms Symposium Apr. 1990 p 259-271 (For primary document see N90-22079 15-39)
Avail: NTIS HC A16/MF A03 CSCL 14B

N90-22104*# Thiokol Corp., Cape Canaveral AFS, FL. Space Services Div.
CIRCULARITY MEASURING SYSTEM: A SHAPE GAUGE DESIGNED ESPECIALLY FOR USE ON LARGE OBJECTS
G. R. RohrKaste *In* NASA, John F. Kennedy Space Center, The 24th Aerospace Mechanisms Symposium Apr. 1990 p 341-351 (For primary document see N90-22079 15-39)
Avail: NTIS HC A16/MF A03 CSCL 14B

36 LASERS AND MASERS

Includes parametric amplifiers.
For related information see also *76 Solid-State Physics.*

N90-22028 Alabama Univ., Huntsville.
HIGH POWER CO2 LASER INSTABILITY AND ITS CORRECTIONS Ph.D. Thesis
Kenneth L. Webster 1989 112 p
Avail: Univ. Microfilms Order No. DA8925809

A high power CO2 laser beam is known to deteriorate after a few micro-seconds due to a mode-medium interaction (MMI) which results from an intensity dependent heating rate related to the vibrational-to-translational decay of the upper and lower CO2 lasing levels. An iterative numerical technique is developed to model the time evolution of the beam as it is affected by the MMI. The technique is used to study the MMI in an unstable CO2 resonator with a hard-edge output mirror for different parameters like the Fresnel number and the density of CO2. The major contribution is the use of a Gaussian-reflectivity and a phase-conjugate mirror to correct the MMI. These mirrors are shown to produce a smoother intensity profile which significantly reduces the negative effects of the MMI. Quantitative results on peak density variation, beam quality, and total output power are presented. Dissert. Abstr.

N90-22029 Cornell Univ., Ithaca, NY.
DEVELOPMENT AND APPLICATIONS OF A COUPLED CAVITY SODIUM-CHLORIDE LASER Ph.D. Thesis
Christopher Paul Yakymyshyn 1989 194 p
Avail: Univ. Microfilms Order No. DA8924550

Coupled cavity modelocking is a technique for generating ultrashort optical pulses. By adding to a conventional modelocked laser cavity a second resonant coupled cavity containing a short piece of optical fiber, laser pulses less than 100 fsec long can be generated while maintaining excellent temporal and spectral pulse quality. The external fiber creates a phase chirped pulse (through self-phase modulation) that, when interferometrically recombined with an unchirped intracavity laser pulse at the output coupler, results in a shortened pulse being reflected back into the laser cavity. The external cavity and output coupler taken together form a nonlinear termination with an intensity-dependent reflectivity. Also known as Additive Pulse Modelocking (APM), the technique is wavelength insensitive, and therefore allows continuous tuning of the laser over a large fraction of the grain bandwidth. This thesis reviews the development of an APM laser based on the NaCl:OH(-) color center laser. Pulses as short as 75 fsec achieved with peak powers of over 20 kW. The laser is tunable from 1.48 to 1.69 microns. Applications of the laser are also discussed. Second harmonic generation resulted in sub-100 fsec pulses tunable from 755 nm to 820 nm with over 5 mW of average power. Soliton compression in a second optical fiber generated pulses as short as 26 fsec. Finally, application of the NaCl:OH(-) APM laser to pump-probe experiments in GaInAs is described. Preliminary results demonstrate the laser's ability to generate data suitable for extracting hot electron relaxation rates in GaInAs. Dissert. Abstr.

N90-22030*# Hampton Inst., VA. Dept. of Physics.
DIRECT SOLAR-PUMPED IODINE LASER AMPLIFIER Final Report, 1 Mar. 1984 - 28 Feb. 1990
Kwang S. Han and In Heon Hwang Mar. 1990 17 p
(Grant NAG1-441)
(NASA-CR-186442; NAS 1.26:186442) Avail: NTIS HC A03/MF A01 CSCL 20E

The optimum conditions of a solar pumped iodine laser are found in this research for the case of a continuous wave operation and a pulsed operation. The optimum product of the pressure(p) inside the laser tube and the tube diameter(d) was pd=40 approx. 50 torr-cm on the contrary to the case of a high intensity flashlamp pumped iodine laser where the optimum value of the product is known to be pd=150 torr-cm. The pressure-diameter product is less than 1/3 of that of the high power iodine laser. During the research period, various laser materials were also studied for solar pumping. Among the laser materials, Nd:YAG is found to have the lowest laser threshold pumping intensity of about 200 solar constant. The Rhodamine 6G was also tested as the solar pumped laser material. The threshold pumping power was measured to be about 20,000 solar constant. The amplification experiment for a continuously pumped iodine laser amplifier was performed using Vortek solar simulator and the amplification factors were measured for single pass amplification and triple pass amplification of the 15 cm long amplifier tube. The amplification of 5 was obtained for the triple pass amplification. Author

N90-22031*# Hampton Inst., VA. Dept. of Physics.
DEVELOPMENT OF MID-INFRARED SOLID STATE LASERS FOR SPACEBORNE LIDAR Final Report, 13 Apr. 1988 - 31 Jan. 1990
Donald A. Whitney Jan. 1990 51 p
(Grant NAG1-877)
(NASA-CR-185095; NAS 1.26:185095) Avail: NTIS HC A04/MF A01 CSCL 20E

Researchers investigated laser performance of Ho(3+):Tm(3+):Cr(3+):YAG crystals under both Cr:GSAG laser and flashlamp pumping. A flashlamp pumped Cr:GSAG laser was built to simulate high power quasi-CW laser diode pumping of a 2.1 micron holmium laser. The 2.1 micron output laser energy exceeded more than 14 mJ, the highest value reported to date under laser pumping near 785 nm. This was obtained in a pulse length of nearly 650 microns from a 3 x 3 mm Ho:Tm:Cr:YAG rod by using the flashlamp-pumped Cr:GSAG laser as a pumping source at the diode laser wavelength, 785 microns. In addition, Ho:Tm:Cr:YAG crystals with various Tm(3+) concentrations have been evaluated for flashlamp-pumped normal mode and Q-switched 2.1 micron laser operations under a wide variety of experimental conditions in order to understand internal dynamic processes among the ions and to determine an optimum lasing condition. An increase of the laser slope efficiency was observed with the increase of the Tm(3+) concentration from 2.5 atomic percent to 4.5 atomic percent. The thermal dependence of the laser performance was also investigated. Q-switched laser output energies corresponding to nearly 100 percent of the normal-mode laser energies were obtained in a strong single spike of 200 ns pulse length by optimizing the opening time of a lithium niobate Q-switch. Author

N90-22032# Sandia National Labs., Albuquerque, NM. Fluid and Thermal Sciences Dept.
HEAT-TRANSFER REGIMES IN NUCLEAR-REACTOR-PUMPED GAS LASERS
J. R. Torczynski 1990 27 p Presented at the 5th AIPA/ASME Thermophysics and Heat Transfer Conference, Seattle, WA, 18-20 Jun. 1990
(Contract DE-AC04-76DP-00789)
(DE90-002904; SAND-89-2425C; CONF-900619-1) Avail: NTIS HC A03/MF A01

The flow induced in nuclear-reactor-pumped gas lasers by the competing effects of spatially nonuniform fission-fragment heating (pumping) and heat transfer to the walls is examined. The equations of motion are acoustically filtered (low Mach number approximation), and the resulting equations are seen to have three timescales: the duration of the heating, the time required by the heating to produce a pressure rise comparable to the initial pressure, and the time for the thermal boundary layer to grow into the center of the laser cell. Three distinct regimes emerge from consideration of the relative magnitudes of these timescales. In the negligible-conduction regime, thermal-conduction effects are small, and the motion is determined by the spatial nonuniformity of the heating. In the dominant-conduction regime, thermal-conduction effects govern the motion. In the mixed regime, the effects of thermal conduction and heating nonuniformity are comparable, but since they are oppositely directed, a complex gas motion results. Analytical solutions to the equations of motion are presented for the negligible-conduction and dominant-conduction regimes, and examples are given for all three regimes. Plots of the second spatial derivative of the density field (a quantity often used in optical analyses) are given for the negligible-conduction and the dominant-conduction regimes as functions of the appropriate similarity parameters. DOE

N90-22033# Kansas State Univ., Manhattan. Dept. of Chemistry.
REACTIONS OF N2A3 SIGMA u + AND CANDIDATES FOR SHORT WAVELENGTHS LASERS Final Report, 1 Jun. 1986 - 30 Sep. 1989
D. W. Setser 1990 159 p Prepared for Lawrence Livermore National Lab., CA
(Contract W-7405-eng-48)
(DE90-009514; UCRL-CR-103371) Avail: NTIS HC A08/MF A01

The technique for generating SO(X) and the quenching rate constants for SO(A) were reported in Chem. Phys. Lett. 149, 384 (1988). The new spectroscopic data, the spin-orbit state relaxation rates and some additional electronic quenching data is reported. A summary is provided for the relaxation and quenching rate constants of SO(A). From the scientific point of view, the results are quite interesting since reliable data for (sup 3)II(sub 0,1,2) electronic states are scarce. Unfortunately, from the energy storage point of view, the quenching rates of SO(A) by He and Ar are too large for SO(A) to be a good energy storage candidate. DOE

N90-22034# Lawrence Livermore National Lab., CA.
INJECTION-SEEDED Nd:YAG LASER LINEWIDTH MEASUREMENT USING SATURATION SPECTROSCOPY IN IODINE
Gregory W. Faris and Mark J. Dyer (SRI International Corp., Menlo Park, CA.) 7 Dec. 1989 6 p
(Contract W-7405-eng-48)
(DE90-009537; UCRL-CR-103293) Avail: NTIS HC A02/MF A01

The application is described of two laser saturation spectroscopy in iodine for the measurement of the time-averaged linewidth of an injection-seeded Nd:YAG laser. Linewidths as narrow as 23 MHz were measured. DOE

N90-22035# Idaho National Engineering Lab., Idaho Falls.
BEAM PROPAGATION IN DIRECT NUCLEAR PUMPED LASER AMPLIFIERS
W. A. Neuman, J. R. Fincke, G. D. Lassahn, and L. M. Montierth 1989 11 p Presented at the International Conference on Lasers, New Orleans, LA, 3-8 Dec. 1989
(Contract DE-AC07-76ID-01570)
(DE90-009613; EGG-M-89350; CONF-891261-9) Avail: NTIS HC A03/MF A01

Thermal distortions in transverse flow, direct nuclear pumped laser amplifiers and the resulting effect on beam propagation is investigated. Nuclear pumping occurs from surfaces, either from plates parallel to the flow direction, from screens or porous material perpendicular to the flow direction, or from the combination of the two. The analysis presented is topically divided into the analysis of the energy deposition of the energetic charged particles in the amplifying media and the analysis of the beam propagation in the amplifier and to the far field. The spatially varying energy deposition produces large index of refraction variations in the nuclear pumped amplifier. These variations are modeled by a Zernike polynomial expansion and their effect on the propagation of a uniform intensity plane wave is discussed. For purposes of illustration, an amplifier with a 1 m gain length and a 1 atm (101 kPa) argon gas flowing at 100 m/s is presented. With approximately 150 W/cu cm average charged particle pumping in the amplifier the beam qualities range from 7 to 27 times diffraction limited when the primary (tilt and focus) aberrations in the amplifier are corrected. DOE

N90-22036 California Inst. of Tech., Pasadena.
LINEAR, NONLINEAR, AND TUNABLE GUIDED WAVE MODES FOR HIGH-POWER (GaAl)As SEMICONDUCTOR LASERS Ph.D. Thesis
David Glenn Mehuys 1990 221 p
Avail: Univ. Microfilms Order No. DA9009387

High power, coherent radiation from semiconductor lasers is attractive for such diverse applications as free space communication, optical data storage, and microsurgery. However, several factors conspire to prevent near ideal performance from broad area devices and laser arrays. Waveguides wider than a few microns support many lateral modes with poor gain discrimination. Consequently, such modes are easily mixed by perturbations in gain and refractive index caused by gain saturation, thermal gradients, and inhomogeneities due to imperfect crystal growth. This causes spatially localized modes, multimode operation, and reduced spatial coherence, all of which lead to farfield patterns broader than the diffraction limit. The influence of gain saturation on the lateral modes of broad area structures and laser arrays was investigated. Analytical and numerical techniques were developed to solve self consistently for mode shapes and propagation constants as a function of injected current density above threshold. In gain guided, quantum well lasers, the nonlinear broad area modes are observed to oscillate into narrow, single-lobed farfields which broaden only slightly with increased power output up to the 500 mW level. In contrast, the lateral modes of laser arrays were found to be unstable with increased current injection. Waveguides which are phase matched below threshold become detuned under the influence of gain saturation, so that interguide power transfer is reduced. This diminishes the injection locking bandwidth, and ultimately, the spatial coherence. Dissert. Abstr.

N90-21905*# Jet Propulsion Lab., California Inst. of Tech., Pasadena.
AN 8.4-GHz DUAL-MASER FRONT-END SYSTEM FOR PARKES REIMPLEMENTATION
D. L. Trowbridge, J. R. Loreman, T. J. Brunzie, and R. Quinn *In its* The Telecommunications and Data Acquisition Report 15 Feb. 1990 p 301-319 (For primary document see N90-21880 15-32)
Avail: NTIS HC A15/MF A02 CSCL 20E

N90-21924# Yale Univ., New Haven, CT. Dept. of Applied Physics.
HIGH INTENSITY LASER BEAM INTERACTIONS WITH SINGLE DROPLETS
Richard K. Chang and Alfred S. Kwok *In* AGARD, Atmospheric Propagation in the UV, Visible, IR, and MM-Wave Region and Related Systems Aspects Mar. 1990 12 p (For primary document see N90-21907 15-32)
(Contract DAAL03-88-K-0040; AF-AFOSR-0100-88)
Copyright Avail: NTIS HC A16/MF A03; Non-NATO Nationals requests available only from AGARD/Scientific Publications Executive

37 MECHANICAL ENGINEERING

Includes auxiliary systems (nonpower); machine elements and processes; and mechanical equipment.

N90-22037 Colorado Univ., Boulder.
NONLINEAR STABILITY ANALYSIS AND CONTROL OF DYNAMICAL ROBOTIC SYSTEMS Ph.D. Thesis
Jamil Mosallam Bakhashwain 1989 197 p
Avail: Univ. Microfilms Order No. DA8923479

The manipulator control problem is the problem of finding appropriate torques or forces that will drive the actuators in order for the manipulator to follow the specified trajectory. Adaptive model-following control based on the Popov hyperstability approach is first used for the control of a robotic manipulator. A continuous controller is considered and used to achieve the desired performance provided by the reference model. As a result of this approach, the controller avoids the problems reported in the literature where a discontinuous controller is used which employs the unit vector adaptation algorithm and chatters at a theoretically infinite frequency. The discontinuous controller also requires the linearization of the nonlinear system dynamics with respect to a typical configuration, i.e., an operating point. The Lyapunov direct method is then used. A method is developed that generates a Lyapunov function for nonlinear systems that are described by m first order vector Energy Metric Algorithm. The Lyapunov function generated by this method has a functional relationship with the original nonlinear system and therefore is expected to produce the largest region of attraction. The stability of the robot system is investigated in light of this new algorithm, where different non-adaptive control laws are developed and considered for stabilization, regulation, and tracking of a robotic manipulator. An important feature of the method is that it provides means for comparing the convergence rate for different control laws and for improving the transient response. Dissert. Abstr.

N90-22038 California Univ., Davis.
PRACTICAL NONLINEAR SIMULATION OF ROTATING MACHINERY DYNAMICS WITH APPLICATION TO TURBINE BLADE RUBBING Ph.D. Thesis
Rory Ronald Davis 1989 483 p
Avail: Univ. Microfilms Order No. DA9002729

The design of rotating machinery elements is often performed without consideration of the effect of unsteady dynamic loading that may have a significant bearing on component life and durability. Unsteady loads are experienced in events of start and stop transients, rotative speed traverses, turbine blade or shaft rubbing, and unsteady fluid/structure interaction. Although there are some tools available to help address these types of events analytically, they are difficult to apply to realistic systems. Practical methods of performing unsteady nonlinear analysis of rotating machinery systems are investigated, with emphasis on generality of structural and nonlinear effects modeling, accuracy of models for unsteady 3-D motion, and utilization of and implementation with already available finite element and transient simulation tools. Structural modeling generality is achieved by using matrix and modal models from finite element programs for rotating shafts, flexible or rigid disks, housings, and any other structures of interest in a system. For the nonlinear phenomenon of rubbing, a general rub state algorithm including 3-D rigid body and flexural motion of both rubbing parts is developed. For flexible disks, the use of substructure, normal modes, cylindrical coordinate, and cyclic sector models are all addressed in detail. The effect of shaft torque is investigated and reformulated for practical incorporation in simulations. Computer subroutines to implement the formulations developed are presented and demonstrated on a set of realistic sample models with rigid and flexible disks for unsteady events of start transients, sudden imbalance shaft whirl, and rigid disk and flexible blade tip rubs. Dissert. Abstr.

N90-22039 California Inst. of Tech., Pasadena.
EXPERIMENTAL INVESTIGATION OF THE EFFECT OF CAVITATION ON THE ROTORDYNAMIC FORCES ON A WHIRLING CENTRIFUGAL PUMP IMPELLER Ph.D. Thesis
Ronald John Franz 1989 178 p
Avail: Univ. Microfilms Order No. DA9000563

The interaction of a rotating impeller and the working fluid introduce forces on the rotor. These fluid-induced forces can cause self-excited whirl, where the rotor moves away from and whirls along a trajectory eccentric to its undeflected position. When designing a turbomachine, particularly one which is to operate at high speed, it is important to be able to predict the fluid-induced forces, both steady and unsteady, acting on the various components of the machine. The fluid-induced rotordynamic forces acting upon the impeller and therefore on the bearings was investigated for a centrifugal impeller in a spiral volute in the presence of cavitation. An experiment in forced vibration was made to study the fluid-induced rotordynamic force on an impeller whirling around its machine axis of rotation in water. The whirl trajectory of the rotor is prescribed to be a circular orbit of a fixed radius. A dynamometer mounted behind the rotor and rotating with it measures the force on the impeller. The force measured is a combination of a steady radial force due to volute asymmetries and an unsteady force due to the eccentric motion of the rotor. These measurements were carried out over a full range of whirl/impeller speed ratios at different flow coefficients for various turbomachines. A destabilizing force was observed over a region of positive whirl ratio. Cavitation corresponding to a three percent head loss did not have a significant effect upon this destabilizing force. However, a lesser degree of cavitation at the design point for the impeller-volute combination tested increased this destabilizing force for a particular set of whirl ratios.
Dissert. Abstr.

N90-22040 Ohio State Univ., Columbus.
FINITE ELEMENT ANALYSIS OF ELASTIC CONTACT PROBLEMS WITH FRICTION Ph.D. Thesis
Jong-Tae Jinn 1989 291 p
Avail: Univ. Microfilms Order No. DA9001969

The objectives are to develop a variational principle incorporating the path-dependence of friction and an effective computational model for two-dimensional elastostatic contact problems involving friction. The accuracy of solution for these frictional contact problems and the convergence of the associated iteration scheme are investigated in detail. A general mathematical structure of contact problems with Coulomb's friction law is initially studied within the framework of nonlinear continuum mechanics field theory. A semi-implicit scheme is proposed for the effective numerical integration of contact problems. A variation principle is proposed for incremental contact problems with friction on the basis of mini-max principles in mechanics. Both displacement and contact traction vectors are taken as independent state variables. As an integral part of the developed numerical scheme, the method of embedding the contact conditions into discretized governing contact equations is presented. The associated nonlinear subjective mapping is called the embedding map. With the help of the imbedding map, the formulated problem can be represented in the form of a fixed point problem for the nodal contact force vector. The existence of the solutions are studied using the Banach fixed point theorem. An iterative scheme based on the block Gauss-Seidel method is proposed for solving the aforementioned nonlinear fixed point problem. The convergence criteria for the proposed iterative scheme are also studied. Finally, the validity and applicability of the developed solution method are demonstrated by means of several diverse applications. Various factors influencing the accuracy of the solution are identified and numerically investigated. Dissert. Abstr.

N90-22041*# National Aeronautics and Space Administration. Lewis Research Center, Cleveland, OH.
BEARING ELASTOHYDRODYNAMIC LUBRICATION: A COMPLEX CALCULATION MADE SIMPLE
Erwin V. Zaretsky Apr. 1990 11 p
(NASA-TM-102575; E-5360; NAS 1.15:102575) Avail: NTIS HC A03/MF A01 CSCL 11H

The lubricant elastohydrodynamic (EHD) film thickness formula is reduced to a simplified form whereby only the rolling-element bearing inside and outside diameters and speed (in revolutions per minute) and the lubricant type and viscosity (in centipoise) at temperature are required for its use. Additionally, a graph is provided for the first time that is based upon experimental data giving an EHD film reduction factor as a function of contact lubricant flow number. This reduction factor accounts for lubricant starvation within the Hertzian contact. A graph relating the ratio of minimum film thickness to composite surface roughness and a lubrication-life correction factor is also provided. The life correction factor is used to determine resultant bearing life. Author

N90-22042* National Aeronautics and Space Administration. Langley Research Center, Hampton, VA.
LIGHTWEIGHT PISTON ARCHITECTURE Patent
Allan H. Taylor, inventor (to NASA) and Philip O. Ransone, inventor (to NASA) 20 Mar. 1990 5 p Filed 28 Sep. 1988
(NASA-Case-LAR-13926-1; US-Patent-4,909,133; US-Patent-Appl-SN-250469; US-Patent-Class-92-212; US-Patent-Class-92-213; US-Patent-Class-92-222; US-Patent-Class-92-248; US-Patent-Class-123-193P; US-Patent-Class-29-888.046) Avail: US Patent and Trademark Office CSCL 13I

The invention is an improvement in a lightweight carbon-carbon composite piston, the improvement uses near-net shape knitted or warp-interlock preforms to improve the structural qualities of the piston. In its preferred embodiment, a one piece, tubular, closed-ended, knitted preform (a sock) of carbon fibers embedded within the matrix of the piston structure forms the crown, side wall, skirt and inner surface of the piston, and wrap-interlock preforms strengthen the piston crown and wrist pin bosses.
Official Gazette of the U.S. Patent and Trademark Office

N90-22043*# National Aeronautics and Space Administration. Marshall Space Flight Center, Huntsville, AL.
DEFINITION OF LARGE COMPONENTS ASSEMBLED ON-ORBIT AND ROBOT COMPATIBLE MECHANICAL JOINTS
J. Williamsen, F. Thomas, J. Finckenor, and B. Spiegel Apr. 1990 43 p
(NASA-TM-100395; NAS 1.15:100395) Avail: NTIS HC A03/MF A01 CSCL 13I

One of four major areas of project Pathfinder is in-space assembly and construction. The task of in-space assembly and construction is to develop the requirements and the technology needed to build elements in space. A 120-ft diameter tetrahedral aerobrake truss is identified as the focus element. A heavily loaded mechanical joint is designed to robotically assemble the defined aerobrake element. Also, typical large components such as habitation modules, storage tanks, etc., are defined, and attachment concepts of these components to the tetrahedral truss are developed. Author

N90-22044# Los Alamos National Lab., NM.
EVALUATING THERMOGRAPHIC PHOSPHORS IN AN OPERATING TURBINE ENGINE
B. W. Noel, H. M. Borella, W. Lewis, W. D. Turley, D. L. Beshears, G. J. Capps, M. R. Cates, J. D. Muhs, and K. W. Tobin 1989 13 p Presented at the 35th International Gas Turbine and Aeroengine Congress and Exposition (TURBO Expo), Brussels,

Belgium, 11-14 Jun. 1990
(Contract W-7405-eng-36)
(DE90-004874; LA-UR-89-4275; CONF-900615-2) Avail: NTIS HC A03/MF A01

The results of a field test in a commercial turbine engine showed that we can remotely measure the temperature of engine components in operating engines using thermographic phosphors. The remote measurement method exploits the temperature dependence of the characteristic decay time of the laser-induced fluorescence of thermographic phosphors. This paper summarizes recent work leading up to and including a successful test of the thermographic-phosphor method in an operating turbine engine. DOE

N90-22045# Oak Ridge National Lab., TN. Center for Engineering Systems Advanced Research.

AN ALTERNATIVE METHOD TO SOLVING THE KINEMATICS OF A REDUNDANT ROBOT

Philippe Belmans and Jean-Christophe Culioli 1990 6 p Presented at the American Nuclear Society Annual Meeting, Nashville, TN, 10-14 Jun. 1990
(Contract DE-AC05-84OR-21400)
(DE90-006892; CONF-900608-10) Avail: NTIS HC A02/MF A01

The state occupied by an m degrees of freedom robot is determined by an articular joint position-vector q of R(sup m), but usually the specification of a task by its task-vector X takes place in the operational space R(sup n). Controlling the kinematics of a robot requires to find q as a function of X. In most of the cases, it is impossible to obtain this relationship analytically and globally. The problem is solved by linearization of the geometric model of the robot X = F(q) in the neighborhood of the point q, introducing the (n x m) Jacobian matrix: Delta X = J(q) Delta q; Delta q epsilon R(sup m); Delta X epsilon R(sup n); where Delta X is the variation of task-vector, Delta q is the corresponding small variation of the articular position. DOE

N90-22046# Sandia National Labs., Albuquerque, NM. Experimental Mechanics Dept.

DATA AND CONCLUSIONS FROM TESTS ON SMALL SCREWS

J. L. Cawlfield, T. L. Ernest, and R. T. Reese 1990 8 p Presented at the International Conference on Micromechanics of Failure of Quasi-Brittle Materials, Albuquerque, NM, 7-8 Jun. 1990
(Contract DE-AC04-76DP-00789)
(DE90-007500; SAND-90-0534C; CONF-9006122-3) Avail: NTIS HC A02/MF A01

The integrity of many mechanical assemblies and electrical components depends on small threaded fasteners. The design standards for small (less than (1/4) inch in diameter) screws made of stainless steel are not as well developed as those for larger sizes of high strength steels. The typical design approach is based on the application of static design principals. Steady state accelerations are applied to the component or assembly and sufficient screws are installed in mounting hardware for attachment to the next assembly. These design principals have been used successfully for years in a wide variety of applications. As the parts requiring small screws have continued to decrease in size, some design requirements include greater thread depths and adherence to strict interpretation of the governing thread standards. These design requirements have their origins in the lack of adequate definitions and standards for designs using small threaded fasteners. These design practices have led to significant problems in manufacturing parts with small threaded fasteners by requiring thread dgpths to four and more diameters of engagement while maintaining thread heights (radial engagement) of 75 percent throughout the thread interfaces. A test program was developed to address questions regarding design and manufacturing issues involving small threaded fasteners. DOE

N90-22047# Oak Ridge National Lab., TN. Center for Engineering Systems Advanced Research.

TRAJECTORY GENERATION FOR CAR-LIKE ROBOTS

Hubert A. Vasseur and Francois G. Pin 1990 13 p Presented at the American Nuclear Society Annual Meeting, Nashville, TN, 10-14 Jun. 1990
(Contracts DE-AC05-84OR-21400; DAAG08-83-C-0011)
(DE90-008407; CONF-900608-11) Avail: NTIS HC A03/MF A01

Autonomous robots or remotely operated vehicles have raised high hopes in the military and industrial communities because of the potential safety improvement and gain of productivity they may provide. Waste management on nuclear sites, pallet manipulation in factories, interventions on battle fields, etc., are actively studied. A lot of these applications require powerful four wheel vehicles, the kinematics of which is similar to that of a car. Such vehicles have three degrees of freedom: the (x,y) positions in a plane and the orientation of the vehicle. Path planning is often understood as only changing the position of the vehicle, whereas the tasks performed by this kind of robot requires a perfect orientation of the vehicle: forklifting a pallet or docking at a loading or unloading station requires accuracy in the orientation of the vehicle. It is this requirement and the kinematic constraints of the motion mode which have led to the path-planning algorithm presented. The velocity of the robot belongs to a 2-D vectorial space. However, it is assumed that there is no slipping of the wheels. Therefore, at a given position, the direction of the velocity of the rear axle, is colinear with that of the vehicle. The equation conveying this constraint is not integrable and affects the velocity but not the space of the configurations of the robot: it is a non-holonomic constraint. If the steering angle of the front wheels is constant, the vehicle moves along a circle. Since the steering angle of the car-like robots is limited, the radius of the circle is always greater than a certain value which is the minimum radius of curvature of any achievable trajectory. DOE

N90-22048# Oak Ridge National Lab., TN.

ROBOTS FOR AIRCRAFT COATINGS REMOVAL: PARAMETERS AND REQUIREMENTS

Uri Gat 1990 3 p Presented at the DOD Conference on Industry Advanced Coatings Removal, Atlanta, GA, 1-3 May 1990
(Contract DE-AC05-84OR-21400)
(DE90-009429; CONF-9005155-1) Avail: NTIS HC A01/MF A01

The chemical stripping of coatings of aircraft is being phased out, primarily for environmental reasons. The search is on for methods that are more economical, more efficient, non-damaging and environmentally acceptable. Two of several prime candidates for the new methods are laser stripping and media stripping. Amongst the media stripping methods several are being considered, some of which are plastic media, bicarbonates, and frozen carbon dioxide. To achieve better quality, uniformity, efficiency, and economy and to reduce to a minimum any possible environmental hazards, it is desirable to utilize robots and automatic methods for the aircraft stripping. It is desirable that the robots be flexible and versatile to the extent possible. The flexibility and versatility refers to the ability to recognize and adjust to: variations within an aircraft type; different types of aircraft, including segments of aircraft; accommodation of different stripping methods, primarily laser stripping and plastic media blasting (PMB). However it is realized that flexability or versatility may not be available. Furthermore no practical robots or even partial levels of automation may be readily available for implementation. This paper summarizes desired features and characteristics for robots for coatings removals from aircraft. DOE

N90-22049*# Thiokol Corp., Brigham City, UT. Joints and Seals Design.

FLIGHT SET 360T004 (STS-30) Final Report

Lowell V. Nelsen Mar. 1990 141 p
(Contract NAS8-30490)
(NASA-CR-183927; NAS 1.26:183927; TWR-17543-Vol-4) Avail: NTIS HC A07/MF A01 CSCL 13I

The performance of 360T004, Forth Flight, Redesigned Solid Rocket Motors (RSRM) is assessed in respect to joint sealing issues as seen from post-test inspection of the seals and sealing surfaces. The factory joint disassembly inspections for this flight set were omitted. The decision was based on the rational that there is sufficient information in the present data base, and this would give H-7 refurbishment operations faster turn around time for this set of hardware. The factory joint disassembly inspections will resume for 360H005, Fifth Flight, through 360L007, Seventh Flight, due to a new grease application being in effect during the assembly process. The left hand nozzle was forced into the snubbed position upon splash down. This required unique tooling to be manufactured to perform the disassembly of the internal nozzle joints. This was completed on February 5 and 6, 1990 at the H-5 Clearfield, Utah facility. The RSRM consisting of capture feature, field joints with the J-joint insulation configuration is illustrated. The nozzle-to-case joint design, which includes 100, 7/8-inch radial bolts in conjunction with a wiper O-ring and modified insulation design is also illustrated, as is the ignition system seals and a cross section of the igniter. The configuration of all internal nozzle joints is shown. Author

N90-22050# Technische Univ., Delft (Netherlands). Faculty of Aerospace Engineering.

REVIEW OF ANALYSIS METHODS FOR MECHANICALLY FASTENED JOINTS IN COMPOSITES

W. J. Slagter Jul. 1989 39 p

(LR-599; ETN-90-96354) Avail: NTIS HC A03/MF A01

A literature review of analysis methods for mechanically fastened joints in composites is presented. Typical analytical procedures such as that for load distribution in the joint are described. Detailed stress analysis in the vicinity of fastener holes and static strength prediction are discussed. The advantages and shortcomings of these different procedures and various other state of the art design codes are outlined. Experimental data on failure modes and failure criteria is reviewed. ESA

N90-22051# Technische Univ., Delft (Netherlands). Faculty of Technical Mathematics and Informatics.

ELASTIC AND VISCOELASTIC ANALYSIS OF TWO MULTIPLY LAYERED CYLINDERS ROLLING OVER EACH OTHER WITH COULOMB FRICTION

J. J. Kalker 1989 48 p

(Rept-89-50; ISSN-0922-5461; ETN-90-96366) Copyright Avail: NTIS HC A03/MF A01

A linear analysis of the friction between two coated cylinders is presented. An influence function is used in the analysis. These functions are the displacement-stress field in the half space due to a normal and a shearing standard loading. They move over the viscoelastic half-space with rolling velocity. A complex Fourier transform is used to determine these values. The two influence functions are each convoluted by a weight function. The weight functions are found with the aid of algorithms used by Kalker. Loadings due to partial slip in the contact is determined. The displacement-stress field both on and inside the half-space is computed. ESA

N90-22052# Oxford Univ. (England). Dept. of Engineering Science.

CALCULATING THE TIME DOMAIN AVERAGE OF GEAR VIBRATION DATA SAMPLED AT LESS THAN THE NYQUIST FREQUENCY

P. D. McFadden 1989 23 p

(OUEL-1768/89; ETN-90-96406) Avail: NTIS HC A03/MF A01

The calculation of the time domain average of the tooth meshing vibration of an individual gear in a complex gearbox from vibration data sampled at less than the Nyquist frequency is examined. It is shown that by sampling at a fraction of the usual sampling rate, the periodic vibration signals produced by the gear of interest may be passed without attenuation, but that some unwanted periodic signals, such as might be produced by other gears in the same gearbox, may be aliased to frequencies which will be passed with only limited attenuation. These findings are demonstrated by numerical examples. ESA

N90-22053# Oxford Univ. (England). Robotics Research Group.

PERTURBATION TECHNIQUES IN THE DYNAMICS AND CONTROL OF FLEXIBLE MANIPULATORS Ph.D. Thesis

Anthony Robin Fraser and R. W. Daniel 1989 253 p

(OUEL-1772/89; ETN-90-96407) Avail: NTIS HC A12/MF A02

Efficient dynamic models are developed for both single-link and multi-link flexible robot manipulators, based on the natural modes of the arm or a set of assumed modes. The minimum number of modes that can be used in the model is determined by the bandwidth of the controller, actuators and sensors of the arm. A reduced-order dynamic model for an experimental single-link arm is developed and used to design fixed-parameter controllers for the arm. The controller perform very well at the design conditions but their performance deteriorates significantly as the arm is loaded. A general nonlinear model of a planar two-link arm is developed and used to demonstrate similar effects in multi-link arms. Here the deterioration in performance arises from configuration as well as loading changes. A technique is developed to update the controller parameters and maintain the arm performance for changing loads and configuration which is based on a perturbation analysis of the arm dynamics and is designed to satisfy the practical restrictions of realtime implementation. The method is successfully demonstrated on the single-link arm and, via simulation, on the planar two-link arm. ESA

N90-22054*# National Aeronautics and Space Administration. Lewis Research Center, Cleveland, OH.

COMPUTERIZED INSPECTION OF GEAR TOOTH SURFACES

Faydor L. Litvin, Zhang Yi, Jonathan Kieffer, Robert F. Handschuh (Army Research and Technology Labs., Cleveland, OH.), and John J. Coy 1989 18 p Presented at the SIAM Conference on Geometric Design, Tempe, AZ, 6-10 Nov. 1989

(DA Proj. 1L1-62209-AH-47-A)

(NASA-TM-102395; E-5113; NAS 1.15:102395; AVSCOM-TR-89-C-011) Avail: NTIS HC A03/MF A01 CSCL 13I

An approach is proposed that uses coordinate measurements of the real surface of spiral bevel gears to determine the actual machine tool setting applied during the gear manufacturing process. The deviations of the real surface from the theoretical one are also determined. Adjustments are then applied by machine tool corrections to minimize these surface deviations. This is accomplished by representing the real surface analytically in the same Gaussian coordinates as the theoretical surface. Author

N90-22088*# Fairchild Space Co., Germantown, MD.

A ROBOT END EFFECTOR EXCHANGE MECHANISM FOR SPACE APPLICATIONS

Barney F. Gorin *In* NASA, John F. Kennedy Space Center, The 24th Aerospace Mechanisms Symposium Apr. 1990 p 121-126 (For primary document see N90-22079 15-39)

Avail: NTIS HC A16/MF A03 CSCL 13I

N90-22089*# Jet Propulsion Lab., California Inst. of Tech., Pasadena.

A NEW SIX-DEGREE-OF-FREEDOM FORCE-REFLECTING HAND CONTROLLER FOR SPACE TELEROBOTICS

Douglas McAffee, Edward Snow, William Townsend, Lee Robinson, and Joe Hanson *In* NASA, John F. Kennedy Space Center, The 24th Aerospace Mechanisms Symposium Apr. 1990 p 127-141 (For primary document see N90-22079 15-39)

Avail: NTIS HC A16/MF A03 CSCL 13I

N90-22090*# Fairchild Space Co., Germantown, MD.

THE RESUPPLY INTERFACE MECHANISM RMS COMPATIBILITY TEST

Stewart W. Jackson and Frank G. Gallo *In* NASA, John F. Kennedy Space Center, The 24th Aerospace Mechanisms Symposium Apr. 1990 p 143-156 (For primary document see N90-22079 15-39)

Avail: NTIS HC A16/MF A03 CSCL 13I

N90-22091*# AEC-Able Engineering Co., Inc., Goleta, CA.
RELATCHABLE LAUNCH RESTRAINT MECHANISM FOR DEPLOYABLE BOOMS
Robert M. Warden *In* NASA, John F. Kennedy Space Center, The 24th Aerospace Mechanisms Symposium Apr. 1990 p 157-170 (For primary document see N90-22079 15-39)
Avail: NTIS HC A16/MF A03 CSCL 13I

N90-22092*# National Aeronautics and Space Administration. Goddard Space Flight Center, Greenbelt, MD.
THE CONNECTOR SPACE REDUCTION MECHANISM
M. Bruce Milam *In* NASA, John F. Kennedy Space Center, The 24th Aerospace Mechanisms Symposium Apr. 1990 p 171-186 (For primary document see N90-22079 15-39)
Avail: NTIS HC A16/MF A03 CSCL 13I

N90-22093*# Lockheed Missiles and Space Co., Sunnyvale, CA. Astronautics Div.
DRIVING AND LATCHING OF THE STARLAB POINTING MIRROR DOORS
Herbert R. Beaven, Jr. and Raymond R. Avina *In* NASA, John F. Kennedy Space Center, The 24th Aerospace Mechanisms Symposium Apr. 1990 p 187-205 (For primary document see N90-22079 15-39)
Avail: NTIS HC A16/MF A03 CSCL 13I

N90-22094*# National Aeronautics and Space Administration. Marshall Space Flight Center, Huntsville, AL.
ORBITAL MANEUVERING VEHICLE (OMV) THREE-POINT DOCKING LATCH
W. Neill Myers, John C. Forbes, and Wayne L. Barnes *In* NASA, John F. Kennedy Space Center, The 24th Aerospace Mechanisms Symposium Apr. 1990 p 207-212 (For primary document see N90-22079 15-39)
Avail: NTIS HC A16/MF A03 CSCL 13I

N90-22095*# Hughes Aircraft Co., El Segundo, CA. Space and Communications Group.
EXPERIENCE WITH SYNTHETIC FLUORINATED FLUID LUBRICANTS
Peter L. Conley and John J. Bohner *In* NASA, John F. Kennedy Space Center, The 24th Aerospace Mechanisms Symposium Apr. 1990 p 213-230 (For primary document see N90-22079 15-39)
Avail: NTIS HC A16/MF A03 CSCL 13I

N90-22096*# National Research Council of Canada, Victoria (British Columbia). Tribology and Mechanics Lab.
TRIBOMATERIAL FACTORS IN SPACE MECHANISM BRAKE PERFORMANCE
H. M. Hawthorne *In* NASA, John F. Kennedy Space Center, The 24th Aerospace Mechanisms Symposium Apr. 1990 p 231-241 Sponsored in part by Spar Aerospace Ltd. (For primary document see N90-22079 15-39)
Avail: NTIS HC A16/MF A03 CSCL 13I

N90-22097*# Honeywell, Inc., Glendale, AZ. Satellite Systems Operations.
POSITIVE LUBRICATION SYSTEM
Dennis W. Smith and Fred L. Hooper *In* NASA, John F. Kennedy Space Center, The 24th Aerospace Mechanisms Symposium Apr. 1990 p 243-258 (For primary document see N90-22079 15-39)
Avail: NTIS HC A16/MF A03 CSCL 13I

N90-22099*# Teldix Luftfahrt-Ausruestungs G.m.b.H., Heidelberg (Germany, F.R.).
TEST RESULTS AND FLIGHT EXPERIENCE OF BALL BEARING MOMENTUM AND REACTION WHEELS
W. Auer *In* NASA, John F. Kennedy Space Center, The 24th Aerospace Mechanisms Symposium Apr. 1990 p 273-287 (For primary document see N90-22079 15-39)
Avail: NTIS HC A16/MF A03 CSCL 13I

N90-22100*# MPB Corp., Keene, NH. Miniature Precision Bearings Div.
ON THE DESIGN AND DEVELOPMENT OF A MINIATURE CERAMIC GIMBAL BEARING
Robert A. Hanson, Barry ODwyer, Keith M. Gordon, and Edward W. Jarvis *In* NASA, John F. Kennedy Space Center, The 24th Aerospace Mechanisms Symposium Apr. 1990 p 289-300 (For primary document see N90-22079 15-39)
Avail: NTIS HC A16/MF A03 CSCL 13I

N90-22105*# National Aeronautics and Space Administration. Langley Research Center, Hampton, VA.
DEVELOPMENT OF CABLE DRIVE SYSTEMS FOR AN AUTOMATED ASSEMBLY PROJECT
Charles A. Monroe, Jr. *In* NASA, John F. Kennedy Space Center, The 24th Aerospace Mechanisms Symposium Apr. 1990 p 353-367 (For primary document see N90-22079 15-39)
Avail: NTIS HC A16/MF A03 CSCL 13I

38 QUALITY ASSURANCE AND RELIABILITY

Includes product sampling procedures and techniques; and quality control.

N90-22055# National Inst. of Standards and Technology, Gaithersburg, MD.
INSTITUTE FOR MATERIALS SCIENCE AND ENGINEERING, NONDESTRUCTIVE EVALUATION: TECHNICAL ACTIVITIES Annual Report, FY 1989
H. Thomas Yolken, ed. Nov. 1989 77 p
(PB90-132739; NISTIR-89/4147) Avail: NTIS HC A05/MF A01 CSCL 14D

A review of the Nondestructive Evaluation Program at NIST is presented. Topics include the following: Intelligent processing of rapidly solidified metal powders; Nondestructive characterization of ceramic sintering; Monitoring of machined ceramic surfaces by thermal waves; Eddy current temperature sensing; Ultrasonic sensor for sheet metal formability; Ultrasonic metrology for surface finish and part thickness; Measurement and control of polymer processing parameters using fluorescence spectroscopy; Nondestructive evaluation of diamond films; Transient elastic waves in laminates; Intelligent processing of solder joint connections for printed wiring assemblies; Ultrasonics and acoustic emission; Real-time x ray radioscopy; Magnetic methods and standards for NDE; Eddy current techniques; New standard test methods for characterizing performance of thermal imaging systems; and Capacitive array research for characterization of ceramics.
Author

N90-22056 United Kingdom Atomic Energy Authority, Harwell (England). Neural Network Applications Initiative.
THE CLASSIFICATION OF DEFECTS FROM ULTRASONIC MEASUREMENTS
Colin G. Windsor 1988 10 p
(AERE-R-13306) Copyright Avail: Issuing Activity

The Rumelhart back propagation and Hopfield algorithms were used to classify the nature of the defects found in steel pressure vessels. Ultrasonic data from some 83 defects of known type had previously been processed into six feature parameters describing the ultrasonic reflections. Both neural network methods performed as well as a weighted minimum distance algorithm in classifying the defect type.
Author

N90-22057# Imatran Voima Oy, Helsinki (Finland).
RELIABILITY IMPORTANCE MEASURES AND THEIR CALCULATION
Risto Andsten and Jussi Vaurio Jan. 1989 43 p
(DE90-620391; IVO-A-01/89; ISBN-951-8928-07-X; ISSN-0782-7415) Avail: NTIS (US Sales Only) HC A03/MF A01

The importance of a component to the system reliability of availability and to the system failure rate can be measured by a number of importance measures. Such measures can be used to guide the system design improvement actions as well as the diagnostic and repair actions. This report developes relationships between several importance measures, illustrates their meaning with interpretations and applications, and describes the computer program called IMPO that calculates importance measures when the system minimum cat sets and component parameters are five. A user's manual is included with illustrative examples. DOE

N90-22058 Princeton Univ., NJ.
A METHODOLOGY FOR KNOWLEDGE-BASED RESTRUCTURABLE CONTROL TO ACCOMMODATE SYSTEM FAILURES Ph.D. Thesis
Chien Yu Huang 1989 212 p
Avail: Univ. Microfilms Order No. DA9008352

The problem of dealing with unanticipated failures of dynamic systems is addressed. The solution centers on developing a knowledge based approach to perform online failure isolation and system reconfiguration. The failure analysis employs inference mechanisms and causal relationships among the devices to generate probable failure models, which are pruned and ranked by the use of heuristic measures. Hypotheses for other probable causes are made if the failure model does not adequately account for the anomalies. After the source of the failure is identified, the system knowledge is updated and the impact of failure is assessed. Any degradation of the system performance caused by failures is restored by restructuring the control. This issue is studied in depth and addressed by the analysis and design of an implicit model following control law. The concepts and methodologies of the approach are illustrated via many examples and further substantiated using a number of failure scenarios involving a tandem rotor helicopter. The results show that by providing a form of intelligent self organization, the knowledge based restructurable control approach potentially is capable of accommodating unanticipated failures. Dissert. Abstr.

39 STRUCTURAL MECHANICS

Includes structural element design and weight analysis; fatigue; and thermal stress.

For applications see *05 Aircraft Design, Testing and Performance* and *18 Spacecraft Design, Testing and Performance.*

N90-22059# Vibration Inst., Clarendon Hills, IL.
THE SHOCK AND VIBRATION DIGEST, VOLUME 21, NO. 2 Monthly Report
Vicki M. Pate, ed. Feb. 1989 76 p
Avail: NTIS HC A05/MF A01

A feature article on vibration analysis of systems with random parametric excitations is presented. A book on the rotordynamics of turbomachinery is reviewed. Abstracts dealing with such shock and vibration related topics as machine tools, bridges, automobiles, gears, beams, mechanical properties, fatigue tests, computational methods and modeling techniques are given For individual titles, see N90-22060 through N90-22060.

N90-22060# University of Western Ontario, London. Dept. of Mechanical Engineering.
VIBRATION ANALYSIS OF SYSTEMS WITH RANDOM PARAMETRIC EXCITATIONS
C. W. S. To *In* Vibration Inst., The Shock and Vibration Digest, Volume 21, No. 2 Feb. 1989 p 3-12 (For primary document see N90-22059 15-39)
Avail: NTIS HC A05/MF A01

Systems subjected to random parametric excitations are considered. Both quantitative and qualitative aspects of the analysis are included. The quantitative analysis techniques reviewed are the Fokker-Planck equation approaches, methods of stochastic averaging, truncated hierarchy techniques and various other methods Author

N90-22061# Vibration Inst., Clarendon Hills, IL.
THE SHOCK AND VIBRATION DIGEST, VOLUME 21, NO. 1 Monthly Report
Vicki M. Pate, ed. Jan. 1989 84 p
Avail: NTIS HC A05/MF A01

A feature article on recent advances in structural control, a review of approximate methods for determining the vibration modes of membranes, and a review of the 59th Shock and Vibration Symposium are given. Abstracts are given in the areas of machines, structures, vehicles, testing systems, mechanical and structural components, mechanical properties, experimental techniques and tests, acoustic environments, mathematical and computational methods, modeling techniques, and optimum design. For individual titles, see N90-22062 through N90-22063.

N90-22062# State Univ. of New York, Buffalo. Dept. of Civil Engineering.
RECENT ADVANCES IN STRUCTURAL CONTROL
A. M. Reinhorn and G. D. Manolis *In* Vibration Inst., The Shock and Vibration Digest, Volume 21, No. 1 Jan. 1989 p 3-8 (For primary document see N90-22061 15-39)
Avail: NTIS HC A05/MF A01

Interest in structural control has been growing with the emphasis now placed on experimental programs that will substantiate the various theories and designs that are currently proposed. The key idea behind structural control is to keep the response of a structure within certain bounds dictated by serviceability. This can be achieved by passive control, active control, or the combination of these two basic approaches. It is asserted that the concepts behind passive and active structural control are sound, and for the most part, well understood. In support of implementing these concepts in everyday practice, experimental studies on more realistic structural models followed by full-scale testing either in the laboratory or in the field are most essential. Author

N90-22063# Adelaide Univ. (Australia). Dept. of Applied Mathematics.
A REVIEW OF APPROXIMATE METHODS FOR DETERMINING THE VIBRATIONAL MODES OF MEMBRANES
J. Mazumdar *In* Vibration Inst., The Shock and Vibration Digest, Volume 21, No. 1 Jan. 1989 p 9-13 (For primary document see N90-22061 15-39)
Avail: NTIS HC A05/MF A01

Various approximate methods for the study of membrane vibrations published during the past three or four years are reviewed. Recent research on nonlinear effects, forced vibrations, material anisotropy, and many other complicating factors is summarized. Author

N90-22064# Vibration Inst., Clarendon Hills, IL.
THE SHOCK AND VIBRATION DIGEST, VOLUME 21, NO. 3 Monthly Report
Vicki M. Pate, ed. Mar. 1989 72 p
Avail: NTIS HC A04/MF A01

A feature article on rotor to stationary element rub-related vibration phenomena in rotating machinery is presented. A book concerned with the dynamics of multibody systems is reviewed. Abstracts on shock and vibration related topics such as mechanical drives, towers, automobiles, expert systems, gears, beams, mechanical properties, vibration tests, computational methods and modeling techniques are given. For individual titles, see N90-22065 through N90-22065.

N90-22065# Bently Rotor Dynamics Research Corp., Minden, NV.
ROTOR-TO-STATIONARY ELEMENT RUB-RELATED VIBRATION PHENOMENA IN ROTATING MACHINERY: LITERATURE SURVEY
A. Muszynska *In* Vibration Inst., The Shock and Vibration Digest, Volume 21, No. 3 Mar. 1989 p 3-11 (For primary document see N90-22064 15-39)
(Contract NAS8-36719)
Avail: NTIS HC A04/MF A01

Rotor to stationary element rub is a serious malfunction in rotating machinery that may lead to catastrophic failure. Dynamic phenomena occurring during rubbing such as friction, impacting, stiffening and coupling effects are discussed. A literature survey on rub-related phenomena in rotating machinery is presented.
Author

N90-22066# Vibration Inst., Clarendon Hills, IL.
THE SHOCK AND VIBRATION DIGEST, VOLUME 21, NO. 7 Monthly Report
Judith Nagle-Eshleman, ed. Jul. 1989 76 p
Avail: NTIS HC A05/MF A01

A feature article on the optimal design of structures subjected to shock and vibration environments is given. A book on the vibrations of structures and applications in civil engineering is reviewed. The 35th annual meeting of the Institute of Environmental Sciences is reviewed. Abstracts of shock and vibration related articles are given. Topics include machine tools, bridges, helicopters, gears, beams, mechanical properties fatigue tests, computational methods and modeling techniques. For individual titles, see N90-22067 through N90-22067.

N90-22067# Purdue Univ., West Lafayette, IN. School of Mechanical Engineering.
OPTIMUM DESIGN OF STRUCTURES UNDER SHOCK AND VIBRATION ENVIRONMENT
S. S. Rao *In* Vibration Inst., The Shock and Vibration Digest, Volume 21, No. 7 Jul. 1989 p 3-15 (For primary document see N90-22066 15-39)
Avail: NTIS HC A05/MF A01

The problems of optimal design of structures subjected to shock and vibration are classified according to the physical nature of the problem and the major behavior constraint involved. A summary of recent work in each class of problems is presented. Also presented is recent research in structural optimization methods, including multiobjective strategies, multilevel approaches, and stochastic models, aspects of sensitivity analysis and approximation techniques in optimization and structural optimization problems in need of further investigation.
Author

N90-22068# Vibration Inst., Clarendon Hills, IL.
THE SHOCK AND VIBRATION DIGEST, VOLUME 21, NO. 8 Monthly Report
Vicki M. Pate, ed. Aug. 1989 68 p
Avail: NTIS HC A04/MF A01

A feature article on recent progress in the dynamic plastic behavior of structures is presented. Several book reviews on such topics as structural dynamics, vibration measurement, noise reduction, expert systems in structural engineering, and structural failure are given. Abstracts of articles on such shock and vibration topics as machine tools, bridges, gears, beams, mechanical properties, vibration tests, computational methods, and mathematical models are given. For individual title see N90-22069.

N90-22069# Liverpool Univ. (England). Dept. of Mechanical Engineering.
RECENT PROGRESS IN THE DYNAMIC PLASTIC BEHAVIOR OF STRUCTURES, PART 5
Norman Jones *In* Vibration Inst., The Shock and Vibration Digest, Volume 21, No. 8 Aug. 1989 p 3-13 (For primary document see N90-22068 15-39)
Avail: NTIS HC A04/MF A01

The literature published since 1985 on the dynamic plastic behavior of structures is reviewed. The focus is on recent developments in the rigid-plastic methods of analysis, dynamic crushing, similitude and experimental techniques. Comments on dynamic plastic buckling, numerical studies, beams and plates and dynamic failure are also offered.
Author

N90-22070 Michigan Technological Univ., Houghton.
ELASTIC STABILITY AND NONLINEAR BEHAVIOR OF IMPERFECT SHELLS WITH INITIAL STRESSES Ph.D. Thesis
Xiang Ju 1988 164 p
Avail: Univ. Microfilms Order No. DA8924448

A computer software program based on the total Lagrangian description of motion, the DMV theory of thin shells and the finite difference energy method was developed to be able to perform the geometrically nonlinear analysis of thin imperfect shells. Some numerical procedures such as the Newton-Raphson and modified constant arc-length method of Riks/Wempner are used to trace the nonlinear behavior including the effect of initial (residual) stresses which are caused by elastic-plastic loading and elastic unloading in a certain sheet metal forming process. The Galerkin's approach was used to estimate the elastic stability and post-buckling behavior of simply supported shallow shells of rectangular planform with initial stresses. Results from the finite difference energy method and the Galerkin's approach are comparable.
Dissert. Abstr.

N90-22071 Wayne State Univ., Detroit, MI.
NUMERICAL SOLUTIONS OF THE NONLINEAR THEORY OF CURVED BEAMS Ph.D. Thesis
Ta-Ming Liu 1989 200 p
Avail: Univ. Microfilms Order No. DA8922767

Based on the nonlinear curved-beam theory developed by Cohen-Whitman-DeSilva, the numerical solutions of the plane motion of beams or beam-columns in static equilibrium were obtained by using the finite difference method and the Newton-Raphson method. Two classes of beam problems are considered i.e., an initially circular curved cantilever beam acted on by a concentrated vertical load at the free end, the angle subtended by the span of the beam ranging from 0 (i.e., straight beam) to 3 pi/8, and an initially straight simply supported beam-column acted on by a terminal moment and an axial horizontal load at the righthand-side movable end. For each class of beam problem, the numerical solutions obtained included the deflection curves at the different loading conditions, the axial force, shear force, and bending moment diagrams, and the non-dimensional relations between the deformation (vertical deflection, axial stretch, and rotational angle of cross section) with respect to the loading conditions. Also for each class of beam the following effects on the beam deformation are treated: (1) the change of the direction of the vertical (or horizontal) concentrated load during deformation is considered. For the follower load condition, the direction of the concentrated force is kept always perpendicular to the d sub 3 (or d sub 2) direction (for straight beam); and (2) the axial stretch and shear deformation are concerned. Note that the direction of the normal reaction force at the simply supported end is assumed always kept in the vertical direction, not perpendicular to the centroidal axis of the beam during deformation.
Dissert. Abstr.

N90-22072 Bradford Univ. (England).
FAILURE MECHANISMS UNDER COMPLEX LOADING OF GLASS-REINFORCED POLYESTER COMPOSITES AND THEIR MATRICES: THE EFFECT OF SUPERPOSED HYDROSTATIC PRESSURES UP TO 300 MPa ON AXIAL TENSILE AND COMPRESSIVE STRENGTHS, AND IN-PLANE SHEAR PROPERTIES OF UNIDIRTIONALLY REINFORCED GLASS-POLYESTER COMPOSITES AND THE RELEVANT POLYESTERS Ph.D. Thesis
Ruth Helen Sigley 1988 240 p
Avail: Univ. Microfilms Order No. BRDX86518

Failure mechanisms of uniaxial glass-polyester composites were investigated in tensions, compression, diametral compression, and in-plane shear under superposed pressures up to 300 MPa. Relevant matrices were tested in tension and compression under the same pressure regime. Yielding of resins took place only under axial compression. The yield surface could be represented by a three-parameter pyramid. In the extensile mode, even when all principle stresses were compressive, brittle fracture, associated with a strain energy or tensile strain criterion was observed. In composites under load, groups of somewhat curved fibers (bundles) tended to act as microstructural units, and many failures occurred at these bundle interfaces. Ultimate failure in axial tension was controlled by the fibers, whose brittle strength was found not to be governed by a critical tensile stress. Criteria involving deviatoric stress, strain and strain energy and total strain energy are discussed. Failure in axial compression was through debonding and buckling of surface bundles, and appeared to be controlled by the transverse tensile strain for bundling debonding. Failures in in-plane shear and diametral compression occurred at fiber-matrix interfaces. The latter process is postulated to be controlled by a critical tensile strain; with pressurizing fluid interaction , this changed to, tentatively, a deviatoric tensile strain criterion. Attempts are made to discuss micromechanisms relating to the various types and stages of failure. Behavior under pressure of these commercial glass-polyesters is more complex than epoxy composites with which results are compared. Dissert. Abstr.

N90-22073# Vibration Inst., Clarendon Hills, IL.
THE SHOCK AND VIBRATION DIGEST, VOLUME 22, NO. 1 Monthly Report
Vicki M. Pate, ed. Jan. 1990 68 p
Avail: NTIS HC A04/MF A01

A feature article on the stable response of damped mechanical systems is presented. A book on stochastic methods in structural dynamics is reviewed, as well as the 60th Shock and Vibration Symposium. Abstracts on such shock and vibration related topics as machine tools, bridges, automobiles, beams, mechanical properties, vibration tests, computational methods, and mathematical models are given. For individual title see N90-22074.

N90-22074# Stevens Inst. of Tech., Hoboken, NJ. Dept. of Mechanical Engineering.
STABLE RESPONSE OF DAMPED MECHANICAL SYSTEMS, 4
D. Nicholson *In* Vibration Inst., The Shock and Vibration Digest, Volume 22, No. 1 Jan. 1990 p 3-11 (For primary document see N90-22073 15-39)
Avail: NTIS HC A04/MF A01

Selected recent literature is surveyed on several topics pertaining to the time response of a discrete, time-invariant, linear, multiple degree of freedom mechanical system. Emphasis is on asymmetric systems. Several specific results are described. Topics covered include conditions for asymptotic stability, localization of system eigenvalues, response bounds under various types of excitation and the relation between system stability and numerical stability of time integration methods for calculating the system response. Author

N90-22075 Michigan Univ., Ann Arbor.
NATURAL MODES OF CRACKED BEAMS AND IDENTIFICATION OF CRACKS Ph.D. Thesis
Mo-How Herman Shen 1989 231 p
Avail: Univ. Microfilms Order No. DA9001709

A method is presented for both the detection and monitoring of structural cracks, based on measurements of dynamic response. The technique is to analytically model the structural dynamics based on cracked beam theories derived under the Bernoulli-Euler assumption. Crack properties are related to the natural frequencies and mode shapes of the beam via this model. This model is incorporated into a system for the determination of crack damage through an identification process. First, an approximate Galerkin solution to the one-dimensional cracked beam theory for the free bending motion of beams with pairs of symmetric crack is suggested. This approach provides for the determination of the natural frequencies and mode shapes of the cracked beam. To validate the computational model, a two-dimensional finite element approach is proposed, which also allows one to determine the parameter that controls the stress concentration profile near the crack-tip in the theoretical formulation. Existing crack beam theory for a pair of symmetric cracks is extended to cover the free vibration of beams with a single edge crack. The natural frequencies and mode shapes of simply supported and cantilevered beams are computed for both symmetric and one-sided cracks. These predictions are confirmed by comparison to experimental and finite element results for both kinds of cracks. An identification procedure is developed to determine the crack characteristics from dynamic measurements. This procedure is based on minimization of either the mean square or the max measure of difference between measurement data and the corresponding predictions obtained from the computational model. Necessary conditions are obtained for both formulations. The method was tested for simulated damage in the form of a simply-supported beam. Dissert. Abstr.

N90-22076 Northwestern Univ., Evanston, IL.
CONTACT MECHANICS FOR THREE-DIMENSIONAL GEOMETRIES Ph.D. Thesis
Mark Tod Hanson 1989 161 p
Avail: Univ. Microfilms Order No. DA9002492

A three-dimensional analysis is used to study components subjected to heavily loaded concentrated contacts. Two particular aspects are analyzed in detail. First, three dimensional fracture mechanics is utilized to develop an analytical model for the fatigue crack propagation phase of contract fatigue surface pitting failure. Using three-dimensional fracture mechanics coupled with a phenomenological crack growth law, an estimation of crack growth life is obtained. The fluid pressure mechanism for fatigue crack propagation is analyzed by considering the two limiting cases of uniform and linear fluid pressure inside the crack. The results illustrate the need for fluid pressure to propagate a crack as well as the effects of varying fluid pressure on crack growth life. The second aspect investigated is the effect of a vertical free surface near the contact region in heavily loaded contacts. A two-dimensional quarter plane is considered first in order to understand the physical behavior of contact near a free surface and to reveal the mathematical complexities involved in such an analysis. The three-dimensional problem is then analyzed by extending the two-dimensional theory to a quarter space geometry. Contact is modeled with ellipsoidal distributions of shear and normal tractions in the vicinity of the edge. The free surface effect on the internal stress field in the quarter space is considered. Mechanical failure in the form of plastic yielding is considered by analyzing the von Mises yield parameter for several typical contact loadings. Dissert. Abstr.

N90-22077 Kentucky Univ., Lexington.
ELASTODYNAMIC SCATTERING AND TRANSMISSION PROBLEMS IN THREE DIMENSIONS BY THE BOUNDARY INTEGRAL EQUATION METHOD Ph.D. Thesis
Ivan Rosario Gonsalves 1989 205 p
Avail: Univ. Microfilms Order No. DA9002080

The direct Boundary Integral Equation Method (BIEM) is used to formulate and obtain the numerical solution for the three-dimensional, steady-state (time-harmonic) elastodynamic response of an elastic medium containing inhomogeneities consisting of elastic inclusions and/or cavities and rigid inclusions. The inclusions are assumed to be perfectly bonded to the surrounding embedding medium. For a finite embedding medium, the problem considered is the (harmonically) forced vibrations of the composite nonhomogeneous body. Both radiation and scattering problems are considered when the embedding medium is a full-space of infinite extent. The unprescribed and/or continuous displacements and tractions on the inclusion boundaries appear explicitly as the only unknown in the integral equations. Consequently, all modeling for numerical purposes is confined to finite boundaries only. The numerical solution procedure, which uses quadratic isoparametric elements for modeling purposes, is based on nodal collocation of BIEs free from principal-value integrals. A modification of the CHIEF formulation of acoustics is used to overcome the nonuniqueness of the full-space BIE solution at the fictitious eigenfrequencies. For scattering and radiation problems in a uniform elastic half-space, only rigid inclusions and cavities are considered. Integral formulations, free from principal-value integrals, are presented with Stokes' (full space) and Lamb's (half-space) fundamental tensors (Green's functions) for flush footings as well as for partially or fully embedded inclusions. Whereas the Stokes'-tensor BIE requires modeling of the infinite half-space surface, all modeling is confined to finite boundaries of the inclusions when Lamb's tensors were used. The validity and accuracy of the BIEM formulations are demonstrated by comparing the BIEM solutions with available analytical and numerical solutions. Dissert. Abstr.

N90-22078# Northwestern Univ., Evanston, IL.
ELASTO-PLASTIC ANALYSIS FOR CONTACT FATIGUE FAILURE Ph.D. Thesis
Viraj Vithoontien 1989 94 p
Avail: Univ. Microfilms Order No. DA9001878

A scheme of combining analytical and finite element methods is developed for the analysis of repeated rolling and sliding contacts on an elastic-plastic half plane. The element size used for subdividing the finite element domain was carefully selected to assure the accuracy of the finite element results. The present result of an elastic plastic indentation was shown to be accurate when compared with those obtained by another finite element scheme considered highly reliable. Repeated rolling and sliding contacts for elastic-perfectly plastic and elastic-linear kinematic hardening materials are reexamined by the present finite element scheme. The results are extensively compared with experimental measurements and computational results. The evaluation of residual stresses and strains induced by 2-D repeated rolling and sliding contacts was made for 52100 steel. The finite element results are employed for predicting a number of loading cycles required for microcrack to be initiated for various loading conditions on the basis of the modified initiation life model of Tanaka and Mura. The dark and light etching regions observed experimentally are theoretically shown to be generated by the plastic deformation. An excessive accumulation of plastic work during contact fatigue is responsible for the formation of shear bands. The dependency of the direction of shear bands on the surface traction is confirmed by the present results. The present results are applicable for the initiation life and the orientation of a near-surface fatigue crack originated by asperities that are transversely oriented to the rolling direction. Dissert. Abstr.

N90-22079*# National Aeronautics and Space Administration. John F. Kennedy Space Center, Cocoa Beach, FL.
THE 24TH AEROSPACE MECHANISMS SYMPOSIUM
Washington Apr. 1990 370 p Symposium held at Kennedy Space Center, FL, 18-20 Apr. 1990; sponsored by NASA, Washington, California Inst. of Tech., Pasadena, and LMSC, Sunnyvale, CA
(NASA-CP-3062; NAS 1.55:3062) Avail: NTIS HC A16/MF A03 CSCL 20K

The proceedings of the symposium are reported. Technological areas covered include actuators, aerospace mechanism applications for ground support equipment, lubricants, latches, connectors, and other mechanisms for large space structures. For individual titles, see N90-22080 through N90-22105.

N90-22080*# National Aeronautics and Space Administration. Ames Research Center, Moffett Field, CA.
CYCLE LIFE MACHINE FOR AX-5 SPACE SUIT
Deborah S. Schenberger *In* NASA, John F. Kennedy Space Center, The 24th Aerospace Mechanisms Symposium Apr. 1990 p 1-8 (For primary document see N90-22079 15-39)
Avail: NTIS HC A16/MF A03 CSCL 20K

In order to accurately test the AX-5 space suit, a complex series of motions needed to be performed which provided a unique opportunity for mechanism design. The cycle life machine design showed how 3-D computer images can enhance mechanical design as well as help in visualizing mechanisms before manufacturing them. In the early stages of the design, potential problems in the motion of the joint and in the four bar linkage system were resolved using CAD. Since these problems would have been very difficult and tedious to solve on a drawing board, they would probably not have been addressed prior to fabrication, thus limiting the final design or requiring design modification after fabrication. Author

N90-22081*# Jet Propulsion Lab., California Inst. of Tech., Pasadena.
DEVELOPMENT OF SHAPE MEMORY METAL AS THE ACTUATOR OF A FAIL SAFE MECHANISM
V. G. Ford, M. R. Johnson, and S. D. Orlosky (TiNi Alloy Co., Oakland, CA.) *In* NASA, John F. Kennedy Space Center, The 24th Aerospace Mechanisms Symposium Apr. 1990 p 9-24 (For primary document see N90-22079 15-39)
Avail: NTIS HC A16/MF A03 CSCL 20K

A small, compact, lightweight device was developed using shape memory alloy (SMA) in wire form to actuate a pin-puller that decouples the flanges of two shafts. When the SMA is heated it contracts producing a useful force and stroke. As it cools, it can be reset (elongated in this case) by applying a relatively small force. Resistive heating is accomplished by running a current through the SMA wire for a controlled length of time. The electronics to drive the device are not elaborate or complicated, consisting of a timed current source. The total available contraction is 3 percent of the length of the wire. This device, the engineering properties of the SMA, and the tests performed to verify the design concept are described. Author

N90-22082*# Centre National d'Etudes Spatiales, Toulouse (France).
SPOT 4 SPACE MAGNETIC RECORDER MECHANISMS c35
A. Borrien, E. Vialatoux, J. L. Lhermet, and A. Didier (Schlumberger Industries, Velizy, France) *In* NASA, John F. Kennedy Space Center, The 24th Aerospace Mechanisms Symposium Apr. 1990 p 25-39 (For primary document see N90-22079 15-39)
Avail: NTIS HC A16/MF A03 CSCL 14B

The design of the SPOT 4 satellite will be quite different from the previous ones. The design of the new magnetic tape recorder, which was derived from industrial knowledge and mission requirements; the main technical characteristics of the recorder; and the mechanical subsystems of the recorder and their locations and contributions to the final performance are all discussed. The philosophy of the development program, required to achieve the desired performance and reliability for each flight model, is described, and information on the schedule and current development is presented. The components of the tape plate system, (the transmission belts, tape rollers of the recorders, and reel hub ball bearings) which are subjected to heavy mechanical operation, fatigue, and wear in the thermal environment of the mission, are discussed. For each of the components, a description of its function in the recorder is given, as well as the mechanical stress imposed during the various operational phases. The quality testing program, which was used to verify the design safety margins, is described. Finally, the first test results of a functioning model of the flight system are presented. Author

N90-22083*# Lockheed Aircraft Corp., Palo Alto, CA. Research Lab.
DEVELOPMENT OF THE CLAES INSTRUMENT APERTURE DOOR SYSTEM c35
D. M. Stubbs *In* NASA, John F. Kennedy Space Center, The 24th Aerospace Mechanisms Symposium Apr. 1990 p 41-56 (For primary document see N90-22079 15-39)
Avail: NTIS HC A16/MF A03 CSCL 14B

The design, assembly, and test processes followed in developing a space-qualified aperture door system are described. A blackbody calibration source is mounted inside the door, requiring the assembly to open and close a minimum of 150 cycles for instrument recalibration. Within the door system are four separate mechanisms, three of which are redundant; a pyro launch latch, a hinge bearing assembly, and a pair of pivot mechanisms. Decoupling devices within the pivot mechanisms allow an active drive unit to automatically overdrive a failed drive unit. The door is also stowable for possible Shuttle retrieval and re-entry. Illustrations and photographs of the flight hardware help acquaint the reader with the design. The aim is to pass on lessons learned in all phases of developing this spaceflight mechanism. Author

N90-22084*# Jet Propulsion Lab., California Inst. of Tech., Pasadena.

A SOFT ACTUATION SYSTEM FOR SEGMENTED REFLECTOR ARTICULATION AND ISOLATION **c74**

Michael L. Agronin and Louise Jandura *In* NASA, John F. Kennedy Space Center, The 24th Aerospace Mechanisms Symposium Apr. 1990 p 57-73 (For primary document see N90-22079 15-39)

Avail: NTIS HC A16/MF A03 CSCL 20F

Segmented reflectors have been proposed for space based applications such as optical communication and large diameter telescopes. An actuation system for mirrors in a space based segmented mirror array was developed as part of NASA's Precision Segmented Reflector program. The actuation system, called the Articulated Panel Module (APM), provides 3 degrees of freedom mirror articulation, gives isolation from structural motion, and simplifies space assembly of the mirrors to the reflector backup truss. A breadboard of the APM was built and is described. Author

N90-22085*# Centre National d'Etudes Spatiales, Toulouse (France).

A DYNAMIC MOTION SIMULATOR FOR FUTURE EUROPEAN DOCKING SYSTEMS **c14**

G. Brondino, Ph. Marchal, D. Grimbert, and P. Noirault (MATRA Espace, Paris-Velizy, France) *In* NASA, John F. Kennedy Space Center, The 24th Aerospace Mechanisms Symposium Apr. 1990 p 75-87 (For primary document see N90-22079 15-39)

Avail: NTIS HC A16/MF A03 CSCL 14B

Europe's first confrontation with docking in space will require extensive testing to verify design and performance and to qualify hardware. For this purpose, a Docking Dynamics Test Facility (DDTF) was developed. It allows reproduction on the ground of the same impact loads and relative motion dynamics which would occur in space during docking. It uses a 9 degree of freedom, servo-motion system, controlled by a real time computer, which simulates the docking spacecraft in a zero-g environment. The test technique involves and active loop based on six axis force and torque detection, a mathematical simulation of individual spacecraft dynamics, and a 9 degree of freedom servomotion of which 3 DOFs allow extension of the kinematic range to 5 m. The configuration was checked out by closed loop tests involving spacecraft control models and real sensor hardware. The test facility at present has an extensive configuration that allows evaluation of both proximity control and docking systems. It provides a versatile tool to verify system design, hardware items and performance capabilities in the ongoing HERMES and COLUMBUS programs. The test system is described and its capabilities are summarized. Author

N90-22086*# Lockheed Missiles and Space Co., Sunnyvale, CA.

THE DEVELOPMENT OF A COMPLEMENTARY EXPENDABLE LAUNCH VEHICLE INTERFACE FOR AN STS DEPLOYABLE PAYLOAD **c15**

Ed Eubanks and John Gibb *In* NASA, John F. Kennedy Space Center, The 24th Aerospace Mechanisms Symposium Apr. 1990 p 89-104 (For primary document see N90-22079 15-39)

Avail: NTIS HC A16/MF A03 CSCL 22B

The development is described of an interface, the Titan Payload Adapter (TPA), between a Space Transportation System (STS) deployable payload and an expendable launch vehicle (ELV). Separate ascent and separation constraint systems allow a payload with integral trunnions to retain its originally designed, boost-phase load structure, yet also allow the expendable booster vehicle to separate from the payload via retro-rockets. Design requirements as well as development problems and their solutions are discussed. Author

N90-22087*# Toshiba Corp., Kawasaki (Japan). Mechanical Engineering Lab.

DEVELOPMENT OF A MULTIPURPOSE HAND CONTROLLER FOR JEMRMS **c54**

Nobuto Matsuhira, Shoichi Iikura, Makoto Asakura, and Yasuo Shinomiya *In* NASA, John F. Kennedy Space Center, The 24th Aerospace Mechanisms Symposium Apr. 1990 p 105-120 (For primary document see N90-22079 15-39)

Avail: NTIS HC A16/MF A03 CSCL 05H

A prototype multipurpose hand controller for the JEMRMS (Japanese Experiment Module Remote Manipulator System) was developed. The hand controller (H/C) is an orthogonal type, with 6 degrees of freedom (DOF) and small size. The orthogonal type H/C is very simple for coordinate transformations and can easily control any type of manipulators. In fact, the JEMRMS is planned to have two manipulators controlled by a common H/C at this stage. The H/C was able to be used as a rate control joystick and a force reflection master arm, using an experimental 6 DOF manipulator. Good maneuverability was confirmed in the verification test. The orthogonal type H/C is suitable for use as a common H/C for the two manipulators of the JEMRMS. Author

N90-22088*# Fairchild Space Co., Germantown, MD.

A ROBOT END EFFECTOR EXCHANGE MECHANISM FOR SPACE APPLICATIONS **c37**

Barney F. Gorin *In* NASA, John F. Kennedy Space Center, The 24th Aerospace Mechanisms Symposium Apr. 1990 p 121-126 (For primary document see N90-22079 15-39)

Avail: NTIS HC A16/MF A03 CSCL 13I

Efficient robot operation requires the use of specialized end effectors or tools for tasks. In spacecraft applications, the microgravity environment precludes the use of gravitational forces to retain the tools in holding fixture. As a result of this, a retention mechanism which forms a part of the tool storage container is required. A unique approach to this problem has resulted in the development of an end effector exchange mechanism that meets the requirements for spaceflight applications while avoiding the complexity usually involved. This mechanism uses multiple latching cams both on the manipulator and in the tool storage container, combined with a system of catch rings to provide retention in both locations and the required failure tolerance. Because of the cam configuration the mechanism operates passively, requiring no electrical commands except those needed to move the manipulator into position. Similarly, it inherently provides interlocks to prevent the release of one cam before its opposite number is engaged. Author

N90-22089*# Jet Propulsion Lab., California Inst. of Tech., Pasadena.

A NEW SIX-DEGREE-OF-FREEDOM FORCE-REFLECTING HAND CONTROLLER FOR SPACE TELEROBOTICS **c37**

Douglas McAffee, Edward Snow, William Townsend, Lee Robinson, and Joe Hanson *In* NASA, John F. Kennedy Space Center, The 24th Aerospace Mechanisms Symposium Apr. 1990 p 127-141 (For primary document see N90-22079 15-39)

Avail: NTIS HC A16/MF A03 CSCL 13I

A new 6 degree of freedom universal Force Reflecting Hand Controller (FRHC) was designed for use as the man-machine interface in teleoperated and telerobotic flight systems. The features of this new design include highly intuitive operation, excellent kinesthetic feedback, high fidelity force/torque feedback, a kinematically simple structure, mechanically decoupled motion in all 6 DOF, good back-drivability, and zero backlash. In addition, the new design has a much larger work envelope, smaller stowage volume, greater stiffness and responsiveness, and better overlap of the human operator's range of motion than do previous designs. The utility and basic operation of a new, flight prototype FRHC called the Model X is briefly discussed. The design heritage, general design goals, and design implementation of this advanced new generation of FRHCs are presented, followed by a discussion of basic features and the results of initial testing. Author

N90-22090*# Fairchild Space Co., Germantown, MD.

THE RESUPPLY INTERFACE MECHANISM RMS COMPATIBILITY TEST **c37**

Stewart W. Jackson and Frank G. Gallo *In* NASA, John F. Kennedy Space Center, The 24th Aerospace Mechanisms

Symposium Apr. 1990 p 143-156 (For primary document see N90-22079 15-39)
Avail: NTIS HC A16/MF A03 CSCL 13I

Spacecraft on-orbit servicing consists of exchanging components such as payloads, orbital replacement units (ORUs), and consumables. To accomplish the exchange of consumables, the receiving vehicle must mate to the supplier vehicle. Mating can be accomplished by a variety of docking procedures. However, these docking schemes are mission dependent and can vary from shuttle bay berthing to autonomous rendezvous and docking. Satisfying the many docking conditions will require use of an innovative docking device. The device must provide fluid, electrical, pneumatic and data transfer between vehicles. Also, the proper stiffness must be obtained and sustained between the vehicles. A device to accomplish this, the resupply interface mechanism (RIM), was developed. The RIM is a unique device because it grasps the mating vehicle, draws the two vehicles together, simultaneously mates all connectors, and rigidizes the mating devices. The NASA-Johnson Manipulator Development Facility was used to study how compatible the RIM is to on orbit docking and berthing. The facility contains a shuttle cargo bay mockup with a remote manipulator system (RMS). This RMS is used to prepare crew members for shuttle missions involving spacecraft berthing operations. The MDF proved to be an excellant system for testing the RIM/RMS compatibility. The elements examined during the RIM JSC test were: RIM gross and fine alignment; berthing method sequence; visual cuing aids; utility connections; and RIM overall performance. The results showed that the RIM is a good device for spacecraft berthing operations. Mating was accomplished during every test run and all test operators (crew members) felt that the RIM is an effective device. The purpose of the JSC RIM test and its results are discussed. Author

N90-22091*# AEC-Able Engineering Co., Inc., Goleta, CA.
RELATCHABLE LAUNCH RESTRAINT MECHANISM FOR DEPLOYABLE BOOMS **c37**
Robert M. Warden *In* NASA, John F. Kennedy Space Center, The 24th Aerospace Mechanisms Symposium Apr. 1990 p 157-170 (For primary document see N90-22079 15-39)
Avail: NTIS HC A16/MF A03 CSCL 13I

A new Relatchable Launch Mechanism was developed which enables a deployable system to be restrained and released repeatedly rather than the normal one shot release systems of the past. The deployable systems are of the self extending type which rely on a lanyard attached to a drive motor to control the deployment and retraction. The Relatch Mechanism uses the existing drive motor to also actuate the latch. The design and kinematics of the Relatch Mechanism as used on two flight programs are described. Author

N90-22092*# National Aeronautics and Space Administration. Goddard Space Flight Center, Greenbelt, MD.
THE CONNECTOR SPACE REDUCTION MECHANISM **c37**
M. Bruce Milam *In* NASA, John F. Kennedy Space Center, The 24th Aerospace Mechanisms Symposium Apr. 1990 p 171-186 (For primary document see N90-22079 15-39)
Avail: NTIS HC A16/MF A03 CSCL 13I

The Connector Space Reduction Mechanism (CSRM) is a simple device that can reduce the number of electromechanical devices on the Payload Interface Adapter/Station Interface Adapter (PIA/SIA) from 4 to 1. The device uses simplicity to attack the heart of the connector mating problem for large interfaces. The CSRM allows blind mate connector mating with minimal alignment required over short distances. This eliminates potential interface binding problems and connector damage. The CSRM is compatible with G and H connectors and Moog Rotary Shutoff fluid couplings. The CSRM can be used also with less forgiving connectors, as was demonstrated in the lab. The CSRM is NASA-Goddard exclusive design with patent applied for. The CSRM is the correct mechanism for the PIA/SIA interface as well as other similar berthing interfaces. Author

N90-22093*# Lockheed Missiles and Space Co., Sunnyvale, CA. Astronautics Div.
DRIVING AND LATCHING OF THE STARLAB POINTING MIRROR DOORS **c37**
Herbert R. Beaven, Jr. and Raymond R. Avina *In* NASA, John F. Kennedy Space Center, The 24th Aerospace Mechanisms Symposium Apr. 1990 p 187-205 (For primary document see N90-22079 15-39)
Avail: NTIS HC A16/MF A03 CSCL 13I

The Starlab Experiment, a major SDIO technology initiative, is an attached payload which will be delivered into Earth orbit aboard NASA's Space Shuttle in 1991. Starlab will generate and aim an 80 cm diameter laser beam into space through a large opening in the structure which houses the pointing mirror. Two doors, each somewhat larger than a desktop, cover the opening when the laser optics system is nonoperational. Latch Mechanism Assemblies hold the doors shut during liftoff and ascent and, again, during Orbiter reentry. Each door is powered by a Door Drive System during the many open/close cycles between various experiments. The design, testing, and resultant failure modes of these mechanisms are examined. Author

N90-22094*# National Aeronautics and Space Administration. Marshall Space Flight Center, Huntsville, AL.
ORBITAL MANEUVERING VEHICLE (OMV) THREE-POINT DOCKING LATCH **c37**
W. Neill Myers, John C. Forbes, and Wayne L. Barnes *In* NASA, John F. Kennedy Space Center, The 24th Aerospace Mechanisms Symposium Apr. 1990 p 207-212 (For primary document see N90-22079 15-39)
Avail: NTIS HC A16/MF A03 CSCL 13I

The primary purpose of the OMV is to dock with orbiting payloads and then either transfer them to a different orbit or return them to the Space Shuttle for servicing. Some such missions will involve docking with payloads equipped with a Flight Support System (FSS) type of interface; an example is the Hubble Space Telescope (HST). The design and development of a mechanism to be used for testing this docking concept on the NASA-Marshall test beds is described. The test results to date are also presented. Author

N90-22095*# Hughes Aircraft Co., El Segundo, CA. Space and Communications Group.
EXPERIENCE WITH SYNTHETIC FLUORINATED FLUID LUBRICANTS **c37**
Peter L. Conley and John J. Bohner *In* NASA, John F. Kennedy Space Center, The 24th Aerospace Mechanisms Symposium Apr. 1990 p 213-230 (For primary document see N90-22079 15-39)
Avail: NTIS HC A16/MF A03 CSCL 13I

Since the late 1970's, the wet lubricant of choice for space mechanisms has been one of the family of synthetic perfluoro polyalkylether (PEPE) compounds, namely Fomblin Z-25 (Bray-815Z) or DuPont's Krytox 143xx series. While offering the advantages of extremely low vapor pressures and wide temperature ranges, these oils and derived greases have a complex chemistry compared to the more familiar natural and synthetic hydrocarbons. Many aerospace companies have conducted test programs to characterize the behavior of these compounds in a space environment, resulting in a large body of hard knowledge as well as considerable space lore concerning the suitability of the lubricants for particular applications and techniques for successful application. The facts are summarized and a few myths about the compounds are dispelled, and some performance guidelines for the mechanism design engineer are provided. Author

N90-22096*# National Research Council of Canada, Victoria (British Columbia). Tribology and Mechanics Lab.
TRIBOMATERIAL FACTORS IN SPACE MECHANISM BRAKE PERFORMANCE **c37**
H. M. Hawthorne *In* NASA, John F. Kennedy Space Center, The 24th Aerospace Mechanisms Symposium Apr. 1990

p 231-241 Sponsored in part by Spar Aerospace Ltd. (For primary document see N90-22079 15-39)
Avail: NTIS HC A16/MF A03 CSCL 13I

The asbestos/phenolic pads of Shuttle Remote Manipulator System (SRMS) brakes are unsuitable for use in long life space mechanisms because their friction decreases on extended sliding in high vacuum. Dehydration of the material and accumulation of wear debris in the conforming interface of this tribosystem induces the permanent friction changes. Other polymer and some ceramic based materials exhibit similar frictional torque behavior due to the development of minimal contact patches by the interfacial debris. In contrast, high friction occurs when other ceramics form many small contacts throughout fine debris beds. Generating this latter interfacial structure during run-in ensures that the in-vacuo friction remains stable thereafter. Such materials with low wear rates are potential candidates for friction elements in SSRMS and similar mechanisms. Author

N90-22097*# Honeywell, Inc., Glendale, AZ. Satellite Systems Operations.

POSITIVE LUBRICATION SYSTEM c37

Dennis W. Smith and Fred L. Hooper *In* NASA, John F. Kennedy Space Center, The 24th Aerospace Mechanisms Symposium Apr. 1990 p 243-258 (For primary document see N90-22079 15-39)
Avail: NTIS HC A16/MF A03 CSCL 13I

As part of the development of an autonomous lubrication system for spin bearings, a system was developed to deliver oil to grease-lubricated bearings upon demand. This positive oil delivery system (PLUS) consists of a pressurized reservoir with a built-in solenoid valve that delivers a predictable quantity of oil to the spin bearing through a system of stainless steel tubes. Considerable testing was performed on the PLUS to characterize its performance and verify its effectiveness, along with qualifying it for flight. Additional development is underway that will lead to the fully autonomous active lubrication system. Author

N90-22098*# TRW Space Technology Labs., Redondo Beach, CA.

ACTIVE CONTROL OF BEARING PRELOAD USING PIEZOELECTRIC TRANSLATORS c35

Ted W. Nye *In* NASA, John F. Kennedy Space Center, The 24th Aerospace Mechanisms Symposium Apr. 1990 p 259-271 (For primary document see N90-22079 15-39)
Avail: NTIS HC A16/MF A03 CSCL 14B

In many spacecraft applications, mechanisms are required to perform precision pointing operations or to sometimes dither about or track a moving object. These mechanisms perform in a predictable and repeatable manner in benign temperature environments. Severe thermal gradients experienced in actual space applications however, cause assemblies to expand and contract around their bearings. This results in unpredictable changes in bearing preload, and hence bearing friction. This becomes a limitation for servos controlling pointing accuracy. Likewise, uncontrollable vibrations may couple into fixed preload (hence, fixed stiffness) mechanisms and limit pointing accuracy. Consequently, a complex problem faced today is how to design mechanisms that remain insensitive to changing thermal and vibrational spacecraft environments. Research presented involves the simplified modeling and test results of an actuator module that used piezoelectrically preload controlled bearings. The feasibility of actively controlling bearing preload was demonstrated. Because bearing friction is related to preload, a thermally active system designed with aluminum components and a 440 C bearing, was friction tested at temperatures ranging from 0 to 70 C (32 to 158 F). Effectiveness of the translators were demonstrated by mapping a controllable friction range throughout tested temperatures. It was learned that constant preload for this system could be maintained over an approximate 44 C (79 F) temperature span. From testing, it was also discovered that at the more deviate temperatures, expansions were so large that radial clearances were taken up and the duplex bearing became radially preloaded. Thus, active control of bearing preload is feasible but may be limited by inherent geometry constraints and materials used in the system. Author

N90-22099*# Teldix Luftfahrt-Ausruestungs G.m.b.H., Heidelberg (Germany, F.R.).

TEST RESULTS AND FLIGHT EXPERIENCE OF BALL BEARING MOMENTUM AND REACTION WHEELS c37

W. Auer *In* NASA, John F. Kennedy Space Center, The 24th Aerospace Mechanisms Symposium Apr. 1990 p 273-287 (For primary document see N90-22079 15-39)
Avail: NTIS HC A16/MF A03 CSCL 13I

The required satellite mission durations and levels of reliability have been considerably increased: While in the beginning of the 70's 3 to 5 year missions were planned, the standard is now 10 years with an expansion to 15 years and more for such programs as INTELSAT VII. Based on a 20 year test and flight experience with basically the same design, ball bearing momentum and reaction wheels with the required 15 year mission capability can be provided. Author

N90-22100*# MPB Corp., Keene, NH. Miniature Precision Bearings Div.

ON THE DESIGN AND DEVELOPMENT OF A MINIATURE CERAMIC GIMBAL BEARING c37

Robert A. Hanson, Barry ODwyer, Keith M. Gordon, and Edward W. Jarvis *In* NASA, John F. Kennedy Space Center, The 24th Aerospace Mechanisms Symposium Apr. 1990 p 289-300 (For primary document see N90-22079 15-39)
Avail: NTIS HC A16/MF A03 CSCL 13I

A review is made of a program to develop ceramic gimbal bearings for a miniaturized missile guidance system requiring nonmagnetic properties and higher load capacity than possible with conventional AISI 440C stainless steel bearings. A new gimbal design concept is described which utilizes the compressive strength and nonmagnetic properties of silicon nitride (Si3N4) ceramics for the gimbal bearing. Considerable manufacturing development has occurred in the last 5 years making ceramic bearings a viable option in the gimbal design phase. A preliminary study into the feasibility of the proposed design is summarized. Finite element analysis of the brittle ceramic bearing components under thermal stress and high acceleration loading were conducted to ensure the components will not fail catastrophically in service. Finite element analysis was also used to optimize the adhesive joint design. Bearing torque tests run at various axial loads indicate that the average running torque of ceramic bearings varies with load similarly to that of conventional steel bearings. Author

N90-22101*# National Aeronautics and Space Administration. Ames Research Center, Moffett Field, CA.

AX-5 SPACE SUIT BEARING TORQUE INVESTIGATION c54

Stuart Loewenthal, Vic Vykukal, Robert MacKendrick, and Philip Culbertson, Jr. (Sterling Federal Systems, Inc., Palo Alto, CA.) *In* NASA, John F. Kennedy Space Center, The 24th Aerospace Mechanisms Symposium Apr. 1990 p 301-312 (For primary document see N90-22079 15-39)
Avail: NTIS HC A16/MF A03 CSCL 05H

The symptoms and eventual resolution of a torque increase problem occurring with ball bearings in the joints of the AX-5 space suit are described. Starting torques that rose 5 to 10 times initial levels were observed in crew evaluation tests of the suit in a zero-g water tank. This bearing problem was identified as a blocking torque anomaly, observed previously in oscillatory gimbal bearings. A large matrix of lubricants, ball separator designs and materials were evaluated. None of these combinations showed sufficient tolerance to lubricant washout when repeatedly cycled in water. The problem was resolved by retrofitting a pressure compensated, water exclusion seal to the outboard side of the bearing cavity. The symptoms and possible remedies to blocking are discussed. Author

N90-22102*# National Aeronautics and Space Administration. John F. Kennedy Space Center, Cocoa Beach, FL.

DESIGN OF A TELESCOPING TUBE SYSTEM FOR ACCESS AND HANDLING EQUIPMENT c54

Alan C. Littlefield *In its* The 24th Aerospace Mechanisms Symposium Apr. 1990 p 313-327 (For primary document see N90-22079 15-39)

Avail: NTIS HC A16/MF A03 CSCL 05H

Spacecraft processing presents unique problems for the design of ground support equipment. A telescoping tube system consists of a number of nested structural tubes that can be extended and retracted (telescoped) while supporting a load. A typical telescoping tube system provides lateral, torsional, and vertical support for an access platform. Several concepts for improved telescoping tubes were developed with emphasis placed on reliability, ease of maintenance, and cost effectiveness. The most promising prototype design utilizes adjustable rollers running on tracks bolted to the tube sections. A wire rope deployment system ensures that all tube sections are controlled during extension and retraction. Track shimming and roller adjustment allow for fabrication of a high precision tube assembly that does not require extensive machining or unusually large shop equipment. The use of rolling contact eliminates the contamination problems encountered with sliding tubes in previous designs. The prototype design is suitable for indoor or outdoor use. A prototype tube assembly was fabricated and tested for strength, stiffness, maintainability, and endurance. Author

N90-22103*# Lockheed Space Operations Co., Cocoa Beach, FL.

CLEAN ACCESS PLATFORM FOR ORBITER c14

H. Morrison and J. Harris *In* NASA, John F. Kennedy Space Center, The 24th Aerospace Mechanisms Symposium Apr. 1990 p 329-340 (For primary document see N90-22079 15-39)

Avail: NTIS HC A16/MF A03 CSCL 14B

The design of the Clean Access Platform at the Kennedy Space Center, beginning with the design requirements and tracing the effort throughout development and manufacturing is described. Also examined are: (1) A system description; (2) Testing requirements and conclusions; (3) Safety and reliability features; (4) Major problems experienced during the project; and (5) Lessons learned, including features necessary for the effective design of mechanisms used in clean systems. Author

N90-22104*# Thiokol Corp., Cape Canaveral AFS, FL. Space Services Div.

CIRCULARITY MEASURING SYSTEM: A SHAPE GAUGE DESIGNED ESPECIALLY FOR USE ON LARGE OBJECTS c35

G. R. RohrKaste *In* NASA, John F. Kennedy Space Center, The 24th Aerospace Mechanisms Symposium Apr. 1990 p 341-351 (For primary document see N90-22079 15-39)

Avail: NTIS HC A16/MF A03 CSCL 14B

The Circularity Measuring System (CMS) was developed to make an in-situ determination of shape similarity for selected fit large cylinders (RSRM segments). It does this to a repeatable accuracy of 0.10 mm (0.004 inch). This is less that the goal of 0.07 mm (0.003 inch), but was determined adequate because of the addition of an assembly aid that increased the entry chamfer of the clevis side of the joint. The usefulness of the CMS is demonstrated by the application to measurements other than its specified design purpose, such as submarine hull circularity, SRM mid-case circularity, as well as circularity of interfacing SRM tooling, specifically the rounding devices and horizontal disassembly devices. Commercialization of the tool is being pursued, since it is an enhancement of metrology technology for circularity determination. The most accurate in-situ technology it replaces is determined from a template. The CMS is an improvement in accuracy and operation. Author

N90-22105*# National Aeronautics and Space Administration. Langley Research Center, Hampton, VA.

DEVELOPMENT OF CABLE DRIVE SYSTEMS FOR AN AUTOMATED ASSEMBLY PROJECT c37

Charles A. Monroe, Jr. *In* NASA, John F. Kennedy Space Center, The 24th Aerospace Mechanisms Symposium Apr. 1990 p 353-367 (For primary document see N90-22079 15-39)

Avail: NTIS HC A16/MF A03 CSCL 13I

In a robotic assembly project, a method was needed to accurately position a robot and a structure which the robot was to assemble. The requirements for high precision and relatively long travel distances dictated the use of cable drive systems. The design of the mechanisms used in translating the robot and in rotating the assembly under construction is discussed. The design criteria are discussed, and the effect of particular requirements on the design is noted. Finally, the measured performance of the completed mechanism is compared with design requirements. Author

N90-22106# National Inst. of Standards and Technology, Boulder, CO. Fracture and Deformation Div.

INSTITUTE FOR MATERIALS SCIENCE AND ENGINEERING, FRACTURE AND DEFORMATION DIVISION: TECHNICAL ACTIVITIES, 1989

H. I. McHenry, ed. Dec. 1989 84 p

(PB90-155359; NISTIR-89/4149) Avail: NTIS HC A05/MF A01 CSCL 20K

The principle accomplishments in three general research areas: materials performance, properties, and processing are summarized. The Fracture Mechanics, Fracture Physics, Nondestructive Evaluation, and Composite Materials groups work together to detect damage in metals and composite materials and to assess the significance of the damage with respect to service performance. The Cryogenic Materials and Physical Properties groups investigates the behavior of materials at low temperature and measure and model the physical properties of advanced materials, including composites, ceramics and the new high critical temperature superconductors. The Welding and Thermomechanical Processing groups investigate the nonequilibrium metallurgical changes that occur during processing and affect the quality, microstructure, properties and performance of metals. GRA

N90-22107# Princeton Univ., NJ. Dept. of Civil Engineering and Operations Research.

SCATTERING OF WAVES BY INCLUSIONS IN A NONHOMOGENEOUS ELASTIC HALF SPACE SOLVED BY BOUNDARY ELEMENT METHODS

P. K. Hadley, A. Askar (Bogazici Univ., Istanbul, Turkey), and A. S. Cakmak 15 Jun. 1989 131 p

(Contract SUNYRF-88-3002; NSF ECE-86-07591)

(PB90-145699; NCEER-89-0027) Avail: NTIS HC A07/MF A01 CSCL 20K

A technique is presented for examining the interaction of soil layers and structures in a two-dimensional profile subjected to incident SH waves. The analysis is carried out in the frequency domain where the response at any frequency in the spectrum is computed by the boundary element method. This enables the efficient solution of complex geometries, including lenses, tunnels, foundations, and cavities. Results are presented which show that the interaction of closely spaced structures is significant. Author

N90-22108 Wyoming Univ., Laramie.

NONLINEAR FRACTURE MECHANICS USING SEMICIRCULAR SPECIMENS AND TENSION-SOFTENING BEHAVIOR Ph.D. Thesis

Kim D. Basham 1989 290 p

Avail: Univ. Microfilms Order No. DA9003785

The critical stress-intensity factors, K(sub Ic); (also referred to as toughness values) were measured for core-derived semi-circular bend specimens of Berea Sandstone and eastern basalt, using both LEFM and nonlinear fracture mechanic concepts. The K(sub Ic) values obtained from the stress intensity method are compared to true or actual fracture toughness values deduced from a new experimental technique based on the nonlinear J-integral and tension-softening behavior. Tension-softening is the gradual decrease in the tensile strength as the material separates across an eventual failure surface. The critical energy release rate, J(sub

c), is related to the area under the tension-softening curve. From J(sub c), a size-independent fracture toughness is computed. Experimental data based on LEFM underestimate true fracture toughness for laboratory size specimens characterized by quasi-brittle fracture behavior, such as rocks. Two semi-circular bend specimens with slightly different notch lengths were loaded to failure. The load, load line displacement, and crack tip opening displacement were simultaneously recorded throughout the loading process by a fully automated data acquisition/reduction system involving a Keithly System 500 and a Zenith Z-248 computer. An Instron 1332, closed-loop, servohydraulic testing machine and an improved method of machine control was used to record true post-peak load behavior. A FORTRAN program that processes all raw data is presented. The program computes the stress-separation curve and the size-independent fracture toughness. Also, a new and more efficient method of deducing the stress-operation curve is presented. The stress intensity factor method (LEFM) also is discussed in detail. All theoretical concepts and experimental techniques are presented and discussed. The K(sub Ic) values; characteristic lengths, l(sub ch); ligament distances; and specimen dimensions are compared. All results are presented and conclusions are made concerning the application of LEFM and nonlinear fracture mechanic concepts to geomaterials.
Dissert. Abstr.

N90-22109 Pennsylvania Univ., Philadelphia.
A STUDY OF CREEP DAMAGE USING MICRORADIOGRAPHY AND CONTINUUM DAMAGE MECHANICS Ph.D. Thesis
John Edward Benci 1989 205 p
Avail: Univ. Microfilms Order No. DA9004765

The development of intergranular creep damage was investigated in several alloys using the synchrotron x ray microradiography, an x ray imaging technique utilizing the transmitted beam. The technique of synchrotron microradiography was developed and refined. A 100-fold improvement in the resolution of the technique was realized, and features on the order of microns can now be routinely observed. The resolution which can be achieved as well as the factors influencing resolution and sensitivity were determined. The technique was then applied to the study of the development of creep damage around notches in three metals. Notched tensile samples of copper, iron, and a low alloy steel were subjected to slow strain rate tensile testing at 500 or 700 C. The tests were interrupted at various fractions of the creep life. The density and distribution of creep damage was measured from the microradiographs with an image analysis system; and the results from the image analysis were compared to damage predictions from a continuum damage mechanics model of the damage process. Creep damage in the copper alloy was concentrated in a fairly narrow band around the plane of minimum cross-section in the samples. This is in stark contrast to the results from iron and the low alloy steel. The creep damage in these materials developed at fairly sharp angles to the notch or crack plane. The results show that the damage processes in iron and this steel are controlled by the equivalent stress, consistent with a plasticity mechanism of cavity growth. The formation of damage in copper is controlled by the maximum principal or hydrostatic stress, confirming a diffusive creep damage growth process.
Dissert. Abstr.

N90-22110# Queensland Univ., Brisbane (Australia). Dept. of Civil Engineering.
COORDINATE SYSTEMS FOR PLASTIC YIELD SURFACES STRESS AND STRAIN SPACE THEORIES
J. L. Meek and Su Yinong Dec. 1988 45 p
(PB90-164765; RR-CE98; ISBN-0-86776-318-3) Avail: NTIS HC A03/MF A01 CSCL 20K

In stress space, the expressions for yield criteria are given as functions of the principal stresses sigma 1, sigma 2, and sigma 3, or alternatively, the cartesian components sigma ij, and in strain space as functions of epsilon 1, epsilon 2, and epsilon 3 or epsilon ij. Because the yield surfaces are associated with components in the pi plane, these functions are not always easily obtained. Intermediate variables X1, X2, X3 associated with the pi plane are introduced (X3 being coincident with the deviatoric axis). It is found that the yield functions are easily expressed in the chosen coordinate system. These coordinate axes may be used to obtain the expressions for the elastoplastic constitutive matrices used in the finite element analysis. The theory is developed for both stress space and strain space as it is anticipated that the later formulation has an important place in the application of elasto-plastic analysis.
Author

N90-22111# Sandia National Labs., Albuquerque, NM.
COMBINING ACOUSTIC EMISSION LOCATIONS AND A MICROCRACK DAMAGE MODEL TO STUDY DEVELOPMENT OF DAMAGE IN BRITTLE MATERIALS
David J. Holcomb, Charles M. Stone, and Laurence S. Costin 1990 8 p Presented at the 31st US Symposium on Rock Mechanics, Golden, CO, 18-20 Jun. 1990
(Contract DE-AC04-76DP-00789)
(DE90-005195; SAND-89-2913C; CONF-900646-3) Avail: NTIS HC A02/MF A01

Under compressive stresses, brittle polycrystalline materials fail as the result of the growth, interaction and coalescence of microcracks. To predict the deformation of damaging material, constitutive laws developed for such materials must incorporate the effects of crack size, density, orientation, and interaction. A method of incorporating the accumulation and growth of microcracks into a continuum model is to use a measure of microcrack growth and interaction defined as damage. Although a number of damage theories have been proposed, there is no generally accepted experimental technique for detecting and measuring damage. Acoustic emissions (AE) have been correlated with microcrack nucleation and growth. We propose that AE locations and density are useful measures of damage that can be correlated with calculated damage. Our approach is to use acoustic emissions (AE) and computer modeling to study the development of damage in geomaterials.
DOE

N90-22112# Sandia National Labs., Albuquerque, NM. Applied Mechanics III Div.
A CONTINUUM DAMAGE MODEL FOR THE QUASI-STATIC RESPONSE OF BRITTLE MATERIALS
E. P. Chen and D. Y. Tzou (New Mexico Univ., Albuquerque.) 1990 7 p Presented at the International Conference on Micromechanics of Failure of Quasi-Brittle Materials, Albuquerque, NM, 7-8 Jun. 1990
(Contract DE-AC04-76DP-00789)
(DE90-007681; SAND-90-0541C; CONF-9006122-1) Avail: NTIS HC A02/MF A01

An isotropic continuum damage theory which accounts for the degradation of material strength under quasi-static loading conditions has been developed in the present investigation. The damage mechanism in this theory has been selected to be the interaction and growth of subscale cracks. The development of the theory follows closely the strain-rate dependent dynamic model advanced by the first author and his coworkers. Briefly, the cracks are activated by the maximum principal tensile strain and the density of activated cracks is described by a Weibull statistical distribution. The moduli of a cracked solid derived by Budiansky and O'Connell are then used to represent the global material degradation due to subscale cracking. Two additional material constants have been introduced in this model. These constants are determined from uniaxial tensile test data. The model has been implemented into a finite element code. Sample calculations involving the uniaxial and biaxial responses of plain concrete panels are presented to demonstrate the utility of the model.
DOE

N90-22113# Sandia National Labs., Albuquerque, NM. Applied Mechanics Div.
SEVERE SHOCK AND VIBRATION ENVIRONMENTS FOR ELECTRONIC COMPONENTS
David R. Martinez 1990 16 p Presented at the 4th International SAMPE Electronic Materials and Processes Conference, Albuquerque, NM, 12-14 Jun. 1990

(Contract DE-AC04-76DP-00789)
(DE90-007686; SAND-89-2730C; CONF-9006121-1) Avail: NTIS HC A03/MF A01

Electronic components used in system applications must be qualified to mechanical shock and vibration environments. Often these environments are severe, requiring the development and use of special test techniques and procedures. Environmental specifications are based upon analytical model predictions and measured test data. Test specifications are determined after careful consideration of simulation techniques, input levels, dynamic behavior of the test fixturing, as well as an assessment of the degree of conservatism imposed by the specification and testing procedures. The process of determining component shock and vibration specifications is discussed, beginning with the initial description of system and subsystem level environments, and concluding with component level test specifications. Included is a discussion of the difference between environmental specifications and test specifications, and the instrumentation/measurement problems associated with obtaining valid field measurements for severe shock data. The role of finite element analysis in predicting the dynamic structural response of components is also explained. Shock data analysis techniques are described including both time-domain and frequency-domain characterizations of the data. The resonant plate shock testing technique for simulating severe shock environments is presented, including difficulties that arise in practical applications. DOE

N90-22114# Sandia National Labs., Albuquerque, NM. Applied Mechanics Div.

DYNAMIC RESPONSE OF A COMPLEX ENCAPSULATED ELECTRONIC ASSEMBLY SUBJECTED TO A SEVERE SHOCK ENVIRONMENT

Steven N. Burchett 1990 8 p Presented at the 4th International SAMPE Electronic Materials and Processes Conference, Albuquerque, NM, 12-14 Jun. 1990
(Contract DE-AC04-76DP-00789)
(DE90-007689; SAND-89-2617C; CONF-9006121-2) Avail: NTIS HC A02/MF A01

Several complex encapsulated electronic assemblies electrically failed after they were exposed to very severe mechanical shock tests. Postmortem examination showed that a microcomputer ceramic substrate in each assembly was cracked. The stress history in the ceramic substrate was determined using finite element computer analyses to assist in the evaluation of the failures. The purposes of the analyses were: (1) to determine the cause of the failures, (2) to evaluate contributing factors, and (3) to evaluate possible design changes. The results of the analyses compared favorably with experimental results and clearly indicated that ceramic substrate failure during the shock test was possible. The analyses indicated that the natural frequency of the encapsulated assembly was essentially tuned to the resonant plate primary frequency causing amplified responses and high stresses. Additional calculations provided guidance for design improvements that reduced stress levels generated by the severe shock environment. DOE

N90-22115# Sandia National Labs., Albuquerque, NM. Experimental Mechanics Dept.

CONTINUED RESEARCH ON THE STRAIN TO FAILURE OF THICK-WALLED CYLINDERS SUBJECTED TO INTERNAL PRESSURE

Dennis P. Roach and Thomas G. Priddy 1990 22 p Presented at the Pressure Vessels and Piping Conference: Be in Tune for the 90's, Nashville, TN, 17-21 Jun. 1990
(Contract DE-AC04-76DP-00789)
(DE90-008952; SAND-89-2505C; CONF-900617-6) Avail: NTIS HC A03/MF A01

The determination of the fully plastic response and pressure limit of a pressure vessel is of considerable importance in design. In-house experience in weapon development, new aerospace applications and autofrettage operations all require in-depth knowledge of the strength of high pressure containment structures. This paper presents additional results to support the strain-to-failure analysis of thick-walled cylindrical vessels. Both aluminum and steel, with material properties ranging from ductile to brittle, were tested at stress levels through plastic and strain hardening ranges to fracture. From these tests, the pressure-expansion and through thickness yielding characteristics were determined for these specimens. The critical effective plastic strain depends on the level of tensile stress triaxiality which varies through the wall thickness. It is shown that the proposed strain-to-failure criterion is based on this triaxiality of stress in the critical region and can be used to predict the complete pressure versus strain relations and maximum pressure for the test cylinders. DOE

N90-22116# Oak Ridge National Lab., TN.

INCLUSION OF UNSTABLE DUCTILE TEARING AND EXTRAPOLATED CRACK-ARREST TOUGHNESS DATA IN PWR VESSEL INTEGRITY ASSESSMENT

T. L. Dickson, R. D. Cheverton, and D. K. Shum 1990 10 p Presented at the Pressure Vessels and Piping Conference: Be in Tune for the 90's, Nashville, TN, 17-21 Jun. 1990
(Contract DE-AC05-84OR-21400)
(DE90-009427; CONF-900617-8) Avail: NTIS HC A02/MF A01

Over the past several years, the Heavy-Section Steel Technology Program at Oak Ridge National Laboratory has performed a series of large-scale fracture-mechanics experiments. These experiments have demonstrated that prototypical nuclear reactor vessel steels can exhibit crack-arrest toughness values considerably above 220 MPa(center dot)(radical) m, although arrest can be followed immediately by unstable ductile tearing. This report evaluates the influence of the crack-arrest toughness above 220 MPa(center dot)(radical) m on the integrity assessments of nuclear reactor pressure vessels for pressurized-thermal shock (PTS) loading conditions, taking into account the potential for unstable ductile tearing following arrest. The influence of the high crack-arrest toughness data and unstable ductile tearing on pressurized-water reactor vessel integrity assessment is PTS transient dependent. However, it appears that the potential benefit from crack-arrest events corresponding to toughness values above 240 MPa(center dot)(radical) m for low-upper-shelf weld (LUSW) material and above 370 MPa(center dot)(radical) m for those vessels not containing LUSW material will usually be negated by unstable tearing. DOE

N90-22117*# National Aeronautics and Space Administration. Lewis Research Center, Cleveland, OH.

FATIGUE CRACK GROWTH IN UNIDIRECTIONAL METAL MATRIX COMPOSITE

Louis J. Ghosn (Sverdrup Technology, Inc., Cleveland, OH.), Jack Telesman, and Peter Kantzos 1990 9 p Proposed for presentation at the International Fatigue Series, Honolulu, HI, 15-20 Jul. 1990
(NASA-TM-103102; E-5426; NAS 1.15:103102) Avail: NTIS HC A02/MF A01 CSCL 20K

The weight function method was used to determine the effective stress intensity factor and the crack opening profile for a fatigue tested composite which exhibited fiber bridging. The bridging mechanism was modeled using two approaches; the crack closure approach and the shear lag approach. The numerically determined stress intensity factor values from both methods were compared and correlated with the experimentally obtained crack growth rates for SiC/Ti-15-3 (0)(sub 8) oriented composites. The near crack tip opening profile was also determined for both methods and compared with the experimentally obtained measurements. Author

N90-22118# Technische Univ., Delft (Netherlands). Faculty of Aerospace Engineering.

FATIGUE CRACK GROWTH PREDICTIONS FOR VARIABLE-AMPLITUDE AND SPECTRUM LOADING

J. Schijve May 1987 35 p Presented at 3rd International Conference on Fatigue and Fatigue Thresholds, Charlottesville, VA, 28 Jun. - 3 Jul. 1987
(LR-526; ETN-90-96333) Avail: NTIS HC A03/MF A01

A survey of various aspects related to the prediction of fatigue crack growth under variable amplitude loading is presented. Several interaction effects, including crack closure related phenomena, are discussed. Different categories of prediction models and the results of two round-robin programs are discussed. Methods which can be used to check prediction models in detail and criteria to be satisfied are described. Further developments in the field are discussed. ESA

N90-22119# Technische Univ., Delft (Netherlands). Faculty of Aerospace Engineering.
ANILISA: COMPUTATIONAL MODULE FOR KOITER'S IMPERFECTION SENSITIVITY THEORY
J. Arbocz and J. M. A. M. Hol Jan. 1989 91 p
(LR-582; ETN-90-96346) Avail: NTIS HC A05/MF A01

The development of the Delft Interactive Shell Design Code (DISDECO) is described. ANILISA, a part of DISDECO extended to studying anisotropic shell structures under combined loading, is discussed. Nonlinear Donnell type anisotropic shell equations are used. The circumferential dependence is eliminated by Fourier decomposition. The resulting sets of ordinary differential equations are solved numerically via the shooting method. Specified boundary conditions can thus be enforced rigorously not only in prebuckling problems but in buckling and post-buckling problems. Initial results are presented which indicate that in order to obtain reliable results for anisotropic shells, rigorous enforcing of edge restraint and boundary conditions is vital. ESA

N90-22120# Technische Univ., Delft (Netherlands). Faculty of Aerospace Engineering.
COMPUTATIONAL METHODS AND PLASTICITY
Z. Waszczyszyn (Technical Univ. of Cracow, Poland) Feb. 1989 217 p
(LR-583; ETN-90-96347) Avail: NTIS HC A10/MF A02

A series of lecture notes on the plastic properties of metals and alloys are presented. Mathematical models of the deformation process are discussed. The processes of viscoplasticity, elastoplasticity and elastic-viscoplasticity are addressed. Experiments used to identify model parameters are described. A comparison of simple hardening rules is presented. Limit and shakedown analysis of structures by linear programming is discussed. Static, finite element analysis of elastic-plastic structures is outlined. Thermo-elastoplastic creep and viscoplastic analysis is discussed. Buckling of elastic-plastic structures is reviewed. ESA

N90-22121# Technische Univ., Delft (Netherlands). Faculty of Technical Mathematics and Informatics.
DYNAMICS OF AN OSCILLATOR WITH THREE-DEGREES-OF-FREEDOM IN A UNIFORM WINDFIELD
C. G. A. vanderBeek 1989 24 p Sponsored by Netherlands Foundation for Mathematics and Netherlands Organization for Scientific Research
(Rept-89-56; ISSN-0922-5461; ETN-90-96371) Copyright Avail: NTIS HC A03/MF A01

The equations of motion for an oscillator with three degrees of freedom in a uniform windfield are derived. For higher order frequency ratios, the influence of the coupling terms on the occurrence and local stability of periodic motions is studied. The global behavior of the solutions is investigated. A comparison is made with the results of a two degrees of freedom model in order to investigate the influence of the additional degree of freedom. A detailed diagram of the aeroelastic oscillator is presented. A comparison of the results predicted and the actual motion of the oscillator is outlined. ESA

N90-22122# Technische Univ., Delft (Netherlands). Lab. for Engineering Mechanics.
GRAPHS OF THE STATE OF STRESS AT ROUNDED CORNERS
J. P. Benthem and T. Douma 1988 37 p
(MEMT-1; ISBN-90-370-0019-3; ETN-90-96374) Copyright Avail: NTIS HC A03/MF A01

The state of stress around a crack front is investigated. It is well defined by the stress identity factor. The degree to which the stress is diminished by giving a rounded shape to the sharp crack is quantified. Numerical solutions corresponding to wedges of arbitrary angles are presented. The rounding of sharp corners in practice is discussed. Rounding of such corners does not give an exactly hyperbolic shape. It is concluded that smooth curves with the same radius at the top and the same directions of the asymptotes as those of a hyperbola will not differ very much from the hyperbolas used in the study. ESA

N90-22123# Oxford Univ. (England). Dept. of Engineering Science.
TRANSIENT RESPONSE OF A CYLINDRICAL SHELL OF FINITE LENGTH TO TRANSVERSE IMPACT
S. M. Li (Beijing Inst. of Tech., China), H. Z. Zhong, and C. Ruiz 1989 27 p Sponsored by the British Council
(OUEL-1780/89; ETN-90-96410) Avail: NTIS HC A03/MF A01

An exact analytical solution within the linear framework is developed for the transient dynamic impact response of a two-end simply supported cylindrical shell of finite length. The solution obtained is shown to consist in a remarkably simple analytical expression. Several examples of impact loadings are calculated. The results show excellent agreement with those of the computer code ABAQUS. ESA

N90-22124 Connecticut Univ., Storrs.
FREE WAVE PROPAGATION IN ORTHOGONALLY STIFFENED CYLINDERS Ph.D. Thesis
Mark Spencer Bennett 1989 119 p
Avail: Univ. Microfilms Order No. DA9010171

A finite element based methodology is developed to evaluate elastic wave propagation characteristics of orthogonally stiffened circular cylinders. It is assumed that shell stiffeners are spaced at regular intervals; therefore, the structure is spatially periodic in two dimensions. It is known that periodic structures behave as mechanical filters which permit propagating waves to exist only in certain frequency bands. The proposed methodology allows the structural-acoustic analyst to predict the location of these propagation zones and, therefore, design an intrinsically tuned structure. The methodology utilizes periodicity to substantially reduce the number of degrees of freedom required in a finite element analysis of the structure. The method is completely general and allows for detailed modeling of both the shell and its stiffeners. The method is applicable to a variety of stiffened shell structures and is computationally more efficient than a conventional finite element analysis. Numerical examples are presented to verify the technique. A discussion of simple 1-D periodic structures, and a review of the literature relevant to the investigation is also presented. Dissert. Abstr.

N90-22125 California Inst. of Tech., Pasadena.
DYNAMIC RESPONSE OF STRUCTURES WITH UNCERTAIN PARAMETERS Ph.D. Thesis
Hector Antonio Jensen 1990 164 p
Avail: Univ. Microfilms Order No. DA9009380

A technique for obtaining the response of linear structural systems with parameter uncertainties subjected to either deterministic or random excitation is presented. The parameter uncertainties are modeled as random variables or random fields, and are assumed to be time-independent. The new method is an extension of the deterministic finite element method to the space of random functions. First, the general formulation of the method is developed, in the case where the excitation is deterministic in time. Next, the application of this formulation to systems satisfying the 1-D wave equation with uncertainty in their physical properties is described. A particular physical conceptualization of this equation is chosen for study, and some engineering applications are discussed in both an earthquake ground motion and a structural context. Finally, the formulation of the new method is extended to include cases where the excitation is random in time. Application of this formulation to the random response of a primary-secondary system is described. It is found that parameter uncertainties can

have a strong effect on the system response characteristics.
Dissert. Abstr.

N90-22126 Rutgers - The State Univ., New Brunswick, NJ.
THE STRESS FIELD DUE TO AN EDGE DISLOCATION AND SOME FRACTURE PROBLEMS FOR A THREE-PHASE COMPOSITE CYLINDER MODEL Ph.D. Thesis
Haian Luo 1989 175 p
Avail: Univ. Microfilms Order No. DA9008917

An exact solution is given for the stress field due to an edge dislocation embedded in a three-phase composite cylinder. The force on the dislocation is then derived, from which a set of simple approximate formulae is also suggested. It is shown that, in comparison with the two-phase model adopted by Dundurs and Mura (1964), the three-phase model allows the dislocation to have a stable equilibrium position under much less stringent combinations of the material constants. Also, the analysis and calculation show that in the three-phase model the orientation of Burgers vector has only limited effects on the stability of dislocation. Using the derived stress distribution induced by a unit dislocation as the Green's function, the problem of matrix-cracking is analyzed. In the analyses, a radial matrix-crack is assumed to be near a fiber and subjected to several loading conditions. The resultant singular integral equations are solved numerically. The results show that volume concentration of the fiber has nonnegligible influence on the stress intensity factors of the crack. Finally, the arc-shaped interface crack problem in the fiber-reinforced composite materials is investigated. The three-phase composite cylinder model is adopted to take into account the effect of surrounding fibers. Using Muskhelishvili's complex variable method, an exact elastic solution is derived based on the conventional crack opening assumption. The complex stress intensity factors for the interface crack, in the sense defined by Hutchinson, Mear and Rice, are determined.
Dissert. Abstr.

N90-22127 Connecticut Univ., Storrs.
ANALYSIS OF A FINITE TWO-DIMENSIONAL SOLID WITH AN INCLINED CRACK AND A RIGID INCLUSION Ph.D. Thesis
Metin Ozen 1989 219 p
Avail: Univ. Microfilms Order No. DA9010695

The stress field for a two-dimensional, finite solid with a subsurface crack parallel to the contact surface and an inclined crack and a rigid inclusion, was derived. On the contact surface, a Hertzian load was applied to simulate a rolling/sliding contact. The crack tip stress intensity factors, normal and tangential displacement differences at the crack, contact surface normal displacement, and the normal derivatives of the thin shell surrounding the rigid inclusion were chosen as the unknowns. Finite two-dimensional Fourier transformation, in conjunction with the Green-Gauss theorem, was applied to the Navier's equations. The unknowns were expanded into regular Fourier series and Fourier series with square root singular terms. The collocation method was used to solve the system of integral equations resulting from the application of the boundary conditions. This operation lead to an infinite system of linear algebraic equations with respect to the Fourier coefficients of the unknown functions. The stress intensity factors at the crack tips, discontinuities of the displacements across the crack, and the displacement of the load edge were calculated for the subsurface crack case. These results showed very good agreement with the results from a finite element model. Numerical results from the inclined crack and inclusion case could not be presented due to numerical difficulties encountered during the solution phase. Dissert. Abstr.

N90-22128 Illinois Univ., Urbana-Champaign.
THE MECHANICS OF SHEAR BAND FORMATION IN THERMAL VISCOPLASTIC MATERIALS AT HIGH RATES OF LOADING Ph.D. Thesis
Raed A. Sherif 1989 246 p
Avail: Univ. Microfilms Order No. DA9011018

The mechanics of adiabatic shear bands are investigated through the study of a 1-D simple shearing model. The materials considered are assumed to exhibit strain rate hardening, thermal softening, and strain hardening or softening. The mechanism leading to shear band formation is assumed to be a thermo-mechanical mechanism. First, the different stages associated with the localization of plastic flow are identified. The limits of validity of the thermo-mechanical mechanism are then discussed. The existence and uniqueness of a homogeneous, spatially independent solution to the problem is investigated. Accordingly, a distinction between the notions of shear instability and shear localization is presented. Necessary and sufficient conditions for shear instability are derived. The necessary and sufficient conditions for the homogeneous deformation to localize through the use of a linear stability theory are investigated. The analysis is supported by numerical solutions to the nonlinear system of governing equations. The behavior is then investigated of the field variables at the late stages of deformation. An exact steady state formulation is presented for the nonlinear problem. Exact and asymptotic solutions are obtained for the steady state problem. Dissert. Abstr.

N90-22129 Northwestern Univ., Evanston, IL.
GREEN'S FUNCTIONS FOR THE ELASTIC ANNULUS AND THEIR APPLICATION TO VARIOUS CRACK PROBLEMS Ph.D. Thesis
Rebecca Elaine Worden 1989 123 p
Avail: Univ. Microfilms Order No. DA9009694

An analysis of two-dimensional annular regions whose inner boundary is that of either a hole or a perfectly bonded, rigid inclusion is presented. The special case of a disk is also considered. Fast-converging Green's functions for the point load and the dislocation on the annulus are determined and used to build solutions for problems of loaded annular bodies containing a crack. Results are presented for the stresses on the annulus with applied point loads and for crack propagating under the influence of these loads. Problems of cracks propagating in regions where the direction of the principle stresses is changing are examined and curved crack paths are found using a criterion of maximum energy release rate in the direction of crack propagation. Also, included in an appendix, is an examination of the numerical methods used to evaluate the singular integral equations that arise in crack problems and some of the difficulties that are encountered when these methods are used to solve equations containing generalized Cauchy kernels. Dissert. Abstr.

N90-22130 Houston Univ., TX.
AN INVESTIGATION INTO THE FOUNDATIONS OF ELASTIC-PLASTIC FRACTURE MECHANICS Ph.D. Thesis
Yanqiu Zhang 1989 140 p
Avail: Univ. Microfilms Order No. DA9009490

The present dissertation is composed of two parts. In Part 1 the near field at a crack tip contained in elastic-plastic materials under the plane stress and small yielding conditions is investigated using the finite element method. To make the numerical simulation approach a real-life crack problem, a finite strength incremental plasticity theory was employed in the investigation; also a very fine mesh was used to study the large stress gradients near the tip. A comparison of the numerical results with the asymptotic solutions of Hutchinson and of Rice and Rosengren (HRR field) showed that there was no common area near the crack tip in which all of the stress and deformation field components could be characterized by the HRR theory. In Part 2, the optical method of caustics, commonly used in experimental investigations of fracture, was examined both analytically and numerically. Simulations of the caustics were obtained using both the asymptotic HRR field and the numerical results in Part 1. A general method for the determination of the plastic intensity factor at the crack tip and the mode mixity from caustic measurements is proposed.
Dissert. Abstr.

N90-22131 Purdue Univ., West Lafayette, IN.
A SPECTRAL ANALYSIS APPROACH TO WAVE PROPAGATION IN LAYERED SOLIDS Ph.D. Thesis
Stephen Anthony Rizzi 1989 207 p
Avail: Univ. Microfilms Order No. DA9008685

The impact resistance of a structure depends in part on its ability to propagate energy away from the impact site. Further, many situations arise when a detailed analysis of the local behavior is necessary. This is especially true in layered media because the interaction of stress waves with various interface boundaries can generate highly localized wave behavior. A spectrally formulated element designed expressly for solving these types of problems in a highly efficient manner is developed. The spectral formulation is first applied to the problem of a line load on the half plane with particular attention paid to the generation of Rayleigh surface waves. It is then used to study the effect of free, fixed, and elastic boundaries on incident waves. Finally, the case of waves in multi-layered solids is treated. These analytical studies are complemented at each stage by experimental studies using strain gage and accelerometer histories, plus an ultra-high speed camera for dynamic photoelasticity. The availability of this data affords the opportunity to use it actively as input to the spectral tools to solve inverse problems. This synergy of experiment and spectral analysis forms a very powerful tool. Dissert. Abstr.

N90-22132 Purdue Univ., West Lafayette, IN.
THREE-DIMENSIONAL FINITE ELEMENT FORMULATIONS FOR THICK AND THIN LAMINATED PLATES Ph.D. Thesis
Steven Paul Wanthal 1989 155 p
Avail: Univ. Microfilms Order No. DA9008710

Aiming at satisfying the need for modeling the effects of transverse shear and transverse normal stress in thin and thick laminated plates, a family of three quadrilateral displacement finite elements are formulated. The family includes: a 16 node, 40 degree-of-freedom; a 16 node, 48 degree-of-freedom; and a 25 node, 64 degree-of-freedom quadrilateral element for modeling each layer of the laminate. To evaluate the formulation and applicability the present elements are used to model a range of example problems of thin and thick laminated plates in bending and stretching, and the results are compared with alternative solutions. Examples show that these three types of finite elements are capable of modeling, to various degrees, the effects of transverse shear and interlaminar stresses which can cause delamination. Dissert. Abstr.

N90-22133 Akron Univ., OH.
INTERNAL FRACTURES IN MODEL ELASTOMERIC COMPOSITES Ph.D. Thesis
Yuh-Chin Hwang 1990 154 p
Avail: Univ. Microfilms Order No. DA9010643

Finite element methods (FEM) were employed to calculate the stresses set up in a thin rubber layer, bonded between two rigid spheres, when small tensile or compressive deflections are imposed. Values of stiffness were calculated for various spacings of the spheres, i.e., for various thicknesses of the rubber layer. They are in good agreement with earlier experimental measurements of compression stiffness and with the predictions of an approximate theoretical treatment. However, they are strongly affected by small departures of the rubber layer from complete incompressibility. The highest dilatant stress (in tension) is found to be set up on the central axis, near the bonded surfaces, where internal fracture has been observed to occur in similar bonded layers. For moderately thick layers, the axial tensile stress in the center of the layer is substantially higher than the lateral stresses. This feature suggests that the initiation of fracture in this location may not obey the same criterion as for an isotropic stress field, and that a crack, once formed here, will propagate as a tear across the axis of symmetry. FEM was used to calculate the rate of release of strain energy caused by growth of an internal crack in the same model elastic composite under tension. The reduction in strain energy caused by a small circular crack at the interface was found to be only about one half of that due to a similar crack in the center of the layer. A crack in a thin layer caused a much larger rate of energy release, depending on the radius of the layer relative to its minimum thickness. The stress required for growth of an initial crack was therefore relatively small. But the rate of release of energy decreased as the crack grew, indicating that the crack would stabilize at a finite size without severing the specimen in two. Dissert. Abstr.

N90-22134 Northwestern Univ., Evanston, IL.
PROBABILISTIC FINITE ELEMENTS: APPLICATIONS TO FRACTURE AND FATIGUE Ph.D. Thesis
Glen Howard Besterfield 1989 158 p
Avail: Univ. Microfilms Order No. DA9009624

The fusion of the probabilistic finite element method (PFEM) and reliability analysis for probabilistic fracture mechanics (PFM) is presented. The PFEM is extended to PFM using an enriched element to model the singular strain field at the crack-tip. Statistical moments of stress intensity factors are calculated for uncertainties in load, material properties including fracture toughness, component geometry, and crack geometry. The first-order probability of brittle fracture is calculated via an optimization procedure to determine the reliability index. A comprehensive method for determining the probability of fatigue failure for mixed-mode cyclic loading is also presented. The loading is mixed-mode with randomness in the initial and final crack lengths, initial crack angle, and initial crack position, material properties, crack growth law, crack direction law, and loading. The methodology consists of calculating the reliability index, which is used to calculate the probability of fatigue failure. Performance of the methodologies presented are demonstrated on classical mode 1 fracture problems for both brittle fracture and fatigue crack growth. The fusion of PFEM and reliability analysis for PFM is computationally quite efficient and provides a powerful tool for the design engineer. Dissert. Abstr.

N90-22135*# National Aeronautics and Space Administration. Langley Research Center, Hampton, VA.
THE COMPUTATIONAL STRUCTURAL MECHANICS TESTBED DATA LIBRARY DESCRIPTION
Caroline B. Stewart, comp. (Analytical Services and Materials, Inc., Hampton, VA.) Oct. 1988 158 p Revised
(NASA-TM-100645-Rev-1; NAS 1.15:100645-Rev-1) Avail: NTIS HC A08/MF A01 CSCL 20K

The datasets created and used by the Computational Structural Mechanics Testbed software system are documented by this manual. A description of each dataset including its form, contents, and organization is presented. Author

N90-21902*# Jet Propulsion Lab., California Inst. of Tech., Pasadena.
STRUCTURAL FATIGUE IN THE 34-METER HA-DEC ANTENNAS
R. A. VanHek and B. P. Saldua *In its* The Telecommunications and Data Acquisition Report 15 Feb. 1990 p 252-262 (For primary document see N90-21880 15-32)
Avail: NTIS HC A15/MF A02 CSCL 20K

42 GEOSCIENCES (GENERAL)

No abstracts in this category.

43 EARTH RESOURCES AND REMOTE SENSING

Includes remote sensing of earth resources by aircraft and spacecraft; photogrammetry; and aerial photography.

For instrumentation see *35 Instrumentation and Photography.*

N90-22136 Washington Univ., Seattle.
MODELING THE LATERAL DIFFUSION OF FLUORESCENT PARTICLES WITHIN A FOREST CANOPY Ph.D. Thesis

Mark Douglas Schaaf 1989 252 p
Avail: Univ. Microfilms Order No. DA9000307

The objectives were: (1) to develop one or more models that predict the crosswind spread (i.e., sigma(sup 2)(sub y) of gases of small particles released instantaneously from point sources within the stem space of a forest, and (2) to evaluate the accuracy of the proposed models by comparing predicted and observed values of lateral diffusion and dosage using data reported in existing canopy diffusion studies. Three models of sigma(sub 2)(sub y) were developed based on diffusion models for the surface-boundary layer. The models were validated using fluorescent particle diffusion data collected in a Douglas-fir forest by Fritschen et al. (1970). The problem definition and applications are contained. Pertinent literature is reviewed. The development of the three diffusion models are summarized. The methods used to validate the diffusion models are also summarized. The results of the model validation are presented. The conclusions and recommendations are given.
Dissert. Abstr.

N90-22137 State Univ. of New York, Stony Brook.
APPLICATIONS OF REMOTE SENSING TO STUDIES OF OCEANIC UPPER MIXED LAYER DYNAMICS Ph.D. Thesis
Xiao-Hai Yan 1989 229 p
Avail: Univ. Microfilms Order No. DA8926293

Two mixed layer thermal inertia (MLTI) models and one image processing model were developed to measure the thermal inertia of the mixed layer from satellites. Temporal variations in the spatial distribution of the thermal inertia of the mixed layer provide information application to studies of variations in the upper ocean diurnal mixed layer depth in regions of the ocean where diurnal variations in the thermal structure of the upper layer due to horizontal advection and horizontal diffusion are small. One model is numerical, and the other is analytical. Both MLTI models were developed to use remotely-sensed values of sea surface temperature, albedo, and surface wind speeds to calculate the thermal inertia and to predict changes in subsurface diurnal mixed layer depth. The principle of the MLTI model depends on the fact that the diurnal sea surface temperature fluctuation is primarily a function of the thermal inertia and thickness of the diurnal mixed layer, local meteorological conditions, and physical characteristics of the sea surface. The image processing model included automatic geometric rectification and registration, radiometric correction for atmospheric attenuation, pattern recognition for cloud detection and land flagging, and an inverse process for generating a calibration function for image mapping. MLTI models and image processing model were tested using data from LOTUS buoys located in the Sargasso Sea around 34 deg N, 70 deg W. The mixed-layer depths predicted by the MLTI models agree well with data gathered at the LOTUS mooring. Dissert. Abstr.

N90-22138# Instituto de Pesquisas Espaciais, Sao Jose dos Campos (Brazil).
SPECTRAL RESPONSE OF WHEAT AND ITS RELATIONSHIP WITH AGRONOMIC VARIABLES IN THE TROPICAL REGION
Bernardo Friedrich T Rudorff and Getulio Teixeira Batista Dec. 1989 52 p Submitted for publication Sponsored by Fundacao Banco do Brasil
(INPE-5018-RPE/612) Avail: NTIS HC A04/MF A01

The spectral behavior of three varieties of wheat (Anahuac, IAC-24, and BH-1146) was analyzed using field radiometry throughout the 1988 growing season, in the region of Assis, SP. The field radiometric data were obtained in the visible and near infrared portion of the electromagnetic spectrum of 30 sampled fields distributed in commercially planted fields of four farms. The radiometric data were transformed into vegetation indices which are expected to represent crop growing conditions and development. These indice were related to agronomic variables (grain yield, green phytomass, dry phytomass, canopy height, etc.) obtained in ten measurement missions carried out weekly beginning at initial stages of growing (approx. 30 days after planting) until harvesting. The main objective was to verify the potential of spectral data to estimate grain yield of wheat growing in tropical region. It was observed that the vegetation index obtained at rooting to beginning of flowering stages was quite well related to the final grain yield and correlation coefficients of 0.82 to 0.93 were obtained. The radiometric data were analyzed multitemporally also, where the vegetation indices were integrated throughout the growing cycle and related to the final yield. Another analysis, included the incorporation of spectral data into a yield estimation model denominated agrometeorological-spectral model. This model was developed to provide an assessment of the growing conditions of a crop through meteorological and spectral variables. Results obtained clearly indicated that the reflected energy at certain stages of the crop development and at certain wavelength bands are well related to the final grain yield. Therefore, spectral data, transformed into vegetation indices have great potential to be used in yield predicting models for wheat growing in tropical regions.
Author

N90-22139# Instituto de Pesquisas Espaciais, Sao Jose dos Campos (Brazil).
FIELD REPORTS ON RADIOMETRIC CAMPAIGNS OF SOYBEANS IN THE FEDERAL DISTRICT: SAFRA 88/89 [RELATORIO DA CAMPANHA DE MEDIDAS RADIOMETRICAS DA SOJA NO DISTRITO FEDERAL - SAFRA 88/89]
Bernardo Friedrich T Rudorff, Getulio Teixeira Batista, Eduardo Delgado Assad, Eric Stoner, Lucimar Moreira, Plinio Itamar, and Jamil Macedo Feb. 1990 89 p In PORTUGUESE; ENGLISH summary Sponsored by Banco do Brasil
(INPE-5021-RPE/615) Avail: NTIS HC A05/MF A01

Activities involved in the radiometric campaigns carried out throughout the growing season of soybeans in the crop year of 1988 to 1989, in the Federal District of Brazil are discussed. A preliminary analysis of the relationship between spectral data and agronomic parameters is given. The radiometric measurements were acquired by using a spectral radiometer which measures the reflected energy by the crop in the visible and near infrared portion of the electromagnetic spectrum. Data were collected over 30 selected fields from which 20 were over commercial production fields and 10 were in an experimental station. The radiometric (spectral) data were transformed into vegetation indices which represents the growing conditions of the crop. These indices were related to agronomic measurements (yield, fresh biomass, and dry biomass), obtained during six radiometric/agronomic campaigns. The trajectory of the vegetation index (ND) throughout the growing cycle had the expected behavior. The analyses of the relationship between the vegetation indices and agronomic parameters were performed by grouping the fields according to the number of days after planting and reasonable results were obtained for samples with 45 to 55 days after planting. The correlation coefficients between the vegetation index and fresh and dry biomass were 0.69 and 0.57, respectively, considering the entire set of samples of all six campaigns. Author

N90-22140# Beleidscommissie Remote Sensing, Delft (Netherlands).
THE AGRISCATT-87 CAMPAIGN: PROCESSING OF THE DUTSCAT DATA Final Report
P. Snoeij and P. J. F. Swart (Technische Univ., Delft, Netherlands) Oct. 1989 157 p
(BCRS-89-20; ETN-90-96395) Avail: NTIS HC A08/MF A01

The AGRISCATT-87 airborne campaign was completed in Sep. 1987. The data acquired with the multifrequency microwave scatterometer Dutscat is processed and distributed to scientific investigators for assessment. The results for frequency 4 are strongly affected by hardware problems which were not solved until the 6th sortie. A study of the surplus value of reprocessing forested areas is started. The AGRISCATT-87 results are used in a definition study concerning desirable Dutscat modifications and future development. ESA

44 ENERGY PRODUCTION AND CONVERSION

Includes specific energy conversion systems, e.g., fuel cells; global sources of energy; geophysical conversion; and windpower.

For related information see also *07 Aircraft Propulsion and Power, 20 Spacecraft Propulsion and Power,* and *28 Propellants and Fuels.*

N90-22141# Manufacturing and Technolgy Conversion International, Inc., Columbia, MD.
TESTING OF AN ADVANCED THERMOCHEMICAL CONVERSION REACTOR SYSTEM
Jan. 1990 177 p Prepared for Pacific Northwest Lab., Richland, WA
(Contracts DE-AC06-76RL-01830; CEC-500-86-012; PNL-007109-A-C)
(DE90-007989; PNL-7245) Avail: NTIS HC A09/MF A01

This report presents the results of work conducted by MTCI to verify and confirm experimentally the ability of the MTCI gasification process to effectively generate a high-quality, medium-Btu gas from a wider variety of feedstock and waste than that attainable in air-blown, direct gasification systems. The system's overall simplicity, due to the compact nature of the pulse combustor, and the high heat transfer rates attainable within the pulsating flow resonance tubes, provide a decided and near-term potential economic advantage for the MTCI indirect gasification system. The primary objective was the design, construction, and testing of a Process Design Verification System for an indirectly heated, thermochemical fluid-bed reactor and a pulse combustor an an integrated system that can process alternative renewable sources of energy such as biomass, black liquor, municipal solid waste and waste hydrocarbons, including heavy oils into a useful product gas. The test objectives for the biomass portion of this program were to establish definitive performance data on biomass feedstocks covering a wide range of feedstock qualities and characteristics. The test objectives for the black liquor portion of this program were to verify the operation of the indirect gasifier on commercial black liquor containing 65 percent solids at several temperature levels and to characterize the bed carbon content, bed solids particle size and sulfur distribution as a function of gasification conditions. DOE

N90-22142# Midwest Research Inst., Golden, CO.
PHOTOVOLTAIC PROGRAM BRANCH Annual Report, FY 1989
K. A. Summers, ed. Mar. 1990 280 p
(Contract DE-AC02-83CH-10093)
(DE90-000318; SERI/TP-211-3643) Avail: NTIS HC A13/MF A02

This report summarizes the progress of the Photovoltaic (PV) Program Branch of the Solar Energy Research Institute (SERI) from October 1, 1988, through September 30, 1989. The branch is responsible for managing the subcontracted portion of SERI's PV Advanced Research and Development Project. In fiscal year (FY) 1989, this included nearly 50 subcontracts, with a total annualized funding of approximately $13.1 million. Approximately two-thirds of the subcontracts were with universities, at a total funding of nearly $4 million. The six technical sections of the report cover the main areas of the subcontracted program: Amorphous Silicon Research, Polycrystalline Thin Films, Crystalline Silicon Materials Research, High-Efficiency Concepts, New Ideas, and University Participation. Technical summaries of each of the subcontracted programs provide a discussion of approaches, major accomplishments in FY 1989, and future research directions. Each report will be cataloged individually. DOE

N90-22143# Oregon State Univ., Corvallis. Wind Resources Assessment Lab.
REGIONAL WIND ENERGY ASSESSMENT Final Progress Report, Jun. 1988 - May 1989
John E. Wade, Robert W. Baker, and Stel N. Walker Oct. 1989 111 p Prepared for Bonneville Power Administration, Portland, OR
(Contract DE-AI79-86BP-63406)
(DE90-009439; DOE/BP-63406/12; BPA-89-33) Avail: NTIS HC A06

The purpose is to discuss the status of Bonneville Power Administrations wind monitoring program and the data collected from June 1988 through May 1989. The wind monitoring program has been on-going since 1976. The annual summary of this data provides BPA with a periodic status report on both the equipment and wind resonance being measured. There were nine active sites this year. Three sites were instrumented at more than one level. One site, Hampton Butte, apparently failed in November of 1988 and was removed in May of 1989. The data recovery rate for all nine sites over their entire period of record was 82 percent. For each site, data are summarized for the past year. The statistics used to characterize the wind resource include: mean wind speed; peak gust; available energy; Weibull parameters; available energy; data recovery rate; and estimated turbine energy output for eight selected wind turbines. The appendices include summarized data for the entire period of record at these sites. These summaries provide the most important wind speed statistics required by potential wind developers. DOE

N90-22144# Risoe National Lab., Roskilde (Denmark). Test Station for Windmills.
AERODYNAMICS OF A FULL-SCALE, NON ROTATING WIND TURBINE BLADE UNDER NATURAL WIND CONDITIONS
U. S. Paulsen May 1989 6 p
(Risoe-M-2768) Avail: NTIS HC A02/MF A01

Experiments on aerodynamic behavior are carried out under natural wind conditions on a full-scale NACA 44XX series airfoil blade, with a 6.4 m span and a linear variation of taper, thickness and geometrical twist. Bending moments in two directions perpendicular to each other are measured. Bending moments are analyzed in directions parallel and perpendicular to the onset flow and to the chord at the tipsection, and results are compared with different theoretical models using 2-D airfoil section characteristics gathered from wind tunnel (WT) tests. The obtained chord Reynolds Number (Re) ranges between 500,000 and 1,000,000, and the influence on the aerodynamic characteristics is discussed. The onset flow is measured 2 m in front of the blade, at a height of approximately 15.8 m above ground level. The comparison between the experimental and theoretical approaches show significant deviations on drag and lift effects for the blade considered. The main deviation between airfoil characteristics measured in natural wind and those obtained from WT measurements are found in the region where stall occurs. The particular measurements demonstrate at angles of attack after stall that more lift and less drag can be achieved than under WT test conditions. The airfoil-characteristics are analyzed through parameters describing variations governed by shifts in wind direction and wind speed, and through the blade bending motion. Author

N90-22145# Risoe National Lab., Roskilde (Denmark).
ROTOR LOADING ON A THREE-BLADED WIND TURBINE
Peter Hauge Madsen and Flemming Rasmussen [1989] 6 p
Sponsored by Danish Ministry of Energy
Avail: NTIS HC A02/MF A01

For a well designed and adjusted horizontal axis wind turbine, the turbulence in the wind is one of the primary sources of cyclic loading. Wind turbulence not only causes blade loads, but is responsible for the major part of the cyclic rotor loads which are transferred through the rotor shaft. In order to predict the cyclic part of the primary structural rotor loads, the thrust, the yaw and the tilt moment, a model was developed. The model works in the frequency domain and uses the standard engineering representation of turbulence in terms of a coherence function and a power spectrum. The model which accounts for the rotational sampling of the turbulent wind field, shows good agreement with the results of testing programs on wind turbines which are tested at The Test Station for Windmills at Risoe National Laboratory. The comparison is made in terms of both the frequency content of the turbulence induced loads as well as the associated fatigue damage. A parametric study demonstrates the effect of the tower bending and tower torsion flexibility on the magnitude of the cyclic rotor loads. Author

N90-22146# Risoe National Lab., Roskilde (Denmark). Dept. of Meteorology and Wind Energy.
OPTIMIZATION OF POWER OUTPUT FROM WIND TURBINES
Sten Frandsen and Peter Hauge Madsen [1989] 7 p
Avail: NTIS HC A02/MF A01

In high wind climates, the standard wind turbine is not optimized relative to the wind speed distribution, i.e., the machine extracts a lower fraction of the energy available in the wind than theoretically possible. It is demonstrated by an example that the over-all efficiency may be as low as 15 percent while under other circumstances a modern wind turbine is expected to utilize more than 30 percent of the wind energy. Thus, for the same external geometry of the wind turbine, the output may be doubled. The basic mean to increase the over-all-efficiency in high wind speed climates is to increase the rpm of the machine (the present trend in wind turbine optimization is actually the opposite: increasing the swept area by means of blade extenders together with decreased rpm). For stall regulated machines, the consequences of increased rpm include higher rated power and larger aerodynamic loads. The technical impact is analyzed in terms of increase in materials' consumption and the economic benefits obtained by the suggested improvement of efficiency are briefly indicated. The potential cost effectiveness is found to be significant. Author

45 ENVIRONMENT POLLUTION

Includes atmospheric, noise, thermal, and water pollution.

N90-22147*# National Aeronautics and Space Administration, Washington, DC.
FINAL ENVIRONMENTAL IMPACT STATEMENT FOR THE GALILEO MISSION (TIER 2)
May 1989 297 p
(NASA-TM-102925; NAS 1.15:102925) Avail: NTIS HC A13/MF A02 CSCL 13B

This Final Environmental Impact Statement (FEIS) addresses the proposed action of completing the preparation and operation of the Galileo spacecraft, including its planned launch on the Space Transportation System (STS) Shuttle in October 1989, and the alternative of canceling further work on the mission. The only expected environmental effects of the proposed action are associated with normal launch vehicle operation, and are treated in published National Environmental Policy Act (NEPA) documents on the Shuttle (NASA 1978) and the Kennedy Space Center (NASA 1979), and in the KSC Environmental Resources Document (NASA 1986) and the Galileo Tier 1 EIS (NASA 1988a). The environmental impacts of a normal launch were deemed insufficient to preclude Shuttle operations. Environmental impacts may also result from launch or mission accidents that could release plutonium fuel used in the Galileo power system. Intensive analysis of the possible accidents associated with the proposed action reveal small health or environmental risks. There are no environmental impacts in the no-action alternative. The remote possibility of environmental impacts of the proposed action must be weighed against the large adverse fiscal and programmatic impacts inherent in the no-action alternative. Author

N90-22148*# National Aeronautics and Space Administration, Washington, DC.
DRAFT ENVIRONMENTAL IMPACT STATEMENT FOR THE GALILEO MISSION (TIER 2)
Dec. 1988 431 p
(NASA-TM-102926; NAS 1.15:102926) Avail: NTIS HC A19/MF A03 CSCL 13B

This Draft Environmental Impact Statement (DEIS) addresses the environmental impacts which may be caused by the preparation and operation of the Ulysses spacecraft, including its planned launch on the Space Transportation System (STS) Shuttle and the alternative of canceling further work on the mission. The launch configuration will use the STS/Inertial Upper Stage (IUS)/Payload Assist Module-Special (PAM-S) combination. The Tier 1 EIS included a delay alternative which considered the Titan 4 launch vehicle as an alternative booster stage for launch in 1991 or later. However, the U.S. Air Force, which procures the Titan 4 for NASA, could not provide a Titan 4 vehicle for the 1991 launch opportunity because of high priority Department of Defense requirements. The only expected environmental effects of the proposed action are associated with normal Shuttle launch operations. These impacts are limited largely to the near-field at the launch pad, except for temporary stratospheric ozone effects during launch and occasional sonic boom effects near the landing site. These effects have been judged insufficient to preclude Shuttle launches. In the event of: (1) an accident during launch, or (2) reentry of the spacecraft from earth orbit, there are potential adverse health and environmental effects associated with the possible release of plutonium dioxide from the spacecraft's radioisotope thermoelectric generators (RTG). Author

N90-22149 Georgia Inst. of Tech., Atlanta.
THE INTERPRETATION OF SAGE 2 OZONE MEASUREMENTS IN THE LOWER MESOSPHERE Ph.D. Thesis
Ding-Chong Allen Chu 1989 123 p
Avail: Univ. Microfilms Order No. DA8925449

SAGE 2 observations of ozone at sunrise and sunset (solar zenith angle = 90 deg) at approximately the same tropical latitude and on the same day exhibit larger concentrations at sunrise than at sunset between 55 and 65 km altitude. Because of rapid conversion of atomic oxygen to ozone at sunset and the reverse at sunrise, the onion peeling assumption of constant ozone in the SAGE 2 retrievals is invalid in this altitude range. The observations are compared against predictions from a one-dimensional model by deriving simulated ozone profiles obtained by applying the onion peel procedure to model results. Good agreement between the observed and modeled sunrise/sunset ratios is then obtained. The results indicate that the SAGE 2 ozone retrievals overestimate by a factor of 1.3 at sunrise and 1.1 at sunset at 65 km. Between 55 and 60 km altitude the Chapman reactions produce an adequate simulation of the sunrise and sunset ratio, but between 60 and 65 km this ratio is affected by the destruction of O(x) by HO(x) during the first part of the night. SAGE 2 ozone profiles between 60 and 65 km altitude thus provide information on mesospheric HO(x) chemistry not only through profiles averages but also through the sunrise/sunset ratio. The observations, for example, indicate an OH concentration at 65 km altitude in the tropics an hour after dark of approximately 8 x 10(exp 6)/cu cm. Dissert. Abstr.

N90-22150 Oregon Graduate Center for Study and Research, Portland.
GLOBAL DISTRIBUTION OF ORGANO-BROMINE GASES Ph.D. Thesis
Rohith Gunawardena 1989 255 p
Avail: Univ. Microfilms Order No. DA8923577

Both man-made and natural trace organo-bromine gases are present in the atmosphere in minute quantities. The man-made species CBrF3 and CBrClF2 are believed to be an important source of bromine to the stratosphere where they act as catalysts in the chlorofluorocarbon-ozone-depletion hypothesis. A high resolution capillary colum EC-GC method with and O2 doped detector was developed, System 5, to measure these and related organo-bromine gases in the atmosphere. It was developed from a packed column EC-GC method, System 1, that was used to measure CH3I at sub pptv levels but could measure only one organo-bromine gas, CBrClF2. The development work to improve upon System 1 involved testing and matching different types of columns, carrier gases, make-up gases to the detector temperatures to obtain operating conditions with optimum resolution, very high sensitivity and sufficiently stable baseline to measure atmospheric organo-bromine gases. Nine organo-bromine gases were identified in clean background air. The precision of analysis of each system used was sufficient to determine the distributions and time course behavior of the species studied. Dissert. Abstr.

N90-22151 Michigan Univ., Ann Arbor.
THE CALCULATION OF INFRARED LIMB EMISSION BY OZONE IN THE TERRESTRIAL MIDDLE ATMOSPHERE Ph.D. Thesis
Martin Gerard Mlynczak 1989 137 p
Avail: Univ. Microfilms Order No. DA9001685

The calculation of infrared limb emission from the middle atmosphere to space by ozone in the 9 to 11 microns spectral region is discussed. The departure from local thermodynamic equilibrium (LTE) in the vibration-rotation bands of zone is investigated, considering the process of collisional excitation, collisional quenching, chemical pumping, photochemical reaction loss, radiative emission and radiative absorption. As the database of kinetic and spectroscopic rates necessary to construct statistical equilibrium models is very sparse, three different models are developed and their results are compared. The source functions for the nu(sub 3) hot bands and combination bands are calculated from the surface to 110 km in altitude for noon and midnight conditions during mid-latitude winter. The radiance emitted by ozone is calculated for six bands for two of the three statistical equilibrium models considered using a high-resolution, line-by-line infrared emission model. A maximum 32 percent difference in the spectrally integrated radiance between 925 and 1141/cm exists between the two sets of model radiances for tangent paths in the upper mesosphere. The difference in radiance is primarily the result of the differences in the hot band emission. The agreement between the radiances predicted by these two models is best in the lower thermosphere where radiative processes control the populations and also in the middle stratosphere where collisional effects control the populations. The contribution to the total radiance due to emission from two combination bands of carbon dioxide that emit in the 9 to 11 micron spectral region is also calculated. Author

N90-22152# Los Alamos National Lab., NM. Center for National Security Studies.
PROCEEDINGS OF THE CONFERENCE ON TECHNOLOGY-BASED CONFIDENCE BUILDING: ENERGY AND ENVIRONMENT
John C. Allred, ed., Roger C. Eckhardt, ed., and Arthur S. Nichols, ed. Nov. 1989 533 p Conference held in Santa Fe, NM, 9-14 Jul. 1989; sponsored by California Univ.
(CNSS-Papers-22) Avail: NTIS HC A23/MF A03

The aim of the conference was to survey programs of international cooperation in pertinent areas of mutual concern to all nations and to identify new initiatives that could contribute to enhanced international stability, with emphasis on cooperation between the U.S. and the U.S.S.R. Topics addressed include: energy production; nuclear reactor technology; reactor safety; agriculture; global warming; energy use; cooperative ventures; global change; air pollution; scientific exchanges; and geothermal energy technology. For individual titles, see N90-22153 through N90-22154.

N90-22153# US International Space Year Association, Washington, DC.
MISSION TO PLANET EARTH
John L. McLucas *In* LANL, Proceedings of the Conference on Technology-Based Confidence Building: Energy and Environment, Nov. 1989 p 266-274 (For primary document see N90-22152 15-45)
Avail: NTIS HC A23/MF A03 CSCL 13B

The use of space assets to improve the knowledge of dealing with environment change is discussed. Mission to Planet Earth is a research program aimed at knowing the Earth and the changes that are taking place. The Mission of Planet Earth must be supplemented by measurements made on land and in airplanes, sounding rockets, shore stations, and buoys to yield a complete picture. All this must be accompanied by the development of more realistic mathematical models and extensive interdisciplinary analysis, with results compiled to view the environment from a worldwide perspective. A broad interdisciplinary effort is the only hope for dealing with environmental problems on the scale that is required to achieve success, and only by laying out a clear plan for action can the necessary international cooperation be enlisted. Only by having the complete picture can an explanation be made to political leaders around the world as to what is happening, what must be done to curb harmful actions, and how to balance the use of the Earth's resources with the ability of nature to sustain them. B.G.

N90-22154# Houston Univ., TX. Dept. of Physics.
OPPORTUNITIES FOR US-USSR COOPERATION IN THE INVESTIGATION OF ARCTIC STRATOSPHERIC OZONE
W. R. Sheldon *In* LANL, Proceedings of the Conference on Technology-Based Confidence Building: Energy and Environment Nov. 1989 p 349-354 (For primary document see N90-22152 15-45)
Avail: NTIS HC A23/MF A03 CSCL 13B

The model of the polar atmosphere that was developed to account for the Antarctic ozone hole is described, and the northern polar region is shown to be equally vulnerable to episodes of significant ozone depletion, if only very small changes were to occur in Artic weather patterns. In situ investigtion of the stratosphere north of the Arctic circle was the focus of several major campaigns conducted in eary 1989. The results of these efforts are recounted briefly, with emphasis on the CNES stratospheric balloon campaign at Esrange in January 1989, an expedition which provided observations of the initial phase of an ozone hole. Northern polar atmospheric circulation patterns are shown to behave such that ozone hole formation was terminated at an early stage in 1989. However, the point is made that conditions in the northern stratosphere are perilously close to creating an Arctic ozone hole as large as any observed in the Southern Hemisphere. The results could be an ecological disaster north of latitude 65 deg, with the greatest probable threat to Scandinavia and the U.S.S.R. Possible cooperative research programs with the U.S.S.R. to investigate relevant aspects of the polar stratosphere are discussed. Author

N90-22155# National Oceanic and Atmospheric Administration, Silver Spring, MD. Air Resources Lab.
AEROSOL SEPARATOR FOR USE IN AIRCRAFT
Joe F. Boatman, Dennis L. Wellman, William D. Keene, and James N. Galloway (Virginia Univ., Charlottesville.) Dec. 1989 26 p
(PB90-142217; NOAA-TM-ERL-ARL-179) Avail: NTIS HC A03/MF A01 CSCL 13B

When sampling atmospheric aerosols using aircraft, it is sometimes advantageous to separate a portion of the aerosol from the sample stream. During flights through clouds, one may wish to separate all cloud water from the air stream so that interstitial aerosol particles and gases can be measured. Alternately, when flying within the marine boundary layer, one may wish to separate large sea-salt particles from the air stream in order to increase resolution in the calculation of non-sea-salt constituents. The goal of the work was to build and test an aerosol separator. To achieve this goal, a separator was developed, tested in the laboratory and during flights aboard the National Oceanic and Atmospheric Administration King Air research aircraft. The results of the effort are summarized. Author

N90-22156# Environmental Protection Agency, Washington, DC. Office of Toxic Substances.
DETERMINATION OF RATES OF REACTION IN THE GAS-PHASE IN THE TROPOSPHERE: THEORY AND PRACTICE. 2: RATE OF DIRECT PHOTOREACTION: SCREENING-LEVEL TEST GUIDELINE-SPECTROSCOPIC DETERMINATION OF THE CROSS SECTION AND THE MAXIMUM RATE OF DIRECT PHOTOREACTION IN SUNLIGHT
Asa Leifer Nov. 1989 55 p
(PB90-146291; EPA/560/5-89/007) Avail: NTIS HC A04/MF A01 CSCL 13B

A simple and cost effective screening test for estimating an environmentally relevant maximum rate constant and minimum half life for direct photoreaction of a chemical in the gas phase in the troposphere is described in detail. The theory and development of the screening test is discussed and detailed procedures are described for measuring the cross section of a chemical in the gas phase in the laboratory by spectroscopic techniques and data reporting for sections 4 and 5 of TSCA (Toxic Substance and Control Act.) Tables of solar irradiance (J(sub lambda)) are given from 0 to 70 deg North latitude in 10 deg increments as a function of season of the year to cover the continental United States and other parts of the U.S., such as Alaska and Hawaii. An example is given to illustrate the use of the experimental cross section data and solar irradiance data (J(sub lambda)) to estimate the maximum rate of direct photoreaction (kdE)max and the minimum half life t(sub 1/2 E) (sub/min). Author

N90-22157# Environmental Protection Agency, Research Triangle Park, NC. Atmospheric Research and Exposure Assessment Lab.

THE LAMINAR FLOW ELEMENT: ITS USE AS A FLOW STANDARD

William F. Barnard 1990 12 p Presented at the 8th World Clean Air Congress
(PB90-129677; EPA/600/D-89/176) Avail: NTIS HC A03/MF A01 CSCL 13B

A standard device to measure flows accurately and precisely was required by the U.S. Environmental Protection Agency (EPA) to establish an air pollution field auditing system capable of generating pollutant concentrations in the parts per million and parts per billion range. The establishment of a standard normally requires the device possess accuracy and precision specifications at least an order of magnitude (one decade) better than the devices to be calibrated. In the measurement of low flows (less than twenty liters per minute) there are many devices capable of 1 to 2 percent accuracies. The figure generally represents a percentage of full scale. When properly calibrated, the laminar flow element (LFE) is capable of obtaining accuracies better than .3 percent of reading. The LFE's characteristics, calibrations, limitations, and usage in EPA's National Performance Audit Program are presented. Author

N90-22158# National Center for Atmospheric Research, Boulder, CO.

THE SOURCES AND CHEMISTRY OF LATE WINTER ARCTIC TROPOSPHERIC AEROSOLS Ph.D. Thesis

Shao-Meng Li 1989 222 p Prepared in cooperation with Florida State Univ., Tallahassee
(Grant NSF ATM-87-09659)
(PB90-131988; NCAR/CT-122) Avail: NTIS HC A10/MF A02 CSCL 13B

Aerosols at Barrow from 16 March to 7 May 1986 were studied for natural components and pollutants by ion chromatography (IC) and proton induced X ray emission (PIXE) and a receptor model. Organic acid concentrations were high, likely due to condensation. Twenty percent of nonsea salt apparently came from marine organosulfur, traced by methanesulfonate, and 80 percent from NH4HSO4. Combustion aerosols resembled condensates and originated in Europe during a haze event. Sea salt originated in the Beaufort Sea or the North Pacific. Eolian dust was even present. Another aerosol component contained bromine. Ozone varied inversely with bromine when nitrate was low, arguing for a chemical link; otherwise ozone had a pollution origin and was affected by dynamics. Author

N90-22159# Oak Ridge National Lab., TN.

SITE VISIT TO US ANTARCTIC PROGRAM (USAP) FACILITIES AND THE RESEARCH VESSEL POLAR DUKE

Robert M. Reed Apr. 1990 16 p
(Contract DE-AC05-84OR-21400)
(DE90-009396; ORNL/FTR-3571) Avail: NTIS HC A03/MF A01

Site visit to the U.S. Antarctic Program (USAP) Facilities at Palmer Station and the Research Vessel Polar Duke: information collection for an environmental impact statement. Data was collected by interviews with National Science Foundation and ITT/Antarctic Services Staff responsible for environmental management functions. Tours were conducted of the facilities and discussions were held with facility engineers. DOE

N90-22160# Technische Univ., Delft (Netherlands). Faculty of Technical Mathematics and Informatics.

UNCERTAINTY ANALYSIS OF THE ACCIDENT EFFECT AREA OF A BLEVE

Roger Cooke and Hans Meeuwissen 1989 23 p
(Rept-89-49; ISSN-0922-5461; ETN-90-96365) Copyright Avail: NTIS HC A03/MF A01

An uncertainty analysis of models for environmental impact analysis of large accidents involving chemical plants is presented. As the data available for large accidents is unreliable, various parameters in the models are identified as being uncertain. The effect of this parameter uncertainty and modeling uncertainty on the uncertainty of the outcomes of the accident effect area models is investigated. A Monte Carlo simulation is used to study the modeling dependencies between uncertain parameters. It is concluded that the accident area of a Boiling Liquid Expanding Vapor Explosion (BLEVE) has been underestimated by a factor of two in the environmental impact models used to date. ESA

N90-22161 Royal Netherlands Meteorological Inst., De Bilt. Afdeling Fysische Meteorologie.

FROM PENMAN TO MAKKINK: A NEW METHOD FOR THE CALCULATION OF THE CLIMATOLOGICAL EVAPORATION NUMBERS [VAN PENMAN NAAR MAKKINK: EEN NIEUWE BEREKENINGSWIJZE VOOR DE KLIMATOLOGISCHE VERDAMPINGSGETALLEN]

J. C. Hooghart and W. N. Lablans 1988 69 p In DUTCH
(KNMI-TR-111; ISSN-0169-1708; ETN-90-96394) Copyright
Avail: Royal Netherlands Meteorological Inst., Postbus 201, 3730 AE DeBilt, Wilhelminalaan, Netherlands

The calculation of the evaporation numbers following the Penman formula and the Makkink formula was examined. The formulas of Penman, Makkink and Priestley-Taylor are outlined and compared. The method using routinely determined evaporation numbers for the estimation of the evaporation of vegetation based on the so-called vegetation factors, is explained. The evaporation from surface water and the evaporation under special circumstances such as dry periods or winter, is treated. The practical calculation and procurement of evaporation numbers is discussed. Some practical recommendations are given. ESA

N90-22162*# National Aeronautics and Space Administration, Washington, DC.

FINAL ENVIRONMENTAL IMPACT STATEMENT FOR THE ULYSSES MISSION (TIER 2)

Jun. 1990 341 p
(NASA-TM-101104; NAS 1.15:101104) Avail: NTIS HC A15/MF A02 CSCL 13B

This Final (Tier 2) Environmental Impact Statement (FEIS) addresses the environmental impacts which may be caused by implementation of the Ulysses mission, a space flight mission to observe the polar regions of the Sun. The proposed action is completion of preparation and operation of the Ulysses spacecraft, including its planned launch at the earliest available launch opportunity on the Space Transportation System (STS) Shuttle in October 1990 or in the backup opportunity in November 1991. The alternative is canceling further work on the mission. The Tier 1 EIS included a delay alternative which considered the Titan 4 launch vehicle as an alternative booster stage for launch in 1991 or later. This alternative was further evaluated and eliminated from consideration when, in November 1988, the U.S. Air Force, which procures the Titan 4, notified that it could not provide a Titan 4 vehicle for the 1991 launch opportunity because of high priority Department of Defense requirements. The Titan 4 launch vehicle is no longer a feasible alternative to the STS/Inertial Upper Stage (IUS)/Payload Assist Module-Special (PAM-S) for the November 1991 launch opportunity. The only expected environment effects of the proposed action are associated with normal launch vehicle operation and are treated elsewhere. The environmental impacts of normal Shuttle launches were addressed in existing NEPA documentation and are briefly summarized. These impacts are limited largely to the near-field at the launch pad, except for temporary stratospheric ozone effects during launch and occasional sonic boom effects near the landing site. These effects were judged insufficient to preclude Shuttle launches. There could also be environmental impacts associated with the accidental release of radiological material during launch, deployment, or interplanetary trajectory injection of the Ulysses spacecraft. Intensive analysis indicates that the probability of release is small. There are no environmental impacts in the no-action alternative; however, the U.S. Government and the European Space Agency would suffer adverse fiscal and programmatic impacts if this alternative were adopted. The scientific benefits of the mission would be delayed and possibly lost. There could be significant impacts on the ability of the U.S. to negotiate international agreements for cooperative space activities. Author

N90-21908# Admiralty Research Establishment, Portsdown (England).
A SURVEY OF THE MARITIME-AEROSOL DATA COLLECTED AT SOUTH UIST AND THE IMPLICATIONS FOR THE LOWTRAN MARITIME AEROSOL MODEL
N. P. Tolliday, M. H. Smith, P. M. Park, and I. E. Consterdine (Manchester Univ., England) *In* AGARD, Atmospheric Propagation in the UV, Visible, IR, and MM-Wave Region and Related Systems Aspects Mar. 1990 11 p (For primary document see N90-21907 15-32)
Copyright Avail: NTIS HC A16/MF A03; Non-NATO Nationals requests available only from AGARD/Scientific Publications Executive

N90-21909# Centre National de la Recherche Scientifique, Paris (France).
THE MEDITERRANEAN MARINE ENVIRONMENT AND ITS EFFECTS ON AEROSOLS AND INFRARED TRANSMISSION Thesis
Mireille Tanguy *In* AGARD, Atmospheric Propagation in the UV, Visible, IR, and MM-Wave Region and Related Systems Aspects Mar. 1990 13 p In FRENCH (For primary document see N90-21907 15-32)
Copyright Avail: NTIS HC A16/MF A03; Non-NATO Nationals requests available only from AGARD/Scientific Publications Executive

N90-21910*# National Aeronautics and Space Administration. Langley Research Center, Hampton, VA.
NEW SPECTRAL FEATURES OF STRATOSPHERIC TRACE GASES
A. Goldman, F. J. Murcray, R. D. Blatherwick, J. J. Kosters, F. H. Murcray, D. G. Murcray (Denver Univ., CO.), and C. P. Rinsland *In* AGARD, Atmospheric Propagation in the UV, Visible, IR, and MM-Wave Region and Related Systems Aspects Mar. 1990 13 p (For primary document see N90-21907 15-32)
Copyright Avail: NTIS HC A16/MF A03; Non-NATO Nationals requests available only from AGARD/Scientific Publications Executive CSCL 04A

N90-21911# Science Applications International Corp., Billerica, MA.
MINIMIZING THE EFFECTS OF THE ATMOSPHERE IN THE OBSERVATION OF ULTRAVIOLET RADIATION
A. V. Dentamaro, C. G. Stergis, and V. C. Baisley (Air Force Geophysics Lab., Hanscom AFB, MA.) *In* AGARD, Atmospheric Propagation in the UV, Visible, IR, and MM-Wave Region and Related Systems Aspects Mar. 1990 11 p (For primary document see N90-21907 15-32)
Copyright Avail: NTIS HC A16/MF A03; Non-NATO Nationals requests available only from AGARD/Scientific Publications Executive

N90-21912# National Oceanic and Atmospheric Administration, Boulder, CO. Wave Propagation Lab.
SCINTILLATION OF MILLIMETER-WAVE INTENSITY AND PHASE CAUSED BY TURBULENCE AND PRECIPITATION
R. J. Hill, S. F. Clifford, R. J. Lataitis, and A. D. Sarma *In* AGARD, Atmospheric Propagation in the UV, Visible, IR, and MM-Wave Region and Related Systems Aspects Mar. 1990 6 p Sponsored in part by National Research Council (For primary document see N90-21907 15-32)
(Contract MIPR-125-88)
Copyright Avail: NTIS HC A16/MF A03; Non-NATO Nationals requests available only from AGARD/Scientific Publications Executive

46 GEOPHYSICS

Includes aeronomy; upper and lower atmosphere studies; ionospheric and magnetospheric physics; and geomagnetism.

For space radiation see *93 Space Radiation.*

N90-22163 Colorado Univ., Boulder.
SEMIGEOSTROPHIC FLOW OVER OROGRAPHY IN A STRATIFIED ROTATING ATMOSPHERE Ph.D. Thesis
Brian David Gross 1989 146 p
Avail: Univ. Microfilms Order No. DA8923498

Nonuniform flow over orography is examined by means of a semi-geostrophic model. The flow is adiabatic, inviscid, and hydrostatic. A steady solution is presented for flow over an isolated mountain in a uniform potential vorticity model. The decomposition of the physical space solution into fields of translation, rotation, divergence, and deformation forms the basis of the analysis. The principal features associated with the solution are a region of relatively strong cyclonic vorticity in the lee of the mountain, accompanied by convergence, and a region of weaker cyclonic vorticity on the windward slope, accompanied by divergence. Vorticity enhancement by vertical vortex-tube stretching is evaluated as a possible mechanism that may initiate lee cyclogenesis. A time-dependent, isentropic coordinate model is characterized by nonuniform potential vorticity. Steady flow characteristics in the presence of boundary potential temperature gradients are examined by means of a uniform potential vorticity model of linear shear flow over a two-dimensional ridge. Dissert. Abstr.

N90-22164 Maryland Univ., College Park.
ON THREE-DIMENSIONAL SCALING AND CONSISTENT TRUNCATION OF GLOBAL ATMOSPHERIC MODELS Ph.D. Thesis
Ming Ji 1989 137 p
Avail: Univ. Microfilms Order No. DA8924173

A three dimensional scale index based on spherical domain and quasi-geostrophic scale analysis indicates a truncation limit of global atmospheric models which includes both horizontal and vertical dimensions. Based on such a scale index, a numerical experiment is designed using a simplified adiabatic version of the NCAR community climate model (CCMOB) to examine, incorporating nonlinear dynamics alone, whether an optimal horizontal resolution for a nine vertical level (modes) global GCM model can be achieved. In establishing appropriate vertical modes which are independent, can be uniquely scaled, and are physically relevant, an optimal distribution of levels, which was developed is utilized in the experiment. The experimental results which consist of a total of 120 eight day integrations of the CCMOB with ten initial states for each of six horizontal truncations, appear to agree with the conclusions implied by the above referenced three dimensional scale index, considering however only the nonlinear dynamical aspect. It should be noted that due to the simplifications and idealizations made to carry out the experiment, additional studies under more realistic atmospheric conditions are necessary and are encouraged based on the results presented to further validate the existence of the consistency of three dimensional model resolutions. Dissert. Abstr.

N90-22165 Georgia Inst. of Tech., Atlanta.
THE RELATIONSHIP BETWEEN THE BUOYANCY OF NEAR-SURFACE AIR AND THE POTENTIAL TEMPERATURE OF THE TROPOPAUSE Ph.D. Thesis
Robert James Rossi 1989 190 p
Avail: Univ. Microfilms Order No. DA8925462

It was hypothesized that the mixing that defines the upper limit of the troposphere is associated with severe storms. Further, that the air at, and just below, the tropopause is surface air of maximum thermodynamic energy content, drawn into the cores of severe convective cells and rising without dilution to its level of buoyant equilibrium. A quantitative investigation of the hypothesis is reported. It was found that the potential temperature of tropopause air was indeed very similar to the effective potential temperature of air near the surface at the same location or somewhat upwind. The local relationship was found almost throughout the year (centered around the summer) at stations in the northern, western, tropical Pacific and during the summer in Florida and Puerto Rico. This relationship was not found at all at Hilo, Hawaii and over most of the stations on the United States Pacific Coast and over the continental United States. Analysis of sea surface temperatures and convective activity indicated that various Southern Hemisphere tropical areas were the likely source of relatively warm tropopause air observed over the United States Pacific stations. The results presented here indicate that the character of lower tropospheric air plays a large role in determining the depth of the troposphere and that more research on this subject is justified. Dissert. Abstr.

N90-22166*# Lunar and Planetary Inst., Houston, TX.
TOPICAL CONFERENCE ON THE ORIGIN OF THE EARTH
1988 121 p Conference held in Berkeley, CA, 1-3 Dec. 1988; sponsored by Lunar and Planetary Inst. and NASA Johnson Space Center
(Contract NASw-4066)
(NASA-CR-185061; NAS 1.26:185061; LPI-681) Avail: NTIS HC A06/MF A01 CSCL 08G

The abstracts are presented on the topic of the origin of the Earth. The subject of planetary evolution from inner solar system plantesimals through the formation and composition of the Earth's atmosphere and the physical structure of the Earth and the Moon is explored in great variety. B.H.A.

N90-22167 Washington Univ., Seattle.
THE OBSERVED THREE-DIMENSIONAL STRUCTURE OF BAROCLINIC WAVES IN THE NORTHERN HEMISPHERE WINTER AS REVEALED IN A LINEAR REGRESSION ANALYSIS Ph.D. Thesis
Gyu Ho Lim 1989 180 p
Avail: Univ. Microfilms Order No. DA9006974

Transient disturbances with periods shorter than seven days in time series of various meteorological variables from operational analyses are studied for nine winters. The structure of the disturbances was documented using one-point regression maps and cross section assembled from them. The regression coefficients are computed between the unfiltered field time series of meteorological variables and highpass filtered, normalized time series at selected base gridpoints in the oceans. The westward tilt of the axes, wavelength and propagation speed of the disturbances, and their evolution in time, evident in the simultaneous and lag regressions, all are in agreement with those of baroclinic waves in previous theoretical and observational studies. However, the secondary or ageostrophic circulation in baroclinic waves does not comprise a complete circulation on the vertical plane along the axis of the baroclinic wavetrain as common in textbook descriptions. The direction of the ageostrophic wind, near the earth's surface, is perpendicular rather than parallel to the axis of the wavetrain in the real atmosphere. The causes and implications of such orientation of the ageostrophic winds are clarified in view of the dynamics of baroclinic waves. The relative importance of various dynamical processes in baroclinic waves was diagnosed by comparing the regressions of time series of terms in the simplified vorticity and thermodynamic energy equations and the quasigeostrophic tendency and omega equations. Dissert. Abstr.

N90-22168 Pennsylvania State Univ., University Park.
LAGRANGIAN MODEL SIMULATION OF THE TURBULENT TRANSPORT OF EVAPORATING JET DROPLETS Ph.D. Thesis
James Bearer Edson 1989 154 p
Avail: Univ. Microfilms Order No. DA9007844

The HEXOS (Humidity EXchange Over the Sea) subprograms HEXIST (HEXOS EXperiment in Simulation Tunnel) and CLUSE (Couche Limite Unidimensionnelle Stationaire d'Embruns) were designed to investigate the generation, turbulent transport, and evaporation of droplets ejected by bursting bubbles within the air-sea simulation tunnel at Institute de Mecanique Statistique de la Turbulence. Droplet concentration size spectra and turbulence characteristics were measured under various conditions to study the effects of wind speed and humidity on the above processes. The bubbles were produced by aeration devices to insure repeatability when necessary. The Lagrangian model developed as part of this investigation simulates the generation and advection of evaporating jet drops. The technique used to advect the droplets is similar to Langevin simulations of vertical dispersion. However, the approach differs significantly in that the particles (i.e., jet drops) are not constrained to follow the turbulent motion of the wind field exactly. This was accomplished by deriving an expression for the particle's vertical velocity which includes a mean fall velocity, reduced velocity variance, and a particle integral time scale which includes parameters to account for inertial effects and nonzero fall velocity. The source function is derived from an assumed bubble spectrum of the form dN/dr=Cr(-beta), where C and beta are chosen to best fit the measured data. Once chosen, these parameters are fixed so that true comparisons can be between modeled and measured data. The droplets are released at their ejection heights so that droplet production is treated as an elevated source. Profiles of droplet size spectra are then calculated downwind of the source by keeping track of the particle's size and position. These profiles show excellent agreement with those measured during HEXIST and CLUSE. Dissert. Abstr.

N90-22169# Sandia National Labs., Albuquerque, NM. Geomechanics Div.
SURFACE ROUGHNESS AND THE PHYSICAL PROPERTIES OF FRACTURES
Stephen R. Brown 1990 9 p Presented at the 31st US Symposium on Rock Mechanics, Golden, CO, 18-20 Jun. 1990
(Contract DE-AC04-76DP-00789)
(DE90-006046; SAND-89-2126C; CONF-900646-5) Avail: NTIS HC A02/MF A01

This paper presents a brief review of previous work on the effect of surface roughness on the physical properties of fractures. DOE

N90-22170# Los Alamos National Lab., NM.
THE PRESSURE DILATION OF A DEEP, JOINTED REGION OF THE EARTH
Donald W. Brown and Bruce A. Robinson 1990 8 p Presented at the International Conference on Rock Joints, Loen, Norway, 4-6 Jun. 1990
(Contract W-7405-eng-36)
(DE90-007537; LA-UR-90-505; CONF-900640-3) Avail: NTIS HC A02/MF A01

A series of pressurization tests of a 3.5-km deep body of jointed crystalline rock has shown that both the pressure deformation (i.e., dilation) of the region and the boundary permeation are nonlinear functions of the effective stress. This is because the apertures for both the joints and microcracks are strong functions of the effective normal stress acting to close them. For a surface pressure increase from zero to 7.5 MPa, the fluid storage in the natural joints and microcracks in this 0.3 cu m volume of rock increased by 1470 cu m. The corresponding increase in fluid storage between 7.5 and 15 MPa was 1090 cu m. However, even at a surface pressure level of 15 MPa, the permeation loss rate from this large volume of rock is only 0.3 l/s after six months of pressure maintenance. Using transient nonlinear numerical modeling, it is shown that the pressure-dependent fracture permeability model of Gangi, and the fracture porosity equivalent, adequately represent the measured permeability and porosity data obtained to date from this continuing series of pressurization experiments. DOE

N90-22171# California Univ., Berkeley. Lawrence Berkeley Lab. Earth Sciences Div.

EFFECTS OF SINGLE FRACTURES ON SEISMIC WAVE PROPAGATION

L. R. Myer, L. J. Pyrak-Nolte (Purdue Univ., West Lafayette, IN.), and N. G. W. Cook Jan. 1990 8 p Presented at the International Conference on Rock Joints, Loen, Norway, 4-6 Jun. 1990
(Contract DE-AC03-76SF-00098)
(DE90-009191; LBL-28442; CONF-900640-4) Avail: NTIS HC A02/MF A01

Detection and characterization of fractures, joints and faults remains an important problem in mining and geotechnical engineering, as well as in petroleum reservoir engineering. A theoretical model has been developed which predicts the amplitude and group time delay of the transmitted, reflected, and converted waves resulting from a plane wave incident upon a single fracture. It is assumed that seismic stresses are continuous across the interface. Seismic particle displacements, however, are assumed to be discontinuous. For completely dry conditions, the magnitude of the displacement discontinuity is given by the ratio of the seismic stress to the stiffness, (kappa), of the fracture. If a fluid is present in the fracture, we postulate that, in addition to the displacement discontinuity, a velocity discontinuity exists which is equal to the ratio of the seismic stress to specific viscosity, (eta). The wave equation has been solved for two sets of boundary conditions, with each set incorporating both specific stiffness and specific viscosity. These boundary conditions have been designated as Kelvin and Maxwell models. DOE

N90-22172# California Univ., Berkeley. Lawrence Berkeley Lab. Earth Sciences Div.

THE EFFECTS OF TORTUOSITY ON FLOW THROUGH A NATURAL FRACTURE

A. M. Cook, L. R. Myer, N. G. W. Cook, and F. M. Doyle (California Univ., Berkeley.) Jan. 1990 9 p Presented at the 31st US Symposium on Rock Mechanics, Golden, CO, 18-20 Jun. 1990
(Contract DE-AC03-76SF-00098)
(DE90-009193; LBL-28443; CONF-900646-11) Avail: NTIS HC A02/MF A01

Fractures can play a dominant role in the movement of fluid through rock media. As a result, much work has been done, both theoretically and experimentally, on laminar fluid flow through open fractures consisting of parallel plates of varying degrees of surface roughness. In many cases the behavior of the fluid can be described using the expression developed by Lomize (1951) and used by others such as Witherspoon et al. (1980). This equation has become generally known as the cubic law equation because flow rate is proportional to the cube of the aperture. Although the relation of fracture aperture to flow is obvious, tortuosity of the flow paths in a fracture may also have a significant effect on flow. In this paper the results of a series of flow tests performed on a naturally fractured siltstone sample taken at depth from an oil reservoir are presented. The results of flow measurements over a wide range of apertures showed that tortuosity was a primary factor in explaining the difference between the measured flow rates and those predicted by the cubic law equation. DOE

N90-22173# California Univ., Berkeley. Lawrence Berkeley Lab. Earth Sciences Div.

IN-SITU FRACTURE STIFFNESS DETERMINATION

G. J. Hesler, III, Z. Zheng (Terra Tek, Inc., Salt Lake City, UT.), and L. R. Myer Jan. 1990 7 p Presented at the International Conference on Rock Joints, Loen, Norway, 4-6 Jun. 1990 Sponsored in part by Swiss National Cooperative for Nuclear Waste Storage
(Contract DE-AC03-76SF-00098)
(DE90-009202; LBL-28444; CONF-900640-4) Avail: NTIS HC A02/MF A01

In-situ experiments to determine the hydrologic and mechanical characteristics of large naturally occurring fractures were conducted at the NAGRA test site in Grimsel, Switzerland. In addition to seismic measurements across a fracture zone in the FRI test area and flow measurements into the zone, deformation of the fracture resulting from pressurization of the zone was also measured. The deformation is modeled in three different ways: as a mathematical crack employing linear elastic fracture mechanics; as a mathematical crack with an additional restraining stiffness between the faces of the crack, and as a row of coplanar two-dimensional cracks. DOE

N90-22174# California Univ., Berkeley. Lawrence Berkeley Lab. Earth Sciences Div.

COUPLED BEHAVIOR OF ROCK JOINTS

Chin-Fu Tsang Feb. 1990 35 p Presented at the International Conference on Rock Joints, Loen, Norway, 4-6 Jun. 1990 Sponsored by Swedish Nuclear Power Inspectorate, Stockholm
(Contract DE-AC03-76SF-00098)
(DE90-009222; LBL-28600; CONF-900640-5) Avail: NTIS HC A03/MF A01

The behavior of rock joints under various coupled processes is reviewed under four broad categories: hydromechanical processes, thermohydromechanical processes, hydromechanical-chemical processes, and thermomechanical-hydrochemical processes. The state-of-the-art and possible directions of further research in these coupled processes are discussed. Rock joint behaviors considered include not only dilation, closure, shear and joint propagation, but also changes in flow permeability and chemical sorption and retardation capabilities. These properties are of critical concern in practical considerations of the rock mass as a medium to store and isolate chemical and radioactive wastes. Investigations of coupled processes in two-fracture systems and multi-fracture systems are pointed out as interesting areas for future research. The need to consider coupled processes in borehole testing procedures involving rock joints is emphasized. DOE

N90-22175 California Univ., Los Angeles.

FORMULATION OF NON-REFLECTING BOUNDARY CONDITIONS IN NUMERICAL MODELS OF THE ATMOSPHERE Ph.D. Thesis

Sajal Kumar Kar 1989 298 p
Avail: Univ. Microfilms Order No. DA9012997

To eliminate/minimize spurious reflections of small-scale gravity-inertia waves at the material-surface upper boundary of a numerical model of the atmosphere, an energy-absorbing sponge layer is formulated. The sponge layer is designed for forced internal gravity-inertia waves in a resting isothermal atmosphere on an f-plane. The sponge layer is introduced immediately below the material-surface upper boundary. The sponge terms appear as linear damping of the vorticity, divergence, and temperature perturbations inside the sponge layer. The damping coefficient (L) is same for all sponge terms. For small-scale gravity-inertia waves that are most effective in propagating vertical wave energy upwards, two approximate forms of L, namely L(sub 1) and L(sub 2) are derived, neither of which explicitly depend on the sign of frequency and equivalent depth, and as such either can be readily implemented into a time-dependent model. The sponge layer with the coefficient L(sub 1) is designed for a spectral model. The sponge layer with the coefficient L(sub 2), on the other hand, is designed for a finite-difference. The sponge layers in linear time-dependent models were implemented and tested. A lateral sponge layer is designed for linear one-dimensional shallow-water gravity waves. The damping terms inside the sponge layer can selectively damp the characteristic variable advected back (or reflected) into the model domain from the lateral boundary. The lateral sponge layer was implemented in a linear time-dependent model. Dissert. Abstr.

N90-22176 California Univ., Los Angeles.
A NEW STABILITY CRITERION IN THE SHALLOW-WATER SYSTEM FOR TWO-DIMENSIONAL COHERENT EDDIES IN THE ATMOSPHERE AND OCEANS Ph.D. Thesis
Hirofumi Sakuma 1989 78 p
Avail: Univ. Microfilms Order No. DA9010633

A new Lyapunov stability condition is formulated for the shallow water equations, using a gauge variable formalism. This sufficient condition is derived for the class of perturbations that conserve the total mass of the fluid. It is weaker than existing stability criteria, i.e., it applies to a wider class of flows. Formal stability with respect to infinitesimally-small perturbations of arbitrary shape, i.e., the positive definiteness of the second variation of the gauge independent part of a Lyapunov functional, is obtained for two classes of large scale geophysical flows: pseudo eastward flow with constant shear, and localized coherent structures of modon type. Thereby the linear stability of eastward propagating modons, which was hitherto an open question, is proved. The modons whose stability is demonstrated are solutions to the shallow water equations (SWE), while the original modons were derived as solutions for the (potential) vorticity equation of the SWE only. The differences and similarities between these two types of solutions are discussed. Dissert. Abstr.

N90-21919# Air Force Geophysics Lab., Hanscom AFB, MA.
MODELS OF AEROSOLS, CLOUDS, AND PRECIPITATION FOR ATMOSPHERIC PROPAGATION STUDIES
Eric P. Shettle *In* AGARD, Atmospheric Propagation in the UV, Visible, IR, and MM-Wave Region and Related Systems Aspects Mar. 1990 14 p (For primary document see N90-21907 15-32)
Copyright Avail: NTIS HC A16/MF A03; Non-NATO Nationals requests available only from AGARD/Scientific Publications Executive

N90-21921# Naval Research Lab., Washington, DC.
THE NAVAL OCEANIC VERTICAL AEROSOL MODEL Progress Report
Stuart G. Gathman, Gerrit deLeeuw, Kenneth L. Davidson, and Douglas R. Jensen (Naval Ocean Systems Center, San Diego, CA.) *In* AGARD, Atmospheric Propagation in the UV, Visible, IR, and MM-Wave Region and Related Systems Aspects Mar. 1990 11 p Sponsored in part by National Research Council (For primary document see N90-21907 15-32)
Copyright Avail: NTIS HC A16/MF A03; Non-NATO Nationals requests available only from AGARD/Scientific Publications Executive

47 METEOROLOGY AND CLIMATOLOGY

Includes weather forecasting and modification.

N90-22177 Saint Louis Univ., MO.
DYNAMIC AND MICROPHYSICAL CHARACTERISTICS OF CIRRUS CLOUDS AS REVEALED BY AIRCRAFT, LIDAR, AND OTHER OBSERVATIONS DURING FIRE Ph.D. Thesis
Ismail Gultepe 1989 320 p
Avail: Univ. Microfilms Order No. DA9000911

Data on cirrus clouds collected by aircraft, Doppler lidar, satellites, and rawinsondes during the First International Satellite Cloud Climatology Regional Experiment (FIRE) were used. These data, gathered over Wisconsin on 28 and 31 October 1986, were utilized to understand the microphysical, dynamical, and radiative characteristics of cirrus clouds. Aircraft data were collected in the step-up and Lagrangian spiral descent flight patterns for 31 October only. The NOAA Doppler lidar collected backscattering power in the velocity azimuth display (VAD) mode from which Doppler velocities were obtained. Aircraft measurements were not sufficiently accurate to observe vertical velocities (omega) within the cloud; therefore, two techniques were used to obtain omega from divergence. One was the spiral technique which integrated the lateral wind component around a closed flight path to obtain the net divergence. The other technique was the VAD technique which calculated divergences from the Fourier coefficients. The omega was then obtained from the divergence after employing the anelastic continuity equation. Vertical velocities on a large scale were calculated using the isentropic analysis. The large-scale omega's in the vicinity of the cirrus cloud were also estimated from the three radiosondes. Finally, the cloud-scale omega's using the steady-state and mass-flux techniques were calculated from the aircraft measurements. Results showed that the cirrus cloud on 31 October formed in a stable atmosphere and on 28 October they formed within an unstable atmosphere. The local cooling rate because of IR radiative flux in a layer close to the cirrus top on 31 October was about 14 C/day. Moisture and heat advections played important roles in the development of the cirrus cloud; latent heat release did not. Vertical velocities from different techniques ranged from 1 to 2 cm/s at large-scale to 50 cm/s at cloud-scale. Dissert. Abstr.

N90-22178 Washington Univ., Seattle.
CHARACTERISTICS OF CUMULUS BANDCLOUDS OFF THE EAST COAST OF HAWAII Ph.D. Thesis
Graciela Binimelis Raga 1989 162 p
Avail: Univ. Microfilms Order No. DA9000302

A comprehensive study was performed on the thermodynamic and dynamic characteristics of tradewind cumulus clouds off the East coast of Hawaii. The study was based on the analysis of aircraft data collected during the Joint Hawaii Warm Rain Project in 1985. Presented are data from seventeen case studies. The results from individual clouds are combined to obtain a composite picture of the typical Hawaiian cloud. Thermodynamic analysis is used to investigate the sources of the air that is entrained into the clouds. Entrainment was found to occur at all levels; an entrainment rate is estimated from the observations. A simple parcel model with constant lateral entrainment was used to represent the composite Hawaiian cloud, and was found to give good agreement with observations below the trade inversion. An attempt is made to estimate the effect of the presence of the bandclouds on the surrounding environment. Estimates are made of the net divergence of mass, and therefore of moisture and heat, from the system formed by the bands and their near environment. The analysis of the clear air soundings near the bandclouds showed evidence of a decoupling of the trade layer into two sublayers. The role that the clouds play in the determination of these sublayers is discussed. The analysis suggests that the presence of precipitating particles within the bandclouds, and more importantly the loss of water by precipitation, is a possible mechanism for the observed decoupling in the environmental sounding. Author

N90-22179 Saint Louis Univ., MO.
A LINEAR ANALYSIS OF MONSOON BASE STATES ASSOCIATED WITH BANDED CONVECTION Ph.D. Thesis
John Russell Roadcap 1989 265 p
Avail: Univ. Microfilms Order No. DA9000932

The response of a linearized system of anelastic perturbation equations to varied wind, temperature, moisture, and diabatic heating profiles representative of base states found during the Arabian Sea monsoon is investigated as an eigenvalue problem. The diabatic heating profile for deep convection is parameterized using the Anthes scheme which is driven by a 1DSS cloud model. Shallow non-precipitating convection is parameterized using the Betts two layer cloud model. The base state wind profiles are fit with a least squares curve whose order may vary. Eddy diffusion coefficients are determined from the cloud model using a Smagorinsky-Lilly type formulation. Moisture is accessed into the linear model via either boundary layer moisture accession or the vertically-integrated advection over the cloud depth. Sensible warming, a consequence of environmental subsidence, and cooling in the cloud layer below 2 km, a result of the moist downdrafts, are included in the calculations. Results suggest the shapes of the convective heating and horizontal wind profiles are crucial in determining the onset of the longitudinal stationary mode as the precipitation efficiency is increased. Stationary longitudinal modes are associated with a minimum of flux Richardson number in the wavenumber domain. Analysis of the energy transfer spectra suggests that kinetic energy conversion is down-scale for both longitudinal and transverse modes prior to the critical point but becomes up-scale for transverse modes after the onset of stationarity. Dissert. Abstr.

N90-22180 Colorado State Univ., Fort Collins.
SATELLITE VERSUS GCM-SIMULATED RADIATION BALANCE: COMPARISONS AND IMPLICATIONS FOR CLIMATE MODELING Ph.D. Thesis
Laura Dorothy Smith 1989 328 p
Avail: Univ. Microfilms Order No. DA9000490

Measurements of the earth radiation budget (ERB) from spaceborne instruments and long-term simulations of climate with general circulation models (GCMs) make complementary contributions to improve the understanding of cloud-radiation-climate interactions and the role of clouds in the atmospheric general circulation. The global distributions of the planetary radiation balance components and cloudiness computed from long-term climate simulations with the NCAR Community Climate Model (NCAR CCM) were compared against those measured during the Nimbus-7 satellite mission. The latest version of the NCAR CCM, also known as version CCM1, was used. Daily broad-spectral-band narrow angle field-of-view ERB measurements and estimates of cloud amounts derived from satellite radiances were taken during the time period between May 1979 and June 1980. The comparison between model-generated and satellite-observed radiation fields helped identify a major discrepancy in the simulation of climate with NCAR CCM. Analyses of the model-generated cloudiness and its forcing on radiation demonstrated that the high frequency of occurrence of clouds explained most of the difference in the temporal variability between model and observations. It was shown that the prediction of clouds in term of the large-scale relative humidity field and the atmospheric stability, and the treatment of condensation as a complete rainout process, maintained a decoupling between clouds, radiation, and the hydrologic cycle. The impacts of the cloud prediction scheme and the parameterization of the interactions between clouds, and the radiative, dynamic, and thermodynamic processes were separately analyzed from two different climate experiments with CCM1. Dissert. Abstr.

N90-22181# State Univ. of New York, Stony Brook.
SOUTHERN OSCILLATION SIMULATION IN COUPLED OCEAN/ATMOSPHERE GLOBAL CLIMATE MODELS Ph.D. Thesis
Kenneth Robert Sperber 1989 175 p
Avail: Univ. Microfilms Order No. DA8926294

The Southern Oscillation is a major component in the interannual variations of global climate. The Oregon State University Global Climate model with a dynamically interactive upper ocean reproduces in qualitatively correct fashion the major characteristics of the Southern Oscillation. This model stimulates the observed anti-correlation of annually averaged sea-level pressure between the eastern Pacific and the Indonesian region, the primary atmospheric signal of the Southern Oscillation. During the first half of the calender year, positive sea-surface temperature (SST) anomalies propagate eastward towards South America from the tropical western Pacific. These SST anomalies develop in conjunction with the eastward mixed layer current anomalies in the tropical Pacific. In the late summer/early fall anomalously warm water near South America develops and moves westward to merge with the central Pacific anomalies. The decay of the warm phase occurs in mid/late northern winter. The cold phase of the Southern Oscillation enhancement of the zonal circulation, evolves in a fashion similar to the warm phase with the sign of the anomalies reversed, similar to observations. Comparison with a slab version (no ocean dynamics) of the GCM indicates that the Southern Oscillation has its genesis in the atmosphere during northern spring and dynamic ocean interactions act to propagate this atmospheric impetus to other seasons. Southern Oscillation generation in the GCMs indicates that high frequency ocean wave are not necessary for this phenomenon to occur as suggested by Pacific Basin Models. These results also show that ocean/atmosphere global climate models are useful tools investigation of time dependent changes on the interannual timescale in addition to their hitherto accepted use for studying equilibrium properties of climate. Dissert. Abstr.

N90-22182# Oregon State Univ., Corvallis.
CLOUD CHEMISTRY AND OCCURRENCE IN THE WESTERN UNITED STATES: A SYNOPSIS OF CURRENT INFORMATION
Patricia S. Muir and Margi Boehm (NSI Technology Services Corp., Corvallis, OR.) 1989 34 p Presented at the Air Pollution Control Association Annual Meeting, Anaheim, CA, Jun. 1989 Sponsored by EPA and National Acid Precipitation Assessment Program
(PB90-134248; EPA/600/D-89/217) Avail: NTIS HC A03/MF A01 CSCL 04B

Published data on the inorganic chemistry and occurrence of clouds and fogs in the western U.S. in summarized. Cloudwater chemistry differs among regions (southern CA to coastal AK). Most variability in the data can be attributed to differences in total dissolved ionic concentrations among sites. Ionic concentrations generally decrease from urban/industrial sites in southern CA toward forested sites in more remote, northern areas. Differences in cloudwater chemistry among sites generally appear greater than differences among events at a given site. Samples from southern CA are generally more acidic than those from the more northern sites. Most cloud interception is anticipated along the Pacific coast in the Coast Range of northern CA, OR, and WA and along the western slopes of the Cascades. The available data on cloudwater chemistry indicate that these regions experience clouds of relatively low ionic concentrations. However, the limited data should be supplemented to substantiate these results. Author

N90-22183# National Weather Service, Garden City, NY.
SECOND NATIONAL WINTER WEATHER WORKSHOP CONDUCTED BY THE NATIONAL WEATHER SERVICE
Laurence G. Lee, ed. 1988 309 p Workshop held in Raleigh, NC, 26-30 Sep. 1988
(PB90-147414; NOAA-TM-NWS-ER-82) Avail: NTIS HC A14/MF A02 CSCL 04B

Areas of discussion at this workshop include: Synoptic studies of major east coast snowstorms; Model diagnostics of east coast storms; Winter forecast problems associated with light to moderate snow events in the Mid-Atlantic states on 14 and 22 February 1986; Instability bursts and heavy precipitation from extratropical cyclone systems (ECSs); Satellite view of convective type clouds and heavy snow; A method to determine the width of a snow band associated with winter storms by using infrared satellite data; Winter east coast lightning data and survey of lightning strikes in storms; Skill in prediction of explosive cyclogenesis over the western North Atlantic Ocean; Patterns of thickness anomaly for explosive cyclogenesis over the west-central North Atlantic Ocean; The role of melting in determining precipitation type in eastern New York during the storm of October 4th, 1987; A procedure for forecasting precipitation type using NGM low level temperatures and LFM MOS frozen precipitation forecasts; Local objective guidance for predicting precipitation type (LOG/PT) in North Carolina... an alternative to MOS guidance; Winter precipitation type; The operational dilemma of huge numerical model differences; Snow forecasting using physical parameters; Concerning Q-vectors; Major arctic outbreaks affecting Louisiana. GRA

N90-22184 Wisconsin Univ., Madison.
HAIL GROWTH IN A HIGHLY-GLACIATED CENTRAL HIGH PLAINS MULTI-CELLULAR HAILSTORM Ph.D. Thesis
Jerry Michael Straka 1989 425 p
Avail: Univ. Microfilms Order No. DA8914541

The question of how storm kinematics, microphysics, and their interactions affect the production of hail in a multi-cellular, central high plains hailstorm has yet to be satisfactorily answered. One interesting observation in these storms is that they tend to be extremely inefficient precipitation producers, and that they produce very little large hail. During the National Hail Research field project the largest dimensions of the hailstorms observed in the network were only 30 to 35 mm. In this study, a three-dimensional cloud model with detailed hail microphysics was developed to replicate the observed features of one of these hailstorms. The model results have provided details of hailstorms not previously available. With the model results, and comparisons of these results with available observations, a description is provided of how storm kinematics, low density growth, interactions between different hydrometers, and interactions between the microphysics and kinematics result in making northeastern Colorado hailstorms inefficient producers of precipitation and large hail sizes. Important features were related to: (1) that air passes through these storms quite rapidly, and more importantly, (2) that these storms are very highly glaciated. Simulation results suggest that more than 90 percent of the precipitate mass in these storms is ice. Powerful updrafts in the storm core, and the low sticking efficiencies of ice at cold temperatures resulted in a lack of large hydrometeor formation. Observations of several central high plains hailstorms supported these results. Dissert. Abstr.

N90-22185 State Univ. of New York, Albany.
A CASE STUDY OF CLOUD-TO-GROUND LIGHTNING DURING THE GALE PROGRAM Ph.D. Thesis
Thomas J. Kopp 1989 235 p
Avail: Univ. Microfilms Order No. DA9003270

Cloud-to-ground (CG) lightning within a pair of squall lines which propagated through North Carolina, South Carolina, and adjacent off-shore waters on 14 March 1986 were investigated through mesoscale sounding, a single-Doppler radar and lightning direction finder (DF) data. The squall lines passed through a dense network of information gathering systems associated with the Genesis of Atlantic Lows Experiment (GALE), allowing for an analysis of thunderstorms on a variety of different scales. The timing and location of negative and positive CG flashes was then examined with respect to environmental characteristics and storm structure. The squall lines developed ahead of a frontal zone with an associated deepening area of low pressure. The environment in which the thunderstorm cells developed was characterized by conditional instability and warm temperatures at low-levels. The State University of New York's DF network recorded over 8500 CG flashes, of which 15 percent lowered positive charge to ground. This percentage is higher than observed for most thunderstorms. Negative CG flashes occurred primarily in the convective portion of the storm, within areas of higher reflectivity and higher cloud tops. These CG flashes exhibited a striated pattern when plotted over time as they followed the cells within the squall line. Growth of the coldest cloud tops were associated with the highest rates of negative CG flash production. Positive CG flashes primarily occurred under the anvil and within stratiform portions of the storm. They clearly avoided the highest reflectivity regions. The results indicate positive CG flashes occur in regions with small vertical motions and clouds with smaller thicknesses. Considerations of possible charging mechanisms within the stratiform region, where many positive CG flashes occur, implies that both the transport of charge and the production of charge may be important.
Dissert. Abstr.

N90-22186 Pennsylvania State Univ., University Park.
TROPOPAUSE UNDULATIONS AND THE DEVELOPMENT OF EXTRATROPICAL CYCLONES Ph.D. Thesis
Paul Arthur Hirschberg 1989 662 p
Avail: Univ. Microfilms Order No. DA9007868

The hypothesis that the development of extratropical cyclones is influenced by the evolution of temperature anomalies associated with meso-alpha scale tropopause undulations is evaluated. A diagnostic analysis of an observed cyclone is used to show that the three-dimensional distribution of height change is sensitive to the distribution of temperature change in the lower stratosphere, especially near 200 mb. Quantitative analysis of the storm with a geopotential height tendency equation indicates that a synergistic process developed between the upper and lower levels whereby the vertical motion pattern maintained and indentified the lower-stratospheric temperature anomalies while the subsequent upper-level warm advection led to an enhanced vertical circulation. Using the results of this diagnostic study, a physically appealing conceptual model is constructed. The conceptual model is based on the hydrostatic and vertical motion adjustments that occur as tropopause undulations propagate over favored regions of tropospheric warm advection and less stable air. In the second part of the study, an analytic five-layer model is developed to examine the governing hypothesis and the conceptual model. The analytic model yields nonlinear diagnostic solutions to simple initial-value problems. Results of series of model experiments substantiate the results of the case study and many aspects of the new conceptual model. Specifically, it is found that tropospheric cold core baroclinic systems do not show their traditionally observed characteristics unless certain lower-stratospheric temperature configurations associated with tropopause undulations are present. Furthermore, for given tropospheric temperature structures, there are particular lower-stratospheric temperature configurations which optimize the development of the 1000 mb model low. Another important finding from the model study is that altering the baroclinity of the PBL does not significantly affect the instantaneous quasi-geostrophic dynamics. Dissert. Abstr.

N90-22187 Reading Univ. (England).
FRONTAL STRUCTURE IN A MESOSCALE MODEL Ph.D. Thesis
P. D. Ferris 1989 216 p
Avail: Univ. Microfilms Order No. BRDX86895

The results of integrations of a three-dimensional mesoscale model are presented and discussed. The model is used to simulate two observed cases of cold fronts over the British Isles, and also frontogenesis in a deformation field. In the real data cases the model reproduces features of observed frontal regions. Sensitivity experiments show that their presence is due to a combination of the synoptic scale forcing and the local effect of the physical processes. In the idealized simulations the initial state is a two-dimensional baroclinic region in a deformation field. In the absence of physical processes the forming front remains straight and two-dimensional. The frontal gradients are only limited by the model's horizontal diffusion. Some observed features of fronts are reproduced, but there are also some shortcomings. When physical processes are included in the idealized simulations more similarities with observed frontal zones arise. This is in agreement with the real data integrations. In longer integrations with moist processes included some along front asymmetry develops. This is not adequately explained by frontal instability theories. It obtains its energy primarily from convective latent heating and has a short (250 km) along front wavelength. This wavelength is related to the rotationally controlled lengthscale over which the atmosphere reponds to the latent heating. When a perturbation in the form of a low level vortex is imposed on the idealized front, some three dimensional structure develops. At first this is local to the perturbation, but it propagates along the front by the neutral eddy wave mechanism. When the same type of perturbation is applied in a model simulation of an observed quasi-two dimensional front no three dimensional structure amplifies as it is not supported by the two dimensional large scale forcing. Dissert. Abstr.

N90-22188# National Inst. of Polar Research, Tokyo (Japan). Japanese Antarctic Research Expedition.
JARE DATA REPORTS, NO. 140 (METEOROLOGY 21): METEOROLOGICAL DATA AT ASUKA CAMP, ANTARCTICA IN 1987
Takashi Yamanouchi, Kazuo Shibuya, and Ryoki Sakai Nov. 1988 107 p
(ISSN-0075-3343) Avail: NTIS HC A06/MF A01

Surface meteorological observations were made continuously since January 1987 at Asuka Camp. The camp was established as the third Japanese Antarctic station in December 1984. The surface synoptic data taken by the 28th Japanese Antarctic

Research Expedition (JARE) in 1987 is contained. From March 1, surface synoptic reports (FM12-VIII-EXT-SYNOP) at 00, 06, and 12 GMT and monthly summaries (FM71-VI-CLIMAT) were sent to Melbourne, Australia through Syowa and Mawson Stations. The automatic meteorology observation system is composed of sensors and data recording units. Atmospheric pressure, temperature, dew-point temperature, wind direction and speed, and global solar radiation are measured automatically. A windmill type anemometer with a wind vane (aerovane) was installed on a meteorological tower at a height of 10 m above the snow surface. A platinum resistance typer thermometer to measure the air temperature was placed inside an instrument shelter mounted in a ventilated cylinder at a height of 1.5 m above the snow surface. A Dewcel type dew-point thermometer was also placed inside the shelter. The instrument shelter was installed on the snow surface equipped with a lifting mechanism to maintain the height above the surface in case of a rise of the snow surface by a snow drift. A pyranometer to measure the global radiation is mounted on the roof of the observation hut and a barometer is set inside the hut together with recording instruments. Analog signals from the sensors are converted to digital data through transducers and collected by the data logger and recorded on the floppy disk and printer every hour. The analog data are also monitored by the pen recorder. The visibility, cloud amount, genue of cloud and weather phenomena are observed visually according to the WMO standards, at least twice a day at 09 and 15 LT. Author

N90-22189# Los Alamos National Lab., NM.

AN ANOMALOUS WIND BETWEEN VALLEYS: ITS CHARACTERISTICS AND A PROPOSED EXPLANATION

G. L. Stone and D. E. Hoard (Amparo Corp., Santa Fe, NM.) 1990 19 p Presented at the 5th Conference on Mountain Meteorology, Boulder, CO, 26-29 Jun. 1990
(Contract W-7405-eng-36)
(DE90-008965; LA-UR-90-721; CONF-9006111-3) Avail: NTIS HC A03/MF A01

Beginning in 1986, the U.S. Army engaged the Los Alamos National Laboratory to study meteorological operations at several sites where toxic materials are stored. The main objective was to develop recommendations for a system that could forecast the transport and dispersion of airborne materials in the event of an accident. In the course of that project, detailed meteorological and tracer experiments were conducted at the Army's Tooele Depot, 60 km southwest of Salt Lake City, Utah. During these investigations we observed that the direction of near-surface flow through low passes connecting two adjacent valleys is often opposite to the prevailing gradient flow. In this sense, the wind was considered anomalous. The statistical properties of this intervalley flow were discussed and a case study was used to illustrate its vertical structure in relation to the surrounding terrain and the overlying gradient flow. A simplified analysis of the thermal energy changes in the valley atmospheres is used to explain the origin of this local flow. DOE

N90-22190# Los Alamos National Lab., NM.

DAYTIME WIND VALLEYS ADJACENT TO THE GREAT SALT LAKE

G. L. Stone and D. E. Hoard (Amparo Corp., Santa Fe, NM.) 1990 22 p Presented at the 5th Conference on Mountain Meteorology, Boulder, CO, 26-29 Jun. 1990
(Contract W-7405-eng-36)
(DE90-008991; LA-UR-90-720; CONF-9006111-2) Avail: NTIS HC A03/MF A01

In 1986 Los Alamos National Laboratory was engaged by the U.S. Army to study the meteorological aspects of emergency preparedness at several sites where toxic materials are stored and handled. The project included a series of tracer and meteorological field experiments in the vicinity of the Tooele Army Depot. These experiments generated a large data set for validating numerical simulations and for empirical analyses of the local meteorology. The main characteristics of the daytime, up-valley flow at the Utah site, including frequency of occurrence, horizontal and vertical structure, and temporal evolution were discussed. Some parameters controlling the variability in onset time for up-valley flow are identified, and an empirical forecasting scheme is discussed. DOE

N90-22191# Los Alamos National Lab., NM.

THE ASCOT 1988 VALLEY/TRIBUTARY INTERACTION STUDY

William M. Porch and William E. Clements 1990 32 p Presented at the 5th Conference on Mountain Meteorology, Boulder, CO, 26-29 Jun. 1990
(Contract W-7405-eng-36)
(DE90-009043; LA-UR-90-53; CONF-9006111-1) Avail: NTIS HC A03/MF A01

This paper describes a regular oscillation observed in nighttime valley air flows under relatively light upper level wind conditions. The period of these oscillations is about 20 minutes with at least one harmonic at about 10 minutes. These oscillations are important to pollutant dispersion in valley flows at night. The strong coherence of tributary flow and main valley oscillations and the fact that tributary oscillations lead valley oscillation indicate the importance of tributaries as major contributors to the cold air flow in valleys. DOE

N90-22192# Oregon State Univ., Corvallis. Wind Resources Assessment Lab.

REGIONAL WIND ENERGY ASSESSMENT Final Progress Report, Jun. 1987 - May 1988

John E. Wade and Stel N. Walker Sep. 1989 146 p Prepared for Bonneville Power Administration, Portland, OR
(Contract DE-AI79-86BP-63406)
(DE90-009380; DOE/BP-63406/6; BPA-88-28) Avail: NTIS HC A07

The purpose of this report is to discuss the status of Bonneville Power Administrations wind monitoring program and the data collected from 1987 through May 1988. The wind monitoring program has been on-going since 1976. The annual summary of this data provides BPA with a periodic status report on both the equipment and wind resource being measured. There were 12 active sites this year. Three sites were instrumented at more than one level and one site, Cape Blanco, had anemometers at two different locations. The second Cape Blanco anemometer was taken out in January and the Albion Butte site failed in February and was removed in July of 1988. The data recovery rate for all sites this past year was 80 percent. Two sites were inactive for half the year, Albion Butte and Spring Creek. The Spring Creek site experienced reoccurring failure of the data logger cassette interface. Pequop Summit and Upper Pyle also had low data rates because of problems with the cassette tape reader. For each site data are summarized for the entire period of record in the report's Appendices. For three sites there are 12 years of record. These summaries provide the most important wind speed statistics required by potential wind developers. In addition, the appendices contain pressure and temperature data for each site. DOE

N90-22193# Oregon State Univ., Corvallis. Energy Resources Research Lab.

WIND FORECASTING FOR UTILITY OPERATIONS Final Report

John E. Wade, Robert W. Baker, and Stel N. Walker Nov. 1989 62 p Prepared for Bonneville Power Administration, Portland, OR
(Contract DE-AI79-86BP-63406)
(DE90-009466; DOE/BP-63406/9; BPA-89-30) Avail: NTIS HC A04/MF A01

Winds are an important climatic variable in utility operational planning. Light winds reduce air quality, severe winds represent a threat to structures, and dispatchers must know the wind speed if wind energy conversion facility output is to be anticipated. This report examines two wind forecasting problems: forecasting wind energy output and forecasting extremely strong winds. Utilities have long used weather forecasts in making load projections. However, the problem of forecasting wind energy availability presents a new challenge. Wind is one of the hardest weather variables to forecast. In addition, the wind turbine's response to variations in the wind is very nonlinear. To be useful, studies have shown that wind forecasts must be accurate to within 2 mph. The current state of the art appears to be a forecasting error of about 3 mph. DOE

N90-22194# Colorado State Univ., Fort Collins. Dept. of Atmospheric Science.
FORECAST OF ATLANTIC SEASONAL HURRICANE ACTIVITY FOR 1990
William M. Gray 5 Jun. 1990 15 p
Avail: NTIS HC A03/MF A01

Details of a forecast of tropical cyclone activity for the Atlantic Ocean region (including the Caribbean Sea and the Gulf of Mexico) during 1990 are presented. This forecast is based on the ongoing research which relates the amount of seasonal Atlantic tropical cyclone activity to five factors: (1) the El Nino (EN); (2) the Quasi-Biennial Oscillation of equatorial stratospheric wind (QBO); (3) Gulf of Mexico and Caribbean Basin Sea-Level Pressure Anomalies (SLPA); (4) lower latitude Caribbean Basin 200 mb Zonal Wind Anomalies (ZWA); and (5) July-September West African rainfall (AR) amount. Information received up to 4 June 1990 indicates that the 1990 hurricane season can be expected to have about 7 hurricanes, 11 total named storms of at least tropical storm intensity, about 30 hurricane days and a Hurricane Destruction Potential of 90. It is also expected that there should be three major hurricanes of Saffir/Simpson intensity category 3, 4 or 5. This means that the 1990 Atlantic hurricane season will likely be an above average hurricane season, especially as regards to the average hurricane activity of the 1970s and 1980s. This season's hurricane enhancement is due to the expected favorable influences of a westerly phase stratospheric QBO and expected near normal African rainfall. Drought conditions prevailed in Africa from 1970 to 1987. Author

N90-21920# Defence Research Establishment Valcartier (Quebec).
INTERPRETING METEOROLOGICAL DATA REPORTS FOR LOWTRAN NAVY AEROSOL MODEL EXTINCTION CALCULATIONS
A. J. Beaulieu *In* AGARD, Atmospheric Propagation in the UV, Visible, IR, and MM-Wave Region and Related Systems Aspects Mar. 1990 9 p (For primary document see N90-21907 15-32)
Copyright Avail: NTIS HC A16/MF A03; Non-NATO Nationals requests available only from AGARD/Scientific Publications Executive

N90-21923# Forschungsinstitut fuer Optik, Tuebingen (Germany, F.R.).
MODELLING OF OPTICALLY AND IR EFFECTIVE ATMOSPHERIC TURBULENCE
V. Thiermann and A. Kohnle *In* AGARD, Atmospheric Propagation in the UV, Visible, IR, and MM-Wave Region and Related Systems Aspects Mar. 1990 12 p (For primary document see N90-21907 15-32)
Copyright Avail: NTIS HC A16/MF A03; Non-NATO Nationals requests available only from AGARD/Scientific Publications Executive

48 OCEANOGRAPHY

Includes biological, dynamic, and physical oceanography; and marine resources.

For related information see also *43 Earth Resources and Remote Sensing.*

N90-22195# Proudman Oceanographic Lab., Birkenhead (England).
AN INVESTIGATION OF METEOROLOGICAL EFFECTS ON CURRENTS IN THE SHELF AND CONTINENTAL SLOPE SEAS NORTHWEST OF THE UNITED KINGDOM. 2: RELATIONSHIPS BETWEEN CURRENTS AT DIFFERENT LOCATIONS AND WITH OTHER VARIABLES
J. M. Huthnance, D. L. Blackman, M. Dolman, S. Eastman, D. C. MacDonald, C. Stainthorpe, and J. Wolf 1989 116 p
Sponsored by DOE, London, England
(PB90-151911; Rept-6) Avail: NTIS HC A06/MF A01 CSCL 08C

Data from the continental shelf and slope northwest of the UK in the period 19 August 1982 to 23 March 1983, notably from the Continental Slope Experiment (CONSLEX), is given. The development is from previous analysis for individual current meter moorings to consideration of wider groups of data. These include spatial structure across current meter moorings, and relationships between currents and other variables such as temperature, ocean bottom, sea level and meteorological variables. Author

N90-22196# Proudman Oceanographic Lab., Birkenhead (England).
EUROPEAN NETWORK OF INTEREST IN THE MEASUREMENT AND ANALYSIS OF MEAN SEA LEVELS FROM TIDE GAUGE RECORDS
P. L. Woodworth, N. E. Spencer, and G. A. Alcock 1989 45 p
Sponsored by Commission of the European Communities
Prepared in cooperation with Bidston Observatory, Merseyside, England
(PB90-151929; Rept-7) Avail: NTIS HC A03/MF A01 CSCL 08C

A representative current network or community of engineers and scientists engaged in the measurement and analysis of European mean sea levels is listed. Addresses are provided for Permanent Service for Mean Sea Level data suppliers, for Global Level of Sea Surface global network contacts and for individual researchers. Author

N90-22197# Delaware Univ., Newark. Dept. of Mathematical Sciences.
GENERALIZED HERGLOTZ FUNCTIONS AND INVERSE SCATTERING PROBLEM IN A FINITE DEPTH OCEAN
Robert P. Gilbert and Yongzhi Xu Oct. 1989 26 p
(Grant NOAA-NA-86AADSG040)
(PB90-150996; DEL-SG-31-89) Avail: NTIS HC A03/MF A01 CSCL 08C

In an investigation of an underwater acoustic wave inverse scattering problem, namely to recover the shape of a scatterer from the far field pattern of the scattered wave, it was found that, besides the difficulty that the problem is nonlinear and improperly posed, the most difficult point of the problem comes from the fact that the scattered wave field and the far field is not one to one related. The researchers continue the investigation of the problem by seeking an optimal solution in the orthogonal complement of the closure of the set of far field patterns. Author

N90-22198# Beleidscommissie Remote Sensing, Delft (Netherlands).
PRE-STUDY LASER BATHYMETRY
R. W. J. Dirks, H. Hofstraat, D. Spitzer, G. J. Kunz, C. W. Lamberts, G. W. M. vanMierlo, F. P. P. deVries, C. Smorenburg, and H. Visser (Physics and Electronics Lab. TNO, The Hague, Netherlands) Oct. 1989 258 p
(BCRS-89-26; ETN-90-96396) Avail: NTIS HC A12/MF A02

In the framework of the Euromar Advanced Airborne Instrumentation project, pre-study was performed concerning the applicability of the laser bathymetry in Dutch coastal regions. Radiative transfer model of pulsed laser light in the watercolumn is presented, including the bottom effects, using a second order scatter approach. In a parallel study, basic interaction principles of the laser beam with atmosphere, water surface, water bulk and the bottom are described. A concise literature survey is presented of existing laser bathymetry systems with emphasis on hardware specifications. This survey led to a generic set up, which was taken as a starting point for a preliminary design incorporating several novel features. An analysis is given of the software needed for the data acquisition, the in-flight and the off-flight data processing. As a result, a preliminary estimate of the effort involved is given. A number of feasibility studies are suggested for the evaluation of a bathymetric system for the coastal waters of the North Sea. The pre-study supplies basic information for the next execution phase concerning the definition and feasibility of the bathymetric system. ESA

N90-22199# Institute of Oceanographic Sciences, Wormley (England). Deacon Lab.
MEASUREMENT OF THE REFLECTANCE RATIO OF NATURAL LIGHT IN THE SEA
B. Booty 1989 23 p
(IOS-265; ETN-90-96420) Avail: NTIS HC A03/MF A01; Inst. of Oceanographic Sciences, Deacon Lab., Wormley, Godalming, Surrey, GU8 5UB, England, 11 sterling pounds

Theoretical and instrumental aspects of the measurement of reflectance ratios in the sea were considered. Problems were identified and an instrument, designed to avoid fundamental difficulties inherent in this type of measurement, was built. Pre-design experiments and experience at sea with the prototype instrument provided supporting evidence for hypotheses. The thinking is outlined and the main conclusions reached regarding the measurement of sub-surface reflectance ratios are summarized. A brief description of the instrument, designed and constructed for use as a tool for the further development of optical methods for the identification and quantification of materials suspended or dissolved in the sea, is given. ESA

N90-22200# Institute of Oceanographic Sciences, Wormley (England). Deacon Lab.
SURVEY OF INSTRUMENTAL METHODS FOR THE DETERMINATION OF THE HIGH FREQUENCY WAVE SPECTRUM
C. H. Clayson 1989 68 p
(IOS-267; ETN-90-96421) Avail: NTIS HC A04/MF A01; Inst. of Oceanographic Sciences, Deacon Lab., Wormley, Godalming, Surrey, GU8 5UB, England, 19 sterling pounds

Interest in the high frequency wave spectrum has increased because of the importance of decimetric and centimetric wavelength sea surface waves in microwave scattering processes. Existing contact (surface-piercing) and non-contact (remote) sensing techniques for observing high frequency waves both in the time domain and spatially is examined. The defects and limitations of such techniques and how these might be overcome by alternative, largely untried, techniques, are considered. While apparently adequate instruments exist for time domain measurements in laboratory tanks, reservoirs, or small lakes, the observed nature of high frequency waves suggests that an adequate description of the processes can only be achieved by spatial measurements using, for example, high resolution stereophotography, in the open sea. ESA

N90-22201# Institute of Oceanographic Sciences, Wormley (England). Deacon Lab.
A FREE SURFACE BRYAN-COX-SEMTNER MODEL
P. D. Killworth, D. Stainforth, D. J. Webb, and S. M. Paterson 1989 172 p
(IOS-270; ETN-90-96422) Avail: NTIS HC A08/MF A01; Inst. of Oceanographic Sciences, Deacon Lab., Wormley, Godalming, Surrey, GU8 5UB, England, 40 sterling pounds

A version of the Cox numerical ocean general circulation model, adapted to include a free surface, is described and documented in detail. The model is designed for the following uses: tidal studies (a tidal option is explicitly included); assimilation of satellite altimetric data (since the surface elevation is now a prognostic variable); and in situations where accurate relaxation to obtain the stream function in the original model is too time-consuming. The model has been produced using the Cox update scheme, making it simple to use by modelers already in a position to use the Cox model. A full listing is, however, also included. Example output is provided, and computations are compared with the equivalent Cox runs. ESA

51 LIFE SCIENCES (GENERAL)

N90-22202*# Texas Univ. Health Science Center, Houston. Bioprocessing Research Center.
RESEARCH IN BIOLOGICAL SEPARATIONS AND CELL CULTURE Annual Report No. 3, 1 Jun. 1987 - 31 May 1988
L. Scott Rodkey Jun. 1988 172 p
(Contract NAS9-17403)
(NASA-CR-172060; NAS 1.26:172060) Avail: NTIS HC A08/MF A01 CSCL 06C

During the final months, some experiments were initiated in an effort to study the nonreproducibility of cell separations that were attempted up to that time. During the final month, data was collected which clearly shows that the lack of precision and resolution in cell separations is a direct function of the inappropriate buffers that were chosen to be used in the McDonnell Douglas continuous flow electrophoresis system. The nonreproducibility and poor resolution of cell separation systems which had been an ongoing problem for many years was solved. The correct buffer is, at present, unkown. However, it is now quite clear that the next logical effort in the area of cell separations by continuous flow electrophoresis needs to be in finding an appropriate buffer system which buffers at the pH at which the system operates. Task 4, studies of recycling isoelectric focusing, progressed very well. Studies were completed in comparing the McDonnell Douglas continuous flow electrophoresis system with the recycling isoelectric focusing system and the results are unequivocal. During the year, ampholyte synthesis was refined and extended so that new classes of ampholytes are now available for high resolution work. Studies of electrodissolution were performed, as were studies of ampholyte-protein interactions. Finally, a new design of recycling isoelectric focusing hardware was built and tested. Three of the tasks within the Bioprocessing Research Center (7, 8, and 9) were performed. These studies generally encompass the area of bioreactor design and function. Studies in this category include work on fluid dynamics that occur in bioreactors, design of bioreactor control systems, and identification and assessment of stress forces on cells. Author

N90-22203* Lockheed Engineering and Sciences Co., Washington, DC.
USSR SPACE LIFE SCIENCES DIGEST, ISSUE 25
Lydia Razran Hooke, ed., Ronald Teeter, ed., Victoria Garshnek, ed., and Joseph Rowe, ed. (Library of Congress, Washington, DC.) Washington NASA Jan. 1990 107 p
(Contract NASw-4292)
(NASA-CR-3922(29); NAS 1.26:3922(29)) Avail: NTIS HC A06/MF A01 CSCL 06C

This is the twenty-fifth issue of NASA's Space Life Sciences Digest. It contains abstracts of 42 journal papers or book chapters published in Russian and of 3 Soviet monographs. Selected abstracts are illustrated with figures and tables from the original. The abstracts in this issue have been identified as relevant to 26 areas of space biology and medicine. These areas include: adaptation, body fluids, botany, cardiovascular and respiratory systems, developmental biology, endocrinology, enzymology, equipment and instrumentation, exobiology, gravitational biology, habitability and environmental effects, human performance, immunology, life support systems, man-machine systems, mathematical modeling, metabolism, microbiology, musculoskeletal system, neurophysiology, nutrition, operational medicine, psychology, radiobiology, reproductive system, and space biology and medicine. Author

N90-22204 New South Wales Univ., Sydney (Australia).
EXCITATORY AND INHIBITORY BACKWARD CONDITIONING IN THE RAT Ph.D. Thesis Abstract Only
Stephen C. Provost May 1988 4 p
Avail: Issuing Activity

The experiments sought to test the explanations provided by theories of conditioning for the outcome of a backward conditioning arrangement. The experiments all employed a conditioned emotional response (CER) procedure with rat subjects. The nature of the variables responsible for the development of inhibitory conditioning in a backward arrangement was examined in Experiments 1 to 5. Experiments 1, 2, and 3 demonstrated that both the consistency of the intertrial intervals (ITIs) separating U.S. presentations, and the length of the backward interstimulus interval (ISI) separating the CS from the U.S., were involved in the determination of inhibitory strength. Experiment 4 was designed to provide evidence that might support an explanation for the role of the backward ISI in terms of formal theories of conditioning. Experiment 5 was an attempt to provide an explanation for the role of the ITI in terms of opponent-process theories of conditioning. Although the evidence from both experiments was inconclusive, Experiment 5 provided some evidence that excitatory backward conditioning was possible in this preparation. Experiment 6 confirmed this possibility with a more intense U.S. than Experiments 1 to 5, and showed that excitatory backward conditioning was not effected by the presence of a signal for the U.S. Experiments 7 and 8 demonstrated that excitatory backward conditioning also was not influenced by the consistency of the ITIs separating U.S. presentations. Opponent-process theories provide the most adequate explanation for the evidence obtained, although no single experiment provided a critical test of any theory. The fundamental issue which must be addressed by an opponent-process theory for it to provide a complete account of backward conditioning is the involvement of the ITI in inhibitory conditioning. At least one possible account, which points to the possibility of forward trace conditioning taking place when the ITI is varied, seems implausible given the results of these experiments. An alternative account, based upon Star's critical decay duration hypothesis, is suggested: Variability of the ITI may have a direct effect upon growth of opponent processes. The implications of this view for future investigations of backward conditioning, and opponent-process theory in general, are considered. Dissert. Abstr.

N90-22205*# Alabama Univ., Birmingham. Dept. of Biochemistry.
THE CHEMICAL BASIS FOR THE ORIGIN OF THE GENETIC CODE AND THE PROCESS OF PROTEIN SYNTHESIS Final Report
James C. Lacey, Jr. 16 May 1990 74 p
(Grant NGR-01-010-001)
(NASA-CR-186590; NAS 1.26:186590) Avail: NTIS HC A04/MF A01 CSCL 06C

A model for the origin of protein synthesis. The essential features of the model are that 5'-AMP and perhaps other monoribonucleotides can serve as catalysts for the selective synthesis of L-based peptides. A unique set of characteristics of 5'-AMP is responsible for the selective catalysts and these characteristics are described in detail. The model involves the formation of diesters as intermediates and selectivity for use of the L-isomer occurs principally at the step of forming the diester. However, in the formation of acetyl phenylalanine-AMP monoester there is a selectivity for esterification by the D-isomer. Data showing this selectivity is presented. This selectivity for D-isomer disappears after the first step. The identity was confirmed of all four of possible diesters of acetyl-D- and -L phenylaline with 5'-AMP by nuclear magnetic resonance (NMR). The data using flourescence and NMR show the Trp ring can associate with the adenine ring more strongly when the D-isomer is in the 2' position than it can when in the 3' position. These same data also suggest a molecular mechanisim for the faster esterificaton of 5'-AMP by acetyl-D-phenylaline. Some new data is also presented on the possible structure of the 2' isomer of acetyl-D-tryptophan-AMP monoester. The HPLC elution times of all four possible acetyl diphenylalanine esters of 5'-AMP were studied, these peptidyl esters will be products in the studies of peptide formation on the ribose of 5'-AMP. Other studies were on the rate of synthesis and the identity of the product when producing 3'Ac-Phe-2'tBOC-Phe-AMP diester. HPLC purification and identification of this product were accomplished. Author

N90-22206# Paraiba Univ., Joao Pessoa (Brazil).
PROCEEDINGS OF THE 6TH REGIONAL SYMPOSIUM ON BIOPHYSICS
1988 67 p In PORTUGESE Symposium held in Joao Pessoa, Brazil, 8-10 Dec. 1988
(DE90-619618; INIS-BR-1797; CONF-8812131) Avail: NTIS (US Sales Only) HC A04/MF A01

Topics addressed include: molecular biophysics, radiobiology, photobiology, and biophysics of processes and systems. DOE

52 AEROSPACE MEDICINE

Includes physiological factors; biological effects of radiation; and effects of weightlessness on man and animals.

N90-22207*# National Aeronautics and Space Administration, Washington, DC.
AEROSPACE MEDICINE AND BIOLOGY: A CONTINUING BIBLIOGRAPHY WITH INDEXES (SUPPLEMENT 334)
Feb. 1989 50 p
(NASA-SP-7011(334); NAS 1.21:7011(334)) Avail: NTIS HC A03; NTIS standing order as PB90-912300; $11.50 domestic, $23.00 foreign CSCL 06E

This bibliography lists 254 reports, articles and other documents introduced into the NASA Scientific and Technical Information System during February, 1990. Subject coverage includes: aerospace medicine and psychology, life support systems and controlled environments, safety equipment, exobiology and extraterrestrial life, and flight crew behavior and performance. Author

N90-22208* National Aeronautics and Space Administration, Washington, DC.
AEROSPACE MEDICINE AND BIOLOGY: A CONTINUING BIBLIOGRAPHY WITH INDEXES (SUPPLEMENT 335)
Feb. 1989 58 p
(NASA-SP-7011(335); NAS 1.21:7011(335)) Avail: NTIS HC A04; NTIS standing order as PB89-912300, $11.50 domestic, $23.00 foreign CSCL 06E

This bibliography lists 143 reports, articles and other documents introduced into the NASA Scientific and Technical Information System during March, 1990. Subject coverage includes: aerospace medicine and psychology, life support systems and controlled environments, safety equipment, exobiology and extraterrestrial life, and flight crew behavior and performance. Author

N90-22209 New South Wales Univ., Kensington (Australia). Centre for Biomedical Engineering.
THE EFFECTS OF LINEAR ACCELERATION ON PERCEPTION AND NYSTAGMUS Abstract Only Ph.D. Thesis
Mingjia Dai 1988 3 p
Avail: Issuing Activity

The role of otolith function was tested in two different experimental paradigms. One involved measurement of the perceived posture of the subject with respect to inertial space. The other paradigm involved the measurement of vestibular induced eye movements. All the experiments were conducted on a fixed-chair centrifuge. Perceptual experiments were conducted in three groups: normal subjects, bilateral vestibular neurectomy patients (BSNPs), and unilateral vestibular neurectomy patients (UVNPs). Two mathematical models of roll-tilt perception in different situations were devised. The perceived horizontal (PH) for normals was accurate; BVNPs showed a reduced response to the roll-tilt stimulus; UVNPs showed a static PH shift (visual bias) directed towards the operated side and a response asymmetry in roll-tilt perception. The visual bias and response asymmetry diminished with time but was still marked for some UVNPs six months after the operation. Independent measurement of ocular torsion showed that the visual bias was associated with ocular torsion. In addition the delay of roll-tilt perception and sensory conflict due to visual input for normal subjects was studied. The effects of off-center rotation on nystagmus were studied for normal subjects. The preliminary findings were: (1) linear acceleration changed the gain and postrotatory time constant of canal evoked lateral VOR nystagmus; (2) the nystagmus component on Z-axis tended to vector the resultant nystagmus onto gravito-inertial horizontal; and (3) a secondary nystagmus appeared after substantially suppressed VOR. A mathematical model was established to describe the reduced LVOR as a result of this interaction. These findings suggest that the otoliths are necessary for roll-tilt perception and for modifying canal evoked nystagmus, and that Ewald's second law is applicable to a single set of otoliths. Author

N90-22210# Midwest Research Inst., Kansas City, MO.
STUDIES OF 60-Hz EXPOSURE EFFECTS ON HUMAN FUNCTION Quarterly Report No. 3, 1 Jan. - 31 Mar. 1990
Charles Graham and Harvey D. Cohen 16 Apr. 1990 5 p
(Contract DE-FG01-89CE-34025; MRI Proj. RA-111-C)
(DE90-009473; DOE/CE-34025/T3) Avail: NTIS HC A01/MF A01

Public concern is expressed about possible health risks arising from exposure to the electric and magnetic fields generated by power distribution systems. This project is addressing this concern through a laboratory research program designed to evaluate the effects of brief exposure to known field conditions on multiple measures of human function. In previous research, it was found that such exposure had statistically significant effects on physiological measures of cardiac and brain activity, and on performance measures of reaction time and performance accuracy. These effects were seen more clearly under intermittent exposure conditions, and at certain levels of electric and magnetic field strength. In the current effort, a series of exploratory studies, followed by a confirmatory experiment, are planned to determine if the above physiological effects differ as a function of exposure to the electric and magnetic fields separately and combined, time of day, and rate of intermittent exposure. Further studies will explore the mechanisms underlying these effects. The information developed will be of value in risk assessment, and in basic research programs aimed at identifying specific factors involved in the interaction of powerline fields with the human system. During the present reporting period, funding was awarded to continue this research effort at a reduced level until December 31, 1990. The goals for this reporting period were to: complete exploratory Study 1; participate in a project review meeting at MRI; and begin additional exploratory studies. DOE

N90-22211 Massachusetts Univ., Amherst.
THE PREDICTABILITY AND EFFICIENCY OF HUMAN WALKING: METABOLIC, MECHANICAL, AND BIOPHYSICAL CONSIDERATIONS Ph.D. Thesis
Kenneth George Holt 1989 196 p
Avail: Univ. Microfilms Order No. DA9011741

The major purpose was to compare the stride frequency predicted by a model of human walking based on the resonant frequency for a force-driven harmonic oscillator (FDHO) with that chosen by subjects when asked to walk at a comfortable rate on a treadmill (Preferred Stride Frequency - PSF). A second purpose was to determine if differences existed between the metabolic and mechanical costs and efficiency of the two (FDHO and PSF), and frequencies above and below the preferred. Eight adult subjects were tested on three days. On the first day preferred walking frequency was obtained, and from anthropometric measures of a segment lengths a predicted frequency was obtained. On the second and third days subjects were required to walk on a treadmill to a metronome at the preferred and predicted frequencies and at frequencies +/- 5, +/- 10, and +/- 15 strides per minute around the PSF obtained on the first day. Oxygen consumption was used to represent the metabolic cost at steady state. From the kinematic data mechanical work done by each segment and the head, arms and trunk were calculated. To produce an efficiency calculation the metabolic data were converted to a work equivalent and divided into the mechanical work. Results indicated that the preferred stride frequency was extremely consistent across days as were the metabolic and mechanical costs associated with it. The preferred and predicted stride frequencies were not significantly different indicating that the FDHO is a good predictive model of walking frequency. The metabolic and mechanical costs and efficiency were also not different between the two, suggesting that the resonant frequency of the limbs as biological oscillators produces minimal metabolic cost. This is supported by the finding that the curves resulted in a strongly quadratic trend with minimum for metabolic work and a maximum for efficiency at the PSF. Dissert. Abstr.

53 BEHAVIORAL SCIENCES

Includes psychological factors; individual and group behavior; crew training and evaluation; and psychiatric research.

N90-22212*# Essex Corp., Orlando, FL.
ISSUES IN DEVELOPMENT, EVALUATION, AND USE OF THE NASA PREFLIGHT ADAPTATION TRAINER (PAT)
Norman E. Lane and Robert S. Kennedy Jul. 1988 50 p
Prepared for Miami Univ., Oxford, OH
(Contract NAS9-17413)
(NASA-CR-185608; NAS 1.26:185608; EOTR-88-9) Avail: NTIS HC A03/MF A01 CSCL 05I

The Preflight Adaptation Trainer (PAT) is intended to reduce or alleviate space adaptation syndrome by providing opportunities for portions of that adaptation to occur under normal gravity conditions prior to space flight. Since the adaptation aspects of the PAT objectives involve modification not only of the behavior of the trainee, but also of sensiomotor skills which underly the behavioral generation, the defining of training objectives of the PAT utilizes four mechanisms: familiarization, demonstration, training and adaptation. These mechanisms serve as structural reference points for evaluation, drive the content and organization of the training procedures, and help to define the roles of the PAT instructors and operators. It was determined that three psychomotor properties are most critical for PAT evaluation: reliability; sensitivity; and relevance. It is cause for concern that the number of measures available to examine PAT effects exceed those that can be properly studied with the available sample sizes; special attention will be required in selection of the candidate measure set. The issues in PAT use and application within a training system context are addressed through linking the three training related mechanisms of familiarization, demonstration and training to the fourth mechanism, adaptation. B.H.A.

N90-22213*# National Aeronautics and Space Administration. Ames Research Center, Moffett Field, CA.
THE PSYCHOLOGY OF COMPUTER DISPLAYS IN THE MODERN MISSION CONTROL CENTER
Michael M. Granaas (South Dakota Univ., Vermillion.) and Donald C. Rhea Oct. 1988 6 p Previously announced in IAA as A88-37951
(NASA-TM-100451; H-1507; NAS 1.15:100451) Avail: NTIS HC A02/MF A01 CSCL 05I

Work at NASA's Western Aeronautical Test Range (WATR) has demonstrated the need for increased consideration of psychological factors in the design of computer displays for the WATR mission control center. These factors include color perception, memory load, and cognitive processing abilities. A review of relevant work in the human factors psychology area is provided to demonstrate the need for this awareness. The information provided should be relevant in control room settings where computerized displays are being used. Author

N90-22214# Idaho National Engineering Lab., Idaho Falls.
INSIGHTS INTO COMPLEX HUMAN PERFORMANCE
Heidi Ann Hahn and Harold S. Blackman 1990 7 p Presented at the American Nuclear Society Topical Meeting on Human Factors, Snowbird, 10-14 Jun. 1990
(Contract DE-AC07-76ID-01570)
(DE90-006957; EGG-M-89492; CONF-9006115-1) Avail: NTIS HC A02/MF A01

A research program was implemented to investigate the applicability of verbal protocol analysis to identify operator strategies for task performance and to assess how well strategies further define the performance of humans in complex systems. This research was conducted in two environments: control rooms of nuclear power plants and cockpits of civilian aircraft. Results are presented regarding the specific technique of applying verbal protocol methods as well as the importance of strategies in human performance in complex systems. DOE

54 MAN/SYSTEM TECHNOLOGY AND LIFE SUPPORT

Includes human engineering; biotechnology; and space suits and protective clothing.

For related information see also *16 Space Transportation.*

N90-22215*# Old Dominion Coll., Norfolk, VA. Dept. of Mechanical Engineering and Mechanics.
EXPERT SYSTEMS FOR AUTOMATED MAINTENANCE OF A MARS OXYGEN PRODUCTION SYSTEM Final Report, period ending 30 Nov. 1989
Robert L. Ash, Jen-Kuang Huang, and Ming-Tsang Ho Oct. 1989 169 p
(Grant NAG9-308)
(NASA-CR-186209; NAS 1.26:186209) Avail: NTIS HC A08/MF A01 CSCL 06K

A prototype expert system was developed for maintaining autonomous operation of a Mars oxygen production system. Normal operation conditions and failure modes according to certain desired criteria are tested and identified. Several schemes for failure detection and isolation using forward chaining, backward chaining, knowledge-based and rule-based are devised to perform several housekeeping functions. These functions include self-health checkout, an emergency shut down program, fault detection and conventional control activities. An effort was made to derive the dynamic model of the system using Bond-Graph technique in order to develop the model-based failure detection and isolation scheme by estimation method. Finally, computer simulations and experimental results demonstrated the feasibility of the expert system and a preliminary reliability analysis for the oxygen production system is also provided. Author

N90-22216*# National Aeronautics and Space Administration. Ames Research Center, Moffett Field, CA.
VISION SCIENCE AND TECHNOLOGY AT NASA: RESULTS OF A WORKSHOP
Andrew B. Watson, ed. and Jeffrey B. Mulligan, ed. Feb. 1990 68 p Workshop held at Moffett Field, CA, 30 Nov. - 2 Dec. 1988 Revised
(NASA-TM-102214-Rev-1; A-89211-Rev-1; NAS 1.15:102214-Rev-1) Avail: NTIS HC A04/MF A01 CSCL 05H

A broad review is given of vision science and technology within NASA. The subject is defined and its applications in both NASA and the nation at large are noted. A survey of current NASA efforts is given, noting strengths and weaknesses of the NASA program. For individual titles, see N90-22217 through N90-22246.

N90-22217*# National Aeronautics and Space Administration. Ames Research Center, Moffett Field, CA.
SAMPLING AND NOISE IN VISION NETWORKS Abstract Only
Albert J. Ahumada, Jr. *In its* Vision Science and Technology at NASA: Results of a Workshop Feb. 1990 p 19-20 (For primary document see N90-22216 15-54)
Avail: NTIS HC A04/MF A01 CSCL 05H

This research is part of the Human Interface Research Branch-Vision Group's program to develop computable models of biological solutions to general vision system problems. Two problem areas are addressed: effects of discrete sampling by receptors, and effects of visual system noise. Author

N90-22218*# National Aeronautics and Space Administration. Ames Research Center, Moffett Field, CA.
NETWORKS FOR IMAGE ACQUISITION, PROCESSING AND DISPLAY Abstract Only
Albert J. Ahumada, Jr. *In its* Vision Science and Technology at NASA: Results of a Workshop Feb. 1990 p 21 (For primary document see N90-22216 15-54)
Avail: NTIS HC A04/MF A01 CSCL 05H

The human visual system comprises layers of networks which sample, process, and code images. Understanding these networks is a valuable means of understanding human vision and of designing autonomous vision systems based on network processing. Ames Research Center has an ongoing program to develop computational models of such networks. The models predict human performance in detection of targets and in discrimination of displayed information. In addition, the models are artificial vision systems sharing properties with biological vision that has been tuned by evolution for high performance. Properties include variable density sampling, noise immunity, multi-resolution coding, and fault-tolerance. The research stresses analysis of noise in visual networks, including sampling, photon, and processing unit noises. Specific accomplishments include: models of sampling array growth with variable density and irregularity comparable to that of the retinal cone mosaic; noise models of networks with signal-dependent and independent noise; models of network connection development for preserving spatial registration and interpolation; multi-resolution encoding models based on hexagonal arrays (HOP transform); and mathematical procedures for simplifying analysis of large networks. Author

N90-22219*# Microtronics Associates, Pittsburgh, PA.
PARALLEL ASYNCHRONOUS HARDWARE IMPLEMENTATION OF IMAGE PROCESSING ALGORITHMS Abstract Only c61
Darryl D. Coon and A. G. U. Perera *In* NASA, Ames Research Center, Vision Science and Technology at NASA: Results of a Workshop Feb. 1990 p 22 (For primary document see N90-22216 15-54)
(Contract NAS1-18645)
Avail: NTIS HC A04/MF A01 CSCL 09B

Research is being carried out on hardware for a new approach to focal plane processing. The hardware involves silicon injection mode devices. These devices provide a natural basis for parallel asynchronous focal plane image preprocessing. The simplicity and novel properties of the devices would permit an independent analog processing channel to be dedicated to every pixel. A laminar architecture built from arrays of the devices would form a two-dimensional (2-D) array processor with a 2-D array of inputs located directly behind a focal plane detector array. A 2-D image data stream would propagate in neuron-like asynchronous pulse-coded form through the laminar processor. No multiplexing, digitization, or serial processing would occur in the preprocessing state. High performance is expected, based on pulse coding of input currents down to one picoampere with noise referred to input of about 10 femtoamperes. Linear pulse coding has been observed for input currents ranging up to seven orders of magnitude. Low power requirements suggest utility in space and in conjunction with very large arrays. Very low dark current and multispectral capability are possible because of hardware compatibility with the cryogenic environment of high performance detector arrays. The aforementioned hardware development effort is aimed at systems which would integrate image acquisition and image processing. Author

N90-22220*# National Aeronautics and Space Administration. Ames Research Center, Moffett Field, CA.
VISIONS OF VISUALIZATION AIDS: DESIGN PHILOSOPHY AND EXPERIMENTAL RESULTS Abstract Only
Stephen R. Ellis *In its* Vision Science and Technology at NASA: Results of a Workshop Feb. 1990 p 23 (For primary document see N90-22216 15-54)
Avail: NTIS HC A04/MF A01 CSCL 05H

Aids for the visualization of high-dimensional scientific or other data must be designed. Simply casting multidimensional data into a two- or three-dimensional spatial metaphor does not guarantee that the presentation will provide insight or parsimonious description of the phenomena underlying the data. Indeed, the communication of the essential meaning of some multidimensional data may be obscured by presentation in a spatially distributed format. Useful visualization is generally based on pre-existing theoretical beliefs concerning the underlying phenomena which guide selection and formatting of the plotted variables. Two examples from chaotic dynamics are used to illustrate how a visulaization may be an aid to insight. Two examples of displays to aid spatial maneuvering are described. The first, a perspective format for a commercial air traffic display, illustrates how geometric distortion may be introduced to insure that an operator can understand a depicted three-dimensional situation. The second, a display for planning small spacecraft maneuvers, illustrates how the complex counterintuitive character of orbital maneuvering may be made more tractable by removing higher-order nonlinear control dynamics, and allowing independent satisfaction of velocity and plume impingement constraints on orbital changes. Author

N90-22221*# National Aeronautics and Space Administration. Lyndon B. Johnson Space Center, Houston, TX.

VISION SCIENCE AND TECHNOLOGY FOR SUPERVISED INTELLIGENT SPACE ROBOTS Abstract Only **c63**

Jon D. Erickson *In* NASA, Ames Research Center, Vision Science and Technology at NASA: Results of a Workshop Feb. 1990 p 24 (For primary document see N90-22216 15-54)
Avail: NTIS HC A04/MF A01 CSCL 09B

The focus of recent work in robotic vision for application in intelligent space robots such as the Extravehicular Activity (EVA) Retriever is in visual function, that is, how information about the space world is derived and then conveyed to cognition. The goal of this work in visual function is first to understand how the relevant structure of the surrounding world is evidenced by regularities among the pixels of images, then to understand how these regularities are mapped on the premises that form the primitive elements of cognition, and then to apply these understandings with the elements of visual processing (algorithms) and visual mechanism (machine organization) to intelligent space robot simulations and test beds. Since visual perception is the process of recognizing regularities in images that are known on the basis of a model of the world to be reliable related to causal structure in the environment (because perception attaches meaning to the link between a conception of the environment and the objective environment), the work involves understanding generic, generally applicable models of world structure (not merely objects) and how that structure evidences itself in images. Author

N90-22222*# National Aeronautics and Space Administration. Goddard Space Flight Center, Greenbelt, MD.

COMPUTATION AND PARALLEL IMPLEMENTATION FOR EARLY VISION Abstract Only **c61**

J. Anthony Gualtieri *In* NASA, Ames Research Center, Vision Science and Technology at NASA: Results of a Workshop Feb. 1990 p 25-26 (For primary document see N90-22216 15-54)
Avail: NTIS HC A04/MF A01 CSCL 09B

The problem of early vision is to transform one or more retinal illuminance images-pixel arrays-to image representations built out of such primitive visual features such as edges, regions, disparities, and clusters. These transformed representations form the input to later vision stages that perform higher level vision tasks including matching and recognition. Researchers developed algorithms for: (1) edge finding in the scale space formulation; (2) correlation methods for computing matches between pairs of images; and (3) clustering of data by neural networks. These algorithms are formulated for parallel implementation of SIMD machines, such as the Massively Parallel Processor, a 128 x 128 array processor with 1024 bits of local memory per processor. For some cases, researchers can show speedups of three orders of magnitude over serial implementations. Author

N90-22223*# Odetics, Inc., Anaheim, CA.

INTENSITY DEPENDENT SPREAD THEORY Abstract Only

Richard Holben *In* NASA, Ames Research Center, Vision Science and Technology at NASA: Results of a Workshop Feb. 1990 p 27 (For primary document see N90-22216 15-54)
Avail: NTIS HC A04/MF A01 CSCL 05H

The Intensity Dependent Spread (IDS) procedure is an image-processing technique based on a model of the processing which occurs in the human visual system. IDS processing is relevant to many aspects of machine vision and image processing. For quantum limited images, it produces an ideal trade-off between spatial resolution and noise averaging, performs edge enhancement thus requiring only mean-crossing detection for the subsequent extraction of scene edges, and yields edge responses whose amplitudes are independent of scene illumination, depending only upon the ratio of the reflectance on the two sides of the edge. These properties suggest that the IDS process may provide significant bandwidth reduction while losing only minimal scene information when used as a preprocessor at or near the image plane. Author

N90-22224*# National Aeronautics and Space Administration. Langley Research Center, Hampton, VA.

IMAGE GATHERING, CODING, AND PROCESSING: END-TO-END OPTIMIZATION FOR EFFICIENT AND ROBUST ACQUISITION OF VISUAL INFORMATION Abstract Only

Friedrich O. Huck and Carl L. Fales *In* NASA, Ames Research Center, Vision Science and Technology at NASA: Results of a Workshop Feb. 1990 p 28-29 (For primary document see N90-22216 15-54)
Avail: NTIS HC A04/MF A01 CSCL 05H

Researchers are concerned with the end-to-end performance of image gathering, coding, and processing. The applications range from high-resolution television to vision-based robotics, wherever the resolution, efficiency and robustness of visual information acquisition and processing are critical. For the presentation at this workshop, it is convenient to divide research activities into the following two overlapping areas: The first is the development of focal-plane processing techniques and technology to effectively combine image gathering with coding, with an emphasis on low-level vision processing akin to the retinal processing in human vision. The approach includes the familiar Laplacian pyramid, the new intensity-dependent spatial summation, and parallel sensing/processing networks. Three-dimensional image gathering is attained by combining laser ranging with sensor-array imaging. The second is the rigorous extension of information theory and optimal filtering to visual information acquisition and processing. The goal is to provide a comprehensive methodology for quantitatively assessing the end-to-end performance of image gathering, coding, and processing. Author

N90-22225*# National Aeronautics and Space Administration. Lyndon B. Johnson Space Center, Houston, TX.

HYBRID VISION ACTIVITIES AT NASA JOHNSON SPACE CENTER Abstract Only

Richard D. Juday *In* NASA, Ames Research Center, Vision Science and Technology at NASA: Results of a Workshop Feb. 1990 p 30 (For primary document see N90-22216 15-54)
Avail: NTIS HC A04/MF A01 CSCL 05H

NASA's Johnson Space Center in Houston, Texas, is active in several aspects of hybrid image processing. (The term hybrid image processing refers to a system that combines digital and photonic processing). The major thrusts are autonomous space operations such as planetary landing, servicing, and rendezvous and docking. By processing images in non-Cartesian geometries to achieve shift invariance to canonical distortions, researchers use certain aspects of the human visual system for machine vision. That technology flow is bidirectional; researchers are investigating the possible utility of video-rate coordinate transformations for human low-vision patients. Man-in-the-loop teleoperations are also supported by the use of video-rate image-coordinate transformations, as researchers plan to use bandwidth compression tailored to the varying spatial acuity of the human operator. Technological elements being developed in the program include upgraded spatial light modulators, real-time coordinate transformations in video imagery, synthetic filters that robustly allow estimation of object pose parameters, convolutionally blurred filters that have continuously selectable invariance to such image changes as magnification and rotation, and optimization of optical correlation done with spatial light modulators that have limited range and couple both phase and amplitude in their response. Author

N90-22226*# National Aeronautics and Space Administration. Ames Research Center, Moffett Field, CA.
HUMAN MOTION PERCEPTION: HIGHER-ORDER ORGANIZATION Abstract Only
Mary K. Kaiser and Dennis R. Proffitt (Virginia Univ., Charlottesville.) *In its* Vision Science and Technology at NASA: Results of a Workshop Feb. 1990 p 31-32 (For primary document see N90-22216 15-54)
Avail: NTIS HC A04/MF A01 CSCL 05H

An overview is given of higher-order motion perception and organization. It is argued that motion is sufficient to fully specify a number of environmental properties, including: depth order, three-dimensional form, object displacement, and dynamics. A grammar of motion perception is proposed; applications of this work for display design are discussed. Author

N90-22227*# National Aeronautics and Space Administration. Ames Research Center, Moffett Field, CA.
TWO-DIMENSIONAL SHAPE RECOGNITION USING SPARSE DISTRIBUTED MEMORY Abstract Only
Pentti Kanerva and Bruno Olshausen *In its* Vision Science and Technology at NASA: Results of a Workshop Feb. 1990 p 33 (For primary document see N90-22216 15-54)
Avail: NTIS HC A04/MF A01 CSCL 05H

Researchers propose a method for recognizing two-dimensional shapes (hand-drawn characters, for example) with an associative memory. The method consists of two stages: first, the image is preprocessed to extract tangents to the contour of the shape; second, the set of tangents is converted to a long bit string for recognition with sparse distributed memory (SDM). SDM provides a simple, massively parallel architecture for an associative memory. Long bit vectors (256 to 1000 bits, for example) serve as both data and addresses to the memory, and patterns are grouped or classified according to similarity in Hamming distance. At the moment, tangents are extracted in a simple manner by progressively blurring the image and then using a Canny-type edge detector (Canny, 1986) to find edges at each stage of blurring. This results in a grid of tangents. While the technique used for obtaining the tangents is at present rather ad hoc, researchers plan to adopt an existing framework for extracting edge orientation information over a variety of resolutions, such as suggested by Watson (1987, 1983), Marr and Hildreth (1980), or Canny (1986). Author

N90-22228*# Odetics, Inc., Anaheim, CA.
THE INTENSITY DEPENDENT SPREAD MODEL AND COLOR CONSTANCY Abstract Only
Ellie Kurrasch *In* NASA, Ames Research Center, Vision Science and Technology at NASA: Results of a Workshop Feb. 1990 p 34 (For primary document see N90-22216 15-54)
Avail: NTIS HC A04/MF A01 CSCL 05H

Odetics is investigating the use of the intensity dependent spread (IDS) model for determining color constancy. Object segmentation is performed effortlessly by the human visual systems, but creating computer vision that takes an image as input and performs object identification on the basis of color has some difficulties. The unknown aspects of the light illuminating a scene in space or anywhere can seriously interfere with the use of color for object identification. The color of an image depends not only on the physical characteristics of the object, but also on the wavelength composition of the incident illumination. IDS processing provides the extraction of edges and of reflectance changes across edges, independent of variations in scene illumination. IDS depends solely on the ratio of the reflectances on the two sides of the edge. Researchers are in the process of using IDS to recover the reflectance image. Author

N90-22229*# National Aeronautics and Space Administration. Ames Research Center, Moffett Field, CA.
FILLING IN THE RETINAL IMAGE Abstract Only
James Larimer and Thomas Piantanida (SRI International Corp., Menlo Park, CA.) *In its* Vision Science and Technology at NASA: Results of a Workshop Feb. 1990 p 35 (For primary document see N90-22216 15-54)
Avail: NTIS HC A04/MF A01 CSCL 05H

The optics of the eye form an image on a surface at the back of the eyeball called the retina. The retina contains the photoreceptors that sample the image and convert it into a neural signal. The spacing of the photoreceptors in the retina is not uniform and varies with retinal locus. The central retinal field, called the macula, is densely packed with photoreceptors. The packing density falls off rapidly as a function of retinal eccentricity with respect to the macular region and there are regions in which there are no photoreceptors at all. The retinal regions without photoreceptors are called blind spots or scotomas. The neural transformations which convert retinal image signals into percepts fills in the gaps and regularizes the inhomogeneities of the retinal photoreceptor sampling mosaic. The filling-in mechamism plays an important role in understanding visual performance. The filling-in mechanism is not well understood. A systematic collaborative research program at the Ames Research Center and SRI in Menlo Park, California, was designed to explore this mechanism. It was shown that the perceived fields which are in fact different from the image on the retina due to filling-in, control some aspects of performance and not others. Researchers have linked these mechanisms to putative mechanisms of color coding and color constancy. Author

N90-22230*# National Aeronautics and Space Administration. Ames Research Center, Moffett Field, CA.
A3I VISIBILITY MODELING PROJECT Abstract Only
James Larimer, Aries Arditi, James Bergen, and Norman Badler (Pennsylvania Univ., Philadelphia.) *In its* Vision Science and Technology at NASA: Results of a Workshop Feb. 1990 p 36 (For primary document see N90-22216 15-54)
Avail: NTIS HC A04/MF A01 CSCL 05H

The Army-NASA Aircrew Aircraft Integration program is supporting a joint project to build a visibility computer-aided design (CAD) tool. CAD has become an essential tool in modern engineering applications. CAD tools are used to create engineering drawings and to evaluate potential designs before they are physically realized. The visibility CAD tool will provide the design engineer with a tool to aid in the location and specification of windows, displays, and control in crewstations. In an aircraft cockpit the location of instruments and the emissive and reflective characteristics of the surfaces must be determined to assure adequate aircrew performance. The visibility CAD tool will allow the designer to ask and answer many of these questions in the context of a three-dimensional graphical representation of the cockpit. The graphic representation of the cockpit is a geometrically valid model of the cockpit design. A graphic model of a pilot, called the pilot manikin, can be placed naturalistically in the cockpit model. The visibility tool has the capability of mapping the cockpit surfaces and other objects modeled in this graphic design space onto the simulated pilot's retinas for a given visual fixation. Author

N90-22231*# National Aeronautics and Space Administration. Goddard Space Flight Center, Greenbelt, MD.
MOTION DETECTION IN ASTRONOMICAL AND ICE FLOE IMAGES Abstract Only
M. Manohar, H. K. Ramapriyan, and J. P. Strong *In* NASA, Ames Research Center, Vision Science and Technology at NASA: Results of a Workshop Feb. 1990 p 37 (For primary document see N90-22216 15-54)
Avail: NTIS HC A04/MF A01 CSCL 05H

Two approaches are presented for establishing correspondence between small areas in pairs of successive images for motion detection. The first one, based on local correlation, is used on a pair of successive Voyager images of the Jupiter which differ mainly in locally variable translations. This algorithm is implemented on a sequential machine (VAX 780) as well as the Massively Parallel Processor (MPP). In the case of the sequential algorithm, the pixel correspondence or match is computed on a sparse grid of points using nonoverlapping windows (typically 11 x 11) by local correlations over a predetermined search area. The displacement of the corresponding pixels in the two images is called the disparities to cubic surfaces. The disparities at points where the error between the computed values and the surface values exceeds a particular threshold are replaced by the surface values. A bilinear interpolation is then used to estimate disparities at all other pixels between the grid points. When this algorithm was applied at the red spot in the Jupiter image, the rotating velocity field of the storm was determined. The second method of motion detection is applicable to pairs of images in which corresponding areas can experience considerable translation as well as rotation. Author

N90-22232*# Georgia Inst. of Tech., Atlanta.
PASSIVE NAVIGATION USING IMAGE IRRADIANCE TRACKING **c04**
P. K. A. Menon (National Aeronautics and Space Administration. Ames Research Center, Moffett Field, CA.) *In* NASA, Ames Research Center, Vision Science and Technology at NASA: Results of a Workshop Feb. 1990 p 38 (For primary document see N90-22216 15-54)
(Grant NAG2-463)
Avail: NTIS HC A04/MF A01 CSCL 17G

Rotorcraft operating at low altitudes require navigational schemes for detecting terrain and obstacles. Due to the nature of the missions to be accomplished and available power onboard, a passive navigation scheme is desirable in this situation. The development of a passive navigation scheme using optical image sequences and vehicle motion variables from an onboard inertial navigation scheme is described. This approach combines the geometric properties of perspective projection and a feedback irradiance tracking scheme at each pixel in the image to determine the range to various objects within the field-of-view. Derivation of the numerical algorithm and simulation results are given. Due to the feedback nature of the implementation, the computational scheme is robust. Other applications of the proposed approach include navigation for autonomous planetary rovers and telerobots. Author

N90-22233*# National Aeronautics and Space Administration. Ames Research Center, Moffett Field, CA.
FACTORS AFFECTING THE PERCEPTION OF TRANSPARENT MOTION Abstract Only
Jeffrey B. Mulligan *In its* Vision Science and Technology at NASA: Results of a Workshop Feb. 1990 p 38 (For primary document see N90-22216 15-54)
Avail: NTIS HC A04/MF A01 CSCL 05H

It is possible to create a perception of transparency by combining patterns having different motions. Two particular combination rules, have specific interpretations in terms of physical phenomena: additive (specular reflection) and multiplicative (shadow illumination). Arbitrary combination rules applied to random patterns generate percepts in which the motions of the two patterns are visible, but have super-imposed noise. It is also possible to combine the patterns (using an exclusive-OR rule) so that only noise is visible. Within a one-dimensional family of combination rules which include addition and multiplication, there is a range where smooth motions are seen with no superimposed noise; this range is centered about the additive combination. This result suggests that the motion system deals with a linear representation of luminance, and is consistent with the analysis of motion by linear sensors. This research gives tentative validation the use in beam splitters (which combine images additively) in the construction of heads-up aviation displays. Further work is needed to determine if the superiority of additive combination generalizes to the case of full-color imagery (there are results in the literature suggesting that subtractive color mixture yields the best legibility of overlapping alphanumerics). Author

N90-22234*# National Aeronautics and Space Administration. Ames Research Center, Moffett Field, CA.
PHOTONIC PROCESSING AT NASA AMES RESEARCH CENTER Abstract Only
Ellen Ochoa and Max Reid *In its* Vision Science and Technology at NASA: Results of a Workshop Feb. 1990 p 39 (For primary document see N90-22216 15-54)
Avail: NTIS HC A04/MF A01 CSCL 05H

The Photonic Processing group is engaged in applied research on optical processors in support of the Ames vision to lead the development of autonomous intelligent systems. Optical processors, in conjunction with numeric and symbolic processors, are needed to provide the powerful processing capability that is required for many future agency missions. The research program emphasizes application of analog optical processing, where free-space propagation between components allows natural implementations of algorithms requiring a large degree of parallel computation. Special consideration is given in the Ames program to the integration of optical processors into larger, heterogeneous computational systems. Demonstration of the effective integration of optical processors within a broader knowledge-based system is essential to evaluate their potential for dependable operation in an autonomous environment such as space. The Ames Photonics program is currently addressing several areas of interest. One of the efforts is to develop an optical correlator system with two programmable spatial light modulators (SLMs) to perform distortion invariant pattern recognition. Another area of research is optical neural networks, also for use in distortion-invariant pattern recognition. Author

N90-22235*# National Aeronautics and Space Administration. Ames Research Center, Moffett Field, CA.
SPARSE DISTRIBUTED MEMORY OVERVIEW Abstract Only
Mike Raugh *In its* Vision Science and Technology at NASA: Results of a Workshop Feb. 1990 p 40-41 (For primary document see N90-22216 15-54)
Avail: NTIS HC A04/MF A01 CSCL 05H

The Sparse Distributed Memory (SDM) project is investigating the theory and applications of massively parallel computing architecture, called sparse distributed memory, that will support the storage and retrieval of sensory and motor patterns characteristic of autonomous systems. The immediate objectives of the project are centered in studies of the memory itself and in the use of the memory to solve problems in speech, vision, and robotics. Investigation of methods for encoding sensory data is an important part of the research. Examples of NASA missions that may benefit from this work are Space Station, planetary rovers, and solar exploration. Sparse distributed memory offers promising technology for systems that must learn through experience and be capable of adapting to new circumstances, and for operating any large complex system requiring automatic monitoring and control. Sparse distributed memory is a massively parallel architecture motivated by efforts to understand how the human brain works. Sparse distributed memory is an associative memory, able to retrieve information from cues that only partially match patterns stored in the memory. It is able to store long temporal sequences derived from the behavior of a complex system, such as progressive records of the system's sensory data and correlated records of the system's motor controls. Author

N90-22236*# Jet Propulsion Lab., California Inst. of Tech., Pasadena.
ALGORITHMS AND ARCHITECTURES FOR ROBOT VISION Abstract Only **c63**
Paul S. Schenker *In* NASA, Ames Research Center, Vision Science and Technology at NASA: Results of a Workshop Feb. 1990 p 42-43 (For primary document see N90-22216 15-54)
Avail: NTIS HC A04/MF A01 CSCL 09B

The scope of the current work is to develop practical sensing implementations for robots operating in complex, partially unstructured environments. A focus in this work is to develop object models and estimation techniques which are specific to requirements of robot locomotion, approach and avoidance, and grasp and manipulation. Such problems have to date received limited attention in either computer or human vision - in essence, asking not only how perception is in general modeled, but also what is the functional purpose of its underlying representations. As in the past, researchers are drawing on ideas from both the psychological and machine vision literature. Of particular interest is the development 3-D shape and motion estimates for complex objects when given only partial and uncertain information and when such information is incrementally accrued over time. Current studies consider the use of surface motion, contour, and texture information, with the longer range goal of developing a fused sensing strategy based on these sources and others. Author

N90-22237*# National Aeronautics and Space Administration. Ames Research Center, Moffett Field, CA.

COMPUTER VISION TECHNIQUES FOR ROTORCRAFT LOW ALTITUDE FLIGHT

Banavar Sridhar *In its* Vision Science and Technology at NASA: Results of a Workshop Feb. 1990 p 45-46 (For primary document see N90-22216 15-54)

Avail: NTIS HC A04/MF A01 CSCL 05H

Rotorcraft operating in high-threat environments fly close to the earth's surface to utilize surrounding terrain, vegetation, or manmade objects to minimize the risk of being detected by an enemy. Increasing levels of concealment are achieved by adopting different tactics during low-altitude flight. Rotorcraft employ three tactics during low-altitude flight: low-level, contour, and nap-of-the-earth (NOE). The key feature distinguishing the NOE mode from the other two modes is that the whole rotorcraft, including the main rotor, is below tree-top whenever possible. This leads to the use of lateral maneuvers for avoiding obstacles, which in fact constitutes the means for concealment. The piloting of the rotorcraft is at best a very demanding task and the pilot will need help from onboard automation tools in order to devote more time to mission-related activities. The development of an automation tool which has the potential to detect obstacles in the rotorcraft flight path, warn the crew, and interact with the guidance system to avoid detected obstacles, presents challenging problems. Research is described which applies techniques from computer vision to automation of rotorcraft navigtion. The effort emphasizes the development of a methodology for detecting the ranges to obstacles in the region of interest based on the maximum utilization of passive sensors. The range map derived from the obstacle-detection approach can be used as obstacle data for the obstacle avoidance in an automatic guidance system and as advisory display to the pilot. The lack of suitable flight imagery data presents a problem in the verification of concepts for obstacle detection. This problem is being addressed by the development of an adequate flight database and by preprocessing of currently available flight imagery. The presentation concludes with some comments on future work and how research in this area relates to the guidance of other autonomous vehicles. Author

N90-22238*# National Aeronautics and Space Administration. Ames Research Center, Moffett Field, CA.

KALMAN FILTER BASED RANGE ESTIMATION FOR AUTONOMOUS NAVIGATION USING IMAGING SENSORS c04

Banavar Sridhar *In its* Vision Science and Technology at NASA: Results of a Workshop Feb. 1990 p 47-48 (For primary document see N90-22216 15-54)

Avail: NTIS HC A04/MF A01 CSCL 17G

Rotorcraft operating in high-threat environments fly close to the surface of the earth to utilize surrounding terrain, vegetation, or man-made objects to minimize the risk of being detected by the enemy. Two basic requirements for obstacle avoidance are detection and range estimation of the object from the current rotorcraft position. There are many approaches to the estimation of range using a sequence of images. The approach used in this analysis differes from previous methods in two significant ways: an attempt is not made to estimate the rotorcraft's motion from the images; and the interest lies in recursive algorithms. The rotorcraft parameters are assumed to be computed using an onboard inertial navigation system. Given a sequence of images, using image-object differential equations, a Kalman filter (Sridhar and Phatak, 1988) can be used to estimate both the relative coordinates and the earth coordinates of the objects on the ground. The Kalman filter can also be used in a predictive mode to track features in the images, leading to a significant reduction of search effort in the feature extraction step of the algorithm. The purpose is to summarize early results obtained in extending the Kalman filter for use with actual image sequences. The experience gained from the application of this algorithm to real images is very valuable and is a necessary step before proceeding to the estimation of range during low-altitude curvilinear flight. A simple recursive method is presented to estimate range to objects using a sequence of images. The method produces good range estimates using real images in a laboratory set up and needs to be evaluated further using several different image sequences to test its robustness. The feature generation part of the algorithm requires further refinement on the strategies to limit the number of features (Sridhar and Phatak, 1989). The extension of the work reported here to curvilinear flight may require the use of the extended Kalman filter. Author

N90-22239*# California Univ., Berkeley. Telerobotics Unit.

INSTRUMENTATION AND ROBOTIC IMAGE PROCESSING USING TOP-DOWN MODEL CONTROL Abstract Only

Lawrence Stark, Barbara Mills, An H. Nguyen, and Huy X. Ngo *In* NASA, Ames Research Center, Vision Science and Technology at NASA: Results of a Workshop Feb. 1990 p 49 (For primary document see N90-22216 15-54)

Avail: NTIS HC A04/MF A01 CSCL 05H

A top-down image processing scheme is described. A three-dimensional model of a robotic working environment, with robot manipulators, workpieces, cameras, and on-the-scene visual enhancements is employed to control and direct the image processing, so that rapid, robust algorithms act in an efficient manner to continually update the model. Only the model parameters are communicated, so that savings in bandwidth are achieved. This image compression by modeling is especially important for control of space telerobotics. The background for this scheme lies in an hypothesis of human vision put forward by the senior author and colleagues almost 20 years ago - the Scanpath Theory. Evidence was obtained that repetitive sequences of saccadic eye movements, the scanpath, acted as the checking phase of visual pattern recognition. Further evidence was obtained that the scanpaths were apparently generated by a cognitive model and not directly by the visual image. This top-down theory of human vision was generalized in some sense to the frame in artificial intelligence. Another source of the concept arose from bioengineering instrumentation for measuring the pupil and eye movements with infrared video cameras and special-purpose hardware. Author

N90-22240*# National Aeronautics and Space Administration. Marshall Space Flight Center, Huntsville, AL.

COMPUTER VISION RESEARCH AT MARSHALL SPACE FLIGHT CENTER Abstract Only c63

Frank L. Vinz *In* NASA, Ames Research Center, Vision Science and Technology at NASA: Results of a Workshop Feb. 1990 p 50 (For primary document see N90-22216 15-54)

Avail: NTIS HC A04/MF A01 CSCL 09B

Orbital docking, inspection, and sevicing are operations which have the potential for capability enhancement as well as cost reduction for space operations by the application of computer vision technology. Research at MSFC has been a natural outgrowth of orbital docking simulations for remote manually controlled vehicles such as the Teleoperator Retrieval System and the Orbital Maneuvering Vehicle (OMV). Baseline design of the OMV dictates teleoperator control from a ground station. This necessitates a high data-rate communication network and results in several seconds of time delay. Operational costs and vehicle control difficulties could be alleviated by an autonomous or semi-autonomous control system onboard the OMV which would be based on a computer vision system having capability to recognize video images in real time. A concept under development

at MSFC with these attributes is based on syntactic pattern recognition. It uses tree graphs for rapid recognition of binary images of known orbiting target vehicles. This technique and others being investigated at MSFC will be evaluated in realistic conditions by the use of MSFC orbital docking simulators. Computer vision is also being applied at MSFC as part of the supporting development for Work Package One of Space Station Freedom.
Author

N90-22241*# Stanford Univ., CA.

STANFORD/NASA-AMES CENTER OF EXCELLENCE IN MODEL-BASED HUMAN PERFORMANCE Abstract Only

Brian A. Wandell *In* NASA, Ames Research Center, Vision Science and Technology at NASA: Results of a Workshop Feb. 1990 p 51 (For primary document see N90-22216 15-54)
Avail: NTIS HC A04/MF A01 CSCL 05H

The human operator plays a critical role in many aeronautic and astronautic missions. The Stanford/NASA-Ames Center of Excellence in Model-Based Human Performance (COE) was initiated in 1985 to further our understanding of the performance capabilities and performance limits of the human component of aeronautic and astronautic projects. Support from the COE is devoted to those areas of experimental and theoretical work designed to summarize and explain human performance by developing computable performance models. The ultimate goal is to make these computable models available to other scientists for use in design and evaluation of aeronautic and astronautic instrumentation. Within vision science, two topics have received particular attention. First, researchers did extensive work analyzing the human ability to recognize object color relatively independent of the spectral power distribution of the ambient lighting (color constancy). The COE has supported a number of research papers in this area, as well as the development of a substantial data base of surface reflectance functions, ambient illumination functions, and an associated software package for rendering and analyzing image data with respect to these spectral functions. Second, the COE supported new empirical studies on the problem of selecting colors for visual display equipment to enhance human performance in discrimination and recognition tasks. Author

N90-22242*# National Aeronautics and Space Administration. Ames Research Center, Moffett Field, CA.

AMES VISION GROUP RESEARCH OVERVIEW Abstract Only

Andrew B. Watson *In its* Vision Science and Technology at NASA: Results of a Workshop Feb. 1990 p 52 (For primary document see N90-22216 15-54)
Avail: NTIS HC A04/MF A01 CSCL 05H

A major goal of the reseach group is to develop mathematical and computational models of early human vision. These models are valuable in the prediction of human performance, in the design of visual coding schemes and displays, and in robotic vision. To date researchers have models of retinal sampling, spatial processing in visual cortex, contrast sensitivity, and motion processing. Based on their models of early human vision, researchers developed several schemes for efficient coding and compression of monochrome and color images. These are pyramid schemes that decompose the image into features that vary in location, size, orientation, and phase. To determine the perceptual fidelity of these codes, researchers developed novel human testing methods that have received considerable attention in the research community. Researchers constructed models of human visual motion processing based on physiological and psychophysical data, and have tested these models through simulation and human experiments. They also explored the application of these biological algorithms to applications in automated guidance of rotorcraft and autonomous landing of spacecraft. Researchers developed networks for inhomogeneous image sampling, for pyramid coding of images, for automatic geometrical correction of disordered samples, and for removal of motion artifacts from unstable cameras. Author

N90-22243*# National Aeronautics and Space Administration. Ames Research Center, Moffett Field, CA.

PYRAMID IMAGE CODES Abstract Only

Andrew B. Watson *In its* Vision Science and Technology at NASA: Results of a Workshop Feb. 1990 p 53 (For primary document see N90-22216 15-54)
Avail: NTIS HC A04/MF A01 CSCL 05H

All vision systems, both human and machine, transform the spatial image into a coded representation. Particular codes may be optimized for efficiency or to extract useful image features. Researchers explored image codes based on primary visual cortex in man and other primates. Understanding these codes will advance the art in image coding, autonomous vision, and computational human factors. In cortex, imagery is coded by features that vary in size, orientation, and position. Researchers have devised a mathematical model of this transformation, called the Hexagonal oriented Orthogonal quadrature Pyramid (HOP). In a pyramid code, features are segregated by size into layers, with fewer features in the layers devoted to large features. Pyramid schemes provide scale invariance, and are useful for coarse-to-fine searching and for progressive transmission of images. The HOP Pyramid is novel in three respects: (1) it uses a hexagonal pixel lattice, (2) it uses oriented features, and (3) it accurately models most of the prominent aspects of primary visual cortex. The transform uses seven basic features (kernels), which may be regarded as three oriented edges, three oriented bars, and one non-oriented blob. Application of these kernels to non-overlapping seven-pixel neighborhoods yields six oriented, high-pass pyramid layers, and one low-pass (blob) layer. Author

N90-22244*# Odetics, Inc., Anaheim, CA.

INTENSITY DEPENDENT SPREAD PROCESSOR AND WORKSTATION Abstract Only **c60**

George Westrom *In* NASA, Ames Research Center, Vision Science and Technology at NASA: Results of a Workshop Feb. 1990 p 54 (For primary document see N90-22216 15-54)
Avail: NTIS HC A04/MF A01 CSCL 09B

The Intensity Dependent Spread (IDS) is an adaptive algorithm which is modified according to the local intensity in the scene. (This results in a nonlinear process which cannot take advantage of rather nice linear transform methods.) The computation is similar to a neural net whereby intensity information is moving from each input pixel to a set of surrounding output pixels in a manner described by Cornsweet and Yellott. A prototype of a very large scale integration IDS processor is being developed and implemented in a workstation environment. The workstation consists of a SUN 3/260 and a DATACUBE pipeline processor. The IDS prototype is a board set which operates in the DATA CUBE processor. The SUN 3/260 performs control, background processing, IDS simulation and image display functions. Author

N90-22245*# National Aeronautics and Space Administration. Goddard Space Flight Center, Greenbelt, MD.

SPACE ENVIRONMENT ROBOT VISION SYSTEM Abstract Only **c63**

H. John Wood and William L. Eichhorn *In* NASA, Ames Research Center, Vision Science and Technology at NASA: Results of a Workshop Feb. 1990 p 55 (For primary document see N90-22216 15-54)
Avail: NTIS HC A04/MF A01 CSCL 09B

A prototype twin-camera stereo vision system for autonomous robots has been developed at Goddard Space Flight Center. Standard charge coupled device (CCD) imagers are interfaced with commercial frame buffers and direct memory access to a computer. The overlapping portions of the images are analyzed using photogrammetric techniques to obtain information about the position and orientation of objects in the scene. The camera head consists of two 510 x 492 x 8-bit CCD cameras mounted on individually adjustable mounts. The 16 mm efl lenses are designed for minimum geometric distortion. The cameras can be rotated in the pitch, roll, and yaw (pan angle) directions with respect to their optical axes. Calibration routines have been developed which automatically determine the lens focal lengths and pan angle between the two cameras. The calibration utilizes observations of a calibration structure with known geometry. Test results show the precision attainable is plus or minus 0.8 mm in range at 2 m distance using a camera separation of 171 mm. To demonstrate a task needed on Space Station Freedom, a target structure with a movable I beam was built. The camera head can autonomously direct actuators to dock the I-beam to another one so that they could be bolted together. Author

N90-22246*# National Aeronautics and Space Administration. Goddard Space Flight Center, Greenbelt, MD.
SELF-CALIBRATION OF ROBOT-SENSOR SYSTEM Abstract Only c63
Pen-Shu Yeh *In* NASA, Ames Research Center, Vision Science and Technology at NASA: Results of a Workshop Feb. 1990 p 56 (For primary document see N90-22216 15-54)
Avail: NTIS HC A04/MF A01 CSCL 09B

The process of finding the coordinate transformation between a robot and an external sensor system has been addressed. This calibration is equivalent to solving a nonlinear optimization problem for the parameters that characterize the transformation. A two-step procedure is herein proposed for solving the problem. The first step involves finding a nominal solution that is a good approximation of the final solution. A varational problem is then generated to replace the original problem in the next step. With the assumption that the variational parameters are small compared to unity, the problem that can be more readily solved with relatively small computation effort. Author

N90-22087*# Toshiba Corp., Kawasaki (Japan). Mechanical Engineering Lab.
DEVELOPMENT OF A MULTIPURPOSE HAND CONTROLLER FOR JEMRMS
Nobuto Matsuhira, Shoichi Iikura, Makoto Asakura, and Yasuo Shinomiya *In* NASA, John F. Kennedy Space Center, The 24th Aerospace Mechanisms Symposium Apr. 1990 p 105-120 (For primary document see N90-22079 15-39)
Avail: NTIS HC A16/MF A03 CSCL 05H

N90-22101*# National Aeronautics and Space Administration. Ames Research Center, Moffett Field, CA.
AX-5 SPACE SUIT BEARING TORQUE INVESTIGATION
Stuart Loewenthal, Vic Vykukal, Robert MacKendrick, and Philip Culbertson, Jr. (Sterling Federal Systems, Inc., Palo Alto, CA.) *In* NASA, John F. Kennedy Space Center, The 24th Aerospace Mechanisms Symposium Apr. 1990 p 301-312 (For primary document see N90-22079 15-39)
Avail: NTIS HC A16/MF A03 CSCL 05H

N90-22102*# National Aeronautics and Space Administration. John F. Kennedy Space Center, Cocoa Beach, FL.
DESIGN OF A TELESCOPING TUBE SYSTEM FOR ACCESS AND HANDLING EQUIPMENT
Alan C. Littlefield *In its* The 24th Aerospace Mechanisms Symposium Apr. 1990 p 313-327 (For primary document see N90-22079 15-39)
Avail: NTIS HC A16/MF A03 CSCL 05H

55 SPACE BIOLOGY

Includes exobiology; planetary biology; and extraterrestrial life.

No abstracts in this category.

59 MATHEMATICAL AND COMPUTER SCIENCES (GENERAL)

No abstracts in this category.

60 COMPUTER OPERATIONS AND HARDWARE

Includes hardware for computer graphics, firmware, and data processing.

For components see *33 Electronics and Electrical Engineering.*

N90-22247*# National Aeronautics and Space Administration. Langley Research Center, Hampton, VA.
GRAPHICS MINI MANUAL
Nancy L. Taylor, Donald P. Randall, John T. Bowen, Mary M. Johnson, Vincent R. Roland, Christine G. Matthews, Raymond L. Gates, Kristi M. Skeens, Scott R. Nolf, and Dana P. Hammond (Computer Sciences Corp., Hampton, VA.) et al Feb. 1990 67 p Revised
(NASA-TM-87622-Rev; NAS 1.15:87622-Rev; CSCC-G-1a-Rev)
Avail: NTIS HC A04/MF A01 CSCL 09B

The computer graphics capabilities available at the Center are introduced and their use is explained. More specifically, the manual identifies and describes the various graphics software and hardware components, details the interfaces between these components, and provides information concerning the use of these components at LaRC. Author

N90-22248# Texas A&M Univ., College Station. Transportation Inst.
GRAPHICALLY-ORIENTED NONLINEAR ANALYSIS OF STATICALLY LOADED PLANE FRAMES ON MICROCOMPUTERS Final Report, Sep. 1987 - Aug. 1989
Paul N. Roschke and Syed Aftab May 1989 54 p Sponsored by Federal Highway Administration, Austin, TX and Texas State Dept. of Highways and Public Transportation, Austin
(PB90-165945; TTI-2-5-88-1183-2; RR-1183-2; FHWA/TX-90/1183-2) Avail: NTIS HC A04/MF A01 CSCL 09B

Computer program FRAME51 performs a nonlinear analysis of statically loaded plane frames using a discrete element model. Enhancements are made to an existing FORTRAN code using currently available hardware and software. The original code runs on a minicomputer with alphanumeric terminals, while the enhanced version runs on a microcomputer with an improved user interface that includes panel-oriented input and extensive use of graphics. Low level assembly language routines are written to provide functions for manipulating screens, and calls to a commercial software package provide functions for graphical capabilities. The existing code is integrated with the new program as subroutines, but no other modifications are made to facilitate avoidance of new error sources. Panel-oriented input eases the user's burden of creating and editing problems. Graphical representation of input data allows error-checking before execution of the code. In addition to the conventional numerical presentation, output data from analysis is also displayed graphically. Author

N90-22249# Sandia National Labs., Albuquerque, NM.
AN ACOUSTO-OPTIC IMAGE CORRELATOR WITH A THROUGHPUT RATE OF 1000 TEMPLATES PER SECOND
Perry A. Molley 28 Mar. 1990 18 p Presented at the 8th SPIE's Applications of Artificial Intelligence Conference, Orlando, FL, 17-19 Apr. 1990
(Contract DE-AC04-76DP-00789)

(DE90-009323; SAND-89-2383C; CONF-9004125-3) Avail: NTIS HC A03/MF A01

A two-dimensional image correlator based on acousto-optic (AO) and charge-coupled devices (CCDs) is described that can be built with existing technology to provide 1000 frames per second operation. In recent years, architectures have been developed that perform the two-dimensional correlation utilizing one-dimensional input devices. The input scene is loaded into the acousto-optic device (AOD) one line at time. This line is then correlated against all of the rows of a reference template introduced into the optical system using a one-dimensional array of LEDs or laser diodes. However, it generally takes a much greater time to load the AO cell than it does to process the information. This latency time severely limits the maximum throughput rate of the processor. This paper introduces a new acousto-optic correlator implementation that overcomes this bottleneck so that processing can occur close to 100 percent of the time. A grayscale image correlator is proposed that can be built using present technology that can realistically achieve throughput rates on the order of 10(exp 12) operations per second. This translates to over 1000 correlations per second for input scenes with dimensions of 512 times 512 pixels and reference templates of size 64 times 64 pixels. DOE

N90-22250# Edgerton, Germeshausen and Grier, Inc., Idaho Falls, ID. Computer Applications and Technology Transfer Group.
VCS: A NETWORKED VERSION CONTROL SYSTEM
D. G. Barber Feb. 1990 26 p
(Contract DE-AC07-76ID-01570)
(DE90-009805; EGG-CATT-8926) Avail: NTIS HC A03/MF A01

Version Control System (VCS) is a portable source control system which is based on the generic Source Code Control System (SCCS) provided with many Unix systems. It extends the SCCS capabilities and provides support for networked application development. The networking support is provided through TCP/IP facilities. VCS includes functions for version control, change control, base-lining and status reporting. Audit trail, project management, and application development tools are also provided. DOE

N90-22251# Oak Ridge National Lab., TN.
UNDERSTANDING THE COMPUTING SYSTEM DOMAIN OF ADVANCED COMPUTING WITH MICROCOMPUTERS
Kerry A. Hake 1990 24 p Presented at the Advanced Computing for the Social Sciences Conference, Williamsburg, VA, 10-12 Apr. 1990
(Contract DE-AC05-84OR-21400)
(DE90-009825; CONF-9004177-1) Avail: NTIS HC A03/MF A01

Accepting the challenge by the Executive Office of the President, Office of Science and Technology Policy for research to keep pace with technology, the author surveys the knowledge domain of advanced microcomputers. The paper provides a general background for social scientists in technology traditionally relegated to computer science and engineering. The concept of systems integration serves as a framework of understanding for the various elements of the knowledge domain of advanced microcomputing. The systems integration framework is viewed as a series of interrelated building blocks composed of the domain elements. These elements are: the processor platform, operating system, display technology, mass storage, application software, and human-computer interface. References come from recent articles in popular magazines and journals to help emphasize the easy access of this information, its appropriate technical level for the social scientist, and its transient currency. DOE

N90-22244*# Odetics, Inc., Anaheim, CA.
INTENSITY DEPENDENT SPREAD PROCESSOR AND WORKSTATION Abstract Only
George Westrom *In* NASA, Ames Research Center, Vision Science and Technology at NASA: Results of a Workshop Feb. 1990 p 54 (For primary document see N90-22216 15-54)
Avail: NTIS HC A04/MF A01 CSCL 09B

61 COMPUTER PROGRAMMING AND SOFTWARE

Includes computer programs, routines, alogorithms, and specific applications, e.g., CAD/CAM.

N90-22252# National Inst. of Standards and Technology, Gaithersburg, MD. Applied and Computational Mathematics Div.
SUPERCOMPUTERS NEED SUPER ARITHMETIC Final Report
D. W. Lozier and P. R. Turner (Naval Academy, Annapolis, MD.) Oct. 1989 31 p
(PB90-130253; NISTIR-89/4135) Avail: NTIS HC A03/MF A01 CSCL 09B

The parallel computation of vector norms and inner products in floating-point for vector and parallel computers is discussed. The vectorization of algorithms for the operations is examined and a new form of computer arithmetic, the symmetric level-index system, is proposed. Author

N90-22253# National Inst. of Standards and Technology, Gaithersburg, MD. Applied and Computational Mathematics Div.
OPTIMAL 3-DIMENSIONAL METHODS FOR LINEAR PROGRAMMING
Paul D. Domich, Paul T. Boggs, Janet R. Donaldson (National Inst. of Standards and Technology, Boulder, CO.), and Christoph Witzgall Dec. 1989 25 p
(Contract N00014-87-F-0053)
(PB90-155391; NISTIR-89/4225) Avail: NTIS HC A03/MF A01 CSCL 09B

Interior point algorithms for solving linear programming problems are considered. An optimal three-dimensional method is developed that, at each iteration, solves a sub-problem based on minimizing the cost function on low-dimensional cross sections of the feasible region. The generators for the original two-dimensional subproblems are derived from either a discrete or a continuous version of Huard's method of centers. The generators for the optimal three-dimensional subproblem included the dual affine search direction, and two higher order search directions. One of the higher order directions is a third order correction to the Newton recentering direction, and the other is a correction to the dual affine direction that is motivated by the use of rank-one updates of the second derivative information. Numerical results are presented for the optimal three-dimensional method that indicate almost a 23 percent reduction in CPU time compared to the best dual affine implementation. Author

N90-22254# National Inst. of Standards and Technology, Gaithersburg, MD. Applied and Computational Mathematics Div.
AN ALGORITHM AND COMPUTER PROGRAM FOR THE CALCULATION OF ENVELOPE CURVES
M. McClain, A. Feldman, D. Kahaner, and X. T. Ying Dec. 1989 26 p
(PB90-155409; NISTIR-89/4210) Avail: NTIS HC A03/MF A01 CSCL 09B

A procedure was developed to numerically calculate the envelope functions of an oscillatory curve. The method is shown to be applicable to optical transmission data, but it is general enough to be used for many other data sets. The program is available on request. Author

N90-22255*# Missouri Univ., Columbia. Dept. of Industrial Engineering.
ENGINEERING SPECIFICATION AND SYSTEM DESIGN FOR CAD/CAM OF CUSTOM SHOES: UMC PROJECT EFFORT Progress Report, 1 Aug. - 31 Dec. 1989
Han P. Bao May 1990 68 p
(Grant NAG1-875)
(NASA-CR-186547; NAS 1.26:186547; UMC-IE-5-0590) Avail: NTIS HC A04/MF A01 CSCL 09B

Further experimentations were made to improve the design and fabrication techniques of the integrated sole. The sole design is shown to be related to the foot position requirements and the actual shape of the foot including presence of neurotropic ulcers or other infections. Factors for consideration were: heel pitch, balance line, and rigidity conditions of the foot. Machining considerations were also part of the design problem. Among these considerations, widths of each contour, tool motion, tool feed rate, depths of cut, and slopes of cut at the boundary were the key elements. The essential fabrication techniques evolved around the idea of machining a mold then, using quick-firm latex material, casting the sole through the mold. Two main mold materials were experimented with: plaster and wood. Plaster was very easy to machine and shape but could barely support the pressure in the hydraulic press required by the casting process. Wood was found to be quite effective in terms of relative cost, strength, and surface smoothness except for the problem of cutting against the fibers which could generate ragged surfaces. The programming efforts to convert the original dBase programs into C programs so that they could be executed on the SUN Computer at North Carolina State University are discussed. Author

N90-22256# Oak Ridge National Lab., TN. Engineering Physics and Mathematics Div.
SYMBOLIC PATTERN PROCESSING SYSTEM FOR PLANAR SPATIAL STRUCTURES
Nageswara S. V. Rao (Old Dominion Univ., Norfolk, VA.) and Charles W. Glover 1990 17 p Presented at the 10th International Conference on Pattern Recognition, Atlantic City, NJ, 17-21 Jun. 1990
(Contract DE-AC05-84OR-21400)
(DE90-001598; CONF-900652-1) Avail: NTIS HC A03/MF A01

A symbolic pattern processing system that recognizes when composite planar structures are present in a 2-D spatial pattern is described. The composite objects are composed and identified by the arrangement of elementary objects (such as rectangles, squares, circles, etc.). The composite planar structures are represented by a special class of graphs where the nodes satisfy a 2-D ordering. Straightforward algorithms are used to generate these graphs from an image (obtained using a vision system) that was preprocessed by a system of low level neural networks. The graphs are generated for all arrangements of elementary objects in an image, and the resulting graphs are compared with predetermined models of composite objects in order to determine if the composite object is present in the image. An algorithm is presented to find out if two given graphs match within a specified tolerance given by the pair (l,d). A similarity measure between two graphs based on two different linearizations of 2-D lattice points is developed. A decision making module, based on empirical rules, decides if the image contains any instances of the prestored models of composite objects. DOE

N90-22257# Lawrence Livermore National Lab., CA.
SISAL 1.2: AN ALTERNATIVE TO FORTRAN FOR SHARED MEMORY MULTIPROCESSORS
David Cann and John Feo 20 Nov. 1989 12 p Presented at the ACM SIGPLAN 1990 Conference on Programming Language Design and Implementation, White Plains, NY, 20-22 Jun. 1990 Revised Submitted for publication
(Contract W-7405-eng-48)
(DE90-005181; UCRL-102263-Rev-1; CONF-9006101-1-Rev-1)
Avail: NTIS HC A03/MF A01

The acquisition of parallel processors in the scientific community is increasing, but the difficulties of programming parallel machines persist. Two approaches have emerged: automatic parallelizing compilers for extant languages, and new languages that provide an easier-to-use and cleaner parallel programming model. Unfortunately most new languages have acquired a reputation for inefficiency because of their semantics. This paper compares the performance of SISAL 1.2, an applicative language for parallel numerical computations, and FORTRAN using the Livermore Loops. We show that applicative programs when compiled using a set of powerful yet simple optimization techniques can achieve execution speeds comparable to FORTRAN, and can effectively exploit shared memory multiprocessors. DOE

N90-22258# Edgerton, Germeshausen and Grier, Inc., Idaho Falls, ID. Computer Applications and Technology Transfer Group.
FORTRAN CODING GUIDELINES
D. M. Cook, N. H. Marshall, E. S. Marwil, S. D. Matthews, and G. A. Mortensen Feb. 1990 13 p
(Contract DE-AC07-76ID-01570)
(DE90-009804; EGG-CATT-8898) Avail: NTIS HC A03/MF A01

This report describes the FORTRAN coding guidelines used by the Scientific Computing Unit at EG and G Idaho, Inc. All new software development of FORTRAN codes employs these guidelines. Existing software which undergoes adaptive or perfective maintenance is upgraded to meet these guidelines whenever possible. These guidelines are based on adherence to the FORTRAN language standard and utilization of good programming practices to achieve consistency within each software project. DOE

N90-22259# Sandia National Labs., Albuquerque, NM.
MOLECULAR DYNAMICS SIMULATIONS OF SHORT-RANGE FORCE SYSTEMS ON 1024-NODE HYPERCUBES
Steven J. Plimpton 1990 6 p Presented at the 5th Distributed Memory Computing Conference, Charleston, SC, 9-12 Apr. 1990
(Contract DE-AC04-76DP-00789)
(DE90-009833; SAND-89-2918C; CONF-9004159-3) Avail: NTIS HC A02/MF A01

Two parallel algorithms for classical molecular dynamics are presented. The first assigns each processor to a subset of particles; the second assigns each to a fixed region of 3d space. The algorithms are implemented on 1024-node hypercubes for problems characterized by short-range forces, diffusion (so that each particle's neighbors change in time), and problem size ranging from 250 to 10000 particles. Timings for the algorithms on the 1024-node NCUBE/ten and the newer NCUBE 2 hypercubes are given. The latter is found to be competitive with a CRAY-XMP, running an optimized serial algorithm. For smaller problems the NCUBE 2 and CRAY-XMP are roughly the same; for larger ones the NCUBE 2 (with 1024 nodes) is up to twice as fast. Parallel efficiencies of the algorithms and communication parameters for the two hypercubes are also examined. DOE

N90-22260# Sandia National Labs., Albuquerque, NM. Applied Mechanics Div.
PAVING: A NEW APPROACH TO AUTOMATED QUADRILATERAL MESH GENERATION
Ted D. Blacker and Michael B. Stephenson (Brigham Young Univ., Provo, UT.) Mar. 1990 56 p
(Contract DE-AC04-76DP-00789)
(DE90-010244; SAND-90-0249) Avail: NTIS HC A04/MF A01

This paper presents a new mesh generation technique, Paving, which meshes arbitrary 2-D geometries with an all-quadrilateral mesh. Paving allows varying element size distributions on the boundary as well as the interior of a region. The generated mesh is well-formed (i.e., nearly square elements, elements perpendicular to boundaries, etc.) and geometrically pleasing (i.e., mesh contours tend to follow geometric contours of the boundary). In this paper we describe the theory behind this algorithmic/heuristic technique, evaluate the performance of the approach, and present examples of automatically generated meshes. DOE

N90-22261*# Hawaii Univ., Maui. Dept. of Electrical Engineering.
ON DECODING OF MULTI-LEVEL MPSK MODULATION CODES
Shu Lin and Alok Kumar Gupta 20 May 1990 113 p
(Grant NAG5-931)
(NASA-CR-186601; NAS 1.26:186601; NASA-Rept-90-003)
Avail: NTIS HC A06/MF A01 CSCL 09B

The decoding problem of multi-level block modulation codes is investigated. The hardware design of soft-decision Viterbi decoder for some short length 8-PSK block modulation codes is presented. An effective way to reduce the hardware complexity of the decoder by reducing the branch metric and path metric, using a non-uniform floating-point to integer mapping scheme, is proposed and discussed. The simulation results of the design are presented. The multi-stage decoding (MSD) of multi-level modulation codes is also investigated. The cases of soft-decision and hard-decision MSD are considered and their performance are evaluated for several codes of different lengths and different minimum squared Euclidean distances. It is shown that the soft-decision MSD reduces the decoding complexity drastically and it is suboptimum. The hard-decision MSD further simplifies the decoding while still maintaining a reasonable coding gain over the uncoded system, if the component codes are chosen properly. Finally, some basic 3-level 8-PSK modulation codes using BCH codes as component codes are constructed and their coding gains are found for hard decision multistage decoding. Author

N90-22262*# National Aeronautics and Space Administration. Lewis Research Center, Cleveland, OH.

GRID2D/3D: A COMPUTER PROGRAM FOR GENERATING GRID SYSTEMS IN COMPLEX-SHAPED TWO- AND THREE-DIMENSIONAL SPATIAL DOMAINS. PART 1: THEORY AND METHOD

T. I.-P. Shih, R. T. Bailey (Florida Univ., Gainesville.), H. L. Nguyen, and R. J. Roelke Mar. 1990 103 p
(Grants NAG3-929; NAG3-997)
(NASA-TM-102453; E-5241; NAS 1.15:102453) Avail: NTIS HC A06/MF A01 CSCL 09B

An efficient computer program, called GRID2D/3D was developed to generate single and composite grid systems within geometrically complex two- and three-dimensional (2- and 3-D) spatial domains that can deform with time. GRID2D/3D generates single grid systems by using algebraic grid generation methods based on transfinite interpolation in which the distribution of grid points within the spatial domain is controlled by stretching functions. All single grid systems generated by GRID2D/3D can have grid lines that are continuous and differentiable everywhere up to the second-order. Also, grid lines can intersect boundaries of the spatial domain orthogonally. GRID2D/3D generates composite grid systems by patching together two or more single grid systems. The patching can be discontinuous or continuous. For continuous composite grid systems, the grid lines are continuous and differentiable everywhere up to the second-order except at interfaces where different single grid systems meet. At interfaces where different single grid systems meet, the grid lines are only differentiable up to the first-order. For 2-D spatial domains, the boundary curves are described by using either cubic or tension spline interpolation. For 3-D spatial domains, the boundary surfaces are described by using either linear Coon's interpolation, bi-hyperbolic spline interpolation, or a new technique referred to as 3-D bi-directional Hermite interpolation. Since grid systems generated by algebraic methods can have grid lines that overlap one another, GRID2D/3D contains a graphics package for evaluating the grid systems generated. With the graphics package, the user can generate grid systems in an interactive manner with the grid generation part of GRID2D/3D. GRID2D/3D is written in FORTRAN 77 and can be run on any IBM PC, XT, or AT compatible computer. In order to use GRID2D/3D on workstations or mainframe computers, some minor modifications must be made in the graphics part of the program; no modifications are needed in the grid generation part of the program. This technical memorandum describes the theory and method used in GRID2D/3D. Author

N90-22263# Technische Univ., Delft (Netherlands). Faculty of Technical Mathematics and Informatics.

LOCAL MODE SMOOTHING ANALYSIS FOR VARIOUS INCOMPLETE FACTORIZATION ITERATIVE METHODS IN THREE DIMENSIONS

M. Khalil 1989 46 p
(Rept-89-38; ISSN-0922-5461; ETN-90-96355) Copyright Avail: NTIS HC A03/MF A01

Algorithms for various 3-D incomplete factorization iterative methods are described. The local mode smoothing factors for each method are presented. The boundary conditions are taken into account in an approximate way. A robust but costly smoother is found. A simpler but weaker smoother is proposed. Practical tests with a cell-centered multigrid method are carried out using this smoother. Acceleration by Orthomin is used to improve the efficiency of the multigrid in case of bad smoothing. ESA

N90-22264# Technische Univ., Delft (Netherlands). Faculty of Technical Mathematics and Informatics.

SOFTWARE QUALITY ASSURANCE: TOWARDS A MEASURABLE QUALITY IMPROVEMENT [SOFTWARE QUALITY ASSURANCE: NAAR EEN MEETBARE KWALITEITSVERBETERING]

Jacco Wesselius and Frans Ververs 1989 21 p In DUTCH
(Rept-89-42; ISSN-0920-2358; ETN-90-96358) Copyright Avail: NTIS HC A03/MF A01

The requirements for the organization of the software development process for dangerous or privacy-sensitive environments are analyzed with a view to a more active role of the SQA (Software Quality Assurance) division. The concept of software quality is outlined. The requirements for the organization of the software development process which have to be fulfilled to guarantee the quality of the final product already during the development are discussed. It is concluded that the present software development methods do not offer sufficient possibilities to guarantee the quality. A development model has to be developed allowing a frequent quality control, and using formal notation forms to avoid ambiguities. ESA

N90-22265# Technische Univ., Delft (Netherlands). Faculty of Technical Mathematics and Informatics.

LONG STEPS WITH THE LOGARITHMIC PENALTY BARRIER FUNCTION IN LINEAR PROGRAMMING

C. Roos and J.-P. Vial 1989 13 p
(Grant FNSRS-1-467-0-86)
(Rept-89-44; ISSN-0922-5641; ETN-90-96360) Copyright Avail: NTIS HC A03/MF A01

A polynomial implementation of the classical logarithmic barrier function approach is presented. A series of long steps are taken between successive reductions of the penalty parameter. The long steps are used as a means of getting back to the vincinity of the trajectory of centers. The algorithm requires at most O(nL) iterations. In terms of complexity of operation, the inner steps constitute the bulk of the computational effort. The results put the classical barrier method on par with the projective algorithm of Karmarkar. ESA

N90-22266# Technische Univ., Delft (Netherlands). Faculty of Technical Mathematics and Informatics.

AN INTRODUCTION TO MONTAGUE GRAMMAR

Maria Polkowska-Semeniuk and Lech T. Polkowski 1989 51 p
(Rept-89-46; ISSN-0922-5461; ETN-90-96362) Copyright Avail: NTIS HC A04/MF A01

A review of some formal models of language proposed by Richard Montague is presented. Techniques used by Montague and presented in the papers: English as a formal language and a proper treatment of quantification are discussed. Means of generating a subset of English along with semantics for the subset are outlined. Montagues approach to syntax as generally formalized in Universal Grammar is discussed. The Tarski notion of satisfiability is introduced. Literature dealing with Montague grammer is listed and summarized. ESA

N90-22267# Technische Univ., Delft (Netherlands). Faculty of Technical Mathematics and Informatics.

SOME REMARKS ON TREATMENT OF be IN MONTAGUE'S PTQ

Maria Polkowska-Semeniuk and Lech T. Polkowski 1989 16 p
(Rept-89-40; ISSN-0922-5641; ETN-90-96373) Copyright Avail: NTIS HC A03/MF A01

A formula of intensional logic rendering the 2-place verb be is presented. It is shown that under some natural assumptions as to the nature of the terms involved, the expression is equivalent to the original rendering of be as proposed by Montague. The basic notions of intensional logic are reviewed. A restricted non-tensed variant of intensional logic used is described. The dividing of expressions into classes of indexed types in intensional logic is explained. The logical steps involved in the rendering of the verb be are described in detail. ESA

N90-22268# Nationaal Inst. voor Kernfysica en Hoge Energiefysica, Amsterdam (Netherlands).
NEW ALGORITHMS FOR ONE-LOOP INTEGRALS
G. J. vanOldenborgh and J. A. M. Vermaseren 6 Oct. 1989 31 p
(NIKHEF-H/89-17; ETN-90-96385) Avail: NTIS HC A03/MF A01

New algorithms are presented for evaluating the scalar one loop integrals for three and four point functions for arbitrary masses and external momenta. These formulations are useful both for analytic integration and for numerical evaluation in a computer program. The expressions are very compact and provide for an easy isolation of asymptotic behavior and potential numerical problems. The tensor integrals were also rewritten according to new algorithms, making it very easy to express amplitudes in terms of scalar loop integrals. ESA

N90-22269# Universiteit Twente, Enschede (Netherlands). Dept. of Computer Science.
INCOMPARABLE ELEMENTS IN ALGEBRAIC LATTICES WITH APPLICATIONS TO FORMAL LANGUAGE THEORY
Peter R. J. Asveld Oct. 1989 25 p
(Grant NWO-62-58)
(Memo-INF-89-54; ISSN-0923-1714; ETN-90-96387) Avail: NTIS HC A03/MF A01

Two special types of algebraic (or compactly generated) lattices called A1 and A2 lattices are introduced. These lattices are uncountable and each element in these lattices, apart from the zero and the unit, possesses an incomparable element. The main results characterize those elements that have a largest incomparable element. Two particular kinds of algebras called A1 and A2 algebra are defined and it is shown that the lattice of subalgebras of an A1 algebra (A2 algebra) is an A1 lattice (A2 lattice, respectively). These results are established in order to apply them in formal language theory; they yield necessary and sufficient conditions for a language family to possess a largest incomparable similar language family. On the other hand formal language theory provides language families that may serve as (counter) example in algebra. In this way it is shown that, although each A2 algebra (A2 lattice) is an A1 algebra (A1 lattice, repectively), the converse implication does not hold. ESA

N90-22270# Rijkswaterstaat, Delft (Netherlands).
INVENTORY OF PROGRAM PACKAGES RELATED TO THE PROJECT SIMONA [INVENTARISATIE VAN PROGRAMMAPAKKETTEN IN VERBAND MET HET PROJEKT SIMONA]
G. Segal 1989 38 p In DUTCH
(ETN-90-96397) Avail: NTIS HC A03/MF A01

An inventory of different program packages and user wishes was made with a view to the establishment of a general, modular infrastructure for SIMONA (simulation models of the Wet Department for the Maintenance of Dikes, Roads, Bridges and the Navigability of Canals). The emphasis was on packages related to water motion and transport problems. Preprocessing, computations, postprocessing, and data bases were treated separately. Some aspects of the management of SIMONA are discussed. ESA

N90-22271# Oxford Univ. (England). Robotics Research Group.
EDGE RECOGNITION USING IMAGE-PROCESSING HARDWARE
Alan M. McIvor 1989 11 p
(OUEL-1777/89; ETN-90-96409) Avail: NTIS HC A03/MF A01

The implementation of several edge recognition systems is discussed: Sobel, Laplacian of Gaussian, and Canny, on commercially available Datacube Max Video image-processing hardware at or near frame rate. Any approximations necessary to operate at these throughput rates are described and a comparison made between the output of these systems and slower implementations on general-purpose machines. As is normal with these systems, there is a tradeoff between the size of the system and the throughput achievable. All three can be implemented at frame-rate. ESA

N90-22272# Oxford Univ. (England). Robotics Research Group.
IMPLEMENTING THE CANNY EDGE RECOGNIZER WITH DATACUBE IMAGE-PROCESSING HARDWARE
Alan M. McIvor 1989 33 p
(OUEL-1786/89; ETN-90-96414) Avail: NTIS HC A03/MF A01

The implementation of the Canny edge recognition system on commercially available Datacube MaxVideo image-processing hardware at or near frame rate is demonstrated. The approximations needed to do so and the performance of the system are discussed. It is shown that the system can implement the edge recognizer at 5 fps, although this is slowed to 1 fps by the transfer of edge lists to the host. Given a larger system, it would be possible to implement the edge recognizer at frame rate. ESA

N90-22273# Oxford Univ. (England). Robotics Research Group.
A CSP MODEL FOR DISTRIBUTED CONTROL SOFTWARE DESIGN
Y. K. H. Lau and R. W. Daniel 1989 89 p Sponsored by Croucher Foundation
(OUEL-1789/89; ETN-90-96415) Avail: NTIS HC A05/MF A01

The difficulty of implementing error free and deadlock free realtime code even for trivial systems, encountered in the development of software for distributed computer control systems is addressed. A formal system of CSP (communicating sequential processes) is used. A nested hierarchy of subsystems, each described by a functional module, is used as the distributed system. The functional properties of the overall system are derived by describing each module in the style of a program block and the modular structure of a system corresponds to a factorization of its overall specification. Before the stage of implementation, such system specification will be analyzed, correctly proved and finally refined into applicable software. ESA

N90-22274# Royal Signals and Radar Establishment, Malvern (England).
PERFORMANCE OF THE IMP ARRAY PROCESSING ALGORITHM: FIRST RESULTS
J. L. Mather Jul. 1989 52 p
(RSRE-Memo-4291; BR111534; ETN-90-96425) Copyright Avail: NTIS HC A04/MF A01

The Incremental Multi-Parameter (IMP) algorithm is described from the point of view of analyzing data from arrays of sensors. This algorithm makes use of the conventional beamformer as a key component of an iterative analysis of the data, yet is able to outperform alternative high resolution estimators such as MUSIC by 10 to 15 dB. The algorithm is suitable for general array geometries, and is also capable of handling single snapshot data and coherent signals. Preliminary results from Monte Carlo analyses of the performance of IMP are presented in comparison with MUSIC and RootMUSIC. An accelerated beam space version of the algorithm, Eigenvector Projection Method/IMP (EPM/IMP), is introduced, and its performance evaluated against EPM/MUSIC and EPM/RootMUSIC. Conclusions are drawn regarding the reasons for the high performance of IMP. ESA

N90-22275# Royal Signals and Radar Establishment, Malvern (England).
AN INTRODUCTION TO SELECTED STRUCTURED METHODS
G. P. Randell Jun. 1989 51 p
(RSRE-Memo-4294; BR111474; ETN-90-96426) Copyright Avail: NTIS HC A04/MF A01

Concise descriptions of five structured methods are presented as part of a work program looking into the integration of structured and formal methods for the development of software based systems. The structured methods are: Structured Systems Analysis and Design Method (SSADM), Jackson System Development (JSD), Yourdon, Controlled Requirements Expression (CORE) and the Soft Systems Approach. Diagrams describing the stages of SSADM broken down into steps are included. ESA

N90-22276# Royal Signals and Radar Establishment, Malvern (England).
A STUDY OF CACHING IN CAPABILITY COMPUTERS
J. G. Haines (Newcastle-upon-Tyne Univ., England) Sep. 1989 49 p
(RSRE-89015; BR112197; ETN-90-96428) Copyright Avail: NTIS HC A03/MF A01

An investigation into the use of cache memories in capability architectures is described. A theory to describe the relationship between the size of cache and its efficiency is proposed. The use of a simulator to test the theory and compare various cache management policies is described, and the results obtained are discussed. Conclusions are drawn as to the best caching strategy for the SMITE capability computer. ESA

N90-21901*# Jet Propulsion Lab., California Inst. of Tech., Pasadena.
IMPROVING A DATA-ACQUISITION SOFTWARE SYSTEM WITH ABSTRACT DATA TYPE COMPONENTS
S. D. Howard *In its* The Telecommunications and Data Acquisition Report 15 Feb. 1990 p 248-251 (For primary document see N90-21880 15-32)
Avail: NTIS HC A15/MF A02 CSCL 09B

N90-21987# Politecnico di Torino (Italy). Dept. of Aerospace Engineering.
THREE-DIMENSIONAL ADAPTIVE GRIDS WITH LIMITED SKEWNESS
Renzo Arina *In* AGARD, Applications of Mesh Generation to Complex 3-D Configurations Mar. 1990 8 p (For primary document see N90-21975 15-34)
Copyright Avail: NTIS HC A14/MF A02; Non-NATO Nationals requests available only from AGARD/Scientific Publications Executive

N90-21995# Princeton Univ., NJ. Dept. of Mechanical and Aerospace Engineering.
UNSTRUCTURED MESH GENERATION BY A GENERALIZED DELAUNAY ALGORITHM
Timothy J. Baker *In* AGARD, Applications of Mesh Generation to Complex 3-D Configurations Mar. 1990 10 p Sponsored in part by IBM (For primary document see N90-21975 15-34)
Copyright Avail: NTIS HC A14/MF A02; Non-NATO Nationals requests available only from AGARD/Scientific Publications Executive

N90-22219*# Microtronics Associates, Pittsburgh, PA.
PARALLEL ASYNCHRONOUS HARDWARE IMPLEMENTATION OF IMAGE PROCESSING ALGORITHMS Abstract Only
Darryl D. Coon and A. G. U. Perera *In* NASA, Ames Research Center, Vision Science and Technology at NASA: Results of a Workshop Feb. 1990 p 22 (For primary document see N90-22216 15-54)
(Contract NAS1-18645)
Avail: NTIS HC A04/MF A01 CSCL 09B

N90-22222*# National Aeronautics and Space Administration. Goddard Space Flight Center, Greenbelt, MD.
COMPUTATION AND PARALLEL IMPLEMENTATION FOR EARLY VISION Abstract Only
J. Anthony Gualtieri *In* NASA, Ames Research Center, Vision Science and Technology at NASA: Results of a Workshop Feb. 1990 p 25-26 (For primary document see N90-22216 15-54)
Avail: NTIS HC A04/MF A01 CSCL 09B

62 COMPUTER SYSTEMS

Includes computer networks and special application computer systems.

N90-22277# Stanford Linear Accelerator Center, CA.
SCALABLE COHERENT INTERFACE
Knut Alnaes, Ernst H. Kristiansen, David B. Gustavson, and David V. James (Apple Computer, Cupertino, CA.) Jan. 1990 7 p Presented at the CompEuro '90 Conference, Tel Aviv, Israel, 7-9 May 1990
(Contract DE-AC03-76SF-00515)
(DE90-008011; SU-SLAC-PUB-5184; CONF-9005132-1) Avail: NTIS HC A02/MF A01

The Scalable Coherent Interface (IEEE P1596) is establishing an interface standard for very high performance multiprocessors, supporting a cache-coherent-memory model scalable to systems with up to 64 K nodes. This Scalable Coherent Interface (SCI) will supply a peak bandwidth per node of 1 GigaByte/second. The SCI standard should facilitate assembly of processor, memory, I/O and bus bridge cards from multiple vendors into massively parallel systems with throughput far above what is possible today. The SCI standard encompasses two levels of interface, a physical level and a logical level. The physical level specifies electrical, mechanical and thermal characteristics of connectors and cards that meet the standard. The logical level describes the address space, data transfer protocols, cache coherence mechanisms, synchronization primitives and error recovery. In this paper we address logical level issues such as packet formats, packet transmission, transaction handshake, flow control, and cache coherence. DOE

N90-22278*# Old Dominion Univ., Norfolk, VA. Dept. of Computer Science.
EXTREMELY HIGH DATA-RATE, RELIABLE NETWORK SYSTEMS RESEARCH Annual Progress Report, 15 Aug. 1989 - 15 Aug. 1990
E. C. Foudriat, Kurt J. Maly, R. Mukkamala, Nicholas D. Murray (National Aeronautics and Space Administration. Langley Research Center, Hampton, VA.), and C. Michael Overstreet May 1990 182 p
(Grant NAG1-908)
(NASA-CR-186359; NAS 1.26:186359) Avail: NTIS HC A09/MF A01 CSCL 09B

Significant progress was made over the year in the four focus areas of this research group: gigabit protocols, extensions of metropolitan protocols, parallel protocols, and distributed simulations. Two activities, a network management tool and the Carrier Sensed Multiple Access Collision Detection (CSMA/CD) protocol, have developed to the point that a patent is being applied for in the next year; a tool set for distributed simulation using the language SIMSCRIPT also has commercial potential and is to be further refined. The year's results for each of these areas are summarized and next year's activities are described. For individual titles, see N90-22279 through N90-22288.

N90-22279*# Old Dominion Univ., Norfolk, VA. Dept. of Computer Science.
TRAFFIC PLACEMENT POLICIES FOR A MULTI-BAND NETWORK
Kurt J. Maly, E. C. Foudriat, David Game, R. Mukkamala, and C. Michael Overstreet *In its* Extremely High Data-Rate, Reliable Network Systems Research May 1990 13 p (For primary document see N90-22278 15-62)
(Contract NAG1-908; CITT-596041)
Avail: NTIS HC A09/MF A01 CSCL 09B

Recently protocols were introduced that enable the integration of synchronous traffic (voice or video) and asynchronous traffic (data) and extend the size of local area networks without loss in speed or capacity. One of these is DRAMA, a multiband protocol based on broadband technology. It provides dynamic allocation of bandwidth among clusters of nodes in the total network. A number of traffic placement policies for such networks are proposed and evaluated. Metrics used for performance evaluation include average network access delay, degree of fairness of access among the nodes, and network throughput. The feasibility of the DRAMA protocol is established through simulation studies. DRAMA provides effective integration of synchronous and asychronous traffic due to its ability to separate traffic types. Under the suggested traffic placement policies, the DRAMA protocol is shown to handle diverse loads, mixes of traffic types, and numbers of nodes, as well as modifications to the network structure and momentary traffic overloads. Author

N90-22280*# Old Dominion Univ., Norfolk, VA.

CSMA/RN: A UNIVERSAL PROTOCOL FOR GIGABIT NETWORKS

E. C. Foudriat, Kurt J. Maly, C. Michael Overstreet, S. Khanna, and Frank Paterra *In its* Extremely High Data-Rate, Reliable Network Systems Research May 1990 12 p (For primary document see N90-22278 15-62)

Avail: NTIS HC A09/MF A01 CSCL 09B

Networks must provide intelligent access for nodes to share the communications resources. In the range of 100 Mbps to 1 Gbps, the demand access class of protocols were studied extensively. Many use some form of slot or reservation system and many the concept of attempt and defer to determine the presence or absence of incoming information. The random access class of protocols like shared channel systems (Ethernet), also use the concept of attempt and defer in the form of carrier sensing to alleviate the damaging effects of collisions. In CSMA/CD, the sensing of interference is on a global basis. All systems discussed above have one aspect in common, they examine activity on the network either locally or globally and react in an attempt and whatever mechanism. Of the attempt + mechanisms discussed, one is obviously missing; that is attempt and truncate. Attempt and truncate was studied in a ring configuration called the Carrier Sensed Multiple Access Ring Network (CSMA/RN). The system features of CSMA/RN are described including a discussion of the node operations for inserting and removing messages and for handling integrated traffic. The performance and operational features based on analytical and simulation studies which indicate that CSMA/RN is a useful and adaptable protocol over a wide range of network conditions are discussed. Finally, the research and development activities necessary to demonstrate and realize the potential of CSMA/RN as a universal, gigabit network protocol is outlined. Author

N90-22281*# Old Dominion Univ., Norfolk, VA.

DISTRIBUTED SIMULATION, NO SPECIAL TOOLS REQUIRED

Frank Paterra, C. Michael Overstreet, and Kurt J. Maly *In its* Extremely High Data-Rate, Reliable Network Systems Research May 1990 11 p (For primary document see N90-22278 15-62)

(Grants NAG1-908; CIT-INF-89-002-01; RF Proj. 596043)

Avail: NTIS HC A09/MF A01 CSCL 09B

A tool kit of C language functions that can be linked with SIMSCRIPT programs to provide the data communication primitives necessary for distributed simulation is presented. A test case is discussed and some timing data are presented. Additionally some metrics, developed to determine the applicability of the server model decomposition for particular simulations, are discussed. Author

N90-22282*# Old Dominion Univ., Norfolk, VA. Dept. of Computer Science.

ALTERNATIVE PARALLEL RING PROTOCOLS

R. Mukkamala, E. C. Foudriat, Kurt J. Maly, and V. Kale *In its* Extremely High Data-Rate, Reliable Network Systems Research May 1990 18 p (For primary document see N90-22278 15-62)

(Grants NAG1-908; CIT-INF-89-002-01; RF Proj. 596043)

Avail: NTIS HC A09/MF A01 CSCL 09B

Communication protocols are know to influence the utilization and performance of communication network. The effect of two token ring protocols on a gigabit network with multiple ring structure is investigated. In the first protocol, a mode sends at most one message on receiving a token. In the second protocol, a mode sends all the waiting messages when a token is received. The behavior of these protocols is shown to be highly dependent on the number of rings as well as the load in the network. Author

N90-22283*# Old Dominion Univ., Norfolk, VA. Dept. of Computer Science.

PERFORMANCE OF GIGABIT FDDI

David Game and Kurt J. Maly *In its* Extremely High Data-Rate, Reliable Network Systems Research May 1990 9 p (For primary document see N90-22278 15-62)

(Grants NAG1-908; CIT-RF-89-002-01; RF Proj. 596043)

Avail: NTIS HC A09/MF A01 CSCL 09B

Great interest exists in developing high speed protocols which will be able to support data rates at gigabit speeds. Hardware currently exists which can experimentally transmit at data rates exceeding a gigabit per second, but it is not clear as to what types of protocols will provide the best performance. One possibility is to examine current protocols and their extensibility to these speeds. Scaling of Fiber Distributed Data Interface (FDDI) to gigabit speeds is studied. More specifically, delay statistics are included to provide insight as to which parameters (network length, packet length or number of nodes) have the greatest effect on performance. Author

N90-22284*# Old Dominion Univ., Norfolk, VA.

DISTRIBUTED SIMULATION OF NETWORK PROTOCOLS

Frank Paterra, C. Michael Overstreet, and Kurt J. Maly *In its* Extremely High Data-Rate, Reliable Network Systems Research May 1990 12 p (For primary document see N90-22278 15-62)

(Grants NAG1-908; CIT-INF-89-002-01; RF Proj. 596043)

Avail: NTIS HC A09/MF A01 CSCL 09B

Simulations of high speed network protocols are very CPU intensive operations requiring very long run times. Very high speed network protocols (Gigabit/sec rates) require longer simulation runs in order to reach a steady state, while at the same time requiring additional CPU processing for each unit of time because of the data rates for the traffic being simulated. As protocol development proceeds and simulations provide insights into any problems associated with the protocol, the simulation model often must be changed to generate additional or finer statistical performance information. Iterating on this process is very time consuming due to the required run times for the simulation models. The results of the efforts to distribute a high speed ring network protocol, Carrier Sensed Multiple Access/Ring Network (CSMA/RN), are presented. Author

N90-22285*# Old Dominion Univ., Norfolk, VA.

MODELLING HIGH DATA RATE COMMUNICATION NETWORK ACCESS PROTOCOL

S. Khanna, E. C. Foudriat, Frank Paterra, Kurt J. Maly, and C. Michael Overstreet *In its* Extremely High Data-Rate, Reliable Network Systems Research May 1990 11 p (For primary document see N90-22278 15-62)

(Grants NAG1-908; CIT-INF-89-002-01; RF Proj. 596043)

Avail: NTIS HC A09/MF A01 CSCL 09B

Modeling of high data rate communication systems is different from the low data rate systems. Three simulations were built during the development phase of Carrier Sensed Multiple Access/Ring Network (CSMA/RN) modeling. The first was a model using SIMCRIPT based upon the determination and processing of each event at each node. The second simulation was developed in C based upon isolating the distinct object that can be identified as the ring, the message, the node, and the set of critical events. The third model further identified the basic network functionality by creating a single object, the node which includes the set of critical events which occur at the node. The ring structure is implicit in the node structure. This model was also built in C. Each model is discussed and their features compared. It should be stated that the language used was mainly selected by the model developer because of his past familiarity. Further the models were not built with the intent to compare either structure or language but because the complexity of the problem and initial results contained obvious errors, so alternative models were built to isolate, determine, and correct programming and modeling errors. The CSMA/RN protocol is discussed in sufficient detail to understand modeling complexities. Each model is described along with its features and problems. The models are compared and concluding observations and remarks are presented. Author

N90-22286*# Old Dominion Univ., Norfolk, VA. Dept. of Computer Science.

EXTENSIBILITY AND LIMITATIONS OF FDDI

David Game and Kurt J. Maly *In its* Extremely High Data-Rate, Reliable Network Systems Research May 1990 24 p (For primary document see N90-22278 15-62)
(Grants NAG1-908; CIT-RF-89-002-01; RF Proj. 596043)
Avail: NTIS HC A09/MF A01 CSCL 09B

Recently two standards for Metropolitan Area Networks (MANs), Fiber Distributed Data Interface (FDDI) and Distributed Queue Dual Bus (DQDB), have emerged as the primary competitors for the MAN arena. Great interest exists in building higher speed networks which support large numbers of node and greater distance, and it is not clear what types of protocols are needed for this type of environment. There is some question as to whether or not these MAN standards can be extended to such environments. The extensibility of FDDI to the Gbps range and a long distance environment is investigated. Specification parameters which affect performance are shown and a measure is provided for predicting utilization of FDDI. A comparison of FDDI at 100 Mbps and 1 Gbps is presented. Some specific problems with FDDI are addressed and modifications which improve the viability of FDDI in such high speed networks are investigated. Author

N90-22287*# Old Dominion Univ., Norfolk, VA. Dept. of Computer Science.

FAIRNESS PROBLEMS AT THE MEDIA ACCESS LEVEL FOR HIGH-SPEED NETWORKS

Kurt J. Maly, L. Zhang, and David Game *In its* Extremely High Data-Rate, Reliable Network Systems Research May 1990 29 p (For primary document see N90-22278 15-62)
(Grants NAG1-908; CIT-RF-89-002-01; RF Proj. 596043)
Avail: NTIS HC A09/MF A01 CSCL 09B

Most lower speed (approx. 10 Mbps) local area networks use adaptive or random access protocols like Ethernet. Others at higher speed use demand assignment like token or slotted rings. These include Cambridge ring and electronic token ring systems. Fairness issues in representatives of such protocols are discussed. In particular, Fiber Distributed Data Interface (FDDI) was selected as a demand access protocol using tokens, Carrier Sensed Multiple Access/Ring Network (CSMA/RN) a random access protocol, and Distributed Queue Dual Bus (DQDB) a demand access protocol using reservations. Fairness at the media access level was the focus, i.e., attaining access or being excessively delayed when a message is queued to be sent as a function of network location. Within that framework, the essential fairness of FDDI was observed along with severe fairness problems in DQDB and some problems for CSMA/RN. Several modifications were investigated and their ameliorative effect is shown. Finally, a unified presentation which allows comparisons of the three protocols' fairness when normalized to their capacity is given. Author

N90-22288*# Old Dominion Univ., Norfolk, VA. Dept. of Computer Science.

A CARRIER SENSED MULTIPLE ACCESS PROTOCOL FOR HIGH DATA BASE RATE RING NETWORKS

E. C. Foudriat, Kurt J. Maly, C. Michael Overstreet, S. Khanna, and Frank Paterra *In its* Extremely High Data-Rate, Reliable Network Systems Research May 1990 28 p (For primary document see N90-22278 15-62)
(Grants NAG1-908; CIT-INF-89-002-01; RF Proj. 596044)
Avail: NTIS HC A09/MF A01 CSCL 09B

The results of the study of a simple but effective media access protocol for high data rate networks are presented. The protocol is based on the fact that at high data rates networks can contain multiple messages simultaneously over their span, and that in a ring, nodes used to detect the presence of a message arriving from the immediate upstream neighbor. When an incoming signal is detected, the node must either abort or truncate a message it is presently sending. Thus, the protocol with local carrier sensing and multiple access is designated CSMA/RN. The performance of CSMA/RN with TTattempt and truncate is studied using analytic and simulation models. Three performance factors, wait or access time, service time and response or end-to-end travel time are presented. The service time is basically a function of the network rate, it changes by a factor of 1 between no load and full load. Wait time, which is zero for no load, remains small for load factors up to 70 percent of full load. Response time, which adds travel time while on the network to wait and service time, is mainly a function of network length, especially for longer distance networks. Simulation results are shown for CSMA/RN where messages are removed at the destination. A wide range of local and metropolitan area network parameters including variations in message size, network length, and node count are studied. Finally, a scaling factor based upon the ratio of message to network length demonstrates that the results, and hence, the CSMA/RN protocol, are applicable to wide area networks. Author

N90-22289# Technische Univ., Delft (Netherlands). Faculty of Technical Mathematics and Informatics.

TOWARDS A SARKOVSKI ORDER FOR THE EMBEDDING OF DISKS MAINTAINING THEIR ORIENTATION [VERS UN ORDRE DE SARKOVSKII POUR LES PLONGEMENTS DU DISQUE PRESERVANT L'ORIENTATION]

Jean-Marc Gambaudo, Sebastian vanStrien, and Charles Tresser (Nice Univ., France) 1989 11 p In FRENCH; ENGLISH summary
(Rept-89-43; ISSN-0922-5461; ETN-90-96359) Copyright Avail: NTIS HC A03/MF A01

A periodic orbit O with a C1 orientation is characterized. It preserves embedding in the D2 disk such that the isotopic class of this embedding in the punctured disk is of D2-O. The existence of periodic orbits with a period of 3 is shown. Such an orbit contains the periodic orbits of all other periodicities. This is shown to be an analog of a well known result in endomorphism interval studies. Ways in which the results can be applied to other periodic orbits are discussed. ESA

N90-22290# Technische Univ., Delft (Netherlands). Faculty of Technical Mathematics and Informatics.

PARALLEL NON-LINEAR OPTIMIZATION

Freerk A. Lootsma 1989 38 p
(Rept-89-45; ISSN-0922-5461; ETN-90-96361) Copyright Avail: NTIS HC A03/MF A01

Three classes of nonlinear optimization methods suitable for implementation on parallel computers are described. Newton and quasi-Newton methods are concentrated on in the area of unconstrained optimization. They have the advantage of being readily convertible into synchronous and asynchronous algorithms. Promising methods of constrained minimization, the so-called dual algorithms for separable and partially separable problems, are discussed. Decomposition techniques for block angular problems with a small number of linking variables or linking constraints are described. The possible benefits of parallel computing in the field of nonlinear optimization are outlined. ESA

N90-22291# Oxford Univ. (England). Dept. of Engineering Science.

THE WAVE MODEL FOR ADVANCED KNOWLEDGE PROCESSING

Peter S. Sapaty (Academy of Sciences of the Ukrainian SSR, Kiev.) 1989 35 p Sponsored by Alexander von Humboldt Foundation
(OUEL-1803/89; ETN-90-96417) Avail: NTIS HC A03/MF A01

A completely new concept of a universal parallel graph machine is proposed. Its underlying activity is not a program in the usual sense, but a highly organized network-structured active data of large volume which directly interprets strings of the powerful general purpose WAVE metalanguage. The WAVE strings, together with the transit information, propagate in a distributed data space in an asynchronous wavefront mode, colonizing the appropriate regions in it and activating a variety of parallel processes for solving the most diverse classes of graph and network problems. This logic-flow organization, where algorithms exist and develop directly in a large data space, dynamically matching themselves with the distributed data, permits the creation of radically new and powerful computers for advanced knowledge processing. Not being burdened with the traditional centralized control, communication or algorithmic resources, they may include large numbers of processing elements and efficiently exploit the advantages of the VLSI (Very Large Scale Integration) technology. ESA

N90-22292*# National Aeronautics and Space Administration. Langley Research Center, Hampton, VA.
THE ART OF FAULT-TOLERANT SYSTEM RELIABILITY MODELING
Ricky W. Butler and Sally C. Johnson Mar. 1990 132 p
(NASA-TM-102623; NAS 1.15:102623) Avail: NTIS HC A07/MF A01 CSCL 09B

A step-by-step tutorial of the methods and tools used for the reliability analysis of fault-tolerant systems is presented. Emphasis is on the representation of architectural features in mathematical models. Details of the mathematical solution of complex reliability models are not presented. Instead the use of several recently developed computer programs—SURE, ASSIST, STEM, PAWS—which automate the generation and solution of these models is described. Author

63 CYBERNETICS

Includes feedback and control theory, artificial intelligence, robotics and expert systems.

For related information see also *54 Man/System Technology and Life Support.*

N90-22293 Maryland Univ., College Park.
ADAPTIVE CONTROL OF A FLEXIBLE MANIPULATOR WITH UNKNOWN CHANGING LOADS Ph.D. Thesis
Tzung-Cheng Yang 1989 161 p
Avail: Univ. Microfilms Order No. DA8924261

A new adaptive control scheme for the tip position control of a single link flexible manipulator handling unknown changing loads and its experimental verification is presented. The major portion of the new adaptive control scheme consists of a recursive control algorithm (RCA) combined with parameter estimate resetting; acting together, the RCA and the parameter estimate resetting eliminate undesirable transients. The parameter estimate resetting is to memorize the parameter estimate vector obtained from system identification before a payload is picked up and then to use this vector to reset the estimated parameters before the payload is released. Besides the RCA with parameter estimate resetting, the new adaptive control scheme has two other components, namely a new modified Luenberger observer control structure for pole placement and the Fortescue's algorithm for system identification. The modified Luenberger observer control structure applies intergral action on the Luenberger observer structure and is shown both in theory and in simulation to have better performance than the commonly used error driven control structure. The Fortescue's algorithm is used to suppress the transient when the setpoint is changed after the payload is picked up. Dissert. Abstr.

N90-22294*# National Aeronautics and Space Administration. Goddard Space Flight Center, Greenbelt, MD.
THE 1990 GODDARD CONFERENCE ON SPACE APPLICATIONS OF ARTIFICIAL INTELLIGENCE
James L. Rash, ed. May 1990 342 p Conference held in Greenbelt, MD, 1-2 May 1990
(NASA-CP-3068; Rept-90B00078; NAS 1.55:3068) Avail: NTIS HC A15/MF A02 CSCL 09B

The papers presented at the 1990 Goddard Conference on Space Applications of Artificial Intelligence are given. The purpose of this annual conference is to provide a forum in which current research and development directed at space applications of artificial intelligence can be presented and discussed. The proceedings fall into the following areas: Planning and Scheduling, Fault Monitoring/Diagnosis, Image Processing and Machine Vision, Robotics/Intelligent Control, Development Methodologies, Information Management, and Knowledge Acquisition. For individual titles, see N90-22295 through N90-22321.

N90-22295*# National Aeronautics and Space Administration. Goddard Space Flight Center, Greenbelt, MD.
THE APPLICATION OF CONNECTIONISM TO QUERY PLANNING/SCHEDULING IN INTELLIGENT USER INTERFACES
Nicholas Short, Jr. and Lokendra Shastri (Pennsylvania Univ., Philadelphia.) *In its* The 1990 Goddard Conference on Space Applications of Artificial Intelligence May 1990 p 3-16 (For primary document see N90-22294 15-63)
Avail: NTIS HC A15/MF A02 CSCL 09B

In the mid nineties, the Earth Observing System (EOS) will generate an estimated 10 terabytes of data per day. This enormous amount of data will require the use of sophisticated technologies from real time distributed Artificial Intelligence (AI) and data management. Without regard to the overall problems in distributed AI, efficient models were developed for doing query planning and/or scheduling in intelligent user interfaces that reside in a network environment. Before intelligent query/planning can be done, a model for real time AI planning and/or scheduling must be developed. As Connectionist Models (CM) have shown promise in increasing run times, a connectionist approach to AI planning and/or scheduling is proposed. The solution involves merging a CM rule based system to a general spreading activation model for the generation and selection of plans. The system was implemented in the Rochester Connectionist Simulator and runs on a Sun 3/260. Author

N90-22296*# Jet Propulsion Lab., California Inst. of Tech., Pasadena.
RESOURCE ALLOCATION PLANNING HELPER (RALPH): LESSONS LEARNED
Ralph Durham, Norman B. Reilly, and Joe B. Springer *In* NASA, Goddard Space Flight Center, The 1990 Goddard Conference on Space Applications of Artificial Intelligence May 1990 p 17-28 (For primary document see N90-22294 15-63)
Avail: NTIS HC A15/MF A02 CSCL 09B

The current task of Resource Allocation Process includes the planning and apportionment of JPL's Ground Data System composed of the Deep Space Network and Mission Control and Computing Center facilities. The addition of the data driven, rule based planning system, RALPH, has expanded the planning horizon from 8 weeks to 10 years and has resulted in large labor savings. Use of the system has also resulted in important improvements in science return through enhanced resource utilization. In addition, RALPH has been instrumental in supporting rapid turn around for an increased volume of special what if studies. The status of RALPH is briefly reviewed and important lessons learned from the creation of an highly functional design team are focused on through an evolutionary design and implementation period in which an AI shell was selected, prototyped, and ultimately abandoned, and through the fundamental changes to the very process that spawned the tool kit. Principal topics include proper integration of software tools within the planning environment, transition from prototype to delivered to delivered software, changes in the planning methodology as a result of evolving software capabilities and creation of the ability to develop and process generic requirements to allow planning flexibility. Author

N90-22297*# Martin Marietta Corp., Denver, CO. Information Systems Group.
THE ROLE OF ARTIFICIAL INTELLIGENCE TECHNIQUES IN SCHEDULING SYSTEMS

Amy L. Geoffroy, Daniel L. Britt, and John R. Gohring *In* NASA, Goddard Space Flight Center, The 1990 Goddard Conference on Space Applications of Artificial Intelligence May 1990 p 29-41 (For primary document see N90-22294 15-63)
Avail: NTIS HC A15/MF A02 CSCL 09B

Artificial Intelligence (AI) techniques provide good solutions for many of the problems which are characteristic of scheduling applications. However, scheduling is a large, complex heterogeneous problem. Different applications will require different solutions. Any individual application will require the use of a variety of techniques, including both AI and conventional software methods. The operational context of the scheduling system will also play a large role in design considerations. The key is to identify those places where a specific AI technique is in fact the preferable solution, and to integrate that technique into the overall architecture. Author

N90-22298*# Jet Propulsion Lab., California Inst. of Tech., Pasadena.

PLAN-IT-2: THE NEXT GENERATION PLANNING AND SCHEDULING TOOL

William C. Eggemeyer and Jennifer W. Cruz *In* NASA, Goddard Space Flight Center, The 1990 Goddard Conference on Space Applications of Artificial Intelligence May 1990 p 43-61 (For primary document see N90-22294 15-63)
Avail: NTIS HC A15/MF A02 CSCL 09B

PLAN-IT is a scheduling program which has been demonstrated and evaluated in a variety of scheduling domains. The capability enhancements being made for the next generation of PLAN-IT, called PLAN-IT-2 is discussed. PLAN-IT-2 represents a complete rewrite of the original PLAN-IT incorporating major changes as suggested by the application experiences with the original PLAN-IT. A few of the enhancements described are additional types of constraints, such as states and resettable-depletables (batteries), dependencies between constraints, multiple levels of activity planning during the scheduling process, pattern constraint searching for opportunities as opposed to just minimizing the amount of conflicts, additional customization construction features for display and handling of diverse multiple time systems, and reduction in both the size and the complexity for creating the knowledge-base to address the different problem domains. Author

N90-22299*# Space Telescope Science Inst., Baltimore, MD.

AN APPROACH TO RESCHEDULING ACTIVITIES BASED ON DETERMINATION OF PRIORITY AND DISRUPTIVITY

Jeffrey L. Sponsler and Mark D. Johnston *In* NASA, Goddard Space Flight Center, The 1990 Goddard Conference on Space Applications of Artificial Intelligence May 1990 p 63-74 (For primary document see N90-22294 15-63)
Avail: NTIS HC A15/MF A02 CSCL 09B

A constraint-based scheduling system called SPIKE is being used to create long term schedules for the Hubble Space Telescope. Feedback for the spacecraft or from other ground support systems may invalidate some scheduling decisions and those activities concerned must be reconsidered. A function rescheduling priority is defined which for a given activity performs a heuristic analysis and produces a relative numerical value which is used to rank all such entities in the order that they should be rescheduled. A function disruptivity is also defined that is used to place a relative numeric value on how much a pre-existing schedule would be changed in order to reschedule an activity. Using these functions, two algorithms (a stochastic neural network approach and an exhaustive search approach) are proposed to find the best place to reschedule an activity. Prototypes were implemented and preliminary testing reveals that the exhaustive technique produces only marginally better results at much greater computational cost. Author

N90-22300*# General Electric Co., Moorestown, NJ. Advanced Technology Labs.

SPACE COMMUNICATIONS SCHEDULER: A RULE-BASED APPROACH TO ADAPTIVE DEADLINE SCHEDULING

Nicholas Straguzzi *In* NASA, Goddard Space Flight Center, The 1990 Goddard Conference on Space Applications of Artificial Intelligence May 1990 p 75-93 (For primary document see N90-22294 15-63)
Avail: NTIS HC A15/MF A02 CSCL 09B

Job scheduling is a deceptively complex subfield of computer science. The highly combinatorial nature of the problem, which is NP-complete in nearly all cases, requires a scheduling program to intelligently transverse an immense search tree to create the best possible schedule in a minimal amount of time. In addition, the program must continually make adjustments to the initial schedule when faced with last-minute user requests, cancellations, unexpected device failures, quests, cancellations, unexpected device failures, etc. A good scheduler must be quick, flexible, and efficient, even at the expense of generting slightly less-than-optimal schedules. The Space Communication Scheduler (SCS) is an intelligent rule-based scheduling system. SCS is an adaptive deadline scheduler which allocates modular communications resources to meet an ordered set of user-specified job requests on board the NASA Space Station. SCS uses pattern matching techniques to detect potential conflicts through algorithmic and heuristic means. As a result, the system generates and maintains high density schedules without relying heavily on backtracking or blind search techniques. SCS is suitable for many common real-world applications. Author

N90-22301*# Rockwell International Corp., Houston, TX. Space Operations.

CONSTRAINT-BASED EVALUATION OF SEQUENTIAL PROCEDURES

Matthew R. Barry *In* NASA, Goddard Space Flight Center, The 1990 Goddard Conference on Space Applications of Artificial Intelligence May 1990 p 95-103 (For primary document see N90-22294 15-63)
Avail: NTIS HC A15/MF A02 CSCL 09B

Constraining the operation of an agent requires knowledge of the restrictions to physical and temporal capabilities of that agent, as well as an inherent understanding of the desires being processed by that agent. Usually a set of constraints are available that must be adhered to in order to foster safe operations. In the worst case, violation of a constraint may be cause to terminate operation. If the agent is carrying out a plan, then a method for predicting the agent's desires, and therefore possible constraint violations, is required. The conceptualization of constraint-based reasoning used herein assumes that a system knows how to select a constraint for application as well as how to apply that constraint once it is selected. The application of constraint-based reasoning for evaluating certain kinds of plans known as sequential procedures is discussed. By decomposing these plans, it is possible to apply context dependent constraints in production system fashion without incorporating knowledge of the original planning process. Author

N90-22302*# Colorado Univ., Boulder. Lab. for Atmospheric and Space Physics.

SURE (SCIENCE USER RESOURCE EXPERT): A SCIENCE PLANNING AND SCHEDULING ASSISTANT FOR A RESOURCE BASED ENVIRONMENT

Nancy E. Thalman and Thomas P. Sparn *In* NASA, Goddard Space Flight Center, The 1990 Goddard Conference on Space Applications of Artificial Intelligence May 1990 p 105-113 (For primary document see N90-22294 15-63)
Avail: NTIS HC A15/MF A02 CSCL 09B

SURE (Science User Resource Expert) is one of three components that compose the SURPASS (Science User Resource Planning and Scheduling System). This system is a planning and scheduling tool which supports distributed planning and scheduling, based on resource allocation and optimization. Currently SURE is being used within the SURPASS by the UARS (Upper Atmospheric Research Satellite) SOLSTICE instrument to build a daily science plan and activity schedule and in a prototyping effort with NASA GSFC to demonstrate distributed planning and scheduling for the SOLSTICE II instrument on the EOS platform. For the SOLSTICE application the SURE utilizes a rule-based system. Development of a rule-based program using Ada CLIPS as opposed to using conventional programming, allows for capture of the science planning and scheduling heuristics in rules and provides flexibility in inserting or removing rules as the scientific objectives and mission constraints change. The SURE system's role as a component in the SURPASS, the purpose of the SURE planning and scheduling tool, the SURE knowledge base, and the software architecture of the SURE component are described. Author

N90-22303*# Howard Univ., Washington, DC. Dept. of Electrical Engineering.

A KNOWLEDGE-BASED APPROACH TO IMPROVING OPTIMIZATION TECHNIQUES IN SYSTEM PLANNING

J. A. Momoh and Z. Z. Zhang *In* NASA, Goddard Space Flight Center, The 1990 Goddard Conference on Space Applications of Artificial Intelligence May 1990 p 115-122 Sponsored by DOE and Los Angeles Dept. of Water and Power, CA (For primary document see N90-22294 15-63)
(Grant NSF ECS-86-57559)
Avail: NTIS HC A15/MF A02 CSCL 09B

A knowledge-based (KB) approach to improve mathematical programming techniques used in the system planning environment is presented. The KB system assists in selecting appropriate optimization algorithms, objective functions, constraints and parameters. The scheme is implemented by integrating symbolic computation of rules derived from operator and planner's experience and is used for generalized optimization packages. The KB optimization software package is capable of improving the overall planning process which includes correction of given violations. The method was demonstrated on a large scale power system discussed in the paper. Author

N90-22304*# Martin Marietta Corp., Denver, CO. Information Systems Group.

MANAGING TEMPORAL RELATIONS

Daniel L. Britt, Amy L. Geoffroy, and John R. Gohring *In* NASA, Goddard Space Flight Center, The 1990 Goddard Conference on Space Applications of Artificial Intelligence May 1990 p 123-134 (For primary document see N90-22294 15-63)
Avail: NTIS HC A15/MF A02 CSCL 09B

Various temporal constraints on the execution of activities are described, and their representation in the scheduling system MAESTRO is discussed. Initial examples are presented using a sample activity described. Those examples are expanded to include a second activity, and the types of temporal constraints that can obtain between two activities are explored. Soft constraints, or preferences, in activity placement are discussed. Multiple performances of activities are considered, with respect to both hard and soft constraints. The primary methods used in MAESTRO to handle temporal constraints are described as are certain aspects of contingency handling with respect to temporal constraints. A discussion of the overall approach, with indications of future directions for this research, concludes the study. Author

N90-22305*# Ford Aerospace Corp., Seabrook, MD.

NASA GROUND TERMINAL COMMUNICATION EQUIPMENT AUTOMATED FAULT ISOLATION EXPERT SYSTEMS

Y. K. Tang and C. R. Wetzel *In* NASA, Goddard Space Flight Center, The 1990 Goddard Conference on Space Applications of Artificial Intelligence May 1990 p 139-145 (For primary document see N90-22294 15-63)
Avail: NTIS HC A15/MF A02 CSCL 09B

The prototype expert systems are described that diagnose the Distribution and Switching System I and II (DSS1 and DSS2), Statistical Multiplexers (SM), and Multiplexer and Demultiplexer systems (MDM) at the NASA Ground Terminal (NGT). A system level fault isolation expert system monitors the activities of a selected data stream, verifies that the fault exists in the NGT and identifies the faulty equipment. Equipment level fault isolation expert systems are invoked to isolate the fault to a Line Replaceable Unit (LRU) level. Input and sometimes output data stream activities for the equipment are available. The system level fault isolation expert system compares the equipment input and output status for a data stream and performs loopback tests (if necessary) to isolate the faulty equipment. The equipment level fault isolation system utilizes the process of elimination and/or the maintenance personnel's fault isolation experience stored in its knowledge base. The DSS1, DSS2 and SM fault isolation systems, using the knowledge of the current equipment configuration and the equipment circuitry issues a set of test connections according to the predefined rules. The faulty component or board can be identified by the expert system by analyzing the test results. The MDM fault isolation system correlates the failure symptoms with the faulty component based on maintenance personnel experience. The faulty component can be determined by knowing the failure symptoms. The DSS1, DSS2, SM, and MDM equipment simulators are implemented in PASCAL. The DSS1 fault isolation expert system was converted to C language from VP-Expert and integrated into the NGT automation software for offline switch diagnoses. Potentially, the NGT fault isolation algorithms can be used for the DSS1, SM, amd MDM located at Goddard Space Flight Center (GSFC). Author

N90-22306*# National Aeronautics and Space Administration. Lewis Research Center, Cleveland, OH.

AUTONOMOUS POWER EXPERT SYSTEM

Jerry L. Walters, Edward J. Petrik, Mary Ellen Roth, Long Van Truong, Todd Quinn, and Walter M. Krawczonek (Sverdrup Technology, Inc., Cleveland, OH.) *In* NASA, Goddard Space Flight Center, The 1990 Goddard Conference on Space Applications of Artificial Intelligence May 1990 p 147-156 (For primary document see N90-22294 15-63)
Avail: NTIS HC A15/MF A02 CSCL 09B

The Autonomous Power Expert (APEX) system was designed to monitor and diagnose fault conditions that occur within the Space Station Freedom Electrical Power System (SSF/EPS) Testbed. APEX is designed to interface with SSF/EPS testbed power management controllers to provide enhanced autonomous operation and control capability. The APEX architecture consists of three components: (1) a rule-based expert system, (2) a testbed data acquisition interface, and (3) a power scheduler interface. Fault detection, fault isolation, justification of probable causes, recommended actions, and incipient fault analysis are the main functions of the expert system component. The data acquisition component requests and receives pertinent parametric values from the EPS testbed and asserts the values into a knowledge base. Power load profile information is obtained from a remote scheduler through the power scheduler interface component. The current APEX design and development work is discussed. Operation and use of APEX by way of the user interface screens is also covered. Author

N90-22307*# TRW, Inc., Redondo Beach, CA.

SPACECRAFT COMMAND VERIFICATION: THE AI SOLUTION

Lorraine M. Fesq, Amy Stephan, and Brian K. Smith (California Univ., Los Angeles.) *In* NASA, Goddard Space Flight Center, The 1990 Goddard Conference on Space Applications of Artificial Intelligence May 1990 p 157-163 (For primary document see N90-22294 15-63)
Avail: NTIS HC A15/MF A02 CSCL 09B

Recently, a knowledge-based approach was used to develop a system called the Command Constraint Checker (CCC) for TRW. CCC was created to automate the process of verifying spacecraft command sequences. To check command files by hand for timing and sequencing errors is a time-consuming and error-prone task. Conventional software solutions were rejected when it was estimated that it would require 36 man-months to build an automated tool to check constraints by conventional methods. Using rule-based representation to model the various timing and sequencing constraints of the spacecraft, CCC was developed and tested in only three months. By applying artificial intelligence techniques, CCC designers were able to demonstrate the viability of AI as a tool to transform difficult problems into easily managed tasks. The design considerations used in developing CCC are discussed and the potential impact of this system on future satellite programs is examined. Author

N90-22308*# Rockwell International Corp., Houston, TX. Space Operations.

ANALYZING SPACECRAFT CONFIGURATIONS THROUGH SPECIALIZATION AND DEFAULT REASONING

Matthew R. Barry and Carlyle M. Lowe *In* NASA, Goddard Space Flight Center, The 1990 Goddard Conference on Space Applications of Artificial Intelligence May 1990 p 165-179 (For primary document see N90-22294 15-63)
Avail: NTIS HC A15/MF A02 CSCL 09B

For an intelligent system to describe a real-world situation using as few statements as possible, it is necessary to make inferences based on observed data and to incorporate general knowledge of the reasoning domain into the description. These reasoning processes must reduce several levels of specific descriptions into only those few that most precisely describe the situation. Moreover, the system must be able to generate descriptions in the absence of data, as instructed by certain rules of inference. The deductions applied by the system, then, generate a high-level description from the low-level evidence provided by the real and default data sources. An implementation of these ideas in a real-world situation is described. The application concerns evaluation of Space Shuttle electromechanical system configurations by console operators in the Mission Control Center. A production system provides the reasoning mechanism through which the default assignments and specializations occur. Examples are provided within this domain for each type of inference, and the suitability is discussed of each toward achieving the goal of describing a situation in the fewest statements possible. Finally, several enhancements are suggested that will further increase the intelligence of similar spacecraft monitoring applications. Author

N90-22309*# College of William and Mary, Williamsburg, VA. Dept. of Computer Science.

SIMULATION-BASED REASONING ABOUT THE PHYSICAL PROPAGATION OF FAULT EFFECTS

Stefan Feyock and Dalu Li *In* NASA, Goddard Space Flight Center, The 1990 Goddard Conference on Space Applications of Artificial Intelligence May 1990 p 181-189 (For primary document see N90-22294 15-63)
(Contract NCC1-122)
Avail: NTIS HC A15/MF A02 CSCL 09B

The research described deals with the effects of faults on complex physical systems, with particular emphasis on aircraft and spacecraft systems. Given that a malfunction has occurred and been diagnosed, the goal is to determine how that fault will propagate to other subsystems, and what the effects will be on vehicle functionality. In particular, the use of qualitative spatial simulation to determine the physical propagation of fault effects in 3-D space is described. Author

N90-22310*# Howard Univ., Washington, DC. Dept. of Electrical Engineering.

KNOWLEDGE-BASED AND INTEGRATED MONITORING AND DIAGNOSIS IN AUTONOMOUS POWER SYSTEMS

J. A. Momoh and Z. Z. Zhang *In* NASA, Goddard Space Flight Center, The 1990 Goddard Conference on Space Applications of Artificial Intelligence May 1990 p 191-199 Sponsored by DOE and Los Angeles Dept. of Water and Power, CA (For primary document see N90-22294 15-63)
(Grant NSF ECS-86-57559)
Avail: NTIS HC A15/MF A02 CSCL 09B

A new technique of knowledge-based and integrated monitoring and diagnosis (KBIMD) to deal with abnormalities and incipient or potential failures in autonomous power systems is presented. The KBIMD conception is discussed as a new function of autonomous power system automation. Available diagnostic modelling, system structure, principles and strategies are suggested. In order to verify the feasibility of the KBIMD, a preliminary prototype expert system is designed to simulate the KBIMD function in a main electric network of the autonomous power system. Author

N90-22311*# National Aeronautics and Space Administration. Goddard Space Flight Center, Greenbelt, MD.

THE PROCEDURE SAFETY SYSTEM

Maureen E. OBrien *In its* The 1990 Goddard Conference on Space Applications of Artificial Intelligence May 1990 p 201-209 (For primary document see N90-22294 15-63)
Avail: NTIS HC A15/MF A02 CSCL 09B

Telerobotic operations, whether under autonomous or teleoperated control, require a much more sophisticated safety system than that needed for most industrial applications. Industrial robots generally perform very repetitive tasks in a controlled, static environment. The safety system in that case can be as simple as shutting down the robot if a human enters the work area, or even simply building a cage around the work space. Telerobotic operations, however, will take place in a dynamic, sometimes unpredictable environment, and will involve complicated and perhaps unrehearsed manipulations. This creates a much greater potential for damage to the robot or objects in its vicinity. The Procedural Safety System (PSS) collects data from external sensors and the robot, then processes it through an expert system shell to determine whether an unsafe condition or potential unsafe condition exists. Unsafe conditions could include exceeding velocity, acceleration, torque, or joint limits, imminent collision, exceeding temperature limits, and robot or sensor component failure. If a threat to safety exists, the operator is warned. If the threat is serious enough, the robot is halted. The PSS, therefore, uses expert system technology to enhance safety thus reducing operator work load, allowing him/her to focus on performing the task at hand without the distraction of worrying about violating safety criteria. Author

N90-22312*# National Aeronautics and Space Administration. John F. Kennedy Space Center, Cocoa Beach, FL.

THE JPL/KSC TELEROBOTIC INSPECTION DEMONSTRATION

David Mittman, Bruce Bon, Carol Collins, Gerry Fleischer, Todd Litwin, Jack Morrison, Jacquie OMeara, Stephen Peters (Jet Propulsion Lab., California Inst. of Tech., Pasadena.), John Brogdon, and Bob Humeniuk et al *In* NASA, Goddard Space Flight Center, The 1990 Goddard Conference on Space Applications of Artificial Intelligence May 1990 p 213-222 (For primary document see N90-22294 15-63)
Avail: NTIS HC A15/MF A02 CSCL 09B

An ASEA IRB90 robotic manipulator with attached inspection cameras was moved through a Space Shuttle Payload Assist Module (PAM) Cradle under computer control. The Operator and Operator Control Station, including graphics simulation, gross-motion spatial planning, and machine vision processing, were located at JPL. The Safety and Support personnel, PAM Cradle, IRB90, and image acquisition system, were stationed at the Kennedy Space Center (KSC). Images captured at KSC were used both for processing by a machine vision system at JPL, and for inspection by the JPL Operator. The system found collision-free paths through the PAM Cradle, demonstrated accurate knowledge of the location of both objects of interest and obstacles, and operated with a communication delay of two seconds. Safe operation of the IRB90 near Shuttle flight hardware was obtained both through the use of a gross-motion spatial planner developed at JPL using artificial intelligence techniques, and infrared beams and pressure sensitive strips mounted to the critical surfaces of the flight hardward at KSC. The Demonstration showed that telerobotics is effective for real tasks, safe for personnel and hardware, and highly productive and reliable for Shuttle payload operations and Space Station external operations. Author

N90-22313*# Jet Propulsion Lab., California Inst. of Tech., Pasadena. Sequence Automation Research Group.

SYSTEM CONTROL OF AN AUTONOMOUS PLANETARY MOBILE SPACECRAFT

William C. Dias and Barbara A. Zimmerman *In* NASA, Goddard Space Flight Center, The 1990 Goddard Conference on Space Applications of Artificial Intelligence May 1990 p 223-237 (For primary document see N90-22294 15-63)
Avail: NTIS HC A15/MF A02 CSCL 09B

The goal is to suggest the scheduling and control functions necessary for accomplishing mission objectives of a fairly autonomous interplanetary mobile spacecraft, while maximizing reliability. Goals are to provide an extensible, reliable system conservative in its use of on-board resources, while getting full value from subsystem autonomy, and avoiding the lure of ground micromanagement. A functional layout consisting of four basic elements is proposed: GROUND and SYSTEM EXECUTIVE system functions and RESOURCE CONTROL and ACTIVITY MANAGER subsystem functions. The system executive includes six subfuctions: SYSTEM MANAGER, SYSTEM FAULT PROTECTION, PLANNER, SCHEDULE ADAPTER, EVENT MONITOR and RESOURCE MONITOR. The full configuration is needed for autonomous operation on Moon or Mars, whereas a reduced version without the planning, schedule adaption and event monitoring functions could be appropriate for lower-autonomy use on the Moon. An implementation concept is suggested which is conservative in use of system resources and consists of modules combined with a network communications fabric. A language concept termed a scheduling calculus for rapidly performing essential on-board schedule adaption functions is introduced.
Author

N90-22314*# TRW, Inc., Redondo Beach, CA.

AUTOMATED PROCEDURE EXECUTION FOR SPACE VEHICLE AUTONOMOUS CONTROL

Thomas A. Broten and David A. Brown *In* NASA, Goddard Space Flight Center, The 1990 Goddard Conference on Space Applications of Artificial Intelligence May 1990 p 239-250 (For primary document see N90-22294 15-63)
Avail: NTIS HC A15/MF A02 CSCL 09B

Increased operational autonomy and reduced operating costs have become critical design objectives in next-generation NASA and DoD space programs. The objective is to develop a semi-automated system for intelligent spacecraft operations support. The Spacecraft Operations and Anomaly Resolution System (SOARS) is presented as a standardized, model-based architecture for performing High-Level Tasking, Status Monitoring and automated Procedure Execution Control for a variety of spacecraft. The particular focus is on the Procedure Execution Control module. A hierarchical procedure network is proposed as the fundamental means for specifying and representing arbitrary operational procedures. A separate procedure interpreter controls automatic execution of the procedure, taking into account the current status of the spacecraft as maintained in an object-oriented spacecraft model.
Author

N90-22315*# National Aeronautics and Space Administration. Goddard Space Flight Center, Greenbelt, MD.

USING EXPERT SYSTEMS TO IMPLEMENT A SEMANTIC DATA MODEL OF A LARGE MASS STORAGE SYSTEM

Larry H. Roelofs (Computer Technology Associates, Inc., Rockville, MD.) and William J. Campbell *In its* The 1990 Goddard Conference on Space Applications of Artificial Intelligence May 1990 p 253-270 (For primary document see N90-22294 15-63)
Avail: NTIS HC A15/MF A02 CSCL 09B

The successful development of large volume data storage systems will depend not only on the ability of the designers to store data, but on the ability to manage such data once it is in the system. The hypothesis is that mass storage data management can only be implemented successfully based on highly intelligent meta data management services. There now exists a proposed mass store system standard proposed by the IEEE that addresses many of the issues related to the storage of large volumes of data, however, the model does not consider a major technical issue, namely the high level management of stored data. However, if the model were expanded to include the semantics and pragmatics of the data domain using a Semantic Data Model (SDM) concept, the result would be data that is expressive of the Intelligent Information Fusion (IIF) concept and also organized and classified in context to its use and purpose. The results are presented of a demonstration prototype SDM implemented using the expert system development tool NEXPERT OBJECT. In the prototype, a simple instance of a SDM was created to support a hypothetical application for the Earth Observing System, Data Information System (EOSDIS). The massive amounts of data that EOSDIS will manage requires the definition and design of a powerful information management system in order to support even the most basic needs of the project. The application domain is characterized by a semantic like network that represents the data content and the relationships between the data based on user views and the more generalized domain architectural view of the information world. The data in the domain are represented by objects that define classes, types and instances of the data. In addition, data properties are selectively inherited between parent and daughter relationships in the domain. Based on the SDM a simple information system design is developed from the low level data storage media, through record management and meta data management to the user interface.
Author

N90-22316*# Martin Marietta Corp., Denver, CO. Information and Communications Systems.

KNOWLEDGE STRUCTURE REPRESENTATION AND AUTOMATED UPDATES IN INTELLIGENT INFORMATION MANAGEMENT SYSTEMS

Stephen Corey and Richard S. Carnahan, Jr. *In* NASA, Goddard Space Flight Center, The 1990 Goddard Conference on Space Applications of Artificial Intelligence May 1990 p 271-285 (For primary document see N90-22294 15-63)
Avail: NTIS HC A15/MF A02 CSCL 09B

A continuing effort to apply rapid prototyping and Artificial Intelligence techniques to problems associated with projected Space Station-era information management systems is examined. In particular, timely updating of the various databases and knowledge structures within the proposed intelligent information management system (IIMS) is critical to support decision making processes. Because of the significantly large amounts of data entering the IIMS on a daily basis, information updates will need to be automatically performed with some systems requiring that data be incorporated and made available to users within a few hours. Meeting these demands depends first, on the design and implementation of information structures that are easily modified and expanded, and second, on the incorporation of intelligent automated update techniques that will allow meaningful information relationships to be established. Potential techniques are studied for developing such an automated update capability and IIMS update requirements are examined in light of results obtained from the IIMS prototyping effort.
Author

N90-22317*# Naval Research Lab., Washington, DC.

ADAPTIVE PATTERN RECOGNITION BY MINI-MAX NEURAL NETWORKS AS A PART OF AN INTELLIGENT PROCESSOR

Harold H. Szu *In* NASA, Goddard Space Flight Center, The 1990 Goddard Conference on Space Applications of Artificial Intelligence May 1990 p 287-306 (For primary document see N90-22294 15-63)
Avail: NTIS HC A15/MF A02 CSCL 09B

In this decade and progressing into 21st Century, NASA will have missions including Space Station and the Earth related Planet Sciences. To support these missions, a high degree of sophistication in machine automation and an increasing amount of data processing throughput rate are necessary. Meeting these challenges requires intelligent machines, designed to support the necessary automations in a remote space and hazardous environment. There are two approaches to designing these intelligent machines. One of these is the knowledge-based expert system approach, namely AI. The other is a non-rule approach based on parallel and distributed computing for adaptive fault-tolerances, namely Neural or Natural Intelligence (NI). The union of AI and NI is the solution to the problem stated above. The NI segment of this unit extracts features automatically by applying Cauchy simulated annealing to a mini-max cost energy function. The feature discovered by NI can then be passed to the AI system for future processing, and vice versa. This passing increases reliability, for AI can follow the NI formulated algorithm exactly, and can provide the context knowledge base as the constraints of neurocomputing. The mini-max cost function that solves the unknown feature can furthermore give us a top-down architectural design of neural networks by means of Taylor series expansion of the cost function. A typical mini-max cost function consists of the sample variance of each class in the numerator, and separation of the center of each class in the denominator. Thus, when the total cost energy is minimized, the conflicting goals of intraclass clustering and interclass segregation are achieved simultaneously. Author

N90-22318*# Texas Univ., Austin. Dept. of Computer Sciences.

BOUNDED-TIME FAULT-TOLERANT RULE-BASED SYSTEMS

James C. Browne, Allen Emerson, Mohamed Gouda, Daniel Miranker, Aloysius Mok, and Louis Rosier *In* NASA, Goddard Space Flight Center, The 1990 Goddard Conference on Space Applications of Artificial Intelligence May 1990 p 307-321 Sponsored in part by Texas Instruments, Inc. (For primary document see N90-22294 15-63)
(Contracts N00014-89-J-1913; N00014-89-J-1472)
Avail: NTIS HC A15/MF A02 CSCL 09B

Two systems concepts are introduced: bounded response-time and self-stabilization in the context of rule-based programs. These concepts are essential for the design of rule-based programs which must be highly fault tolerant and perform in a real time environment. The mechanical analysis of programs for these two properties is discussed. The techniques are used to analyze a NASA application. Author

N90-22319*# Quebec Univ., Montreal.

A KNOWLEDGE-BASED SYSTEM WITH LEARNING FOR COMPUTER COMMUNICATION NETWORK DESIGN

Samuel Pierre, Hai Hoc Hoang (Montreal Univ., Quebec), and Evelyne Tropper-Hausen *In* NASA, Goddard Space Flight Center, The 1990 Goddard Conference on Space Applications of Artificial Intelligence May 1990 p 323-337 (For primary document see N90-22294 15-63)
Avail: NTIS HC A15/MF A02 CSCL 09B

Computer communication network design is well-known as complex and hard. For that reason, the most effective methods used to solve it are heuristic. Weaknesses of these techniques are listed and a new approach based on artificial intelligence for solving this problem is presented. This approach is particularly recommended for large packet switched communication networks, in the sense that it permits a high degree of reliability and offers a very flexible environment dealing with many relevant design parameters such as link cost, link capacity, and message delay. Author

N90-22320*# Computer Sciences Corp., Beltsville, MD.

EVALUATION OF A PROPOSED EXPERT SYSTEM DEVELOPMENT METHODOLOGY: TWO CASE STUDIES

Lewey Gilstrap *In* NASA, Goddard Space Flight Center, The 1990 Goddard Conference on Space Applications of Artificial Intelligence May 1990 p 339-347 (For primary document see N90-22294 15-63)
Avail: NTIS HC A15/MF A02 CSCL 09B

Two expert system development projects were studied to evaluate a proposed Expert Systems Development Methodology (ESDM). The ESDM was developed to provide guidance to managers and technical personnel and serve as a standard in the development of expert systems. It was agreed that the proposed ESDM must be evaluated before it could be adopted; therefore a study was planned for its evaluation. This detailed study is now underway. Before the study began, however, two ongoing projects were selected for a retrospective evaluation. They were the Ranging Equipment Diagnostic Expert System (REDEX) and the Backup Control Mode Analysis and Utility System (BCAUS). Both projects were approximately 1 year into development. Interviews of project personnel were conducted, and the resulting data was used to prepare the retrospective evaluation. Decision models of the two projects were constructed and used to evaluate the completeness and accuracy of key provisions of ESDM. A major conclusion reached from these case studies is that suitability and risk analysis should be required for all AI projects, large and small. Further, the objectives of each stage of development during a project should be selected to reduce the next largest area of risk or uncertainty on the project. Author

N90-22321*# Ford Aerospace Corp., Seabrook, MD.

SATELLITE IMAGE ANALYSIS USING NEURAL NETWORKS

Roger A. Sheldon *In* NASA, Goddard Space Flight Center, The 1990 Goddard Conference on Space Applications of Artificial Intelligence May 1990 p 349-355 (For primary document see N90-22294 15-63)
Avail: NTIS HC A15/MF A02 CSCL 09B

The tremendous backlog of unanalyzed satellite data necessitates the development of improved methods for data cataloging and analysis. Ford Aerospace has developed an image analysis system, SIANN (Satellite Image Analysis using Neural Networks) that integrates the technologies necessary to satisfy NASA's science data analysis requirements for the next generation of satellites. SIANN will enable scientists to train a neural network to recognize image data containing scenes of interest and then rapidly search data archives for all such images. The approach combines conventional image processing technology with recent advances in neural networks to provide improved classification capabilities. SIANN allows users to proceed through a four step process of image classification: filtering and enhancement, creation of neural network training data via application of feature extraction algorithms, configuring and training a neural network model, and classification of images by application of the trained neural network. A prototype experimentation testbed was completed and applied to climatological data. Author

N90-22322*# National Aeronautics and Space Administration. Ames Research Center, Moffett Field, CA.

PRELIMINARY DEVELOPMENT OF AN INTELLIGENT COMPUTER ASSISTANT FOR ENGINE MONITORING

James D. Disbrow (PRC Systems Services Co., Edwards, CA.), Eugene L. Duke, and Ronald J. Ray Aug. 1989 12 p Previously announced in IAA as A89-46910
(NASA-TM-101702; H-1553; NAS 1.15:101702) Avail: NTIS HC A03/MF A01 CSCL 09B

As part of the F-18 high-angle-of-attack vehicle program, an AI method was developed for the real time monitoring of the propulsion system and for the identification of recovery procedures for the F404 engine. The aim of the development program is to provide enhanced flight safety and to reduce the duties of the propulsion engineers. As telemetry data is received, the results are continually displayed in a number of different color graphical formats. The system makes possible the monitoring of the engine state and the individual parameters. Anomaly information is immediately displayed to the engineer. Author

N90-22323*# National Aeronautics and Space Administration. Lewis Research Center, Cleveland, OH.

ELECTRIC POWER SCHEDULING: A DISTRIBUTED PROBLEM-SOLVING APPROACH

Pamela A. Mellor, James L. Dolce, and Joseph C. Krupp (Decision-Science Applications, Inc., Arlington, VA.) 1990 8 p Proposed for presentation at the 25th Intersociety Energy Conversion Engineering Conference, Reno, NV, 12-17 Aug. 1990; cosponsored by AIChE, SAE, ACS, AIAA, ASME, and IEEE
(NASA-TM-103149; E-5503; NAS 1.15:103149) Avail: NTIS HC A02/MF A01 CSCL 09B

Space Station Freedom's power system, along with the spacecraft's other subsystems, needs to carefully conserve its resources and yet strive to maximize overall Station productivity. Due to Freedom's distributed design, each subsystem must work cooperatively within the Station community. There is a need for a scheduling tool which will preserve this distributed structure, allow each subsystem the latitude to satisfy its own constraints, and preserve individual value systems while maintaining Station-wide integrity. The value-driven free-market economic model is such a tool. Author

N90-22324*# National Aeronautics and Space Administration. Lewis Research Center, Cleveland, OH.

AUTOMATING SECURITY MONITORING AND ANALYSIS FOR SPACE STATION FREEDOM'S ELECTRIC POWER SYSTEM

James L. Dolce, Dejan J. Sobajic, and Yoh-Han Pao (Case Western Reserve Univ., Cleveland, OH.) 1990 10 p Proposed for presentation at the 25th Intersociety Energy Conversion Engineering Conference, Reno, NV, 12-17 Aug. 1990; cosponsored by AIChE, SAE, ACS, AIAA, ASME, and IEEE
(NASA-TM-103148; E-5502; NAS 1.15:103148) Avail: NTIS HC A02/MF A01 CSCL 09B

Operating a large, space power system requires classifying the system's status and analyzing its security. Conventional algorithms are used by terrestrial electric utilities to provide such information to their dispatchers, but their application aboard Space Station Freedom will consume too much processing time. A new approach for monitoring and analysis using adaptive pattern techniques is presented. This approach yields an on-line security monitoring and analysis algorithm that is accurate and fast; and thus, it can free the Space Station Freedom's power control computers for other tasks. Author

N90-22325*# National Aeronautics and Space Administration. Lewis Research Center, Cleveland, OH.

AN EXPERT SYSTEM FOR SIMULATING ELECTRIC LOADS ABOARD SPACE STATION FREEDOM

George Kukich (Analytical Engineering Corp., North Olmsted, OH.) and James L. Dolce 1990 7 p Proposed for presentation at the 25th Intersociety Energy Conversion Engineering Conference, Reno, NV, 12-17 Aug. 1990; cosponsored by AIChE, SAE, ACS, AIAA, ASME, and IEEE
(NASA-TM-103150; E-5504; NAS 1.15:103150) Avail: NTIS HC A02/MF A01 CSCL 09B

Space Station Freedom will provide an infrastructure for space experimentation. This environment will feature regulated access to any resources required by an experiment. Automated systems are being developed to manage the electric power so that researchers can have the flexibility to modify their experiment plan for contingencies or for new opportunities. To define these flexible power management characteristics for Space Station Freedom, a simulation is required that captures the dynamic nature of space experimentation; namely, an investigator is allowed to restructure his experiment and to modify its execution. This changes the energy demands for the investigator's range of options. An expert system competent in the domain of cryogenic fluid management experimentation was developed. It will be used to help design and test automated power scheduling software for Freedom's electric power system. The expert system allows experiment planning and experiment simulation. The former evaluates experimental alternatives and offers advice on the details of the experiment's design. The latter provides a real-time simulation of the experiment replete with appropriate resource consumption. Author

N90-22326# Technische Univ., Delft (Netherlands). Faculty of Technical Mathematics and Informatics.

GUIDE TO RMS-LITERATURE

L. Stakenborg 1989 44 p
(Rept-89-52; ISSN-0922-5461; ETN-90-96368) Copyright Avail: NTIS HC A03/MF A01

An overview of the literature on the subject of Reason Maintenance Systems (RMS) is presented. A deductive system operating in a situation of incomplete knowledge must speculate in order to deduce plausible information. A conclusion may be withdrawn as soon as new information contradicting the conclusion becomes available. Techniques developed to support a deductive system's belief revision process are described. The architecture and applications of RMS-based problem solvers are described. A formalization of the RMS is presented. Two different types of RMS systems are discussed: justification based truth maintenance systems and assumption based truth maintenance systems. A bibliography containing references to the original papers is included. ESA

N90-22327# Oxford Univ. (England). Dept. of Engineering Science.

A FRAME APPROACH TO THE H-INFINITY SUPER-OPTIMAL SOLUTION

D.-W. Gu, M. C. Tsai, and I. Postlethwaite 1989 24 p
(OUEL-1761/89; ETN-90-96403) Avail: NTIS HC A03/MF A01

A frame approach to the H infinity super-optimal solution is given which offers computational improvements over existing algorithms. The approach is based on interpreting s-numbers (defined in the introduction) as largest gains between appropriately defined spaces. Some useful bounds on Hankel singular values and s-numbers are derived. Related definitions and preliminary results are included. ESA

N90-22328# Oxford Univ. (England). Dept. of Engineering Science.

THE ROLE OF INPUT WEIGHTING AND BOUNDING IN THE CHARACTERISTIC GPC METHOD

B. Kouvaritakis and J. A. Rossiter 1989 35 p
(OUEL-1762/89; ETN-90-96404) Avail: NTIS HC A03/MF A01

Transcribing the characteristic decomposition of a transfer function matrix of a discrete time multivariable system from the frequency domain to the time domain provides a convenient means of breaking down complex multivariable GPC (Generalized Predictive Control) problems into a set of simple scalar characteristic GPC problems, but a difficulty arises that in so doing one ends up costing the activity of a fictitious set of inputs in place of the inputs into the actual systems. A study which aims to overcome this difficulty and to propose suitable extensions is presented. The means of bounding inputs from below in order to avoid non-minimum phase behavior (which is inherent in GPC) and from above in order to avoid overfiring which could come into conflict with physical/economic constraint is considered. Some suitable extensions that overcome these problems are given. The efficacy of the results is demonstrated by means of two illustrative examples. ESA

N90-22329# Oxford Univ. (England). Dept. of Engineering Science.

BRANCH POINT PLACEMENT

B. Kouvaritakis and J. A. Rossiter 1989 33 p Sponsored by United Kingdom Science and Engineering Research Center and Central Electricity Generating Board
(OUEL-1767/89; ETN-90-96405) Avail: NTIS HC A03/MF A01

A study of the feedback stability and relative stability margins of a multivariable system is presented. Aims were to identify the branch point properties that minimize the sensitivity problem and maximize the degree of controller commutativity and to propose algorithms for the systematic placement of branch points. Branch point placement improved the sensitivity properties of two different polynomial matrices, one without and one with unstable branch points, and enabled deep truncation of the eigenvalue/eigenvector sequences with minimal error. ESA

N90-22330# Oxford Univ. (England). Dept. of Engineering Science.

A ROBUST STABILITY RESULT FOR GENERALISED PREDICTIVE CONTROL

B. D. Robinson and D. W. Clarke 1989 17 p
(OUEL-1773/89; ETN-90-96408) Avail: NTIS HC A03/MF A01

Based on a stability theorem for pole-placement control a result is derived for generalized predictive control which gives a sufficient condition for closed loop stability in the presence of unmodeled dynamics. The choice of controller design parameters under which this can be applied is presented. Suitable processes with which the result can be used are discussed. The steady plate gain of the model is demonstrated to be an important element in guaranteeing stability. ESA

N90-22331# Oxford Univ. (England). Dept. of Engineering Science.
BICAUSAL REPRESENTATIONS AND MULTIVARIABLE GENERALIZED PREDICTIVE CONTROL
B. Kouvaritakis and J. A. Rossiter 1989 23 p Sponsored by United Kingdom Science and Engineering Research Council and Central Electricity Generating Board
(OUEL-1781/89; ETN-90-96411) Avail: NTIS HC A03/MF A01

The generalization of the generalized predictive control to the multivariable case is addressed. It is shown that under some mild conditions, the characteristic sub-systems admit a bi-causal representation which can be made as accurate as desired. Bicausality does not constitute a problem in predictive control and a suitable multivariable self-tuning algorithm is proposed. The superiority of the derived results is demonstrated by means of a design study. ESA

N90-22332# Instituto de Pesquisas Espaciais, Sao Jose dos Campos (Brazil).
AN INTELLIGENT INTERFACE FOR THE DESIGN OF OPTIMAL CONTROL SYSTEMS
Ricardo Acerbi, Paulo Ouvera Simoni, and Eleri Cardoso (Instituto Tecnologico de Aeronautica, Sao Jose dos Campos, Brazil) Nov. 1989 8 p Presented at the 2nd International Conference on Industrial and Engineering Applications of Artificial Intelligence and Expert Systems, Tullahoma, TN, 6-9 Jun. 1989
(INPE-4917-PRE/1516) Avail: NTIS HC A02/MF A01

An interface for giving suggestions about how to modify weighting matrices which appear in the formulation of optimal control problems with quadratic performance index is described. The suggestions come both from heuristics for choosing the matrix elements, some of them being obtained through simulations for several systems, and also from criteria for improving the system in relation to the specification of some parameters. Author

N90-22333# Instituto de Pesquisas Espaciais, Sao Jose dos Campos (Brazil). Departamento de Processamento de Imagens.
OBJECT DETECTION USING STRUCTURAL MATCHING
Leonardo SantannaBins, Flavio Roberto D. Velasco, and Antonio Miguel Vieir Monteiro Nov. 1989 17 p Presented at the 6th Simposio Brasileiro de Inteligencia Artificial, Rio de Janeiro, Brazil, 6-9 Nov. 1989 Sponsored by SID Informatica
(INPE-4954-PRE/1532) Avail: NTIS HC A03/MF A01

An object can be represented by its structural description, i.e., its simple parts and the relationships between these parts. Detecting objects through structural matching can be achieved by establishing the correspondence between the object description, and the model description previously stored. This work proposes: the use of an extended model of relaxation (that includes some amount of global information) to obtain the best matching between object and model structures; the use of good continuity principle to deal with partially occluded parts. Results of experiments with some images of industrial tools with occluded parts are shown. An appropriate choice of the relationships to be used in structural descriptions allows the detection to be rotation invariant. Author

N90-22334 Arizona State Univ., Tempe.
CONTROL OF HUMAN ARM MOVEMENT VIA OPTIMIZATION Ph.D. Thesis
Amir-Hossein Seif-Naraghi 1989 303 p
Avail: Univ. Microfilms Order No. DA9006008

After a survey of the single- and multi-joint goal-directed human movement literature, it is clear that there is no single hypothesis that explains the strategies of everyday movement. This study is based on the idea that goal-directed movements are in some sense optimal. In order to investigate the optimal control of single-joint elbow movements, an eighth-order nonlinear Hill-based antagonistic muscle pair model, which includes important nonlinear muscle and passive joint properties and neural processes, is utilized. A general performance criterion which includes kinematic as well as neuromuscular measures determines the goal of the movement task, while a global optimization algorithm provides the solution. The systematic variations in relative weights of competing subcriteria result in a continuum of movements at various kinematic and neuromuscular costs and speed. Inclusion of small amounts of neuromuscular costs is very effective in reducing all other costs, with little increase in movement time. Minimum jerk subcriterion matches the kinematics of reported experimental results, but does not match the control strategy. A combination of neuromuscular effort and jerk weighted against a measure of time-optimality is suggested to be a likely candidate for optimization of moderate to fast movements by the nervous system. The simulation results for wrist flexion-extension and head horizontal models concur with the major trends for elbow flexion-extension movements. The effects of inertial and isotonic joint loading and external perturbations, as well as task-specific linearization on control strategies, demonstrate the importance of nonlinear properties of musculoskeletal system in the study of motor control. Dissert. Abstr.

N90-22221*# National Aeronautics and Space Administration. Lyndon B. Johnson Space Center, Houston, TX.
VISION SCIENCE AND TECHNOLOGY FOR SUPERVISED INTELLIGENT SPACE ROBOTS Abstract Only
Jon D. Erickson *In* NASA, Ames Research Center, Vision Science and Technology at NASA: Results of a Workshop Feb. 1990 p 24 (For primary document see N90-22216 15-54)
Avail: NTIS HC A04/MF A01 CSCL 09B

N90-22236*# Jet Propulsion Lab., California Inst. of Tech., Pasadena.
ALGORITHMS AND ARCHITECTURES FOR ROBOT VISION Abstract Only
Paul S. Schenker *In* NASA, Ames Research Center, Vision Science and Technology at NASA: Results of a Workshop Feb. 1990 p 42-43 (For primary document see N90-22216 15-54)
Avail: NTIS HC A04/MF A01 CSCL 09B

N90-22240*# National Aeronautics and Space Administration. Marshall Space Flight Center, Huntsville, AL.
COMPUTER VISION RESEARCH AT MARSHALL SPACE FLIGHT CENTER Abstract Only
Frank L. Vinz *In* NASA, Ames Research Center, Vision Science and Technology at NASA: Results of a Workshop Feb. 1990 p 50 (For primary document see N90-22216 15-54)
Avail: NTIS HC A04/MF A01 CSCL 09B

N90-22245*# National Aeronautics and Space Administration. Goddard Space Flight Center, Greenbelt, MD.
SPACE ENVIRONMENT ROBOT VISION SYSTEM Abstract Only
H. John Wood and William L. Eichhorn *In* NASA, Ames Research Center, Vision Science and Technology at NASA: Results of a Workshop Feb. 1990 p 55 (For primary document see N90-22216 15-54)
Avail: NTIS HC A04/MF A01 CSCL 09B

N90-22246*# National Aeronautics and Space Administration. Goddard Space Flight Center, Greenbelt, MD.
SELF-CALIBRATION OF ROBOT-SENSOR SYSTEM Abstract Only
Pen-Shu Yeh *In* NASA, Ames Research Center, Vision Science and Technology at NASA: Results of a Workshop Feb. 1990 p 56 (For primary document see N90-22216 15-54)
Avail: NTIS HC A04/MF A01 CSCL 09B

64 NUMERICAL ANALYSIS

Includes iteration, difference equations, and numerical approximation.

N90-22335# Tilburg Univ. (Netherlands). Dept. of Economics.
ON THE EXISTENCE OF A POSITIVE DEFINITE SOLUTION OF THE MATRIX EQUATION X + A(SUP TAU)X(EXP -1)A = I
Jacob C. Engwerda 1989 29 p

(PB90-133976; FEW-397) Avail: NTIS HC A03/MF A01 CSCL 12A

The question is raised under which conditions on the real (square) matrix A, the matrix equation X + A sup (tau) X sup (-1) A = I has a real symmetric positive definite solution X. Both necessary and sufficient solvability conditions on A are derived. Moreover, an algorithm is given to calculate the solution. For a number of special cases, an analytic solution is also presented. Author

N90-22336# National Inst. of Standards and Technology, Gaithersburg, MD. Applied and Computational Mathematics Div.

ORTHOGONAL DISTANCE REGRESSION

Paul T. Boggs and Janet R. Donaldson (National Inst. of Standards and Technology, Boulder, CO.) Nov. 1989 18 p
(PB90-151747; NISTIR-89/4197) Avail: NTIS HC A03/MF A01 CSCL 12A

Orthogonal Distance Regression (ODR) is the name given to the computational problem associated with finding the maximum likelihood estimators of measurement error models in the case of normally distributed errors. The stable and efficient algorithm of Boggs et al. for finding the solution of the problem when the underlying model is assumed to be nonlinear in both the independent variable and the parameters is examined. Also described is the associated public domain software package, ODRPACK. The results of a baseline simulation study that compares ODR with ordinary least squares (OLS) are reviewed. New results of an extension to the study are presented. Finally, the use of the asymptotic convariance matrix for computing confidence regions and intervals for the estimated parameters is discussed. The conclusions are that ODR is better than OLS for the criteria considered, and that ODRPACK can provide effective solutions and useful statistical information for nonlinear ODR problems. GRA

N90-22337# Los Alamos National Lab., NM.

AN ANALYSIS OF THE FINITE-DIFFERENCED, EVEN-PARITY DISCRETE-ORDINATES EQUATIONS IN SLAB GEOMETRY

W. F. Miller, Jr. 31 Jan. 1990 6 p Presented at the American Nuclear Society Annual Meeting, Nashville, TN, 10-15 Jun. 1990
(Contract W-7405-eng-36)
(DE90-006479; LA-UR-90-97-Rev; CONF-900608-9-Rev) Avail: NTIS HC A02/MF A01

Considerable effort was expended in recent years in finding improved spatial differencing schemes for the neutron and radiation transport equations. Standard criteria used to select a candidate scheme are its order of spatial convergence for small mesh size and its positivity in the sense that positive solutions emerge from positive input data. More recently, it has become clear that truly robust schemes must behave well in diffusing regions and must be compatible with an effective iteration acceleration method. Recently, Morel and Larsen reported their work on a promising new method called the multiple balance method that has virtually all the desirable characteristics. Here we study a different approach to the problem by considering discrete-ordinates approximations to the even-parity transport equations. Three spatial difference approaches were analyzed: diamond differencing, cell-edge differencing, and cell-center differencing. For the case of isotropic scattering and sources, the latter two approaches are shown to be strictly positive, to be second-order accurate, to be compatible with derived diffusion synthetic acceleration methods, and to possess the necessary diffusion limits. Unlike previous work with the even-parity equation, finite elements or variational principles were not used. DOE

N90-22338# Sandia National Labs., Albuquerque, NM.

SPLINE FUNCTION SMOOTHING AND DIFFERENTIATION OF NOISY DATA ON A RECTANGULAR GRID

Clark R. Dohrmann and Henry R. Busby (Ohio State Univ., Columbus.) 1990 19 p Presented at the Society for Experimental Mechanics Conference, Albuquerque, NM, 4-6 Jun. 1990
(Contract DE-AC04-76DP-00789)
(DE90-009319; SAND-89-2244C; CONF-9006124-2) Avail: NTIS HC A03/MF A01

A method is presented for smoothing and differentiating noisy data given on a rectangular grid. The method makes use of a one-dimensional smoothing algorithm to construct the solution to an associated two-dimensional problem. Smoothing parameter selection is automated using a technique that does not require prior knowledge of the amount of noise in the data. Numerical examples are provided demonstrating the application of the method. DOE

N90-22339*# National Aeronautics and Space Administration. Ames Research Center, Moffett Field, CA.

DYNAMICAL APPROACH STUDY OF SPURIOUS STEADY-STATE NUMERICAL SOLUTIONS OF NONLINEAR DIFFERENTIAL EQUATIONS. PART 1: THE ODE CONNECTION AND ITS IMPLICATIONS FOR ALGORITHM DEVELOPMENT IN COMPUTATIONAL FLUID DYNAMICS

H. C. Yee, P. K. Sweby, and D. F. Griffiths (Dundee Univ., Scotland) Apr. 1990 110 p Proposed for presentation at the 12th International Conference on Numerical Methods in Fluid Dynamics, Oxford, England, 9-13 Jul. 1990
(NASA-TM-102820; A-90149; NAS 1.15:102820) Avail: NTIS HC A06/MF A01 CSCL 12A

Spurious stable as well as unstable steady state numerical solutions, spurious asymptotic numerical solutions of higher period, and even stable chaotic behavior can occur when finite difference methods are used to solve nonlinear differential equations (DE) numerically. The occurrence of spurious asymptotes is independent of whether the DE possesses a unique steady state or has additional periodic solutions and/or exhibits chaotic phenomena. The form of the nonlinear DEs and the type of numerical schemes are the determining factor. In addition, the occurrence of spurious steady states is not restricted to the time steps that are beyond the linearized stability limit of the scheme. In many instances, it can occur below the linearized stability limit. Therefore, it is essential for practitioners in computational sciences to be knowledgeable about the dynamical behavior of finite difference methods for nonlinear scalar DEs before the actual application of these methods to practical computations. It is also important to change the traditional way of thinking and practices when dealing with genuinely nonlinear problems. In the past, spurious asymptotes were observed in numerical computations but tended to be ignored because they all were assumed to lie beyond the linearized stability limits of the time step parameter delta t. As can be seen from the study, bifurcations to and from spurious asymptotic solutions and transitions to computational instability not only are highly scheme dependent and problem dependent, but also initial data and boundary condition dependent, and not limited to time steps that are beyond the linearized stability limit. Author

N90-22340*# National Aeronautics and Space Administration. Ames Research Center, Moffett Field, CA.

ON SPURIOUS STEADY-STATE SOLUTIONS OF EXPLICIT RUNGE-KUTTA SCHEMES

P. K. Sweby, H. C. Yee, and D. F. Griffiths (Dundee Univ., Scotland) Apr. 1990 33 p Presented at the 3rd International Conference on Hyperbolic Problems, Uppsala, Sweden, 11-15 Jun. 1990
(NASA-TM-102819; A-90148; NAS 1.15:102819) Avail: NTIS HC A03/MF A01 CSCL 12A

The bifurcation diagram associated with the logistic equation v sup n+1 = av sup n (1-v sup n) is by now well known, as is its equivalence to solving the ordinary differential equation u prime = alpha u (1-u) by the explicit Euler difference scheme. It has also been noted by Iserles that other popular difference schemes may not only exhibit period doubling and chaotic phenomena but also possess spurious fixed points. Runge-Kutta schemes applied to both the equation u prime = alpha u (1-u) and the cubic equation u prime = alpha u (1-u)(b-u) were studied computationally and analytically and their behavior was contrasted with the explicit Euler scheme. Their spurious fixed points and periodic orbits were noted. In particular, it was observed that these may appear below the linearized stability limits of the scheme and, consequently, computation may lead to erroneous results. Author

N90-22341# Technische Univ., Delft (Netherlands). Faculty of Aerospace Engineering.

DISCRETE VARIABLE STRUCTURAL OPTIMIZATION BY THE COMPLEX METHOD

P. G. vanBladel Jun. 1989 33 p
(LR-597; ETN-90-96352) Avail: NTIS HC A03/MF A01

The use of the complex method for discrete variable optimization problems is proposed. The basic complex method and the required modifications for discrete variables are presented. Three examples of structural optimization problems are solved to show the potential of the method. Results obtained show that the method can usefully be applied to discrete variable problems of modest size. ESA

N90-22342# Technische Univ., Delft (Netherlands). Faculty of Technical Mathematics and Informatics.

A CHINESE BIBLIOGRAPHY ON QUADRATIC SYSTEMS OF DIFFERENTIAL EQUATIONS

R. E. Kooij 1989 35 p
(Rept-89-39; ISSN-0922-5461; ETN-90-96356) Copyright Avail: NTIS HC A03/MF A01

A bibliography of work on quadratic systems by Chinese mathematicians is presented. For each article, the author, title, and magazine in which the article was published are identified. For some articles, the source is given. This is the case for articles appearing in the Mathematical Review, Zentralblatt fur Mathematik and Current Mathematical Publications. The language in which the articles and summaries are written is identified. The articles are listed by order of publication date from 1957 to 1989. ESA

N90-22343# Technische Univ., Delft (Netherlands). Faculty of Technical Mathematics and Informatics.

NORMAL FORMS FOR WEAKLY NON-LINEAR PERTURBED WAVE EQUATIONS

C. G. A. vanderBeek 1989 30 p Sponsored by the Netherlands Foundation for Mathematics and the Netherlands Organization for Scientific Research
(Rept-89-41; ISSN-0922-5461; ETN-90-96357) Copyright Avail: NTIS HC A03/MF A01

A concept of normal forms applicable to a class of weakly nonlinear perturbed wave equations is introduced. An algorithm used in calculating the normal form associated with this class of equations is presented. Some properties of the normal form are discussed. An initial boundary value problem for the Rayleigh wave equation is discussed in detail as an application of the theory. The relationship between the normal form concept and the normal form concept for ordinary differential equations is discussed. It is shown that the energy of the truncated first order normal form of the Rayleigh wave equations has a similar behavior as the energy of the truncated first order normal form of the Rayleigh equation. ESA

N90-22344# Technische Univ., Delft (Netherlands). Faculty of Technical Mathematics and Informatics.

ON A THIRD q-BESSEL FUNCTION

Rene F. Swarttouw 1989 20 p
(Rept-89-48; ISSN-0922-5641; ETN-90-96364) Copyright Avail: NTIS HC A03/MF A01

The relationship between the little q-Jacobi polynomials and a third q-Bessel function is demonstrated. Other relations of the q-Bessel functions are derived. Work by Exton is cited. Some q-extensions of formulas involving derivatives of the Bessel function are presented. The q-difference operator is used to point out the relationships. ESA

N90-22345# Technische Univ., Delft (Netherlands). Faculty of Technical Mathematics and Informatics.

GENERALIZATIONS OF A Q-ANALOGUE OF LAGUERRE POLYNOMIALS

Roelof Koekoek 1989 27 p
(Rept-89-51; ISSN-0922-5461; ETN-90-96367) Copyright Avail: NTIS HC A03/MF A01

Laguerre polynomials which are orthogonal with respect to the inner product are studied. These polynomials have properties which differ from those of classical orthogonal polynomials. The properties of Koornwinder's generalized Laguerre polynomials are summarized. A q-analog of these polynomials is studied. Generalizations of Moak's q-Laguerre polynomials are described. Further generalizations of these polynomials are studied. The q-analog of the polynomials in the general case are investigated. ESA

N90-22346# Technische Univ., Delft (Netherlands). Faculty of Technical Mathematics and Informatics.

PREFERENCE NUMBERS AND FUNNEL DIMENSION

J. M. Aarts and H. vanMaaren 1989 14 p
(Rept-89-57; ISSN-0922-5461; ETN-90-96372) Avail: NTIS HC A03/MF A01

The concept of funnel dimension of a topological space is introduced. Relations with existing notions of dimension are established. Funnel dimension is used to discuss a problem of mathematical economics. The problem is concerned with the characterization of topological spaces admitting the performance of a generalized pivoting algorithm. Such an algorithm approximates solutions to fixed point, optimization or feasibility problems. The connection between such an algorithm and the topology and dimension theory involved in the concept of funnel dimension, is described. ESA

N90-22347# Universiteit Twente, Enschede (Netherlands). Faculty of Applied Mathematics.

HOPF BIFURCATION WITH NONSEMISIMPLE 1:1 RESONANCE E

S. A. VanGils, M. P. Krupa, and W. F. Langford (Guelph Univ., Ontario) Sep. 1989 29 p Sponsored in part by Canadian Natural Sciences and Engineering Research Council
(MEMO-808; ETN-90-96386) Avail: NTIS HC A03/MF A01

The generalized Hopf bifurcation corresponding to non-semisimple double imaginary eigenvalues (case of 1 to 1 resonance) is analyzed using a normal form approach. This bifurcation has codimension 3, and a center subspace of dimension 4. Due to a phase-shift symmetry, the four-dimensional normal form equations may be reduced to a three-dimensional system. There may be 0, 1, or 2 small periodic solutions. There are parameter values for which the three-dimensional system has a degenerate bifurcation associated with eigenvalues. The unfoldings of this degenerate bifurcation give conditions for invariant two tori and three tori in the original system. A further degeneracy in the amplitude equations for the reduced three-dimensional system implies even richer dynamics in the full equations. ESA

N90-22348# Leiden Univ. (Netherlands). Dept. of Mathematics and Computer Science.

EFFICIENT ESTIMATION IN THE CLAYTON-CUZICK MODEL FOR SURVIVAL DATA

Chris A. J. Klaassen 1988 29 p
(TW-88-06; ETN-90-96388) Copyright Avail: NTIS HC A03/MF A01

Some general class of semiparametric transformation models is considered. A second order differential equation is derived which typically determines the efficient influence function for estimation of the real parameter involved. A model of Clayton and Cuzick for survival data is studied in some detail. ESA

N90-22349# Leiden Univ. (Netherlands). Dept. of Mathematics and Computer Science.

THE THETA-METHODS IN THE NUMERICAL SOLUTION OF DELAY DIFFERENTIAL EQUATIONS

Karel J. intHout and Marc N. Spijker 1989 8 p
(TW-89-03; ETN-90-96389) Copyright Avail: NTIS HC A02/MF A01

Initial value problems for delay differential equations are addressed. Two theta methods to deal with stability questions in the numerical solution of Stiff problems are used: a one stage Runge-Kutta or one-leg method and a two stage Runge-Kutta or linear multistep method. The two stage method is concluded as exhibiting a better stability problem than the one stage method. ESA

N90-22350# Leiden Univ. (Netherlands). Dept. of Mathematics and Computer Science.

STABILITY RADIUS OF POLYNOMIALS OCCURRING IN THE NUMERICAL SOLUTION OF INITIAL VALUE PROBLEMS

Roeland vanderMarel 1989 21 p Submitted for publication
(TW-89-04; ETN-90-96390) Copyright Avail: NTIS HC A03/MF A01

Polynomial approximations phi(x) to the exponential function exp(x) related to numerical procedures for solving initial value problems are addressed. Motivated by stability requirements, a numerical study of the largest disk contained in a stability region is presented. Several conjectures about the radius of this largest disk are made on the basis of numerical study. ESA

N90-22351# Leiden Univ. (Netherlands). Dept. of Mathematics and Computer Science.

STABILITY CRITERIA IN THE NUMERICAL SOLUTION OF INITIAL VALUE PROBLEMS

Marc N. Spijker 1989 11 p Submitted for publication
(TW-89-05; ETN-90-96391) Copyright Avail: NTIS HC A03/MF A01

The stability analysis of one-step methods for solving stiff initial value problems is addressed. The first part of the study concerns highly nonlinear differential equations. For such equations a stability analysis based on the test equation U'(t) = AU(t), with constant matrix A, is deceptive. Reliable stability criteria for Runge-Kutta methods are reviewed using the concept of algebraic stability introduced by Burrage, Butcher and Crouzeix. The second part concerns linear differential equations U'(t) = AU(t) with A as above. Here a stability analysis based on the simple test equations U'(t) = lambda U(t) with lambda a complex constant, can also be deceptive. For such situations, reliable stability criteria that can be applied to general one-step methods for solving U'(t) = AU(t) are discussed. ESA

N90-22352# Leiden Univ. (Netherlands). Dept. of Mathematics and Computer Science.

CONTRACTIVITY IN THE MAXIMUM NORM FOR RUNGE-KUTTA METHODS

J. F. B. M. Kraaijevanger 1989 13 p Submitted for publication Sponsored by Netherlands Organization for Scientific Research and Royal Netherlands Academy of Sciences
(TW-89-06; ETN-90-96392) Copyright Avail: NTIS HC A03/MF A01

Conditions for contractivity in the stability analysis of a Runge-Kutta method are considered. Norms generated by an inner product, and norms such as the maximum norms, are dealt with. The linear autonomous case U'(t) = LU(t) and the general nonlinear non autonomous case U'(t) = f(t, U(t)) are considered. A distinction between unconditional contractivity (for all stepsizes) and conditional contractivity (under stepsize restriction) is made. ESA

N90-22353# Leiden Univ. (Netherlands). Dept. of Mathematics and Computer Science.

STABILITY ANALYSIS OF NUMERICAL METHODS FOR DELAY DIFFERENTIAL EQUATIONS

Karel J. intHout and Marc N. Spijker 1989 16 p
(TW-89-09; ETN-90-96393) Copyright Avail: NTIS HC A03/MF A01

The stability analysis of step-by-step methods for the numerical solution of delay differential equations is addressed. The behavior of such methods when they are applied to the linear test problem U'(t) = lambda U(t) + mu U(t - upsilon) with upsilon greater than 0 and lambda, mu complex is focussed on. A general theorem is presented which can be used to obtain complete characterizations of the stability regions of these methods. ESA

N90-22354# National Physical Lab., Teddington (England). Div. of Information Technology and Computing.

THE APPROXIMATION OF A COMPOSITE BEZIER CUBIC CURVE BY A COMPOSITE BEZIER QUADRATIC CURVE

M. G. Cox and P. M. Harris Oct. 1989 25 p Presented at Institute of Mathematics and its Applications Silver Jubilee Conference, 5-6 Sep. 1989
(NPL-DITC-147/89; ISSN-0262-5369; ETN-90-96431) Copyright Avail: NTIS HC A03/MF A01

In the context of the computer representation of textual characters, an algorithm for approximating a composite Bezier cubic curve by a composite Bezier quadratic curve is described. The knots or breakpoints of the approximating function are determined such that the error of approximation does not exceed a specified value. The number of breakpoints, and hence the number of arcs of the approximation, is not in general optimal but can be expected to be small. The work is clearly relevant to other application areas. ESA

N90-22355# National Physical Lab., Teddington (England). Div. of Information Technology and Computing.

THE USE OF LOCAL POLYNOMIAL APPROXIMATIONS IN A KNOT-PLACEMENT STRATEGY FOR LEAST SQUARES SPLINE FITTING

Helen M. Anthony, M. G. Cox, and P. M. Harris Oct. 1989 19 p
(NPL-DITC-148/89; ISSN-0262-5369; ETN-90-96432) Copyright Avail: NTIS HC A03/MF A01

The use of univariate spline functions to obtain least-squares fits to noisy data is investigated. When defining the linear space of approximating functions from which a fit is to be taken, there is freedom both in the number and locations of the interior knots. These knots can have a profound influence on how well the spline fits the data. An algorithm is described for determining an initial estimate of the number of knots, and their distribution, from which an initial fit to the data is obtained. The algorithm exploits in a natural way the piecewise polynomial nature of the approximating function by isolating subsets of the data which are adequately described by simple polynomials. Once an initial set of knots is known, adaptive knot placement strategies may be used to improve this set. ESA

N90-22356# National Physical Lab., Teddington (England). Div. of Information Technology and Computing.

NEURAL IMPLEMENTATION OF A METHOD FOR SOLVING SYSTEMS OF LINEAR ALGEBRAIC EQUATIONS

A. B. Forbes and A. J. Mansfield Nov. 1989 16 p
(NPL-DITC-155/89; ISSN-0262-5369; ETN-90-96433) Copyright Avail: NTIS HC A03/MF A01

It is shown that a direct method for finding the general solution to a system of linear equations can be implemented in a simple neural network using only features found in many neural models. Thus it is likely that this algorithm will have a parallel implementation using purpose-built neural hardware. Moreover, the neural implementation of the algorithm gives a training method for an associative network without hidden units. A comparison with other training methods is made. ESA

N90-22357# National Physical Lab., Teddington (England). Div. of Materials Applications.

THE ANALYSIS OF STRESS RELAXATION ON INDENTATION OF A RIGID PUNCH INTO A VISCOELASTIC SHEET OF FINITE THICKNESS

D. H. Ferriss Aug. 1989 23 p
(NPL-DMA(A)-193; ISSN-0143-7313; ETN-90-96436) Copyright Avail: NTIS HC A03/MF A01

As a first stage, the problem of a rigid punch indenting into an elastic sheet of finite thickness is treated using a Hankel transform of the stress function. The problem is reduced to a Fredholm integral equation of the second kind. It is shown how the total load under the punch can be determined from numerical solution of this equation. In a second stage the analysis is extended to allow for the effects of viscoelasticity of the indented sheet by assuming a simple linear model for the material behavior and invoking the correspondence principle. ESA

65 STATISTICS AND PROBABILITY

Includes data sampling and smoothing; Monte Carlo method; and stochastic processes.

N90-22358# Technische Univ., Delft (Netherlands).
CLUSTERING AND UNIQUENESS IN MATHEMATICAL MODELS OF PERCOLATION PHENOMENA Ph.D. Thesis
Alberto Gandolfi 1989 116 p Sponsored by CNR
(ETN-90-96400) Copyright Avail: NTIS HC A08/MF A01

The models of major interest in the theory of percolation and in statistical mechanics, are reviewed. The results presented are placed in the wider context of the knowledge of these models. The relation between percolation and the random graphs is discussed. A random graph is obtained when the graph is given and the random subgraph of it is described by a probability measure. The random graph is said to be totally connected if the subgraph contains all vertices of the original graph, with probability one. Examples and conditions for a graph to be totally connected are given. The contribution of the work to random graph theory consists of simplified proofs that certain conditions are sufficient to ensure that a graph is totally connected. The supercritical phase and its recent results are stressed. ESA

66 SYSTEMS ANALYSIS

Includes mathematical modeling; network analysis; and operations research.

N90-22359# Science Applications International Corp., Orlando, FL.
ENGAGEMENT ANALYSIS STUDY Final Report
29 Sep. 1989 67 p Prepared for LLNL, CA
(Contract W-7405-eng-48)
(DE90-009529; UCRL-21237) Avail: NTIS HC A04/MF A01

The engagement analysis effort since the initial report is documented herein. This work was in two phases, and supported LLNL in guidance and engagement analysis efforts of interest to them. The initial efforts consisted of analysis of a ground launched midcourse phase interceptor. During the later phases of the subcontract, emphasis shifted toward an innovative space based engagement concept. Both efforts are documented herein. Part 2 includes the results of simulation modifications and guidance analyses. Additional case runs and the 6 DOF results were generated under this LLNL subcontract. DOE

67 THEORETICAL MATHEMATICS

Includes topology and number theory.

N90-22360# Stanford Univ., CA. Systems Optimization Lab.
A GENERALIZED COMPLEMENTARITY PROBLEM IN HILBERT SPACE
Jen-Chih Yao Mar. 1990 5 p
(Contracts DE-FG03-87ER-25028; N00014-89-J-1659; NSF DMS-89-13089)
(DE90-009576; SU-SOL-90-5) Avail: NTIC HC A01/MF A01

An existence theorem for a generalized complementarity problem over arbitrary closed convex cone in a Hilbert space is proved. DOE

70 PHYSICS (GENERAL)

For precision time and time interval (PTTI) see *35 Instrumentation and Photography;* for geophysics, astrophysics or solar physics see *46 Geophysics, 90 Astrophysics,* or *92 Solar Physics.*

N90-22361# Oak Ridge National Lab., TN. Mathematical Sciences Section.
A WEAK FORMULATION FOR PHASE-CHANGE PROBLEMS WITH BULK MOVEMENT DUE TO UNEQUAL DENSITIES
Vasilios Alexiades (Tennessee Univ., Knoxville.) and John B. Drake 1990 6 p Presented at the 5th International Colloquium on Free Boundary Problems: Theory and Applications, Montreal, Quebec, 13-22 Jun. 1990
(Contract DE-AC05-84OR-21400)
(DE90-009398; CONF-900684-2) Avail: NTIS HC A02/MF A01

When the densities of solid and liquid are different, a change of phase induces a volume change, forcing movement of the bulk phases. Conservation of total energy across the interface leads to a modified Stefan Condition, which contains a term cubic in the interfacial speed. We present a weak formulation for the conservation of mass, momentum and energy and study numerically a 1-phase, one-dimensional example. DOE

N90-22362# Technische Univ., Delft (Netherlands). Faculty of Technical Mathematics and Informatics.
ON THE STRUCTURE OF MANDELBROT'S PERCOLATION PROCESS AND OTHER RANDOM CANTOR SETS
F. M. Dekking and R. W. J. Meester 1989 25 p
(Rept-89-54; ISSN-0922-5461; ETN-90-96369) Copyright Avail: NTIS HC A03/MF A01

Generalizations of Mandelbrot's percolation process are discussed. A process called the random Sierpinski carpet is given particular attention. The process passes through several different phases as its parameters increase from zero to one. The final percolation phase is described in detail. Mandelbrot's implementation of Hoyle's model of galaxies is presented as an example of a percolation. Random sets with a statistically self-similar structure were called canonical curdling by Mandelbrot. Chayes, Chayes and Durrette renamed the process Mandelbrot percolation. Ways of generating the classical Cantor set by means of substitution are shown. ESA

71 ACOUSTICS

Includes sound generation, transmission and attenuation. For noise pollution see *45 Environmental Pollution.*

N90-22363# Vibration Inst., Clarendon Hills, IL.
THE SHOCK AND VIBRATION DIGEST, VOLUME 21, NO. 6 Monthly Report
Judith Nagle-Eshleman, ed. Jun. 1989 76 p
Avail: NTIS HC A05/MF A01

A feature article on noise transmission into propeller-driven airplanes, a review of a book on composite structures, and a bibliography of shock and vibration related topics are included. The bibliography covers such areas of interest as: machine tools, bridges, helicopters, gears, beams, mechanical properties, computational methods and modeling techniques. For individual title see N90-22364.

N90-22364# Atlantic Applied Research Corp., Van Nuys, CA.
NOISE TRANSMISSION INTO PROPELLER-DRIVEN AIRPLANES
J. F. Wilby *In* Vibration Inst., The Shock and Vibration Digest, Volume 21, No. 6 Jun. 1989 p 3-10 (For primary document see N90-22363 15-71)
Avail: NTIS HC A05/MF A01

Recent progress in the understanding of noise transmission in propeller-driven airplnes since 1985 is reviewed. The discussion includes airborne and structure-borne noise transmission and passive and active noise control. It is concluded that the following work is required before current results can be implemented in an actual airplane environment: (1) development of a detailed structure-borne noise model for typical airplane structures, (2) development of improved passive noise control treatments tuned to propeller noise harmonic components, (3) implementation of active noise control methods in typical aircraft environments, and (4) improved understanding of noise transmission through aircraft structures made from composite materials. Author

N90-22365 Georgetown Univ., Washington, DC.

POLARIZATION COUPLING IN THE ACOUSTO-OPTIC INTERACTION OF SURFACE WAVES Ph.D. Thesis

William Robert Graver 1988 174 p

Avail: Univ. Microfilms Order No. DA8923232

Optical wave depolarization resulting from an interaction with a surface acoustic wave was analyzed for conditions where the acoustic beam does not lie in the optical plane of incidence. The depolarization resulting from the acousto-optic interaction is predicted from the scattered optical field as a function of the optical incident angle, theta, and the acoustic incident angle, phi. The acoustic contributions to the scattered optical field considered in the analysis include the corrugation of the surface and the elasto-optic effect near the surface. In the physical case modeled, the acoustic wave propagates in fused silica and the optical wave propagates in air. The contributions from acoustic-to-optical wave number ratio, K/k, and acoustically-driven corrugation and elasto-optic surface amplitude effects are investigated with regard to incident-to-scattered polarization states: S to S, S to P, P to S, and P to P. A general scattering cross-section model is used to predict depolarization over -90 is less than theta is less than +90 degrees. Scattering cross-sections for 0 is less than K/k is less than or = to 0.1 are modeled by computer analysis for coplanar and noncoplanar cases. The presence of incident-to-scattered polarization, initially identified as a complementary change in the non-coplanar cross-section values for scattered S and P states, is also investigated by the Jones method of optical matrices. Using Jones notation to describe the initial-to-scattered polarization states, an optical analog method was developed with transfer matrix coefficients defined by the scattered light field from the general scattering cross-section model. The optical analog model was then modified, using the coefficients of the Jones matrix, to generate a Stokes transfer matrix describing the interaction. Re-defining the incident S- and P-states in Stokes notation, the change in scattered optical intensity was tested for similar cases of depolarization studied by the Jones method. Dissert. Abstr.

N90-22366 Georgetown Univ., Washington, DC.

DIFFRACTION OF LIGHT BY ULTRASONIC PULSES Ph.D. Thesis

John William Wolf 1988 169 p

Avail: Univ. Microfilms Order No. DA8923228

An experimental setup was designed and constructed to verify the predictions of a recently developed theory of light diffraction by pulsed ultrasonic waves. The computer-controlled apparatus uses a long optical path to resolve diffraction orders produced by low MHz center frequency pulses with repetition frequencies as low as 40 KHz. The experiment is the first to accurately measure light patterns produced by ultrasonic pulses of such low repetition frequencies. The primary result of the experiment is a technique to model an ultrasonic pulse in a liquid medium, given the center and repetition frequencies and pulse duration. An empirical model of the transducer response to continuous waves was developed and used to predict the Fourier spectrum of a pulse in the liquid. This pulse spectrum is used as input for the diffraction model to predict the shape of the resultant light diffraction pattern. Finite amplitude pulses were propagated and examined with the diffraction apparatus. The nonlinear theory describing finite amplitude acoustic waves was applied to ultrasonic pulses and combined with the pulse spectrum and light diffraction models. Ultrasonic pulses, reflected and transmitted from a brass plate, were examined with the light diffraction apparatus. The theory describing reflection and transmission of ultrasonic beams from plates immersed in liquid media was applied to ultrasonic pulses and incorporated into the pulse spectrum, nonlinear propagation, and light diffraction models. Dissert. Abstr.

N90-22367 Stanford Univ., CA.

NONLINEAR ACOUSTIC INTERACTIONS IN SUPERFLUID HELIUM Ph.D. Thesis

Donald Rex Wright 1989 107 p

Avail: Univ. Microfilms Order No. DA8925978

Studies of nonlinear acoustic interactions in superfluid helium at temperatures below 0.2 K have culminated in the construction of an all-acoustic parametric amplifier at gigahertz frequencies. This amplifier represents the shortest wavelength parametric amplifier ever made, with signal wavelengths shorter than 1000A and pump wavelengths shorter than 600A. Begun as part of a program to extend the frequency range, and hence improve the resolution, of the scanning acoustic microscope while maintaining an adequate signal-to-noise ratio, the early work on nonlinearity concentrated on the very high power densities achieved at the focus of an acoustic lens. In a pressure range where the dispersion forbids three phonon processes, indirect evidence of four phonon mixing is observed. In the parametric amplifier experiment, plane waves are mixed at a predefined angle in the superfluid helium. Two gain regimes are observed. The first regime is a four phonon collinear process, in which gain on the signal is created by the second-harmonic of the pump. The second regime is a noncollinear phase matched process, in which the signal phonon stimulates decay of the pump phonon to create gain at the signal frequency. Dissert. Abstr.

N90-22368 Pennsylvania State Univ., University Park.

AN INVESTIGATION OF THE GENERATION AND RADIATION OF AERODYNAMIC NOISE IN REAL PIPING SYSTEMS Ph.D. Thesis

William Carl Ward 1989 262 p

Avail: Univ. Microfilms Order No. DA9007942

The response of finite length cylindrical shells to excitation by broadband, aerodynamically generated internal sound flow was investigated. The response is shown to be damping controlled; the nonresonant coincidence response can be modeled by an exponential buildup over the acoustic propagation time in the shell: t = c/l. For an infinite pipe or when the coincidence frequency closely matches a finite length resonance, the response approaches the damping limit. A simple theory for the narrowband transmission loss, termed the Damping Controlled Arbitrary Length Coincidence method (DCALC), is proposed and verified experimentally. By modeling each coincidence as a simple damped oscillator, the method gives the off-resonance and near-resonance limits of the transmission loss, as well as the approximate shape of the transmission loss dips and the maximum values between adjacent coincidences. Knowledge of the pipe resonances is not required, and the calculation effort for the method is less than for statistical methods, even though a narrowband prediction is obtained. The DCALC method was evaluated through wall response measurements of industrial steel pipes, ranging from 0.5 to 3 meters in length, driven by throttling noise from a globe valve over a variety of flow conditions. The measured pipe responses showed good agreement with theory, and the results demonstrate the limits of accuracy for transmission loss predictions. Dissert. Abstr.

N90-22369 College of William and Mary, Williamsburg, VA.

NONLINEARITY PARAMETERS OF POLYMERS Ph.D. Thesis

Meng-Chou Wu 1989 110 p

Avail: Univ. Microfilms Order No. DA9008532

Three types of acoustic nonlinearity parameters for solids are discussed. The results of measurements of these parameters for three polymers - polymethyl methacrylate, Polystyrene, and polysulfone - are presented. A new technique was developed, using piezoelectric transducers directly bonded to the specimens, which allows the measurements of fundamental and second harmonics generated in the solids, and thereby the determination of nonlinearity parameter beta(sub 3), which is the ratio of a linear combination of second- and third-elastic coefficients to the

second-order elastic coefficient. The second nonlinearity parameter, B/A can be determined from the temperature and pressure derivatives of the sound velocity. Its exact relationship for the case of solids was derived. The results from the two techniques are shown to be consistent. The pressure derivative of the sound velocity is also related to the Grueneisen parameter, which can be used to describe the anharmonicity of interactions in polymer molecules, especially of interchain vibrations. The interchain specific heat for these polymers is then calculated from the Grueneisen parameters; and the characterization of polymers by using these thermoacoustic parameters is discussed.
Dissert. Abstr.

72 ATOMIC AND MOLECULAR PHYSICS

Includes atomic structure, electron properties, and molecular spectra.

N90-22370# California Univ., Davis. Dept. of Physics.
CORRELATED ELECTRON PROCESSES IN ION-ATOM COLLISIONS Final Report, 8 Sep. 1988 - 31 Aug. 1989
Douglas W. McColm 1 Feb. 1990 13 p Prepared for Lawrence Livermore National Lab., CA
(Contract W-7405-eng-48)
(DE90-009477; UCRL-CR-103380) Avail: NTIS HC A03/MF A01

Electron processes occurring in collisions between heavy ions and atoms were studied. The doubly differential secondary electron yield following the impact of 3.5 to 8 MeV/uU(sup q+)(q = 38,68) ion impact on thin carbon foil targets was investigated experimentally. The absolute electron emission yields were determined for ejection angles varied between 22.5 and 157 deg and electron energies ranging from 10 eV to 8 keV. The electron spectra are compared to previous investigations and new experimental data using lighter ion impact at MeV projectile energies. DOE

N90-22371*# National Aeronautics and Space Administration. Marshall Space Flight Center, Huntsville, AL.
NEW CALCULATIONS AND MEASUREMENTS OF THE COULOMB CROSS-SECTION FOR THE PRODUCTION OF DIRECT ELECTRON PAIRS BY HIGH ENERGY NUCLEI
J. H. Derrickson, S. Dake, B. L. Dong, P. B. Eby, W. F. Fountain, M. Fuki, J. C. Gregory, T. Hayashi, A. Iyono, and D. T. King (Tennessee Univ., Knoxville.) et al [1989] 4 p Prepared in cooperation with Osaka Univ., Japan
(Grant NAGw-1231)
(NASA-TM-101280; NAS 1.15:101280) Avail: NTIS HC A01/MF A01 CSCL 20H

Recently, new calculations were made of the direct Coulomb pair cross section that rely less in arbitrary parameters. More accurate calculations of the cross section down to low pair energies were made. New measurements of the total direct electron pair yield, and the energy and angular distribution of the electron pairs in emulsion were made for O-16 at 60 and 200 GeV/amu at S-32 at 200 GeV/amu which give satisfactory agreement with the new calculations. These calculations and measurements are presented along with previous accelerator measurements made of this effect during the last 40 years. The microscope scanning criteria used to identify the direct electron pairs is described. Prospects for application of the pair method to cosmic ray energy measurements in the region 10 (exp 13) to 10 (exp 15) eV/amu are discussed.
Author

N90-22372# Nationaal Inst. voor Kernfysica en Hoge Energiefysica, Amsterdam (Netherlands).
QCD COMPTON SCATTERING AT HERA ENERGY
J. J. Engelen, S. J. deJong, R. Laterveer, and J. A. M. Vermaseren Feb. 1989 13 p
(NIKHEF-H/89-3; ETN-90-96380) Avail: NTIS HC A03/MF A01

Total and differential cross sections for quantum chromodynamics (QCD) Compton scattering in electron proton collisions at HERA energy are presented. The electron photon vertex is taken into account explicitly. The Q (exp 2) of the exchanged photon ranges from nearly zero (almost real photon) to the kinematically allowed maximum. The QCD scale is set by the invariant mass of the quark and gluon produced. It is concluded that at high jet transverse momentum a relatively pure sample of QCD Compton events can be isolated. ESA

N90-22373# Nationaal Inst. voor Kernfysica en Hoge Energiefysica, Amsterdam (Netherlands).
THEORY OF A CHARGED SPINNING PARTICLE IN A GRAVITATIONAL AND ELECTROMAGNETIC FIELD
J. W. vanHolten Feb. 1989 15 p Presented at Landelijk Seminarium Mathematische Methoden in de Veldentheorie, Netherlands, 12 Dec. 1986
(NIKHEF-H/89-4; ETN-90-96381) Avail: NTIS HC A03/MF A01

The classical and quantum mechanics of a charged spinning particle, such as an electron, in arbitrary gravitational and electromagnetic background fields is presented. The classical theory is shown to possess supersymmetry. The equivalent Dirac formulation of the quantum theory is derived. The canonical structure of the theory is presented. The spectrum of states in the quantum theory is described. Applications of the Dirac operator index to obtain the value of the chiral anomaly are explained.
ESA

N90-22374# Nationaal Inst. voor Kernfysica en Hoge Energiefysica, Amsterdam (Netherlands).
OPERATOR ALGEBRA FROM FUSION RULES: THE INFINITE NUMBER OF ISING THEORIES
Juergen Fuchs Mar. 1989 28 p
(NIKHEF-H/89-7; ETN-90-96382) Avail: NTIS HC A03/MF A01

A technique for using the fusion rules of a conformal field theory to derive differential equations for the four point functions of the theory is described. The use of these equations in determining the operator product coefficients for primary fields is outlined. The results are applied to the Ising fusion rules. A set of theories possessing these fusion rules is described. The set is labelled by two discrete parameters. For a specific value of one of the parameters, it is shown that they represent an infinite number of inequivalent theories. This is the case for the level one spin Wess-Zumino-Witten theories. ESA

N90-22375# Nationaal Inst. voor Kernfysica en Hoge Energiefysica, Amsterdam (Netherlands).
GENERALIZED KILLING EQUATIONS AND SYMMETRIES OF SPINNING SPACE
R. H. Rietdijk and J. W. vanHolten Apr. 1989 14 p Sponsored in part by Stichting voor Fundamenteel Onderzoek der Materie
(NIKHEF-H/89-8; ETN-90-96383) Avail: NTIS HC A03/MF A01

A set of general conditions for the isometrics of d-dimensional spinning space is derived. These equations constitute a Grassmann valued extension of the Killing equations for ordinary space. They are developed as invariances of spinning particle actions. Solutions for extended Killing equations in arbitrary curved space are presented. The spinning particles in d-dimensions are shown to possess new types of supersymmetries which transform the commuting and anti-commuting coordinates linearly and nonlinearly. The algebra of these nonlinear transformations is presented. A complete solution of the generalized Killing equations is outlined. An infinite set of conserved charges is constructed. ESA

N90-22376# Nationaal Inst. voor Kernfysica en Hoge Energiefysica, Amsterdam (Netherlands).
EXCLUSIVE PRODUCTION OF p, p-, pi, AND pi- IN PHOTON PHOTON COLLISIONS
H. Aihara, M. Alston-Garnjost, R. E. Avery, A. Barbaro-Galtieri, A. R. Barker, B. A. Barnett, D. A. Bauer, A. Bay, G. J. Bobbink, and C. D. Buchanan (California Univ., Los Angeles.) et al Apr. 1989

19 p Sponsored in part by by DOE; NSF; Joint Japanese United States Collaboration in High Energy Physics; and Stichting voor Fundamenteel Onderzoek der Materie
(NIKHEF-H/89-9; ETN-90-96384) Avail: NTIS HC A03/MF A01

A measurement of the positron-electron (e+e-) interaction leading to (e+e-, p ,p-, pi, pi-) process with a Time Projection Chamber (TPC)/Two Gamma facility at the e+e- storage ring is reported. 45 (p, p-, pi, pi-) events were identified in data corresponding to an integrated e+e- luminosity of 142 p (l/b). The cross section for photon photon collision leading to (p, p-, pi, pi-) is given as a function of the photon photon center of mass energy, between 2.5 to 5.5 GeV, and as a function of the invariant mass squared of one of the photons. This cross section falls much more rapidly than that for a similar process, photon photon collision leading to (p, p-). No delta particle production is observed and only a small fraction of the events at low center of mass energy is consistent with photon photon collision leading to delta particles. In an expanded search through the same data, 4 events compatible with lambda particle production were found. ESA

N90-22377# Amsterdam Univ. (Netherlands).
INVESTIGATION OF CORRELATIONS IN NUCLEI WITH THE (e,e'X) REACTION Ph.D. Thesis
Rolf Ent 1989 103 p
(ETN-90-96398) Avail: NTIS HC A06/MF A01

Some (e, e'd) experiments on He-4, Li-6, and C-12, and a first (e, e'alpha) experiment on Li-6, are described. The aim is to study the mechanism of (e, e'X) reactions and to extract useful spectroscopic information, that is, the probability of finding a cluster X inside a nucleus and the cluster bound-state wave function. The special detector used for the latter reaction which is capable of detecting low energetic particles is described. An extensive review of the experiments including reaction mechanism and spectroscopic results is given. ESA

N90-22378# National Physical Lab., Teddington (England). Div. of Radiation Science and Acoustics.
NON-RANDOM UNCERTAINTIES IN THE CALIBRATION OF PROTECTION-LEVEL SECONDARY STANDARDS
C. Cross and M. J. Rossiter Dec. 1988 31 p
(NPL-RS(EXT)-110; ISSN-0143-7135; ETN-90-96429) Copyright
Avail: NTIS HC A03/MF A01

The non-random uncertainties are considered in the following categories: the various corrections applied to the primary standard response in order to realize the quantity exposure; conversion to air kerma; the uncertainties associated with the physical data, and the comparison procedure. The study is presented in three sections: the first covers the non-random uncertainties applicable to protection-level calibrations at low energies, that is using x rays with generating voltages up to 50 kV (mean energies 8 to 38 keV); the second covers non-random uncertainties in protection-level calibrations using the ISO (International Organization for Standardization) narrow spectrum series of x ray qualities (mean energies 33 to 247 keV), and the third part deals with the non-random uncertainties applicable to protection-level calibrations in the Co-60 and Cs-137 gamma ray beams. ESA

73 NUCLEAR AND HIGH-ENERGY PHYSICS

Includes elementary and nuclear particles; and reactor theory.

For space radiation see *93 Space Radiation.*

N90-22379# General Electric Co., Philadelphia, PA. Astro-Space Div.
GENERAL PURPOSE HEAT SOURCE RADIOISOTOPE THERMOELECTRIC GENERATOR PROGRAM. BOOK 1: ACCIDENT ANALYSIS Safety Status Report
Jan. 1990 131 p
(Contract DE-AC01-79ET-32043)
(Rept-90SDS4202-Bk-1) Avail: NTIS HC A07/MF A01

The status of the accident analysis for the Ulysses outer planetary space science mission is presented. This mission employs a Radioisotope Thermoelectric Generator (RTG) as the prime electrical power source for the spacecraft. The RTG employs silicon-germanium thermoelectric couples to produce electricity from the heat energy that results from the decay of the radioisotope fuel, Plutonium-238, used in the RTG heat source. The heat source configuration used in the RTG is termed General Purpose Heat Source (GPHS), and the RTG is designated GPHS-RTG. The results of a rigorous safety assessment, including substantial analyses and testing, of the launch and deployment of the RTG for the Ulysses mission are given. A summary is given of the potential accident and failure sequences which might result in fuel release, the analysis and testing methods employed, and the predicted source terms. Each source term consists of a quantity of fuel released, the location of release and the physical characteristics of the fuel released. Each source term has an associated probability of occurrence. The purpose is to: (1) identify all potential single or multiple malfunctions during the complete mission profile which can possibly affect nuclear safety; and (2) provide estimates of probabilities of occurrence associated with each type of accident. Author

N90-22380# General Electric Co., Philadelphia, PA. Astro-Space Div.
GENERAL PURPOSE HEAT SOURCE RADIOISOTOPE THERMOELECTRIC GENERATOR. BOOK 2: ACCIDENT ANALYSIS, APPENDICES
Jan. 1990 634 p
(Contract DE-AC01-79ET-32043)
(Rept-90SDS4202-Bk-2) Avail: NTIS HC A99/MF A04

The purpose is to document the accident scenarios and failure probabilities defined by NASA for the Space Transportation System (the Shuttle Data Book NSTS-08116 and supporting documentation) and used in the Ulysses Mission Safety Status Report (SSR). NASA utilized a systematic approach to identify the credible accident scenarios that might pose a threat to the radioisotope thermoelectric generator (RTG). First, the Shuttle system was divided into the following seven elements: (1) Launch Support Equipment (LSE); (2) Payload; (3) Orbiter; (4) External Tank (ET); (5) Solid Rocket Boosters (SRB); (6) Space Shuttle Main Engines (SSME); and (7) Range Safety System (RSS). Each element was further divided into its major components, and these components were then subdivided until all known failure modes were identified. The approach used to develop the different accident scenarios was to divide the mission into phases and subphases as necessary. The phases were keyed to specific events that resulted in significant changes in vehicle configuration and/or in the potential consequences to the RTG. After the phases were defined, the accident scenarios for each phase were analyzed by developing detailed fault trees for each of the seven major systems as applicable. Author

N90-22381# Richland Operations Office (AEC), WA.
PREVENTION OF SIGNIFICANT DETERIORATION APPLICATION FOR APPROVAL TO CONSTRUCT SP-100 GROUND ENGINEERING SYSTEM TEST SITE
Apr. 1990 73 p
(Contract DE-AC06-87RL-10930)
(DE90-007986; DOE/RL-90-14) Avail: NTIS HC A04/MF A01

The following application is being submitted by the U.S. Department of Energy, Richland Operations Office, P.O. Box 550, Richland, Washington 99352, pursuant to WAC 173-403-080, and in compliance with the Department of Ecology Guide to Processin g a Prevention of Significant Deterioration (PSD) Permit for a new source of airborne radionuclide emissions at the Hanford Site in Washington State. The new source, the SP-100 Ground Engineering System (GES) Test Site, will be located in the 309 Building of the 300 Area. The U.S. Department of Energy (DOE), the National Aeronautics and Space Administration (NASA), and the U.S. Department of Defense (DOD) have entered into an agreement to jointly develop space nuclear reactor power system technology. The DOE has primary responsibility for developing and ground testing the nuclear subsystem. A ground test of a reactor is necessary to demonstrate technology readiness of this major subsystem before proceeding with the flight system development and demonstration. The SP-100 GES Test Site will provide a location for the operation and testing of a prototype space-based, liquid metal-cooled, fast flux nuclear reactor in an environment closely simulating the vacuum and temperature conditions of space operations. The purpose of the GES is to develop safe, compact, light-weight and durable space reactor power system technology. DOE

N90-22382# National Physical Lab., Teddington (England). Div. of Radiation Science and Acoustics.
DERIVATION OF RADIATION BEAM NON-UNIFORMITY CORRECTIONS FOR THE CALIBRATION OF LARGE VOLUME IONISATION CHAMBERS
G. A. Bass, M. J. Rossiter, and T. T. Williams Nov. 1989 32 p
(NPL-RSA(EXT)-11; ISSN-0955-9655; ETN-90-96430) Copyright
Avail: NTIS HC A03/MF A01

Work undertaken, using a radionuclide source irradiation unit, to accurately measure the beam uniformity of each reference radiation in the narrow series and of the gamma ray beams produced by the radionuclide sources of highest activity is presented. Measurements were extended to the x rays beams of protection-level series in the range 50 to 280 kV. The methods used to calculate non-uniformity corrections for various types of ionization chamber are shown and the results discussed. ESA

74 OPTICS

Includes light phenomena; and optical devices.
For lasers see *36 Lasers and Masers.*

N90-22383* National Aeronautics and Space Administration. John F. Kennedy Space Center, Cocoa Beach, FL.
OPTICAL SHUTTER SWITCHING MATRIX Patent
Charles H. Grove, inventor (to NASA) 20 Mar. 1990 12 p
Filed 21 Oct. 1988
(NASA-Case-KSC-11392-1; US-Patent-4,910,396; US Patent-Appl-SN-262851; US-Patent-Class-250-229; US-Patent-Class-350-356) Avail: US Patent and Trademark Office CSCL 20F

A switching matrix enables switching of optical signals from any of a plurality of optical input paths to selected optical output paths, without requiring physical reconnecting of the inputs or outputs. Plural broadband optical waveguides are defined preferably in otherwise non-transmissive quartz crystalline wafers, to provide relatively high signal isolation. The wafers are fused to electronic shutter windows situated in an array and discretely operable under processor x-y address control. Optical signals passed through actuated electronic shutter windows are summed in output wafers, having waveguide structure generally reverse to that of the input quartz wafers. Through selected segment actuation, optical signals from selected optical input paths may be transmitted or blocked at the electronically controlled shutter array, for being output on selected optical output paths. Alternatively, fiber optic bundles may replace input or output quartz wafers. The switching matrix is useful as a switching module which may be variously associated in series and/or parallel connections for obtaining a desired number of switching channels, and required levels of signal separation therewith. Input/output signal characteristics and parameters are maintained by power summation at the outputs with automatic gain control, regardless of the number of paths or the like selectively summed in a given output. Connectors may be used in conjunction with the optical input and output paths, whereby both electrical and optical signals may be switched. Various modules may include converters as built-in features, so as to meet particular applications.

Official Gazette of the U.S. Patent and Trademark Office

N90-22384# Oxford Univ. (England). Robotics Research Group.
LOW ORDER FIR AND IIR FILTERS IN DYNAMIC VISION
Alan M. McIvor 1989 18 p
(OUEL-1785/89; ETN-90-96413) Avail: NTIS HC A03/MF A01

The easy application of low order FIR (finite impulse response) and IIR (infinite impulse response) filters at each pixel location in an image sequence at frame rates with current technology is addressed. An evaluation of their performance and limitations using theoretical, simulation and experimental methods is presented. ESA

N90-21883*# Jet Propulsion Lab., California Inst. of Tech., Pasadena.
MICROWAVE ANALOG FIBER-OPTIC LINK FOR USE IN THE DEEP SPACE NETWORK
R. T. Logan, Jr., G. F. Lutes, and L. Maleki *In its* The Telecommunications and Data Acquisition Report 15 Feb. 1990 p 21-33 (For primary document see N90-21880 15-32)
Avail: NTIS HC A15/MF A02 CSCL 20F

N90-22084*# Jet Propulsion Lab., California Inst. of Tech., Pasadena.
A SOFT ACTUATION SYSTEM FOR SEGMENTED REFLECTOR ARTICULATION AND ISOLATION
Michael L. Agronin and Louise Jandura *In* NASA, John F. Kennedy Space Center, The 24th Aerospace Mechanisms Symposium Apr. 1990 p 57-73 (For primary document see N90-22079 15-39)
Avail: NTIS HC A16/MF A03 CSCL 20F

75 PLASMA PHYSICS

Includes magnetohydrodynamics and plasma fusion.
For ionospheric plasmas see *46 Geophysics.* For space plasmas see *90 Astrophysics.*

N90-22385# Ceskoslovenska Akademie Ved, Prague. Inst. of Plasma Physics.
GAS-PUFF Z-PINCH EXPERIMENT
A. Krejci Nov. 1988 23 p
(IPPCZ-286) Avail: NTIS HC A03/MF A01

The fast linear Z-pinch was experimentally investigated using a pulse high current generator (10.8 micro F, 5 to 10 kJ, 150 to 250 kA) and a pulse injection of argon and neon. Measured electrical characteristics of the discharge (current shape and risetime, inductance) and calculated dynamic parameters of plasma implosion (accelerated mass, radial plasma velocity) are presented. X ray diagnostics with temporal resolution (vacuum x ray diodes, semiconductor detectors) were utilized. The temperature and the density of pinch plasma as well as its other parameters (size, lifetime) were estimated. Total energy emitted by pinch in ultra-soft x ray region during approx. 200 ns pulse achieves 125 J/4 pi. Author

N90-22386# Ceskoslovenska Akademie Ved, Prague. Inst. of Plasma Physics.
THE INTRINSIC STOCHASTICITY OF NEAR-INTEGRABLE HAMILTONIAN SYSTEMS
L. Krlin Jun. 1988 59 p
(IPPCZ-282) Avail: NTIS HC A04/MF A01

Under certain conditions, the dynamics of near-integrable Hamiltonian systems appears to be stochastic. This stochasticity (intrinsic stochasticity, or deterministic chaos) is closely related to the Kolgomorov-Arnold-Moser (KAM) theorem of the stability of near-integrable multiperiodic Hamiltonian systems. The effect of the intrinsic stochasticity attracts still growing attention both in theory and in various applications in contemporary physics. The relation of the intrinsic stochasticity to the modern ergodic theory and to the KAM theorem is discussed and some numerical experiments on related astrophysical and high-temperature plasma problems are described. Author

N90-22387 California Univ., Los Angeles.
HYBRID MODELING OF PLASMAS AND APPLICATIONS TO FUSION AND SPACE PHYSICS Ph.D. Thesis
Farzad Kazeminejad 1989 216 p
Avail: Univ. Microfilms Order No. DA8926470

Since the early days of controlled fusion research, plasma physicists have encountered great challenges in obtaining solutions to the highly nonlinear equations which govern the behavior of fusion plasmas; with the growth of other applications of plasma physics these problems have grown in importance. Obtaining reasonable solutions to the nonlinear equations is crucial to understanding the behavior of plasmas. With the advent of high speed computers, computer modeling of plasmas has moved into the front row of the tools used in research of their nonlinear plasma dynamics. There are roughly speaking two types of plasma models, particle models and fluid models. Particle models in general require larger memory for the computer due to the massive amounts of data associated with the particles' kinematical variables. Fluid models are better fit to handle large scales and long times. The drawback of fluid models however, is that they miss the physical phenomena taking place at the microscale and these phenomena can influence the properties of the fluids. Another approach is to start with fluid models and incorporate more physics. Such models are referred to as hybrid models: two such models are discussed. They are then applied to two problems; the first is a simulation of the artificial comet generated by the AMPTE experiment; the second is the production of enhanced noise in fusion plasmas by injected energetic ions or by fusion reaction products. In both cases, the models demonstrate qualitative agreement with the experimental observations. Dissert. Abstr.

N90-22388 California Univ., Los Angeles.
THE MHD STRUCTURE OF AN OPEN MAGNETOTAIL BOUNDARY Ph.D. Thesis
Ennio Rodolfo Sanchez 1989 225 p
Avail: Univ. Microfilms Order No. DA9001752

The results of a theoretical and observational study of an open magnetotail boundary are presented. An MHD (magnetohydrodynamics) model for the complete magnetotail boundary is presented. The tailward evolution of the rational discontinuity-slow expansion fan model is quantitatively obtained for different magnetosheath magnetic field strengths and orientations. Its properties are studied. Two observational studies of the IMP 8 magnetotail boundary crossings were carried out using an analysis that combines plasma and magnetic field measurements. Dissert. Abstr.

N90-22389*# Colorado State Univ., Fort Collins. Dept. of Mechanical Engineering.
PLASMA CONTACTOR RESEARCH, 1989 Annual Report, 1 Jan. 1989 - 1 Jan. 1990
John D. Williams Feb. 1990 67 p
(Grant NAG3-776)
(NASA-CR-185212; NAS 1.26:185212) Avail: NTIS HC A04/MF A01 CSCL 20I

The characteristics of double layers observed by researchers investigating magnetospheric phenomena are contrasted to those observed in plasma contacting experiments. Experiments in the electron collection mode of the plasma contacting process were performed and the results confirm a simple model of this process for current levels ranging to 3 A. Experimental results were also obtained in a study of the process of electron emission from a hollow cathode plasma contactor. High energy ions are observed coming from the cathode in addition to the electrons and a phenomenological model that suggests a mechanism by which this could occur is presented. Experimental results showing the effects of the design parameters of the ambient plasma simulator on the plasma potential, electron temperature, electron density and plasma noise levels induced in plasma contacting experiments are presented. A preferred simulator design is selected on the basis of these results. Author

N90-22390 Princeton Univ., NJ.
RIGOROUS UPPER BOUNDS FOR TURBULENT TRANSPORT IN BOUNDED SYSTEMS: PASSIVE ADVECTION AND REVERSED-FIELD PINCHES Ph.D. Thesis
Chang-Bae Kim 1989 137 p
Avail: Univ. Microfilms Order No. DA9007162

Upper bounds are considered for steady-state transport in turbulent bounded systems, for both passive advection and self-consistent cylindrical plasmas. Specifically, the work of Krommes and Smith on passive advection is extended in two directions: (1) For their reference model improved upper bounds are obtained by including the effects of cross-correlations up to fourth order. Numerical solutions of the model stochastic differential equation are also obtained; they show that the new bounds compare quite favorably with the exact results, even at large Reynolds and Kubo numbers; (2) The problem of particle transport due to statistically specified stochastic magnetic fields in a collisionless turbulent plasma is revisited to take account of a finite spatial autocorrelation length L(sub c). A bound is obtained which reduces for small L(sub c) to the quasilinear limit and for large L(sub c) to the strong turbulence limit, and which provides a reasonable and rigorous interpolation for intermediate values of L(sub c). Then, a self-consistent problem is treated by considering upper bounds for the turbulently generated electromotive force along the axial direction in a magnetized cylindrical plasma bounded by a perfectly conducting wall. One goal in particular is to obtain rigorous results about relaxation in reversed-field pinches. It is assumed that the plasma is driven by an external electric field and has reached a possibly turbulent steady state in which the total current is fixed and in which the conservation laws of energy and magnetic helicity are enforced. For simplicity, incompressible, resistive magnetohydrodynamic (MHD) equations are used. A bounding curve is obtained without the helicity constraint, used with the Hartmann number. Features of the maximal-emf state corresponding to the reversed-field state are discussed. Dissert. Abstr.

N90-22391 Wisconsin Univ., Madison.
MAGNETIC TURBULENCE VERSUS SAFETY FACTOR IN THE TOKAPOLE 2 TOKAMAK Ph.D. Thesis
Dale Edward Graessle 1989 154 p
Avail: Univ. Microfilms Order No. DA8914515

Low-frequency (omega much less than omega(sub ci)) radial magnetic turbulence was measured over the full minor radius (r = 0 to 18 cm) for discharges in Tokapole 2. It was also scaled over the range of edge safety factor 0.6 less than or = q(sub a) less than or = 5.0. It was found that q(sub a) served as a control parameter for both the magnetic function amplitude and the global confinement time. As q(sub a) is reduced from 5 to 0.6 the turbulence level increases by a factor of fifty while the confinement time decreases by more than a factor of ten. The turbulent amplitude 1 cm inside the separatrix is nearly large enough for q(sub a) less than or = 1 to account for the global confinement by means of collisionless stochastic magnetic transport. Frequency spectra were obtained reliably from 10 to 400 kHz. For all q(sub a) most of the fluctuation power appears below 100 kHz. This low-frequency structure changes as the safety factor is varied. Although the spectra do not always have clearly-defined peaks in this range of f, radial coherence lengths at these frequencies are very long, indicating global modes with a broadband structure. For f greater than or = 100 kHz, the spectra becomes featureless, with a power-law frequency decay. For q(sub a) less than or = 3, the spectra decay as f(-1.4) in all cases. For higher q(sub a), a new power law decay of f(-2.3) appears. Radial, poloidal, and parallel correlation analysis was done for the full range of q(sub a). The parallel correlation length is estimated to be 150 + or - 50 cm. Radial and poloidal coherence lengths are of the order of the machine dimensions for frequencies below 100 kHz for all q(sub a). For f greater than or = 100 kHZ, radial coherence lengths are .5 to 2.5 cm for q(sub a) less than or = 3. Poloidal coherence lengths are independent of minor radius, and smaller for low q, indicating low q discharges have broader m-spectra. This might explain the increase in fluctuation amplitude as q(sub

a) decreases. It is suggested that the turbulence for all discharges with q(sub a) less than or = 3 is due to the same underlying cause or set of causes, and that the differences result from geometric effects associated with the variation in q(sub a).
Dissert. Abstr.

N90-22392# Foreign Applied Sciences Assessment Center, La Jolla, CA.
JAPANESE MAGNETIC CONFINEMENT FUSION RESEARCH
R. C. Davidson, M. A. Abdou, L. A. Berry, C. W. Horton, J. F. Lyon, and P. H. Rutherford Jan. 1990 334 p
Avail: NTIS HC A15/MF A02

Six U.S. scientists surveyed and assessed Japanese research and development in magnetic fusion. The technical accomplishments from the early 1980s through June 1989 are reviewed, and the Japanese capabilities and outlook for future contributions are assessed. Detailed evaluations are provided in the areas of basic and applied plasma physics, tokamak confinement, alternate confinement approaches, plasma technology, and fusion nuclear technology and materials. Author

N90-22393# Lawrence Livermore National Lab., CA.
PRODUCING DENSE PLASMAS WITH X RAYS Final Report, Jan. - Dec. 1989
Dennis Matthews, J. C. Trebes, Roger W. Falcone (California Univ., Berkeley.), and L. B. DaSilva Mar. 1990 4 p
(Contract W-7405-eng-48)
(DE90-009539; UCRL-CR-103211) Avail: NTIS HC A02/MF A01

Plasmas generated by x ray irradiation rather than optical lasers achieve density and temperatures of interest to astrophysics, inertial confinement fusion and atomic physics. In the past year we have developed and characterized a facility capable of focusing broadband x rays from a laser produced plasma to flux levels of approx 10(exp 4) J/sq cm. DOE

N90-22394# Avco-Everett Research Lab., MA.
MHD CHANNEL DEVELOPMENT, PART 1 Final Report, 25 Apr. 1984 - 31 Dec. 1988
Dec. 1989 363 p
(Contract DE-AC22-84PC-70507)
(DE90-009549; DOE/PC-70507/T2-Pt-1) Avail: NTIS HC A16/MF A02

This is the final report of work performed by Avco Research Laboratory, Inc. for the U.S. Department of Energy, Pittsburgh Energy Technology Center. The overall objectives of this program were: to contribute, by appropriate systematic experimental and analytical investigations, to the engineering data base necessary for the design and construction of MHD generators at the 50 MW(sub th) and ultimately at commercial sizes; and to design and fabricate specific hardware items to be tested at a site to be specified by DOE. The program consisted of a series of related tasks, which are described in subsequent sections of this report. Section 2.0 summarizes the important results of the entire program. Sections 3.0 through 7.0 describe the work in detail, and are organized as follows: Section 3.0, MHD Channel Design and Performance, reports experimental and analytical investigations related to MHD channel design and performance. Section 4.0, MHD Channel Construction and Lifetime, reports experimental investigations related to MHD channel reliability and lifetime. Section 5.0, MHD Channel Loading and Control, reports on the analysis, testing and fabrication of channel loading and control circuits. Section 6.0, Facility Operation, describes the facilities and operation and maintenance of the Mk VI and VII test bays. Section 7.0, DOE Test Facility Technical Support, reports on the results of the data reduction and analysis of the CDIF generator test data. DOE

N90-22395# Avco-Everett Research Lab., MA.
MHD CHANNEL DEVELOPMENT, PART 2 Final Report, 25 Apr. 1984 - 31 Dec. 1988
Dec. 1989 366 p
(Contract DE-AC22-84PC-70507)
(DE90-009550; DOE/PC-70507/T2-Pt-2) Avail: NTIS HC A16/MF A01

This is the final report of work performed by Avco Research Laboratory, Inc. for the U.S. Department of Energy, Pittsburgh Energy Technology Center. The overall objectives of this program were: to contribute, by appropriate systematic experimental and analytical investigations, to the engineering data base necessary for the design and construction of MHD generators at the 50 MW(sub th) and ultimately at commercial sizes; and to design and fabricate specific hardware items to be tested at a site to be specified by DOE. The program consisted of a series of related tasks, which are described in subsequent sections of this report. Section 2.0 summarizes the important results of the entire program. DOE

N90-22396# Avco-Everett Research Lab., MA.
MHD CHANNEL DEVELOPMENT, PART 3 Final Report, 25 Apr. 1984 - 31 Dec. 1988
Dec. 1989 165 p
(Contract DE-AC22-84PC-70507)
(DE90-009551; DOE/PC-70507/T2-Pt-3) Avail: NTIS HC A08/MF A01

This is the final report of work performed by Avco Research Laboratory, Inc. for the U.S. Department of Energy, Pittsburgh Energy Technology Center. The overall objectives of this program were: to contribute, by appropriate systematic experimental and analytical investigations, to the engineering data base necessary for the design and construction of MHD generators at the 50 MW(sub th) and ultimately at commercial sizes; and to design and fabricate specific hardware items to be tested at a site to be specified by DOE. Section 3.0, MHD Channel Design and Performance, reports experimental and analytical investigations related to MHD channel design and performance. DOE

N90-22397# Avco-Everett Research Lab., MA.
MHD CHANNEL DEVELOPMENT, PART 4 Final Report, 25 Apr. 1984 - 31 Dec. 1988
Dec. 1989 323 p
(Contract DE-AC22-84PC-70507)
(DE90-009552; DOE/PC-70507/T2-Pt-4) Avail: NTIS HC A14/MF A02

This is the final report of work performed by Avco Research Laboratory, Inc. for the U.S. Department of Energy, Pittsburgh Energy Technology Center. The overall objectives of this program were: to contribute, by appropriate systematic experimental and analytical investigations, to the engineering data base necessary for the design and construction of MHD generators at the 50 MW(sub th) and ultimately at commercial sizes; and to design and fabricate specific hardware items to be tested at a site to be specified by DOE. The program consisted of a series of related tasks, which are described in subsequent sections of this report. Section 4.0, MHD Channel Construction and Lifetime, reports experimental investigations related to MHD channel reliability and lifetime, where the principal aim is to improve the constructability, maintainability, and reliability of coal-fired, long-duration MHD channels. DOE

N90-22398# General Atomic Co., San Diego, CA.
THREE-DIMENSIONAL SIMULATIONS OF SIMPLE ELECTRON DRIFT WAVE TURBULENCE IN TOKAMAK GEOMETRY
R. E. Waltz Mar. 1990 18 p Presented at the Conference on Research Trends in Nonlinear and Relativistic Plasma Physics, San Diego, CA, 5-8 Feb. 1990 Submitted for publication
(Contract DE-AC03-89ER-53277)
(DE90-009581; GA-A-20024; CONF-900237-1) Avail: NTIS HC A03/MF A01

A 3-D code is used to study the scaling of an electrostatic electron drift wave turbulence with respect to shear and curvature of the tokamak magnetic field as well as the driving strength. The electrons are modeled with a simple formula for the deviation from a near Boltzmann response and the ions are modeled as a nonlinear fluid. For sheared slab geometry suppressing curvature (or toroidal) effects, the turbulence level and transport scale according to the mixing length given by the linear normal mode widths and the poloidal wavelengths scaled to the ion gyroradius. Toroidal coupling results in a more complex behavior. DOE

N90-22399# International Atomic Energy Agency, Vienna (Austria).
IMPURITY CONTROL IN TOROIDAL DEVICES
Jan. 1990 173 p Presented at the IAEA Technical Committee Meeting on Impurity Control, Naka, Japan, 13-15 Feb. 1989
(DE90-618585; IAEA-TECDOC-536; CONF-8902101) Avail: NTIS (US Sales Only) HC A08/MF A01

This summary report on the Technical Committee Meeting organized by the IAEA provides an overview of the results presented. Of the twenty-three papers presented, sixteen were devoted to tokamak experiments. These presented data of plasma behavior in the scrape-off layer and divertor regions, as well as effects of impurities on the core plasma; these are summarized here. Other papers summarized deal with plasma-wall interactions, including wall material behavior. Still others deal with theoretical work on physics modelling in the edge region. DOE

N90-22400# Oxford Univ. (England). Dept. of Engineering Science.
ON THE THEORY OF HEISER AND SHERCLIFF EXPERIMENT. PART 1: MHD FLOW IN AN OPEN CHANNEL IN STRONG UNIFORM MAGNETIC FIELD
S. Y. Molokov and J. E. Allen 1989 24 p
(OUEL-1804/89-Pt-1; ETN-90-96418) Avail: NTIS HC A03/MF A01

Magnetohydrodynamic (MHD) flows of viscous incompressible fluid in strong magnetic fields parallel to a free surface of fluid are investigated. The problem of flow in an open channel due to a moving side wall in uniform magnetic field is considered, and treated by means of matched asymptotic expansions method. The flow region is divided into various subregions and leading terms of asymptotic expansions as M tends towards infinity (M is the Hartmann number) of solutions of correspondent problems in each subregion are obtained. An exact analytic solution of equations governing the free-surface layer of thickness of order M to the minus 1/2 power is obtained. ESA

N90-22401# Oxford Univ. (England). Dept. of Engineering Science.
ON THE THEORY OF HEISER AND SHERCLIFF EXPERIMENT. PART 2: MHD FLOW BETWEEN TWO CYLINDERS IN STRONG RADICAL MAGNETIC FIELD
S. Y. Molokov and J. E. Allen 1989 17 p
(OUEL-1805/89-Pt-2; ETN-90-96419) Avail: NTIS HC A03/MF A01

A magnetohydrodynamic (MHD) flow of conducting fluid between two concentric insulating cylinders in strong radial magnetic field which is parallel to a free surface of a fluid is investigated by means of matched asymptotic expansions method. The flow region is divided into various subregions and leading terms of asymptotic expansions as M tends towards infinity (M is the Hartmann number) of solutions of problems governing flow in these subregions are obtained. ESA

N90-22402*# Stanford Univ., CA. Center for Space Science and Astrophysics.
CYCLOTRON MASER AND PLASMA WAVE GROWTH IN MAGNETIC LOOPS
Russell J. Hamilton and Vahe Petrosian 25 May 1990 30 p
(Grants NsG-7092; NSF ATM-87-05084)
(NASA-CR-179862; NAS 1.26:179862) Avail: NTIS HC A03/MF A01 CSCL 20I

Cyclotron maser and plasma wave growth which results from electrons accelerated in magnetic loops are studied. The evolution of the accelerated electron distribution is determined by solving the kinetic equation including Coulomb collisions and magnetic convergence. It is found that for modest values of the column depth of the loop the growth rates of instabilities are significantly reduced and that the reduction is much larger for the cyclotron modes than for the plasma wave modes. The large decrease in the growth rate with column depth suggests that solar coronal densities must be much lower than commonly accepted in order for the cyclotron maser to operate. The density depletion has to be similar to that which occurs during auroral kilometric radiation events in the magnetosphere. The resulting distributions are much more complicated than the idealized distributions used in many theoretical studies, but the fastest growing mode can still simply be determined by the ratio of electron plasma to gyrofrequency, U=omega(sub p)/Omega(sub e). However, the dominant modes are different than for the idealized situations with growth of the z-mode largest for U approximately less than 0.5, and second harmonic x-mode (s=2) or fundamental o-mode (s=1) the dominant modes for 0.5 approximately less than U approximately less than 1. The electron distributions typically contain more than one inverted feature which could give rise to wave growth. It is shown that this can result in simultaneous amplification of more than one mode with each mode driven by a different feature and can be observed, for example, by differences in the rise times of the right and left circularly polarized components of the associated spike bursts. Author

76 SOLID-STATE PHYSICS

Includes superconductivity.
For related information, see also *33 Electronics and Electrical Engineering* and *36 Lasers and Masers.*

N90-22403 Illinois Univ. at Urbana-Champaign, Savoy.
TRANSPORT AND RELAXATION PROPERTIES IN ANISOTROPIC SUPERCONDUCTORS Ph.D. Thesis
Hocine Bahlouli 1988 175 p
Avail: Univ. Microfilms Order No. DA8908616

The nature of the superconducting state formed in some of the heavy fermion (HF) metals remains a subject of debate. A theoretical analysis is given of some experiments which can help to decide the issue. A detailed calculation of the nuclear spin relaxation time T(sub 1) is given in anisotropic superconductors. The magnetic field effect on T(sub 1) is also studied, and it is found that for high enough fields a new process, the pair creation process, will dominate the relaxation which results in a Korringa-like behavior. More importantly it was found that due to the competition between the usual spin-flip contribution and the anomalous pair-creation contribution at very low temperatures, the nuclear-spin relaxation time develops a minimum which scales with the applied magnetic field. Besides, the possible orientation dependence of T(sub 1) if the dipolar interaction gives the dominant contribution was studied. Results were examined explicitly using some of the allowed group theoretical states in HF superconductors. Heavy fermion metals are peculiar in many respects, two of which are of interest: The normal state thermopower coefficient is large, signaling the presence of a substantial particle-hole asymmetry in the normal density of states; and transport properties seem to be dominated by non-magnetic impurity scattering close to the resonant limit. In the superconducting state, the second aspect results in a particle-hole asymmetry in the scattering amplitude which gives rise to an anomalously large thermoelectric coefficient if the normal state scattering phase shift is different from pi/2. Finally, some further possible experimental means of probing the anisotropy of the gap by applying a magnetic field or a supercurrent flow to our superconductor and varying its direction are suggested. Dissert Abstr.

N90-22404 Illinois Univ., Urbana-Champaign.
TRANSPORT PROPERTIES OF ANISOTROPIC SUPERCONDUCTORS Ph.D. Thesis
Badredine Arfi 1988 169 p
Avail: Univ. Microfilms Order No. DA8908613

The experimental data on ultrasonic attenuation and thermal conduction in the superconducting phase of U Pt3 do not behave as expected if the electron-impurity phase shift were small, and

therefore, assuming electron-impurity scattering to be the dominant process, transport coefficients were calculated for a range of phase shifts, and for three anisotropic superconducting states, the axial and polar p-wave states, and a d-wave state consistent with cubic and hexagonal crystal symmetries. The amplitude for an impurity to scatter a quasiparticle by taking into account repeated scattering of a quasiparticle by a single impurity was calculated and it is found that for phase shifts which are not small, the superconducting correlations can give rise to a very different energy dependence of the quasiparticle mean free path in the superconducting state, as compared with its behavior in the normal state. The calculated ultrasonic attenuation and thermal-conductivity agree much better with the data for U Pt3 if the normal-state phase shift is taken to be resonant (close to pi/2), and if the superconducting state has a nodal line at the equator of the Fermi surface. For phase shifts which are neither small, nor resonant, the mean free times for quasiparticle-like excitations differ from the quasihole-like ones, which leads to an enhancement of the thermoelectric effect in the superconducting state by a factor of order T sub F/T sub c. There is an angular symmetry of the scattering amplitude with respect to reflection of the final momentum and the symmetry axis of the gap. The angular symmetry leads to new tensor components of transport coefficients which are non-zero only if the parity of the superconducting order parameters is the same as that of the current or currents entering the transport coefficient. Experimental detection of these new coefficients would therefore serve to determine the parity of the order parameter.
Dissert. Abstr.

N90-22405 Oxford Univ. (England).
LOW TEMPERATURE PROPERTIES OF AMORPHOUS SOLIDS
Ph.D. Thesis
J. N. Page 1987 181 p
Avail: Univ. Microfilms Order No. BRD-85918

The low temperature properties of amorphous solids are still not well understood. The two-level states (TLS) model was generally accepted as explaining the behavior of glasses below 1 K, in particular the linear contribution to the specific heat capacity, but there remain anomalies above 1 K. This behavior was examined in epoxy resin systems which were chosen not so much for their technological importance but for their ease of preparation and hence the case with which their characteristics can systematically be changed. Specifically the proportion of diamine hardener needed to cure the samples was varied well as the diamine chain length. The vibrational density of states at low energies was derived from inelastic neutron scattering data and was compared with the predictions of the fractal model for amorphous systems. The experimental results showed the behavior expected on the basis of this model, namely: Debye-like behavior with Z(omega) varies as omega squared at the lowest energies; a breakaway to a dependence above omega squared at a crossover frequency; and Z(omega) varies as omega squared at higher energies with 0.8 is less than or = to x is less than or = to 1.0. It is shown that this form of the density of states, when coupled with the fractal model, may explain the low temperature anomalies mentioned. Measurements of the ultrasonic sound velocity were performed to help with the neutron scattering data analysis. In order to test a prediction of the fractal model that the thermal conductivity of amorphous materials was proportional to temperature above the plateau, the thermal conductivity of the epoxy resin samples and also a family of Se-Te glassy alloys was measured in the range of 4 to 110 K. Kappa varies as T above 30 K. Alternatives to the fractal model are discussed.
Dissert. Abstr.

N90-22406 Georgia Inst. of Tech., Atlanta.
AN INVESTIGATION OF NARROW-BANDGAP SEMICONDUCTORS: DEVICES, CIRCUITS, AND SYSTEMS
Ph.D. Thesis
Brian Keith Butka 1989 226 p
Avail: Univ. Microfilms Order No. DA8925446

Semiconductor infrared imaging systems for the 3 to 12 micron region are typically constructed utilizing hybrid circuits consisting of a silicon signal processor and a narrow-bandgap charge-coupled-device CCD imaging array. With the demonstration of MISFET operation in narrow-bandgap semiconductors, it is now possible to monolithically fabricate the necessary signal processing circuitry in the narrow-bandgap material. Beginning with fundamental physics without material-specific assumptions, device models are developed which reflect the physics of narrow-bandgap materials. Using these models, the performance of narrow-bandgap diodes and MISFETs is examined with respect to doping, bandgap, and operating temperature variations and a set of optimum device parameters is proposed. The models are also used to examine the design constraints of narrow-bandgap circuits. Circuits operating on a charge-transfer principle are shown to be feasible in narrow-bandgap materials. Differential amplifier, A/D converter, and digital logic circuit designs are proposed and verified using the developed device models. Monolithic imaging systems are found to have less parasitic capacitance attached to the CCD output circuitry. This reduced capacitance results in a larger output signal from a monolithic imaging system. In addition, the maximum imaging array size that can be fabricated as a monolithic imaging system is shown to be larger than the maximum array size of a hybrid system. If the entire imaging system cannot be fabricated monolithically, substantial gains in performance can be achieved by fabricating the correlated-double sampling circuitry and the differential amplifier in the narrow-bandgap material.
Author

N90-22407# Brown Univ., Providence, RI. Dept. of Chemistry.
PREPARATION AND CHARACTERIZATION OF Cu2ZnGeS(4-y)Se(Y)
K. Doverspike, K. Dwight, and A. Wold 15 Jan. 1990 23 p
(Contract N00014-85-K-0177)
(AD-A217469; TR-14) Avail: NTIS HC A03/MF A01 CSCL 07/2

Copper Zinc Germanium Selenide can be prepared in both tetragonal stannite and orthorhombic wurtz-stannite phases, whereas Cu2ZnGeSe4 only exists in the tetragonal phase. Selenium can be substituted for sulfur up to 100 percent in the tetragonal structure of Cu2ZnGeS(4-y)Se(y) prepared at 700 C, and up to 75 percent in the orthorhombic structure prepared at 900 C. The temperature at which the phase transformation takes place was found to increase with higher selenium concentration. Iron was substituted into both forms of Cu2Zn(1-x)Fe(x)GeS(4-y)Se(y) and the resulting magnetic properties indicated that the FeFe superexchange interactions are the same in both structures.
GRA

N90-22408*# National Inst. of Standards and Technology, Gaithersburg, MD. Applied and Computational Mathematics Div.
EFFECT OF A CRYSTAL-MELT INTERFACE ON TAYLOR-VORTEX FLOW
G. B. McFadden, S. R. Coriell, B. T. Murray, M. E. Glicksman, and M. E. Selleck (Rensselaer Polytechnic Inst., Troy, NY.) Oct. 1989 22 p Sponsored by NASA; Microgravity Sciences and Applications Program; and DARPA
(NASA-CR-186512; NAS 1.26:186512; PB90-130261; NISTIR-89/4192) Avail: NTIS HC A03/MF A01 CSCL 20L

The linear stability of circular Couette flow between concentric infinite cylinders is considered for the case that the stationary outer cylinder is a crystal-melt interface rather than a rigid surface. A radial temperature difference is maintained across the liquid gap, and equations for heat transport in the crystal and melt phases are included to extend the ordinary formulation of the problem. The stability of the two-phase system depends on the Prandtl number. For small Prandtl number the linear stability of the two-phase system is given by the classical results for a rigid-walled system. For increasing values of the Prandtl number, convective heat transport becomes significant and the system becomes increasingly less stable. Previous results in a narrow-gap approximation are extended to the case of a finite gap, and both axisymmetric and non-axisymmetric disturbance modes are considered. The two-phase system becomes less stable as the finite gap tends to the narrow-gap limit. The two-phase system is more stable to non-axisymmetric modes with azimuthal wavenumber n = 1; the stability of these n = 1 modes is sensitive to the latent heat of fusion. Author

N90-22409*# Loyola Coll., Baltimore, MD.
JETC (JAPANESE TECHNOLOGY EVALUATION CENTER) PANEL REPORT ON HIGH TEMPERATURE SUPERCONDUCTIVITY IN JAPAN
Duane Shelton and George Gamota (Mitre Corp., Bedford, MA.) Nov. 1989 240 p Sponsored by NASA; NSF; DARPA; and DOE
(NASA-CR-180413; NAS 1.26:180413; PB90-123126) Avail: NTIS HC A11/MF A02 CSCL 20L

The Japanese regard success in R and D in high temperature superconductivity as an important national objective. The results of a detailed evaluation of the current state of Japanese high temperature superconductivity development are provided. The analysis was performed by a panel of technical experts drawn from U.S. industry and academia, and is based on reviews of the relevant literature and visits to Japanese government, academic and industrial laboratories. Detailed appraisals are presented on the following: Basic research; superconducting materials; large scale applications; processing of superconducting materials; superconducting electronics and thin films. In all cases, comparisons are made with the corresponding state-of-the-art in the United States. GRA

N90-22410# Helsinki Univ. of Technology, Espoo (Finland). Lab. of Physics.
POSITRON TRAPPING IN SEMICONDUCTORS
M. J. Puska, C. Corbel (Commissariat a l'Energie Atomique, Saclay, France), and R. M. Nieminen 17 Oct. 1989 47 p
(PB90-165606; Rept-194; ISSN-0359-6214) Avail: NTIS HC A03/MF A01 CSCL 20L

Positron trapping into vacancies in semiconductors is studied on the basis of Golden Rule calculations. The emphasis is put on the comparison of the trapping properties defects in different charge states. In particular, the temperature dependences are investigated. Important features for vacancy-type defects in semiconductors are the localized electron states within the forbidden energy gap and (in the case of negatively charged defects) the weakly bound Rydberg states for positrons. Compared to vacancy-type defects in metals, these features enable new kinds of trapping mechanisms with electron-hole and phonon excitations. For charged defects the Coulomb wave character of the delocalized positron states before trapping determines the amplitude of the wave function at the defect and thereby affects strongly the magnitude of the trapping rate. As a result, trapping into positively charged defects shows remarkable properties which differ from the picture established for positron trapping in metals. The trapping rate into negative defects increases strongly with decreasing temperature, and at very low temperatures giant values may result. Author

N90-22411# Brookhaven National Lab., Upton, NY.
REPORT ON THE FIFTH WORKSHOP ON SYNCHROTRON X RAY LITHOGRAPHY
G. P. Williams, J. B. Godel, G. S. Brown, and W. Liebmann (Karl-Suss America, Essex Junction, VT.) 1989 15 p Presented at the 5th Brookhaven National Laboratory Workshop on Synchrotron X ray Lithography, Upton, NY, 16-17 Nov. 1989
(Contract DE-AC02-76CH-00016)
(DE90-007903; BNL-52230; CONF-891195-Summ) Avail: NTIS HC A03/MF A01

Semiconductors comprise a greater part of the United States economy than the aircraft, steel, and automobile industries combined. In future the semiconductor manufacturing industry will be forced to switch away from present optical manufacturing methods in the early to mid 1990s. X ray lithography has emerged as the leading contender for continuing production below the 0.4 micron level. Brookhaven National Laboratory began a series of workshops on x ray lithography in 1986 to examine key issues and in particular to enable United States industry to take advantage of the technical base established in this field. Since accelerators provide the brightest sources for x ray lithography, most of the research and development to date has taken place at large accelerator-based research centers such as Brookhaven, the University of Wisconsin, and Stanford. The goals of this Fifth Brookhaven Workshop were to review progress and goals since the last workshop and to establish a blueprint for the future. The meeting focused on the exposure tool, that is, a term defined as the source plus beamline and stepper. In order to assess the appropriateness of schedules for the development of this tool, other aspects of the required technology such as masks, resists and inspection and repair were also reviewed. To accomplish this, two working groups were set up, one to review the overall aspects of x ray lithography and set a time frame, the other to focus on sources. DOE

N90-22412# Sandia National Labs., Albuquerque, NM.
A REFRIGERATED DEWAR FOR THE JOSEPHSON ARRAY VOLTAGE CALIBRATION SYSTEM
Robert V. Duncan 1989 3 p Presented at the Conference on Precision Electromagnetic Measurements, Ottawa, Ontario, 11-14 Jun. 1990
(Contract DE-AC04-76DP-00789)
(DE90-005237; SAND-89-3134C; CONF-900689-2) Avail: NTIS HC A01/MF A01

A refrigerated Dewar has been used successfully with the Josephson array voltage calibration system. It has been used to re-liquefy helium with no degradation of the calibration system's performance. The independence of the array voltage from temperature has been confirmed to three parts in 10(exp 8) per Kelvin using this Dewar. DOE

N90-22413# Los Alamos National Lab., NM.
PULSED LASER PROCESSING OF HIGH TEMPERATURE SUPERCONDUCTING THIN FILMS
R. E. Muenchausen, R. C. Dye, R. C. Estler, S. Foltyn, A. R. Garcia, K. M. Hubbard, N. S. Nogar, X. D. Wu, A. Carim, and A. Mukherjee (New Mexico Univ., Albuquerque.) et al 1990 15 p Presented at the 4th International SAMPE Electronic Materials and Processes Conference, Albuquerque, NM, 12-14 Jun. 1990
(Contract W-7405-eng-36)
(DE90-008928; LA-UR-90-933; CONF-9006121-5) Avail: NTIS HC A03/MF A01

Systematic studies of the effects of pulsed laser deposition processing parameters on plume dynamics and resultant film properties have been performed. Plume angular distributions, cos(sup m)(theta), were observed to be variable between 1 is greater than m is greater than 10 depending on laser energy density and spot size. Under optimized conditions, epitaxial, superconducting thin films could be grown in-situ on a variety of single-crystal substrates. High quality, 200 nm thick films were obtained at deposition rates approaching 15 nm/sec. Additionally, the patterning of YBa2Cu3O(7-x) thin films was achieved by a process which combines thermal oxygen diffusion and laser annealing. This process is performed under relatively mild conditions which allows the structural integrity of the films to be preserved. DOE

N90-22414# Los Alamos National Lab., NM.
OVERVIEW OF CURRENT BULK AND THICK FILM HIGH TEMPERATURE SUPERCONDUCTOR PROCESSING STRATEGIES
Kevin C. Ott and Rod K. Quinn 1990 12 p Presented at the 4th International SAMPE Electronic Materials and Processes Conference, Albuquerque, NM, 12-14 Jun. 1990
(Contract W-7405-eng-36)
(DE90-008949; LA-UR-90-756; CONF-9006121-4) Avail: NTIS HC A03/MF A01

A review of processing strategies to prepare conductor-configured high temperature superconductors is presented along with a tabulation of recent results obtained using a variety of processing procedures to produce wires, tapes, monoliths, and thick films of high temperature superconducting material. DOE

N90-22415# Lawrence Livermore National Lab., CA.
IMPROVED CRYSTAL BENDING TECHNIQUES APPLIED TO THE LLNL DUAL-ARM JOHANN MOUNTING X RAY SPECTROMETER Final Report
J. D. Silver and C. T. Chantler (Oxford Univ., England) 1990 19 p
(Contract W-7405-eng-48)
(DE90-009528; UCRL-21296) Avail: NTIS HC A03/MF A01

Earlier investigations using the LLNL Spectrometer have revealed several limitations to the resolution of observed spectral lines. The first is the broadening due to the finite target source, together with secondary effects due to the bowing of the target. Other limitations relate to the target and spectrometer geometry, and in particular to the small (2R = 30cm) Rowland Circle radius. At small radii the production of a perfect curvature becomes increasingly difficult as distortions of the mosaic spread of crystallite angles are introduced by the stress. This is particularly true of lattice planes with three non-zero Miller indices (e.g., Si111 compared to Si220) and of stiff or thick crystals (e.g., silicon and quartz, which will shatter if greater than 0.2mm crystals are bent to this radius), but small broadening and asymmetrical shifts are also introduced for other crystals. Conversely, soft crystals (such as thin PET) will bend readily to the radius but distort and relax in mountings with fixed bending forces. A set of improvements to the bending techniques for both soft and stiff crystals is addressed. The first and most important development is the use of parallel, vertical posts and (symmetrical) bending points driven by micrometers instead of the earlier formed (i.e., pressed) crystals. The primary advantage is that the curvature from a small number of stress points is calculable, reproducible and does not introduce random stresses and distortions over the surface. The major methods used include the 2-point, 2-bar mount and the 4-point, 4-bar method. Various 4-point, 2-bar methods were also used. DOE

N90-22416# Oak Ridge National Lab., TN. Solid State Div.
SUPERCONDUCTING AND SEMICONDUCTING THIN FILMS OF La(SUB 123) AND Y(SUB 123) AND THEIR SUPERLATTICES
L. Ganapathi, Ashok Kumar, J. Narayan (North Carolina State Univ., Raleigh.), and O. W. Holland 1989 5 p Presented at the Materials Research Society Fall Meeting, Boston, MA, 27 Nov. - 2 Dec. 1989
(Contract DE-AC05-84OR-21400; NSF MSM-88-18994)
(DE90-009565; CONF-891119-120) Avail: NTIS HC A01/MF A01

Thin films of La(sub 123) and their superlattice with Y(sub 123) are deposited on various substrates for the first time. Thin films of La(sub 123) can be made semiconducting or superconducting within a small range of oxygen stoichiometry. A multiple target holder was used for in situ processing of superlattice thin films. The ability of the La(sub 123) compound to exhibit either semiconductivity or superconductivity was utilized to construct semiconductor/superconductor superlattice structures with Y(sub 123). X ray diffraction studies have shown clearly the presence of two distinct type layers in the superlattice films with an individual layer thickness of approx. 120 and 300A, although this did not happen for approx. 24A thickness of the individual layers. Rutherford backscattering experiments showed good quality of the films with channeling yields less than 10 percent. Resistivity measurements showed a (Tc) (onset) = 90 K and (Tc) (zero) = 85 K for the La(sub 123) as well as superlattice thin films. DOE

N90-22417# Oak Ridge National Lab., TN. Metal and Ceramics Div.
GRAIN BOUNDARY INTERMETALLIC PHASES IN ALLOY 718
M. G. Burke (Westinghouse Electric Corp., Pittsburgh, PA.) and M. K. Miller 1990 5 p Presented at the Spring Meeting of the Materials Research Society, San Francisco, CA, 16-21 Apr. 1990
(Contract DE-AC05-84OR-21400)
(DE90-009812; CONF-900466-5) Avail: NTIS HC A01/MF A01

A nickel base superalloy which is widely used in power generation applications, Alloy 718, was studied by analytical electron microscopy in order to elucidate the development of the complex microstructure which is produced during a typical multistage thermal treatment. The distribution of delta, gamma (double prime), gamma (prime) and Laves phases was found to be strongly dependent on aging treatment. DOE

N90-22418# Oak Ridge National Lab., TN. Solid State Div.
IN-SITU PULSED LASER DEPOSITION OF HIGH-T(SUB c) YBa(SUB 2)Cu(SUB 3)O(SUB 7) SUPERCONDUCTING THIN FILMS ON (100) LaAlO3 SUBSTRATES
P. Tiwari, S. Sharan, R. K. Singh, O. W. Holland, and J. Narayan (North Carolina State Univ., Raleigh.) 1989 5 p Presented at the Materials Research Society Fall Meeting, Boston, MA, 27 Nov. - 2 Dec. 1989
(Contract DE-AC05-84OR-21400)
(DE90-009861; CONF-891119-122) Avail: NTIS HC A01

The formation of superconducting thin films on lanthanum aluminate substrates is very important for high frequency applications. The fabrication is discussed of epitaxial superconducting YBa2Cu3O7 thin films on (100)LaAlO3 substrates, which exhibit excellent dielectric properties required for high frequency applications. The films were deposited by the biased pulsed laser evaporation technique (PLE) at substrate temperatures between 500 to 650 C and exhibit excellent crystallinity with best minimum ion channeling yields corresponding to approximately 3 percent. The superconducting transition temperatures varied from 88 to 92 K with critical current densities at 77 K and zero magnetic field greater than 4 to 5 x 10(exp 6) Amps/sq cm. DOE

N90-22419# Gosudarstvennyi Komitet po Ispolzovaniyu Atomnoi Energii, Serpukhov (USSR). Inst. Fiziki Vysokikh Ehnergij.
DEVELOPMENT OF THE METHODS AND MEANS OF PRECISE FORMING AND GEOMETRY CONTROL OF SUPERCONDUCTING CURRENT-CARRYING ELEMENT FOR THE UNR PULSED DIPOLES
E. R. Borisov, A. N. Surkov, and N. V. Taran 1989 13 p In RUSSIAN; ENGLISH summary
(DE90-620108; IFVE-OUNK-89-23) Avail: NTIS (US Sales Only) HC A03/MF A01

Control features and methods for obtaining precise-accurate trapezoidal cross sections in superconducting stranded cables are described. Devices for control and molding provide the output of stranded cables of the value with mean-square deviation from the size along the middle line of a trapezoid equalling 3 microns. DOE

N90-22420# Gosudarstvennyi Komitet po Ispolzovaniyu Atomnoi Energii, Serpukhov (USSR). Inst. Fiziki Vysokikh Ehnergij.
HEAT LEAK MEASUREMENTS IN SUPERCONDUCTING DIPOLE MAGNET SUPPORTS
S. S. Kozub and Ya. V. Shpakovich 1989 9 p In RUSSIAN; ENGLISH summary
(DE90-620109; IFVE-OUNK-89-24) Avail: NTIS (US Sales Only) HC A02/MF A01

The methods and results of measuring heat leak in the UNK, superconducting (SC) dipole magnet with a warm magnetic shield are described. Proceeding from the thermal conduction of the materials used for fabrication of the SP magnet supports, the measured values for the heat leak in the supports and outlined the ways of its reduction are analyzed. DOE

N90-22421*# National Aeronautics and Space Administration. Lewis Research Center, Cleveland, OH.
GROWTH AND PATTERNING OF LASER ABLATED SUPERCONDUCTING YBa2Cu3O7 FILMS ON LaAlO3 SUBSTRATES
J. D. Warner, K. B. Bhasin, N. C. Varaljay, D. Y. Bohman, and C. M. Chorey (Sverdrup Technology, Inc., Cleveland, OH.) 1989 8 p Presented at the 36th National Symposium and Topical Conference, Boston, MA, 23-27 Oct. 1989; sponsored by American Vacuum Society
(NASA-TM-102436; E-5205; NAS 1.15:102436) Avail: NTIS HC A02/MF A01 CSCL 20L

A high quality superconducting film on a substrate with a low dielectric constant is desired for passive microwave circuit applications. In addition, it is essential that the patterning process does not effect the superconducting properties of the thin films to achieve the highest circuit operating temperatures. YBa2Cu3O7 superconducting films were grown on lanthanum aluminate substrates using laser ablation with resulting maximum transition temperature (T sub c) of 90 K. The films were grown on a LaAlO3 which was at 775 C and in 170 mtorr of oxygen and slowly cooled to room temperature in 1 atm of oxygen. These films were then processed using photolithography and a negative photoresist with an etch solution of bromine and ethanol. Results are presented on the effect of the processing on T(sub c) of the film and the microwave properties of the patterned films. Author

N90-22422# Royal Signals and Radar Establishment, Malvern (England).
UV PHOTO-ENHANCED MOCVD OF CADMIUM AND CADMIUM TELLURIDE Ph.D. Thesis - Birmingham Univ.
Sajad Haq Apr. 1988 214 p
(RSRE-Memo-4208; BR111416; ETN-90-96423) Copyright
Avail: NTIS HC A10/MF A02

The UV photolysis of dimethylcadmium (Me2Cd) and diethyltelluride (Et2Te) were investigated using high pressure mercury arc lamps. Metallic Cd films were deposited onto gallium arsenide, silicon and sapphire substrates in order to investigate nucleation mechanisms and film growth models. Cadmium telluride epitaxial layers were grown onto (100) gallium arsenide substrates both with and without UV illumination. Film quality and structure were studied using transmission electron microscopy, x ray diffraction, scanning electron microscopy and secondary ion mass spectrometry. ESA

N90-22423# Royal Signals and Radar Establishment, Malvern (England).
OPTICAL PROPERTIES OF ZINC SELENIDE GROWN USING MOLECULAR BEAM DEPOSITION TECHNIQUES
K. Welford Jun. 1989 37 p
(RSRE-Memo-4269; BR111748; ETN-90-96424) Copyright
Avail: NTIS HC A03/MF A01

The refractive index of MBD (molecular beam deposition) grown ZnSe films was measured for three different growth temperatures and the wavelength and temperature dispersions were quantified. Permanent absorption, but not refractive index, changes were identified for the first time. Possible origins of the changes are conjectured along with the significant effects they will cause in optically bistable devices. Future studies are outlined which it is hoped will go some way towards producing better quality material and thus devices. ESA

N90-22424 Alabama Univ., Huntsville.
OPTICAL BISTABILITY IN SEMICONDUCTING MATERIAL Ph.D. Thesis
Yi-Qiang Li 1989 120 p
Avail: Univ. Microfilms Order No. DA9008446

Several topics, including the study of mirrorless optical bistability systems of various mechanisms, theoretical modeling of the self electro optic effect device, and the investigation of nonlinear properties of composite materials are discussed. A model for mirrorless optical bistability in a multiple quantum well structure (MQWS) is discussed. The band gap of the semiconductor GaAs/GaAlAs MQWS material is considered to be temperature dependent in this model. A set of Maxwell's equations for the electric field and the heat conduction equation for the temperature are solved numerically with appropriate boundary conditions for the electric field as well as the temperature. Optical bistability is obtained from the boundary condition for the heat conduction equation. A quantitative theoretical model for the important device, self electro optic effect device is developed by setting up Maxwell's equation and the circuit equation appropriate for a PIN photodiode. Numerical results are obtained for several different values of cross voltage and incident light frequency. A comparison between the theoretical results and experimental results shows very good agreement. Recent speculations on the useful applications of composite materials in optical bistability provide the motivation for the last part of the research work, where the nonlinear properties of a composite material are studied. Because of the local field effect, the effective dielectric constant shows multiple values. A discontinuity is present in the dielectric constant, and shows that OB is observed for the boundary value of the electric field. A two dimensional case is also considered and numerical results are obtained. Dissert. Abstr.

77 THERMODYNAMICS AND STATISTICAL PHYSICS

Includes quantum mechanics; theoretical physics; and Bose and Fermi statistics.

For related information see also *25 Inorganic and Physical Chemistry* and *34 Fluid Mechanics and Heat Transfer.*

N90-22425 Illinois Univ., Urbana-Champaign.
THE SYNERGISM OF ANALYTIC AND NUMERICAL TECHNIQUES IN GENERAL RELATIVITY: CALCULATION OF RADIATIVE SPACETIMES Ph.D. Thesis
Andrew M. Abrahams 1988 135 p
Avail: Univ. Microfilms Order No. DA8908603

The theoretical difficulty of identifying the radiative component of a general spacetime is manifested in numerical relativity as the problem of extracting asymptotic gravitational radiation wave-forms at finite radii during simulations on spacelike slices. These wave-forms can be contaminated by linear effects due to the choice of gauge and the wave's near zone field as well as by non-linear interactions. A synergistic approach is taken, where a numerical solution of the Einstein equations, coupled with hydrodynamics for the source and strong-field region, is matched in the near zone or local wave zone onto a linear analytic solution used for the exterior region. General solutions to the linearized vacuum Einstein equations expanded in multipole moments are developed. These solutions are employed in three matching schemes for extracting waveforms: an infinitesimal gauge transformation is used to express the analytic solution in several gauges useful for numerical relativity and gauge-independent combination of multipole amplitudes are formed; variables are constructed which are invariant under gauge-transformations; and surface integrals of Riemann tensor components are used to avoid gauge effects. In all three methods the near-zone field terms are separated off with an ordinary differential equation (ODE) integration over a timelike cylinder. A prescription for calculating initial values for these ODEs from data on a spacelike hypersurface is provided. These procedures are tested using simulated sinusoidal and non-sinusoidal pulsating neutron-star spacetimes. An application of these methods to Brill wave spacetimes and a discussion of non-linear effects in these spacetimes are included. Dissert. Abstr.

N90-22426*# Fermi National Accelerator Lab., Batavia, IL.
BIG-BANG NUCLEOSYNTHESIS REVISITED
Keith A. Olive, David N. Schramm, Gary Steigman, and Terry P. Walker (Harvard-Smithsonian Center for Astrophysics, Cambridge, MA.) Dec. 1989 14 p Sponsored in part by Presidential Young Investigator award
(Contracts NAGw-1321; NAGw-1340; NASG-931; DE-AC02-83ER-40105; DE-AC02-76ER-01545; NSF AST-88-20595)
(NASA-CR-186256; NAS 1.26:186256; FERMILAB-Pub-89/262-A; CFA-89-2985; UMN-TH-816/89) Avail: NTIS HC A03/MF A01 CSCL 20C

The homogeneous big-bang nucleosynthesis yields of D, He-3, He-4, and Li-7 are computed taking into account recent measurements of the neutron mean-life as well as updates of several nuclear reaction rates which primarily affect the production of Li-7. The extraction of primordial abundances from observation and the likelihood that the primordial mass fraction of He-4, Y(sub p) is less than or equal to 0.24 are discussed. Using the primordial abundances of D + He-3 and Li-7 we limit the baryon-to-photon ratio (eta in units of 10 exp -10) 2.6 less than or equal to eta(sub 10) less than or equal to 4.3; which we use to argue that baryons contribute between 0.02 and 0.11 to the critical energy density of the universe. An upper limit to Y(sub p) of 0.24 constrains the number of light neutrinos to N(sub nu) less than or equal to 3.4, in excellent agreement with the LEP and SLC collider results. We turn this argument around to show that the collider limit of 3 neutrino species can be used to bound the primordial abundance of He-4: 0.235 less than or equal to Y(sub p) less than or equal to 0.245. Author

N90-22427 Drexel Univ., Philadelphia, PA.
NUMERICAL INVESTIGATIONS OF NONLINEAR BEHAVIOR IN THE EINSTEIN EQUATIONS Ph.D. Thesis
Peter Anninos 1989 209 p
Avail: Univ. Microfilms Order No. DA9004591

The complexity of the Einstein equations of General Relativity poses great challenges to investigators who want to explore and understand the nature of the basic nonlinear physics of the gravitational field. To address this problem, a numerical code was developed as a tool to investigate fully nonlinear behavior in the simplified 1-D vacuum cosmology. In particular, the initial value construction and evolution was studied of linear and nonlinear plane symmetric gravitational waves in an expanding universe as described by the Gowdy T cubed class of metrics. A perturbative treatment of the Einstein equations was carried out to obtain analytic descriptions of the gravitational field in both the linear and weakly nonlinear second order regimes. In so doing, conditions necessary for the linearization stability of these solutions were derived. The fully nonlinear equations were solved by testing the code against the exact and perturbative analytic solutions. The 3 + 1 split of spacetime and the York formalism was used to decompose the metric and momentum variables into their freely specifiable and constrained pieces. Linear and nonlinear solutions are presented for free data in the form of standing waves and localized packets or pulses. In the studies of standing waves, the essential nonlinearity of the gravitational self interaction was demonstrated to be the generation of frequencies harmonic to those present in the free data. In studying traveling waves pulses, no evidence was found of nonlinear wave propagation. For the class of metrics it was shown that the nonlinearity of the Einstein equations lies in the Coulomb or nonradiative components of the Riemann curvature tensor. Dissert. Abstr.

80 SOCIAL SCIENCES (GENERAL)

Includes educational matters.

No abstracts in this category.

81 ADMINISTRATION AND MANAGEMENT

Includes management planning and research.

N90-22428*# National Aeronautics and Space Administration, Washington, DC.
SPACE STATION WORKSHOP: COMMERCIAL MISSIONS AND USER REQUIREMENTS
23 Feb. 1988 326 p Workshop held in Nashville, TN, 3-5 Nov. 1987
(NASA-TM-102912; NAS 1.15:102912) Avail: NTIS HC A15/MF A02 CSCL 05A

The topics of discussion addressed during a three day workshop on commercial application in space are presented. Approximately half of the program was directed towards an overview and orientation to the Space Station Project; the technical attributes of space; and present and future potential commercial opportunies. The remaining time was spent addressing technological issues presented by previously-formed industry working groups, who attempted to identify the technology needs, problems or issues faced and/or anticipated by the following industries: extraction (mining, agriculture, petroleum, fishing, etc.); fabrication (manufacturing, automotive, aircraft, chemical, pharmaceutical and electronics); and services (communications, transportation and retail robotics). After the industry groups presented their technology issues, the workshop divided into smaller discussion groups composed of: space experts from NASA; academia; industry experts in the appropriate disciplines; and other workshop participants. The needs identified by the industry working groups, space station technical requirements, proposed commercial ventures and other issues related to space commercialization were discussed. The material summarized and reported are the consensus from the discussion groups. B.H.A.

N90-22429# Office of Management and Budget, Washington, DC.
MANAGING FEDERAL INFORMATION RESOURCES Annual Report No. 7
6 Dec. 1989 64 p
(PB90-100173) Avail: NTIS HC A04/MF A01 CSCL 05B

An annual report to Congress is presented on the Office of Management and Budget's (OMB's) activities Under the Paperwork Reduction Act. OMB's progress is described in managing and overseeing many of the information gathering, processing and dissemination functions of the Federal government. Author

82 DOCUMENTATION AND INFORMATION SCIENCE

Includes information management; information storage and retrieval technology; technical writing; graphic arts; and micrography.

For computer documentation see *61 Computer Programming and Software.*

N90-22430*# National Aeronautics and Space Administration, Washington, DC.
INDEX TO NASA NEWS RELEASES AND SPEECHES, 1986
May 1987 209 p
(NASA-TM-101899; NAS 1.15:101899) Avail: NTIS HC A10/MF A02 CSCL 05B

This issue of the Index to NASA News Releases and Speeches contains a listing of news releases distributed by the Office of Public Affairs, NASA Headquarters, and a selected listing of speeches presented by members of the Headquarters staff during 1986. The index is arranged in six sections: Subject Index, Personal Names Index, News Release Number Index, Accession Number Index, and Speeches and News Releases. M.G.

N90-22431*# National Aeronautics and Space Administration, Washington, DC.
INDEX TO NASA NEWS RELEASES AND SPEECHES, 1987
Apr. 1988 75 p
(NASA-TM-101900; NAS 1.15:101900) Avail: NTIS HC A04/MF A01 CSCL 05B

This issue of the Index to NASA News Releases and Speeches contains a listing of news releases distributed by the Office of Public Affairs, NASA Headquarters, and a selected listing of speeches presented by members of the Headquarters staff during 1987. The index is arranged in six sections: Subject Index, Personal Names Index, News Release Number Index, Accession Number Index, and Speeches and News Releases. M.G.

N90-22432*# National Aeronautics and Space Administration, Washington, DC.
INDEX TO NASA NEWS RELEASES AND SPEECHES, 1988
Apr. 1989 61 p

(NASA-TM-101901; NAS 1.15:101901) Avail: NTIS HC A04/MF A01 CSCL 05B

This issue of the Index to NASA News Releases and Speeches contains a listing of news releases distributed by the Office of Public Affairs, NASA Headquarters, and a selected listing of speeches presented by members of the Headquarters staff during 1988. The index is arranged in six sections: Subject Index, Personal Names Index, News Release Number Index, Accession Number Index, and Speeches and News Releases. M.G.

N90-22433# Defense Technical Information Center, Alexandria, VA.

HOW TO GET IT: A GUIDE TO DEFENSE-RELATED INFORMATION RESOURCES

Gretchen A. Schlag and Charles E. Reed Jan. 1989 626 p (AD-A201600; DTIC/TR-89/1; IDA-Paper-P-1500) Avail: NTIS HC A99/MF A04 CSCL 05/2

A reference tool to identify and/or acquire government published or sponsored documents, maps, patents, specifications or standards and other resources of interest to the defense community is presented. Entries are arranged alphabetically in a single dictionary listing, by document type, source, acronym, series designation, or short title. Each entry consists of an identification of the item and detailed acquisition information such as source, order forms necessary, if there is a cost, where it is indexed, and telephone numbers for additional information. A detailed introduction, glossary and bibliography are included. Author

N90-22434 Drexel Univ., Philadelphia, PA.

A STUDY OF MENTAL MODELS THROUGH COMMUNICATION BETWEEN USERS AND ADVISORS SOLVING SOFTWARE MANIPULATION PROBLEMS Ph.D. Thesis

Parto Dehdashti 1989 257 p
Avail: Univ. Microfilms Order No. DA8926526

Mental models, as defined by Norman (1983), using analysis of face-to-face communication between users and advisors are examined. The premise was that congruence between the advisor's understanding of the user's views (advisor's meta model) and the user's mental model would contribute to obtaining a solution to the user's software manipulation problem. Four components of software, as defined by Riley (1986), objects, actions, syntax, and semantics, were represented by a set of terms to measure the congruence. The user's judgement of the relevance of the terms to the problem and solution was compared with the advisor's meta model of the relevance of the terms. The resulting congruence index was then compared with the user's satisfaction which was determined from the user's responses to interview questions. No statistically significant relationship was detected between the congruence measure and user satisfaction. Regression analysis showed that congruence in combination with advisor's expertise better explained the user's satisfaction. Analysis of conversation transcripts indicated that although users may have considered problems solved, many had not learned from the interaction with the advisors. Types of software manipulation problems and the use of four components of software were incidentally studied. Qualitative and quantitative analysis together contributed to a better understanding of mental models in face-to-face interactions. Dissert. Abstr.

N90-22435 Arizona Univ., Tucson.

FACILITATING KNOWLEDGE SHARING IN ORGANIZATIONS: SEMIAUTONOMOUS AGENTS THAT LEARN TO GATHER, CLASSIFY, AND DISTRIBUTE ENVIRONMENTAL SCANNING KNOWLEDGE Ph.D. Thesis

Gregg Steven Elofson 1989 275 p
Avail: Univ. Microfilms Order No. DA9000123

Evaluating patterns of indicators is often the first step an organization takes in scanning the environment. Not surprisingly, the experts that evaluate these patterns are not equally adept across all disciplines. While one expert is particularly skilled at recognizing the potential for political turmoil in a foreign nation, another is best at recognizing how Japanese government de-regulation is meant to complement the development of some new product. Moreover, the experts often benefit from one another's skills and knowledge in assessing activity in the environment external to the organization. One problem in this process occurs when the expert is unavailable and knowledge cannot be shared. Addressing the problem of knowledge sharing, of distributing expertise, is the focus. A technical approach is adapted in this effort - an architecture and a prototype are described that provide the capability of capturing, organizing, and delivering the knowledge used by experts in classifying patterns of qualitative indicators about the business environment. Using a combination of artificial intelligence and machine learning techniques, a collection of objects termed Apprentices are employed to do the work of gathering, classifying, and distributing the expertise of knowledge workers in environmental scanning. Furthermore, an archival case study is provided to illustrate the operations of an Apprentice using real world data. Dissert. Abstr.

N90-22436 Washington Univ., Seattle.

EVALUATION OF OPTICAL STORAGE TECHNOLOGY FOR DECISION SUPPORT DATABASES Ph.D. Thesis

Tse-Yih Bernard Han 1989 177 p
Avail: Univ. Microfilms Order No. DA9000243

Most current applications of optional digital disks (ODDs) are best suited for environments where additions to the databases are common but record changes are few. In contrast, this research considers environments with a moderate level of updates which must be available for on-line access within a short time after they occur. A hybrid system, combining write-once, read-many ODDs and magnetic disks (MDs), is proposed to exploit advantages of both storage technologies. The hybrid system uses the low cost, large capacity ODDs for base files with distributed free space, and the conventional MDs to buffer updates so as to avoid costly small writes to the ODD. Periodically, updates on the MD are moved to the ODD to refresh base files. When available free space on the ODD is exhausted, files and updates are reorganized onto new ODD media. Two optimization models are developed for the evaluation and management of files stored on the hybrid system. The first model is used to approximate the average file cost for a homogeneous file group. Results indicate that the hybrid system is cost effective for files with large size, low volatility, high degree of sequential I/O access, and rapid growth. The second model is a heterogeneous files model, which determines the optimum mix of pure MD and by hybrid devices and determines the placements for files characterized by various size, volatility, growth, and I/O demand. Model analysis considers environments with only space constraints or both size and I/O capacity constraints for ODD devices. The conclusion is that cost savings on the order of 30 to 40 percent can be realized in a typical decision support environment by using the mix of hybrid and conventional storage devices proscribed by the optimization models developed. Dissert. Abstr.

N90-22437 Wisconsin Univ., Milwaukee.

KNOWLEDGE-BASED SEMANTIC QUERY PROCESSING: AN OPTIMAL TRANSFORMATION APPROACH Ph.D. Thesis

Tung-Ching Lin 1989 313 p
Avail: Univ. Microfilms Order No. DA9003101

Database plays a major role in all information systems, such as transaction processing system, management information system and decision support system. The efficiency of database depends on the Query Optimization Subsystem (QOS). The major function of the QOS is to select a cheapest access plan for a given query. There are two inherent limitations in the conventional QOS, the first is that the information used to evaluate the query comes only from the physical level. The second is that there exists only one query representation form. An expert system named QUOTA (QUery Optimization Transformation Approach) is developed which can be embedded in the relational query optimization subsystem, to relax the two limitations of the conventional technique. The major idea of QUOTA is to use Semantic Integrity Constraint rules (SIC) to transform the original query into several semantically equivalent queries (SEQ). It is hoped that less expensive access plans, which were missed by conventional techniques, might be

found among these. The major steps of QUOTA are as follows: the related SIC rules are selected from the knowledge base: Two groups of knowledge were established to reduce the search space. The conflict among the SIC rules were detected and resolved: all possible conflicts and the heuristic rules to resolve them were identified in this step. The best SEQ was created: a search technique called ABCR (All Benefit and Conflict Resolution) was created to search the solution efficiently and effectively. A CARGO-SHIPPING relational database, in which forty five cases are used is chosen to test the efficacy of QUOTA.
Dissert. Abstr.

N90-22438*# National Aeronautics and Space Administration, Washington, DC.
NASA THESAURUS SUPPLEMENT: A FOUR PART CUMULATIVE SUPPLEMENT TO THE 1988 EDITION OF THE NASA THESAURUS (SUPPLEMENT 3) Semiannual Report
Mar. 1989 33 p
(NASA-SP-7064-Suppl-3; NAS 1.21:7064-Suppl-3) Avail: NTIS HC A03/MF A01 CSCL 05B

The four-part cumulative supplement to the 1988 edition of the NASA Thesaurus includes the Hierarchical Listing (Part 1), Access Vocabulary (Part 2), Definitions (Part 3), and Changes (Part 4). The semiannual supplement gives complete hierarchies and accepted upper/lowercase forms for new terms. Author

N90-22439# Office of Management and Budget, Washington, DC. Office of Information and Regulatory Affairs.
CURRENT INFORMATION TECHNOLOGY RESOURCE REQUIREMENTS OF THE FEDERAL GOVERNMENT: MAJOR SYSTEMS ACQUISITIONS AND PLANNED RESOURCES
12 Jan. 1990 693 p
(PB90-146820) Avail: NTIS HC A99/MF A04; also available in set of 2 reports HC E99/MF E99 as PB90-149980 CSCL 05B

The document is based on information submitted in support of the Budget of the United States Government for Fiscal Year 1990 and consists of a compilation of individual agency information technology acquisition plans for the period 1989 through 1994. It should be noted that resources information is subject to change as congressional action on the budget and other changes cause priorities to be reevaluated and allocations to shift. GRA

N90-22440# Advisory Group for Aerospace Research and Development, Neuilly-Sur-Seine (France). Technical Information Panel.
ELECTRONIC TRANSFER OF INFORMATION AND ITS IMPACT ON AEROSPACE AND DEFENCE RESEARCH AND DEVELOPMENT
Mar. 1990 190 p Meeting held in Brussels, Belgium, 17-19 Oct. 1989
(AGARD-CP-466; ISBN-92-835-0550-6) Copyright Avail: NTIS HC A09/MF A02; Non-NATO Nationals requests available only from AGARD/Scientific Publications Executive

Topics discussed include the present state and trends in the electronic transfer of information in Europe, North America, and Japan; operational and experimental systems for electronic storage and delivery of information; operational and experimental systems of electronic publishing and communication; and applications in the aerospace community. Included are papers on proposed telecommunications networks, Integrated Services Digital Network (ISDN) and satellite networks, plans for an integrated system for a large technical library, automation plans of the European Patent Office, optical disc systems, desk-top publishing, Standard Generalized Markup Language (SGML), electronic mail, computer conferencing and the U.S. Defense Department's Computer-aided Acquisition and Logistics Support (CALS) program. For individual titles, see N90-22441 through N90-22455.

N90-22441# Commission of the European Communities (Luxembourg). Directorate General Telecommunications.
TECHNOLOGIES FOR ELECTRONIC TRANSFER OF INFORMATION: THE PRESENT STATE AND TRENDS IN EUROPE
F. Mastroddi *In* AGARD, Electronic Transfer of Information and its Impact on Aerospace and Defence Research and Development Mar. 1990 10 p (For primary document see N90-22440 15-82)
Copyright Avail: NTIS HC A09/MF A02; Non-NATO Nationals requests available only from AGARD/Scientific Publications Executive

The emergence of new data storage and transfer media is having a growing effect on the electronic information industry. Two decades ago, there were only a handful of bibliographic databases, operated over dedicated online networks. Today the mass storage possibilities of new technologies, potential cost/benefit ratios, integration with personal computers and telecommunications networks are typical perceived benefits. There are several hundred optical disc applications running in Europe, in business, in education, leisure and research. A Commission of the European Community (CEC)-sponsored survey has identified many of these, and has gathered the opinions of market leaders on present and future trends. The consensus of opinion points to a promising market potential for this sector, depending on overcoming a set of key barriers - technical, economic and organizational and on the introduction of new telecommunications facilities. The European Commission (EC), under its new telecommunications and information market programs, aims to encourage the rapid development of this sector and to help overcome the barriers to growth. A call for proposals for pilot/demonstration projects held in early 1989 is one example of EC action. Author

N90-22442# National Federation of Abstracting and Indexing Services, Philadelphia, PA.
TECHNOLOGY FOR ELECTRONIC TRANSFER OF INFORMATION: THE PRESENT AND FUTURE IN NORTH AMERICA
Betty Unruh *In* AGARD, Electronic Transfer of Information and Its Impact on Aerospace and Defence Research and Development Mar. 1990 11 p (For primary document see N90-22440 15-82)
Copyright Avail: NTIS HC A09/MF A02; Non-NATO Nationals requests available only from AGARD/Scientific Publications Executive

Developments in the electronic transfer of information are largely led by advances in technology. This has been true and continues to be so today. The technologies of today, how they have advanced, and what effect those advancements have had on the products being delivered as well as on the information industry and its member companies are addressed. The successful delivery of information, however, is not completely dependent on technology. Successful products (and the technologies they utilize) are firmly rooted in the markets they serve. The importance of a product meeting a market need cannot be overlooked. How products, born of technology, have addressed market demands (when successful) or not addressed (when unsuccessful) will be included for both the past and present with an eye to what the lessons learned portend for the future. Author

N90-22443# GMD Bureau Tokyo, Akasaka (Japan). Deutsches Kulturzentrum.
TECHNOLOGIES FOR ELECTRONIC TRANSFER OF INFORMATION: THE PRESENT STATE AND TRENDS IN JAPAN
U. Wattenberg *In* AGARD, Electronic Transfer of Information and its Impact on Aerospace and Defence Research and Development Mar. 1990 10 p (For primary document see N90-22440 15-82)
Copyright Avail: NTIS HC A09/MF A02; Non-NATO Nationals requests available only from AGARD/Scientific Publications Executive

A full picture of electronic transfer of information in Japan is given. The huge number (6000) of Kanji characters caused many difficulties for the information industry: a Japanese-Japanese dictionary is needed for inputting characters via the keyboard; the characters require high resolution screens, etc. Having solved these problems, Japan has turned such disadvantages into advantages: it is leading in the production of high resolution screens and fax machines. Together with China and Korea, Japan is establishing a 2-byte standard character set for up to 65000 characters. The Japan Information Center of Science and Technology (JICST) is one of the largest hosts and document supply centers in the world. The JICST file on science and technology e.g., grows by 700,000 documents per year and the number of documents copied per year 700,000 too. 100,000 documents per year are translated into machine English; machine translation systems are applied mainly for translations from English into Japanese. JICST hosts one of the STN nodes (Columbus, Karlsruhe, Tokyo) through which the JICST databases are worldwide accessible, those in English really, and those in Japanese in principle. Of high importance are also the activities of the Japan Patent Information Organization (JAPIO) which cooperates with the U.S. Patent and Trade Mark Office and the European Patent Office in establishing a worldwide image file of all patents since 1920. Instead of the traditional 16 mm microfilm and microfiche the JAPIO now distributes to its subscribers 12 cm CD-ROM including full text images and index data. There is a sophisticated retrieval system for trade marks. And patents can be applied now either online, or on floppy disk, or in printed form. Japanese newspaper companies now hold their journals in electronic form. There is a data base with 500,000 photos on CD-ROM. Each day 500 new photos enter the database. Author

N90-22444# British Telecom, London (England).

INNOVATIONS IN TELECOMMUNICATIONS NETWORKS

Chris Holmes *In* AGARD, Electronic Transfer of Information and its Impact on Aerospace and Defence Research and Development Mar. 1990 12 p (For primary document see N90-22440 15-82)

Copyright Avail: NTIS HC A09/MF A02; Non-NATO Nationals requests available only from AGARD/Scientific Publications Executive

A public telecomms carrier has 6 main roles in the IT marketplace: a user; a vendor of telecommunications networks for voice, data and information services (both public and private); a vendor for components of IT systems, personal computers, UNIX machines, multiplexes, modems, etc.; a systems integrator offering complete customer solutions with adaptive engineering to meet specific customer needs; a conformance tester; and a standards maker. The major innovations in the first 3 of these roles in the field of electronic transfer of information are briefly examined. Inevitably it is biased towards the activities of the company but where appropriate the national and international linkages are explored. Author

N90-22445# Ministere de l'Education Nationale, Paris (France).

MEGATENDANCES [MAGATENDANCES]

S. Chambaud *In* AGARD, Electronic Transfer of Information and its Impact on Aerospace and Defence Research and Development Mar. 1990 10 p In FRENCH (For primary document see N90-22440 15-82)

Copyright Avail: NTIS HC A09/MF A02; Non-NATO Nationals requests available only from AGARD/Scientific Publications Executive

Five megatrends from the area of electronic transfer of information are identified: Three are from a technological discipline, one raises socioeconomic aspects, and the last is dependent on the results of research. This analysis predicts the use of information systems in the future. Transl. by E.R.

N90-22446# Commission of the European Communities (Luxembourg). Directorate General Telecommunications.

DOCUMENT DELIVERY VIA ISDN OR SATELLITE NETWORKS

Anthony J. Dunning *In* AGARD, Electronic Transfer of Information and its Impact on Aerospace and Defence Research and Development (SEE N90-22440 15-82) Mar. 1990 (For primary document see N90-22440 15-82)

Copyright Avail: NTIS HC A09/MF A02; Non-NATO Nationals requests available only from AGARD/Scientific Publications Executive

As a preliminary to discussing telecommunications networks and services, the main characteristics of documents and document delivery systems are presented from a theoretical viewpoint. The physical and functional characteristics of archives and document receiving terminals are also presented. An outline review of voice and data communications networks in W. Europe is presented. The plans for the introduction of ISDN services, and the facilities offered by experimental and operational satellite services are discussed. Standards aspects of telecomms services are considered, in particular the layer 7 protocol elements. The emergence of open distributed processing in ECMA and ISO and the associated client/server model are mentioned in this context. Author

N90-22447# Air Force Weapons Lab., Kirtland AFB, NM. Technical Processing Section.

THE WEAPONS LABORATORY TECHNICAL LIBRARY: AUTOMATING WITH STILAS

Barbara I. Newton and Janet M. Jourdain *In* AGARD, Electronic Transfer of Information and its Impact on Aerospace and Defence Research and Development (SEE N90-22440 15-82) Mar. 1990 (For primary document see N90-22440 15-82)

Copyright Avail: NTIS HC A09/MF A02; Non-NATO Nationals requests available only from AGARD/Scientific Publications Executive

In 1983, the United States Air Force Weapons Laboratory Technical Library formally recognized the requirement to manage its large diversified collections by automating several functions. This awareness coincided with the initiation of a joint Library of Congress - Defense Technical Information Center (DTIC) procurement program for an automated library system to serve the sophisticated needs of Department of Defense scientific libraries. Prototypes of the DTIC-sponsored project were described in the literature as The Local Automation Model. The Weapons Laboratory agreed to install the first production version of the system that was renamed the Scientific and Technical Information Library Automated System (STILAS). STILAS incorporates the features of an integrated library system with gateway reference access to an assortment of remote data bases, allowing library staff members and end-users to access up to four data base systems simultaneously. In addition to this reference function, STILAS performs all of the traditional library management functions of circulation, serials control, acquisitions, and inventory control. STILAS access is provided to Kirtland Air Force Base and its tenant organizations. Author

N90-22448# European Patent Office, Rijswijk (Netherlands). Principal Directorate Classification Documentation.

THE AUTOMATION PLAN OF THE GENERAL DIRECTORATE 1 (SEARCH) OF THE EUROPEAN PATENT OFFICE

Robert Bare *In* AGARD, Electronic Transfer of Information and its Impact on Aerospace and Defence Research and Development Mar. 1990 7 p (For primary document see N90-22440 15-82)

Copyright Avail: NTIS HC A09/MF A02; Non-NATO Nationals requests available only from AGARD/Scientific Publications Executive

The European Patent Office is actually realizing a huge automation project corresponding to an investment of about 300 million DM. This project is undertaken to cope with the ever increasing number of patent applications and volume of documents to be searched. The automation effort will be conducted in three directions: processing of textual information (Epoque); processing of images (Bacon); and personal systems. Author

N90-22449# Electronic Publishing Digital Equipment Co. Ltd., Basing View (England).

DESK TOP PUBLISHING: WHAT YOU NEED TO KNOW

Malcolm Taylor *In* AGARD, Electronic Transfer of Information and its Impact on Aerospace and Defence Research and Development Mar. 1990 25 p (For primary document see N90-22440 15-82)

Copyright Avail: NTIS HC A09/MF A02; Non-NATO Nationals requests available only from AGARD/Scientific Publications Executive

A comprehensive view on desk top publishing (DTP) is given. DTP is the way many people can use some of the traditional publishing skills. DTP can cope with different types of input (text, images, etc.), is easier to read, more authoritative, more effective in communicating, uses less paper, and facilitates multiple and multimedia output. When the documentation of a device (e.g., an aircraft) outweighs the device itself and when the documentation needs frequent updating then DTP can save much money. The minimum requirements for DTP are a PC, a screen to show input or output, a printer (preferably a laser printer) to print the output, a keyboard, a mouse and some DTP software. In addition to creating pages the software should support document retrieval, document management, revision control, revision tracking, distribution, and distribution control. The system should accept texts from other devices such as networks, should permit optical as well as intelligent character reading, should accept images such as line drawings and photographs, and should permit the creation of graphics. Publishing standards and architectures such as the Standard Generalized Markup Language (SGML) and the Office Document Architecture (ODA) play an increasing role in DTP. Author

N90-22450# MID Information Logistics Group G.m.b.H., Heidelberg (Germany, F.R.).

ELECTRONIC PUBLISHING WITH STANDARD GENERALIZED MARKUP LANGUAGE (SGML)

Manfred Krueger *In* AGARD, Electronic Transfer of Information and its Impact on Aerospace and Defence Research and Development Mar. 1990 8 p (For primary document see N90-22440 15-82)

Copyright Avail: NTIS HC A09/MF A02; Non-NATO Nationals requests available only from AGARD/Scientific Publications Executive

Electronic publishing of information made up of complex structured text (including technical and scientific notations, graphics and images) in large volumes with a long life cycle and suited for multiple forms of output is examined. In such a scenario, Standard Generalized Markup Language (SGML) serves as the basic tool in order to achieve a new quality of organizational control and managerial flexibility. The specific features of SGML will be demonstrated describing applications developed within the Association of American Publishers (AAP), the International Organization for Standardization (ISO) and the CALS initiative (Computer-aided Acquisition and Logistics Support) of the U.S. Department of Defense. Author

N90-22451# Information Technology Applications S.A. (Luxembourg).

ELECTRONIC MAIL SYSTEMS

Barry Mahon *In* AGARD, Electronic Transfer of Information and its Impact on Aerospace and Defence Research and Development Mar. 1990 3 p (For primary document see N90-22440 15-82)

Copyright Avail: NTIS HC A09/MF A02; Non-NATO Nationals requests available only from AGARD/Scientific Publications Executive

Electronic mail, or the use of computers and telecommunications networks for transferring messages, has been available to users of computer systems for a number of years. It's early availability was restricted to specialists and to those who had ready access to telecommunications facilities. More recently it has become widely available with a number of competing public services, many originating in the USA. A new CCITT/ISO standard known as X400 was agreed which is designed to facilitate the interaction between previously incompatible electronic messaging systems. It is expected that the availability of services supporting the X400 standard will contribute to the wider use of electronic messaging as a business and technical communication tool. However, in the same time frame, the general availability of equipment for productivity enhancement based on microprocessors, generally classified as the Information Technologies, has left many users or potential users of messaging systems with a bewildering choice of facilities. The developments are briefly reviewed and then the integration of message handling in the more advanced systems is presented. In so doing the emphasis is on the different functions which can be and should be covered by planners of messaging services. Direct services such as telex, fax, and interpersonal messaging are treated as well as the indirect facilities of gateways to external databases, intelligent interfacing and personal information management. A number of different scenarios are presented which illustrate how existing equipment and infrastructure can be more efficiently utilized to provide integrated services. Author

N90-22452# Guelph Univ. (Ontario).

COMPUTER CONFERENCING: MINDS MEETING ANYWHERE ANYTIME

John B. Black and Ellen Pearson *In* AGARD, Electronic Transfer of Information and its Impact on Aerospace and Defence Research and Development Mar. 1990 4 p (For primary document see N90-22440 15-82)

Copyright Avail: NTIS HC A09/MF A02; Non-NATO Nationals requests available only from AGARD/Scientific Publications Executive

Computer conferencing systems provide an effective means of group communication without the limitations posed by real-time interactions (e.g., audio and video tele-conferences) or physical location (e.g., face-to-face traditional meetings). Using various components of the myriad of telecommunications facilities available today, they provide a means of sharing the collective memory of a discussion among two, two hundred or two thousand participants who may be scattered around the globe. A description of this concept is provided, potential applications are discussed, and key factors required to make computer conferencing successful are indicated. Author

N90-22453# Defense Technical Information Center, Alexandria, VA.

APPLICATIONS TO THE AEROSPACE AND DEFENSE R AND D COMMUNITY: THE DOD COMPUTER-AIDED ACQUISITION AND LOGISTICS SUPPORT (CALS) INITIATIVE

Kurt N. Molholm *In* AGARD, Electronic Transfer of Information and its Impact on Aerospace and Defence Research and Development Mar. 1990 8 p (For primary document see N90-22440 15-82)

Copyright Avail: NTIS HC A09/MF A02; Non-NATO Nationals requests available only from AGARD/Scientific Publications Executive

The U.S. Department of Defense (DoD) Computer-aided Acquisition and Logistics support (CALS) initiative is directed toward improving the design, development, and support of weapons systems through the use of current and emerging computer technology. CALS emphasizes greater utilization of information contained in DoD and contractor databases to provide optimum, economic weapon system support using electronic transfer of information to the maximum amount possible. Author

N90-22454# Aerospatiale, Suresnes (France). Centre dInformation Documentaire Commun.

ELECTRONIC TRANSFER OF INFORMATION APPLICATIONS IN THE SOCIETE AEROSPATIALE [TRANSFERT ELECTRONIQUE DE L'INFORMATION APPLICATIONS DANS LA SOCIETE AEROSPATIALE]

Oleg Lavroff *In* AGARD, Electronic Transfer of Information and its Impact on Aerospace and Defence Research and Development Mar. 1990 5 p In FRENCH (For primary document see N90-22440 15-82)

Copyright Avail: NTIS HC A09/MF A02; Non-NATO Nationals requests available only from AGARD/Scientific Publications Executive

The applications of electronic information transfer in Aerospatiale, a French company with 33,000 employees, a turnover of 28 billion French Francs, and involved in the production of the Concorde, Airbus and Ariane is described. A number of electronic information projects are being studied or implemented: a bibliographic database in the field of technics for internal (knowhow of company) and external (patents etc.) information which should obviate the intermediaries; a database on macroeconomics; a database on internal and external standards; a database on multilingual terminology, stored on CD-ROM, as an aid for translation; technical documentation, stored on optical media, for use by clients, in particular a maintenance information planning system; computer assisted aircraft trouble shooting; an aircraft document retrieval system (more than 200,000 pages text and images); an advanced project for European information exchange on technical documentation; and a system for automated online order processing, e.g., for ordering spare parts. With 70 percent of the production being exported, automatic translation of technical documentation is of utmost importance. Author

N90-22455# British Aerospace Public Ltd. Co., Preston (England). Project Management Systems.
INFORMATION TECHNOLOGY APPLICATIONS: A BRITISH AEROSPACE MILITARY AIRCRAFT LTD VIEW
K. Hall *In* AGARD, Electronic Transfer of Information and its Impact on Aerospace and Defence Research and Development Mar. 1990 16 p (For primary document see N90-22440 15-82)
Copyright Avail: NTIS HC A09/MF A02; Non-NATO Nationals requests available only from AGARD/Scientific Publications Executive

A view of the use and impact of information technology in BAe Military Aircraft Ltd is presented. A precis of the current and expected business market place is included to give perspective to the importance of this industrial sector. The current situation is described with reference to typical conflicting requirements and the dynamic, competitive background. An example of a high level integrated business architecture is included which comprises a basic element of information flow in a company. Many of the components of an IT system focus in the project management activity, and consequently a system used for the management of projects is described in more detail. This illustrates in more depth the nature and complexity of one of the main activities in aerospace, and gives in addition an indication of the investment and timescales involved in such large - scale projects. Some conclusions are presented for consideration as policy guidelines for adoption by the AGARD panel. Author

N90-22456*# National Aeronautics and Space Administration. Goddard Space Flight Center, Greenbelt, MD.
NSSDC DATA LISTING
Richard Horowitz and Joseph H. King Feb. 1990 116 p
(NASA-TM-102989; NAS 1.15:102989; NSSDC/WDC-A-R/S-90-06) Avail: NTIS HC A06/MF A01 CSCL 05B

In a highly summarized way, data available from the National Space Science Data Center (NSSDC) is identified. Most data are offline data sets (on magnetic tape or as film/print products of various sizes) from individual instruments carried on spacecraft; these compose the Satellite Data Listing. Descriptive names, time spans, data form, and quantity of these data sets are identified in the listing, which is sorted alphabetically-first by spacecraft name and then by the principal investigator's or team leader's last name. Several data sets held at NSSDC, not associated with individual spaceflight instruments, are identified in separate listings following the Satellite Data Listing. These data sets make up the Supplementary Data Listings and include composite spacecraft data sets, ground-based data, models, and computer routines. The identifiers used in the Supplementary Data Listings were created by NSSDC and are explained in the pages preceding the listings. Data set form codes are listed. NSSDC offers primarily archival, retrieval, replication, and dissemination services associated with the data sets discussed in the two major listings identified above. NSSDC also provides documentation which enables the data recipient to use the data received. NSSDC is working toward expanding presently limited capabilities for data subsetting and for promotion of data files to online residence for user downloading. NSSDC data holdings span the range of scientific disciplines in which NASA is involved, and include astrophysics, lunar and planetary science, solar physics, space plasma physics, and Earth science. In addition to the functions mentioned above, NSSDC offers data via special services and systems in a number of areas, including Astronomical Data Center (ADC), Coordinated Data Analysis Workshops (CDAWs), NASA Climate Data System (NCDS), Pilot Land Data System (PLDS), and Crustal Dynamics Data Information System (CDDIS). Furthermore, NSSDC has a no-password account on its SPAN/Telenet-accessible VAX through which the NASA Master Directory and selected online data bases are accessible and through which any data described here may be ordered. Astrophysics data support by NSSDC is not limited to the ADC. Each of these special services/systems is described briefly. Author

N90-22457# Instituto de Pesquisas Espaciais, Sao Paulo (Brazil).
GEOGRAPHIC INFORMATION SYSTEM: CODED DATA OF AGROCATTLE-RAISING PROJECTS IN THE AMAZON [SISTEMA DE NFORMACOES GEOGRAFICAS: CODIFICANDO DADOS DE PROJETOS AGROPECUARIOS NA AMAZONIA]
Jose Simeao deMedeiros and Roberto W. OliveiraDias (Organization of American States.) Oct. 1989 7 p In PORTUGUESE; ENGLISH summary Presented at the 5th Brazilian Symposium on Remote Sensing, Natal, Brazil, Oct. 1989
(INPE-4978-PRE/1543) Avail: NTIS HC A02/MF A01

Experimentally the geocoding, storage, and the data integration are presented from various sources by using Geographical Information System 1.1 version (GIS) developed by INPE. The test site selected was Quixada, Para Bovina Farm with 30,500 ha of total area, located in Santa do Araguaia, Para State. The thematic map from TM LANDSAT images interpretation with topographic isolines, drainage net, roads, and firebreaks, were digitalized in different data plans at a 1:100,000 scale. These data plans were overlayed among themselves in different maps, creating totally and/or in part the farm maps. These tests were useful to evaluate the GIS potential of data geocoding, storage, combinations, and edition of agrocattle-raising projects in Amazon Region. Author

N90-22458# Oklahoma Geological Survey, Norman.
NATURAL RESOURCES INFORMATION SYSTEM FOR THE STATE OF OKLAHOMA Quarterly Report, Jan. - Mar. 1990
Charles J. Mankin May 1990 14 p
(Contract DE-FG22-89BC-14483)
(DE90-009483; DOE/BC-14483/4) Avail: NTIS HC A03/MF A01

The objective of this research program is to continue developing, editing, maintaining, utilizing, and making publicly available the Natural Resources Information System (NRIS) for the State of Oklahoma. The Oklahoma Geological survey, working with Geological Information Systems at the University of Oklahoma, has undertaken to construct this information system in response to the need for a computerized, centrally located library containing accurate, detailed information on the state's natural resources. Particular emphasis during this phase of development is being placed on computerizing information related to the energy needs of the nation, specifically oil and gas. Progress is described. DOE

N90-22459# Technische Univ., Delft (Netherlands). Faculty of Technical Mathematics and Informatics.
OBJECT-ORIENTED DATABASES: HOW ARE THEY DIFFERENT AND WHAT DIFFERNECE DOES IT MAKE
D. J. McConalogue 1989 29 p Revised
(Rept-89-55; ISSN-0922-5461; ETN-90-96370) Copyright Avail: NTIS HC A03/MF A01

The role of object-oriented paradigms in database technology is discussed. The use of such paradigms in overcoming the data modeling and performance of traditional systems is described. They are shown to be particularly useful when faced with the demands of a number of new applications areas that involve complex entities. Other ways in which an object-oriented database is better able to meet the needs of new applications are described. Object-oriented programming and systems are outlined. Object-oriented languages are described. Data manipulation in object-oriented databases is discussed. ESA

N90-22460# National Physical Lab., Teddington (England). Div. of Materials Applications.
SGTE DATA FOR PURE ELEMENTS
A. T. Dinsdale Sep. 1989 298 p
(NPL-DMA(A)-195; ISSN-0143-7313; ETN-90-96437) Copyright
Avail: NTIS HC A13/MF A02

Scientific Group Thermodata Europe (SGTE) is a consortium of seven organizations in western Europe engaged in the compilation of a comprehensive, self consistent and authoritative thermochemical database for inorganic and metallurgical systems. A list of the data currently being used by SGTE for the condensed phases of the pure elements is presented. The data for each phase of each element considered are presented as expressions showing, as a function of temperature, the variation of G-Hser, the Gibbs energy relative to the enthalpy of the Standard Element Reference (the reference phase for the element at 298.15K) and the difference in Gibbs energy between each phase and this reference phase (lattice stability). The variation of the heat capacity of the various phases and the Gibbs energy difference phases are shown graphically. ESA

83 ECONOMICS AND COST ANALYSIS

Includes cost effectiveness studies.

No abstracts in this category.

84 LAW, POLITICAL SCIENCE AND SPACE POLICY

Includes NASA appropriation hearings; aviation law; space law and policy; international law; international cooperation; and patent policy.

N90-22461# General Accounting Office, Washington, DC. National Security and International Affairs Div.
SPACE SHUTTLE, NASA'S MAJOR CHANGES TO FLIGHT HARDWARE: FACT SHEET FOR THE CHAIRMAN, COMMITTEE ON SCIENCE, SPACE, AND TECHNOLOGY, HOUSE OF REPRESENTATIVES
Jun. 1988 32 p
(GAO/NSIAD-88-173FS; B-229005) Avail: NTIS HC A03/MF A01

Selected changes made by NASA to the space shuttle's flight hardware are noted. Here, information presented during a briefing of representatives of the House Subcommittee on Space Science and Applications is given. Fifty-six changes made to the space shuttle flight hardware are noted. Changes were made to the Orbiter, the solid rocket booster assembly, the solid rocket motor, and the space shuttle main engines. The costs of changes are quoted. Information is given in tabular form. R.J.F.

N90-22462# Executive Office of the President, Washington, DC.
AERONAUTICS AND SPACE REPORT OF THE PRESIDENT: 1987 ACTIVITIES
1989 183 p
Avail: NTIS HC A09/MF A01

United States aeronautics and space activities for the calender year 1987 are summarized in the areas of space science and applications; communications; space transportation; safety, reliability, and quality assurance; commercial use of space; the Space Station; space operations; aeronautics; and space research and technology. The activities of each of the following organizations are described: National Aeronautics and Space Administration, Department of Defense, Department of Commerce, Department of Energy, Department of the Interior, Department of Agriculture, Federal Communications Commission, Department of Transportation, Environmental Protection Agency, National Science Foundation, Smithsonian Institution, Department of State, Arms Control and Disarmament Agency, and the United States Information Agency. M.G.

N90-22463# Oak Ridge National Lab., TN.
INTERNATIONAL SCIENCE AND TECHNOLOGY POLICIES: TESTIMONY BEFORE THE SUBCOMMITTEE ON INTERNATIONAL SCIENTIFIC COOPERATION, COMMITTEE ON SCIENCE, SPACE, AND TECHNOLOGY, UNITED STATES HOUSE OF REPRESENTATIVES
Alvin W. Trivelpiece 4 Apr. 1990 13 p
(Contract DE-AC05-84OR-21400)
(DE90-009416; DOE/OR-21400/T418) Avail: NTIS HC A03/MF A01

This paper reflects testimony before a congressional committee on International Science and Technology Policies. DOE

85 URBAN TECHNOLOGY AND TRANSPORTATION

Includes applications of space technology to urban problems; technology transfer; technology assessment; and surface and mass transportation.

For related information see also *03 Air Transportation and Safety, 16 Space Transportation,* and *44 Energy Production and Conversion.*

No abstracts in this category.

88 SPACE SCIENCES (GENERAL)

N90-22464*# National Aeronautics and Space Administration. Lewis Research Center, Cleveland, OH.
EXTRATERRESTRIAL LIFE IN THE UNIVERSE
Robert W. Graham Feb. 1990 10 p Presented at the Lewis Special Summer Lecture Series, Cleveland, OH, 18 Jul. 1989
(NASA-TM-102363; E-5080; NAS 1.15:102363) Avail: NTIS HC A02/MF A01 CSCL 06C

The possibility that life exists elsewhere in the universe, even in our own planetary system, has intrigued scientists, philosophers, and theologians for centuries. The spaceflight programs of NASA have provided much new information about our planetary neighbors and have put to rest some speculations about the existence of life on those planets or their satellites. However, there are still undetermined questions about the possibility of some form of life existing in the far distant past in our planetary system. Beyond our planetary system, the astronomical quest for scientific clues about life continues, largely via the radio telescope. Thus far there is no conclusive evidence. Here, some of the recent findings about our planetary neighbors are reviewed and the question about life elsewhere in the universe is addressed. Author

89 ASTRONOMY

Includes radio, gamma-ray, and infrared astronomy, and astrometry.

N90-22465 Arizona Univ., Tucson.
SEARCH FOR RAPIDLY STAR FORMING GALAXIES AT HIGH REDSHIFT Ph.D. Thesis

Richard Joseph Elston 1988 161 p
Avail: Univ. Microfilms Order No. DA8906385

Three surveys were conducted to try and locate distant star forming galaxies. The most general survey used deep 2 mu images with optical CCD photometry to locate objects with peculiar spectral energy distributions (SEDs). Using the IR data, rapidly star forming galaxies to $z = 25$ should be located. With a 3 sigma detection limit of 18.5 at K, no objects were found with z is greater than 5 but several blue objects were found at z is less than 4 in 26 min squared of sky. This suggests that there is no extremely luminous early phase of galaxy formation. Several blue objects were found at z is less than 4 in 10 min squared of sky. Of particular interest is an object which has a flat SED from V to K but shows a strong spectral break between B and V and a weaker break at 5800 A. It is suggested that these may be Lyman limit and Lyman alpha forest absorption at $z = 3.8$ in a galaxy forming approximately equal to 400 solar masses/year of stars. A large sample of galaxies selected to have similar properties was also found. From this sample it appears this possible high redshift star forming phase only contributes 1/10 of the metal present in disks or spheroids. Thirty Lyman alpha emission line companions to 12 $z = 3$ quasars were also found. These objects have Lyman alpha equivalent widths and luminosities consistent with galaxies forming approximately equal to 100 solar masses/year of stars. Also, 2 of the quasars have 8 companions and may be in cluster environments. A final survey analyzed optical to IR SEDs of luminous blue radio galaxies at z is greater than 1. In these objects SEDs were found indicative of star formation rates between 10 and 100 solar masses/year, but interpretation is difficult due to the AGN component of the sources. While these data seem to suggest a significant star forming phase taking place in galaxies at z is approximately equal to 3 to 4, interpreting this result is difficult since it cannot be determined if disk or spheroidal populations are being observed. Consideration of their dense environments and current epoch morphology suggest that these may be spheroids but these galaxies may not be typical. Dissert. Abstr.

N90-22466 Harvard Univ., Cambridge, MA.

RECOMBINATION LINES OF C I AND N II IN THE INTERSTELLAR MEDIUM Ph.D. Thesis

Vladimir EscalanteRamirez 1988 514 p
Avail: Univ. Microfilms Order No. DA8908965

A model potential method was used to calculate non-hydrogenic transition probabilities and radiative electron recombination coefficients of singly excited states of C I and N II. The results are applied to the calculation of the emission spectrum produced by recombination in the interstellar medium. The spectrum produced by resonant fluorescence from the ground and metastable states is also calculated for comparison with the recombination spectrum. The calculated emission rates are used to interpret observations of forbidden and permitted lines of C I and N II in planetary nebulae, H II regions, and nova shells using a minimum number of assumptions concerning the physical conditions in those objects. Comparison of relative line intensities allows the determination of the excitation mechanism in cases in which several lines of the same ion were observed. When the excitation is by recombination, an abundance, which is weakly dependent on temperature, can be determined. Dissert. Abstr.

N90-22467*# Columbia Univ., New York, NY. Dept. of Astronomy and Physics.

PHYSICS OF SYSTEMS CONTAINING NEUTRON STARS Semiannual Technical Report, 1 Mar. - 31 Aug. 1989

Jacob Shaham Nov. 1989 34 p
(Grant NAGw-1618)
(NASA-CR-186002; NAS 1.26:186002; CAL-1793) Avail: NTIS HC A03/MF A01 CSCL 03A

The following is a summary of work done during the period of Mar. to Oct. 1989. Three major topics were extensively looked into during this time: the reported 2,000 Hz optical signal from the direction of SNR1987A, the possibility that neutron stellar surface magnetic fields do not decay except when the star is accreting, and the 6 Hz QPOs of LMXBs. For individual titles, see N90-22468 through N90-22470.

N90-22468*# Columbia Univ., New York, NY. Astrophysics Lab.

DOES SN 1987A CONTAIN A RAPIDLY VIBRATING NEUTRON STAR

Q. Wang, K. Chen, T. T. Hamilton, M. Ruderman, and Jacob Shaham *In its* Physics of Systems Containing Neutron Stars Nov. 1989 6 p Previously announced in IAA as A89-36039 Submitted for publication (For primary document see N90-22467 15-89)
(Grants NAG8-497; NAGw-567; NSF AST-86-02831)
(CAL-371) Avail: NTIS HC A03/MF A01 CSCL 03A

If the recently reported 0.5 ms-period pulsed optical signal from the direction of Supernova 1987A originated in a young neutron star, its interpretation as a rotational period has difficulties. The surface magnetic field would have to be much lower than expected, and the high rotation rate may rule out preferred nuclear equations of state. It is pointed out here that a remnant radial vibration of a neutron star, excited in the supernova event, may survive for several years with about the observed (gravitationally redshifted) period. Heavy ions at the low-density stellar surface, periodically shocked by the vibration, may efficiently produce narrow pulses of optical cyclotron radiation in a surface field of about a trillion gauss. Author

N90-22469*# Columbia Univ., New York, NY. Astrophysics Lab.

ORIGIN OF PULSED EMISSION FROM THE YOUNG SUPERNOVA REMNANT SN 1987A

M. Ruderman, W. Kluzniak, and Jacob Shaham *In its* Physics of Systems Containing Neutron Stars Nov. 1989 10 p (For primary document see N90-22467 15-89)
(Grants NAGw-567; NAGw-1618; NSF AST-86-02831)
(CAL-377) Avail: NTIS HC A03/MF A01 CSCL 03A

To overcome difficulties in understanding the origin of the submillisecond optical pulses from SN 1987A a model similar to that of Kundt and Krotscheck for pulsed synchrotron emission from the Crab was applied. The interaction of the expected ultrarelativistic e(sup + or -) pulsar wind with the pulsar dipole electromagnetic wave reflected from the walls of a pulsar cavity within the SN 1987A nubula can generate pulsed optical emission with efficiency at most eta(sub max) is approximately equal to 10(exp -3). The maximum luminosity of the source is reproduced and other observational constraints can be satisfied for an average wind energy flow is approximately equal to 10(exp 38) erg/(s steradian) and for electron Lorentz factor gamma is approximately equal to 10(exp 5). This model applied to the Crab yields pulsations of much lower luminosity and frequency. Author

N90-22470*# Rikkyo Univ., Tokyo (Japan). Dept. of Physics.

DOES MASS ACCRETION LEAD TO FIELD DECAY IN NEUTRON STARS

N. Shibazaki, T. Murakami, Jacob Shaham, and K. Nomoto (Tokyo Univ., Japan) *In* Columbia Univ., Physics of Systems Containing Neutron Stars Nov. 1989 9 p Sponsored in cooperation with the Ministry of Education, Science, and Culture (For primary document see N90-22467 15-89)
(Grant NAGw-1618)
(CAL-394) Avail: NTIS HC A03/MF A01 CSCL 03A

The recent discovery of cyclotron lines from gamma-ray bursts indicates that the strong magnetic fields of isolated neutron stars might not decay. The possible inverse correlation between the strength of the magnetic field and the mass accreted by the neutron star suggests that mass accretion itself may lead to the decay of the magnetic field. The spin and magnetic field evolution of the neutron star was calculated under the hypothesis of the accretion-induced field decay. It is shown that the calculated results are consistent with the observations of binary and millisecond radio pulsars. Author

N90-22471 Pennsylvania Univ., Philadelphia.
A THREE-YEAR STUDY OF THE OH MASERS IN ORION-KL AND A STUDY OF THE (3,2) TRANSITION OF AMMONIA Ph.D. Thesis
Victor Migenes 1989 266 p
Avail: Univ. Microfilms Order No. DA8922570

The hydroxyl masers towards Orion-KL were mapped at three epochs, January 1985, April 1986, and October 1987, by the Very Large Array (VLA). At each epoch approximately 170 OH maser features with velocities between -12 to +30 km/s were found surrounding the IR sources IRc2, IRc6 and IRc7. These masers are located in an east-west distribution of 14 arc seconds in length, along a ridge defined by the NH3 emission associated with the dense hot core region. The OH masers appear to be in clumps, with diameters of approximately 0.5 to 3 arc sec and with dispersion velocities of 2 to 10 km/s and are probably formed in turbulent regions near the edges of shock fronts. In general the proper motions of the masers are higher than expected, but these could be interpreted as due to the turbulent motion of the material very close to young stellar objects. In addition, in January 1987, the (J,K) = (3,2) inversion line of ammonia toward Orion-KL was mapped. The VLA maps show that the emission is clumped on approximately equal to 1 arc sec scales. Most of these clumps appear to be collapsing and may be protostar candidates. The width of these clumps is considerably smaller than the widths measured with single-dish radio telescopes, allowing for a qualitatively different picture of the fragmentation process on scales of 10(exp 16) cm. The non-metastable and metastable NH3 lines are formed in different regions of the hot core. The OH clusters and the NH3 clumps are spatially correlated and both offer a consistent picture of the turbulent core of the Orion-KL nebula. The expanding-cylinder model for the ammonia emission can be seen as a cross section of the torus geometry delineated by masers and other molecular emission. There is a strong power-law correlation between the dispersion velocity of the NH3 and OH condensations and their sizes. This correlation is consistent with results obtained from similar studies of larger size-scale structure.
Author

N90-22472 Florida Univ., Gainesville.
ANALYSIS OF GAMMA SQUARED VELORUM PHOTOMETRY FROM THE SOUTH POLE Ph.D. Thesis
MaryJane Taylor 1988 190 p
Avail: Univ. Microfilms Order No. DA8924033

Several hundred photometric observations of the Wolf-Rayet star, gamma squared Vel, were obtained with the South Pole Optical Telescope using filters centered on the He II and C III emission lines at 4686 A as the comparison source. Two independent techniques are used to determine periodic behavior of variations in the strengths of these emission lines. The first of these methods uses power spectrum analysis based on Deeming's method of Fast Fourier Transforms. The second process involves fitting a first-order sine wave to the data using least-squares analysis. The results of the analysis of the He II feature indicate a fundamental period of 1.20 hours with an amplitude of fluctuation of a few percent. Several harmonics and subharmonics of this period are also detected. The presence of a 1.20 hour period of variability has certain theoretical implications which are discussed in the context of recent theoretical developments. It is suggested that these spectral changes are due to radial pulsations of gamma squared Vel. An attempt is made to arrive at satisfactory models to describe intensity variations of the C III emission line. Despite the weakness of this feature, periods are determined which indicate slightly more rapid fluctuations than those found to describe variations in the corresponding helium data. It is suggested that this result may provide clues indicating the relative locations of line formation in the extended wind. In addition to the analysis of narrowband photometry, observations in the visual and blue filters are reduced to photometric magnitudes using comparison star HR3452. The analysis of these data do not reveal any evidence of an optical eclipse in the gamma squared Vel system, at least within the limitations of these data. Dissert. Abstr.

N90-22473 California Univ., Berkeley.
A HIGH GALACTIC LATITUDE SURVEY OF FAR ULTRAVIOLET EXCESS OBJECTS Ph.D. Thesis
Jay Virgil Bixler 1988 177 p
Avail: Univ. Microfilms Order No. DA8916584

Two closely related efforts in astrophysical instrumentation and observation are described with the objective of performing a high galactic latitude survey of faint objects in the far ultraviolet. The avenues of research possible with data obtained from space based ultraviolet surveys are discussed and a summary of past, present and planned instruments capable of such survey work presented. The Faust telescope, an eight degree field of view imaging instrument with peak sensitivity at 1700A, designed for survey work is described. An imaging, active readout detector and associated ground support equipment were designed, constructed, and calibrated to replace the original photographic detector. The present state of observational data relevant to determining the atmospheric parameters of subdwarf B and O stars, and their mid-Galactic plane density and scale height was reviewed. Theoretical explanations of their evolutionary status were proposed. The optical observations and spectral reductions performed on objects included in a catalog of far ultraviolet bright, high galactic latitude objects are described. These observations provide a sample of subdwarf O and B stars free of brightness and temperature selection effects. A model atmospheres analysis was performed on the subdwarf sample to determine the temperature, gravity and helium to hydrogen ratio of the individual objects. The results show a smooth distribution of objects on the gravity versus temperature diagram near the theoretical location of the extended horizontal branch.
Author

N90-22474 California Univ., Los Angeles.
THE EMISSION LINES IN THE ULTRA-VIOLET SPECTRUM OF BETA LYRAE Ph.D. Thesis
Paolo Alberto Mazzali 1989 234 p
Avail: Univ. Microfilms Order No. DA8926447

The properties of the non-degenerate interacting binary system of beta Lyrae was investigated by studying its mass loss features. After reviewing the most noteworthy characteristics of this famously peculiar object, the typical wind signatures were examined: the UV emission lines, observed in high dispersion by IUE. These lines can be divided into two groups: one includes the superionized hot star wind resonances, displaying P-Cygni profiles superimposed to broad emission features; the other includes lines of moderately ionized species, showing pure P-Cygni profiles. After reviewing the theories of radiatively driven stellar winds and line formation, the 3D extension of Sobolev theory, designed to calculate radiative transfer and emerging line profiles in winds where stellar rotation and angular momentum conservation in the flow are included, was described. This model represents more accurately the physics of beta Lyrae. The models are able to predict the stellar rotational rate from the shape of the profiles, showing that rotation cannot be neglected in the modelling of P-Cygni lines. Finally, applying the self-consistent NLTE and hydrodynamic codes developed by Kudritzki, Pauldrach and Puls at the Munich Sternwarte, the winds of the two stars in the system were modeled. Dissert. Abstr.

N90-22475 California Inst. of Tech., Pasadena.
DIFFRACTION-LIMITED IMAGING ON THE 200-INCH TELESCOPE Ph.D. Thesis
Tadashi Nakajima 1989 162 p
Avail: Univ. Microfilms Order No. DA9000586

The technique of non-redundant masking at the Palomar 200-inch telescope and radio VLBI imaging software was used to make optical aperture synthesis maps of two binary stars, Beta Corona Borealis and Sigma Herculis. The dynamic range of the map of Beta CrB, a binary star with a separation of 230 milliarcseconds is 50:1. For Sigma Her, a separation of 70 milliarcseconds was found and the dynamic range of the image is 30:1. These demonstrate the potential of the non-redundant masking technique for diffraction limited imaging of astronomical objects with high dynamic range. It was found that the optimal integration time for measuring the closure phase is longer than

that for measuring the fringe amplitude. There is not a close relationship between amplitude errors and phase errors, as is found in radio interferometry. Amplitude self calibration is less effective at optical wavelengths than at radio wavelengths. Primary beam sensitivity correction made in radio aperture is not necessary in optical aperture synthesis. Effects of atmospheric disturbances on optical aperture synthesis were studied by Monte Carlo simulations based on the Kolmogorov theory of refractive-index fluctuations. For the non-redundant masking technique with r sub c-sized apertures, the simulated fringe amplitude gives an upper bound of the observed fringe amplitude. Monte Carlo simulations are also made to study the sensitivity and resolution of the bispectral analysis of speckle interferometry. The bispectral modulation transfer function and its signal-to-noise ratio at high light levels is presented. The signal-to-noise ratio of the bispectrum at arbitrary light levels is derived in the mid-spatial-frequency range.
Dissert. Abstr.

N90-22476 California Inst. of Tech., Pasadena.
EXPERIMENTS WITH A LASER INTERFEROMETRIC GRAVITATIONAL WAVE ANTENNA Ph.D. Thesis
Michael Edward Zucker 1989 184 p
Avail: Univ. Microfilms Order No. DA9000612

Sources and effects of astrophysical gravitational radiation are explained briefly to motivate discussion of the Caltech 40 meter antenna, which employs laser interferometry to monitor proper distances between inertial test masses. Practical considerations in construction of the apparatus are described. Redesign of test mass systems resulted in a reduction of noise from internal mass vibrations by up to two orders of magnitude at some frequencies. A laser frequency stabilization system was developed which corrects the frequency of an argon ion laser to a residual fluctuation level bounded by the spectral density square root of S sub upsilon(f) less than or equal to 60 microHz/square root of Hz, at fluctuation frequencies near 1.2 kHz. These and other improvements have contributed to reducing the spectral density of equivalent gravitational wave strain noise to square root of S sub h(f) approx. equal 10(exp -19)/square root of Hz at these frequencies. Finally, observations made with the antenna in February and March of 1987 are described. Kilohertz-band gravitational waves produced by the remnant of the recent supernova are shown to be theoretically unlikely at the strength required for confident detection in this antenna (then operating at poorer sensitivity than that quoted above). A search for periodic waves in the recorded data, comprising Fourier analysis of four 105-second samples of the antenna strain signal, was used to place new upper limits on periodic gravitational radiation at frequencies between 305 Hz and 5 kHz. Dissert. Abstr.

N90-22477# Chalmers Univ. of Technology, Goeteborg (Sweden).
A COMPARISON OF PHOTOSPHERIC AND CIRCUMSTELLAR (HCN)/(CO)-RATIOS FOR BRIGHT CARBON STARS
H. Olofsson, K. Eriksson, and B. Gustafsson (Astronomical Observatory, Uppsala, Sweden) 1989 24 p Submitted for publication Sponsored by Swedish Natural Science Research Council, Stockholm
(PB90-151101; Rept-89/29) Avail: NTIS HC A03/MF A01 CSCL 03A

Measures of circumstellar HCN/CO abundance ratios for carbon stars are compared with corresponding ratios estimated from photospheric abundance analysis. A satisfactory agreement is found for most stars. However, V Hya and two 60 micrometer-excess sources have significantly lower circumstellar ratios than expected, and for the (13)C-rich stars the ratios are somewhat higher. Author

N90-22478 Council for National Academic Awards (England).
PHOTOMETRIC MONITORING OF EARLY TYPE EMISSION LINE STARS Ph.D. Thesis
John Keith Davies 1988 345 p
Avail: Univ. Microfilms Order No. BRDX87675

A program of simultaneous optical (UBVRI) and infrared (JHKLMNQ) photometry of early type, emission line, stars is described. Particular emphasis is placed on observations of suspected pre-main sequence objects such as Herbig Ae/Be stars. The observations, together with data from the IRAS point source catalogue, are analyzed to probe the circumstellar environments of these objects and to determine the extent and causes of optical variability in such stars. It is found that many of these stars are associated with warm circumstellar dust and that the mean temperature of that dust is higher than the characteristic temperature of dust associated with T Tauri stars. It is shown that many of the stars in the program display variability at optical and infrared wavelengths, but that no single mechanism can account for the variability. The main variability mechanisms found are obscuration by circumstellar dust and changes in the underlying star. In some cases, more than one mechanism operates at different times in a single star. It is also shown that the class of objects described as Herbig Ae/Be stars is very heterogeneous and that trends of variability range with spectral type reported by other authors may be illusory. Some unusual stars, including V644 Cen and HD97048 are identified and examined in detail. Suggestions are made for future work. A brief spectrophotometric survey of similar stars is also reported. Author

N90-22479*# Sussex Univ., Brighton (England). Astronomy Centre.
FAST SPECTROSCOPIC VARIATIONS ON RAPIDLY-ROTATING, COOL DWARFS. 3: MASSES OF CIRCUMSTELLAR ABSORBING CLOUDS ON AB DORADUS
A. Collier Cameron, D. K. Duncan, P. Ehrenfreund, B. H. Foing, K. D. Kuntz, M. V. Penston, R. D. Robinson, and D. R. Soderblom (Space Telescope Science Inst., Baltimore, MD.) 20 Dec. 1989 79 p Sponsored in part by Science and Engineering Research Council and Commission of the European Communities
(Grant NAG5-1076)
(NASA-CR-186563; NAS 1.26:186563) Avail: NTIS HC A05/MF A01 CSCL 03A

New time-resolved H alpha, Ca II H and K and Mg II h and k spectra of the rapidly-rotating K0 dwarf star AB Doradus (= HD 36705). The transient absorption features seen in the H alpha line are also present in the Ca II and Mg II resonance lines. New techniques are developed for measuring the average strength of the line absorption along lines of sight intersecting the cloud. These techniques also give a measure of the projected cloud area. The strength of the resonance line absorption provides useful new constraints on the column densities, projected surface areas, temperatures and internal turbulent velocity dispersions of the circumstellar clouds producing the absorption features. At any given time the star appears to be surrounded by at least 6 to 10 clouds with masses in the range 2 to 6 x 10(exp 17) g. The clouds appear to have turbulent internal velocity dispersions of order 3 to 20 km/s, comparable with the random velocities of discrete filamentary structures in solar quiescent prominences. Night-to-night changes in the amount of Ca II resonance line absorption can be explained by changes in the amplitude of turbulent motions in the clouds. The corresponding changes in the total energy of the internal motions are of order 10(exp 29) erg per cloud. Changes of this magnitude could easily be activated by the frequent energetic (approximately 10(exp 34) erg) x ray flares seen on this star. Author

N90-22480# Lawrence Livermore National Lab., CA.
UPDATE ON THE OPAL OPACITY CODE
F. J. Rogers, C. A. Iglesias, and B. G. Wilson 23 Feb. 1990 11 p Presented at the Atomic Processes in Plasmas, Gaithersburg, MD, 2-5 Oct. 1989
(Contract W-7405-eng-48)
(DE90-009946; UCRL-JC-103348; CONF-891052-2) Avail: NTIS HC A03/MF A01

Persisting discrepancies between theory and observation in a number of astrophysical properties has led to the conjecture that opacity databases may be inaccurate. The OPAL opacity code was developed to address this question. The physical basis of OPAL removes several of the approximations present in past calculations. For example, it utilizes a much larger and more detailed set of atomic data than was used to construct the Los Alamos Astrophysical Library. This data is generated online, in LS or intermediate coupling, from prefitted analytic effective potentials and is of similar quality as single configuration, relativistic, self consistent field calculations. The OPAL code was used to calculate opacities for the solar core and for Cepheid variable stars. In both cases, significant increases in the opacity compared to the Los Alamos Astrophysical Library were found. DOE

N90-22481 Princeton Univ., NJ.

THE OPTICAL NIGHT SKY AT LOW SURFACE BRIGHTNESS: HIGH LATITUDE DUST AND FAINT FIELD GALAXIES Ph.D. Thesis

Puragra Guhathakurta 1989 209 p

Avail: Univ. Microfilms Order No. DA9012721

Deep CCD imaging in U, B(sub j), R, and I, over angular scales ranging from a few arcseconds to over 30 arcminutes, is used to study two classes of astronomical objects that produce fluctuations in the dark night sky background: interstellar dust clouds at high Galactic latitudes, initially identified by their thermal re-radiation of ambient starlight as IRAS 100 microns cirrus; and a population of faint blue field galaxies, which, at 30 B(subj) mag/arcsec, begin to fill up the field of view. A CCD mosaicing technique, designed to allow imaging of large areas of the sky at low light levels, was used to study the cirrus morphology. The scattering and re-emission of optical radiation from the cirrus are investigated, with the goal of learning more about the environment of these clouds and the physical processes involved. The cirrus is extremely red in both B(sub j)-R and R-I, much redder than a simple scattering model predicts. The excess R and I band flux is probably the result of luminescence in small hydrogenated dust grains. This very red color appears to be a universal signature of optically thin dust clouds at high latitudes, and should enable them to be distinguished from the second component, aggregates of faint blue galaxies. These galaxies dominate the number counts in the field, and the U band count slope is even steeper than that in B(sub j). The colors, over the wavelength range 3600 A to 1 micron, are indicative of fairly recent evolution. Dissert. Abstr.

N90-22482 Minnesota Univ., Minneapolis.

THE MODELING OF IRAS DETECTIONS OF CLASSICAL NOVAE AND RELATED OBJECTS Ph.D. Thesis

Thomas Edward Harrison 1989 248 p

Avail: Univ. Microfilms Order No. DA9008278

Data on classical novae were extracted from the Infrared Astronomical Satellite (IRAS) database, and models were developed to explain the resulting detections. Data were also extracted on objects which have behavior similar to classical novae. For the 105 novae or suspected novae in the sample, detections are reported for 53 of them. Eleven of these appear to be false detections of the galactic cirrus. To explain the remaining detections, several computer programs were developed that model the ejected gas using published data on the conditions expected in post-outburst nova ejecta. The result of these programs is a prediction of the far-infrared line spectrum emitted by the gas ejected in the nova explosion. A number of the detections made by IRAS are explainable this way. In several cases, emission from dust or free-free processes can be invoked to explain the IRAS data. Information was also extracted from the IRAS database for 116 objects related to novae. Such objects as dwarf novae, nova-like variables, symbiotic stars and cataclysmic planetary nebulae are included as related objects. Many of these objects were detected (93), and the resultant energy distributions were compared to those found for novae to determine if there are similarities among the different classes of cataclysmic variables. The source of the infrared energy for the dwarf novae and nova-like variables remains difficult to explain. Dissert. Abstr.

90 ASTROPHYSICS

Includes cosmology; celestial mechanics; space plasmas; and interstellar and interplanetary gases and dust.

For related information see also *75 Plasma Physics.*

N90-22483 Texas Univ., Austin.

COMPUTER SIMULATION OF TIME-DEPENDENT SPHERICALLY SYMMETRIC SPACETIMES CONTAINING RADIATING FLUIDS: FORMALISM AND CODE TESTS Ph.D. Thesis

Anthony Mezzacappa 1988 178 p

Avail: Univ. Microfilms Order No. DA8909715

General equations are presented for general relativistic radiation hydrodynamics. The 3 + 1 Einstein equations including a radiation component in the energy-momentum tensor are derived and these equations are specialized to spherical symmetric spacetimes and the isotropic gauge. The 3 + 1 equations are derived for general relativistic hydrodynamics, including the radiation 4-force density, and the 3 + 1 general relativistic Boltzmann equation, all for spherical symmetric spacetimes. These equations are then specialized to the isotropic gauge. The implicit finite differencing of the Boltzmann equation and of the radiation contribution to the hydrodynamics equations are described. A new implicit numerical scheme is presented for the matter-radiation coupling, that is, for the collision term in the Boltzmann equation and the radiation 4-force density in the hydrodynamics equations. This scheme allows analytic matrix inversion of the finite difference equations for these terms and does not rely on partial temperatures. Evans' hydrodynamics code for spherically symmetric spacetimes, which is used in conjunction with the radiation code is described. The results of a code test for the radiation transport and matter-radiation coupling that serves as a benchmark for the code is presented. Finally, the results of a general relativistic example and code tests which was developed is described. A star was constructed in general relativistic hydrodynamic and thermodynamic equilibrium by solving the Oppenheimer-Volkoff equations coupled to the equations for thermodynamic equilibrium. The methods used to numerically integrate this system of ordinary differential equations are discussed. Dissert. Abstr.

N90-22484 Arizona Univ., Tucson.

THE PRODUCTION AND SPATIAL DISTRIBUTION OF NEUTRAL AND IONIZED WATER VAPOR IN COMET P/HALLEY Ph.D. Thesis

Michael Antonio DiSanti 1989 171 p

Avail: Univ. Microfilms Order No. DA8915955

The problem of water vapor production and distribution in comet P/Halley, based upon interpretation of observational data obtained during the recent 1985 to 1986 apparition is addressed. The data was acquired using the Lunar and Planetary Laboratory charge-coupled device (CCD) on the 154 cm Catalina telescope of the University of Arizona Observatories. The data acquisition system was employed in two modes. The long-slit spectroscopy mode covered the wavelength range 5200 to 10400 A at a spectral resolution approximately 14 A. The narrow band filter imaging mode allowed two-dimensional mapping of selected cometary emission features, as well as the continuum, with a field of view of roughly 10 arc-min. The 1986 March 5 long-slit spatial profiles showed a central dip in the water ion (H2O+) column density, of order 30 percent in the inner coma, which filled in farther tailward. Vega-1 spacecraft measurements (March 6) revealed a decrease in local ion density, of roughly 60 percent at closest approach R is approximate or equal to 9000 km sunward of the nucleus, relative to an inbound maximum R is approximate or equal to 12000 km. Our filter images (March 6), centered on the H2O+ 0, 8, 0 band, showed that the falloff in ions was relatively rapid sunward of the nucleus. In the anti-solar direction the decrease was much more gradual, due to the solar wind sweeping ions from the head of the comet into the plasma tail, whose width was of order 10(exp 5) km in the inner coma, diverging slowly and breaking up into a ray pattern farther tailward. The distribution of neutral water was mapped out using the O I wavelength 6300 emission as diagnostic probe. In contrast to the ions, the H2O molecules were confined mainly to the inner few x 10(exp 4) km of the coma, and exhibited a much more symmetrical distribution. Integration of the O I slit profiles, assuming azimuthal symmetry, allowed calculation of the H2O production rate, which ranged from approximately 10(exp 28) molecules/s, when Halley was at a distance r is approximately or greater than 2 AU from the sun, to approximately 1.5 x 10(exp 30) molecules/s from 1986 March 5. Author

N90-22485 Colorado Univ., Boulder.

INTERACTIONS OF MASSIVE STARS WITH THE INTERSTELLAR MEDIUM: BOW SHOCKS AND SUPERBUBBLES Ph.D. Thesis

Mordecai-Mark MacLow 1989 126 p

Avail: Univ. Microfilms Order No. DA8923511

Stellar winds and supernovae from massive stars carry most of the energy transferred from stars to the interstellar medium. The structures created by these processes reveal glimpses of the movement of mass between stars and the galactic ecological cycle. Two such structures are modeled bow shocks and superbubbles. Multiple supernovae and winds from OB associations carve large holes filled with hot gas in the galactic disk. These superbubbles sweep up thin, cold, dense shells that eventually grow large enough to blow out of the disk, venting hot gas into the galactic halo. To model superbubbles, the blast waves from supernovae within them are analytically described, showing they become subsonic before reaching the walls or cooling radiatively. The Kompaneets or thin-shell approximation are used to numerically model the growth of superbubbles in stratified disks until they become Raleigh-Taylor unstable. ZEUS, a two-dimensional hydrodynamics code was used to follow the breakup of the shell. The differences between the results and previous models are explained. Considering stars with strong winds leads to an explanation for ultracompact H II regions (USHRs). It was proposed that UCHRs are trapped in bow shocks swept up by the winds of massive stars moving supersonically through molecular clouds. A thin shell approximation was used to find the shape of such bow shocks. Simulated maps were produced and compared to G12.21 - 0.01, G29.96 - 0.02, G34.26 + 0.15, and G43.89 - 0.78. Dissert. Abstr.

N90-22486 Indiana Univ., Bloomington.

THE EVOLUTION OF THE SUPERNOVA REMNANT IC 443 Ph.D. Thesis

Michael Leon McCollough 1989 330 p

Avail: Univ. Microfilms Order No. DA8925113

The evolution and appearance of a supernova remnant (SNR) can be greatly affected by the nature and makeup of the interstellar medium (ISM) into which the SNR is evolving. The effect of multiphase nature of the ISM on the evolution and appearance of a SNR is examined. Multiwavelength observations consisting of high resolution images made in the radio, infrared, optical, and x ray were obtained of the SNC IC 443. From these images and previous research done on IC 443, analytic and numerical hydrodynamics models have allowed assessment of various parameters. The x ray data indicate the age (t is approximately 5000 years), initial energy (is approximately (3-7) x 10(exp 50) ergs), and current density (1-2/cu cm) of the shocked intercloud gas. The radio and optical observations indicate that small scale radio/optical structure is due to isothermal shocks moving through dense clouds. The bulk of the radio emissions arises in large scale structure from the intercloud gas. The IR indicates that dust and line emission are important in the cooling of the remnant. It was found that IC 443 is evolving in a very complex region of the ISM. The intercloud medium into which the SNR is expanding is typical of a H II region containing low and high density clouds. There appears to be a factor of 2 variation in the average ambient density across the remnant. Across the front and along the east of the remnant a collision with a molecular cloud is occurring. Emission from the shock heated dust and the IR lines serves as the major source of energy loss in the remnant. Much of IC 443s appearance may be the result of the prior interaction of the supernova progenitor with the molecular cloud. It is apparent that the appearance and evolution of IC 443 is being shaped by the environment into which IC 443 is expanding. Dissert. Abstr.

N90-22487 Manchester Univ. (England).

HERBIG-HARO OBJECTS AND STELLAR JETS Ph.D. Thesis

T. N. Wilkins 1988 286 p

Avail: Univ. Microfilms Order No. BRD-86506

The current state of knowledge on Herbig-Haro objects and stellar jets is summarized. The software is discussed with a brief mention of previously existing programs. Long-slit and TAURUS observations of the region of HH 29 and L1551 IRS 5 jet are presented. Observations of the jet probably associated with a VLA source near HL Tau are discussed. Long-slit observations of HH 1 and 2 are examined. Gaussians were fitted to the profiles to obtain accurate radial velocities, widths, etc. These show a considerable variety of velocities and electron densities. Long-slit observations are described for the nebula surrounding the symbiotic star R Aquarii. This shows a complicated flow pattern, and results are in the main consistent with Solf and Ulrich's (1985) model, in terms of the ejection of two shells. Achievements in data reduction techniques are summarized and future plans outlined. Dissert. Abstr.

N90-22488*# National Aeronautics and Space Administration. Lewis Research Center, Cleveland, OH.

SPACE STATION FREEDOM SOLAR ARRAY PANELS PLASMA INTERACTION TEST FACILITY

Donald F. Martin and Kenneth D. Mellott 1989 14 p Presented at the Spacecraft Charging Technology Conference, Monterey, CA, 31 Oct. - 3 Nov. 1989; sponsored by Naval Postgraduate School (NASA-TM-102475; E-5262; NAS 1.15:102475) Avail: NTIS HC A03/MF A01 CSCL 03B

The Space Station Freedom Power System will make extensive use of photovoltaic (PV) power generation. The phase 1 power system consists of two PV power modules each capable of delivering 37.5 KW of conditioned power to the user. Each PV module consists of two solar arrays. Each solar array is made up of two solar blankets. Each solar blanket contains 82 PV panels. The PV power modules provide a 160 V nominal operating voltage. Previous research has shown that there are electrical interactions between a plasma environment and a photovoltaic power source. The interactions take two forms: parasitic current loss (occurs when the currect produced by the PV panel leaves at a high potential point and travels through the plasma to a lower potential point, effectively shorting that portion of the PV panel); and arcing (occurs when the PV panel electrically discharges into the plasma). The PV solar array panel plasma interaction test was conceived to evaluate the effects of these interactions on the Space Station Freedom type PV panels as well as to conduct further research. The test article consists of two active solar array panels in series. Each panel consists of two hundred 8 cm x 8 cm silicon solar cells. The test requirements dictated specifications in the following areas: plasma environment/plasma sheath; outgassing; thermal requirements; solar simulation; and data collection requirements. B.H.A.

N90-22489# Virginia Univ., Charlottesville.

THE DISTRIBUTION OF MOLECULAR CLOUDS IN SPIRAL GALAXIES Ph.D. Thesis

David Scott Adler 1989 230 p

Avail: Univ. Microfilms Order No. DA8919116

The distribution of molecular clouds in spiral galaxies is studied via numerical simulations of cloud/particle systems and millimeter-wave observations of carbon monoxide in external galaxies. Particular attention is paid to the dynamics of clouds in and around the spiral arm regions. Algorithms that calculate the gravitational force on a cloud from the remainder of the cloud ensemble are added to an existing N-body code. Fourier transform techniques are utilized to calculate the forces, cutting down on the problems a Newtonian calculation would create. Extensive testing is done to ensure that the method provides an adequate approximation of self-gravitational forces. Clouds are seen to congregate quite naturally in the spiral arms of the model disk even with the exclusion of cloud collisions or self-gravity. The model disk is used to investigate the validity of using longitude-velocity diagrams to identify Galactic GMCs. The reference point is put into an evolved model disk at a point similar to the Sun's position in the Galaxy. It is found that concentrations of clouds in the l-v diagram do not always correspond to complexes of clouds in the disk. Detection of CO in four previously unstudied galaxies occurred during a background search of nearly disk galaxies. Major axis-minor axis information was obtained from M74 (NGC 628). The CO intensity falls off as a function of radius, consistent with most other observed external galaxies. The CO rotation curve is in general agreement with the HI rotation curve. Higher resolution observations were done on M51, NGC 6946, and IC 342. Integrations were taken along and across an arm, as well as parallel to it, in an attempt to see density and velocity contrasts between the arm and interarm regions. Dissert. Abstr.

N90-22490 Michigan Univ., Ann Arbor.
SPECTRUM FORMATION IN ACTIVE GALACTIC NUCLEI AND TYPE 2 SUPERNOVAE Ph.D. Thesis
Ronald Gene Eastman 1989 133 p
Avail: Univ. Microfilms Order No. DA9001622

Three separate but related problems of spectrum formation in Seyfert galaxies, quasars, and Type 2 supernovae are studied. The observed steepening of quasar continua for frequencies above the Ly alpha rest frequency is reproduced by absorption in marginally optically thin cloudlets moving away from quasars with a suitable velocity distribution. The calculations take into account Ly alpha, Ly beta, and Lyman continuum absorption and also reemission back into the line of sight. For a reasonable match with observations, which extend nearly to 400 A in the rest frame of one quasar, a neutral hydrogen column density of approximately 10(sup 17)/sq cm is needed. An investigation is made of the He II Ly alpha transfer problem and the related O III and N III Bowen fluorescence mechanisms for detailed photoionization models of emission-line clouds in Seyfert galaxies and quasars. Transfer results and/or predicted relative intensities of He II or O III far ultraviolet lines are presented for calculations employing various atomic densities, ionizing radiation field characteristics, ionization parameters, chemical abundances, and gas velocity structures. A code was developed which simultaneously solves the non-LTE equations of statistical equilibrium and the time independent equations of radiation transport in an expanding atmosphere. This was applied to the study of the spectrum of SN 1987A. The behavior of a model atmosphere in which the density structure is a power law function of radius was studied and compared closely with SN87A data. This model atmosphere is employed to derive corrections to the Expanding Photosphere Method for determining distances to supernovae. Dissert. Abstr.

N90-22491 Auburn Univ., AL.
CURRENT DRIVE IN A SUPERNOVA Ph.D. Thesis
Hideya Kishi 1989 147 p
Avail: Univ. Microfilms Order No. DA8925629

The current generation rate due to the scattering of neutrinos of charged particles in a supernova plasma with temperature and density gradients and differential rotation was calculated. The motivation is to understand the potential effect of the magnetic field generated by the neutrino scattering off charged particles on the supernova explosion. For a long time, this phenomenon was difficult to explain, despite the efforts of many theoretical astrophysicists. Earlier workers have found that magnetic fields of more than 10(exp 15) Gauss are needed in the supernova explosion. Results show the generated magnetic field is large enough to help the supernova explosion. The time scale of the acceleration of electrons by the scattering neutrinos (.01 to .001 sec) is comparable to the times scale of the gravitational collapse (.01 to .001 sec). The results also show that electrons contribute dominantly to the current generation rate. This fact led to the investigation of the deceleration of electrons by heavy ions through Coulomb interaction. Results show that the Coulomb relaxation process is inefficient because electron degeneracy suppresses the deceleration of electrons. Therefore, the current generation is still effective and the generated magnetic field is large enough to affect the supernova explosion. The finding of a source of a strong magnetic field suggests further study of the processes in the nonlinear regime. The nonlinear processes include the effect of the magnetic field on the current generation process; the effect of the magnetic field on the differential rotation, which is an essential part of the current drive; and the effect of the magnetic field on the buoyancy instability and subsequent convective motion of infalling material. Dissert. Abstr.

N90-22492 California Univ., Los Angeles.
INVESTIGATION OF THE LATE STAGES OF STELLAR EVOLUTION: MASS LOSS FROM EVOLVED STARS Ph.D. Thesis
Lauren Jones Likkel 1989 224 p
Avail: Univ. Microfilms Order No. DA8926436

In order to investigate the latest stages of stellar evolution, objects with IRAS flux densities similar to those of evolved stars with cold circumstellar material were studied. The selected objects, mostly previously unidentified, were observed for CO emission, and for H2O (22 GHz) and OH (1.6 GHz) maser emission. At least 38 of the 77 objects in the sample are evolved stars with molecular circumstellar envelopes, including 22 OH/IR stars; 22 of the evolved stars are suggested to be pre-planetary nebulae. The pre-planetary nebulae candidates in the sample fall into one or more of three groups: intermediate spectral type stars with expanding molecular shells, irregular or non-variable OH/IR stars, or oxygen-rich stars with cold circumstellar envelopes that show CO emission but not OH emission. Analysis of the OH/IR stars in the sample and similar but warmer OH/IR stars indicates that the reddest OH/IR stars have a lower scale height, and thus a larger progenitor mass, than the other OH/IR stars. The results indicate that only the reddest OH/IR stars have a scale height consistant with the previously accepted value for progenitor mass of approximately 2 to 5 solar masses and that the progenitor mass for a typical OH/IR star is approximately 1 solar mass. Three objects are discussed in detail. IRAS09371+1212, nicknamed the Frosty Leo Nebula, was identified as an evolved star by its CO profile. IRAS21282+5050 is a planetary nebula. IRAS1634-3814 was found to have an extremely unusual OH emission profile. Dissert. Abstr.

N90-22493 Massachusetts Univ., Amherst.
THE SAGITTARIUS B2 MOLECULAR CLOUD: AN EXTREME CASE OF A GALACTIC CENTER GIANT MOLECULAR CLOUD Ph.D. Thesis
Dariusz Cezary Lis 1989 289 p
Avail: Univ. Microfilms Order No. DA9001532

A model was developed of the Sagittarius B2 molecular cloud based on the J = 1 yields 0 and 2 yields 1 transitions of (13)CO and C(18)O, as well as on the far infrared and submillimeter continuum emission from the dust, in order to determine the physical conditions in this source. The total mass of the cloud is dominated by an envelope which consists of a constant density component and a power law component with a radial exponent of -2. The virial mass of the cloud is a factor of approx. 2 higher than the molecular mass, suggesting that Sgr B2 is close to virial equilibrium. The Sgr B2(M) and (N) continuum sources are situated inside small dense cores embedded in the extended clouds. The middle source is much more luminous than the northern source. The observed change in the middle-to-north peak flux ratio between 350 mu and 1300 mu is primarily a result of the difference in luminosity. In order to compare Sgr B2 with other Galactic Center clouds, the J = 1 yields 0 transition of (13)CO was observed in two selected Galactic Center fields centered on the G1.1 to 0.1 and G359.4 to 0.1 continuum sources. The molecular clouds observed there seem to be distinctively different from Sgr B2. Dissert. Abstr.

N90-22494 Brigham Young Univ., Provo, UT.
A THEORETICAL SCENARIO FOR THE DYNAMICS OF FORMATION AND EARLY EVOLUTION OF GLOBULAR

CLUSTERS IN GALAXIES Ph.D. Thesis

Fabrizio Pinto 1989 238 p

Avail: Univ. Microfilms Order No. DA9004119

The formation of globular clusters was a key cosmological process related to the physical state of the universe shortly after the Big Bang. For this reason, globular clusters can be used as probes to study the environments where galaxies formed, and in order to better understand the formation of these objects, the problem was approached from two different points of view. The former approach has been that of using young globular clusters in the Large Magellanic Cloud as a laboratory to study the formation of massive star clusters. An analytic model was devised to describe these objects. An estimate of the star formation efficiency was obtained which is in agreement with the observations. Even if these results can be extended to the primeval case only with great caution, this approach was quite fruitful in helping constrain the values of some otherwise arbitrary parameters. The latter approach was that of modeling in greater detail some important phases of star formation and dynamical evolution in the Galaxy. In particular, the phase of gas expulsion from a newly formed cluster was studied analytically in the impulsive approximation. This has yielded interesting new results concerning the roles possibly played by the magnetic field and by the turbulence in protoclouds. A theoretical model was devised to describe the formation of star clusters based on the hypothesis that the process is triggered by cloud-cloud collisions. This model has helped better clarify what physical parameters may have had an important role in shaping the cluster population. Dissert. Abstr.

N90-22495 Massachusetts Univ., Amherst.

KINEMATIC MODELS OF COMETARY COMAE Ph.D. Thesis

Lowell Evan Tacconi-Garman 1989 208 p

Avail: Univ. Microfilms Order No. DA9001572

As a first step towards understanding the kinematics of cometary comae, an analysis was undertaken of the 18-cm OH lines in comets. This work builds on past OH excitation and kinematic studies to meld them into a complete and self-consistent model for a cometary coma. The kinematics were modeled via the vectorial formalism and the powerful Monte Carlo technique was used in an effort to reproduce the high sensitivity, high spectral resolution 18-cm OH line profiles of Comets Halley, Giacobini-Zinner, Hartley-Good, Thiele, and Wilson which were obtained at the 43 meter telescope of the National Radio Astronomy Observatory at Green Bank, West Virginia. For the first time a zeroth order A-doublet quenching correction was applied to the 18-cm data and the long standing UV/radio gas production rate disparity was accounted for. Gas expansion velocities and coma anisotropies were derived from observations covering a wide range of heliocentric distances and gas production rates. The inferred ratio of dayside gas emission to nightside gas emission for all comets in this study, except P/Giacobini-Zinner, is approx. two. This value is consistent with that derived from in situ observations of the neutral gas in the coma of Comet Halley and is independent of both gas productivity and heliocentric distance. For P/Giacobini-Zinner, anomalously high gas outflow anisotropies were inferred for which there is no clear explanation.
Dissert. Abstr.

N90-22496 Arizona Univ., Tucson.

THE MASS OF THE COMA CLUSTER Ph.D. Thesis

Lih-Sin The 1989 103 p

Avail: Univ. Microfilms Order No. DA9000149

The dynamical mass determination of galaxies and systems of galaxies shows a large excess of mass above what is directly observed. This excess of mass indicates the presence of dark matter. The nature of this dark matter is still unknown and dark matter in the outer regions of large stellar structures such as clusters of galaxies might provide enough matter to close the universe. The mass distribution of the Coma cluster is investigated. It is shown that optical data alone are unable to distinguish between a wide range of possible mass distribution for the Coma cluster. Low-mass models must have larger density than high-mass models and require that the galaxies move on near-circular orbits, whereas high-mass models require the galaxy orbits to be predominantly radial. The optical data constrain the amount of dark matter very poorly. The x ray data can also be used for a mass determination of the Coma cluster. These data may require the mass of the cluster to be more concentrated to the core than a light-traces-mass model if the central temperature of the gas is high. The above analysis, and most other approaches, assume the existence of dark matter. An alternative approach was proposed by Milgrom (1983a,b,c): the Newtonian law of motion breaks down in a weak field, and must be modified. The present analysis shows that this model is also consistent with optical and x ray data on the Coma cluster, although a good fit required values for Milgrom's universal parameter a(sub o) to be 2h(sup 1.5) (H sub o) = 50 h km/s/Mpc) higher than those inferred from the rotation curves of spiral galaxies. Finally, whether the model of an expanding cluster dominated by a massive binary galaxy is consistent with optical data on the surface density and velocity dispersion of the Coma cluster is investigated. The evolution of the model is simulated for a wide variety of initial conditions. This model is not a viable representation of the Coma cluster. Dissert. Abstr.

N90-22497 Washington Univ., Seattle.

THE ASSOCIATION OF SUPERNOVAE WITH REGIONS OF RECENT STAR FORMATION IN LATE-TYPE GALAXIES Ph.D. Thesis

Schuyler Dana VanDyk 1989 311 p

Avail: Univ. Microfilms Order No. DA9000328

The association of supernovae of the four major types (Ia, Ib, II, and II pec) with regions of the recent star formation in their parent late-type galaxies is established. The purpose is to place constraints on quantitative analysis of both photographic and CCD H alpha images of the galaxies. The CCD images of several parent galaxies were especially obtained. The geometries of detected giant H II regions on these images near the supernovae sites are determined and compared to the H II region-supernova separation, in order to establish physical association. The specific problems of supernova classification and positional uncertainties, as well as the probability of chance super-position, are considered in this work. In addition, calibrated surface brightness profiles and integrated physical properties are presented for the associated H II regions. For the supernova sites imaged with CCDs, broad-band B images were also obtained, in order to map the distribution of blue stellar populations in the supernovae environments. The results of this study are: from the lack of association with H II regions or bright OB associations, Type Ia supernovae are not likely to be associated with a young massive population, with mass M is greater than or = to 8 solar masses (which supports the currently popular model of an evolved binary system involving critical mass transfer on a white dwarf); Type Ib, II and II pec supernovae, however, are very likely to be associated with massive stellar populations, as theoretically expected; and, the very massive Wolf-Rayet star progenitor model for Type Ib supernovae is not strongly supported. Dissert. Abstr.

N90-22498 California Inst. of Tech., Pasadena.

THE Al-26(RHO, GAMMA)SI-27 REACTION: STELLAR ORIGINS OF GALACTIC Al-26 Ph.D. Thesis

Robert Bruce Vogelaar 1989 163 p

Avail: Univ. Microfilms Order No. DA9000608

To explain the Mg-26 isotopic anomaly seen in meteorites (Al-26 daughter) as well as the observation of 1809-keV gamma rays in the interstellar medium (live decay of Al-26) one must know, among other things the destruction rate of Al-26. Properties of states in Si-27 just above the Al-27 + p mass were investigated to determine the destruction rate of Al-26 via the Al-26(rho, gamma)Si-27 reaction at astrophysical temperatures. Twenty micrograms of Al-26 were used to produce two types of Al2O3 targets by evaporation of the oxide. One was onto a thick platinum backing suitable for (rho, gamma) work, and the other onto a thin carbon foil for the (He-3, d) reaction. The Al-26(rho, gamma)Si-27 excitation function, obtained using a germanium detector and voltage-ramped target, confirmed known resonances and revealed new ones at 770, 847, 876, 917, and 928 keV. Possible resonances below the lowest observed on at E(sub p) = 286 keV were investigated using the Al-26(He-3, d)Si-27 proton-transfer reaction. States in Si-27 corresponding to 196 and 286 keV proton resonances were observed. A possible resonance at 130 keV (postulated in prior work) was shown to have a strength of omega gamma is less than 0.02 microe V. By arranging four large NaI detector as a 4 pi calorimeter, the 196-keV proton resonance, and one at 247 keV, were observed directly, having omega gamma = 55 + or - 9 and 10 + or - 5 microe V respectively. Large uncertainties in the reaction rate have been reduced. At novae temperatures, the rate is about 100 times faster than that used in recent model calculations, casting some doubt on novae production of galactic Al-26. Dissert. Abstr.

N90-22499 California Univ., Berkeley.
THE RATIO OF NEUTRAL HYDROGEN TO NEUTRAL HELIUM IN THE LOCAL INTERSTELLAR MEDIUM Ph.D. Thesis
James Carswell Green 1989 129 p
Avail: Univ. Microfilms Order No. DA9006336

The results are described from a sounding rocket borne EUV spectrometer that was designed and built. This instrument operated from 400 to 1150A with a spectral resolution of approx. 15A. The instrument effective area was about 1 sq cm. The instrument was successfully launched, and observed the nearby DA white dwarf G191-B2B. From this observation, it was determined that the stellar effective temperature is 61,000 + or -4000 to 6000K, and the ratio of helium to hydrogen in the stellar photosphere is 1.0 + or -0.68 to 2.2 x 10(exp -4). Additionally, the neutral column densities of helium and hydrogen were measured to the star. The neutral helium column density was determined from the first observation of the interstellar absorption edge at 504A. The ratio of neutral helium to neutral hydrogen constrains the mean ionization of the warm gas along the line of sight to G191-B2B. The fractional ionization of hydrogen (H II/H) is approx. less than 20 percent, unless significant helium ionization is present as well. The scenario where the fractional ionization of hydrogen is high (H II/H) approx. less than 40 percent and the helium is neutral is ruled out with 99 percent certainty. This result is consistent with some recent theoretical calculations. Using these results, a self-consistent model of the local interstellar medium along the line of sight to G191-B2B is developed. In addition, an unexpected emission feature at 584A was detected in this observation with a high level of significance. Possible sources of this emission are examined, including the companion K dwarf G191-B2A, and an emission nebula near or around G191-B2B. Dissert. Abstr.

N90-22500 Texas Univ., Austin.
MODELLING LATE-TIME ATMOSPHERES OF SUPERNOVAE Ph.D. Thesis
Douglas Alexander Swartz 1989 294 p
Avail: Univ. Microfilms Order No. DA9005676

Supernovae result from the explosion of stars. The majority of the knowledge of these objects comes from analysis of their spectra. The most useful approach in the analysis is to construct model atmospheres. A theoretical spectrum derived from a model atmosphere can be compared to observation and the proper physical description deduced. A computational method for solving the supernova model atmosphere problem applicable at late times is developed and applied. A complete physical description of supernovae in the late-time stage of evolution is presented. The radiation field is shown to be transparent in the continuum but optically thick in allowed line transitions. These properties, and the fact that the atmosphere is in a state of rapid and differential expansion, permit the transfer equations to be solved using the Sobolev approximation. A new technique is developed to solve the resulting coupled radiative transfer and statistical equilibrium equations. The first comprehensive comparison of theoretical and observed spectra of a hydrogen-rich supernova, namely SN 1987A, is presented. The best fitting models are obtained when the radioactive Co-56 is distributed throughout a large fraction of the atmosphere and when the remaining composition retains its original stratification. Applications are also made to analytic and semi-analytic models to establish a groundwork for understanding the response of the resulting spectrum to variations in input model parameters. The numerical methods presented provide a reasonably complete description of supernovae. The methods can constrain the composition, radioactive cobalt distribution, and density structure of these objects. Dissert. Abstr.

N90-22501# Instituto de Pesquisas Espaciais, Sao Jose dos Campos (Brazil).
UD FILTERING AND SMOOTHING APPLIED TO ORBIT DETERMINATION
Helio Koiti Kuga, Atair Rios-Neto, and Valcir Orlando Aug. 1989 18 p Presented at the International Symposium on Space Dynamics, Toulouse, France, 6-10 Nov. 1989
(INPE-4966-PRE/1535) Avail: NTIS HC A03/MF A01

The performance is described of filtering and smoothing techniques applied to orbit determination of earth satellites. A (forward pass) Kalman filter along with an adaptive procedure for estimating the dynamic noise level which prevents the divergence of estimates due to inaccurate modelling of the orbital motion is implemented in the UD factorization form. The backward smoother is a numerically efficient version of the Rauch-Tung-Striebel (RTS) smoother. This smoother, developed in the UD form, has proven to be economical, compact and competitive for computer implementation. Digital simulations are performed for 2 situations of orbit determination: short arc orbit determination with favorably tracking geometry; and long arc orbit determination with existing tracking stations. Tests containing many levels of modelling degradation are carried out. The forward pass adaptive UD filter behaves so as to deal with these modelling nuisances and does not allow the divergence phenomenon to occur. In no real time operations, the backward UD smoother is used to improve the accuracy of the estimates and of the covariances resulting from the filtering phase. The results show, in the main, that the UD smoother can enhance the accuracy of the forward pass filter, sometimes by an order of magnitude. For post-flight analysis, the UD smoother is a useful tool when one aims at reconstituting the entire trajectory of the orbital motion covered by the tracking data. Author

N90-22502*# Osservatorio Astronomico, Rome (Italy).
STABILITY OF COMPACTIFICATION DURING INFLATION
Luca Amendola, Edward W. Kolb (Fermi National Accelerator Lab., Batavia, IL.), Marco Littero, and Franco Occhionero Mar. 1990 22 p
(Grant NAGw-1340)
(NASA-CR-186597; NAS 1.26:186597; FERMILAB-Pub-90/47-A)
Avail: NTIS HC A03/MF A01 CSCL 03B

The possibility that inflation may trigger an instability in compactification of extra spatial dimensions is considered. In old, new, or extended inflation, the false vacuum energy results in a semiclassical instability in which the scalar field representing the radius of the extra dimensions may tunnel through a potential barrier leading to an expansion of the internal space. In chaotic inflation, if the initial value of the scalar field responsible for inflation is large enough, the internal space becomes classically unstable to ever increasing expansion. Restrictions on inflationary models necessary to keep the extra dimensions small are discussed. Author

N90-22503*# Chicago Univ., IL. Astronomy and Astrophysics Center.
GRAVITATIONAL EFFECTS OF GLOBAL TEXTURES
Dirk Noetzold Mar. 1990 10 p Prepared in cooperation with Fermi National Accelerator Lab., Batavia, IL
(Grant NAGw-1340)
(NASA-CR-186596; NAS 1.26:186596; FERMILAB-Pub-90/64-A)
Avail: NTIS HC A02/MF A01 CSCL 03B

A solution for the dynamics of global textures is obtained. Their gravitational field during the collapse and the subsequent evolution is found to be given solely by a space-time dependent deficit solid angle. The frequency shift of photons traversing this gravitational field is calculated. The space-time dependent texture metric locally contracts the volume of three-space and thereby induces overdensities in homogeneous matter distributions. There are no gravitational forces unless matter has a nonzero angular momentum with respect to the texture origin which would be the case for moving textures. Author

N90-22504*# Carnegie-Mellon Univ., Pittsburgh, PA. Dept. of Physics.
GRAVITATIONAL COUPLINGS OF THE INFLATION IN EXTENDED INFLATION
Richard Holman, Edward W. Kolb, and Yun Wang (Chicago Univ., IL.) Feb. 1990 10 p
(Grant NAGw-1340)
(NASA-CR-186595; NAS 1.26:186595; FERMILAB-Pub-90/44-A; CMU-HEP90-03) Avail: NTIS HC A02/MF A01 CSCL 03B

A new extended inflationary scenario evading the difficulties of the original model is discussed. The model can thermalize the energy in the bubble walls by the necessary epoch, and establish a Robertson-Walker frame in the bubble clusters. The essential new ingredient in the model is the observation that the coupling of inflation to the Jordan-Brans-Dicke field is expected to be different from that of visible matter. Author

N90-22505*# Sussex Univ., Brighton (England). Dept. of Physics.
TOPOLOGICAL DEFECTS IN EXTENDED INFLATION
Edmund J. Copeland, Edward W. Kolb (Fermi National Accelerator Lab., Batavia, IL.), and Andrew R. Liddle Apr. 1990 11 p
(Grant NAGw-1340)
(NASA-CR-186594; NAS 1.26:186594; SUSSEX-AST-90/4-1; FNAL-Pub-90/56-A) Avail: NTIS HC A03/MF A01 CSCL 03B

The production of topological defects, especially cosmic strings, in extended inflation models was considered. In extended inflation, the Universe passes through a first-order phase transition via bubble percolation, which naturally allows defects to form at the end of inflation. The correlation length, which determines the number density of the defects, is related to the mean size of bubbles when they collide. This mechanism allows a natural combination of inflation and large scale structure via cosmic strings. Author

N90-22506*# Waseda Univ., Tokyo (Japan). Dept. of Physics.
SOFT INFLATION
Andrew L. Berkin, Kei-Ichi Maeda, and Junichi Yokoyama (Tokyo Univ., Japan) Apr. 1990 12 p
(Grant NAGw-1340)
(NASA-CR-186593; NAS 1.26:186593; WU-AP/07/90; UTAP-107/90; FERMILAB-Pub-90/52-A) Avail: NTIS HC A03/MF A01 CSCL 03B

The cosmology resulting from two coupled scalar fields was studied, one which is either a new inflation or chaotic type inflation, and the other which has an exponentially decaying potential. Such a potential may appear in the conformally transformed frame of generalized Einstein theories like the Jordan-Brans-Dicke theory. The constraints necessary for successful inflation are examined. Conventional GUT models such as SU(5) were found to be compatible with new inflation, while restrictions on the self-coupling constant are significantly loosened for chaotic inflation. Author

N90-22507# Academy of Sciences of the Ukrainian SSR, Kharkov. Inst. of Radio Astronomy.
WIND INSTABILITY AS A POSSIBLE CAUSE OF THE SPIRAL STRUCTURE FORMATION IN THE GASEOUS SUBSYSTEM OF GALAXIES WITH THE CIRCULAR MAGNETIC FIELD
S. G. Gestrin 1988 19 p In RUSSIAN; ENGLISH summary
(DE90-618944; INIS-SU-155) Avail: NTIS (US Sales Only) HC A03/MF A01

The wind instability as the possible cause of the spiral structure in the gaseous subsystems of galaxies with the circular magnetic field is examined. It is shown that in the presence of a sufficiently strong circular magnetic field typical for some galaxies, a very weak peculiarity on the rotation curve which is provided for the existence of the localized surface mode is required for the development of the wind instability. This peculiarity is the jump of the second derivative from the angular velocity. It is necessary also that magnetic fields grow or fall down slower than 1/r with the distance from the galactic center. In this case the spiral structure arises with the number of arms being defined by the ratio between the rotation velocity near the pecularity and the Alfven speed in the disc. DOE

N90-22508 Princeton Univ., NJ.
A GALAXY FORMATION COOKBOOK: RECIPES AND UTENSILS Ph.D. Thesis
Neal Steven Katz 1989 298 p
Avail: Univ. Microfilms Order No. DA9008355

Numerical simulations of hierarchial galaxy formation including gas dynamics are presented. These simulations are conducted using a general-purpose program for evolving self-gravitating systems in three dimensions. The gravitational forces are calculated using a hierarchial tree algorithm while the gas dynamic properties are determined using smoothed particle hydrodynamics. Since in this method the complete thermodynamic state of the gas is known everywhere, dissipational effects can be included by allowing the gas to cool radiatively, using standard cooling curves, and star formation can be prescribed in a physical manner. The simulations model the collapse of isolated constant density perturbations, made of dark and baryonic matter in a 10 to 1 ratio, initially in solid rotation and in Hubble flow. Small scale power is added using the Zel'dovich approximation assuming a power law slope of either -2.5 or 0. The simulations are successful in making systems that resemble spirals and ellipticals. Of the parameters that are investigated - the small scale power amplitude, the initial angular momentum, and the star formation rate - it is the amplitude of the small scale power that is most important in determining the final Hubble type. Systems form through the merger of sub-clumps. The systems with larger small scale power have clumps with higher central densities. Higher density clumps retain their identities longer than lower density clumps and are able to lose more angular momentum. These systems form ellipticals. Spirals form when these clumps are not very distinct and little angular momentum transport occurs. Since the Hubble type is determined by how much small scale power is present when compared to the height of the galaxy-sized peak, the density-morphology relation is easily explained. The formation and equilibrium characteristics of systems formed through dissipationless collapse using similar initial conditions are also studied. Dissert. Abstr.

N90-22509 California Inst. of Tech., Pasadena.
MULTIPOLE MOMENTS IN GENERAL RELATIVITY AND DYNAMICAL PERTURBATIONS OF BLACK-HOLE MAGNETOSPHERES Ph.D. Thesis
Xiao-He Zhang 1990 197 p
Avail: Univ. Microfilms Order No. DA9009395

In part 1 the generic, vacuum, dynamical gravitational field of the exterior universe in the vicinity of a freely moving body is expanded in positive powers of the distance r away from the body's spatial origin. The expansion coefficients, called external multipole movements, are defined covariantly in terms of the body's central world line. The expansion is used to derive higher-order corrections to previously known laws of motion and precession for black holes and other bodies. In part 2, the interaction of magnetohydrodynamic (MHD) waves in a black-hole magnetosphere with the 'dragging of inertial frames' effect of the hole's rotation is studied. The laws of perfect general relativistic magnetohydrodynamics (GRMHD) are rewritten in 3 + 1 language in a general spacetime, and the GRMHD equations are reduced to a set of algebraic equations for stationary spacetimes and MHD flows with one arbitrary spatial symmetry. Then in a model spacetime with two spatial symmetries, which captures the key features of the Kerr geometry, the Fourier-analyzed GRMHD equations are derived which govern weak, linearized perturbations of a stationary magnetosphere with outflowing jet. These equations are subsequently solved numerically. It is found that when an oscillatory external force is applied to the region of the magnetosphere where plasma (e+ e-) is being created, the magnetosphere responds especially strongly at a particular, resonant, driving frequency. The magnetosphere of a rotating black hole, when perturbed by nonaxisymmetric magnetic fields, might exhibit an analogous resonance. If so then the hole's outflowing jet might be modulated at resonant frequencies omega is approx. = (m/2)Omega(sub H) where m is an integer and Omega(sub H) is the hole's angular velocity. Dissert. Abstr.

N90-22510*# Smithsonian Astrophysical Observatory, Cambridge, MA.
AN ASTROPHYSICS DATA PROGRAM INVESTIGATION OF CLUSTER EVOLUTION Semiannual Report No. 1, 1 Aug. 1989 - 31 Jan. 1990
Edwin M. Kellogg Jun. 1990 25 p
(Grant NAG5-1200)
(NASA-CR-181296; NAS 1.26:181296) Avail: NTIS HC A03/MF A01 CSCL 03B

A preliminary status report is given on studies using the Einstein x ray observations of distant clusters of galaxies that are also candidates for gravitational lenses. The studies will determine the location and surface brightness distribution of the x ray emission from clusters associated with selected gravitational lenses. The x ray emission comes from hot gas that traces out the total gravitational potential in the cluster, so its distribution is approximately the same as the mass distribution causing gravitational lensing. Core radii and x ray virial masses can be computed for several of the brighter Einstein sources, and preliminary results are presented on A2218. Preliminary status is also reported on a study of the optical data from 0024+16. A provisional value of 1800 to 2200 km/s for the equivalent velocity dispersion is obtained. The ultimate objective is to extract the mass of the gravitational lens, and perhaps more detailed information on the distribution of matter as warranted. A survey of the Einstein archive shows that the clusters A520, A1704, 3C295, A2397, A1722, SC5029-247, A3186 and A370 have enough x ray counts observed to warrant more detailed optical observations of arcs for comparison. Mass estimates for these clusters can therefore be obtained from three independent sources: the length scale (core radius) that characterizes the density dropoff of the x ray emitting hot gas away from its center, the velocity dispersion of the galaxies moving in the cluster potential, and gravitational bending of light by the total cluster mass. This study will allow the comparison of these three techniques and ultimately improve the knowledge of cluster masses. Author

91 LUNAR AND PLANETARY EXPLORATION

Includes planetology; and manned and unmanned flights.
For spacecraft design or space stations see *18 Spacecraft Design, Testing and Performance.*

N90-22511 Stanford Univ., CA.
WAVES IN SATURN'S RINGS PROBED BY RADIO OCCULTATION Ph.D. Thesis
Paul Alan Rosen 1989 324 p
Avail: Univ. Microfilms Order No. DA8912933

Thirty wave features, observed in 3.6 and 13 cm-wavelength optical depth profiles of Saturn's rings obtained by Voyager 1 radio occultation, are analyzed individually and comparatively. A new technique for locating waveform extrema, which fits a sinusoid to each half cycle of wave data, quantifies the wavelength variation across a feature. Fitting dispersion models to the derived wavelengths provides new estimates of ambient surface mass density sigma in each wave region. For 14 weak density waves in Ring A, modelling of the waveform near resonance with linear density wave theory gives independent estimates of sigma, as well as reliable estimates of resonance location. Measurements of wave amplitude damping give an upper bound for ring thickness 2H, where H is the ring scale height. Mass loading estimates from waveform modelling are 20 to 40 percent larger than dispersion-derived values, suggesting accumulation of mass in the wave regions. The average offset of derived wave location from theoretical resonance is about 1 km. In Ring C, dispersion analysis indicates that the most prominent wave feature, previously unidentified, is a one-armed spiral wave at Titan's -1:0 nodal inner vertical resonance, the first wave of this kind identified in nature. Eight other wave features in Ring C remain unexplained. The locations of all identified Ring C resonances stronger than the Mimas 4:1 inner Lindblad resonance (ILR) coincide with gap-ringlet features. If these features are created by the resonances, the required deficit of viscous torque relative to satellite torque limits the ring thickness to 2H less than or approximately equal to 1 m. From wave damping lengths in Ring C, 2H less than or approximately equal to 5 m at least locally. Dissert. Abstr.

N90-22512 Georgia Inst. of Tech., Atlanta.
A THEORETICAL INVESTIGATION OF GRAVITY-WAVE-GENERATED STRESS AND VORTICITY IN THE PLANETARY BOUNDARY LAYER Ph.D. Thesis
Carmen Joseph Nappo 1989 229 p
Avail: Univ. Microfilms Order No. DA8925460

Vertically propagating gravity waves are generated whenever a stable atmospheric flows passes over a terrain obstacle of sufficiently large horizontal size. These waves act to propagate mean-flow horizontal momentum to the ground surface. This downward flux of momentum represents a Reynolds stress, but this stress can only act on the atmosphere if the gravity waves are absorbed by the mean flow. Wave absorption will occur near a critical level where the phase speed of the wave equals the component of the background flow parallel to the wave vector. For the case of terrain-generated waves, critical levels will exist where the component of the background flow directed over the obstacle reverses its direction. Within the Planetary Boundary Layer (PBL) over regions of complex terrain, wind reversals frequently occur. Thus it is expected that wave stresses will have an effect on the PBL dynamics. However, conventional PBL theory does not account for gravity-wave stress, and so it is important to evaluate the magnitude of the wave stress relative to the friction stress. Using simple linear theory, the wave stresses and wave drags over two-dimensional and three-dimensional hills were evaluated for typical stable PBL conditions. Dissert. Abstr.

N90-22513 Brown Univ., Providence, RI.
GEOLOGY OF CORONAE AND DOMAL STRUCTURES ON VENUS AND MODELS OF THEIR ORIGIN Ph.D. Thesis
Ellen Renee Stofan 1989 260 p
Avail: Univ. Microfilms Order No. DA9002303

Coronae (160 to 670 km across) and domal structures (greater than 1000 km across) are complex topographic highs on Venus that were affected by volcanic and topographic processes. The geology of coronae and a major domal structure, Beta Regio, are documented using Pioneer Venus, Arecibo, and Venera 15/16 data. The evolution and possible models of origin of these features are also investigated. Beta Regio is a 2000 x 2300 km topographic high located in the equatorial region of Venus that rises over 5 km above the surrounding region. Within Beta Regio lie two large volcanic shields, Theia and Rhea Mons. Coronae are circular to elongate structures on Venus, characterized by an annulus of concentric compressional ridges and relatively raised topography surrounded by a peripheral trough. Volcanic domes, flows and edifices, as well as tectonic lineaments characterize the interiors of coronae. Thirty one coronae were detected on Venus. Two analytical models were developed that are consistent with the general characteristics and evolution of coronae: hotspot or rising mantle diapir model and sinking mantle diapir model. Coronae appear to be part of a continuum of thermally produced features on Venus, along with volcanic complexes and domal structures such as Beta Regio. Dissert. Abstr.

N90-22514 California Inst. of Tech., Pasadena.
QUANTITATIVE STUDIES OF THE MARTIAN SOUTH POLAR REGION USING SPACECRAFT IMAGES Ph.D. Thesis
Kenneth Edward Herkenhoff 1989 297 p
Avail: Univ. Microfilms Order No. DA9000568

Mariner 9 images were processed for comparison with nearly simultaneous infrared spectra of the south polar cap of Mars. Combined analysis of these observations indicate that the southern residual cap was covered by carbon dioxide frost throughout the summer of 1971 to 1972. Five color/albedo units were recognized and mapped in the southern layered deposits on Mars. Shadow brightness were measured and modeled in order to correct for the effects of atmospheric scattering and quantify the albedo and color of the surface. The layered deposits appear to be mantled by red dust except where eolian stripping has exposed the darker, less red underlying bedrock. Frost and bare ground are mixed below the resolution of the images in many areas, some of which appear to be younger than the surrounding layered terrain. Maximum slopes of 10 to 20 degrees occur on an exposure of layered deposits within the south polar residual cap of Mars. A new photoclinometric technique is used to produce profiles of slope and albedo using high resolution Mariner 9 images. Stereophotogrammetry is also used to constrain the photoclinometric solutions, which resolve layer thicknesses of 100 to 300 meters. Albedo variations are correlated with slope, indicating that frost is present on level areas. Weathering of the layered deposits by sublimation of water ice can account for the data presented and previous observations of the north polar deposits. The non-volatile component of the layered deposits appears to consist mainly of bright red dust, with small amounts of dark dust or sand. Dark dust, perhaps similar to the magnetic material found at the Viking Lander sites, may preferentially form filamentary residue particles upon weathering of the deposits. Once eroded, these particles may saltate to form the dark dunes found in both polar regions. Eventual destruction of the particles could allow recycling of the dark dust into the layered deposits via atmospheric suspension. Dissert. Abstr.

N90-22515 Lancaster Univ. (England).
SULPHUR SILICATE INTERACTIONS ON THE JOVIAN SATELLITE Io Ph.D. Thesis
Ashley Gerard Davies 1988 466 p
Avail: Univ. Microfilms Order No. BRDX87340

Io, which has the highest level of volcanic activity of any planet in the Solar System, has an upper crust rich in sulphur compounds and a silicate interior. A model is developed in which volatiles for the large Pele-type plumes are mobilized by the interaction between intrusive silicate magma bodies and the sulphur-rich crust. Heat transfer during such an interaction is strongly dependent on the ability of a molten sulphur layer above an intrusion to remove heat by convection. The controlling factors on the amount of sulphur mobilized are the sill surface temperature and the temperature of the host material into which the sill in intruded; the deeper the intrusion depth, the greater amount of sulphur mobilized. For any depth of intrusion, the maximum amount of sulphur that can be mobilized and the rate of production of molten sulphur are calculated. The volumes of sulphur produced in this way are shown to be sufficient to supply Pele-type plumes at their calculated mass eruption rates for their eruptive lifetimes, and the Pele-type plumes are shown to be an efficient means of removing heat from the interior of Io. Extrusive silicate activity through a sulphur layer can also take place. Existing models of the ascent and eruption of basaltic magma are applied to terrestrial eruptions and modified for Ionian planetary conditions. Film footage of phase 23 of the Pu'u 'O'o eruption of Kilauea, Hawaii, is analyzed to determine velocities in a fire fountain, and using a model of the eruption of basalt, the magma volatile content and the pressure and flow velocity in the vent are determined. Such sulphur-silicate interactions can explain some of the features on the surface of Io. A photoclinometric model is developed and used to determine the topography of two volcanic calderas. It is postulated that one of these calderas is the result of a Pele-type plume eruption. Dissert. Abstr.

N90-22516# Oak Ridge National Lab., TN. Chemical Technology and Health Div.
THE ROLE OF AUTOMATION AND ROBOTICS IN THE LUNAR-BASED CHEMICAL ANALYSIS LABORATORY
Carl A. Burtis 1989 9 p Presented at the 9th College Park Colloquium: A Lunar-based Chemical Analysis Laboratory, College Park, 30-31 Oct. 1989
(Contract DE-AC05-84OR-21400)
(DE90-009401; CONF-8910387-1) Avail: NTIS HC A02/MF A01

The Lunar-Based Chemical Analysis Laboratory (LBCAL) will be required to provide a wide range of analytical services in an environment of limited physical and human resources. In order to provide these services, it will have to rely on and utilize automated equipment. A wide array of automated analytical equipment is currently available and will have to be evaluated for its suitability for operation in the reduced-gravity conditions of a lunar base. In some cases, specific (e.g., the Medical Demonstration Unit) or core equipment (e.g., centrifugal analyzer) will have to be developed or existing systems modified. In addition, heavy reliance on robotics, both preprogrammed and remotely controlled via a telecommunications linkage (e.g., telerobotics), will be required to compensate for the limited human resources that will be experienced at the lunar base. DOE

N90-22517# Academy of Sciences of the Ukrainian SSR, Kharkov. Inst. of Radio Astronomy.
JUPITER'S DRIFTING DECAMETRIC BURSTS WITH THE CHANGING TIME SCALE
N. N. Gerasimova 1988 21 p In RUSSIAN; ENGLISH summary
(DE90-618870; INIS-SU-156) Avail: NTIS (US Sales Only) HC A03/MF A01

The drifting burst class with the changing time scale for each event is selected from the observational data of the Jovian decametric emission obtained with the radiotelescope UTR-2. The burst duration at fixed frequency changes from few seconds (or fractions of a second) at frequencies $f = 10$ to 12 MHz to less than 0.02 s (the time constant of the registration) at frequencies $f = 12$ to 17 MHz. The model in which electron beams streaming from the planet generate plasma neutral oscillations at the frequency around the electron gyrofrequency is proposed. Presence of the regular and irregular inhomogeneities of the magnetic field and density could provide both hydrodynamic and kinetic character of the instability during the individual event. This fact leads to the sharp change of the time scales in the limits of one event. DOE

N90-22518 Colorado Univ., Boulder.
AURORAL ULTRAVIOLET DARKENING ON THE OUTER PLANETS Ph.D. Thesis
Wayne Robert Pryor 1989 220 p
Avail: Univ. Microfilms Order No. DA9009177

The Voyager 2 Photopolarimeter Subsystem (PPS) has made photometric observations of Jupiter at 2400 A and photometric and polarimetric observations of Saturn and Uranus at 2650 A. At these wavelengths the instrument is observing each planet's stratosphere and upper troposphere. The most striking features are that both poles of Jupiter and the observed northern pole of Saturn are very dark, while Uranus has a uniformly bright appearance. All three planets show evidence for a stratospheric haze. Simple vertically homogeneous multiple scattering models are used to characterize these stratospheric hazes. Emphasis is placed on establishing their latitudinal distribution. Auroras occur at high latitudes on Jupiter and Saturn and at low latitudes on Uranus. The asymmetric polar darkening on Jupiter seen by PPS is roughly matched by the asymmetry in the auroral zones. Historical data suggest that the haze asymmetry is persistent. The dark north polar cap seen by PPS at Saturn is small and close to the pole, which corresponds to the small auroral zone close to the pole. A model is examined which attributes the darkening to auroral bombardment initiating methane chemistry that makes dark hydrocarbon particles. Possible chemical pathways are discussed, and mass balance calculations are presented for Jupiter, Saturn, and Uranus. The model is quantitatively plausible for Jupiter and Saturn. The lack of localized darkening on Uranus can be explained in this model by noting that weak vertical mixing and methane condensation near the 1-bar level lead to negligible methane

abundances at auroral altitudes. The auroras must reach the methane for dark material to form. The thin haze that is seen on Uranus is ascribed to photochemical processes. Voyager 2 will reach Neptune this year. Ground-based observers have reported vigorous vertical mixing and large amounts of stratospheric methane there. If there is an aurora reaching this stratospheric methane, the model predicts that a dark zone will be seen there.
Dissert. Abstr.

92 SOLAR PHYSICS

Includes solar activity, solar flares, solar radiation and sunspots.

For related information see *93 Space Radiation.*

N90-22519 Arizona Univ., Tucson.
THE OBSERVED PROPERTIES OF THE INTERMEDIATE-DEGREE GRAVITY MODES AND THEIR RELEVANCE TO THE SOLAR NEUTRINO PARADOX Ph.D. Thesis
Gregory Francis Rabaey 1989 129 p
Avail: Univ. Microfilms Order No. DA8919052

Intermediate-degree g-modes (those with angular order (l) is approximately equal to 30) were first observed in the late 1970s. However, it wasn't until 1986 that a preliminary survey was made of the 1979 differential radius observations and a set of four multiplets exhibiting mode-locking was classified. These multiplets with angular order (l) is approximately equal to 30 and the eigenfrequencies of approximately 350 microHz were used as a starting point for the cumulative analysis discussed. This comprehensive study culminated in the classification of a set of 20 intermediate-degree g-mode multiplets containing over 600 normal modes of oscillation. Two significant consequences will be discussed. Because these modes of oscillation are localized within the inner 50 percent of the Sun by radius and because of their large temperature eigenfunctions implied by the observed phase-locking, these modes of oscillation provide a modification of the effective temperature profile defined for a given process in the Sun. One of these processes is the observed 8-B neutrino production. The second consequence of these observations is a predicted periodic modulation of the neutrino production rates. The existence of a large set of mode-coupled gravity modes will lead to a low-frequency modulation of neutrino production rates which may account for the observed periodicity in the 8-B neutrino production. The prediction of this periodicity in the neutrino production rates is unique among all the competing theories that resolve the solar neutrino paradox and is testable by the new generation of solar neutrino detectors. Dissert. Abstr.

N90-22520# National Geophysical Data Center, Boulder, CO.
SOLAR-GEOPHYSICAL DATA NUMBER 542, OCTOBER 1989. PART 1: (PROMPT REPORTS). DATA FOR SEPTEMBER, AUGUST 1989, AND LATE DATA
Helen E. Coffey, ed. Oct. 1989 177 p
(PB90-148669; SGD-542-Pt-1; ISSN-0038-0911; LC-79-640375)
Avail: NTIS HC A09/MF A01 CSCL 03B

Some areas of discussion are: Detailed index for 1989; Data for September 1989 - Solar-terrestrial environment, IUWDS alert periods (advance and worldwide), Solar activity indices, Solar flares, Solar radio emission, Stanford mean solar magnetic field; Data for August 1989 - Solar active regions, Sudden ionospheric disturbances, Solar radio spectral observations, Cosmic ray measurements by neutron monitor, Geomagnetic indices; Late Data - Cosmic ray measurements by neutron monitor Huancayo June 1989, inferred interplanetary magnetic field 1984 to 1988, Geomagnetic activity indices July 1989. GRA

N90-22521# National Geophysical Data Center, Boulder, CO.
SOLAR-GEOPHYSICAL DATA NUMBER 542, OCTOBER 1989. PART 2: (COMPREHENSIVE REPORTS). DATA FOR APRIL 1989 AND MISCELLANEOUS
Helen E. Coffey, ed. Oct. 1989 102 p
(PB90-148677; SGD-542-Pt-2; ISSN-0038-0911; LC-79-640375)
Avail: NTIS HC A06/MF A01 CSCL 03B

Some data presented are: Detailed index for 1989; Data for April 1989 - Solar flares, Solar radio bursts at fixed frequencies, interplanetary solar particles and plasma, Solar x ray radiation from GOES satellite, Mass ejections from the sun, Active prominences and filaments; Miscellaneous data - Meudon Carte Synoptique Carrington rotations 1811-1812, Solar ultraviolet radiation Nimbus 7 November 1978 to October 1984. GRA

N90-22522*# Texas Univ., Austin. Inst. for Fusion Studies.
SLOW SHOCKS IN CORONAL MASS EJECTIONS
R. S. Steinolfson [1989] 4 p Sponsored in part by NSF (Grant NAG5-761)
(NASA-CR-186578; NAS 1.26:186578) Avail: NTIS HC A01/MF A01 CSCL 03B

The possibility that slow-mode shock compression may produce at least some of the increased brightness observed at the leading edge of coronal mass ejections is investigated. Among the reasons given for the possible existence of slow shocks are the following: (1) transient velocities are often greater than the upstream sound speed but less than the Alfven speed, (2) the presence of a slow shock is consistent with the flat top observed in some transients, and (3) the lateral extension of slow shocks may be responsible for distributing adjacent structures as also seen on the observations. It is shown that there may be some difficulties with this suggestion for transients originating inside the closed-field region at the base of a preexisting coronal streamer. First of all, slow mode characteristics have difficulty emerging from the closed-field region at the streamer base so they can merge to form a slow shock, unless a preceding, large-amplitude disturbance opens the field lines. In addition, a slow shock cannot exist at the center of the streamer current sheet. Finally, numerical simulations demonstrate that at least the last two (and possibly all) of the above reasons for slow shocks can be satisfied by a disturbance whose leading edge propagates at the local fast-mode speed without any shocks. The leading portion of the transient that would be seen in white-light coronagraphs propagates at a speed either less than or equal to the fast-mode speed. Author

93 SPACE RADIATION

Includes cosmic radiation; and inner and outer earth's radiation belts.

For biological effects of radiation see *52 Aerospace Medicine*. For theory see *73 Nuclear and High-Energy Physics.*

N90-22523 California Univ., Berkeley.
EXTENDED OPTICAL EMISSION IN 3CR RADIO GALAXIES Ph.D. Thesis
Patrick Joseph McCarthy 1988 311 p
Avail: Univ. Microfilms Order No. DA8916787

The results of an investigation of the optical properties of radio galaxies drawn from the 3CR galaxies are combined with a survey spanning the entire redshift range of the catalog. The aim is to examine the emission line and optical continuum properties of powerful radio sources, their relation to the radio properties, and their evolution with cosmic time. The bulk of this work is concerned with the optical properties of high luminosity radio galaxies. A sample of 52 radio galaxies spanning the redshift range from 0.05 and 2.0 were observed. This gives an unprecedented opportunity to examine how the optical properties of radio galaxies, and their relations to the radio source properties, change over a range in cosmic time that is comparable to the Hubble time.
Dissert. Abstr.

N90-22524 Durham Univ. (England).
GAMMA RAYS, COSMIC RAYS, AND LOCAL MOLECULAR CLOUDS Ph.D. Thesis

Kenneth Michael Richardson 1988 113 p
Avail: Univ. Microfilms Order No. BRD-86636

An estimate of the CO-to-N(H2) conversion factor X was obtained using gamma ray data from local molecular clouds at medium latitudes. Evidence is found for the production of low-energy cosmic rays in the cloud environs which complicates the derivation of X, but an interpretation of the results that is consistent with extinction and optically thin molecular emission data is possible and suggests X is approximately (1-2) x 10(exp 20) mol/sq cm/(K/kms). Some variations in the cosmic ray intensity not associated with the clouds but in the same line-of-sight may be indicated by the gamma ray analysis. Differences between the value proposed by COS-B (X = 2.6 x 10(exp 20) in the Orion molecular cloud) and the present work are ascribed to their disregard for the production of cosmic rays in or around the clouds. Several models that might account for the cosmic ray excess are examined in detail. The most promising is that by Morfill (1982) in which electrons are convected into the cloud by Alfven waves generated by a few GeV protons. The Massachusetts-Stony Brook virial analysis of inner Galaxy giant molecular clouds is reappraised, leading to X is approximately less than 1 x 10(exp 20) after allowance was made for saturation broadening of the CO emission line. Dissert. Abstr.

N90-22525*# Chicago Univ., IL. Astronomy and Astrophysics Center.
ULTRAHIGH-ENERGY PARTICLE FLUX FROM COSMIC STRINGS
Pijushpani Bhattacharjee and N. C. Rana (Tata Inst. of Fundamental Research, Bombay, India) Apr. 1990 13 p
(Grant NAGw-1340)
(NASA-CR-186592; NAS 1.26:186592; FERMILAB-Pub-90/69-A)
Avail: NTIS HC A03/MF A01 CSCL 03B

The expected flux is estimated of ultrahigh energy (greater than 10(exp 18) eV) protons in the present epoch due to a process which involves collapse or multiple self-intersections of a special class of closed cosmic string loops in the universe. This flux is compared with the observed flux of ultrahigh energy cosmic rays, and the implications are discussed. Author

N90-22526*# National Aeronautics and Space Administration. Marshall Space Flight Center, Huntsville, AL.
GAMMA RAY BURSTS: CURRENT STATUS OF OBSERVATIONS AND THEORY
Charles A. Meegan Apr. 1990 23 p
(NASA-TM-100398; NAS 1.15:100398) Avail: NTIS HC A03/MF A01 CSCL 03B

Gamma ray bursts display a wide range of temporal and spectral characteristics, but typically last several seconds and emit most of their energy in a low energy, gamma ray region. The burst sources appear to be isotropically distributed on the sky. Several lines of evidence suggest magnetic neutron stars as sources for bursts. A variety of energy sources and emission mechanisms are proposed. Author

N90-22527 Arizona Univ., Tucson.
VERY HIGH ENERGY GAMMA RAYS FROM THE CRAB NEBULA AND PULSAR Ph.D. Thesis
Ping Wai Kwok 1989 195 p
Avail: Univ. Microfilms Order No. DA9010482

This project is to search for very high energy (VHE) (10(exp 11) to 10(exp 14)eV) gamma rays from the Crab nebula and pulsar using the atmospheric Cherenkov imaging technique. The technique uses an array of 37 photomultiplier tubes to record the images of the Cherenkov light pulses generated by energetic particles in the air showers initiated by VHE gamma rays or charged cosmic rays. Gamma ray like events are selected from numerous cosmic ray events based on the predicted properties of the image, such as the size, shape, and orientation with respect to the axis of the detector. A steady weak flux of VHE gamma rays from the Crab is detected at high statistical significance (9 sigma), which is not usually achieved in VHE gamma ray astronomy. No strong evidence of pulsed emission is found when the same data is folded at the Crab pulsar's radio ephemeris. The angular resolution of the technique cannot separate the emission coming from the nebula from that from the pulsar. Although it is generally believed that the unpulsed emission is coming from the nebula, there may be an unpulsed component coming at only a couple of light cylinder radii away from the pulsar too. Using the outer gap model of pulsar, the spectrum is derived and is found to be compatible with the observations. Dissert. Abstr.

99 GENERAL

N90-22528*# National Aeronautics and Space Administration, Washington, DC.
RESEARCH AND TECHNOLOGY OBJECTIVES AND PLANS SUMMARY (RTOPS) Research and Technology Program, FY 1988
Jan. 1988 200 p
(NASA-TM-89662; NAS 1.15:89662) Avail: NTIS HC A09/MF A02 CSCL 05A

This publication represents the NASA research and technology program for FY88. It is a compilation of the Summary portions of each of the RTOPs (Research and Technology Objectives and Plans) used for management review and control of research currently in progress throughout NASA. The RTOP Summary is designed to facilitate communication and coordination among concerned technical personnel in government, in industry, and in universities. The first section containing citations and abstracts of the RTOPs is followed by four indexes: Subject, Technical Monitor, Responsible NASA Organization, and RTOP Number. Author

N90-22529*# National Aeronautics and Space Administration, Washington, DC.
NASA INFORMATION SCIENCES AND HUMAN FACTORS PROGRAM Annual Report, 1989
Lee Holcomb, Ray Hood, Melvin Montemerlo, James Jenkins, Paul Smith, John DiBattista, Ramon DePaula, and Paul Hunter 1990 270 p
(NASA-TM-4190; NAS 1.15:4190) Avail: NTIS HC A12/MF A02 CSCL 05H

Fiscal year 1989 descriptions of technical accomplishments in seven sections are presented: automation and robotics; communications; computer sciences; controls and guidance; data systems; human factors; and sensor technology. Author

SUBJECT INDEX

SCIENTIFIC AND TECHNICAL AEROSPACE REPORTS VOLUME 28 NUMBER 15

Typical Subject Index Listing

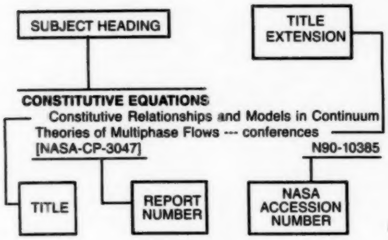

The subject heading is a key to the subject content of the document. Titles, report numbers, and accession numbers of pertinent documents are provided under each subject heading. When the title is insufficiently descriptive of the document content, a title extension has been added, separated from the title by three hyphens. The report number helps to indicate the type of document cited (e.g., NASA report, NASA translation, NASA contractor report). The NASA accession number is the number by which the document abstracts are arranged in this journal and by which the document is sold or requested. The titles, with title extensions if present, are arranged under each subject heading in ascending accession number order. The subject headings have been selected from the latest revision of the *NASA Thesaurus* (NASA SP-7064).

A

ABLATION

Growth and patterning of laser ablated superconducting YBa2Cu3O7 films on LaAlO3 substrates
[NASA-TM-102436] N90-22421

ABSORPTION SPECTROSCOPY

Infrared absorption spectroscopy and chemical kinetics of free radicals
[DE90-009469] N90-21837

Saturated fluorescence measurements of the hydroxyl radical in laminar high-pressure flames
[NASA-CR-185218] N90-22022

ABSTRACTS

Topical Conference on the Origin of the Earth
[NASA-CR-185061] N90-22166

ACCELERATION (PHYSICS)

The vibro-acoustic mapping of low gravity trajectories on a Learjet aircraft
[NASA-TM-103103] N90-21723

Active primary lithium thionyl chloride battery for artillery applications
[DE90-009511] N90-21955

Severe shock and vibration environments for electronic components
[DE90-007686] N90-22113

Engagement analysis study
[DE90-009529] N90-22359

ACCELERATION TOLERANCE

The effects of linear acceleration on perception and nystagmus N90-22209

ACCESS CONTROL

CSMA/RN: A universal protocol for gigabit networks N90-22280

ACCESS TIME

A carrier sensed multiple access protocol for high data base rate ring networks N90-22288

ACCIDENT INVESTIGATION

General purpose heat source radioisotope thermoelectric generator program. Book 1: Accident analysis
[REPT-90SDS4202-BK-1] N90-22379

General purpose heat source radioisotope thermoelectric generator. Book 2: Accident analysis, appendices
[REPT-90SDS4202-BK-2] N90-22380

ACCIDENTS

Final (Tier 1) environmental impact statement for the Galileo and Ulysses Missions
[NASA-TM-102917] N90-21779

Final environmental impact statement for the Galileo Mission (Tier 2)
[NASA-TM-102925] N90-22147

General purpose heat source radioisotope thermoelectric generator program. Book 1: Accident analysis
[REPT-90SDS4202-BK-1] N90-22379

ACCRETION DISKS

Does mass accretion lead to field decay in neutron stars
[CAL-394] N90-22470

ACCURACY

Wind forecasting for utility operations
[DE90-009466] N90-22193

ACIDITY

Cloud chemistry and occurrence in the western United States: A synopsis of current information
[PB90-134248] N90-22182

ACOUSTIC EMISSION

Impact tolerant material
[NASA-CASE-LAR-12887-3] N90-21822

Propagation environments, effects, and decision aids N90-21918

Combining acoustic emission locations and a microcrack damage model to study development of damage in brittle materials
[DE90-005195] N90-22111

Polarization coupling in the acousto-optic interaction of surface waves N90-22365

ACOUSTIC IMPEDANCE

Impact tolerant material
[NASA-CASE-LAR-12887-3] N90-21822

ACOUSTIC MICROSCOPES

Nonlinear acoustic interactions in superfluid helium N90-22367

ACOUSTIC PROPAGATION

Propagation of transient acoustic waves in porous media
[ETN-90-96401] N90-22015

An investigation of the generation and radiation of aerodynamic noise in real piping systems N90-22368

ACOUSTIC SCATTERING

Generalized Herglotz functions and inverse scattering problem in a finite depth ocean
[PB90-150996] N90-22197

ACOUSTICS

The vibro-acoustic mapping of low gravity trajectories on a Learjet aircraft
[NASA-TM-103103] N90-21723

ACOUSTO-OPTICS

An acousto-optic image correlator with a throughput rate of 1000 templates per second
[DE90-009323] N90-22249

Polarization coupling in the acousto-optic interaction of surface waves N90-22365

ACRYLIC RESINS

Thermomechanical properties of polymeric materials and related stresses
[NASA-TM-100758] N90-21864

ACTIVATION ENERGY

Testing carbon fabric for oxidation mass loss N90-21819

ACTIVE CONTROL

Advances in optimal active control techniques for aerospace systems; application to aircraft active landing gear N90-21769

Bi-directional thruster development and test report
[NASA-CR-182013] N90-21785

Modern developments in shear flow control with swirl
[NASA-CR-186586] N90-22000

The Shock and Vibration Digest, volume 21, no. 1 N90-22061

Recent advances in structural control N90-22062

Active control of bearing preload using piezoelectric translators N90-22098

The Shock and Vibration Digest, volume 21, no. 6 N90-22363

Noise transmission into propeller-driven airplanes N90-22364

ACTIVE GALACTIC NUCLEI

Spectrum formation in active galactic nuclei and Type 2 supernovae N90-22490

ACTS

The Advanced Communications Technology Satellite (ACTS) capabilities for serving science
[NASA-CR-186584] N90-21789

ACTUATORS

Bi-directional thruster development and test report
[NASA-CR-182013] N90-21785

The 24th Aerospace Mechanisms Symposium
[NASA-CP-3062] N90-22079

Development of shape memory metal as the actuator of a fail safe mechanism N90-22081

A soft actuation system for segmented reflector articulation and isolation N90-22084

Active control of bearing preload using piezoelectric translators N90-22098

ADAPTERS

The connector space reduction mechanism N90-22092

ADAPTIVE CONTROL

An adaptive human response mechanism controlling the V/STOL aircraft. Appendix 3: The adaptive control model of a pilot in V/STOL aircraft control loops
[NASA-CR-186599] N90-21777

Three-dimensional adaptive grids with limited skewness N90-21987

Nonlinear stability analysis and control of dynamical robotic systems N90-22037

A methodology for knowledge-based restructurable control to accommodate system failures N90-22058

Adaptive control of a flexible manipulator with unknown changing loads N90-22293

The role of input weighting and bounding in the characteristic GPC method
[OUEL-1762/89] N90-22328

A robust stability result for generalised predictive control
[OUEL-1773/89] N90-22330

Bicausal representations and multivariable generalized predictive control
[OUEL-1781/89] N90-22331

ADAPTIVE FILTERS

UD filtering and smoothing applied to orbit determination
[INPE-4966-PRE/1535] N90-22501

ADHESION

Interfacial studies in fiber-reinforced thermoplastic-matrix composites N90-21814

ADHESION TESTS

Interfacial studies in fiber-reinforced thermoplastic-matrix composites N90-21814

ADHESIVE BONDING

On the design and development of a miniature ceramic gimbal bearing N90-22100

ADHESIVES

The controlled-damage concept in design of laminated composites N90-21830

ADVECTION

Rigorous upper bounds for turbulent transport in bounded systems: Passive advection and reversed-field pinches N90-22390

AEROASSIST

Optimal trajectories for the aeroassisted flight experiment. Part 4: Data, tables, and graphs
[NASA-CR-186164] N90-21780

AERODYNAMIC BRAKES

Tribomaterial factors in space mechanism brake performance N90-22096

AERODYNAMIC CHARACTERISTICS
Prediction of forces and moments for flight vehicle control effectors. Part 1: Validation of methods for predicting hypersonic vehicle controls forces and moments
[NASA-CR-186571] N90-21734
On the way to an integrated mesh generation system for industrial applications N90-21969
Application of the TRANAIR rectangular grid approach to the aerodynamic analysis of complex configurations
N90-21996
Aerodynamics of a full-scale, non rotating wind turbine blade under natural wind conditions
[RISOE-M-2768] N90-22144
AERODYNAMIC COEFFICIENTS
Slotted-wall research with disk and parachute models in a low-speed wind tunnel
[DE90-002989] N90-21737
AERODYNAMIC CONFIGURATIONS
Prediction of forces and moments for flight vehicle control effectors. Part 1: Validation of methods for predicting hypersonic vehicle controls forces and moments
[NASA-CR-186571] N90-21734
Geometry and grids of complex configurations for aerodynamic calculation N90-21980
AERODYNAMIC DRAG
On the use of external burning to reduce aerospace vehicle transonic drag
[NASA-TM-103107] N90-21762
AERODYNAMIC LOADS
Airloads, wakes, and aeroelasticity
[NASA-CR-177551] N90-21738
Aeroelastic simulation of higher harmonic control
N90-21768
AERODYNAMIC NOISE
An investigation of the generation and radiation of aerodynamic noise in real piping systems N90-22368
AERODYNAMIC STABILITY
Prediction of forces and moments for flight vehicle control effectors. Part 2: An analysis of delta wing aerodynamic control effectiveness in ground effect
[NASA-CR-186572] N90-21735
AERODYNAMICS
Aeronautical engineering: A continuing bibliography with indexes (supplement 250)
[NASA-SP-7037(250)] N90-21722
Prediction of forces and moments for flight vehicle control effectors. Part 2: An analysis of delta wing aerodynamic control effectiveness in ground effect
[NASA-CR-186572] N90-21735
Modeling of vortex-induced oscillations based on indicial response approach
[NASA-CR-186560] N90-21736
Aerodynamics of a full-scale, non rotating wind turbine blade under natural wind conditions
[RISOE-M-2768] N90-22144
AEROELASTICITY
Airloads, wakes, and aeroelasticity
[NASA-CR-177551] N90-21738
Identification of XV-15 aeroelastic modes using frequency-domain methods
[NASA-TM-101021] N90-21756
Aeroelastic simulation of higher harmonic control
N90-21768
AERONAUTICAL ENGINEERING
Aeronautical engineering: A continuing bibliography with indexes (supplement 250)
[NASA-SP-7037(250)] N90-21722
Aeronautics and space report of the President: 1987 activities N90-22462
AERONAUTICS
Research and Technology Objectives and Plans Summary (RTOPS)
[NASA-TM-89662] N90-22528
AEROSOLS
A survey of the maritime-aerosol data collected at South Uist and the implications for the LOWTRAN maritime aerosol model N90-21908
The Mediterranean marine environment and its effects on aerosols and infrared transmission N90-21909
Models of aerosols, clouds, and precipitation for atmospheric propagation studies N90-21919
Interpreting meteorological data reports for LOWTRAN Navy aerosol model extinction calculations N90-21920
The naval oceanic vertical aerosol model N90-21921
Inclusion of clouds and rain in atmospheric slant path calculations N90-21925
Cirrus cloud optical properties measured with the University of Wisconsin high spectral resolution and volume imaging lidars N90-21932
Technique for selecting an aerosol model useful for infrared atmospheric transmittance calculations
N90-21934
Aerosol separator for use in aircraft
[PB90-142217] N90-22155
The sources and chemistry of late winter Arctic tropospheric aerosols
[PB90-131988] N90-22158
AEROSPACE ENGINEERING
The 24th Aerospace Mechanisms Symposium
[NASA-CP-3062] N90-22079
Aeronautics and space report of the President: 1987 activities N90-22462
Research and Technology Objectives and Plans Summary (RTOPS)
[NASA-TM-89662] N90-22528
AEROSPACE ENVIRONMENTS
Experience with synthetic fluorinated fluid lubricants
N90-22095
AEROSPACE INDUSTRY
Electronic Transfer of Information and its Impact on Aerospace and Defence Research and Development
[AGARD-CP-466] N90-22440
AEROSPACE MEDICINE
USSR Space Life Sciences Digest, issue 25
[NASA-CR-3922(29)] N90-22203
Aerospace medicine and biology: A continuing bibliography with indexes (supplement 334)
[NASA-SP-7011(334)] N90-22207
Aerospace medicine and biology: A continuing bibliography with indexes (supplement 335)
[NASA-SP-7011(335)] N90-22208
AEROSPACE PLANES
Numerical simulation of hypersonic flow around a space plane. Part 2: Application to high angles of attack flow
[NAL-TR-1011T] N90-21726
AEROSPACE SCIENCES
NASA Thesaurus supplement: A four part cumulative supplement to the 1988 edition of the NASA Thesaurus (supplement 3)
[NASA-SP-7064-SUPPL-3] N90-22438
Research and Technology Objectives and Plans Summary (RTOPS)
[NASA-TM-89662] N90-22528
AEROSPACE SYSTEMS
Advances in optimal active control techniques for aerospace systems; application to aircraft active landing gear N90-21769
Large space systems antenna technology
N90-21798
AEROSPACE VEHICLES
On the use of external burning to reduce aerospace vehicle transonic drag
[NASA-TM-103107] N90-21762
AFTERBODIES
The interaction between a plane shock wave and a cylindrical afterbody N90-21728
AFTERBURNING
Exhaust environment measurements of a turbofan engine equipped with an afterburner and 2D nozzle
[NASA-CR-4289] N90-21760
AGING (MATERIALS)
Grain boundary intermetallic phases in alloy 718
[DE90-009812] N90-22417
AGING (METALLURGY)
The effect of aging at 343 C on type 308 stainless steel weldments
[DE90-009232] N90-21853
AGRICULTURE
Spectral response of wheat and its relationship with agronomic variables in the tropical region
[INPE-5018-RPE/612] N90-22138
Field reports on radiometric campaigns of soybeans in the Federal district: Safra 88/89
[INPE-5021-RPE/615] N90-22139
Proceedings of the Conference on Technology-Based Confidence Building: Energy and Environment
[CNSS-PAPERS-22] N90-22152
AGROCLIMATOLOGY
From Penman to Makkink: A new method for the calculation of the climatological evaporation numbers
[KNMI-TR-111] N90-22161
AILERONS
Prediction of forces and moments for flight vehicle control effectors. Part 1: Validation of methods for predicting hypersonic vehicle controls forces and moments
[NASA-CR-186571] N90-21734
AIR
WINCOF-I code for prediction of fan compressor unit with water ingestion
[NASA-CR-185157] N90-21724
AIR FILTERS
Aerosol separator for use in aircraft
[PB90-142217] N90-22155
AIR FLOW
Fire propagation in concurrent flows
[PB90-151754] N90-21834
Aerosol separator for use in aircraft
[PB90-142217] N90-22155
An anomalous wind between valleys: Its characteristics and a proposed explanation
[DE90-008965] N90-22189
Daytime wind valleys adjacent to the Great Salt Lake
[DE90-008991] N90-22190
The ASCOT 1988 valley/tributary interaction study
[DE90-009043] N90-22191
AIR MASSES
Optimal control of an aircraft flying through a downburst N90-21765
Calculation of IR propagation statistics in the eastern Atlantic for surveillance system performance assessment N90-21938
AIR POLLUTION
Proceedings of the Conference on Technology-Based Confidence Building: Energy and Environment
[CNSS-PAPERS-22] N90-22152
The laminar flow element: Its use as a flow standard
[PB90-129677] N90-22157
The sources and chemistry of late winter Arctic tropospheric aerosols
[PB90-131988] N90-22158
AIR QUALITY
Global distribution of organo-bromine gases
N90-22150
Prevention of significant deterioration application for approval to construct SP-100 Ground Engineering System Test Site
[DE90-007986] N90-22381
AIR SAMPLING
Aerosol separator for use in aircraft
[PB90-142217] N90-22155
AIR TRAFFIC CONTROL
A conflict analysis of 4D descent strategies in a metered, multiple-arrival route environment
[NASA-CR-182019] N90-21772
AIR TRANSPORTATION
Aeronautics and space report of the President: 1987 activities N90-22462
AIR WATER INTERACTIONS
The Mediterranean marine environment and its effects on aerosols and infrared transmission N90-21909
The naval oceanic vertical aerosol model N90-21921
Infrared propagation in the air-sea boundary layer
N90-21926
The relationship between the buoyancy of near-surface air and the potential temperature of the tropopause
N90-22165
Lagrangian model simulation of the turbulent transport of evaporating jet droplets N90-22168
Southern oscillation simulation in coupled ocean/atmosphere global climate models N90-22181
AIRBORNE LASERS
Pre-study laser bathymetry
[BCRS-89-26] N90-22198
AIRBORNE/SPACEBORNE COMPUTERS
A comparison of time-optimal interception trajectories for the F-8 and F-15
[NASA-CR-186300] N90-21753
Preliminary development of an intelligent computer assistant for engine monitoring
[NASA-TM-101702] N90-22322
AIRCRAFT ACCIDENT INVESTIGATION
Aircraft accident report, United Airlines Flight 811, Boeing 747-122, N4713U, Honolulu, Hawaii, February 24, 1989
[PB90-910401] N90-21748
AIRCRAFT ACCIDENTS
Aircraft accident report, United Airlines Flight 811, Boeing 747-122, N4713U, Honolulu, Hawaii, February 24, 1989
[PB90-910401] N90-21748
Optimal control of an aircraft flying through a downburst N90-21765
AIRCRAFT COMPARTMENTS
The Shock and Vibration Digest, volume 21, no. 6
N90-22363
Noise transmission into propeller-driven airplanes
N90-22364
AIRCRAFT CONFIGURATIONS
Prediction of forces and moments for flight vehicle control effectors. Part 1: Validation of methods for predicting hypersonic vehicle controls forces and moments
[NASA-CR-186571] N90-21734
Grid patching approaches for complex three-dimensional configurations N90-21985
Multiblock topology specification and grid generation for complete aircraft configurations N90-21986
A discussion on issues relating to multiblock grid generation N90-21991
Automatic grid generation in complex three-dimensional configurations using a frontal system N90-21992
Unstructured finite element mesh generation and adaptive procedures for CFD N90-21993

AIRCRAFT CONTROL
Optimization and guidance of flight trajectories in the presence of windshear
[NASA-CR-186163] N90-21747
The insertion of human dynamics models in the flight control loops of V/STOL research aircraft. Appendix 2: The optimal control model of a pilot in V/STOL aircraft control loops
[NASA-CR-186598] N90-21776
An adaptive human response mechanism controlling the V/STOL aircraft. Appendix 3: The adaptive control model of a pilot in V/STOL aircraft control loops
[NASA-CR-186599] N90-21777

AIRCRAFT DESIGN
Conceptual design optimization study
[NASA-CR-4298] N90-21755
Applications of Mesh Generation to Complex 3-D Configurations
[AGARD-CP-464] N90-21975
Design and testing of a multiblock grid-generation procedure for aircraft design and research N90-21984
Multiblock topology specification and grid generation for complete aircraft configurations N90-21986
Feature-associated mesh embedding for complex configurations N90-21988
A3I visibility modeling project N90-22230

AIRCRAFT ENGINES
Control of flow separation and mixing by aerodynamic excitation
[NASA-TM-103131] N90-21733
Preliminary development of an intelligent computer assistant for engine monitoring
[NASA-TM-101702] N90-22322

AIRCRAFT LANDING
Optimization and guidance of flight trajectories in the presence of windshear
[NASA-CR-186163] N90-21747

AIRCRAFT NOISE
The Shock and Vibration Digest, volume 21, no. 6
N90-22363
Noise transmission into propeller-driven airplanes
N90-22364

AIRCRAFT POWER SUPPLIES
Preliminary design of a long-endurance Mars aircraft
[NASA-CR-185243] N90-21763

AIRCRAFT SAFETY
Aircraft accident report, United Airlines Flight 811, Boeing 747-122, N4713U, Honolulu, Hawaii, February 24, 1989
[PB90-910401] N90-21748

AIRCRAFT STRUCTURES
Robots for aircraft coatings removal: Parameters and requirements
[DE90-009429] N90-22048

AIRFOIL PROFILES
Graphs of the state of stress at rounded corners
[MEMT-1] N90-22122
Aerodynamics of a full-scale, non rotating wind turbine blade under natural wind conditions
[RISOE-M-2768] N90-22144

AIRFOILS
Control of flow separation and mixing by aerodynamic excitation
[NASA-TM-103131] N90-21733

AIRSPEED
Optimal control of an aircraft flying through a downburst N90-21765

ALBEDO
Quantitative studies of the Martian south polar region using spacecraft images N90-22514

ALGAE
Photosynthetic water splitting, phase 2
[PB90-132671] N90-21833

ALGEBRA
Finding the complete path and weight enumerators of convolutional codes N90-21897
Algebraic block-structured grid generation based on a macro-block concept N90-21978
Applications of algebraic grid generation N90-21979
Incomparable elements in algebraic lattices with applications to formal language theory
[MEMO-INF-89-54] N90-22269
Operator algebra from fusion rules: The infinite number of Ising theories
[NIKHEF-H/89-7] N90-22374
Generalized killing equations and symmetries of spinning space
[NIKHEF-H/89-8] N90-22375

ALGORITHMS
Extension of a streamwise upwind algorithm to a moving grid system
[NASA-TM-102800] N90-21739
First-order weight corrections for real-time flight path management
[LR-580] N90-21751
Accurate nonlinear control for satellites using reaction wheels
[INPE-4983-PRE/1546] N90-21787
A trajectory generation and system characterization model for cislunar low-thrust spacecraft. Volume 2: Technical manual
[NASA-CR-185172] N90-21807
Framework for a space shuttle main engine health monitoring system
[NASA-CR-185224] N90-21809
Finding the complete path and weight enumerators of convolutional codes N90-21897
Adaptive frequency estimation by MUSIC (Multiple Signal Classification) method
[PB90-166794] N90-21943
Convergence acceleration of upwind relaxation methods for the Navier-Stokes equations N90-21973
Applications of Mesh Generation to Complex 3-D Configurations
[AGARD-CP-464] N90-21975
Three-dimensional adaptive grids with limited skewness N90-21987
Unstructured mesh generation by a generalized Delaunay algorithm N90-21995
Nonlinear stability analysis and control of dynamical robotic systems N90-22037
Trajectory generation for car-like robots
[DE90-008407] N90-22047
The classification of defects from ultrasonic measurements
[AERE-R-13306] N90-22056
Parallel asynchronous hardware implementation of image processing algorithms N90-22219
Computation and parallel implementation for early vision N90-22222
Algorithms and architectures for robot vision
N90-22236
Kalman filter based range estimation for autonomous navigation using imaging sensors N90-22238
Intensity dependent spread processor and workstation
N90-22244
Optimal 3-dimensional methods for linear programming
[PB90-155391] N90-22253
An algorithm and computer program for the calculation of envelope curves
[PB90-155409] N90-22254
Symbolic pattern processing system for planar spatial structures
[DE90-001598] N90-22256
Molecular dynamics simulations of short-range force systems on 1024-node hypercubes
[DE90-009833] N90-22259
On decoding of multi-level MPSK modulation codes
[NASA-CR-186601] N90-22261
Local mode smoothing analysis for various incomplete factorization iterative methods in three dimensions
[REPT-89-38] N90-22263
An approach to rescheduling activities based on determination of priority and disruptivity N90-22299
Space communications scheduler: A rule-based approach to adaptive deadline scheduling N90-22300
Bounded-time fault-tolerant rule-based systems
N90-22318
Automating security monitoring and analysis for Space Station Freedom's electric power system
[NASA-TM-103148] N90-22324
Branch point placement
[OUEL-1767/89] N90-22329
Control of human arm movement via optimization
N90-22334
On the existence of a positive definite solution of the matrix equation X + A(sup tau)X(exp -1)A = I
[PB90-133976] N90-22335
Orthogonal distance regression
[PB90-151747] N90-22336
Spline function smoothing and differentiation of noisy data on a rectangular grid
[DE90-009319] N90-22338
Dynamical approach study of spurious steady-state numerical solutions of nonlinear differential equations. Part 1: The ODE connection and its implications for algorithm development in computational fluid dynamics
[NASA-TM-102820] N90-22339
Normal forms for weakly non-linear perturbed wave equations
[REPT-89-41] N90-22343
Preference numbers and funnel dimension
[REPT-89-57] N90-22346
Neural implementation of a method for solving systems of linear algebraic equations
[NPL-DITC-155/89] N90-22356
Update on the OPAL opacity code
[DE90-009946] N90-22480

ALIGNMENT
Induction-type metal detector with increased scanning area capability
[NASA-CASE-KSC-11386-1] N90-22023

ALLOYS
Fracture toughness and tensile properties of alloy HT9 in thin sections under high neutron fluences
[DE90-008386] N90-21851
Computational methods and plasticity
[LR-583] N90-22120

ALTERNATING DIRECTION IMPLICIT METHODS
Three-dimensional simulation of vortex breakdown
[NASA-TM-102664] N90-21744

ALUMINATES
Growth and patterning of laser ablated superconducting YBa2Cu3O7 films on LaAlO3 substrates
[NASA-TM-102436] N90-22421

ALUMINIDES
Microstructure and mechanical properties of nickel aluminide powders consolidated by extrusion and hot isostatic pressing
[DE90-009777] N90-21855

ALUMINUM ISOTOPES
The Al-26(rho, gamma)Si-27 reaction: Stellar origins of galactic Al-26 N90-22498

ALUMINUM OXIDES
New corrosion resistant ceramic coatings by laser processing
[AERE-R-13166] N90-21863
In-situ pulsed laser deposition of high-T(sub c) YBa(sub 2)Cu(sub 3)O(sub 7) superconducting thin films on (100) LaAlO3 substrates
[DE90-009861] N90-22418

AMAZON REGION (SOUTH AMERICA)
Geographic information system: Coded data of agrocattle-raising projects in the Amazon
[INPE-4978-PRE/1543] N90-22457

AMMONIA
A three-year study of the OH masers in Orion-KL and a study of the (3,2) transition of ammonia N90-22471

AMMONIUM COMPOUNDS
Studies on the use of supercritical ammonia for ceramic nitride synthesis and fabrication
[NASA-TM-102570] N90-21843

AMMONOLYSIS
Studies on the use of supercritical ammonia for ceramic nitride synthesis and fabrication
[NASA-TM-102570] N90-21843

AMMUNITION
Extraction of recovery of plasticizers from solid propellants and munitions
[AD-D014433] N90-21868

AMORPHOUS MATERIALS
Low temperature properties of amorphous solids
N90-22405

AMOUNT
An introduction to Montague grammar
[REPT-89-46] N90-22266

AMPLIFICATION
Direct solar-pumped iodine laser amplifier
[NASA-CR-186442] N90-22030

ANALOG SIMULATION
Polarization coupling in the acousto-optic interaction of surface waves N90-22365

ANALOGIES
Frontal structure in a mesoscale model N90-22187

ANALYSIS (MATHEMATICS)
On the existence of a positive definite solution of the matrix equation X + A(sup tau)X(exp -1)A = I
[PB90-133976] N90-22335
Discrete variable structural optimization by the complex method
[LR-597] N90-22341

ANELASTICITY
Dynamic and microphysical characteristics of cirrus clouds as revealed by aircraft, lidar, and other observations during FIRE N90-22177

ANGLE OF ATTACK
Numerical simulation of hypersonic flow around a space plane. Part 2: Application to high angles of attack flow
[NAL-TR-1011T] N90-21726

ANISOTROPIC MEDIA
Transport properties of anisotropic superconductors
N90-22404

ANISOTROPIC SHELLS
ANILISA: Computational module for Koiter's imperfection sensitivity theory
[LR-582] N90-22119

ANISOTROPY
Transport and relaxation properties in anisotropic superconductors N90-22403

ANNULI
Green's functions for the elastic annulus and their application to various crack problems N90-22129

ANOMALIES

Southern oscillation simulation in coupled ocean/atmosphere global climate models N90-22181

Tropopause undulations and the development of extratropical cyclones N90-22186

Low temperature properties of amorphous solids N90-22405

The Al-26(rho, gamma)Si-27 reaction: Stellar origins of galactic Al-26 N90-22498

ANTARCTIC REGIONS

Opportunities for US-USSR cooperation in the investigation of Arctic stratospheric ozone N90-22154

Site visit to US Antarctic Program (USAP) facilities and the Research Vessel Polar Duke [DE90-009396] N90-22159

JARE data reports, no. 140 (meteorology 21): Meteorological data at Asuka Camp, Antarctica in 1987 [ISSN-0075-3343] N90-22188

ANTENNA ARRAYS

Large space systems antenna technology N90-21798

A real-time signal combining system for Ka-band feed arrays using maximum-likelihood weight estimates N90-21888

ANTENNA DESIGN

Millimeter wavelength rectenna development N90-21797

Inflatable antennas for microwave pwoer transmission N90-21799

Dual-shaped offset reflector antenna designs from solutions of the geometrical optics first-order partial differential equations N90-21887

Passive shape control of space antennas with determinate truss support structures N90-21949

ANTENNA FEEDS

Ultralow noise performance of an 8.4-GHz maser-feedhorn system N90-21889

An 8.4-GHz dual-maser front-end system for Parkes reimplementation N90-21905

ANTENNA RADIATION PATTERNS

Analysis of a high harmonic rectangular gyrotron using ribbon beams N90-21801

ANTENNAS

Structural fatigue in the 34-meter HA-Dec antennas N90-21902

ANTHROPOMETRY

The predictability and efficiency of human walking: Metabolic, mechanical, and biophysical considerations N90-22211

ANTIMONY COMPOUNDS

Ternary reactions among polymer substrate-organohalogen-antimony oxides under pyrolytic, oxidative and flaming conditions [PB90-154766] N90-21861

APERTURES

Development of the CLAES instrument aperture door system N90-22083

APPLICATIONS OF MATHEMATICS

Preference numbers and funnel dimension [REPT-89-57] N90-22346

APPLICATIONS PROGRAMS (COMPUTERS)

Automated analysis of measured turbulent boundary flow [PB90-147844] N90-21970

Design and testing of a multiblock grid-generation procedure for aircraft design and research N90-21984

The computational structural mechanics testbed data library description [NASA-TM-100645-REV-1] N90-22135

Graphically-oriented nonlinear analysis of statically loaded plane frames on microcomputers [PB90-165945] N90-22248

APPROXIMATION

A review of approximate methods for determining the vibrational modes of membranes N90-22063

Stability radius of polynomials occurring in the numerical solution of initial value problems [TW-89-04] N90-22350

The approximation of a composite Bezier cubic curve by a composite Bezier quadratic curve [NPL-DITC-147/89] N90-22354

AQUATIC PLANTS

Utilization of water hyacinths to upgrade heavily loaded wastewater treatment plant effluents N90-21873

ARCHITECTURE (COMPUTERS)

Parallel asynchronous hardware implementation of image processing algorithms N90-22219

Sparse distributed memory overview N90-22235

Algorithms and architectures for robot vision N90-22236

VCS: A networked Version Control System [DE90-009805] N90-22250

Understanding the computing system domain of advanced computing with microcomputers [DE90-009825] N90-22251

Scalable coherent interface [DE90-008011] N90-22277

The art of fault-tolerant system reliability modeling [NASA-TM-102623] N90-22292

The 1990 Goddard Conference on Space Applications of Artificial Intelligence [NASA-CP-3068] N90-22294

Resource Allocation Planning Helper (RALPH): Lessons learned N90-22296

The role of artificial intelligence techniques in scheduling systems N90-22297

SURE (Science User Resource Expert): A science planning and scheduling assistant for a resource based environment N90-22302

Managing temporal relations N90-22304

Autonomous power expert system N90-22306

Spacecraft command verification: The AI solution N90-22307

Adaptive pattern recognition by mini-max neural networks as a part of an intelligent processor N90-22317

Guide to RMS-literature [REPT-89-52] N90-22326

An intelligent interface for the design of optimal control systems [INPE-4917-PRE/1516] N90-22332

Facilitating knowledge sharing in organizations: Semiautonomous agents that learn to gather, classify, and distribute environmental scanning knowledge N90-22435

Update on the OPAL opacity code [DE90-009946] N90-22480

ARCTIC REGIONS

Opportunities for US-USSR cooperation in the investigation of Arctic stratospheric ozone N90-22154

The sources and chemistry of late winter Arctic tropospheric aerosols [PB90-131988] N90-22158

AREA NAVIGATION

A conflict analysis of 4D descent strategies in a metered, multiple-arrival route environment [NASA-CR-182019] N90-21772

ARIANE LAUNCH VEHICLE

The initial imperfection databank at the Delft University of Technology, part 3 [LR-568] N90-21783

ARRAYS

Performance of the IMP array processing algorithm: First results [RSRE-MEMO-4291] N90-22274

ARTIFICIAL INTELLIGENCE

Vision Science and Technology at NASA: Results of a Workshop [NASA-TM-102214-REV-1] N90-22216

Sparse distributed memory overview N90-22235

The 1990 Goddard Conference on Space Applications of Artificial Intelligence [NASA-CP-3068] N90-22294

The application of connectionism to query planning/scheduling in intelligent user interfaces N90-22295

Resource Allocation Planning Helper (RALPH): Lessons learned N90-22296

The role of artificial intelligence techniques in scheduling systems N90-22297

PLAN-IT-2: The next generation planning and scheduling tool N90-22298

Space communications scheduler: A rule-based approach to adaptive deadline scheduling N90-22300

Constraint-based evaluation of sequential procedures N90-22301

Managing temporal relations N90-22304

Spacecraft command verification: The AI solution N90-22307

Analyzing spacecraft configurations through specialization and default reasoning N90-22308

Simulation-based reasoning about the physical propagation of fault effects N90-22309

The JPL/KSC telerobotic inspection demonstration N90-22312

System control of an autonomous planetary mobile spacecraft N90-22313

Automated procedure execution for space vehicle autonomous control N90-22314

Knowledge structure representation and automated updates in intelligent information management systems N90-22316

Bounded-time fault-tolerant rule-based systems N90-22318

A knowledge-based system with learning for computer communication network design N90-22319

Guide to RMS-literature [REPT-89-52] N90-22326

Facilitating knowledge sharing in organizations: Semiautonomous agents that learn to gather, classify, and distribute environmental scanning knowledge N90-22435

ARTIFICIAL SATELLITES

Analysis, selection, and implementation of procedures which approve optimal artificial satellite maneuvers [INPE-5003-TDL/397] N90-21786

ARTILLERY

Active primary lithium thionyl chloride battery for artillery applications [DE90-009511] N90-21955

ASBESTOS

Tribomaterial factors in space mechanism brake performance N90-22096

ASCENT

Optimal trajectories for the aeroassisted flight experiment. Part 4: Data, tables, and graphs [NASA-CR-186164] N90-21780

ASTROMETRY

A higher density VLBI catalog for navigating Magellan and Galileo N90-21904

ASTRONAUT PERFORMANCE

Issues in development, evaluation, and use of the NASA Preflight Adaptation Trainer (PAT) [NASA-CR-185608] N90-22212

ASTRONAUT TRAINING

Issues in development, evaluation, and use of the NASA Preflight Adaptation Trainer (PAT) [NASA-CR-185608] N90-22212

ASTRONOMICAL MODELS

Numerical investigations of nonlinear behavior in the Einstein equations N90-22427

Origin of pulsed emission from the young supernova remnant SN 1987A [CAL-377] N90-22469

A three-year study of the OH masers in Orion-KL and a study of the (3,2) transition of ammonia N90-22471

The emission lines in the ultra-violet spectrum of Beta Lyrae N90-22474

The modeling of IRAS detections of classical novae and related objects N90-22482

Herbig-Haro objects and stellar jets N90-22487

The distribution of molecular clouds in spiral galaxies N90-22489

The Sagittarius B2 molecular cloud: An extreme case of a galactic center giant molecular cloud N90-22493

Kinematic models of cometary comae N90-22495

The mass of the Coma cluster N90-22496

A galaxy formation cookbook: Recipes and utensils N90-22508

ASTRONOMICAL PHOTOGRAPHY

Diffraction-limited imaging on the 200-inch telescope N90-22475

ASTRONOMY

Motion detection in astronomical and ice floe images N90-22231

NSSDC data listing [NASA-TM-102989] N90-22456

The optical night sky at low surface brightness: High latitude dust and faint field galaxies N90-22481

ASTROPHYSICS

NSSDC data listing [NASA-TM-102989] N90-22456

Physics of systems containing neutron stars [NASA-CR-186002] N90-22467

A high galactic latitude survey of far ultraviolet excess objects N90-22473

The Al-26(rho, gamma)Si-27 reaction: Stellar origins of galactic Al-26 N90-22498

An astrophysics data program investigation of cluster evolution [NASA-CR-181296] N90-22510

ASYMMETRY

Analytical study of the origin and behavior of asymmetric vortices [NASA-TM-102796] N90-21746

Experimental investigation of the effect of cavitation on the rotordynamic forces on a whirling centrifugal pump impeller N90-22039

ASYMPTOTIC METHODS

An unsteady time asymptotic flow in the square driven cavity [NASA-TM-103141] N90-22016

On the theory of Heiser and Shercliff experiment. Part 1: MHD flow in an open channel in strong uniform magnetic field [OUEL-1804/89-PT-1] N90-22400

On the theory of Heiser and Shercliff experiment. Part 2: MHD flow between two cylinders in strong radical magnetic field [OUEL-1805/89-PT-2] N90-22401

ASYMPTOTIC PROPERTIES

The synergism of analytic and numerical techniques in general relativity: Calculation of radiative spacetimes N90-22425

ATLANTIC OCEAN
Forecast of Atlantic seasonal hurricane activity for 1990 N90-22194
An investigation of meteorological effects on currents in the shelf and continental slope seas northwest of the United Kingdom. 2: Relationships between currents at different locations and with other variables [PB90-151911] N90-22195
ATMOSPHERIC ATTENUATION
LOWTRAN 7: Status, review, and impact for short-to-long-wavelength infrared applications N90-21917
Millimetre-wave propagation in the evaporation duct N90-21929
Applications of remote sensing to studies of oceanic upper mixed layer dynamics N90-22137
ATMOSPHERIC BOUNDARY LAYER
Infrared propagation in the air-sea boundary layer N90-21926
Effect of atmospheric turbulence on electro-optical systems N90-21940
A linear analysis of monsoon base states associated with banded convection N90-22179
ATMOSPHERIC CHEMISTRY
The sources and chemistry of late winter Arctic tropospheric aerosols [PB90-131988] N90-22158
Cloud chemistry and occurrence in the western United States: A synopsis of current information [PB90-134248] N90-22182
ATMOSPHERIC CIRCULATION
An investigation of turbulence structure in a low Reynolds number incompressible turbulent boundary layer N90-21966
An anomalous wind between valleys: Its characteristics and a proposed explanation [DE90-008965] N90-22189
ATMOSPHERIC COMPOSITION
New spectral features of stratospheric trace gases N90-21910
Global distribution of organo-bromine gases N90-22150
Opportunities for US-USSR cooperation in the investigation of Arctic stratospheric ozone N90-22154
The sources and chemistry of late winter Arctic tropospheric aerosols [PB90-131988] N90-22158
ATMOSPHERIC EFFECTS
Atmospheric Propagation in the UV, Visible, IR, and mm-Wave Region and Related Systems Aspects [AGARD-CP-454] N90-21907
The Mediterranean marine environment and its effects on aerosols and infrared transmission N90-21909
Minimizing the effects of the atmosphere in the observation of ultraviolet radiation N90-21911
Report on STC/Technische Universiteit (TU) Delft Extremely High Frequency (EHF) radio relay study N90-21915
Propagation environments, effects, and decision aids N90-21918
Interpreting meteorological data reports for LOWTRAN Navy aerosol model extinction calculations N90-21920
Modeling millimeter-wave propagation effects in the atmosphere N90-21922
Lidar measurements of the optical propagation environment N90-21930
Effect of atmospheric turbulence on electro-optical systems N90-21940
Atmospheric modelling studies: A modelling comparison between IR and millimetric atmospheric propagation N90-21941
Fast method for computing infrared transmission, computation examples N90-21942
An experimental investigation of mixing in buoyant flows N90-21963
ATMOSPHERIC GENERAL CIRCULATION MODELS
On three-dimensional scaling and consistent truncation of global atmospheric models N90-22164
Satellite versus GCM-simulated radiation balance: Comparisons and implications for climate modeling N90-22180
Southern oscillation simulation in coupled ocean/atmosphere global climate models N90-22181
ATMOSPHERIC MODELS
Atmospheric Propagation in the UV, Visible, IR, and mm-Wave Region and Related Systems Aspects [AGARD-CP-454] N90-21907
A survey of the maritime-aerosol data collected at South Uist and the implications for the LOWTRAN maritime aerosol model N90-21908
Models of aerosols, clouds, and precipitation for atmospheric propagation studies N90-21919
Interpreting meteorological data reports for LOWTRAN Navy aerosol model extinction calculations N90-21920
The naval oceanic vertical aerosol model N90-21921
Modeling millimeter-wave propagation effects in the atmosphere N90-21922
Inclusion of clouds and rain in atmospheric slant path calculations N90-21925
A temperature-dependent regular infrared band model for absorption and dispersion N90-21927
Millimetre-wave propagation in the evaporation duct N90-21929
Technique for selecting an aerosol model useful for infrared atmospheric transmittance calculations N90-21934
Atmospheric modelling studies: A modelling comparison between IR and millimetric atmospheric propagation N90-21941
Modeling the lateral diffusion of fluorescent particles within a forest canopy N90-22136
Opportunities for US-USSR cooperation in the investigation of Arctic stratospheric ozone N90-22154
Formulation of non-reflecting boundary conditions in numerical models of the atmosphere N90-22175
Characteristics of cumulus bandclouds off the east coast of Hawaii N90-22178
A linear analysis of monsoon base states associated with banded convection N90-22179
Hail growth in a highly-glaciated central high plains multi-cellular hailstorm N90-22184
A high galactic latitude survey of far ultraviolet excess objects N90-22473
Spectrum formation in active galactic nuclei and Type 2 supernovae N90-22490
Modelling late-time atmospheres of supernovae N90-22500
Auroral ultraviolet darkening on the outer planets N90-22518
ATMOSPHERIC MOISTURE
A linear analysis of monsoon base states associated with banded convection N90-22179
ATMOSPHERIC PHYSICS
Hybrid modeling of plasmas and applications to fusion and space physics N90-22387
ATMOSPHERIC PRESSURE
JARE data reports, no. 140 (meteorology 21): Meteorological data at Asuka Camp, Antarctica in 1987 [ISSN-0075-3343] N90-22188
ATMOSPHERIC RADIATION
Modelling UV-visible radiation observed from space N90-21937
ATMOSPHERIC REFRACTION
Infrared propagation in the air-sea boundary layer N90-21926
ATMOSPHERIC SCATTERING
Quantitative studies of the Martian south polar region using spacecraft images N90-22514
ATMOSPHERIC TEMPERATURE
Millimetric, infrared, and optical propagation studies over a 500 m path N90-21913
Tropopause undulations and the development of extratropical cyclones N90-22186
ATMOSPHERIC TURBULENCE
Millimetric, infrared, and optical propagation studies over a 500 m path N90-21913
Modelling of optically and IR effective atmospheric turbulence N90-21923
Effect of atmospheric turbulence on electro-optical systems N90-21940
ATTITUDE (INCLINATION)
Accurate nonlinear control for satellites using reaction wheels [INPE-4963-PRE/1546] N90-21787
Towards a Sarkovski order for the embedding of disks maintaining their orientation [REPT-89-43] N90-22289
ATTITUDE CONTROL
Direct inversion of rigid-body rotational dynamics [NASA-TM-102798] N90-21773
Numerical simulation model of hydrazine attitude control thrusters [INPE-4965-PRE/1534] N90-21848
AUGER SPECTROSCOPY
Long term intensity stability of Auger electron spectrometers: Instructions for the interlaboratory comparison [NPL-DMM(A)-1] N90-22027
AURORAS
Auroral ultraviolet darkening on the outer planets N90-22518
AUTOMATIC CONTROL
Development of cable drive systems for an automated assembly project N90-22105
Paving: A new approach to automated quadrilateral mesh generation [DE90-010244] N90-22260
A CSP model for distributed control software design [OUEL-1789/89] N90-22273
The procedure safety system N90-22311
Automated procedure execution for space vehicle autonomous control N90-22314
AUTOMATIC FLIGHT CONTROL
First-order weight corrections for real-time flight path management [LR-580] N90-21751
AUTONOMOUS NAVIGATION
Kalman filter based range estimation for autonomous navigation using imaging sensors N90-22238
AUTONOMY
Publications of the NASA Controlled Ecological Life Support System (CELSS) Program, 1979-1989 [NASA-CR-4297] N90-21754
Positive lubrication system N90-22097
Autonomous power expert system N90-22306
System control of an autonomous planetary mobile spacecraft N90-22313
AXISYMMETRIC BODIES
Numerical study of laminar and turbulent flows past two-dimensional and axisymmetric bodies N90-22020
AXISYMMETRIC FLOW
Theory and numerical analysis of single and multi-element nozzle propellers [LR-579] N90-21741

B

B STARS
A high galactic latitude survey of far ultraviolet excess objects N90-22473
Interactions of massive stars with the interstellar medium: Bow shocks and superbubbles N90-22485
The Sagittarius B2 molecular cloud: An extreme case of a galactic center giant molecular cloud N90-22493
BACKSCATTERING
UV spectral simulations using LOWTRAN 7 N90-21928
Lidar measurements of the optical propagation environment N90-21930
Cirrus cloud optical properties measured with the University of Wisconsin high spectral resolution and volume imaging lidars N90-21932
Millimeter-wave bistatic scattering by terrain N90-21936
BACKUPS
Impact tolerant material [NASA-CASE-LAR-12887-3] N90-21822
BALL BEARINGS
Positive lubrication system N90-22097
Test results and flight experience of ball bearing momentum and reaction wheels N90-22099
AX-5 space suit bearing torque investigation N90-22101
BALLISTIC TRAJECTORIES
The vibro-acoustic mapping of low gravity trajectories on a Learjet aircraft [NASA-TM-103103] N90-21723
BANDWIDTH
Radar RFI at Goldstone DSS 12 and DSS 16 N90-21900
BARIUM OXIDES
Growth and patterning of laser ablated superconducting YBa2Cu3O7 films on LaAlO3 substrates [NASA-TM-102436] N90-22421
BAROCLINIC WAVES
The observed three-dimensional structure of baroclinic waves in the Northern Hemisphere winter as revealed in a linear regression analysis N90-22167
BARRELS (CONTAINERS)
The influence of large, cold objects on engulfing fire environments [DE90-003342] N90-21875
BATHYMETERS
Pre-study laser bathymetry [BCRS-89-26] N90-22198
BEAM INJECTION
PIC code modeling of spacecraft charging potential during electron beam injection into a background of neutral gas and plasma, part 1 [NASA-CR-186602] N90-21792
BEAM INTERACTIONS
High intensity laser beam interactions with single droplets N90-21924
BEAMS (SUPPORTS)
Towards a unified analysis methodology for composite rotor blades N90-21730
The Shock and Vibration Digest, volume 21, no. 8 N90-22068
Recent progress in the dynamic plastic behavior of structures, part 5 N90-22069
BEARINGS
Bearing elastohydrodynamic lubrication: A complex calculation made simple [NASA-TM-102575] N90-22041

BELLOWS
Pressurized bellows flat contact heat exchanger interface
[NASA-CASE-MSC-21271-1] N90-21999
BENDING
Natural modes of cracked beams and identification of cracks N90-22075
Rotor loading on a three-bladed wind turbine N90-22145
Improved crystal bending techniques applied to the LLNL dual-arm Johann mounting x ray spectrometer
[DE90-009526] N90-22415
BENZENE
Detailed mechanism for oxidation of benzene
[NASA-TM-102443] N90-21842
BESSEL FUNCTIONS
Multiwave diffraction analysis of transmission phase gratings
[RSRE-MEMO-4325] N90-21948
On a third q-Bessel function
[REPT-89-48] N90-22344
BIBLIOGRAPHIES
Aeronautical engineering: A continuing bibliography with indexes (supplement 250)
[NASA-SP-7037(250)] N90-21722
Publications of the NASA Controlled Ecological Life Support System (CELSS) Program, 1979-1989
[NASA-CR-4297] N90-21754
The Shock and Vibration Digest, volume 21, no. 2 N90-22059
The Shock and Vibration Digest, volume 21, no. 1 N90-22061
The Shock and Vibration Digest, volume 21, no. 7 N90-22066
The Shock and Vibration Digest, volume 21, no. 8 N90-22068
The Shock and Vibration Digest, volume 22, no. 1 N90-22073
Aerospace medicine and biology: A continuing bibliography with indexes (supplement 334)
[NASA-SP-7011(334)] N90-22207
Aerospace medicine and biology: A continuing bibliography with indexes (supplement 335)
[NASA-SP-7011(335)] N90-22208
A Chinese bibliography on quadratic systems of differential equations
[REPT-89-39] N90-22342
The Shock and Vibration Digest, volume 21, no. 6 N90-22363
Electronic transfer of information applications in the Societe Aerospatiale N90-22454
BIG BANG COSMOLOGY
Big-bang nucleosynthesis revisited
[NASA-CR-186256] N90-22426
BINARY MIXTURES
Molecular theory of fluid phase equilibria
[PB90-131277] N90-21832
BINARY STARS
The emission lines in the ultra-violet spectrum of Beta Lyrae N90-22474
Diffraction-limited imaging on the 200-inch telescope N90-22475
BIOASTRONAUTICS
USSR Space Life Sciences Digest, issue 25
[NASA-CR-3922(29)] N90-22203
Aerospace medicine and biology: A continuing bibliography with indexes (supplement 334)
[NASA-SP-7011(334)] N90-22207
Aerospace medicine and biology: A continuing bibliography with indexes (supplement 335)
[NASA-SP-7011(335)] N90-22208
BIOCHEMISTRY
Studies of 60-Hz exposure effects on human function
[DE90-009473] N90-22210
BIOENGINEERING
Instrumentation and robotic image processing using top-down model control N90-22239
BIOLOGICAL EFFECTS
Proceedings of the 6th Regional Symposium on Biophysics
[DE90-619618] N90-22206
Aerospace medicine and biology: A continuing bibliography with indexes (supplement 334)
[NASA-SP-7011(334)] N90-22207
Aerospace medicine and biology: A continuing bibliography with indexes (supplement 335)
[NASA-SP-7011(335)] N90-22208
Studies of 60-Hz exposure effects on human function
[DE90-009473] N90-22210
BIOMASS ENERGY PRODUCTION
Testing of an advanced thermochemical conversion reactor system
[DE90-007989] N90-22141
BIOPHYSICS
Proceedings of the 6th Regional Symposium on Biophysics
[DE90-619618] N90-22206
The predictability and efficiency of human walking: Metabolic, mechanical, and biophysical considerations N90-22211
BIOPROCESSING
Research in biological separations and cell culture
[NASA-CR-172060] N90-22202
BIOREACTORS
Research in biological separations and cell culture
[NASA-CR-172060] N90-22202
BLACK HOLES (ASTRONOMY)
Multipole moments in general relativity and dynamical perturbations of black-hole magnetospheres N90-22509
BLADE-VORTEX INTERACTION
Airloads, wakes, and aeroelasticity
[NASA-CR-177551] N90-21738
BOEING 747 AIRCRAFT
Aircraft accident report, United Airlines Flight 811, Boeing 747-122, N4713U, Honolulu, Hawaii, February 24, 1989
[PB90-910401] N90-21748
BOILING
Flow boiling with enhancement devices for cold plate coolant channel design
[NASA-CR-186358] N90-21961
BOLTED JOINTS
Experimental determination of thermal conductance in bolted joint impact in satellites
[INPE-4989-PRE/1551] N90-21788
Review of analysis methods for mechanically fastened joints in composites
[LR-599] N90-22050
BOOSTER ROCKET ENGINES
Draft environmental impact statement for the Galileo Mission (Tier 2)
[NASA-TM-102926] N90-22148
BOUNDARIES
A structured approach to interactive multiple block grid generation N90-21983
BOUNDARY ELEMENT METHOD
Scattering of waves by inclusions in a nonhomogeneous elastic half space solved by boundary element methods
[PB90-145699] N90-22107
BOUNDARY INTEGRAL METHOD
Elastodynamic scattering and transmission problems in three dimensions by the boundary integral equation method N90-22077
BOUNDARY LAYER FLOW
An investigation of turbulence structure in a low Reynolds number incompressible turbulent boundary layer N90-21966
Automated analysis of measured turbulent boundary flow
[PB90-147844] N90-21970
Experimental observations on transition to turbulence in confined coaxial jets and other boundary layer flows
[DE90-008939] N90-22005
BOUNDARY LAYER SEPARATION
Control of flow separation and mixing by aerodynamic excitation
[NASA-TM-103131] N90-21733
Numerical investigation of some control methods for 3-D turbulent interactions due to sharp fins N90-21764
Low temperature properties of amorphous solids N90-22405
BOUNDARY VALUE PROBLEMS
Experimental and analytical investigations of granular materials: Shear flow and convective heat transfer N90-21968
The solution of scattering and radiation problems for complex configurations based on 3-D grid and patch models N90-21997
Analysis of a finite two-dimensional solid with an inclined crack and a rigid inclusion N90-22127
Formulation of non-reflecting boundary conditions in numerical models of the atmosphere N90-22175
Tropopause undulations and the development of extratropical cyclones N90-22186
Normal forms for weakly non-linear perturbed wave equations
[REPT-89-41] N90-22343
The theta-methods in the numerical solution of delay differential equations
[TW-89-03] N90-22349
Stability radius of polynomials occurring in the numerical solution of initial value problems
[TW-89-04] N90-22350
Stability criteria in the numerical solution of initial value problems
[TW-89-05] N90-22351
BRAIN
Sparse distributed memory overview N90-22235
Pyramid image codes N90-22243
BRANCHING (MATHEMATICS)
Branch point placement
[OUEL-1767/89] N90-22329
Bicausal representations and multivariable generalized predictive control
[OUEL-1781/89] N90-22331
Hopf bifurcation with nonsemisimple 1:1 resonance e
[MEMO-808] N90-22347
BRANCHING (PHYSICS)
Bifurcations in viscous flow fields. On the genesis and development of topologically complicated separated flow structures
[PB90-167156] N90-22012
BRAYTON CYCLE
Analysis of thermal energy storage material with change-of-phase volumetric effects
[NASA-TM-102457] N90-21974
BRAZIL
Field reports on radiometric campaigns of soybeans in the Federal district: Safra 88/89
[INPE-5021-RPE/615] N90-22139
BREADBOARD MODELS
A soft actuation system for segmented reflector articulation and isolation N90-22084
BRIDGES (STRUCTURES)
Inventory of program packages related to the project SIMONA
[ETN-90-96397] N90-22270
BRIGHTNESS
The association of supernovae with regions of recent star formation in late-type galaxies N90-22497
BRILLOUIN EFFECT
Transient effects in Brillouin gain spectroscopy in solids
[DE90-009476] N90-21839
High resolution stimulated Raman-Brillouin spectroscopy in gases and solids
[DE90-009535] N90-21840
BRITTLE MATERIALS
Combining acoustic emission locations and a microcrack damage model to study development of damage in brittle materials
[DE90-005195] N90-22111
A continuum damage model for the quasi-static response of brittle materials
[DE90-007681] N90-22112
BRITTLENESS
Combining acoustic emission locations and a microcrack damage model to study development of damage in brittle materials
[DE90-005195] N90-22111
BROADBAND
Computation of broad spectral band electro-optical system transmittance response characteristics to military smokes and obscurants using field test data from transmissometer system measurements N90-21939
BROADCASTING
Broadcast file distribution on packet satellite networks N90-21906
BROMINE
Global distribution of organo-bromine gases N90-22150
BUBBLES
Numerical simulation of liquid circulation in a bubbly column
[DE90-005226] N90-22002
Gravitational couplings of the inflation in extended inflation
[NASA-CR-186595] N90-22504
Soft inflation
[NASA-CR-186593] N90-22506
BUCKLING
Recent progress in the dynamic plastic behavior of structures, part 5 N90-22069
ANILISA: Computational module for Koiter's imperfection sensitivity theory
[LR-582] N90-22119
BUOYANCY
An experimental investigation of mixing in buoyant flows N90-21963
The relationship between the buoyancy of near-surface air and the potential temperature of the tropopause N90-22165
Current drive in a supernova N90-22491
BUTANES
A comparison of the autoignition chemistry of n-butane and isobutane in an internal combustion engine
[DE90-009474] N90-21838

C

C (PROGRAMMING LANGUAGE)
Distributed simulation, no special tools required N90-22281

CABLES (ROPES)
Development of cable drive systems for an automated assembly project N90-22105
CADMIUM
UV photo-enhanced MOCVD of cadmium and cadmium telluride
[RSRE-MEMO-4208] N90-22422
CADMIUM TELLURIDES
UV photo-enhanced MOCVD of cadmium and cadmium telluride
[RSRE-MEMO-4208] N90-22422
CALIBRATING
Precise estimation of tropospheric path delays with GPS techniques N90-21881
Lidar measurements of the optical propagation environment N90-21930
Radar scatterometry and polarimetry at 220 GHz N90-21935
Millimeter-wave bistatic scattering by terrain N90-21936
Computation of broad spectral band electro-optical system transmittance response characteristics to military smokes and obscurants using field test data from transmissometer system measurements N90-21939
Homogeneous dilute turbulent particle-laden water flows N90-21965
The calibration and measuring procedure of a five-hole hemispherical head probe in compressible flow
[LR-585] N90-22013
Development of the CLAES instrument aperture door system N90-22083
Self-calibration of robot-sensor system N90-22246
A refrigerated Dewar for the Josephson array voltage calibration system
[DE90-005237] N90-22412
CALIFORNIA
Evaporation duct effects at millimeter wavelengths N90-21914
The naval oceanic vertical aerosol model N90-21921
CAMERAS
Space environment robot vision system N90-22245
CAMS
A robot end effector exchange mechanism for space applications N90-22088
CANONICAL FORMS
On the structure of Mandelbrot's percolation process and other random Cantor sets
[REPT-89-54] N90-22362
CANOPIES (VEGETATION)
Millimeter-wave bistatic scattering by terrain N90-21936
Modeling the lateral diffusion of fluorescent particles within a forest canopy N90-22136
Spectral response of wheat and its relationship with agronomic variables in the tropical region
[INPE-5018-RPE/612] N90-22138
CANTILEVER BEAMS
Natural modes of cracked beams and identification of cracks N90-22075
CAPILLARY FLOW
Development and integration of the capillary pumped loop GAS and Hitchhiker flight experiments
[NASA-TM-100756] N90-21790
Plane Stokes flow driven by capillarity on a free surface: Overview and status
[DE90-009186] N90-22008
Plane Stokes flow driven by capillarity on a free surface: Overview and status
[DE90-009290] N90-22009
CAPILLARY WAVES
Survey of instrumental methods for the determination of the high frequency wave spectrum
[IOS-267] N90-22200
CARBON
Testing carbon fabric for oxidation mass loss N90-21819
Mechanical properties of carbon-implanted niobium
[DE90-009864] N90-21823
Recombination lines of C I and N II in the interstellar medium N90-22466
Analysis of gamma squared Velorum photometry from the South Pole N90-22472
CARBON DIOXIDE LASERS
High power CO2 laser instability and its corrections N90-22028
CARBON FIBER REINFORCED PLASTICS
Failure analysis of woven hybrid composite using a finite element method
[OUEL-1791/89] N90-21828
CARBON FIBERS
Proceedings of the Advisory Committee on Standardization of Carbon-Phenolic Test Methods and Specifications
[NASA-CR-186478] N90-21817
Development of low thermal conductivity pan-based carbon fibers for solid rocket motor nozzle applications N90-21818
CARBON MONOXIDE
A comparison of photospheric and circumstellar (HCN)/(CO)-ratios for bright carbon stars
[PB90-151101] N90-22477
The distribution of molecular clouds in spiral galaxies N90-22489
CARBON STARS
A comparison of photospheric and circumstellar (HCN)/(CO)-ratios for bright carbon stars
[PB90-151101] N90-22477
CARBON-CARBON COMPOSITES
Lightweight piston architecture
[NASA-CASE-LAR-13926-1] N90-22042
CARIBBEAN REGION
Forecast of Atlantic seasonal hurricane activity for 1990 N90-22194
CARRIER FREQUENCIES
QPSK carrier-acquisition performance in the advanced receiver 2 N90-21892
Radar RFI at Goldstone DSS 12 and DSS 16 N90-21900
CARTESIAN COORDINATES
Coordinate systems for plastic yield surfaces stress and strain space theories
[PB90-164765] N90-22110
CASSEGRAIN OPTICS
Dual-shaped offset reflector antenna designs from solutions of the geometrical optics first-order partial differential equations N90-21887
CATALOGS
The Weapons Laboratory technical library: Automating with STILAS N90-22447
CATALOGS (PUBLICATIONS)
A higher density VLBI catalog for navigating Magellan and Galileo N90-21904
Photometric monitoring of early type emission line stars N90-22478
Extended optical emission in 3CR radio galaxies N90-22523
CATALYSTS
The chemical basis for the origin of the genetic code and the process of protein synthesis
[NASA-CR-186590] N90-22205
CATHODES
Advanced electric propulsion research, 1989
[NASA-CR-185237] N90-21810
Method of making a cathode from tungsten powder
[AD-D014434] N90-21850
Hollow cathode operation at high discharge currents
[NASA-CR-185238] N90-21953
MHD channel development, part 1
[DE90-009549] N90-22394
CAUCHY PROBLEM
Green's functions for the elastic annulus and their application to various crack problems N90-22129
CAVITATION FLOW
Experimental investigation of the effect of cavitation on the rotordynamic forces on a whirling centrifugal pump impeller N90-22039
CAVITIES
Current management for improved railgun performance N90-21781
An unsteady time asymptotic flow in the square driven cavity
[NASA-TM-103141] N90-22016
Origin of pulsed emission from the young supernova remnant SN 1987A
[CAL-377] N90-22469
CAVITY RESONATORS
Development and applications of a coupled cavity sodium-chloride laser N90-22029
CELLS (BIOLOGY)
Research in biological separations and cell culture
[NASA-CR-172060] N90-22202
CENTER OF MASS
Exclusive production of p, p-, pi, and pi- in photon photon collisions
[NIKHEF-H/89-9] N90-22376
CENTRIFUGAL PUMPS
Experimental investigation of the effect of cavitation on the rotordynamic forces on a whirling centrifugal pump impeller N90-22039
CERAMIC COATINGS
New corrosion resistant ceramic coatings by laser processing
[AERE-R-13166] N90-21863
CERAMICS
Studies on the use of supercritical ammonia for ceramic nitride synthesis and fabrication
[NASA-TM-102570] N90-21843
Polysiloxanes derived from the controlled hydrolysis of tetraethoxysilane as precursors to silica for use in ceramic processing
[NASA-TM-102489] N90-21858
A stress-strength interference approach to fast and delayed fracture reliability analysis for ceramic components N90-21859
Fracture mechanics of monolithic ceramic materials under small scale microcracking conditions N90-21860
Institute for Materials Science and Engineering, nondestructive evaluation: Technical activities
[PB90-132739] N90-22055
On the design and development of a miniature ceramic gimbal bearing N90-22100
Institute for Materials Science and Engineering, Fracture and Deformation Division: Technical activities, 1989
[PB90-155359] N90-22106
Dynamic response of a complex encapsulated electronic assembly subjected to a severe shock environment
[DE90-007689] N90-22114
CERENKOV RADIATION
Very high energy gamma rays from the Crab nebula and pulsar N90-22527
CHANNEL CAPACITY
Traffic placement policies for a multi-band network N90-22279
CHANNEL FLOW
Flow boiling with enhancement devices for cold plate coolant channel design
[NASA-CR-186358] N90-21961
Automated analysis of measured turbulent boundary flow
[PB90-147844] N90-21970
CHANNELS (DATA TRANSMISSION)
Traffic placement policies for a multi-band network N90-22279
Alternative parallel ring protocols N90-22282
CHAOS
The intrinsic stochasticity of near-integrable Hamiltonian systems
[IPPCZ-282] N90-22386
CHARACTER RECOGNITION
Performance of the IMP array processing algorithm: First results
[RSRE-MEMO-4291] N90-22274
CHARACTERIZATION
Development of ultrasonic nondestructive methods for defect and damage characterization in composite materials N90-21816
Development of low thermal conductivity pan-based carbon fibers for solid rocket motor nozzle applications N90-21818
Preparation and characterization of Cu2ZnGeS(4-y)Se(y)
[AD-A217469] N90-22407
CHARGE COUPLED DEVICES
Space environment robot vision system N90-22245
CHARGED PARTICLES
Beam propagation in direct nuclear pumped laser amplifiers
[DE90-009613] N90-22035
CHEMICAL ANALYSIS
Aging characteristics of Li/SO(sub 2) cells
[NASA-CR-180432] N90-21954
Reactions of N2A3 sigma u + and candidates for short wavelengths lasers
[DE90-009514] N90-22033
Testing of an advanced thermochemical conversion reactor system
[DE90-007989] N90-22141
The role of automation and robotics in the Lunar-Based Chemical Analysis Laboratory
[DE90-009401] N90-22516
CHEMICAL BONDS
A comparison of the autoignition chemistry of n-butane and isobutane in an internal combustion engine
[DE90-009474] N90-21838
CHEMICAL COMPOSITION
Welding behavior and welding metallurgy of ductile intermetallic alloys
[DE90-008908] N90-21852
CHEMICAL PROPERTIES
Surface structure and chemistry of high surface area silica gels
[DE90-007684] N90-21865
CHEMICAL REACTIONS
Studies on reactive flows N90-21831
Infrared absorption spectroscopy and chemical kinetics of free radicals
[DE90-009469] N90-21837
An experimental investigation of mixing in buoyant flows N90-21963
CHEMICAL REACTORS
Testing of an advanced thermochemical conversion reactor system
[DE90-007989] N90-22141

CHINA
A Chinese bibliography on quadratic systems of differential equations
[REPT-89-39] N90-22342

CHLORIDES
Active primary lithium thionyl chloride battery for artillery applications
[DE90-009511] N90-21955

CHROMIUM OXIDES
New corrosion resistant ceramic coatings by laser processing
[AERE-R-13166] N90-21863

CIRCUITS
New flexible circuit material evaluation
[DE90-008313] N90-21866

CIRCULAR CYLINDERS
Free wave propagation in orthogonally stiffened cylinders N90-22124

CIRCUMFERENCES
Circularity measuring system: A shape gauge designed especially for use on large objects N90-22104

CIRRUS CLOUDS
Cirrus cloud optical properties measured with the University of Wisconsin high spectral resolution and volume imaging lidars N90-21932
Dynamic and microphysical characteristics of cirrus clouds as revealed by aircraft, lidar, and other observations during FIRE N90-22177

CISLUNAR SPACE
A trajectory generation and system characterization model for cislunar low-thrust spacecraft. Volume 2: Technical manual
[NASA-CR-185172] N90-21807

CLASSIFICATIONS
Recognition and analysis of aircraft targets by radar, using structural pattern representations derived from polarimetric signatures N90-21879
The association of supernovae with regions of recent star formation in late-type galaxies N90-22497

CLEAN ROOMS
Clean access platform for orbiter N90-22103

CLEANING
Clean access platform for orbiter N90-22103

CLEANLINESS
Clean access platform for orbiter N90-22103

CLEAR AIR TURBULENCE
Effect of atmospheric turbulence on electro-optical systems N90-21940

CLIMATE
Optimization of power output from wind turbines N90-22146
On three-dimensional scaling and consistent truncation of global atmospheric models N90-22164
Satellite versus GCM-simulated radiation balance: Comparisons and implications for climate modeling N90-22180
Southern oscillation simulation in coupled ocean/atmosphere global climate models N90-22181

CLIMATOLOGY
Evaporation duct effects at millimeter wavelengths N90-21914
From Penman to Makkink: A new method for the calculation of the climatological evaporation numbers
[KNMI-TR-111] N90-22161
Dynamic and microphysical characteristics of cirrus clouds as revealed by aircraft, lidar, and other observations during FIRE N90-22177
Southern oscillation simulation in coupled ocean/atmosphere global climate models N90-22181

CLOSED ECOLOGICAL SYSTEMS
Publications of the NASA Controlled Ecological Life Support System (CELSS) Program, 1979-1989
[NASA-CR-4297] N90-21754

CLOUD COVER
Satellite versus GCM-simulated radiation balance: Comparisons and implications for climate modeling N90-22180

CLOUD PHYSICS
Cirrus cloud optical properties measured with the University of Wisconsin high spectral resolution and volume imaging lidars N90-21932
Cloud chemistry and occurrence in the western United States: A synopsis of current information
[PB90-134248] N90-22182
Hail growth in a highly-glaciated central high plains multi-cellular hailstorm N90-22184

CLOUDS (METEOROLOGY)
Models of aerosols, clouds, and precipitation for atmospheric propagation studies N90-21919
Lidar measurement of concentration and turbulence in battlefield obscurants N90-21931

CLUSTER ANALYSIS
Clustering and uniqueness in mathematical models of percolation phenomena
[ETN-90-96400] N90-22358

COANDA EFFECT
Control of flow separation and mixing by aerodynamic excitation
[NASA-TM-103131] N90-21733

COASTS
Evaporation duct effects at millimeter wavelengths N90-21914
Characteristics of cumulus bandclouds off the east coast of Hawaii N90-22178

COAXIAL FLOW
Experimental observations on transition to turbulence in confined coaxial jets and other boundary layer flows
[DE90-008939] N90-22005

COBALT ISOTOPES
Modelling late-time atmospheres of supernovae N90-22500

COCKPITS
A3I visibility modeling project N90-22230

CODERS
A VLSI decomposition of the deBruijn graph N90-21895

CODING
An adaptive vector quantization scheme N90-21898
Algebraic block-structured grid generation based on a macro-block concept N90-21978
Networks for image acquisition, processing and display N90-22218
Image gathering, coding, and processing: End-to-end optimization for efficient and robust acquisition of visual information N90-22224
Ames vision group research overview N90-22242
Pyramid image codes N90-22243
FORTRAN coding guidelines
[DE90-009804] N90-22258
Geographic information system: Coded data of agrocattle-raising projects in the Amazon
[INPE-4978-PRE/1543] N90-22457

COGNITION
Visions of visualization aids: Design philosophy and experimental results N90-22220
Vision science and technology for supervised intelligent space robots N90-22221
Sparse distributed memory overview N90-22235

COHERENT RADIATION
Linear, nonlinear, and tunable guided wave modes for high-power (GaAl)As semiconductor lasers N90-22036

COLD FRONTS
Frontal structure in a mesoscale model N90-22187

COLLIMATION
Performance of the IMP array processing algorithm: First results
[RSRE-MEMO-4291] N90-22274

COLLISIONLESS PLASMAS
Rigorous upper bounds for turbulent transport in bounded systems: Passive advection and reversed-field pinches N90-22390

COLLISIONS
Computer simulation of time-dependent spherically symmetric spacetimes containing radiating fluids: Formalism and code tests N90-22483

COLOR
The intensity dependent spread model and color constancy N90-22228

COLOR VISION
Stanford/NASA-Ames Center of Excellence in model-based human performance N90-22241
Ames vision group research overview N90-22242

COMBUSTION
On the use of external burning to reduce aerospace vehicle transonic drag
[NASA-TM-103107] N90-21762
Saturated fluorescence measurements of the hydroxyl radical in laminar high-pressure flames
[NASA-CR-185218] N90-22022

COMBUSTION CHAMBERS
On the direct simulation of vortex shedding
[LR-513] N90-21743
The pyrolysis of polymethylmethacrylate during combustion in a solid fuel combustion chamber
[LR-531] N90-21845
Solid fuel combustion chamber
[LR-562] N90-21846
Solid fuel combustion chamber
[LR-591] N90-21847

COMBUSTION CHEMISTRY
Studies on reactive flows N90-21831
Ternary reactions among polymer substrate-organohalogen-antimony oxides under pyrolytic, oxidative and flaming conditions
[PB90-154766] N90-21861

COMBUSTION PRODUCTS
Device for quickly sensing the amount of O2 in a combustion product gas
[NASA-CASE-LAR-13816-1] N90-22025

COMET TAILS
The production and spatial distribution of neutral and ionized water vapor in Comet P/Halley N90-22484

COMETARY ATMOSPHERES
Kinematic models of cometary comae N90-22495

COMMERCIAL AIRCRAFT
Aircraft accident report, United Airlines Flight 811, Boeing 747-122, N4713U, Honolulu, Hawaii, February 24, 1989
[PB90-910401] N90-21748
First-order weight corrections for real-time flight path management
[LR-580] N90-21751

COMMUNICATING
Desk top publishing: What you need to know N90-22449

COMMUNICATION
NASA Information Sciences and Human Factors Program
[NASA-TM-4190] N90-22529

COMMUNICATION NETWORKS
Alternative parallel ring protocols N90-22282
Modelling high data rate communication network access protocol N90-22285
Extensibility and limitations of FDDI N90-22286
Fairness problems at the media access level for high-speed networks N90-22287
A knowledge-based system with learning for computer communication network design N90-22319
Document delivery via ISDN or satellite networks N90-22446

COMPLEX SYSTEMS
Insights into complex human performance
[DE90-006957] N90-22214

COMPLEX VARIABLES
Discrete variable structural optimization by the complex method
[LR-597] N90-22341

COMPONENT RELIABILITY
A stress-strength interference approach to fast and delayed fracture reliability analysis for ceramic components N90-21859
Reliability importance measures and their calculation
[DE90-620391] N90-22057

COMPOSITE MATERIALS
Review of analysis methods for mechanically fastened joints in composites
[LR-599] N90-22050
Institute for Materials Science and Engineering, Fracture and Deformation Division: Technical activities, 1989
[PB90-155359] N90-22106

COMPOSITE STRUCTURES
Elastodynamic scattering and transmission problems in three dimensions by the boundary integral equation method N90-22077

COMPRESSED GAS
Martensitic transformation induced by stress pulses
[DE90-009534] N90-21854

COMPRESSIBILITY
Failure mechanisms under complex loading of glass-reinforced polyester composites and their matrices: The effect of superposed hydrostatic pressures up to 300 MPa on axial tensile and compressive strengths, and in-plane shear properties of unidirtionally reinforced glass-polyester composites and the relevant polyesters N90-22072
Internal fractures in model elastomeric composites N90-22133

COMPRESSIBLE BOUNDARY LAYER
Development of a defect stream function, law of the wall/wake method for compressible turbulent boundary layers N90-22019

COMPRESSIBLE FLOW
Numerical investigation of separated transonic turbulent flows with a multiple-time-scale turbulence model
[NASA-TM-102499] N90-21962
Partial acoustic filtering applied to the equations of compressible flow
[DE90-000673] N90-22001
The calibration and measuring procedure of a five-hole hemispherical head probe in compressible flow
[LR-585] N90-22013

COMPRESSORS
WINCOF-I code for prediction of fan compressor unit with water ingestion
[NASA-CR-185157] N90-21724

COMPTON EFFECT
QCD Compton scattering at HERA energy
[NIKHEF-H/89-3] N90-22372

COMPUTATION
Fast method for computing infrared transmission, computation examples N90-21942
Bearing elastohydrodynamic lubrication: A complex calculation made simple
[NASA-TM-102575] N90-22041

The Shock and Vibration Digest, volume 21, no. 2 N90-22059

Computation and parallel implementation for early vision N90-22222

COMPUTATIONAL FLUID DYNAMICS

Numerical simulation of hypersonic flow around a space plane. Part 2: Application to high angles of attack flow [NAL-TR-1011T] N90-21726

Swept wing ice accretion modeling [NASA-TM-103114] N90-21727

Extension of a streamwise upwind algorithm to a moving grid system [NASA-TM-102800] N90-21739

Three-dimensional simulation of vortex breakdown [NASA-TM-102664] N90-21744

A multiblock/multizone code (PAB 3D-v2) for the three-dimensional Navier-Stokes equations: Preliminary applications [NASA-CR-182032] N90-21745

Analytical study of the origin and behavior of asymmetric vortices [NASA-TM-102796] N90-21746

An upwind-differencing scheme for the incompressible Navier-Stokes equations [NASA-TM-101051] N90-21757

A dual potential formulation of the Navier-Stokes equations N90-21972

Convergence acceleration of upwind relaxation methods for the Navier-Stokes equations N90-21973

Applications of Mesh Generation to Complex 3-D Configurations [AGARD-CP-464] N90-21975

Recent developments in grid generation N90-21976

Applications of algebraic grid generation N90-21979

Geometry and grids of complex configurations for aerodynamic calculation N90-21980

Mesh generation for flow computation in turbomachine N90-21981

Unsteady Euler solutions on dynamic blocked grids for complex configurations N90-21982

A structured approach to interactive multiple block grid generation N90-21983

Design and testing of a multiblock grid-generation procedure for aircraft design and research N90-21984

Grid patching approaches for complex three-dimensional configurations N90-21985

Multiblock topology specification and grid generation for complete aircraft configurations N90-21986

Three-dimensional adaptive grids with limited skewness N90-21987

Feature-associated mesh embedding for complex configurations N90-21988

On the way to an integrated mesh generation system for industrial applications N90-21989

Generation, optimization, and adaptation of multidomain meshes around complex configurations N90-21990

A discussion on issues relating to multiblock grid generation N90-21991

Automatic grid generation in complex three-dimensional configurations using a frontal system N90-21992

Unstructured finite element mesh generation and adaptive procedures for CFD N90-21993

Generation and adaptation of 3-D unstructured grids for transient problems N90-21994

Unstructured mesh generation by a generalized Delaunay algorithm N90-21995

Application of the TRANAIR rectangular grid approach to the aerodynamic analysis of complex configurations N90-21996

The solution of scattering and radiation problems for complex configurations based on 3-D grid and patch models N90-21997

High order P-G finite elements for convection-dominated problems [DE90-614743] N90-21998

Development of a computational fluid dynamics and chemistry model for the fouling of jet fuels [DE90-005664] N90-22003

Computational modeling and validation for hypersonic inlets [NASA-TM-103111] N90-22011

European research on viscous flow (EuroVisc) [NLR-TP-89077-U] N90-22014

Numerical study of laminar and turbulent flows past two-dimensional and axisymmetric bodies N90-22020

GRID2D/3D: A computer program for generating grid systems in complex-shaped two- and three-dimensional spatial domains. Part 1: Theory and method [NASA-TM-102453] N90-22262

Dynamical approach study of spurious steady-state numerical solutions of nonlinear differential equations. Part 1: The ODE connection and its implications for algorithm development in computational fluid dynamics [NASA-TM-102820] N90-22339

COMPUTATIONAL GEOMETRY

Unstructured finite element mesh generation and adaptive procedures for CFD N90-21993

COMPUTATIONAL GRIDS

Extension of a streamwise upwind algorithm to a moving grid system [NASA-TM-102800] N90-21739

Three-dimensional simulation of vortex breakdown [NASA-TM-102664] N90-21744

A multiblock/multizone code (PAB 3D-v2) for the three-dimensional Navier-Stokes equations: Preliminary applications [NASA-CR-182032] N90-21745

Applications of Mesh Generation to Complex 3-D Configurations [AGARD-CP-464] N90-21975

Recent developments in grid generation N90-21976

General structured grid generation systems N90-21977

Geometry and grids of complex configurations for aerodynamic calculation N90-21980

Mesh generation for flow computation in turbomachine N90-21981

Unsteady Euler solutions on dynamic blocked grids for complex configurations N90-21982

A structured approach to interactive multiple block grid generation N90-21983

Design and testing of a multiblock grid-generation procedure for aircraft design and research N90-21984

Grid patching approaches for complex three-dimensional configurations N90-21985

Three-dimensional adaptive grids with limited skewness N90-21987

Feature-associated mesh embedding for complex configurations N90-21988

On the way to an integrated mesh generation system for industrial applications N90-21989

Generation, optimization, and adaptation of multidomain meshes around complex configurations N90-21990

A discussion on issues relating to multiblock grid generation N90-21991

Automatic grid generation in complex three-dimensional configurations using a frontal system N90-21992

Unstructured finite element mesh generation and adaptive procedures for CFD N90-21993

Generation and adaptation of 3-D unstructured grids for transient problems N90-21994

Unstructured mesh generation by a generalized Delaunay algorithm N90-21995

Application of the TRANAIR rectangular grid approach to the aerodynamic analysis of complex configurations N90-21996

The solution of scattering and radiation problems for complex configurations based on 3-D grid and patch models N90-21997

Paving: A new approach to automated quadrilateral mesh generation [DE90-010244] N90-22260

GRID2D/3D: A computer program for generating grid systems in complex-shaped two- and three-dimensional spatial domains. Part 1: Theory and method [NASA-TM-102453] N90-22262

Local mode smoothing analysis for various incomplete factorization iterative methods in three dimensions [REPT-89-38] N90-22263

Spline function smoothing and differentiation of noisy data on a rectangular grid [DE90-009319] N90-22338

COMPUTER AIDED DESIGN

Conceptual design optimization study [NASA-CR-4298] N90-21755

Geometry and grids of complex configurations for aerodynamic calculation N90-21980

A3I visibility modeling project N90-22230

Graphically-oriented nonlinear analysis of statically loaded plane frames on microcomputers [PB90-165945] N90-22248

Engineering specification and system design for CAD/CAM of custom shoes: UMC project effort [NASA-CR-186547] N90-22255

COMPUTER AIDED MANUFACTURING

Development, implementation and test of a computer program for the production of axisymmetric pattern moulds on a numerically controlled milling machine [LR-593] N90-21877

Computerized inspection of gear tooth surfaces [NASA-TM-102395] N90-22054

Engineering specification and system design for CAD/CAM of custom shoes: UMC project effort [NASA-CR-186547] N90-22255

COMPUTER GRAPHICS

The psychology of computer displays in the modern mission control center [NASA-TM-100451] N90-22213

A3I visibility modeling project N90-22230

Graphics mini manual [NASA-TM-87622-REV] N90-22247

Graphically-oriented nonlinear analysis of statically loaded plane frames on microcomputers [PB90-165945] N90-22248

Preliminary development of an intelligent computer assistant for engine monitoring [NASA-TM-101702] N90-22322

COMPUTER NETWORKS

VCS: A networked Version Control System [DE90-009805] N90-22250

Extremely high data-rate, reliable network systems research [NASA-CR-186359] N90-22278

CSMA/RN: A universal protocol for gigabit networks N90-22280

Performance of gigabit FDDI N90-22283

Distributed simulation of network protocols N90-22284

Extensibility and limitations of FDDI N90-22286

A carrier sensed multiple access protocol for high data base rate ring networks N90-22288

SURE (Science User Resource Expert): A science planning and scheduling assistant for a resource based environment N90-22302

A knowledge-based system with learning for computer communication network design N90-22319

COMPUTER PROGRAMMING

Improving a data-acquisition software system with abstract data type components N90-21901

Resource Allocation Planning Helper (RALPH): Lessons learned N90-22296

Knowledge-based and integrated monitoring and diagnosis in autonomous power systems N90-22310

Evaluation of a proposed expert system development methodology: Two case studies N90-22320

Object-oriented databases: How are they different and what differnece does it make [REPT-89-55] N90-22459

COMPUTER PROGRAMS

WINCOF-I code for prediction of fan compressor unit with water ingestion [NASA-CR-185157] N90-21724

Prediction of forces and moments for flight vehicle control effectors. Part 2: An analysis of delta wing aerodynamic control effectiveness in ground effect [NASA-CR-186572] N90-21735

A computer program for the prediction of nozzle-propeller performance [LR-578] N90-21740

A multiblock/multizone code (PAB 3D-v2) for the three-dimensional Navier-Stokes equations: Preliminary applications [NASA-CR-182032] N90-21745

Computational simulation of structural fracture in fiber composites [NASA-TM-102505] N90-21821

METCAN verification status [NASA-TM-103119] N90-21824

Probabilistic analysis of bladed turbine disks and the effect of mistuning [NASA-TM-102564] N90-21871

Development, implementation and test of a computer program for the production of axisymmetric pattern moulds on a numerically controlled milling machine [LR-593] N90-21877

Finding the complete path and weight enumerators of convolutional codes N90-21897

A survey of the maritime-aerosol data collected at South Uist and the implications for the LOWTRAN maritime aerosol model N90-21908

The Mediterranean marine environment and its effects on aerosols and infrared transmission N90-21909

LOWTRAN 7: Status, review, and impact for short-to-long-wavelength infrared applications N90-21917

Propagation environments, effects, and decision aids N90-21918

Models of aerosols, clouds, and precipitation for atmospheric propagation studies N90-21919

Interpreting meteorological data reports for LOWTRAN Navy aerosol model extinction calculations N90-21920

Modeling millimeter-wave propagation effects in the atmosphere N90-21922

UV spectral simulations using LOWTRAN 7 N90-21928

Technique for selecting an aerosol model useful for infrared atmospheric transmittance calculations N90-21934

Calculation of IR propagation statistics in the eastern Atlantic for surveillance system performance assessment N90-21938

Atmospheric modelling studies: A modelling comparison between IR and millimetric atmospheric propagation N90-21941

Theory of a periodic cylindrical waveguide with a nonuniform metal-dielectric filling
[DE90-620099] N90-21945
General structured grid generation systems N90-21977
Algebraic block-structured grid generation based on a macro-block concept N90-21978
Mesh generation for flow computation in turbomachine N90-21981
Numerical simulation of liquid circulation in a bubbly column
[DE90-005226] N90-22002
Reliability importance measures and their calculation
[DE90-620391] N90-22057
Elastic stability and nonlinear behavior of imperfect shells with initial stresses N90-22070
Nonlinear fracture mechanics using semicircular specimens and tension-softening behavior N90-22108
ANILISA: Computational module for Koiter's imperfection sensitivity theory
[LR-582] N90-22119
A free surface Bryan-Cox-Seminer model
[IOS-270] N90-22201
Graphics mini manual
[NASA-TM-87622-REV] N90-22247
An algorithm and computer program for the calculation of envelope curves
[PB90-155409] N90-22254
Paving: A new approach to automated quadrilateral mesh generation
[DE90-010244] N90-22260
GRID2D/3D: A computer program for generating grid systems in complex-shaped two- and three-dimensional spatial domains. Part 1: Theory and method
[NASA-TM-102453] N90-22262
Software quality assurance: Towards a measurable quality improvement
[REPT-89-42] N90-22264
New algorithms for one-loop integrals
[NIKHEF-H/89-17] N90-22268
Inventory of program packages related to the project SIMONA
[ETN-90-96397] N90-22270
Traffic placement policies for a multi-band network N90-22279
Distributed simulation, no special tools required N90-22281
The WAVE model for advanced knowledge processing
[OUEL-1803/89] N90-22291
The art of fault-tolerant system reliability modeling
[NASA-TM-102623] N90-22292
PLAN-IT-2: The next generation planning and scheduling tool N90-22298
Space communications scheduler: A rule-based approach to adaptive deadline scheduling N90-22300
Simulation-based reasoning about the physical propagation of fault effects N90-22309
Automated procedure execution for space vehicle autonomous control N90-22314
Bounded-time fault-tolerant rule-based systems N90-22318
The Weapons Laboratory technical library: Automating with STILAS N90-22447
Update on the OPAL opacity code
[DE90-009946] N90-22480
The modeling of IRAS detections of classical novae and related objects N90-22482

COMPUTER STORAGE DEVICES
Two-dimensional shape recognition using sparse distributed memory N90-22227
Sparse distributed memory overview N90-22235
Understanding the computing system domain of advanced computing with microcomputers
[DE90-009825] N90-22251

COMPUTER SYSTEMS DESIGN
Resource Allocation Planning Helper (RALPH): Lessons learned N90-22296
The role of artificial intelligence techniques in scheduling systems N90-22297
Evaluation of a proposed expert system development methodology: Two case studies N90-22320
Applications to the aerospace and defense R and D community: The DOD computer-aided acquisition and logistics support (CALS) initiative N90-22453

COMPUTER SYSTEMS PERFORMANCE
Extremely high data-rate, reliable network systems research
[NASA-CR-186359] N90-22278
Performance of gigabit FDDI N90-22283
Distributed simulation of network protocols N90-22284
A carrier sensed multiple access protocol for high data base rate ring networks N90-22288
NASA ground terminal communication equipment automated fault isolation expert systems N90-22305
Simulation-based reasoning about the physical propagation of fault effects N90-22309
Evaluation of a proposed expert system development methodology: Two case studies N90-22320

COMPUTER SYSTEMS PROGRAMS
Software quality assurance: Towards a measurable quality improvement
[REPT-89-42] N90-22264
An introduction to selected structured methods
[RSRE-MEMO-4294] N90-22275

COMPUTER TECHNIQUES
A study of caching in capability computers
[RSRE-89015] N90-22276
The role of artificial intelligence techniques in scheduling systems N90-22297
Polarization coupling in the acousto-optic interaction of surface waves N90-22365
Electronic Transfer of Information and its Impact on Aerospace and Defence Research and Development
[AGARD-CP-466] N90-22440
Electronic publishing with Standard Generalized Markup Language (SGML) N90-22450
Applications to the aerospace and defense R and D community: The DOD computer-aided acquisition and logistics support (CALS) initiative N90-22453
Electronic transfer of information applications in the Societe Aerospatiale N90-22454
NASA Information Sciences and Human Factors Program
[NASA-TM-4190] N90-22529

COMPUTER VISION
Vision Science and Technology at NASA: Results of a Workshop
[NASA-TM-102214-REV-1] N90-22216
Parallel asynchronous hardware implementation of image processing algorithms N90-22219
Vision science and technology for supervised intelligent space robots N90-22221
Computation and parallel implementation for early vision N90-22222
Intensity dependent spread theory N90-22223
Image gathering, coding, and processing: End-to-end optimization for efficient and robust acquisition of visual information N90-22224
Hybrid vision activities at NASA Johnson Space Center N90-22225
Two-dimensional shape recognition using sparse distributed memory N90-22227
The intensity dependent spread model and color constancy N90-22228
Algorithms and architectures for robot vision N90-22236
Computer vision techniques for rotorcraft low altitude flight N90-22237
Computer vision research at Marshall Space Flight Center N90-22240
Ames vision group research overview N90-22242
Space environment robot vision system N90-22245
Object detection using structural matching
[INPE-4954-PRE/1532] N90-22333

COMPUTERIZED SIMULATION
Swept wing ice accretion modeling
[NASA-TM-103114] N90-21727
Three-dimensional simulation of vortex breakdown
[NASA-TM-102664] N90-21744
A comparison of time-optimal interception trajectories for the F-8 and F-15
[NASA-CR-186300] N90-21753
Quiet mode for nonlinear rotor models
[NASA-TM-102236] N90-21758
Optimal control of an aircraft flying through a downburst N90-21765
Computational simulation of structural fracture in fiber composites
[NASA-TM-102505] N90-21821
Progression of damage and fracture in composites under dynamic loading
[NASA-TM-103118] N90-21825
QPSK carrier-acquisition performance in the advanced receiver 2 N90-21892
UV spectral simulations using LOWTRAN 7 N90-21928
Computer simulation of ionospheric radio frequency heating
[DE90-009478] N90-21944
Experimental and analytical investigations of granular materials: Shear flow and convective heat transfer N90-21968
A dual potential formulation of the Navier-Stokes equations N90-21972
Design and testing of a multiblock grid-generation procedure for aircraft design and research N90-21984
Generation and adaptation of 3-D unstructured grids for transient problems N90-21994
Practical nonlinear simulation of rotating machinery dynamics with application to turbine blade rubbing N90-22038
Lagrangian model simulation of the turbulent transport of evaporating jet droplets N90-22168
Southern oscillation simulation in coupled ocean/atmosphere global climate models N90-22181
Frontal structure in a mesoscale model N90-22187
Molecular dynamics simulations of short-range force systems on 1024-node hypercubes
[DE90-009833] N90-22259
Inventory of program packages related to the project SIMONA
[ETN-90-96397] N90-22270
Extremely high data-rate, reliable network systems research
[NASA-CR-186359] N90-22278
Traffic placement policies for a multi-band network N90-22279
Distributed simulation, no special tools required N90-22281
Alternative parallel ring protocols N90-22282
Distributed simulation of network protocols N90-22284
Modelling high data rate communication network access protocol N90-22285
Adaptive control of a flexible manipulator with unknown changing loads N90-22293
Simulation-based reasoning about the physical propagation of fault effects N90-22309
An expert system for simulating electric loads aboard Space Station Freedom
[NASA-TM-103150] N90-22325
Engagement analysis study
[DE90-009529] N90-22359
Hybrid modeling of plasmas and applications to fusion and space physics N90-22387
Three-dimensional simulations of simple electron drift wave turbulence in tokamak geometry
[DE90-009581] N90-22398
Computer simulation of time-dependent spherically symmetric spacetimes containing radiating fluids: Formalism and code tests N90-22483
A galaxy formation cookbook: Recipes and utensils N90-22508

COMPUTERS
Graphics mini manual
[NASA-TM-87622-REV] N90-22247
Computer conferencing: Minds meeting anywhere anytime N90-22452

CONCENTRIC CYLINDERS
Effect of a crystal-melt interface on Taylor-vortex flow
[NASA-CR-186512] N90-22408

CONDITIONING (LEARNING)
Excitatory and inhibitory backward conditioning in the rat N90-22204

CONDUCTIVE HEAT TRANSFER
Inverse problems of heat conduction N90-21969

CONDUCTORS
Current management for improved railgun performance N90-21781

CONES (VOLCANOES)
Geology of coronae and domal structures on Venus and models of their origin N90-22513

CONFERENCES
Free-Space Power Transmission
[NASA-CP-10016] N90-21795
Proceedings of the Advisory Committee on Standardization of Carbon-Phenolic Test Methods and Specifications
[NASA-CR-186478] N90-21817
Applications of Mesh Generation to Complex 3-D Configurations
[AGARD-CP-464] N90-21975
Recent developments in grid generation N90-21976
The 24th Aerospace Mechanisms Symposium
[NASA-CP-3062] N90-22079
Proceedings of the Conference on Technology-Based Confidence Building: Energy and Environment
[CNSS-PAPERS-22] N90-22152
Topical Conference on the Origin of the Earth
[NASA-CR-185061] N90-22166
Proceedings of the 6th Regional Symposium on Biophysics
[DE90-619618] N90-22206
Vision Science and Technology at NASA: Results of a Workshop
[NASA-TM-102214-REV-1] N90-22216
The 1990 Goddard Conference on Space Applications of Artificial Intelligence
[NASA-CP-3068] N90-22294
Impurity control in toroidal devices
[DE90-618585] N90-22399
Space Station Workshop: Commercial Missions and User Requirements
[NASA-TM-102912] N90-22428

Computer conferencing: Minds meeting anywhere anytime N90-22452

CONFIDENCE LIMITS
Uncertainty analysis of the accident effect area of a BLEVE [REPT-89-49] N90-22160

CONFIGURATION MANAGEMENT
A soft actuation system for segmented reflector articulation and isolation N90-22084
Analyzing spacecraft configurations through specialization and default reasoning N90-22308

CONFINEMENT
Thermomechanically-induced convective motion and natural convection in confined gaseous helium subjected to boundary heating N90-21960
Laser Doppler anemometry measurements of a confined turbulent water jet with a uniform background flow N90-21971
Experimental observations on transition to turbulence in confined coaxial jets and other boundary layer flows [DE90-008939] N90-22005

CONFORMAL MAPPING
Generation, optimization, and adaptation of multidomain meshes around complex configurations N90-21990

CONGRESSIONAL REPORTS
Managing Federal information resources [PB90-100173] N90-22429

CONICAL SHELLS
The initial imperfection databank at the Delft University of Technology, part 3 [LR-568] N90-21783

CONNECTORS
The resupply interface mechanism RMS compatibility test N90-22090
The connector space reduction mechanism N90-22092

CONSERVATION EQUATIONS
Prediction of length scales in a Mach reflection flowfield N90-21959

CONSERVATION LAWS
Numerical simulation model of hydrazine attitude control thrusters [INPE-4965-PRE/1534] N90-21848
Topics in vortex methods for the computation of three- and two-dimensional incompressible unsteady flows N90-21967
A weak formulation for phase-change problems with bulk movement due to unequal densities [DE90-009398] N90-22361

CONSTRAINTS
Constraint-based evaluation of sequential procedures N90-22301

CONSTRUCTION
A robotically constructed production and supply base on Phobos [NASA-CR-186234] N90-21872

CONTACT LOADS
Analysis of a finite two-dimensional solid with an inclined crack and a rigid inclusion N90-22127

CONTAMINATION
Clean access platform for orbiter N90-22103

CONTINENTAL SHELVES
An investigation of meteorological effects on currents in the shelf and continental slope seas northwest of the United Kingdom. 2: Relationships between currents at different locations and with other variables [PB90-151911] N90-22195

CONTINUUM MECHANICS
Finite element analysis of elastic contact problems with friction N90-22040
A study of creep damage using microradiography and continuum damage mechanics N90-22109

CONTINUUM MODELING
A continuum damage model for the quasi-static response of brittle materials [DE90-007681] N90-22112

CONTOURS
Topics in vortex methods for the computation of three- and two-dimensional incompressible unsteady flows N90-21967

CONTROL EQUIPMENT
Prediction of forces and moments for flight vehicle control effectors. Part 1: Validation of methods for predicting hypersonic vehicle controls forces and moments [NASA-CR-186571] N90-21734
Prediction of forces and moments for flight vehicle control effectors. Part 2: An analysis of delta wing aerodynamic control effectiveness in ground effect [NASA-CR-186572] N90-21735
Development of the methods and means of precise forming and geometry control of superconducting current-carrying element for the UNR pulsed dipoles [DE90-620108] N90-22419

CONTROL STABILITY
A robust stability result for generalised predictive control [OUEL-1773/89] N90-22330

CONTROL STICKS
Development of a multipurpose hand controller for JEMRMS N90-22087

CONTROL SURFACES
Prediction of forces and moments for flight vehicle control effectors. Part 1: Validation of methods for predicting hypersonic vehicle controls forces and moments [NASA-CR-186571] N90-21734

CONTROL SYSTEMS DESIGN
Microwave Landing System (MLS) remote monitoring subsystem/remote maintenance monitoring system [DOT/FAA/PS-89/2] N90-21749
Advances in optimal active control techniques for aerospace systems; application to aircraft active landing gear N90-21769
A decentralized linear quadratic control design method for flexible structures N90-21770
Balanced bridge feedback control system [NASA-CASE-NPO-17430-1-CU] N90-21951
A methodology for knowledge-based restructurable control to accommodate system failures N90-22058
Relatchable launch restraint mechanism for deployable booms N90-22091
VCS: A networked Version Control System [DE90-009805] N90-22250
The art of fault-tolerant system reliability modeling [NASA-TM-102623] N90-22292
Adaptive control of a flexible manipulator with unknown changing loads N90-22293
System control of an autonomous planetary mobile spacecraft N90-22313
An intelligent interface for the design of optimal control systems [INPE-4917-PRE/1516] N90-22332

CONTROL THEORY
Optimal and near-optimal medium range air-to-air missile guidance against maneuvering targets N90-21766
Advances in optimal active control techniques for aerospace systems; application to aircraft active landing gear N90-21769
Nonlinear stability analysis and control of dynamical robotic systems N90-22037
Perturbation techniques in the dynamics and control of flexible manipulators [OUEL-1772/89] N90-22053
On the existence of a positive definite solution of the matrix equation X + A(sup tau)X(exp -1)A = I [PB90-133976] N90-22335

CONTROLLED FUSION
Hybrid modeling of plasmas and applications to fusion and space physics N90-22387

CONTROLLERS
A comparison of time-optimal interception trajectories for the F-8 and F-15 [NASA-CR-186300] N90-21753
A decentralized linear quadratic control design method for flexible structures N90-21770
Bi-directional thruster development and test report [NASA-CR-182013] N90-21785
An 8.4-GHz dual-maser front-end system for Parkes reimplementation N90-21905
Nonlinear stability analysis and control of dynamical robotic systems N90-22037
Development of a multipurpose hand controller for JEMRMS N90-22087
A new six-degree-of-freedom force-reflecting hand controller for space telerobotics N90-22089

CONVECTION
Analytical study of the origin and behavior of asymmetric vortices [NASA-TM-102796] N90-21746
Thermomechanically-induced convective motion and natural convection in confined gaseous helium subjected to boundary heating N90-21960
The relationship between the buoyancy of near-surface air and the potential temperature of the tropopause N90-22165
Current drive in a supernova N90-22491

CONVECTION CLOUDS
Second National Winter Weather Workshop Conducted by the National Weather Service [PB90-147414] N90-22183

CONVECTIVE FLOW
High order P-G finite elements for convection-dominated problems [DE90-614743] N90-21998
A linear analysis of monsoon base states associated with banded convection N90-22179

CONVECTIVE HEAT TRANSFER
Experimental and analytical investigations of granular materials: Shear flow and convective heat transfer N90-21968
Frontal structure in a mesoscale model N90-22187
Effect of a crystal-melt interface on Taylor-vortex flow [NASA-CR-186512] N90-22408
Sulphur silicate interactions on the Jovian satellite Io N90-22515

CONVERGENCE
Convergence acceleration of upwind relaxation methods for the Navier-Stokes equations N90-21973
High order P-G finite elements for convection-dominated problems [DE90-614743] N90-21998

CONVERSATION
A study of mental models through communication between users and advisors solving software manipulation problems N90-22434

COOLING SYSTEMS
Flow boiling with enhancement devices for cold plate coolant channel design [NASA-CR-186358] N90-21961

COORDINATE TRANSFORMATIONS
Self-calibration of robot-sensor system N90-22246
Generalized killing equations and symmetries of spinning space [NIKHEF-H/89-8] N90-22375

COPOLYMERS
Stability studies of a pH-sensitive polymer matrix: Applications to fiber optic pH sensors [DE90-009579] N90-21867

COPPER
Preparation and characterization of Cu2ZnGeS(4-y)Se(y) [AD-A217469] N90-22407

COPPER OXIDES
Growth and patterning of laser ablated superconducting YBa2Cu3O7 films on LaAlO3 substrates [NASA-TM-102436] N90-22421

CORNER FLOW
Graphs of the state of stress at rounded corners [MEMT-1] N90-22122

CORONAL LOOPS
Cyclotron maser and plasma wave growth in magnetic loops [NASA-CR-179862] N90-22402

CORONAS
Geology of coronae and domal structures on Venus and models of their origin N90-22513
Slow shocks in coronal mass ejections [NASA-CR-186578] N90-22522

CORRECTION
First-order weight corrections for real-time flight path management [LR-580] N90-21751
Computerized inspection of gear tooth surfaces [NASA-TM-102395] N90-22054

CORRELATION
Motion detection in astronomical and ice floe images N90-22231

CORRELATION COEFFICIENTS
Spectral response of wheat and its relationship with agronomic variables in the tropical region [INPE-5018-RPE/612] N90-22138
Field reports on radiometric campaigns of soybeans in the Federal district: Safra 88/89 [INPE-5021-RPE/615] N90-22139

CORROSION PREVENTION
New corrosion resistant ceramic coatings by laser processing [AERE-R-13166] N90-21863

CORROSION RESISTANCE
New corrosion resistant ceramic coatings by laser processing [AERE-R-13166] N90-21863

COSMIC DUST
The optical night sky at low surface brightness: High latitude dust and faint field galaxies N90-22481
The Sagittarius B2 molecular cloud: An extreme case of a galactic center giant molecular cloud N90-22493

COSMIC RAY SHOWERS
Very high energy gamma rays from the Crab nebula and pulsar N90-22527

COSMIC RAYS
Gamma rays, cosmic rays, and local molecular clouds N90-22524
Ultrahigh-energy particle flux from cosmic strings [NASA-CR-186592] N90-22525
Very high energy gamma rays from the Crab nebula and pulsar N90-22527

COSMOLOGY
Numerical investigations of nonlinear behavior in the Einstein equations N90-22427
Stability of compactification during inflation [NASA-CR-186597] N90-22502

Gravitational effects of global textures [NASA-CR-186596] N90-22503
Gravitational couplings of the inflation in extended inflation [NASA-CR-186595] N90-22504
Topological defects in extended inflation [NASA-CR-186594] N90-22505
Soft inflation [NASA-CR-186593] N90-22506
Ultrahigh-energy particle flux from cosmic strings [NASA-CR-186592] N90-22525

COST EFFECTIVENESS
Optimization of power output from wind turbines N90-22146
Evaluation of optical storage technology for decision support databases N90-22436

COSTS
An all electronic transportation system from LEO to GEO and beyond N90-21796
Space Shuttle, NASA's major changes to flight hardware: Fact sheet for the Chairman, Committee on Science, Space, and Technology, House of Representatives [GAO/NSIAD-88-173FS] N90-22461

COUETTE FLOW
Effect of a crystal-melt interface on Taylor-vortex flow [NASA-CR-186512] N90-22408

COULOMB COLLISIONS
Current drive in a supernova N90-22491

COULOMB POTENTIAL
Elastic and viscoelastic analysis of two multiply layered cylinders rolling over each other with Coulomb friction [REPT-89-50] N90-22051
New calculations and measurements of the Coulomb cross-section for the production of direct electron pairs by high energy nuclei [NASA-TM-101280] N90-22371

COUNTER ROTATION
Studies on reactive flows N90-21831
Unsteady Euler solutions on dynamic blocked grids for complex configurations N90-21982

COUNTERMEASURES
Atmospheric Propagation in the UV, Visible, IR, and mm-Wave Region and Related Systems Aspects [AGARD-CP-454] N90-21907
Computation of broad spectral band electro-optical system transmittance response characteristics to military smokes and obscurants using field test data from transmissometer system measurements N90-21939

COUPLING
Relatchable launch restraint mechanism for deployable booms N90-22091

COUPLINGS
The connector space reduction mechanism N90-22092

CRAB NEBULA
Very high energy gamma rays from the Crab nebula and pulsar N90-22527

CRACK CLOSURE
Three-dimensional fatigue crack closure behavior of metals N90-21857

CRACK PROPAGATION
Energy release rate analysis of interfacial cracks in composites N90-21829
Contact mechanics for three-dimensional geometries N90-22076
Combining acoustic emission locations and a microcrack damage model to study development of damage in brittle materials [DE90-005195] N90-22111
A continuum damage model for the quasi-static response of brittle materials [DE90-007681] N90-22112
Inclusion of unstable ductile tearing and extrapolated crack-arrest toughness data in PWR vessel integrity assessment [DE90-009427] N90-22116
Fatigue crack growth in unidirectional metal matrix composite [NASA-TM-103102] N90-22117
Fatigue crack growth predictions for variable-amplitude and spectrum loading [LR-526] N90-22118
Green's functions for the elastic annulus and their application to various crack problems N90-22129

CRACK TIPS
Energy release rate analysis of interfacial cracks in composites N90-21829
Natural modes of cracked beams and identification of cracks N90-22075
Analysis of a finite two-dimensional solid with an inclined crack and a rigid inclusion N90-22127
An investigation into the foundations of elastic-plastic fracture mechanics N90-22130

CRACKS
Structural fatigue in the 34-meter HA-Dec antennas N90-21902
The classification of defects from ultrasonic measurements [AERE-R-13306] N90-22056
Natural modes of cracked beams and identification of cracks N90-22075
Contact mechanics for three-dimensional geometries N90-22076
Combining acoustic emission locations and a microcrack damage model to study development of damage in brittle materials [DE90-005195] N90-22111
Dynamic response of a complex encapsulated electronic assembly subjected to a severe shock environment [DE90-007689] N90-22114
Inclusion of unstable ductile tearing and extrapolated crack-arrest toughness data in PWR vessel integrity assessment [DE90-009427] N90-22116
The stress field due to an edge dislocation and some fracture problems for a three-phase composite cylinder model N90-22126
Analysis of a finite two-dimensional solid with an inclined crack and a rigid inclusion N90-22127
Green's functions for the elastic annulus and their application to various crack problems N90-22129
An investigation into the foundations of elastic-plastic fracture mechanics N90-22130

CREEP PROPERTIES
A study of creep damage using microradiography and continuum damage mechanics N90-22109

CREW PROCEDURES (INFLIGHT)
Simulation-based reasoning about the physical propagation of fault effects N90-22309

CRITERIA
Green's functions for the elastic annulus and their application to various crack problems N90-22129

CRITICAL LOADING
Failure mechanisms under complex loading of glass-reinforced polyester composites and their matrices: The effect of superposed hydrostatic pressures up to 300 MPa on axial tensile and compressive strengths, and in-plane shear properties of unidirtionally reinforced glass-polyester composites and the relevant polyesters N90-22072

CROSS FLOW
The interaction between a plane shock wave and a cylindrical afterbody N90-21728

CRUISING FLIGHT
An approach to on-board optimization of cruise at constant altitude [LR-581] N90-21752

CRUSTAL FRACTURES
In-situ fracture stiffness determination [DE90-009202] N90-22173

CRYOGENIC EQUIPMENT
A refrigerated Dewar for the Josephson array voltage calibration system [DE90-005237] N90-22412

CRYOGENIC FLUIDS
Scattered-light scanner measurements of cryogenic liquid-jet breakup [NASA-TM-102432] N90-22021

CRYOGENICS
Ultralow noise performance of an 8.4-GHz maser-feedhorn system N90-21889
Institute for Materials Science and Engineering, Fracture and Deformation Division: Technical activities, 1989 [PB90-155359] N90-22106
A refrigerated Dewar for the Josephson array voltage calibration system [DE90-005237] N90-22412

CRYSTAL GROWTH
Linear, nonlinear, and tunable guided wave modes for high-power (GaAl)As semiconductor lasers N90-22036
UV photo-enhanced MOCVD of cadmium and cadmium telluride [RSRE-MEMO-4208] N90-22422

CRYSTAL LATTICES
Improved crystal bending techniques applied to the LLNL dual-arm Johann mounting x ray spectrometer [DE90-009528] N90-22415

CRYSTAL STRUCTURE
In-situ pulsed laser deposition of high-T(sub c) YBa(sub 2)Cu(sub 3)O(sub 7) superconducting thin films on (100) LaAlO3 substrates [DE90-009861] N90-22418

CRYSTALLIZATION
Interfacial studies in fiber-reinforced thermoplastic-matrix composites N90-21814

CRYSTALS
Transient effects in Brillouin gain spectroscopy in solids [DE90-009476] N90-21839
High resolution stimulated Raman-Brillouin spectroscopy in gases and solids [DE90-009535] N90-21840
Brillouin gain spectroscopy in glasses and crystals [DE90-009536] N90-21841
Photovoltaic Program Branch [DE90-000318] N90-22142
Effect of a crystal-melt interface on Taylor-vortex flow [NASA-CR-186512] N90-22408
Improved crystal bending techniques applied to the LLNL dual-arm Johann mounting x ray spectrometer [DE90-009528] N90-22415

CULTURE TECHNIQUES
Research in biological separations and cell culture [NASA-CR-172060] N90-22202

CUMULUS CLOUDS
Characteristics of cumulus bandclouds off the east coast of Hawaii N90-22178

CURRENT CONVERTERS (AC TO DC)
Voltage source ac-to-dc converters for high-power transmitters N90-21886

CURRENT DENSITY
Hollow cathode operation at high discharge currents [NASA-CR-185238] N90-21953
MHD channel development, part 1 [DE90-009549] N90-22394

CURRENT SHEETS
Slow shocks in coronal mass ejections [NASA-CR-186578] N90-22522

CURVE FITTING
Identification of XV-15 aeroelastic modes using frequency-domain methods [NASA-TM-101021] N90-21756
An algorithm and computer program for the calculation of envelope curves [PB90-155409] N90-22254
The approximation of a composite Bezier cubic curve by a composite Bezier quadratic curve [NPL-DITC-147/89] N90-22354

CURVED BEAMS
Numerical solutions of the nonlinear theory of curved beams N90-22071

CYANIDES
A comparison of photospheric and circumstellar (HCN)/(CO)-ratios for bright carbon stars [PB90-151101] N90-22477

CYBERNETICS
Guide to RMS-literature [REPT-89-52] N90-22326

CYCLIC LOADS
Cycle life machine for AX-5 space suit N90-22080
Probabilistic finite elements: Applications to fracture and fatigue N90-22134
Rotor loading on a three-bladed wind turbine N90-22145

CYCLOGENESIS
Semigeostrophic flow over orography in a stratified rotating atmosphere N90-22163
Second National Winter Weather Workshop Conducted by the National Weather Service [PB90-147414] N90-22183

CYCLONES
Tropopause undulations and the development of extratropical cyclones N90-22186

CYCLOTRON RADIATION
Operation of a step tunable megawatt gyrotron N90-21802
Cyclotron maser and plasma wave growth in magnetic loops [NASA-CR-179862] N90-22402

CYCLOTRON RESONANCE DEVICES
Free-Space Power Transmission [NASA-CP-10016] N90-21795
Analysis of a high harmonic rectangular gyrotron using ribbon beams N90-21801
Operation of a step tunable megawatt gyrotron N90-21802
The 10-100 kW submillimeter gyrotron N90-21803
High power millimeter wave source development program N90-21805

CYLINDRICAL BODIES
The interaction between a plane shock wave and a cylindrical afterbody N90-21728
Theory of a periodic cylindrical waveguide with a nonuniform metal-dielectric filling [DE90-620099] N90-21945
On the theory of Heiser and Shercliff experiment. Part 2: MHD flow between two cylinders in strong radical magnetic field [OUEL-1805/89-PT-2] N90-22401

CYLINDRICAL PLASMAS
Rigorous upper bounds for turbulent transport in bounded systems: Passive advection and reversed-field pinches N90-22390

CYLINDRICAL SHELLS
Transient response of a cylindrical shell of finite length to transverse impact [OUEL-1780/89] N90-22123

D

DAMAGE
Advances in optimal active control techniques for aerospace systems; application to aircraft active landing gear N90-21769
Current management for improved railgun performance N90-21781
Progression of damage and fracture in composites under dynamic loading
[NASA-TM-103118] N90-21825
An assessment of the hardness of miniature vacuum tubes to high-voltage transients
[DE90-009541] N90-21956
Natural modes of cracked beams and identification of cracks N90-22075
A continuum damage model for the quasi-static response of brittle materials
[DE90-007681] N90-22112

DAMAGE ASSESSMENT
The controlled-damage concept in design of laminated composites N90-21830
A study of creep damage using microradiography and continuum damage mechanics N90-22109

DAMPING
Robust control of flexible structures N90-21784
The Shock and Vibration Digest, volume 21, no. 1 N90-22061
Elastic stability and nonlinear behavior of imperfect shells with initial stresses N90-22070
An investigation of the generation and radiation of aerodynamic noise in real piping systems N90-22368

DARK MATTER
The mass of the Coma cluster N90-22496

DARKENING
Auroral ultraviolet darkening on the outer planets N90-22518

DATA ACQUISITION
Enhanced Low Level Wind Shear (LLWAS) 6-sensor improvement user's manual for data processing of field data
[DOT/FAA/CT-TN90/8] N90-21759
The Telecommunications and Data Acquisition Report
[NASA-CR-186479] N90-21880
Improving a data-acquisition software system with abstract data type components N90-21901
Small strain gage applications 2
[DE90-008312] N90-22026
The AGRISCATT-87 campaign: Processing of the Dutscat data
[BCRS-89-20] N90-22140
Site visit to US Antarctic Program (USAP) facilities and the Research Vessel Polar Duke
[DE90-009396] N90-22159
Regional wind energy assessment
[DE90-009380] N90-22192
Networks for image acquisition, processing and display N90-22218
How to get it: A guide to defense-related information resources
[AD-A201600] N90-22433

DATA BASE MANAGEMENT SYSTEMS
Object-oriented databases: How are they different and what differnece does it make
[REPT-89-55] N90-22459

DATA BASES
The initial imperfection databank at the Delft University of Technology, part 3
[LR-568] N90-21783
Calculation of IR propagation statistics in the eastern Atlantic for surveillance system performance assessment N90-21938
The computational structural mechanics testbed data library description
[NASA-TM-100645-REV-1] N90-22135
Computer vision techniques for rotorcraft low altitude flight N90-22237
Evaluation of optical storage technology for decision support databases N90-22436
The Weapons Laboratory technical library: Automating with STILAS N90-22447
Electronic mail systems N90-22451
Applications to the aerospace and defense R and D community: The DOD computer-aided acquisition and logistics support (CALS) initiative N90-22453
Electronic transfer of information applications in the Societe Aerospatiale N90-22454
NSSDC data listing
[NASA-TM-102989] N90-22456
Object-oriented databases: How are they different and what differnece does it make
[REPT-89-55] N90-22459
SGTE data for pure elements
[NPL-DMA(A)-195] N90-22460
Update on the OPAL opacity code
[DE90-009946] N90-22480
The modeling of IRAS detections of classical novae and related objects N90-22482

DATA LINKS
Microwave Landing System (MLS) remote monitoring subsystem/remote maintenance monitoring system
[DOT/FAA/PS-89/2] N90-21749
Microwave Landing System (MLS) multiple system design interoperability interface control report
[DOT/FAA/SA-89/2] N90-21750

DATA MANAGEMENT
A study of caching in capability computers
[RSRE-89015] N90-22276
The application of connectionism to query planning/scheduling in intelligent user interfaces N90-22295
Using expert systems to implement a semantic data model of a large mass storage system N90-22315

DATA PROCESSING
Enhanced Low Level Wind Shear (LLWAS) 6-sensor improvement user's manual for data processing of field data
[DOT/FAA/CT-TN90/8] N90-21759
The AGRISCATT-87 campaign: Processing of the Dutscat data
[BCRS-89-20] N90-22140
The WAVE model for advanced knowledge processing
[OUEL-1803/89] N90-22291
Spline function smoothing and differentiation of noisy data on a rectangular grid
[DE90-009319] N90-22338
The approximation of a composite Bezier cubic curve by a composite Bezier quadratic curve
[NPL-DITC-147/89] N90-22354
The use of local polynomial approximations in a knot-placement strategy for least squares spline fitting
[NPL-DITC-148/89] N90-22355
The automation plan of the General Directorate 1 (search) of the European Patent Office N90-22448

DATA REDUCTION
A VLSI design for a systolic Viterbi decoder N90-21899

DATA SAMPLING
Calculating the time domain average of gear vibration data sampled at less than the Nyquist frequency
[OUEL-1768/89] N90-22052

DATA SMOOTHING
Local mode smoothing analysis for various incomplete factorization iterative methods in three dimensions
[REPT-89-38] N90-22263

DATA STORAGE
Using expert systems to implement a semantic data model of a large mass storage system N90-22315

DATA STRUCTURES
Knowledge structure representation and automated updates in intelligent information management systems N90-22316
Document delivery via ISDN or satellite networks N90-22446

DATA SYSTEMS
NSSDC data listing
[NASA-TM-102989] N90-22456
NASA Information Sciences and Human Factors Program
[NASA-TM-4190] N90-22529

DATA TRANSMISSION
Microwave Landing System (MLS) remote monitoring subsystem/remote maintenance monitoring system
[DOT/FAA/PS-89/2] N90-21749
Scalable coherent interface
[DE90-008011] N90-22277
Extremely high data-rate, reliable network systems research
[NASA-CR-186359] N90-22278
Performance of gigabit FDDI N90-22283
Modelling high data rate communication network access protocol N90-22285
Extensibility and limitations of FDDI N90-22286
A carrier sensed multiple access protocol for high data base rate ring networks N90-22288
Technologies for electronic transfer of information: The present state and trends in Europe N90-22441
Technology for electronic transfer of information: The present and future in North America N90-22442
Megatendances N90-22445
Document delivery via ISDN or satellite networks N90-22446

DAYTIME
Daytime wind valleys adjacent to the Great Salt Lake
[DE90-008991] N90-22190

DECAMETRIC WAVES
Jupiter's drifting decametric bursts with the changing time scale
[DE90-618870] N90-22517

DECISION MAKING
Insights into complex human performance
[DE90-006957] N90-22214

DECISION THEORY
Recognition and analysis of aircraft targets by radar, using structural pattern representations derived from polarimetric signatures N90-21879

DECLINATION
Galileo Earth approach navigation using connected-element interferometer phase-delay tracking N90-21884

DECODERS
A VLSI decomposition of the deBruijn graph N90-21895
Validity of the two-level model for Viterbi decoder gap-cycle performance N90-21896
Finding the complete path and weight enumerators of convolutional codes N90-21897
A VLSI design for a systolic Viterbi decoder N90-21899

DECODING
A VLSI decomposition of the deBruijn graph N90-21895
An adaptive vector quantization scheme N90-21898
A VLSI design for a systolic Viterbi decoder N90-21899
On decoding of multi-level MPSK modulation codes
[NASA-CR-186601] N90-22261

DECOMPOSITION
Conceptual design optimization study
[NASA-CR-4298] N90-21755
A discussion on issues relating to multiblock grid generation N90-21991

DECOUPLING
Relatchable launch restraint mechanism for deployable booms N90-22091

DEEP SPACE NETWORK
The Telecommunications and Data Acquisition Report
[NASA-CR-186479] N90-21880
Precise estimation of tropospheric path delays with GPS techniques N90-21881
The determination of maximum deep space station slew rates for a high Earth orbiter N90-21882
Microwave analog fiber-optic link for use in the deep space network N90-21883
Galileo Earth approach navigation using connected-element interferometer phase-delay tracking N90-21884
Voltage source ac-to-dc converters for high-power transmitters N90-21886
A real-time signal combining system for Ka-band feed arrays using maximum-likelihood weight estimates N90-21888
Radiometric tests on wet and dry antenna reflector surface panels N90-21890
A functional description of the advanced receiver N90-21891
A VLSI decomposition of the deBruijn graph N90-21895
Radar RFI at Goldstone DSS 12 and DSS 16 N90-21900
Structural fatigue in the 34-meter HA-Dec antennas N90-21902
A higher density VLBI catalog for navigating Magellan and Galileo N90-21904
An 8.4-GHz dual-maser front-end system for Parkes reimplementation N90-21905

DEFECTS
The initial imperfection databank at the Delft University of Technology, part 3
[LR-568] N90-21783
Development of ultrasonic nondestructive methods for defect and damage characterization in composite materials N90-21816
The classification of defects from ultrasonic measurements
[AERE-R-13306] N90-22056
Positron trapping in semiconductors
[PB90-165606] N90-22410
Topological defects in extended inflation
[NASA-CR-186594] N90-22505

DEFENSE PROGRAM
The Weapons Laboratory technical library: Automating with STILAS N90-22447

DEFLECTION
Internal fractures in model elastomeric composites N90-22133

DEFORMATION
Residual stresses in laminated thermoplastic matrix composites N90-21815
The effect of hydrogen and microstructure on the deformation and fracture behavior of a single crystal nickel-base superalloy
[NASA-CR-185219] N90-21849
Nonlinear spline operator interpolation and sliding control of deformable maneuvering bodies N90-21878

Combining acoustic emission locations and a microcrack damage model to study development of damage in brittle materials
[DE90-005195] N90-22111
Coupled behavior of rock joints
[DE90-009222] N90-22174

DEGREES OF FREEDOM
Dynamics of an oscillator with three-degrees-of-freedom in a uniform windfield
[REPT-89-56] N90-22121

DELAMINATING
Energy release rate analysis of interfacial cracks in composites N90-21829
The controlled-damage concept in design of laminated composites N90-21830
Three-dimensional finite element formulations for thick and thin laminated plates N90-22132

DELAY
A stress-strength interference approach to fast and delayed fracture reliability analysis for ceramic components N90-21859

DELIVERY
Document delivery via ISDN or satellite networks N90-22446

DELTA WINGS
Prediction of forces and moments for flight vehicle control effectors. Part 2: An analysis of delta wing aerodynamic control effectiveness in ground effect
[NASA-CR-186572] N90-21735
A video-based experimental investigation of wing rock N90-21771

DEMODULATION
A functional description of the advanced receiver N90-21891

DENSE PLASMAS
Producing dense plasmas with x rays
[DE90-009539] N90-22393

DENSITY (MASS/VOLUME)
A weak formulation for phase-change problems with bulk movement due to unequal densities
[DE90-009398] N90-22361

DENSITY DISTRIBUTION
Inclusion of clouds and rain in atmospheric slant path calculations N90-21925
A study of creep damage using microradiography and continuum damage mechanics N90-22109

DEPOSITION
Development of a computational fluid dynamics and chemistry model for the fouling of jet fuels
[DE90-005664] N90-22003

DESCENT
Optimal control of an aircraft flying through a downburst N90-21765
A conflict analysis of 4D descent strategies in a metered, multiple-arrival route environment
[NASA-CR-182019] N90-21772

DESIGN ANALYSIS
Conceptual design optimization study
[NASA-CR-4298] N90-21755
Operation of a step tunable megawatt gyrotron N90-21802
The 10-100 kW submillimeter gyrotron N90-21803
Principles of Very Large Scale Integrated (VLSI) system planning N90-21950
Thermomechanically-induced convective motion and natural convection in confined gaseous helium subjected to boundary heating N90-21960
Application of the TRANAIR rectangular grid approach to the aerodynamic analysis of complex configurations N90-21996
Review of analysis methods for mechanically fastened joints in composites
[LR-599] N90-22050
Clean access platform for orbiter N90-22103
Human motion perception: Higher-order organization N90-22226
An investigation of narrow-bandgap semiconductors: Devices, circuits, and systems N90-22406

DESORPTION
Production and analysis by mass spectrometry of beams of polyglycol ions N90-21835

DESTABILIZATION
Instabilities and subharmonic resonances of subsonic heated round jets, volume 2
[NASA-CR-186058] N90-22017

DETECTION
Device for quickly sensing the amount of O2 in a combustion product gas
[NASA-CASE-LAR-13816-1] N90-22025
Motion detection in astronomical and ice floe images N90-22231

DEW POINT
JARE data reports, no. 140 (meteorology 21): Meteorological data at Asuka Camp, Antarctica in 1987
[ISSN-0075-3343] N90-22188

DIAMONDS
Institute for Materials Science and Engineering, nondestructive evaluation: Technical activities
[PB90-132739] N90-22055

DIATOMIC MOLECULES
Molecular theory of fluid phase equilibria
[PB90-131277] N90-21832

DIELECTRICS
Theory of a periodic cylindrical waveguide with a nonuniform metal-dielectric filling
[DE90-620099] N90-21945

DIFFERENCE EQUATIONS
On spurious steady-state solutions of explicit Runge-Kutta schemes
[NASA-TM-102819] N90-22340

DIFFERENTIAL EQUATIONS
Electromagnetic inverse profiling of stratified media
[ETN-90-96402] N90-21947
Instabilities and subharmonic resonances of subsonic heated round jets, volume 2
[NASA-CR-186058] N90-22017
Dynamical approach study of spurious steady-state numerical solutions of nonlinear differential equations. Part 1: The ODE connection and its implications for algorithm development in computational fluid dynamics
[NASA-TM-102820] N90-22339
On spurious steady-state solutions of explicit Runge-Kutta schemes
[NASA-TM-102819] N90-22340
A Chinese bibliography on quadratic systems of differential equations
[REPT-89-39] N90-22342
Normal forms for weakly non-linear perturbed wave equations
[REPT-89-41] N90-22343
On a third q-Bessel function
[REPT-89-48] N90-22344
Efficient estimation in the Clayton-Cuzick model for survival data
[TW-88-06] N90-22348
The theta-methods in the numerical solution of delay differential equations
[TW-89-03] N90-22349
Stability criteria in the numerical solution of initial value problems
[TW-89-05] N90-22351
Stability analysis of numerical methods for delay differential equations
[TW-89-09] N90-22353

DIFFRACTION LIMITED CAMERAS
Diffraction-limited imaging on the 200-inch telescope N90-22475

DIFFRACTION PATTERNS
Diffraction of light by ultrasonic pulses N90-22366

DIFFRACTION RADIATION
Multiwave diffraction analysis of transmission phase gratings
[RSRE-MEMO-4325] N90-21948

DIFFUSION
An experimental investigation of mixing in buoyant flows N90-21963
On dual Lagrangian hyperbolic models for one dimensional two phase flow problems
[DE90-007012] N90-22004
Modeling the lateral diffusion of fluorescent particles within a forest canopy N90-22136

DIFFUSION COEFFICIENT
The temperature variation of hydrogen diffusion coefficients in metal alloys
[NASA-TM-100397] N90-21836

DIFFUSION FLAMES
Studies on reactive flows N90-21831

DIGITAL COMPUTERS
Parallel asynchronous hardware implementation of image processing algorithms N90-22219

DIGITAL ELECTRONICS
An investigation of narrow-bandgap semiconductors: Devices, circuits, and systems N90-22406

DIGITAL FILTERS
Low order FIR and IIR filters in dynamic vision
[OUEL-1785/89] N90-22384

DIGITAL SIMULATION
UD filtering and smoothing applied to orbit determination
[INPE-4966-PRE/1535] N90-22501

DIGITAL SYSTEMS
A real-time signal combining system for Ka-band feed arrays using maximum-likelihood weight estimates N90-21888
Geographic information system: Coded data of agrocattle-raising projects in the Amazon
[INPE-4978-PRE/1543] N90-22457

DILUTION
Molecular theory of fluid phase equilibria
[PB90-131277] N90-21832

DIMENSIONS
Preference numbers and funnel dimension
[REPT-89-57] N90-22346
Stability of compactification during inflation
[NASA-CR-186597] N90-22502

DIPOLES
Development of the methods and means of precise forming and geometry control of superconducting current-carrying element for the UNR pulsed dipoles
[DE90-620108] N90-22419

DIRAC EQUATION
Theory of a charged spinning particle in a gravitational and electromagnetic field
[NIKHEF-H/89-4] N90-22373

DISCONTINUITY
Algebraic block-structured grid generation based on a macro-block concept N90-21978

DISCRETE FUNCTIONS
An analysis of the finite-differenced, even-parity discrete-ordinates equations in slab geometry
[DE90-006479] N90-22337
Discrete variable structural optimization by the complex method
[LR-597] N90-22341

DISK GALAXIES
The distribution of molecular clouds in spiral galaxies N90-22489

DISKS (SHAPES)
Towards a Sarkovski order for the embedding of disks maintaining their orientation
[REPT-89-43] N90-22289

DISPERSING
A temperature-dependent regular infrared band model for absorption and dispersion N90-21927
The ASCOT 1986 valley/tributary interaction study
[DE90-009043] N90-22191

DISPLACEMENT MEASUREMENT
Circularity measuring system: A shape gauge designed especially for use on large objects N90-22104

DISPLAY DEVICES
The psychology of computer displays in the modern mission control center
[NASA-TM-100451] N90-22213
Visions of visualization aids: Design philosophy and experimental results N90-22220
Human motion perception: Higher-order organization N90-22226
Stanford/NASA-Ames Center of Excellence in model-based human performance N90-22241

DISTANCE
Orthogonal distance regression
[PB90-151747] N90-22336

DISTORTION
High intensity laser beam interactions with single droplets N90-21924

DISTRIBUTED PROCESSING
Two-dimensional shape recognition using sparse distributed memory N90-22227
A CSP model for distributed control software design
[OUEL-1789/89] N90-22273
Distributed simulation, no special tools required N90-22281

DISTRIBUTION FUNCTIONS
Molecular theory of fluid phase equilibria
[PB90-131277] N90-21832
A stress-strength interference approach to fast and delayed fracture reliability analysis for ceramic components N90-21859

DIVERGENT NOZZLES
Exhaust environment measurements of a turbofan engine equipped with an afterburner and 2D nozzle
[NASA-CR-4289] N90-21760

DOCUMENTS
Document delivery via ISDN or satellite networks N90-22446
The automation plan of the General Directorate 1 (search) of the European Patent Office N90-22448
Desk top publishing: What you need to know N90-22449

DONNELL EQUATIONS
ANILISA: Computational module for Koiter's imperfection sensitivity theory
[LR-582] N90-22119

DOORS
Aircraft accident report, United Airlines Flight 811, Boeing 747-122, N4713U, Honolulu, Hawaii, February 24, 1989
[PB90-910401] N90-21748
Development of the CLAES instrument aperture door system N90-22083
Driving and latching of the Starlab pointing mirror doors N90-22093

DOPPLER EFFECT
Digital Doppler extraction demonstration with the advanced receiver N90-21893

DOPPLER NAVIGATION
Using connected-element interferometer phase-delay data for Magellan navigation in Venus orbit N90-21885
DOPPLER RADAR
Dynamic and microphysical characteristics of cirrus clouds as revealed by aircraft, lidar, and other observations during FIRE N90-22177
DOWN-CONVERTERS
An 8.4-GHz dual-maser front-end system for Parkes reimplementation N90-21905
DRAG REDUCTION
On the use of external burning to reduce aerospace vehicle transonic drag
[NASA-TM-103107] N90-21762
DRAINAGE
Geographic information system: Coded data of agrocattle-raising projects in the Amazon
[INPE-4978-PRE/1543] N90-22457
DROP SIZE
Scattered-light scanner measurements of cryogenic liquid-jet breakup
[NASA-TM-102432] N90-22021
DROPS (LIQUIDS)
High intensity laser beam interactions with single droplets N90-21924
DRY HEAT
Pressurized bellows flat contact heat exchanger interface
[NASA-CASE-MSC-21271-1] N90-21999
DRYING
Spectral response of wheat and its relationship with agronomic variables in the tropical region
[INPE-5018-RPE/612] N90-22138
DUCTILITY
Welding behavior and welding metallurgy of ductile intermetallic alloys
[DE90-008908] N90-21852
Inclusion of unstable ductile tearing and extrapolated crack-arrest toughness data in PWR vessel integrity assessment
[DE90-009427] N90-22116
DURABILITY
Computational simulation of structural fracture in fiber composites
[NASA-TM-102505] N90-21821
Progression of damage and fracture in composites under dynamic loading
[NASA-TM-103118] N90-21825
DUST
Photometric monitoring of early type emission line stars N90-22478
The evolution of the supernova remnant IC 443 N90-22486
DWARF NOVAE
The modeling of IRAS detections of classical novae and related objects N90-22482
DWARF STARS
Fast spectroscopic variations on rapidly-rotating, cool dwarfs. 3: Masses of circumstellar absorbing clouds on AB Doradus
[NASA-CR-186563] N90-22479
DYNAMIC CHARACTERISTICS
Towards a unified analysis methodology for composite rotor blades N90-21730
Severe shock and vibration environments for electronic components
[DE90-007686] N90-22113
Dynamics of an oscillator with three-degrees-of-freedom in a uniform windfield
[REPT-89-56] N90-22121
Dynamic and microphysical characteristics of cirrus clouds as revealed by aircraft, lidar, and other observations during FIRE N90-22177
Characteristics of cumulus bandclouds off the east coast of Hawaii N90-22178
A galaxy formation cookbook: Recipes and utensils N90-22508
DYNAMIC CONTROL
Robust control of flexible structures N90-21784
DYNAMIC LOADS
Progression of damage and fracture in composites under dynamic loading
[NASA-TM-103118] N90-21825
Practical nonlinear simulation of rotating machinery dynamics with application to turbine blade rubbing N90-22038
DYNAMIC MODELS
Perturbation techniques in the dynamics and control of flexible manipulators
[OUEL-1772/89] N90-22053
DYNAMIC RESPONSE
Development and application of a generalized dynamic wake theory for lifting rotors N90-21731
Natural modes of cracked beams and identification of cracks N90-22075
Dynamic response of a complex encapsulated electronic assembly subjected to a severe shock environment
[DE90-007689] N90-22114
Dynamic response of structures with uncertain parameters N90-22125
DYNAMIC STRUCTURAL ANALYSIS
Development and application of a generalized dynamic wake theory for lifting rotors N90-21731
Airloads, wakes, and aeroelasticity
[NASA-CR-177551] N90-21738
Progression of damage and fracture in composites under dynamic loading
[NASA-TM-103118] N90-21825
A review of approximate methods for determining the vibrational modes of membranes N90-22063
Optimum design of structures under shock and vibration environment N90-22067
Natural modes of cracked beams and identification of cracks N90-22075
DYNAMICAL SYSTEMS
Nonlinear stability analysis and control of dynamical robotic systems N90-22037
The Shock and Vibration Digest, volume 22, no. 1 N90-22073
Stable response of damped mechanical systems, 4 N90-22074

E

EARLY STARS
Photometric monitoring of early type emission line stars N90-22478
EARTH ATMOSPHERE
Modelling UV-visible radiation observed from space N90-21937
EARTH CRUST
Surface roughness and the physical properties of fractures
[DE90-006046] N90-22169
EARTH MAGNETOSPHERE
Equilibrium and stability analysis of magnetospheric plasmas N90-21782
EARTH OBSERVING SYSTEM (EOS)
SURE (Science User Resource Expert): A science planning and scheduling assistant for a resource based environment N90-22302
EARTH PLANETARY STRUCTURE
Topical Conference on the Origin of the Earth
[NASA-CR-185061] N90-22166
EARTH RADIATION BUDGET
Satellite versus GCM-simulated radiation balance: Comparisons and implications for climate modeling N90-22180
EARTH RESOURCES
Mission to planet Earth N90-22153
Natural resources information system for the state of Oklahoma
[DE90-009483] N90-22458
EARTHQUAKES
Scattering of waves by inclusions in a nonhomogeneous elastic half space solved by boundary element methods
[PB90-145699] N90-22107
ECONOMIC ANALYSIS
International science and technology policies: Testimony before the Subcommittee on International Scientific Cooperation, Committee on Science, Space, and Technology, United States House of Representatives
[DE90-009416] N90-22463
ECONOMICS
Preference numbers and funnel dimension
[REPT-89-57] N90-22346
ECOSYSTEMS
Publications of the NASA Controlled Ecological Life Support System (CELSS) Program, 1979-1989
[NASA-CR-4297] N90-21754
Site visit to US Antarctic Program (USAP) facilities and the Research Vessel Polar Duke
[DE90-009396] N90-22159
EDDY CURRENTS
Institute for Materials Science and Engineering, nondestructive evaluation: Technical activities
[PB90-132739] N90-22055
EDDY VISCOSITY
Development of a defect stream function, law of the wall/wake method for compressible turbulent boundary layers N90-22019
EDGE DETECTION
Computation and parallel implementation for early vision N90-22222
Intensity dependent spread theory N90-22223
Edge recognition using image-processing hardware
[OUEL-1777/89] N90-22271
Implementing the Canny edge recognizer with datacube image-processing hardware
[OUEL-1786/89] N90-22272
EDGE DISLOCATIONS
The stress field due to an edge dislocation and some fracture problems for a three-phase composite cylinder model N90-22126
EFFICIENCY
Test method for fire extinguishing powder, Nordtest project 675-87
[PB90-166984] N90-21874
EFFLUENTS
Utilization of water hyacinths to upgrade heavily loaded wastewater treatment plant effluents N90-21873
EIGENVALUES
Bicausal representations and multivariable generalized predictive control
[OUEL-1781/89] N90-22331
EIGENVECTORS
Adaptive frequency estimation by MUSIC (Multiple Signal Classification) method
[PB90-166794] N90-21943
Bicausal representations and multivariable generalized predictive control
[OUEL-1781/89] N90-22331
EINSTEIN EQUATIONS
The synergism of analytic and numerical techniques in general relativity: Calculation of radiative spacetimes N90-22425
Numerical investigations of nonlinear behavior in the Einstein equations N90-22427
EJECTION
Herbig-Haro objects and stellar jets N90-22487
ELASTIC MEDIA
Elastodynamic scattering and transmission problems in three dimensions by the boundary integral equation method N90-22077
ELASTIC PROPERTIES
Towards a unified analysis methodology for composite rotor blades N90-21730
ELASTIC WAVES
Partial acoustic filtering applied to the equations of compressible flow
[DE90-000673] N90-22001
Institute for Materials Science and Engineering, nondestructive evaluation: Technical activities
[PB90-132739] N90-22055
Free wave propagation in orthogonally stiffened cylinders N90-22124
ELASTOHYDRODYNAMICS
Bearing elastohydrodynamic lubrication: A complex calculation made simple
[NASA-TM-102575] N90-22041
ELASTOMERS
Internal fractures in model elastomeric composites N90-22133
ELASTOPLASTICITY
Elastic stability and nonlinear behavior of imperfect shells with initial stresses N90-22070
Elasto-plastic analysis for contact fatigue failure N90-22078
Coordinate systems for plastic yield surfaces stress and strain space theories
[PB90-164765] N90-22110
An investigation into the foundations of elastic-plastic fracture mechanics N90-22130
ELASTOSTATICS
Finite element analysis of elastic contact problems with friction N90-22040
ELECTRIC AUTOMOBILES
Laboratory testing of Energy Research Corporation ERC 160 NiCd 6 volt traction battery
[DE90-009629] N90-21957
Laboratory testing of Saft SEH-5-200 6 volt traction battery
[DE90-009787] N90-21958
ELECTRIC BATTERIES
Active primary lithium thionyl chloride battery for artillery applications
[DE90-009511] N90-21955
ELECTRIC CURRENT
Current management for improved railgun performance N90-21781
Development of the methods and means of precise forming and geometry control of superconducting current-carrying element for the UNR pulsed dipoles
[DE90-620108] N90-22419
ELECTRIC GENERATORS
Assessment of High Temperature Superconducting (HTS) electric motors for rotorcraft propulsion
[NASA-CR-185222] N90-21761
ELECTRIC MOTOR VEHICLES
Analytical and experimental study of high phase order induction motors
[NASA-CR-186580] N90-21952
ELECTRIC MOTORS
Assessment of High Temperature Superconducting (HTS) electric motors for rotorcraft propulsion
[NASA-CR-185222] N90-21761

ELECTRIC POTENTIAL
Voltage source ac-to-dc converters for high-power transmitters N90-21886
Induction-type metal detector with increased scanning area capability
[NASA-CASE-KSC-11386-1] N90-22023
Device for quickly sensing the amount of O2 in a combustion product gas
[NASA-CASE-LAR-13816-1] N90-22025
A refrigerated Dewar for the Josephson array voltage calibration system
[DE90-005237] N90-22412
ELECTRIC POWER TRANSMISSION
An expert system for simulating electric loads aboard Space Station Freedom
[NASA-TM-103150] N90-22325
ELECTRIC PROPULSION
Advanced electric propulsion research, 1989
[NASA-CR-185237] N90-21810
ELECTRICAL FAULTS
Knowledge-based and integrated monitoring and diagnosis in autonomous power systems N90-22310
ELECTRICAL PROPERTIES
New flexible circuit material evaluation
[DE90-008313] N90-21866
Active primary lithium thionyl chloride battery for artillery applications
[DE90-009511] N90-21955
Laboratory testing of Energy Research Corporation ERC 160 NiCd 6 volt traction battery
[DE90-009629] N90-21957
Laboratory testing of Saft SEH-5-200 6 volt traction battery
[DE90-009787] N90-21958
ELECTRO-OPTICAL EFFECT
Propagation environments, effects, and decision aids
N90-21918
ELECTRO-OPTICS
Modelling of optically and IR effective atmospheric turbulence N90-21923
Computation of broad spectral band electro-optical system transmittance response characteristics to military smokes and obscurants using field test data from transmissometer system measurements N90-21939
Effect of atmospheric turbulence on electro-optical systems N90-21940
Atmospheric modelling studies: A modelling comparison between IR and millimetric atmospheric propagation
N90-21941
Optical bistability in semiconducting material
N90-22424
ELECTROCHEMISTRY
Electrochemical impregnation and cycle life of lightweight nickel electrodes for nickel-hydrogen cells
[NASA-TM-103140] N90-21844
ELECTRODES
Effect of LEO cycling on 125 Ah advanced design IPV nickel-hydrogen battery cells
[NASA-TM-103128] N90-21808
Electrochemical impregnation and cycle life of lightweight nickel electrodes for nickel-hydrogen cells
[NASA-TM-103140] N90-21844
Stability studies of a pH-sensitive polymer matrix: Applications to fiber optic pH sensors
[DE90-009579] N90-21867
MHD channel development, part 2
[DE90-009550] N90-22395
MHD channel development, part 3
[DE90-009551] N90-22396
ELECTRODISSOLUTION
Research in biological separations and cell culture
[NASA-CR-172060] N90-22202
ELECTRODYNAMICS
Theory of a periodic cylindrical waveguide with a nonuniform metal-dielectric filling
[DE90-620099] N90-21945
ELECTROLYSIS
Impact of low gravity on water electrolysis operation
[NASA-CR-185521] N90-21870
ELECTROLYTES
Effect of LEO cycling on 125 Ah advanced design IPV nickel-hydrogen battery cells
[NASA-TM-103128] N90-21808
ELECTROMAGNETIC FIELDS
Electromagnetic inverse profiling of stratified media
[ETN-90-96402] N90-21947
Studies of 60-Hz exposure effects on human function
[DE90-009473] N90-22210
Theory of a charged spinning particle in a gravitational and electromagnetic field
[NIKHEF-H/89-4] N90-22373
ELECTROMAGNETIC INTERACTIONS
Computer simulation of ionospheric radio frequency heating
[DE90-009478] N90-21944
ELECTROMAGNETIC PROPULSION
A superconducting quenchgun for delivering lunar derived oxygen to lunar orbit
[NASA-CR-185161] N90-21806
ELECTROMAGNETIC PULSES
Development and applications of a coupled cavity sodium-chloride laser N90-22029
Origin of pulsed emission from the young supernova remnant SN 1987A
[CAL-377] N90-22469
ELECTROMAGNETIC RADIATION
Induction-type metal detector with increased scanning area capability
[NASA-CASE-KSC-11386-1] N90-22023
ELECTROMAGNETIC WAVE TRANSMISSION
Multiwave diffraction analysis of transmission phase gratings
[RSRE-MEMO-4325] N90-21948
ELECTROMECHANICAL DEVICES
The connector space reduction mechanism
N90-22092
ELECTRON BEAMS
PIC code modeling of spacecraft charging potential during electron beam injection into a background of neutral gas and plasma, part 1
[NASA-CR-186602] N90-21792
Jupiter's drifting decametric bursts with the changing time scale
[DE90-618870] N90-22517
ELECTRON DENSITY (CONCENTRATION)
Plasma contactor research, 1989
[NASA-CR-185212] N90-22389
ELECTRON EMISSION
Correlated electron processes in ion-atom collisions
[DE90-009477] N90-22370
Plasma contactor research, 1989
[NASA-CR-185212] N90-22389
ELECTRON ENERGY
New calculations and measurements of the Coulomb cross-section for the production of direct electron pairs by high energy nuclei
[NASA-TM-101280] N90-22371
ELECTRON PLASMA
Cyclotron maser and plasma wave growth in magnetic loops
[NASA-CR-179862] N90-22402
ELECTRON RECOMBINATION
Recombination lines of C I and N II in the interstellar medium N90-22466
ELECTRON SCATTERING
Correlated electron processes in ion-atom collisions
[DE90-009477] N90-22370
Transport properties of anisotropic superconductors
N90-22404
ELECTRON SPIN
Theory of a charged spinning particle in a gravitational and electromagnetic field
[NIKHEF-H/89-4] N90-22373
ELECTRON STATES
Positron trapping in semiconductors
[PB90-165606] N90-22410
ELECTRONIC MAIL
Technologies for electronic transfer of information: The present state and trends in Europe N90-22441
Technology for electronic transfer of information: The present and future in North America N90-22442
Innovations in telecommunications networks
N90-22444
Megatendances N90-22445
Document delivery via ISDN or satellite networks
N90-22446
Electronic mail systems N90-22451
ELECTRONIC PACKAGING
Severe shock and vibration environments for electronic components
[DE90-007686] N90-22113
Dynamic response of a complex encapsulated electronic assembly subjected to a severe shock environment
[DE90-007689] N90-22114
ELECTROPHORESIS
Research in biological separations and cell culture
[NASA-CR-172060] N90-22202
ELEMENTARY EXCITATIONS
Transport properties of anisotropic superconductors
N90-22404
ELEMENTARY PARTICLE INTERACTIONS
Exclusive production of p, p-, pi, and pi- in photon photon collisions
[NIKHEF-H/89-9] N90-22376
ELUTION
The chemical basis for the origin of the genetic code and the process of protein synthesis
[NASA-CR-186590] N90-22205
EMBEDDING
Feature-associated mesh embedding for complex configurations N90-21988
Towards a Sarkovski order for the embedding of disks maintaining their orientation
[REPT-89-43] N90-22289
EMISSION SPECTRA
Spectral response of wheat and its relationship with agronomic variables in the tropical region
[INPE-5018-RPE/612] N90-22138
Field reports on radiometric campaigns of soybeans in the Federal district: Safra 88/89
[INPE-5021-RPE/615] N90-22139
The emission lines in the ultra-violet spectrum of Beta Lyrae N90-22474
EMITTERS
Production and analysis by mass spectrometry of beams of polyglycol ions N90-21835
EMOTIONAL FACTORS
Excitatory and inhibitory backward conditioning in the rat N90-22204
EMULSIONS
New calculations and measurements of the Coulomb cross-section for the production of direct electron pairs by high energy nuclei
[NASA-TM-101280] N90-22371
ENCAPSULATING
Dynamic response of a complex encapsulated electronic assembly subjected to a severe shock environment
[DE90-007689] N90-22114
END EFFECTORS
A robot end effector exchange mechanism for space applications N90-22088
ENERGY ABSORPTION
Formulation of non-reflecting boundary conditions in numerical models of the atmosphere N90-22175
ENERGY DISSIPATION
The evolution of the supernova remnant IC 443
N90-22486
ENERGY DISTRIBUTION
New calculations and measurements of the Coulomb cross-section for the production of direct electron pairs by high energy nuclei
[NASA-TM-101280] N90-22371
ENERGY GAPS (SOLID STATE)
An investigation of narrow-bandgap semiconductors: Devices, circuits, and systems N90-22406
ENERGY METHODS
Elastic stability and nonlinear behavior of imperfect shells with initial stresses N90-22070
ENERGY SPECTRA
Long term intensity stability of Auger electron spectrometers: Instructions for the interlaboratory comparison
[NPL-DMM(A)-1] N90-22027
The modeling of IRAS detections of classical novae and related objects N90-22482
ENERGY STORAGE
Analysis of thermal energy storage material with change-of-phase volumetric effects
[NASA-TM-102457] N90-21974
Reactions of N2A3 sigma u + and candidates for short wavelengths lasers
[DE90-009514] N90-22033
ENGINE FAILURE
Framework for a space shuttle main engine health monitoring system
[NASA-CR-185224] N90-21809
ENGINE INLETS
Control of flow separation and mixing by aerodynamic excitation
[NASA-TM-103131] N90-21733
ENGINE MONITORING INSTRUMENTS
Framework for a space shuttle main engine health monitoring system
[NASA-CR-185224] N90-21809
Preliminary development of an intelligent computer assistant for engine monitoring
[NASA-TM-101702] N90-22322
ENGLISH LANGUAGE
An introduction to Montague grammar
[REPT-89-46] N90-22266
ENTRAINMENT
An experimental investigation of mixing in buoyant flows N90-21963
Laser Doppler anemometry measurements of a confined turbulent water jet with a uniform background flow
N90-21971
ENVIRONMENT EFFECTS
Final environmental impact statement for the Galileo Mission (Tier 2)
[NASA-TM-102925] N90-22147
Draft environmental impact statement for the Galileo Mission (Tier 2)
[NASA-TM-102926] N90-22148
Site visit to US Antarctic Program (USAP) facilities and the Research Vessel Polar Duke
[DE90-009396] N90-22159

Uncertainty analysis of the accident effect area of a BLEVE
[REPT-89-49] N90-22160
Final Environmental Impact Statement for the Ulysses Mission (Tier 2)
[NASA-TM-101104] N90-22162

ENVIRONMENT MODELS
Uncertainty analysis of the accident effect area of a BLEVE
[REPT-89-49] N90-22160

ENVIRONMENT POLLUTION
Uncertainty analysis of the accident effect area of a BLEVE
[REPT-89-49] N90-22160

ENVIRONMENTAL MONITORING
Mission to planet Earth N90-22153

ENVIRONMENTAL SURVEYS
Final (Tier 1) environmental impact statement for the Galileo and Ulysses Missions
[NASA-TM-102917] N90-21779
Final environmental impact statement for the Galileo Mission (Tier 2)
[NASA-TM-102925] N90-22147
Draft environmental impact statement for the Galileo Mission (Tier 2)
[NASA-TM-102926] N90-22148
Site visit to US Antarctic Program (USAP) facilities and the Research Vessel Polar Duke
[DE90-009396] N90-22159
Final Environmental Impact Statement for the Ulysses Mission (Tier 2)
[NASA-TM-101104] N90-22162

EQUATIONS OF MOTION
Homogeneous dilute turbulent particle-laden water flows N90-21965
Mathematical modeling of fluid-solid mixtures
[DE90-009152] N90-22007
Dynamics of an oscillator with three-degrees-of-freedom in a uniform windfield
[REPT-89-56] N90-22121

EQUATIONS OF STATE
Update on the OPAL opacity code
[DE90-009946] N90-22480

EQUATORIAL REGIONS
Geology of coronae and domal structures on Venus and models of their origin N90-22513

EQUILIBRIUM EQUATIONS
Modelling late-time atmospheres of supernovae
N90-22500

EQUILIBRIUM FLOW
Equilibrium and stability analysis of magnetospheric plasmas N90-21782

EQUIVALENT CIRCUITS
Analytical and experimental study of high phase order induction motors
[NASA-CR-186580] N90-21952

ERGODIC PROCESS
The intrinsic stochasticity of near-integrable Hamiltonian systems
[IPPCZ-282] N90-22386

EROSION
Advanced electric propulsion research, 1989
[NASA-CR-185237] N90-21810
Hollow cathode operation at high discharge currents
[NASA-CR-185238] N90-21953

ERROR ANALYSIS
Engagement analysis study
[DE90-009529] N90-22359

ERRORS
Interpreting meteorological data reports for LOWTRAN Navy aerosol model extinction calculations N90-21920

ESTIMATES
Adaptive frequency estimation by MUSIC (Multiple Signal Classification) method
[PB90-166794] N90-21943
Efficient estimation in the Clayton-Cuzick model for survival data
[TW-88-06] N90-22348

ESTIMATING
Exact closed-form expressions for the performance of the split-symbol moments estimator of signal-to-noise ratio N90-21894

ETHERS
Experience with synthetic fluorinated fluid lubricants
N90-22095

EULER EQUATIONS OF MOTION
Applications of Mesh Generation to Complex 3-D Configurations
[AGARD-CP-464] N90-21975
Unsteady Euler solutions on dynamic blocked grids for complex configurations N90-21982
Grid patching approaches for complex three-dimensional configurations N90-21985
Feature-associated mesh embedding for complex configurations N90-21988
Generation and adaptation of 3-D unstructured grids for transient problems N90-21994

EULER-LAGRANGE EQUATION
Perturbation techniques in the dynamics and control of flexible manipulators
[OUEL-1772/89] N90-22053
Lagrangian model simulation of the turbulent transport of evaporating jet droplets N90-22168

EUROPE
The automation plan of the General Directorate 1 (search) of the European Patent Office N90-22448

EVAPORATION
Evaporation duct effects at millimeter wavelengths
N90-21914
Millimetre-wave propagation in the evaporation duct
N90-21929
An experimental investigation of mixing in buoyant flows N90-21963
From Penman to Makkink: A new method for the calculation of the climatological evaporation numbers
[KNMI-TR-111] N90-22161
Lagrangian model simulation of the turbulent transport of evaporating jet droplets N90-22168
The Al-26(rho, gamma)Si-27 reaction: Stellar origins of galactic Al-26 N90-22498

EVAPORATIVE COOLING
An experimental investigation of mixing in buoyant flows N90-21963

EXCITATION
Vibration analysis of systems with random parametric excitations N90-22060
Dynamic response of structures with uncertain parameters N90-22125
The Al-26(rho, gamma)Si-27 reaction: Stellar origins of galactic Al-26 N90-22498

EXHAUST FLOW SIMULATION
On the direct simulation of vortex shedding
[LR-513] N90-21743
Analysis of a six-component, flow-through, strain-gage, force balance used for hypersonic wind tunnel models with scramjet exhaust flow simulation
[NASA-CR-186585] N90-21775

EXHAUST GASES
Exhaust environment measurements of a turbofan engine equipped with an afterburner and 2D nozzle
[NASA-CR-4289] N90-21760

EXHAUST NOZZLES
Performance characteristics of a one-third-scale, vectorable ventral nozzle for SSTOVL aircraft
[NASA-TM-103120] N90-21725
Exhaust environment measurements of a turbofan engine equipped with an afterburner and 2D nozzle
[NASA-CR-4289] N90-21760
Shelf life extension for the lot AAE nozzle severance LSCs
[NASA-CR-183878] N90-21813

EXOBIOLOGY
USSR Space Life Sciences Digest, issue 25
[NASA-CR-3922(29)] N90-22203
Aerospace medicine and biology: A continuing bibliography with indexes (supplement 334)
[NASA-SP-7011(334)] N90-22207
Aerospace medicine and biology: A continuing bibliography with indexes (supplement 335)
[NASA-SP-7011(335)] N90-22208

EXPANDABLE STRUCTURES
Design of a telescoping tube system for access and handling equipment N90-22102

EXPANSION
Stability of compactification during inflation
[NASA-CR-186597] N90-22502

EXPEDITIONS
JARE data reports, no. 140 (meteorology 21): Meteorological data at Asuka Camp, Antarctica in 1987
[ISSN-0075-3343] N90-22188

EXPENDABLE STAGES (SPACECRAFT)
The development of a complementary expendable launch vehicle interface for an STS deployable payload
N90-22086

EXPERIMENT DESIGN
High power millimeter wave source development program N90-21805

EXPERT SYSTEMS
Expert systems for automated maintenance of a Mars oxygen production system
[NASA-CR-186209] N90-22215
Photonic processing at NASA Ames Research Center
N90-22234
The WAVE model for advanced knowledge processing
[OUEL-1803/89] N90-22291
A knowledge-based approach to improving optimization techniques in system planning N90-22303
NASA ground terminal communication equipment automated fault isolation expert systems N90-22305
Autonomous power expert system N90-22306
Knowledge-based and integrated monitoring and diagnosis in autonomous power systems N90-22310
The procedure safety system N90-22311
Using expert systems to implement a semantic data model of a large mass storage system N90-22315
Adaptive pattern recognition by mini-max neural networks as a part of an intelligent processor
N90-22317
A knowledge-based system with learning for computer communication network design N90-22319
Evaluation of a proposed expert system development methodology: Two case studies N90-22320
Preliminary development of an intelligent computer assistant for engine monitoring
[NASA-TM-101702] N90-22322
An expert system for simulating electric loads aboard Space Station Freedom
[NASA-TM-103150] N90-22325
An intelligent interface for the design of optimal control systems
[INPE-4917-PRE/1516] N90-22332
Neural implementation of a method for solving systems of linear algebraic equations
[NPL-DITC-155/89] N90-22356
Facilitating knowledge sharing in organizations: Semiautonomous agents that learn to gather, classify, and distribute environmental scanning knowledge
N90-22435
Knowledge-based semantic query processing: An optimal transformation approach N90-22437

EXPLOSIONS
Modelling late-time atmospheres of supernovae
N90-22500

EXPOSURE
Studies of 60-Hz exposure effects on human function
[DE90-009473] N90-22210

EXTERNAL TANKS
Space Shuttle, NASA's major changes to flight hardware: Fact sheet for the Chairman, Committee on Science, Space, and Technology, House of Representatives
[GAO/NSIAD-88-173FS] N90-22461

EXTINCTION
Interpreting meteorological data reports for LOWTRAN Navy aerosol model extinction calculations N90-21920

EXTINGUISHING
Test method for fire extinguishing powder, Nordtest project 675-87
[PB90-166984] N90-21874

EXTRACTION
Studies on the use of supercritical ammonia for ceramic nitride synthesis and fabrication
[NASA-TM-102570] N90-21843

EXTRATERRESTRIAL LIFE
Extraterrestrial life in the universe
[NASA-TM-102363] N90-22464

EXTRAVEHICULAR ACTIVITY
Vision science and technology for supervised intelligent space robots N90-22221

EXTREME ULTRAVIOLET RADIATION
The ratio of neutral hydrogen to neutral helium in the local interstellar medium N90-22499

EXTREMELY HIGH FREQUENCIES
A real-time signal combining system for Ka-band feed arrays using maximum-likelihood weight estimates
N90-21886

EXTRUDING
Microstructure and mechanical properties of nickel aluminide powders consolidated by extrusion and hot isostatic pressing
[DE90-009777] N90-21855

EYE (ANATOMY)
Sampling and noise in vision networks N90-22217

F

F-8 AIRCRAFT
A comparison of time-optimal interception trajectories for the F-8 and F-15
[NASA-CR-186300] N90-21753

F-15 AIRCRAFT
A comparison of time-optimal interception trajectories for the F-8 and F-15
[NASA-CR-186300] N90-21753

FABRICATION
Studies on the use of supercritical ammonia for ceramic nitride synthesis and fabrication
[NASA-TM-102570] N90-21843
Development of the methods and means of precise forming and geometry control of superconducting current-carrying element for the UNR pulsed dipoles
[DE90-620108] N90-22419

FABRICS
Testing carbon fabric for oxidation mass loss
N90-21819

FACTORIZATION
UD filtering and smoothing applied to orbit determination
[INPE-4966-PRE/1535] N90-22501

FAIL-SAFE SYSTEMS
Development of shape memory metal as the actuator of a fail safe mechanism N90-22081

FAILURE
Evaluation of a prototype lighted ball marker for powerline obstructions
[DOT/FAA/CT-TN90/12] N90-21774
Dynamic response of a complex encapsulated electronic assembly subjected to a severe shock environment
[DE90-007689] N90-22114
Continued research on the strain to failure of thick-walled cylinders subjected to internal pressure
[DE90-008952] N90-22115
General purpose heat source radioisotope thermoelectric generator program. Book 1: Accident analysis
[REPT-90SDS4202-BK-1] N90-22379
General purpose heat source radioisotope thermoelectric generator. Book 2: Accident analysis, appendices
[REPT-90SDS4202-BK-2] N90-22380

FAILURE ANALYSIS
Strength in notched and impact-damaged laminates N90-21820
Review of analysis methods for mechanically fastened joints in composites
[LR-599] N90-22050
A methodology for knowledge-based restructurable control to accommodate system failures N90-22058
Elasto-plastic analysis for contact fatigue failure N90-22078
SPOT 4 space magnetic recorder mechanisms N90-22082
Knowledge-based and integrated monitoring and diagnosis in autonomous power systems N90-22310

FAILURE MODES
Framework for a space shuttle main engine health monitoring system
[NASA-CR-185224] N90-21809
Strength in notched and impact-damaged laminates N90-21820
Fracture toughness and tensile properties of alloy HT9 in thin sections under high neutron fluences
[DE90-008386] N90-21851
Failure mechanisms under complex loading of glass-reinforced polyester composites and their matrices: The effect of superposed hydrostatic pressures up to 300 MPa on axial tensile and compressive strengths, and in-plane shear properties of unidirtionally reinforced glass-polyester composites and the relevant polyesters N90-22072
Expert systems for automated maintenance of a Mars oxygen production system
[NASA-CR-186209] N90-22215
General purpose heat source radioisotope thermoelectric generator. Book 2: Accident analysis, appendices
[REPT-90SDS4202-BK-2] N90-22380

FAINT OBJECTS
A high galactic latitude survey of far ultraviolet excess objects N90-22473

FANS
WINCOF-I code for prediction of fan compressor unit with water ingestion
[NASA-CR-185157] N90-21724

FAR ULTRAVIOLET RADIATION
A high galactic latitude survey of far ultraviolet excess objects N90-22473

FAST FOURIER TRANSFORMATIONS
Analysis of gamma squared Velorum photometry from the South Pole N90-22472

FASTENERS
Review of analysis methods for mechanically fastened joints in composites
[LR-599] N90-22050

FATIGUE (MATERIALS)
Development of ultrasonic nondestructive methods for defect and damage characterization in composite materials N90-21816
Three-dimensional fatigue crack closure behavior of metals N90-21857
Contact mechanics for three-dimensional geometries N90-22076
Cycle life machine for AX-5 space suit N90-22080
Fatigue crack growth in unidirectional metal matrix composite
[NASA-TM-103102] N90-22117
Fatigue crack growth predictions for variable-amplitude and spectrum loading
[LR-526] N90-22118
Rotor loading on a three-bladed wind turbine N90-22145

FAULT TOLERANCE
The art of fault-tolerant system reliability modeling
[NASA-TM-102623] N90-22292
The 1990 Goddard Conference on Space Applications of Artificial Intelligence
[NASA-CP-3068] N90-22294
NASA ground terminal communication equipment automated fault isolation expert systems N90-22305
Autonomous power expert system N90-22306
Adaptive pattern recognition by mini-max neural networks as a part of an intelligent processor N90-22317
Bounded-time fault-tolerant rule-based systems N90-22318

FAULTS
NASA ground terminal communication equipment automated fault isolation expert systems N90-22305

FEASIBILITY ANALYSIS
Testing of an advanced thermochemical conversion reactor system
[DE90-007989] N90-22141

FEDERAL BUDGETS
Current information technology resource requirements of the Federal government: Major systems acquisitions and planned resources
[PB90-146820] N90-22439

FEED SYSTEMS
Hybrid propulsion technology program. Volume 1: Conceptional design package
[NASA-CR-183953] N90-21793
Hybrid propulsion technology program. Volume 2: Technology definition package
[NASA-CR-183954] N90-21794

FEEDBACK
Passive navigation using image irradiance tracking N90-22232

FEEDBACK CONTROL
Balanced bridge feedback control system
[NASA-CASE-NPO-17430-1-CU] N90-21951
High order P-G finite elements for convection-dominated problems
[DE90-614743] N90-21998
A new six-degree-of-freedom force-reflecting hand controller for space telerobotics N90-22089
Branch point placement
[OUEL-1767/89] N90-22329
An intelligent interface for the design of optimal control systems
[INPE-4917-PRE/1516] N90-22332
Engagement analysis study
[DE90-009529] N90-22359

FEET (ANATOMY)
Engineering specification and system design for CAD/CAM of custom shoes: UMC project effort
[NASA-CR-186547] N90-22255

FERMI SURFACES
Transport properties of anisotropic superconductors N90-22404

FERRITES
The effect of aging at 343 C on type 308 stainless steel weldments
[DE90-009232] N90-21853

FIBER COMPOSITES
Interfacial studies in fiber-reinforced thermoplastic-matrix composites N90-21814
Computational simulation of structural fracture in fiber composites
[NASA-TM-102505] N90-21821
METCAN verification status
[NASA-TM-103119] N90-21824
Matrix density effects on the mechanical properties of SiC/RBSN composites
[NASA-TM-103098] N90-21826
Failure mechanisms under complex loading of glass-reinforced polyester composites and their matrices: The effect of superposed hydrostatic pressures up to 300 MPa on axial tensile and compressive strengths, and in-plane shear properties of unidirtionally reinforced glass-polyester composites and the relevant polyesters N90-22072
The stress field due to an edge dislocation and some fracture problems for a three-phase composite cylinder model N90-22126

FIBER OPTICS
Microwave Landing System (MLS) multiple system design interoperability interface control report
[DOT/FAA/SA-89/2] N90-21750
Microwave analog fiber-optic link for use in the deep space network N90-21883
Optical shutter switching matrix
[NASA-CASE-KSC-11392-1] N90-22383

FIBER ORIENTATION
Fatigue crack growth in unidirectional metal matrix composite
[NASA-TM-103102] N90-22117

FIBER STRENGTH
Matrix density effects on the mechanical properties of SiC/RBSN composites
[NASA-TM-103098] N90-21826

FIELD EMISSION
An assessment of the hardness of miniature vacuum tubes to high-voltage transients
[DE90-009541] N90-21956

FIELD THEORY (ALGEBRA)
Operator algebra from fusion rules: The infinite number of Ising theories
[NIKHEF-H/89-7] N90-22374
Generalized killing equations and symmetries of spinning space
[NIKHEF-H/89-8] N90-22375

FIELD THEORY (PHYSICS)
Theory of a charged spinning particle in a gravitational and electromagnetic field
[NIKHEF-H/89-4] N90-22373

FILLETS
Effective methods of controlling a junction vortex system in an incompressible, three-dimensional, turbulent flow N90-21732

FINE STRUCTURE
The observed properties of the intermediate-degree gravity modes and their relevance to the solar neutrino paradox N90-22519

FINITE DIFFERENCE THEORY
An upwind-differencing scheme for the incompressible Navier-Stokes equations
[NASA-TM-101051] N90-21757
Experimental determination of thermal conductance in bolted joint impact in satellites
[INPE-4989-PRE/1551] N90-21786
Elastic stability and nonlinear behavior of imperfect shells with initial stresses N90-22070
Numerical solutions of the nonlinear theory of curved beams N90-22071
An analysis of the finite-differenced, even-parity discrete-ordinates equations in slab geometry
[DE90-006479] N90-22337
Dynamical approach study of spurious steady-state numerical solutions of nonlinear differential equations. Part 1: The ODE connection and its implications for algorithm development in computational fluid dynamics
[NASA-TM-102820] N90-22339
Computer simulation of time-dependent spherically symmetric spacetimes containing radiating fluids: Formalism and code tests N90-22483

FINITE ELEMENT METHOD
Towards a unified analysis methodology for composite rotor blades N90-21730
A decentralized linear quadratic control design method for flexible structures N90-21770
Computational simulation of structural fracture in fiber composites
[NASA-TM-102505] N90-21821
Modelling of the impact response of fibre-reinforced composites
[OUEL-1784/89] N90-21827
Failure analysis of woven hybrid composite using a finite element method
[OUEL-1791/89] N90-21828
Energy release rate analysis of interfacial cracks in composites N90-21829
Numerical simulation model of hydrazine attitude control thrusters
[INPE-4965-PRE/1534] N90-21848
Three-dimensional fatigue crack closure behavior of metals N90-21857
A stress-strength interference approach to fast and delayed fracture reliability analysis for ceramic components N90-21859
Fracture mechanics of monolithic ceramic materials under small scale microcracking conditions N90-21860
Applications of Mesh Generation to Complex 3-D Configurations
[AGARD-CP-464] N90-21975
Automatic grid generation in complex three-dimensional configurations using a frontal system N90-21992
Unstructured finite element mesh generation and adaptive procedures for CFD N90-21993
Application of the TRANAIR rectangular grid approach to the aerodynamic analysis of complex configurations N90-21996
High order P-G finite elements for convection-dominated problems
[DE90-614743] N90-21998
Practical nonlinear simulation of rotating machinery dynamics with application to turbine blade rubbing N90-22038
Finite element analysis of elastic contact problems with friction N90-22040
Natural modes of cracked beams and identification of cracks N90-22075

- Elasto-plastic analysis for contact fatigue failure N90-22078
- On the design and development of a miniature ceramic gimbal bearing N90-22100
- Coordinate systems for plastic yield surfaces stress and strain space theories [PB90-164765] N90-22110
- Computational methods and plasticity [LR-583] N90-22120
- Free wave propagation in orthogonally stiffened cylinders N90-22124
- Dynamic response of structures with uncertain parameters N90-22125
- Analysis of a finite two-dimensional solid with an inclined crack and a rigid inclusion N90-22127
- An investigation into the foundations of elastic-plastic fracture mechanics N90-22130
- Three-dimensional finite element formulations for thick and thin laminated plates N90-22132
- Internal fractures in model elastomeric composites N90-22133
- Probabilistic finite elements: Applications to fracture and fatigue N90-22134
- Paving: A new approach to automated quadrilateral mesh generation [DE90-010244] N90-22260

FINITE VOLUME METHOD
- Numerical simulation of hypersonic flow around a space plane. Part 2: Application to high angles of attack flow [NAL-TR-1011T] N90-21726

FINS
- Numerical investigation of some control methods for 3-D turbulent interactions due to sharp fins N90-21764

FIREBREAKS
- Geographic information system: Coded data of agrocattle-raising projects in the Amazon [INPE-4978-PRE/1543] N90-22457

FIRES
- Test method for fire extinguishing powder, Nordtest project 675-87 [PB90-166984] N90-21874
- The influence of large, cold objects on engulfing fire environments [DE90-003342] N90-21875

FIXED POINT ARITHMETIC
- Finite element analysis of elastic contact problems with friction N90-22040

FLAME PROPAGATION
- Studies on reactive flows N90-21831
- Fire propagation in concurrent flows [PB90-151754] N90-21834
- The influence of large, cold objects on engulfing fire environments [DE90-003342] N90-21875

FLAME RETARDANTS
- Ternary reactions among polymer substrate-organohalogen-antimony oxides under pyrolytic, oxidative and flaming conditions [PB90-154766] N90-21861

FLAME STABILITY
- On the use of external burning to reduce aerospace vehicle transonic drag [NASA-TM-103107] N90-21762

FLAMES
- Saturated fluorescence measurements of the hydroxyl radical in laminar high-pressure flames [NASA-CR-185218] N90-22022

FLAT PLATES
- An investigation of turbulence structure in a low Reynolds number incompressible turbulent boundary layer N90-21966

FLEXIBILITY
- New flexible circuit material evaluation [DE90-008313] N90-21866
- Rotor loading on a three-bladed wind turbine N90-22145

FLEXIBLE BODIES
- A decentralized linear quadratic control design method for flexible structures N90-21770
- Robust control of flexible structures N90-21784
- Nonlinear spline operator interpolation and sliding control of deformable maneuvering bodies N90-21878

FLIGHT CONTROL
- The insertion of human dynamics models in the flight control loops of V/STOL research aircraft. Appendix 2: The optimal control model of a pilot in V/STOL aircraft control loops [NASA-CR-186598] N90-21776

FLIGHT MANAGEMENT SYSTEMS
- First-order weight corrections for real-time flight path management [LR-580] N90-21751
- A conflict analysis of 4D descent strategies in a metered, multiple-arrival route environment [NASA-CR-182019] N90-21772

FLIGHT MECHANICS
- Optimization and guidance of flight trajectories in the presence of windshear [NASA-CR-186163] N90-21747
- A comparison of time-optimal interception trajectories for the F-8 and F-15 [NASA-CR-186300] N90-21753

FLIGHT OPTIMIZATION
- An approach to on-board optimization of cruise at constant altitude [LR-581] N90-21752

FLIGHT PATHS
- A comparison of time-optimal interception trajectories for the F-8 and F-15 [NASA-CR-186300] N90-21753
- Optimal control of an aircraft flying through a downburst N90-21765
- Dynamic and microphysical characteristics of cirrus clouds as revealed by aircraft, lidar, and other observations during FIRE N90-22177
- Computer vision techniques for rotorcraft low altitude flight N90-22237

FLIGHT SIMULATION
- Aeroelastic simulation of higher harmonic control N90-21768
- Unsteady separated flows produced by complex harmonic motions: Investigation of wing-flow interactions elicited by a mechanical model simulating dragonfly wing kinematics N90-22018

FLIGHT TESTS
- Severe shock and vibration environments for electronic components [DE90-007686] N90-22113

FLOATING POINT ARITHMETIC
- Supercomputers need super arithmetic [PB90-130253] N90-22252

FLOW CHARACTERISTICS
- Experimental and analytical investigations of granular materials: Shear flow and convective heat transfer N90-21968

FLOW DISTORTION
- Wind tunnel investigation of three sonic anemometers [PB90-149808] N90-21729
- Theoretical and experimental study of flow-control devices for inlets of indraft wind tunnels [NASA-TM-100050] N90-21778

FLOW DISTRIBUTION
- Wind tunnel investigation of three sonic anemometers [PB90-149808] N90-21729
- Effective methods of controlling a junction vortex system in an incompressible, three-dimensional, turbulent flow N90-21732
- Extension of a streamwise upwind algorithm to a moving grid system [NASA-TM-102800] N90-21739
- An upwind-differencing scheme for the incompressible Navier-Stokes equations [NASA-TM-101051] N90-21757
- Numerical investigation of some control methods for 3-D turbulent interactions due to sharp fins N90-21764
- An experimental investigation of the physical mechanisms controlling the asymmetric flow past slender bodies at large angles of attack N90-21767
- Theoretical and experimental study of flow-control devices for inlets of indraft wind tunnels [NASA-TM-100050] N90-21778
- Prediction of length scales in a Mach reflection flowfield N90-21959
- Interaction of a turbulent round jet with the free surface N90-21964
- Recent developments in grid generation N90-21976
- A structured approach to interactive multiple block grid generation N90-21983
- A discussion on issues relating to multiblock grid generation N90-21991
- Bifurcations in viscous flow fields. On the genesis and development of topologically complicated separated flow structures [PB90-167156] N90-22012
- The calibration and measuring procedure of a five-hole hemispherical head probe in compressible flow [LR-585] N90-22013
- Herbig-Haro objects and stellar jets N90-22487

FLOW EQUATIONS
- Partial acoustic filtering applied to the equations of compressible flow [DE90-000673] N90-22001

FLOW GEOMETRY
- Analytical study of the origin and behavior of asymmetric vortices [NASA-TM-102796] N90-21746

FLOW MEASUREMENT
- The calibration and measuring procedure of a five-hole hemispherical head probe in compressible flow [LR-585] N90-22013

FLOW STABILITY
- Analytical study of the origin and behavior of asymmetric vortices [NASA-TM-102796] N90-21746
- Modern developments in shear flow control with swirl [NASA-CR-186586] N90-22000
- A new stability criterion in the shallow-water system for two-dimensional coherent eddies in the atmosphere and oceans N90-22176
- Effect of a crystal-melt interface on Taylor-vortex flow [NASA-CR-186512] N90-22408

FLOW THEORY
- Mathematical modeling of fluid-solid mixtures [DE90-009152] N90-22007

FLOW VELOCITY
- Fire propagation in concurrent flows [PB90-151754] N90-21834
- Automated analysis of measured turbulent boundary flow [PB90-147844] N90-21970
- On dual Lagrangian hyperbolic models for one dimensional two phase flow problems [DE90-007012] N90-22004
- Experimental observations on transition to turbulence in confined coaxial jets and other boundary layer flows [DE90-008939] N90-22005

FLOW VISUALIZATION
- Interaction of a turbulent round jet with the free surface N90-21964
- Experimental observations on transition to turbulence in confined coaxial jets and other boundary layer flows [DE90-008939] N90-22005

FLUID DYNAMICS
- WINCOF-I code for prediction of fan compressor unit with water ingestion [NASA-CR-185157] N90-21724
- Modeling of vortex-induced oscillations based on indicial response approach [NASA-CR-186560] N90-21736
- The effects of tortuosity on flow through a natural fracture [DE90-009193] N90-22172

FLUID FLOW
- A multiblock/multizone code (PAB 3D-v2) for the three-dimensional Navier-Stokes equations: Preliminary applications [NASA-CR-182032] N90-21745
- Numerical simulation model of hydrazine attitude control thrusters [INPE-4965-PRE/1534] N90-21848
- Applications of algebraic grid generation N90-21979
- Heat-transfer regimes in nuclear-reactor-pumped gas lasers [DE90-002904] N90-22032
- Beam propagation in direct nuclear pumped laser amplifiers [DE90-009613] N90-22035
- The effects of tortuosity on flow through a natural fracture [DE90-009193] N90-22172
- In-situ fracture stiffness determination [DE90-009202] N90-22173

FLUID MECHANICS
- Development and application of a generalized dynamic wake theory for lifting rotors N90-21731

FLUIDS
- Computer simulation of time-dependent spherically symmetric spacetimes containing radiating fluids: Formalism and code tests N90-22483

FLUORESCENCE
- Evaluating thermographic phosphors in an operating turbine engine [DE90-004874] N90-22044
- Institute for Materials Science and Engineering, nondestructive evaluation: Technical activities [PB90-132739] N90-22055
- Modeling the lateral diffusion of fluorescent particles within a forest canopy N90-22136
- Spectrum formation in active galactic nuclei and Type 2 supernovae N90-22490

FLUOROCARBONS
- Experimental performance of ozone-safe alternative refrigerants: Experimental performance comparisons of R32, R125, R143a, R218, R134a, R152a, R124, R142b, RC318 and R143 in a refrigeration circuit [DE90-009227] N90-21876

FLUX VECTOR SPLITTING
- An upwind-differencing scheme for the incompressible Navier-Stokes equations [NASA-TM-101051] N90-21757

FOCAL PLANE DEVICES
- Parallel asynchronous hardware implementation of image processing algorithms N90-22219

FOKKER-PLANCK EQUATION
- Vibration analysis of systems with random parametric excitations N90-22060

FOLIAGE
Millimeter-wave bistatic scattering by terrain N90-21936

FORCE DISTRIBUTION
Analysis of a six-component, flow-through, strain-gage, force balance used for hypersonic wind tunnel models with scramjet exhaust flow simulation [NASA-CR-186585] N90-21775

FORCED VIBRATION
A video-based experimental investigation of wing rock N90-21771
Experimental investigation of the effect of cavitation on the rotordynamic forces on a whirling centrifugal pump impeller N90-22039
Elastodynamic scattering and transmission problems in three dimensions by the boundary integral equation method N90-22077

FORECASTING
Millimetre-wave propagation in the evaporation duct N90-21929
Aging characteristics of Li/SO(sub 2) cells [NASA-CR-180432] N90-21954
An anomalous wind between valleys: Its characteristics and a proposed explanation [DE90-008965] N90-22189
Daytime wind valleys adjacent to the Great Salt Lake [DE90-008991] N90-22190
Wind forecasting for utility operations [DE90-009466] N90-22193
Forecast of Atlantic seasonal hurricane activity for 1990 N90-22194

FORESTS
Millimeter-wave bistatic scattering by terrain N90-21936
Modeling the lateral diffusion of fluorescent particles within a forest canopy N90-22136
Cloud chemistry and occurrence in the western United States: A synopsis of current information [PB90-134248] N90-22182

FORMALISM
Incomparable elements in algebraic lattices with applications to formal language theory [MEMO-INF-89-54] N90-22269

FORMULAS (MATHEMATICS)
From Penman to Makkink: A new method for the calculation of the climatological evaporation numbers [KNMI-TR-111] N90-22161

FORTRAN
TOODEE: A two-dimensional, time-dependent heat conduction program [DE90-009631] N90-22010
FORTRAN coding guidelines [DE90-009604] N90-22258

FORWARD SCATTERING
Millimeter-wave bistatic scattering by terrain N90-21936

FOULING
Development of a computational fluid dynamics and chemistry model for the fouling of jet fuels [DE90-005664] N90-22003

FOURIER ANALYSIS
On dual Lagrangian hyperbolic models for one dimensional two phase flow problems [DE90-007012] N90-22004
Severe shock and vibration environments for electronic components [DE90-007686] N90-22113

FOURIER SERIES
Analysis of a finite two-dimensional solid with an inclined crack and a rigid inclusion N90-22127
Dynamic and microphysical characteristics of cirrus clouds as revealed by aircraft, lidar, and other observations during FIRE N90-22177

FOURIER TRANSFORMATION
Propagation of transient acoustic waves in porous media [ETN-90-96401] N90-22015
The distribution of molecular clouds in spiral galaxies N90-22489

FRACTALS
Low temperature properties of amorphous solids N90-22405

FRACTURE MECHANICS
Computational simulation of structural fracture in fiber composites [NASA-TM-102505] N90-21821
Energy release rate analysis of interfacial cracks in composites N90-21829
The effect of hydrogen and microstructure on the deformation and fracture behavior of a single crystal nickel-base superalloy [NASA-CR-185219] N90-21849
Fracture toughness and tensile properties of alloy HT9 in thin sections under high neutron fluences [DE90-008386] N90-21851
Fracture mechanics of monolithic ceramic materials under small scale microcracking conditions N90-21860
Contact mechanics for three-dimensional geometries N90-22076
Institute for Materials Science and Engineering, Fracture and Deformation Division: Technical activities, 1989 [PB90-155359] N90-22106
Nonlinear fracture mechanics using semicircular specimens and tension-softening behavior N90-22108
Continued research on the strain to failure of thick-walled cylinders subjected to internal pressure [DE90-008952] N90-22115
Inclusion of unstable ductile tearing and extrapolated crack-arrest toughness data in PWR vessel integrity assessment [DE90-009427] N90-22116
An investigation into the foundations of elastic-plastic fracture mechanics N90-22130
Probabilistic finite elements: Applications to fracture and fatigue N90-22134
In-situ fracture stiffness determination [DE90-009202] N90-22173

FRACTURE STRENGTH
Fracture toughness and tensile properties of alloy HT9 in thin sections under high neutron fluences [DE90-008386] N90-21851
Nonlinear fracture mechanics using semicircular specimens and tension-softening behavior N90-22108

FRACTURES (MATERIALS)
A continuum damage model for the quasi-static response of brittle materials [DE90-007681] N90-22112
Internal fractures in model elastomeric composites N90-22133
Surface roughness and the physical properties of fractures [DE90-006046] N90-22169
Effects of single fractures on seismic wave propagation [DE90-009191] N90-22171

FRACTURING
Computational simulation of structural fracture in fiber composites [NASA-TM-102505] N90-21821
Progression of damage and fracture in composites under dynamic loading [NASA-TM-103118] N90-21825
A stress-strength interference approach to fast and delayed fracture reliability analysis for ceramic components N90-21859
The stress field due to an edge dislocation and some fracture problems for a three-phase composite cylinder model N90-22126
Probabilistic finite elements: Applications to fracture and fatigue N90-22134
The effects of tortuosity on flow through a natural fracture [DE90-009193] N90-22172

FRAGMENTATION
Production and analysis by mass spectrometry of beams of polyglycol ions N90-21835

FRAMES
Graphically-oriented nonlinear analysis of statically loaded plane frames on microcomputers [PB90-165945] N90-22248

FRAMES (DATA PROCESSING)
Implementing the Canny edge recognizer with datacube image-processing hardware [OUEL-1786/89] N90-22272

FREDHOLM EQUATIONS
The analysis of stress relaxation on indentation of a rigid punch into a viscoelastic sheet of finite thickness [NPL-DMA(A)-193] N90-22357

FREE BOUNDARIES
A spectral analysis approach to wave propagation in layered solids N90-22131

FREE ELECTRON LASERS
Free-Space Power Transmission [NASA-CP-10016] N90-21795
Free electron lasers driven by linear induction accelerators: High power radiation sources N90-21800

FREE JETS
Interaction of a turbulent round jet with the free surface N90-21964

FREE RADICALS
Infrared absorption spectroscopy and chemical kinetics of free radicals [DE90-009469] N90-21837

FREQUENCIES
Adaptive frequency estimation by MUSIC (Multiple Signal Classification) method [PB90-166794] N90-21943

FREQUENCY MODULATION
Multiresolution and time-frequency representations of signals [REPT-89-47] N90-21946

FREQUENCY RANGES
Nonlinear acoustic interactions in superfluid helium N90-22367

FREQUENCY STABILITY
Experiments with a laser interferometric gravitational wave antenna N90-22476

FRICTION
Numerical simulation model of hydrazine attitude control thrusters [INPE-4965-PRE/1534] N90-21848
Finite element analysis of elastic contact problems with friction N90-22040
Rotor-to-stationary element rub-related vibration phenomena in rotating machinery: Literature survey N90-22065
Tribomaterial factors in space mechanism brake performance N90-22096
Active control of bearing preload using piezoelectric translators N90-22098

FRICTION FACTOR
Tribomaterial factors in space mechanism brake performance N90-22096
AX-5 space suit bearing torque investigation N90-22101

FRICTION MEASUREMENT
Elastic and viscoelastic analysis of two multiply layered cylinders rolling over each other with Coulomb friction [REPT-89-50] N90-22051

FRONTS (METEOROLOGY)
A case study of cloud-to-ground lightning during the GALE program N90-22185

FUEL COMBUSTION
Detailed mechanism for oxidation of benzene [NASA-TM-102443] N90-21842
High speed commercial transport fuels considerations and research needs [NASA-TM-102535] N90-21869

FUEL CONSUMPTION
An approach to on-board optimization of cruise at constant altitude [LR-581] N90-21752
Analysis, selection, and implementation of procedures which approve optimal artificial satellite maneuvers [INPE-5003-TDL/397] N90-21786

FUEL PRODUCTION
Photosynthetic water splitting, phase 2 [PB90-132671] N90-21833
A robotically constructed production and supply base on Phobos [NASA-CR-186234] N90-21872

FUEL SYSTEMS
MHD channel development, part 4 [DE90-009552] N90-22397

FUELS
A comparison of the autoignition chemistry of n-butane and isobutane in an internal combustion engine [DE90-009474] N90-21838

FUNCTIONAL DESIGN SPECIFICATIONS
An introduction to selected structured methods [RSRE-MEMO-4294] N90-22275

FUNCTIONS (MATHEMATICS)
Generalized Herglotz functions and inverse scattering problem in a finite depth ocean [PB90-150996] N90-22197
New algorithms for one-loop integrals [NIKHEF-H/89-17] N90-22268

FUNNELS
Preference numbers and funnel dimension [REPT-89-57] N90-22346

G

GALACTIC CLUSTERS
A theoretical scenario for the dynamics of formation and early evolution of globular clusters in galaxies N90-22494
The mass of the Coma cluster N90-22496
An astrophysics data program investigation of cluster evolution [NASA-CR-181296] N90-22510

GALACTIC EVOLUTION
Search for rapidly star forming galaxies at high redshift N90-22465
Wind instability as a possible cause of the spiral structure formation in the gaseous subsystem of galaxies with the circular magnetic field [DE90-618944] N90-22507
A galaxy formation cookbook: Recipes and utensils N90-22508

GALACTIC STRUCTURE
Wind instability as a possible cause of the spiral structure formation in the gaseous subsystem of galaxies with the circular magnetic field [DE90-618944] N90-22507

GALAXIES

The optical night sky at low surface brightness: High latitude dust and faint field galaxies N90-22481

The association of supernovae with regions of recent star formation in late-type galaxies N90-22497

A galaxy formation cookbook: Recipes and utensils N90-22508

Gamma rays, cosmic rays, and local molecular clouds N90-22524

GALERKIN METHOD

Numerical simulation model of hydrazine attitude control thrusters
[INPE-4965-PRE/1534] N90-21848

Natural modes of cracked beams and identification of cracks N90-22075

GALILEO PROJECT

Final (Tier 1) environmental impact statement for the Galileo and Ulysses Missions
[NASA-TM-102917] N90-21779

Finding the complete path and weight enumerators of convolutional codes N90-21897

Final environmental impact statement for the Galileo Mission (Tier 2)
[NASA-TM-102925] N90-22147

Draft environmental impact statement for the Galileo Mission (Tier 2)
[NASA-TM-102926] N90-22148

GALILEO SPACECRAFT

Final (Tier 1) environmental impact statement for the Galileo and Ulysses Missions
[NASA-TM-102917] N90-21779

Galileo Earth approach navigation using connected-element interferometer phase-delay tracking N90-21884

A VLSI decomposition of the deBruijn graph N90-21895

A higher density VLBI catalog for navigating Magellan and Galileo N90-21904

Final environmental impact statement for the Galileo Mission (Tier 2)
[NASA-TM-102925] N90-22147

GAMMA RAY BEAMS

Non-random uncertainties in the calibration of protection-level secondary standards
[NPL-RS(EXT)-110] N90-22378

Derivation of radiation beam non-uniformity corrections for the calibration of large volume ionisation chambers
[NPL-RSA(EXT)-11] N90-22382

GAMMA RAY BURSTS

Gamma ray bursts: Current status of observations and theory
[NASA-TM-100398] N90-22526

GAMMA RAYS

Gamma rays, cosmic rays, and local molecular clouds N90-22524

Very high energy gamma rays from the Crab nebula and pulsar N90-22527

GAS ANALYSIS

Device for quickly sensing the amount of O2 in a combustion product gas
[NASA-CASE-LAR-13816-1] N90-22025

GAS DYNAMICS

Partial acoustic filtering applied to the equations of compressible flow
[DE90-000673] N90-22001

A galaxy formation cookbook: Recipes and utensils N90-22508

GAS FLOW

Numerical simulation of liquid circulation in a bubbly column
[DE90-005226] N90-22002

On dual Lagrangian hyperbolic models for one dimensional two phase flow problems
[DE90-007012] N90-22004

Scattered-light scanner measurements of cryogenic liquid-jet breakup
[NASA-TM-102432] N90-22021

GAS INJECTION

Analysis of a six-component, flow-through, strain-gage, force balance used for hypersonic wind tunnel models with scramjet exhaust flow simulation
[NASA-CR-186585] N90-21775

GAS JETS

Instabilities and subharmonic resonances of subsonic heated round jets, volume 2
[NASA-CR-186058] N90-22017

GAS LASERS

Heat-transfer regimes in nuclear-reactor-pumped gas lasers
[DE90-002904] N90-22032

GAS TURBINE ENGINES

Evaluating thermographic phosphors in an operating turbine engine
[DE90-004874] N90-22044

GAS VALVES

Zero-G phase detector and separator
[NASA-CASE-LEW-14844-1] N90-22024

GASEOUS DIFFUSION

The temperature variation of hydrogen diffusion coefficients in metal alloys
[NASA-TM-100397] N90-21836

GASEOUS FUELS

Testing of an advanced thermochemical conversion reactor system
[DE90-007989] N90-22141

GASIFICATION

Testing carbon fabric for oxidation mass loss N90-21819

GEAR TEETH

Calculating the time domain average of gear vibration data sampled at less than the Nyquist frequency
[OUEL-1768/89] N90-22052

Computerized inspection of gear tooth surfaces
[NASA-TM-102395] N90-22054

GENETIC CODE

The chemical basis for the origin of the genetic code and the process of protein synthesis
[NASA-CR-186590] N90-22205

GEODYNAMICS

NSSDC data listing
[NASA-TM-102989] N90-22456

GEOGRAPHIC INFORMATION SYSTEMS

Geographic information system: Coded data of agrocattle-raising projects in the Amazon
[INPE-4978-PRE/1543] N90-22457

GEOLOGY

An anomalous wind between valleys: Its characteristics and a proposed explanation
[DE90-008965] N90-22189

Natural resources information system for the state of Oklahoma
[DE90-009483] N90-22458

Geology of coronae and domal structures on Venus and models of their origin N90-22513

GEOMAGNETIC TAIL

The MHD structure of an open magnetotail boundary N90-22388

GEOMAGNETISM

Solar-geophysical data number 542, October 1989. Part 1: (Prompt reports). Data for September, August 1989, and late data
[PB90-148669] N90-22520

GEOMETRICAL OPTICS

Dual-shaped offset reflector antenna designs from solutions of the geometrical optics first-order partial differential equations N90-21887

The solution of scattering and radiation problems for complex configurations based on 3-D grid and patch models N90-21997

GEOMETRY

An analysis of the finite-differenced, even-parity discrete-ordinates equations in slab geometry
[DE90-006479] N90-22337

GEOPHYSICS

Topical Conference on the Origin of the Earth
[NASA-CR-185061] N90-22166

Solar-geophysical data number 542, October 1989. Part 1: (Prompt reports). Data for September, August 1989, and late data
[PB90-148669] N90-22520

Solar-geophysical data number 542, October 1989. Part 2: (Comprehensive reports). Data for April 1989 and miscellaneous
[PB90-148677] N90-22521

GEOPOTENTIAL HEIGHT

Tropopause undulations and the development of extratropical cyclones N90-22186

GEOSTROPHIC WIND

Semigeostrophic flow over orography in a stratified rotating atmosphere N90-22163

GEOTECHNICAL ENGINEERING

Effects of single fractures on seismic wave propagation
[DE90-009191] N90-22171

GEOTHERMAL ENERGY UTILIZATION

The pressure dilation of a deep, jointed region of the earth
[DE90-007537] N90-22170

GEOTHERMAL RESOURCES

The pressure dilation of a deep, jointed region of the earth
[DE90-007537] N90-22170

GEOTHERMAL TECHNOLOGY

The pressure dilation of a deep, jointed region of the earth
[DE90-007537] N90-22170

GERMANIUM

Preparation and characterization of Cu2ZnGeS(4-y)Se(y)
[AD-A217469] N90-22407

GIBBS FREE ENERGY

SGTE data for pure elements
[NPL-DMA(A)-195] N90-22460

GIMBALS

On the design and development of a miniature ceramic gimbal bearing N90-22100

GIOTTO MISSION

An 8.4-GHz dual-maser front-end system for Parkes reimplementation N90-21905

GLASS

High resolution stimulated Raman-Brillouin spectroscopy in gases and solids
[DE90-009535] N90-21840

Brillouin gain spectroscopy in glasses and crystals
[DE90-009536] N90-21841

Homogeneous dilute turbulent particle-laden water flows N90-21965

GLASS FIBER REINFORCED PLASTICS

Failure analysis of woven hybrid composite using a finite element method
[OUEL-1791/89] N90-21828

GLASS TRANSITION TEMPERATURE

Thermomechanical properties of polymeric materials and related stresses
[NASA-TM-100758] N90-21864

GLOBAL POSITIONING SYSTEM

Precise estimation of tropospheric path delays with GPS techniques N90-21881

GLOBAL WARMING

Proceedings of the Conference on Technology-Based Confidence Building: Energy and Environment
[CNSS-PAPERS-22] N90-22152

GLOBULAR CLUSTERS

A theoretical scenario for the dynamics of formation and early evolution of globular clusters in galaxies N90-22494

GLYCOLS

Production and analysis by mass spectrometry of beams of polyglycol ions N90-21835

GOVERNMENT PROCUREMENT

Current information technology resource requirements of the Federal government: Major systems acquisitions and planned resources
[PB90-146820] N90-22439

GRADIENTS

Electromagnetic inverse profiling of stratified media
[ETN-90-96402] N90-21947

GRAIN BOUNDARIES

Grain boundary intermetallic phases in alloy 718
[DE90-009812] N90-22417

GRAMMARS

An introduction to Montague grammar
[REPT-89-46] N90-22266

Some remarks on treatment of be in Montague's PTQ — Proper Treatment of Quantification (PTQ)
[REPT-89-40] N90-22267

GRANULAR MATERIALS

Experimental and analytical investigations of granular materials: Shear flow and convective heat transfer N90-21968

GRAPH THEORY

A VLSI decomposition of the deBruijn graph N90-21895

Clustering and uniqueness in mathematical models of percolation phenomena
[ETN-90-96400] N90-22358

GRAPHIC ARTS

Graphics mini manual
[NASA-TM-87622-REV] N90-22247

GRAPHITE-EPOXY COMPOSITES

Development of ultrasonic nondestructive methods for defect and damage characterization in composite materials N90-21816

Energy release rate analysis of interfacial cracks in composites N90-21829

The controlled-damage concept in design of laminated composites N90-21830

GRATINGS (SPECTRA)

Multiwave diffraction analysis of transmission phase gratings
[RSRE-MEMO-4325] N90-21948

GRAVITATION

Stability of compactification during inflation
[NASA-CR-186597] N90-22502

GRAVITATION THEORY

Generalized killing equations and symmetries of spinning space
[NIKHEF-H/89-8] N90-22375

GRAVITATIONAL COLLAPSE

Gravitational effects of global textures
[NASA-CR-186596] N90-22503

Ultrahigh-energy particle flux from cosmic strings
[NASA-CR-186592] N90-22525

GRAVITATIONAL EFFECTS

Thermomechanically-induced convective motion and natural convection in confined gaseous helium subjected to boundary heating N90-21960

A robot end effector exchange mechanism for space applications N90-22088

Gravitational effects of global textures [NASA-CR-186596] N90-22503

GRAVITATIONAL FIELDS

Theory of a charged spinning particle in a gravitational and electromagnetic field [NIKHEF-H/89-4] N90-22373

Numerical investigations of nonlinear behavior in the Einstein equations N90-22427

Gravitational effects of global textures [NASA-CR-186596] N90-22503

Gravitational couplings of the inflation in extended inflation [NASA-CR-186595] N90-22504

GRAVITATIONAL LENSES

An astrophysics data program investigation of cluster evolution [NASA-CR-181296] N90-22510

GRAVITATIONAL WAVES

The synergism of analytic and numerical techniques in general relativity: Calculation of radiative spacetimes N90-22425

Experiments with a laser interferometric gravitational wave antenna N90-22476

GRAVITY ANOMALIES

The observed properties of the intermediate-degree gravity modes and their relevance to the solar neutrino paradox N90-22519

GRAVITY WAVES

Formulation of non-reflecting boundary conditions in numerical models of the atmosphere N90-22175

A theoretical investigation of gravity-wave-generated stress and vorticity in the planetary boundary layer N90-22512

GREAT SALT LAKE (UT)

Daytime wind valleys adjacent to the Great Salt Lake [DE90-008991] N90-22190

GREEN'S FUNCTIONS

Green's functions for the elastic annulus and their application to various crack problems N90-22129

GREENHOUSE EFFECT

Experimental performance of ozone-safe alternative refrigerants: Experimental performance comparisons of R32, R125, R143a, R218, R134a, R152a, R124, R142b, RC318 and R143 in a refrigeration circuit [DE90-009227] N90-21876

GREENLAND

Calculation of IR propagation statistics in the eastern Atlantic for surveillance system performance assessment N90-21936

GREGORIAN ANTENNAS

Dual-shaped offset reflector antenna designs from solutions of the geometrical optics first-order partial differential equations N90-21887

GRID GENERATION (MATHEMATICS)

Applications of Mesh Generation to Complex 3-D Configurations [AGARD-CP-464] N90-21975

Recent developments in grid generation N90-21976

General structured grid generation systems N90-21977

Algebraic block-structured grid generation based on a macro-block concept N90-21978

Applications of algebraic grid generation N90-21979

Geometry and grids of complex configurations for aerodynamic calculation N90-21980

Mesh generation for flow computation in turbomachine N90-21981

A structured approach to interactive multiple block grid generation N90-21983

Grid patching approaches for complex three-dimensional configurations N90-21985

Multiblock topology specification and grid generation for complete aircraft configurations N90-21986

Three-dimensional adaptive grids with limited skewness N90-21987

On the way to an integrated mesh generation system for industrial applications N90-21989

Generation, optimization, and adaptation of multidomain meshes around complex configurations N90-21990

A discussion on issues relating to multiblock grid generation N90-21991

Automatic grid generation in complex three-dimensional configurations using a frontal system N90-21992

Unstructured finite element mesh generation and adaptive procedures for CFD N90-21993

Generation and adaptation of 3-D unstructured grids for transient problems N90-21994

Unstructured mesh generation by a generalized Delaunay algorithm N90-21995

GRID2D/3D: A computer program for generating grid systems in complex-shaped two- and three-dimensional spatial domains. Part 1: Theory and method [NASA-TM-102453] N90-22262

GROUND EFFECT (AERODYNAMICS)

Prediction of forces and moments for flight vehicle control effectors. Part 2: An analysis of delta wing aerodynamic control effectiveness in ground effect [NASA-CR-186572] N90-21735

GROUND SUPPORT EQUIPMENT

The 24th Aerospace Mechanisms Symposium [NASA-CP-3062] N90-22079

Design of a telescoping tube system for access and handling equipment N90-22102

NASA ground terminal communication equipment automated fault isolation expert systems N90-22305

GROWTH

Spectral response of wheat and its relationship with agronomic variables in the tropical region [INPE-5018-RPE/612] N90-22138

Field reports on radiometric campaigns of soybeans in the Federal district: Safra 88/89 [INPE-5021-RPE/615] N90-22139

GRUNEISEN CONSTANT

Nonlinearity parameters of polymers N90-22369

GUIDE VANES

Theoretical and experimental study of flow-control devices for inlets of indraft wind tunnels [NASA-TM-100050] N90-21778

GUN LAUNCHERS

A superconducting quenchgun for delivering lunar derived oxygen to lunar orbit [NASA-CR-185161] N90-21806

H

H ALPHA LINE

Fast spectroscopic variations on rapidly-rotating, cool dwarfs. 3: Masses of circumstellar absorbing clouds on AB Doradus [NASA-CR-186563] N90-22479

H II REGIONS

Recombination lines of C I and N II in the interstellar medium N90-22466

Interactions of massive stars with the interstellar medium: Bow shocks and superbubbles N90-22485

The evolution of the supernova remnant IC 443 N90-22486

The association of supernovae with regions of recent star formation in late-type galaxies N90-22497

HAIL

Hail growth in a highly-glaciated central high plains multi-cellular hailstorm N90-22184

HAILSTORMS

Hail growth in a highly-glaciated central high plains multi-cellular hailstorm N90-22184

HALF PLANES

Elasto-plastic analysis for contact fatigue failure N90-22078

HALF SPACES

Elastodynamic scattering and transmission problems in three dimensions by the boundary integral equation method N90-22077

Scattering of waves by inclusions in a nonhomogeneous elastic half space solved by boundary element methods [PB90-145699] N90-22107

HALIDES

Studies on the use of supercritical ammonia for ceramic nitride synthesis and fabrication [NASA-TM-102570] N90-21843

HALLEY'S COMET

The production and spatial distribution of neutral and ionized water vapor in Comet P/Halley N90-22484

HAMILTONIAN FUNCTIONS

The intrinsic stochasticity of near-integrable Hamiltonian systems [IPPCZ-282] N90-22386

HANKEL FUNCTIONS

A frame approach to the H-infinity super-optimal solution [OUEL-1761/89] N90-22327

The analysis of stress relaxation on indentation of a rigid punch into a viscoelastic sheet of finite thickness [NPL-DMA(A)-193] N90-22357

HARDENING (MATERIALS)

Elasto-plastic analysis for contact fatigue failure N90-22078

HARDNESS

Mechanical properties of carbon-implanted niobium [DE90-009864] N90-21823

HARMONIC CONTROL

Aeroelastic simulation of higher harmonic control N90-21768

HARMONIC GENERATIONS

Development and applications of a coupled cavity sodium-chloride laser N90-22029

HARMONIC MOTION

Unsteady separated flows produced by complex harmonic motions: Investigation of wing-flow interactions elicited by a mechanical model simulating dragonfly wing kinematics N90-22018

HARMONICS

Quiet mode for nonlinear rotor models [NASA-TM-102236] N90-21756

Nonlinearity parameters of polymers N90-22369

Analysis of gamma squared Velorum photometry from the South Pole N90-22472

HARTMANN FLOW

On the theory of Heiser and Shercliff experiment. Part 1: MHD flow in an open channel in strong uniform magnetic field [OUEL-1804/89-PT-1] N90-22400

On the theory of Heiser and Shercliff experiment. Part 2: MHD flow between two cylinders in strong radical magnetic field [OUEL-1805/89-PT-2] N90-22401

HAWAII

Characteristics of cumulus bandclouds off the east coast of Hawaii N90-22178

HEAT EXCHANGERS

Pressurized bellows flat contact heat exchanger interface [NASA-CASE-MSC-21271-1] N90-21999

HEAT FLUX

Flow boiling with enhancement devices for cold plate coolant channel design [NASA-CR-186358] N90-21961

An anomalous wind between valleys: Its characteristics and a proposed explanation [DE90-008965] N90-22189

HEAT MEASUREMENT

Interfacial studies in fiber-reinforced thermoplastic-matrix composites N90-21814

HEAT SOURCES

General purpose heat source radioisotope thermoelectric generator program. Book 1: Accident analysis [REPT-90SDS4202-BK-1] N90-22379

General purpose heat source radioisotope thermoelectric generator. Book 2: Accident analysis, appendices [REPT-90SDS4202-BK-2] N90-22380

HEAT STORAGE

Analysis of thermal energy storage material with change-of-phase volumetric effects [NASA-TM-102457] N90-21974

HEAT TRANSFER

WINCOF-I code for prediction of fan compressor unit with water ingestion [NASA-CR-185157] N90-21724

Development and integration of the capillary pumped loop GAS and Hitchhiker flight experiments [NASA-TM-100756] N90-21790

Numerical simulation model of hydrazine attitude control thrusters [INPE-4965-PRE/1534] N90-21848

Flow boiling with enhancement devices for cold plate coolant channel design [NASA-CR-186358] N90-21961

Pressurized bellows flat contact heat exchanger interface [NASA-CASE-MSC-21271-1] N90-21999

On dual Lagrangian hyperbolic models for one dimensional two phase flow problems [DE90-007012] N90-22004

TOODEE: A two-dimensional, time-dependent heat conduction program [DE90-009631] N90-22010

Heat-transfer regimes in nuclear-reactor-pumped gas lasers [DE90-002904] N90-22032

Testing of an advanced thermochemical conversion reactor system [DE90-007989] N90-22141

Dynamic and microphysical characteristics of cirrus clouds as revealed by aircraft, lidar, and other observations during FIRE N90-22177

A linear analysis of monsoon base states associated with banded convection N90-22179

Heat leak measurements in superconducting dipole magnet supports [DE90-620109] N90-22420

HEATING

Thermomechanically-induced convective motion and natural convection in confined gaseous helium subjected to boundary heating N90-21960

HELICOPTER CONTROL

Aeroelastic simulation of higher harmonic control N90-21768

HELIUM

Thermomechanically-induced convective motion and natural convection in confined gaseous helium subjected to boundary heating N90-21960

Analysis of gamma squared Velorum photometry from the South Pole N90-22472

The ratio of neutral hydrogen to neutral helium in the local interstellar medium N90-22499

HERBIG-HARO OBJECTS

Herbig-Haro objects and stellar jets N90-22487

HEURISTIC METHODS

An approach to rescheduling activities based on determination of priority and disruptivity N90-22299

Space communications scheduler: A rule-based approach to adaptive deadline scheduling N90-22300

Knowledge-based semantic query processing: An optimal transformation approach N90-22437

HIGH CURRENT

Gas-puff z-pinch experiment [IPPCZ-286] N90-22385

HIGH FREQUENCIES

Report on STC/Technische Universiteit (TU) Delft Extremely High Frequency (EHF) radio relay study N90-21915

Survey of instrumental methods for the determination of the high frequency wave spectrum [IOS-267] N90-22200

HIGH POWER LASERS

High intensity laser beam interactions with single droplets N90-21924

High power CO2 laser instability and its corrections N90-22028

Direct solar-pumped iodine laser amplifier [NASA-CR-186442] N90-22030

Development of mid-infrared solid state lasers for spaceborne lidar [NASA-CR-185095] N90-22031

Linear, nonlinear, and tunable guided wave modes for high-power (GaAl)As semiconductor lasers N90-22036

HIGH TEMPERATURE

Fracture toughness and tensile properties of alloy HT9 in thin sections under high neutron fluences [DE90-008386] N90-21851

HIGH TEMPERATURE PLASMAS

The intrinsic stochasticity of near-integrable Hamiltonian systems [IPPCZ-282] N90-22386

HIGH TEMPERATURE PROPELLANTS

Extraction of recovery of plasticizers from solid propellants and munitions [AD-D014433] N90-21868

HIGH TEMPERATURE SUPERCONDUCTORS

Assessment of High Temperature Superconducting (HTS) electric motors for rotorcraft propulsion [NASA-CR-185222] N90-21761

JETC (Japanese Technology Evaluation Center) Panel Report on High Temperature Superconductivity in Japan [NASA-CR-180413] N90-22409

Pulsed laser processing of high temperature superconducting thin films [DE90-008928] N90-22413

Overview of current bulk and thick film high temperature superconductor processing strategies [DE90-008949] N90-22414

In-situ pulsed laser deposition of high-T(sub c) YBa(sub 2)Cu(sub 3)O(sub 7) superconducting thin films on (100) LaAlO3 substrates [DE90-009861] N90-22418

HIGH VOLTAGES

Evaluation of a prototype lighted ball marker for powerline obstructions [DOT/FAA/CT-TN90/12] N90-21774

HILBERT SPACE

A generalized complementarity problem in Hilbert space [DE90-009576] N90-22360

HINGES

Development of the CLAES instrument aperture door system N90-22083

HOLES (ELECTRON DEFICIENCIES)

Positron trapping in semiconductors [PB90-165606] N90-22410

HOLLOW CATHODES

Advanced electric propulsion research, 1989 [NASA-CR-185237] N90-21810

Hollow cathode operation at high discharge currents [NASA-CR-185238] N90-21953

Plasma contactor research, 1989 [NASA-CR-185212] N90-22389

HORSESHOE VORTICES

Effective methods of controlling a junction vortex system in an incompressible, three-dimensional, turbulent flow N90-21732

HOT ISOSTATIC PRESSING

Microstructure and mechanical properties of nickel aluminide powders consolidated by extrusion and hot isostatic pressing [DE90-009777] N90-21855

HOT PRESSING

Microstructure and mechanical properties of nickel aluminide powders consolidated by extrusion and hot isostatic pressing [DE90-009777] N90-21855

HOT STARS

The emission lines in the ultra-violet spectrum of Beta Lyrae N90-22474

HUMAN BEHAVIOR

The insertion of human dynamics models in the flight control loops of V/STOL research aircraft. Appendix 2: The optimal control model of a pilot in V/STOL aircraft control loops [NASA-CR-186598] N90-21776

HUMAN BEINGS

Networks for image acquisition, processing and display N90-22218

Human motion perception: Higher-order organization N90-22226

HUMAN FACTORS ENGINEERING

The insertion of human dynamics models in the flight control loops of V/STOL research aircraft. Appendix 2: The optimal control model of a pilot in V/STOL aircraft control loops [NASA-CR-186598] N90-21776

Insights into complex human performance [DE90-006957] N90-22214

Pyramid image codes N90-22243

NASA Information Sciences and Human Factors Program [NASA-TM-4190] N90-22529

HUMAN PERFORMANCE

Insights into complex human performance [DE90-006957] N90-22214

Networks for image acquisition, processing and display N90-22218

Stanford/NASA-Ames Center of Excellence in model-based human performance N90-22241

HUMAN REACTIONS

An adaptive human response mechanism controlling the V/STOL aircraft. Appendix 3: The adaptive control model of a pilot in V/STOL aircraft control loops [NASA-CR-186599] N90-21777

HUMAN TOLERANCES

Studies of 60-Hz exposure effects on human function [DE90-009473] N90-22210

HUMIDITY

Lagrangian model simulation of the turbulent transport of evaporating jet droplets N90-22168

HURRICANES

Forecast of Atlantic seasonal hurricane activity for 1990 N90-22194

HYBRID CIRCUITS

An investigation of narrow-bandgap semiconductors: Devices, circuits, and systems N90-22406

HYBRID PROPULSION

Hybrid propulsion technology program. Volume 1: Conceptional design package [NASA-CR-183953] N90-21793

Hybrid propulsion technology program. Volume 2: Technology definition package [NASA-CR-183954] N90-21794

HYDRAULIC JETS

Laser Doppler anemometry measurements of a confined turbulent water jet with a uniform background flow N90-21971

HYDRAZINES

Numerical simulation model of hydrazine attitude control thrusters [INPE-4965-PRE/1534] N90-21848

HYDROCARBON FUELS

Hybrid propulsion technology program. Volume 1: Conceptional design package [NASA-CR-183953] N90-21793

HYDRODYNAMICS

Computer simulation of time-dependent spherically symmetric spacetimes containing radiating fluids: Formalism and code tests N90-22483

Interactions of massive stars with the interstellar medium: Bow shocks and superbubbles N90-22485

The evolution of the supernova remnant IC 443 N90-22486

A galaxy formation cookbook: Recipes and utensils N90-22508

HYDROGEN

On the use of external burning to reduce aerospace vehicle transonic drag [NASA-TM-103107] N90-21762

Photosynthetic water splitting, phase 2 [PB90-132671] N90-21833

The temperature variation of hydrogen diffusion coefficients in metal alloys [NASA-TM-100397] N90-21836

The effect of hydrogen and microstructure on the deformation and fracture behavior of a single crystal nickel-base superalloy [NASA-CR-185219] N90-21849

The ratio of neutral hydrogen to neutral helium in the local interstellar medium N90-22499

HYDROGEN COMPOUNDS

A comparison of photospheric and circumstellar (HCN)/(CO)-ratios for bright carbon stars [PB90-151101] N90-22477

HYDROGEN FUELS

Photosynthetic water splitting, phase 2 [PB90-132671] N90-21833

HYDROGEN PRODUCTION

Photosynthetic water splitting, phase 2 [PB90-132671] N90-21833

Impact of low gravity on water electrolysis operation [NASA-CR-185521] N90-21870

HYDROLOGY

In-situ fracture stiffness determination [DE90-009202] N90-22173

HYDROLYSIS

Polysiloxanes derived from the controlled hydrolysis of tetraethoxysilane as precursors to silica for use in ceramic processing [NASA-TM-102489] N90-21858

Surface structure and chemistry of high surface area silica gels [DE90-007684] N90-21865

HYDROSTATICS

Failure mechanisms under complex loading of glass-reinforced polyester composites and their matrices: The effect of superposed hydrostatic pressures up to 300 MPa on axial tensile and compressive strengths, and in-plane shear properties of unidirtionally reinforced glass-polyester composites and the relevant polyesters N90-22072

A study of creep damage using microradiography and continuum damage mechanics N90-22109

Semigeostrophic flow over orography in a stratified rotating atmosphere N90-22163

HYDROXYL EMISSION

A three-year study of the OH masers in Orion-KL and a study of the (3,2) transition of ammonia N90-22471

Kinematic models of cometary comae N90-22495

HYDROXYL RADICALS

Saturated fluorescence measurements of the hydroxyl radical in laminar high-pressure flames [NASA-CR-185218] N90-22022

Kinematic models of cometary comae N90-22495

HYPERBOLIC COORDINATES

Graphs of the state of stress at rounded corners [MEMT-1] N90-22122

HYPERCUBE MULTIPROCESSORS

Molecular dynamics simulations of short-range force systems on 1024-node hypercubes [DE90-009833] N90-22259

HYPERGEOMETRIC FUNCTIONS

On a third q-Bessel function [REPT-89-48] N90-22344

HYPERSONIC AIRCRAFT

Prediction of forces and moments for flight vehicle control effectors. Part 1: Validation of methods for predicting hypersonic vehicle controls forces and moments [NASA-CR-186571] N90-21734

Prediction of forces and moments for flight vehicle control effectors. Part 2: An analysis of delta wing aerodynamic control effectiveness in ground effect [NASA-CR-186572] N90-21735

HYPERSONIC FLOW

Numerical simulation of hypersonic flow around a space plane. Part 2: Application to high angles of attack flow [NAL-TR-1011T] N90-21726

HYPERSONIC INLETS

Computational modeling and validation for hypersonic inlets [NASA-TM-103111] N90-22011

HYPERSONICS

Prediction of forces and moments for flight vehicle control effectors. Part 1: Validation of methods for predicting hypersonic vehicle controls forces and moments [NASA-CR-186571] N90-21734

HYPERSPACES

On a third q-Bessel function [REPT-89-48] N90-22344

I

ICE CLOUDS
Inclusion of clouds and rain in atmospheric slant path calculations N90-21925
ICE FORMATION
Swept wing ice accretion modeling
[NASA-TM-103114] N90-21727
IDEAL GAS
Partial acoustic filtering applied to the equations of compressible flow
[DE90-000673] N90-22001
IDENTIFYING
The intensity dependent spread model and color constancy N90-22228
IGNITION
A comparison of the autoignition chemistry of n-butane and isobutane in an internal combustion engine
[DE90-009474] N90-21838
Detailed mechanism for oxidation of benzene
[NASA-TM-102443] N90-21842
ILLUMINATING
Factors affecting the perception of transparent motion N90-22233
IMAGE ANALYSIS
Multiresolution and time-frequency representations of signals
[REPT-89-47] N90-21946
A study of creep damage using microradiography and continuum damage mechanics N90-22109
Algorithms and architectures for robot vision N90-22236
Satellite image analysis using neural networks N90-22321
IMAGE CORRELATORS
An acousto-optic image correlator with a throughput rate of 1000 templates per second
[DE90-009323] N90-22249
IMAGE MOTION COMPENSATION
Passive navigation using image irradiance tracking N90-22232
IMAGE PROCESSING
Applications of remote sensing to studies of oceanic upper mixed layer dynamics N90-22137
Vision Science and Technology at NASA: Results of a Workshop
[NASA-TM-102214-REV-1] N90-22216
Networks for image acquisition, processing and display N90-22218
Parallel asynchronous hardware implementation of image processing algorithms N90-22219
Computation and parallel implementation for early vision N90-22222
Intensity dependent spread theory N90-22223
Image gathering, coding, and processing: End-to-end optimization for efficient and robust acquisition of visual information N90-22224
Hybrid vision activities at NASA Johnson Space Center N90-22225
Two-dimensional shape recognition using sparse distributed memory N90-22227
The intensity dependent spread model and color constancy N90-22228
Motion detection in astronomical and ice floe images N90-22231
Photonic processing at NASA Ames Research Center N90-22234
Instrumentation and robotic image processing using top-down model control N90-22239
Computer vision research at Marshall Space Flight Center N90-22240
Ames vision group research overview N90-22242
Pyramid image codes N90-22243
Intensity dependent spread processor and workstation N90-22244
Space environment robot vision system N90-22245
An acousto-optic image correlator with a throughput rate of 1000 templates per second
[DE90-009323] N90-22249
Symbolic pattern processing system for planar spatial structures
[DE90-001598] N90-22256
Edge recognition using image-processing hardware
[OUEL-1777/89] N90-22271
Implementing the Canny edge recognizer with datacube image-processing hardware
[OUEL-1786/89] N90-22272
Satellite image analysis using neural networks N90-22321
Low order FIR and IIR filters in dynamic vision
[OUEL-1785/89] N90-22384
IMAGERY
Computer vision techniques for rotorcraft low altitude flight N90-22237
IMAGES
Sampling and noise in vision networks N90-22217
Computation and parallel implementation for early vision N90-22222
Image gathering, coding, and processing: End-to-end optimization for efficient and robust acquisition of visual information N90-22224
Motion detection in astronomical and ice floe images N90-22231
Passive navigation using image irradiance tracking N90-22232
Factors affecting the perception of transparent motion N90-22233
IMAGING TECHNIQUES
Cirrus cloud optical properties measured with the University of Wisconsin high spectral resolution and volume imaging lidars N90-21932
Institute for Materials Science and Engineering, nondestructive evaluation: Technical activities
[PB90-132739] N90-22055
A study of creep damage using microradiography and continuum damage mechanics N90-22109
Kalman filter based range estimation for autonomous navigation using imaging sensors N90-22238
Object detection using structural matching
[INPE-4954-PRE/1532] N90-22333
An investigation of narrow-bandgap semiconductors: Devices, circuits, and systems N90-22406
A high galactic latitude survey of far ultraviolet excess objects N90-22473
The optical night sky at low surface brightness: High latitude dust and faint field galaxies N90-22481
The production and spatial distribution of neutral and ionized water vapor in Comet P/Halley N90-22484
IMPACT
Transient response of a cylindrical shell of finite length to transverse impact
[OUEL-1780/89] N90-22123
IMPACT DAMAGE
Development of ultrasonic nondestructive methods for defect and damage characterization in composite materials N90-21816
Impact tolerant material
[NASA-CASE-LAR-12887-3] N90-21822
The controlled-damage concept in design of laminated composites N90-21830
IMPACT LOADS
Martensitic transformation induced by stress pulses
[DE90-009534] N90-21854
A dynamic motion simulator for future European docking systems N90-22085
Severe shock and vibration environments for electronic components
[DE90-007686] N90-22113
Dynamic response of a complex encapsulated electronic assembly subjected to a severe shock environment
[DE90-007689] N90-22114
IMPURITIES
Impurity control in toroidal devices
[DE90-618585] N90-22399
IN-FLIGHT MONITORING
Preliminary development of an intelligent computer assistant for engine monitoring
[NASA-TM-101702] N90-22322
INCLUSIONS
Scattering of waves by inclusions in a nonhomogeneous elastic half space solved by boundary element methods
[PB90-145699] N90-22107
INCOMPRESSIBLE BOUNDARY LAYER
An investigation of turbulence structure in a low Reynolds number incompressible turbulent boundary layer N90-21966
INCOMPRESSIBLE FLOW
Effective methods of controlling a junction vortex system in an incompressible, three-dimensional, turbulent flow N90-21732
Modeling of vortex-induced oscillations based on indicial response approach
[NASA-CR-186560] N90-21736
An upwind-differencing scheme for the incompressible Navier-Stokes equations
[NASA-TM-101051] N90-21757
Plane Stokes flow driven by capillarity on a free surface: Overview and status
[DE90-009186] N90-22008
An unsteady time asymptotic flow in the square driven cavity
[NASA-TM-103141] N90-22016
INCONEL (TRADEMARK)
Grain boundary intermetallic phases in alloy 718
[DE90-009812] N90-22417
INDEXES (DOCUMENTATION)
Aeronautical engineering: A continuing bibliography with indexes (supplement 250)
[NASA-SP-7037(250)] N90-21722
European network of interest in the measurement and analysis of mean sea levels from tide gauge records
[PB90-151929] N90-22196
Aerospace medicine and biology: A continuing bibliography with indexes (supplement 334)
[NASA-SP-7011(334)] N90-22207
Aerospace medicine and biology: A continuing bibliography with indexes (supplement 335)
[NASA-SP-7011(335)] N90-22208
Index to NASA news releases and speeches, 1986
[NASA-TM-101899] N90-22430
Index to NASA news releases and speeches, 1987
[NASA-TM-101900] N90-22431
Index to NASA news releases and speeches, 1988
[NASA-TM-101901] N90-22432
NASA Thesaurus supplement: A four part cumulative supplement to the 1988 edition of the NASA Thesaurus (supplement 3)
[NASA-SP-7064-SUPPL-3] N90-22438
INDUCTANCE
Gas-puff z-pinch experiment
[IPPCZ-286] N90-22385
INDUCTION
Free electron lasers driven by linear induction accelerators: High power radiation sources N90-21800
Induction-type metal detector with increased scanning area capability
[NASA-CASE-KSC-11386-1] N90-22023
A knowledge-based system with learning for computer communication network design N90-22319
INDUCTION MOTORS
Analytical and experimental study of high phase order induction motors
[NASA-CR-186580] N90-21952
INDUSTRIES
Technology for electronic transfer of information: The present and future in North America N90-22442
INELASTIC SCATTERING
QCD Compton scattering at HERA energy
[NIKHEF-H/89-3] N90-22372
Low temperature properties of amorphous solids N90-22405
INERTIAL NAVIGATION
Passive navigation using image irradiance tracking N90-22232
INFERENCE
Analyzing spacecraft configurations through specialization and default reasoning N90-22308
Knowledge structure representation and automated updates in intelligent information management systems N90-22316
INFINITY
A frame approach to the H-infinity super-optimal solution
[OUEL-1761/89] N90-22327
INFLATABLE STRUCTURES
Free-Space Power Transmission
[NASA-CP-10016] N90-21795
Inflatable antennas for microwave pwoer transmission N90-21799
INFLATING
Gravitational couplings of the inflation in extended inflation
[NASA-CR-186595] N90-22504
INFORMATION
Applications to the aerospace and defense R and D community: The DOD computer-aided acquisition and logistics support (CALS) initiative N90-22453
INFORMATION DISSEMINATION
Facilitating knowledge sharing in organizations: Semiautonomous agents that learn to gather, classify, and distribute environmental scanning knowledge N90-22435
Technologies for electronic transfer of information: The present state and trends in Europe N90-22441
Technology for electronic transfer of information: The present and future in North America N90-22442
INFORMATION FLOW
Information technology applications: A British Aerospace Military Aircraft Ltd view N90-22455
INFORMATION MANAGEMENT
Using expert systems to implement a semantic data model of a large mass storage system N90-22315
Knowledge structure representation and automated updates in intelligent information management systems N90-22316
Managing Federal information resources
[PB90-100173] N90-22429
How to get it: A guide to defense-related information resources
[AD-A201600] N90-22433
Electronic mail systems N90-22451
INFORMATION RETRIEVAL
How to get it: A guide to defense-related information resources
[AD-A201600] N90-22433

NASA Thesaurus supplement: A four part cumulative supplement to the 1988 edition of the NASA Thesaurus (supplement 3) [NASA-SP-7064-SUPPL-3] N90-22438
Desk top publishing: What you need to know N90-22449
Electronic transfer of information applications in the Societe Aerospatiale N90-22454

INFORMATION SYSTEMS
Managing Federal information resources [PB90-100173] N90-22429
Current information technology resource requirements of the Federal government: Major systems acquisitions and planned resources [PB90-146820] N90-22439
Electronic Transfer of Information and its Impact on Aerospace and Defence Research and Development [AGARD-CP-466] N90-22440
Innovations in telecommunications networks N90-22444
Megatendances N90-22445
The Weapons Laboratory technical library: Automating with STILAS N90-22447
The automation plan of the General Directorate 1 (search) of the European Patent Office N90-22448
Electronic transfer of information applications in the Societe Aerospatiale N90-22454
Information technology applications: A British Aerospace Military Aircraft Ltd view N90-22455
NSSDC data listing [NASA-TM-102989] N90-22456
Natural resources information system for the state of Oklahoma [DE90-009483] N90-22458

INFORMATION THEORY
Vision science and technology for supervised intelligent space robots N90-22221
Image gathering, coding, and processing: End-to-end optimization for efficient and robust acquisition of visual information N90-22224
How to get it: A guide to defense-related information resources [AD-A201600] N90-22433
Current information technology resource requirements of the Federal government: Major systems acquisitions and planned resources [PB90-146820] N90-22439

INFORMATION TRANSFER
Electronic transfer of information applications in the Societe Aerospatiale N90-22454

INFRARED ABSORPTION
Infrared absorption spectroscopy and chemical kinetics of free radicals [DE90-009469] N90-21837
A temperature-dependent regular infrared band model for absorption and dispersion N90-21927

INFRARED INSTRUMENTS
Calculation of IR propagation statistics in the eastern Atlantic for surveillance system performance assessment N90-21938
Atmospheric modelling studies: A modelling comparison between IR and millimetric atmospheric propagation N90-21941

INFRARED LASERS
Development of mid-infrared solid state lasers for spaceborne lidar [NASA-CR-185095] N90-22031

INFRARED PHOTOMETRY
Photometric monitoring of early type emission line stars N90-22478

INFRARED RADIATION
Atmospheric Propagation in the UV, Visible, IR, and mm-Wave Region and Related Systems Aspects [AGARD-CP-454] N90-21907
The Mediterranean marine environment and its effects on aerosols and infrared transmission N90-21909
Millimetric, infrared, and optical propagation studies over a 500 m path N90-21913
LOWTRAN 7: Status, review, and impact for short-to-long-wavelength infrared applications N90-21917
Infrared propagation in the air-sea boundary layer N90-21926
Technique for selecting an aerosol model useful for infrared atmospheric transmittance calculations N90-21934
Fast method for computing infrared transmission, computation examples N90-21942
The calculation of infrared limb emission by ozone in the terrestrial middle atmosphere N90-22151
The modeling of IRAS detections of classical novae and related objects N90-22482

INFRARED STARS
Investigation of the late stages of stellar evolution: Mass loss from evolved stars N90-22492

INHIBITION (PSYCHOLOGY)
Excitatory and inhibitory backward conditioning in the rat N90-22204

INJECTION LOCKING
Linear, nonlinear, and tunable guided wave modes for high-power (GaAl)As semiconductor lasers N90-22036

INLET FLOW
Control of flow separation and mixing by aerodynamic excitation [NASA-TM-103131] N90-21733
Theoretical and experimental study of flow-control devices for inlets of indraft wind tunnels [NASA-TM-100050] N90-21778
Computational modeling and validation for hypersonic inlets [NASA-TM-103111] N90-22011

INORGANIC CHEMISTRY
Cloud chemistry and occurrence in the western United States: A synopsis of current information [PB90-134248] N90-22182

INSECTS
Unsteady separated flows produced by complex harmonic motions: Investigation of wing-flow interactions elicited by a mechanical model simulating dragonfly wing kinematics N90-22018

INSPECTION
Computerized inspection of gear tooth surfaces [NASA-TM-102395] N90-22054
The JPL/KSC telerobotic inspection demonstration N90-22312

INTEGRAL EQUATIONS
Elastodynamic scattering and transmission problems in three dimensions by the boundary integral equation method N90-22077

INTEGRALS
New algorithms for one-loop integrals [NIKHEF-H/89-17] N90-22268

INTERACTIONS
Numerical investigation of some control methods for 3-D turbulent interactions due to sharp fins N90-21764

INTERACTIVE CONTROL
Applications of algebraic grid generation N90-21979

INTERCEPTION
A comparison of time-optimal interception trajectories for the F-8 and F-15 [NASA-CR-186300] N90-21753

INTERFACES
Scalable coherent interface [DE90-008011] N90-22277

INTERFACIAL TENSION
Energy release rate analysis of interfacial cracks in composites N90-21829
VAMAS project on variable weld penetration: Surface tension of the steels [NPL-DMA(A)-188] N90-21856

INTERFERENCE DRAG
Slotted-wall research with disk and parachute models in a low-speed wind tunnel [DE90-002989] N90-21737

INTERFEROMETERS
Galileo Earth approach navigation using connected-element interferometer phase-delay tracking N90-21884
Using connected-element interferometer phase-delay data for Magellan navigation in Venus orbit N90-21885

INTERMETALLICS
Welding behavior and welding metallurgy of ductile intermetallic alloys [DE90-008908] N90-21852
Grain boundary intermetallic phases in alloy 718 [DE90-009812] N90-22417

INTERNAL COMBUSTION ENGINES
Lightweight piston architecture [NASA-CASE-LAR-13926-1] N90-22042

INTERNAL PRESSURE
Continued research on the strain to failure of thick-walled cylinders subjected to internal pressure [DE90-008952] N90-22115

INTERNAL WAVES
Formulation of non-reflecting boundary conditions in numerical models of the atmosphere N90-22175

INTERNATIONAL COOPERATION
Proceedings of the Conference on Technology-Based Confidence Building: Energy and Environment [CNSS-PAPERS-22] N90-22152
Mission to planet Earth N90-22153

INTERPLANETARY SPACECRAFT
System control of an autonomous planetary mobile spacecraft N90-22313

INTERPOLATION
Quiet mode for nonlinear rotor models [NASA-TM-102236] N90-21758
Nonlinear spline operator interpolation and sliding control of deformable maneuvering bodies N90-21878
Inclusion of clouds and rain in atmospheric slant path calculations N90-21925
Algebraic block-structured grid generation based on a macro-block concept N90-21978
Motion detection in astronomical and ice floe images N90-22231
An algorithm and computer program for the calculation of envelope curves [PB90-155409] N90-22254

INTERSTELLAR GAS
Interactions of massive stars with the interstellar medium: Bow shocks and superbubbles N90-22485

INTERSTELLAR MASERS
A three-year study of the OH masers in Orion-KL and a study of the (3,2) transition of ammonia N90-22471
Investigation of the late stages of stellar evolution: Mass loss from evolved stars N90-22492

INTERSTELLAR MATTER
Recombination lines of C I and N II in the interstellar medium N90-22466
The optical night sky at low surface brightness: High latitude dust and faint field galaxies N90-22481
The evolution of the supernova remnant IC 443 N90-22486
The Al-26(rho, gamma)Si-27 reaction: Stellar origins of galactic Al-26 N90-22498
The ratio of neutral hydrogen to neutral helium in the local interstellar medium N90-22499

INVARIANCE
Hopf bifurcation with nonsemisimple 1:1 resonance e [MEMO-808] N90-22347

INVENTORIES
Inventory of program packages related to the project SIMONA [ETN-90-96397] N90-22270

INVERSE SCATTERING
Generalized Herglotz functions and inverse scattering problem in a finite depth ocean [PB90-150996] N90-22197

INVERSIONS
Characteristics of cumulus bandclouds off the east coast of Hawaii N90-22178
A three-year study of the OH masers in Orion-KL and a study of the (3,2) transition of ammonia N90-22471

INVERTERS
MHD channel development, part 3 [DE90-009551] N90-22396

INVISCID FLOW
Prediction of length scales in a Mach reflection flowfield N90-21959

IO
Sulphur silicate interactions on the Jovian satellite Io N90-22515

IODINE
Injection-seeded Nd:YAG laser linewidth measurement using saturation spectroscopy in iodine [DE90-009537] N90-22034

IODINE LASERS
Direct solar-pumped iodine laser amplifier [NASA-CR-186442] N90-22030

ION DENSITY (CONCENTRATION)
The production and spatial distribution of neutral and ionized water vapor in Comet P/Halley N90-22484

ION IMPLANTATION
Mechanical properties of carbon-implanted niobium [DE90-009864] N90-21823

ION PRODUCTION RATES
Advanced electric propulsion research, 1989 [NASA-CR-185237] N90-21810

ION PROPULSION
Advanced electric propulsion research, 1989 [NASA-CR-185237] N90-21810
Hollow cathode operation at high discharge currents [NASA-CR-185238] N90-21953

ION SCATTERING
Computer simulation of ionospheric radio frequency heating [DE90-009478] N90-21944

IONIC COLLISIONS
Production and analysis by mass spectrometry of beams of polyglycol ions N90-21835

IONIZATION CHAMBERS
Derivation of radiation beam non-uniformity corrections for the calibration of large volume ionisation chambers [NPL-RSA(EXT)-11] N90-22382

IONOSPHERIC CURRENTS
Equilibrium and stability analysis of magnetospheric plasmas N90-21782

IONOSPHERIC HEATING
Computer simulation of ionospheric radio frequency heating [DE90-009478] N90-21944

IONS
Production and analysis by mass spectrometry of beams of polyglycol ions N90-21835
Hollow cathode operation at high discharge currents [NASA-CR-185238] N90-21953

IRON ALLOYS
Martensitic transformation induced by stress pulses [DE90-009534] N90-21854
IRRADIANCE
Measurement of the reflectance ratio of natural light in the sea [IOS-265] N90-22199
Passive navigation using image irradiance tracking N90-22232
IRRADIATION
Fracture toughness and tensile properties of alloy HT9 in thin sections under high neutron fluences [DE90-008386] N90-21851
High intensity laser beam interactions with single droplets N90-21924
Producing dense plasmas with x rays [DE90-009539] N90-22393
IRREGULARITIES
The initial imperfection databank at the Delft University of Technology, part 3 [LR-568] N90-21783
ISING MODEL
Operator algebra from fusion rules: The infinite number of Ising theories [NIKHEF-H/89-7] N90-22374
ISOMERS
The chemical basis for the origin of the genetic code and the process of protein synthesis [NASA-CR-186590] N90-22205
ISOPARAMETRIC FINITE ELEMENTS
Elastodynamic scattering and transmission problems in three dimensions by the boundary integral equation method N90-22077
ISOTOPE EFFECT
Towards a Sarkovski order for the embedding of disks maintaining their orientation [REPT-89-43] N90-22289
ITERATION
Towards a unified analysis methodology for composite rotor blades N90-21730
Analysis, selection, and implementation of procedures which approve optimal artificial satellite maneuvers [INPE-5003-TDL/397] N90-21786
Passive shape control of space antennas with determinate truss support structures N90-21949
Optimal 3-dimensional methods for linear programming [PB90-155391] N90-22253
Incomparable elements in algebraic lattices with applications to formal language theory [MEMO-INF-89-54] N90-22269
ITERATIVE SOLUTION
Local mode smoothing analysis for various incomplete factorization iterative methods in three dimensions [REPT-89-38] N90-22263
Performance of the IMP array processing algorithm: First results [RSRE-MEMO-4291] N90-22274

J

J INTEGRAL
Nonlinear fracture mechanics using semicircular specimens and tension-softening behavior N90-22108
JAPAN
Japanese magnetic confinement fusion research N90-22392
Technologies for electronic transfer of information: The present state and trends in Japan N90-22443
JET AIRCRAFT NOISE
Exhaust environment measurements of a turbofan engine equipped with an afterburner and 2D nozzle [NASA-CR-4289] N90-21760
JET ENGINE FUELS
Development of a computational fluid dynamics and chemistry model for the fouling of jet fuels [DE90-005664] N90-22003
JET ENGINES
WINCOF-I code for prediction of fan compressor unit with water ingestion [NASA-CR-185157] N90-21724
JET FLOW
Interaction of a turbulent round jet with the free surface N90-21964
Herbig-Haro objects and stellar jets N90-22487
JOINTS (ANATOMY)
Control of human arm movement via optimization N90-22334
JOINTS (JUNCTIONS)
Definition of large components assembled on-orbit and robot compatible mechanical joints [NASA-TM-100395] N90-22043
Cycle life machine for AX-5 space suit N90-22080
AX-5 space suit bearing torque investigation N90-22101
Circularity measuring system: A shape gauge designed especially for use on large objects N90-22104
JOSEPHSON JUNCTIONS
A refrigerated Dewar for the Josephson array voltage calibration system [DE90-005237] N90-22412
JUPITER (PLANET)
Equilibrium and stability analysis of magnetospheric plasmas N90-21782
Jupiter's drifting decametric bursts with the changing time scale [DE90-618870] N90-22517
Auroral ultraviolet darkening on the outer planets N90-22518

K

K-EPSILON TURBULENCE MODEL
Numerical study of laminar and turbulent flows past two-dimensional and axisymmetric bodies N90-22020
KALMAN FILTERS
An adaptive human response mechanism controlling the V/STOL aircraft. Appendix 3: The adaptive control model of a pilot in V/STOL aircraft control loops [NASA-CR-186599] N90-21777
Kalman filter based range estimation for autonomous navigation using imaging sensors N90-22238
UD filtering and smoothing applied to orbit determination [INPE-4966-PRE/1535] N90-22501
KINEMATICS
Direct inversion of rigid-body rotational dynamics [NASA-TM-102798] N90-21773
Unsteady separated flows produced by complex harmonic motions: Investigation of wing-flow interactions elicited by a mechanical model simulating dragonfly wing kinematics N90-22018
An alternative method to solving the kinematics of a redundant robot [DE90-006892] N90-22045
Elasto-plastic analysis for contact fatigue failure N90-22078
Control of human arm movement via optimization N90-22334
Kinematic models of cometary comae N90-22495
KINETIC ENERGY
Scaling of nonnuclear kinetic-energy antisatellites [DE90-009758] N90-21791
KINETICS
Development of a computational fluid dynamics and chemistry model for the fouling of jet fuels [DE90-005664] N90-22003
KLYSTRONS
Radar RFI at Goldstone DSS 12 and DSS 16 N90-21900
KNOWLEDGE BASES (ARTIFICIAL INTELLIGENCE)
A methodology for knowledge-based restructurable control to accommodate system failures N90-22058
PLAN-IT-2: The next generation planning and scheduling tool N90-22298
SURE (Science User Resource Expert): A science planning and scheduling assistant for a resource based environment N90-22302
A knowledge-based approach to improving optimization techniques in system planning N90-22303
Knowledge-based and integrated monitoring and diagnosis in autonomous power systems N90-22310
KNOWLEDGE REPRESENTATION
Knowledge structure representation and automated updates in intelligent information management systems N90-22316

L

LABORATORIES
International science and technology policies: Testimony before the Subcommittee on International Scientific Cooperation, Committee on Science, Space, and Technology, United States House of Representatives [DE90-009416] N90-22463
The role of automation and robotics in the Lunar-Based Chemical Analysis Laboratory [DE90-009401] N90-22516
LAGUERRE FUNCTIONS
Generalizations of a q-analogue of Laguerre polynomials [REPT-89-51] N90-22345
LAMINAR FLOW
An experimental investigation of the physical mechanisms controlling the asymmetric flow past slender bodies at large angles of attack N90-21767
European research on viscous flow (EuroVisc) [NLR-TP-89077-U] N90-22014
Saturated fluorescence measurements of the hydroxyl radical in laminar high-pressure flames [NASA-CR-185218] N90-22022
The laminar flow element: Its use as a flow standard [PB90-129677] N90-22157
LAMINAR MIXING
Experimental observations on transition to turbulence in confined coaxial jets and other boundary layer flows [DE90-008939] N90-22005
LAMINATES
Residual stresses in laminated thermoplastic matrix composites N90-21815
Strength in notched and impact-damaged laminates N90-21820
Computational simulation of structural fracture in fiber composites [NASA-TM-102505] N90-21821
Modelling of the impact response of fibre-reinforced composites [OUEL-1784/89] N90-21827
Failure analysis of woven hybrid composite using a finite element method [OUEL-1791/89] N90-21828
The controlled-damage concept in design of laminated composites N90-21830
Institute for Materials Science and Engineering, nondestructive evaluation: Technical activities [PB90-132739] N90-22055
Three-dimensional finite element formulations for thick and thin laminated plates N90-22132
LANDING GEAR
Advances in optimal active control techniques for aerospace systems; application to aircraft active landing gear N90-21769
LANDING SITES
Quantitative studies of the Martian south polar region using spacecraft images N90-22514
LANGUAGE PROGRAMMING
Incomparable elements in algebraic lattices with applications to formal language theory [MEMO-INF-89-54] N90-22269
LANTHANUM
Growth and patterning of laser ablated superconducting YBa2Cu3O7 films on LaAlO3 substrates [NASA-TM-102436] N90-22421
LANTHANUM OXIDES
Superconducting and semiconducting thin films of La(sub 123) and Y(sub 123) and their superlattices [DE90-009565] N90-22416
In-situ pulsed laser deposition of high-T(sub c) YBa(sub 2)Cu(sub 3)O(sub 7) superconducting thin films on (100) LaAlO3 substrates [DE90-009861] N90-22418
LAPLACE TRANSFORMATION
Propagation of transient acoustic waves in porous media [ETN-90-96401] N90-22015
The analysis of stress relaxation on indentation of a rigid punch into a viscoelastic sheet of finite thickness [NPL-DMA(A)-193] N90-22357
LARGE SPACE STRUCTURES
Large space systems antenna technology N90-21798
Inflatable antennas for microwave pwoer transmission N90-21799
Definition of large components assembled on-orbit and robot compatible mechanical joints [NASA-TM-100395] N90-22043
The 24th Aerospace Mechanisms Symposium [NASA-CP-3062] N90-22079
LASER ANEMOMETERS
Laser Doppler anemometry measurements of a confined turbulent water jet with a uniform background flow N90-21971
LASER ANNEALING
Pulsed laser processing of high temperature superconducting thin films [DE90-008928] N90-22413
LASER APPLICATIONS
New corrosion resistant ceramic coatings by laser processing [AERE-R-13166] N90-21863
Reactions of N2A3 sigma u + and candidates for short wavelengths lasers [DE90-009514] N90-22033
LASER BEAMS
New corrosion resistant ceramic coatings by laser processing [AERE-R-13166] N90-21863
High intensity laser beam interactions with single droplets N90-21924
High power CO2 laser instability and its corrections N90-22028
LASER CAVITIES
Development and applications of a coupled cavity sodium-chloride laser N90-22029

LASER INDUCED FLUORESCENCE
Saturated fluorescence measurements of the hydroxyl radical in laminar high-pressure flames
[NASA-CR-185218] N90-22022
LASER INTERFEROMETRY
Experiments with a laser interferometric gravitational wave antenna N90-22476
LASER MATERIALS
Direct solar-pumped iodine laser amplifier
[NASA-CR-186442] N90-22030
LASER MODE LOCKING
Development and applications of a coupled cavity sodium-chloride laser N90-22029
LASER OUTPUTS
Effect of atmospheric turbulence on electro-optical systems N90-21940
Development of mid-infrared solid state lasers for spaceborne lidar
[NASA-CR-185095] N90-22031
LASER POWER BEAMING
Solar-pumped laser for free space power transmission
N90-21804
LASER PUMPING
Direct solar-pumped iodine laser amplifier
[NASA-CR-186442] N90-22030
Development of mid-infrared solid state lasers for spaceborne lidar
[NASA-CR-185095] N90-22031
LASER SPECTROSCOPY
Transient effects in Brillouin gain spectroscopy in solids
[DE90-009476] N90-21839
Reactions of N2A3 sigma u + and candidates for short wavelengths lasers
[DE90-009514] N90-22033
Injection-seeded Nd:YAG laser linewidth measurement using saturation spectroscopy in iodine
[DE90-009537] N90-22034
Evaluating thermographic phosphors in an operating turbine engine
[DE90-004874] N90-22044
LASER STABILITY
Experiments with a laser interferometric gravitational wave antenna N90-22476
LASERS
Growth and patterning of laser ablated superconducting YBa2Cu3O7 films on LaAlO3 substrates
[NASA-TM-102436] N90-22421
International science and technology policies: Testimony before the Subcommittee on International Scientific Cooperation, Committee on Science, Space, and Technology, United States House of Representatives
[DE90-009416] N90-22463
LASING
Solar-pumped laser for free space power transmission
N90-21804
High power CO2 laser instability and its corrections
N90-22028
LATCHES
A robot end effector exchange mechanism for space applications N90-22088
Relatchable launch restraint mechanism for deployable booms N90-22091
Driving and latching of the Starlab pointing mirror doors N90-22093
Orbital Maneuvering Vehicle (OMV) three-point docking latch N90-22094
LATTICES (MATHEMATICS)
Incomparable elements in algebraic lattices with applications to formal language theory
[MEMO-INF-89-54] N90-22269
LAUNCH VEHICLES
The development of a complementary expendable launch vehicle interface for an STS deployable payload
N90-22086
LAUNCHING
Current management for improved railgun performance N90-21781
LEAKAGE
Heat leak measurements in superconducting dipole magnet supports
[DE90-620109] N90-22420
LEAST SQUARES METHOD
The use of local polynomial approximations in a knot-placement strategy for least squares spline fitting
[NPL-DITC-148/89] N90-22355
LECTURES
Index to NASA news releases and speeches, 1986
[NASA-TM-101899] N90-22430
Index to NASA news releases and speeches, 1987
[NASA-TM-101900] N90-22431
Index to NASA news releases and speeches, 1988
[NASA-TM-101901] N90-22432
LENNARD-JONES POTENTIAL
Molecular theory of fluid phase equilibria
[PB90-131277] N90-21832
LIAPUNOV FUNCTIONS
Nonlinear stability analysis and control of dynamical robotic systems N90-22037
A new stability criterion in the shallow-water system for two-dimensional coherent eddies in the atmosphere and oceans N90-22176
LIFE (DURABILITY)
Electrochemical impregnation and cycle life of lightweight nickel electrodes for nickel-hydrogen cells
[NASA-TM-103140] N90-21844
Practical nonlinear simulation of rotating machinery dynamics with application to turbine blade rubbing
N90-22038
LIFE SCIENCES
USSR Space Life Sciences Digest, issue 25
[NASA-CR-3922(29)] N90-22203
LIFE SUPPORT SYSTEMS
Publications of the NASA Controlled Ecological Life Support System (CELSS) Program, 1979-1989
[NASA-CR-4297] N90-21754
LIFTING ROTORS
Development and application of a generalized dynamic wake theory for lifting rotors N90-21731
LIGHT AMPLIFIERS
Direct solar-pumped iodine laser amplifier
[NASA-CR-186442] N90-22030
Beam propagation in direct nuclear pumped laser amplifiers
[DE90-009613] N90-22035
LIGHT EMISSION
Extended optical emission in 3CR radio galaxies
N90-22523
LIGHT SCATTERING
Brillouin gain spectroscopy in glasses and crystals
[DE90-009536] N90-21841
Measurement of the reflectance ratio of natural light in the sea
[IOS-265] N90-22199
LIGHTNING
Second National Winter Weather Workshop Conducted by the National Weather Service
[PB90-147414] N90-22183
A case study of cloud-to-ground lightning during the GALE program N90-22185
LIMB BRIGHTENING
The calculation of infrared limb emission by ozone in the terrestrial middle atmosphere N90-22151
LINE CURRENT
Voltage source ac-to-dc converters for high-power transmitters N90-21886
LINE SPECTRA
Injection-seeded Nd:YAG laser linewidth measurement using saturation spectroscopy in iodine
[DE90-009537] N90-22034
Improved crystal bending techniques applied to the LLNL dual-arm Johann mounting x ray spectrometer
[DE90-009528] N90-22415
Kinematic models of cometary comae N90-22495
LINEAR ACCELERATORS
Free electron lasers driven by linear induction accelerators: High power radiation sources N90-21800
LINEAR EVOLUTION EQUATIONS
The synergism of analytic and numerical techniques in general relativity: Calculation of radiative spacetimes
N90-22425
LINEAR PROGRAMMING
Computational methods and plasticity
[LR-583] N90-22120
Optimal 3-dimensional methods for linear programming
[PB90-155391] N90-22253
Symbolic pattern processing system for planar spatial structures
[DE90-001598] N90-22256
Long steps with the logarithmic penalty barrier function in linear programming
[REPT-89-44] N90-22265
Contractivity in the maximum norm for Runge-Kutta methods
[TW-89-06] N90-22352
LINEAR QUADRATIC REGULATOR
A decentralized linear quadratic control design method for flexible structures N90-21770
LINEAR SYSTEMS
Dynamic response of structures with uncertain parameters N90-22125
LINKAGES
Cycle life machine for AX-5 space suit N90-22080
LINKS
Computer conferencing: Minds meeting anywhere anytime N90-22452
LIQUEFIED GASES
High speed commercial transport fuels considerations and research needs
[NASA-TM-102535] N90-21869
LIQUID ATOMIZATION
Scattered-light scanner measurements of cryogenic liquid-jet breakup
[NASA-TM-102432] N90-22021
LIQUID HELIUM
Nonlinear acoustic interactions in superfluid helium
N90-22367
LIQUID OXYGEN
A superconducting quenchgun for delivering lunar derived oxygen to lunar orbit
[NASA-CR-185161] N90-21806
LIQUID PHASES
Molecular theory of fluid phase equilibria
[PB90-131277] N90-21832
LIQUID-GAS MIXTURES
An experimental investigation of the physical mechanisms controlling the asymmetric flow past slender bodies at large angles of attack N90-21767
LIQUID-VAPOR INTERFACES
Numerical simulation of liquid circulation in a bubbly column
[DE90-005226] N90-22002
LIQUIDS
A weak formulation for phase-change problems with bulk movement due to unequal densities
[DE90-009398] N90-22361
LITHIUM
Active primary lithium thionyl chloride battery for artillery applications
[DE90-009511] N90-21955
LITHIUM ISOTOPES
Investigation of correlations in nuclei with the (e,e'X) reaction
[ETN-90-96398] N90-22377
LITHIUM SULFUR BATTERIES
Aging characteristics of Li/SO(sub 2) cells
[NASA-CR-180432] N90-21954
LITHOGRAPHY
Report on the fifth workshop on synchrotron x ray lithography
[DE90-007903] N90-22411
LOAD DISTRIBUTION (FORCES)
Numerical solutions of the nonlinear theory of curved beams N90-22071
LOAD TESTING MACHINES
Cycle life machine for AX-5 space suit N90-22080
A dynamic motion simulator for future European docking systems N90-22085
LOADS (FORCES)
Passive shape control of space antennas with determinate truss support structures N90-21949
Nonlinear fracture mechanics using semicircular specimens and tension-softening behavior N90-22108
ANILISA: Computational module for Koiter's imperfection sensitivity theory
[LR-582] N90-22119
Adaptive control of a flexible manipulator with unknown changing loads N90-22293
An expert system for simulating electric loads aboard Space Station Freedom
[NASA-TM-103150] N90-22325
LOCAL AREA NETWORKS
Traffic placement policies for a multi-band network
N90-22279
Fairness problems at the media access level for high-speed networks N90-22287
LOGARITHMS
Long steps with the logarithmic penalty barrier function in linear programming
[REPT-89-44] N90-22265
LOGIC CIRCUITS
An investigation of narrow-bandgap semiconductors: Devices, circuits, and systems N90-22406
LOGIC PROGRAMMING
An introduction to selected structured methods
[RSRE-MEMO-4294] N90-22275
LOGISTICS
Electronic publishing with Standard Generalized Markup Language (SGML) N90-22450
Applications to the aerospace and defense R and D community: The DOD computer-aided acquisition and logistics support (CALS) initiative N90-22453
LONG TERM EFFECTS
Long term intensity stability of Auger electron spectrometers: Instructions for the interlaboratory comparison
[NPL-DMM(A)-1] N90-22027
LOSSES
Testing carbon fabric for oxidation mass loss
N90-21819
LOW ALTITUDE
Computer vision techniques for rotorcraft low altitude flight N90-22237

LOW CONDUCTIVITY
Development of low thermal conductivity pan-based carbon fibers for solid rocket motor nozzle applications N90-21818

LOW REYNOLDS NUMBER
An investigation of turbulence structure in a low Reynolds number incompressible turbulent boundary layer N90-21966

LOW TEMPERATURE
The influence of large, cold objects on engulfing fire environments [DE90-003342] N90-21875
Low temperature properties of amorphous solids N90-22405

LOW THRUST
A trajectory generation and system characterization model for cislunar low-thrust spacecraft. Volume 2: Technical manual [NASA-CR-185172] N90-21807

LUBRICANTS
Self-lubricating polymer composites and polymer transfer film lubrication for space applications [NASA-TM-102492] N90-21862
Bearing elastohydrodynamic lubrication: A complex calculation made simple [NASA-TM-102575] N90-22041
Experience with synthetic fluorinated fluid lubricants N90-22095
AX-5 space suit bearing torque investigation N90-22101

LUBRICATING OILS
Experience with synthetic fluorinated fluid lubricants N90-22095
Positive lubrication system N90-22097

LUBRICATION
Bearing elastohydrodynamic lubrication: A complex calculation made simple [NASA-TM-102575] N90-22041

LUBRICATION SYSTEMS
Positive lubrication system N90-22097

LUMINOSITY
Search for rapidly star forming galaxies at high redshift N90-22465
Extended optical emission in 3CR radio galaxies N90-22523

LUNAR BASES
The role of automation and robotics in the Lunar-Based Chemical Analysis Laboratory [DE90-009401] N90-22516

LUNAR ORBITS
A superconducting quenchgun for delivering lunar derived oxygen to lunar orbit [NASA-CR-185161] N90-21806

LYRA CONSTELLATION
The emission lines in the ultra-violet spectrum of Beta Lyrae N90-22474

M

MACH NUMBER
Instabilities and subharmonic resonances of subsonic heated round jets, volume 2 [NASA-CR-186058] N90-22017

MACH REFLECTION
Prediction of length scales in a Mach reflection flowfield N90-21959

MACHINE TOOLS
Computerized inspection of gear tooth surfaces [NASA-TM-102395] N90-22054

MACHINE TRANSLATION
Technologies for electronic transfer of information: The present state and trends in Japan N90-22443

MACHINING
Data and conclusions from tests on small screws [DE90-007500] N90-22046

MAGELLAN PROJECT (NASA)
Using connected-element interferometer phase-delay data for Magellan navigation in Venus orbit N90-21885

MAGELLAN SPACECRAFT (NASA)
A higher density VLBI catalog for navigating Magellan and Galileo N90-21904

MAGELLANIC CLOUDS
A theoretical scenario for the dynamics of formation and early evolution of globular clusters in galaxies N90-22494

MAGMA
Sulphur silicate interactions on the Jovian satellite Io N90-22515

MAGNESIUM ISOTOPES
The Al-26(rho, gamma)Si-27 reaction: Stellar origins of galactic Al-26 N90-22498

MAGNETIC DIPOLES
Heat leak measurements in superconducting dipole magnet supports [DE90-620109] N90-22420

MAGNETIC DISKS
Evaluation of optical storage technology for decision support databases N90-22436

MAGNETIC EFFECTS
Current drive in a supernova N90-22491

MAGNETIC FIELD CONFIGURATIONS
Hollow cathode operation at high discharge currents [NASA-CR-185238] N90-21953

MAGNETIC FIELDS
Magnetic turbulence versus safety factor in the Tokapole 2 tokamak N90-22391
On the theory of Heiser and Shercliff experiment. Part 1: MHD flow in an open channel in strong uniform magnetic field [OUEL-1804/89-PT-1] N90-22400
On the theory of Heiser and Shercliff experiment. Part 2: MHD flow between two cylinders in strong radical magnetic field [OUEL-1805/89-PT-2] N90-22401
A theoretical scenario for the dynamics of formation and early evolution of globular clusters in galaxies N90-22494
Wind instability as a possible cause of the spiral structure formation in the gaseous subsystem of galaxies with the circular magnetic field [DE90-618944] N90-22507

MAGNETIC FLUX
The MHD structure of an open magnetotail boundary N90-22388

MAGNETIC PROPERTIES
Preparation and characterization of Cu2ZnGeS(4-y)Se(y) [AD-A217469] N90-22407

MAGNETIC RECORDING
SPOT 4 space magnetic recorder mechanisms N90-22082

MAGNETIC STARS
Gamma ray bursts: Current status of observations and theory [NASA-TM-100398] N90-22526

MAGNETIC SWITCHING
Free electron lasers driven by linear induction accelerators: High power radiation sources N90-21800

MAGNETOHYDRODYNAMIC FLOW
On the theory of Heiser and Shercliff experiment. Part 1: MHD flow in an open channel in strong uniform magnetic field [OUEL-1804/89-PT-1] N90-22400
On the theory of Heiser and Shercliff experiment. Part 2: MHD flow between two cylinders in strong radical magnetic field [OUEL-1805/89-PT-2] N90-22401
Multipole moments in general relativity and dynamical perturbations of black-hole magnetospheres N90-22509

MAGNETOHYDRODYNAMIC GENERATORS
MHD channel development, part 1 [DE90-009549] N90-22394
MHD channel development, part 2 [DE90-009550] N90-22395
MHD channel development, part 3 [DE90-009551] N90-22396
MHD channel development, part 4 [DE90-009552] N90-22397

MAGNETOHYDRODYNAMIC STABILITY
Equilibrium and stability analysis of magnetospheric plasmas N90-21782
Magnetic turbulence versus safety factor in the Tokapole 2 tokamak N90-22391
Wind instability as a possible cause of the spiral structure formation in the gaseous subsystem of galaxies with the circular magnetic field [DE90-618944] N90-22507
Jupiter's drifting decametric bursts with the changing time scale [DE90-618870] N90-22517

MAGNETOHYDRODYNAMIC WAVES
Slow shocks in coronal mass ejections [NASA-CR-186578] N90-22522
Gamma rays, cosmic rays, and local molecular clouds N90-22524

MAGNETOHYDRODYNAMICS
The MHD structure of an open magnetotail boundary N90-22388
MHD channel development, part 1 [DE90-009549] N90-22394
MHD channel development, part 2 [DE90-009550] N90-22395
MHD channel development, part 3 [DE90-009551] N90-22396
MHD channel development, part 4 [DE90-009552] N90-22397

MAGNETOSHEATH
The MHD structure of an open magnetotail boundary N90-22388

MAGNETOSPHERES
Multipole moments in general relativity and dynamical perturbations of black-hole magnetospheres N90-22509

MAINTENANCE
Microwave Landing System (MLS) remote monitoring subsystem/remote maintenance monitoring system [DOT/FAA/PS-89/2] N90-21749
Advances in optimal active control techniques for aerospace systems; application to aircraft active landing gear N90-21769
Reliability importance measures and their calculation [DE90-620391] N90-22057
Expert systems for automated maintenance of a Mars oxygen production system [NASA-CR-186209] N90-22215

MALFUNCTIONS
Rotor-to-stationary element rub-related vibration phenomena in rotating machinery: Literature survey N90-22065

MAN MACHINE SYSTEMS
An adaptive human response mechanism controlling the V/STOL aircraft. Appendix 3: The adaptive control model of a pilot in V/STOL aircraft control loops [NASA-CR-186599] N90-21777
Insights into complex human performance [DE90-006957] N90-22214
Hybrid vision activities at NASA Johnson Space Center N90-22225

MAN-COMPUTER INTERFACE
Understanding the computing system domain of advanced computing with microcomputers [DE90-009825] N90-22251
The application of connectionism to query planning/scheduling in intelligent user interfaces N90-22295

MANAGEMENT INFORMATION SYSTEMS
Knowledge-based semantic query processing: An optimal transformation approach N90-22437

MANAGEMENT METHODS
Current management for improved railgun performance N90-21781
Electronic publishing with Standard Generalized Markup Language (SGML) N90-22450
Information technology applications: A British Aerospace Military Aircraft Ltd view N90-22455

MANEUVERS
Optimal and near-optimal medium range air-to-air missile guidance against maneuvering targets N90-21766
Nonlinear spline operator interpolation and sliding control of deformable maneuvering bodies N90-21878

MANIPULATORS
Nonlinear stability analysis and control of dynamical robotic systems N90-22037
The Shock and Vibration Digest, volume 21, no. 3 N90-22064
Development of a multipurpose hand controller for JEMRMS N90-22087
The resupply interface mechanism RMS compatibility test N90-22090
Vision science and technology for supervised intelligent space robots N90-22221
Instrumentation and robotic image processing using top-down model control N90-22239
Adaptive control of a flexible manipulator with unknown changing loads N90-22293
The JPL/KSC telerobotic inspection demonstration N90-22312

MANNED ORBITAL LABORATORIES
Space Station Workshop: Commercial Missions and User Requirements [NASA-TM-102912] N90-22428

MANNED SPACE FLIGHT
A robotically constructed production and supply base on Phobos [NASA-CR-186234] N90-21872
Aeronautics and space report of the President: 1987 activities N90-22462

MANUAL CONTROL
Development of a multipurpose hand controller for JEMRMS N90-22087
A new six-degree-of-freedom force-reflecting hand controller for space telerobotics N90-22089

MANUALS
FORTRAN coding guidelines [DE90-009804] N90-22258

MANUFACTURING
Aging characteristics of Li/SO(sub 2) cells [NASA-CR-180432] N90-21954
Laboratory testing of Saft SEH-5-200 6 volt traction battery [DE90-009787] N90-21958
Data and conclusions from tests on small screws [DE90-007500] N90-22046

MANY BODY PROBLEM
The distribution of molecular clouds in spiral galaxies N90-22489
MAPPING
A three-year study of the OH masers in Orion-KL and a study of the (3,2) transition of ammonia N90-22471
MARINE ENVIRONMENTS
The Mediterranean marine environment and its effects on aerosols and infrared transmission N90-21909
MARINE METEOROLOGY
A survey of the maritime-aerosol data collected at South Uist and the implications for the LOWTRAN maritime aerosol model N90-21908
The Mediterranean marine environment and its effects on aerosols and infrared transmission N90-21909
The naval oceanic vertical aerosol model N90-21921
Infrared propagation in the air-sea boundary layer N90-21926
Aerosol separator for use in aircraft [PB90-142217] N90-22155
MARKERS
Evaluation of a prototype lighted ball marker for powerline obstructions [DOT/FAA/CT-TN90/12] N90-21774
MARKET RESEARCH
Technology for electronic transfer of information: The present and future in North America N90-22442
MARS (PLANET)
A robotically constructed production and supply base on Phobos [NASA-CR-186234] N90-21872
Quantitative studies of the Martian south polar region using spacecraft images N90-22514
MARS ATMOSPHERE
Preliminary design of a long-endurance Mars aircraft [NASA-CR-185243] N90-21763
Expert systems for automated maintenance of a Mars oxygen production system [NASA-CR-186209] N90-22215
MARS PHOTOGRAPHS
Quantitative studies of the Martian south polar region using spacecraft images N90-22514
MARS SURFACE
Quantitative studies of the Martian south polar region using spacecraft images N90-22514
MARTENSITIC TRANSFORMATION
Martensitic transformation induced by stress pulses [DE90-009534] N90-21854
MASERS
Operation of a step tunable megawatt gyrotron N90-21802
The 10-100 kW submillimeter gyrotron N90-21803
An 8.4-GHz dual-maser front-end system for Parkes reimplementation N90-21905
Cyclotron maser and plasma wave growth in magnetic loops [NASA-CR-179862] N90-22402
MASS DISTRIBUTION
Inclusion of clouds and rain in atmospheric slant path calculations N90-21925
The mass of the Coma cluster N90-22496
An astrophysics data program investigation of cluster evolution [NASA-CR-181296] N90-22510
MASS SPECTROSCOPY
Production and analysis by mass spectrometry of beams of polyglycol ions N90-21835
MASS TRANSFER
WINCOF-I code for prediction of fan compressor unit with water ingestion [NASA-CR-185157] N90-21724
Investigation of the late stages of stellar evolution: Mass loss from evolved stars N90-22492
The association of supernovae with regions of recent star formation in late-type galaxies N90-22497
MATCHING
Object detection using structural matching [INPE-4954-PRE/1532] N90-22333
MATHEMATICAL LOGIC
Some remarks on treatment of be in Montague's PTQ --- Proper Treatment of Quantification (PTQ) [REPT-89-40] N90-22267
MATHEMATICAL MODELS
Development and application of a generalized dynamic wake theory for lifting rotors N90-21731
Modeling of vortex-induced oscillations based on indicial response approach [NASA-CR-186560] N90-21736
Analytical study of the origin and behavior of asymmetric vortices [NASA-TM-102796] N90-21746
Conceptual design optimization study [NASA-CR-4298] N90-21755
Quiet mode for nonlinear rotor models [NASA-TM-102236] N90-21758
A decentralized linear quadratic control design method for flexible structures N90-21770
A conflict analysis of 4D descent strategies in a metered, multiple-arrival route environment [NASA-CR-182019] N90-21772
The insertion of human dynamics models in the flight control loops of V/STOL research aircraft. Appendix 2: The optimal control model of a pilot in V/STOL aircraft control loops [NASA-CR-186598] N90-21776
Strength in notched and impact-damaged laminates N90-21820
Studies on reactive flows N90-21831
Numerical simulation model of hydrazine attitude control thrusters [INPE-4965-PRE/1534] N90-21848
Nonlinear spline operator interpolation and sliding control of deformable maneuvering bodies N90-21878
Evaporation duct effects at millimeter wavelengths N90-21914
Lidar measurement of concentration and turbulence in battlefield obscurants N90-21931
Modelling UV-visible radiation observed from space N90-21937
Computation of broad spectral band electro-optical system transmittance response characteristics to military smokes and obscurants using field test data from transmissometer system measurements N90-21939
Effect of atmospheric turbulence on electro-optical systems N90-21940
Passive shape control of space antennas with determinate truss support structures N90-21949
Experimental and analytical investigations of granular materials: Shear flow and convective heat transfer N90-21968
Numerical simulation of liquid circulation in a bubbly column [DE90-005226] N90-22002
Mathematical modeling of fluid-solid mixtures [DE90-009152] N90-22007
Nonlinear stability analysis and control of dynamical robotic systems N90-22037
Practical nonlinear simulation of rotating machinery dynamics with application to turbine blade rubbing N90-22038
An alternative method to solving the kinematics of a redundant robot [DE90-006892] N90-22045
Computerized inspection of gear tooth surfaces [NASA-TM-102395] N90-22054
The Shock and Vibration Digest, volume 21, no. 2 N90-22059
Contact mechanics for three-dimensional geometries N90-22076
A continuum damage model for the quasi-static response of brittle materials [DE90-007681] N90-22112
Severe shock and vibration environments for electronic components [DE90-007686] N90-22113
The stress field due to an edge dislocation and some fracture problems for a three-phase composite cylinder model N90-22126
Analysis of a finite two-dimensional solid with an inclined crack and a rigid inclusion N90-22127
The mechanics of shear band formation in thermal viscoplastic materials at high rates of loading N90-22128
Three-dimensional finite element formulations for thick and thin laminated plates N90-22132
The interpretation of SAGE 2 ozone measurements in the lower mesosphere N90-22149
The calculation of infrared limb emission by ozone in the terrestrial middle atmosphere N90-22151
Mission to planet Earth N90-22153
Formulation of non-reflecting boundary conditions in numerical models of the atmosphere N90-22175
Second National Winter Weather Workshop Conducted by the National Weather Service [PB90-147414] N90-22183
The effects of linear acceleration on perception and nystagmus N90-22209
The art of fault-tolerant system reliability modeling [NASA-TM-102623] N90-22292
Object detection using structural matching [INPE-4954-PRE/1532] N90-22333
Efficient estimation in the Clayton-Cuzick model for survival data [TW-88-06] N90-22348
Clustering and uniqueness in mathematical models of percolation phenomena [ETN-90-96400] N90-22358
On the structure of Mandelbrot's percolation process and other random Cantor sets [REPT-89-54] N90-22362
Diffraction of light by ultrasonic pulses N90-22366
An investigation of the generation and radiation of aerodynamic noise in real piping systems N90-22368
Hybrid modeling of plasmas and applications to fusion and space physics N90-22387
Impurity control in toroidal devices [DE90-618585] N90-22399
Optical bistability in semiconducting material N90-22424
The evolution of the supernova remnant IC 443 N90-22486
Modelling late-time atmospheres of supernovae N90-22500
Stability of compactification during inflation [NASA-CR-186597] N90-22502
Gravitational couplings of the inflation in extended inflation [NASA-CR-186595] N90-22504
Soft inflation [NASA-CR-186593] N90-22506
Geology of coronae and domal structures on Venus and models of their origin N90-22513
MATHEMATICAL PROGRAMMING
A knowledge-based approach to improving optimization techniques in system planning N90-22303
MATRICES (CIRCUITS)
Optical shutter switching matrix [NASA-CASE-KSC-11392-1] N90-22383
MATRICES (MATHEMATICS)
METCAN verification status [NASA-TM-103119] N90-21824
On the existence of a positive definite solution of the matrix equation X + A(sup tau)X(exp -1)A = I [PB90-133976] N90-22335
MATRIX MATERIALS
Interfacial studies in fiber-reinforced thermoplastic-matrix composites N90-21814
Matrix density effects on the mechanical properties of SiC/RBSN composites [NASA-TM-103098] N90-21826
MAXIMUM LIKELIHOOD ESTIMATES
A real-time signal combining system for Ka-band feed arrays using maximum-likelihood weight estimates N90-21888
Orthogonal distance regression [PB90-151747] N90-22336
MEASURING INSTRUMENTS
Circularity measuring system: A shape gauge designed especially for use on large objects N90-22104
MECHANICAL DRIVES
The Shock and Vibration Digest, volume 21, no. 3 N90-22064
Development of cable drive systems for an automated assembly project N90-22105
MECHANICAL PROPERTIES
Development of low thermal conductivity pan-based carbon fibers for solid rocket motor nozzle applications N90-21818
Severe shock and vibration environments for electronic components [DE90-007686] N90-22113
MECHANICAL SHOCK
The Shock and Vibration Digest, volume 21, no. 2 N90-22059
The Shock and Vibration Digest, volume 21, no. 1 N90-22061
The Shock and Vibration Digest, volume 21, no. 3 N90-22064
The Shock and Vibration Digest, volume 21, no. 7 N90-22066
Optimum design of structures under shock and vibration environment N90-22067
The Shock and Vibration Digest, volume 21, no. 8 N90-22068
The Shock and Vibration Digest, volume 22, no. 1 N90-22073
The Shock and Vibration Digest, volume 21, no. 6 N90-22363
MEDITERRANEAN SEA
The Mediterranean marine environment and its effects on aerosols and infrared transmission N90-21909
MELTS (CRYSTAL GROWTH)
Effect of a crystal-melt interface on Taylor-vortex flow [NASA-CR-186512] N90-22408
MEMBRANE STRUCTURES
The Shock and Vibration Digest, volume 21, no. 1 N90-22061
A review of approximate methods for determining the vibrational modes of membranes N90-22063
MEMORY (COMPUTERS)
An adaptive vector quantization scheme N90-21898
Sparse distributed memory overview N90-22235
MENTAL PERFORMANCE
A study of mental models through communication between users and advisors solving software manipulation problems N90-22434

MERCURY ARCS
UV photo-enhanced MOCVD of cadmium and cadmium telluride [RSRE-MEMO-4208] N90-22422
MESOSCALE PHENOMENA
A case study of cloud-to-ground lightning during the GALE program N90-22185
Frontal structure in a mesoscale model N90-22187
MESOSPHERE
The interpretation of SAGE 2 ozone measurements in the lower mesosphere N90-22149
MESSAGE PROCESSING
CSMA/RN: A universal protocol for gigabit networks N90-22280
Alternative parallel ring protocols N90-22282
Modelling high data rate communication network access protocol N90-22285
Fairness problems at the media access level for high-speed networks N90-22287
A carrier sensed multiple access protocol for high data base rate ring networks N90-22288
A knowledge-based system with learning for computer communication network design N90-22319
Electronic mail systems N90-22451
MESSAGES
Electronic mail systems N90-22451
METABOLISM
The predictability and efficiency of human walking: Metabolic, mechanical, and biophysical considerations N90-22211
METAL FATIGUE
Structural fatigue in the 34-meter HA-Dec antennas N90-21902
METAL MATRIX COMPOSITES
METCAN verification status [NASA-TM-103119] N90-21824
Fatigue crack growth in unidirectional metal matrix composite [NASA-TM-103102] N90-22117
METAL POWDER
Method of making a cathode from tungsten powder [AD-D014434] N90-21850
Microstructure and mechanical properties of nickel aluminide powders consolidated by extrusion and hot isostatic pressing [DE90-009777] N90-21855
Institute for Materials Science and Engineering, nondestructive evaluation: Technical activities [PB90-132739] N90-22055
METAL-GAS SYSTEMS
The temperature variation of hydrogen diffusion coefficients in metal alloys [NASA-TM-100397] N90-21836
METALLIC GLASSES
Low temperature properties of amorphous solids N90-22405
METALS
Three-dimensional fatigue crack closure behavior of metals N90-21857
METEOROLOGICAL PARAMETERS
A survey of the maritime-aerosol data collected at South Uist and the implications for the LOWTRAN maritime aerosol model N90-21908
Millimetric, infrared, and optical propagation studies over a 500 m path N90-21913
Evaporation duct effects at millimeter wavelengths N90-21914
Interpreting meteorological data reports for LOWTRAN Navy aerosol model extinction calculations N90-21920
The naval oceanic vertical aerosol model N90-21921
Lidar measurements of the optical propagation environment N90-21930
Lidar measurement of concentration and turbulence in battlefield obscurants N90-21931
Technique for selecting an aerosol model useful for infrared atmospheric transmittance calculations N90-21934
Calculation of IR propagation statistics in the eastern Atlantic for surveillance system performance assessment N90-21938
Atmospheric modelling studies: A modelling comparison between IR and millimetric atmospheric propagation N90-21941
The observed three-dimensional structure of baroclinic waves in the Northern Hemisphere winter as revealed in a linear regression analysis N90-22167
JARE data reports, no. 140 (meteorology 21): Meteorological data at Asuka Camp, Antarctica in 1987 [ISSN-0075-3343] N90-22188
METEOROLOGY
Minimizing the effects of the atmosphere in the observation of ultraviolet radiation N90-21911
Evaporation duct effects at millimeter wavelengths N90-21914
Report on STC/Technische Universiteit (TU) Delft Extremely High Frequency (EHF) radio relay study N90-21915
Propagation environments, effects, and decision aids N90-21918
On three-dimensional scaling and consistent truncation of global atmospheric models N90-22164
JARE data reports, no. 140 (meteorology 21): Meteorological data at Asuka Camp, Antarctica in 1987 [ISSN-0075-3343] N90-22188
An investigation of meteorological effects on currents in the shelf and continental slope seas northwest of the United Kingdom. 2: Relationships between currents at different locations and with other variables [PB90-151911] N90-22195
METHANE
High speed commercial transport fuels considerations and research needs [NASA-TM-102535] N90-21869
MICROCOMPUTERS
Graphically-oriented nonlinear analysis of statically loaded plane frames on microcomputers [PB90-165945] N90-22248
Understanding the computing system domain of advanced computing with microcomputers [DE90-009825] N90-22251
MICROCRACKS
Fracture mechanics of monolithic ceramic materials under small scale microcracking conditions N90-21860
Elasto-plastic analysis for contact fatigue failure N90-22078
Combining acoustic emission locations and a microcrack damage model to study development of damage in brittle materials [DE90-005195] N90-22111
The pressure dilation of a deep, jointed region of the earth [DE90-007537] N90-22170
MICROMECHANICS
Failure mechanisms under complex loading of glass-reinforced polyester composites and their matrices: The effect of superposed hydrostatic pressures up to 300 MPa on axial tensile and compressive strengths, and in-plane shear properties of unidirtionally reinforced glass-polyester composites and the relevant polyesters N90-22072
MICROMETEOROLOGY
Scintillation of millimeter-wave intensity and phase caused by turbulence and precipitation N90-21912
MICROSTRUCTURE
The effect of hydrogen and microstructure on the deformation and fracture behavior of a single crystal nickel-base superalloy [NASA-CR-185219] N90-21849
Welding behavior and welding metallurgy of ductile intermetallic alloys [DE90-008908] N90-21852
The effect of aging at 343 C on type 308 stainless steel weldments [DE90-009232] N90-21853
Microstructure and mechanical properties of nickel aluminide powders consolidated by extrusion and hot isostatic pressing [DE90-009777] N90-21855
Failure mechanisms under complex loading of glass-reinforced polyester composites and their matrices: The effect of superposed hydrostatic pressures up to 300 MPa on axial tensile and compressive strengths, and in-plane shear properties of unidirtionally reinforced glass-polyester composites and the relevant polyesters N90-22072
Improved crystal bending techniques applied to the LLNL dual-arm Johann mounting x ray spectrometer [DE90-009528] N90-22415
Grain boundary intermetallic phases in alloy 718 [DE90-009812] N90-22417
MICROWAVE ANTENNAS
A real-time signal combining system for Ka-band feed arrays using maximum-likelihood weight estimates N90-21888
MICROWAVE EQUIPMENT
Method of making a cathode from tungsten powder [AD-D014434] N90-21850
MICROWAVE LANDING SYSTEMS
Microwave Landing System (MLS) remote monitoring subsystem/remote maintenance monitoring system [DOT/FAA/PS-89/2] N90-21749
Microwave Landing System (MLS) multiple system design interoperability interface control report [DOT/FAA/SA-89/2] N90-21750
MICROWAVE SCATTERING
The AGRISCATT-87 campaign: Processing of the Dutscat data [BCRS-89-20] N90-22140
MICROWAVE TRANSMISSION
Inflatable antennas for microwave pwoer transmission N90-21799
Microwave analog fiber-optic link for use in the deep space network N90-21883
MICROWAVES
Microwave analog fiber-optic link for use in the deep space network N90-21883
MIDCOURSE GUIDANCE
Engagement analysis study [DE90-009529] N90-22359
MIDCOURSE TRAJECTORIES
A trajectory generation and system characterization model for cislunar low-thrust spacecraft. Volume 2: Technical manual [NASA-CR-185172] N90-21807
MIDDLE ATMOSPHERE
The calculation of infrared limb emission by ozone in the terrestrial middle atmosphere N90-22151
MIE SCATTERING
The naval oceanic vertical aerosol model N90-21921
Inclusion of clouds and rain in atmospheric slant path calculations N90-21925
Modelling UV-visible radiation observed from space N90-21937
MILITARY TECHNOLOGY
Electronic Transfer of Information and its Impact on Aerospace and Defence Research and Development [AGARD-CP-466] N90-22440
Information technology applications: A British Aerospace Military Aircraft Ltd view N90-22455
MILLIMETER WAVES
Millimeter wavelength rectenna development N90-21797
High power millimeter wave source development program N90-21805
Atmospheric Propagation in the UV, Visible, IR, and mm-Wave Region and Related Systems Aspects [AGARD-CP-454] N90-21907
Scintillation of millimeter-wave intensity and phase caused by turbulence and precipitation N90-21912
Evaporation duct effects at millimeter wavelengths N90-21914
The mm-wave region propagation experiments by satellite N90-21916
Modeling millimeter-wave propagation effects in the atmosphere N90-21922
Millimetre-wave propagation in the evaporation duct N90-21929
Millimeter-wave bistatic scattering by terrain N90-21936
Atmospheric modelling studies: A modelling comparison between IR and millimetric atmospheric propagation N90-21941
MILLING MACHINES
Development, implementation and test of a computer program for the production of axisymmetric pattern moulds on a numerically controlled milling machine [LR-593] N90-21877
MINIATURIZATION
An assessment of the hardness of miniature vacuum tubes to high-voltage transients [DE90-009541] N90-21956
Small strain gage applications 2 [DE90-008312] N90-22026
On the design and development of a miniature ceramic gimbal bearing N90-22100
MINIMAX TECHNIQUE
Robust control of flexible structures N90-21784
MINING
A robotically constructed production and supply base on Phobos [NASA-CR-186234] N90-21872
MIRRORS
A soft actuation system for segmented reflector articulation and isolation N90-22084
Driving and latching of the Starlab pointing mirror doors N90-22093
MISSILE CONTROL
Optimal and near-optimal medium range air-to-air missile guidance against maneuvering targets N90-21766
Engagement analysis study [DE90-009529] N90-22359
MISSION PLANNING
Using connected-element interferometer phase-delay data for Magellan navigation in Venus orbit N90-21885
MIXING
Control of flow separation and mixing by aerodynamic excitation [NASA-TM-103131] N90-21733
The relationship between the buoyancy of near-surface air and the potential temperature of the tropopause N90-22165
MIXING LAYERS (FLUIDS)
An experimental investigation of mixing in buoyant flows N90-21963

Applications of remote sensing to studies of oceanic upper mixed layer dynamics N90-22137

MIXTURES

WINCOF-I code for prediction of fan compressor unit with water ingestion
[NASA-CR-185157] N90-21724

Mathematical modeling of fluid-solid mixtures
[DE90-009152] N90-22007

MODELS

Aeroelastic simulation of higher harmonic control N90-21768

Unsteady separated flows produced by complex harmonic motions: Investigation of wing-flow interactions elicited by a mechanical model simulating dragonfly wing kinematics N90-22018

The chemical basis for the origin of the genetic code and the process of protein synthesis
[NASA-CR-186590] N90-22205

A study of mental models through communication between users and advisors solving software manipulation problems N90-22434

MODULATION

Radar RFI at Goldstone DSS 12 and DSS 16 N90-21900

On decoding of multi-level MPSK modulation codes
[NASA-CR-186601] N90-22261

MODULUS OF ELASTICITY

Matrix density effects on the mechanical properties of SiC/RBSN composites
[NASA-TM-103098] N90-21826

MOLDS

Development, implementation and test of a computer program for the production of axisymmetric pattern moulds on a numerically controlled milling machine
[LR-593] N90-21877

MOLECULAR BEAM EPITAXY

Optical properties of zinc selenide grown using molecular beam deposition techniques
[RSRE-MEMO-4269] N90-22423

MOLECULAR CLOUDS

Interactions of massive stars with the interstellar medium: Bow shocks and superbubbles N90-22485

The evolution of the supernova remnant IC 443 N90-22486

The distribution of molecular clouds in spiral galaxies N90-22489

The Sagittarius B2 molecular cloud: An extreme case of a galactic center giant molecular cloud N90-22493

Gamma rays, cosmic rays, and local molecular clouds N90-22524

MOLECULAR DIFFUSION

Molecular dynamics simulations of short-range force systems on 1024-node hypercubes
[DE90-009833] N90-22259

MOLECULAR RELAXATION

Transport and relaxation properties in anisotropic superconductors N90-22403

MOLECULAR STRUCTURE

A comparison of the autoignition chemistry of n-butane and isobutane in an internal combustion engine
[DE90-009474] N90-21838

Surface structure and chemistry of high surface area silica gels
[DE90-007684] N90-21865

MOLECULAR THEORY

Molecular theory of fluid phase equilibria
[PB90-131277] N90-21832

MOLECULES

Molecular theory of fluid phase equilibria
[PB90-131277] N90-21832

Molecular dynamics simulations of short-range force systems on 1024-node hypercubes
[DE90-009833] N90-22259

Nonlinearity parameters of polymers N90-22369

MOM (SEMICONDUCTORS)

Millimeter wavelength rectenna development N90-21797

MOMENTUM

Test results and flight experience of ball bearing momentum and reaction wheels N90-22099

MOMENTUM THEORY

A dual potential formulation of the Navier-Stokes equations N90-21972

MONITORS

An 8.4-GHz dual-maser front-end system for Parkes reimplementation N90-21905

The laminar flow element: Its use as a flow standard
[PB90-129677] N90-22157

Automating security monitoring and analysis for Space Station Freedom's electric power system
[NASA-TM-103148] N90-22324

MONSOONS

A linear analysis of monsoon base states associated with banded convection N90-22179

MONTE CARLO METHOD

A conflict analysis of 4D descent strategies in a metered, multiple-arrival route environment
[NASA-CR-182019] N90-21772

Recognition and analysis of aircraft targets by radar, using structural pattern representations derived from polarimetric signatures N90-21879

Diffraction-limited imaging on the 200-inch telescope N90-22475

MORPHOLOGY

Interfacial studies in fiber-reinforced thermoplastic-matrix composites N90-21814

Production and analysis by mass spectrometry of beams of polyglycol ions N90-21835

Search for rapidly star forming galaxies at high redshift N90-22465

MOTION

Motion detection in astronomical and ice floe images N90-22231

MOTION PERCEPTION

Human motion perception: Higher-order organization N90-22226

Factors affecting the perception of transparent motion N90-22233

Ames vision group research overview N90-22242

MOTION SICKNESS

Issues in development, evaluation, and use of the NASA Preflight Adaptation Trainer (PAT)
[NASA-CR-185608] N90-22212

MOTION SIMULATION

Homogeneous dilute turbulent particle-laden water flows N90-21965

MOTION SIMULATORS

A dynamic motion simulator for future European docking systems N90-22085

MOTORS

Extraction of recovery of plasticizers from solid propellants and munitions
[AD-D014433] N90-21868

MOUNTAINS

Verification of Klett's method by comparison of lidar and transmissometer measurements N90-21933

An anomalous wind between valleys: Its characteristics and a proposed explanation
[DE90-008965] N90-22189

MULTIPHASE FLOW

Scattered-light scanner measurements of cryogenic liquid-jet breakup
[NASA-TM-102432] N90-22021

MULTIPLE ACCESS

Extremely high data-rate, reliable network systems research
[NASA-CR-186359] N90-22278

CSMA/RN: A universal protocol for gigabit networks N90-22280

A carrier sensed multiple access protocol for high data base rate ring networks N90-22288

MULTIPLIERS

An 8.4-GHz dual-maser front-end system for Parkes reimplementation N90-21905

MULTIPOLES

Multipole moments in general relativity and dynamical perturbations of black-hole magnetospheres N90-22509

MULTIPROCESSING (COMPUTERS)

SISAL 1.2: An alternative to FORTRAN for shared memory multiprocessors
[DE90-005181] N90-22257

MULTISENSOR APPLICATIONS

The AGRISCATT-87 campaign: Processing of the Dutscat data
[BCRS-89-20] N90-22140

MULTISTATIC RADAR

Millimeter-wave bistatic scattering by terrain N90-21936

MUSCULAR FUNCTION

Control of human arm movement via optimization N90-22334

N

NAP-OF-THE-EARTH NAVIGATION

Computer vision techniques for rotorcraft low altitude flight N90-22237

NASA PROGRAMS

Vision Science and Technology at NASA: Results of a Workshop
[NASA-TM-102214-REV-1] N90-22216

Index to NASA news releases and speeches, 1986
[NASA-TM-101899] N90-22430

Index to NASA news releases and speeches, 1987
[NASA-TM-101900] N90-22431

Index to NASA news releases and speeches, 1988
[NASA-TM-101901] N90-22432

Aeronautics and space report of the President: 1987 activities N90-22462

Research and Technology Objectives and Plans Summary (RTOPS)
[NASA-TM-89662] N90-22528

NAVIER-STOKES EQUATION

Numerical simulation of hypersonic flow around a space plane. Part 2: Application to high angles of attack flow
[NAL-TR-1011T] N90-21726

Modeling of vortex-induced oscillations based on indicial response approach
[NASA-CR-186560] N90-21736

Three-dimensional simulation of vortex breakdown
[NASA-TM-102664] N90-21744

A multiblock/multizone code (PAB 3D-v2) for the three-dimensional Navier-Stokes equations: Preliminary applications
[NASA-CR-182032] N90-21745

Analytical study of the origin and behavior of asymmetric vortices
[NASA-TM-102796] N90-21746

An upwind-differencing scheme for the incompressible Navier-Stokes equations
[NASA-TM-101051] N90-21757

A dual potential formulation of the Navier-Stokes equations N90-21972

Convergence acceleration of upwind relaxation methods for the Navier-Stokes equations N90-21973

Mesh generation for flow computation in turbomachine N90-21981

Grid patching approaches for complex three-dimensional configurations N90-21985

Generation and adaptation of 3-D unstructured grids for transient problems N90-21994

Computational modeling and validation for hypersonic inlets
[NASA-TM-103111] N90-22011

Bifurcations in viscous flow fields. On the genesis and development of topologically complicated separated flow structures
[PB90-167156] N90-22012

An unsteady time asymptotic flow in the square driven cavity
[NASA-TM-103141] N90-22016

Numerical study of laminar and turbulent flows past two-dimensional and axisymmetric bodies N90-22020

NAVIGATION

Optimal and near-optimal medium range air-to-air missile guidance against maneuvering targets N90-21766

The determination of maximum deep space station slew rates for a high Earth orbiter N90-21882

A higher density VLBI catalog for navigating Magellan and Galileo N90-21904

Passive navigation using image irradiance tracking N90-22232

NAVIGATION SATELLITES

Precise estimation of tropospheric path delays with GPS techniques N90-21881

NEBULAE

A three-year study of the OH masers in Orion-KL and a study of the (3,2) transition of ammonia N90-22471

NEODYMIUM LASERS

Injection-seeded Nd:YAG laser linewidth measurement using saturation spectroscopy in iodine
[DE90-009537] N90-22034

NEPTUNE (PLANET)

Auroral ultraviolet darkening on the outer planets N90-22518

NETWORK ANALYSIS

Networks for image acquisition, processing and display N90-22218

NEURAL NETS

The classification of defects from ultrasonic measurements
[AERE-R-13306] N90-22056

An approach to rescheduling activities based on determination of priority and disruptivity N90-22299

Adaptive pattern recognition by mini-max neural networks as a part of an intelligent processor N90-22317

Satellite image analysis using neural networks N90-22321

Neural implementation of a method for solving systems of linear algebraic equations
[NPL-DITC-155/89] N90-22356

NEUTRAL GASES

PIC code modeling of spacecraft charging potential during electron beam injection into a background of neutral gas and plasma, part 1
[NASA-CR-186602] N90-21792

Spectrum formation in active galactic nuclei and Type 2 supernovae N90-22490

The ratio of neutral hydrogen to neutral helium in the local interstellar medium N90-22499

NEUTRINOS

Current drive in a supernova N90-22491

NEUTRON SCATTERING

Low temperature properties of amorphous solids N90-22405

NEUTRON STARS

Physics of systems containing neutron stars [NASA-CR-186002] N90-22467

Does SN 1987A contain a rapidly vibrating neutron star [CAL-371] N90-22468

Does mass accretion lead to field decay in neutron stars [CAL-394] N90-22470

Gamma ray bursts: Current status of observations and theory [NASA-TM-100398] N90-22526

NEUTRONS

Fracture toughness and tensile properties of alloy HT9 in thin sections under high neutron fluences [DE90-008386] N90-21851

An analysis of the finite-differenced, even-parity discrete-ordinates equations in slab geometry [DE90-006479] N90-22337

Physics of systems containing neutron stars [NASA-CR-186002] N90-22467

NEWS

Index to NASA news releases and speeches, 1986 [NASA-TM-101899] N90-22430

Index to NASA news releases and speeches, 1987 [NASA-TM-101900] N90-22431

Index to NASA news releases and speeches, 1988 [NASA-TM-101901] N90-22432

NEWTON METHODS

Parallel non-linear optimization [REPT-89-45] N90-22290

NEWTON-RAPHSON METHOD

Elastic stability and nonlinear behavior of imperfect shells with initial stresses N90-22070

Numerical solutions of the nonlinear theory of curved beams N90-22071

NICKEL

Microstructure and mechanical properties of nickel aluminide powders consolidated by extrusion and hot isostatic pressing [DE90-009777] N90-21855

NICKEL ALLOYS

The temperature variation of hydrogen diffusion coefficients in metal alloys [NASA-TM-100397] N90-21836

The effect of hydrogen and microstructure on the deformation and fracture behavior of a single crystal nickel-base superalloy [NASA-CR-185219] N90-21849

NICKEL CADMIUM BATTERIES

Laboratory testing of Energy Research Corporation ERC 160 NiCd 6 volt traction battery [DE90-009629] N90-21957

Laboratory testing of Saft SEH-5-200 6 volt traction battery [DE90-009787] N90-21958

NICKEL HYDROGEN BATTERIES

Effect of LEO cycling on 125 Ah advanced design IPV nickel-hydrogen battery cells [NASA-TM-103128] N90-21808

Photovoltaic power for Space Station Freedom [NASA-TM-102569] N90-21812

Electrochemical impregnation and cycle life of lightweight nickel electrodes for nickel-hydrogen cells [NASA-TM-103140] N90-21844

Analysis of thermal energy storage material with change-of-phase volumetric effects [NASA-TM-102457] N90-21974

NIGHT SKY

The optical night sky at low surface brightness: High latitude dust and faint field galaxies N90-22481

NIOBIUM

Mechanical properties of carbon-implanted niobium [DE90-009864] N90-21823

NITRIDES

Studies on the use of supercritical ammonia for ceramic nitride synthesis and fabrication [NASA-TM-102570] N90-21843

NITROGEN

Recombination lines of C I and N II in the interstellar medium N90-22466

NOISE INTENSITY

Prediction of length scales in a Mach reflection flowfield N90-21959

NOISE MEASUREMENT

Exhaust environment measurements of a turbofan engine equipped with an afterburner and 2D nozzle [NASA-CR-4289] N90-21760

NOISE REDUCTION

The Shock and Vibration Digest, volume 21, no. 8 N90-22068

Spline function smoothing and differentiation of noisy data on a rectangular grid [DE90-009319] N90-22338

The Shock and Vibration Digest, volume 21, no. 6 N90-22363

Noise transmission into propeller-driven airplanes N90-22384

NOISE TEMPERATURE

Ultralow noise performance of an 8.4-GHz maser-feedhorn system N90-21889

Radiometric tests on wet and dry antenna reflector surface panels N90-21890

NONDESTRUCTIVE TESTS

Development of ultrasonic nondestructive methods for defect and damage characterization in composite materials N90-21816

Institute for Materials Science and Engineering, nondestructive evaluation: Technical activities [PB90-132739] N90-22055

Institute for Materials Science and Engineering, Fracture and Deformation Division: Technical activities, 1989 [PB90-155359] N90-22106

NONLINEAR EQUATIONS

Parallel non-linear optimization [REPT-89-45] N90-22290

A generalized complementarity problem in Hilbert space [DE90-009576] N90-22360

Numerical investigations of nonlinear behavior in the Einstein equations N90-22427

NONLINEAR PROGRAMMING

Analysis, selection, and implementation of procedures which approve optimal artificial satellite maneuvers [INPE-5003-TDL/397] N90-21786

NONLINEAR SYSTEMS

Quiet mode for nonlinear rotor models [NASA-TM-102236] N90-21758

Direct inversion of rigid-body rotational dynamics [NASA-TM-102798] N90-21773

Nonlinear fracture mechanics using semicircular specimens and tension-softening behavior N90-22108

NONLINEARITY

Accurate nonlinear control for satellites using reaction wheels [INPE-4983-PRE/1546] N90-21787

Nonlinear spline operator interpolation and sliding control of deformable maneuvering bodies N90-21878

Nonlinear stability analysis and control of dynamical robotic systems N90-22037

Practical nonlinear simulation of rotating machinery dynamics with application to turbine blade rubbing N90-22038

On three-dimensional scaling and consistent truncation of global atmospheric models N90-22164

Graphically-oriented nonlinear analysis of statically loaded plane frames on microcomputers [PB90-165945] N90-22248

Nonlinearity parameters of polymers N90-22369

NONUNIFORM FLOW

Flow boiling with enhancement devices for cold plate coolant channel design [NASA-CR-186358] N90-21961

NORMS

Contractivity in the maximum norm for Runge-Kutta methods [TW-89-06] N90-22352

NORTH AMERICA

Technology for electronic transfer of information: The present and future in North America N90-22442

NORTHERN HEMISPHERE

The observed three-dimensional structure of baroclinic waves in the Northern Hemisphere winter as revealed in a linear regression analysis N90-22167

NOSES (FOREBODIES)

Effective methods of controlling a junction vortex system in an incompressible, three-dimensional, turbulent flow N90-21732

NOTCH TESTS

Strength in notched and impact-damaged laminates N90-21820

NOVAE

The Al-26(rho, gamma)Si-27 reaction: Stellar origins of galactic Al-26 N90-22498

NOZZLE DESIGN

A computer program for the prediction of nozzle-propeller performance [LR-578] N90-21740

Theory and numerical analysis of single and multi-element nozzle propellers [LR-579] N90-21741

Recent improvements in the scope and accuracy of the performance prediction of nozzle propellers [LR-598] N90-21742

NOZZLE EFFICIENCY

Theory and numerical analysis of single and multi-element nozzle propellers [LR-579] N90-21741

NUCLEAR ASTROPHYSICS

Big-bang nucleosynthesis revisited [NASA-CR-186256] N90-22426

NUCLEAR ELECTRIC PROPULSION

A trajectory generation and system characterization model for cislunar low-thrust spacecraft. Volume 2: Technical manual [NASA-CR-185172] N90-21807

NUCLEAR FUSION

Operator algebra from fusion rules: The infinite number of Ising theories [NIKHEF-H/89-7] N90-22374

Japanese magnetic confinement fusion research N90-22392

Big-bang nucleosynthesis revisited [NASA-CR-186256] N90-22426

NUCLEAR PUMPED LASERS

Beam propagation in direct nuclear pumped laser amplifiers [DE90-009613] N90-22035

NUCLEAR PUMPING

Heat-transfer regimes in nuclear-reactor-pumped gas lasers [DE90-002904] N90-22032

Beam propagation in direct nuclear pumped laser amplifiers [DE90-009613] N90-22035

NUCLEAR REACTIONS

Investigation of correlations in nuclei with the (e,e'X) reaction [ETN-90-96398] N90-22377

NUCLEAR REACTORS

Proceedings of the Conference on Technology-Based Confidence Building: Energy and Environment [CNSS-PAPERS-22] N90-22152

NUCLEAR SPIN

Transport and relaxation properties in anisotropic superconductors N90-22403

NUCLEATION

Interfacial studies in fiber-reinforced thermoplastic-matrix composites N90-21814

Martensitic transformation induced by stress pulses [DE90-009534] N90-21854

UV photo-enhanced MOCVD of cadmium and cadmium telluride [RSRE-MEMO-4208] N90-22422

NUCLEI (NUCLEAR PHYSICS)

New calculations and measurements of the Coulomb cross-section for the production of direct electron pairs by high energy nuclei [NASA-TM-101280] N90-22371

Investigation of correlations in nuclei with the (e,e'X) reaction [ETN-90-96398] N90-22377

NUMERICAL ANALYSIS

Theory and numerical analysis of single and multi-element nozzle propellers [LR-579] N90-21741

Experimental determination of thermal conductance in bolted joint impact in satellites [INPE-4989-PRE/1551] N90-21788

Computational methods and plasticity [LR-583] N90-22120

Stability radius of polynomials occurring in the numerical solution of initial value problems [TW-89-04] N90-22350

The synergism of analytic and numerical techniques in general relativity: Calculation of radiative spacetimes N90-22425

NUMERICAL CONTROL

Development, implementation and test of a computer program for the production of axisymmetric pattern moulds on a numerically controlled milling machine [LR-593] N90-21877

Computerized inspection of gear tooth surfaces [NASA-TM-102395] N90-22054

NUMERICAL INTEGRATION

Finite element analysis of elastic contact problems with friction N90-22040

NUMERICAL STABILITY

Dynamical approach study of spurious steady-state numerical solutions of nonlinear differential equations. Part 1: The ODE connection and its implications for algorithm development in computational fluid dynamics [NASA-TM-102820] N90-22339

The theta-methods in the numerical solution of delay differential equations [TW-89-03] N90-22349

Stability radius of polynomials occurring in the numerical solution of initial value problems [TW-89-04] N90-22350

Stability analysis of numerical methods for delay differential equations
[TW-89-09] N90-22353

NYQUIST DIAGRAM
A robust stability result for generalised predictive control
[OUEL-1773/89] N90-22330

NYQUIST FREQUENCIES
Calculating the time domain average of gear vibration data sampled at less than the Nyquist frequency
[OUEL-1768/89] N90-22052

O

O RING SEALS
Flight set 360T004 (STS-30)
[NASA-CR-183927] N90-22049

O STARS
A high galactic latitude survey of far ultraviolet excess objects N90-22473
Interactions of massive stars with the interstellar medium: Bow shocks and superbubbles N90-22485

OBJECT PROGRAMS
Object-oriented databases: How are they different and what differnece does it make
[REPT-89-55] N90-22459

OBSERVATORIES
The determination of maximum deep space station slew rates for a high Earth orbiter N90-21882

OBSTACLE AVOIDANCE
Kalman filter based range estimation for autonomous navigation using imaging sensors N90-22238

OCEAN CURRENTS
An investigation of meteorological effects on currents in the shelf and continental slope seas northwest of the United Kingdom. 2: Relationships between currents at different locations and with other variables
[PB90-151911] N90-22195

OCEAN DYNAMICS
Applications of remote sensing to studies of oceanic upper mixed layer dynamics N90-22137

OCEAN MODELS
Applications of remote sensing to studies of oceanic upper mixed layer dynamics N90-22137
A free surface Bryan-Cox-Semtner model
[IOS-270] N90-22201

OCEAN SURFACE
European network of interest in the measurement and analysis of mean sea levels from tide gauge records
[PB90-151929] N90-22196

OCEAN TEMPERATURE
An investigation of meteorological effects on currents in the shelf and continental slope seas northwest of the United Kingdom. 2: Relationships between currents at different locations and with other variables
[PB90-151911] N90-22195

OCEANOGRAPHY
European network of interest in the measurement and analysis of mean sea levels from tide gauge records
[PB90-151929] N90-22196
Pre-study laser bathymetry
[BCRS-89-26] N90-22198

OCEANS
A new stability criterion in the shallow-water system for two-dimensional coherent eddies in the atmosphere and oceans N90-22176
Generalized Herglotz functions and inverse scattering problem in a finite depth ocean
[PB90-150996] N90-22197

OKLAHOMA
Natural resources information system for the state of Oklahoma
[DE90-009483] N90-22458

ON-LINE SYSTEMS
Nonlinear spline operator interpolation and sliding control of deformable maneuvering bodies N90-21878
Automating security monitoring and analysis for Space Station Freedom's electric power system
[NASA-TM-103148] N90-22324
Evaluation of optical storage technology for decision support databases N90-22436
Technologies for electronic transfer of information: The present state and trends in Europe N90-22441

ONBOARD DATA PROCESSING
An approach to on-board optimization of cruise at constant altitude
[LR-581] N90-21752

ONBOARD EQUIPMENT
Passive navigation using image irradiance tracking N90-22232

OPACITY
Update on the OPAL opacity code
[DE90-009946] N90-22480

OPERATING SYSTEMS (COMPUTERS)
Innovations in telecommunications networks N90-22444

OPERATORS (MATHEMATICS)
Nonlinear spline operator interpolation and sliding control of deformable maneuvering bodies N90-21878

OPTICAL BISTABILITY
Optical properties of zinc selenide grown using molecular beam deposition techniques
[RSRE-MEMO-4269] N90-22423
Optical bistability in semiconducting material N90-22424

OPTICAL COMMUNICATION
Optical shutter switching matrix
[NASA-CASE-KSC-11392-1] N90-22383

OPTICAL DATA PROCESSING
Photonic processing at NASA Ames Research Center N90-22234

OPTICAL DEPOLARIZATION
Polarization coupling in the acousto-optic interaction of surface waves N90-22365

OPTICAL EQUIPMENT
An acousto-optic image correlator with a throughput rate of 1000 templates per second
[DE90-009323] N90-22249

OPTICAL FIBERS
Stability studies of a pH-sensitive polymer matrix: Applications to fiber optic pH sensors
[DE90-009579] N90-21867

OPTICAL MEASUREMENT
A video-based experimental investigation of wing rock N90-21771

OPTICAL MEMORY (DATA STORAGE)
Evaluation of optical storage technology for decision support databases N90-22436
Technologies for electronic transfer of information: The present state and trends in Japan N90-22443
Electronic transfer of information applications in the Societe Aerospatiale N90-22454

OPTICAL PATHS
Diffraction of light by ultrasonic pulses N90-22366
Optical shutter switching matrix
[NASA-CASE-KSC-11392-1] N90-22383

OPTICAL PROPERTIES
Cirrus cloud optical properties measured with the University of Wisconsin high spectral resolution and volume imaging lidars N90-21932
Extended optical emission in 3CR radio galaxies N90-22523

OPTICAL RADAR
Atmospheric Propagation in the UV, Visible, IR, and mm-Wave Region and Related Systems Aspects
[AGARD-CP-454] N90-21907
Lidar measurements of the optical propagation environment N90-21930
Lidar measurement of concentration and turbulence in battlefield obscurants N90-21931
Cirrus cloud optical properties measured with the University of Wisconsin high spectral resolution and volume imaging lidars N90-21932
Verification of Klett's method by comparison of lidar and transmissometer measurements N90-21933
Development of mid-infrared solid state lasers for spaceborne lidar
[NASA-CR-185095] N90-22031
Dynamic and microphysical characteristics of cirrus clouds as revealed by aircraft, lidar, and other observations during FIRE N90-22177

OPTICAL SCANNERS
Induction-type metal detector with increased scanning area capability
[NASA-CASE-KSC-11386-1] N90-22023

OPTICAL SWITCHING
Optical shutter switching matrix
[NASA-CASE-KSC-11392-1] N90-22383

OPTICAL THICKNESS
Cirrus cloud optical properties measured with the University of Wisconsin high spectral resolution and volume imaging lidars N90-21932

OPTIMAL CONTROL
Optimal control of an aircraft flying through a downburst N90-21765
Optimal and near-optimal medium range air-to-air missile guidance against maneuvering targets N90-21766
Advances in optimal active control techniques for aerospace systems; application to aircraft active landing gear N90-21769
A decentralized linear quadratic control design method for flexible structures N90-21770
The insertion of human dynamics models in the flight control loops of V/STOL research aircraft. Appendix 2: The optimal control model of a pilot in V/STOL aircraft control loops
[NASA-CR-186598] N90-21776
Analysis, selection, and implementation of procedures which approve optimal artificial satellite maneuvers
[INPE-5003-TDL/397] N90-21786
The Shock and Vibration Digest, volume 21, no. 1 N90-22061
Recent advances in structural control N90-22062
A frame approach to the H-infinity super-optimal solution
[OUEL-1761/89] N90-22327
The role of input weighting and bounding in the characteristic GPC method
[OUEL-1762/89] N90-22328
Branch point placement
[OUEL-1767/89] N90-22329
An intelligent interface for the design of optimal control systems
[INPE-4917-PRE/1516] N90-22332
Control of human arm movement via optimization N90-22334
Low order FIR and IIR filters in dynamic vision
[OUEL-1785/89] N90-22384

OPTIMIZATION
Recent improvements in the scope and accuracy of the performance prediction of nozzle propellers
[LR-598] N90-21742
Optimization and guidance of flight trajectories in the presence of windshear
[NASA-CR-186163] N90-21747
A comparison of time-optimal interception trajectories for the F-8 and F-15
[NASA-CR-186300] N90-21753
Conceptual design optimization study
[NASA-CR-4298] N90-21755
Optimal control of an aircraft flying through a downburst N90-21765
Optimal and near-optimal medium range air-to-air missile guidance against maneuvering targets N90-21766
Optimal trajectories for the aeroassisted flight experiment. Part 4: Data, tables, and graphs
[NASA-CR-186164] N90-21780
Electromagnetic inverse profiling of stratified media
[ETN-90-96402] N90-21947
Generation, optimization, and adaptation of multidomain meshes around complex configurations N90-21990
Optimum design of structures under shock and vibration environment N90-22067
Optimization of power output from wind turbines N90-22146
Global distribution of organo-bromine gases N90-22150
Parallel non-linear optimization
[REPT-89-45] N90-22290
A knowledge-based approach to improving optimization techniques in system planning N90-22303
Control of human arm movement via optimization N90-22334
On the existence of a positive definite solution of the matrix equation X + A(sup tau)X(exp -1)A = I
[PB90-133976] N90-22335
Discrete variable structural optimization by the complex method
[LR-597] N90-22341
Knowledge-based semantic query processing: An optimal transformation approach N90-22437
Object-oriented databases: How are they different and what differnece does it make
[REPT-89-55] N90-22459

ORBIT CALCULATION
Using connected-element interferometer phase-delay data for Magellan navigation in Venus orbit N90-21885
UD filtering and smoothing applied to orbit determination
[INPE-4966-PRE/1535] N90-22501

ORBITAL ASSEMBLY
Definition of large components assembled on-orbit and robot compatible mechanical joints
[NASA-TM-100395] N90-22043
Development of cable drive systems for an automated assembly project N90-22105

ORBITAL MANEUVERING VEHICLES
Orbital Maneuvering Vehicle (OMV) three-point docking latch N90-22094
Computer vision research at Marshall Space Flight Center N90-22240

ORBITAL MANEUVERS
Orbital Maneuvering Vehicle (OMV) three-point docking latch N90-22094

ORBITAL RENDEZVOUS
The resupply interface mechanism RMS compatibility test N90-22090

ORBITAL SERVICING
Definition of large components assembled on-orbit and robot compatible mechanical joints
[NASA-TM-100395] N90-22043
The resupply interface mechanism RMS compatibility test N90-22090

Orbital Maneuvering Vehicle (OMV) three-point docking latch N90-22094

ORBITS

Towards a Sarkovski order for the embedding of disks maintaining their orientation
[REPT-89-43] N90-22289

UD filtering and smoothing applied to orbit determination
[INPE-4966-PRE/1535] N90-22501

ORGANIZATIONS

Facilitating knowledge sharing in organizations: Semiautonomous agents that learn to gather, classify, and distribute environmental scanning knowledge N90-22435

OROGRAPHY

Semigeostrophic flow over orography in a stratified rotating atmosphere N90-22163

ORTHOGONAL FUNCTIONS

Orthogonal distance regression
[PB90-151747] N90-22336

Generalizations of a q-analogue of Laguerre polynomials
[REPT-89-51] N90-22345

ORTHOPEDICS

Engineering specification and system design for CAD/CAM of custom shoes: UMC project effort
[NASA-CR-186547] N90-22255

OSCILLATING FLOW

Extension of a streamwise upwind algorithm to a moving grid system
[NASA-TM-102800] N90-21739

OSCILLATIONS

Modeling of vortex-induced oscillations based on indicial response approach
[NASA-CR-186560] N90-21736

OSCILLATORS

An 8.4-GHz dual-maser front-end system for Parkes reimplementation N90-21905

Dynamics of an oscillator with three-degrees-of-freedom in a uniform windfield
[REPT-89-56] N90-22121

OTOLITH ORGANS

The effects of linear acceleration on perception and nystagmus N90-22209

OXIDATION

Testing carbon fabric for oxidation mass loss N90-21819

Detailed mechanism for oxidation of benzene
[NASA-TM-102443] N90-21842

Ternary reactions among polymer substrate-organohalogen-antimony oxides under pyrolytic, oxidative and flaming conditions
[PB90-154766] N90-21861

OXYGEN

Device for quickly sensing the amount of O2 in a combustion product gas
[NASA-CASE-LAR-13816-1] N90-22025

OXYGEN ATOMS

The interpretation of SAGE 2 ozone measurements in the lower mesosphere N90-22149

OXYGEN CONSUMPTION

The predictability and efficiency of human walking: Metabolic, mechanical, and biophysical considerations N90-22211

OXYGEN PRODUCTION

Impact of low gravity on water electrolysis operation
[NASA-CR-185521] N90-21870

Expert systems for automated maintenance of a Mars oxygen production system
[NASA-CR-186209] N90-22215

OXYGEN SUPPLY EQUIPMENT

Hybrid propulsion technology program. Volume 1: Conceptional design package
[NASA-CR-183953] N90-21793

Hybrid propulsion technology program. Volume 2: Technology definition package
[NASA-CR-183954] N90-21794

OZONE

The interpretation of SAGE 2 ozone measurements in the lower mesosphere N90-22149

The calculation of infrared limb emission by ozone in the terrestrial middle atmosphere N90-22151

Opportunities for US-USSR cooperation in the investigation of Arctic stratospheric ozone N90-22154

OZONE DEPLETION

Experimental performance of ozone-safe alternative refrigerants: Experimental performance comparisons of R32, R125, R143a, R218, R134a, R152a, R124, R142b, RC318 and R143 in a refrigeration circuit
[DE90-009227] N90-21876

Opportunities for US-USSR cooperation in the investigation of Arctic stratospheric ozone N90-22154

P

PACKET SWITCHING

Scalable coherent interface
[DE90-008011] N90-22277

PACKET TRANSMISSION

Broadcast file distribution on packet satellite networks N90-21906

PACKETS (COMMUNICATION)

Broadcast file distribution on packet satellite networks N90-21906

PAINTS

Radiometric tests on wet and dry antenna reflector surface panels N90-21890

Robots for aircraft coatings removal: Parameters and requirements
[DE90-009429] N90-22048

PAIR PRODUCTION

New calculations and measurements of the Coulomb cross-section for the production of direct electron pairs by high energy nuclei
[NASA-TM-101280] N90-22371

PANEL METHOD (FLUID DYNAMICS)

Application of the TRANAIR rectangular grid approach to the aerodynamic analysis of complex configurations N90-21996

PANELS

Experimental determination of thermal conductance in bolted joint impact in satellites
[INPE-4989-PRE/1551] N90-21788

Radiometric tests on wet and dry antenna reflector surface panels N90-21890

PARALLEL COMPUTERS

Supercomputers need super arithmetic
[PB90-130253] N90-22252

PARALLEL FLOW

Instabilities and subharmonic resonances of subsonic heated round jets, volume 2
[NASA-CR-186058] N90-22017

PARALLEL PROCESSING (COMPUTERS)

Parallel asynchronous hardware implementation of image processing algorithms N90-22219

Computation and parallel implementation for early vision N90-22222

Image gathering, coding, and processing: End-to-end optimization for efficient and robust acquisition of visual information N90-22224

Photonic processing at NASA Ames Research Center N90-22234

Sparse distributed memory overview N90-22235

SISAL 1.2: An alternative to FORTRAN for shared memory multiprocessors
[DE90-005181] N90-22257

Molecular dynamics simulations of short-range force systems on 1024-node hypercubes
[DE90-009833] N90-22259

Scalable coherent interface
[DE90-008011] N90-22277

Parallel non-linear optimization
[REPT-89-45] N90-22290

PARALLEL PROGRAMMING

SISAL 1.2: An alternative to FORTRAN for shared memory multiprocessors
[DE90-005181] N90-22257

PARAMETER IDENTIFICATION

Uncertainty analysis of the accident effect area of a BLEVE
[REPT-89-49] N90-22160

Performance of the IMP array processing algorithm: First results
[RSRE-MEMO-4291] N90-22274

Autonomous power expert system N90-22306

PARAMETERIZATION

Operation of a step tunable megawatt gyrotron N90-21802

Modelling of optically and IR effective atmospheric turbulence N90-21923

Nonlinearity parameters of polymers N90-22369

PARAMETRIC AMPLIFIERS

Nonlinear accustic interactions in superfluid helium N90-22367

PARTIAL DIFFERENTIAL EQUATIONS

Numerical simulation model of hydrazine attitude control thrusters
[INPE-4965-PRE/1534] N90-21848

Dual-shaped offset reflector antenna designs from solutions of the geometrical optics first-order partial differential equations N90-21887

On the way to an integrated mesh generation system for industrial applications N90-21989

PARTICLE ACCELERATION

Current drive in a supernova N90-22491

PARTICLE COLLISIONS

Correlated electron processes in ion-atom collisions
[DE90-009477] N90-22370

PARTICLE ENERGY

Exclusive production of p, p-, pi, and pi- in photon photon collisions
[NIKHEF-H/89-9] N90-22376

PARTICLE INTERACTIONS

PIC code modeling of spacecraft charging potential during electron beam injection into a background of neutral gas and plasma, part 1
[NASA-CR-186602] N90-21792

QCD Compton scattering at HERA energy
[NIKHEF-H/89-3] N90-22372

Investigation of correlations in nuclei with the (e,e'X) reaction
[ETN-90-96398] N90-22377

PARTICLE PRODUCTION

The observed properties of the intermediate-degree gravity modes and their relevance to the solar neutrino paradox N90-22519

PARTICLE SPIN

Operator algebra from fusion rules: The infinite number of Ising theories
[NIKHEF-H/89-7] N90-22374

PARTICLE TRAJECTORIES

Swept wing ice accretion modeling
[NASA-TM-103114] N90-21727

PARTICLES

Mathematical modeling of fluid-solid mixtures
[DE90-009152] N90-22007

PATENT APPLICATIONS

The automation plan of the General Directorate 1 (search) of the European Patent Office N90-22448

PATENTS

The automation plan of the General Directorate 1 (search) of the European Patent Office N90-22448

Electronic transfer of information applications in the Societe Aerospatiale N90-22454

PATTERN RECOGNITION

Applications of remote sensing to studies of oceanic upper mixed layer dynamics N90-22137

Photonic processing at NASA Ames Research Center N90-22234

Algorithms and architectures for robot vision N90-22236

Instrumentation and robotic image processing using top-down model control N90-22239

Computer vision research at Marshall Space Flight Center N90-22240

An acousto-optic image correlator with a throughput rate of 1000 templates per second
[DE90-009323] N90-22249

Symbolic pattern processing system for planar spatial structures
[DE90-001598] N90-22256

Adaptive pattern recognition by mini-max neural networks as a part of an intelligent processor N90-22317

Satellite image analysis using neural networks N90-22321

Object detection using structural matching
[INPE-4954-PRE/1532] N90-22333

PAYLOAD INTEGRATION

The development of a complementary expendable launch vehicle interface for an STS deployable payload N90-22086

Driving and latching of the Starlab pointing mirror doors N90-22093

PENALTY FUNCTION

Long steps with the logarithmic penalty barrier function in linear programming
[REPT-89-44] N90-22265

PENETRATION

VAMAS project on variable weld penetration: Surface tension of the steels
[NPL-DMA(A)-188] N90-21856

PERCOLATION

Clustering and uniqueness in mathematical models of percolation phenomena
[ETN-90-96400] N90-22358

On the structure of Mandelbrot's percolation process and other random Cantor sets
[REPT-89-54] N90-22362

PERFLUORO COMPOUNDS

Experience with synthetic fluorinated fluid lubricants N90-22095

PERFORMANCE PREDICTION

Recent improvements in the scope and accuracy of the performance prediction of nozzle propellers
[LR-598] N90-21742

Validity of the two-level model for Viterbi decoder gap-cycle performance N90-21896

The predictability and efficiency of human walking: Metabolic, mechanical, and biophysical considerations N90-22211

Networks for image acquisition, processing and display N90-22218

PERFORMANCE TESTS
Flight motor set 360L002 (STS-27R). Volume 5: Nozzle component
[NASA-CR-183945] N90-21811
Aging characteristics of Li/SO(sub 2) cells
[NASA-CR-180432] N90-21954
Laboratory testing of Energy Research Corporation ERC 160 NiCd 6 volt traction battery
[DE90-009629] N90-21957
Laboratory testing of Saft SEH-5-200 6 volt traction battery
[DE90-009787] N90-21958

PERIOD DOUBLING
On spurious steady-state solutions of explicit Runge-Kutta schemes
[NASA-TM-102819] N90-22340

PERIODIC VARIATIONS
Towards a Sarkovski order for the embedding of disks maintaining their orientation
[REPT-89-43] N90-22289

PERTURBATION
Effect of atmospheric turbulence on electro-optical systems N90-21940
Normal forms for weakly non-linear perturbed wave equations
[REPT-89-41] N90-22343
Multipole moments in general relativity and dynamical perturbations of black-hole magnetospheres
N90-22509

PERTURBATION THEORY
An experimental investigation of the physical mechanisms controlling the asymmetric flow past slender bodies at large angles of attack N90-21767
Perturbation techniques in the dynamics and control of flexible manipulators
[OUEL-1772/89] N90-22053
A new stability criterion in the shallow-water system for two-dimensional coherent eddies in the atmosphere and oceans N90-22176

PH FACTOR
Stability studies of a pH-sensitive polymer matrix: Applications to fiber optic pH sensors
[DE90-009579] N90-21867

PHASE CHANGE MATERIALS
Analysis of thermal energy storage material with change-of-phase volumetric effects
[NASA-TM-102457] N90-21974

PHASE DETECTORS
Zero-G phase detector and separator
[NASA-CASE-LEW-14844-1] N90-22024

PHASE DIAGRAMS
Molecular theory of fluid phase equilibria
[PB90-131277] N90-21832

PHASE MODULATION
Multiwave diffraction analysis of transmission phase gratings
[RSRE-MEMO-4325] N90-21948

PHASE RULE
SGTE data for pure elements
[NPL-DMA(A)-195] N90-22460

PHASE SEPARATION (MATERIALS)
Grain boundary intermetallic phases in alloy 718
[DE90-009812] N90-22417

PHASE SHIFT
Transport and relaxation properties in anisotropic superconductors N90-22403
Transport properties of anisotropic superconductors
N90-22404

PHASE SHIFT KEYING
QPSK carrier-acquisition performance in the advanced receiver 2 N90-21892
On decoding of multi-level MPSK modulation codes
[NASA-CR-186601] N90-22261

PHASE TRANSFORMATIONS
Welding behavior and welding metallurgy of ductile intermetallic alloys
[DE90-008908] N90-21852
Extraction of recovery of plasticizers from solid propellants and munitions
[AD-D014433] N90-21868
A weak formulation for phase-change problems with bulk movement due to unequal densities
[DE90-009398] N90-22361
Preparation and characterization of Cu2ZnGeS(4-y)Se(y)
[AD-A217469] N90-22407
Topological defects in extended inflation
[NASA-CR-186594] N90-22505

PHASE VELOCITY
Instabilities and subharmonic resonances of subsonic heated round jets, volume 2
[NASA-CR-186058] N90-22017
A theoretical investigation of gravity-wave-generated stress and vorticity in the planetary boundary layer
N90-22512

PHENOLIC RESINS
Proceedings of the Advisory Committee on Standardization of Carbon-Phenolic Test Methods and Specifications
[NASA-CR-186478] N90-21817
Tribomaterial factors in space mechanism brake performance N90-22096

PHOBOS
A robotically constructed production and supply base on Phobos
[NASA-CR-186234] N90-21872

PHOSPHORS
Evaluating thermographic phosphors in an operating turbine engine
[DE90-004874] N90-22044

PHOTOCHEMICAL REACTIONS
Determination of rates of reaction in the gas-phase in the troposphere: Theory and practice. 2: Rate of direct photoreaction: Screening-level test guideline-spectroscopic determination of the cross section and the maximum rate of direct photoreaction in sunlight
[PB90-146291] N90-22156
Auroral ultraviolet darkening on the outer planets
N90-22518

PHOTOELASTICITY
A spectral analysis approach to wave propagation in layered solids N90-22131

PHOTOELECTRICITY
QCD Compton scattering at HERA energy
[NIKHEF-H/89-3] N90-22372

PHOTOGRAMMETRY
Space environment robot vision system N90-22245

PHOTOIONIZATION
Spectrum formation in active galactic nuclei and Type 2 supernovae N90-22490

PHOTOLYSIS
Infrared absorption spectroscopy and chemical kinetics of free radicals
[DE90-009469] N90-21837
UV photo-enhanced MOCVD of cadmium and cadmium telluride
[RSRE-MEMO-4208] N90-22422

PHOTOMETRY
Analysis of gamma squared Velorum photometry from the South Pole N90-22472

PHOTONS
Exclusive production of p, p-, pi, and pi- in photon photon collisions
[NIKHEF-H/89-9] N90-22376

PHOTORECEPTORS
Filling in the retinal image N90-22229

PHOTOSENSITIVITY
Stability studies of a pH-sensitive polymer matrix: Applications to fiber optic pH sensors
[DE90-009579] N90-21867

PHOTOSPHERE
A comparison of photospheric and circumstellar (HCN)/(CO)-ratios for bright carbon stars
[PB90-151101] N90-22477

PHOTOSYNTHESIS
Photosynthetic water splitting, phase 2
[PB90-132671] N90-21833

PHOTOVOLTAIC CELLS
Analysis of thermal energy storage material with change-of-phase volumetric effects
[NASA-TM-102457] N90-21974

PHOTOVOLTAIC CONVERSION
Space Station Freedom solar array panels plasma interaction test facility
[NASA-TM-102475] N90-22488

PHOTOVOLTAIC EFFECT
Photovoltaic Program Branch
[DE90-000318] N90-22142

PHYSIOLOGY
Studies of 60-Hz exposure effects on human function
[DE90-009473] N90-22210

PIEZOELECTRICITY
Active control of bearing preload using piezoelectric translators N90-22098

PIONEER 10 SPACE PROBE
Digital Doppler extraction demonstration with the advanced receiver N90-21893

PIPE FLOW
On the way to an integrated mesh generation system for industrial applications N90-21989
Turbulence in slurry pipe flow
[DE90-008940] N90-22006
Mathematical modeling of fluid-solid mixtures
[DE90-009152] N90-22007

PIPELINING (COMPUTERS)
Intensity dependent spread processor and workstation
N90-22244

PIPES (TUBES)
Turbulence in slurry pipe flow
[DE90-008940] N90-22006
Mathematical modeling of fluid-solid mixtures
[DE90-009152] N90-22007
Design of a telescoping tube system for access and handling equipment N90-22102
An investigation of the generation and radiation of aerodynamic noise in real piping systems N90-22368

PISTONS
Lightweight piston architecture
[NASA-CASE-LAR-13926-1] N90-22042

PLANAR STRUCTURES
Graphically-oriented nonlinear analysis of statically loaded plane frames on microcomputers
[PB90-165945] N90-22248
Symbolic pattern processing system for planar spatial structures
[DE90-001598] N90-22256
Polarization coupling in the acousto-optic interaction of surface waves N90-22365

PLANE STRESS
An investigation into the foundations of elastic-plastic fracture mechanics N90-22130

PLANE WAVES
The interaction between a plane shock wave and a cylindrical afterbody N90-21728

PLANETARY ATMOSPHERES
Jupiter's drifting decametric bursts with the changing time scale
[DE90-618870] N90-22517
Auroral ultraviolet darkening on the outer planets
N90-22518

PLANETARY BOUNDARY LAYER
A theoretical investigation of gravity-wave-generated stress and vorticity in the planetary boundary layer
N90-22512

PLANETARY COMPOSITION
Topical Conference on the Origin of the Earth
[NASA-CR-185061] N90-22166

PLANETARY EVOLUTION
Topical Conference on the Origin of the Earth
[NASA-CR-185061] N90-22166

PLANETARY GEOLOGY
Topical Conference on the Origin of the Earth
[NASA-CR-185061] N90-22166
Quantitative studies of the Martian south polar region using spacecraft images N90-22514

PLANETARY MAGNETIC FIELDS
Equilibrium and stability analysis of magnetospheric plasmas N90-21782

PLANETARY NEBULAE
Recombination lines of C I and N II in the interstellar medium N90-22466
Investigation of the late stages of stellar evolution: Mass loss from evolved stars N90-22492

PLANETS
Extraterrestrial life in the universe
[NASA-TM-102363] N90-22464

PLANFORMS
Prediction of forces and moments for flight vehicle control effectors. Part 2: An analysis of delta wing aerodynamic control effectiveness in ground effect
[NASA-CR-186572] N90-21735

PLANNING
Principles of Very Large Scale Integrated (VLSI) system planning N90-21950
The 1990 Goddard Conference on Space Applications of Artificial Intelligence
[NASA-CP-3068] N90-22294
The application of connectionism to query planning/scheduling in intelligent user interfaces
N90-22295
SURE (Science User Resource Expert): A science planning and scheduling assistant for a resource based environment N90-22302
A knowledge-based approach to improving optimization techniques in system planning N90-22303

PLANTING
Spectral response of wheat and its relationship with agronomic variables in the tropical region
[INPE-5018-RPE/612] N90-22138

PLASMA CONTROL
Magnetic turbulence versus safety factor in the Tokapole 2 tokamak N90-22391
Japanese magnetic confinement fusion research
N90-22392
Impurity control in toroidal devices
[DE90-618585] N90-22399

PLASMA DRIFT
Three-dimensional simulations of simple electron drift wave turbulence in tokamak geometry
[DE90-009581] N90-22398

PLASMA DYNAMICS
Hybrid modeling of plasmas and applications to fusion and space physics N90-22387

PLASMA INTERACTIONS
Space Station Freedom solar array panels plasma interaction test facility
[NASA-TM-102475] N90-22488
PLASMA PHYSICS
Hybrid modeling of plasmas and applications to fusion and space physics N90-22387
Plasma contactor research, 1989
[NASA-CR-185212] N90-22389
NSSDC data listing
[NASA-TM-102989] N90-22456
PLASMA POTENTIALS
Plasma contactor research, 1989
[NASA-CR-185212] N90-22389
PLASMA WAVES
Cyclotron maser and plasma wave growth in magnetic loops
[NASA-CR-179862] N90-22402
PLASMAS (PHYSICS)
Equilibrium and stability analysis of magnetospheric plasmas N90-21782
Gas-puff z-pinch experiment
[IPPCZ-286] N90-22385
Hybrid modeling of plasmas and applications to fusion and space physics N90-22387
The MHD structure of an open magnetotail boundary N90-22388
Plasma contactor research, 1989
[NASA-CR-185212] N90-22389
PLASTIC DEFORMATION
Contact mechanics for three-dimensional geometries N90-22076
The mechanics of shear band formation in thermal viscoplastic materials at high rates of loading N90-22128
PLASTIC FLOW
The mechanics of shear band formation in thermal viscoplastic materials at high rates of loading N90-22128
PLASTIC PROPERTIES
Three-dimensional fatigue crack closure behavior of metals N90-21857
The Shock and Vibration Digest, volume 21, no. 8 N90-22068
Recent progress in the dynamic plastic behavior of structures, part 5 N90-22069
A study of creep damage using microradiography and continuum damage mechanics N90-22109
PLASTICIZERS
Extraction of recovery of plasticizers from solid propellants and munitions
[AD-D014433] N90-21868
PLATES
Pressurized bellows flat contact heat exchanger interface
[NASA-CASE-MSC-21271-1] N90-21999
PLATES (STRUCTURAL MEMBERS)
Progression of damage and fracture in composites under dynamic loading
[NASA-TM-103118] N90-21825
The Shock and Vibration Digest, volume 21, no. 8 N90-22068
Recent progress in the dynamic plastic behavior of structures, part 5 N90-22069
PLUMES
Sulphur silicate interactions on the Jovian satellite Io N90-22515
PLUTONIUM OXIDES
Final Environmental Impact Statement for the Ulysses Mission (Tier 2)
[NASA-TM-101104] N90-22162
PLY ORIENTATION
Residual stresses in laminated thermoplastic matrix composites N90-21815
PNEUMATIC CONTROL
Bi-directional thruster development and test report
[NASA-CR-182013] N90-21785
PNEUMATIC EQUIPMENT
Bi-directional thruster development and test report
[NASA-CR-182013] N90-21785
PNEUMATIC PROBES
The calibration and measuring procedure of a five-hole hemispherical head probe in compressible flow
[LR-585] N90-22013
POINT SOURCES
Photometric monitoring of early type emission line stars N90-22478
POINTING CONTROL SYSTEMS
Nonlinear spline operator interpolation and sliding control of deformable maneuvering bodies N90-21878
Balanced bridge feedback control system
[NASA-CASE-NPO-17430-1-CU] N90-21951
Driving and latching of the Starlab pointing mirror doors N90-22093
Active control of bearing preload using piezoelectric translators N90-22098
POINTS (MATHEMATICS)
Branch point placement
[OUEL-1767/89] N90-22329
POISSON EQUATION
On the way to an integrated mesh generation system for industrial applications N90-21989
POISSON RATIO
Failure analysis of woven hybrid composite using a finite element method
[OUEL-1791/89] N90-21828
POLAR CAPS
Quantitative studies of the Martian south polar region using spacecraft images N90-22514
POLAR REGIONS
A high galactic latitude survey of far ultraviolet excess objects N90-22473
The optical night sky at low surface brightness: High latitude dust and faint field galaxies N90-22481
POLARIMETERS
Radar scatterometry and polarimetry at 220 GHz N90-21935
POLARIZATION CHARACTERISTICS
Recognition and analysis of aircraft targets by radar, using structural pattern representations derived from polarimetric signatures N90-21879
POLICIES
International science and technology policies: Testimony before the Subcommittee on International Scientific Cooperation, Committee on Science, Space, and Technology, United States House of Representatives
[DE90-009416] N90-22463
POLLUTION MONITORING
The laminar flow element: Its use as a flow standard
[PB90-129677] N90-22157
POLLUTION TRANSPORT
Global distribution of organo-bromine gases N90-22150
The ASCOT 1988 valley/tributary interaction study
[DE90-009043] N90-22191
POLYACRYLONITRILE
Development of low thermal conductivity pan-based carbon fibers for solid rocket motor nozzle applications N90-21818
POLYCARBONATES
Thermomechanical properties of polymeric materials and related stresses
[NASA-TM-100758] N90-21864
POLYCRYSTALS
Mechanical properties of carbon-implanted niobium
[DE90-009864] N90-21823
Photovoltaic Program Branch
[DE90-000318] N90-22142
POLYESTERS
Failure mechanisms under complex loading of glass-reinforced polyester composites and their matrices: The effect of superposed hydrostatic pressures up to 300 MPa on axial tensile and compressive strengths, and in-plane shear properties of unidirtionally reinforced glass-polyester composites and the relevant polyesters N90-22072
POLYMER CHEMISTRY
Polysiloxanes derived from the controlled hydrolysis of tetraethoxysilane as precursors to silica for use in ceramic processing
[NASA-TM-102489] N90-21858
POLYMER MATRIX COMPOSITES
Self-lubricating polymer composites and polymer transfer film lubrication for space applications
[NASA-TM-102492] N90-21862
POLYMERIZATION
Polysiloxanes derived from the controlled hydrolysis of tetraethoxysilane as precursors to silica for use in ceramic processing
[NASA-TM-102489] N90-21858
Nonlinearity parameters of polymers N90-22369
POLYMETHYL METHACRYLATE
Fire propagation in concurrent flows
[PB90-151754] N90-21834
The pyrolysis of polymethylmethacrylate during combustion in a solid fuel combustion chamber
[LR-531] N90-21845
POLYNOMIALS
Generalizations of a q-analogue of Laguerre polynomials
[REPT-89-51] N90-22345
Stability radius of polynomials occurring in the numerical solution of initial value problems
[TW-89-04] N90-22350
POLYURETHANE RESINS
Thermomechanical properties of polymeric materials and related stresses
[NASA-TM-100758] N90-21864
POROUS BOUNDARY LAYER CONTROL
Propagation of transient acoustic waves in porous media
[ETN-90-96401] N90-22015
POSITRONS
Positron trapping in semiconductors
[PB90-165606] N90-22410
POSTFLIGHT ANALYSIS
Flight motor set 360L002 (STS-27R). Volume 5: Nozzle component
[NASA-CR-183945] N90-21811
UD filtering and smoothing applied to orbit determination
[INPE-4966-PRE/1535] N90-22501
POSTMISSION ANALYSIS (SPACECRAFT)
Flight motor set 360L002 (STS-27R). Volume 5: Nozzle component
[NASA-CR-183945] N90-21811
POSTURE
The effects of linear acceleration on perception and nystagmus N90-22209
POTASSIUM HYDROXIDES
Effect of LEO cycling on 125 Ah advanced design IPV nickel-hydrogen battery cells
[NASA-TM-103128] N90-21808
POTENTIAL FLOW
A dual potential formulation of the Navier-Stokes equations N90-21972
POWDER (PARTICLES)
Test method for fire extinguishing powder, Nordtest project 675-87
[PB90-166984] N90-21874
POWDER METALLURGY
Microstructure and mechanical properties of nickel aluminide powders consolidated by extrusion and hot isostatic pressing
[DE90-009777] N90-21855
POWER CONDITIONING
Electric power scheduling: A distributed problem-solving approach
[NASA-TM-103149] N90-22323
POWER TRANSMISSION
Free-Space Power Transmission
[NASA-CP-10016] N90-21795
PRANDTL NUMBER
Effect of a crystal-melt interface on Taylor-vortex flow
[NASA-CR-186512] N90-22408
PRE-MAIN SEQUENCE STARS
Photometric monitoring of early type emission line stars N90-22478
PRECIPITATION (METEOROLOGY)
Scintillation of millimeter-wave intensity and phase caused by turbulence and precipitation N90-21912
Models of aerosols, clouds, and precipitation for atmospheric propagation studies N90-21919
PREDICTION ANALYSIS TECHNIQUES
Recent improvements in the scope and accuracy of the performance prediction of nozzle propellers
[LR-598] N90-21742
Millimetric, infrared, and optical propagation studies over a 500 m path N90-21913
Modelling of optically and IR effective atmospheric turbulence N90-21923
UV spectral simulations using LOWTRAN 7 N90-21928
Multiblock topology specification and grid generation for complete aircraft configurations N90-21986
Review of analysis methods for mechanically fastened joints in composites
[LR-599] N90-22050
Fatigue crack growth predictions for variable-amplitude and spectrum loading
[LR-526] N90-22118
Uncertainty analysis of the accident effect area of a BLEVE
[REPT-88-49] N90-22160
On three-dimensional scaling and consistent truncation of global atmospheric models N90-22164
Satellite versus GCM-simulated radiation balance: Comparisons and implications for climate modeling N90-22180
The Shock and Vibration Digest, volume 21, no. 6 N90-22363
Noise transmission into propeller-driven airplanes N90-22364
PREDICTIONS
Prediction of forces and moments for flight vehicle control effectors. Part 1: Validation of methods for predicting hypersonic vehicle controls forces and moments
[NASA-CR-186571] N90-21734
The solution of scattering and radiation problems for complex configurations based on 3-D grid and patch models N90-21997
The role of input weighting and bounding in the characteristic GPC method
[OUEL-1762/89] N90-22328
A robust stability result for generalised predictive control
[OUEL-1773/89] N90-22330

Bicausal representations and multivariable generalized predictive control
[OUEL-1781/89] N90-22331

PREFORMS
Lightweight piston architecture
[NASA-CASE-LAR-13926-1] N90-22042

PREMIXED FLAMES
Studies on reactive flows N90-21831

PRESSURE DISTRIBUTION
An experimental investigation of the physical mechanisms controlling the asymmetric flow past slender bodies at large angles of attack N90-21767

PRESSURE EFFECTS
The pressure dilation of a deep, jointed region of the earth
[DE90-007537] N90-22170

PRESSURE MEASUREMENT
Exhaust environment measurements of a turbofan engine equipped with an afterburner and 2D nozzle
[NASA-CR-4289] N90-21760
The calibration and measuring procedure of a five-hole hemispherical head probe in compressible flow
[LR-585] N90-22013

PRESSURE VESSELS
Effect of LEO cycling on 125 Ah advanced design IPV nickel-hydrogen battery cells
[NASA-TM-103128] N90-21808
Continued research on the strain to failure of thick-walled cylinders subjected to internal pressure
[DE90-008952] N90-22115

PRESTRESSING
Active control of bearing preload using piezoelectric translators N90-22098

PRINTED CIRCUITS
Report on the fifth workshop on synchrotron x ray lithography
[DE90-007903] N90-22411

PRINTING
Desk top publishing: What you need to know N90-22449
Electronic publishing with Standard Generalized Markup Language (SGML) N90-22450

PROBABILITY THEORY
A stress-strength interference approach to fast and delayed fracture reliability analysis for ceramic components N90-21859
Calculation of IR propagation statistics in the eastern Atlantic for surveillance system performance assessment N90-21938
Probabilistic finite elements: Applications to fracture and fatigue N90-22134
General purpose heat source radioisotope thermoelectric generator program. Book 1: Accident analysis
[REPT-90SDS4202-BK-1] N90-22379
General purpose heat source radioisotope thermoelectric generator. Book 2: Accident analysis, appendices
[REPT-90SDS4202-BK-2] N90-22380
The association of supernovae with regions of recent star formation in late-type galaxies N90-22497

PROBLEM SOLVING
Neural implementation of a method for solving systems of linear algebraic equations
[NPL-DITC-155/89] N90-22356
A generalized complementarity problem in Hilbert space
[DE90-009576] N90-22360
A study of mental models through communication between users and advisors solving software manipulation problems N90-22434

PROCESS CONTROL (INDUSTRY)
Overview of current bulk and thick film high temperature superconductor processing strategies
[DE90-008949] N90-22414

PROGRAM VERIFICATION (COMPUTERS)
METCAN verification status
[NASA-TM-103119] N90-21824
Spacecraft command verification: The AI solution N90-22307

PROGRAMMING LANGUAGES
SISAL 1.2: An alternative to FORTRAN for shared memory multiprocessors
[DE90-005181] N90-22257
Electronic publishing with Standard Generalized Markup Language (SGML) N90-22450

PROGRESS
Solid fuel combustion chamber
[LR-562] N90-21846

PROJECT MANAGEMENT
Solid fuel combustion chamber
[LR-562] N90-21846
Solid fuel combustion chamber
[LR-591] N90-21847
Information technology applications: A British Aerospace Military Aircraft Ltd view N90-22455

PROJECT PLANNING
Large space systems antenna technology N90-21798
Solid fuel combustion chamber
[LR-591] N90-21847

PROJECTILES
Current management for improved railgun performance N90-21781
Active primary lithium thionyl chloride battery for artillery applications
[DE90-009511] N90-21955

PROJECTS
The AGRISCATT-87 campaign: Processing of the Dutscat data
[BCRS-89-20] N90-22140
Pre-study laser bathymetry
[BCRS-89-26] N90-22198

PROP-FAN TECHNOLOGY
Unsteady Euler solutions on dynamic blocked grids for complex configurations N90-21982

PROPANE
Test method for fire extinguishing powder, Nordtest project 675-87
[PB90-166984] N90-21874

PROPELLANT COMBUSTION
Extraction of recovery of plasticizers from solid propellants and munitions
[AD-D014433] N90-21868

PROPELLER EFFICIENCY
A computer program for the prediction of nozzle-propeller performance
[LR-578] N90-21740
Theory and numerical analysis of single and multi-element nozzle propellers
[LR-579] N90-21741

PROPELLER FANS
Unsteady Euler solutions on dynamic blocked grids for complex configurations N90-21982

PROPELLER SLIPSTREAMS
Recent improvements in the scope and accuracy of the performance prediction of nozzle propellers
[LR-598] N90-21742

PROPELLERS
Theory and numerical analysis of single and multi-element nozzle propellers
[LR-579] N90-21741

PROPULSION SYSTEM PERFORMANCE
Assessment of High Temperature Superconducting (HTS) electric motors for rotorcraft propulsion
[NASA-CR-185222] N90-21761
Preliminary design of a long-endurance Mars aircraft
[NASA-CR-185243] N90-21763

PROTEIN SYNTHESIS
The chemical basis for the origin of the genetic code and the process of protein synthesis
[NASA-CR-186590] N90-22205

PROTOCOL (COMPUTERS)
Broadcast file distribution on packet satellite networks N90-21906
Scalable coherent interface
[DE90-008011] N90-22277
Extremely high data-rate, reliable network systems research
[NASA-CR-186359] N90-22278
Traffic placement policies for a multi-band network N90-22279
CSMA/RN: A universal protocol for gigabit networks N90-22280
Alternative parallel ring protocols N90-22282
Performance of gigabit FDDI N90-22283
Distributed simulation of network protocols N90-22284
Modelling high data rate communication network access protocol N90-22285
Extensibility and limitations of FDDI N90-22286
Fairness problems at the media access level for high-speed networks N90-22287
A carrier sensed multiple access protocol for high data base rate ring networks N90-22288

PROTON RESONANCE
The Al-26(rho, gamma)Si-27 reaction: Stellar origins of galactic Al-26 N90-22498

PROTONS
Ultrahigh-energy particle flux from cosmic strings
[NASA-CR-186592] N90-22525

PROTOTYPES
Measurement of the reflectance ratio of natural light in the sea
[IOS-265] N90-22199
Facilitating knowledge sharing in organizations: Semiautonomous agents that learn to gather, classify, and distribute environmental scanning knowledge N90-22435

PSYCHOLOGICAL FACTORS
The psychology of computer displays in the modern mission control center
[NASA-TM-100451] N90-22213

PUBLIC HEALTH
Studies of 60-Hz exposure effects on human function
[DE90-009473] N90-22210

PUBLIC RELATIONS
Index to NASA news releases and speeches, 1986
[NASA-TM-101899] N90-22430
Index to NASA news releases and speeches, 1987
[NASA-TM-101900] N90-22431
Index to NASA news releases and speeches, 1988
[NASA-TM-101901] N90-22432

PULSARS
Does mass accretion lead to field decay in neutron stars
[CAL-394] N90-22470
Very high energy gamma rays from the Crab nebula and pulsar N90-22527

PULSE DIFFRACTION
Diffraction of light by ultrasonic pulses N90-22366

PULSE DURATION
Diffraction of light by ultrasonic pulses N90-22366

PULSE GENERATORS
Gas-puff z-pinch experiment
[IPPCZ-286] N90-22385

PULSED LASERS
Pulsed laser processing of high temperature superconducting thin films
[DE90-008928] N90-22413
In-situ pulsed laser deposition of high-T(sub c) YBa(sub 2)Cu(sub 3)O(sub 7) superconducting thin films on (100) LaAlO3 substrates
[DE90-009861] N90-22418

PULSES
Martensitic transformation induced by stress pulses
[DE90-009534] N90-21854

PUMP IMPELLERS
Experimental investigation of the effect of cavitation on the rotordynamic forces on a whirling centrifugal pump impeller N90-22039

PURIFICATION
The chemical basis for the origin of the genetic code and the process of protein synthesis
[NASA-CR-186590] N90-22205

PYROLYSIS
Fire propagation in concurrent flows
[PB90-151754] N90-21834
The pyrolysis of polymethylmethacrylate during combustion in a solid fuel combustion chamber
[LR-531] N90-21845
Ternary reactions among polymer substrate-organohalogen-antimony oxides under pyrolytic, oxidative and flaming conditions
[PB90-154766] N90-21861

PYROTECHNICS
Extraction of recovery of plasticizers from solid propellants and munitions
[AD-D014433] N90-21868

Q

Q SWITCHED LASERS
Development of mid-infrared solid state lasers for spaceborne lidar
[NASA-CR-185095] N90-22031

Q VALUES
Generalizations of a q-analogue of Laguerre polynomials
[REPT-89-51] N90-22345

QUADRATIC EQUATIONS
A Chinese bibliography on quadratic systems of differential equations
[REPT-89-39] N90-22342

QUADRATURES
QPSK carrier-acquisition performance in the advanced receiver 2 N90-21892

QUALITY CONTROL
Testing of an advanced thermochemical conversion reactor system
[DE90-007989] N90-22141
Software quality assurance: Towards a measurable quality improvement
[REPT-89-42] N90-22264
Natural resources information system for the state of Oklahoma
[DE90-009483] N90-22458

QUANTUM CHROMODYNAMICS
QCD Compton scattering at HERA energy
[NIKHEF-H/89-3] N90-22372

QUANTUM WELLS
Optical bistability in semiconducting material N90-22424

QUASARS
Spectrum formation in active galactic nuclei and Type 2 supernovae N90-22490
QUATERNIONS
Direct inversion of rigid-body rotational dynamics
[NASA-TM-102798] N90-21773
QUENCHING (ATOMIC PHYSICS)
Reactions of N2A3 sigma u + and candidates for short wavelengths lasers
[DE90-009514] N90-22033
QUERY LANGUAGES
Knowledge-based semantic query processing: An optimal transformation approach N90-22437

R

RACKS (FRAMES)
A robot end effector exchange mechanism for space applications N90-22068
RADAR ASTRONOMY
The Telecommunications and Data Acquisition Report
[NASA-CR-186479] N90-21880
RADAR DATA
Improving a data-acquisition software system with abstract data type components N90-21901
RADAR MEASUREMENT
Lidar measurements of the optical propagation environment N90-21930
Lidar measurement of concentration and turbulence in battlefield obscurants N90-21931
Verification of Klett's method by comparison of lidar and transmissometer measurements N90-21933
RADAR TARGETS
Recognition and analysis of aircraft targets by radar, using structural pattern representations derived from polarimetric signatures N90-21879
RADIANCE
LOWTRAN 7: Status, review, and impact for short-to-long-wavelength infrared applications
N90-21917
Models of aerosols, clouds, and precipitation for atmospheric propagation studies N90-21919
UV spectral simulations using LOWTRAN 7
N90-21928
Long term intensity stability of Auger electron spectrometers: Instructions for the interlaboratory comparison
[NPL-DMM(A)-1] N90-22027
RADIATION
An analysis of the finite-differenced, even-parity discrete-ordinates equations in slab geometry
[DE90-006479] N90-22337
RADIATION DISTRIBUTION
Analysis of a high harmonic rectangular gyrotron using ribbon beams N90-21801
Modelling UV-visible radiation observed from space
N90-21937
Satellite versus GCM-simulated radiation balance: Comparisons and implications for climate modeling
N90-22180
Spectrum formation in active galactic nuclei and Type 2 supernovae N90-22490
RADIATION EFFECTS
Proceedings of the 6th Regional Symposium on Biophysics
[DE90-619618] N90-22206
Experiments with a laser interferometric gravitational wave antenna N90-22476
RADIATION HARDENING
An assessment of the hardness of miniature vacuum tubes to high-voltage transients
[DE90-009541] N90-21956
RADIATION HAZARDS
Final environmental impact statement for the Galileo Mission (Tier 2)
[NASA-TM-102925] N90-22147
Draft environmental impact statement for the Galileo Mission (Tier 2)
[NASA-TM-102926] N90-22148
Final Environmental Impact Statement for the Ulysses Mission (Tier 2)
[NASA-TM-101104] N90-22162
General purpose heat source radioisotope thermoelectric generator program. Book 1: Accident analysis
[REPT-90SDS4202-BK-1] N90-22379
RADIATION MEASUREMENT
Non-random uncertainties in the calibration of protection-level secondary standards
[NPL-RS(EXT)-110] N90-22378
Derivation of radiation beam non-uniformity corrections for the calibration of large volume ionisation chambers
[NPL-RSA(EXT)-11] N90-22382
RADIATION PROTECTION
General purpose heat source radioisotope thermoelectric generator program. Book 1: Accident analysis
[REPT-90SDS4202-BK-1] N90-22379
Prevention of significant deterioration application for approval to construct SP-100 Ground Engineering System Test Site
[DE90-007986] N90-22381
RADIATION SHIELDING
Prevention of significant deterioration application for approval to construct SP-100 Ground Engineering System Test Site
[DE90-007986] N90-22381
RADIATION SOURCES
Free electron lasers driven by linear induction accelerators: High power radiation sources N90-21800
Minimizing the effects of the atmosphere in the observation of ultraviolet radiation N90-21911
The synergism of analytic and numerical techniques in general relativity: Calculation of radiative spacetimes
N90-22425
RADIATION TRANSPORT
Computer simulation of time-dependent spherically symmetric spacetimes containing radiating fluids: Formalism and code tests N90-22483
RADIATIVE RECOMBINATION
Recombination lines of C I and N II in the interstellar medium N90-22466
RADIATIVE TRANSFER
Propagation environments, effects, and decision aids
N90-21918
The emission lines in the ultra-violet spectrum of Beta Lyrae N90-22474
Modelling late-time atmospheres of supernovae
N90-22500
RADIO ASTRONOMY
The Telecommunications and Data Acquisition Report
[NASA-CR-186479] N90-21880
Jupiter's drifting decametric bursts with the changing time scale
[DE90-618870] N90-22517
RADIO FREQUENCIES
The mm-wave region propagation experiments by satellite N90-21916
RADIO FREQUENCY HEATING
Computer simulation of ionospheric radio frequency heating
[DE90-009478] N90-21944
RADIO FREQUENCY INTERFERENCE
Radar RFI at Goldstone DSS 12 and DSS 16
N90-21900
RADIO GALAXIES
Search for rapidly star forming galaxies at high redshift N90-22465
Extended optical emission in 3CR radio galaxies
N90-22523
RADIO NAVIGATION
The Telecommunications and Data Acquisition Report
[NASA-CR-186479] N90-21880
RADIO OCCULTATION
Waves in Saturn's rings probed by radio occultation
N90-22511
RADIO PHYSICS
Extended optical emission in 3CR radio galaxies
N90-22523
RADIO RELAY SYSTEMS
Report on STC/Technische Universiteit (TU) Delft Extremely High Frequency (EHF) radio relay study
N90-21915
RADIO WAVES
Modeling millimeter-wave propagation effects in the atmosphere N90-21922
RADIOACTIVE CONTAMINANTS
Final Environmental Impact Statement for the Ulysses Mission (Tier 2)
[NASA-TM-101104] N90-22162
RADIOACTIVE DECAY
Does mass accretion lead to field decay in neutron stars
[CAL-394] N90-22470
RADIOACTIVE WASTES
In-situ fracture stiffness determination
[DE90-009202] N90-22173
RADIOBIOLOGY
Proceedings of the 6th Regional Symposium on Biophysics
[DE90-619618] N90-22206
RADIOISOTOPE BATTERIES
Preliminary design of a long-endurance Mars aircraft
[NASA-CR-185243] N90-21763
Draft environmental impact statement for the Galileo Mission (Tier 2)
[NASA-TM-102926] N90-22148
Final Environmental Impact Statement for the Ulysses Mission (Tier 2)
[NASA-TM-101104] N90-22162
General purpose heat source radioisotope thermoelectric generator program. Book 1: Accident analysis
[REPT-90SDS4202-BK-1] N90-22379
General purpose heat source radioisotope thermoelectric generator. Book 2: Accident analysis, appendices
[REPT-90SDS4202-BK-2] N90-22380
RADIOMETERS
Radiometric tests on wet and dry antenna reflector surface panels N90-21890
Spectral response of wheat and its relationship with agronomic variables in the tropical region
[INPE-5018-RPE/612] N90-22138
Field reports on radiometric campaigns of soybeans in the Federal district: Safra 88/89
[INPE-5021-RPE/615] N90-22139
RADIOMETRIC CORRECTION
Applications of remote sensing to studies of oceanic upper mixed layer dynamics N90-22137
RADIOMETRIC RESOLUTION
Multiresolution and time-frequency representations of signals
[REPT-89-47] N90-21946
RAILGUN ACCELERATORS
Current management for improved railgun performance N90-21781
RAIN
Inclusion of clouds and rain in atmospheric slant path calculations N90-21925
RAMAN SPECTRA
High resolution stimulated Raman-Brillouin spectroscopy in gases and solids
[DE90-009535] N90-21840
Brillouin gain spectroscopy in glasses and crystals
[DE90-009536] N90-21841
RANDOM ACCESS
CSMA/RN: A universal protocol for gigabit networks
N90-22280
Fairness problems at the media access level for high-speed networks N90-22287
RANDOM ACCESS MEMORY
A study of caching in capability computers
[RSRE-89015] N90-22276
RANDOM ERRORS
The use of local polynomial approximations in a knot-placement strategy for least squares spline fitting
[NPL-DITC-148/89] N90-22355
RANDOM NUMBERS
On the structure of Mandelbrot's percolation process and other random Cantor sets
[REPT-89-54] N90-22362
RANDOM VARIABLES
Dynamic response of structures with uncertain parameters N90-22125
RANDOM VIBRATION
Probabilistic analysis of bladed turbine disks and the effect of mistuning
[NASA-TM-102564] N90-21871
RANGE FINDERS
Vision science and technology for supervised intelligent space robots N90-22221
RANGEFINDING
Minimizing the effects of the atmosphere in the observation of ultraviolet radiation N90-21911
The optical night sky at low surface brightness: High latitude dust and faint field galaxies N90-22481
RATS
Excitatory and inhibitory backward conditioning in the rat N90-22204
RAYLEIGH EQUATIONS
Normal forms for weakly non-linear perturbed wave equations
[REPT-89-41] N90-22343
RAYLEIGH SCATTERING
Modelling UV-visible radiation observed from space
N90-21937
RAYLEIGH WAVES
Normal forms for weakly non-linear perturbed wave equations
[REPT-89-41] N90-22343
REACTION KINETICS
On the use of external burning to reduce aerospace vehicle transonic drag
[NASA-TM-103107] N90-21762
Testing carbon fabric for oxidation mass loss
N90-21819
Studies on reactive flows N90-21831
Infrared absorption spectroscopy and chemical kinetics of free radicals
[DE90-009469] N90-21837

A comparison of the autoignition chemistry of n-butane and isobutane in an internal combustion engine [DE90-009474] N90-21838

Detailed mechanism for oxidation of benzene [NASA-TM-102443] N90-21842

Determination of rates of reaction in the gas-phase in the troposphere: Theory and practice. 2: Rate of direct photoreaction: Screening-level test guideline-spectroscopic determination of the cross section and the maximum rate of direct photoreaction in sunlight [PB90-146291] N90-22156

The Al-26(rho, gamma)Si-27 reaction: Stellar origins of galactic Al-26 N90-22498

REACTION WHEELS

Accurate nonlinear control for satellites using reaction wheels [INPE-4983-PRE/1546] N90-21787

Test results and flight experience of ball bearing momentum and reaction wheels N90-22099

REACTIVITY

Testing carbon fabric for oxidation mass loss N90-21819

Studies on reactive flows N90-21831

Experience with synthetic fluorinated fluid lubricants N90-22095

REACTOR CORES

Prevention of significant deterioration application for approval to construct SP-100 Ground Engineering System Test Site [DE90-007986] N90-22381

REACTOR DESIGN

Photosynthetic water splitting, phase 2 [PB90-132671] N90-21833

REACTOR SAFETY

Proceedings of the Conference on Technology-Based Confidence Building: Energy and Environment [CNSS-PAPERS-22] N90-22152

Prevention of significant deterioration application for approval to construct SP-100 Ground Engineering System Test Site [DE90-007986] N90-22381

Magnetic turbulence versus safety factor in the Tokapole 2 tokamak N90-22391

REACTOR TECHNOLOGY

TOODEE: A two-dimensional, time-dependent heat conduction program [DE90-009631] N90-22010

Proceedings of the Conference on Technology-Based Confidence Building: Energy and Environment [CNSS-PAPERS-22] N90-22152

READ-ONLY MEMORY DEVICES

Technologies for electronic transfer of information: The present state and trends in Japan N90-22443

Electronic transfer of information applications in the Societe Aerospatiale N90-22454

REAL TIME OPERATION

A real-time signal combining system for Ka-band feed arrays using maximum-likelihood weight estimates N90-21888

The application of connectionism to query planning/scheduling in intelligent user interfaces N90-22295

Computer conferencing: Minds meeting anywhere anytime N90-22452

RECEIVERS

A functional description of the advanced receiver N90-21891

QPSK carrier-acquisition performance in the advanced receiver 2 N90-21892

Digital Doppler extraction demonstration with the advanced receiver N90-21893

Broadcast file distribution on packet satellite networks N90-21906

RECOGNITION

Edge recognition using image-processing hardware [OUEL-1777/89] N90-22271

Implementing the Canny edge recognizer with datacube image-processing hardware [OUEL-1786/89] N90-22272

RECTENNAS

Millimeter wavelength rectenna development N90-21797

RECTIFICATION

Applications of remote sensing to studies of oceanic upper mixed layer dynamics N90-22137

RECURSIVE FUNCTIONS

Adaptive control of a flexible manipulator with unknown changing loads N90-22293

RED SHIFT

Search for rapidly star forming galaxies at high redshift N90-22465

Extended optical emission in 3CR radio galaxies N90-22523

REDUCED GRAVITY

The vibro-acoustic mapping of low gravity trajectories on a Learjet aircraft [NASA-TM-103103] N90-21723

Development and integration of the capillary pumped loop GAS and Hitchhiker flight experiments [NASA-TM-100756] N90-21790

Issues in development, evaluation, and use of the NASA Preflight Adaptation Trainer (PAT) [NASA-CR-185608] N90-22212

REDUNDANCY

Relatchable launch restraint mechanism for deployable booms N90-22091

The art of fault-tolerant system reliability modeling [NASA-TM-102623] N90-22292

REENTRY VEHICLES

Lidar measurements of the optical propagation environment N90-21930

REFLECTANCE

Radar scatterometry and polarimetry at 220 GHz N90-21935

Measurement of the reflectance ratio of natural light in the sea [IOS-265] N90-22199

The intensity dependent spread model and color constancy N90-22228

REFLECTOR ANTENNAS

Dual-shaped offset reflector antenna designs from solutions of the geometrical optics first-order partial differential equations N90-21887

Radiometric tests on wet and dry antenna reflector surface panels N90-21890

REFLECTORS

A soft actuation system for segmented reflector articulation and isolation N90-22084

REFRACTION

A temperature-dependent regular infrared band model for absorption and dispersion N90-21927

REFRACTIVITY

Millimetric, infrared, and optical propagation studies over a 500 m path N90-21913

Modelling of optically and IR effective atmospheric turbulence N90-21923

Effect of atmospheric turbulence on electro-optical systems N90-21940

An algorithm and computer program for the calculation of envelope curves [PB90-155409] N90-22254

Optical properties of zinc selenide grown using molecular beam deposition techniques [RSRE-MEMO-4269] N90-22423

REFRIGERANTS

Experimental performance of ozone-safe alternative refrigerants: Experimental performance comparisons of R32, R125, R143a, R218, R134a, R152a, R124, R142b, RC318 and R143 in a refrigeration circuit [DE90-009227] N90-21876

REGENERATION (ENGINEERING)

Publications of the NASA Controlled Ecological Life Support System (CELSS) Program, 1979-1989 [NASA-CR-4297] N90-21754

REGRESSION ANALYSIS

The observed three-dimensional structure of baroclinic waves in the Northern Hemisphere winter as revealed in a linear regression analysis N90-22167

Orthogonal distance regression [PB90-151747] N90-22336

REINFORCED PLASTICS

Modelling of the impact response of fibre-reinforced composites [OUEL-1784/89] N90-21827

RELATIVITY

The synergism of analytic and numerical techniques in general relativity: Calculation of radiative spacetimes N90-22425

Numerical investigations of nonlinear behavior in the Einstein equations N90-22427

Multipole moments in general relativity and dynamical perturbations of black-hole magnetospheres N90-22509

RELAXATION METHOD (MATHEMATICS)

Convergence acceleration of upwind relaxation methods for the Navier-Stokes equations N90-21973

Object detection using structural matching [INPE-4954-PRE/1532] N90-22333

RELIABILITY

Evaluation of a prototype lighted ball marker for powerline obstructions [DOT/FAA/CT-TN90/12] N90-21774

Regional wind energy assessment [DE90-009439] N90-22143

RELIABILITY ANALYSIS

Probabilistic finite elements: Applications to fracture and fatigue N90-22134

The art of fault-tolerant system reliability modeling [NASA-TM-102623] N90-22292

RELIABILITY ENGINEERING

SPOT 4 space magnetic recorder mechanisms N90-22082

Development of the CLAES instrument aperture door system N90-22083

REMOTE CONTROL

Microwave Landing System (MLS) remote monitoring subsystem/remote maintenance monitoring system [DOT/FAA/PS-89/2] N90-21749

A new six-degree-of-freedom force-reflecting hand controller for space telerobotics N90-22089

REMOTE MANIPULATOR SYSTEM

Development of a multipurpose hand controller for JEMRMS N90-22087

The resupply interface mechanism RMS compatibility test N90-22090

REMOTE SENSING

Modelling UV-visible radiation observed from space N90-21937

Applications of remote sensing to studies of oceanic upper mixed layer dynamics N90-22137

Field reports on radiometric campaigns of soybeans in the Federal district: Safra 88/89 [INPE-5021-RPE/615] N90-22139

Mission to planet Earth N90-22153

REMOTELY PILOTED VEHICLES

Preliminary design of a long-endurance Mars aircraft [NASA-CR-185243] N90-21763

REMOVAL

Robots for aircraft coatings removal: Parameters and requirements [DE90-009429] N90-22048

RESEARCH

The Advanced Communications Technology Satellite (ACTS) capabilities for serving science [NASA-CR-186584] N90-21789

RESEARCH AIRCRAFT

Aerosol separator for use in aircraft [PB90-142217] N90-22155

RESEARCH AND DEVELOPMENT

Solid fuel combustion chamber [LR-562] N90-21846

Pre-study laser bathymetry [BCRS-89-26] N90-22198

Technologies for electronic transfer of information: The present state and trends in Japan N90-22443

Applications to the aerospace and defense R and D community: The DOD computer-aided acquisition and logistics support (CALS) initiative N90-22453

International science and technology policies: Testimony before the Subcommittee on International Scientific Cooperation, Committee on Science, Space, and Technology, United States House of Representatives [DE90-009416] N90-22463

Research and Technology Objectives and Plans Summary (RTOPS) [NASA-TM-89662] N90-22528

RESEARCH FACILITIES

Research in biological separations and cell culture [NASA-CR-172060] N90-22202

Hybrid vision activities at NASA Johnson Space Center N90-22225

RESEARCH MANAGEMENT

Research and Technology Objectives and Plans Summary (RTOPS) [NASA-TM-89662] N90-22528

RESIDUAL STRESS

Residual stresses in laminated thermoplastic matrix composites N90-21815

Elastic stability and nonlinear behavior of imperfect shells with initial stresses N90-22070

RESONANCE

Hopf bifurcation with nonsemisimple 1:1 resonance e [MEMO-808] N90-22347

RESONANT FREQUENCIES

Identification of XV-15 aeroelastic modes using frequency-domain methods [NASA-TM-101021] N90-21756

Probabilistic analysis of bladed turbine disks and the effect of mistuning [NASA-TM-102564] N90-21871

Optimum design of structures under shock and vibration environment N90-22067

Dynamic response of a complex encapsulated electronic assembly subjected to a severe shock environment [DE90-007689] N90-22114

RESOURCE ALLOCATION

Resource Allocation Planning Helper (RALPH): Lessons learned N90-22296

RESOURCES MANAGEMENT

Regional wind energy assessment [DE90-009439] N90-22143

RESPONSE TIME (COMPUTERS)

Bounded-time fault-tolerant rule-based systems N90-22318

RETINA
Filling in the retinal image N90-22229
A3I visibility modeling project N90-22230
RETRACTABLE EQUIPMENT
Design of a telescoping tube system for access and handling equipment N90-22102
REVERSE FIELD PINCH
Rigorous upper bounds for turbulent transport in bounded systems: Passive advection and reversed-field pinches N90-22390
REVISIONS
Guide to RMS-literature [REPT-89-52] N90-22326
Evaluation of optical storage technology for decision support databases N90-22436
Space Shuttle, NASA's major changes to flight hardware: Fact sheet for the Chairman, Committee on Science, Space, and Technology, House of Representatives [GAO/NSIAD-88-173FS] N90-22461
REYNOLDS STRESS
A theoretical investigation of gravity-wave-generated stress and vorticity in the planetary boundary layer N90-22512
RHEA (ASTRONOMY)
Geology of coronae and domal structures on Venus and models of their origin N90-22513
RHEOLOGY
Experimental and analytical investigations of granular materials: Shear flow and convective heat transfer N90-21968
RIBBONS
Analysis of a high harmonic rectangular gyrotron using ribbon beams N90-21801
RIEMANN MANIFOLD
Multipole moments in general relativity and dynamical perturbations of black-hole magnetospheres N90-22509
RIGID STRUCTURES
Direct inversion of rigid-body rotational dynamics [NASA-TM-102798] N90-21773
RISK
Final environmental impact statement for the Galileo Mission (Tier 2) [NASA-TM-102925] N90-22147
Computer vision techniques for rotorcraft low altitude flight N90-22237
Kalman filter based range estimation for autonomous navigation using imaging sensors N90-22238
ROADS
Inventory of program packages related to the project SIMONA [ETN-90-96397] N90-22270
Geographic information system: Coded data of agrocattle-raising projects in the Amazon [INPE-4978-PRE/1543] N90-22457
ROBOT ARMS
Perturbation techniques in the dynamics and control of flexible manipulators [OUEL-1772/89] N90-22053
The JPL/KSC telerobotic inspection demonstration N90-22312
ROBOT SENSORS
The procedure safety system N90-22311
ROBOTICS
Robust control of flexible structures N90-21784
A robotically constructed production and supply base on Phobos [NASA-CR-186234] N90-21872
Nonlinear stability analysis and control of dynamical robotic systems N90-22037
An alternative method to solving the kinematics of a redundant robot [DE90-006892] N90-22045
A new six-degree-of-freedom force-reflecting hand controller for space telerobotics N90-22089
Development of cable drive systems for an automated assembly project N90-22105
Instrumentation and robotic image processing using top-down model control N90-22239
Space environment robot vision system N90-22245
The procedure safety system N90-22311
The JPL/KSC telerobotic inspection demonstration N90-22312
The role of automation and robotics in the Lunar-Based Chemical Analysis Laboratory [DE90-009401] N90-22516
NASA Information Sciences and Human Factors Program [NASA-TM-4190] N90-22529
ROBOTS
A robotically constructed production and supply base on Phobos [NASA-CR-186234] N90-21872
Definition of large components assembled on-orbit and robot compatible mechanical joints [NASA-TM-100395] N90-22043
Trajectory generation for car-like robots [DE90-008407] N90-22047
Robots for aircraft coatings removal: Parameters and requirements [DE90-009429] N90-22048
The Shock and Vibration Digest, volume 21, no. 3 N90-22064
A robot end effector exchange mechanism for space applications N90-22088
Vision Science and Technology at NASA: Results of a Workshop [NASA-TM-102214-REV-1] N90-22216
Vision science and technology for supervised intelligent space robots N90-22221
Algorithms and architectures for robot vision N90-22236
Ames vision group research overview N90-22242
Space environment robot vision system N90-22245
Self-calibration of robot-sensor system N90-22246
International science and technology policies: Testimony before the Subcommittee on International Scientific Cooperation, Committee on Science, Space, and Technology, United States House of Representatives [DE90-009416] N90-22463
The role of automation and robotics in the Lunar-Based Chemical Analysis Laboratory [DE90-009401] N90-22516
ROBUSTNESS (MATHEMATICS)
Robust control of flexible structures N90-21784
ROCK MECHANICS
The effects of tortuosity on flow through a natural fracture [DE90-009193] N90-22172
Coupled behavior of rock joints [DE90-009222] N90-22174
ROCKET ENGINES
Hybrid propulsion technology program. Volume 1: Conceptional design package [NASA-CR-183953] N90-21793
Hybrid propulsion technology program. Volume 2: Technology definition package [NASA-CR-183954] N90-21794
ROCKET NOZZLES
Flight motor set 360L002 (STS-27R). Volume 5: Nozzle component [NASA-CR-183945] N90-21811
Shelf life extension for the lot AAE nozzle severance LSCs [NASA-CR-183878] N90-21813
ROCKS
The pressure dilation of a deep, jointed region of the earth [DE90-007537] N90-22170
Coupled behavior of rock joints [DE90-009222] N90-22174
ROLLING
Elastic and viscoelastic analysis of two multiply layered cylinders rolling over each other with Coulomb friction [REPT-89-50] N90-22051
ROLLING MOMENTS
A video-based experimental investigation of wing rock N90-21771
ROTARY WING AIRCRAFT
Development and application of a generalized dynamic wake theory for lifting rotors N90-21731
Quiet mode for nonlinear rotor models [NASA-TM-102236] N90-21758
Assessment of High Temperature Superconducting (HTS) electric motors for rotorcraft propulsion [NASA-CR-185222] N90-21761
Passive navigation using image irradiance tracking N90-22232
Computer vision techniques for rotorcraft low altitude flight N90-22237
Kalman filter based range estimation for autonomous navigation using imaging sensors N90-22238
ROTARY WINGS
Airloads, wakes, and aeroelasticity [NASA-CR-177551] N90-21738
ROTATING FLUIDS
Semigeostrophic flow over orography in a stratified rotating atmosphere N90-22163
ROTATING SHAFTS
Practical nonlinear simulation of rotating machinery dynamics with application to turbine blade rubbing N90-22038
The Shock and Vibration Digest, volume 21, no. 3 N90-22064
Rotor-to-stationary element rub-related vibration phenomena in rotating machinery: Literature survey N90-22065
ROTATION
Experimental investigation of the effect of cavitation on the rotordynamic forces on a whirling centrifugal pump impeller N90-22039
Wind instability as a possible cause of the spiral structure formation in the gaseous subsystem of galaxies with the circular magnetic field [DE90-618944] N90-22507
ROTOR AERODYNAMICS
The Shock and Vibration Digest, volume 21, no. 2 N90-22059
ROTOR BLADES
Towards a unified analysis methodology for composite rotor blades N90-21730
ROTOR DYNAMICS
Quiet mode for nonlinear rotor models [NASA-TM-102236] N90-21758
Probabilistic analysis of bladed turbine disks and the effect of mistuning [NASA-TM-102564] N90-21871
Experimental investigation of the effect of cavitation on the rotordynamic forces on a whirling centrifugal pump impeller N90-22039
ROTORS
The Shock and Vibration Digest, volume 21, no. 2 N90-22059
The Shock and Vibration Digest, volume 21, no. 3 N90-22064
Rotor-to-stationary element rub-related vibration phenomena in rotating machinery: Literature survey N90-22065
Aerodynamics of a full-scale, non rotating wind turbine blade under natural wind conditions [RISOE-M-2768] N90-22144
Rotor loading on a three-bladed wind turbine N90-22145
RUDDERS
Prediction of forces and moments for flight vehicle control effectors. Part 1: Validation of methods for predicting hypersonic vehicle controls forces and moments [NASA-CR-186571] N90-21734
RUN TIME (COMPUTERS)
Distributed simulation, no special tools required N90-22281
Performance of gigabit FDDI N90-22283
Distributed simulation of network protocols N90-22284
Extensibility and limitations of FDDI N90-22286
RUNGE-KUTTA METHOD
On spurious steady-state solutions of explicit Runge-Kutta schemes [NASA-TM-102819] N90-22340
The theta-methods in the numerical solution of delay differential equations [TW-89-03] N90-22349
Stability criteria in the numerical solution of initial value problems [TW-89-05] N90-22351
Contractivity in the maximum norm for Runge-Kutta methods [TW-89-06] N90-22352
Stability analysis of numerical methods for delay differential equations [TW-89-09] N90-22353

S

S MATRIX THEORY
Recognition and analysis of aircraft targets by radar, using structural pattern representations derived from polarimetric signatures N90-21879
Radar scatterometry and polarimetry at 220 GHz N90-21935
SAFETY
Final (Tier 1) environmental impact statement for the Galileo and Ulysses Missions [NASA-TM-102917] N90-21779
The procedure safety system N90-22311
General purpose heat source radioisotope thermoelectric generator program. Book 1: Accident analysis [REPT-90SDS4202-BK-1] N90-22379
SAFETY FACTORS
Magnetic turbulence versus safety factor in the Tokapole 2 tokamak N90-22391
SAGE SATELLITE
The interpretation of SAGE 2 ozone measurements in the lower mesosphere N90-22149
SAGITTARIUS CONSTELLATION
The Sagittarius B2 molecular cloud: An extreme case of a galactic center giant molecular cloud N90-22493
SAMPLING
Aerosol separator for use in aircraft [PB90-142217] N90-22155
Sampling and noise in vision networks N90-22217
Networks for image acquisition, processing and display N90-22218

SATELLITE ALTIMETRY
A free surface Bryan-Cox-Semtner model [IOS-270] N90-22201
SATELLITE IMAGERY
Modelling UV-visible radiation observed from space N90-21937
Satellite image analysis using neural networks N90-22321
SATELLITE NETWORKS
Broadcast file distribution on packet satellite networks N90-21906
Electronic Transfer of Information and its Impact on Aerospace and Defence Research and Development [AGARD-CP-466] N90-22440
Document delivery via ISDN or satellite networks N90-22446
SATELLITE-BORNE INSTRUMENTS
The mm-wave region propagation experiments by satellite N90-21916
SATURN (PLANET)
Auroral ultraviolet darkening on the outer planets N90-22518
SATURN RINGS
Waves in Saturn's rings probed by radio occultation N90-22511
SCALARS
Soft inflation [NASA-CR-186593] N90-22506
SCATTERING
The solution of scattering and radiation problems for complex configurations based on 3-D grid and patch models N90-21997
Elastodynamic scattering and transmission problems in three dimensions by the boundary integral equation method N90-22077
Current drive in a supernova N90-22491
SCATTEROMETERS
Radar scatterometry and polarimetry at 220 GHz N90-21935
SCHEDULING
The 1990 Goddard Conference on Space Applications of Artificial Intelligence [NASA-CP-3068] N90-22294
The application of connectionism to query planning/scheduling in intelligent user interfaces N90-22295
The role of artificial intelligence techniques in scheduling systems N90-22297
PLAN-IT-2: The next generation planning and scheduling tool N90-22298
An approach to rescheduling activities based on determination of priority and disruptivity N90-22299
Space communications scheduler: A rule-based approach to adaptive deadline scheduling N90-22300
SURE (Science User Resource Expert): A science planning and scheduling assistant for a resource based environment N90-22302
Managing temporal relations N90-22304
System control of an autonomous planetary mobile spacecraft N90-22313
Electric power scheduling: A distributed problem-solving approach [NASA-TM-103149] N90-22323
An expert system for simulating electric loads aboard Space Station Freedom [NASA-TM-103150] N90-22325
SCIENTISTS
European network of interest in the measurement and analysis of mean sea levels from tide gauge records [PB90-151929] N90-22196
SCINTILLATION
Scintillation of millimeter-wave intensity and phase caused by turbulence and precipitation N90-21912
The mm-wave region propagation experiments by satellite N90-21916
SCREWS
Data and conclusions from tests on small screws [DE90-007500] N90-22046
SEA ICE
Motion detection in astronomical and ice floe images N90-22231
SEA LEVEL
European network of interest in the measurement and analysis of mean sea levels from tide gauge records [PB90-151929] N90-22196
SEA SURFACE TEMPERATURE
Applications of remote sensing to studies of oceanic upper mixed layer dynamics N90-22137
The relationship between the buoyancy of near-surface air and the potential temperature of the tropopause N90-22165
SEA WATER
Measurement of the reflectance ratio of natural light in the sea [IOS-265] N90-22199
SEALING
Flight set 360T004 (STS-30) [NASA-CR-183927] N90-22049
SEARCH PROFILES
Space communications scheduler: A rule-based approach to adaptive deadline scheduling N90-22300
SEAS
Calculation of IR propagation statistics in the eastern Atlantic for surveillance system performance assessment N90-21938
SECURITY
Automating security monitoring and analysis for Space Station Freedom's electric power system [NASA-TM-103148] N90-22324
SEISMIC WAVES
Effects of single fractures on seismic wave propagation [DE90-009191] N90-22171
SEISMOLOGY
Effects of single fractures on seismic wave propagation [DE90-009191] N90-22171
SELF LUBRICATION
Self-lubricating polymer composites and polymer transfer film lubrication for space applications [NASA-TM-102492] N90-21862
SELF ORGANIZING SYSTEMS
Guide to RMS-literature [REPT-89-52] N90-22326
SEMANTICS
An introduction to Montague grammar [REPT-89-46] N90-22266
Some remarks on treatment of be in Montague's PTQ — Proper Treatment of Quantification (PTQ) [REPT-89-40] N90-22267
Using expert systems to implement a semantic data model of a large mass storage system N90-22315
Knowledge-based semantic query processing: An optimal transformation approach N90-22437
SEMICONDUCTING FILMS
Superconducting and semiconducting thin films of La(sub 123) and Y(sub 123) and their superlattices [DE90-009565] N90-22416
SEMICONDUCTOR DEVICES
An assessment of the hardness of miniature vacuum tubes to high-voltage transients [DE90-009541] N90-21956
SEMICONDUCTOR DIODES
Millimeter wavelength rectenna development N90-21797
SEMICONDUCTOR LASERS
Development of mid-infrared solid state lasers for spaceborne lidar [NASA-CR-185095] N90-22031
Linear, nonlinear, and tunable guided wave modes for high-power (GaAl)As semiconductor lasers N90-22036
An acousto-optic image correlator with a throughput rate of 1000 templates per second [DE90-009323] N90-22249
SEMICONDUCTORS (MATERIALS)
An investigation of narrow-bandgap semiconductors: Devices, circuits, and systems N90-22406
Positron trapping in semiconductors [PB90-165606] N90-22410
Report on the fifth workshop on synchrotron x ray lithography [DE90-007903] N90-22411
Optical bistability in semiconducting material N90-22424
SEPARATED FLOW
Control of flow separation and mixing by aerodynamic excitation [NASA-TM-103131] N90-21733
Numerical investigation of some control methods for 3-D turbulent interactions due to sharp fins N90-21764
Numerical investigation of separated transonic turbulent flows with a multiple-time-scale turbulence model [NASA-TM-102499] N90-21962
Bifurcations in viscous flow fields. On the genesis and development of topologically complicated separated flow structures [PB90-167156] N90-22012
Unsteady separated flows produced by complex harmonic motions: Investigation of wing-flow interactions elicited by a mechanical model simulating dragonfly wing kinematics N90-22018
SEPARATORS
Zero-G phase detector and separator [NASA-CASE-LEW-14844-1] N90-22024
Research in biological separations and cell culture [NASA-CR-172060] N90-22202
SEQUENCING
Passive navigation using image irradiance tracking N90-22232
Kalman filter based range estimation for autonomous navigation using imaging sensors N90-22238
A CSP model for distributed control software design [OUEL-1789/89] N90-22273
Constraint-based evaluation of sequential procedures N90-22301
Spacecraft command verification: The AI solution N90-22307
SEQUENTIAL COMPUTERS
A CSP model for distributed control software design [OUEL-1789/89] N90-22273
SERIES EXPANSION
Adaptive pattern recognition by mini-max neural networks as a part of an intelligent processor N90-22317
SERVICE LIFE
Test results and flight experience of ball bearing momentum and reaction wheels N90-22099
Design of a telescoping tube system for access and handling equipment N90-22102
SERVOCONTROL
Bi-directional thruster development and test report [NASA-CR-182013] N90-21785
SERVOMECHANISMS
Bi-directional thruster development and test report [NASA-CR-182013] N90-21785
SEYFERT GALAXIES
Spectrum formation in active galactic nuclei and Type 2 supernovae N90-22490
SH WAVES
Scattering of waves by inclusions in a nonhomogeneous elastic half space solved by boundary element methods [PB90-145699] N90-22107
SHADOWS
Factors affecting the perception of transparent motion N90-22233
SHAFTS (MACHINE ELEMENTS)
Assessment of High Temperature Superconducting (HTS) electric motors for rotorcraft propulsion [NASA-CR-185222] N90-21761
The development of a complementary expendable launch vehicle interface for an STS deployable payload N90-22086
SHALLOW WATER
A new stability criterion in the shallow-water system for two-dimensional coherent eddies in the atmosphere and oceans N90-22176
SHAPE CONTROL
Robust control of flexible structures N90-21784
Passive shape control of space antennas with determinate truss support structures N90-21949
SHAPE MEMORY ALLOYS
Development of shape memory metal as the actuator of a fail safe mechanism N90-22081
SHAPED CHARGES
Shelf life extension for the lot AAE nozzle severance LSCs [NASA-CR-183878] N90-21813
SHAPES
Molecular theory of fluid phase equilibria [PB90-131277] N90-21832
The solution of scattering and radiation problems for complex configurations based on 3-D grid and patch models N90-21997
Lightweight piston architecture [NASA-CASE-LAR-13926-1] N90-22042
Circularity measuring system: A shape gauge designed especially for use on large objects N90-22104
Two-dimensional shape recognition using sparse distributed memory N90-22227
Development of the methods and means of precise forming and geometry control of superconducting current-carrying element for the UNR pulsed dipoles [DE90-620108] N90-22419
SHEAR FLOW
Control of flow separation and mixing by aerodynamic excitation [NASA-TM-103131] N90-21733
Experimental and analytical investigations of granular materials: Shear flow and convective heat transfer N90-21968
Automated analysis of measured turbulent boundary flow [PB90-147844] N90-21970
Modern developments in shear flow control with swirl [NASA-CR-186586] N90-22000
Unsteady separated flows produced by complex harmonic motions: Investigation of wing-flow interactions elicited by a mechanical model simulating dragonfly wing kinematics N90-22018
Semigeostrophic flow over orography in a stratified rotating atmosphere N90-22163
SHEAR LAYERS
Control of flow separation and mixing by aerodynamic excitation [NASA-TM-103131] N90-21733

SHEAR PROPERTIES

Failure mechanisms under complex loading of glass-reinforced polyester composites and their matrices: The effect of superposed hydrostatic pressures up to 300 MPa on axial tensile and compressive strengths, and in-plane shear properties of unidirtionally reinforced glass-polyester composites and the relevant polyesters N90-22072

Coupled behavior of rock joints [DE90-009222] N90-22174

SHEAR STRESS

Development of a defect stream function, law of the wall/wake method for compressible turbulent boundary layers N90-22019

Three-dimensional finite element formulations for thick and thin laminated plates N90-22132

SHEARING

Energy release rate analysis of interfacial cracks in composites N90-21829

The mechanics of shear band formation in thermal viscoplastic materials at high rates of loading N90-22128

SHELL STABILITY

ANILISA: Computational module for Koiter's imperfection sensitivity theory [LR-582] N90-22119

SHIELDING

Scaling of nonnuclear kinetic-energy antisatellites [DE90-009758] N90-21791

Fracture mechanics of monolithic ceramic materials under small scale microcracking conditions N90-21860

SHOCK LAYERS

Numerical investigation of some control methods for 3-D turbulent interactions due to sharp fins N90-21764

SHOCK LOADS

Slow shocks in coronal mass ejections [NASA-CR-186578] N90-22522

SHOCK TESTS

Dynamic response of a complex encapsulated electronic assembly subjected to a severe shock environment [DE90-007689] N90-22114

SHOCK WAVE INTERACTION

Numerical investigation of separated transonic turbulent flows with a multiple-time-scale turbulence model [NASA-TM-102499] N90-21962

Computational modeling and validation for hypersonic inlets [NASA-TM-103111] N90-22011

SHOCK WAVES

The interaction between a plane shock wave and a cylindrical afterbody N90-21728

Impact tolerant material [NASA-CASE-LAR-12887-3] N90-21822

SHOES

Engineering specification and system design for CAD/CAM of custom shoes: UMC project effort [NASA-CR-186547] N90-22255

SHORT TAKEOFF AIRCRAFT

Performance characteristics of a one-third-scale, vectorable ventral nozzle for SSTOVL aircraft [NASA-TM-103120] N90-21725

SHROUDED PROPELLERS

A computer program for the prediction of nozzle-propeller performance [LR-578] N90-21740

Recent improvements in the scope and accuracy of the performance prediction of nozzle propellers [LR-598] N90-21742

SIGNAL DETECTION

Sampling and noise in vision networks N90-22217

SIGNAL PROCESSING

Microwave Landing System (MLS) multiple system design interoperability interface control report [DOT/FAA/SA-89/2] N90-21750

A functional description of the advanced receiver N90-21891

Digital Doppler extraction demonstration with the advanced receiver N90-21893

Mark 4-A DSCC (Magellan-era) telemetry system description N90-21903

The mm-wave region propagation experiments by satellite N90-21916

LOWTRAN 7: Status, review, and impact for short-to-long-wavelength infrared applications N90-21917

Multiresolution and time-frequency representations of signals [REPT-89-47] N90-21946

Balanced bridge feedback control system [NASA-CASE-NPO-17430-1-CU] N90-21951

Zero-G phase detector and separator [NASA-CASE-LEW-14844-1] N90-22024

Calculating the time domain average of gear vibration data sampled at less than the Nyquist frequency [OUEL-1768/89] N90-22052

Sampling and noise in vision networks N90-22217

An investigation of narrow-bandgap semiconductors: Devices, circuits, and systems N90-22406

SIGNAL TO NOISE RATIOS

A real-time signal combining system for Ka-band feed arrays using maximum-likelihood weight estimates N90-21888

QPSK carrier-acquisition performance in the advanced receiver 2 N90-21892

Exact closed-form expressions for the performance of the split-symbol moments estimator of signal-to-noise ratio N90-21894

Validity of the two-level model for Viterbi decoder gap-cycle performance N90-21896

SIGNATURE ANALYSIS

Recognition and analysis of aircraft targets by radar, using structural pattern representations derived from polarimetric signatures N90-21879

SILICA GEL

Surface structure and chemistry of high surface area silica gels [DE90-007684] N90-21865

SILICATES

Sulphur silicate interactions on the Jovian satellite Io N90-22515

SILICON DIOXIDE

Polysiloxanes derived from the controlled hydrolysis of tetraethoxysilane as precursors to silica for use in ceramic processing [NASA-TM-102489] N90-21858

SILICON NITRIDES

Matrix density effects on the mechanical properties of SiC/RBSN composites [NASA-TM-103098] N90-21826

On the design and development of a miniature ceramic gimbal bearing N90-22100

SILOXANES

Polysiloxanes derived from the controlled hydrolysis of tetraethoxysilane as precursors to silica for use in ceramic processing [NASA-TM-102489] N90-21858

SIMULATION

New spectral features of stratospheric trace gases N90-21910

Millimetre-wave propagation in the evaporation duct N90-21929

The interpretation of SAGE 2 ozone measurements in the lower mesosphere N90-22149

The role of input weighting and bounding in the characteristic GPC method [OUEL-1762/89] N90-22328

An intelligent interface for the design of optimal control systems [INPE-4917-PRE/1516] N90-22332

Orthogonal distance regression [PB90-151747] N90-22336

SIMULATORS

Plasma contactor research, 1989 [NASA-CR-185212] N90-22389

SINE WAVES

Adaptive frequency estimation by MUSIC (Multiple Signal Classification) method [PB90-166794] N90-21943

SINGLE CRYSTALS

The effect of hydrogen and microstructure on the deformation and fracture behavior of a single crystal nickel-base superalloy [NASA-CR-185219] N90-21849

SINGULAR INTEGRAL EQUATIONS

Green's functions for the elastic annulus and their application to various crack problems N90-22129

SINTERING

Institute for Materials Science and Engineering, nondestructive evaluation: Technical activities [PB90-132739] N90-22055

SIZE DISTRIBUTION

Inclusion of clouds and rain in atmospheric slant path calculations N90-21925

SKEWNESS

Three-dimensional adaptive grids with limited skewness N90-21987

SKY BRIGHTNESS

The optical night sky at low surface brightness: High latitude dust and faint field galaxies N90-22481

SLABS

An analysis of the finite-differenced, even-parity discrete-ordinates equations in slab geometry [DE90-006479] N90-22337

SLAGS

MHD channel development, part 4 [DE90-009552] N90-22397

SLENDER BODIES

An experimental investigation of the physical mechanisms controlling the asymmetric flow past slender bodies at large angles of attack N90-21767

SLEWING

The determination of maximum deep space station slew rates for a high Earth orbiter N90-21882

SLIDING

Nonlinear spline operator interpolation and sliding control of deformable maneuvering bodies N90-21878

SLOTTED WIND TUNNELS

Slotted-wall research with disk and parachute models in a low-speed wind tunnel [DE90-002989] N90-21737

SLURRIES

Turbulence in slurry pipe flow [DE90-008940] N90-22006

SMOOTHING

Spline function smoothing and differentiation of noisy data on a rectangular grid [DE90-009319] N90-22338

UD filtering and smoothing applied to orbit determination [INPE-4966-PRE/1535] N90-22501

SNOWSTORMS

Second National Winter Weather Workshop Conducted by the National Weather Service [PB90-147414] N90-22183

SODIUM CHLORIDES

Development and applications of a coupled cavity sodium-chloride laser N90-22029

SOFTWARE ENGINEERING

Improving a data-acquisition software system with abstract data type components N90-21901

Software quality assurance: Towards a measurable quality improvement [REPT-89-42] N90-22264

A CSP model for distributed control software design [OUEL-1789/89] N90-22273

A study of caching in capability computers [RSRE-89015] N90-22276

SOFTWARE TOOLS

Distributed simulation, no special tools required N90-22281

Resource Allocation Planning Helper (RALPH): Lessons learned N90-22296

SOIL SCIENCE

Scattering of waves by inclusions in a nonhomogeneous elastic half space solved by boundary element methods [PB90-145699] N90-22107

Spectral response of wheat and its relationship with agronomic variables in the tropical region [INPE-5018-RPE/612] N90-22138

SOILS

Scattering of waves by inclusions in a nonhomogeneous elastic half space solved by boundary element methods [PB90-145699] N90-22107

SOLAR ARRAYS

Preliminary design of a long-endurance Mars aircraft [NASA-CR-185243] N90-21763

Photovoltaic power for Space Station Freedom [NASA-TM-102569] N90-21812

Analysis of thermal energy storage material with change-of-phase volumetric effects [NASA-TM-102457] N90-21974

Space Station Freedom solar array panels plasma interaction test facility [NASA-TM-102475] N90-22488

SOLAR CELLS

Photovoltaic Program Branch [DE90-000318] N90-22142

Automating security monitoring and analysis for Space Station Freedom's electric power system [NASA-TM-103148] N90-22324

Space Station Freedom solar array panels plasma interaction test facility [NASA-TM-102475] N90-22488

SOLAR CORONA

Cyclotron maser and plasma wave growth in magnetic loops [NASA-CR-179862] N90-22402

SOLAR DYNAMIC POWER SYSTEMS

Photovoltaic power for Space Station Freedom [NASA-TM-102569] N90-21812

SOLAR ENERGY CONVERSION

Photosynthetic water splitting, phase 2 [PB90-132671] N90-21833

Electric power scheduling: A distributed problem-solving approach [NASA-TM-103149] N90-22323

SOLAR FLARES

Solar-geophysical data number 542, October 1989. Part 1: (Prompt reports). Data for September, August 1989, and late data [PB90-148669] N90-22520

Solar-geophysical data number 542, October 1989. Part 2: (Comprehensive reports). Data for April 1989 and miscellaneous [PB90-148677] N90-22521

SOLAR GENERATORS

Automating security monitoring and analysis for Space Station Freedom's electric power system
[NASA-TM-103148] N90-22324

SOLAR MAGNETIC FIELD

Cyclotron maser and plasma wave growth in magnetic loops
[NASA-CR-179862] N90-22402

Solar-geophysical data number 542, October 1989. Part 1: (Prompt reports). Data for September, August 1989, and late data
[PB90-148669] N90-22520

SOLAR NEUTRINOS

The observed properties of the intermediate-degree gravity modes and their relevance to the solar neutrino paradox N90-22519

SOLAR PHYSICS

NSSDC data listing
[NASA-TM-102989] N90-22456

Solar-geophysical data number 542, October 1989. Part 1: (Prompt reports). Data for September, August 1989, and late data
[PB90-148669] N90-22520

Solar-geophysical data number 542, October 1989. Part 2: (Comprehensive reports). Data for April 1989 and miscellaneous
[PB90-148677] N90-22521

SOLAR RADIATION

Determination of rates of reaction in the gas-phase in the troposphere: Theory and practice. 2: Rate of direct photoreaction: Screening-level test guideline-spectroscopic determination of the cross section and the maximum rate of direct photoreaction in sunlight
[PB90-146291] N90-22156

JARE data reports, no. 140 (meteorology 21): Meteorological data at Asuka Camp, Antarctica in 1987
[ISSN-0075-3343] N90-22188

SOLAR RADIO BURSTS

Solar-geophysical data number 542, October 1989. Part 2: (Comprehensive reports). Data for April 1989 and miscellaneous
[PB90-148677] N90-22521

SOLAR RADIO EMISSION

Solar-geophysical data number 542, October 1989. Part 1: (Prompt reports). Data for September, August 1989, and late data
[PB90-148669] N90-22520

SOLAR SIMULATION

The synergism of analytic and numerical techniques in general relativity: Calculation of radiative spacetimes
N90-22425

SOLAR SIMULATORS

Direct solar-pumped iodine laser amplifier
[NASA-CR-186442] N90-22030

SOLAR SYSTEM

Improving a data-acquisition software system with abstract data type components N90-21901

SOLAR WIND

The production and spatial distribution of neutral and ionized water vapor in Comet P/Halley N90-22484

SOLAR-PUMPED LASERS

Free-Space Power Transmission
[NASA-CP-10016] N90-21795

Solar-pumped laser for free space power transmission
N90-21804

SOLID PROPELLANT COMBUSTION

On the direct simulation of vortex shedding
[LR-513] N90-21743

The pyrolysis of polymethylmethacrylate during combustion in a solid fuel combustion chamber
[LR-531] N90-21845

Solid fuel combustion chamber
[LR-562] N90-21846

Solid fuel combustion chamber
[LR-591] N90-21847

SOLID PROPELLANT ROCKET ENGINES

Flight motor set 360L002 (STS-27R). Volume 5: Nozzle component
[NASA-CR-183945] N90-21811

Shelf life extension for the lot AAE nozzle severance LSCs
[NASA-CR-183878] N90-21813

Development of low thermal conductivity pan-based carbon fibers for solid rocket motor nozzle applications
N90-21818

Solid fuel combustion chamber
[LR-591] N90-21847

Flight set 360T004 (STS-30)
[NASA-CR-183927] N90-22049

SOLID ROCKET PROPELLANTS

Solid fuel combustion chamber
[LR-562] N90-21846

SOLID STATE

Ternary reactions among polymer substrate-organohalogen-antimony oxides under pyrolytic, oxidative and flaming conditions
[PB90-154766] N90-21861

SOLID STATE LASERS

Development of mid-infrared solid state lasers for spaceborne lidar
[NASA-CR-185095] N90-22031

SOLIDS

Transient effects in Brillouin gain spectroscopy in solids
[DE90-009476] N90-21839

High resolution stimulated Raman-Brillouin spectroscopy in gases and solids
[DE90-009535] N90-21840

A spectral analysis approach to wave propagation in layered solids N90-22131

A weak formulation for phase-change problems with bulk movement due to unequal densities
[DE90-009398] N90-22361

SONIC ANEMOMETERS

Wind tunnel investigation of three sonic anemometers
[PB90-149808] N90-21729

SOUND TRANSMISSION

The Shock and Vibration Digest, volume 21, no. 6
N90-22363

Noise transmission into propeller-driven airplanes
N90-22364

SOUND WAVES

Impact tolerant material
[NASA-CASE-LAR-12887-3] N90-21822

Propagation environments, effects, and decision aids
N90-21918

SOURCE PROGRAMS

High power millimeter wave source development program N90-21805

SOUTH AMERICA

Southern oscillation simulation in coupled ocean/atmosphere global climate models N90-22181

SOUTHERN OSCILLATION

Southern oscillation simulation in coupled ocean/atmosphere global climate models N90-22181

SOYBEANS

Field reports on radiometric campaigns of soybeans in the Federal district: Safra 88/89
[INPE-5021-RPE/615] N90-22139

SPACE ADAPTATION SYNDROME

Issues in development, evaluation, and use of the NASA Preflight Adaptation Trainer (PAT)
[NASA-CR-185608] N90-22212

SPACE BASES

A robotically constructed production and supply base on Phobos
[NASA-CR-186234] N90-21872

SPACE COMMERCIALIZATION

Space Station Workshop: Commercial Missions and User Requirements
[NASA-TM-102912] N90-22428

Aeronautics and space report of the President: 1987 activities N90-22462

SPACE COMMUNICATION

The Telecommunications and Data Acquisition Report
[NASA-CR-186479] N90-21880

Mark 4-A DSCC (Magellan-era) telemetry system description N90-21903

The mm-wave region propagation experiments by satellite N90-21916

SPACE FLIGHT

NSSDC data listing
[NASA-TM-102989] N90-22456

Extraterrestrial life in the universe
[NASA-TM-102363] N90-22464

SPACE MANUFACTURING

Space Station Workshop: Commercial Missions and User Requirements
[NASA-TM-102912] N90-22428

SPACE NAVIGATION

Galileo Earth approach navigation using connected-element interferometer phase-delay tracking
N90-21884

Using connected-element interferometer phase-delay data for Magellan navigation in Venus orbit N90-21885

SPACE PERCEPTION

The effects of linear acceleration on perception and nystagmus N90-22209

SPACE PLASMAS

Equilibrium and stability analysis of magnetospheric plasmas N90-21782

The intrinsic stochasticity of near-integrable Hamiltonian systems
[IPPCZ-282] N90-22386

Plasma contactor research, 1989
[NASA-CR-185212] N90-22389

NSSDC data listing
[NASA-TM-102989] N90-22456

Space Station Freedom solar array panels plasma interaction test facility
[NASA-TM-102475] N90-22488

Solar-geophysical data number 542, October 1989. Part 2: (Comprehensive reports). Data for April 1989 and miscellaneous
[PB90-148677] N90-22521

SPACE POWER REACTORS

Prevention of significant deterioration application for approval to construct SP-100 Ground Engineering System Test Site
[DE90-007986] N90-22381

SPACE PROCESSING

Space Station Workshop: Commercial Missions and User Requirements
[NASA-TM-102912] N90-22428

SPACE PROGRAMS

Aeronautics and space report of the President: 1987 activities N90-22462

SPACE SHUTTLE BOOSTERS

Space Shuttle, NASA's major changes to flight hardware: Fact sheet for the Chairman, Committee on Science, Space, and Technology, House of Representatives
[GAO/NSIAD-88-173FS] N90-22461

SPACE SHUTTLE MAIN ENGINE

Framework for a space shuttle main engine health monitoring system
[NASA-CR-185224] N90-21809

Space Shuttle, NASA's major changes to flight hardware: Fact sheet for the Chairman, Committee on Science, Space, and Technology, House of Representatives
[GAO/NSIAD-88-173FS] N90-22461

SPACE SHUTTLE ORBITERS

Prediction of forces and moments for flight vehicle control effectors. Part 1: Validation of methods for predicting hypersonic vehicle controls forces and moments
[NASA-CR-186571] N90-21734

SPACE SHUTTLE PAYLOADS

Impact of low gravity on water electrolysis operation
[NASA-CR-185521] N90-21870

Space Station Workshop: Commercial Missions and User Requirements
[NASA-TM-102912] N90-22428

SPACE SHUTTLES

General purpose heat source radioisotope thermoelectric generator. Book 2: Accident analysis, appendices
[REPT-90SDS4202-BK-2] N90-22380

Space Shuttle, NASA's major changes to flight hardware: Fact sheet for the Chairman, Committee on Science, Space, and Technology, House of Representatives
[GAO/NSIAD-88-173FS] N90-22461

SPACE SIMULATORS

Issues in development, evaluation, and use of the NASA Preflight Adaptation Trainer (PAT)
[NASA-CR-185608] N90-22212

SPACE STATION PAYLOADS

Space Station Workshop: Commercial Missions and User Requirements
[NASA-TM-102912] N90-22428

SPACE STATION POLAR PLATFORMS

Space Station Freedom solar array panels plasma interaction test facility
[NASA-TM-102475] N90-22488

SPACE STATION POWER SUPPLIES

Photovoltaic power for Space Station Freedom
[NASA-TM-102569] N90-21812

Electric power scheduling: A distributed problem-solving approach
[NASA-TM-103149] N90-22323

Space Station Freedom solar array panels plasma interaction test facility
[NASA-TM-102475] N90-22488

SPACE STATIONS

Photovoltaic power for Space Station Freedom
[NASA-TM-102569] N90-21812

The determination of maximum deep space station slew rates for a high Earth orbiter N90-21882

Automating security monitoring and analysis for Space Station Freedom's electric power system
[NASA-TM-103148] N90-22324

An expert system for simulating electric loads aboard Space Station Freedom
[NASA-TM-103150] N90-22325

Space Station Workshop: Commercial Missions and User Requirements
[NASA-TM-102912] N90-22428

Aeronautics and space report of the President: 1987 activities N90-22462

SPACE SUITS

Cycle life machine for AX-5 space suit N90-22080

AX-5 space suit bearing torque investigation
N90-22101

SPACE TRANSPORTATION
Aeronautics and space report of the President: 1987 activities N90-22462
SPACE TRANSPORTATION SYSTEM
An all electronic transportation system from LEO to GEO and beyond N90-21796
General purpose heat source radioisotope thermoelectric generator. Book 2: Accident analysis, appendices
[REPT-90SDS4202-BK-2] N90-22380
SPACE TRANSPORTATION SYSTEM FLIGHTS
Final environmental impact statement for the Galileo Mission (Tier 2)
[NASA-TM-102925] N90-22147
SPACE WEAPONS
Scaling of nonnuclear kinetic-energy antisatellites
[DE90-009758] N90-21791
SPACE-TIME FUNCTIONS
Propagation of transient acoustic waves in porous media
[ETN-90-96401] N90-22015
Computer simulation of time-dependent spherically symmetric spacetimes containing radiating fluids: Formalism and code tests N90-22483
SPACEBORNE EXPERIMENTS
Impact of low gravity on water electrolysis operation
[NASA-CR-185521] N90-21870
An expert system for simulating electric loads aboard Space Station Freedom
[NASA-TM-103150] N90-22325
Space Station Workshop: Commercial Missions and User Requirements
[NASA-TM-102912] N90-22428
SPACEBORNE LASERS
Solar-pumped laser for free space power transmission N90-21804
SPACECRAFT CHARGING
PIC code modeling of spacecraft charging potential during electron beam injection into a background of neutral gas and plasma, part 1
[NASA-CR-186602] N90-21792
SPACECRAFT COMMUNICATION
The Advanced Communications Technology Satellite (ACTS) capabilities for serving science
[NASA-CR-186584] N90-21789
SPACECRAFT CONFIGURATIONS
Analyzing spacecraft configurations through specialization and default reasoning N90-22308
SPACECRAFT CONTROL
Direct inversion of rigid-body rotational dynamics
[NASA-TM-102798] N90-21773
A dynamic motion simulator for future European docking systems N90-22085
Spacecraft command verification: The AI solution N90-22307
System control of an autonomous planetary mobile spacecraft N90-22313
Automated procedure execution for space vehicle autonomous control N90-22314
SPACECRAFT DOCKING
A dynamic motion simulator for future European docking systems N90-22085
The resupply interface mechanism RMS compatibility test N90-22090
Orbital Maneuvering Vehicle (OMV) three-point docking latch N90-22094
Computer vision research at Marshall Space Flight Center N90-22240
SPACECRAFT LAUNCHING
Final (Tier 1) environmental impact statement for the Galileo and Ulysses Missions
[NASA-TM-102917] N90-21779
Final environmental impact statement for the Galileo Mission (Tier 2)
[NASA-TM-102925] N90-22147
Draft environmental impact statement for the Galileo Mission (Tier 2)
[NASA-TM-102926] N90-22148
Final Environmental Impact Statement for the Ulysses Mission (Tier 2)
[NASA-TM-101104] N90-22162
General purpose heat source radioisotope thermoelectric generator program. Book 1: Accident analysis
[REPT-90SDS4202-BK-1] N90-22379
General purpose heat source radioisotope thermoelectric generator. Book 2: Accident analysis, appendices
[REPT-90SDS4202-BK-2] N90-22380
SPACECRAFT MANEUVERS
Analysis, selection, and implementation of procedures which approve optimal artificial satellite maneuvers
[INPE-5003-TDL/397] N90-21786
Accurate nonlinear control for satellites using reaction wheels
[INPE-4983-PRE/1546] N90-21787
SPACECRAFT PERFORMANCE
Automated procedure execution for space vehicle autonomous control N90-22314
SPACECRAFT POWER SUPPLIES
Effect of LEO cycling on 125 Ah advanced design IPV nickel-hydrogen battery cells
[NASA-TM-103128] N90-21808
Draft environmental impact statement for the Galileo Mission (Tier 2)
[NASA-TM-102926] N90-22148
Final Environmental Impact Statement for the Ulysses Mission (Tier 2)
[NASA-TM-101104] N90-22162
Automating security monitoring and analysis for Space Station Freedom's electric power system
[NASA-TM-103148] N90-22324
SPACECRAFT TRACKING
Precise estimation of tropospheric path delays with GPS techniques N90-21881
The determination of maximum deep space station slew rates for a high Earth orbiter N90-21882
Galileo Earth approach navigation using connected-element interferometer phase-delay tracking N90-21884
Digital Doppler extraction demonstration with the advanced receiver N90-21893
SPACECRAFT TRAJECTORIES
Galileo Earth approach navigation using connected-element interferometer phase-delay tracking N90-21884
SPATIAL DISTRIBUTION
The production and spatial distribution of neutral and ionized water vapor in Comet P/Halley N90-22484
SPECTRA
Radar RFI at Goldstone DSS 12 and DSS 16 N90-21900
Spectral response of wheat and its relationship with agronomic variables in the tropical region
[INPE-5018-RPE/612] N90-22138
An algorithm and computer program for the calculation of envelope curves
[PB90-155409] N90-22254
SPECTRAL BANDS
New spectral features of stratospheric trace gases N90-21910
Computation of broad spectral band electro-optical system transmittance response characteristics to military smokes and obscurants using field test data from transmissometer system measurements N90-21939
The calculation of infrared limb emission by ozone in the terrestrial middle atmosphere N90-22151
SPECTRAL EMISSION
Non-random uncertainties in the calibration of protection-level secondary standards
[NPL-RS(EXT)-110] N90-22378
SPECTRAL ENERGY DISTRIBUTION
Search for rapidly star forming galaxies at high redshift N90-22465
SPECTRAL RESOLUTION
Cirrus cloud optical properties measured with the University of Wisconsin high spectral resolution and volume imaging lidars N90-21932
SPECTROMETERS
Development of the CLAES instrument aperture door system N90-22083
Improved crystal bending techniques applied to the LLNL dual-arm Johann mounting x ray spectrometer
[DE90-009528] N90-22415
SPECTROSCOPY
Transient effects in Brillouin gain spectroscopy in solids
[DE90-009476] N90-21839
High resolution stimulated Raman-Brillouin spectroscopy in gases and solids
[DE90-009535] N90-21840
Brillouin gain spectroscopy in glasses and crystals
[DE90-009536] N90-21841
Institute for Materials Science and Engineering, nondestructive evaluation: Technical activities
[PB90-132739] N90-22055
SPECTRUM ANALYSIS
New spectral features of stratospheric trace gases N90-21910
A spectral analysis approach to wave propagation in layered solids N90-22131
Analysis of gamma squared Velorum photometry from the South Pole N90-22472
Fast spectroscopic variations on rapidly-rotating, cool dwarfs. 3: Masses of circumstellar absorbing clouds on AB Doradus
[NASA-CR-186563] N90-22479
SPIN DYNAMICS
Direct inversion of rigid-body rotational dynamics
[NASA-TM-102798] N90-21773
Generalized killing equations and symmetries of spinning space
[NIKHEF-H/89-8] N90-22375
SPIRAL GALAXIES
The distribution of molecular clouds in spiral galaxies N90-22489
Wind instability as a possible cause of the spiral structure formation in the gaseous subsystem of galaxies with the circular magnetic field
[DE90-618944] N90-22507
SPLINE FUNCTIONS
GRID2D/3D: A computer program for generating grid systems in complex-shaped two- and three-dimensional spatial domains. Part 1: Theory and method
[NASA-TM-102453] N90-22262
Spline function smoothing and differentiation of noisy data on a rectangular grid
[DE90-009319] N90-22338
The approximation of a composite Bezier cubic curve by a composite Bezier quadratic curve
[NPL-DITC-147/89] N90-22354
The use of local polynomial approximations in a knot-placement strategy for least squares spline fitting
[NPL-DITC-148/89] N90-22355
SPLINES
Nonlinear spline operator interpolation and sliding control of deformable maneuvering bodies N90-21878
SPOT (FRENCH SATELLITE)
SPOT 4 space magnetic recorder mechanisms N90-22082
SQUALLS
A case study of cloud-to-ground lightning during the GALE program N90-22185
STABILITY
Verification of Klett's method by comparison of lidar and transmissometer measurements N90-21933
Inverse problems of heat conduction N90-21969
Instabilities and subharmonic resonances of subsonic heated round jets, volume 2
[NASA-CR-186058] N90-22017
Long term intensity stability of Auger electron spectrometers: Instructions for the interlaboratory comparison
[NPL-DMM(A)-1] N90-22027
High power CO2 laser instability and its corrections N90-22028
Nonlinear stability analysis and control of dynamical robotic systems N90-22037
Orthogonal distance regression
[PB90-151747] N90-22336
Stability criteria in the numerical solution of initial value problems
[TW-89-05] N90-22351
Stability of compactification during inflation
[NASA-CR-186597] N90-22502
A theoretical investigation of gravity-wave-generated stress and vorticity in the planetary boundary layer N90-22512
STABILIZATION
Accurate nonlinear control for satellites using reaction wheels
[INPE-4983-PRE/1546] N90-21787
STACKS
Failure analysis of woven hybrid composite using a finite element method
[OUEL-1791/89] N90-21828
STAGE SEPARATION
The development of a complementary expendable launch vehicle interface for an STS deployable payload N90-22086
STAINLESS STEELS
The effect of aging at 343 C on type 308 stainless steel weldments
[DE90-009232] N90-21853
VAMAS project on variable weld penetration: Surface tension of the steels
[NPL-DMA(A)-188] N90-21856
STANDARDIZATION
Proceedings of the Advisory Committee on Standardization of Carbon-Phenolic Test Methods and Specifications
[NASA-CR-186478] N90-21817
STANDARDS
The laminar flow element: Its use as a flow standard
[PB90-129677] N90-22157
STAR CLUSTERS
Interactions of massive stars with the interstellar medium: Bow shocks and superbubbles N90-22485
The association of supernovae with regions of recent star formation in late-type galaxies N90-22497
STAR FORMATION
A theoretical scenario for the dynamics of formation and early evolution of globular clusters in galaxies N90-22494
The association of supernovae with regions of recent star formation in late-type galaxies N90-22497

STAR FORMATION RATE
Search for rapidly star forming galaxies at high redshift N90-22465
STARK EFFECT
High resolution stimulated Raman-Brillouin spectroscopy in gases and solids
[DE90-009535] N90-21840
STARS
The Al-26(rho, gamma)Si-27 reaction: Stellar origins of galactic Al-26 N90-22498
STATE ESTIMATION
Direct inversion of rigid-body rotational dynamics
[NASA-TM-102798] N90-21773
STATIC LOADS
Development of ultrasonic nondestructive methods for defect and damage characterization in composite materials N90-21816
STATISTICAL ANALYSIS
Molecular theory of fluid phase equilibria
[PB90-131277] N90-21832
A real-time signal combining system for Ka-band feed arrays using maximum-likelihood weight estimates N90-21888
Exact closed-form expressions for the performance of the split-symbol moments estimator of signal-to-noise ratio N90-21894
Millimetric, infrared, and optical propagation studies over a 500 m path N90-21913
Adaptive frequency estimation by MUSIC (Multiple Signal Classification) method
[PB90-166794] N90-21943
Inverse problems of heat conduction N90-21969
Orthogonal distance regression
[PB90-151747] N90-22336
An investigation of the generation and radiation of aerodynamic noise in real piping systems N90-22368
The MHD structure of an open magnetotail boundary N90-22388
Managing Federal information resources
[PB90-100173] N90-22429
STATISTICAL DISTRIBUTIONS
Clustering and uniqueness in mathematical models of percolation phenomena
[ETN-90-96400] N90-22358
STATORS
Analytical and experimental study of high phase order induction motors
[NASA-CR-186580] N90-21952
Rotor-to-stationary element rub-related vibration phenomena in rotating machinery: Literature survey N90-22065
STEADY FLOW
Prediction of length scales in a Mach reflection flowfield N90-21959
STEADY STATE
On spurious steady-state solutions of explicit Runge-Kutta schemes
[NASA-TM-102819] N90-22340
STEELS
Structural fatigue in the 34-meter HA-Dec antennas N90-21902
STELLAR COLOR
The association of supernovae with regions of recent star formation in late-type galaxies N90-22497
STELLAR COMPOSITION
A comparison of photospheric and circumstellar (HCN)/(CO)-ratios for bright carbon stars
[PB90-151101] N90-22477
STELLAR ENVELOPES
A comparison of photospheric and circumstellar (HCN)/(CO)-ratios for bright carbon stars
[PB90-151101] N90-22477
Photometric monitoring of early type emission line stars N90-22478
Fast spectroscopic variations on rapidly-rotating, cool dwarfs. 3: Masses of circumstellar absorbing clouds on AB Doradus
[NASA-CR-186563] N90-22479
Herbig-Haro objects and stellar jets N90-22487
Investigation of the late stages of stellar evolution: Mass loss from evolved stars N90-22492
STELLAR EVOLUTION
Physics of systems containing neutron stars
[NASA-CR-186002] N90-22467
Investigation of the late stages of stellar evolution: Mass loss from evolved stars N90-22492
Topological defects in extended inflation
[NASA-CR-186594] N90-22505
Soft inflation
[NASA-CR-186593] N90-22506
STELLAR LUMINOSITY
Origin of pulsed emission from the young supernova remnant SN 1987A
[CAL-377] N90-22469
Gamma rays, cosmic rays, and local molecular clouds N90-22524
STELLAR MAGNETIC FIELDS
Physics of systems containing neutron stars
[NASA-CR-186002] N90-22467
STELLAR MASS
Does mass accretion lead to field decay in neutron stars
[CAL-394] N90-22470
Investigation of the late stages of stellar evolution: Mass loss from evolved stars N90-22492
The association of supernovae with regions of recent star formation in late-type galaxies N90-22497
STELLAR MASS EJECTION
Slow shocks in coronal mass ejections
[NASA-CR-186578] N90-22522
STELLAR MODELS
Modelling late-time atmospheres of supernovae N90-22500
STELLAR OSCILLATIONS
Physics of systems containing neutron stars
[NASA-CR-186002] N90-22467
Does SN 1987A contain a rapidly vibrating neutron star
[CAL-371] N90-22468
STELLAR RADIATION
Does SN 1987A contain a rapidly vibrating neutron star
[CAL-371] N90-22468
STELLAR ROTATION
The emission lines in the ultra-violet spectrum of Beta Lyrae N90-22474
STELLAR SPECTRA
Fast spectroscopic variations on rapidly-rotating, cool dwarfs. 3: Masses of circumstellar absorbing clouds on AB Doradus
[NASA-CR-186563] N90-22479
STELLAR SPECTROPHOTOMETRY
Photometric monitoring of early type emission line stars N90-22478
STELLAR STRUCTURE
The mass of the Coma cluster N90-22496
STELLAR TEMPERATURE
The ratio of neutral hydrogen to neutral helium in the local interstellar medium N90-22499
STELLAR WINDS
Interactions of massive stars with the interstellar medium: Bow shocks and superbubbles N90-22485
Wind instability as a possible cause of the spiral structure formation in the gaseous subsystem of galaxies with the circular magnetic field
[DE90-618944] N90-22507
STEP FUNCTIONS
Long steps with the logarithmic penalty barrier function in linear programming
[REPT-89-44] N90-22265
STEREOPHOTOGRAPHY
Survey of instrumental methods for the determination of the high frequency wave spectrum
[IOS-267] N90-22200
STEREOSCOPIC VISION
Space environment robot vision system N90-22245
STIFFNESS
In-situ fracture stiffness determination
[DE90-009202] N90-22173
STIMULATED EMISSION
High intensity laser beam interactions with single droplets N90-21924
STOCHASTIC PROCESSES
Homogeneous dilute turbulent particle-laden water flows N90-21965
Vibration analysis of systems with random parametric excitations N90-22060
The Shock and Vibration Digest, volume 22, no. 1 N90-22073
An approach to rescheduling activities based on determination of priority and disruptivity N90-22299
The intrinsic stochasticity of near-integrable Hamiltonian systems
[IPPCZ-282] N90-22386
STOKES FLOW
Plane Stokes flow driven by capillarity on a free surface: Overview and status
[DE90-009186] N90-22008
Plane Stokes flow driven by capillarity on a free surface: Overview and status
[DE90-009290] N90-22009
STORAGE BATTERIES
Photovoltaic power for Space Station Freedom
[NASA-TM-102569] N90-21812
STORAGE RINGS (PARTICLE ACCELERATORS)
Exclusive production of p, p-, pi, and pi- in photon photon collisions
[NIKHEF-H/89-9] N90-22376
STORAGE STABILITY
Shelf life extension for the lot AAE nozzle severance LSCs
[NASA-CR-183878] N90-21813
STORMS
Tropopause undulations and the development of extratropical cyclones N90-22186
STRAIN ENERGY RELEASE RATE
Energy release rate analysis of interfacial cracks in composites N90-21829
STRAIN GAGE BALANCES
Analysis of a six-component, flow-through, strain-gage, force balance used for hypersonic wind tunnel models with scramjet exhaust flow simulation
[NASA-CR-186585] N90-21775
STRAIN GAGES
Small strain gage applications 2
[DE90-008312] N90-22026
STRAIN RATE
The mechanics of shear band formation in thermal viscoplastic materials at high rates of loading N90-22128
STRATA
Electromagnetic inverse profiling of stratified media
[ETN-90-96402] N90-21947
STRATOSPHERE
New spectral features of stratospheric trace gases N90-21910
Opportunities for US-USSR cooperation in the investigation of Arctic stratospheric ozone N90-22154
Forecast of Atlantic seasonal hurricane activity for 1990 N90-22194
STRESS ANALYSIS
Strength in notched and impact-damaged laminates N90-21820
Fracture toughness and tensile properties of alloy HT9 in thin sections under high neutron fluences
[DE90-008386] N90-21851
A stress-strength interference approach to fast and delayed fracture reliability analysis for ceramic components N90-21859
Data and conclusions from tests on small screws
[DE90-007500] N90-22046
Dynamic response of a complex encapsulated electronic assembly subjected to a severe shock environment
[DE90-007689] N90-22114
Continued research on the strain to failure of thick-walled cylinders subjected to internal pressure
[DE90-008952] N90-22115
The computational structural mechanics testbed data library description
[NASA-TM-100645-REV-1] N90-22135
STRESS DISTRIBUTION
Residual stresses in laminated thermoplastic matrix composites N90-21815
Elastic and viscoelastic analysis of two multiply layered cylinders rolling over each other with Coulomb friction
[REPT-89-50] N90-22051
Contact mechanics for three-dimensional geometries N90-22076
Graphs of the state of stress at rounded corners
[MEMT-1] N90-22122
The stress field due to an edge dislocation and some fracture problems for a three-phase composite cylinder model N90-22126
Analysis of a finite two-dimensional solid with an inclined crack and a rigid inclusion N90-22127
An investigation into the foundations of elastic-plastic fracture mechanics N90-22130
Internal fractures in model elastomeric composites N90-22133
STRESS INTENSITY FACTORS
Nonlinear fracture mechanics using semicircular specimens and tension-softening behavior N90-22108
Fatigue crack growth in unidirectional metal matrix composite
[NASA-TM-103102] N90-22117
The stress field due to an edge dislocation and some fracture problems for a three-phase composite cylinder model N90-22126
Analysis of a finite two-dimensional solid with an inclined crack and a rigid inclusion N90-22127
Probabilistic finite elements: Applications to fracture and fatigue N90-22134
STRESS RELAXATION
Residual stresses in laminated thermoplastic matrix composites N90-21815
The analysis of stress relaxation on indentation of a rigid punch into a viscoelastic sheet of finite thickness
[NPL-DMA(A)-193] N90-22357
STRESS WAVES
A spectral analysis approach to wave propagation in layered solids N90-22131
STRESS-STRAIN RELATIONSHIPS
Three-dimensional fatigue crack closure behavior of metals N90-21857
Coordinate systems for plastic yield surfaces stress and strain space theories
[PB90-164765] N90-22110

STRING THEORY
Gravitational couplings of the inflation in extended inflation
[NASA-CR-186595] N90-22504
Topological defects in extended inflation
[NASA-CR-186594] N90-22505
Ultrahigh-energy particle flux from cosmic strings
[NASA-CR-186592] N90-22525
STRUCTURAL ANALYSIS
Towards a unified analysis methodology for composite rotor blades N90-21730
Computational simulation of structural fracture in fiber composites
[NASA-TM-102505] N90-21821
Surface structure and chemistry of high surface area silica gels
[DE90-007684] N90-21865
Review of analysis methods for mechanically fastened joints in composites
[LR-599] N90-22050
The Shock and Vibration Digest, volume 21, no. 8 N90-22068
Recent progress in the dynamic plastic behavior of structures, part 5 N90-22069
The Shock and Vibration Digest, volume 22, no. 1 N90-22073
Scattering of waves by inclusions in a nonhomogeneous elastic half space solved by boundary element methods
[PB90-145699] N90-22107
Free wave propagation in orthogonally stiffened cylinders N90-22124
The computational structural mechanics testbed data library description
[NASA-TM-100645-REV-1] N90-22135
Graphically-oriented nonlinear analysis of statically loaded plane frames on microcomputers
[PB90-165945] N90-22248
STRUCTURAL DESIGN
The 10-100 kW submillimeter gyrotron N90-21803
STRUCTURAL ENGINEERING
The Shock and Vibration Digest, volume 21, no. 1 N90-22061
Recent advances in structural control N90-22062
The Shock and Vibration Digest, volume 21, no. 7 N90-22066
Optimum design of structures under shock and vibration environment N90-22067
The Shock and Vibration Digest, volume 21, no. 8 N90-22068
STRUCTURAL FAILURE
Advances in optimal active control techniques for aerospace systems; application to aircraft active landing gear N90-21769
STRUCTURAL MEMBERS
Structural fatigue in the 34-meter HA-Dec antennas N90-21902
STRUCTURAL PROPERTIES (GEOLOGY)
Geology of coronae and domal structures on Venus and models of their origin N90-22513
STRUCTURAL STABILITY
Fatigue crack growth predictions for variable-amplitude and spectrum loading
[LR-526] N90-22118
STRUCTURAL VIBRATION
Exhaust environment measurements of a turbofan engine equipped with an afterburner and 2D nozzle
[NASA-CR-4289] N90-21760
Robust control of flexible structures N90-21784
The Shock and Vibration Digest, volume 21, no. 2 N90-22059
Vibration analysis of systems with random parametric excitations N90-22060
The Shock and Vibration Digest, volume 21, no. 1 N90-22061
A review of approximate methods for determining the vibrational modes of membranes N90-22063
The Shock and Vibration Digest, volume 21, no. 7 N90-22066
Optimum design of structures under shock and vibration environment N90-22067
The Shock and Vibration Digest, volume 21, no. 8 N90-22068
The Shock and Vibration Digest, volume 22, no. 1 N90-22073
Stable response of damped mechanical systems, 4 N90-22074
The Shock and Vibration Digest, volume 21, no. 6 N90-22363
STRUCTURAL WEIGHT
Electrochemical impregnation and cycle life of lightweight nickel electrodes for nickel-hydrogen cells
[NASA-TM-103140] N90-21844
SUBDWARF STARS
A high galactic latitude survey of far ultraviolet excess objects N90-22473
SUBMILLIMETER WAVES
The 10-100 kW submillimeter gyrotron N90-21803
The Sagittarius B2 molecular cloud: An extreme case of a galactic center giant molecular cloud N90-22493
SUBSONIC FLOW
Instabilities and subharmonic resonances of subsonic heated round jets, volume 2
[NASA-CR-186058] N90-22017
SUBSTRATES
Dynamic response of a complex encapsulated electronic assembly subjected to a severe shock environment
[DE90-007689] N90-22114
Growth and patterning of laser ablated superconducting YBa2Cu3O7 films on LaAlO3 substrates
[NASA-TM-102436] N90-22421
SULFUR
Sulphur silicate interactions on the Jovian satellite Io N90-22515
SULFUR OXIDES
Reactions of N2A3 sigma u + and candidates for short wavelengths lasers
[DE90-009514] N90-22033
SUNLIGHT
Determination of rates of reaction in the gas-phase in the troposphere: Theory and practice. 2: Rate of direct photoreaction: Screening-level test guideline-spectroscopic determination of the cross section and the maximum rate of direct photoreaction in sunlight
[PB90-146291] N90-22156
SUPERCOMPUTERS
Supercomputers need super arithmetic
[PB90-130253] N90-22252
SUPERCONDUCTING FILMS
JETC (Japanese Technology Evaluation Center) Panel Report on High Temperature Superconductivity in Japan
[NASA-CR-180413] N90-22409
Pulsed laser processing of high temperature superconducting thin films
[DE90-008928] N90-22413
Superconducting and semiconducting thin films of La(sub 123) and Y(sub 123) and their superlattices
[DE90-009565] N90-22416
In-situ pulsed laser deposition of high-T(sub c) YBa(sub 2)Cu(sub 3)O(sub 7) superconducting thin films on (100) LaAlO3 substrates
[DE90-009861] N90-22418
Growth and patterning of laser ablated superconducting YBa2Cu3O7 films on LaAlO3 substrates
[NASA-TM-102436] N90-22421
SUPERCONDUCTING MAGNETS
Heat leak measurements in superconducting dipole magnet supports
[DE90-620109] N90-22420
SUPERCONDUCTIVITY
A superconducting quenchgun for delivering lunar derived oxygen to lunar orbit
[NASA-CR-185161] N90-21806
Transport and relaxation properties in anisotropic superconductors N90-22403
JETC (Japanese Technology Evaluation Center) Panel Report on High Temperature Superconductivity in Japan
[NASA-CR-180413] N90-22409
Development of the methods and means of precise forming and geometry control of superconducting current-carrying element for the UNR pulsed dipoles
[DE90-620108] N90-22419
Growth and patterning of laser ablated superconducting YBa2Cu3O7 films on LaAlO3 substrates
[NASA-TM-102436] N90-22421
International science and technology policies: Testimony before the Subcommittee on International Scientific Cooperation, Committee on Science, Space, and Technology, United States House of Representatives
[DE90-009416] N90-22463
SUPERCONDUCTORS
Transport and relaxation properties in anisotropic superconductors N90-22403
Transport properties of anisotropic superconductors N90-22404
SUPERFLUIDITY
Nonlinear acoustic interactions in superfluid helium N90-22367
SUPERHIGH FREQUENCIES
Radiometric tests on wet and dry antenna reflector surface panels N90-21890
SUPERLATTICES
Superconducting and semiconducting thin films of La(sub 123) and Y(sub 123) and their superlattices
[DE90-009565] N90-22416
SUPERNOVA REMNANTS
The evolution of the supernova remnant IC 443 N90-22486
SUPERNOVA 1987A
Does SN 1987A contain a rapidly vibrating neutron star
[CAL-371] N90-22468
Origin of pulsed emission from the young supernova remnant SN 1987A
[CAL-377] N90-22469
Modelling late-time atmospheres of supernovae N90-22500
SUPERNOVAE
Interactions of massive stars with the interstellar medium: Bow shocks and superbubbles N90-22485
Spectrum formation in active galactic nuclei and Type 2 supernovae N90-22490
Current drive in a supernova N90-22491
The association of supernovae with regions of recent star formation in late-type galaxies N90-22497
SUPERSONIC FLOW
Prediction of length scales in a Mach reflection flowfield N90-21959
SUPERSONIC SPEED
High speed commercial transport fuels considerations and research needs
[NASA-TM-102535] N90-21869
SUPERSYMMETRY
Generalized killing equations and symmetries of spinning space
[NIKHEF-H/89-8] N90-22375
SUPPORT INTERFERENCE
Wind tunnel investigation of three sonic anemometers
[PB90-149808] N90-21729
SUPPORTS
Heat leak measurements in superconducting dipole magnet supports
[DE90-620109] N90-22420
SURFACE FINISHING
Institute for Materials Science and Engineering, nondestructive evaluation: Technical activities
[PB90-132739] N90-22055
SURFACE PROPERTIES
Surface structure and chemistry of high surface area silica gels
[DE90-007684] N90-21865
Inverse problems of heat conduction N90-21969
Computerized inspection of gear tooth surfaces
[NASA-TM-102395] N90-22054
The effects of tortuosity on flow through a natural fracture
[DE90-009193] N90-22172
SURFACE ROUGHNESS
Bearing elastohydrodynamic lubrication: A complex calculation made simple
[NASA-TM-102575] N90-22041
Surface roughness and the physical properties of fractures
[DE90-006046] N90-22169
SURFACE TEMPERATURE
Sulphur silicate interactions on the Jovian satellite Io N90-22515
SURFACE WAVES
Interaction of a turbulent round jet with the free surface N90-21964
Polarization coupling in the acousto-optic interaction of surface waves N90-22365
SURFACES
Coordinate systems for plastic yield surfaces stress and strain space theories
[PB90-164765] N90-22110
SURVEILLANCE
Calculation of IR propagation statistics in the eastern Atlantic for surveillance system performance assessment N90-21938
SURVEYS
A survey of the maritime-aerosol data collected at South Uist and the implications for the LOWTRAN maritime aerosol model N90-21908
Search for rapidly star forming galaxies at high redshift N90-22465
A high galactic latitude survey of far ultraviolet excess objects N90-22473
An astrophysics data program investigation of cluster evolution
[NASA-CR-181296] N90-22510
SWEPT WINGS
Swept wing ice accretion modeling
[NASA-TM-103114] N90-21727
SWIRLING
Modern developments in shear flow control with swirl
[NASA-CR-186586] N90-22000
SWITCHING CIRCUITS
An assessment of the hardness of miniature vacuum tubes to high-voltage transients
[DE90-009541] N90-21956
Optical shutter switching matrix
[NASA-CASE-KSC-11392-1] N90-22383
SWIVELS
Performance characteristics of a one-third-scale, vectorable ventral nozzle for SSTOVL aircraft
[NASA-TM-103120] N90-21725

SYMBOLS
Exact closed-form expressions for the performance of the split-symbol moments estimator of signal-to-noise ratio N90-21894
Technologies for electronic transfer of information: The present state and trends in Japan N90-22443
SYMMETRY
The production and spatial distribution of neutral and ionized water vapor in Comet P/Halley N90-22484
SYNCHROTRON RADIATION
Origin of pulsed emission from the young supernova remnant SN 1987A
[CAL-377] N90-22469
SYNCHROTRONS
Report on the fifth workshop on synchrotron x ray lithography
[DE90-007903] N90-22411
SYNTAX
An introduction to Montague grammar
[REPT-89-46] N90-22266
Some remarks on treatment of be in Montague's PTQ — Proper Treatment of Quantification (PTQ)
[REPT-89-40] N90-22267
Knowledge structure representation and automated updates in intelligent information management systems N90-22316
SYNTHESIS (CHEMISTRY)
Method of making a cathode from tungsten powder
[AD-D014434] N90-21850
Polysiloxanes derived from the controlled hydrolysis of tetraethoxysilane as precursors to silica for use in ceramic processing
[NASA-TM-102489] N90-21858
Preparation and characterization of Cu2ZnGeS(4-y)Se(y)
[AD-A217469] N90-22407
SYNTHETIC APERTURE RADAR
Using connected-element interferometer phase-delay data for Magellan navigation in Venus orbit N90-21885
SYNTHETIC APERTURES
Diffraction-limited imaging on the 200-inch telescope N90-22475
SYSTEM FAILURES
Reliability importance measures and their calculation
[DE90-620391] N90-22057
A methodology for knowledge-based restructurable control to accommodate system failures N90-22058
NASA ground terminal communication equipment automated fault isolation expert systems N90-22305
SYSTEM IDENTIFICATION
Adaptive control of a flexible manipulator with unknown changing loads N90-22293
SYSTEMS ANALYSIS
Computation of broad spectral band electro-optical system transmittance response characteristics to military smokes and obscurants using field test data from transmissometer system measurements N90-21939
Insights into complex human performance
[DE90-006957] N90-22214
An introduction to selected structured methods
[RSRE-MEMO-4294] N90-22275
Electric power scheduling: A distributed problem-solving approach
[NASA-TM-103149] N90-22323
SYSTEMS ENGINEERING
An all electronic transportation system from LEO to GEO and beyond N90-21796
Solar-pumped laser for free space power transmission N90-21804
Progression of damage and fracture in composites under dynamic loading
[NASA-TM-103118] N90-21825
Vibration analysis of systems with random parametric excitations N90-22060
Understanding the computing system domain of advanced computing with microcomputers
[DE90-009825] N90-22251
SYSTEMS INTEGRATION
An introduction to selected structured methods
[RSRE-MEMO-4294] N90-22275

T

TACTICS
Computer vision techniques for rotorcraft low altitude flight N90-22237
TAKEOFF
Optimization and guidance of flight trajectories in the presence of windshear
[NASA-CR-186163] N90-21747
TAPE RECORDERS
SPOT 4 space magnetic recorder mechanisms N90-22082
TARGET RECOGNITION
Recognition and analysis of aircraft targets by radar, using structural pattern representations derived from polarimetric signatures N90-21879
TARGETS
Optimal and near-optimal medium range air-to-air missile guidance against maneuvering targets N90-21766
TEARING
Inclusion of unstable ductile tearing and extrapolated crack-arrest toughness data in PWR vessel integrity assessment
[DE90-009427] N90-22116
TECHNOLOGIES
International science and technology policies: Testimony before the Subcommittee on International Scientific Cooperation, Committee on Science, Space, and Technology, United States House of Representatives
[DE90-009416] N90-22463
TECHNOLOGY ASSESSMENT
An all electronic transportation system from LEO to GEO and beyond N90-21796
Aging characteristics of Li/SO(sub 2) cells
[NASA-CR-180432] N90-21954
Trajectory generation for car-like robots
[DE90-008407] N90-22047
Low order FIR and IIR filters in dynamic vision
[OUEL-1785/89] N90-22384
Japanese magnetic confinement fusion research N90-22392
JETC (Japanese Technology Evaluation Center) Panel Report on High Temperature Superconductivity in Japan
[NASA-CR-180413] N90-22409
TECHNOLOGY TRANSFER
How to get it: A guide to defense-related information resources
[AD-A201600] N90-22433
International science and technology policies: Testimony before the Subcommittee on International Scientific Cooperation, Committee on Science, Space, and Technology, United States House of Representatives
[DE90-009416] N90-22463
TECHNOLOGY UTILIZATION
Induction-type metal detector with increased scanning area capability
[NASA-CASE-KSC-11386-1] N90-22023
Information technology applications: A British Aerospace Military Aircraft Ltd view N90-22455
TECTONICS
Geology of coronae and domal structures on Venus and models of their origin N90-22513
TELECOMMUNICATION
The Telecommunications and Data Acquisition Report
[NASA-CR-186479] N90-21880
Atmospheric Propagation in the UV, Visible, IR, and mm-Wave Region and Related Systems Aspects
[AGARD-CP-454] N90-21907
Electronic Transfer of Information and its Impact on Aerospace and Defence Research and Development
[AGARD-CP-466] N90-22440
Technologies for electronic transfer of information: The present state and trends in Europe N90-22441
Innovations in telecommunications networks N90-22444
Electronic mail systems N90-22451
Computer conferencing: Minds meeting anywhere anytime N90-22452
TELEMETRY
Digital Doppler extraction demonstration with the advanced receiver N90-21893
Mark 4-A DSCC (Magellan-era) telemetry system description N90-21903
An 8.4-GHz dual-maser front-end system for Parkes reimplementation N90-21905
TELEOPERATORS
A new six-degree-of-freedom force-reflecting hand controller for space telerobotics N90-22089
Development of cable drive systems for an automated assembly project N90-22105
Hybrid vision activities at NASA Johnson Space Center N90-22225
Instrumentation and robotic image processing using top-down model control N90-22239
Computer vision research at Marshall Space Flight Center N90-22240
The JPL/KSC telerobotic inspection demonstration N90-22312
TELESCOPES
A soft actuation system for segmented reflector articulation and isolation N90-22084
Diffraction-limited imaging on the 200-inch telescope N90-22475
TEMPERATURE CONTROL
Development and integration of the capillary pumped loop GAS and Hitchhiker flight experiments
[NASA-TM-100756] N90-21790
TEMPERATURE DEPENDENCE
Detailed mechanism for oxidation of benzene
[NASA-TM-102443] N90-21842
A temperature-dependent regular infrared band model for absorption and dispersion N90-21927
Evaluating thermographic phosphors in an operating turbine engine
[DE90-004874] N90-22044
Optical bistability in semiconducting material N90-22424
TEMPERATURE DISTRIBUTION
Inverse problems of heat conduction N90-21969
TEMPERATURE EFFECTS
Analysis of a six-component, flow-through, strain-gage, force balance used for hypersonic wind tunnel models with scramjet exhaust flow simulation
[NASA-CR-186585] N90-21775
METCAN verification status
[NASA-TM-103119] N90-21824
The temperature variation of hydrogen diffusion coefficients in metal alloys
[NASA-TM-100397] N90-21836
Development of shape memory metal as the actuator of a fail safe mechanism N90-22081
TEMPERATURE GRADIENTS
TOODEE: A two-dimensional, time-dependent heat conduction program
[DE90-009631] N90-22010
Scattered-light scanner measurements of cryogenic liquid-jet breakup
[NASA-TM-102432] N90-22021
Linear, nonlinear, and tunable guided wave modes for high-power (GaAl)As semiconductor lasers N90-22036
Effect of a crystal-melt interface on Taylor-vortex flow
[NASA-CR-186512] N90-22408
TEMPERATURE INVERSIONS
Infrared propagation in the air-sea boundary layer N90-21926
Inverse problems of heat conduction N90-21969
TEMPERATURE MEASUREMENT
Inverse problems of heat conduction N90-21969
TEMPERATURE PROFILES
The observed properties of the intermediate-degree gravity modes and their relevance to the solar neutrino paradox N90-22519
TENSILE DEFORMATION
Continued research on the strain to failure of thick-walled cylinders subjected to internal pressure
[DE90-008952] N90-22115
TENSILE PROPERTIES
Fracture toughness and tensile properties of alloy HT9 in thin sections under high neutron fluences
[DE90-008386] N90-21851
Data and conclusions from tests on small screws
[DE90-007500] N90-22046
TENSILE STRENGTH
Strength in notched and impact-damaged laminates N90-21820
Matrix density effects on the mechanical properties of SiC/RBSN composites
[NASA-TM-103098] N90-21826
The effect of aging at 343 C on type 308 stainless steel weldments
[DE90-009232] N90-21853
Nonlinear fracture mechanics using semicircular specimens and tension-softening behavior N90-22108
TENSILE STRESS
Modelling of the impact response of fibre-reinforced composites
[OUEL-1784/89] N90-21827
TENSILE TESTS
Interfacial studies in fiber-reinforced thermoplastic-matrix composites N90-21814
Failure analysis of woven hybrid composite using a finite element method
[OUEL-1791/89] N90-21828
TENSORS
New algorithms for one-loop integrals
[NIKHEF-H/89-17] N90-22268
TERMINOLOGY
NASA Thesaurus supplement: A four part cumulative supplement to the 1988 edition of the NASA Thesaurus (supplement 3)
[NASA-SP-7064-SUPPL-3] N90-22438
TERRAIN
Millimeter-wave bistatic scattering by terrain N90-21936
TEST FACILITIES
A dynamic motion simulator for future European docking systems N90-22085
Prevention of significant deterioration application for approval to construct SP-100 Ground Engineering System Test Site
[DE90-007986] N90-22381
MHD channel development, part 4
[DE90-009552] N90-22397

TEST RANGES
The psychology of computer displays in the modern mission control center
[NASA-TM-100451] N90-22213
TETRAHEDRONS
Unstructured mesh generation by a generalized Delaunay algorithm N90-21995
TEXTS
Desk top publishing: What you need to know
N90-22449
Electronic publishing with Standard Generalized Markup Language (SGML) N90-22450
TEXTURES
Gravitational effects of global textures
[NASA-CR-186596] N90-22503
THEOREMS
The intrinsic stochasticity of near-integrable Hamiltonian systems
[IPPCZ-282] N90-22386
THERMAL ANALYSIS
The influence of large, cold objects on engulfing fire environments
[DE90-003342] N90-21875
THERMAL CONDUCTIVITY
Experimental determination of thermal conductance in bolted joint impact in satellites
[INPE-4989-PRE/1551] N90-21788
Development of low thermal conductivity pan-based carbon fibers for solid rocket motor nozzle applications
N90-21818
TOODEE: A two-dimensional, time-dependent heat conduction program
[DE90-009631] N90-22010
Low temperature properties of amorphous solids
N90-22405
Heat leak measurements in superconducting dipole magnet supports
[DE90-620109] N90-22420
THERMAL DIFFUSIVITY
Flow boiling with enhancement devices for cold plate coolant channel design
[NASA-CR-186358] N90-21961
THERMAL EMISSION
Applications of remote sensing to studies of oceanic upper mixed layer dynamics N90-22137
THERMAL ENERGY
Flow boiling with enhancement devices for cold plate coolant channel design
[NASA-CR-186358] N90-21961
THERMAL EXPANSION
Thermomechanical properties of polymeric materials and related stresses
[NASA-TM-100758] N90-21864
Thermomechanically-induced convective motion and natural convection in confined gaseous helium subjected to boundary heating N90-21960
THERMAL STABILITY
High speed commercial transport fuels considerations and research needs
[NASA-TM-102535] N90-21869
THERMAL STRESSES
Thermomechanical properties of polymeric materials and related stresses
[NASA-TM-100758] N90-21864
SPOT 4 space magnetic recorder mechanisms
N90-22082
THERMAL VACUUM TESTS
Space Station Freedom solar array panels plasma interaction test facility
[NASA-TM-102475] N90-22488
THERMOCHEMICAL PROPERTIES
SGTE data for pure elements
[NPL-DMA(A)-195] N90-22460
THERMOCHEMISTRY
Testing of an advanced thermochemical conversion reactor system
[DE90-007989] N90-22141
THERMODYNAMIC EQUILIBRIUM
The calculation of infrared limb emission by ozone in the terrestrial middle atmosphere N90-22151
Computer simulation of time-dependent spherically symmetric spacetimes containing radiating fluids: Formalism and code tests N90-22483
THERMODYNAMIC PROPERTIES
Development of low thermal conductivity pan-based carbon fibers for solid rocket motor nozzle applications
N90-21818
Inverse problems of heat conduction N90-21969
THERMODYNAMICS
Molecular theory of fluid phase equilibria
[PB90-131277] N90-21832
Thermomechanical properties of polymeric materials and related stresses
[NASA-TM-100758] N90-21864
TOODEE: A two-dimensional, time-dependent heat conduction program
[DE90-009631] N90-22010
Heat-transfer regimes in nuclear-reactor-pumped gas lasers
[DE90-002904] N90-22032
The mechanics of shear band formation in thermal viscoplastic materials at high rates of loading
N90-22128
The relationship between the buoyancy of near-surface air and the potential temperature of the tropopause
N90-22165
Characteristics of cumulus bandclouds off the east coast of Hawaii N90-22178
Overview of current bulk and thick film high temperature superconductor processing strategies
[DE90-008949] N90-22414
A galaxy formation cookbook: Recipes and utensils
N90-22508
THERMOELASTICITY
Residual stresses in laminated thermoplastic matrix composites N90-21815
THERMOELECTRIC GENERATORS
Final environmental impact statement for the Galileo Mission (Tier 2)
[NASA-TM-102925] N90-22147
Draft environmental impact statement for the Galileo Mission (Tier 2)
[NASA-TM-102926] N90-22148
Final Environmental Impact Statement for the Ulysses Mission (Tier 2)
[NASA-TM-101104] N90-22162
General purpose heat source radioisotope thermoelectric generator program. Book 1: Accident analysis
[REPT-90SDS4202-BK-1] N90-22379
General purpose heat source radioisotope thermoelectric generator. Book 2: Accident analysis, appendices
[REPT-90SDS4202-BK-2] N90-22380
THERMOELECTRICITY
Transport and relaxation properties in anisotropic superconductors N90-22403
THERMOGRAPHY
Evaluating thermographic phosphors in an operating turbine engine
[DE90-004874] N90-22044
THERMOMECHANICAL TREATMENT
Thermomechanically-induced convective motion and natural convection in confined gaseous helium subjected to boundary heating N90-21960
THERMOPLASTICITY
Residual stresses in laminated thermoplastic matrix composites N90-21815
THESAURI
NASA Thesaurus supplement: A four part cumulative supplement to the 1988 edition of the NASA Thesaurus (supplement 3)
[NASA-SP-7064-SUPPL-3] N90-22438
THICK FILMS
Overview of current bulk and thick film high temperature superconductor processing strategies
[DE90-008949] N90-22414
THICK PLATES
Three-dimensional finite element formulations for thick and thin laminated plates N90-22132
THIN FILMS
New flexible circuit material evaluation
[DE90-008313] N90-21866
Photovoltaic Program Branch
[DE90-000318] N90-22142
Pulsed laser processing of high temperature superconducting thin films
[DE90-008928] N90-22413
Superconducting and semiconducting thin films of La(sub 123) and Y(sub 123) and their superlattices
[DE90-009565] N90-22416
In-situ pulsed laser deposition of high-T(sub c) YBa(sub 2)Cu(sub 3)O(sub 7) superconducting thin films on (100) LaAlO3 substrates
[DE90-009861] N90-22418
Growth and patterning of laser ablated superconducting YBa2Cu3O7 films on LaAlO3 substrates
[NASA-TM-102436] N90-22421
THIN PLATES
Three-dimensional finite element formulations for thick and thin laminated plates N90-22132
THIN WALLED SHELLS
Elastic stability and nonlinear behavior of imperfect shells with initial stresses N90-22070
Interactions of massive stars with the interstellar medium: Bow shocks and superbubbles N90-22485
THREE DIMENSIONAL BOUNDARY LAYER
Numerical investigation of some control methods for 3-D turbulent interactions due to sharp fins N90-21764
Local mode smoothing analysis for various incomplete factorization iterative methods in three dimensions
[REPT-89-38] N90-22263
THREE DIMENSIONAL FLOW
Swept wing ice accretion modeling
[NASA-TM-103114] N90-21727
Effective methods of controlling a junction vortex system in an incompressible, three-dimensional, turbulent flow
N90-21732
THREE DIMENSIONAL MODELS
Swept wing ice accretion modeling
[NASA-TM-103114] N90-21727
Three-dimensional simulation of vortex breakdown
[NASA-TM-102664] N90-21744
General structured grid generation systems
N90-21977
Grid patching approaches for complex three-dimensional configurations N90-21985
The solution of scattering and radiation problems for complex configurations based on 3-D grid and patch models N90-21997
Contact mechanics for three-dimensional geometries
N90-22076
On three-dimensional scaling and consistent truncation of global atmospheric models N90-22164
Hail growth in a highly-glaciated central high plains multi-cellular hailstorm N90-22184
Frontal structure in a mesoscale model N90-22187
Three-dimensional simulations of simple electron drift wave turbulence in tokamak geometry
[DE90-009581] N90-22398
THRUST
Optimal control of an aircraft flying through a downburst N90-21765
Hybrid propulsion technology program. Volume 1: Conceptional design package
[NASA-CR-183953] N90-21793
Hybrid propulsion technology program. Volume 2: Technology definition package
[NASA-CR-183954] N90-21794
THRUST CONTROL
A comparison of time-optimal interception trajectories for the F-8 and F-15
[NASA-CR-186300] N90-21753
THRUSTORS
Bi-directional thruster development and test report
[NASA-CR-182013] N90-21785
THUNDERSTORMS
A case study of cloud-to-ground lightning during the GALE program N90-22185
TIDES
A free surface Bryan-Cox-Semtner model
[IOS-270] N90-22201
TILTING ROTORS
Identification of XV-15 aeroelastic modes using frequency-domain methods
[NASA-TM-101021] N90-21756
TIME DEPENDENCE
Plane Stokes flow driven by capillarity on a free surface: Overview and status
[DE90-009290] N90-22009
Computer simulation of time-dependent spherically symmetric spacetimes containing radiating fluids: Formalism and code tests N90-22483
TIME DISCRIMINATION
Multiresolution and time-frequency representations of signals
[REPT-89-47] N90-21946
TIME LAG
Precise estimation of tropospheric path delays with GPS techniques N90-21881
TIME MARCHING
Extension of a streamwise upwind algorithm to a moving grid system
[NASA-TM-102800] N90-21739
TIME SERIES ANALYSIS
The observed three-dimensional structure of baroclinic waves in the Northern Hemisphere winter as revealed in a linear regression analysis N90-22167
TITAN LAUNCH VEHICLES
Draft environmental impact statement for the Galileo Mission (Tier 2)
[NASA-TM-102926] N90-22148
TOKAMAK DEVICES
Magnetic turbulence versus safety factor in the Tokapole 2 tokamak N90-22391
Three-dimensional simulations of simple electron drift wave turbulence in tokamak geometry
[DE90-009581] N90-22398
TOOLS
Report on the fifth workshop on synchrotron x ray lithography
[DE90-007903] N90-22411

TOPOGRAPHY
Surface roughness and the physical properties of fractures
[DE90-006046] N90-22169
Geographic information system: Coded data of agrocattle-raising projects in the Amazon
[INPE-4978-PRE/1543] N90-22457
Geology of coronae and domal structures on Venus and models of their origin N90-22513
Sulphur silicate interactions on the Jovian satellite Io N90-22515
TOPOLOGY
Algebraic block-structured grid generation based on a macro-block concept N90-21978
Multiblock topology specification and grid generation for complete aircraft configurations N90-21986
Bifurcations in viscous flow fields. On the genesis and development of topologically complicated separated flow structures
[PB90-167156] N90-22012
Preference numbers and funnel dimension
[REPT-89-57] N90-22346
TOROIDAL PLASMAS
Impurity control in toroidal devices
[DE90-618585] N90-22399
TORQUE
AX-5 space suit bearing torque investigation N90-22101
TORSION
Rotor loading on a three-bladed wind turbine N90-22145
TORUSES
Hopf bifurcation with nonsemisimple 1:1 resonance e
[MEMO-808] N90-22347
TOUGHNESS
Inclusion of unstable ductile tearing and extrapolated crack-arrest toughness data in PWR vessel integrity assessment
[DE90-009427] N90-22116
TOWERS
Rotor loading on a three-bladed wind turbine N90-22145
TOXIC HAZARDS
Daytime wind valleys adjacent to the Great Salt Lake
[DE90-008991] N90-22190
TRACE ELEMENTS
New spectral features of stratospheric trace gases N90-21910
Global distribution of organo-bromine gases N90-22150
TRACKING (POSITION)
Passive navigation using image irradiance tracking N90-22232
TRACTION
Finite element analysis of elastic contact problems with friction N90-22040
TRAINING ANALYSIS
Issues in development, evaluation, and use of the NASA Preflight Adaptation Trainer (PAT)
[NASA-CR-185608] N90-22212
TRAINING DEVICES
Visions of visualization aids: Design philosophy and experimental results N90-22220
TRAINING SIMULATORS
Issues in development, evaluation, and use of the NASA Preflight Adaptation Trainer (PAT)
[NASA-CR-185608] N90-22212
TRAJECTORIES
Optimization and guidance of flight trajectories in the presence of windshear
[NASA-CR-186163] N90-21747
First-order weight corrections for real-time flight path management
[LR-580] N90-21751
A comparison of time-optimal interception trajectories for the F-8 and F-15
[NASA-CR-186300] N90-21753
Optimal trajectories for the aeroassisted flight experiment. Part 4: Data, tables, and graphs
[NASA-CR-186164] N90-21780
UD filtering and smoothing applied to orbit determination
[INPE-4966-PRE/1535] N90-22501
TRAJECTORY OPTIMIZATION
An approach to on-board optimization of cruise at constant altitude
[LR-581] N90-21752
Trajectory generation for car-like robots
[DE90-008407] N90-22047
TRANSDUCERS
MHD channel development, part 2
[DE90-009550] N90-22395
TRANSFER FUNCTIONS
The role of input weighting and bounding in the characteristic GPC method
[OUEL-1762/89] N90-22328
A robust stability result for generalised predictive control
[OUEL-1773/89] N90-22330
TRANSFER ORBITS
An all electronic transportation system from LEO to GEO and beyond N90-21796
TRANSFORMATIONS (MATHEMATICS)
Efficient estimation in the Clayton-Cuzick model for survival data
[TW-88-06] N90-22348
TRANSFORMERS
Voltage source ac-to-dc converters for high-power transmitters N90-21886
TRANSIENT RESPONSE
Transient response of a cylindrical shell of finite length to transverse impact
[OUEL-1780/89] N90-22123
TRANSITION FLOW
European research on viscous flow (EuroVisc)
[NLR-TP-89077-U] N90-22014
TRANSITION PROBABILITIES
Recombination lines of C I and N II in the interstellar medium N90-22466
TRANSMISSION LOSS
Evaporation duct effects at millimeter wavelengths N90-21914
Report on STC/Technische Universiteit (TU) Delft Extremely High Frequency (EHF) radio relay study N90-21915
The mm-wave region propagation experiments by satellite N90-21916
Propagation environments, effects, and decision aids N90-21918
Modeling millimeter-wave propagation effects in the atmosphere N90-21922
A temperature-dependent regular infrared band model for absorption and dispersion N90-21927
Radar scatterometry and polarimetry at 220 GHz N90-21935
Calculation of IR propagation statistics in the eastern Atlantic for surveillance system performance assessment N90-21938
An investigation of the generation and radiation of aerodynamic noise in real piping systems N90-22368
TRANSMISSOMETERS
Verification of Klett's method by comparison of lidar and transmissometer measurements N90-21933
TRANSMITTANCE
Minimizing the effects of the atmosphere in the observation of ultraviolet radiation N90-21911
LOWTRAN 7: Status, review, and impact for short-to-long-wavelength infrared applications N90-21917
UV spectral simulations using LOWTRAN 7 N90-21928
Technique for selecting an aerosol model useful for infrared atmospheric transmittance calculations N90-21934
Computation of broad spectral band electro-optical system transmittance response characteristics to military smokes and obscurants using field test data from transmissometer system measurements N90-21939
Fast method for computing infrared transmission, computation examples N90-21942
An algorithm and computer program for the calculation of envelope curves
[PB90-155409] N90-22254
TRANSMITTERS
Voltage source ac-to-dc converters for high-power transmitters N90-21886
TRANSONIC FLOW
Numerical investigation of separated transonic turbulent flows with a multiple-time-scale turbulence model
[NASA-TM-102499] N90-21962
A discussion on issues relating to multiblock grid generation N90-21991
TRANSPARENCE
High intensity laser beam interactions with single droplets N90-21924
Factors affecting the perception of transparent motion N90-22233
Modelling late-time atmospheres of supernovae N90-22500
TRANSPORT AIRCRAFT
High speed commercial transport fuels considerations and research needs
[NASA-TM-102535] N90-21869
TRANSPORT PROPERTIES
Inventory of program packages related to the project SIMONA
[ETN-90-96397] N90-22270
Transport and relaxation properties in anisotropic superconductors N90-22403
Transport properties of anisotropic superconductors N90-22404
TRANSPORT THEORY
Millimeter-wave bistatic scattering by terrain N90-21936
Rigorous upper bounds for turbulent transport in bounded systems: Passive advection and reversed-field pinches N90-22390
TRANSVERSE OSCILLATION
Transient response of a cylindrical shell of finite length to transverse impact
[OUEL-1780/89] N90-22123
TRAPPING
Positron trapping in semiconductors
[PB90-165606] N90-22410
TRAVELING WAVE MASERS
Ultralow noise performance of an 8.4-GHz maser-feedhorn system N90-21889
TREADMILLS
The predictability and efficiency of human walking: Metabolic, mechanical, and biophysical considerations N90-22211
TRENDS
Electronic Transfer of Information and its Impact on Aerospace and Defence Research and Development
[AGARD-CP-466] N90-22440
Technologies for electronic transfer of information: The present state and trends in Europe N90-22441
Technologies for electronic transfer of information: The present state and trends in Japan N90-22443
Megatendances N90-22445
TRIANGULATION
Unstructured mesh generation by a generalized Delaunay algorithm N90-21995
TRIBOLOGY
Self-lubricating polymer composites and polymer transfer film lubrication for space applications
[NASA-TM-102492] N90-21862
The 24th Aerospace Mechanisms Symposium
[NASA-CP-3062] N90-22079
Tribomaterial factors in space mechanism brake performance N90-22096
TRIGONOMETRIC FUNCTIONS
Transient response of a cylindrical shell of finite length to transverse impact
[OUEL-1780/89] N90-22123
TROPICAL REGIONS
Spectral response of wheat and its relationship with agronomic variables in the tropical region
[INPE-5018-RPE/612] N90-22136
The interpretation of SAGE 2 ozone measurements in the lower mesosphere N90-22149
The relationship between the buoyancy of near-surface air and the potential temperature of the tropopause N90-22165
Southern oscillation simulation in coupled ocean/atmosphere global climate models N90-22181
TROPICAL STORMS
Forecast of Atlantic seasonal hurricane activity for 1990 N90-22194
TROPOPAUSE
The relationship between the buoyancy of near-surface air and the potential temperature of the tropopause N90-22165
Tropopause undulations and the development of extratropical cyclones N90-22186
TROPOSPHERE
Precise estimation of tropospheric path delays with GPS techniques N90-21881
Lidar measurements of the optical propagation environment N90-21930
Determination of rates of reaction in the gas-phase in the troposphere: Theory and practice. 2: Rate of direct photoreaction: Screening-level test guideline-spectroscopic determination of the cross section and the maximum rate of direct photoreaction in sunlight
[PB90-146291] N90-22156
The sources and chemistry of late winter Arctic tropospheric aerosols
[PB90-131988] N90-22158
TROUGHS
Geology of coronae and domal structures on Venus and models of their origin N90-22513
TRUSSES
Passive shape control of space antennas with determinate truss support structures N90-21949
TUNGSTEN
Method of making a cathode from tungsten powder
[AD-D014434] N90-21850
TURBINE BLADES
Probabilistic analysis of bladed turbine disks and the effect of mistuning
[NASA-TM-102564] N90-21871
Practical nonlinear simulation of rotating machinery dynamics with application to turbine blade rubbing N90-22038

Aerodynamics of a full-scale, non rotating wind turbine blade under natural wind conditions
[RISOE-M-2768] N90-22144

TURBINE WHEELS

Probabilistic analysis of bladed turbine disks and the effect of mistuning
[NASA-TM-102564] N90-21871

TURBOFAN ENGINES

Exhaust environment measurements of a turbofan engine equipped with an afterburner and 2D nozzle
[NASA-CR-4289] N90-21760

TURBOGENERATORS

The role of input weighting and bounding in the characteristic GPC method
[OUEL-1762/89] N90-22328

TURBOJET ENGINES

On the use of external burning to reduce aerospace vehicle transonic drag
[NASA-TM-103107] N90-21762

TURBOMACHINERY

Mesh generation for flow computation in turbomachine N90-21981

Experimental investigation of the effect of cavitation on the rotordynamic forces on a whirling centrifugal pump impeller N90-22039

The Shock and Vibration Digest, volume 21, no. 2 N90-22059

TURBOPROP ENGINES

The Shock and Vibration Digest, volume 21, no. 6 N90-22363

Noise transmission into propeller-driven airplanes N90-22364

TURBULENCE

Numerical investigation of some control methods for 3-D turbulent interactions due to sharp fins N90-21764

Studies on reactive flows N90-21831

Fire propagation in concurrent flows
[PB90-151754] N90-21834

Scintillation of millimeter-wave intensity and phase caused by turbulence and precipitation N90-21912

Millimetre-wave propagation in the evaporation duct N90-21929

Lidar measurement of concentration and turbulence in battlefield obscurants N90-21931

An experimental investigation of mixing in buoyant flows N90-21963

An investigation of turbulence structure in a low Reynolds number incompressible turbulent boundary layer N90-21966

Experimental observations on transition to turbulence in confined coaxial jets and other boundary layer flows
[DE90-008939] N90-22005

Turbulence in slurry pipe flow
[DE90-008940] N90-22006

Scattered-light scanner measurements of cryogenic liquid-jet breakup
[NASA-TM-102432] N90-22021

Regional wind energy assessment
[DE90-009439] N90-22143

Rotor loading on a three-bladed wind turbine N90-22145

Magnetic turbulence versus safety factor in the Tokapole 2 tokamak N90-22391

Three-dimensional simulations of simple electron drift wave turbulence in tokamak geometry
[DE90-009581] N90-22398

A three-year study of the OH masers in Orion-KL and a study of the (3,2) transition of ammonia N90-22471

Fast spectroscopic variations on rapidly-rotating, cool dwarfs. 3: Masses of circumstellar absorbing clouds on AB Doradus
[NASA-CR-186563] N90-22479

A theoretical scenario for the dynamics of formation and early evolution of globular clusters in galaxies N90-22494

TURBULENCE EFFECTS

Control of flow separation and mixing by aerodynamic excitation
[NASA-TM-103131] N90-21733

Rigorous upper bounds for turbulent transport in bounded systems: Passive advection and reversed-field pinches N90-22390

TURBULENCE MODELS

A multiblock/multizone code (PAB 3D-v2) for the three-dimensional Navier-Stokes equations: Preliminary applications
[NASA-CR-182032] N90-21745

Numerical investigation of separated transonic turbulent flows with a multiple-time-scale turbulence model
[NASA-TM-102499] N90-21962

Computational modeling and validation for hypersonic inlets
[NASA-TM-103111] N90-22011

Development of a defect stream function, law of the wall/wake method for compressible turbulent boundary layers N90-22019

TURBULENT BOUNDARY LAYER

Numerical investigation of separated transonic turbulent flows with a multiple-time-scale turbulence model
[NASA-TM-102499] N90-21962

An investigation of turbulence structure in a low Reynolds number incompressible turbulent boundary layer N90-21966

Automated analysis of measured turbulent boundary flow
[PB90-147844] N90-21970

European research on viscous flow (EuroVisc)
[NLR-TP-89077-U] N90-22014

Development of a defect stream function, law of the wall/wake method for compressible turbulent boundary layers N90-22019

TURBULENT DIFFUSION

A linear analysis of monsoon base states associated with banded convection N90-22179

TURBULENT FLOW

Numerical investigation of separated transonic turbulent flows with a multiple-time-scale turbulence model
[NASA-TM-102499] N90-21962

Homogeneous dilute turbulent particle-laden water flows N90-21965

Numerical study of laminar and turbulent flows past two-dimensional and axisymmetric bodies N90-22020

TURBULENT HEAT TRANSFER

Computer simulation of ionospheric radio frequency heating
[DE90-009478] N90-21944

TURBULENT JETS

Interaction of a turbulent round jet with the free surface N90-21964

Laser Doppler anemometry measurements of a confined turbulent water jet with a uniform background flow N90-21971

Modern developments in shear flow control with swirl
[NASA-CR-186586] N90-22000

Lagrangian model simulation of the turbulent transport of evaporating jet droplets N90-22168

TVD SCHEMES

Numerical simulation of hypersonic flow around a space plane. Part 2: Application to high angles of attack flow
[NAL-TR-1011T] N90-21726

TWO DIMENSIONAL BODIES

Numerical study of laminar and turbulent flows past two-dimensional and axisymmetric bodies N90-22020

TWO DIMENSIONAL FLOW

Topics in vortex methods for the computation of three- and two-dimensional incompressible unsteady flows N90-21967

TWO DIMENSIONAL MODELS

Topics in vortex methods for the computation of three- and two-dimensional incompressible unsteady flows N90-21967

TWO PHASE FLOW

An experimental investigation of the physical mechanisms controlling the asymmetric flow past slender bodies at large angles of attack N90-21767

Development and integration of the capillary pumped loop GAS and Hitchhiker flight experiments
[NASA-TM-100756] N90-21790

Flow boiling with enhancement devices for cold plate coolant channel design
[NASA-CR-186358] N90-21961

On dual Lagrangian hyperbolic models for one dimensional two phase flow problems
[DE90-007012] N90-22004

Mathematical modeling of fluid-solid mixtures
[DE90-009152] N90-22007

U

U.S.S.R.

Opportunities for US-USSR cooperation in the investigation of Arctic stratospheric ozone N90-22154

USSR Space Life Sciences Digest, issue 25
[NASA-CR-3922(29)] N90-22203

UBV SPECTRA

Photometric monitoring of early type emission line stars N90-22478

ULTRASONIC FLAW DETECTION

Development of ultrasonic nondestructive methods for defect and damage characterization in composite materials N90-21816

The classification of defects from ultrasonic measurements
[AERE-R-13306] N90-22056

ULTRASONIC RADIATION

Diffraction of light by ultrasonic pulses N90-22366

ULTRASONICS

Institute for Materials Science and Engineering, nondestructive evaluation: Technical activities
[PB90-132739] N90-22055

ULTRAVIOLET DETECTORS

UV photo-enhanced MOCVD of cadmium and cadmium telluride
[RSRE-MEMO-4208] N90-22422

ULTRAVIOLET RADIATION

Atmospheric Propagation in the UV, Visible, IR, and mm-Wave Region and Related Systems Aspects
[AGARD-CP-454] N90-21907

Minimizing the effects of the atmosphere in the observation of ultraviolet radiation N90-21911

Modelling UV-visible radiation observed from space N90-21937

The emission lines in the ultra-violet spectrum of Beta Lyrae N90-22474

ULTRAVIOLET SPECTRA

UV spectral simulations using LOWTRAN 7 N90-21928

ULTRAVIOLET SPECTROMETERS

The ratio of neutral hydrogen to neutral helium in the local interstellar medium N90-22499

ULYSSES MISSION

Final (Tier 1) environmental impact statement for the Galileo and Ulysses Missions
[NASA-TM-102917] N90-21779

Draft environmental impact statement for the Galileo Mission (Tier 2)
[NASA-TM-102926] N90-22148

Final Environmental Impact Statement for the Ulysses Mission (Tier 2)
[NASA-TM-101104] N90-22162

General purpose heat source radioisotope thermoelectric generator program. Book 1: Accident analysis
[REPT-90SDS4202-BK-1] N90-22379

General purpose heat source radioisotope thermoelectric generator. Book 2: Accident analysis, appendices
[REPT-90SDS4202-BK-2] N90-22380

UNDERWATER ACOUSTICS

Generalized Herglotz functions and inverse scattering problem in a finite depth ocean
[PB90-150996] N90-22197

UNIFORM FLOW

Laser Doppler anemometry measurements of a confined turbulent water jet with a uniform background flow N90-21971

UNITED KINGDOM

Frontal structure in a mesoscale model N90-22187

UNITED STATES

Opportunities for US-USSR cooperation in the investigation of Arctic stratospheric ozone N90-22154

UNIVERSE

Big-bang nucleosynthesis revisited
[NASA-CR-186256] N90-22426

Extraterrestrial life in the universe
[NASA-TM-102363] N90-22464

The mass of the Coma cluster N90-22496

Multipole moments in general relativity and dynamical perturbations of black-hole magnetospheres N90-22509

UNIX (OPERATING SYSTEM)

Graphics mini manual
[NASA-TM-87622-REV] N90-22247

UNSTEADY AERODYNAMICS

Development and application of a generalized dynamic wake theory for lifting rotors N90-21731

Control of flow separation and mixing by aerodynamic excitation
[NASA-TM-103131] N90-21733

Airloads, wakes, and aeroelasticity
[NASA-CR-177551] N90-21738

Aeroelastic simulation of higher harmonic control N90-21768

UNSTEADY FLOW

Extension of a streamwise upwind algorithm to a moving grid system
[NASA-TM-102800] N90-21739

Topics in vortex methods for the computation of three- and two-dimensional incompressible unsteady flows N90-21967

An unsteady time asymptotic flow in the square driven cavity
[NASA-TM-103141] N90-22016

Unsteady separated flows produced by complex harmonic motions: Investigation of wing-flow interactions elicited by a mechanical model simulating dragonfly wing kinematics N90-22018

Analysis of gamma squared Velorum photometry from the South Pole N90-22472

UPSTREAM

Studies on reactive flows N90-21831

URANIUM

Correlated electron processes in ion-atom collisions
[DE90-009477] N90-22370

URANUS (PLANET)
Auroral ultraviolet darkening on the outer planets N90-22518

USER MANUALS (COMPUTER PROGRAMS)
Enhanced Low Level Wind Shear (LLWAS) 6-sensor improvement user's manual for data processing of field data [DOT/FAA/CT-TN90/8] N90-21759
Reliability importance measures and their calculation [DE90-620391] N90-22057

USER REQUIREMENTS
A study of mental models through communication between users and advisors solving software manipulation problems N90-22434
Desk top publishing: What you need to know N90-22449

UTAH
An anomalous wind between valleys: Its characteristics and a proposed explanation [DE90-008965] N90-22189

V

V/STOL AIRCRAFT
The insertion of human dynamics models in the flight control loops of V/STOL research aircraft. Appendix 2: The optimal control model of a pilot in V/STOL aircraft control loops [NASA-CR-186598] N90-21776
An adaptive human response mechanism controlling the V/STOL aircraft. Appendix 3: The adaptive control model of a pilot in V/STOL aircraft control loops [NASA-CR-186599] N90-21777

VACUUM
Numerical investigations of nonlinear behavior in the Einstein equations N90-22427
Stability of compactification during inflation [NASA-CR-186597] N90-22502

VACUUM TUBES
An assessment of the hardness of miniature vacuum tubes to high-voltage transients [DE90-009541] N90-21956

VALLEYS
An anomalous wind between valleys: Its characteristics and a proposed explanation [DE90-008965] N90-22189
Daytime wind valleys adjacent to the Great Salt Lake [DE90-008991] N90-22190
The ASCOT 1988 valley/tributary interaction study [DE90-009043] N90-22191

VAPOR PHASES
Determination of rates of reaction in the gas-phase in the troposphere: Theory and practice. 2: Rate of direct photoreaction: Screening-level test guideline-spectroscopic determination of the cross section and the maximum rate of direct photoreaction in sunlight [PB90-146291] N90-22156

VARIABLE PITCH PROPELLERS
A computer program for the prediction of nozzle-propeller performance [LR-578] N90-21740

VARIATIONAL PRINCIPLES
Towards a unified analysis methodology for composite rotor blades N90-21730
Finite element analysis of elastic contact problems with friction N90-22040
Self-calibration of robot-sensor system N90-22246

VECTOR QUANTIZATION
An adaptive vector quantization scheme N90-21898

VELOCITY DISTRIBUTION
Theoretical and experimental study of flow-control devices for inlets of indraft wind tunnels [NASA-TM-100050] N90-21778
A dual potential formulation of the Navier-Stokes equations N90-21972

VELOCITY MEASUREMENT
Laser Doppler anemometry measurements of a confined turbulent water jet with a uniform background flow N90-21971

VENUS (PLANET)
Using connected-element interferometer phase-delay data for Magellan navigation in Venus orbit N90-21885

VENUS SURFACE
Geology of coronae and domal structures on Venus and models of their origin N90-22513

VERTICAL LANDING
Performance characteristics of a one-third-scale, vectorable ventral nozzle for SSTOVL aircraft [NASA-TM-103120] N90-21725

VERTICAL MOTION
Tropopause undulations and the development of extratropical cyclones N90-22186

VERY LARGE ARRAY (VLA)
Validity of the two-level model for Viterbi decoder gap-cycle performance N90-21896
Herbig-Haro objects and stellar jets N90-22487

VERY LARGE SCALE INTEGRATION
A VLSI decomposition of the deBruijn graph N90-21895
A VLSI design for a systolic Viterbi decoder N90-21899
Principles of Very Large Scale Integrated (VLSI) system planning N90-21950
The WAVE model for advanced knowledge processing [OUEL-1803/89] N90-22291

VERY LONG BASE INTERFEROMETRY
The determination of maximum deep space station slew rates for a high Earth orbiter N90-21882
Using connected-element interferometer phase-delay data for Magellan navigation in Venus orbit N90-21885
A higher density VLBI catalog for navigating Magellan and Galileo N90-21904
Diffraction-limited imaging on the 200-inch telescope N90-22475

VESTIBULAR NYSTAGMUS
The effects of linear acceleration on perception and nystagmus N90-22209

VIBRATION
Aeroelastic simulation of higher harmonic control N90-21768
The Shock and Vibration Digest, volume 21, no. 3 N90-22064
Nonlinearity parameters of polymers N90-22369
Low temperature properties of amorphous solids N90-22405
Experiments with a laser interferometric gravitational wave antenna N90-22476

VIBRATION DAMPING
The vibro-acoustic mapping of low gravity trajectories on a Learjet aircraft [NASA-TM-103103] N90-21723
Development and application of a generalized dynamic wake theory for lifting rotors N90-21731
Identification of XV-15 aeroelastic modes using frequency-domain methods [NASA-TM-101021] N90-21756
Recent advances in structural control N90-22062
Optimum design of structures under shock and vibration environment N90-22067
The Shock and Vibration Digest, volume 22, no. 1 N90-22073
Stable response of damped mechanical systems, 4 N90-22074

VIBRATION EFFECTS
The Shock and Vibration Digest, volume 21, no. 3 N90-22064

VIBRATION MEASUREMENT
Calculating the time domain average of gear vibration data sampled at less than the Nyquist frequency [OUEL-1768/89] N90-22052
The Shock and Vibration Digest, volume 21, no. 1 N90-22061
The Shock and Vibration Digest, volume 21, no. 8 N90-22068

VIBRATION MODE
Instabilities and subharmonic resonances of subsonic heated round jets, volume 2 [NASA-CR-186058] N90-22017
A review of approximate methods for determining the vibrational modes of membranes N90-22063
Natural modes of cracked beams and identification of cracks N90-22075
The observed properties of the intermediate-degree gravity modes and their relevance to the solar neutrino paradox N90-22519

VISCOELASTIC CYLINDERS
Elastic and viscoelastic analysis of two multiply layered cylinders rolling over each other with Coulomb friction [REPT-89-50] N90-22051

VISCOELASTICITY
Computational methods and plasticity [LR-583] N90-22120
The analysis of stress relaxation on indentation of a rigid punch into a viscoelastic sheet of finite thickness [NPL-DMA(A)-193] N90-22357

VISCOPLASTICITY
Computational methods and plasticity [LR-583] N90-22120
The mechanics of shear band formation in thermal viscoplastic materials at high rates of loading N90-22128

VISCOUS FLOW
Plane Stokes flow driven by capillarity on a free surface: Overview and status [DE90-009186] N90-22008
Bifurcations in viscous flow fields. On the genesis and development of topologically complicated separated flow structures [PB90-167156] N90-22012
European research on viscous flow (EuroVisc) [NLR-TP-89077-U] N90-22014

VISIBILITY
A3I visibility modeling project N90-22230

VISION
Sampling and noise in vision networks N90-22217
Networks for image acquisition, processing and display N90-22218
Visions of visualization aids: Design philosophy and experimental results N90-22220
Human motion perception: Higher-order organization N90-22226
Filling in the retinal image N90-22229
Instrumentation and robotic image processing using top-down model control N90-22239
Pyramid image codes N90-22243

VISUAL DISCRIMINATION
Networks for image acquisition, processing and display N90-22218
Two-dimensional shape recognition using sparse distributed memory N90-22227
Stanford/NASA-Ames Center of Excellence in model-based human performance N90-22241

VISUAL FIELDS
Filling in the retinal image N90-22229

VISUAL OBSERVATION
A high galactic latitude survey of far ultraviolet excess objects N90-22473

VISUAL PERCEPTION
Filling in the retinal image N90-22229

VITERBI DECODERS
On decoding of multi-level MPSK modulation codes [NASA-CR-186601] N90-22261

VOLCANOES
Sulphur silicate interactions on the Jovian satellite Io N90-22515

VORTEX ALLEVIATION
Effective methods of controlling a junction vortex system in an incompressible, three-dimensional, turbulent flow N90-21732

VORTEX BREAKDOWN
Three-dimensional simulation of vortex breakdown [NASA-TM-102664] N90-21744
Modern developments in shear flow control with swirl [NASA-CR-186586] N90-22000

VORTEX FILAMENTS
Topics in vortex methods for the computation of three- and two-dimensional incompressible unsteady flows N90-21967

VORTEX RINGS
Topics in vortex methods for the computation of three- and two-dimensional incompressible unsteady flows N90-21967

VORTEX SHEDDING
On the direct simulation of vortex shedding [LR-513] N90-21743

VORTICES
Effective methods of controlling a junction vortex system in an incompressible, three-dimensional, turbulent flow N90-21732
Modeling of vortex-induced oscillations based on indicial response approach [NASA-CR-186560] N90-21736
On the direct simulation of vortex shedding [LR-513] N90-21743
Analytical study of the origin and behavior of asymmetric vortices [NASA-TM-102796] N90-21746
Topics in vortex methods for the computation of three- and two-dimensional incompressible unsteady flows N90-21967
Instabilities and subharmonic resonances of subsonic heated round jets, volume 2 [NASA-CR-186058] N90-22017
Semigeostrophic flow over orography in a stratified rotating atmosphere N90-22163
A new stability criterion in the shallow-water system for two-dimensional coherent eddies in the atmosphere and oceans N90-22176
Effect of a crystal-melt interface on Taylor-vortex flow [NASA-CR-186512] N90-22408

VORTICITY
An experimental investigation of mixing in buoyant flows N90-21963
Unsteady separated flows produced by complex harmonic motions: Investigation of wing-flow interactions elicited by a mechanical model simulating dragonfly wing kinematics N90-22018
Semigeostrophic flow over orography in a stratified rotating atmosphere N90-22163
A theoretical investigation of gravity-wave-generated stress and vorticity in the planetary boundary layer N90-22512

VOYAGER 1 SPACECRAFT
Waves in Saturn's rings probed by radio occultation N90-22511

VOYAGER 2 SPACECRAFT
Digital Doppler extraction demonstration with the advanced receiver N90-21893

W

WAFERS
Optical shutter switching matrix [NASA-CASE-KSC-11392-1] N90-22383
WAKES
Development and application of a generalized dynamic wake theory for lifting rotors N90-21731
Effective methods of controlling a junction vortex system in an incompressible, three-dimensional, turbulent flow N90-21732
Airloads, wakes, and aeroelasticity [NASA-CR-177551] N90-21738
WALKING
The predictability and efficiency of human walking: Metabolic, mechanical, and biophysical considerations N90-22211
WALL FLOW
Development of a defect stream function, law of the wall/wake method for compressible turbulent boundary layers N90-22019
WASTE DISPOSAL
In-situ fracture stiffness determination [DE90-009202] N90-22173
WASTE WATER
Utilization of water hyacinths to upgrade heavily loaded wastewater treatment plant effluents N90-21873
WATER
WINCOF-I code for prediction of fan compressor unit with water ingestion [NASA-CR-185157] N90-21724
Radiometric tests on wet and dry antenna reflector surface panels N90-21890
Experimental observations on transition to turbulence in confined coaxial jets and other boundary layer flows [DE90-008939] N90-22005
Inventory of program packages related to the project SIMONA [ETN-90-96397] N90-22270
WATER FLOW
Homogeneous dilute turbulent particle-laden water flows N90-21965
WATER SPLITTING
Photosynthetic water splitting, phase 2 [PB90-132671] N90-21833
Impact of low gravity on water electrolysis operation [NASA-CR-185521] N90-21870
WATER TREATMENT
Utilization of water hyacinths to upgrade heavily loaded wastewater treatment plant effluents N90-21873
WATER TUNNEL TESTS
A video-based experimental investigation of wing rock N90-21771
WATER VAPOR
The production and spatial distribution of neutral and ionized water vapor in Comet P/Halley N90-22484
WATERWAYS
Inventory of program packages related to the project SIMONA [ETN-90-96397] N90-22270
WAVE DIFFRACTION
Diffraction of light by ultrasonic pulses N90-22366
Extended optical emission in 3CR radio galaxies N90-22523
WAVE DISPERSION
Topics in vortex methods for the computation of three- and two-dimensional incompressible unsteady flows N90-21967
WAVE EQUATIONS
Propagation of transient acoustic waves in porous media [ETN-90-96401] N90-22015
WAVE EXCITATION
Modern developments in shear flow control with swirl [NASA-CR-186586] N90-22000
WAVE INTERACTION
The interaction between a plane shock wave and a cylindrical afterbody N90-21728
WAVE PROPAGATION
Precise estimation of tropospheric path delays with GPS techniques N90-21881
Atmospheric Propagation in the UV, Visible, IR, and mm-Wave Region and Related Systems Aspects [AGARD-CP-454] N90-21907
The mm-wave region propagation experiments by satellite N90-21916
LOWTRAN 7: Status, review, and impact for short-to-long-wavelength infrared applications N90-21917
Models of aerosols, clouds, and precipitation for atmospheric propagation studies N90-21919
Modeling millimeter-wave propagation effects in the atmosphere N90-21922
Atmospheric modelling studies: A modelling comparison between IR and millimetric atmospheric propagation N90-21941
Theory of a periodic cylindrical waveguide with a nonuniform metal-dielectric filling [DE90-620099] N90-21945
Partial acoustic filtering applied to the equations of compressible flow [DE90-000673] N90-22001
Beam propagation in direct nuclear pumped laser amplifiers [DE90-009613] N90-22035
Free wave propagation in orthogonally stiffened cylinders N90-22124
A spectral analysis approach to wave propagation in layered solids N90-22131
Effects of single fractures on seismic wave propagation [DE90-009191] N90-22171
WAVE REFLECTION
The classification of defects from ultrasonic measurements [AERE-R-13306] N90-22056
WAVE SCATTERING
Scattering of waves by inclusions in a nonhomogeneous elastic half space solved by boundary element methods [PB90-145699] N90-22107
WAVEGUIDES
An 8.4-GHz dual-maser front-end system for Parkes reimplementation N90-21905
Theory of a periodic cylindrical waveguide with a nonuniform metal-dielectric filling [DE90-620099] N90-21945
WAVELENGTHS
Survey of instrumental methods for the determination of the high frequency wave spectrum [IOS-267] N90-22200
WEAPON SYSTEMS
The Weapons Laboratory technical library: Automating with STILAS N90-22447
WEAR
Self-lubricating polymer composites and polymer transfer film lubrication for space applications [NASA-TM-102492] N90-21862
SPOT 4 space magnetic recorder mechanisms N90-22082
Positive lubrication system N90-22097
WEATHER
Minimizing the effects of the atmosphere in the observation of ultraviolet radiation N90-21911
Scintillation of millimeter-wave intensity and phase caused by turbulence and precipitation N90-21912
Propagation environments, effects, and decision aids N90-21918
Modelling of optically and IR effective atmospheric turbulence N90-21923
Calculation of IR propagation statistics in the eastern Atlantic for surveillance system performance assessment N90-21938
JARE data reports, no. 140 (meteorology 21): Meteorological data at Asuka Camp, Antarctica in 1987 [ISSN-0075-3343] N90-22188
An anomalous wind between valleys: Its characteristics and a proposed explanation [DE90-008965] N90-22189
WEATHER FORECASTING
Second National Winter Weather Workshop Conducted by the National Weather Service [PB90-147414] N90-22183
WEATHERING
Quantitative studies of the Martian south polar region using spacecraft images N90-22514
WEAVING
Failure analysis of woven hybrid composite using a finite element method [OUEL-1791/89] N90-21828
WEDGE FLOW
Graphs of the state of stress at rounded corners [MEMT-1] N90-22122
WEDGES
Prediction of length scales in a Mach reflection flowfield N90-21959
WEIGHTING FUNCTIONS
High order P-G finite elements for convection-dominated problems [DE90-614743] N90-21998
Fatigue crack growth in unidirectional metal matrix composite [NASA-TM-103102] N90-22117
WEIGHTLESSNESS
Zero-G phase detector and separator [NASA-CASE-LEW-14844-1] N90-22024
WEIGHTLESSNESS SIMULATION
The vibro-acoustic mapping of low gravity trajectories on a Learjet aircraft [NASA-TM-103103] N90-21723
WELD STRENGTH
VAMAS project on variable weld penetration: Surface tension of the steels [NPL-DMA(A)-188] N90-21856
WELDABILITY
Welding behavior and welding metallurgy of ductile intermetallic alloys [DE90-008908] N90-21852
WELDED JOINTS
The effect of aging at 343 C on type 308 stainless steel weldments [DE90-009232] N90-21853
WELDING
Welding behavior and welding metallurgy of ductile intermetallic alloys [DE90-008908] N90-21852
Institute for Materials Science and Engineering, Fracture and Deformation Division: Technical activities, 1989 [PB90-155359] N90-22106
WHEAT
Spectral response of wheat and its relationship with agronomic variables in the tropical region [INPE-5018-RPE/612] N90-22138
WHITE NOISE
Adaptive frequency estimation by MUSIC (Multiple Signal Classification) method [PB90-166794] N90-21943
Sampling and noise in vision networks N90-22217
WIND (METEOROLOGY)
Regional wind energy assessment [DE90-009439] N90-22143
An anomalous wind between valleys: Its characteristics and a proposed explanation [DE90-008965] N90-22189
Daytime wind valleys adjacent to the Great Salt Lake [DE90-008991] N90-22190
The ASCOT 1988 valley/tributary interaction study [DE90-009043] N90-22191
Wind forecasting for utility operations [DE90-009466] N90-22193
WIND DIRECTION
Aerodynamics of a full-scale, non rotating wind turbine blade under natural wind conditions [RISOE-M-2768] N90-22144
JARE data reports, no. 140 (meteorology 21): Meteorological data at Asuka Camp, Antarctica in 1987 [ISSN-0075-3343] N90-22188
WIND EFFECTS
Lagrangian model simulation of the turbulent transport of evaporating jet droplets N90-22166
WIND PROFILES
A linear analysis of monsoon base states associated with banded convection N90-22179
The emission lines in the ultra-violet spectrum of Beta Lyrae N90-22474
WIND SHEAR
Optimization and guidance of flight trajectories in the presence of windshear [NASA-CR-186163] N90-21747
Enhanced Low Level Wind Shear (LLWAS) 6-sensor improvement user's manual for data processing of field data [DOT/FAA/CT-TN90/8] N90-21759
WIND TUNNEL MODELS
Slotted-wall research with disk and parachute models in a low-speed wind tunnel [DE90-002989] N90-21737
WIND TUNNEL TESTS
Numerical simulation of hypersonic flow around a space plane. Part 2: Application to high angles of attack flow [NAL-TR-1011T] N90-21726
Wind tunnel investigation of three sonic anemometers [PB90-149808] N90-21729
Slotted-wall research with disk and parachute models in a low-speed wind tunnel [DE90-002989] N90-21737
A video-based experimental investigation of wing rock N90-21771
Analysis of a six-component, flow-through, strain-gage, force balance used for hypersonic wind tunnel models with scramjet exhaust flow simulation [NASA-CR-186585] N90-21775
Aerodynamics of a full-scale, non rotating wind turbine blade under natural wind conditions [RISOE-M-2768] N90-22144
WIND TUNNEL WALLS
Slotted-wall research with disk and parachute models in a low-speed wind tunnel [DE90-002989] N90-21737

WIND TUNNELS
Theoretical and experimental study of flow-control devices for inlets of indraft wind tunnels
[NASA-TM-100050] N90-21778
An investigation of turbulence structure in a low Reynolds number incompressible turbulent boundary layer
N90-21966

WIND TURBINES
Regional wind energy assessment
[DE90-009439] N90-22143
Aerodynamics of a full-scale, non rotating wind turbine blade under natural wind conditions
[RISOE-M-2768] N90-22144
Rotor loading on a three-bladed wind turbine
N90-22145
Optimization of power output from wind turbines
N90-22146

WIND VANES
JARE data reports, no. 140 (meteorology 21): Meteorological data at Asuka Camp, Antarctica in 1987
[ISSN-0075-3343] N90-22188

WIND VARIATIONS
Regional wind energy assessment
[DE90-009380] N90-22192
Wind forecasting for utility operations
[DE90-009466] N90-22193

WIND VELOCITY
A survey of the maritime-aerosol data collected at South Uist and the implications for the LOWTRAN maritime aerosol model N90-21908
Aerodynamics of a full-scale, non rotating wind turbine blade under natural wind conditions
[RISOE-M-2768] N90-22144
Lagrangian model simulation of the turbulent transport of evaporating jet droplets N90-22168
Wind forecasting for utility operations
[DE90-009466] N90-22193

WIND VELOCITY MEASUREMENT
Regional wind energy assessment
[DE90-009380] N90-22192

WINDMILLS (WINDPOWERED MACHINES)
Rotor loading on a three-bladed wind turbine
N90-22145

WINDPOWER UTILIZATION
Regional wind energy assessment
[DE90-009439] N90-22143
Optimization of power output from wind turbines
N90-22146
Regional wind energy assessment
[DE90-009380] N90-22192

WING OSCILLATIONS
A video-based experimental investigation of wing rock
N90-21771

WINGS
Extension of a streamwise upwind algorithm to a moving grid system
[NASA-TM-102800] N90-21739
Conceptual design optimization study
[NASA-CR-4298] N90-21755
Unsteady separated flows produced by complex harmonic motions: Investigation of wing-flow interactions elicited by a mechanical model simulating dragonfly wing kinematics N90-22018

WINTER
The sources and chemistry of late winter Arctic tropospheric aerosols
[PB90-131988] N90-22158
The observed three-dimensional structure of baroclinic waves in the Northern Hemisphere winter as revealed in a linear regression analysis N90-22167

WIRE
Development of shape memory metal as the actuator of a fail safe mechanism N90-22081

WOLF-RAYET STARS
Analysis of gamma squared Velorum photometry from the South Pole N90-22472

WORDS (LANGUAGE)
Some remarks on treatment of be in Montague's PTQ — Proper Treatment of Quantification (PTQ)
[REPT-89-40] N90-22267

WORK
The predictability and efficiency of human walking: Metabolic, mechanical, and biophysical considerations
N90-22211

WORKSTATIONS
Intensity dependent spread processor and workstation
N90-22244

X

X RAY IMAGERY
A study of creep damage using microradiography and continuum damage mechanics N90-22109

X RAY SOURCES
Report on the fifth workshop on synchrotron x ray lithography
[DE90-007903] N90-22411

X RAY SPECTROSCOPY
Improved crystal bending techniques applied to the LLNL dual-arm Johann mounting x ray spectrometer
[DE90-009528] N90-22415

X RAYS
Non-random uncertainties in the calibration of protection-level secondary standards
[NPL-RS(EXT)-110] N90-22378
Derivation of radiation beam non-uniformity corrections for the calibration of large volume ionisation chambers
[NPL-RSA(EXT)-11] N90-22382
Producing dense plasmas with x rays
[DE90-009539] N90-22393
An astrophysics data program investigation of cluster evolution
[NASA-CR-181296] N90-22510

X-15 AIRCRAFT
Prediction of forces and moments for flight vehicle control effectors. Part 1: Validation of methods for predicting hypersonic vehicle controls forces and moments
[NASA-CR-186571] N90-21734

XV-15 AIRCRAFT
Identification of XV-15 aeroelastic modes using frequency-domain methods
[NASA-TM-101021] N90-21756

Y

YAG LASERS
Injection-seeded Nd:YAG laser linewidth measurement using saturation spectroscopy in iodine
[DE90-009537] N90-22034

YTTRIUM OXIDES
Superconducting and semiconducting thin films of La(sub 123) and Y(sub 123) and their superlattices
[DE90-009565] N90-22416
Growth and patterning of laser ablated superconducting YBa2Cu3O7 films on LaAlO3 substrates
[NASA-TM-102436] N90-22421

Z

ZEEMAN EFFECT
Modeling millimeter-wave propagation effects in the atmosphere N90-21922

ZETA PINCH
Gas-puff z-pinch experiment
[IPPCZ-286] N90-22385

ZINC SELENIDES
Preparation and characterization of Cu2ZnGeS(4-y)Se(y)
[AD-A217469] N90-22407
Optical properties of zinc selenide grown using molecular beam deposition techniques
[RSRE-MEMO-4269] N90-22423

PERSONAL AUTHOR INDEX

SCIENTIFIC AND TECHNICAL AEROSPACE REPORTS VOLUME 28 NUMBER 15

Typical Personal Author Index Listing

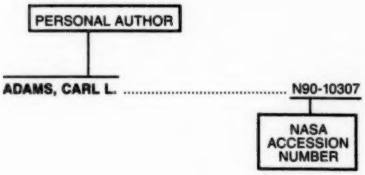

Listings in this index are arranged alphabetically by personal author. The NASA accession number denotes the number by which the citation is identified.

A

AARTS, J. M. N90-22346
ABBOTT, JOHN M. N90-21733
ABDOL-HAMID, KHALED S. N90-21745
ABDOU, M. A. N90-22392
ABRAHAMS, ANDREW M. N90-22425
ABREU, L. W. N90-21917
N90-21928
ACERBI, RICARDO N90-22332
ACREE, CECIL W., JR. N90-21756
ADDAGARLA, S. N90-21838
ADEFF, SERGIO E. N90-21970
ADLER, DAVID SCOTT N90-22489
AFTAB, SYED N90-22248
AGMA, MULJADJI N90-21835
AGRONIN, MICHAEL L. N90-22084
AHN, HOJIN N90-21968
AHUMADA, ALBERT J., JR. N90-22217
N90-22218
AIHARA, H. N90-22376
ALBONE, C. M. N90-21988
ALCOCK, G. A. N90-22196
ALEXANDER, D. J. N90-21853
ALEXANDER, K. B. N90-21853
ALEXIADES, VASILIOS N90-22361
ALKEMADE, J. A. H. N90-21946
ALLEN, J. E. N90-22400
N90-22401
ALLRED, JOHN C. N90-22152
ALLWRIGHT, STEVE N90-21986
ALNAES, KNUT N90-22277
ALSTON-GARNJOST, M. N90-22376
AMBROSEK, RICHARD G. N90-22010
AMENDOLA, A. N90-21984
AMENDOLA, LUCA N90-22502
ANDERSON, D. E., JR. N90-21937
ANDERSON, G. P. N90-21917
N90-21928
ANDERSON, K. D. N90-21914
ANDERSON, T. M. N90-21785
ANDSTEN, RISTO N90-22057
ANGEL, S. MICHAEL N90-21867
ANNINOS, PETER N90-22427
ANSARI, A. A. N90-21863
ANTHONY, HELEN M. N90-22355
ARABSHAHI, ABDOLLAH N90-21982
ARBOCZ, J. N90-22119
ARBOUZ, NASSIM MOHAMMED N90-21784
ARDITI, ARIES N90-22230
ARFI, BADREDINE N90-22404
ARINA, RENZO N90-21987
ARNOLD, S. N90-21896
ASAKURA, MAKOTO N90-22087
ASH, ROBERT L. N90-22215
ASKAR, A. N90-22107
ASSAD, EDUARDO DELGADO N90-22139
ASVELD, PETER R. J. N90-22269
ATILGAN, ALI RANA N90-21730
AUER, W. N90-22099
AVERY, R. E. N90-22376
AVINA, RAYMOND R. N90-22093
AZEVEDO, DAVID JASON N90-21959

B

BACH, RALPH N90-21773
BADILLA, G. N90-21885
BADLER, NORMAN N90-22230
BAHLOULI, HOCINE N90-22403
BAILEY, R. T. N90-22262
BAISLEY, V. C. N90-21911
BAKER, C. BRUCE N90-21729
BAKER, ROBERT W. N90-22143
N90-22193
BAKER, TIMOTHY J. N90-21995
BAKHASHWAIN, JAMIL MOSALLAM N90-22037
BAKKER, PIETER GERRIT N90-22012
BALDWIN, ARLEN R. N90-21955
BANNINK, W. J. N90-22013
BAO, HAN P. N90-22255
BARAONA, COSMO R. N90-21812
BARBARO-GALTIERI, A. N90-22376
BARBER, D. G. N90-22250
BARE, ROBERT N90-22448
BARKER, A. R. N90-22376
BARNARD, WILLIAM F. N90-22157
BARNES, WAYNE L. N90-22094
BARNETT, B. A. N90-22376
BARRY, MATTHEW R. N90-22301
N90-22308
BASHAM, KIM D. N90-22108
BASS, G. A. N90-22382
BASTO, JOSE EDSON N90-21788
BATISTA, GETULIO TEIXEIRA N90-22138
N90-22139
BAUER, B. S. N90-21944
BAUER, D. A. N90-22376
BAY, A. N90-22376
BEAULIEU, A. J. N90-21920
BEAVEN, HERBERT R., JR. N90-22093
BEEMAN, E. R., II N90-21755
BEJAN, ADRIAN N90-22005
BELMANS, PHILIPPE N90-22045
BENCI, JOHN EDWARD N90-22109
BENNETT, M. J. N90-21863
BENNETT, MARK SPENCER N90-22124
BENO, JOSEPH HENRY, JR. N90-21781
BENTHEM, J. P. N90-22122
BERGEN, JAMES N90-22230
BERKIN, ANDREW L. N90-22506
BERRY, L. A. N90-22392
BERTACHINIDEALMEIDAPRADO, ANTONIO FERNANDO N90-21786
BESHEARS, D. L. N90-22044
BESTERFIELD, GLEN HOWARD N90-22134
BEVAN, R. N90-21893
BHASIN, K. B. N90-22421
BHATT, RAMAKRISHNA T. N90-21826
BHATTACHARJEE, PIJUSHPANI N90-22525
BIDWELL, COLIN S. N90-21727
BIETERMAN, MICHAEL B. N90-21996
BILBY, CURT R. N90-21806
N90-21807
BISCHEL, WILLIAM K. N90-21839
N90-21840
BITTKER, DAVID A. N90-21842
BIXLER, JAY VIRGIL N90-22473
BLACK, JOHN B. N90-22452
BLACKER, TED D. N90-22260
BLACKMAN, D. L. N90-22195
BLACKMAN, HAROLD S. N90-22214
BLATHERWICK, R. D. N90-21910
BOATMAN, JOE F. N90-22155
BOBBINK, G. J. N90-22376
BOEHM, FRANZ N90-21859
BOEHM, MARGI N90-22182
BOERSTOEL, J. W. N90-21984
BOGGS, PAUL T. N90-22253
N90-22336
BOHMAN, D. Y. N90-22421
BOHNER, JOHN J. N90-22095
BON, BRUCE N90-22312
BOOTY, B. N90-22199
BORELLA, H. M. N90-22044
BORISOV, E. R. N90-22419
BORRIEN, A. N90-22082
BOUCHARD, DARRYL A. N90-21954
BOUCHARDY, A. M. N90-21942
BOWEN, JOHN T. N90-22247
BOYD, RONALD D., SR. N90-21961
BRADY, RICHARD L. N90-21814
BRANOVICH, LOUIS E. N90-21850
BRASE, L. O. N90-21760
BRAUN, W. CHARLES N90-21930
BRINKER, C. J. N90-21865
BRITT, DANIEL L. N90-22297
N90-22304
BRITTON, DORIS L. N90-21844
BROGDON, JOHN N90-22312
BRONDINO, G. N90-22085
BROOKS, R. F. N90-21856
BROTEN, THOMAS A. N90-22314
BROW, R. K. N90-21865
BROWN, DAVID A. N90-22314
BROWN, DONALD W. N90-22170
BROWN, G. S. N90-22411
BROWN, STEPHEN R. N90-22169
BROWN, WILLIAM C. N90-21796
BROWNE, JAMES C. N90-22318
BRUNZIE, T. J. N90-21905
BUCHANAN, C. D. N90-22376
BUCHELE, DONALD R. N90-22021
BUFFINGTON, R. J. N90-21737
BURCHETT, STEVEN N. N90-22114
BURKE, M. G. N90-22417
BURTIS, CARL A. N90-22516
BUSBY, HENRY R. N90-22338
BUSHNELL, G. S. N90-21785
BUSHONG, WILTON E. N90-22023
BUSSOLETTI, JOHN E. N90-21996
BUTKA, BRIAN KEITH N90-22406
BUTLER, D. N90-21790
BUTLER, RICKY W. N90-22292

C

CAKMAK, A. S. N90-22107
CALISE, ANTHONY J. N90-21753
CAMERON, A. COLLIER N90-22479
CAMPBELL, THOMAS G. N90-21798
CAMPBELL, WILLIAM J. N90-22315
CANAVAN, GREGORY H. N90-21791
CANN, DAVID N90-22257
CANN, M. W. P. N90-21925
CAPPS, G. J. N90-22044
CARDOSO, ELERI N90-22332
CARIM, A. N90-22413
CARNAHAN, RICHARD S., JR. N90-22316
CARNUTH, WALTER N90-21933
CARTER, CAMPBELL D. N90-22022
CARUSO, J. J. N90-21824
CATES, M. R. N90-22044
CAWLFIELD, J. L. N90-22046
CELIK, ISMAIL N90-22002
CERNANSKY, N. P. N90-21838
CHAMBAUD, S. N90-22445
CHAMBERLAIN, NEIL FREDERICK N90-21879
CHAMIS, CHRISTOS C. N90-21821
N90-21824
N90-21825
N90-21871
CHANG, RICHARD K. N90-21924
CHANTLER, C. T. N90-22415
CHASMAN, DANIEL N90-22018
CHAWNER, J. R. N90-21983
CHEN, E. P. N90-22112
CHEN, K. N90-22468
CHETWYND, J. H., JR. N90-21917
N90-21928
CHEUNG, K.-M. N90-21898
CHEVERTON, R. D. N90-22116
CHOI, SEOK KI N90-22020
CHONG, D. N90-21893
CHOREY, C. M. N90-22421
CHU, DING-CHONG ALLEN N90-22149

CLARKE, D. W. N90-22330
CLAYSON, C. H. N90-22200
CLEMENTS, WILLIAM E. N90-22191
CLIFFORD, S. F. N90-21912
CLINTON, R. N90-21818
CLOSE, R. A. N90-21944
CLOUGH, S. A. N90-21917
COFFEY, HELEN E. N90-22520
N90-22521
COHEN, HARVEY D. N90-22210
COLEMAN, NEIL L. N90-21970
COLLINS, CAROL N90-22312
COLLINS, O. N90-21895
COLOZZA, ANTHONY J. N90-21763
CONKLIN, PAUL S. N90-21729
CONLEY, PETER L. N90-22095
CONSTERDINE, I. E. N90-21908
COOK, A. M. N90-22172
COOK, D. M. N90-22258
COOK, M. N90-21813
COOK, H. G. W. N90-22171
N90-22172
COOKE, ROGER N90-22160
COON, DARRYL D. N90-22219
COPELAND, EDMUND J. N90-22505
CORBEL, C. N90-22410
COREY, STEPHEN N90-22316
CORIELL, S. R. N90-22408
CORMIER, R. N90-21886
CORNELL, LINDA N90-21843
COSTIN, LAURENCE S. N90-22111
COUSTEIX, J. N90-22014
COX, M. G. N90-22354
N90-22355
COY, JOHN J. N90-22054
CRAIG, K. H. N90-21929
CROSS, C. N90-22378
CROWE, CLAYTON T. N90-22005
N90-22006
CRUZ, JENNIFER W. N90-22298
CULBERTSON, PHILIP, JR. N90-22101
CULIOLI, JEAN-CHRISTOPHE N90-22045
CURL, ROBERT F. N90-21837

D

DAI, MINGJIA N90-22209
DAKA, J. S. J. N90-21906
DAKE, S. N90-22371
DANFORD, M. D. N90-21836
DANIEL, R. W. N90-22053
N90-22273
DASILVA, L. B. N90-22393
DAVID, S. A. N90-21852
DAVIDSON, KENNETH L. N90-21921
DAVIDSON, R. C. N90-22392
DAVIES, ASHLEY GERARD N90-22515
DAVIES, JOHN KEITH N90-22478
DAVIS, ROGER N90-21939
DAVIS, RORY RONALD N90-22038
DAVIS, WILLIAM T. N90-22025
DAWICKE, DAVID STANLEY N90-21857
DEGANI, DAVID N90-21746
DEHDASHTI, PARTO N90-22434
DEJONG, S. J. N90-22372
DEKKING, F. M. N90-22362
DELCASTILLO, H. N90-21893
DELEEUW, GERRIT N90-21921
DELNICK, FRANK M. N90-21955
DEMEDEIROS, JOSE SIMEAO N90-22457
DENREYER, P. C. N90-21783
DENTAMARO, A. V. N90-21911
DEPAULA, RAMON N90-22529
DERRICKSON, J. H. N90-22371
DEVLOO, PHILIPPE R. B. N90-21848
DEVRIES, F. P. P. N90-22196
DEVRIES, SYTZE MARTEN N90-22015
DEWEY, ALLEN MARK N90-21950
DEWILDE, J. P. N90-21845
N90-21846
N90-21847
DIAS, WILLIAM C. N90-22313
DIBATTISTA, JOHN N90-22529
DICKEY, DUANE P. N90-22023
DICKSON, T. L. N90-22116
DIDIER, A. N90-22082
DIET, JEAN N90-21980
DIJKSTRA, F. N90-21846
N90-21847
DINSDALE, A. T. N90-22460
DIRKS, R. W. J. N90-22198
DISANTI, MICHAEL ANTONIO N90-22484
DISBROW, JAMES D. N90-22322
DOERNBACH, JAY N90-21761
DOHRMANN, CLARK R. N90-22338
DOLCE, JAMES L. N90-22323
N90-22324
N90-22325
DOLINAR, S. N90-21894
N90-21895
N90-21896
DOLMAN, M. N90-22195
DOMICH, PAUL D. N90-22253
DONALDSON, JANET R. N90-22253
N90-22336
DONG, B. L. N90-22371
DOUMA, T. N90-22122
DOVERSPIKE, K. N90-22407
DOYLE, F. M. N90-22172
DRAKE, G. N90-21926
DRAKE, JOHN B. N90-22361
DREWS, M. J. N90-21861
DUBRODOCARMO, EDUARDO N90-21998
DUKE, EUGENE L. N90-22322
DUNCAN, D. K. N90-22479
DUNCAN, L. D. N90-21918
DUNCAN, ROBERT V. N90-22412
DUNNING, ANTHONY J. N90-22446
DURHAM, RALPH N90-22296
DWIGHT, K. N90-22407
DYE, R. C. N90-22413
DYER, MARK J. N90-21839
N90-21840
N90-22034

E

EASTMAN, RONALD GENE N90-22490
EASTMAN, S. N90-22195
EBY, P. B. N90-22371
ECKART, DONALD W. N90-21850
ECKHARDT, ROGER C. N90-22152
EDSON, JAMES BEARER N90-22168
EGGEMEYER, WILLIAM C. N90-22298
EHRENFREUND, P. N90-22479
EICHHORN, WILLIAM L. N90-22245
EISEMAN, PETER R. N90-21979
EKMANN, J. M. N90-22007
EL-ZEIN, MOHAMAD SAMIH N90-21820
ELANDS, P. J. M. N90-21846
N90-21847
ELLIS, STEPHEN R. N90-22220
ELOFSON, GREGG STEVEN N90-22435
ELORANTA, E. W. N90-21932
ELSTON, RICHARD JOSEPH N90-22465
EMERSON, ALLEN N90-22318
ENGELEN, J. J. N90-22372
ENGWERDA, JACOB C. N90-22335
ENT, ROLF N90-22377
ERICKSON, JON D. N90-22221
ERIKSSON, K. N90-22477
ERIKSSON, LARS-ERIK N90-21978
ERNEST, T. L. N90-22046
ESCALANTERAMIREZ, VLADIMIR N90-22466
ESKER, BARBARA S. N90-21725
ESKRIDGE, ROBERT E. N90-21729
ESTEFAN, J. A. N90-21882
ESTLER, R. C. N90-22413
EUBANKS, ED N90-22086
EVANS, B. T. N. N90-21931

F

FALCONE, ROGER W. N90-22393
FALES, CARL L. N90-22224
FARIS, GREGORY W. N90-21839
N90-21840
N90-21841
N90-22034
FARMER, W. MICHAEL N90-21939
FAROKHI, SAEED N90-22000
FELDMAN, A. N90-22254
FELLOWES, F. N90-21863
FEO, JOHN N90-22257
FERENDECI, ALTAN M. N90-21801
FERNANDEZ-PELLO, A. C. N90-21834
FERRIS, P. D. N90-22187
FERRISS, D. H. N90-22357
FESQ, LORRAINE M. N90-22307
FEYOCK, STEFAN N90-22309
FIKES, LOU ANN N90-21819
FINCKE, J. R. N90-22035
FINCKENOR, J. N90-22043
FLACH, GREGORY PAUL N90-21969
FLEISCHER, GERRY N90-22312
FLORIO, ANTONIO N90-21916
FOING, B. H. N90-22479
FOLTYN, S. N90-22413
FORBES, A. B. N90-22356
FORBES, JOHN C. N90-22094
FORD, V. G. N90-22081
FOSSEY, DAVID J. N90-21866
FOUDRIAT, E. C. N90-22278
N90-22279
N90-22280
N90-22282
N90-22285
N90-22288
FOUNTAIN, W. F. N90-22371
FOUTS, C. L. N90-21983
FRANCO, M. M. N90-21890
FRANDSEN, STEN N90-22146
FRANZ, RONALD JOHN N90-22039
FRASER, ANTHONY ROBIN N90-22053
FREEMAN, GERARD L. N90-21850
FRIEDLY, VERLIN JOE N90-21953
FRITZ, W. N90-21989
FUCHS, JUERGEN N90-22374
FUKI, M. N90-22371
FUSARO, ROBERT L. N90-21862

G

GAITONDE, DATTA V. N90-21764
GALEIO, AUGUSTO CESAR N90-21998
GALINAITIS, WILLIAM S. N90-21809
GALINDO-ISRAEL, V. N90-21887
GALLAGHER, JAMES N90-21797
GALLERY, W. O. N90-21917
GALLO, FRANK G. N90-22090
GALLOWAY, JAMES H. N90-22155
GAMBAUDO, JEAN-MARC N90-22289
GAME, DAVID N90-22279
N90-22283
N90-22286
N90-22287
GAMOTA, GEORGE N90-22409
GANAPATHI, L. N90-22416
GANDOLFI, ALBERTO N90-22358
GARCIA, A. R. N90-22413
GARSHNEK, VICTORIA N90-22203
GAT, URI N90-22048
GATES, RAYMOND L. N90-22247
GATHMAN, STUART G. N90-21921
GEGG, STEVEN GERARD N90-21972
GEOFFROY, AMY L. N90-22297
N90-22304
GEORGALA, J. M. N90-21991
GEORGE, T. V. N90-21805
GERASIMOVA, N. N. N90-22517
GESTRIN, S. G. N90-22507
GHOSN, LOUIS J. N90-22117
GIANNAKOPOULOS, ANTONIOS E. N90-21860
GIBB, JOHN N90-22086
GIBBINS, C. J. N90-21913
GIBSON, IVAN S. N90-21740
N90-21741
N90-21742
N90-21877
GILBERT, ROBERT P. N90-22197
GILSTRAP, LEWEY N90-22320
GLASS, G. W. N90-21889
GLASS, GRAHAM P. N90-21837
GLICKSMAN, M. E. N90-22408
GLOVER, CHARLES W. N90-22256
GODEL, J. B. N90-22411
GOHRING, JOHN R. N90-22297
N90-22304
GOLDMAN, A. N90-21910
GONSALVES, IVAN ROSARIO N90-22077
GOODRICH, JOHN W. N90-22016
GOORJIAN, PETER M. N90-21739
GORDON, KEITH M. N90-22100
GORE, ROBERT A. N90-22005
N90-22006
GORIN, BARNEY F. N90-22088
GOUDA, MOHAMED N90-22318
GOUKER, MARK N90-21797
GOUTINES, M. N90-21981
GRAESSLE, DALE EDWARD N90-22391
GRAHAM, CHARLES N90-22210
GRAHAM, ROBERT W. N90-22464
GRANAAS, MICHAEL M. N90-22213
GRAVER, WILLIAM ROBERT N90-22365
GRAY, WILLIAM M. N90-22194
GREEN, JAMES CARSWELL N90-22499
GREEN, R. M. N90-21838
GREENBAUM, E. N90-21833
GREGORY, J. C. N90-22371
GRIFFITHS, D. F. N90-22339
N90-22340
GRIMBERT, D. N90-22085
GRODSINSKY, C. M. N90-21723
GROSS, BRIAN DAVID N90-22163

GROVE, CHARLES H. N90-22383
GRUND, C. J. N90-21932
GU, D.-W. N90-22327
GUALTIERI, J. ANTHONY N90-22222
GUHATHAKURTA, PURAGRA N90-22481
GULTEPE, ISMAIL N90-22177
GUNAWARDENA, ROHITH N90-22150
GUPTA, ALOK KUMAR N90-22261
GURUSWAMY, GURU P. N90-21739
GUSTAFSSON, B. N90-22477
GUSTAVSON, DAVID B. N90-22277

H

HADLEY, P. K. N90-22107
HAEUSER, J. N90-21976
HAH, C. N90-21981
HAHN, HEIDI ANN N90-22214
HAINES, J. G. N90-22276
HAKE, KERRY A. N90-22251
HALL, K. N90-22455
HALL, L. A. N90-21928
HALL, STEPHEN W. N90-21808
HALL, WILLIAM B. N90-21817
N90-21819
HAMILTON, RUSSELL J. N90-22402
HAMILTON, T. T. N90-22468
HAMMOND, DANA P. N90-22247
HAN, KWANG S. N90-22030
HAN, TSE-YIH BERNARD N90-22436
HANDSCHUH, ROBERT F. N90-22054
HANSON, JOE N90-22089
HANSON, MARK TOD N90-22076
HANSON, ROBERT A. N90-22100
HAQ, SAJAD N90-22422
HARDIN, JASPER E. N90-21957
N90-21958
HARDING, J. N90-21827
N90-21828
HARRIS, C. S. N90-21772
HARRIS, J. N90-22103
HARRIS, J. L. N90-21737
HARRIS, P. M. N90-22354
N90-22355
HARRISON, THOMAS EDWARD N90-22482
HARTMANN, G. N90-21985
HAWMAN, MICHAEL W. N90-21809
HAWTHORNE, H. M. N90-22096
HAYASHI, T. N90-22371
HE, CHENGJIAN N90-21731
HEAPS, M. G. N90-21918
HENFLING, J. F. N90-21737
HERKENHOFF, KENNETH EDWARD N90-22514
HESLER, G. J., III N90-22173
HEYMAN, JOSEPH S. N90-21822
HICKMAN, A. PEET N90-21839
N90-21840
HILL, R. J. N90-21912
HINEDI, S. N90-21891
N90-21892
N90-21893
HIRSCHBERG, PAUL ARTHUR N90-22186
HIYAMA, R. M. N90-21755
HO, MING-TSANG N90-22215
HOANG, HAI HOC N90-22319
HOARD, D. E. N90-22189
N90-22190
HOFSTRAAT, H. N90-22198
HOL, J. M. A. M. N90-22119
HOLBEN, RICHARD N90-22223
HOLCOMB, DAVID J. N90-22111
HOLCOMB, LEE N90-22529
HOLLAND, O. W. N90-22416
N90-22418
HOLLOWELL, S. J. N90-21755
HOLMAN, RICHARD N90-22504
HOLMES, CHRIS N90-22444
HOLT, KENNETH GEORGE N90-22211
HOLZMAN, ALLEN L. N90-21793
N90-21794
HOOD, RAY N90-22529
HOOGHART, J. C. N90-22161
HOOKE, LYDIA RAZRAN N90-22203
HOOPER, FRED L. N90-22097
HOOVER, ERIC J. N90-21759
HOPPER, ROBERT W. N90-22008
N90-22009
HOROWITZ, RICHARD N90-22456
HORTON, C. W. N90-22392
HOUSTON, SUSAN H. N90-21749
HOUTMAN, E. M. N90-22013
HOWARD, S. D. N90-21901
HOWELL, HAROLD R. N90-21999
HSU, CHENG-HSING N90-21971
HUANG, CHIEN YU N90-22058
HUANG, F. H. N90-21851
HUANG, J. S. N90-21823
HUANG, JEN-KUANG N90-22215
HUBBARD, K. M. N90-22413
HUCK, FRIEDRICH O. N90-22224
HUET, F. N90-21992
HUFFMAN, R. E. N90-21926
HUFFORD, G. A. N90-21922
HUGHES, HERBERT G. N90-21934
HUMENIUK, BOB N90-22312
HUMPHREY, JOHN N90-21793
N90-21794
HUMPHREYS, D. A. N90-22014
HUNTER, PAUL N90-22529
HUTHNANCE, J. M. N90-22195
HWANG, IN HEON N90-22030
HWANG, YUH-CHIN N90-22133

I

IBRAHIM, MOUNIR B. N90-21974
IGLESIAS, C. A. N90-22480
IIKURA, SHOICHI N90-22087
IMBRIALE, W. N90-21887
INGEBO, ROBERT D. N90-22021
INTHOUT, KAREL J. N90-22349
N90-22353
ITAMAR, PLINIO N90-22139
IYONO, A. N90-22371
IZUMI, K. H. N90-21772

J

JACKSON, STEWART W. N90-22090
JACOBS, C. S. N90-21904
JACOBS, J. M. J. W. N90-21984
JACOT, A. D. N90-21785
JACQUOTTE, OLIVIER-PIERRE N90-21990
JAMES, DAVID V. N90-22277
JANDURA, LOUISE N90-22084
JANUS, J. MARK N90-21982
JARVIS, C. W. N90-21861
JARVIS, EDWARD W. N90-22100
JENKINS, JAMES N90-22529
JENSEN, DOUGLAS R. N90-21921
JENSEN, GORDON E. N90-21793
N90-21794
JENSEN, HECTOR ANTONIO N90-22125
JI, MING N90-22164
JINN, JONG-TAE N90-22040
JOHARI, HAMID N90-21963
JOHNSON, D. L. N90-21889
JOHNSON, FORRESTER T. N90-21996
JOHNSON, M. R. N90-22081
JOHNSON, MARY M. N90-22247
JOHNSON, SALLY C. N90-22292
JOHNSON, WAYNE N90-21738
JOHNSTON, MARK D. N90-22299
JONES, NORMAN N90-22069
JOURDAIN, JANET M. N90-22447
JOUTSENSALO, JYRKI N90-21943
JOYCE, GAYNOR N90-21988
JU, XIANG N90-22070
JUDAY, RICHARD D. N90-22225
JUNCHAT, A. P. N90-21942
JUSINSKI, LEONARD E. N90-21839
N90-21840

K

KACUR, JOHN E. N90-21750
KAHANER, D. N90-22254
KAISER, MARY K. N90-22226
KALE, V. N90-22282
KALKER, J. J. N90-22051
KAMENETZ, JEFFREY N90-21809
KANERVA, PENTTI N90-22227
KANTZOS, PETER N90-22117
KAR, SAJAL KUMAR N90-22175
KARADIMAS, G. N90-21981
KARHUNEN, JUHA N90-21943
KARRAY, FAKHREDDINE N90-21878
KASSIES, A. N90-21984
KATZ, ERIC S. N90-21774
KATZ, NEAL STEVEN N90-22508
KAZANSKI, V. B. N90-21945
KAZEMINEJAD, FARZAD N90-22387
KEENE, WILLIAM D. N90-22155
KEILBACH, JOSEPH N90-21793
N90-21794
KELLOGG, EDWIN M. N90-22510
KENNEDY, ROBERT S. N90-22212
KERSLAKE, THOMAS W. N90-21974
KHALIL, M. N90-22263
KHANNA, S. N90-22280
N90-22285
N90-22288
KIEFFER, JONATHAN N90-22054
KILLWORTH, P. D. N90-22201
KIM, CHANG-BAE N90-22390
KIM, S.-W. N90-21962
KING, D. T. N90-22371
KING, GALEN B. N90-22022
KING, JOSEPH H. N90-22456
KINMAN, P. N90-21893
KIRKPATRICK, R. J. N90-21865
KISER, JAMES D. N90-21826
KISHI, HIDEYA N90-22491
KLAASSEN, CHRIS A. J. N90-22348
KLINGSHIRN, EUGENE A. N90-21952
KLOMPE, A. W. H. N90-21783
KLUZNIAK, W. N90-22469
KNAUTS, H. E. N90-21957
KNEIZYS, F. X. N90-21917
N90-21928
KNIBLOE, J. R. N90-21855
KNISKERN, MARC W. N90-21775
KNOERR, KENNETH R. N90-21729
KOCAROWSKA, I. V. N90-21945
KOEKOEK, ROELOF N90-22345
KOGA, J. K. N90-21792
KOHNLE, A. N90-21923
KOLB, EDWARD W. N90-22502
N90-22504
N90-22505
KOOIJ, R. E. N90-22342
KOPP, THOMAS J. N90-22185
KORDULLA, W. N90-22014
KORSMEYER, DAVID J. N90-21807
KORTING, P. A. O. G. N90-21846
N90-21847
KOSTERS, J. J. N90-21910
KOUVARITAKIS, B. N90-22328
N90-22329
N90-22331
KOVATCH, J. J. N90-21889
KOZUB, S. S. N90-22420
KRAAIJEVANGER, J. F. B. M. N90-22352
KRAWCZONEK, WALTER M. N90-22306
KRAZINSKI, J. L. N90-22003
KREISCHER, K. E. N90-21802
N90-21803
KREJCI, A. N90-22385
KRISTIANSEN, ERNST H. N90-22277
KRLIN, L. N90-22386
KRUEGER, MANFRED N90-22450
KRUER, W. L. N90-21944
KRUPA, M. P. N90-22347
KRUPP, JOSEPH C. N90-22323
KUCUK, SENOL N90-21777
KUGA, HELIO KOITI N90-22501
KUKICH, GEORGE N90-22325
KUMAR, ASHOK N90-22416
KUMAR, RENJITH R. N90-21766
KUNTZ, K. D. N90-22479
KUNZ, G. J. N90-22198
KURRASCH, ELLIE N90-22228
KURUVILA, G. N90-21744
KWAK, DOCHAN N90-21757
KWOK, ALFRED S. N90-21924
KWOK, PING WAI N90-22527

L

LABELLE, R. N90-21893
LABLANS, W. N. N90-22161
LACEY, JAMES C., JR. N90-22205
LAMBERTS, C. W. N90-22198
LANE, NORMAN E. N90-22212
LANGDON, A. B. N90-21944
LANGFORD, W. F. N90-22347
LANGRY, KEVIN N90-21867
LARIMER, JAMES N90-22229
N90-22230
LARSEN, R. N90-21926
LARSON, D. W. N90-21875
LASSAHN, G. D. N90-22035
LATAITIS, R. J. N90-21912
LATERVEER, R. N90-22372
LAU, Y. K. H. N90-22273
LAUGHMAN, ROBERT N90-21939
LAURENDEAU, NORMAND M. N90-22022
LAVROFF, OLEG N90-22454
LEE, C. M. N90-21869
LEE, H.-J. N90-21824
LEE, JA H. N90-21804
LEE, LAURENCE G. N90-22183
LEE, M. G. N90-21870
LEE, SHENG YEN N90-21864

LEE, W. Y. N90-21780
LEICHER, S. N90-21989
LEIFER, ASA N90-22156
LEISCH, STEVEN O. N90-21793
N90-21794
LESKY, EDWARD S. N90-22023
LEVY, M. F. N90-21929
LEVY, SAMUEL C. N90-21954
LEWIS, W. N90-22044
LHERMET, J. L. N90-22082
LI, DALU N90-22309
LI, S. M. N90-22123
LI, SHAO-MENG N90-22158
LI, Y. L. N90-21827
N90-21828
LI, YI-QIANG N90-22424
LICHTEN, S. M. N90-21881
LICKFIELD, G. C. N90-21861
LIDDLE, ANDREW R. N90-22505
LIEBE, H. J. N90-21922
LIEBMANN, W. N90-22411
LIGTHART, L. P. N90-21915
LIKKEL, LAUREN JONES N90-22492
LIM, GYU HO N90-22167
LIN, C. S. N90-21792
LIN, SHU N90-22261
LIN, TUNG-CHING N90-22437
LIN, Y. C. N90-21843
LINDHOUT, J. P. F. N90-22014
LIS, DARIUSZ CEZARY N90-22493
LITTERO, MARCO N90-22502
LITTLEFIELD, ALAN C. N90-22102
LITVIN, FAYDOR L. N90-22054
LITWIN, TODD N90-22312
LIU, TA-MING N90-22071
LOEHNER, RAINALD N90-21994
LOEWENTHAL, STUART N90-22101
LOGAN, R. T., JR. N90-21883
LOOTSMA, FREERK A. N90-22290
LORDON, JEROME N90-21980
LOREMAN, J. R. N90-21905
LOWE, CARLYLE M. N90-22308
LOZIER, D. W. N90-22252
LUI, C. W. N90-21925
LUO, HAIAN N90-22126
LURIE, BORIS J. N90-21951
LUTES, G. F. N90-21883
LYON, J. F. N90-22392

M

MACDONALD, D. C. C. N90-22195
MACEDO, JAMIL N90-22139
MACHA, J. M. N90-21737
MACKENDRICK, ROBERT N90-22101
MACLOW, MORDECAI-MARK N90-22485
MADNIA, KOOROSH N90-21964
MADSEN, PETER HAUGE N90-22145
N90-22146
MADSON, MIKE D. N90-21996
MAEDA, KEI-ICHI N90-22506
MAHON, BARRY N90-22451
MALEKI, L. N90-21883
MALY, KURT J. N90-22278
N90-22279
N90-22280
N90-22281
N90-22282
N90-22283
N90-22284
N90-22285
N90-22286
N90-22287
N90-22288
MANKIN, CHARLES J. N90-22458
MANOHAR, M. N90-22231
MANOHARAN, MUTHUSWAMY GANAPATHY
N90-21829
MANOLIS, G. D. N90-22062
MANSFIELD, A. J. N90-22356
MANSFIELD, N. P. N90-21915
MANTELLI, MARCIA BARBOSA HENRIQUES
N90-21788
MARCHAL, PH. N90-22085
MARLIN, DAVID H. N90-21940
MARSHALL, N. H. N90-22258
MARTIN, DONALD F. N90-22488
MARTINEZ, DAVID R. N90-22113
MARWIL, E. S. N90-22258
MASSOUDI, M. N90-22007
MASTRODDI, F. N90-22441
MATHER, J. L. N90-22274
MATSUHIRA, NOBUTO N90-22087
MATTEDI, ANITA K. N90-21809
MATTHEWS, CHRISTINE G. N90-22247
MATTHEWS, DENNIS N90-22393
MATTHEWS, S. D. N90-22258
MAUGHMER, MARK D. N90-21734
N90-21735
MAZUMDAR, J. N90-22063
MAZZALI, PAOLO ALBERTO N90-22474
MCAFFEE, DOUGLAS N90-22089
MCANALLY, ANTHONY STEPHEN N90-21873
MCARDLE, JACK G. N90-21725
MCCARTHY, PATRICK JOSEPH N90-22523
MCCLAIN, M. N90-22254
MCCLURE, JOHN A. N90-22010
MCCOLLOUGH, MICHAEL LEON N90-22486
MCCOLM, DOUGLAS W. N90-22370
MCCONALOGUE, D. J. N90-22459
MCELIECE, R. N90-21895
MCFADDEN, G. B. N90-22408
MCFADDEN, P. D. N90-22052
MCFARLAND, R. E. N90-21758
MCHENRY, H. I. N90-22106
MCINTOSH, R. N90-21790
MCINTOSH, ROBERT E. N90-21935
MCIVOR, ALAN M. N90-22271
N90-22272
N90-22384
MCLUCAS, JOHN L. N90-22153
MEAD, JAMES B. N90-21935
MEEGAN, CHARLES A. N90-22526
MEEK, J. L. N90-22110
MEESTER, R. W. J. N90-22362
MEEUWISSEN, HANS N90-22160
MEHUYS, DAVID GLENN N90-22036
MELLOR, PAMELA A. N90-22323
MELLOTT, KENNETH D. N90-22488
MELVIN, ROBIN G. N90-21996
MELVIN, WILLIAM S. N90-21868
MENON, P. K. A. N90-22232
MEYER, S. A. N90-21811
MEYER, THOMAS R. N90-21789
MEYERS, M. A. N90-21854
MEZZACAPPA, ANTHONY N90-22483
MIELE, A. N90-21747
N90-21780
MIGENES, VICTOR N90-22471
MILAM, M. BRUCE N90-22092
MILLER, D. L. N90-21838
MILLER, DAVID L. N90-21955
MILLER, M. K. N90-21853
N90-22417
MILLER, W. F., JR. N90-22337
MILLER, WALTER B. N90-21940
MILLS, BARBARA N90-22239
MILLS, K. C. N90-21856
MINNETYAN, LEVON N90-21825
MIRANKER, DANIEL N90-22318
MITTMAN, DAVID N90-22312
MITTRA, R. N90-21887
MJOLHUS, E. N90-21944
MLYNCZAK, MARTIN GERARD N90-22151
MOK, ALOYSIUS N90-22318
MOLHOLM, KURT N. N90-22453
MOLLEY, PERRY A. N90-22249
MOLOKOV, S. Y. N90-22400
N90-22401
MOMOH, J. A. N90-22303
N90-22310
MONROE, CHARLES A., JR. N90-22105
MONSON, PETER A. N90-21832
MONTEIRO, ANTONIO MIGUEL VIEIRA N90-22333
MONTEMERLO, MELVIN N90-22529
MONTIERTH, L. M. N90-22035
MOREIRA, LUCIMAR N90-22139
MORGAN, K. N90-21993
MORRIS, STEVEN LYNN N90-21771
MORRISON, H. N90-22103
MORRISON, JACK N90-22312
MORTENSEN, G. A. N90-22258
MOSKOVITZ, CARY A. N90-21767
MUENCHAUSEN, R. E. N90-22413
MUHS, J. D. N90-22044
MUIR, PATRICIA S. N90-22182
MUKHERJEE, A. N90-22413
MUKKAMALA, R. N90-22278
N90-22279
N90-22282
MULLICAN, A. N90-21724
MULLIGAN, JEFFREY B. N90-22216
N90-22233
MURAKAMI, T. N90-22470
MURCRAY, D. G. N90-21910
MURCRAY, F. H. N90-21910
MURCRAY, F. J. N90-21910
MURRAY, B. T. N90-22408
MURRAY, NICHOLAS D. N90-22278
MURTHY, P. L. N. N90-21821
N90-21824
MURTHY, PAPPU L. N. N90-21825
MURTHY, S. N. B. N90-21724
MUSZYNSKA, A. N90-22065
MYER, L. R. N90-22171
N90-22172
N90-22173
MYERS, W. NEILL N90-22094

N

NAGLE-ESHLEMAN, JUDITH N90-22066
N90-22363
NAGPAL, V. K. N90-21871
NAKAJIMA, TADASHI N90-22475
NANSTAD, R. K. N90-21853
NAPPO, CARMEN JOSEPH N90-22512
NARAYAN, J. N90-22416
N90-22418
NELSEN, LOWELL V. N90-22049
NETO, ANTONIO FELIX MARTINS N90-21787
NEUMAN, W. A. N90-22035
NEWTON, BARBARA I. N90-22447
NG, LIAN LAI N90-22017
NGO, HUY X. N90-22239
NGUYEN, AN H. N90-22239
NGUYEN, H. L. N90-22262
NICHOLLS, R. W. N90-21925
NICHOLS, ARTHUR S. N90-22152
NICHOLSON, D. N90-22074
NICOLETTE, V. F. N90-21875
NIEDZWIECKI, R. W. N90-21869
NIEMEIJER, R. J. N90-21915
NIEMINEN, ESKO N90-21943
NIEMINEN, R. M. N90-22410
NILES, F. E. N90-21918
NOEL, B. W. N90-22044
NOETZOLD, DIRK N90-22503
NOGAR, N. S. N90-22413
NOIRAULT, P. N90-22085
NOLF, SCOTT R. N90-22247
NOMOTO, K. N90-22470
NORMAN, TIMOTHY LEE N90-21830
NORTHRUP, M. ALLEN N90-21867
NOTARI, ANTHONY N90-21930
NOTTKE, NATHAN N90-21806
NOWAK, RICHARD J. N90-21876
NYE, TED W. N90-22098

O

OBAYASHI, SHIGERU N90-21739
OBRIEN, MAUREEN E. N90-22311
OCCHIONERO, FRANCO N90-22502
OCHOA, ELLEN N90-22234
OCONNOR, BRENDAN M. N90-21807
ODWYER, BARRY N90-22100
OLIVE, KEITH A. N90-22426
OLIVEIRADIAS, ROBERTO W. N90-22457
OLOFSSON, H. N90-22477
OLSHAUSEN, BRUNO N90-22227
OMEARA, JACQUIE N90-22312
ONYSZCHUK, I. N90-21897
ORBEKK, ERLAND N90-21978
ORLANDO, VALCIR N90-22501
ORLOSKY, S. D. N90-22081
ORVIS, WILLIAM J. N90-21956
ORZECHOWSKI, T. J. N90-21800
OTOSHI, T. Y. N90-21890
OTT, KEVIN C. N90-22414
OVERSTREET, C. MICHAEL N90-22278
N90-22279
N90-22280
N90-22281
N90-22284
N90-22285
N90-22288
OZEN, METIN N90-22127
OZOROSKI, L. N90-21734
N90-21735
OZOROSKI, T. N90-21734
N90-21735

P

PAGE, J. N. N90-22405
PAIELLI, RUSSELL N90-21773
PAO, YOH-HAN N90-22324
PARANICAS, CHRISTOPHER PETER J. N90-21782
PARK, P. M. N90-21908
PARKYN, ADRIAN TIMOTHY N90-21815
PARSLEY, RANDY N90-21793
N90-21794
PARTHASARATHY, RAMKUMAR N. N90-21965
PATE, VICKI M. N90-22059
N90-22061

N90-22064
N90-22068
N90-22073
PATERRA, FRANK N90-22280
N90-22281
N90-22284
N90-22285
N90-22288
PATERSON, S. M. N90-22201
PAULSEN, U. S. N90-22144
PEARCE, J. A. N90-22003
PEARSON, ELLEN N90-22452
PEIRO, J. N90-21993
PENG, T. K. N90-21900
PENSTON, M. V. N90-22479
PERAIRE, J. N90-21993
PERERA, A. G. U. N90-22219
PERSSON, HENRY N90-21874
PETERS, STEPHEN N90-22312
PETRIK, EDWARD J. N90-22306
PETROSIAN, VAHE N90-22402
PETTENGILL, JAMES B. N90-21753
PETTY, S. M. N90-21889
PHILIPP, WARREN H. N90-21843
N90-21858
PIANTANIDA, THOMAS N90-22229
PIERRE, SAMUEL N90-22319
PIN, FRANCOIS G. N90-22047
PINOLI, PAT C. N90-21818
N90-21819
PINON, ELFEGO, III N90-21807
PINTO, FABRIZIO N90-22494
PITZ, W. J. N90-21838
PLIMPTON, STEVEN J. N90-22259
POLKOWSKA-SEMENIUK, MARIA N90-22266
N90-22267
POLKOWSKI, LECH T. N90-22266
N90-22267
POLLARA, F. N90-21895
PORCH, WILLIAM M. N90-22191
POSNER, E. C. N90-21880
POSTLETHWAITE, I. N90-22327
POTAPCZUK, MARK G. N90-21727
POVINELLI, LOUIS A. N90-22011
POWELL, F. T. N90-21870
POWERS, JANET V. N90-21754
PREEDY, K. A. N90-21926
PRIDDY, THOMAS G. N90-22115
PROFFITT, DENNIS R. N90-22226
PROVOST, STEPHEN C. N90-22204
PRYOR, WAYNE ROBERT N90-22518
PUSKA, M. J. N90-22410
PUSTER, RICHARD L. N90-22025
PYRAK-NOLTE, L. J. N90-22171

Q

QUINN, R. N90-21905
QUINN, ROD K. N90-22414
QUINN, TODD N90-22306

R

RABAEY, GREGORY FRANCIS N90-22519
RAGA, GRACIELA BINIMELIS N90-22178
RAJAGOPAL, K. R. N90-22007
RAMAPRIYAN, H. K. N90-22231
RANA, N. C. N90-22525
RANDALL, DONALD P. N90-22247
RANDELL, G. P. N90-22275
RANOUX, GILBERT N90-21980
RANSONE, PHILIP O. N90-22042
RAO, NAGESWARA S. V. N90-22256
RAO, S. S. N90-22067
RASH, JAMES L. N90-22294
RASMUSSEN, FLEMMING N90-22145
RAUGH, MIKE N90-22235
RAVISHANDRAN, G. N90-21854
RAY, RONALD J. N90-22322
REED, CHARLES E. N90-22433
REED, I. S. N90-21899
REED, ROBERT M. N90-22159
REESE, R. T. N90-22046
REID, ALAN J. N90-22023
REID, MAX N90-22234
REILLY, NORMAN B. N90-22296
REINHORN, A. M. N90-22062
RHEA, DONALD C. N90-22213
RICCI, PAOLO N90-21916
RICE, EDWARD J. N90-21733
RICHARDSON, KENNETH MICHAEL N90-22524
RICKLIN, JENNIFER C. N90-21940
RIDOUT, J. M. N90-21938
RIETDIJK, R. H. N90-22375
RINSLAND, C. P. N90-21910
RIOS-NETO, ATAIR N90-22501
RIZZI, STEPHEN ANTHONY N90-22131
ROACH, DENNIS P. N90-22115
ROADCAP, JOHN RUSSELL N90-22179
ROBINSON, B. D. N90-22330
ROBINSON, BRUCE A. N90-22170
ROBINSON, LAWSON HAYES N90-21768
ROBINSON, LEE N90-22089
ROBINSON, R. D. N90-22479
RODEMICH, E. R. N90-21888
RODKEY, L. SCOTT N90-22202
ROELKE, R. J. N90-22262
ROELOFS, LARRY H. N90-22315
ROGERS, F. J. N90-22480
ROGERS, STUART E. N90-21757
ROHRKASTE, G. R. N90-22104
ROLAND, VINCENT R. N90-22247
RONEY, P. L. N90-21927
ROOS, C. N90-22265
ROQUEMORE, W. M. N90-22003
ROSCHKE, PAUL N. N90-22248
ROSEN, PAUL ALAN N90-22511
ROSIER, LOUIS N90-22318
ROSS, D. L. N90-21903
ROSS, JAMES C. N90-21778
ROSSI, ROBERT JAMES N90-22165
ROSSITER, J. A. N90-22328
N90-22329
N90-22331
ROSSITER, M. J. N90-22378
N90-22382
ROTH, MARY ELLEN N90-22306
ROWE, JOSEPH N90-22203
ROY, G. N90-21931
RUDERMAN, M. N90-22468
N90-22469
RUDORFF, BERNARDO FRIEDRICH THEODOR
N90-22138
N90-22139
RUIZ, C. N90-21827
N90-21828
N90-22123
RUTHERFORD, P. H. N90-22392

S

SACKETT, BRENT J. N90-22010
SAKAI, RYOKI N90-22188
SAKUMA, HIROFUMI N90-22176
SALAS, M. D. N90-21744
SALDUA, B. P. N90-21902
SAMANT, SATISH S. N90-21996
SANCHEZ, ENNIO RODOLFO N90-22388
SAND, JAMES R. N90-21876
SANTANNABINS, LEONARDO N90-22333
SANTELLA, M. L. N90-21852
SAPATY, PETER S. N90-22291
SARMA, A. D. N90-21912
SATORIUS, E. N90-21899
SAUNDERS, S. R. J. N90-21863
SCHAAF, MARK DOUGLAS N90-22136
SCHENBERGER, DEBORAH S. N90-22080
SCHENKER, PAUL S. N90-22236
SCHIJVE, J. N90-22118
SCHLAG, GRETCHEN A. N90-22433
SCHMATZ, M. A. N90-21985
SCHNEIDER, STEVEN J. N90-22024
SCHRAMM, DAVID N. N90-22426
SCHUBERT, F. H. N90-21870
SCHWARZ, W. N90-21985
SEAGRAVES, M. A. N90-21918
SEAH, M. P. N90-22027
SEGAL, G. N90-22270
SEIBERT, W. N90-21989
SEIF-NARAGHI, AMIR-HOSSEIN N90-22334
SELBY, J. E. A. N90-21917
SELLECK, M. E. N90-22408
SETSER, D. W. N90-22033
SHAH, A. R. N90-21871
SHAH, B. N90-21892
SHAHAM, JACOB N90-22467
N90-22468
N90-22469
N90-22470
SHARAN, S. N90-22418
SHASTRI, LOKENDRA N90-22295
SHAW, J. A. N90-21991
SHELDON, ROGER A. N90-22321
SHELDON, W. R. N90-22154
SHELTON, DUANE N90-22409
SHEN, GUO-CHUN N90-21728
SHEN, MO-HOW HERMAN N90-22075
SHERIF, RAED A. N90-22128
SHETTLE, ERIC P. N90-21917
N90-21919
N90-21928
SHEU, WEN-JENN N90-21831
SHIBAZAKI, N. N90-22470
SHIBUYA, KAZUO N90-22188
SHIEH, ARTHUR S.-L. N90-22004
SHIH, M. T. N90-21899
SHIH, T. I.-P. N90-22262
SHIN, JAIWON N90-21732
SHINOMIYA, YASUO N90-22087
SHIRKEY, R. C. N90-21918
SHOGEN, K. N90-21887
SHORT, NICHOLAS, JR. N90-22295
SHPAKOVICH, YA. V. N90-22420
SHUM, D. K. N90-22116
SIGLEY, RUTH HELEN N90-22072
SILVER, J. D. N90-22415
SIMONI, PAULO OUVERA N90-22332
SINGH, JAG J. N90-22025
SINGH, R. K. N90-22418
SINGH, UPENDRA N. N90-21930
SKEENS, KRISTI M. N90-22247
SLAGTER, W. J. N90-22050
SLINGER, C. W. N90-21948
SLOBIN, S. D. N90-21900
SMITH, ALEX E. N90-21749
SMITH, ALVIN N90-21961
SMITH, BERNARD N90-21850
SMITH, BRIAN K. N90-22307
SMITH, DENNIS W. N90-22097
SMITH, G. C. N90-22027
SMITH, LAURA DOROTHY N90-22160
SMITH, M. H. N90-21908
SMITH, P. D. N90-22014
SMITH, PAUL N90-22529
SMITH, ROBERT E. N90-21979
SMITHRICK, JOHN J. N90-21808
SMORENBURG, C. N90-22198
SNOEIJ, P. N90-22140
SNOW, EDWARD N90-22089
SOBAJIC, DEJAN J. N90-22324
SODERBLOM, D. R. N90-22479
SOVERS, O. J. N90-21904
SPARN, THOMAS P. N90-22302
SPENCER, N. E. N90-22196
SPERBER, KENNETH ROBERT N90-22181
SPIEGEL, B. N90-22043
SPIJKER, MARC N. N90-22349
N90-22351
N90-22353
SPIRA, S. N90-21803
SPITZER, D. N90-22198
SPONSLER, JEFFREY L. N90-22299
SPRINGER, JOE B. N90-22296
SRIDHAR, BANAVAR N90-22237
N90-22238
STAINFORTH, D. N90-22201
STAINTHORPE, C. N90-22195
STAKENBORG, L. N90-22326
STARK, LAWRENCE N90-22239
STEEN, W. M. N90-21863
STEIGMAN, GARY N90-22426
STEIN, V. N90-21997
STEINBRENNER, J. P. N90-21983
STEINOLFSON, R. S. N90-22522
STEPHAN, AMY N90-22307
STEPHENSON, MICHAEL B. N90-22260
STERGIS, C. G. N90-21911
STEWART, CAROLINE B. N90-22135
STOFAN, ELLEN RENEE N90-22513
STONE, CHARLES M. N90-22111
STONE, G. L. N90-22189
N90-22190
STONER, ERIC N90-22139
STRAGUZZI, NICHOLAS N90-22300
STRAKA, JERRY MICHAEL N90-22184
STRATARIDAKIS, CONSTANTINE JOHN N90-21966
STRAUSSFOGEL, D. N90-21734
N90-21735
STRICKLAND, D. J. N90-21937
STRONG, J. P. N90-22231
STUBBS, D. M. N90-22083
SU, TZU-JENG N90-21770
SUMMERS, K. A. N90-22142
SURKOV, A. N. N90-22419
SUTLIFF, T. J. N90-21723
SUTRISNO N90-21960
SWART, P. J. F. N90-22140
SWARTTOUW, RENE F. N90-22344
SWARTZ, DOUGLAS ALEXANDER N90-22500
SWEBY, P. K. N90-22339
N90-22340
SZU, HAROLD H. N90-22317

T

TACCONI-GARMAN, LOWELL EVAN N90-22495
TAGHAVI, R. N90-22000
TALLANT, D. R. N90-21865
TANG, Y. K. N90-22305
TANGUY, MIREILLE N90-21909
TARAN, N. V. N90-22419
TAYLOR, ALLAN H. N90-22042
TAYLOR, ARTHUR CANNING, III N90-21973
TAYLOR, MALCOLM N90-22449
TAYLOR, MARYJANE N90-22472
TAYLOR, NANCY L. N90-22247
TEETER, RONALD N90-22203
TELESMAN, JACK N90-22117
TEMKIN, R. J. N90-21802
N90-21803
THALMAN, NANCY E. N90-22302
THE, LIH-SIN N90-22496
THIERMANN, V. N90-21923
THOMAS, F. N90-22043
THOMPSON, JOE F. N90-21977
THURMAN, S. W. N90-21884
N90-21885
TISCHLER, MARK B. N90-21756
TIWARI, P. N90-22418
TO, C. W. S. N90-22060
TOBAK, MURRAY N90-21746
TOBIN, K. W. N90-22044
TOGNACCINI, R. N90-21984
TOLLIDAY, N. P. N90-21908
TOOTH, A. R. N90-21941
TORCZYNSKI, J. R. N90-22001
N90-22032
TOWNSEND, WILLIAM N90-22089
TRAK, AHMET BULENT N90-21949
TREBES, J. C. N90-22393
TREFNY, CHARLES J. N90-21762
TRESSER, CHARLES N90-22289
TRIVELPIECE, ALVIN W. N90-22463
TROPPER-HAUSEN, EVELYNE N90-22319
TROWBRIDGE, D. L. N90-21905
TRUONG, KHIEM VAN N90-21736
TRUONG, LONG VAN N90-22306
TRUONG, T. K. N90-21899
TSAI, M. C. N90-22327
TSANG, CHIN-FU N90-22174
TULPULE, SHARAYU N90-21809
TURLEY, W. D. N90-22044
TURNER, P. R. N90-22252
TUSON, A. T. N90-21863
TZOU, D. Y. N90-22112

U

ULABY, FAWWAZ T. N90-21936
ULVESTAD, J. S. N90-21904
UNRUH, BETTY N90-22442

V

VANBLADEL, P. G. N90-22341
VANDERBEEK, C. G. A. N90-22121
N90-22343
VANDERGELD, C. W. M. N90-21743
VANDERMAREL, ROELAND N90-22350
VANDYK, SCHUYLER DANA N90-22497
VANEVERY, D. N90-21737
VANGILS, S. A. N90-22347
VANHEK, R. A. N90-21902
VANHOLTEN, J. W. N90-22373
N90-22375
VANKA, S. P. N90-22003
VANMAAREN, H. N90-22346
VANMIERLO, G. W. M. N90-22198
VANOLDENBORGH, G. J. N90-22268
VANSINTTRUYEN, J. S. N90-21915
VANSTRIEN, SEBASTIAN N90-22289
VARALJAY, N. C. N90-22421
VASSEUR, HUBERT A. N90-22047
VAURIO, JUSSI N90-22057
VELASCO, FLAVIO ROBERTO D. N90-22333
VERMASEREN, J. A. M. N90-22268
N90-22372
VERMEER, P. L. N90-21946
VERVERS, FRANS N90-22264
VIAL, J.-P. N90-22265
VIALATOUX, E. N90-22082
VILLALOBOS, SONIA M. GOMESDEG. N90-21848
VILNROTTER, V. A. N90-21888
VINCKIER, A. N90-21976
VINEYARD, EDWARD A. N90-21876
VINZ, FRANK L. N90-22240
VISSER, H. N90-22198
VISSER, H. G. N90-21751
N90-21752
VITAGLIANO, P. L. N90-21984
VITHOONTIEN, VIRAJ N90-22078
VOGELAAR, ROBERT BRUCE N90-22498
VOSS, FRED E. N90-21999
VU, KHAI TRAN N90-21769
VYKUKAL, VIC N90-22101

W

WADE, JOHN E. N90-22143
N90-22192
N90-22193
WAHLS, RICHARD ALAN N90-22019
WALKER, STEL N. N90-22143
N90-22192
N90-22193
WALKER, TERRY P. N90-22426
WALLACE, JANICE S. N90-21754
WALSTON, WILLIAM S. N90-21849
WALTERS, JERRY L. N90-22306
WALTZ, R. E. N90-22398
WANDELL, BRIAN A. N90-22241
WANG, H. N90-21780
WANG, Q. N90-22468
WANG, SHU-YI N90-21970
WANG, T. N90-21780
WANG, YI-ZUN N90-22002
WANG, YUN N90-22504
WANTHAL, STEVEN PAUL N90-22132
WARD, WILLIAM CARL N90-22368
WARDEN, ROBERT M. N90-22091
WARNER, J. D. N90-22421
WASZCZYSZYN, Z. N90-22120
WATKINS, WENDALL N90-21939
WATSON, ANDREW B. N90-22216
N90-22242
N90-22243
WATTENBERG, U. N90-22443
WEBB, D. J. N90-22201
WEBSTER, KENNETH L. N90-22028
WELFORD, K. N90-22423
WELLMAN, DENNIS L. N90-22155
WENSKI, EDWARD G. N90-22026
WESSELIUS, JACCO N90-22264
WESTBROOK, C. K. N90-21838
WESTROM, GEORGE N90-22244
WETZEL, C. R. N90-22305
WHITFIELD, DAVID L. N90-21982
WHITNEY, DONALD A. N90-22031
WIJCHERS, T. N90-21846
N90-21847
WILBUR, PAUL J. N90-21810
WILBY, J. F. N90-22364
WILK, R. D. N90-21838
WILKERSON, THOMAS D. N90-21930
WILKINS, T. N. N90-22487
WILLIAMS, G. P. N90-22411
WILLIAMS, GEOFF N90-21799
WILLIAMS, JOHN D. N90-22389
WILLIAMS, T. T. N90-22382
WILLIAMSEN, J. N90-22043
WILLIAMSON, R. L. N90-21855
WILSON, B. G. N90-22480
WINCKELMANS, GREGOIRE STEPHANE N90-21967
WINDSOR, COLIN G. N90-22056
WINGLEE, R. M. N90-21792
WINKLER, ROGER V. N90-21999
WITTENBERG, H. N90-21846
N90-21847
WITZGALL, CHRISTOPH N90-22253
WOLD, A. N90-22407
WOLF, J. N90-22195
WOLF, JOHN WILLIAM N90-22366
WONG, A. Y. N90-21944
WOOD, H. JOHN N90-22245
WOODWORTH, P. L. N90-22196
WOOH, SHI-CHANG N90-21816
WORDEN, REBECCA ELAINE N90-22129
WRIGHT, DONALD REX N90-22367
WRIGHT, R. N. N90-21855
WU, G. D. N90-21780
WU, MENG-CHOU N90-22369
WU, X. D. N90-22413

X

XU, YONGZHI N90-22197

Y

YAKYMYSHYN, CHRISTOPHER PAUL N90-22029
YAMAMOTO, YUKIMITSU N90-21726
YAMANOUCHI, TAKASHI N90-22188
YAN, XIAO-HAI N90-22137
YANG, TZUNG-CHENG N90-22293
YAO, JEN-CHIH N90-22360
YEE, H. C. N90-22339
N90-22340
YEH, PEN-SHU N90-22246
YI, ZHANG N90-22054
YING, X. T. N90-22254
YINONG, SU N90-22110
YOKOYAMA, JUNICHI N90-22506
YOLKEN, H. THOMAS N90-22055
YOUNG, DAVID P. N90-21996

Z

ZANDBERGEN, B. T. C. N90-21846
N90-21847
ZARETSKY, ERWIN V. N90-22041
ZEIJLMANS, MICHAEL COSMAS SILVESTER
N90-21947
ZHANG, L. N90-22287
ZHANG, XIAO-HE N90-22509
ZHANG, YANQIU N90-22130
ZHANG, Z. Z. N90-22303
N90-22310
ZHAO, YI YUAN N90-21765
ZHENG, Z. N90-22173
ZHONG, H. Z. N90-22123
ZILLIAC, GREGORY G. N90-21746
ZIMMERMAN, BARBARA A. N90-22313
ZINKLE, S. J. N90-21823
ZIPF, MARK E. N90-21776
ZUCKER, MICHAEL EDWARD N90-22476

CORPORATE SOURCE INDEX

Typical Corporate Source Index Listing

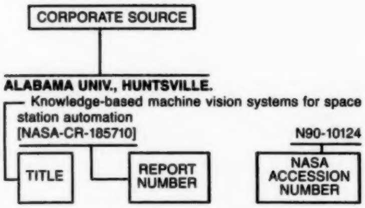
CORPORATE SOURCE
ALABAMA UNIV., HUNTSVILLE.
Knowledge-based machine vision systems for space station automation
[NASA-CR-185710]
N90-10124
TITLE
REPORT NUMBER
NASA ACCESSION NUMBER

Listings in this index are arranged alphabetically by corporate source. The title of the document provides the user with a brief description of the subject matter. The report number helps to indicate the type of document cited (e.g., NASA report, translation, NASA contractor report). The NASA accession number denotes the number by which the citation is identified. The titles are arranged under each corporate source in ascending accession number order.

A

ACADEMY OF SCIENCES OF THE UKRAINIAN SSR, KHARKOV.
Theory of a periodic cylindrical waveguide with a nonuniform metal-dielectric filling
[DE90-620099] N90-21945
Wind instability as a possible cause of the spiral structure formation in the gaseous subsystem of galaxies with the circular magnetic field
[DE90-618944] N90-22507
Jupiter's drifting decametric bursts with the changing time scale
[DE90-618870] N90-22517

ADELAIDE UNIV. (AUSTRALIA).
A review of approximate methods for determining the vibrational modes of membranes N90-22063

ADMIRALTY RESEARCH ESTABLISHMENT, PORTSDOWN (ENGLAND).
A survey of the maritime-aerosol data collected at South Uist and the implications for the LOWTRAN maritime aerosol model N90-21908

ADMIRALTY RESEARCH ESTABLISHMENT, PORTSMOUTH (ENGLAND).
Calculation of IR propagation statistics in the eastern Atlantic for surveillance system performance assessment N90-21938

ADVISORY GROUP FOR AEROSPACE RESEARCH AND DEVELOPMENT, NEUILLY-SUR-SEINE (FRANCE).
Atmospheric Propagation in the UV, Visible, IR, and mm-Wave Region and Related Systems Aspects
[AGARD-CP-454] N90-21907
Applications of Mesh Generation to Complex 3-D Configurations
[AGARD-CP-464] N90-21975
Electronic Transfer of Information and its Impact on Aerospace and Defence Research and Development
[AGARD-CP-466] N90-22440

AEC-ABLE ENGINEERING CO., INC., GOLETA, CA.
Relatchable launch restraint mechanism for deployable booms N90-22091

AEROSPATIALE, CHATILLON (FRANCE).
Geometry and grids of complex configurations for aerodynamic calculation N90-21980

AEROSPATIALE, SURESNES (FRANCE).
Electronic transfer of information applications in the Societe Aerospatiale N90-22454

AIR FORCE GEOPHYSICS LAB., HANSCOM AFB, MA.
LOWTRAN 7: Status, review, and impact for short-to-long-wavelength infrared applications N90-21917
Models of aerosols, clouds, and precipitation for atmospheric propagation studies N90-21919
UV spectral simulations using LOWTRAN 7 N90-21928

AIR FORCE WEAPONS LAB., KIRTLAND AFB, NM.
The Weapons Laboratory technical library: Automating with STILAS N90-22447

AIRCRAFT RESEARCH ASSOCIATION LTD., BEDFORD (ENGLAND).
A discussion on issues relating to multiblock grid generation N90-21991

AKRON UNIV., OH.
Internal fractures in model elastomeric composites N90-22133

ALABAMA UNIV., BIRMINGHAM.
The chemical basis for the origin of the genetic code and the process of protein synthesis
[NASA-CR-186590] N90-22205

ALABAMA UNIV., HUNTSVILLE.
High power CO2 laser instability and its corrections N90-22028
Optical bistability in semiconducting material N90-22424

ALLIED-SIGNAL CORP., KANSAS CITY, MO.
New flexible circuit material evaluation
[DE90-008313] N90-21866
Small strain gage applications 2
[DE90-008312] N90-22026

AMSTERDAM UNIV. (NETHERLANDS).
Investigation of correlations in nuclei with the (e,e'X) reaction
[ETN-90-96398] N90-22377

ANALYTICAL SERVICES AND MATERIALS, INC., HAMPTON, VA.
A multiblock/multizone code (PAB 3D-v2) for the three-dimensional Navier-Stokes equations: Preliminary applications
[NASA-CR-182032] N90-21745

ARGONNE NATIONAL LAB., IL.
Development of a computational fluid dynamics and chemistry model for the fouling of jet fuels
[DE90-005664] N90-22003

ARIZONA STATE UNIV., TEMPE.
Control of human arm movement via optimization N90-22334

ARIZONA UNIV., TUCSON.
Instabilities and subharmonic resonances of subsonic heated round jets, volume 2
[NASA-CR-186058] N90-22017
Facilitating knowledge sharing in organizations: Semiautonomous agents that learn to gather, classify, and distribute environmental scanning knowledge N90-22435
Search for rapidly star forming galaxies at high redshift N90-22465
The production and spatial distribution of neutral and ionized water vapor in Comet P/Halley N90-22484
The mass of the Coma cluster N90-22496
The observed properties of the intermediate-degree gravity modes and their relevance to the solar neutrino paradox N90-22519
Very high energy gamma rays from the Crab nebula and pulsar N90-22527

ARMY AVIATION RESEARCH AND DEVELOPMENT COMMAND, MOFFETT FIELD, CA.
Identification of XV-15 aeroelastic modes using frequency-domain methods
[NASA-TM-101021] N90-21756

ARMY COMMUNICATIONS-ELECTRONICS COMMAND, FORT MONMOUTH, NJ.
Method of making a cathode from tungsten powder
[AD-D014434] N90-21850

ARMY MISSILE COMMAND, REDSTONE ARSENAL, AL.
Extraction of recovery of plasticizers from solid propellants and munitions
[AD-D014433] N90-21868

ATLANTIC APPLIED RESEARCH CORP., VAN NUYS, CA.
Noise transmission into propeller-driven airplanes N90-22364

ATMOSPHERIC SCIENCES LAB., WHITE SANDS MISSILE RANGE, NM.
Propagation environments, effects, and decision aids N90-21918
Effect of atmospheric turbulence on electro-optical systems N90-21940

AUBURN UNIV., AL.
Utilization of water hyacinths to upgrade heavily loaded wastewater treatment plant effluents N90-21873
Current drive in a supernova N90-22491

AVCO-EVERETT RESEARCH LAB., MA.
MHD channel development, part 1
[DE90-009549] N90-22394
MHD channel development, part 2
[DE90-009550] N90-22395
MHD channel development, part 3
[DE90-009551] N90-22396
MHD channel development, part 4
[DE90-009552] N90-22397

AVIONS MARCEL DASSAULT-BREGUET AVIATION, SAINT-CLOUD (FRANCE).
Automatic grid generation in complex three-dimensional configurations using a frontal system N90-21992

B

BELEIDSCOMMISSIE REMOTE SENSING, DELFT (NETHERLANDS).
The AGRISCATT-87 campaign: Processing of the Dutscat data
[BCRS-89-20] N90-22140
Pre-study laser bathymetry
[BCRS-89-26] N90-22198

BENTLY ROTOR DYNAMICS RESEARCH CORP., MINDEN, NV.
Rotor-to-stationary element rub-related vibration phenomena in rotating machinery: Literature survey N90-22065

BIDSTON OBSERVATORY, MERSEYSIDE (ENGLAND).
European network of interest in the measurement and analysis of mean sea levels from tide gauge records
[PB90-151929] N90-22196

BOEING AEROSPACE CO., KENT, WA.
Bi-directional thruster development and test report
[NASA-CR-182013] N90-21785

BOEING COMMERCIAL AIRPLANE CO., SEATTLE, WA.
A conflict analysis of 4D descent strategies in a metered, multiple-arrival route environment
[NASA-CR-182019] N90-21772

BONNEVILLE POWER ADMINISTRATION, PORTLAND, OR.
Regional wind energy assessment
[DE90-009439] N90-22143
Regional wind energy assessment
[DE90-009380] N90-22192
Wind forecasting for utility operations
[DE90-009466] N90-22193

BRADFORD UNIV. (ENGLAND).
Failure mechanisms under complex loading of glass-reinforced polyester composites and their matrices: The effect of superposed hydrostatic pressures up to 300 MPa on axial tensile and compressive strengths, and in-plane shear properties of unidirtionally reinforced glass-polyester composites and the relevant polyesters N90-22072

BRIGHAM YOUNG UNIV., PROVO, UT.
A theoretical scenario for the dynamics of formation and early evolution of globular clusters in galaxies N90-22494

BRITISH AEROSPACE PUBLIC LTD. CO., BRISTOL (ENGLAND).
Atmospheric modelling studies: A modelling comparison between IR and millimetric atmospheric propagation N90-21941

BRITISH AEROSPACE PUBLIC LTD. CO., HATFIELD (ENGLAND).
Multiblock topology specification and grid generation for complete aircraft configurations N90-21986

BRITISH AEROSPACE PUBLIC LTD. CO., PRESTON (ENGLAND).
Information technology applications: A British Aerospace Military Aircraft Ltd view N90-22455

BRITISH TELECOM, LONDON (ENGLAND).
Innovations in telecommunications networks N90-22444

BROOKHAVEN NATIONAL LAB., UPTON, NY.
Report on the fifth workshop on synchrotron x ray lithography
[DE90-007903] N90-22411

BROWN UNIV., PROVIDENCE, RI.
Fracture mechanics of monolithic ceramic materials under small scale microcracking conditions N90-21860
Preparation and characterization of Cu2ZnGeS(4-y)Se(y)
[AD-A217469] N90-22407
Geology of coronae and domal structures on Venus and models of their origin N90-22513

C

CALIFORNIA INST. OF TECH., PASADENA.
Topics in vortex methods for the computation of three- and two-dimensional incompressible unsteady flows N90-21967
Experimental and analytical investigations of granular materials: Shear flow and convective heat transfer N90-21968
Linear, nonlinear, and tunable guided wave modes for high-power (GaAl)As semiconductor lasers N90-22036
Experimental investigation of the effect of cavitation on the rotordynamic forces on a whirling centrifugal pump impeller N90-22039
Dynamic response of structures with uncertain parameters N90-22125
Diffraction-limited imaging on the 200-inch telescope N90-22475
Experiments with a laser interferometric gravitational wave antenna N90-22476
The Al-26(rho, gamma)Si-27 reaction: Stellar origins of galactic Al-26 N90-22498
Multipole moments in general relativity and dynamical perturbations of black-hole magnetospheres N90-22509
Quantitative studies of the Martian south polar region using spacecraft images N90-22514

CALIFORNIA UNIV., BERKELEY.
Fire propagation in concurrent flows
[PB90-151754] N90-21834
Instrumentation and robotic image processing using top-down model control N90-22239
A high galactic latitude survey of far ultraviolet excess objects N90-22473
The ratio of neutral hydrogen to neutral helium in the local interstellar medium N90-22499
Extended optical emission in 3CR radio galaxies N90-22523

CALIFORNIA UNIV., BERKELEY. LAWRENCE BERKELEY LAB.
Effects of single fractures on seismic wave propagation
[DE90-009191] N90-22171
The effects of tortuosity on flow through a natural fracture
[DE90-009193] N90-22172
In-situ fracture stiffness determination
[DE90-009202] N90-22173
Coupled behavior of rock joints
[DE90-009222] N90-22174

CALIFORNIA UNIV., DAVIS.
An investigation of turbulence structure in a low Reynolds number incompressible turbulent boundary layer N90-21966
Practical nonlinear simulation of rotating machinery dynamics with application to turbine blade rubbing N90-22038
Correlated electron processes in ion-atom collisions
[DE90-009477] N90-22370

CALIFORNIA UNIV., LOS ANGELES.
Aeroelastic simulation of higher harmonic control N90-21768
Advances in optimal active control techniques for aerospace systems; application to aircraft active landing gear N90-21769
Formulation of non-reflecting boundary conditions in numerical models of the atmosphere N90-22175
A new stability criterion in the shallow-water system for two-dimensional coherent eddies in the atmosphere and oceans N90-22176
Hybrid modeling of plasmas and applications to fusion and space physics N90-22387
The MHD structure of an open magnetotail boundary N90-22388
The emission lines in the ultra-violet spectrum of Beta Lyrae N90-22474
Investigation of the late stages of stellar evolution: Mass loss from evolved stars N90-22492

CALIFORNIA UNIV., SAN DIEGO, LA JOLLA.
Martensitic transformation induced by stress pulses
[DE90-009534] N90-21854

CARNEGIE-MELLON UNIV., PITTSBURGH, PA.
The effect of hydrogen and microstructure on the deformation and fracture behavior of a single crystal nickel-base superalloy
[NASA-CR-185219] N90-21849
Principles of Very Large Scale Integrated (VLSI) system planning N90-21950
Gravitational couplings of the inflation in extended inflation
[NASA-CR-186595] N90-22504

CASE WESTERN RESERVE UNIV., CLEVELAND, OH.
Analysis of a high harmonic rectangular gyrotron using ribbon beams N90-21801

CENTRE NATIONAL D'ETUDES SPATIALES, TOULOUSE (FRANCE).
SPOT 4 space magnetic recorder mechanisms N90-22082
A dynamic motion simulator for future European docking systems N90-22085

CENTRE NATIONAL DE LA RECHERCHE SCIENTIFIQUE, PARIS (FRANCE).
The Mediterranean marine environment and its effects on aerosols and infrared transmission N90-21909

CESKOSLOVENSKA AKADEMIE VED, PRAGUE.
Gas-puff z-pinch experiment
[IPPCZ-286] N90-22385
The intrinsic stochasticity of near-integrable Hamiltonian systems
[IPPCZ-282] N90-22386

CHALMERS UNIV. OF TECHNOLOGY, GOETEBORG (SWEDEN).
A comparison of photospheric and circumstellar (HCN)/(CO)-ratios for bright carbon stars
[PB90-151101] N90-22477

CHICAGO UNIV., IL.
Gravitational effects of global textures
[NASA-CR-186596] N90-22503
Ultrahigh-energy particle flux from cosmic strings
[NASA-CR-186592] N90-22525

CLEMSON UNIV., SC.
Ternary reactions among polymer substrate-organohalogen-antimony oxides under pyrolytic, oxidative and flaming conditions
[PB90-154766] N90-21861

CLEVELAND STATE UNIV., OH.
Analytical and experimental study of high phase order induction motors
[NASA-CR-186580] N90-21952

COLLEGE OF WILLIAM AND MARY, WILLIAMSBURG, VA.
Simulation-based reasoning about the physical propagation of fault effects N90-22309
Nonlinearity parameters of polymers N90-22369

COLORADO STATE UNIV., FORT COLLINS.
Advanced electric propulsion research, 1989
[NASA-CR-185237] N90-21810
Hollow cathode operation at high discharge currents
[NASA-CR-185238] N90-21953
Satellite versus GCM-simulated radiation balance: Comparisons and implications for climate modeling N90-22180
Forecast of Atlantic seasonal hurricane activity for 1990 N90-22194
Plasma contactor research, 1989
[NASA-CR-185212] N90-22389

COLORADO UNIV., BOULDER.
Robust control of flexible structures N90-21784
The Advanced Communications Technology Satellite (ACTS) capabilities for serving science
[NASA-CR-186584] N90-21789
Thermomechanically-induced convective motion and natural convection in confined gaseous helium subjected to boundary heating N90-21960
Unsteady separated flows produced by complex harmonic motions: Investigation of wing-flow interactions elicited by a mechanical model simulating dragonfly wing kinematics N90-22018
Nonlinear stability analysis and control of dynamical robotic systems N90-22037
Semigeostrophic flow over orography in a stratified rotating atmosphere N90-22163
SURE (Science User Resource Expert): A science planning and scheduling assistant for a resource based environment N90-22302
Interactions of massive stars with the interstellar medium: Bow shocks and superbubbles N90-22485
Auroral ultraviolet darkening on the outer planets N90-22518

COLUMBIA UNIV., NEW YORK, NY.
Equilibrium and stability analysis of magnetospheric plasmas N90-21782
Physics of systems containing neutron stars
[NASA-CR-186002] N90-22467
Does SN 1987A contain a rapidly vibrating neutron star
[CAL-371] N90-22468
Origin of pulsed emission from the young supernova remnant SN 1987A
[CAL-377] N90-22469

COMMISSION OF THE EUROPEAN COMMUNITIES (LUXEMBOURG).
Technologies for electronic transfer of information: The present state and trends in Europe N90-22441
Document delivery via ISDN or satellite networks N90-22446

COMPUTER SCIENCES CORP., BELTSVILLE, MD.
Evaluation of a proposed expert system development methodology: Two case studies N90-22320

CONNECTICUT UNIV., STORRS.
Free wave propagation in orthogonally stiffened cylinders N90-22124
Analysis of a finite two-dimensional solid with an inclined crack and a rigid inclusion N90-22127

CORNELL UNIV., ITHACA, NY.
Development and applications of a coupled cavity sodium-chloride laser N90-22029

COUNCIL FOR NATIONAL ACADEMIC AWARDS (ENGLAND).
The interaction between a plane shock wave and a cylindrical afterbody N90-21728
Photometric monitoring of early type emission line stars N90-22478

D

DEFENCE RESEARCH ESTABLISHMENT VALCARTIER (QUEBEC).
Interpreting meteorological data reports for LOWTRAN Navy aerosol model extinction calculations N90-21920
A temperature-dependent regular infrared band model for absorption and dispersion N90-21927
Lidar measurement of concentration and turbulence in battlefield obscurants N90-21931

DEFENSE TECHNICAL INFORMATION CENTER, ALEXANDRIA, VA.
How to get it: A guide to defense-related information resources
[AD-A201600] N90-22433
Applications to the aerospace and defense R and D community: The DOD computer-aided acquisition and logistics support (CALS) initiative N90-22453

DELAWARE UNIV., NEWARK.
Generalized Herglotz functions and inverse scattering problem in a finite depth ocean
[PB90-150996] N90-22197

DEPARTMENT OF ENERGY, WASHINGTON, DC.
High power millimeter wave source development program N90-21805

DEUTSCHE FORSCHUNGSANSTALT FUER LUFT- UND RAUMFAHRT, OBERPFAFFENHOFEN (GERMANY, F.R.).
The solution of scattering and radiation problems for complex configurations based on 3-D grid and patch models N90-21997

DORNIER-WERKE G.M.B.H., FRIEDRICHSHAFEN (GERMANY, F.R.).
On the way to an integrated mesh generation system for industrial applications N90-21989

DREXEL UNIV., PHILADELPHIA, PA.
Numerical investigations of nonlinear behavior in the Einstein equations N90-22427
A study of mental models through communication between users and advisors solving software manipulation problems N90-22434

DUKE UNIV., DURHAM, NC.
Passive shape control of space antennas with determinate truss support structures N90-21949

DURHAM UNIV. (ENGLAND).
Gamma rays, cosmic rays, and local molecular clouds N90-22524

E

EDGERTON, GERMESHAUSEN AND GRIER, INC., IDAHO FALLS, ID.
Laboratory testing of Energy Research Corporation ERC 160 NiCd 6 volt traction battery
[DE90-009629] N90-21957
Laboratory testing of Saft SEH-5-200 6 volt traction battery
[DE90-009787] N90-21958
On dual Lagrangian hyperbolic models for one dimensional two phase flow problems
[DE90-007012] N90-22004
TOODEE: A two-dimensional, time-dependent heat conduction program
[DE90-009631] N90-22010
VCS: A networked Version Control System
[DE90-009805] N90-22250

FORTRAN coding guidelines
[DE90-009804] N90-22258

ELECTRONIC PUBLISHING DIGITAL EQUIPMENT CO. LTD., BASING VIEW (ENGLAND).
Desk top publishing: What you need to know N90-22449

ELORET CORP., SUNNYVALE, CA.
Modeling of vortex-induced oscillations based on indicial response approach
[NASA-CR-186560] N90-21736

ENVIRONMENTAL PROTECTION AGENCY, RESEARCH TRIANGLE PARK, NC.
The laminar flow element: Its use as a flow standard
[PB90-129677] N90-22157

ENVIRONMENTAL PROTECTION AGENCY, WASHINGTON, DC.
Determination of rates of reaction in the gas-phase in the troposphere: Theory and practice. 2: Rate of direct photoreaction: Screening-level test guideline-spectroscopic determination of the cross section and the maximum rate of direct photoreaction in sunlight
[PB90-146291] N90-22156

ESSEX CORP., ORLANDO, FL.
Issues in development, evaluation, and use of the NASA Preflight Adaptation Trainer (PAT)
[NASA-CR-185608] N90-22212

ESSEX UNIV., COLCHESTER (ENGLAND).
Broadcast file distribution on packet satellite networks N90-21906

EUROPEAN PATENT OFFICE, RIJSWIJK (NETHERLANDS).
The automation plan of the General Directorate 1 (search) of the European Patent Office N90-22448

EUROPEAN SPACE AGENCY. EUROPEAN SPACE RESEARCH AND TECHNOLOGY CENTER, ESTEC, NOORDWIJK (NETHERLANDS).
Recent developments in grid generation N90-21976

EXECUTIVE OFFICE OF THE PRESIDENT, WASHINGTON, DC.
Aeronautics and space report of the President: 1987 activities N90-22462

F

FAIRCHILD SPACE CO., GERMANTOWN, MD.
A robot end effector exchange mechanism for space applications N90-22088
The resupply interface mechanism RMS compatibility test N90-22090

FEDERAL AVIATION ADMINISTRATION, ATLANTIC CITY, NJ.
Enhanced Low Level Wind Shear (LLWAS) 6-sensor improvement user's manual for data processing of field data
[DOT/FAA/CT-TN90/8] N90-21759
Evaluation of a prototype lighted ball marker for powerline obstructions
[DOT/FAA/CT-TN90/12] N90-21774

FERMI NATIONAL ACCELERATOR LAB., BATAVIA, IL.
Big-bang nucleosynthesis revisited
[NASA-CR-186256] N90-22426
Gravitational effects of global textures
[NASA-CR-186596] N90-22503

FLORIDA STATE UNIV., TALLAHASSEE.
The sources and chemistry of late winter Arctic tropospheric aerosols
[PB90-131988] N90-22158

FLORIDA UNIV., GAINESVILLE.
Analysis of gamma squared Velorum photometry from the South Pole N90-22472

FORD AEROSPACE CORP., SEABROOK, MD.
NASA ground terminal communication equipment automated fault isolation expert systems N90-22305
Satellite image analysis using neural networks N90-22321

FOREIGN APPLIED SCIENCES ASSESSMENT CENTER, LA JOLLA, CA.
Japanese magnetic confinement fusion research N90-22392

FORSCHUNGSINSTITUT FUER OPTIK, TUEBINGEN (GERMANY, F.R.).
Modelling of optically and IR effective atmospheric turbulence N90-21923

FRAUNHOFER-INST. FUER ATMOSPHAERISCHE UMWELTFORSCHUNG, GARMISCH-PARTENKIRCHEN (GERMANY, F.R.).
Verification of Klett's method by comparison of lidar and transmissometer measurements N90-21933

G

GEC-MARCONI ELECTRONICS LTD., CHELMSFORD (ENGLAND).
Infrared propagation in the air-sea boundary layer N90-21926

GENERAL ACCOUNTING OFFICE, WASHINGTON, DC.
Space Shuttle, NASA's major changes to flight hardware: Fact sheet for the Chairman, Committee on Science, Space, and Technology, House of Representatives
[GAO/NSIAD-88-173FS] N90-22461

GENERAL ATOMIC CO., SAN DIEGO, CA.
Three-dimensional simulations of simple electron drift wave turbulence in tokamak geometry
[DE90-009581] N90-22398

GENERAL DYNAMICS/FORT WORTH, TX.
A structured approach to interactive multiple block grid generation N90-21983

GENERAL ELECTRIC CO., MOORESTOWN, NJ.
Space communications scheduler: A rule-based approach to adaptive deadline scheduling N90-22300

GENERAL ELECTRIC CO., PHILADELPHIA, PA.
General purpose heat source radioisotope thermoelectric generator program. Book 1: Accident analysis
[REPT-90SDS4202-BK-1] N90-22379
General purpose heat source radioisotope thermoelectric generator. Book 2: Accident analysis, appendices
[REPT-90SDS4202-BK-2] N90-22380

GEORGE WASHINGTON UNIV., WASHINGTON, DC.
Publications of the NASA Controlled Ecological Life Support System (CELSS) Program, 1979-1989
[NASA-CR-4297] N90-21754
Generation and adaptation of 3-D unstructured grids for transient problems N90-21994

GEORGETOWN UNIV., WASHINGTON, DC.
Polarization coupling in the acousto-optic interaction of surface waves N90-22365
Diffraction of light by ultrasonic pulses N90-22366

GEORGIA INST. OF TECH., ATLANTA.
Towards a unified analysis methodology for composite rotor blades N90-21730
Development and application of a generalized dynamic wake theory for lifting rotors N90-21731
A comparison of time-optimal interception trajectories for the F-8 and F-15
[NASA-CR-186300] N90-21753
Millimeter wavelength rectenna development N90-21797
The interpretation of SAGE 2 ozone measurements in the lower mesosphere N90-22149
The relationship between the buoyancy of near-surface air and the potential temperature of the tropopause N90-22165
Passive navigation using image irradiance tracking N90-22232
An investigation of narrow-bandgap semiconductors: Devices, circuits, and systems N90-22406
A theoretical investigation of gravity-wave-generated stress and vorticity in the planetary boundary layer N90-22512

GMD BUREAU TOKYO, AKASAKA (JAPAN).
Technologies for electronic transfer of information: The present state and trends in Japan N90-22443

GOSUDARSTVENNYI KOMITET PO ISPOLZOVANIYU ATOMNOI ENERGII, SERPUKHOV (USSR).
Development of the methods and means of precise forming and geometry control of superconducting current-carrying element for the UNR pulsed dipoles
[DE90-620108] N90-22419
Heat leak measurements in superconducting dipole magnet supports
[DE90-620109] N90-22420

GUELPH UNIV. (ONTARIO).
Computer conferencing: Minds meeting anywhere anytime N90-22452

H

HAMPTON INST., VA.
Direct solar-pumped iodine laser amplifier
[NASA-CR-186442] N90-22030
Development of mid-infrared solid state lasers for spaceborne lidar
[NASA-CR-185095] N90-22031

HARVARD UNIV., CAMBRIDGE, MA.
Recombination lines of C I and N II in the interstellar medium N90-22466

HAWAII UNIV., MAUI.
On decoding of multi-level MPSK modulation codes
[NASA-CR-186601] N90-22261

HELSINKI UNIV. OF TECHNOLOGY, ESPOO (FINLAND).
Adaptive frequency estimation by MUSIC (Multiple Signal Classification) method
[PB90-166794] N90-21943
Positron trapping in semiconductors
[PB90-165606] N90-22410

HONEYWELL, INC., GLENDALE, AZ.
Positive lubrication system N90-22097

HOUSTON UNIV., TX.
An investigation into the foundations of elastic-plastic fracture mechanics N90-22130
Opportunities for US-USSR cooperation in the investigation of Arctic stratospheric ozone N90-22154

HOWARD UNIV., WASHINGTON, DC.
A knowledge-based approach to improving optimization techniques in system planning N90-22303
Knowledge-based and integrated monitoring and diagnosis in autonomous power systems N90-22310

HUGHES AIRCRAFT CO., EL SEGUNDO, CA.
Experience with synthetic fluorinated fluid lubricants N90-22095

I

IDAHO NATIONAL ENGINEERING LAB., IDAHO FALLS.
Microstructure and mechanical properties of nickel aluminide powders consolidated by extrusion and hot isostatic pressing
[DE90-009777] N90-21855
Beam propagation in direct nuclear pumped laser amplifiers
[DE90-009613] N90-22035
Insights into complex human performance
[DE90-006957] N90-22214

ILLINOIS UNIV., URBANA-CHAMPAIGN.
Nonlinear spline operator interpolation and sliding control of deformable maneuvering bodies N90-21878
The mechanics of shear band formation in thermal viscoplastic materials at high rates of loading N90-22128
Transport properties of anisotropic superconductors N90-22404
The synergism of analytic and numerical techniques in general relativity: Calculation of radiative spacetimes N90-22425

ILLINOIS UNIV. AT URBANA-CHAMPAIGN, SAVOY.
Transport and relaxation properties in anisotropic superconductors N90-22403

IMATRAN VOIMA OY, HELSINKI (FINLAND).
Reliability importance measures and their calculation
[DE90-620391] N90-22057

INDIANA UNIV., BLOOMINGTON.
The evolution of the supernova remnant IC 443 N90-22486

INFORMATION TECHNOLOGY APPLICATIONS S.A. (LUXEMBOURG).
Electronic mail systems N90-22451

INSTITUTE FOR SPACE AND TERRESTRIAL SCIENCE, YORK (ONTARIO).
Inclusion of clouds and rain in atmospheric slant path calculations N90-21925

INSTITUTE FOR TELECOMMUNICATION SCIENCES, BOULDER, CO.
Modeling millimeter-wave propagation effects in the atmosphere N90-21922

INSTITUTE OF OCEANOGRAPHIC SCIENCES, WORMLEY (ENGLAND).
Measurement of the reflectance ratio of natural light in the sea
[IOS-265] N90-22199
Survey of instrumental methods for the determination of the high frequency wave spectrum
[IOS-267] N90-22200
A free surface Bryan-Cox-Semtner model
[IOS-270] N90-22201

INSTITUTO DE PESQUISAS ESPACIAIS, SAO JOSE DOS CAMPOS (BRAZIL).
Analysis, selection, and implementation of procedures which approve optimal artificial satellite maneuvers
[INPE-5003-TDL/397] N90-21786
Accurate nonlinear control for satellites using reaction wheels
[INPE-4983-PRE/1546] N90-21787
Experimental determination of thermal conductance in bolted joint impact in satellites
[INPE-4989-PRE/1551] N90-21788
Numerical simulation model of hydrazine attitude control thrusters
[INPE-4965-PRE/1534] N90-21848
Spectral response of wheat and its relationship with agronomic variables in the tropical region
[INPE-5018-RPE/612] N90-22138
Field reports on radiometric campaigns of soybeans in the Federal district: Safra 88/89
[INPE-5021-RPE/615] N90-22139

An intelligent interface for the design of optimal control systems [INPE-4917-PRE/1516] N90-22332
Object detection using structural matching [INPE-4954-PRE/1532] N90-22333
UD filtering and smoothing applied to orbit determination [INPE-4966-PRE/1535] N90-22501

INSTITUTO DE PESQUISAS ESPACIAIS, SAO PAULO (BRAZIL).
Geographic information system: Coded data of agrocattle-raising projects in the Amazon [INPE-4978-PRE/1543] N90-22457

INTERNATIONAL ATOMIC ENERGY AGENCY, VIENNA (AUSTRIA).
Impurity control in toroidal devices [DE90-618585] N90-22399

IOWA STATE UNIV. OF SCIENCE AND TECHNOLOGY, AMES.
A dual potential formulation of the Navier-Stokes equations N90-21972

IOWA UNIV., IOWA CITY.
Numerical study of laminar and turbulent flows past two-dimensional and axisymmetric bodies N90-22020

J

JET PROPULSION LAB., CALIFORNIA INST. OF TECH., PASADENA.
The Telecommunications and Data Acquisition Report [NASA-CR-186479] N90-21880
Precise estimation of tropospheric path delays with GPS techniques N90-21881
The determination of maximum deep space station slew rates for a high Earth orbiter N90-21882
Microwave analog fiber-optic link for use in the deep space network N90-21883
Galileo Earth approach navigation using connected-element interferometer phase-delay tracking N90-21884
Using connected-element interferometer phase-delay data for Magellan navigation in Venus orbit N90-21885
Voltage source ac-to-dc converters for high-power transmitters N90-21886
Dual-shaped offset reflector antenna designs from solutions of the geometrical optics first-order partial differential equations N90-21887
A real-time signal combining system for Ka-band feed arrays using maximum-likelihood weight estimates N90-21888
Ultralow noise performance of an 8.4-GHz maser-feedhorn system N90-21889
Radiometric tests on wet and dry antenna reflector surface panels N90-21890
A functional description of the advanced receiver N90-21891
QPSK carrier-acquisition performance in the advanced receiver 2 N90-21892
Digital Doppler extraction demonstration with the advanced receiver N90-21893
Exact closed-form expressions for the performance of the split-symbol moments estimator of signal-to-noise ratio N90-21894
A VLSI decomposition of the deBruijn graph N90-21895
Validity of the two-level model for Viterbi decoder gap-cycle performance N90-21896
Finding the complete path and weight enumerators of convolutional codes N90-21897
An adaptive vector quantization scheme N90-21898
A VLSI design for a systolic Viterbi decoder N90-21899
Radar RFI at Goldstone DSS 12 and DSS 16 N90-21900
Improving a data-acquisition software system with abstract data type components N90-21901
Structural fatigue in the 34-meter HA-Dec antennas N90-21902
Mark 4-A DSCC (Magellan-era) telemetry system description N90-21903
A higher density VLBI catalog for navigating Magellan and Galileo N90-21904
An 8.4-GHz dual-maser front-end system for Parkes reimplementation N90-21905
Development of shape memory metal as the actuator of a fail safe mechanism N90-22081
A soft actuation system for segmented reflector articulation and isolation N90-22084
A new six-degree-of-freedom force-reflecting hand controller for space telerobotics N90-22089
Algorithms and architectures for robot vision N90-22236
Resource Allocation Planning Helper (RALPH): Lessons learned N90-22296
PLAN-IT-2: The next generation planning and scheduling tool N90-22298
System control of an autonomous planetary mobile spacecraft N90-22313

JOHNSON AERONAUTICS, PALO ALTO, CA.
Airloads, wakes, and aeroelasticity [NASA-CR-177551] N90-21738

K

KANSAS STATE UNIV., MANHATTAN.
Reactions of N2A3 sigma u + and candidates for short wavelengths lasers [DE90-009514] N90-22033

KANSAS UNIV. CENTER FOR RESEARCH, INC., LAWRENCE.
Modern developments in shear flow control with swirl [NASA-CR-186586] N90-22000

KENTUCKY UNIV., LEXINGTON.
Elastodynamic scattering and transmission problems in three dimensions by the boundary integral equation method N90-22077

L

L'GARDE, INC., TUSTIN, CA.
Inflatable antennas for microwave pwoer transmission N90-21799

LABORATORIO DE COMPUTACAO CIENTIFICA, RIO DE JANEIRO (BRAZIL).
High order P-G finite elements for convection-dominated problems [DE90-614743] N90-21998

LANCASTER UNIV. (ENGLAND).
Sulphur silicate interactions on the Jovian satellite Io N90-22515

LARGE SCALE PROGRAMS INST., AUSTIN, TX.
A superconducting quenchgun for delivering lunar derived oxygen to lunar orbit [NASA-CR-185161] N90-21806
A trajectory generation and system characterization model for cislunar low-thrust spacecraft. Volume 2: Technical manual [NASA-CR-185172] N90-21807

LAWRENCE LIVERMORE NATIONAL LAB., CA.
Free electron lasers driven by linear induction accelerators: High power radiation sources N90-21800
A comparison of the autoignition chemistry of n-butane and isobutane in an internal combustion engine [DE90-009474] N90-21838
Transient effects in Brillouin gain spectroscopy in solids [DE90-009476] N90-21839
High resolution stimulated Raman-Brillouin spectroscopy in gases and solids [DE90-009535] N90-21840
Brillouin gain spectroscopy in glasses and crystals [DE90-009536] N90-21841
Martensitic transformation induced by stress pulses [DE90-009534] N90-21854
Stability studies of a pH-sensitive polymer matrix: Applications to fiber optic pH sensors [DE90-009579] N90-21867
Computer simulation of ionospheric radio frequency heating [DE90-009478] N90-21944
An assessment of the hardness of miniature vacuum tubes to high-voltage transients [DE90-009541] N90-21956
Plane Stokes flow driven by capillarity on a free surface: Overview and status [DE90-009186] N90-22008
Plane Stokes flow driven by capillarity on a free surface: Overview and status [DE90-009290] N90-22009
Reactions of N2A3 sigma u + and candidates for short wavelengths lasers [DE90-009514] N90-22033
Injection-seeded Nd:YAG laser linewidth measurement using saturation spectroscopy in iodine [DE90-009537] N90-22034
SISAL 1.2: An alternative to FORTRAN for shared memory multiprocessors [DE90-005181] N90-22257
Engagement analysis study [DE90-009529] N90-22359
Correlated electron processes in ion-atom collisions [DE90-009477] N90-22370
Producing dense plasmas with x rays [DE90-009539] N90-22393
Improved crystal bending techniques applied to the LLNL dual-arm Johann mounting x ray spectrometer [DE90-009528] N90-22415
Update on the OPAL opacity code [DE90-009946] N90-22480

LEIDEN UNIV. (NETHERLANDS).
Efficient estimation in the Clayton-Cuzick model for survival data [TW-88-06] N90-22348
The theta-methods in the numerical solution of delay differential equations [TW-89-03] N90-22349
Stability radius of polynomials occurring in the numerical solution of initial value problems [TW-89-04] N90-22350
Stability criteria in the numerical solution of initial value problems [TW-89-05] N90-22351
Contractivity in the maximum norm for Runge-Kutta methods [TW-89-06] N90-22352
Stability analysis of numerical methods for delay differential equations [TW-89-09] N90-22353

LIFE SYSTEMS, INC., CLEVELAND, OH.
Impact of low gravity on water electrolysis operation [NASA-CR-185521] N90-21870

LIVERPOOL UNIV. (ENGLAND).
Recent progress in the dynamic plastic behavior of structures, part 5 N90-22069

LOCKHEED AIRCRAFT CORP., PALO ALTO, CA.
Development of the CLAES instrument aperture door system N90-22083

LOCKHEED ENGINEERING AND SCIENCES CO., WASHINGTON, DC.
USSR Space Life Sciences Digest, issue 25 [NASA-CR-3922(29)] N90-22203

LOCKHEED MISSILES AND SPACE CO., SUNNYVALE, CA.
The development of a complementary expendable launch vehicle interface for an STS deployable payload N90-22086
Driving and latching of the Starlab pointing mirror doors N90-22093

LOCKHEED SPACE OPERATIONS CO., COCOA BEACH, FL.
Clean access platform for orbiter N90-22103

LOS ALAMOS NATIONAL LAB., NM.
Scaling of nonnuclear kinetic-energy antisatellites [DE90-009758] N90-21791
Experimental observations on transition to turbulence in confined coaxial jets and other boundary layer flows [DE90-008939] N90-22005
Turbulence in slurry pipe flow [DE90-008940] N90-22006
Evaluating thermographic phosphors in an operating turbine engine [DE90-004874] N90-22044
Proceedings of the Conference on Technology-Based Confidence Building: Energy and Environment [CNSS-PAPERS-22] N90-22152
The pressure dilation of a deep, jointed region of the earth [DE90-007537] N90-22170
An anomalous wind between valleys: Its characteristics and a proposed explanation [DE90-008965] N90-22189
Daytime wind valleys adjacent to the Great Salt Lake [DE90-008991] N90-22190
The ASCOT 1988 valley/tributary interaction study [DE90-009043] N90-22191
An analysis of the finite-differenced, even-parity discrete-ordinates equations in slab geometry [DE90-006479] N90-22337
Pulsed laser processing of high temperature superconducting thin films [DE90-008928] N90-22413
Overview of current bulk and thick film high temperature superconductor processing strategies [DE90-008949] N90-22414

LOYOLA COLL., BALTIMORE, MD.
JETC (Japanese Technology Evaluation Center) Panel Report on High Temperature Superconductivity in Japan [NASA-CR-180413] N90-22409

LUNAR AND PLANETARY INST., HOUSTON, TX.
Topical Conference on the Origin of the Earth [NASA-CR-185061] N90-22166

M

MANCHESTER UNIV. (ENGLAND).
Herbig-Haro objects and stellar jets N90-22487

MANUFACTURING AND TECHNOLGY CONVERSION INTERNATIONAL, INC., COLUMBIA, MD.
Testing of an advanced thermochemical conversion reactor system [DE90-007989] N90-22141

MARTIN MARIETTA CORP., DENVER, CO.
The role of artificial intelligence techniques in scheduling systems N90-22297
Managing temporal relations N90-22304
Knowledge structure representation and automated updates in intelligent information management systems N90-22316

MARYLAND UNIV., COLLEGE PARK.
Lidar measurements of the optical propagation environment N90-21930
On three-dimensional scaling and consistent truncation of global atmospheric models N90-22164
Adaptive control of a flexible manipulator with unknown changing loads N90-22293

MASSACHUSETTS INST. OF TECH., CAMBRIDGE.
Operation of a step tunable megawatt gyrotron N90-21802
The 10-100 kW submillimeter gyrotron N90-21803

MASSACHUSETTS UNIV., AMHERST.
Interfacial studies in fiber-reinforced thermoplastic-matrix composites N90-21814
Molecular theory of fluid phase equilibria [PB90-131277] N90-21832
Radar scatterometry and polarimetry at 220 GHz N90-21935
The predictability and efficiency of human walking: Metabolic, mechanical, and biophysical considerations N90-22211
The Sagittarius B2 molecular cloud: An extreme case of a galactic center giant molecular cloud N90-22493
Kinematic models of cometary comae N90-22495

MCDONNELL AIRCRAFT CO., SAINT LOUIS, MO.
Exhaust environment measurements of a turbofan engine equipped with an afterburner and 2D nozzle [NASA-CR-4289] N90-21760

MESSERSCHMITT-BOELKOW-BLOHM G.M.B.H., MUNICH (GERMANY, F.R.).
Grid patching approaches for complex three-dimensional configurations N90-21985

MIAMI UNIV., OXFORD, OH.
Issues in development, evaluation, and use of the NASA Preflight Adaptation Trainer (PAT) [NASA-CR-185608] N90-22212

MICHIGAN TECHNOLOGICAL UNIV., HOUGHTON.
Elastic stability and nonlinear behavior of imperfect shells with initial stresses N90-22070

MICHIGAN UNIV., ANN ARBOR.
Millimeter-wave bistatic scattering by terrain N90-21936
Interaction of a turbulent round jet with the free surface N90-21964
Homogeneous dilute turbulent particle-laden water flows N90-21965
Natural modes of cracked beams and identification of cracks N90-22075
The calculation of infrared limb emission by ozone in the terrestrial middle atmosphere N90-22151
Spectrum formation in active galactic nuclei and Type 2 supernovae N90-22490

MICROTRONICS ASSOCIATES, PITTSBURGH, PA.
Parallel asynchronous hardware implementation of image processing algorithms N90-22219

MID INFORMATION LOGISTICS GROUP G.M.B.H., HEIDELBERG (GERMANY, F.R.).
Electronic publishing with Standard Generalized Markup Language (SGML) N90-22450

MIDWEST RESEARCH INST., GOLDEN, CO.
Photovoltaic Program Branch [DE90-000318] N90-22142

MIDWEST RESEARCH INST., KANSAS CITY, MO.
Studies of 60-Hz exposure effects on human function [DE90-009473] N90-22210

MINISTERE DE L'EDUCATION NATIONALE, PARIS (FRANCE).
Megatendances N90-22445

MINNESOTA UNIV., MINNEAPOLIS.
The modeling of IRAS detections of classical novae and related objects N90-22482

MINORITY SERVICES, INC., WASHINGTON, DC.
Microwave Landing System (MLS) remote monitoring subsystem/remote maintenance monitoring system [DOT/FAA/PS-89/2] N90-21749
Microwave Landing System (MLS) multiple system design interoperability interface control report [DOT/FAA/SA-89/2] N90-21750

MISSISSIPPI STATE UNIV., MISSISSIPPI STATE.
Proceedings of the Advisory Committee on Standardization of Carbon-Phenolic Test Methods and Specifications [NASA-CR-186478] N90-21817
General structured grid generation systems N90-21977
Unsteady Euler solutions on dynamic blocked grids for complex configurations N90-21982

MISSISSIPPI UNIV., UNIVERSITY.
Automated analysis of measured turbulent boundary flow [PB90-147844] N90-21970

MISSOURI UNIV., COLUMBIA.
Engineering specification and system design for CAD/CAM of custom shoes: UMC project effort [NASA-CR-186547] N90-22255

MPB CORP., KEENE, NH.
On the design and development of a miniature ceramic gimbal bearing N90-22100

N

NATIONAAL INST. VOOR KERNFYSICA EN HOGE ENERGIEFYSICA, AMSTERDAM (NETHERLANDS).
New algorithms for one-loop integrals [NIKHEF-H/89-17] N90-22268
QCD Compton scattering at HERA energy [NIKHEF-H/89-3] N90-22372
Theory of a charged spinning particle in a gravitational and electromagnetic field [NIKHEF-H/89-4] N90-22373
Operator algebra from fusion rules: The infinite number of Ising theories [NIKHEF-H/89-7] N90-22374
Generalized killing equations and symmetries of spinning space [NIKHEF-H/89-8] N90-22375
Exclusive production of p, p-, pi, and pi- in photon photon collisions [NIKHEF-H/89-9] N90-22376

NATIONAL AERONAUTICS AND SPACE ADMINISTRATION, WASHINGTON, DC.
Aeronautical engineering: A continuing bibliography with indexes (supplement 250) [NASA-SP-7037(250)] N90-21722
Final (Tier 1) environmental impact statement for the Galileo and Ulysses Missions [NASA-TM-102917] N90-21779
Final environmental impact statement for the Galileo Mission (Tier 2) [NASA-TM-102925] N90-22147
Draft environmental impact statement for the Galileo Mission (Tier 2) [NASA-TM-102926] N90-22148
Final Environmental Impact Statement for the Ulysses Mission (Tier 2) [NASA-TM-101104] N90-22162
Aerospace medicine and biology: A continuing bibliography with indexes (supplement 334) [NASA-SP-7011(334)] N90-22207
Aerospace medicine and biology: A continuing bibliography with indexes (supplement 335) [NASA-SP-7011(335)] N90-22208
Space Station Workshop: Commercial Missions and User Requirements [NASA-TM-102912] N90-22428
Index to NASA news releases and speeches, 1986 [NASA-TM-101899] N90-22430
Index to NASA news releases and speeches, 1987 [NASA-TM-101900] N90-22431
Index to NASA news releases and speeches, 1988 [NASA-TM-101901] N90-22432
NASA Thesaurus supplement: A four part cumulative supplement to the 1988 edition of the NASA Thesaurus (supplement 3) [NASA-SP-7064-SUPPL-3] N90-22438
Research and Technology Objectives and Plans Summary (RTOPS) [NASA-TM-89662] N90-22528
NASA Information Sciences and Human Factors Program [NASA-TM-4190] N90-22529

NATIONAL AERONAUTICS AND SPACE ADMINISTRATION. AMES RESEARCH CENTER, MOFFETT FIELD, CA.
Extension of a streamwise upwind algorithm to a moving grid system [NASA-TM-102800] N90-21739
Analytical study of the origin and behavior of asymmetric vortices [NASA-TM-102796] N90-21746
Identification of XV-15 aeroelastic modes using frequency-domain methods [NASA-TM-101021] N90-21756
An upwind-differencing scheme for the incompressible Navier-Stokes equations [NASA-TM-101051] N90-21757
Quiet mode for nonlinear rotor models [NASA-TM-102236] N90-21758
Direct inversion of rigid-body rotational dynamics [NASA-TM-102798] N90-21773
Theoretical and experimental study of flow-control devices for inlets of indraft wind tunnels [NASA-TM-100050] N90-21778
Application of the TRANAIR rectangular grid approach to the aerodynamic analysis of complex configurations N90-21996
Cycle life machine for AX-5 space suit N90-22080
AX-5 space suit bearing torque investigation N90-22101
The psychology of computer displays in the modern mission control center [NASA-TM-100451] N90-22213
Vision Science and Technology at NASA: Results of a Workshop [NASA-TM-102214-REV-1] N90-22216
Sampling and noise in vision networks N90-22217
Networks for image acquisition, processing and display N90-22218
Visions of visualization aids: Design philosophy and experimental results N90-22220
Human motion perception: Higher-order organization N90-22226
Two-dimensional shape recognition using sparse distributed memory N90-22227
Filling in the retinal image N90-22229
A3I visibility modeling project N90-22230
Factors affecting the perception of transparent motion N90-22233
Photonic processing at NASA Ames Research Center N90-22234
Sparse distributed memory overview N90-22235
Computer vision techniques for rotorcraft low altitude flight N90-22237
Kalman filter based range estimation for autonomous navigation using imaging sensors N90-22238
Ames vision group research overview N90-22242
Pyramid image codes N90-22243
Preliminary development of an intelligent computer assistant for engine monitoring [NASA-TM-101702] N90-22322
Dynamical approach study of spurious steady-state numerical solutions of nonlinear differential equations. Part 1: The ODE connection and its implications for algorithm development in computational fluid dynamics [NASA-TM-102820] N90-22339
On spurious steady-state solutions of explicit Runge-Kutta schemes [NASA-TM-102819] N90-22340

NATIONAL AERONAUTICS AND SPACE ADMINISTRATION. GODDARD SPACE FLIGHT CENTER, GREENBELT, MD.
Development and integration of the capillary pumped loop GAS and Hitchhiker flight experiments [NASA-TM-100756] N90-21790
Thermomechanical properties of polymeric materials and related stresses [NASA-TM-100758] N90-21864
The connector space reduction mechanism N90-22092
Computation and parallel implementation for early vision N90-22222
Motion detection in astronomical and ice floe images N90-22231
Space environment robot vision system N90-22245
Self-calibration of robot-sensor system N90-22246
The 1990 Goddard Conference on Space Applications of Artificial Intelligence [NASA-CP-3068] N90-22294
The application of connectionism to query planning/scheduling in intelligent user interfaces N90-22295
The procedure safety system N90-22311
Using expert systems to implement a semantic data model of a large mass storage system N90-22315
NSSDC data listing [NASA-TM-102989] N90-22456

NATIONAL AERONAUTICS AND SPACE ADMINISTRATION. JOHN F. KENNEDY SPACE CENTER, COCOA BEACH, FL.
Induction-type metal detector with increased scanning area capability [NASA-CASE-KSC-11386-1] N90-22023
The 24th Aerospace Mechanisms Symposium [NASA-CP-3062] N90-22079
Design of a telescoping tube system for access and handling equipment N90-22102
The JPL/KSC telerobotic inspection demonstration N90-22312
Optical shutter switching matrix [NASA-CASE-KSC-11392-1] N90-22383

NATIONAL AERONAUTICS AND SPACE ADMINISTRATION. LYNDON B. JOHNSON SPACE CENTER, HOUSTON, TX.
Pressurized bellows flat contact heat exchanger interface [NASA-CASE-MSC-21271-1] N90-21999

Vision science and technology for supervised intelligent space robots N90-22221
Hybrid vision activities at NASA Johnson Space Center N90-22225

NATIONAL AERONAUTICS AND SPACE ADMINISTRATION. LANGLEY RESEARCH CENTER, HAMPTON, VA.
Three-dimensional simulation of vortex breakdown [NASA-TM-102664] N90-21744
Large space systems antenna technology N90-21798
Solar-pumped laser for free space power transmission N90-21804
Impact tolerant material [NASA-CASE-LAR-12887-3] N90-21822
New spectral features of stratospheric trace gases N90-21910
Applications of algebraic grid generation N90-21979
Device for quickly sensing the amount of O2 in a combustion product gas [NASA-CASE-LAR-13816-1] N90-22025
Lightweight piston architecture [NASA-CASE-LAR-13926-1] N90-22042
Development of cable drive systems for an automated assembly project N90-22105
The computational structural mechanics testbed data library description [NASA-TM-100645-REV-1] N90-22135
Image gathering, coding, and processing: End-to-end optimization for efficient and robust acquisition of visual information N90-22224
Graphics mini manual [NASA-TM-87622-REV] N90-22247
The art of fault-tolerant system reliability modeling [NASA-TM-102623] N90-22292

NATIONAL AERONAUTICS AND SPACE ADMINISTRATION. LEWIS RESEARCH CENTER, CLEVELAND, OH.
The vibro-acoustic mapping of low gravity trajectories on a Learjet aircraft [NASA-TM-103103] N90-21723
Performance characteristics of a one-third-scale, vectorable ventral nozzle for SSTOVL aircraft [NASA-TM-103120] N90-21725
Swept wing ice accretion modeling [NASA-TM-103114] N90-21727
Control of flow separation and mixing by aerodynamic excitation [NASA-TM-103131] N90-21733
On the use of external burning to reduce aerospace vehicle transonic drag [NASA-TM-103107] N90-21762
Free-Space Power Transmission [NASA-CP-10016] N90-21795
Effect of LEO cycling on 125 Ah advanced design IPV nickel-hydrogen battery cells [NASA-TM-103128] N90-21808
Photovoltaic power for Space Station Freedom [NASA-TM-102569] N90-21812
Computational simulation of structural fracture in fiber composites [NASA-TM-102505] N90-21821
METCAN verification status [NASA-TM-103119] N90-21824
Progression of damage and fracture in composites under dynamic loading [NASA-TM-103118] N90-21825
Matrix density effects on the mechanical properties of SiC/RBSN composites [NASA-TM-103098] N90-21826
Detailed mechanism for oxidation of benzene [NASA-TM-102443] N90-21842
Studies on the use of supercritical ammonia for ceramic nitride synthesis and fabrication [NASA-TM-102570] N90-21843
Electrochemical impregnation and cycle life of lightweight nickel electrodes for nickel-hydrogen cells [NASA-TM-103140] N90-21844
Polysiloxanes derived from the controlled hydrolysis of tetraethoxysilane as precursors to silica for use in ceramic processing [NASA-TM-102489] N90-21858
Self-lubricating polymer composites and polymer transfer film lubrication for space applications [NASA-TM-102492] N90-21862
High speed commercial transport fuels considerations and research needs [NASA-TM-102535] N90-21869
Probabilistic analysis of bladed turbine disks and the effect of mistuning [NASA-TM-102564] N90-21871
Numerical investigation of separated transonic turbulent flows with a multiple-time-scale turbulence model [NASA-TM-102499] N90-21962
Analysis of thermal energy storage material with change-of-phase volumetric effects [NASA-TM-102457] N90-21974
Computational modeling and validation for hypersonic inlets [NASA-TM-103111] N90-22011
An unsteady time asymptotic flow in the square driven cavity [NASA-TM-103141] N90-22016
Scattered-light scanner measurements of cryogenic liquid-jet breakup [NASA-TM-102432] N90-22021
Zero-G phase detector and separator [NASA-CASE-LEW-14844-1] N90-22024
Bearing elastohydrodynamic lubrication: A complex calculation made simple [NASA-TM-102575] N90-22041
Computerized inspection of gear tooth surfaces [NASA-TM-102395] N90-22054
Fatigue crack growth in unidirectional metal matrix composite [NASA-TM-103102] N90-22117
GRID2D/3D: A computer program for generating grid systems in complex-shaped two- and three-dimensional spatial domains. Part 1: Theory and method [NASA-TM-102453] N90-22262
Autonomous power expert system N90-22306
Electric power scheduling: A distributed problem-solving approach [NASA-TM-103149] N90-22323
Automating security monitoring and analysis for Space Station Freedom's electric power system [NASA-TM-103148] N90-22324
An expert system for simulating electric loads aboard Space Station Freedom [NASA-TM-103150] N90-22325
Growth and patterning of laser ablated superconducting YBa2Cu3O7 films on LaAlO3 substrates [NASA-TM-102436] N90-22421
Extraterrestrial life in the universe [NASA-TM-102363] N90-22464
Space Station Freedom solar array panels plasma interaction test facility [NASA-TM-102475] N90-22488

NATIONAL AERONAUTICS AND SPACE ADMINISTRATION. MARSHALL SPACE FLIGHT CENTER, HUNTSVILLE, AL.
Development of low thermal conductivity pan-based carbon fibers for solid rocket motor nozzle applications N90-21818
Testing carbon fabric for oxidation mass loss N90-21819
The temperature variation of hydrogen diffusion coefficients in metal alloys [NASA-TM-100397] N90-21836
Definition of large components assembled on-orbit and robot compatible mechanical joints [NASA-TM-100395] N90-22043
Orbital Maneuvering Vehicle (OMV) three-point docking latch N90-22094
Computer vision research at Marshall Space Flight Center N90-22240
New calculations and measurements of the Coulomb cross-section for the production of direct electron pairs by high energy nuclei [NASA-TM-101280] N90-22371
Gamma ray bursts: Current status of observations and theory [NASA-TM-100398] N90-22526

NATIONAL AERONAUTICS AND SPACE ADMINISTRATION. PASADENA OFFICE, CA.
Balanced bridge feedback control system [NASA-CASE-NPO-17430-1-CU] N90-21951

NATIONAL AEROSPACE LAB., AMSTERDAM (NETHERLANDS).
Design and testing of a multiblock grid-generation procedure for aircraft design and research N90-21984
European research on viscous flow (EuroVisc) [NLR-TP-89077-U] N90-22014

NATIONAL AEROSPACE LAB., TOKYO (JAPAN).
Numerical simulation of hypersonic flow around a space plane. Part 2: Application to high angles of attack flow [NAL-TR-1011T] N90-21726

NATIONAL CENTER FOR ATMOSPHERIC RESEARCH, BOULDER, CO.
The sources and chemistry of late winter Arctic tropospheric aerosols [PB90-131988] N90-22158

NATIONAL FEDERATION OF ABSTRACTING AND INDEXING SERVICES, PHILADELPHIA, PA.
Technology for electronic transfer of information: The present and future in North America N90-22442

NATIONAL GEOPHYSICAL DATA CENTER, BOULDER, CO.
Solar-geophysical data number 542, October 1989. Part 1: (Prompt reports). Data for September, August 1989, and late data [PB90-148669] N90-22520
Solar-geophysical data number 542, October 1989. Part 2: (Comprehensive reports). Data for April 1989 and miscellaneous [PB90-148677] N90-22521

NATIONAL INST. OF POLAR RESEARCH, TOKYO (JAPAN).
JARE data reports, no. 140 (meteorology 21): Meteorological data at Asuka Camp, Antarctica in 1987 [ISSN-0075-3343] N90-22188

NATIONAL INST. OF STANDARDS AND TECHNOLOGY, BOULDER, CO.
Institute for Materials Science and Engineering, Fracture and Deformation Division: Technical activities, 1989 [PB90-155359] N90-22106

NATIONAL INST. OF STANDARDS AND TECHNOLOGY, GAITHERSBURG, MD.
Institute for Materials Science and Engineering, nondestructive evaluation: Technical activities [PB90-132739] N90-22055
Supercomputers need super arithmetic [PB90-130253] N90-22252
Optimal 3-dimensional methods for linear programming [PB90-155391] N90-22253
An algorithm and computer program for the calculation of envelope curves [PB90-155409] N90-22254
Orthogonal distance regression [PB90-151747] N90-22336
Effect of a crystal-melt interface on Taylor-vortex flow [NASA-CR-186512] N90-22408

NATIONAL OCEANIC AND ATMOSPHERIC ADMINISTRATION, BOULDER, CO.
Scintillation of millimeter-wave intensity and phase caused by turbulence and precipitation N90-21912

NATIONAL OCEANIC AND ATMOSPHERIC ADMINISTRATION, SILVER SPRING, MD.
Wind tunnel investigation of three sonic anemometers [PB90-149808] N90-21729
Aerosol separator for use in aircraft [PB90-142217] N90-22155

NATIONAL PHYSICAL LAB., TEDDINGTON (ENGLAND).
VAMAS project on variable weld penetration: Surface tension of the steels [NPL-DMA(A)-188] N90-21856
New corrosion resistant ceramic coatings by laser processing [AERE-R-13166] N90-21863
Long term intensity stability of Auger electron spectrometers: Instructions for the interlaboratory comparison [NPL-DMM(A)-1] N90-22027
The approximation of a composite Bezier cubic curve by a composite Bezier quadratic curve [NPL-DITC-147/89] N90-22354
The use of local polynomial approximations in a knot-placement strategy for least squares spline fitting [NPL-DITC-148/89] N90-22355
Neural implementation of a method for solving systems of linear algebraic equations [NPL-DITC-155/89] N90-22356
The analysis of stress relaxation on indentation of a rigid punch into a viscoelastic sheet of finite thickness [NPL-DMA(A)-193] N90-22357
Non-random uncertainties in the calibration of protection-level secondary standards [NPL-RS(EXT)-110] N90-22378
Derivation of radiation beam non-uniformity corrections for the calibration of large volume ionisation chambers [NPL-RSA(EXT)-11] N90-22382
SGTE data for pure elements [NPL-DMA(A)-195] N90-22460

NATIONAL RESEARCH COUNCIL OF CANADA, VICTORIA (BRITISH COLUMBIA).
Tribomaterial factors in space mechanism brake performance N90-22096

NATIONAL TRANSPORTATION SAFETY BOARD, WASHINGTON, DC.
Aircraft accident report, United Airlines Flight 811, Boeing 747-122, N4713U, Honolulu, Hawaii, February 24, 1989 [PB90-910401] N90-21748

NATIONAL WEATHER SERVICE, GARDEN CITY, NY.
Second National Winter Weather Workshop Conducted by the National Weather Service [PB90-147414] N90-22183

NAVAL OCEAN SYSTEMS CENTER, SAN DIEGO, CA.
Evaporation duct effects at millimeter wavelengths N90-21914

Technique for selecting an aerosol model useful for infrared atmospheric transmittance calculations N90-21934

NAVAL RESEARCH LAB., WASHINGTON, DC.
The naval oceanic vertical aerosol model N90-21921
Modelling UV-visible radiation observed from space N90-21937
Adaptive pattern recognition by mini-max neural networks as a part of an intelligent processor N90-22317

NEW SOUTH WALES UNIV., KENSINGTON (AUSTRALIA).
Production and analysis by mass spectrometry of beams of polyglycol ions N90-21835
The effects of linear acceleration on perception and nystagmus N90-22209

NEW SOUTH WALES UNIV., SYDNEY (AUSTRALIA).
Excitatory and inhibitory backward conditioning in the rat N90-22204

NORTH AMERICAN AIRCRAFT OPERATIONS, LOS ANGELES, CA.
Conceptual design optimization study [NASA-CR-4298] N90-21755

NORTH CAROLINA STATE UNIV., RALEIGH.
An experimental investigation of the physical mechanisms controlling the asymmetric flow past slender bodies at large angles of attack N90-21767
Analysis of a six-component, flow-through, strain-gage, force balance used for hypersonic wind tunnel models with scramjet exhaust flow simulation [NASA-CR-186585] N90-21775
Inverse problems of heat conduction N90-21969
Development of a defect stream function, law of the wall/wake method for compressible turbulent boundary layers N90-22019

NORTHWESTERN UNIV., EVANSTON, IL.
Development of ultrasonic nondestructive methods for defect and damage characterization in composite materials N90-21816
Studies on reactive flows N90-21831
A stress-strength interference approach to fast and delayed fracture reliability analysis for ceramic components N90-21859
Contact mechanics for three-dimensional geometries N90-22076
Elasto-plastic analysis for contact fatigue failure N90-22078
Green's functions for the elastic annulus and their application to various crack problems N90-22129
Probabilistic finite elements: Applications to fracture and fatigue N90-22134

O

OAK RIDGE NATIONAL LAB., TN.
Mechanical properties of carbon-implanted niobium [DE90-009864] N90-21823
Photosynthetic water splitting, phase 2 [PB90-132671] N90-21833
Welding behavior and welding metallurgy of ductile intermetallic alloys [DE90-008908] N90-21852
The effect of aging at 343 C on type 308 stainless steel weldments [DE90-009232] N90-21853
Experimental performance of ozone-safe alternative refrigerants: Experimental performance comparisons of R32, R125, R143a, R218, R134a, R152a, R124, R142b, RC318 and R143 in a refrigeration circuit [DE90-009227] N90-21876
An alternative method to solving the kinematics of a redundant robot [DE90-006892] N90-22045
Trajectory generation for car-like robots [DE90-008407] N90-22047
Robots for aircraft coatings removal: Parameters and requirements [DE90-009429] N90-22048
Inclusion of unstable ductile tearing and extrapolated crack-arrest toughness data in PWR vessel integrity assessment [DE90-009427] N90-22116
Site visit to US Antarctic Program (USAP) facilities and the Research Vessel Polar Duke [DE90-009396] N90-22159
Understanding the computing system domain of advanced computing with microcomputers [DE90-009825] N90-22251
Symbolic pattern processing system for planar spatial structures [DE90-001598] N90-22256
A weak formulation for phase-change problems with bulk movement due to unequal densities [DE90-009398] N90-22361
Superconducting and semiconducting thin films of La(sub 123) and Y(sub 123) and their superlattices [DE90-009565] N90-22416
Grain boundary intermetallic phases in alloy 718 [DE90-009812] N90-22417
In-situ pulsed laser deposition of high-T(sub c) YBa(sub 2)Cu(sub 3)O(sub 7) superconducting thin films on (100) LaAlO3 substrates [DE90-009861] N90-22418
International science and technology policies: Testimony before the Subcommittee on International Scientific Cooperation, Committee on Science, Space, and Technology, United States House of Representatives [DE90-009416] N90-22463
The role of automation and robotics in the Lunar-Based Chemical Analysis Laboratory [DE90-009401] N90-22516

ODETICS, INC., ANAHEIM, CA.
Intensity dependent spread theory N90-22223
The intensity dependent spread model and color constancy N90-22228
Intensity dependent spread processor and workstation N90-22244

OFFICE NATIONAL D'ETUDES ET DE RECHERCHES AEROSPATIALES, PARIS (FRANCE).
Fast method for computing infrared transmission, computation examples N90-21942
Generation, optimization, and adaptation of multidomain meshes around complex configurations N90-21990

OFFICE OF MANAGEMENT AND BUDGET, WASHINGTON, DC.
Managing Federal information resources [PB90-100173] N90-22429
Current information technology resource requirements of the Federal government: Major systems acquisitions and planned resources [PB90-146820] N90-22439

OHIO STATE UNIV., COLUMBUS.
Recognition and analysis of aircraft targets by radar, using structural pattern representations derived from polarimetric signatures N90-21879
Finite element analysis of elastic contact problems with friction N90-22040

OKLAHOMA GEOLOGICAL SURVEY, NORMAN.
Natural resources information system for the state of Oklahoma [DE90-009483] N90-22458

OLD DOMINION COLL., NORFOLK, VA.
Expert systems for automated maintenance of a Mars oxygen production system [NASA-CR-186209] N90-22215

OLD DOMINION UNIV., NORFOLK, VA.
Extremely high data-rate, reliable network systems research [NASA-CR-186359] N90-22278
Traffic placement policies for a multi-band network N90-22279
CSMA/RN: A universal protocol for gigabit networks N90-22280
Distributed simulation, no special tools required N90-22281
Alternative parallel ring protocols N90-22282
Performance of gigabit FDDI N90-22283
Distributed simulation of network protocols N90-22284
Modelling high data rate communication network access protocol N90-22285
Extensibility and limitations of FDDI N90-22286
Fairness problems at the media access level for high-speed networks N90-22287
A carrier sensed multiple access protocol for high data base rate ring networks N90-22288

ONSALA SPACE OBSERVATORY (SWEDEN).
A comparison of photospheric and circumstellar (HCN)/(CO)-ratios for bright carbon stars [PB90-151101] N90-22477

OREGON GRADUATE CENTER FOR STUDY AND RESEARCH, PORTLAND.
Global distribution of organo-bromine gases N90-22150

OREGON STATE UNIV., CORVALLIS.
Regional wind energy assessment [DE90-009439] N90-22143
Cloud chemistry and occurrence in the western United States: A synopsis of current information [PB90-134248] N90-22182
Regional wind energy assessment [DE90-009380] N90-22192
Wind forecasting for utility operations [DE90-009466] N90-22193

OSAKA UNIV. (JAPAN).
New calculations and measurements of the Coulomb cross-section for the production of direct electron pairs by high energy nuclei [NASA-TM-101280] N90-22371

OSSERVATORIO ASTRONOMICO, ROME (ITALY).
Stability of compactification during inflation [NASA-CR-186597] N90-22502

OXFORD UNIV. (ENGLAND).
Modelling of the impact response of fibre-reinforced composites [OUEL-1784/89] N90-21827
Failure analysis of woven hybrid composite using a finite element method [OUEL-1791/89] N90-21828
Calculating the time domain average of gear vibration data sampled at less than the Nyquist frequency [OUEL-1768/89] N90-22052
Perturbation techniques in the dynamics and control of flexible manipulators [OUEL-1772/89] N90-22053
Transient response of a cylindrical shell of finite length to transverse impact [OUEL-1780/89] N90-22123
Edge recognition using image-processing hardware [OUEL-1777/89] N90-22271
Implementing the Canny edge recognizer with datacube image-processing hardware [OUEL-1786/89] N90-22272
A CSP model for distributed control software design [OUEL-1789/89] N90-22273
The WAVE model for advanced knowledge processing [OUEL-1803/89] N90-22291
A frame approach to the H-infinity super-optimal solution [OUEL-1761/89] N90-22327
The role of input weighting and bounding in the characteristic GPC method [OUEL-1762/89] N90-22328
Branch point placement [OUEL-1767/89] N90-22329
A robust stability result for generalised predictive control [OUEL-1773/89] N90-22330
Bicausal representations and multivariable generalized predictive control [OUEL-1781/89] N90-22331
Low order FIR and IIR filters in dynamic vision [OUEL-1785/89] N90-22384
On the theory of Heiser and Shercliff experiment. Part 1: MHD flow in an open channel in strong uniform magnetic field [OUEL-1804/89-PT-1] N90-22400
On the theory of Heiser and Shercliff experiment. Part 2: MHD flow between two cylinders in strong radical magnetic field [OUEL-1805/89-PT-2] N90-22401
Low temperature properties of amorphous solids N90-22405

P

PACIFIC NORTHWEST LAB., RICHLAND, WA.
Testing of an advanced thermochemical conversion reactor system [DE90-007989] N90-22141

PARAIBA UNIV., JOAO PESSOA (BRAZIL).
Proceedings of the 6th Regional Symposium on Biophysics [DE90-619618] N90-22206

PENNSYLVANIA STATE UNIV., UNIVERSITY PARK.
Prediction of forces and moments for flight vehicle control effectors. Part 1: Validation of methods for predicting hypersonic vehicle controls forces and moments [NASA-CR-186571] N90-21734
Prediction of forces and moments for flight vehicle control effectors. Part 2: An analysis of delta wing aerodynamic control effectiveness in ground effect [NASA-CR-186572] N90-21735
Lagrangian model simulation of the turbulent transport of evaporating jet droplets N90-22168
Tropopause undulations and the development of extratropical cyclones N90-22186
An investigation of the generation and radiation of aerodynamic noise in real piping systems N90-22368

PENNSYLVANIA UNIV., PHILADELPHIA.
A study of creep damage using microradiography and continuum damage mechanics N90-22109
A three-year study of the OH masers in Orion-KL and a study of the (3,2) transition of ammonia N90-22471

PHOBOS INDUSTRIAL APPLICATIONS CORP., AUSTIN, TX.
A robotically constructed production and supply base on Phobos [NASA-CR-186234] N90-21872

PITTSBURGH ENERGY TECHNOLOGY CENTER, PA.
Mathematical modeling of fluid-solid mixtures [DE90-009152] N90-22007

PITTSBURGH UNIV., PA.
The insertion of human dynamics models in the flight control loops of V/STOL research aircraft. Appendix 2: The optimal control model of a pilot in V/STOL aircraft control loops
[NASA-CR-186598] N90-21776
An adaptive human response mechanism controlling the V/STOL aircraft. Appendix 3: The adaptive control model of a pilot in V/STOL aircraft control loops
[NASA-CR-186599] N90-21777

POLITECNICO DI TORINO (ITALY).
Three-dimensional adaptive grids with limited skewness N90-21987

PRAIRIE VIEW AGRICULTURAL AND MECHANICAL COLL., TX.
Flow boiling with enhancement devices for cold plate coolant channel design
[NASA-CR-186358] N90-21961

PRATT AND WHITNEY AIRCRAFT, WEST PALM BEACH, FL.
Assessment of High Temperature Superconducting (HTS) electric motors for rotorcraft propulsion
[NASA-CR-185222] N90-21761

PRINCETON UNIV., NJ.
Unstructured mesh generation by a generalized Delaunay algorithm N90-21995
A methodology for knowledge-based restructurable control to accommodate system failures N90-22058
Scattering of waves by inclusions in a nonhomogeneous elastic half space solved by boundary element methods
[PB90-145699] N90-22107
Rigorous upper bounds for turbulent transport in bounded systems: Passive advection and reversed-field pinches N90-22390
The optical night sky at low surface brightness: High latitude dust and faint field galaxies N90-22481
A galaxy formation cookbook: Recipes and utensils N90-22508

PRINS MAURITS LAB. TNO, RIJSWIJK (NETHERLANDS).
On the direct simulation of vortex shedding
[LR-513] N90-21743
The pyrolysis of polymethylmethacrylate during combustion in a solid fuel combustion chamber
[LR-531] N90-21845
Solid fuel combustion chamber
[LR-562] N90-21846
Solid fuel combustion chamber
[LR-591] N90-21847

PROUDMAN OCEANOGRAPHIC LAB., BIRKENHEAD (ENGLAND).
An investigation of meteorological effects on currents in the shelf and continental slope seas northwest of the United Kingdom. 2: Relationships between currents at different locations and with other variables
[PB90-151911] N90-22195
European network of interest in the measurement and analysis of mean sea levels from tide gauge records
[PB90-151929] N90-22196

PURDUE UNIV., WEST LAFAYETTE, IN.
WINCOF-I code for prediction of fan compressor unit with water ingestion
[NASA-CR-185157] N90-21724
Energy release rate analysis of interfacial cracks in composites N90-21829
The controlled-damage concept in design of laminated composites N90-21830
Three-dimensional fatigue crack closure behavior of metals N90-21857
Saturated fluorescence measurements of the hydroxyl radical in laminar high-pressure flames
[NASA-CR-185218] N90-22022
Optimum design of structures under shock and vibration environment N90-22067
A spectral analysis approach to wave propagation in layered solids N90-22131
Three-dimensional finite element formulations for thick and thin laminated plates N90-22132

Q

QUEBEC UNIV., MONTREAL.
A knowledge-based system with learning for computer communication network design N90-22319

QUEENSLAND UNIV., BRISBANE (AUSTRALIA).
Coordinate systems for plastic yield surfaces stress and strain space theories
[PB90-164765] N90-22110

R

RAYTHEON CO., WALTHAM, MA.
An all electronic transportation system from LEO to GEO and beyond N90-21796

READING UNIV. (ENGLAND).
Residual stresses in laminated thermoplastic matrix composites N90-21815
Frontal structure in a mesoscale model N90-22187

RICE UNIV., HOUSTON, TX.
Optimization and guidance of flight trajectories in the presence of windshear
[NASA-CR-186163] N90-21747
Optimal trajectories for the aeroassisted flight experiment. Part 4: Data, tables, and graphs
[NASA-CR-186164] N90-21780
Infrared absorption spectroscopy and chemical kinetics of free radicals
[DE90-009469] N90-21837

RICHLAND OPERATIONS OFFICE (AEC), WA.
Prevention of significant deterioration application for approval to construct SP-100 Ground Engineering System Test Site
[DE90-007986] N90-22381

RIJKSWATERSTAAT, DELFT (NETHERLANDS).
Inventory of program packages related to the project SIMONA
[ETN-90-96397] N90-22270

RIKKYO UNIV., TOKYO (JAPAN).
Does mass accretion lead to field decay in neutron stars
[CAL-394] N90-22470

RISOE NATIONAL LAB., ROSKILDE (DENMARK).
Aerodynamics of a full-scale, non rotating wind turbine blade under natural wind conditions
[RISOE-M-2768] N90-22144
Rotor loading on a three-bladed wind turbine N90-22145
Optimization of power output from wind turbines N90-22146

ROCKWELL INTERNATIONAL CORP., HOUSTON, TX.
Constraint-based evaluation of sequential procedures N90-22301
Analyzing spacecraft configurations through specialization and default reasoning N90-22308

ROYAL AEROSPACE ESTABLISHMENT, FARNBOROUGH (ENGLAND).
Feature-associated mesh embedding for complex configurations N90-21988

ROYAL NETHERLANDS METEOROLOGICAL INST., DE BILT.
From Penman to Makkink: A new method for the calculation of the climatological evaporation numbers
[KNMI-TR-111] N90-22161

ROYAL SIGNALS AND RADAR ESTABLISHMENT, MALVERN (ENGLAND).
Multiwave diffraction analysis of transmission phase gratings
[RSRE-MEMO-4325] N90-21948
Performance of the IMP array processing algorithm: First results
[RSRE-MEMO-4291] N90-22274
An introduction to selected structured methods
[RSRE-MEMO-4294] N90-22275
A study of caching in capability computers
[RSRE-89015] N90-22276
UV photo-enhanced MOCVD of cadmium and cadmium telluride
[RSRE-MEMO-4208] N90-22422
Optical properties of zinc selenide grown using molecular beam deposition techniques
[RSRE-MEMO-4269] N90-22423

RUTGERS - THE STATE UNIV., NEW BRUNSWICK, NJ.
The stress field due to an edge dislocation and some fracture problems for a three-phase composite cylinder model N90-22126

RUTGERS UNIV., NEW BRUNSWICK, NJ.
Numerical investigation of some control methods for 3-D turbulent interactions due to sharp fins N90-21764

S

SAINT LOUIS UNIV., MO.
Dynamic and microphysical characteristics of cirrus clouds as revealed by aircraft, lidar, and other observations during FIRE N90-22177
A linear analysis of monsoon base states associated with banded convection N90-22179

SANDIA NATIONAL LABS., ALBUQUERQUE, NM.
Slotted-wall research with disk and parachute models in a low-speed wind tunnel
[DE90-002989] N90-21737
Surface structure and chemistry of high surface area silica gels
[DE90-007684] N90-21865
The influence of large, cold objects on engulfing fire environments
[DE90-003342] N90-21875
Aging characteristics of Li/SO(sub 2) cells
[NASA-CR-180432] N90-21954
Active primary lithium thionyl chloride battery for artillery applications
[DE90-009511] N90-21955
Partial acoustic filtering applied to the equations of compressible flow
[DE90-000673] N90-22001
Heat-transfer regimes in nuclear-reactor-pumped gas lasers
[DE90-002904] N90-22032
Data and conclusions from tests on small screws
[DE90-007500] N90-22046
Combining acoustic emission locations and a microcrack damage model to study development of damage in brittle materials
[DE90-005195] N90-22111
A continuum damage model for the quasi-static response of brittle materials
[DE90-007681] N90-22112
Severe shock and vibration environments for electronic components
[DE90-007686] N90-22113
Dynamic response of a complex encapsulated electronic assembly subjected to a severe shock environment
[DE90-007689] N90-22114
Continued research on the strain to failure of thick-walled cylinders subjected to internal pressure
[DE90-008952] N90-22115
Surface roughness and the physical properties of fractures
[DE90-006046] N90-22169
An acousto-optic image correlator with a throughput rate of 1000 templates per second
[DE90-009323] N90-22249
Molecular dynamics simulations of short-range force systems on 1024-node hypercubes
[DE90-009833] N90-22259
Paving: A new approach to automated quadrilateral mesh generation
[DE90-010244] N90-22260
Spline function smoothing and differentiation of noisy data on a rectangular grid
[DE90-009319] N90-22338
A refrigerated Dewar for the Josephson array voltage calibration system
[DE90-005237] N90-22412

SCIENCE AND TECHNOLOGY CORP., LAS CRUCES, NM.
Computation of broad spectral band electro-optical system transmittance response characteristics to military smokes and obscurants using field test data from transmissometer system measurements N90-21939

SCIENCE APPLICATIONS INTERNATIONAL CORP., BILLERICA, MA.
Minimizing the effects of the atmosphere in the observation of ultraviolet radiation N90-21911

SCIENCE APPLICATIONS INTERNATIONAL CORP., ORLANDO, FL.
Engagement analysis study
[DE90-009529] N90-22359

SCIENCE RESEARCH COUNCIL, DIDCOT (ENGLAND).
Millimetric, infrared, and optical propagation studies over a 500 m path N90-21913
Millimetre-wave propagation in the evaporation duct N90-21929

SELENIA S.P.A., ROME (ITALY).
The mm-wave region propagation experiments by satellite N90-21916

SHAPE TECHNICAL CENTER, THE HAGUE (NETHERLANDS).
Report on STC/Technische Universiteit (TU) Delft Extremely High Frequency (EHF) radio relay study N90-21915

SMITHSONIAN ASTROPHYSICAL OBSERVATORY, CAMBRIDGE, MA.
An astrophysics data program investigation of cluster evolution
[NASA-CR-181296] N90-22510

SOCIETE NATIONALE D'ETUDE ET DE CONSTRUCTION DE MOTEURS D'AVIATION, MOISSY-CRAMAYEL (FRANCE).
Mesh generation for flow computation in turbomachine N90-21981

SOUTHWEST RESEARCH INST., SAN ANTONIO, TX.
PIC code modeling of spacecraft charging potential during electron beam injection into a background of neutral gas and plasma, part 1
[NASA-CR-186602] N90-21792

SPACE TELESCOPE SCIENCE INST., BALTIMORE, MD.
An approach to rescheduling activities based on determination of priority and disruptivity N90-22299

STANFORD LINEAR ACCELERATOR CENTER, CA.
Scalable coherent interface
[DE90-008011] N90-22277

STANFORD UNIV., CA.
Optimal control of an aircraft flying through a downburst N90-21765

Stanford/NASA-Ames Center of Excellence in model-based human performance N90-22241

A generalized complementarity problem in Hilbert space
[DE90-009576] N90-22360

Nonlinear acoustic interactions in superfluid helium
N90-22367

Cyclotron maser and plasma wave growth in magnetic loops
[NASA-CR-179862] N90-22402

Waves in Saturn's rings probed by radio occultation
N90-22511

STATE UNIV. OF NEW YORK, ALBANY.

A case study of cloud-to-ground lightning during the GALE program N90-22185

STATE UNIV. OF NEW YORK, BUFFALO.

Recent advances in structural control N90-22062

STATE UNIV. OF NEW YORK, STONY BROOK.

Applications of remote sensing to studies of oceanic upper mixed layer dynamics N90-22137

Southern oscillation simulation in coupled ocean/atmosphere global climate models N90-22181

STATE UNIV. OF NEW YORK AT BUFFALO, AMHERST.

Prediction of length scales in a Mach reflection flowfield N90-21959

STEVENS INST. OF TECH., HOBOKEN, NJ.

Stable response of damped mechanical systems, 4
N90-22074

SUSSEX UNIV., BRIGHTON (ENGLAND).

Fast spectroscopic variations on rapidly-rotating, cool dwarfs. 3: Masses of circumstellar absorbing clouds on AB Doradus
[NASA-CR-186563] N90-22479

Topological defects in extended inflation
[NASA-CR-186594] N90-22505

SVERDRUP TECHNOLOGY, INC., BROOKPARK, OH.

Preliminary design of a long-endurance Mars aircraft
[NASA-CR-185243] N90-21763

SWEDISH INST. FOR MATERIALS TESTING, BORAS.

Test method for fire extinguishing powder, Nordtest project 675-87
[PB90-166984] N90-21874

T

TECHNISCHE UNIV., DELFT (NETHERLANDS).

A computer program for the prediction of nozzle-propeller performance
[LR-578] N90-21740

Theory and numerical analysis of single and multi-element nozzle propellers
[LR-579] N90-21741

Recent improvements in the scope and accuracy of the performance prediction of nozzle propellers
[LR-598] N90-21742

On the direct simulation of vortex shedding
[LR-513] N90-21743

First-order weight corrections for real-time flight path management
[LR-580] N90-21751

An approach to on-board optimization of cruise at constant altitude
[LR-581] N90-21752

The initial imperfection databank at the Delft University of Technology, part 3
[LR-568] N90-21783

The pyrolysis of polymethylmethacrylate during combustion in a solid fuel combustion chamber
[LR-531] N90-21845

Solid fuel combustion chamber
[LR-562] N90-21846

Solid fuel combustion chamber
[LR-591] N90-21847

Development, implementation and test of a computer program for the production of axisymmetric pattern moulds on a numerically controlled milling machine
[LR-593] N90-21877

Multiresolution and time-frequency representations of signals
[REPT-89-47] N90-21946

Electromagnetic inverse profiling of stratified media
[ETN-90-96402] N90-21947

Bifurcations in viscous flow fields. On the genesis and development of topologically complicated separated flow structures
[PB90-167156] N90-22012

The calibration and measuring procedure of a five-hole hemispherical head probe in compressible flow
[LR-585] N90-22013

Propagation of transient acoustic waves in porous media
[ETN-90-96401] N90-22015

Review of analysis methods for mechanically fastened joints in composites
[LR-599] N90-22050

Elastic and viscoelastic analysis of two multiply layered cylinders rolling over each other with Coulomb friction
[REPT-89-50] N90-22051

Fatigue crack growth predictions for variable-amplitude and spectrum loading
[LR-526] N90-22118

ANILISA: Computational module for Koiter's imperfection sensitivity theory
[LR-582] N90-22119

Computational methods and plasticity
[LR-583] N90-22120

Dynamics of an oscillator with three-degrees-of-freedom in a uniform windfield
[REPT-89-56] N90-22121

Graphs of the state of stress at rounded corners
[MEMT-1] N90-22122

Uncertainty analysis of the accident effect area of a BLEVE
[REPT-89-49] N90-22160

Local mode smoothing analysis for various incomplete factorization iterative methods in three dimensions
[REPT-89-38] N90-22263

Software quality assurance: Towards a measurable quality improvement
[REPT-89-42] N90-22264

Long steps with the logarithmic penalty barrier function in linear programming
[REPT-89-44] N90-22265

An introduction to Montague grammar
[REPT-89-46] N90-22266

Some remarks on treatment of be in Montague's PTQ
[REPT-89-40] N90-22267

Towards a Sarkovski order for the embedding of disks maintaining their orientation
[REPT-89-43] N90-22289

Parallel non-linear optimization
[REPT-89-45] N90-22290

Guide to RMS-literature
[REPT-89-52] N90-22326

Discrete variable structural optimization by the complex method
[LR-597] N90-22341

A Chinese bibliography on quadratic systems of differential equations
[REPT-89-39] N90-22342

Normal forms for weakly non-linear perturbed wave equations
[REPT-89-41] N90-22343

On a third q-Bessel function
[REPT-89-48] N90-22344

Generalizations of a q-analogue of Laguerre polynomials
[REPT-89-51] N90-22345

Preference numbers and funnel dimension
[REPT-89-57] N90-22346

Clustering and uniqueness in mathematical models of percolation phenomena
[ETN-90-96400] N90-22358

On the structure of Mandelbrot's percolation process and other random Cantor sets
[REPT-89-54] N90-22362

Object-oriented databases: How are they different and what differnece does it make
[REPT-89-55] N90-22459

TELDIX LUFTFAHRT-AUSRUESTUNGS G.M.B.H., HEIDELBERG (GERMANY, F.R.).

Test results and flight experience of ball bearing momentum and reaction wheels N90-22099

TEXAS A&M UNIV., COLLEGE STATION.

A video-based experimental investigation of wing rock
N90-21771

Graphically-oriented nonlinear analysis of statically loaded plane frames on microcomputers
[PB90-165945] N90-22248

TEXAS UNIV., AUSTIN.

A decentralized linear quadratic control design method for flexible structures N90-21770

Current management for improved railgun performance N90-21781

Bounded-time fault-tolerant rule-based systems
N90-22318

Computer simulation of time-dependent spherically symmetric spacetimes containing radiating fluids: Formalism and code tests N90-22483

Modelling late-time atmospheres of supernovae
N90-22500

Slow shocks in coronal mass ejections
[NASA-CR-186578] N90-22522

TEXAS UNIV. HEALTH SCIENCE CENTER, HOUSTON.

Research in biological separations and cell culture
[NASA-CR-172060] N90-22202

THIOKOL CORP., BRIGHAM CITY, UT.

Flight motor set 360L002 (STS-27R). Volume 5: Nozzle component
[NASA-CR-183945] N90-21811

Shelf life extension for the lot AAE nozzle severance LSCs
[NASA-CR-183878] N90-21813

Flight set 360T004 (STS-30)
[NASA-CR-183927] N90-22049

THIOKOL CORP., CAPE CANAVERAL AFS, FL.

Circularity measuring system: A shape gauge designed especially for use on large objects N90-22104

TILBURG UNIV. (NETHERLANDS).

On the existence of a positive definite solution of the matrix equation X + A(sup tau)X(exp -1)A = I
[PB90-133976] N90-22335

TOSHIBA CORP., KAWASAKI (JAPAN).

Development of a multipurpose hand controller for JEMRMS N90-22087

TRW, INC., REDONDO BEACH, CA.

Spacecraft command verification: The AI solution
N90-22307

Automated procedure execution for space vehicle autonomous control N90-22314

TRW SPACE TECHNOLOGY LABS., REDONDO BEACH, CA.

Active control of bearing preload using piezoelectric translators N90-22098

U

UNITED KINGDOM ATOMIC ENERGY AUTHORITY, HARWELL (ENGLAND).

The classification of defects from ultrasonic measurements
[AERE-R-13306] N90-22056

UNITED TECHNOLOGIES CORP., SAN JOSE, CA.

Hybrid propulsion technology program. Volume 1: Conceptional design package
[NASA-CR-183953] N90-21793

Hybrid propulsion technology program. Volume 2: Technology definition package
[NASA-CR-183954] N90-21794

UNITED TECHNOLOGIES RESEARCH CENTER, EAST HARTFORD, CT.

Framework for a space shuttle main engine health monitoring system
[NASA-CR-185224] N90-21809

UNIVERSITEIT TWENTE, ENSCHEDE (NETHERLANDS).

Incomparable elements in algebraic lattices with applications to formal language theory
[MEMO-INF-89-54] N90-22269

Hopf bifurcation with nonsemisimple 1:1 resonance e
[MEMO-808] N90-22347

UNIVERSITY COLL. OF SWANSEA (WALES).

Unstructured finite element mesh generation and adaptive procedures for CFD N90-21993

UNIVERSITY OF WESTERN ONTARIO, LONDON.

Vibration analysis of systems with random parametric excitations N90-22060

US INTERNATIONAL SPACE YEAR ASSOCIATION, WASHINGTON, DC.

Mission to planet Earth N90-22153

V

VIBRATION INST., CLARENDON HILLS, IL.

The Shock and Vibration Digest, volume 21, no. 2
N90-22059

The Shock and Vibration Digest, volume 21, no. 1
N90-22061

The Shock and Vibration Digest, volume 21, no. 3
N90-22064

The Shock and Vibration Digest, volume 21, no. 7
N90-22066

The Shock and Vibration Digest, volume 21, no. 8
N90-22068

The Shock and Vibration Digest, volume 22, no. 1
N90-22073

The Shock and Vibration Digest, volume 21, no. 6
N90-22363

VIRGINIA POLYTECHNIC INST. AND STATE UNIV., BLACKSBURG.

Effective methods of controlling a junction vortex system in an incompressible, three-dimensional, turbulent flow
N90-21732

Optimal and near-optimal medium range air-to-air missile guidance against maneuvering targets N90-21766

Strength in notched and impact-damaged laminates
N90-21820

Laser Doppler anemometry measurements of a confined turbulent water jet with a uniform background flow
N90-21971

Convergence acceleration of upwind relaxation methods for the Navier-Stokes equations N90-21973

VIRGINIA UNIV., CHARLOTTESVILLE.

The distribution of molecular clouds in spiral galaxies
N90-22489

VOLVO FLYGMOTOR A.B., TROLLHAETTAN (SWEDEN).
Algebraic block-structured grid generation based on a macro-block concept N90-21978

W

WASEDA UNIV., TOKYO (JAPAN).
Soft inflation
[NASA-CR-186593] N90-22506

WASHINGTON UNIV., SEATTLE.
An experimental investigation of mixing in buoyant flows N90-21963
Modeling the lateral diffusion of fluorescent particles within a forest canopy N90-22136
The observed three-dimensional structure of baroclinic waves in the Northern Hemisphere winter as revealed in a linear regression analysis N90-22167
Characteristics of cumulus bandclouds off the east coast of Hawaii N90-22178
Evaluation of optical storage technology for decision support databases N90-22436
The association of supernovae with regions of recent star formation in late-type galaxies N90-22497

WAYNE STATE UNIV., DETROIT, MI.
Numerical solutions of the nonlinear theory of curved beams N90-22071

WEST VIRGINIA UNIV., MORGANTOWN.
Numerical simulation of liquid circulation in a bubbly column
[DE90-005226] N90-22002

WESTINGHOUSE HANFORD CO., RICHLAND, WA.
Fracture toughness and tensile properties of alloy HT9 in thin sections under high neutron fluences
[DE90-008386] N90-21851

WISCONSIN UNIV., MADISON.
Cirrus cloud optical properties measured with the University of Wisconsin high spectral resolution and volume imaging lidars N90-21932
Hail growth in a highly-glaciated central high plains multi-cellular hailstorm N90-22184
Magnetic turbulence versus safety factor in the Tokapole 2 tokamak N90-22391

WISCONSIN UNIV., MILWAUKEE.
Knowledge-based semantic query processing: An optimal transformation approach N90-22437

WYOMING UNIV., LARAMIE.
Nonlinear fracture mechanics using semicircular specimens and tension-softening behavior N90-22108

Y

YALE UNIV., NEW HAVEN, CT.
High intensity laser beam interactions with single droplets N90-21924

YORK UNIV. (ONTARIO).
Inclusion of clouds and rain in atmospheric slant path calculations N90-21925

CONTRACT NUMBER INDEX

SCIENTIFIC AND TECHNICAL AEROSPACE REPORTS VOLUME 28 NUMBER 15

Typical Contract Number Index Listing

AF-AFOSR-0039-88 .... N90-10330
CONTRACT NUMBER
NASA ACCESSION NUMBER

Listings in this index are arranged alphanumerically by contract number. Under each contract number the NASA accession numbers denoting documents that have been produced as a result of research done under that contract are arranged in ascending order. The NASA accession number denotes the number by which the citation is identified.

AF-AFOSR-0100-88 .... N90-21924
AF-AFOSR-0129-87 .... N90-21827
N90-21828
CEC-500-86-012 .... N90-22141
CIT-INF-89-002-01 .... N90-22281
N90-22282
N90-22284
N90-22285
N90-22288
CIT-RF-89-002-01 .... N90-22283
N90-22286
N90-22287
CITT-596041 .... N90-22279
DA PROJ. 1L1-62209-AH-47-A N90-22054
DAAG08-83-C-0011 .... N90-22047
DAAL03-88-K-0040 .... N90-21924
DE-AC01-79ET-32043 .... N90-22379
N90-22380
DE-AC02-76CH-00016 .... N90-22411
DE-AC02-76ER-01545 .... N90-22426
DE-AC02-83CH-10093 .... N90-22142
DE-AC02-83ER-40105 .... N90-22426
DE-AC03-76SF-00098 .... N90-22171
N90-22172
N90-22173
N90-22174
DE-AC03-76SF-00515 .... N90-22277
DE-AC03-89ER-53277 .... N90-22398
DE-AC04-76DP-00613 .... N90-21866
N90-22026
DE-AC04-76DP-00789 .... N90-21737
N90-21865
N90-21875
N90-21954
N90-21955
N90-22001
N90-22032
N90-22046
N90-22111
N90-22112
N90-22113
N90-22114
N90-22115
N90-22169
N90-22249
N90-22259
N90-22260
N90-22338
N90-22412
DE-AC05-84OR-21400 .... N90-21823
N90-21833
N90-21852
N90-21853
N90-21876
N90-22045
N90-22047
N90-22048
N90-22116
N90-22159
N90-22251
N90-22256
N90-22361
N90-22416
N90-22417
N90-22418
N90-22463
N90-22516
DE-AC06-76RL-01830 .... N90-22141
DE-AC06-87RL-10930 .... N90-21851
N90-22381
DE-AC07-76ID-01570 .... N90-21855
N90-21957
N90-21958
N90-22004
N90-22010
N90-22035
N90-22214
N90-22250
N90-22258
DE-AC22-84PC-70507 .... N90-22394
N90-22395
N90-22396
N90-22397
DE-AI79-86BP-63406 .... N90-22143
N90-22192
N90-22193
DE-FG01-89CE-34025 .... N90-22210
DE-FG03-87ER-25028 .... N90-22360
DE-FG04-87AL-44658 .... N90-21838
DE-FG05-85ER-13439 .... N90-21837
DE-FG22-87PC-79935 .... N90-22002
DE-FG22-89BC-14483 .... N90-22458
DTFA03-83-A-00328 .... N90-21724
FNSRS-1-467-0-86 .... N90-22265
GRI-5083-260-0880 .... N90-21833
GRI-5086-260-1223 .... N90-21832
JPL-956415 .... N90-21780
MIPR-125-88 .... N90-21912
MRI PROJ. RA-111-C N90-22210
NAGW-567 .... N90-22468
N90-22469
NAGW-1105 .... N90-21789
NAGW-1231 .... N90-21792
N90-22371
NAGW-1321 .... N90-22426
NAGW-1340 .... N90-22426
N90-22502
N90-22503
N90-22504
N90-22505
N90-22506
N90-22525
NAGW-1618 .... N90-22467
N90-22469
N90-22470
NAG1-441 .... N90-22030
NAG1-516 .... N90-21747
NAG1-849 .... N90-21734
N90-21735
NAG1-875 .... N90-22255
NAG1-877 .... N90-22031
NAG1-908 .... N90-22278
N90-22279
N90-22281
N90-22282
N90-22283
N90-22284
N90-22285
N90-22286
N90-22287
N90-22288
NAG2-463 .... N90-22232
NAG3-108 .... N90-21952
NAG3-351 .... N90-22022
NAG3-463 .... N90-21849
NAG3-481 .... N90-21724
NAG3-485 .... N90-22017
NAG3-729 .... N90-21776
N90-21777
NAG3-776 .... N90-22389
NAG3-928 .... N90-21806
N90-21807
NAG3-929 .... N90-22262
NAG3-997 .... N90-22262
NAG5-761 .... N90-22522
NAG5-931 .... N90-22261
NAG5-1076 .... N90-22479
NAG5-1200 .... N90-22510
NAG8-497 .... N90-22468
NAG8-545 .... N90-21817
NAG8-755 .... N90-21780
NAG9-308 .... N90-22215
NAG9-310 .... N90-21961
NASA ORDER A-41521 .... N90-21954
NASA ORDER C-99066-G N90-21962
NASG-931 .... N90-22426
NASW-4066 .... N90-22166
NASW-4292 .... N90-22203
NASW-4324 .... N90-21754
NASW-4435 .... N90-21872
NAS1-18015 .... N90-21755
NAS1-18027 .... N90-21772
NAS1-18419 .... N90-21994
NAS1-18599 .... N90-21745
N90-22017
NAS1-18645 .... N90-22219
NAS1-18670 .... N90-21994
NAS1-18762 .... N90-21785
NAS2-11555 .... N90-21738
NAS2-12513 .... N90-21996
NAS3-25117 .... N90-21761
NAS3-25266 .... N90-21763
NAS3-25626 .... N90-21809
NAS8-30490 .... N90-21811
N90-21813
N90-22049
NAS8-36719 .... N90-22065
NAS8-37778 .... N90-21793
N90-21794
NAS9-17403 .... N90-22202
NAS9-17413 .... N90-22212
NAS9-17966 .... N90-21870
NCC1-122 .... N90-22309
NCC1-129 .... N90-21775
NCC2-506 .... N90-21753
NCC2-634 .... N90-21736
NCC3-56 .... N90-22000
NGR-01-010-001 .... N90-22205
NGR-06-002-112 .... N90-21810
N90-21953
NIST 60NANB-4-D0033 .... N90-21861
NIST 60NANB-7-D0737 .... N90-21834
NOAA-NA-86AADSG040 .... N90-22197
NR PROJ. RM-35G80 .... N90-21934
NSF AST-86-02831 .... N90-22468
N90-22469
NSF AST-88-20595 .... N90-22426
NSF ATM-87-05084 .... N90-22402
NSF ATM-87-09659 .... N90-22158
NSF DMS-89-13089 .... N90-22360
NSF ECE-86-07591 .... N90-22107
NSF ECS-86-57559 .... N90-22303
N90-22310
NSF MSM-88-18994 .... N90-22416
NSG-7092 .... N90-22402
NWO-62-58 .... N90-22269
N00014-78-C-0754 .... N90-21944
N00014-85-K-0177 .... N90-22407
N00014-85-K-0582 .... N90-21930
N00014-87-F-0053 .... N90-22253
N00014-89-J-1472 .... N90-22318
N00014-89-J-1659 .... N90-22360
N00014-89-J-1913 .... N90-22318
PNL-007109-A-C N90-22141
RF PROJ. 596043 .... N90-22281
N90-22282
N90-22283
N90-22284
N90-22285
N90-22286
N90-22287
RF PROJ. 596044 .... N90-22288
SUNYRF-88-3002 .... N90-22107
T/RF-35/G0056/G1237 .... N90-21933
W-31-109-ENG-38 .... N90-22003
W-7405-ENG-36 .... N90-21791
N90-22005

N90-22006
N90-22044
N90-22170
N90-22189
N90-22190
N90-22191
N90-22337
N90-22413
N90-22414
W-7405-ENG-48 .... N90-21838
N90-21839
N90-21840
N90-21841
N90-21854
N90-21867
N90-21944
N90-21956
N90-22008
N90-22009
N90-22033
N90-22034
N90-22257
N90-22359
N90-22370
N90-22393
N90-22415
N90-22480
307-51-00 .... N90-22421
314-50-20 .... N90-22213
474-10-52 .... N90-21974
474-46-10 .... N90-22488
488-10-12 .... N90-21806
488-51-03 .... N90-22323
N90-22324
N90-22325
505-60-00 .... N90-21739
N90-21757
N90-22339
N90-22340
505-60-01-01 .... N90-21744
N90-22247
505-60-21 .... N90-21778
505-61-51 .... N90-21738
505-61-71 .... N90-21746
505-62-21 .... N90-21724
N90-21733
N90-21842
N90-21962
N90-22011
N90-22016
N90-22021
505-62-71 .... N90-21725
505-62-91 .... N90-21760
505-63-1B N90-22041
505-63-01-10 .... N90-22135
505-63-11 .... N90-21825
505-63-51 .... N90-22054
505-66-11 .... N90-21773
505-66-21-01 .... N90-22292
505-66-29 .... N90-21758
505-66-41-01 .... N90-21772
505-66-71 .... N90-22322
505-67-00 .... N90-22216
505-68-11 .... N90-21727
505-68-91-06 .... N90-21745
505-69-61 .... N90-21761
505-474-46 .... N90-21812
506-41-21 .... N90-21808
N90-21844
506-42-51 .... N90-22022
506-43-11 .... N90-21862
506-43-41-01 .... N90-21755
506-64-12 .... N90-21807
510-01-0A N90-21821
N90-21824
N90-21826
N90-21843
510-01-01 .... N90-22117
532-06-00 .... N90-21756
535-05-01 .... N90-21858
N90-21869
N90-22262
553-13-00 .... N90-21809
N90-21849
N90-21871
590-14-41-04 .... N90-21785
591-11-31 .... N90-21763
591-22-31 .... N90-22043
694-03-03 .... N90-21723
763-01-21 .... N90-21762

REPORT/ACCESSION NUMBER INDEX

SCIENTIFIC AND TECHNICAL AEROSPACE REPORTS VOLUME 28 NUMBER 15

Typical Report Number Index Listing

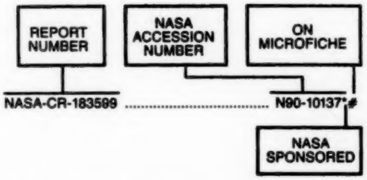

Listings in this index are arranged alphanumerically by report number. The NASA accession number denotes the number by which the citation is identified. An asterisk (*) indicates that the item is a NASA report. A pound sign (#) indicates that the item is available on microfiche.

A-11	N90-21943 #
A-88040	N90-21778* #
A-88268	N90-21756* #
A-89002	N90-21757* #
A-89211-REV-1	N90-22216* #
A-89247	N90-21758* #
A-90089	N90-21746* #
A-90098	N90-21773* #
A-90101	N90-21739* #
A-90148	N90-22340* #
A-90149	N90-22339* #
A-90165	N90-21738* #
AAR-244	N90-21747* #
AD-A201600	N90-22433 #
AD-A217469	N90-22407 #
AD-D014433	N90-21868 #
AD-D014434	N90-21850 #
AERE-R-13166	N90-21863
AERE-R-13306	N90-22056
AERO-ASTRONAUTICS-243-PT-4	N90-21780* #
AGARD-CP-454	N90-21907 #
AGARD-CP-464	N90-21975 #
AGARD-CP-466	N90-22440 #
AIAA-90-0756	N90-21727* #
AIAA-90-1935	N90-21762* #
AIAA-90-2000	N90-21763* #
AIAA-90-2271	N90-21725* #
AVSCOM-TR-89-C-011	N90-22054* #
AVSCOM-TR-90-C-006	N90-21826* #
B-229005	N90-22461 #
BCRS-89-20	N90-22140 #
BCRS-89-26	N90-22198 #
BNL-52230	N90-22411 #
BPA-88-28	N90-22192 #
BPA-89-30	N90-22193 #
BPA-89-33	N90-22143 #
BR111416	N90-22422 #
BR111474	N90-22275 #
BR111534	N90-22274 #
BR111748	N90-22423 #
BR112014	N90-21948 #
BR112197	N90-22276 #
CAL-371	N90-22468* #
CAL-377	N90-22469* #
CAL-394	N90-22470* #
CAL-1793	N90-22467* #
CFA-89-2985	N90-22426* #
CMU-HEP90-03	N90-22504* #
CNSS-PAPERS-22	N90-22152 #
CONF-891052-2	N90-22480 #
CONF-891097-5	N90-21956 #
CONF-891119-120	N90-22416 #
CONF-891119-122	N90-22418 #
CONF-891195-SUMM	N90-22411 #
CONF-891261-9	N90-22035 #
CONF-900140-19	N90-21867 #
CONF-900237-1	N90-22398 #
CONF-900282-3	N90-21838 #
CONF-900466-5	N90-22417 #
CONF-900466-8	N90-21823 #
CONF-900608-9-REV	N90-22337 #
CONF-900608-10	N90-22045 #
CONF-900608-11	N90-22047 #
CONF-900615-1	N90-22003 #
CONF-900615-2	N90-22044 #
CONF-900617-6	N90-22115 #
CONF-900617-7	N90-21853 #
CONF-900617-8	N90-22116 #
CONF-900619-1	N90-22032 #
CONF-900619-2	N90-21875 #
CONF-900623-2	N90-21851 #
CONF-900640-3	N90-22170 #
CONF-900640-4	N90-22171 #
CONF-900640-4	N90-22173 #
CONF-900640-5	N90-22174 #
CONF-900646-3	N90-22111 #
CONF-900646-5	N90-22169 #
CONF-900646-11	N90-22172 #
CONF-900651-1	N90-22001 #
CONF-900651-2	N90-22005 #
CONF-900651-3	N90-22006 #
CONF-900652-1	N90-22256 #
CONF-900672-1	N90-21737 #
CONF-900684-1	N90-22008 #
CONF-900684-1-REV-1	N90-22009 #
CONF-900684-2	N90-22361 #
CONF-900689-2	N90-22412 #
CONF-8812131	N90-22206 #
CONF-8902101	N90-22399 #
CONF-8906295-1	N90-21865 #
CONF-8910387-1	N90-22516 #
CONF-9004125-3	N90-22249 #
CONF-9004159-3	N90-22259 #
CONF-9004177-1	N90-22251 #
CONF-9005132-1	N90-22277 #
CONF-9005155-1	N90-22048 #
CONF-9006101-1-REV-1	N90-22257 #
CONF-9006107-1	N90-22002 #
CONF-9006107-2	N90-22004 #
CONF-9006111-1	N90-22191 #
CONF-9006111-2	N90-22190 #
CONF-9006111-3	N90-22189 #
CONF-9006115-1	N90-22214 #
CONF-9006117-4	N90-21876 #
CONF-9006121-1	N90-22113 #
CONF-9006121-2	N90-22114 #
CONF-9006121-3	N90-21866 #
CONF-9006121-4	N90-22414 #
CONF-9006121-5	N90-22413 #
CONF-9006122-1	N90-22112 #
CONF-9006122-3	N90-22046 #
CONF-9006124-1	N90-22026 #
CONF-9006124-2	N90-22338 #
CONF-9006146-2	N90-21954* #
CONF-9006146-3	N90-21955 #
CONF-9006149-1	N90-21852 #
CSCC-G-1A-REV	N90-22247* #
DEL-SG-31-89	N90-22197 #
DE90-000318	N90-22142 #
DE90-000673	N90-22001 #
DE90-001598	N90-22256 #
DE90-002904	N90-22032 #
DE90-002989	N90-21737 #
DE90-003342	N90-21875 #
DE90-004874	N90-22044 #
DE90-005181	N90-22257 #
DE90-005195	N90-22111 #
DE90-005226	N90-22002 #
DE90-005237	N90-22412 #
DE90-005664	N90-22003 #
DE90-006046	N90-22169 #
DE90-006479	N90-22337 #
DE90-006892	N90-22045 #
DE90-006957	N90-22214 #
DE90-007012	N90-22004 #
DE90-007500	N90-22046 #
DE90-007537	N90-22170 #
DE90-007681	N90-22112 #
DE90-007684	N90-21865 #
DE90-007686	N90-22113 #
DE90-007689	N90-22114 #
DE90-007903	N90-22411 #
DE90-007986	N90-22381 #
DE90-007989	N90-22141 #
DE90-008011	N90-22277 #
DE90-008312	N90-22026 #
DE90-008313	N90-21866 #
DE90-008386	N90-21851 #
DE90-008407	N90-22047 #
DE90-008908	N90-21852 #
DE90-008928	N90-22413 #
DE90-008939	N90-22005 #
DE90-008940	N90-22006 #
DE90-008949	N90-22414 #
DE90-008952	N90-22115 #
DE90-008965	N90-22189 #
DE90-008991	N90-22190 #
DE90-009043	N90-22191 #
DE90-009152	N90-22007 #
DE90-009186	N90-22008 #
DE90-009191	N90-22171 #
DE90-009193	N90-22172 #
DE90-009202	N90-22173 #
DE90-009222	N90-22174 #
DE90-009227	N90-21876 #
DE90-009232	N90-21853 #
DE90-009290	N90-22009 #
DE90-009319	N90-22338 #
DE90-009323	N90-22249 #
DE90-009333	N90-21954* #
DE90-009380	N90-22192 #
DE90-009396	N90-22159 #
DE90-009398	N90-22361 #
DE90-009401	N90-22516 #
DE90-009416	N90-22463 #
DE90-009427	N90-22116 #
DE90-009429	N90-22048 #
DE90-009439	N90-22143 #
DE90-009466	N90-22193 #
DE90-009469	N90-21837 #
DE90-009473	N90-22210 #
DE90-009474	N90-21838 #
DE90-009476	N90-21839 #
DE90-009477	N90-22370 #
DE90-009478	N90-21944 #
DE90-009483	N90-22458 #
DE90-009511	N90-21955 #
DE90-009514	N90-22033 #
DE90-009528	N90-22415 #
DE90-009529	N90-22359 #
DE90-009534	N90-21854 #
DE90-009535	N90-21840 #
DE90-009536	N90-21841 #
DE90-009537	N90-22034 #
DE90-009539	N90-22393 #
DE90-009541	N90-21956 #
DE90-009549	N90-22394 #
DE90-009550	N90-22395 #
DE90-009551	N90-22396 #
DE90-009552	N90-22397 #
DE90-009565	N90-22416 #
DE90-009576	N90-22360 #
DE90-009579	N90-21867 #
DE90-009581	N90-22398 #
DE90-009613	N90-22035 #
DE90-009629	N90-21957 #

DE90-009631 .... N90-22010 #
DE90-009758 .... N90-21791 #
DE90-009777 .... N90-21855 #
DE90-009787 .... N90-21958 #
DE90-009804 .... N90-22258 #
DE90-009805 .... N90-22250 #
DE90-009812 .... N90-22417 #
DE90-009825 .... N90-22251 #
DE90-009833 .... N90-22259 #
DE90-009861 .... N90-22418 #
DE90-009864 .... N90-21823 #
DE90-009946 .... N90-22480 #
DE90-010244 .... N90-22260 #
DE90-614743 .... N90-21998 #
DE90-618585 .... N90-22399 #
DE90-618870 .... N90-22517 #
DE90-618944 .... N90-22507 #
DE90-619618 .... N90-22206 #
DE90-620099 .... N90-21945 #
DE90-620108 .... N90-22419 #
DE90-620109 .... N90-22420 #
DE90-620391 .... N90-22057 #

DOE/BC-14483/4 .... N90-22458 #

DOE/BP-63406/6 .... N90-22192 #
DOE/BP-63406/9 .... N90-22193 #
DOE/BP-63406/12 .... N90-22143 #

DOE/CE-34025/T3 .... N90-22210 #

DOE/ER-13439/5 .... N90-21837 #

DOE/OR-21400/T418 .... N90-22463 #

DOE/PC-70507/T2-PT-1 .... N90-22394 #
DOE/PC-70507/T2-PT-2 .... N90-22395 #
DOE/PC-70507/T2-PT-3 .... N90-22396 #
DOE/PC-70507/T2-PT-4 .... N90-22397 #
DOE/PC-79935/13 .... N90-22002 #

DOE/PETC/TR-90/5 .... N90-22007 #

DOE/RL-90-14 .... N90-22381 #

DOT/FAA/CT-TN89/63 .... N90-21724* #
DOT/FAA/CT-TN90/8 .... N90-21759 #
DOT/FAA/CT-TN90/12 .... N90-21774 #

DOT/FAA/PS-89/2 .... N90-21749 #

DOT/FAA/SA-89/2 .... N90-21750 #

DTIC/TR-89/1 .... N90-22433 #

E-4161 .... N90-21795* #
E-4441 .... N90-21843* #
E-4527 .... N90-21858* #
E-5080 .... N90-22464* #
E-5113 .... N90-22054* #
E-5200 .... N90-22021* #
E-5205 .... N90-22421* #
E-5224 .... N90-21842* #
E-5238 .... N90-21727* #
E-5241 .... N90-22262* #
E-5244 .... N90-21974* #
E-5262 .... N90-22488* #
E-5284 .... N90-21862* #
E-5295 .... N90-21962* #
E-5302 .... N90-21760* #
E-5306 .... N90-21826* #
E-5307 .... N90-21821* #
E-5345 .... N90-21869* #
E-5360 .... N90-22041* #
E-5388 .... N90-21871* #
E-5391 .... N90-21812* #
E-5426 .... N90-22117* #
E-5427 .... N90-21723* #
E-5431 .... N90-21762* #
E-5435 .... N90-22011* #
E-5442 .... N90-21825* #
E-5443 .... N90-21824* #
E-5448 .... N90-21725* #
E-5458 .... N90-21808* #
E-5462 .... N90-21733* #
E-5475 .... N90-21763* #
E-5492 .... N90-21844* #
E-5493 .... N90-22016* #
E-5502 .... N90-22324* #
E-5503 .... N90-22323* #
E-5504 .... N90-22325* #

EGG-CATT-8898 .... N90-22258 #
EGG-CATT-8926 .... N90-22250 #

EGG-EP-8917 .... N90-21958 #
EGG-EP-8918 .... N90-21957 #

EGG-M-89350 .... N90-22035 #
EGG-M-89359 .... N90-22004 #
EGG-M-89492 .... N90-22214 #

EGG-MS-8865 .... N90-21855 #

EGG-NE-8863 .... N90-22010 #

EOTR-88-9 .... N90-22212* #

EPA/560/5-89/007 .... N90-22156 #
EPA/600/D-89/176 .... N90-22157 #
EPA/600/D-89/217 .... N90-22182 #

ETN-90-96333 .... N90-22118 #
ETN-90-96336 .... N90-21783 #
ETN-90-96341 .... N90-22012 #
ETN-90-96342 .... N90-21740 #
ETN-90-96343 .... N90-21741 #
ETN-90-96344 .... N90-21751 #
ETN-90-96345 .... N90-21752 #
ETN-90-96346 .... N90-22119 #
ETN-90-96347 .... N90-22120 #
ETN-90-96348 .... N90-22013 #
ETN-90-96351 .... N90-21877 #
ETN-90-96352 .... N90-22341 #
ETN-90-96353 .... N90-21742 #
ETN-90-96354 .... N90-22050 #
ETN-90-96355 .... N90-22263 #
ETN-90-96356 .... N90-22342 #
ETN-90-96357 .... N90-22343 #
ETN-90-96358 .... N90-22264 #
ETN-90-96359 .... N90-22289 #
ETN-90-96360 .... N90-22265 #
ETN-90-96361 .... N90-22290 #
ETN-90-96362 .... N90-22266 #
ETN-90-96363 .... N90-21946 #
ETN-90-96364 .... N90-22344 #
ETN-90-96365 .... N90-22160 #
ETN-90-96366 .... N90-22051 #
ETN-90-96367 .... N90-22345 #
ETN-90-96368 .... N90-22326 #
ETN-90-96369 .... N90-22362 #
ETN-90-96370 .... N90-22459 #
ETN-90-96371 .... N90-22121 #
ETN-90-96372 .... N90-22346 #
ETN-90-96373 .... N90-22267 #
ETN-90-96374 .... N90-22122 #
ETN-90-96375 .... N90-21743 #
ETN-90-96376 .... N90-21845 #
ETN-90-96377 .... N90-21846 #
ETN-90-96379 .... N90-21847 #
ETN-90-96380 .... N90-22372 #
ETN-90-96381 .... N90-22373 #
ETN-90-96382 .... N90-22374 #
ETN-90-96383 .... N90-22375 #
ETN-90-96384 .... N90-22376 #
ETN-90-96385 .... N90-22268 #
ETN-90-96386 .... N90-22347 #
ETN-90-96387 .... N90-22269 #
ETN-90-96388 .... N90-22348 #
ETN-90-96389 .... N90-22349 #
ETN-90-96390 .... N90-22350 #
ETN-90-96391 .... N90-22351 #
ETN-90-96392 .... N90-22352 #
ETN-90-96393 .... N90-22353 #
ETN-90-96394 .... N90-22161
ETN-90-96395 .... N90-22140 #
ETN-90-96396 .... N90-22198 #
ETN-90-96397 .... N90-22270 #
ETN-90-96398 .... N90-22377 #
ETN-90-96399 .... N90-22014 #
ETN-90-96400 .... N90-22358 #
ETN-90-96401 .... N90-22015 #
ETN-90-96402 .... N90-21947 #
ETN-90-96403 .... N90-22327 #
ETN-90-96404 .... N90-22328 #
ETN-90-96405 .... N90-22329 #
ETN-90-96406 .... N90-22052 #
ETN-90-96407 .... N90-22053 #
ETN-90-96408 .... N90-22330 #
ETN-90-96409 .... N90-22271 #
ETN-90-96410 .... N90-22123 #
ETN-90-96411 .... N90-22331 #
ETN-90-96412 .... N90-21827 #
ETN-90-96413 .... N90-22384 #
ETN-90-96414 .... N90-22272 #
ETN-90-96415 .... N90-22273 #
ETN-90-96416 .... N90-21828 #
ETN-90-96417 .... N90-22291 #
ETN-90-96418 .... N90-22400 #
ETN-90-96419 .... N90-22401 #
ETN-90-96420 .... N90-22199 #
ETN-90-96421 .... N90-22200 #
ETN-90-96422 .... N90-22201 #
ETN-90-96423 .... N90-22422 #
ETN-90-96424 .... N90-22423 #
ETN-90-96425 .... N90-22274 #
ETN-90-96426 .... N90-22275 #
ETN-90-96427 .... N90-21948 #
ETN-90-96428 .... N90-22276 #
ETN-90-96429 .... N90-22378 #
ETN-90-96430 .... N90-22382 #
ETN-90-96431 .... N90-22354 #
ETN-90-96432 .... N90-22355 #
ETN-90-96433 .... N90-22356 #
ETN-90-96434 .... N90-22027 #
ETN-90-96435 .... N90-21856 #
ETN-90-96436 .... N90-22357 #
ETN-90-96437 .... N90-22460 #

FERMILAB-PUB-89/262-A .... N90-22426* #
FERMILAB-PUB-90/44-A .... N90-22504* #
FERMILAB-PUB-90/47-A .... N90-22502* #
FERMILAB-PUB-90/52-A .... N90-22506* #
FERMILAB-PUB-90/64-A .... N90-22503* #
FERMILAB-PUB-90/69-A .... N90-22525* #

FEW-397 .... N90-22335 #

FHWA/TX-90/1183-2 .... N90-22248 #

FNAL-PUB-90/56-A .... N90-22505* #

GA-A-20024 .... N90-22398 #

GAO/NSIAD-88-173FS .... N90-22461 #

GRI-89/0183 .... N90-21832 #
GRI-89/0255 .... N90-21833 #

H-1507 .... N90-22213* #
H-1553 .... N90-22322* #

IAEA-TECDOC-538 .... N90-22399 #

ICOMP-90-04 .... N90-21962* #

IDA-PAPER-P-1500 .... N90-22433 #

IFVE-OUNK-89-23 .... N90-22419 #
IFVE-OUNK-89-24 .... N90-22420 #

INIS-BR-1797 .... N90-22206 #

INIS-SU-154 .... N90-21945 #
INIS-SU-155 .... N90-22507 #
INIS-SU-156 .... N90-22517 #

INPE-4917-PRE/1516 .... N90-22332 #
INPE-4954-PRE/1532 .... N90-22333 #
INPE-4965-PRE/1534 .... N90-21848 #
INPE-4966-PRE/1535 .... N90-22501 #
INPE-4978-PRE/1543 .... N90-22457 #
INPE-4983-PRE/1546 .... N90-21787 #
INPE-4989-PRE/1551 .... N90-21788 #
INPE-5003-TDL/397 .... N90-21786 #
INPE-5018-RPE/612 .... N90-22138 #
INPE-5021-RPE/615 .... N90-22139 #

IOS-265 .... N90-22199 #
IOS-267 .... N90-22200 #
IOS-270 .... N90-22201 #

IPPCZ-282 .... N90-22386 #
IPPCZ-286 .... N90-22385 #

ISBN-0-86776-318-3 .... N90-22110 #
ISBN-90-370-0019-3 .... N90-22122 #
ISBN-91-7848-165-1 .... N90-21874 #
ISBN-92-835-0548-4 .... N90-21907 #
ISBN-92-835-0550-6 .... N90-22440 #
ISBN-92-835-0551-4 .... N90-21975 #
ISBN-951-754-989-X .... N90-21943 #
ISBN-951-8928-07-X .... N90-22057 #

ISSN-0038-0911 .... N90-22520 #
ISSN-0038-0911 .... N90-22521 #
ISSN-0075-3343 .... N90-22188 #
ISSN-0143-7135 .... N90-22378 #
ISSN-0143-7313 .... N90-21856 #
ISSN-0143-7313 .... N90-22027 #
ISSN-0143-7313 .... N90-22357 #
ISSN-0143-7313 .... N90-22460 #
ISSN-0169-1708 .... N90-22161
ISSN-0262-5369 .... N90-22354 #
ISSN-0262-5369 .... N90-22355 #
ISSN-0262-5369 .... N90-22356 #
ISSN-0284-5172 .... N90-21874 #
ISSN-0359-6214 .... N90-22410 #

ISSN-0389-4010 N90-21726 #
ISSN-0782-7415 N90-22057 #
ISSN-0783-7445 N90-21943 #
ISSN-0920-2358 N90-22264 #
ISSN-0922-5461 N90-21946 #
ISSN-0922-5461 N90-22051 #
ISSN-0922-5461 N90-22121 #
ISSN-0922-5461 N90-22160 #
ISSN-0922-5461 N90-22263 #
ISSN-0922-5461 N90-22266 #
ISSN-0922-5461 N90-22289 #
ISSN-0922-5461 N90-22290 #
ISSN-0922-5461 N90-22326 #
ISSN-0922-5461 N90-22342 #
ISSN-0922-5461 N90-22343 #
ISSN-0922-5461 N90-22345 #
ISSN-0922-5461 N90-22346 #
ISSN-0922-5461 N90-22362 #
ISSN-0922-5461 N90-22459 #
ISSN-0922-5641 N90-22265 #
ISSN-0922-5641 N90-22267 #
ISSN-0922-5641 N90-22344 #
ISSN-0923-1714 N90-22269 #
ISSN-0955-9655 N90-22382 #

IVO-A-01/89 N90-22057 #

JPL-TDA-PR-42-100 N90-21880* #

KCP-613-4302 N90-22026 #
KCP-613-4303 N90-21866 #

KNMI-TR-111 N90-22161

KU-FRL-724-4 N90-22000* #

LA-UR-89-4275 N90-22044 #
LA-UR-90-53 N90-22191 #
LA-UR-90-97-REV N90-22337 #
LA-UR-90-505 N90-22170 #
LA-UR-90-720 N90-22190 #
LA-UR-90-721 N90-22189 #
LA-UR-90-756 N90-22414 #
LA-UR-90-856 N90-22006 #
LA-UR-90-857 N90-22005 #
LA-UR-90-933 N90-22413 #

LA-11716-MS N90-21791 #

LBL-28442 N90-22171 #
LBL-28443 N90-22172 #
LBL-28444 N90-22173 #
LBL-28600 N90-22174 #

LC-79-640375 N90-22520 #
LC-79-640375 N90-22521 #

LNCC-020/89 N90-21998 #

LPI-681 N90-22166* #

LR-513 N90-21743 #
LR-526 N90-22118 #
LR-531 N90-21845 #
LR-562 N90-21846 #
LR-568 N90-21783 #
LR-576 N90-22012 #
LR-578 N90-21740 #
LR-579 N90-21741 #
LR-580 N90-21751 #
LR-581 N90-21752 #
LR-582 N90-22119 #
LR-583 N90-22120 #
LR-585 N90-22013 #
LR-591 N90-21847 #
LR-593 N90-21877 #
LR-597 N90-22341 #
LR-598 N90-21742 #
LR-599 N90-22050 #

LSPI-901 N90-21806* #
LSPI-903 N90-21807* #

M/NAFA/89-1 N90-21724* #

MEMO-INF-89-54 N90-22269 #

MEMO-808 N90-22347 #

MEMT-1 N90-22122 #

MP-89-227 N90-21839 #

NA-88-1877 N90-21755* #

NAL-TR-1011T N90-21726 #

NAS 1.15:4190 N90-22529* #
NAS 1.15:87622-REV N90-22247* #
NAS 1.15:89662 N90-22528* #
NAS 1.15:100050 N90-21778* #
NAS 1.15:100395 N90-22043* #
NAS 1.15:100397 N90-21836* #
NAS 1.15:100398 N90-22526* #
NAS 1.15:100451 N90-22213* #
NAS 1.15:100645-REV-1 N90-22135* #
NAS 1.15:100756 N90-21790* #
NAS 1.15:100758 N90-21864* #
NAS 1.15:101021 N90-21756* #
NAS 1.15:101051 N90-21757* #
NAS 1.15:101104 N90-22162* #
NAS 1.15:101280 N90-22371* #
NAS 1.15:101702 N90-22322* #
NAS 1.15:101899 N90-22430* #
NAS 1.15:101900 N90-22431* #
NAS 1.15:101901 N90-22432* #
NAS 1.15:102214-REV-1 N90-22216* #
NAS 1.15:102236 N90-21758* #
NAS 1.15:102363 N90-22464* #
NAS 1.15:102395 N90-22054* #
NAS 1.15:102432 N90-22021* #
NAS 1.15:102436 N90-22421* #
NAS 1.15:102443 N90-21842* #
NAS 1.15:102453 N90-22262* #
NAS 1.15:102457 N90-21974* #
NAS 1.15:102475 N90-22488* #
NAS 1.15:102489 N90-21858* #
NAS 1.15:102492 N90-21862* #
NAS 1.15:102499 N90-21962* #
NAS 1.15:102505 N90-21821* #
NAS 1.15:102535 N90-21869* #
NAS 1.15:102564 N90-21871* #
NAS 1.15:102569 N90-21812* #
NAS 1.15:102570 N90-21843* #
NAS 1.15:102575 N90-22041* #
NAS 1.15:102623 N90-22292* #
NAS 1.15:102664 N90-21744* #
NAS 1.15:102796 N90-21746* #
NAS 1.15:102798 N90-21773* #
NAS 1.15:102800 N90-21739* #
NAS 1.15:102819 N90-22340* #
NAS 1.15:102820 N90-22339* #
NAS 1.15:102912 N90-22428* #
NAS 1.15:102917 N90-21779* #
NAS 1.15:102925 N90-22147* #
NAS 1.15:102926 N90-22148* #
NAS 1.15:102989 N90-22456* #
NAS 1.15:103098 N90-21826* #
NAS 1.15:103102 N90-22117* #
NAS 1.15:103103 N90-21723* #
NAS 1.15:103107 N90-21762* #
NAS 1.15:103111 N90-22011* #
NAS 1.15:103114 N90-21727* #
NAS 1.15:103118 N90-21825* #
NAS 1.15:103119 N90-21824* #
NAS 1.15:103120 N90-21725* #
NAS 1.15:103128 N90-21808* #
NAS 1.15:103131 N90-21733* #
NAS 1.15:103140 N90-21844* #
NAS 1.15:103141 N90-22016* #
NAS 1.15:103148 N90-22324* #
NAS 1.15:103149 N90-22323* #
NAS 1.15:103150 N90-22325* #
NAS 1.21:7011(334) N90-22207* #
NAS 1.21:7011(335) N90-22208*
NAS 1.21:7037(250) N90-21722*
NAS 1.21:7064-SUPPL-3 N90-22438* #
NAS 1.26:3922(29) N90-22203*
NAS 1.26:4289 N90-21760* #
NAS 1.26:4297 N90-21754* #
NAS 1.26:4298 N90-21755* #
NAS 1.26:172060 N90-22202* #
NAS 1.26:177551 N90-21738* #
NAS 1.26:179862 N90-22402* #
NAS 1.26:180413 N90-22409* #
NAS 1.26:180432 N90-21954* #
NAS 1.26:181296 N90-22510* #
NAS 1.26:182013 N90-21785* #
NAS 1.26:182019 N90-21772* #
NAS 1.26:182032 N90-21745* #
NAS 1.26:183878 N90-21813* #
NAS 1.26:183927 N90-22049* #
NAS 1.26:183945 N90-21811* #
NAS 1.26:183953 N90-21793* #
NAS 1.26:183954 N90-21794* #
NAS 1.26:185061 N90-22166* #
NAS 1.26:185095 N90-22031* #
NAS 1.26:185157 N90-21724* #
NAS 1.26:185161 N90-21806* #
NAS 1.26:185172 N90-21807* #
NAS 1.26:185212 N90-22389* #
NAS 1.26:185218 N90-22022* #
NAS 1.26:185219 N90-21849* #
NAS 1.26:185222 N90-21761* #
NAS 1.26:185224 N90-21809* #
NAS 1.26:185237 N90-21810* #
NAS 1.26:185238 N90-21953* #
NAS 1.26:185243 N90-21763* #
NAS 1.26:185521 N90-21870* #
NAS 1.26:185608 N90-22212* #
NAS 1.26:186002 N90-22467* #
NAS 1.26:186058 N90-22017* #
NAS 1.26:186163 N90-21747* #
NAS 1.26:186164 N90-21780* #
NAS 1.26:186209 N90-22215* #
NAS 1.26:186234 N90-21872* #
NAS 1.26:186256 N90-22426* #
NAS 1.26:186300 N90-21753* #
NAS 1.26:186358 N90-21961* #
NAS 1.26:186359 N90-22278* #
NAS 1.26:186442 N90-22030* #
NAS 1.26:186478 N90-21817* #
NAS 1.26:186479 N90-21880* #
NAS 1.26:186512 N90-22408* #
NAS 1.26:186547 N90-22255* #
NAS 1.26:186560 N90-21736* #
NAS 1.26:186563 N90-22479* #
NAS 1.26:186571 N90-21734* #
NAS 1.26:186572 N90-21735* #
NAS 1.26:186578 N90-22522* #
NAS 1.26:186580 N90-21952* #
NAS 1.26:186584 N90-21789* #
NAS 1.26:186585 N90-21775* #
NAS 1.26:186586 N90-22000* #
NAS 1.26:186590 N90-22205* #
NAS 1.26:186592 N90-22525* #
NAS 1.26:186593 N90-22506* #
NAS 1.26:186594 N90-22505* #
NAS 1.26:186595 N90-22504* #
NAS 1.26:186596 N90-22503* #
NAS 1.26:186597 N90-22502* #
NAS 1.26:186598 N90-21776* #
NAS 1.26:186599 N90-21777* #
NAS 1.26:186601 N90-22261* #
NAS 1.26:186602 N90-21792* #
NAS 1.55:3062 N90-22079* #
NAS 1.55:3068 N90-22294* #
NAS 1.55:10016 N90-21795* #

NASA-CASE-KSC-11386-1 N90-22023*
NASA-CASE-KSC-11392-1 N90-22383*

NASA-CASE-LAR-12887-3 N90-21822*
NASA-CASE-LAR-13816-1 N90-22025*
NASA-CASE-LAR-13926-1 N90-22042*

NASA-CASE-LEW-14844-1 N90-22024*

NASA-CASE-MSC-21271-1 N90-21999*

NASA-CASE-NPO-17430-1-CU N90-21951*

NASA-CP-3062 N90-22079* #
NASA-CP-3068 N90-22294* #
NASA-CP-10016 N90-21795* #

NASA-CR-3922(29) N90-22203*
NASA-CR-4289 N90-21760* #
NASA-CR-4297 N90-21754* #
NASA-CR-4298 N90-21755* #
NASA-CR-172060 N90-22202* #
NASA-CR-177551 N90-21738* #
NASA-CR-179862 N90-22402* #
NASA-CR-180413 N90-22409* #
NASA-CR-180432 N90-21954* #
NASA-CR-181296 N90-22510* #
NASA-CR-182013 N90-21785* #
NASA-CR-182019 N90-21772* #
NASA-CR-182032 N90-21745* #
NASA-CR-183878 N90-21813* #
NASA-CR-183927 N90-22049* #
NASA-CR-183945 N90-21811* #
NASA-CR-183953 N90-21793* #
NASA-CR-183954 N90-21794* #
NASA-CR-185061 N90-22166* #
NASA-CR-185095 N90-22031* #
NASA-CR-185157 N90-21724* #
NASA-CR-185161 N90-21806* #
NASA-CR-185172 N90-21807* #
NASA-CR-185212 N90-22389* #
NASA-CR-185218 N90-22022* #
NASA-CR-185219 N90-21849* #
NASA-CR-185222 N90-21761* #
NASA-CR-185224 N90-21809* #
NASA-CR-185237 N90-21810* #
NASA-CR-185238 N90-21953* #
NASA-CR-185243 N90-21763* #
NASA-CR-185521 N90-21870* #
NASA-CR-185608 N90-22212* #

NASA-CR-186002	N90-22467* #
NASA-CR-186058	N90-22017* #
NASA-CR-186163	N90-21747* #
NASA-CR-186164	N90-21760* #
NASA-CR-186209	N90-22215* #
NASA-CR-186234	N90-21872* #
NASA-CR-186256	N90-22426* #
NASA-CR-186300	N90-21753* #
NASA-CR-186358	N90-21961* #
NASA-CR-186359	N90-22278* #
NASA-CR-186442	N90-22030* #
NASA-CR-186478	N90-21817* #
NASA-CR-186479	N90-21880* #
NASA-CR-186512	N90-22408* #
NASA-CR-186547	N90-22255* #
NASA-CR-186560	N90-21736* #
NASA-CR-186563	N90-22479* #
NASA-CR-186571	N90-21734* #
NASA-CR-186572	N90-21735* #
NASA-CR-186578	N90-22522* #
NASA-CR-186580	N90-21952* #
NASA-CR-186584	N90-21789* #
NASA-CR-186585	N90-21775* #
NASA-CR-186586	N90-22000* #
NASA-CR-186590	N90-22205* #
NASA-CR-186592	N90-22525* #
NASA-CR-186593	N90-22506* #
NASA-CR-186594	N90-22505* #
NASA-CR-186595	N90-22504* #
NASA-CR-186596	N90-22503* #
NASA-CR-186597	N90-22502* #
NASA-CR-186598	N90-21776* #
NASA-CR-186599	N90-21777* #
NASA-CR-186601	N90-22261* #
NASA-CR-186602	N90-21792* #
NASA-REPT-90-003	N90-22261* #
NASA-SP-7011(334)	N90-22207* #
NASA-SP-7011(335)	N90-22206*
NASA-SP-7037(250)	N90-21722*
NASA-SP-7064-SUPPL-3	N90-22438* #
NASA-TM-4190	N90-22529* #
NASA-TM-87622-REV	N90-22247* #
NASA-TM-89662	N90-22528* #
NASA-TM-100050	N90-21778* #
NASA-TM-100395	N90-22043* #
NASA-TM-100397	N90-21836* #
NASA-TM-100398	N90-22526* #
NASA-TM-100451	N90-22213* #
NASA-TM-100645-REV-1	N90-22135* #
NASA-TM-100756	N90-21790* #
NASA-TM-100758	N90-21864* #
NASA-TM-101021	N90-21756* #
NASA-TM-101051	N90-21757* #
NASA-TM-101104	N90-22162* #
NASA-TM-101280	N90-22371* #
NASA-TM-101702	N90-22322* #
NASA-TM-101899	N90-22430* #
NASA-TM-101900	N90-22431* #
NASA-TM-101901	N90-22432* #
NASA-TM-102214-REV-1	N90-22216* #
NASA-TM-102236	N90-21758* #
NASA-TM-102363	N90-22464* #
NASA-TM-102395	N90-22054* #
NASA-TM-102432	N90-22021* #
NASA-TM-102436	N90-22421* #
NASA-TM-102443	N90-21842* #
NASA-TM-102453	N90-22262* #
NASA-TM-102457	N90-21974* #
NASA-TM-102475	N90-22468* #
NASA-TM-102489	N90-21858* #
NASA-TM-102492	N90-21862* #
NASA-TM-102499	N90-21962* #
NASA-TM-102505	N90-21821* #
NASA-TM-102535	N90-21869* #
NASA-TM-102564	N90-21871* #
NASA-TM-102569	N90-21812* #
NASA-TM-102570	N90-21843* #
NASA-TM-102575	N90-22041* #
NASA-TM-102623	N90-22292* #
NASA-TM-102664	N90-21744* #
NASA-TM-102796	N90-21746* #
NASA-TM-102798	N90-21773* #
NASA-TM-102800	N90-21739* #
NASA-TM-102819	N90-22340* #
NASA-TM-102820	N90-22339* #
NASA-TM-102912	N90-22428* #
NASA-TM-102917	N90-21779* #
NASA-TM-102925	N90-22147* #
NASA-TM-102926	N90-22148* #
NASA-TM-102989	N90-22456* #
NASA-TM-103098	N90-21826* #
NASA-TM-103102	N90-22117* #
NASA-TM-103103	N90-21723* #
NASA-TM-103107	N90-21762* #
NASA-TM-103111	N90-22011* #
NASA-TM-103114	N90-21727* #
NASA-TM-103118	N90-21825* #
NASA-TM-103119	N90-21824* #
NASA-TM-103120	N90-21725* #
NASA-TM-103128	N90-21808* #
NASA-TM-103131	N90-21733* #
NASA-TM-103140	N90-21844* #
NASA-TM-103141	N90-22016* #
NASA-TM-103148	N90-22324* #
NASA-TM-103149	N90-22323* #
NASA-TM-103150	N90-22325* #
NCAR/CT-122	N90-22158 #
NCEER-89-0027	N90-22107 #
NIKHEF-H/89-3	N90-22372 #
NIKHEF-H/89-4	N90-22373 #
NIKHEF-H/89-7	N90-22374 #
NIKHEF-H/89-8	N90-22375 #
NIKHEF-H/89-9	N90-22376 #
NIKHEF-H/89-17	N90-22268 #
NIST/GCR-89/558	N90-21861 #
NIST/GCR-89/569	N90-21834 #
NISTIR-89/4135	N90-22252 #
NISTIR-89/4147	N90-22055 #
NISTIR-89/4149	N90-22106 #
NISTIR-89/4192	N90-22408* #
NISTIR-89/4197	N90-22336 #
NISTIR-89/4210	N90-22254 #
NISTIR-89/4225	N90-22253 #
NLR-TP-89077-U	N90-22014 #
NOAA-TM-ERL-ARL-178	N90-21729 #
NOAA-TM-ERL-ARL-179	N90-22155 #
NOAA-TM-NWS-ER-82	N90-22183 #
NPL-DITC-147/89	N90-22354 #
NPL-DITC-148/89	N90-22355 #
NPL-DITC-155/89	N90-22356 #
NPL-DMA(A)-188	N90-21856 #
NPL-DMA(A)-193	N90-22357 #
NPL-DMA(A)-195	N90-22460 #
NPL-DMM(A)-1	N90-22027 #
NPL-RS(EXT)-110	N90-22378 #
NPL-RSA(EXT)-11	N90-22382 #
NSSDC/WDC-A-R/S-90-06	N90-22456* #
NTSB/AAR-90/01	N90-21748 #
ORNL/FTR-3571	N90-22159 #
ORNL/TM-11302	N90-21833 #
OUEL-1761/89	N90-22327 #
OUEL-1762/89	N90-22328 #
OUEL-1767/89	N90-22329 #
OUEL-1768/89	N90-22052 #
OUEL-1772/89	N90-22053 #
OUEL-1773/89	N90-22330 #
OUEL-1777/89	N90-22271 #
OUEL-1780/89	N90-22123 #
OUEL-1781/89	N90-22331 #
OUEL-1784/89	N90-21827 #
OUEL-1785/89	N90-22384 #
OUEL-1786/89	N90-22272 #
OUEL-1789/89	N90-22273 #
OUEL-1791/89	N90-21828 #
OUEL-1803/89	N90-22291 #
OUEL-1804/89-PT-1	N90-22400 #
OUEL-1805/89-PT-2	N90-22401 #
PB90-100173	N90-22429 #
PB90-123126	N90-22409* #
PB90-129677	N90-22157 #
PB90-130253	N90-22252 #
PB90-130261	N90-22408* #
PB90-131277	N90-21832 #
PB90-131988	N90-22158 #
PB90-132671	N90-21833 #
PB90-132739	N90-22055 #
PB90-133976	N90-22335 #
PB90-134248	N90-22182 #
PB90-142217	N90-22155 #
PB90-145699	N90-22107 #
PB90-146291	N90-22156 #
PB90-146820	N90-22439 #
PB90-147414	N90-22183 #
PB90-147844	N90-21970 #
PB90-148669	N90-22520 #
PB90-148677	N90-22521 #
PB90-149808	N90-21729 #
PB90-150996	N90-22197 #
PB90-151101	N90-22477 #
PB90-151747	N90-22336 #
PB90-151754	N90-21834 #
PB90-151911	N90-22195 #
PB90-151929	N90-22196 #
PB90-154766	N90-21861 #
PB90-155359	N90-22106 #
PB90-155391	N90-22253 #
PB90-155409	N90-22254 #
PB90-164765	N90-22110 #
PB90-165606	N90-22410 #
PB90-165945	N90-22248 #
PB90-166554	N90-22013 #
PB90-166794	N90-21943 #
PB90-166984	N90-21874 #
PB90-167156	N90-22012 #
PB90-910401	N90-21748 #
PML-1987-C17	N90-21743 #
PML-1987-C142	N90-21845 #
PML-1988-C137	N90-21846 #
PML-1989-C67	N90-21847 #
PNL-7245	N90-22141 #
PROJ-2027-FR-VOL-1	N90-21793* #
PROJ-2027-FR-VOL-2	N90-21794* #
PW-FR-20668	N90-21761* #
REPT-6	N90-22195 #
REPT-7	N90-22196 #
REPT-89-38	N90-22263 #
REPT-89-39	N90-22342 #
REPT-89-40	N90-22267 #
REPT-89-41	N90-22343 #
REPT-89-42	N90-22264 #
REPT-89-43	N90-22289 #
REPT-89-44	N90-22265 #
REPT-89-45	N90-22290 #
REPT-89-46	N90-22266 #
REPT-89-47	N90-21946 #
REPT-89-48	N90-22344 #
REPT-89-49	N90-22160 #
REPT-89-50	N90-22051 #
REPT-89-51	N90-22345 #
REPT-89-52	N90-22326 #
REPT-89-54	N90-22362 #
REPT-89-55	N90-22459 #
REPT-89-56	N90-22121 #
REPT-89-57	N90-22346 #
REPT-89/29	N90-22477 #
REPT-90B00071	N90-21864* #
REPT-90B00078	N90-22294* #
REPT-90B00081	N90-21790* #
REPT-90SDS4202-BK-1	N90-22379 #
REPT-90SDS4202-BK-2	N90-22380 #
REPT-194	N90-22410 #
RISOE-M-2768	N90-22144 #
RR-CE98	N90-22110 #
RR-1183-2	N90-22248 #
RSRE-MEMO-4208	N90-22422 #
RSRE-MEMO-4269	N90-22423 #
RSRE-MEMO-4291	N90-22274 #
RSRE-MEMO-4294	N90-22275 #
RSRE-MEMO-4325	N90-21948 #
RSRE-89015	N90-22276 #
SAND-89-0183C	N90-21865 #
SAND-89-1927C	N90-22001 #
SAND-89-2126C	N90-22169 #
SAND-89-2175C	N90-21875 #
SAND-89-2244C	N90-22338 #
SAND-89-2313C	N90-21954* #
SAND-89-2382C	N90-21955 #
SAND-89-2383C	N90-22249 #
SAND-89-2425C	N90-22032 #
SAND-89-2505C	N90-22115 #
SAND-89-2617C	N90-22114 #
SAND-89-2666C	N90-21737 #
SAND-89-2730C	N90-22113 #
SAND-89-2913C	N90-22111 #
SAND-89-2918C	N90-22259 #

SAND-89-3134C N90-22412 #
SAND-90-0249 N90-22260 #
SAND-90-0534C N90-22046 #
SAND-90-0541C N90-22112 #

SERI/TP-211-3643 N90-22142 #

SFCC-PUBL-40 N90-21743 #
SFCC-PUBL-49 N90-21845 #
SFCC-PUBL-55 N90-21846 #
SFCC-PUBL-56 N90-21847 #

SGD-542-PT-1 N90-22520 #
SGD-542-PT-2 N90-22521 #

SP-RAPP-1989:15 N90-21874 #

SU-SLAC-PUB-5184 N90-22277 #

SU-SOL-90-5 N90-22360 #

SUSSEX-AST-90/4-1 N90-22505* #

TR-14 N90-22407 #
TR-1028-5 N90-21870* #

TTI-2-5-88-1183-2 N90-22248 #

TW-88-06 N90-22348 #
TW-89-03 N90-22349 #
TW-89-04 N90-22350 #
TW-89-05 N90-22351 #
TW-89-06 N90-22352 #
TW-89-09 N90-22353 #

TWR-17541-5 N90-21811* #
TWR-17543-VOL-4 N90-22049* #
TWR-50010 N90-21813* #

UCRL-CR-103211 N90-22393 #
UCRL-CR-103232 N90-21944 #
UCRL-CR-103260 N90-21854 #
UCRL-CR-103293 N90-22034 #
UCRL-CR-103294 N90-21839 #
UCRL-CR-103296 N90-21840 #
UCRL-CR-103297 N90-21841 #
UCRL-CR-103371 N90-22033 #
UCRL-CR-103380 N90-22370 #

UCRL-JC-103167 N90-21867 #
UCRL-JC-103243 N90-22008 #
UCRL-JC-103243-REV-1 N90-22009 #
UCRL-JC-103348 N90-22480 #

UCRL-21237 N90-22359 #
UCRL-21296 N90-22415 #
UCRL-101792 N90-21956 #
UCRL-102263-REV-1 N90-22257 #
UCRL-102784 N90-21838 #

UMC-IE-5-0590 N90-22255* #

UMN-TH-816/89 N90-22426* #

US PATENT-APPL-SN-262851 N90-22383*

US-PATENT-APPL-SN-165945 N90-22025*
US-PATENT-APPL-SN-250469 N90-22042*
US-PATENT-APPL-SN-252077 N90-21999*
US-PATENT-APPL-SN-264107 N90-22023*
US-PATENT-APPL-SN-323236 N90-21822*
US-PATENT-APPL-SN-326766 N90-22024*
US-PATENT-APPL-SN-332677 N90-21951*
US-PATENT-APPL-SN-422161 N90-21868 #
US-PATENT-APPL-SN-468335 N90-21850 #

US-PATENT-CLASS-29-888.046 N90-22042*
US-PATENT-CLASS-55-160 N90-22024*
US-PATENT-CLASS-55-203 N90-22024*
US-PATENT-CLASS-55-204 N90-22024*
US-PATENT-CLASS-89-36.02 N90-21822*
US-PATENT-CLASS-92-212 N90-22042*
US-PATENT-CLASS-92-213 N90-22042*
US-PATENT-CLASS-92-222 N90-22042*
US-PATENT-CLASS-92-248 N90-22042*
US-PATENT-CLASS-123-193P N90-22042*
US-PATENT-CLASS-165-32 N90-21999*
US-PATENT-CLASS-165-46 N90-21999*
US-PATENT-CLASS-165-78 N90-21999*
US-PATENT-CLASS-165-96 N90-21999*
US-PATENT-CLASS-181-286 N90-21822*
US-PATENT-CLASS-181-290 N90-21822*
US-PATENT-CLASS-210-97 N90-22024*
US-PATENT-CLASS-210-512.1 N90-22024*
US-PATENT-CLASS-250-229 N90-22383*
US-PATENT-CLASS-318-434 N90-21951*
US-PATENT-CLASS-318-561 N90-21951*
US-PATENT-CLASS-318-615 N90-21951*
US-PATENT-CLASS-318-618 N90-21951*
US-PATENT-CLASS-324-329 N90-22023*
US-PATENT-CLASS-350-356 N90-22383*
US-PATENT-CLASS-388-821 N90-21951*
US-PATENT-CLASS-422-62 N90-22025*
US-PATENT-CLASS-422-98 N90-22025*
US-PATENT-CLASS-422-111 N90-22025*
US-PATENT-CLASS-422-126 N90-22025*
US-PATENT-CLASS-436-55 N90-22025*
US-PATENT-CLASS-436-137 N90-22025*
US-PATENT-CLASS-436-143 N90-22025*

US-PATENT-4,909,133 N90-22042*
US-PATENT-4,909,313 N90-21999*
US-PATENT-4,910,396 N90-22383*
US-PATENT-4,911,062 N90-21822*
US-PATENT-4,911,738 N90-22024*
US-PATENT-4,911,890 N90-22025*
US-PATENT-4,912,386 N90-21951*
US-PATENT-4,912,414 N90-22023*

USAAVSCOM-CP-89-A-001 N90-21756* #

USAAVSCOM-TM-90-A-005 N90-21738* #

UTAP-107/90 N90-22506* #

UTRC-R90-997978 N90-21809* #

WHC-SA-0475 N90-21851 #

WU-AP/07/90 N90-22506* #

Appendix—About STAR

Scientific and Technical Aerospace Reports (STAR) is a major component of a comprehensive National Aeronautics and Space Administration information system covering aeronautics, space, and supporting disciplines. *STAR* is issued on the 8th and 23rd of each month and announces current publications of the following types:

- NASA, NASA contractor, and NASA grantee reports
- Reports issued by other U.S. Government agencies, domestic and foreign institutions, universities, and private firms
- Translations in report form
- NASA-owned patents and patent applications
- Other U.S. Government agency and foreign patents and patent applications
- Domestic and foreign dissertations and theses

Journal, book, and conference literature, cover-to-cover journal translations, and certain foreign dissertations are announced in a companion journal, *International Aerospace Abstracts (IAA),* available on subscription from the American Institute of Aeronautics and Astronautics, Technical Information Service, 555 West 57th Street, 12th Floor, New York, NY 10019.

SUBJECT SCOPE

The subject scope of *STAR* and *IAA* includes all aspects of aeronautics and space research and development, supporting basic and applied research, and applications. Aerospace aspects of earth resources, energy development, conservation, oceanography, environmental protection, urban transportation, and other topics of high national priority are also covered.

OTHER NASA PUBLICATIONS

Other NASA publications and information services are described in the publication, *The NASA Scientific and Technical Information System ... and How to Use It,* available without charge from the NASA Scientific and Technical Information Facility, P.O. Box 8757, BWI Airport, MD 21240.

HOW TO USE *STAR* SUBJECT CATEGORIES

STAR is categorized by 10 major subject divisions broken down further into 76 specific subject categories and one general division/category. The major subject divisions are listed on page ii in the Table of Contents, together with a note for each that defines its scope and provides any cross-references. For example:

> **AERONAUTICS**
>
> Includes aeronautics (general); aerodynamics; air transportation and safety; aircraft communications and navigation; aircraft design, testing and performance; aircraft instrumentation; aircraft propulsion and power; aircraft stability and control; and research and support facilities (air).
>
> For related information see also *Astronautics.*

Each major division is further divided into as many as nine specific categories, which are identified by category numbers.

Abstracts in *STAR* are grouped by subject category, the categories appearing in sequential order. Category breaks in the abstract section are identified by the category number and title, and a scope note. Cross-references to other categories are provided as appropriate. For example:

> **02 AERODYNAMICS**
>
> Includes aerodynamics of bodies, combinations, wings, rotors, and control surfaces; and internal flow in ducts and turbomachinery.
>
> For related information see also *34 Fluid Mechanics and Heat Transfer.*

CROSS-REFERENCES

Individual *STAR* abstracts are not ordinarily cross-referenced, except for certain conference reports or book translations that have had separate abstracts written for their component papers or chapters. Citations and abstracts of the components follow immediately after those of the parent document. When the subject content of a component differs sufficiently from the general content of the parent, a cross-reference citation also is printed at the end of the category to which it normally would have been assigned if it were independent.

DOCUMENTS ON MICROFICHE

Documents on microfiche(1) are designated by a pound sign (#) following the accession number. The pound sign is used without regard to the source or quality of the microfiche.

LIMITED REPRODUCIBILITY

A Note of Limited Reproducibility appears in the citation, if one or a combination of the following factors affect the reproducibility of more than 20% of the document. These factors include: faint or broken type, color photographs, black and white photographs, foldouts, dot matrix print, charts/graphs with script notation, non-Roman alphabet, or some other factor that limits the reproducibility of that document. This notation also appears on the microfiche header, with the specific causing factor checked off on a list visible in the second frame.

COLOR COPIES

An increasing number of NASA scientific and technical reports are being produced with color graphs, charts, illustrations, and photographs. A message indicating that a document has color pages follows the Sales and Pricing (SAP) information in the *STAR* citation.

Registered users of the NASA Scientific and Technical Information System will receive ordered documents with color at no *additional* cost, as long as stock copies of that document are available. Otherwise, an additional fee of $2.00 per color page, over and above the standard document price will be charged. The NASA STI Facility staff will work with registered users over the telephone to inform and meet each individual's ordering needs.

AVAILABILITIES

One or more sources from which a document announced in *STAR* is available to the public is given in each citation. The most commonly indicated sources and their acronyms or abbreviations are listed below. If the publication is available from a source other than those listed, the publisher and his address will be displayed on the availability line or in combination with the corporate source line.

Avail: NTIS. Sold by the National Technical Information Service. Prices for hard copy (HC) and microfiche (MF) are indicated by a price code following the letters HC or MF in the *STAR* citation. Current values for the price codes are given in the tables on page A-7.

---

(1) A microfiche is a transparent sheet of film, 105 by 148 mm in size, containing as many as 60 to 98 pages of information reduced to micro images (not to exceed 26:1 reduction).

Initially distributed microfiche under the NTIS SRIM (Selected Research in Microfiche) is available at greatly reduced unit prices. For this service and for information concerning subscription to NASA printed reports, consult the NTIS Subscription Section, Springfield, VA 22161.

NOTE ON ORDERING DOCUMENTS: When ordering NASA publications (those followed by the * symbol), use the N accession number. NASA patent applications (only the specifications are offered) should be ordered by the US-Patent-Appl-SN number. Non-NASA publications (no asterisk) should be ordered by the AD, PB, or other *report number* shown on the last line of the citation, not by the N accession number. It is also advisable to cite the title and other bibliographic identification.

Avail: SOD (or GPO). Sold by the Superintendent of Documents, U.S. Government Printing Office, in hard copy. The current price and order number are given following the availability line. (NTIS will fill microfiche requests, as indicated above, for those documents identified by a # symbol.)

Avail: BLL (formerly NLL): British Library Lending Division, Boston Spa, Wetherby, Yorkshire, England. Photocopies available from this organization at the price shown. (If none is given, address inquiry to the BLL.)

Avail: DOE Depository Libraries. Organizations in U.S. cities and abroad that maintain collections of Department of Energy reports, usually in microfiche form, are listed in *Energy Research Abstracts.* Services available from the DOE and its depositories are described in a booklet, *DOE Technical Information Center - Its Functions and Services* (TID-4660), which may be obtained without charge from the DOE Technical Information Center.

Avail: ESDU. Pricing information on specific data, computer programs, and details on Engineering Sciences Data Unit (ESDU) topic categories can be obtained from ESDU International Ltd. Requesters in North America should use the Virginia address while all other requesters should use the London address, both of which are on page A-6.

Avail: Fachinformationszentrum, Karlsruhe. Sold by the Fachinformationszentrum Energie, Physik, Mathematik GMBH, Eggenstein Leopoldshafen, Federal Republic of Germany, at the price shown in deutschmarks (DM).

Avail: HMSO. Publications of Her Majesty's Stationery Office are sold in the U.S. by Pendragon House, Inc. (PHI), Redwood City, CA. The U.S. price (including a service and mailing charge) is given, or a conversion table may be obtained from PHI.

Avail: NASA Public Document Rooms. Documents so indicated may be examined at or purchased from the National Aeronautics and Space Administration, Public Documents Room (Room 126), 600 Independence Ave., S.W., Washington, DC 20546, or public document rooms located at NASA installations, and the NASA Pasadena Office at the Jet Propulsion Laboratory.

Avail: Univ. Microfilms. Documents so indicated are dissertations selected from *Dissertation Abstracts* and are sold by University Microfilms as xerographic copy (HC) and microfilm. All requests should cite the author and the Order Number as they appear in the citation.

Avail: US Patent and Trademark Office. Sold by Commissioner of Patents and Trademarks, U.S. Patent and Trademark Office, at the standard price of

$1.50 each, postage free. (See discussion of NASA patents and patent applications below.)

Avail: (US Sales Only). These foreign documents are available to users within the United States from the National Technical Information Service (NTIS). They are available to users outside the United States through the International Nuclear Information Service (INIS) representative in their country, or by applying directly to the issuing organization.

Avail: USGS. Originals of many reports from the U.S. Geological Survey, which may contain color illustrations, or otherwise may not have the quality of illustrations preserved in the microfiche or facsimile reproduction, may be examined by the public at the libraries of the USGS field offices whose addresses are listed in this Introduction. The libraries may be queried concerning the availability of specific documents and the possible utilization of local copying services, such as color reproduction.

Avail: Issuing Activity, or Corporate Author, or no indication of availability. Inquiries as to the availability of these documents should be addressed to the organization shown in the citation as the corporate author of the document.

NASA PATENTS AND PATENT APPLICATIONS

Patents and patent applications owned by NASA are announced in *STAR* under appropriate subject categories and are referenced in the *STAR* indexes. In the Report/Accession Number Index, patents are indexed by the NASA Case Number (which appears in lieu of the report number in other indexes), the U.S. Patent Number, the U.S. Patent Application Serial Number, and the U.S. Patent Class. Patent applications for which patents have not yet been issued are indexed by the NASA Case Number and the U.S. Patent Application Serial Number.

NASA *patent application specifications* are sold in paper copy and microfiche by the National Technical Information Service (NTIS). The US-Patent-Appl-SN- number should be used in ordering either paper copy or microfiche from NTIS. Printed copies of *patents* (which are not microfiched) are available for purchase from:

Commissioner of Patents and Trademarks
U.S. Patent and Trademark Office
Washington, DC 20231

When ordering patents, the U.S. Patent Number should be used, and payment must be remitted in advance, by money order or check payable to the Commissioner of Patents and Trademarks. Prepaid purchase coupons for ordering are also available from the Patent and Trademark Office. The patents and patent applications announced in *STAR* are owned by NASA and are available for royalty-free licensing. Requests for licensing terms and further information should be addressed to:

Associate General Counsel for Intellectual Property/Code GP
National Aeronautics and Space Administration
Washington, DC 20546

ELIGIBILITY AND REGISTRATION FOR NASA INFORMATION PRODUCTS AND SERVICES

A variety of services is available to organizations of the following types that have registered with NASA to receive specific services or products:

1. NASA offices and installations, contractors, subcontractors, grantees, and consultants;
2. Other U.S. Government agencies and their contractors;
3. Libraries in the United States that have arrangements with NASA to maintain collections of NASA documents for public reference;
4. Other organizations in the United States having a need for NASA documents in work related to aeronautics and space research;
5. Organizations abroad that have established reciprocal document exchange arrangements with NASA.

Only the central service points or central points of document acquisition and control within qualified organizations are eligible to register for NASA products and services. Domestic organizations that may be eligible to receive various classes of NASA publications and services should address their requests for registration or for further information to:

NASA Scientific and Technical Information Facility
ATTN: Registration Services
P.O. Box 8757
BWI Airport, MD 21240
301-621-0153

Organizations abroad should direct requests to Manager, International STI Activities, NTT, NASA Headquarters, Washington, DC 20546.

AVAILABILITY OF *STAR* ABSTRACTS ON MICROFICHE

Microfiche of the abstract sections of this issue and other issues of *STAR* are available on annual subscription from NTIS as PB90-911300, Attn: Subscriptions, 5285 Port Royal Road, Springfield, VA 22161. Annual subscription rates are $75.50 North America; $151.00 foreign. Abstract sections for previous years retroactive to 1964 are available at the current rates. Microfiche for individual *STAR* issue abstract sections are not available.

PUBLIC COLLECTIONS OF NASA DOCUMENTS

DOMESTIC: NASA and NASA-sponsored documents and a large number of aerospace publications are available to the public for reference purposes at the library maintained by the American Institute of Aeronautics and Astronautics, Technical Information Service, 555 West 57th Street, 12th Floor, New York, NY 10019

EUROPEAN: An extensive collection of NASA and NASA-sponsored publications is maintained by the British Library Lending Division, Boston Spa, Wetherby, Yorkshire, England, for public access. The British Library Lending Division also has available many of the non-NASA publications cited in *STAR*. European requesters may purchase facsimile copy or microfiche of NASA and NASA-sponsored documents, those identified by both the symbols # and * from ESA - Information Retrieval Service, European Space Agency, 8-10 rue Mario-Nikis, 75738 Paris CEDEX 15, France.

FEDERAL DEPOSITORY LIBRARY PROGRAM

In order to provide the general public with greater access to U.S. Government publications, Congress established the Federal Depository Library Program under the Government Printing Office (GPO), with 51 regional depositories responsible for permanent retention of material, inter-library loan, and reference services. At least one copy of nearly every NASA and NASA-sponsored publication, either in printed or microfiche format, is received and retained by the 51 regional depositories. A list of the regional GPO libraries, arranged alphabetically by state, appears on the inside back cover. These libraries are *not* sales outlets. A local library can contact a Regional Depository to help locate specific reports, or direct contact may be made by an individual.

ADDRESSES OF ORGANIZATIONS

American Institute of Aeronautics and Astronautics
Technical Information Service
555 West 57th Street, 12th Floor
New York, New York 10019

British Library Lending Division,
Boston Spa, Wetherby, Yorkshire,
England

Commissioner of Patents and Trademarks
U.S. Patent and Trademark Office
Washington, DC 20231

Department of Energy
Technical Information Center
P.O. Box 62
Oak Ridge, Tennessee 37830

European Space Agency-Information Retrieval Service
ESRIN
Via Galileo Galilei
00044 Frascati (Rome) Italy

Engineering Sciences Data Unit International
P.O. Box 1633
Manassas, Virginia 22110

Engineering Sciences Data Unit International, Ltd.
251-259 Regent Street
London, W1R 7AD, England

Fachinformationszentrum Energie, Physik, Mathematik
GMBH
7514 Eggenstein Leopoldshafen
Federal Republic of Germany

Her Majesty's Stationery Office
P.O. Box 569, S.E. 1
London, England

NASA Scientific and Technical Information Facility
P.O. Box 8757
BWI Airport, Maryland 21240

National Aeronautics and Space Administration
Scientific and Technical Information Division (NTT)
Washington, DC 20546

National Technical Information Service
5285 Port Royal Road
Springfield, Virginia 22161

Pendragon House, Inc.
899 Broadway Avenue
Redwood City, California 94063

Superintendent of Documents
U.S. Government Printing Office
Washington, DC 20402

University Microfilms
A Xerox Company
300 North Zeeb Road
Ann Arbor, Michigan 48106

University Microfilms, Ltd.
Tylers Green
London, England

U.S. Geological Survey Library National Center
MS 950
12201 Sunrise Valley Drive
Reston, Virginia 22092

U.S. Geological Survey Library
2255 North Gemini Drive
Flagstaff, Arizona 86001

U.S. Geological Survey
345 Middlefield Road
Menlo Park, California 94025

U.S. Geological Survey Library
Box 25046
Denver Federal Center, MS914
Denver, Colorado 80225

NTIS PRICE SCHEDULES

(Effective January 1, 1990)

Schedule A
STANDARD PRICE DOCUMENTS AND MICROFICHE

PRICE CODE	NORTH AMERICAN PRICE	FOREIGN PRICE
A01	$ 8.00	$ 16.00
A02	11.00	22.00
A03	15.00	30.00
A04-A05	17.00	34.00
A06-A09	23.00	46.00
A10-A13	31.00	62.00
A14-A17	39.00	78.00
A18-A21	45.00	90.00
A22-A25	53.00	106.00
A99	*	*
N01	60.00	120.00
N02	59.00	118.00
N03	20.00	40.00

Schedule E
EXCEPTION PRICE DOCUMENTS AND MICROFICHE

PRICE CODE	NORTH AMERICAN PRICE	FOREIGN PRICE
E01	$10.00	$ 20.00
E02	12.00	24.00
E03	14.00	28.00
E04	16.50	33.00
E05	18.50	37.00
E06	21.50	43.00
E07	24.00	48.00
E08	27.00	54.00
E09	29.50	59.00
E10	32.50	65.00
E11	35.00	70.00
E12	38.50	77.00
E13	41.00	82.00
E14	45.00	90.00
E15	48.50	97.00
E16	53.00	106.00
E17	57.50	115.00
E18	62.00	124.00
E19	69.00	138.00
E20	80.00	160.00
E99	*	*

* Contact NTIS for price quote.

IMPORTANT NOTICE

NTIS Shipping and Handling Charges

U.S., Canada, Mexico — ADD $3.00 per TOTAL ORDER

All Other Countries — ADD $4.00 per TOTAL ORDER

Exceptions — Does NOT apply to:

ORDERS REQUESTING NTIS RUSH HANDLING
ORDERS FOR SUBSCRIPTION OR STANDING ORDER PRODUCTS *ONLY*

NOTE: Each additional delivery address on an order requires a separate shipping and handling charge.

FEDERAL REGIONAL DEPOSITORY LIBRARIES

ALABAMA

AUBURN UNIV. AT MONTGOMERY LIBRARY
Documents Department
Montgomery, AL 36193
(205) 279-9110 ext.253

UNIV. OF ALABAMA LIBRARY
Reference Department/Documents
Box S
Tuscaloosa, AL 35486
(205) 348-6046

ARIZONA

DEPT. OF LIBRARY, ARCHIVES, AND PUBLIC RECORDS
Third Floor State Capitol
1700 West Washington
Phoenix, AZ 85007
(602) 255-4121

ARKANSAS

ARKANSAS STATE LIBRARY
Documents Service Section
One Capitol Mall
Little Rock, AR 72201
(501) 371-2090

CALIFORNIA

CALIFORNIA STATE LIBRARY
Govt. Publications Section
914 Capitol Mall
Sacramento, CA 95814
(916) 322-4572

COLORADO

UNIV. OF COLORADO
Norlin Library
Government Publications Division
Campus Box 184
Boulder, CO 80309
(303) 492-8834

DENVER PUBLIC LIBRARY
Govt. Pub. Department
1357 Broadway
Denver, CO 80203
(303) 571-2346

CONNECTICUT

CONNECTICUT STATE LIBRARY
231 Capitol Avenue
Hartford, CT 06106
(203) 566-4971

FLORIDA

UNIV. OF FLORIDA LIBRARIES
Documents Department
Library West
Gainesville, FL 32611
(904) 392-0367

GEORGIA

UNIV. OF GEORGIA LIBRARIES
Government Documents Dept.
Athens, GA 30602
(404) 542-8949

HAWAII

UNIV. OF HAWAII
Hamilton Library
Government Documents Collection
2550 The Mall
Honolulu, HI 96822
(808) 948-8230

IDAHO

UNIV. OF IDAHO LIBRARY
Documents Section
Moscow, ID 83843
(208) 885-6344

ILLINOIS

ILLINOIS STATE LIBRARY
Federal Documents
Centennial Building
Springfield, IL 62756
(217) 782-5012

INDIANA

INDIANA STATE LIBRARY
Serials Section
140 North Senate Avenue
Indianapolis, IN 46204
(317) 232-3686

IOWA

UNIV. OF IOWA LIBRARIES
Government Publications Dept.
Iowa City, IA 52242
(319) 335-5926

KANSAS

UNIVERSITY OF KANSAS
Spencer Research Library
Government Documents
Lawrence, KS 66045
(913) 864-4662

KENTUCKY

UNIV. OF KENTUCKY LIBRARIES
Government Publications/Maps Dept.
Lexington, KY 40506
(606) 257-8400

LOUISIANA

LOUISIANA STATE UNIVERSITY
Middleton Library
Government Documents Dept.
Baton Rouge, LA 70803
(504) 388-2570

LOUISIANA TECHNICAL UNIV.
Prescott Memorial Library
Government Documents Dept.
Ruston, LA 71272
(318) 257-4962

MAINE

UNIVERSITY OF MAINE
Raymond H. Fogler Library
Govt. Documents & Microforms Dept.
Orono, ME 04469
(207) 581-1680

MARYLAND

UNIVERSITY OF MARYLAND
McKeldin Library
Documents/Maps Room
College Park, MD 20742
(301) 454-3034

MASSACHUSETTS

BOSTON PUBLIC LIBRARY
Government Documents Dept.
666 Boylston Street
Boston, MA 02117
(617) 536-5400 ext.226

MICHIGAN

DETROIT PUBLIC LIBRARY
5201 Woodward Avenue
Detroit, MI 48202
(313) 833-1409

LIBRARY OF MICHIGAN
Government Documents
P.O. Box 30007
735 E. Michigan Avenue
Lansing, MI 48909
(517) 373-1593

MINNESOTA

UNIVERSITY OF MINNESOTA
Wilson Library
Government Publications
309 Nineteenth Avenue South
Minneapolis, MN 55455
(612) 373-7813

MISSISSIPPI

UNIV. OF MISSISSIPPI LIB.
Government Documents Dept.
106 Old Gym Bldg.
University, MS 38677
(601) 232-5857

MISSOURI

University of Missouri at Columbia Library
Government Documents
Columbia, MO 65201
(314) 882-6733

MONTANA

UNIV. OF MONTANA
Mansfield Library
Documents Division
Missoula, MT 59812
(406) 243-6700

NEBRASKA

UNIVERSITY OF NEBRASKA - LINCOLN
Love Memorial Library
Documents Department
Lincoln, NE 68588
(402) 472-2562

NEVADA

UNIV. OF NEVADA-RENO LIB.
Govt. Pub. Department
Reno, NV 89557
(702) 784-6579

NEW JERSEY

NEWARK PUBLIC LIBRARY
U.S. Documents Division
5 Washington Street
P.O. Box 630
Newark, NJ 07101
(201) 733-7812

NEW MEXICO

UNIVERSITY OF NEW MEXICO
General Library
Government Publications/Maps Dept.
Albuquerque, NM 87131
(505) 277-5441

NEW MEXICO STATE LIBRARY
325 Don Gaspar Avenue
Santa Fe, NM 87501
(505) 827-3826

NEW YORK

NEW YORK STATE LIBRARY
Documents Sect. Cultural Educ. Ctr.
Empire State Plaza
Albany, NY 12230
(518) 474-5563

NORTH CAROLINA

UNIVERSITY OF NORTH CAROLINA AT CHAPEL HILL
Davis Library 080A
BA/SS Department Documents
Chapel Hill, NC 27514
(919) 962-1151

NORTH DAKOTA

NORTH DAKOTA STATE UNIVERSITY LIBRARY
Government Documents Dept.
Fargo, ND 58105
(701) 237-8352
In cooperation with Univ. of North Dakota, Chester Fritz Library Grand Forks

OHIO

STATE LIBRARY OF OHIO
Documents Section
65 South Front Street
Columbus, OH 43266
(614) 644-7051

OKLAHOMA

OKLAHOMA DEPT. OF LIBRARIES
Government Documents
200 NE 18th Street
Oklahoma City, OK 73105
(405) 521-2502, ext. 252

OKLAHOMA STATE UNIV. LIB.
Documents Department
Stillwater, OK 74078
(405) 624-0489

OREGON

PORTLAND STATE UNIV.
Millar Library
934 SW Harrison - P.O. Box 1151
Portland, OR 97207
(503) 229-3673

PENNSYLVANIA

STATE LIBRARY OF PENN.
Government Publications Section
Box 1601
Walnut St. & Commonwealth Ave.
Harrisburg, PA 17105
(717) 787-3752

SOUTH CAROLINA

CLEMSON UNIV. COOPER LIB.
Documents Department
Clemson, SC 29634
(803) 656-5174
In cooperation with Univ. of South Carolina, Thomas Cooper Library, Columbia

TEXAS

TEXAS STATE LIBRARY
Public Services Department
P.O. Box 12927 - 1201 Brazos
Austin, TX 78711
(512) 463-5455

TEXAS TECH. UNIV. LIBRARY
Documents Department
Lubbock, TX 79409
(806) 742-2268

UTAH

UTAH STATE UNIVERSITY
Merrill Library & Learning Resources Center, UMC-30
Documents Department
Logan, UT 84322
(801) 750-2682

VIRGINIA

UNIVERSITY OF VIRGINIA
Alderman Library
Government Documents
Charlottesville, VA 22903
(804) 924-3133

WASHINGTON

WASHINGTON STATE LIBRARY
Document Section
Olympia, WA 98504
(206) 753-4027

WEST VIRGINIA

WEST VIRGINIA UNIV. LIB.
Government Documents Section
P.O. Box 6069
Morgantown, WV 26506
(304) 293-3640

WISCONSIN

ST. HIST SOC. OF WISCONSIN LIB.
Government Pub. Section
816 State Street
Madison, WI 53706
(608) 262-2781
In cooperation with Univ. of Wisconsin-Madison, Memorial Library

MILWAUKEE PUBLIC LIBRARY
Documents Division
814 West Wisconsin Avenue
Milwaukee, WI 53233
(414) 278-3065

WYOMING

WYOMING STATE LIBRARY
Supreme Court & Library Bldg.
Cheyenne, WY 82002
(307) 777-5919

National Aeronautics and
Space Administration
Code NTT
Washington, D.C.
20546
Official Business
Penalty for Private Use, $300

SPECIAL FOURTH-CLASS RATE
POSTAGE & FEES PAID
NASA
PERMIT No. G27

POSTMASTER: If Undeliverable (Section 158
Postal Manual) Do Not Return